British Journal of Pharmacology

September 1994

Volume 113 Number 1 pages 1–330

Br. J. Pharmacol. (1994), **113**, 1–2

SPECIAL REPORT

Characterization of the 5-HT receptor potentiating neuromuscular cholinergic transmission in strips of human isolated detrusor muscle

[1]M. Tonini, E. Messori, *G.P. Franceschetti, [2]C.A. Rizzi, A.F. Castoldi, T. Coccini & **S.M. Candura

Department of Internal Medicine and Therapeutics, Division of Pharmacology and Toxicology, University of Pavia, Piazza Botta 10, I-27100 Pavia, Italy; *Division of Urology, Ospedale Civile, Voghera, Italy and **Clinica del Lavoro Foundation, Pavia Medical Centre, Toxicology Unit, Pavia, Italy

In human isolated detrusor strips, submaximal contractile responses evoked by electrical stimulation were resistant to hexamethonium (30 μM) and abolished by tetrodotoxin (0.6 μM) and hyoscine (1 μM), indicating the activation of postganglionic cholinergic nerves. In methysergide (1 μM) and ondansetron (3 μM) pretreated tissues, 5-hydroxytryptamine (5-HT) (0.3 nM–1 μM) caused a concentration-dependent increase in the amplitude of contractions ($pEC_{50} = 8.1$), which was antagonized by the selective 5-HT_4 receptor antagonist GR 113808 (3, 10 and 30 nM) in a competitive manner. Schild analysis yielded a pA_2 estimate of 8.9, a value comparable to that reported for GR 113808 in other animal and human peripheral tissues (8.8–9.7). Our findings indicate that neuromuscular cholinergic transmission in human isolated detrusor muscle is facilitated by neural 5-HT receptors belonging to the 5-HT_4 subtype. The human urinary bladder can thus be regarded as an additional site in which 5-HT_4 receptors are distributed.

Keywords: Human urinary bladder; detrusor strips; neuromuscular cholinergic transmission; 5-hydroxytryptamine; GR 113808; 5-HT_4 receptors

Introduction Excitatory effects elicited by 5-hydroxytryptamine (5-HT) have been described in both unstimulated (Klarskov & Hørby-Petersen, 1986) and electrically stimulated human detrusor strips (Hindmarsh *et al.*, 1977; Corsi *et al.*, 1991). In unstimulated preparations, the 5-HT-induced contractile response is probably mediated by 5-HT_{2A} receptors located on the effector cells, as demonstrated by ketanserin antagonism and by tetrodotoxin resistance (Klarskov & Hørby-Petersen, 1986). In stimulated preparations, 5-HT facilitates neuromuscular cholinergic transmission via receptors different from the 5-HT_1, 5-HT_{2A} and 5-HT_3 subtypes. In fact, the 5-HT_1/5-HT_2 receptor antagonist methysergide and ketanserin were only slightly effective or ineffective (Hindmarsh *et al.*, 1977; Corsi *et al.*, 1991), as was the 5-HT_3 receptor antagonist ondansetron (Corsi *et al.*, 1991). Conversely, the 5-HT potentiating effect was sensitive to micromolar concentrations of tropisetron (Corsi *et al.*, 1991), a low affinity competitive antagonist at central and peripheral 5-HT_4 receptors (Tonini *et al.*, 1991). However, the reported pA_2 value for tropisetron (7.0 instead of 6.5) and a marked reduction of the 5-HT response maximum, have raised some uncertainty as to the type of antagonism observed, as well as on the definition of receptors involved. The need for a careful characterization of this 'atypical' 5-HT receptor has been recently stressed (Ford & Clarke, 1993). The availability of high affinity antagonists at 5-HT_4 receptors, such as GR 113808 (Kaumann, 1993; Gale *et al.*, 1994), prompted us to investigate whether these receptors are involved in the potentiating effect of 5-HT on human isolated detrusor strip contractions to electrical field stimulation.

Methods Specimens from the anterior part of the dome of the urinary bladder were obtained from patients undergoing total cystectomy due to bladder base malignancy. Muscular strips (20 mm long, 4 mm wide) were prepared by removing the serosal and mucosal layers and were mounted isometrically (tension: 20 mN) in a 5 ml bath containing modified Krebs solution gassed with a mixture of 95% O_2 and 5% CO_2 and maintained at 37°C. Methysergide (1 μM) and ondansetron (3 μM) were added to the solution in order to isolate pharmacologically putative 5-HT_4 receptors. After 90 min equilibration, the strips were field stimulated by means of two platinum electrodes connected to a MARB ST 87 stimulator. Trains of electrical pulses at 5 Hz and 5 s in duration were delivered at 1 min intervals, at 0.1 ms pulse width and 60 V. This stimulation evoked reproducible submaximal contractions, the amplitude of which was approximately 30% of that obtained by 20 Hz stimulation (Corsi *et al.*, 1991). Cumulative concentration-response curves to 5-HT were obtained using half logarithmic dosing increments until the maximum effect was reached. Two agonist concentration-response curves were constructed in each tissue. Preliminary experiments showed that the second concentration-response curve was superimposable, providing that there were frequent solution changes (every 5 min) and 60 min intervals between curves. The potentiating effect of 5-HT, either in the absence or in the presence of GR 113808 (3, 10 and 30 nM) (incubation time: 30 min) was studied. Antagonist pA_2 estimate was calculated following Schild regression analysis, using 5-HT concentration-ratios determined at EC_{50} levels in control and test curves. Confidence limits (CL) at 95% probability for the slope of the regression were evaluated by using a computer programme (PHARM/PCS, Version 4.1) based on a manual of pharmacological calculations (Tallarida & Murray, 1986). Results were expressed as means ± s.e.mean of n observations. The modified Krebs solution (pH 7.4) had the following composition (mM): NaCl 120, KCl 4.7, $MgSO_4 \cdot 7H_2O$ 0.6, KH_2PO_4 1.2, $NaHCO_3$ 25, $CaCl_2$ 2.0 and glucose 10. Aqueous solutions of the following drugs were used: hyoscine hydrochloride, hexamethonium bromide and 5-hydroxytryptamine creatinine sulphate (all from Sigma Chemical Co.), tetrodotoxin (TTX) (Sankyo), ondansetron and GR 113808 ([1-[2-[(-methylsulphonyl)amino]ethyl]4-piperidinyl] methyl 1-methyl-1*H*-indole-3-carboxylate) (both synthesized

[1] Author for correspondence.
[2] Permanent address: Department of Pharmacology, Boehringer Ingelheim Italy, Via Serio 15, I-20139 Milan, Italy.

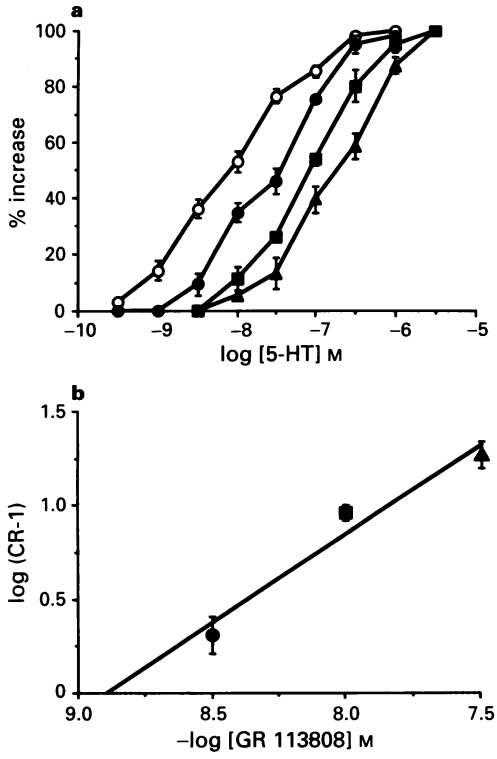

Figure 1 Concentration-response curves for the potentiation of electrically-induced cholinergic contractions of the human isolated detrusor strips by 5-HT. In (a) control curve (○); curves constructed in the presence of 3 (●), 10 (■) and 30 nM (▲) GR 113808. (b) Schild plot of the data in (a). Values are mean ± s.e.mean, $n = 5-9$.

by Boehringer Ingelheim Italy, Milan). Methysergide maleate (Sandoz) was dissolved in methanol and then diluted in distilled water.

Results Electrical field stimulation (5 Hz for 5 s every 60 s, 0.1 ms pulse duration, 60 V) evoked reproducible submaximal contractions, which were unaffected by hexamethonium (30 μM, $n = 5$) and abolished by TTX (0.6 μM, $n = 5$) and hyoscine (1 μM, $n = 5$). Cumulative administration of 5-HT (0.3 nM–1 μM) produced a concentration-dependent increase (maximal increase: 86.6 ± 9.6%, $n = 20$) in the amplitude of stimulated contractions, with a pEC_{50} value of 8.1 ± 0.06 ($n = 20$). In the presence of 5-HT (1 μM), the resulting activity was still resistant to hexamethonium (30 μM, $n = 5$) and completely antagonized by hyoscine (1 μM, $n = 5$). GR 113808 (3, 10 and 30 nM) had no effect on basal contractions, but caused a parallel rightward shift of the 5-HT-induced response, without depression of the maximum (Figure 1a). Schild regression analysis afforded a line (Figure 1b) with a slope of 0.9 (95% CL 0.7–1.1), which was not different from unity, and a pA_2 value of 8.9 ± 0.04 (slope constrained to 1).

Discussion In human isolated detrusor strips, trains of electrical pulses at low frequency (5 Hz) evoked hexamethonium-resistant, TTX- and hyoscine-sensitive contractions, indicating the activation of postganglionic cholinergic nerves (see Maggi *et al.*, 1989). Such contractile responses were enhanced by 5-HT in a concentration-dependent manner, through a hexamethonium-insensitive mechanism and were completely antagonized by hyoscine. This suggests that in the detrusor strips the excitatory effect of 5-HT is dependent on the release of acetylcholine (ACh) from cholinergic motor neurones. GR 113808 produced a concentration-dependent and parallel rightward displacement of the 5-HT response, without depression in maxima. The surmountable nature of antagonism, the unity slope of the Schild plot and the affinity estimate ($pA_2 = 8.9$) are entirely consistent with competitive antagonism at 5-HT_4 receptors. In fact, the latter value is in the range of the affinity estimates of GR 113808 at 5-HT_4 receptors observed in guinea-pig and rat alimentary canal (9.0–9.7) (Gale *et al.*, 1994). Using the same antagonist to counteract the positive inotropic effect caused by 5-HT_4 receptor stimulation in human isolated atrial strips, Kaumann (1993) found a pA_2 value of 8.8. The similarity of pA_2 estimates in isolated detrusor and atrial strips suggests 5-HT_4 receptor homogeneity in human peripheral tissues. Recently, the presence of 5-HT_4 receptors has also been demonstrated in the urinary bladder of two monkeys of the macaque family (Waikar *et al.*, 1994). At variance with human bladder, in monkey bladder these receptors are located post-junctionally, where they cause muscular relaxation through a mechanism antagonized with high affinity by GR 113808 ($pA_2 = 9.5$). In conclusion, our findings indicate that, in electrically stimulated human detrusor strips, the 'atypical' (Corsi *et al.*, 1991) excitatory 5-HT receptor, which promotes ACh release from cholinergic nerves, clearly belongs to the 5-HT_4 subtype. Based on this evidence, selective agonists at 5-HT_4 receptors could be valuable for the pharmacological treatment of micturition disturbances associated with detrusor hypomotility.

References

CORSI, M., PIETRA, C., TOSON, G., TRIST, D., TUCCITTO, G. & ARTIBANI, W. (1991). Pharmacological analysis of 5-hydroxytryptamine effects on electrically stimulated human isolated urinary bladder. *Br. J. Pharmacol.*, **104**, 719–725.

FORD, A.P.D.W. & CLARKE, D.E. (1993). The 5-HT_4 receptor. *Med. Res. Rev.*, **13**, 633–662.

GALE, J.D., GROSSMAN, C.J., WHITEHEAD, J.W.F., OXFORD, A.W., BUNCE, K.T. & HUMPHREY, P.P.A. (1994). GR 113808: a novel, selective antagonist with high affinity at the 5-HT_4 receptor. *Br. J. Pharmacol.*, **111**, 332–338.

HINDMARSH, J.R., IDOWU, O.A., YEATES, W.K. & ZAR, M.A. (1977). Pharmacology of electrically evoked contractions of human bladder. *Br. J. Pharmacol.*, **61**, 115P.

KAUMANN, A.J. (1993). Blockade of human atrial 5-HT_4 receptors by GR 113808. *Br. J. Pharmacol.*, **110**, 1172–1174.

KLARSKOV, P., & HØRBY-PETERSEN, J. (1986). Influence of serotonin on lower urinary tract smooth muscle in vitro. *Br. J. Urol.*, **58**, 507–513.

MAGGI, C.A., PATACCHINI, R., SANTICIOLI, P., TURINI, D., BARBANTI, G., BENEFORTI, P., ROVERO, P. & MELI, A. (1989). Further studies on the motor response of the human isolated bladder to tachykinins, capsaicin and electrical field stimulation. *Gen. Pharmacol.*, **20**, 663–669.

TALLARIDA, R.J. & MURRAY, R.B. (1986). *Manual of Pharmacologic Calculations with Computer Programs.* 2nd ed. New York: Springer-Verlag.

TONINI, M., RIZZI, C.A., MANZO, L. & ONORI, L. (1991). Novel enteric 5-HT_4 receptors and gastrointestinal prokinetic action. *Pharmacol. Res.*, **24**, 5–14.

WAIKAR, M.V., FORD, A.P.D.W. & CLARKE, D.E. (1994). Evidence for an inhibitory 5-HT_4 receptor in urinary bladder of *Rhesus* and *Cynomolgus* monkeys. *Br. J. Pharmacol.*, **111**, 213–218.

(Received April 25, 1994
Accepted May 13, 1994)

Br. J. Pharmacol. (1994), **113**, 3–4

SPECIAL REPORT

The identification of apparently novel cyclic AMP and cyclic GMP phosphodiesterase activities in guinea-pig tracheal smooth muscle

Fiona Burns, Patricia A. Stevens & [1]Nigel J. Pyne

Department of Physiology and Pharmacology, Strathclyde University, 204 George Street, Glasgow, G1 1XW

Phosphodiesterase (PDE) activities that were capable of hydrolysing cyclic AMP ($K_m = 6.8 \pm 2\ \mu M$) and cyclic GMP ($K_m = 6.7 \pm 1.6\ \mu M$) were isolated from tracheal smooth muscle. These enzyme(s) activities were insensitive to stimulation by calcium/calmodulin and to inhibition by cyclic GMP, rolipram (type IV inhibitor) and siguazodan (type III inhibitor). Zaprinast was a relatively poor inhibitor of both cyclic AMP and cyclic GMP hydrolysis ($IC_{50} = 46 \pm 9\ \mu M$ and $45 \pm 14\ \mu M$ respectively). These results suggest that tracheal smooth muscle may contain an apparently novel PDE. However, KCl (30 mM) which facilitates calcium entry in cells, depressed bradykinin-stimulated intracellular cyclic AMP formation, suggesting that the type I PDE may be functionally present. We suggest that considerable caution be exercised in identifying apparently novel PDE isoforms.

Keywords: Phosphodiesterases; tracheal smooth muscle; PDE-I; zaprinast

Introduction A recent special report by Mukai *et al.* (1994) in this journal, identified an apparently novel phosphodiesterase from rat cerebrum which was termed type VIII. This isoform hydrolysed adenosine 3':5'-cyclic monophosphate (cyclic AMP) and guanosine 3':5'-cyclic monophosphate (cyclic GMP) with high affinity, was insensitive to calcium-calmodulin and type III/IV PDE inhibitors. In the present study, we have identified a similar PDE activity from guinea-pig tracheal smooth muscle. However, calcium entry into guinea-pig tracheal smooth muscle cells is associated with depressed agonist-stimulated cyclic AMP responses. The identification of apparently novel phosphodiesterases is discussed in relation to the known effect of proteolysis upon kinetic and inhibitor properties of PDE isoforms.

Methods *Isolation of novel PDE isoforms from guinea-pig tracheal smooth muscle* The study was performed on smooth muscle dissected from trachealis (Pyne & Pyne, 1993). For the cyclic AMP studies, tracheal smooth muscle cells were maintained in culture according to Pyne & Pyne (1993) and cyclic AMP determination performed according to Stevens *et al.* (1994). All isolation procedures were performed at 4°C. Tracheal smooth muscle strips were homogenized in ice-cold isotonic sucrose 0.25 M, EDTA 1 mM, Tris/HCl 10 mM (pH 7.4), benzamidine 2 mM and phenylmethylsulphonylfluoride 0.1 mM, in a turrex homogeniser. The homogenate was immediately centrifuged at 48000 *g* for 20 min and the resulting supernatant removed. The filtered supernatant was loaded onto DEAE-sepharose (1 × 4 ml column), that had been previously equilibrated in buffer A containing Tris/HCl 10 mM (pH 7.4), $MgCl_2$ 5 mM, benzamidine 2 mM and phenylmethylsulphonylfluoride 0.1 mM. The column was then washed with 10 vol of buffer A and PDE activity eluted with a linear NaCl in buffer A gradient (0–0.5 M); 2 ml fractions were collected at a flow rate of 0.5 ml min^{-1}. Fractions containing cyclic GMP PDE activity were loaded onto Affi-gel Blue agarose (1 × 4 ml) that had been pre-equilibrated in buffer A. The column was washed with buffer A which contained EDTA 1 mM, in place of $MgCl_2$.

Analytical methods PDE activity was measured using final concentrations of [^{3}H]-cyclic AMP and [^{3}H]-cyclic GMP of 1 μM, according to Burns & Pyne (1992). Rolipram, siguazodan and zaprinast were dissolved in dimethylsulphoxide to a concentration of 10 mM. Drugs were diluted to the required concentrations and where the final concentration of DMSO was <1%. All assays were performed where <10% of the substrate was utilised.

Materials Rolipram, zaprinast and siguazadon were kind gifts from Dr Torphy (Smith, Kline and Beecham Pharmaceuticals, King of Prussia, U.S.A.). All radioisotopes were from Amersham Int (Bucks, U.K.).

Results *Cyclic AMP PDE activity* We have previously demonstrated that guinea-pig tracheal smooth muscle cells contain type III and IV PDE activities (Burns & Pyne, 1992). We now demonstrate that an apparently novel peak of cyclic AMP phosphodiesterase activity is also eluted from DEAE-sepharose at 0.09 M NaCl. The enzyme activity displayed linear Michaelis-Menten kinetics with a $K_m = 6.8 \pm 2\ \mu M$ ($n = 3$, Table 1). Addition of either calcium (1 mM) and calmodulin (10 units) or cyclic GMP (10 μM) was ineffective in modulating PDE activity (Table 1). The PDE activity was not inhibited by either siguazodan or rolipram (<100 μM, Table 1). Zaprinast was a relatively poor inhibitor of the enzyme activity ($IC_{50} = 46 \pm 9\ \mu M$, $n = 3$, Table 1), whilst IBMX inhibited with an $IC_{50} = 7.8\ \mu M$ ($n = 2$).

Cyclic GMP PDE activity A peak of cyclic GMP PDE activity was eluted from DEAE-sepharose at 0.1 M NaCl. The enzyme activity displayed non-linear Michaelis-Menten kinetics (data not shown). Addition of either calcium (1 mM) and calmodulin (10 units) or cyclic GMP (10 μM) was ineffective in modulating PDE activity (Table 1). From Affi-gel Blue, the type V PDE activity hydrolysed cyclic GMP with linear Michaelis-Menten kinetics ($K_m = 1.7 \pm 0.38\ \mu M$, $n = 6$) and was potently inhibited by zaprinast ($IC_{50} = 1.5 \pm 0.6\ \mu M$, $n = 6$) and IBMX ($IC_{50} = 2.6\ \mu M$, $n = 2$). The apparently novel PDE activity was eluted with EDTA (1 mM). It hydrolysed cyclic GMP with linear kinetics ($K_m = 6.7 \pm 1.6\ \mu M$, $n = 6$, Table 1) and was weakly inhibited by zaprinast ($IC_{50} = 45 \pm 14\ \mu M$, $n = 6$, Table 1) and by IBMX ($IC_{50} = 10\ \mu M$, $n = 2$). The PDE activity was not inhibited by either siguazodan or rolipram (<100 μM, Table 1).

[1] Author for correspondence.

Table 1 Characteristics of novel phosphodiesterose (PDE) activities in tracheal smooth muscle

Cyclic AMP	*Novel PDE*	
[NaCl] elution	0.09 M	
Michaelis-Menten kinetics	linear	
K_m	6.8 ± 2 μM	
IC_{50} (1 μM cyclic AMP)		
Zaprinast	46 ± 2 μM	
Siguazodan	> 100 μM	
Rolipram	> 100 μM	
Effect of Ca/Calmodulin	None	
Effect of cyclic GMP	None	
Cyclic GMP	*Novel PDE*	*type V PDE*
[NaCl] elution	0.1 M	0.1 M
Michaelis-Menten kinetics	linear	linear
K_m	6.7 ± 1.6 μM	1.7 ± 0.4 μM
IC_{50} (1 μM cyclic GMP)		
Zaprinast	46 ± 2 μM	1.5 ± 0.6 μM
Siguazodan	> 100 μM	–
Rolipram	> 100 μM	–
Effect of Ca/Calmodulin	None	None
Effect of cyclic GMP	None	–

All assays of cyclic GMP and cyclic AMP phosphodiesterase activity were performed with 1 μM substrate

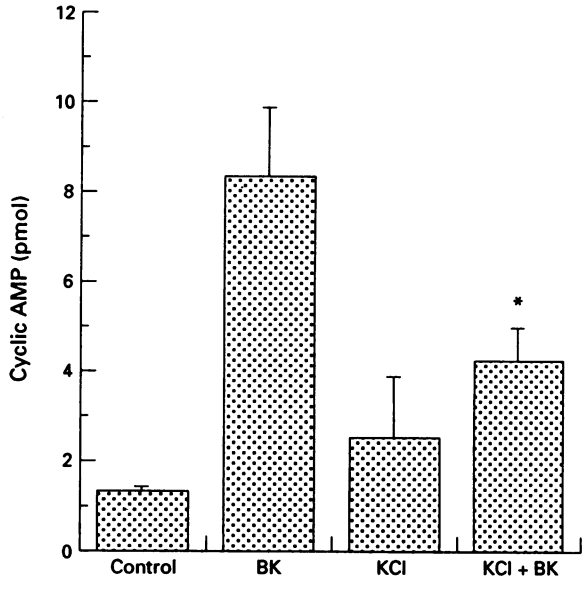

Figure 1 The effect of KCl upon bradykinin (BK)-stimulated intracellular cyclic AMP accumulation in tracheal smooth muscle. The effect of bradykinin (1 μM) and KCl (30 mM) upon intracellular cyclic AMP levels in tracheal smooth muscle cells was measured at $t = 10$ min. Results are expressed as pmol/0.25 × 10^6 cells and are means ± s.d. for $n = 3$ experiments. $^*P < 0.01$ significance versus control values, Students's t test.

Cyclic AMP studies We have previously demonstrated that bradykinin (1 μM) stimulates an intracellular cyclic AMP response in tracheal smooth muscle (Stevens *et al.*, 1994). Whilst, we were unable to identify type I PDE activity, KCl (30 mM) treatment of the cells depressed the bradykinin-stimulated cyclic AMP response (Figure 1).

Discussion This study revealed apparently novel cyclic AMP and cyclic GMP PDE activities in guinea-pig tracheal smooth muscle. This contrasted with the inability to identify a type I calcium/calmodulin sensitive PDE activity. However, Torphy & Cieslinski (1989) have identified the latter isoform in canine trachealis. The novel guinea-pig PDE activities display very similar characteristics to the rat cerebrum isoform (Mukai *et al.*, 1994). Both are pharmacologically distinct from the type I-VII PDEs, and hydrolyse cyclic GMP and cyclic AMP with relatively high-affinity. However, the K_m values for cyclic AMP hydrolysis differ by approximately 10 fold, and the trachealis enzyme is insensitive to cyclic GMP-dependent inhibition of cyclic AMP hydrolysis. Despite the inability to detect type I PDE activity, depolarizing concentrations of KCl and facilitated calcium entry reduced bradykinin-stimulated cyclic AMP formation in tracheal smooth muscle cells. Adenylate cyclase in these cells is not inhibited by calcium (Stevens & Pyne, unpublished) and this suggests that the type I PDE activity may be functionally present in intact cells.

Our studies indicate that the apparent novel PDE activities in airway smooth muscle may be proteolytically derived from the type I PDE. It is well accepted that this results in constitutive activation, with graded alterations in kinetic parameters that are dependent upon the extent of proteolysis. Nicardipine was used as a selective inhibitor of type I PDE activity in the study of Mukai *et al.* (1994) although inhibition occurs via allosteric binding (Wu *et al.*, 1992) and proteolysis of the type I PDE may result in ablated inhibitor sensitivity, as has been described for other PDE isoforms (Price *et al.*, 1987).

In conclusion, we have identified apparently novel PDE activities in tracheal smooth muscle. However, whilst this may provoke interest in their pharmacological specificity and potential therapeutic potential in regulating airway function, we suggest that considerable caution be exercised, as the type I PDE is extremely sensitive to proteolysis and can generate catalytic entities that may appear as novel isoforms.

References

BURNS, F. & PYNE, N.J. (1992). The interaction of the catalytic sub-unit of protein kinase A with the lung type V phosphodiesterase: modulation of a non-catalytic binding site. *Biochem. Biophys. Res. Commun.*, **189**, 1389–1396.

MUKAI, J., ASAI, T., NAKA, M. & TANAKA, T. (1994). Separation and characterization of a novel isoenzyme of cyclic nucleotide phosphodiesterase from rat cerebrum. *Br. J. Pharmacol.*, **111**, 389–390.

PRICE, B., PYNE, N.J. & HOUSLAY, M.D. (1987). Proteolysis of cyclic AMP phosphodiesterase-II attenuates its ability to be inhibited by compounds which exert positive inotropic actions in cardiac tissue. *Biochem. Pharmacol.*, **36**, 4047–4054.

PYNE, S. & PYNE, N.J. (1993). Bradykinin stimulates phospholipase D activity in primary cultures of guinea-pig tracheal smooth muscle. *Biochem. Pharmacol.*, **45**, 593–603.

STEVENS, P., PYNE, S., GRADY, M. & PYNE, N.J. (1994). Bradykinin-dependent activation of adenylate cyclase activity and cyclic AMP accumulation in tracheal smooth muscle occurs via protein kinase C-dependent and independent pathways. *Biochem. J.*, **297**, 333–339.

TORPHY, T.J. & CIESLINSKI, L.B. (1989). Characterisation and selective inhibition of cyclic nucleotide phosphodiesterase isoenzymes in canine tracheal smooth muscle. *Mol. Pharmacol.*, **37**, 206–214.

WU, Z., SHARMA, R.K. & WANG, J.H. (1992). Catalytic and regulatory properties of the calmodulin-stimulated phosphodiesterase isozyme. In *The Biology of Cyclic Nucleotide Phosphodiesterases*. ed. Strada, S.J. & Hidaka, H. pp. 29–44. New York: Raven Press.

(Received April 21, 1994
Accepted June 3, 1994)

Br. J. Pharmacol. (1994), 113, 5–6

SPECIAL REPORT

Close correlation of the cardioprotective effect of FK409, a spontaneous NO releaser, with an increase in plasma cyclic GMP level

[1]Yasuhiro Kita, Toshiko Sugimoto, Yoshimi Hirasawa, Keizo Yoshida & Kazuhiro Maeda

Department of Pharmacology, New Drug Research Laboratories, Fujisawa Pharmaceutical Co., Ltd., 1-6, 2-chome, Kashima, Yodogawa-ku, Osaka 532, Japan

FK409 ((±)-(E)-ethyl-2-[(E)-hydroxyimino]-5-nitro-3-hexeneamide), which has been reported by us to be a new spontaneous nitric oxide (NO) releaser, prevented myocardial infarction following occlusion and reperfusion in rat coronary artery and increased plasma cyclic GMP level in rats, dose-dependently and significantly at 32 mg kg^{-1}. Isosorbide dinitrate (ISDN), which is the most popular orally active NO donor used in the treatment of ischaemic cardiovascular diseases, did not show significant effects at 32 mg kg^{-1} in either experiment. Therefore, it is suggested that FK409 can attenuate myocardial injury during ischaemia and reperfusion in contrast to ISDN and a change in plasma cyclic GMP level may serve as an indicator of the cardioprotective effect of NO-releasing drugs.

Keywords: FK409; ISDN; nitric oxide; cyclic GMP; myocardial infarction

Introduction FK409 ((±)-(E)-ethyl-2-[(E)-hydroxyimino]-5-nitro-3-hexeneamide) is a spontaneous nitric oxide (NO) releaser, which shows potent vasorelaxant and antiplatelet effects (Kita *et al.*, 1994). In our former paper, we have reported that FK409 is the first NO donor which can increase the plasma guanosine 3':5'-cyclic monophosphate (cyclic GMP) level (Kita *et al.*, 1994). Recently, in experiments with isosorbide dinitrate (ISDN) as a NO donor, it has been reported that a change in plasma cyclic GMP level cannot serve as a surrogate measurement of haemodynamic changes because ISDN does not increase the plasma cyclic GMP level at the dose, at which ISDN shows haemodynamic effects (Shotan *et al.*, 1993). However, the correlation between cardioprotective effect and a change in plasma cyclic GMP level by NO donors remains unclear.

In this paper, we evaluated the cardioprotective effect of FK409 during ischaemia and reperfusion in rat coronary artery, applying myocardial infarct areas as the endpoint. Furthermore, we examined whether a change in plasma cyclic GMP level could serve as an indicator of the biological action of NO-releasing drugs.

Methods *Myocardial infarction model* Male SD rats, purchased from Nihon SLC Co. (Sizuoka, Japan) weighing 285–320 g, were fasted for 24 h before the experiment. They were anaesthetized with sodium pentobarbitone (50 mg kg^{-1}, i.p.) and were respired artificially with air through a tracheal cannula. Subsequently the chest was opened. After the heart was exposed, the left coronary artery was ligated for 60 min with a nylon thread and then reperfused for 60 min. Vehicle (0.5% methyl cellulose), FK409 or ISDN (each drug suspended in vehicle) was given orally in a volume of 5 ml kg^{-1}, 30 min before the ligation. Standard second lead of the electrocardiogram (Labo System ZS-501, Fukuda ME Kogyo Co., Tokyo, Japan) was used to evaluate ST segment elevation. Peak ST segment elevation was measured during coronary occlusion. Sixty min after reperfusion, the heart was excised and was divided into six slices perpendicular to the apex-base axis. These were then placed in 0.5% triphenyltetrazolium chloride in phosphate buffered saline without calcium chloride at 37°C for 10 min to dye the normal region. The infarct and normal area were analysed on photographed tissue slices with a digitizer (KD-4300, Graphtec Co., Tokyo, Japan). The myocardial infarct area was expressed as a percentage of the total ventricle area.

Determination of plasma cyclic GMP level Blood from male SD rats weighing 240–325 g, which were anaesthetized with diethyl ether before and 5, 30, 60, 120 and 240 min after the administration of vehicle, FK409 or ISDN, was collected from the abdominal aorta into plastic vessels containing 2% EDTA (20^{-1} volume) on ice. Cyclic GMP levels were determined according to Kita *et al.* (1994). The plasma cyclic GMP level was expressed as a percentage of the pre-administration level.

Materials FK409 and ISDN were synthesized by Fujisawa Pharmaceutical Co. (Osaka, Japan).

Statistical analysis Data are presented as mean ± s.e. mean of the number of experiments as indicated. For multiple comparisons, data were analysed by one-way analysis of variance followed by Dunnett's test.

Results Figure 1a shows the effects of oral FK409 and ISDN on myocardial infarction. FK409 reduced the infarct area dose-dependently and showed significant suppression (45.5% suppression vs. vehicle-treated group) at 32 mg kg^{-1} while ISDN did not reduce the infarct area significantly compared with the vehicle-treated group at 32 mg kg^{-1}.

Figure 1b shows the effects of FK409 and ISDN on plasma cyclic GMP level 5 min after oral administration. Plasma cyclic GMP levels before the administration of vehicle, FK409 (10 and 32 mg kg^{-1}) and ISDN (32 mg kg^{-1}) were 11.7 ± 0.7, 10.1 ± 1.2, 10.3 ± 1.7 and 8.8 ± 1.0 pmol ml^{-1}, respectively. These values were not significantly different. FK409 increased the plasma cyclic GMP level dose-dependently, a significant increase being induced after the administration of 32 mg kg^{-1} FK409. No significant increase in plasma cyclic GMP level was observed after the administration of ISDN, 32 mg kg^{-1}. FK409 increased plasma cyclic GMP level only 5 min after administration, whilst ISDN had no effect at any time (data not shown).

Discussion The data presented in this study clearly showed a beneficial effect of FK409, a new spontaneous NO releaser, on myocardial infarction produced during occlusion and reperfusion in rat coronary artery. The peak ST segment elevations in the electrocardiogram during myocardial

[1] Author for correspondence.

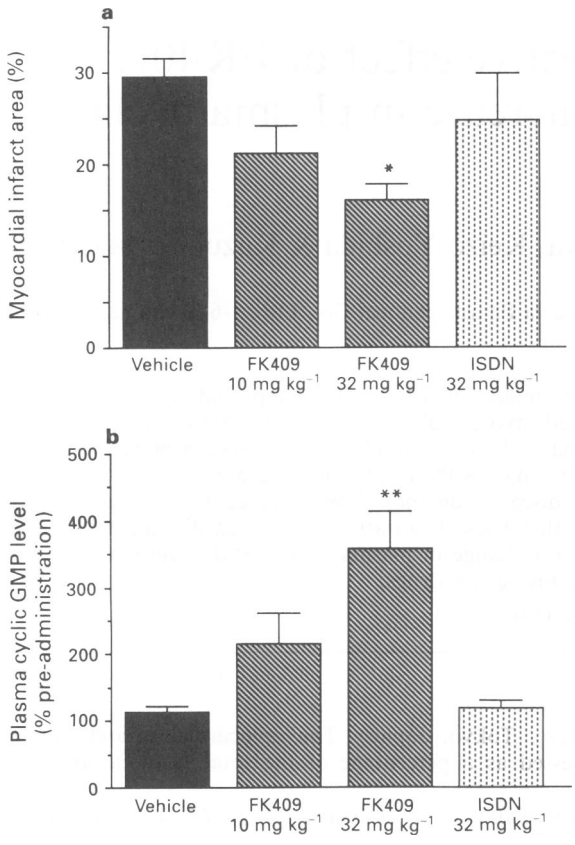

Figure 1 (a) The effects of FK409 and ISDN on myocardial infarction produced during occlusion and reperfusion in rat coronary artery. Each value represents the mean ± s.e.mean of eight and six experiments for vehicle-treated group and drug-treated groups, respectively. $*P<0.05$ compared with vehicle-treated group. (b) The effects of FK409 and ISDN on plasma cyclic GMP level in rats. Each value represents the mean ± s.e.mean of four experiments. $**P<0.01$ compared with vehicle-treated group.

ischaemia were equivalent in both the vehicle-treated and drug-treated groups, indicating a comparable degree of ischaemic insult (data not shown). Nevertheless, FK409 was able to reduce myocardial infarct area dose-dependently and significantly at 32 mg kg^{-1}, while ISDN, which is the most popular orally active NO donor used in the treatment of ischaemic cardiovascular diseases, was not cardioprotective at 32 mg kg^{-1}.

The mechanism of myocardial injury during ischaemia and reperfusion is not fully understood, but thrombus formation (Laws *et al.*, 1983; Bender *et al.*, 1985) and the generation of cardioactive and vasoactive mediators (Stahl *et al.*, 1988; Smith *et al.*, 1989) by activated platelets may be important aspects of this pathogenic mechanism. The reduction of circulating platelets by the treatment with rabbit antiserum against rat platelets has reduced myocardial infarct area in rats (Kanayama *et al.*, 1992). We have reported that FK409 shows much more potent antiplatelet effects than ISDN (Kita *et al.*, 1994). Therefore, the antiplatelet action of FK409 via NO is probably an important factor for the cardioprotective effect of the compound.

FK409 increased the plasma cyclic GMP level dose-dependently and significantly at 32 mg kg^{-1}. FK409 is the first NO donor to be reported to increase plasma cyclic GMP levels *in vivo*. This increase may be attributed to the copious production of intracellular cyclic GMP mediated by NO, which is released spontaneously from FK409. The dose-dependency of FK409-induced cardioprotection coincided with the increase in plasma cyclic GMP level, while ISDN, which can release NO dependently on sulphydryl group (Feelish & Noack, 1987a,b), did not show any increase in plasma cyclic GMP level or a cardioprotective effect at 32 mg kg^{-1}. Thus a change in plasma cyclic GMP level may serve as an indicator of the cardioprotective effect of NO-releasing drugs.

In conclusion, we suggest that FK409, a new spontaneous NO releaser, suppresses myocardial infarction produced during ischaemia and reperfusion. The cardioprotective effect of NO closely correlates with a rapid increase in the plasma cyclic GMP level.

References

BENDER, M., SMITH, B., PINTO, A. & MULLANE, K.M. (1985). Neutrophil depletion suppressed ^{111}In-labeled platelet accumulation in infarcted myocardium. *J. Cardiovasc. Pharmacol.*, **7**, 906–912.

FEELISCH, M. & NOACK, E. (1987a). Nitric oxide (NO) formation from nitrovasodilators occurs independently of hemoglobin or non-heme iron. *Eur. J. Pharmacol.*, **142**, 465–469.

FEELISCH, M. & NOACK, E. (1987b). Correlation between nitric oxide formation during degradation of organic nitrates and activation of guanylate cyclase. *Eur. J. Pharmacol.*, **139**, 19–30.

KANAYAMA, T., KIMURA, Y., TAMAO, Y. & MIZOGAMI, S. (1992). Beneficial effects of a new prostacyclin analogue, KP-10614, on acute myocardial infarction in rats. *J. Cardiovasc. Pharmacol.*, **20**, 630–637.

KITA, Y., HIRASAWA, Y., MAEDA, K., NISHIO, E. & YOSHIDA, K. (1994). Spontaneous nitric oxide release accounts for the potent pharmacological actions of FK409. *Eur. J. Pharmacol.*, **257**, 123–130.

LAWS, K.H., CLANTON, J.A., STARNES, V.A., LUPINETTI, F.H., COLLINS, J.C., OATES, J.A. & HAMMON, Jr., J.W. (1983). Kinetics and imaging of indium-111-labeled autologous platelets in experimental myocardial infarction. *Circulation*, **67**, 110–116.

SHOTAN, A., MEHRA, A., OSTRZEGA, E., HSUEH, W., DO, Y.S., FISHER, D.A., HURST, A., JOHNSON, J.V. & ELKAYAM, U. (1993). Plasma cyclic guanocine monophosphate in chronic heart failure: hemodynamic and neurohormonal correlations and response to nitrate therapy. *Clin. Pharmacol. Ther.*, **54**, 638–644.

SMITH, E.F.III, GRISWOLD, D.E., EGAN, J.W. & HILLEGASS, L.M. (1989). Reduction of myocardial damage and polymorphonuclear leukocyte accumulation following coronary artery occlusion and reperfusion by the thromboxane receptor antagonist BM13.505. *J. Cardiovasc. Pharmacol.*, **13**, 715–722.

STAHL, G.L., TERASHITA, Z.-I. & LEFER, A.M. (1988). Role of platelet activating factor in propagation of cardiac damage during myocardial ischemia. *J. Pharmacol. Exp. Ther.*, **244**, 898–904.

(Received May 5, 1994
Accepted June 7, 1994)

Br. J. Pharmacol (1994), **113**, 7–12

Adenosine-induced hyperpolarization of the membrane voltage in rat mesangial cells in primary culture

[1]Hermann Pavenstädt, Joachim Ruh, *Rainer Greger & Peter Schollmeyer

Department of Medicine, Division of Nephrology, *Department of Physiology, Albert-Ludwigs University, Freiburg, Germany

1 The effect of adenosine on membrane voltage and ion currents was studied in rat mesangial cells in primary culture. Membrane voltage was measured with the patch clamp technique in the slow- or fast whole cell configuration. The resting membrane voltage of mesangial cells was -48 ± 0.5 mV. Adenosine (10^{-8}–10^{-3} M) induced a sustained and concentration-dependent hyperpolarization of membrane voltage ($ED_{50} \approx 6 \times 10^{-7}$ M). Adenosine (10^{-5} M) hyperpolarized the membrane voltage by 14 ± 0.5 mV. During the hyperpolarization ion currents were monitored simultaneously. An increase of the outward current by $51 \pm 11\%$ was observed.

2 An increase of the extracellular K^+ concentration (from 3.6 to 18.6 M) caused a depolarization of membrane voltage to -34 ± 2 mV. In the presence of increased K^+ the hyperpolarization of membrane voltage induced by adenosine was significantly attenuated by $61 \pm 5\%$. The K^+-channel blocker, Ba^{2+} (5×10^{-3} M) depolarized membrane voltage to -24 ± 2 mV. In the presence of Ba^{2+} the adenosine-induced hyperpolarization was significantly inhibited by $72 \pm 8\%$.

3 Preincubation of the adenosine antagonist, 8-phenyltheophylline (10^{-4} M) significantly inhibited the adenosine (10^{-5} M) mediated membrane voltage response by $67 \pm 8\%$. The adenosine agonists 5-N-ethylcarboxamidoadenosine (NECA), **R**-(−)N^6-(2-phenylisopropyl)adenosine (**R**-(−)-PIA), **S**-(+)-N^6-(2-phenylisopropyl)adenosine (**S**-(+)-PIA), N^6-[2-(3,5-dimethoxyphenyl)-2-(2-methylphenyl)-ethyl]adenosine (DPMA), and 2-chloroadenosine (2-CA) also hyperpolarized membrane voltage of mesangial cells. The rank order of potency of the agonists at 10^{-5} M was NECA > adenosine = > **R**-(−)-PIA = DPMA = 2-CA > **S**-(+)-PIA.

4 Stimulation of cyclic AMP by forskolin induced a concentration-dependent hyperpolarization of membrane voltage ($ED_{50} \approx 2 \times 10^{-7}$ M). Application of forskolin (10^{-5} M) in the presence of adenosine (10^{-4} M) had no additive hyperpolarizing effect on the membrane voltage.

5 Activation of protein kinase C by phorbol 12,13 dibutyrate (PDBu) induced a sustained depolarization of membrane voltage ($ED_{50} \approx 5 \times 10^{-9}$ M). In the presence of PDBu, adenosine (10^{-5} M) still hyperpolarized membrane voltage of mesangial cells.

6 The data indicate that adenosine activates K^+-conductance via an A_2 receptor in mesangial cells; the activation of the K^+-conductance, which is probably mediated by cyclic AMP led to a hyperpolarization of membrane voltage.

Keywords: Rat mesangial cell; A_2 receptor; K^+-conductance; cyclic AMP

Introduction

In the kidney, adenosine is capable of influencing many physiological functions. It decreases glomerular filtration rate (GFR) (Osswald *et al.*, 1978), modulates renin secretion (Churchill & Churchill, 1985) and acts as a prejunctional inhibitor of the noradrenaline release (Hedqvist *et al.*, 1978). The mechanisms of the adenosine-induced decrease of GFR are not completely understood. The adenosine-mediated decrease of GFR is due to preglomerular vasoconstriction and postglomerular vasodilatation (Osswald *et al.*, 1978); however, it has been suggested that adenosine may, by mesangial cell contraction, decrease the ultrafiltration coefficient K_f (Olivera *et al.*, 1992). The presence of glomerular adenosine receptors also suggests a potential role for adenosine on glomerular function: A_1 and A_2 receptors have been detected in the glomerulus by autoradiographic binding studies (Palacios *et al.*, 1987; Freismuth *et al.*, 1987) and the presence of a glomerular A_2 receptor was further supported by adenosine 3′:5′-cyclic monophosphate (cyclic AMP) accumulation due to adenosine and specific adenosine analogues (Abboud & Dousa, 1983). On the cellular level it has been shown that mesangial cells possess both, A_1 and A_2 receptors (Olivera *et al.*, 1989; Olivera & Lopez-Novoa, 1992). We have previously shown that extracellular ATP exerts physiological effects, including contraction, an increase in cytosolic calcium activity and stimulation of a Cl^- current via a P_{2y} receptor in mesangial cells (Pavendstädt *et al.*, 1993). In the present study we have investigated whether adenosine modulates membrane voltage and ion currents in mesangial cells. Furthermore, we have begun to characterize the adenosine receptor involved and to examine the possible signal transduction pathway.

[1] Author for correspondence at: Medizinische Klinik, Nephrologische Abteilung, Hugstetterstr. 55, 79106 Freiburg, Germany.

Methods

Cell culture

Mesangial cells were cultured as previously described (Pavenstädt *et al.*, 1993). In brief, rat glomeruli were obtained by the sieve technique and incubated with collagenase IV (1 g l^{-1}, Sigma, Deisenhofen, Germany) for 30 min. Glomeruli cores were suspended in RPMI 1640 medium with 170 g l^{-1} foetal calf serum and plated onto collagen-coated glass cover slips (Greiner, Nürtingen, Germany) and incubated at 37°C in a moist atmosphere containing 5% CO_2. Mesangial cell outgrowth was noted morphologically by phase-contrast microscopy. Immunochemical characterization was performed by the peroxidase-antiperoxidase method (Bross *et al.*, 1978), with positive staining for smooth muscle α-actin, desmin and vimentin. Cytokeratin and factor VIII did not stain,

thus excluding glomerular epithelial- or endothelial cells. Mesangial cells contracted in response to angiotensin II and ATP. Therefore the cells studied showed the morphological, immunological and physiological properties described by others for mesangial cells (Kreisberg & Karnovsky, 1983).

Patch clamp experiments

The patch clamp methods used in these experiments have been described in detail in a previous paper (Greger & Kunzelmann, 1991). Mesangial cells were mounted in a bath chamber on the stage of an inverted microscope, kept at 37°C and superfused with a solution containing (in mM): NaCl 145, K_2HPO_4 1.6, KH_2PO_4 0.4, $CaCl_2$ 1.3, $MgCl_2$ 1, D-glucose 5, pH 7.4. The patch pipettes were filled with a solution containing (in mM) K-gluconate 115, KCl 30, Na_2HPO_4 1.6, NaH_2PO_4 0.4, $CaCl_2$ 0.73, $MgCl_2$ 1.03, EGTA 1, D-glucose 5, pH 7.2, Ca^{2+} activity 10^{-7} M, to which 10–100 mg l^{-1} nystatin was added. The patch pipettes had an input resistance of about 5 MΩ. A flowing (10 μl h^{-1}) KCl (2 M) electrode was used as a reference. The membrane voltage was recorded continuously by a pen recorder (Gould, Seligenstadt, Germany). After achieving a GΩ seal, nystatin slowly permeabilized the cell-attached membrane by inducing a nonselective cation conductance (Marty & Finkelstein, 1975). In a separate series of experiments, larger pipettes (input resistance of 2–3 MΩ) were used and these experiments were performed without nystatin in the fast whole cell configuration. All experiments were done after the cells had been rinsed with the above bath solution for about 5 min or longer. The data were recorded using a LM EPC-7 patch clamp amplifier (List, Darmstadt, Germany) and continuously displayed by a pen recorder. The membrane voltage of the cells was recorded continuously using the current clamp mode of the patch clamp amplifier. Cells were voltage-clamped at the spontaneous membrane voltage and voltage steps of 10 mV to ± 40 mV were applied to estimate ion conductances.

To vary the free Ca^{2+} activity, the solutions were prepared according to established techniques with EGTA and NTA as Ca^{2+} buffers. The Ca^{2+} activity was calculated from a standard equation and was determined with a Ca^{2+} selective electrode (Radiometer, Copenhagen, Denmark).

The following agents were used: adenosine, 5'-N-ethylcarboxamidoadenosine (NECA), R-(−)-N^6-(2-phenylisopropyl) adenosine (R-(−)-PIA), S-(+)-N^6-(2-phenylisopropyl)adenosine (S-(+)-PIA), 2-chloroadenosine (2-CA), N^6-cyclopentyladenosine (CPA), N^6-[2-(3,5-dimethoxyphenyl)-2-(2-methylphenyl)-ethyl]adenosine (DPMA), 8-phenyltheophylline, phorbol 12,13-dibutyrate (PDBu), 4-α-phorbol 12-myristate 13-acetate (4-α-PMA), 8-(−4-chlorophenylthio)-cyclic AMP sodium salt (Biotrend, Köln, Germany), forskolin, 1-9 dideoxyforskolin (Sigma, Deisenhofen, Germany).

Statistics

The data are given as mean values ± s.e. mean (n), where n refers to the number of experiments. Paired t test was used to compare mean values within one experimental series. A P value of <0.05 was acceptable to indicate statistical significance.

Results

Effect of adenosine and adenosine agonists on membrane voltage of mesangial cells

In 248 experiments in the slow- or fast whole cell configuration, membrane voltage was −48 ± 0.5 mV. Addition of adenosine to mesangial cells resulted in a concentration-dependent and sustained hyperpolarization of membrane voltage (Figure 1a). A 10^{-8} M threshold concentration was required to induce a hyperpolarization by adenosine. Half maximal responses were observed at about 6×10^{-7} M adenosine (Figure 1b). Like adenosine, NECA ($n = 36$), and R-(−)PIA ($n = 41$) hyperpolarized membrane voltage of mesangial cells (Figure 1b). In addition, a sustained hyperpolarization was observed with DPMA (10^{-6} M, from −56 ± 3 to −60 ± 2 mV, $n = 6$, significant; 10^{-5} M, from −56 ± 3 to −64 ± 3 mV, $n = 6$, significant), 5-chloroadenosine (10^{-5} M, from −44 ± 3 to −55 ± 3 mV, $n = 5$, significant) and S-(+)-PIA (10^{-5} M, from −43 ± 3 to −45 ± 3 mV, $n = 4$, NS). The rank order of potency of the agonists at 10^{-5} M was NECA > adenosine > R-PIA = DPMA = 2-CA > S-(+)-PIA. The A_1 agonist 5'-(N-cyclopropyl)-carboxamidoadenosine (CPA, 10^{-7} M, $n = 3$) did not influence membrane voltage (data not shown). Preincubation with the adenosine antagonist, 8-phenyltheophylline (10^{-4} M) had no effect on membrane voltage but inhibited significantly the adenosine-induced hyperpolarization by 67 ± 3% ($n = 7$). Figure 2 summarizes the data of the effect of 8-phenyltheophylline in the absence and presence of adenosine.

Adenosine activates K^+ conductance in mesangial cells

In 8 experiments using the fast whole cell technique, membrane voltage and ion currents were monitored simultaneously. During the adenosine-induced hyperpolarization an increase of the outward current by 50 ± 5% ($n = 8$), but no increase of an inward current could be observed. Figure 3 summarizes the effect of adenosine on the outward current. To investigate further whether an activation of a K^+ conductance was responsible for the adenosine-induced hyperpolarization, we examined the influence of an increased extracellular K^+ concentration (from 3.6 to 18.6 mM) on the effect of adenosine. An increase of the extracellular K^+ concentration depolarized membrane voltage to −34 ± 2 mV and attenuated the adenosine-induced hyperpolarization by 61 ± 5% ($n = 7$). Figure 4a shows an original experiment of the effect

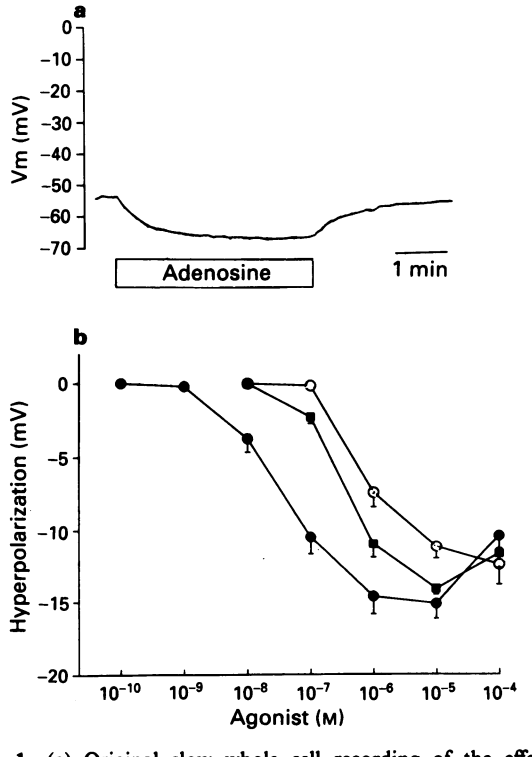

Figure 1 (a) Original slow whole cell recording of the effect of adenosine (10^{-5} M) on membrane voltage (Vm) of mesangial cells. (b) Concentration-response curves of the hyperpolarizing response of membrane voltage to adenosine and adenosine analogues: NECA (●), adenosine (■), R-(−)-PIA (○). For each data point $n = 5$–116. For abbreviations, see text.

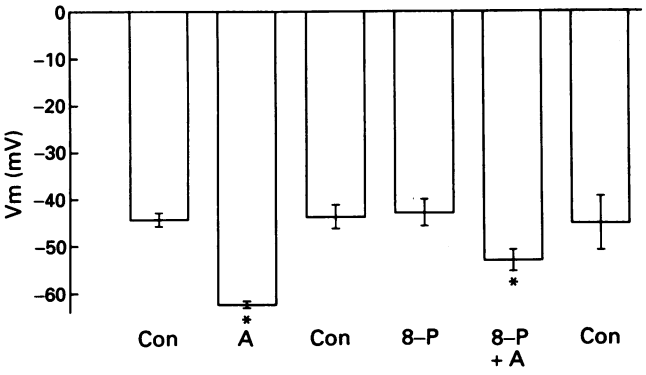

Figure 2 Effect of adenosine (A, 10^{-5} M) in the presence of 8-phenyltheophylline (8-P, 10^{-4} M). Note that hyperpolarization of membrane voltage (Vm) induced by adenosine is significantly inhibited in the presence of 8-phenyltheophylline. $n = 5$.

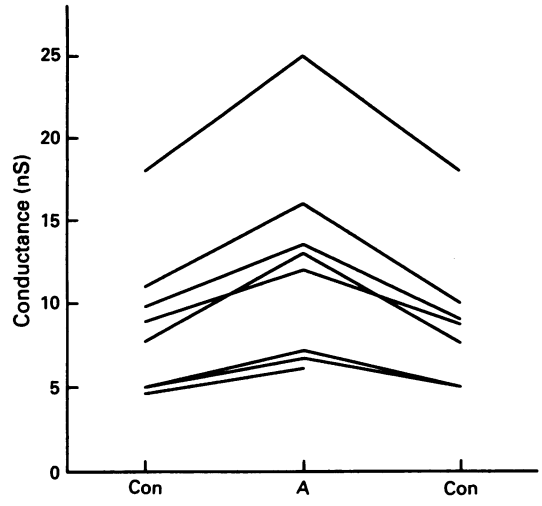

Figure 3 Summary of the effect of adenosine (A, 10^{-5} M) on the outward current of mesangial cells ($n = 8$). Experiments were performed in the fast whole cell configuration and ion currents were registered in the absence (Con) and presence of adenosine. The increase of the outward current was significant and reversible. $n = 8$.

of adenosine in the absence and presence of a high extracellular K^+ concentration, Figure 4b summarizes the data. The K^+-channel blocker, Ba^{2+} (5×10^{-3} M), depolarized membrane voltage significantly to -24 ± 2 mV. In the presence of Ba^{2+} the adenosine-induced hyperpolarization was inhibited by $72 \pm 8\%$ ($n = 4$). Figure 5a shows an original experiment of the effect of Ba^{2+} in the absence and presence of adenosine. Figure 5b summarizes the data.

Forskolin hyperpolarizes membrane voltage of mesangial cells

Stimulation of cyclic AMP production by forskolin resulted in a sustained and concentration-dependent hyperpolariza-

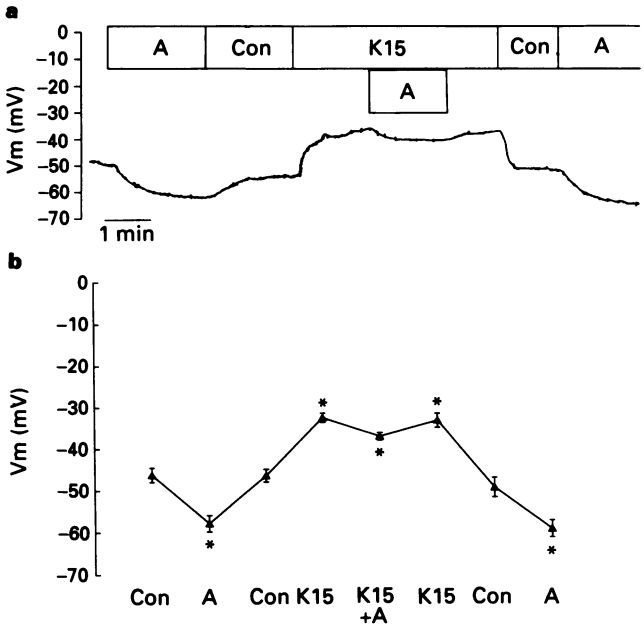

Figure 4 An increase of the extracellular K^+ concentration from 3.6 (Con) to 18.6 mM (K15) depolarized membrane voltage (Vm) and attenuated significantly the hyperpolarization by adenosine (A, 10^{-5} M). (a) Original recording. (b) Summary of 7 paired experiments.

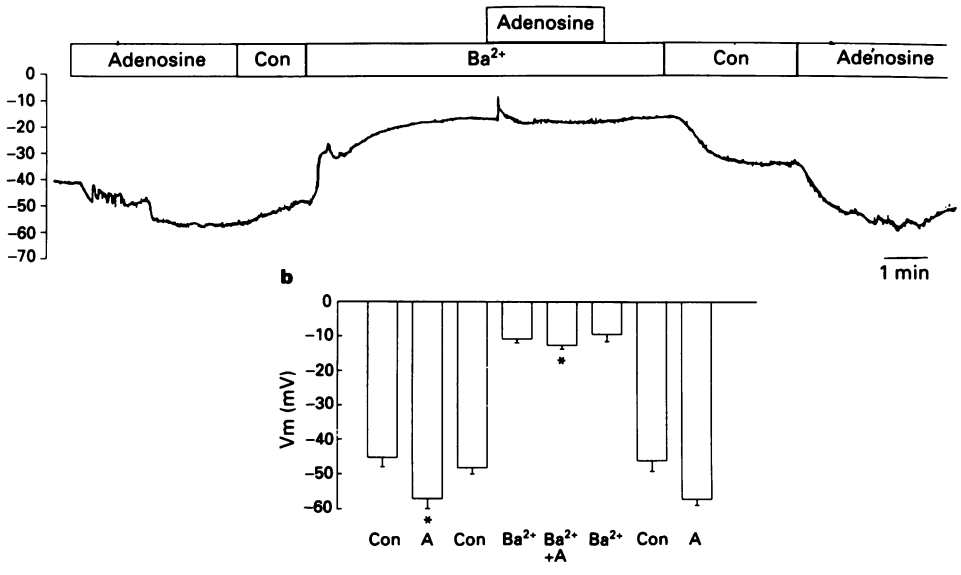

Figure 5 The K^+ channel blocker, Ba^{2+} (5×10^{-3} M), inhibits the adenosine (10^{-5} M)-induced hyperpolarization of membrane voltage (Vm). (a) Original recording of the effect of adenosine in the absence and presence of Ba^{2+}. (b) Summary of 4 paired experiments. Note that Ba^{2+} depolarizes membrane voltage and that in the presence of Ba^{2+} the adenosine (A)-induced hyperpolarization is significantly inhibited.

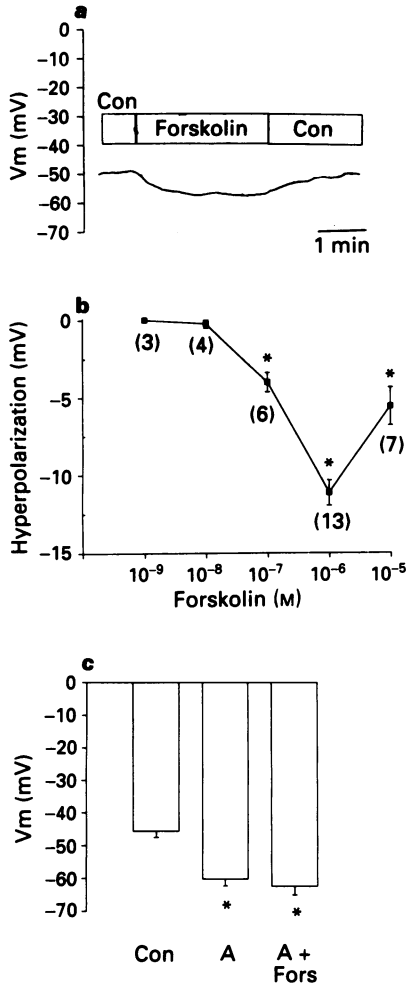

Figure 6 Forskolin hyperpolarizes membrane voltage of mesangial cells. (a) Original record of the effect of forskolin (10^{-5} M) on membrane voltage (Vm) of mesangial cells. (b) Concentration-response curve. (c) Summary of the effect of forskolin (10^{-4} M) in the presence of adenosine (A, 10^{-5} M, $n = 5$).

tion of membrane voltage ($n = 53$, Figure 6a). The inactive 1,9-dideoxyforskolin had no effect on membrane voltage ($n = 5$, data not shown). Half-maximal responses were observed at about 2×10^{-7} M forskolin (Figure 6b). In the presence of an increased extracellular K^+ concentration (from 3.6 to 18.6 M) the effect of forskolin was significantly reduced by $33 \pm 4\%$, $n = 4$. Like forskolin the cyclic AMP analogue 8-(4-chlorophenylthio)-cyclic AMP (10^{-4} M) hyperpolarized membrane voltage significantly from -49 ± 3 mV to -59 ± 3 mV, ($n = 9$, data not shown). Application of adenosine (10^{-5} M) in the presence of forskolin (10^{-4} M) did not result in an additive hyperpolarization of membrane voltage ($n = 7$). Figure 6c summarizes the data of the effect of forskolin in the presence of adenosine.

Stimulation of protein kinase C (PKC) did not inhibit the effect of adenosine on membrane voltage

Stimulation of PKC by phorbol 12,13-dibutyrate (PDBu) led to a sustained and concentration-dependent depolarization of membrane voltage ($ED_{50} \approx 5 \times 10^{-9}$ M, $n = 45$) whereas the inactive phorbol ester, 4-α-PMA had no effect on membrane voltage of mesangial cells ($n = 5$). In the presence of PDBu (10^{-8} M), adenosine (10^{-5} M) still elicited a hyperpolarization of membrane voltage (from -26 ± 3 mV to -50 ± 5 mV, $n = 5$). Figure 7a shows an original recording and Figure 7b the concentration-response curve of the effect of PDBu on membrane voltage of mesangial cells. Figure 7c summarizes the effect of PDBu (10^{-8} M) in the presence and absence of adenosine (10^{-5} M).

Discussion

The present study demonstrates that adenosine induces a sustained hyperpolarization in mesangial cells. It has been reported previously that several vasoactive agonists including angiotensin II (Okuda *et al.*, 1986), vasopressin (Kremer *et al.*, 1989) and extracellular ATP (Pavenstädt *et al.*, 1993) depolarize membrane voltage of mesangial cells, but until now there have been no data demonstrating agonist-induced hyperpolarization in mesangial cells. An adenosine-induced

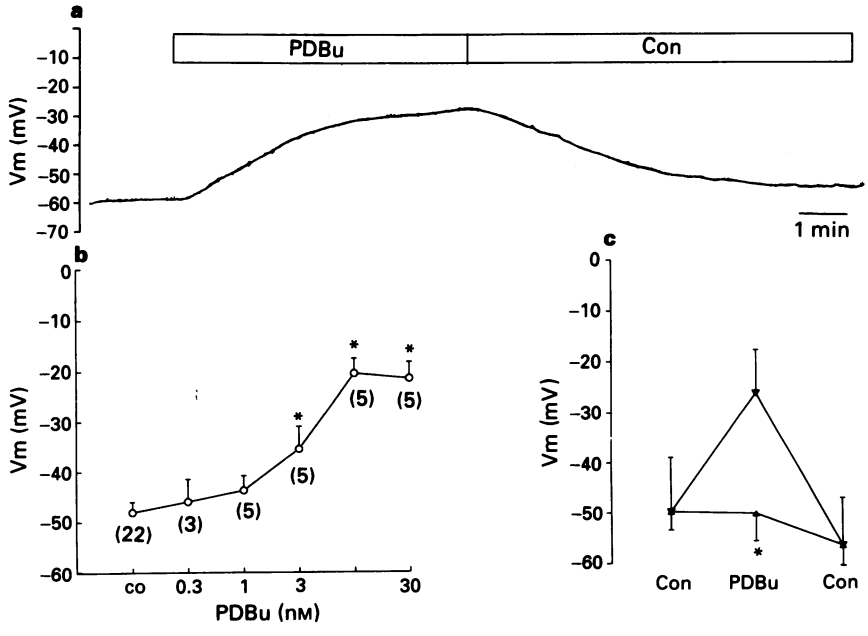

Figure 7 Effect of phorbol 12,13-dibutyrate (PDBu) on membrane voltage (Vm) and the membrane voltage response of mesangial cells to adenosine. (a) Original recording of the effect of PDBu (10^{-8} M) on membrane voltage. (b) Concentration-response curve. (c) Summary of the effect of adenosine (10^{-5} M) (▲) in the presence of PDBu (10^{-8} M). Note that PDBu even at low concentrations induces a sustained and reversible depolarization of membrane voltage and that the adenosine-induced hyperpolarization was not inhibited in the presence of PDBu. $n = 5$.

hyperpolarization has been shown in geniculocortical neurones (Pape, 1992), endothelial cells (Seiss-Geuder *et al.*, 1992) and coronary smooth muscle (Sabouni *et al.*, 1989).

There is a substantial body of evidence that the adenosine-induced hyperpolarization is due to an activation of K^+ conductance. During the hyperpolarization the outward current is increased, the correlation between membrane voltage and the logarithm of the extracellular K^+ concentration is shifted to that predicted by the Nernst voltage for K^+ and the hyperpolarization is blocked by the K^+ channel blocker Ba^{2+} (Kolb, 1990). An activation of potassium conductance by adenosine has also been reported in endothelial cells (Mehrke *et al.*, 1991) and atrial myocytes (Belardinelli & Isenberg, 1983).

The pharmacological effects of adenosine are mediated by specific P_1 purinoceptors, which have been further subdivided into A_1 and A_2 receptors (for review see Kennedy, 1990). A_1 and A_2 receptors differ in their sensitivity to adenosine agonists. Adenosine itself has nanomolar affinity for A_1 receptors but micromolar affinity for A_2 receptors (van Calker *et al.*, 1979) and at the A_1 receptor **R**-PIA is more potent than NECA, whereas at A_2 receptors the potency of these agonists is reversed (Londos *et al.*, 1980). In our experiments NECA was more potent than **R**-(−)-PIA indicating that the adenosine-induced hyperpolarization is probably mediated by an A_2 receptor. However DPMA, which was assumed to act as a selective A_2 agonist (Bridges *et al.*, 1988) was less effective in comparison to NECA. Therefore it is possible that a receptor distinct from the A_2 receptor may be involved in the adenosine-induced hyperpolarization in mesangial cells. Recently it has been shown that NECA, adenosine and **R**-(−)PIA in comparison to our results increased cyclic AMP in mesangial cells with the same rank order of potency (Olivera & Lopez-Novoa, 1992). The relative ineffectiveness of selective antagonists in the latter study also led to the assumption that mesangial cells possess a receptor distinct from the A_1 or A_2 receptor (Olivera & Lopez-Novoa, 1992). An A_1 and A_2 receptor subtype could also not be classified in platelets and in the coronary artery (Forster *et al.*, 1987; Kusachi *et al.*, 1983).

A_1 and A_2 receptors not only differ in their sensitivity to adenosine agonists but also have opposite effects on the generation of cyclic AMP: A_1 receptors mediate inhibition of adenylate cyclase whereas A_2 receptors stimulate the enzyme (van Calker *et al.*, 1979). To test the hypothesis that the adenosine induced hyperpolarization was mediated by cyclic AMP, experiments with forskolin and 8-(4-chlorophenylthio)-cyclic AMP, a cyclic AMP analogue were performed. Both agents induced a sustained hyperpolarization, indicating that cyclic AMP might be the second messenger responsible for the hyperpolarization due to adenosine. Similar results have been reported in vascular smooth muscle- and endothelial cells (Pavenstädt *et al.*, 1991; Graier *et al.*, 1993). Application of both, adenosine and forskolin to mesangial cells had no additive effect on membrane voltage, indicating that under these experimental conditions no further cyclic AMP accumulation leading to a hyperpolarization of membrane voltage occurs. An adenosine-stimulated cyclic AMP accumulation has been shown in glomeruli (Abboud & Dousa, 1983) and in cultured mesangial cells (Olivera & Lopez-Novoa, 1992). An accumulation of cyclic AMP in mesangial cells is known to dissociate stress fibres resulting in a decrease in cell tension and cell relaxation (Schlondorff, 1987). In contrast, it has also been reported that adenosine increases cytosolic free calcium, an event probably leading to mesangial cell contraction (Olivera *et al.*, 1989, 1992). This has led to the assumption that adenosine might regulate GFR by reducing the ultrafiltration coefficient K_f. However, a change of K_f due to adenosine was not found in *in vivo* experiments (Osswald *et al.*, 1978) and adenosine did not stimulate inositol phosphate accumulation in mesangial cells (Pfeilschifter, 1990). We could not observe an adenosine-induced mesangial cell-contraction or an increase of the cytosolic calcium activity in mesangial cells (own unpublished observations). In addition, adenosine did not depolarize membrane voltage, whereas all other calcium mobilizing compounds like ATP, angiotensin II and vasopressin led to a contraction and depolarization of membrane voltage (Gloy *et al.*, 1993; Pavenstädt *et al.*, 1993). In the present study, adenosine induced a cyclic AMP-dependent hyperpolarization of membrane voltage in mesangial cells. An elevation of the cyclic AMP level is known to induce cell relaxation and to antagonize the contractile response of mesangial cells to vasoactive antagonists. Although this is a matter of debate, relaxation of mesangial cells might lead to an increase of the ultrafiltration coefficient K_f (for review see Mené *et al.*, 1989). If this is the case, the adenosine-induced hyperpolarization of mesangial cells might even counteract the effect of adenosine on pre- and post-glomerular vessels leading to a decrease of GFR.

Protein kinase C plays a crucial role in signal transduction of mesangial cells (Pfeilschifter, 1989). Our data indicate that the pharmacological activation of PKC by phorbol ester led to a sustained depolarization of membrane voltage. The PKC-induced depolarization was augmented in a reduced extracellular Cl^- concentration indicating that it was due to an activation of a Cl^- conductance (our unpublished observations). Similar effects of phorbol esters on short term cultured mesangial cells have been observed recently with fluorescent measurements of membrane voltage (Kremer *et al.*, 1992). Recent reports have suggested a PKC-induced phosphorylation of adrenoceptors, resulting in a less efficient activation of adenylate cyclase, whereas in other studies activation of PKC led to a magnification of the stimulation of adenylate cyclase by adrenoceptor agents (Yoshimasa *et al.*, 1987). Therefore, we studied whether activation of PKC by phorbol ester may influence adenosine-induced hyperpolarization. In the presence of PDBu the membrane voltage response to adenosine was still present, indicating that activation of PKC did not inhibit but even might increase the adenosine-induced hyperpolarization. Whether this really reflects an augmented response will have to be clarified on the basis of current measurements.

In summary, the present data indicate that adenosine activates K^+ conductance via an A_2-like receptor in mesangial cells. The activation of the K^+ conductance leads to a hyperpolarization of membrane voltage and this is probably mediated by cyclic AMP.

We thank Mrs Christine Hodler and Mrs Monika von Hofer for their excellent technical assistance. Supported by DFG Pa 483/1-1.

References

ABBOUD, H. & DOUSA, T.P. (1983). Action of adenosine on cyclic 3',5'-nucleotides in glomeruli. *Am. J. Physiol.*, **244**, F633–F638.

BELARDINELLI, L. & ISENBERG, G. (1983). Isolated atrial myocytes: adenosine and acetylcholine increase potassium conductance. *Am. J. Physiol.*, **244**, 734–737.

BRIDGES, A.J., BURNS, R.F., ORTWINE, D.F., PRIEBE, S.R., SZOTEK, D.L. & TRIVEDI, B.K. (1988). N^6-(2-(3,5-dimethyoxyphenyl)-2-(2-methylphenyl)-ethyl)adenosine and its uronamide derivatives. Novel adenosine agonists with both high affinity and high selectivity for the adenosine A_2 receptor. *J. Med. Chem.*, **31**, 1282–1285.

BROSS, K.J., PANGALIS, G.A., STAATZ, C.G. & BLUME, K.G. (1978). Demonstration of cell surface antigens and their antibodies by the peroxidase-antiperoxidase method. *Transplantation*, **25**, 331–334.

CHURCHILL, P.C. & CHURCHILL, M.C. (1985). A_1 and A_2 adenosine receptor activation inhibits and stimulates renin secretion of rat renal cortical slides. *J. Pharmacol. Exp. Ther.*, **232**, 589–594.

FORSTER, M., HORNBY, E.J. & PERRY, C. (1987). Adenosine analogues as inhibitors of human platelet aggregation. *Br. J. Pharmacol.*, **92**, 736P.

FREISMUTH, M., HAUSLEITHNER, V., TUISL, E., NANNOFF, C. & SCHUETZ, W. (1987). Glomeruli and microvessels of the rabbit kidney contain both A_1 and A_2 adenosine receptors. *Naunyn. Schmied. Arch. Pharmacol.*, **335**, 438–444.

GLOY, J., GREGER, R., SCHOLLMEYER, P., HUBER, M. & PAVENSTÄDT, H. (1994). Influence of cell culture conditions and passage number on the response of membrane voltage to ATP and angiotensin II in rat mesangial cells. *Renal Physiol. Biochem.*, **17**, 62–72.

GRAIER, W.F., KUKOVETZ, W.R. & GROSCHNER, K. (1993). Cyclic AMP enhances agonist-induced Ca^{2+} entry into epithelial cells by activation of potassium channels and membrane hyperpolarization. *Biochem. J.*, **291**, 263–267.

GREGER, R. & KUNZELMANN, K. (1991). Simultaneous recording of the cell membrane potential and properties of the cell attached membrane of HT29 colon carcinoma and CF-PAC-cells. *Pflügers Arch.*, **419**, 209–211.

HEDQVIST, P., FREDHOLM, B.B. & OLUNDH, S. (1978). Antagonistic effects of theophylline and adenosine on adrenergic neuroeffector transmission in the rabbit kidney. *Circ. Res.*, **43**, 592–598.

KENNEDY, C. (1990). P_1- and P_2 purinoceptor subtypes – an update. *Arch. Int. Pharmacodyn. Ther.*, **303**, 30–50.

KOLB, H.A. (1990). Potassium channels in excitable and non-excitable cells. *Rev. Physiol. Biochem. Pharmacol.*, **115**, 51–140.

KREISBERG, J.I. & KARNOVSKY, M.J. (1983). Glomerular cells in culture. *Kidney Int.*, **23**, 439–447.

KREMER, S.G., BREUER, W.V. & SKORECKI, K.L. (1989). Vasoconstrictor hormones depolarize renai glomerular mesangial cells by activating chloride channels. *J. Cell. Physiol.*, **138**, 97–105.

KREMER, S.G., ZENG, W., SRIDHARA, S. & SKORECKI, K.L. (1992). Multiple signaling pathways for Cl^- dependent depolarization of mesangial cells: role for Ca^{2+}, PKC and G proteins. *Am. J. Physiol.*, **262**, F668–F678.

KUSACHI, S., THOMPSON, R.D. & OLSSON, R.A. (1983). Ligand selectivity of dog coronary artery adenosine receptor resembles that of adenylate cyclase stimulatory (R_a) receptors. *J. Pharmacol. Exp. Ther.*, **227**, 316–321.

LONDOS, C.D., COOPER, D.M.F & WOLFF, J. (1980). Subclasses of external adenosine receptors. *Proc. Natl. Acad. Sci. USA*, **77**, 2551–2554.

MARTY, A. & FINKELSTEIN, A. (1975). Pores formed in lipid membranes by nystatin. *J. Gen. Physiol.*, **65**, 315–326.

MEHRKE, G., POHL, U. & DAUT, J. (1991). The electrical response of cultured coronary endothelial cells to endothelium-dependent vasodilators. *J. Physiol.*, **439**, 277–299.

MENE, P., SIMONSON, M.S. & DUNN, M.J. (1989). Physiology of the mesangial cell. *Physiol. Rev.*, **69**, 1347–1424.

OKUDA, T., YAMASHITA, N. & KUROKAWA, K. (1986). Angiotensin II and vasopressin stimulate calcium-activated chloride conductance in rat mesangial cells. *J. Clin. Invest.*, **78**, 1443–1448.

OLIVERA, A., LAMAS, S., RODRIGUEZ-PUYOL, D. & LOPEZ-NOVOA, J.M. (1989). Adenosine induces mesangial cell contraction by an A_1-type receptor. *Kidney Int.*, **35**, 1300–1305.

OLIVERA, A. & LOPEZ-NOVOA, M. (1992). Effect of adenosine and adenosine analogues on cyclic AMP accumulation in cultured mesangial cells and isolated glomeruli of the rat. *Br. J. Pharmacol.*, **107**, 341–346.

OLIVERA, A., LOPEZ-RIVAS, A. & LOPEZ-NOVOA, J.M. (1992). Adenosine stimulates Ca^{2+} fluxes and increases cytosolic free Ca^{2+} in cultured rat mesangial cells. *Biochem. J.*, **282**, 871–876.

OSSWALD, H., SPIELMAN, W.S. & KNOX, F.G. (1978). Mechanism of adenosine-mediated decreases in glomerular filtration rate in dogs. *Circ. Res.*, **43**, 465–469.

PALACIOS, J.M., FASTBOOM, J., WIEDERHOLD, K.H. & PROBST, A. (1987). Visualization of adenosine A_1 receptors in the human and the guinea-pig kidney. *Eur. J. Pharmacol.*, **138**, 273–276.

PAPE, H.C. (1992). Adenosine promotes burst activity in guinea-pig geniculocortical neurones through two different ionic mechanisms. *J. Physiol.*, **447**, 729–753.

PAVENSTÄDT, H., GLOY, J., LEIPZIGER, J., KLÄR, B., PFEILSCHIFTER, J., SCHOLLMEYER, P. & GREGER, R. (1993). Effect of extracellular ATP on contraction, cytosolic calcium activity, membrane voltage and ion currents in rat mesangial cells in primary culture. *Br. J. Pharmacol.*, **109**, 953–959.

PAVENSTÄDT, H., LINDEMAN, V., LINDEMAN, S., KUNZELMANN, K., SPÄTH, M. & GREGER, R. (1991). Effect of depolarizing and hyperpolarizing agents on the membrane potential difference of primary cultures of rabbit aorta vascular smooth muscle cells. *Pflügers Arch.*, **419**, 59–65.

PFEILSCHIFTER, J. (1989). Cellular signaling in the kidney. The role of inositol lipids. *Renal. Physiol. Biochem.*, **12**, 1–31.

PFEILSCHIFTER, J. (1990). Extracellular ATP stimulates polyphosphoinositide hydrolysis and prostaglandin synthesis in rat renal mesangial cells. *Cellular Signaling*, **2**, 129–138.

SABOUNI, M.H., HARGITTAI, P.T., LIEBERMAN, E.M. & MUSTAFA, S. (1989). Evidence for adenosine receptor-mediated hyperpolarization in coronary smooth muscle. *Am. J. Physiol.*, **257**, 1750–1752.

SCHLONDORFF, D. (1987). The glomerular mesangial cell: an expanding role for a specialized pericyte. *FASEB J.*, **1**, 272–281.

SEISS-GEUDER, M., MEHRKE, G. & DAUT, J. (1992). Sustained hyperpolarization of cultured guinea pig coronary endothelial cells induced by adenosine. *J. Cardiovasc. Pharmacol.*, **20**, 97–100.

VAN CALKER, D., MÜLLER, M. & HAMPRECHT, B. (1979). Adenosine regulates via two different types of receptors, the accumulation of cyclic AMP in cultured brain cells. *J. Neurochem.*, **33**, 999–1005.

YOSHIMASA, T., SIBLEY, D.R., BOUVIER, M., LEFKOWITZ, R.J. & CARON, G. (1987). Cross-talk between cellular signaling pathways suggested by phorbol-ester-induced adenylate cyclase phosphorylation. *Nature*, **327**, 67–70.

(Received November 18, 1993
Revised April 15, 1994
Accepted April 25, 1994)

Br. J. Pharmacol (1994), **113**, 13–20

The 5-HT_1-like receptor mediating the increase in canine external carotid blood flow: close resemblance to the 5-HT_{1D} subtype

[1]Carlos M. Villalón & José A. Terrón

Sección de Terapéutica Experimental, Departamento de Farmacología y Toxicología, Centro de Investigación y de Estudios Avanzados del Instituto Politécnico Nacional, Apdo. Postal 22026, 14000 México, D.F., México

1 It has recently been shown that the increase in external carotid blood flow induced by 5-hydroxytryptamine (5-HT) in the anaesthetized dog, being mimicked by 5-carboxamidotryptamine (5-CT), inhibited by methiothepin, vagosympathectomy and sympatho-inhibitory drugs, and resistant to blockade by ritanserin and MDL 72222, is mediated by stimulation of prejunctional 5-HT_1-like receptors leading to an inhibitory action on carotid sympathetic nerves; these 5-HT_1-like receptors are unrelated to either the 5-HT_{1A}, 5-HT_{1B} or 5-HT_{1C} (now 5-HT_{2C}) receptor subtypes. Inasmuch as 5-CT, 5-methoxytryptamine, sumatriptan and metergoline display high affinity, amongst other 5-HT binding sites, for the 5-HT_{1D} subtype, in the present study we have used these drugs in an attempt to determine whether the above inhibitory prejunctional 5-HT_1-like receptors correlate with the 5-HT_{1D} subtype.

2 One-minute intracarotid (i.c.) infusions of 5-HT (0.3, 1, 3 and 10 μg), 5-CT (0.01, 0.03, 0.1 and 0.3 μg), 5-methoxytryptamine (1, 3, 10 and 30 μg) and sumatriptan (1, 3, 10, 30 and 100 μg) resulted in dose-dependent increases in external carotid blood flow (without changes in mean arterial blood pressure or heart rate) with the following rank order of agonist potency: 5-CT >> 5-HT > 5-methoxytryptamine ≥ sumatriptan. Interestingly, sumatriptan-induced vasodilatation was followed by a more pronounced vasoconstriction.

3 The external carotid vasodilator effects of 5-HT, 5-CT, 5-methoxytryptamine and sumatriptan were dose-dependently and specifically antagonized by metergoline (10, 30 and/or 100 μg kg^{-1}, i.v.). In addition, 5-methoxytryptamine- and sumatriptan-induced vasodilator effects were, respectively, markedly inhibited or abolished after vagosympathectomy, as previously shown for 5-CT and 5-HT.

4 Sumatriptan showed tachyphylaxis in its vasodilator component and antagonized 5-HT-induced external carotid vasodilatation in a specific manner, suggesting that a common site of action may be involved.

5 Taken together, the above results support our contention that 5-HT, 5-CT, 5-methoxytryptamine and sumatriptan produce external carotid vasodilatation in the dog by an action that might primarily involve a prejunctional inhibition on carotid sympathetic nerves; a secondary component of this vasodilator response may be postsynaptic (endothelium-dependent and/or even directly on the vasculature). Based on the rank order of agonist potency, inhibition by vagosympathectomy and blockade by metergoline, we suggest that the inhibitory prejunctional 5-HT_1-like receptors mediating external carotid vasodilatation in the dog closely resemble the 5-HT_{1D} receptor subtype. The pharmacological profile of these receptors is similar (sympathetic nerves of the rat kidney and human saphenous vein, as well as porcine coronary endothelium) to other putative 5-HT_{1D} receptors mediating vascular responses.

Keywords: Carotid blood flow; 5-hydroxytryptamine; 5-HT_{1D} receptors; metergoline; sumatriptan; vasodilatation

Introduction

Intracarotid infusion of 5-hydroxytryptamine (5-HT) increases the external carotid blood flow in the dog by an inhibitory action on carotid sympathetic nerves, via the stimulation of inhibitory prejunctional 5-HT_1-like receptors unrelated to the 5-HT_{1A}, 5-HT_{1B} or 5-HT_{1C} (now 5-HT_{2C}) subtypes (Villalón *et al.*, 1993a,b). Admittedly, the 5-HT_1 receptor is highly heterogeneous in nature, as five 5-HT_1 binding site subtypes (5-HT_{1A}, 5-HT_{1B}, 5-HT_{1D}, 5-HT_{1E} and 5-HT_{1F}) have been identified (Humphrey *et al.*, 1993), but even these subtypes do not seem to correspond with some 5-HT_1-like receptor-mediated functional responses (Villalón & Saxena, 1992).

Within the 5-HT_1 receptor family, sumatriptan has a relative selectivity for the 5-HT_{1D} subtype (Peroutka & McCarthy, 1989; Schoeffter & Hoyer, 1989). Indeed, some actions of 5-HT and/or sumatriptan, including inhibition of noradrenaline release from sympathetic nerves (Molderings *et al.*, 1990) and contraction (Bax *et al.*, 1992) of the human saphenous vein as well as endothelium-dependent coronary vasodilatation in the pig (Schoeffter & Hoyer, 1990) are mediated by the 5-HT_{1D} (or a similar) receptor. This was suggested by: (i) the blockade of these responses by methiothepin, methysergide and/or metergoline; and (ii) the rank order of agonist potency of 5-carboxamidotryptamine (5-CT) ≥ 5-HT > 5-methoxytryptamine > sumatriptan.

It should be emphasized, notwithstanding, that sumatriptan can activate functional 5-HT_1-like receptors unrelated to the 5-HT_{1D} subtype for example, the increase in resistance within the canine carotid circulation (Perren *et al.*, 1991) and constriction of porcine arteriovenous anastomoses (Den Boer *et al.*, 1992); these effects were not antagonized by metergoline, a compound displaying a very high affinity for the 5-HT_{1D} receptor as well as for the 5-HT_{1A}, 5-HT_{1B}, 5-HT_{1C} (5-HT_{2C}) and 5-HT_2 receptors (Waeber *et al.*, 1988).

On the basis of the above findings, the present study was carried out to characterize further the nature of the inhibitory prejunctional 5-HT_1-like receptors mediating external

[1] Author for correspondence.

carotid vasodilatation in the dog, with particular emphasis on verifying whether these receptors belong to the 5-HT_{1D} subtype. Therefore, we analysed the external carotid vascular effects of the endogenous ligand, 5-HT, and the putative 5-HT_{1D} receptor agonists, 5-CT, 5-methoxytryptamine and sumatriptan (Waeber *et al.*, 1988; Hoyer, 1989; Peroutka & McCarthy, 1989) in the absence or the presence of metergoline. Preliminary results of this investigation have been communicated to the Western Pharmacology Society (Villalón *et al.*, 1993c).

Methods

General

Experiments were carried out in a total of 35 dogs (19.2 ± 0.8 kg) not selected for breed or sex. The animals were anaesthetized with sodium pentobarbitone (30 mg kg^{-1}, i.v.) and additional amounts (1 mg kg^{-1}, i.v.) were provided when required. All dogs were intubated with an endotracheal tube and artificially respired with room air using a Palmer ventilation pump at a rate of 20 strokes min^{-1} and a stroke volume of 13–16 ml kg^{-1}, which was adjusted to maintain arterial pH within normal limits. Moreover, catheters were placed in the inferior vena cava via a femoral vein for the administration of drugs and in the aortic arch via a femoral artery, connected to a Statham pressure transducer (P23 ID) for the measurement of arterial blood pressure. After drug administration, the venous cannula was flushed with 3 ml of physiological saline. Mean arterial blood pressure (MAP) was calculated from the systolic (SAP) and diastolic (DAP) arterial pressures: MAP = DAP + (SAP-DAP)/3. Heart rate was measured with a tachograph (7P4F, Grass Instrument Co., Quincy, MA, U.S.A.) triggered from the blood pressure signal.

The right common carotid artery was dissected for approximately 10 cm proximal to its bifurcation, and the branches originating at this site were identified. In all cases, the corresponding carotid sinus was denervated in order to avoid the reflex cardiovascular effects of 5-HT. Denervation was achieved by carefully stripping the sinus of surrounding tissue, and the adequacy of the procedure was checked by verifying that occlusion of the corresponding common carotid artery did not elicit a pressor response. After ligating the right internal carotid and right occipital arteries, a precalibrated ultrasonic flow probe (4 mm R-Series; Transonic Systems Inc., Ithaca, N.Y., U.S.A.) connected to an ultrasonic T201D flowmeter (Transonic Systems Inc., Ithaca, N.Y., U.S.A.) was placed around the right common carotid artery, 1 or 2 cm proximal to the origin of the cranial thyroid artery. Under these experimental circumstances, the flow through the right common carotid artery was considered to represent the blood flow through the external carotid artery (for detailed considerations see Villalón *et al.*, 1993a,b).

To analyse the effect of agonist drugs on external carotid blood flow, the agonists were administered into the carotid artery by a Harvard model 901 pump (Harvard Apparatus Co. Inc., Millis, MA, U.S.A.) with a cannula inserted into the right cranial thyroid artery. Mean arterial blood pressure, heart rate and external carotid blood flow were recorded simultaneously by a model 7D Grass polygraph (Grass Instrument Co., Quincy, MA, U.S.A.). The body temperature of the animals was maintained between 37–38°C.

Experimental protocol

After the animals had been in a stable haemodynamic condition for at least 30 min, baseline values of blood pressure, heart rate and external carotid blood flow were determined. At this point, the animals were divided into seven groups. The first group ($n = 6$) received consecutive i.c. infusions (during 1 min) of 5-HT (0.3, 1, 3 and 10 μg min^{-1}), 5-carboxamidotryptamine (5-CT; 0.01, 0.03, 0.1 and 0.3 μg min^{-1}) and acetylcholine (0.003, 0.01, 0.03 and 0.1 μg min^{-1}); subsequently, the animals were given metergoline (10, 30 and 100 μg kg^{-1}, i.v.) and the responses to 5-HT, 5-CT and acetylcholine were elicited again after each dose of the antagonist. The other three groups received 1 min i.c. infusions of 5-methoxytryptamine (1, 3, 10 and 30 μg min^{-1}) before and after either physiological saline (0.015, 0.05 and 0.15 ml kg^{-1}, i.v.; $n = 6$), metergoline (10, 30 and 100 μg kg^{-1}, i.v.; $n = 6$) or bilateral cervical vagosympathectomy ($n = 4$; as described by Villalón *et al.*, 1993a,b) respectively. In the saline-treated group, a dose-response curve to 5-HT was elicited before and after the four dose-response curves to 5-methoxytryptamine to investigate any possible interaction between the two agonists.

Finally, the three other groups received 1 min i.c. infusions of sumatriptan (1, 3, 10, 30 and 100 μg min^{-1}) before and after either saline (0.15 ml kg^{-1}, i.v.; $n = 4$), metergoline (100 μg kg^{-1}, i.v.; $n = 5$) or vagosympathectomy ($n = 4$), respectively. In the saline-treated group, the possible interaction of sumatriptan with 5-HT and acetylcholine, respectively, was analysed by eliciting dose-response curves to 5-HT and acetylcholine before and after the first dose-response curve to sumatriptan. Since sumatriptan-induced vasodilator responses showed a fading pattern after repetitive administration, only two dose-response curves to the agonist were obtained.

Each dose of agonist drug was in a solution which was administered at a rate of 1 ml min^{-1} during a period of 1 min, with intervals of 5–45 min. The doses of agonist drugs were selected on the basis of results obtained from preliminary experiments, in which reproducible and consistent dose-dependent responses in external carotid blood flow were elicited with no changes in arterial blood pressure or heart rate (for more details see Villalón *et al.*, 1993a).

The interval between the different doses of the compounds used as agonists and/or antagonists depended on the duration of the effect produced by the preceding dose on the haemodynamic variables. Thus, the dose-intervals between the different doses of agonists (especially 5-CT and sumatriptan) ranged between 5 and 45 min, as in each case we waited until the external carotid blood flow had returned completely to the baseline values; for the antagonists, a period of 10 min was allowed to elapse before the dose-response curves to the agonists were made again. The dosing with all drugs used was sequential.

Data presentation and statistical analysis

All data in the text, figures and tables are presented as mean ± s.e. mean. The peak changes in external carotid blood flow produced by the different doses of agonists were determined. The difference between the variables within one group was evaluated with Duncan's new multiple range test, once an analysis of variance (randomized block design) had revealed that the samples represented different populations (Steel & Torrie, 1980). Where appropriate, Student's paired t test was applied. A P value of 0.05 or less (two-tailed) was considered statistically significant.

Drugs

Apart from the anaesthetic (sodium pentobarbitone), the drugs used in the present study were the following, obtained from the sources indicated: 5-hydroxytryptamine creatinine sulphate (Sigma Chemical Company, St. Louis, MO, U.S.A.); acetylcholine chloride and 5-methoxytryptamine hydrochloride (Research Biochemical Inc., Natick, MA, U.S.A.); 5-carboxamidotryptamine maleate and sumatriptan succinate (gift: Dr P.P.A. Humphrey, Glaxo group research, Ware, U.K.); and metergoline (gift: Farmitalia, Milan, Italy). All compounds were dissolved in physiological saline; when needed, 2% ascorbic acid (metergoline) was added. The

vehicles had no effect on either basal mean arterial blood pressure, heart rate or external carotid blood flow. The doses mentioned in the text refer to the free base of substances.

Results

Systemic haemodynamic variables

The values for blood pressure, heart rate and external carotid blood flow before and after saline or vagosympathectomy are shown in Table 1; similarly, the effects of metergoline are shown in Table 2. After vagosympathectomy, the external carotid blood flow was significantly increased (Table 1); in contrast, all these variables remained essentially unchanged after administration of saline (Table 1), or metergoline (Table 2). Moreover, blood pressure and heart rate were not modified by the i.c. infusions of the various agonists before and after either vagosympathectomy or metergoline (not shown, but baseline values are depicted in Table 1); however, higher doses of the 5-HT agonists tended to produce inconsistent effects on external carotid blood flow.

Initial effects of agonist drugs on external carotid blood flow

The onset of the responses induced by the 5-HT agonists was immediate; thus, Figure 1 shows that i.c. infusions of 5-HT (0.3, 1, 3 and 10 $\mu g\,min^{-1}$), 5-CT (0.01, 0.03, 0.1 and 0.3 $\mu g\,min^{-1}$), 5-methoxytryptamine (1, 3, 10 and 30 $\mu g\,min^{-1}$) and sumatriptan (1, 3, 10, 30 and 100 $\mu g\,min^{-1}$) elicited dose-dependent increases in external carotid blood flow; in no case did the 5-HT agonists significantly change blood pressure or heart rate. The rank order of agonist potency to increase external carotid blood flow was 5-CT >> 5-HT > 5-methoxytryptamine ≥ sumatriptan. At the doses used, the duration of action of 5-CT (2.4 ± 0.6, 3.7 ± 0.6, 5.1 ± 0.8 and 7.3 ± 1.1 min; $n = 6$) and 5-methoxytryptamine (1.3 ± 0.1, 1.7 ± 0.1, 2.1 ± 0.2 and 2.9 ± 0.3 min; $n = 16$) was longer than that of 5-HT, the effects of which lasted only during the period of infusion (1 min) at which time external carotid blood flow returned to the baseline value. Interestingly, 1 min i.c. infusions of sumatriptan (1, 3, 10, 30 and 100 $\mu g\,min^{-1}$) produced dose-dependent biphasic responses, namely, small increases (Figure 1) followed by larger decreases (−2 ± 1, −8 ± 3, −19 ± 4, −46 ± 8 and −64 ± 11 $ml\,min^{-1}$ after sumatriptan, respectively; $n = 6$) in external carotid blood flow; the vasodilator effects of sumatriptan lasted 1 min or less, whilst the vasoconstrictor responses were longer-lasting (2 ± 1, 5 ± 1, 7 ± 1, 15 ± 2 and 24 ± 2 min after sumatriptan, respectively).

Table 1 Mean arterial blood pressure (MAP; mmHg), heart rate (HR; beats min^{-1}) and external carotid blood flow (ECBF; $ml\,min^{-1}$, measured by an ultrasonic flow probe) before and after i.v. administration of saline ($n = 6$) or bilateral cervical vagosympathectomy ($n = 4$)

	Treatment	*Baseline value*	*10 min after treatment*
MAP	Saline[a]	134 ± 5	141 ± 6
	Vagosympathectomy	163 ± 14	169 ± 13
HR	Saline[a]	185 ± 9	175 ± 7
	Vagosympathectomy	151 ± 17	160 ± 14
ECBF	Saline[a]	122 ± 24	115 ± 18
	Vagosympathectomy	118 ± 18	197 ± 25*

[a]Refers to the effect after the third administration of physiological saline. The first and second saline administrations were without significant effects.
*Significantly different ($P < 0.05$) from the baseline value.

Table 2 Mean arterial blood pressure (MAP; mmHg), heart rate (HR; beats min^{-1}) and external carotid blood flow (ECBF; $ml\,min^{-1}$, measured by an ultrasonic flow probe) before and after i.v. administration of metergoline (10, 30 and 100 $\mu g\,kg^{-1}$; $n = 6$)[a]

	Baseline value	*10 min after metergoline (μg kg⁻¹, i.v.) 10*	*30*	*100*
MAP	147 ± 9	146 ± 9	152 ± 8	153 ± 8
HR	171 ± 9	165 ± 11	165 ± 9	156 ± 9
ECBF	113 ± 18	112 ± 18	114 ± 16	118 ± 16

[a]No significant changes in either MAP, HR or ECBF were produced after metergoline (10, 30 or 100 $\mu g\,kg^{-1}$, i.v.).

Effect of metergoline on external carotid vasodilatation to 5-HT, 5-CT and acetylcholine

We have previously reported that the external carotid vasodilatation induced by repeated administrations of 5-HT, 5-CT and acetylcholine remained unchanged in control animals receiving saline (Villalón *et al.*, 1993a). In contrast, the increases in external carotid blood flow induced by 5-HT and 5-CT were dose-dependently antagonized by metergoline (10, 30 and 100 $\mu g\,kg^{-1}$, i.v.), whereas those by acetylcholine remained unaffected (Figure 2). Significantly, not only were the vasodilator responses induced by 5-HT abolished by the highest dose of metergoline, but a dose-dependent vasoconstrictor effect was unmasked.

Effect of physiological saline, metergoline or vagosympathectomy on either 5-methoxytryptamine- or sumatriptan-induced increases in external carotid blood flow

The increases in external carotid blood flow produced by 5-methoxytryptamine, at the doses and time intervals (5–15 min) used in the present study, were reproducible and remained essentially unchanged in control animals receiving 3 subsequent doses (0.015, 0.05 and 0.15 $ml\,kg^{-1}$, i.v.) of saline (Figure 3a). In contrast, the responses to 5-methoxytrypt-

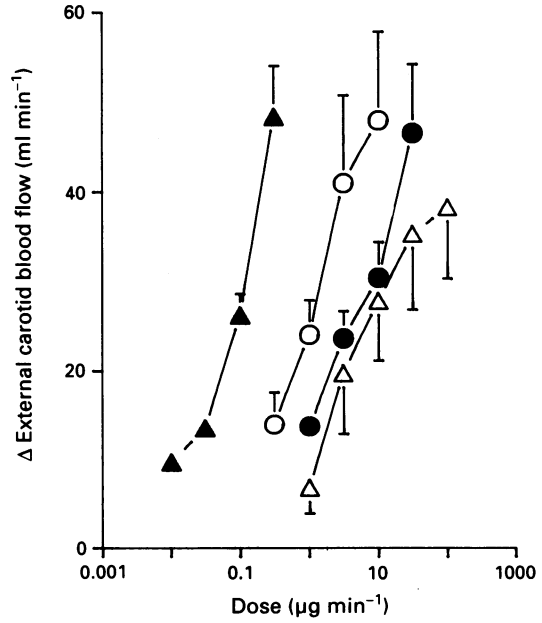

Figure 1 Comparative effects of 1 min i.c. infusions of 5-hydroxytryptamine (○, $n = 6$), 5-carboxamidotryptamine (▲, $n = 6$), 5-methoxytryptamine (●, $n = 6$) and sumatriptan (△, $n = 6$) on the canine external carotid blood flow. Sumatriptan-induced vasodilator effects were followed by larger and longer-lasting vasoconstrictor responses (see Results section).

amine were dose-dependently antagonized by metergoline (10, 30 and 100 $\mu g\ kg^{-1}$, i.v.; Figure 3b) or markedly, but not totally, inhibited after vagosympathectomy (Figure 3c). Moreover, the increases in external carotid blood flow produced by repeated doses of sumatriptan in the control animals were significantly reduced (Figure 4a); nevertheless, external carotid vasodilatation due to sumatriptan was abolished after either metergoline (100 $\mu g\ kg^{-1}$; Figure 4b) or vagosympathectomy (Figure 4c). Although not shown, the vasoconstrictor response that followed sumatriptan-induced vasodilatation was significantly increased after metergoline or vagosympathectomy. In the saline-treated animals, where 5-HT was administered before and after the set of injections of 5-methoxytryptamine (1, 3, 10 and 30 $\mu g\ min^{-1}$; $n = 6$) or sumatriptan (1, 3, 10, 30 and 100 $\mu g\ min^{-1}$; $n = 4$, see Methods), the responses induced by 5-HT (0.3, 1, 3 and 10 $\mu g\ min^{-1}$) remained unchanged after 5-methoxytryptamine (18 ± 3, 30 ± 4, 43 ± 6 and 58 ± 8 ml min^{-1} before and 14 ± 2, 22 ± 1, 37 ± 4 and 54 ± 5 ml min^{-1} after 5-methoxytryptamine, respectively), but were significantly ($P < 0.05$) reduced by sumatriptan (25 ± 3, 39 ± 7, 60 ± 12 and 72 ± 14 ml min^{-1} before and 16 ± 5, 24 ± 4, 33 ± 4 and 40 ± 9 ml min^{-1} after sumatriptan, respectively). It has to be emphasized that the vasodilator effects of 5-HT were not 'masked' by the increase in external carotid blood flow induced by sumatriptan, as the responses to 5-HT were elicited at the time when the effect of sumatriptan had worn off. In this respect, it is important to note that the responses to acetylcholine (0.003, 0.01, 0.03 and 0.1 $\mu g\ min^{-1}$) remained unaltered after sumatriptan (7 ± 2, 14 ± 5, 24 ± 6 and 41 ± 5 ml min^{-1} before and 9 ± 4, 14 ± 5, 24 ± 4 and 37 ± 4 ml min^{-1} after sumatriptan, respectively).

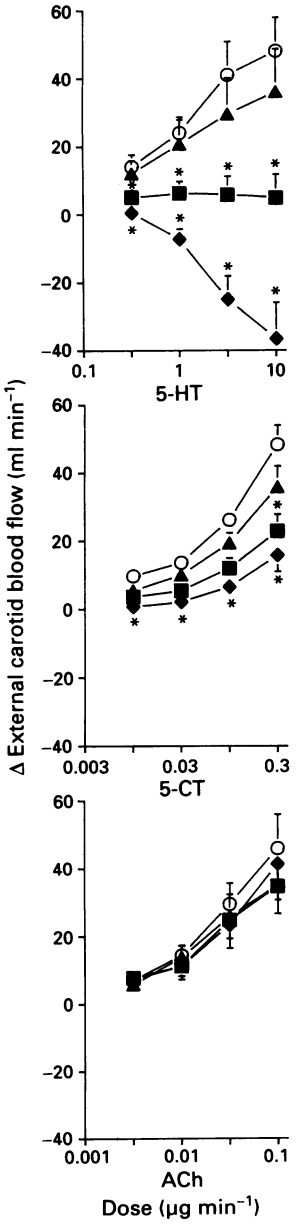

Figure 2 The effects of i.v. bolus injections of metergoline (○, 0 $\mu g\ kg^{-1}$; ▲, 10 $\mu g\ kg^{-1}$; ■, 30 $\mu g\ kg^{-1}$; and ◆, 100 $\mu g\ kg^{-1}$; $n = 6$ each) on the increases in canine external carotid blood flow induced by 1 min i.c. infusions of 5-hydroxytryptamine (5-HT), 5-carboxamidotryptamine (5-CT) and acetylcholine (ACh). $^*P < 0.05$ vs. control.

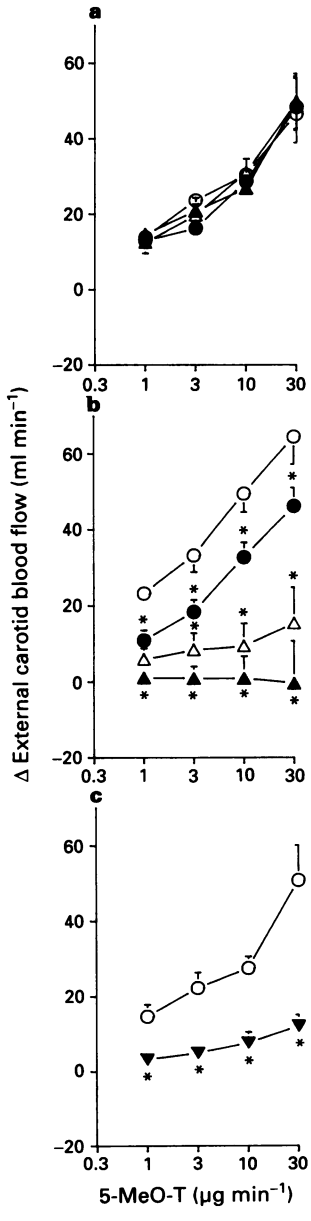

Figure 3 The effects of (a) physiological saline (○, 0 ml kg^{-1}; ●, 0.015 ml kg^{-1}; △, 0.05 ml kg^{-1} and ▲, 0.15 ml kg^{-1}; $n = 6$ each), (b) metergoline (○, 0 $\mu g\ kg^{-1}$; ●, 10 $\mu g\ kg^{-1}$; △, 30 $\mu g\ kg^{-1}$; and ▲, 100 $\mu g\ kg^{-1}$; $n = 6$ each) and (c) bilateral cervical vagosympathectomy (○, before and ▼, after; $n = 4$) on the increases in canine external carotid blood flow induced by 1 min i.c. infusions of 5-methoxytryptamine. $^*P < 0.05$ vs. control.

Discussion

The vasodilator effects of 5-HT on the canine external carotid bed are mediated by 5-HT$_1$-like receptors unrelated to the 5-HT$_{1A}$, 5-HT$_{1B}$ or 5-HT$_{1C}$ (now 5-HT$_{2C}$; Humphrey *et al.*, 1993) receptor subtypes, which mediate a prejunctional inhibitory action on carotid sympathetic nerves (Villalón *et al.*, 1993a,b; Terrón *et al.*, 1994). The present investigation extends these findings and suggests that, apart from the possible involvement of secondary (postjunctional) mechanisms, the prejunctional external carotid 5-HT$_1$-like receptors: (i) can be stimulated by the putative 5-HT$_{1D}$ receptor agonists, 5-methoxytryptamine and sumatriptan, the vasodilator effects of which are markedly inhibited after vagosympathectomy; and (ii) can be specifically antagonized by metergoline which, in addition to displaying a very high affinity for the 5-HT$_{1D}$ receptors (Waeber *et al.*, 1988), is able to block either the prejunctional (Charlton *et al.*, 1986) or postjunctional (Sumner *et al.*, 1989; Schoeffter & Hoyer, 1990; Sumner, 1991) effects of 5-HT and/or 5-CT in other vascular preparations.

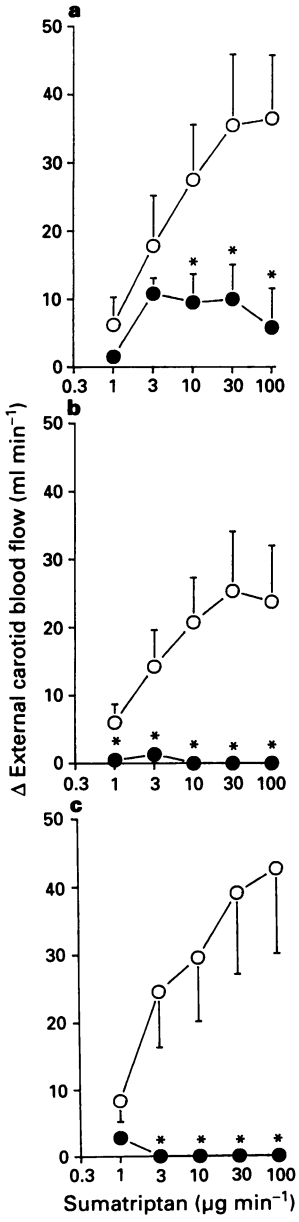

Figure 4 The effects of (a) physiological saline (○, 0 ml kg^{-1} and ●, 0.15 ml kg^{-1}; $n = 4$); (b) metergoline (○, 0 μg kg^{-1} and ●, 100 μg kg^{-1}; $n = 5$); and (c) bilateral cervical vagosympathectomy (○, before and ●, after; $n = 4$) on the increases in canine external carotid blood flow induced by 1 min i.c. infusions of sumatriptan. *$P < 0.05$ vs. control.

Systemic and carotid haemodynamic changes

It has already been shown that the administration of three sequential i.v. bolus injections of saline to the anaesthetized dog produces no substantial changes in either blood pressure, heart rate or external carotid blood flow over a period of about 140–180 min (Villalón *et al.*, 1993a). In the present study, baseline external carotid blood flow was not significantly modified after treatment with saline or metergoline, but was markedly increased after vagosympathectomy, in accordance with previous findings (Mena & Vidrio, 1979; Villalón *et al.*, 1993a,b). That the carotid sympathetic fibres exert a tonic influence in the external carotid bed is further strengthened by the fact that a more accurate indicator of vascular tone, the external carotid conductance, did increase significantly ($P < 0.05$) from 0.62 ± 0.06 to 0.92 ± 0.11 units ($n = 8$), as previously reported (Villalón *et al.*, 1993a).

Agonist action of 5-methoxytryptamine and sumatriptan on the 5-HT receptors mediating external carotid vasodilatation

In addition to recognizing the possible interference by pharmacokinetic factors in our experimental model, we could not, admittedly, reach the maximum effects with the 5-HT agonists used, as higher doses produced inconsistent vasodilator responses (see Experimental protocol). Notwithstanding, our study shows that, like 5-HT and 5-CT (Villalón *et al.*, 1993a; present results), both 5-methoxytryptamine and sumatriptan did increase the external carotid blood flow, although there were important differences in the effects of these drugs.

Accordingly, 5-methoxytryptamine behaved as a potent agonist (being about 0.5 log units less potent than 5-HT) and failed to attenuate the responses to 5-HT; moreover, no evidence of tachyphylaxis was observed since the responses to 5-methoxytryptamine remained unaffected after three consecutive i.v. injections of saline, as shown for 5-HT and 5-CT (Villalón *et al.*, 1993a).

In contrast, sumatriptan was the weakest vasodilator agonist and attenuated the vasodilator responses to 5-HT; this attenuation by sumatriptan (and/or any possible metabolite) is specific as the vasodilatation to acetylcholine, which acts on the vascular endothelium to produce vascular smooth muscle relaxation (Furchgott & Zawadzki, 1980), remained unaffected, thereby implying a common site of action in the effects of sumatriptan and 5-HT. Moreover, the biphasic responses produced by sumatriptan (i.e. external carotid vasodilatation followed by vasoconstriction) are consistent with either the inhibitory action of sumatriptan on the sympathetic nerves of the canine (Humphrey *et al.*, 1988) and human (Molderings *et al.*, 1990) saphenous vein or the vasoconstriction produced by this agonist in the dog common carotid circulation (Feniuk *et al.*, 1989; Perren *et al.*, 1991), responses that involve the activation of 5-HT$_1$-like receptors. Since sumatriptan produces endothelium-dependent relaxation in the coronary artery (Schoeffter & Hoyer, 1990), but not in the vena cava (Sumner, 1991) of the pig, it is difficult to judge to what extent, if any, the vasodilator effect of sumatriptan involves an endothelium dependent (or even a direct) component in our studies.

Antagonism of the vasodilator responses to the 5-HT agonists by metergoline

The blockade of the vasodilatation to 5-HT, 5-CT, 5-methoxytryptamine and sumatriptan by metergoline was specific and unrelated to changes in the baseline haemodynamic parameters. Notwithstanding, the profile of antagonism by

metergoline was different with each 5-HT agonist; thus, the fact that metergoline blocked the responses to 5-methoxytryptamine (Figure 3b) far more effectively than those to 5-CT (Figure 2) may reflect the higher affinity and/or efficacy of 5-CT for 5-HT_1 (including 5-HT_{1D}) binding sites and/or receptors (Hoyer, 1989; Saxena & Villalón, 1990). Indeed, the vasodilator response to 5-CT, and in some cases to 5-methoxytryptamine, remaining after metergoline may be prejunctional since it was abolished after vagosympathectomy (data not given), as shown in control animals (Villalón *et al.*, 1993a).

Role of sympathetic tone on the external carotid vasodilator effects of the 5-HT agonists

Although the vasodilator responses to 5-HT or 5-CT are specifically blocked by methiothepin, vagosympathectomy or sympatholytic drugs (Villalón *et al.*, 1993a; Terrón *et al.*, 1994), we have to recognize that the non-neurogenic vascular tone may also influence the vasodilatation produced by the 5-HT agonists, as suggested by the *inhibition* of 5-HT-induced external carotid vasodilatation by diazoxide (a direct vasodilator agent) in dogs with intact vagosympathetic trunks (Vidrio & Hong, 1976). Hence, it could be argued that the external carotid vasodilatation to 5-HT, 5-CT, 5-methoxytryptamine and sumatriptan was inhibited after vagosympathectomy since the carotid circulation was dilated by this procedure; this seems unlikely, nevertheless, as we have reported that the subsequent restoration of the vascular tone to the prevagosympathectomy level with exogenous noradrenaline did not revert the effects of 5-HT and 5-CT to vasodilatation, with the vasodilator response to acetylcholine remaining unaltered (Villalón *et al.*, 1993a).

Interestingly, both vagosympathectomy and metergoline ($100\,\mu g\,kg^{-1}$) had similar effects on the vasodilator responses to 5-HT and sumatriptan (Villalón *et al.*, 1993a; present results), namely: (i) the responses to both compounds were specifically *abolished*; (ii) a vasoconstrictor effect was unmasked in the case of 5-HT; and (iii) the vasoconstrictor component of the biphasic response to sumatriptan was magnified. Hence, it would seem that only when the vasodilator responses to 5-HT and sumatriptan have been abolished (by vagosympathectomy or metergoline), are their vasoconstrictor components made manifest and/or magnified; thus, if the vasodilator effects of 5-HT and sumatriptan have *postjunctional* (endothelium dependent and/or direct) vasodilator components, as suggested by the 5-methoxytryptamine-induced vasodilator response remaining after vagosympathectomy, they would be precluded by their vasoconstrictor response (absent in the case of 5-CT and 5-methoxytryptamine) which involves postjunctional 5-HT_1-like receptors (Villalón & Terrón, 1994). In line with this assumption, the vasodilator response to 5-methoxytryptamine may consist of a primary inhibitory prejunctional effect (sensitive to vagosympathectomy) which is apparently complemented by a small postjunctional component (resistant to vagosympathectomy), both of which seem to be blocked by metergoline. The above observations, besides being relevant to our notion that the 5-HT_1-like receptors mediating vasodilatation and vasoconstriction of the external carotid bed are heterogeneous (see below), lead us to suggest that, like 5-HT and 5-CT, both 5-methoxytryptamine and sumatriptan are acting prejunctionally, though no direct proof is provided.

Mechanisms involved in the external carotid vasodilator effects of 5-HT, 5-CT, 5-methoxytryptamine and sumatriptan

We have previously shown that 5-HT-, 5-CT- and indorenate-induced external carotid vasodilatation involves the activation of inhibitory prejunctional 5-HT_1-like receptors (Villalón *et al.*, 1993a,b). Several experimental observations, however, have led us to consider the possible participation of additional mechanisms in the external carotid vasodilator effects of 5-HT, 5-CT, 5-methoxytryptamine and sumatriptan. Thus, in addition to an inhibitory action on sympathetic nerves via prejunctional 5-HT_1-like receptors (Charlton *et al.*, 1986; Humphrey *et al.*, 1988; Bond *et al.*, 1989; Molderings *et al.*, 1990; Villalón *et al.*, 1993a,b), 5-HT and some of the above agonists have been shown to induce vasodilatation in other vascular preparations by direct (vascular; Sumner *et al.*, 1989) and indirect (endothelium-dependent; Schoeffter & Hoyer, 1990; Sumner, 1991) effects.

Considering the above information, our results showing the remaining, albeit negligible, vasodilator effect of 5-methoxytryptamine as well as the abolition of 5-HT-, 5-CT- and sumatriptan-induced vasodilator responses after vagosympathectomy, suggest that the former agonist may produce *postjunctional* responses (endothelium-dependent and/or directly on the vasculature); however, these postjunctional effects seem to play a minor, if any, role in the total external carotid vasodilator effect under study (see Figure 3c). Furthermore, the fact that the external carotid vasodilatation induced by sumatriptan was totally blocked by vagosympathectomy or metergoline and that sumatriptan *specifically* attenuated the vasodilator responses to 5-HT, as reported in the perfused rat kidney (Bond *et al.*, 1988), are in keeping with the suggestion that sumatriptan and 5-HT act on a common site of action, presumably, the prejunctional 5-HT_1-like receptors producing external carotid vasodilatation, although, as previously considered, postsynaptic mechanisms cannot be completely ruled out.

Additionally, it is to be remarked that our findings with metergoline, taken individually, cannot provide any evidence on the site of action, as it is capable of blocking either the prejunctional (Charlton *et al.*, 1986) or postjunctional (Sumner *et al.*, 1989; Shoeffter & Hoyer, 1990; Sumner, 1991) effects of 5-HT and/or 5-CT in other vascular preparations.

Taken together, the pharmacological profile displayed by each agonist, as well as the inhibitory effects of vagosympathectomy and metergoline, suggest that the *primary* mechanism involved in the vasodilatation produced by the 5-HT agonists used in the present study is the stimulation of inhibitory prejunctional 5-HT_1-like receptors located on carotid sympathetic nerves, as previously described (Villalón *et al.*, 1993a; Terrón *et al.*, 1994).

Possible resemblance of the inhibitory prejunctional 5-HT_1-like receptors mediating canine external carotid vasodilatation to the 5-HT_{1D} receptor subtype

In previous publications (Villalón *et al.*, 1993a,b; Terrón *et al.*, 1994) we showed that the increases in canine external carotid blood flow produced by 5-HT, 5-CT and indorenate are *not* mimicked by 8-hydroxy-2(di-n-propylamino)tetralin (8-OH-DPAT), buspirone, ipsapirone, 5-methoxy-3-[1,2,3,6-tetrahydro-4-pyridinyl]-1-*H*-indol succinate (RU 24969), 1-(2,5-dimethoxy-4-iodophenyl-)-aminopropane (DOI) or 2-methyl-5-HT. Since, in addition, the vasodilator responses to the above 5-HT receptor agonists are potently and specifically blocked by methiothepin (a 5-HT_1-like receptor antagonist) or vagosympathectomy, but not by drugs that act as antagonists at various receptors [5-HT_{1A} and/or 5-HT_{1B} (spiroxatrine, pindolol and/or cyanopindolol), 5-HT_{1C} and/or 5-HT_2 (ketanserin and/or ritanserin) and 5-HT_3 (MDL 72222)], it was concluded that 5-HT, 5-CT and indorenate increase external carotid blood flow in the dog via prejunctional 5-HT_1-like receptors unrelated to the 5-HT_{1A}, 5-HT_{1B} or 5-HT_{1C} (now 5-HT_{2C}) receptor subtypes (Villalón *et al.*, 1993a,b; Terrón *et al.*, 1994).

The present investigation showed that 5-CT, 5-methoxytryptamine and, to a lesser extent, sumatriptan mimic 5-HT and that low doses (10, 30 and $100\,\mu g\,kg^{-1}$) of metergoline antagonize their respective external carotid vasodilator responses. The high affinity of the above 5-HT agonists for

5-HT_{1D} binding sites (Hoyer, 1989; Peroutka & McCarthy, 1989; Schoeffter & Hoyer, 1989), coupled to the specific attenuation of the 5-HT-induced vasodilator responses by sumatriptan, raises the possibility that the 5-HT_1-like receptors involved in the increase in external carotid blood flow may correspond to the 5-HT_{1D} (or a similar) receptor subtype. Further evidence in support of this possibility is provided by the high antagonist activity of metergoline, a compound displaying the highest affinity for 5-HT_{1D} binding sites (Waeber *et al.*, 1988), against the increases in canine external carotid blood flow produced by 5-HT, 5-CT, 5-methoxytryptamine and sumatriptan; importantly, this blockade was specific since the same doses of metergoline did not modify acetylcholine-induced external carotid vasodilatation.

Although the involvement of inhibitory *prejunctional* 5-HT_{1D} receptors cannot be suggested merely on the antagonism by metergoline of the responses to 5-HT, 5-CT, 5-methoxytryptamine and sumatriptan, we feel that this assumption is strengthened when considering the evidence in its full context (Villalón *et al.*, 1993a,b; present results): (i) complete blockade and even reversal of 5-HT-induced external carotid vasodilatation by vagosympathectomy, methiothepin and metergoline, and resistance to blockade by antagonists at other (sub)types of 5-HT receptors; (ii) the rank order of agonist potency of 5-CT, 5-methoxytryptamine and sumatriptan, which are agonists at functional 5-HT_1-like receptors (Bradley *et al.*, 1986; Humphrey *et al.*, 1988; Feniuk *et al.*, 1989; Saxena & Villalón, 1990) and display high affinity for 5-HT_{1D} binding sites (Hoyer, 1989; Peroutka & McCarthy, 1989); but no effect by agonists at other (sub)types of 5-HT receptors; (iii) inhibition of the responses to 5-CT, 5-methoxytryptamine and sumatriptan by vagosympathectomy or metergoline, which is a potent antagonist at 5-HT_1-like and 5-HT_2 receptors (Saxena & Villalón, 1990) and displays a high affinity for 5-HT_{1D} binding sites (Waeber *et al.*, 1988). Hence, our findings suggest that the prejunctional 5-HT_1-like receptors producing external carotid vasodilatation are similar to the 5-HT_{1D} receptors identified on: (i) sympathetic nerves (Molderings *et al.*, 1990) and vascular smooth muscle (Bax *et al.*, 1992) of the human saphenous vein; and (ii) porcine coronary endothelium (Schoeffter & Hoyer, 1990).

The physiological relevance of a prejunctional inhibitory 5-HT_{1D} receptor in the canine external carotid bed is, to the best of our knowledge, unknown; one possibility exists, however. 5-HT has been shown to be taken-up into and released from sympathetic nerves (see Saxena & Villalón, 1990), and may act, therefore, as a modulator of the neuroeffector transmission; thus, feed-back inhibition of noradrenaline release by 5-HT may be involved, as described for other substances (Rand *et al.*, 1987).

In conclusion, we suggest that the inhibitory prejunctional 5-HT_1-like receptors involved in the primary mechanism mediating external carotid vasodilatation in the dog closely resemble the 5-HT_{1D} receptor subtype. The pharmacological profile of these receptors is similar (sympathetic nerves of the rat kidney and human saphenous vein, as well as porcine coronary endothelium) to other putative 5-HT_{1D} receptors mediating vascular responses. We also acknowledge that the external carotid vasodilatation produced by the 5-HT agonists apparently involves a secondary – though negligible – component at the postsynaptic level.

In connection with the above conclusion, it should be considered that the 5-HT_{1D} receptor represents a heterogeneous subfamily that is comprised of at least two populations, namely one that recognizes sumatriptan and has high affinity for 5-CT, and another that shows little affinity for either sumatriptan or 5-CT (Sumner & Humphrey, 1989; Humphrey *et al.*, 1993). One might further speculate that the high affinity site for sumatriptan and 5-CT might be equivalent to the inhibitory prejunctional 5-HT_{1D}-like receptors that mediate canine external carotid vasodilatation. Undoubtedly, the use of non-selective drugs complicates analysis of the subtypes involved, and progress will be critically dependent upon the discovery of new pharmacological probes which are endowed with high selectivity and potency.

In this regard, it is pertinent to note that methiothepin did completely antagonize the external carotid vasodilator effects of 5-HT and 5-CT at a dose of 30 $\mu g\,kg^{-1}$ (i.v.) (Villalón *et al.*, 1993a); this dose of methiothepin is 0.5 log units lower than the dose of metergoline (100 $\mu g\,kg^{-1}$; i.v.) used in the present study to produce the same effect. Therefore, the need for higher doses of metergoline to produce antagonism in the canine external carotid bed (Figures 2–4) would imply a lower affinity of metergoline for 5-HT_{1D} binding sites; an important discrepancy in this respect is that metergoline ($pK_D = 9.1$) displays higher affinity than methiothepin ($pK_D = 6.3$) for 5-HT_{1D} binding sites (Hoyer, 1989). Nevertheless, two important findings should be considered to explain the above discrepancy. Firstly, methiothepin, but not metergoline, displays very high affinity for α_1-adrenoceptor binding sites (Leysen, 1985); thus, methiothepin, but not metergoline, potently antagonized the external carotid vasoconstrictor responses to the α_1-adrenoceptor agonist, phenylephrine, in dogs pretreated with rauwolscine (Villalón *et al.*, unpublished). Secondly, 5-HT-induced external carotid vasodilatation is inhibited by drugs that decrease the sympathetic outflow, including α_1-adrenoceptor antagonists (Terrón *et al.*, 1994). Accordingly, methiothepin is more potent than metergoline because the former produces blockade of postsynaptic α_1-adrenoceptors. Thus, the higher antagonist potency of methiothepin should not exclude the participation of 5-HT_{1D} receptors.

The technical assistance of Mr Arturo Contreras is gratefully acknowledged. We thank Consejo Nacional de Ciencia y Tecnología (Mexico City, Mexico) for support of this work. 5-Carboxamidotryptamine maleate and sumatriptan succinate as well as metergoline were generous gifts from Glaxo Group Research (Ware, England) and Farmitalia (Milan, Italy), respectively.

References

BAX, W.A., VAN HEUVEN-NOLSEN, D., BOS, E., SIMOONS, M.L. & SAXENA, P.R. (1992). 5-Hydroxytryptamine-induced contractions of the human isolated saphenous vein: involvement of 5-HT_2 and 5-HT_{1D}-like receptors, and a comparison with grafted veins. *Naunyn-Schmied. Arch. Pharmacol.*, **345**, 500–508.

BOND, R.A., CRAIG, D.A., CHARLTON, K.G., ORNSTEIN, A.G. & CLARKE, D.E (1988). Partial agonistic activity of GR43175 at the inhibitory prejunctional 5-HT_1-like receptor in rat kidney. *J. Auton. Pharmacol.*, **9**, 201–210.

BRADLEY, P.B., ENGEL, G., FENIUK, W., FOZARD, J.R., HUMPHREY, P.P.A., MIDDLEMISS, D.N., MYLECHARANE, E.J., RICHARDSON, B.P. & SAXENA, P.R. (1986). Proposals for the classification and nomenclature of functional receptors for 5-hydroxytryptamine. *Neuropharmacology*, **25**, 563–576.

CHARLTON, K.G., BOND, B.A. & CLARKE, D.E. (1986). An inhibitory prejunctional 5-HT_1-like receptor in the isolated perfused rat kidney. *Naunyn-Schmied. Arch. Pharmacol.*, **332**, 8–15.

DEN BOER, M.O., VILLALÓN, C.M. & SAXENA, P.R. (1992). 5-HT_1-like receptor mediated changes in porcine carotid haemodynamics: are 5-HT_{1D} receptors involved? *Naunyn-Schmied. Arch. Pharmacol.*, **345**, 509–515.

FENIUK, W., HUMPHREY, P.P.A. & PERREN, M.J. (1989). The selective carotid arterial vasoconstrictor action of GR43175 in anaesthetized dogs. *Br. J. Pharmacol.*, **96**, 83–90.

FURCHGOTT, R.F. & ZAWADZKI, J.V. (1980). The obligatory role of endothelial cells in the relaxation of arterial smooth muscle by acetylcholine. *Nature*, **288**, 373–376.

HOYER, D. (1989). 5-Hydroxytryptamine receptors and effector coupling mechanisms in peripheral tissues. In *The Peripheral Actions of 5-Hydroxytryptamine*. ed. Fozard, J.R. pp. 73–99. Oxford: Oxford University Press.

HUMPHREY, P.P.A., FENIUK, W., PERREN, M.J., CONNOR, H.E., OXFORD, A.W., COATES, I.H. & BUTINA, D. (1988). GR 43175, a selective agonist for the 5-HT_1-like receptor in dog isolated saphenous vein. *Br. J. Pharmacol.*, **94**, 1123–1132.

HUMPHREY, P.P.A., HARTIG, P. & HOYER, D. (1993). A proposed new nomenclature for 5-HT receptors. *Trends Pharmacol. Sci.*, **14**, 233–236.

LEYSEN, J.E. (1985). Serotonin binding sites. In *Serotonin and the Cardiovascular System*. ed. Vanhoutte, P.M. pp. 43–62. New York: Raven Press.

MENA, M.A. & VIDRIO, H. (1979). Reversal of serotonin vasodilatation in the dog external carotid bed by sympathetic denervation. *J. Cardiovasc. Pharmacol.*, **1**, 149–154.

MOLDERINGS, G.J., WERNER, K., LIKUNGU, J. & GÖTHERT, M. (1990). Inhibition of noradrenaline release from the sympathetic nerves of the human saphenous vein via presynaptic 5-HT receptors similar to the 5-HT_{1D} subtype. *Naunyn-Schmied. Arch. Pharmacol.*, **42**, 371–377.2.

PEROUTKA, S.J. & MCCARTHY, B.G. (1989). Sumatriptan interacts selectively with 5-HT_{1B} and 5-HT_{1D} binding sites. *Eur. J. Pharmacol.*, **163**, 133–136.

PERREN, M.J., FENIUK, W. & HUMPHREY, P.P.A. (1991). Vascular 5-HT_1-like receptors that mediate contraction of the dog isolated saphenous vein and carotid arterial vasoconstriction in anaesthetized dogs are not of the 5-HT_{1A} or 5-HT_{1D} subtype. *Br. J. Pharmacol.*, **102**, 191–197.

RAND, M.J., MAJEWSKI, H., WONG-DUSTING, H., STORY, D.F., LOIACONO, R.E. & ZIOGAS, J. (1987). Modulation of neuroeffector transmission. *J. Cardiovasc. Pharmacol.*, **10** (Suppl. 12), S33–S44.

SAXENA, P.R. & VILLALÓN, C.M. (1990). Cardiovascular effects of serotonin agonists and antagonists. *J. Cardiovasc. Pharmacol.*, **15** (Suppl. 7), S17–S34.

SCHOEFFTER, P. & HOYER, D. (1989). How selective is GR 43175? Interactions with functional 5-HT_{1A}, 5-HT_{1B}, 5-HT_{1C} and 5-HT_{1D} receptors. *Naunyn-Schmied. Arch. Pharmacol.*, **340**, 135–138.

SCHOEFFTER, P. & HOYER, D. (1990). 5-Hydroxytryptamine (5-HT)-induced endothelium-dependent relaxation of pig coronary arteries is mediated by 5-HT receptors similar to the 5-HT_{1D} receptor subtype. *J. Pharmacol. Exp. Ther.*, **252**, 387–395.

STEEL, R.G.D. & TORRIE, J.H. (1980). *Principles and Procedures of Statistics, A Biomedical Approach*, 2nd edn, Tokyo: McGraw-Hill Kogakusha, Ltd.

SUMNER, M.J. (1991). Characterization of the 5-HT receptor mediating endothelium-dependent relaxation in porcine vena cava. *Br. J. Pharmacol.*, **102**, 938–942.

SUMNER, M.J. & HUMPHREY, P.P.A. (1989). 5-HT_{1D} binding sites in porcine brain can be sub-divided by GR43175. *Br. J. Pharmacol.*, **98**, 29–31.

SUMNER, M.J., FENIUK, W. & HUMPHREY, P.P.A. (1989). Further characterization of the 5-HT receptor mediating vascular relaxation and elevation of cyclic AMP in porcine isolated vena cava. *Br. J. Pharmacol.*, **97**, 292–300.

TERRÓN, J.A., HONG, E., LÓPEZ-MUÑOZ, F.J. & VILLALÓN, C.M. (1994). Inhibition of serotonin-induced increase in canine external carotid blood flow by drugs that decrease the sympathetic outflow. *J. Auton. Pharmacol.*, **14**, 165–175.

VIDRIO, H. & HONG, E. (1976). Vascular tone and reactivity to serotonin in the internal and external carotid vascular beds of the dog. *J. Pharmacol. Exp. Ther.*, **197**, 49–56.

VILLALÓN, C.M. & SAXENA, P.R. (1992). Classification of 5-HT receptors. In *Headache and Migraine*. ed. Hogenhuis, L.A.H. & Steiner, T.J. pp. 31–52. Utrecht: Wetenschappelijke uitgeverij Bunge.

VILLALÓN, C.M. & TERRÓN, J.A. (1994). 5-HT_1-like receptors and a novel receptor mediate 5-HT-induced decreases of the canine external carotid blood flow. *Br. J. Pharmacol.*, **112**, 107P.

VILLALÓN, C.M., TERRÓN, J.A. & HONG, E. (1993a). Role of 5-HT_1-like receptors in the increase in external carotid blood flow induced by 5-hydroxytryptamine in the dog. *Eur. J. Pharmacol.*, **240**, 9–20.

VILLALÓN, C.M., TERRÓN, J.A. & HONG, E. (1993b). Further characterization of the 5-HT_1-like receptors mediating the increase in external carotid blood flow in the dog. *Drug Develop. Res.*, **29**, 271–281.

VILLALÓN, C.M., TERRÓN, J.A. & HONG, E. (1993c). Role of 5-HT_{1D}-like receptors in the increase in external carotid blood flow induced by 5-hydroxytryptamine in the dog. *Proceedings of the 1993 Meeting of the Western Pharmacology Society*, Incline Village, Nevada, January 31–February 5, 1993. Abstract No. 24.

WAEBER, C., SCHOEFFTER, P., PALACIOS, J.M. & HOYER, D. (1988). Molecular pharmacology of 5-HT_{1D} recognition sites: radioligand binding studies in human, pig and calf brain membranes. *Naunyn-Schmied. Arch. Pharmacol.*, **337**, 595–601.

(Received December 21, 1993
Revised April 26, 1994
Accepted April 27, 1994)

Br. J. Pharmacol. (1994), **113**, 21–28

Loss of contractile activity of endothelin-1 induced by electrical field stimulation-generated free radicals

Nobuyuki Yasuda, [1]Yoshitoshi Kasuya, Goro Yamada, Hiroshi Hama, *Tomoh Masaki & Katsutoshi Goto

Department of Pharmacology, Institute of Basic Medical Sciences, University of Tsukuba, Tsukuba, Ibaraki 305, Japan and *Department of Pharmacology, Kyoto University Faculty of Medicine, Kyoto 606, Japan

1 Electrical field stimulation (EFS; 10 V, 10 Hz, 2 ms) of porcine coronary artery strips precontracted with 10 nM endothelin-1 (ET-1) for 5 min caused a biphasic response, consisting of a slight contraction during EFS and a marked and irreversible relaxation just after EFS. This irreversible relaxation after EFS has never been investigated. In the present study, we have investigated the mechanism of the relaxation after EFS.

2 The EFS-induced response was not affected by the presence or absence of endothelium and was insensitive to 10 μM tetrodotoxin (TTX).

3 In the presence of free radical scavengers (40 u ml^{-1} superoxide dismutase (SOD), 1200 u ml^{-1} catalase or 80 mM D-mannitol), the relaxation after EFS was significantly inhibited. Moreover, relaxation after EFS was not observed in porcine coronary artery strips precontracted with 20 mM KCl.

4 In a cascade experiment, EFS of Krebs-Ringer solution containing 10 nM ET-1 induced marked suppression of the contractile activity of ET-1 in porcine coronary artery strips, which was in accord with the observed decrease in release of immunoreactive ET-1 (ir-ET-1). This effect of EFS was significantly inhibited by each of the free radical scavengers, 3 mM vitamin C, 40 u ml^{-1} SOD, 1200 u ml^{-1} catalase and 80 mM D-mannitol.

5 The exchange of 95% O_2/5% CO_2 gas for 95% N_2/5% CO_2 gas significantly inhibited the EFS-induced decrease in release of ir-ET-1.

6 Neither superoxide anions generated by xanthine (10 μM) plus xanthine oxidase (0.1 u ml^{-1}) nor hydrogen peroxide (10 μM) exogenously added to Krebs-Ringer solution containing 10 nM ET-1 affected the level of ir-ET-1.

7 Generation of hydroxyl radicals was detected in the EFS-applied Krebs-Ringer solution. The EFS-induced generation of hydroxyl radicals was dependent on the period of stimulation and O_2-bubbling, and significant generation of hydroxyl radicals was detectable with stimulation of over 5 min. Moreover, hydroxyl radicals generated in 50 mM NaCl solution containing 10 nM ET-1 by H_2O_2 plus Fe^{2+}, i.e. the Fenton reaction, significantly decreased the level of ir-ET-1.

8 These findings suggest that oxygen-derived hydroxyl radicals generated by EFS of porcine coronary artery strips inactivate ET-1, probably by structural modification. Thus, porcine coronary artery strips precontracted with ET-1 are potently relaxed by EFS.

Keywords: Coronery artery; endothelin-1; electrical field stimulation; hydroxyl radicals

Introduction

Relaxation of various isolated blood vessels from different species in response to electrical field stimulation (EFS) has been described. Such relaxations are generally thought to be caused either by the activation of postjunctional β-adrenoceptors secondary to release of catecholamines from adrenergic nerve endings (Cohen *et al.*, 1983) or by the release of vasorelaxant substances from noradrenergic and noncholinergic nerves (McCulloch & Edvinsson, 1980; Toda, 1982; Fujimori *et al.*, 1989; Verma *et al.*, 1993) or from the endothelium (Buga & Ignarro, 1992; Van Riper & Bevan, 1992). However, EFS-induced responses in isolated blood vessels show wide variation, depending on the segment of artery, species and stimulation conditions (Rooke *et al.*, 1982; Feletou & Vanhoutte, 1989). Some investigators have recently demonstrated that the production of oxygen-derived free radicals by EFS could provoke vasodilator responses (Lamb & Webb, 1984; Greenberg *et al.*, 1986). Especially, prolonged EFS generates enough oxygen-derived free radicals to produce a change in tone of vascular smooth muscle (Feletou & Vanhoutte, 1987).

Endothelin (ET-1) provokes a strong and sustained contraction in various isolated vascular smooth muscle preparations through the stimulation of ET_A receptor (Kasuya *et al.*, 1992; Sakurai *et al.*, 1992). Thus, ET-1 is a suitable tool to investigate the EFS-induced vasorelaxant response.

In preliminary experiments, we investigated the response of porcine coronary artery strips precontracted with 10 nM ET-1 to prolonged EFS, and observed a marked and irreversible relaxation after EFS. Such relaxations has never been investigated. Thus, the present study was designed to elucidate the mechanism of post-EFS relexation in porcine coronary artery strips.

Methods

Measurement of contraction of arterial strips

Right coronary arteries were isolated from fresh adult porcine hearts obtained from a local slaughterhouse. Arterial segments were cut into 2 × 7 mm helical strips, endothelial cells were removed by rubbing the intimal surface with a cotton swab and the segments were suspended in 20-ml siliconized glass organ chambers filled with Krebs-Ringer solution of the following composition (mM): NaCl 113, KCl

[1] Author for correspondence.

4.8, $CaCl_2$ 2.2, KH_2PO_4 1.2, $MgCl_2$ 1.2, $NaHCO_3$ 25 and glucose 5.5. Depending on the segment used, EFS induced different responses. Thus, we used coronary artery segments restricted to within 2 to 4 cm from the aorta. The solution was maintained at 37°C and gassed with 95% O_2/5% CO_2. Arterial strips were equilibrated at a passive tension of 1.25 g until the contractile tension induced by 50 mM KCl attained a steady state. Isometric contraction was measured by means of a force displacement transducer (Nihon Koden TB-612T) as previously described (Kasuya *et al.*, 1989). In some experiments, artery strips with intact endothelium which showed greater than 75% inhibition of precontraction with prostaglandin $F_{2\alpha}$ ($PGF_{2\alpha}$, 2 μM) in response to ionomycin (10 nM) were used.

Electrical field stimulation

Electrical field stimulation (EFS) was delivered via two parallel platinum electrodes placed 3 mm apart along both sides of the whole length of the strip. The platinum electrodes were connected to a current amplifier and stimulator (Nihon Koden, SEN-7103). EFS was conducted at 10 V at a frequency of 10 Hz in the form of square wave pulses of 2 ms duration. In most experiments, EFS was applied to the strips for a period of 5 min. These parameters for EFS were selected to obtain reproducible responses by conducting preliminary experiments on the frequency-response and voltage-response relationships etc. Stimulation parameters were measured by displaying the pulse wave on an oscilloscope through a small resistor connected in series (Iwatsu, 01445243). TTX and various free radical scavengers were added into the organ bath 15 min before contracting the strips with ET-1.

Cascade experiment

Two organ baths were set up in series. In the upper bath, EFS was applied to Krebs-Ringer solution containing vasoconstrictors (e.g. ET-1) in the absence of the strips. After EFS, the solution in the upper bath was applied to the coronary artery strips in exchange for the surrounding solution in the lower bath, and contractile activity was estimated. As it took about 30 s to exchange the solution, free radicals generated in the upper bath were reduced and thus did not directly affect the coronary artery strips in the lower bath. Thereafter, appropriate free radical scavengers were added to the upper bath prior to EFS and similar cascade experiments were conducted to assess their effect.

Enzyme-linked immunoassay (EIA) of ET-1

According to the procedure previously described (Suzuki *et al.*, 1989), the immunoreactive endothelin-1 (ir-ET-1) level in the bathing solution (normally Krebs-Ringer solution) was determined by sandwich-EIA. A monoclonal anti-endothelin antibody, AwETN 40, which detects the N-terminal portion of ET-1 was used as the immobilized antibody. The Fab' fragment of rabbit antibodies against endothelin C-terminal heptapeptide (15-21) was used as an enzyme-labelled detector antibody after being coupled with horseradish peroxidase (HRP). AwETN40-coated microtiter wells (98 well, NUNC, Denmark) were prepared by adding 20 μg ml^{-1} (100 μl) AwETN40 to each well, followed by 300 μl Block Ace (Snow Brand Milk Products Co., Japan) diluted 4 fold with PBS. Endothelin-1 at various standard concentrations or a 10 μl sample taken from the bathing solutions dissolved in 100 μl buffer D (0.02 M phosphate buffer, pH 7, containing 10% Block Ace, 0.4 M NaCl, and 2 mM EDTA) was added to each well and incubated at room temperature for 1 day. After being washed with PBS, the plate was reacted with 100 μl anti-endothelin (15-21) Fab'-HRP at a dilution of 1/400 in buffer C (0.02 M phosphate buffer, pH 7, containing 1% bovine serum albumin (BSA), 0.4 M NaCl, and 2 mM EDTA) at 4°C for 16 h. After being washed with PBS, the bound enzyme activity was measured using *o*-phenylenediamine as a chromogen at 492 nm.

Generation and measurement of superoxide anions

According to the procedure previously described (Beauchamp & Fridovich, 1971), the accumulation of blue formazan in accordance with reduction of nitro blue tetrazolium (NBT) at 560 nm was taken as an index of superoxide anion production. The reaction was started by addition of 10 μM xanthine and 0.1 u ml^{-1} xanthine oxidase to a bath filled with Krebs-Ringer solution containing 25 μM NBT maintained at 37°C in the absence of the strips. After 20 min, 3.5 ml of the solution was subjected to spectrum determination with a Hitachi spectrophotometer (model DU-7).

Measurement of hydroxyl radicals

p-Nitrosodimethylaniline (*p*-NMA) was used as an effective scavenger of hydroxyl radicals (Minotti & Aust, 1987), and was bleached at 440 nm in proportion to the generation of hydroxyl radicals (Bors *et al.*, 1979). EFS (10 V, 10 Hz, 2 ms) was applied to Krebs-Ringer solution containing 10 μM *p*-NMA maintained at 37°C for various periods (0, 3, 5, 10 min), and 3.5 ml of each solution with a different incubation period was subjected to spectrum determination with a Hitachi spectrophotometer (model DU-7).

Effect of hydroxyl radicals on ir-ET-1

According to the procedure previously described (Minotti & Aust, 1987), 0.1 mM H_2O_2 and 0.2 mM $FeSO_4$ were added to a bath filled with 50 mM NaCl solution containing 10 μM *p*-NMA maintained at 37°C. The generation of hydroxyl radicals following 5 min reaction was detected by assay of *p*-NMA. Thus, 10 nM ET-1 was added to a bath filled with 50 mM NaCl solution containing 10 mM *p*-NMA just before applying 0.1 mM H_2O_2 and 0.2 mM $FeSO_4$, and 100 μl of the solution was subjected to determination of ir-ET-1 by EIA after 5 min.

Drugs

The following drugs were used: *p*-nitrosodimethylaniline, prostaglandin $F_{2\alpha}$ tromethamine, nitro blue tetrazolium, superoxide dismutase, xanthine, tetrodotoxin (TTX), catalase, D-mannitol, sodium-L-ascorbate (vitamin C) and deferoxamine (Wako Pure Chemicals, Osaka, Japan). Xanthine oxidase was from Boehringer Mannheim Yamanouchi (Tokyo, Japan). Endothelin-1 was from the Peptide Institute (Osaka, Japan). Arg^8-vasopressin and angiotensin II were from Sigma Chemical Co., Ltd (St. Louis, MO, U.S.A.).

Statistical analysis

Values are expressed as mean ± s.e. Comparisons were made by one way analysis of variance (ANOVA) followed by Bonferroni correction or Student's *t* test for unpaired values. Differences with *P* values less than 0.05 were considered statistically significant.

Results

Response to EFS

EFS (10 V, 10 Hz, 2 ms, 5 min) caused a biphasic response in porcine coronary artery strips precontracted with 10 nM ET-1, consisting of a slight contraction followed by a marked and irreversible relaxation (Figure 1a). The response induced by EFS was not affected by the presence or absence of endothelium, and was insensitive to 10 μM TTX (Figure 1b,c).

However, each free radical scavenger, 40 u ml^{-1} superoxide dismutase (SOD), 1200 u ml^{-1} catalase and 80 mM D-mannitol, significantly inhibited the relaxation after EFS (Figure 1d,e,f). Furthermore, relaxation after EFS was not observed in porcine coronary artery strips precontracted with 20 mM KCl (Figure 1g).

Effect of EFS on contractile activity and structure of ET-1

To confirm whether free radicals affect coronary artery strips indirectly, i.e., through modification of ET-1, we investigated the effect of EFS on the contractile activity of ET-1 in cascade experiments. As shown in Figure 2, EFS of Krebs-Ringer solution containing 10 nM ET-1 induced marked suppression of the contractile activity of ET-1 in coronary artery strips, although control Krebs–Ringer solution containing 10 nM ET-1 without EFS induced significant contraction. This apparent effect of EFS was significantly inhibited by each of the free radical scavengers, vitamin C (3 mM), SOD (40 u ml^{-1}), catalase (1200 u ml^{-1}) and D-mannitol (80 mM).

To determine whether the suppression of contractile activity of ET-1 in cascade experiments is associated with a change in the structure of the ET-1 molecule, we measured the concentration of immunoreactive ET-1 (ir-ET-1) in the lower bath by the sandwich EIA method as described in Methods. As shown in Figure 3, after EFS of Krebs-Ringer solution containing 10 nM ET-1, the release of ir-ET-1 in the lower bath was reduced to below the detection limit of EIA.

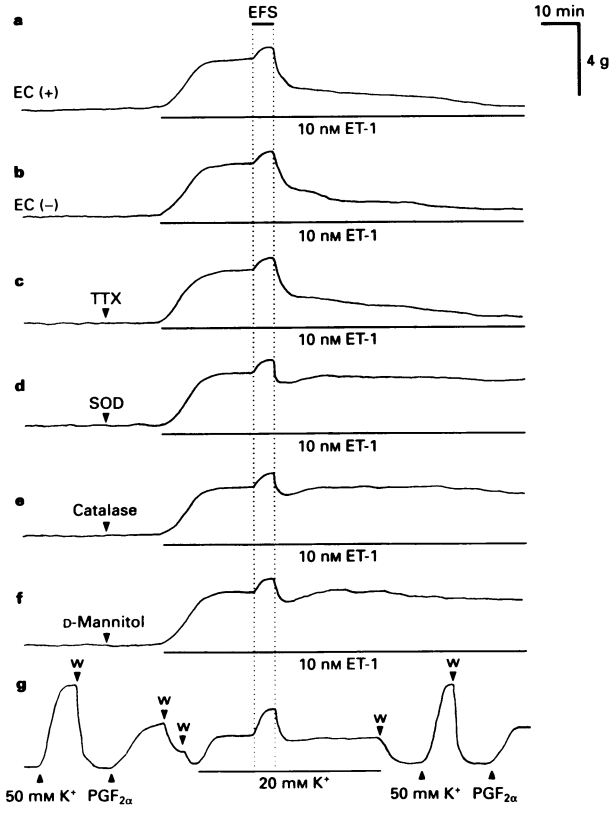

Figure 1 Responses of porcine coronary artery strips precontracted with endothelin-1 (ET-1) or KCl to prolonged EFS (10 V, 10 Hz, 2 ms). EFS was applied to porcine coronary artery strips, with or without endothelium precontracted with 10 nM ET-1 (a,b). The EFS-induced response was not affected by the presence or absence of endothelium. Therefore, porcine coronary artery strips without endothelium were used in the following experiments. EFS was applied to porcine coronary artery strips precontracted with 10 nM ET-1 in the presence of 10 μM tetrodotoxin (TTX) (c) or each radical scavenger (d, 40 u ml^{-1} superoxide dismutase (SOD); e, 1200 u ml^{-1} catalase or f, 80 mM D-mannitol). EFS was applied to porcine coronary artery strips precontracted with 20 mM K^+ (g).

However, the loss of release of ir-ET-1 was significantly inhibited by each free radical scavenger (3 mM vitamin C, 40 u ml^{-1} SOD, 1200 u ml^{-1} catalase and 80 mM D-mannitol).

Measurement of free radicals generated by EFS

To verify the origin of free radicals, we replaced the gas aerating the bath with 95% N_2/5% CO_2 gas to generate a

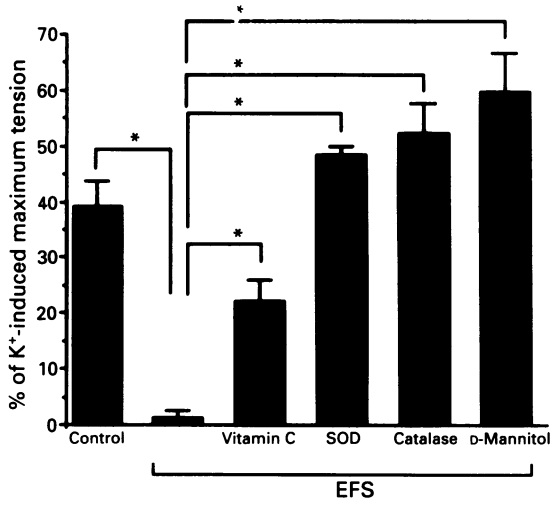

Figure 2 Effect of prolonged EFS on contractile activity of endothelin-1 (ET-1). EFS (10 V, 10 Hz, 2 ms) was applied to Krebs-Ringer solution in the absence or presence of each radical scavenger superoxide-dismutase (SOD (40 u ml^{-1}), vitamin C (3 mM), catalase (1200 u ml^{-1}) or D-mannitol (80 mM)) added just after the addition of 10 nM ET-1. Then, each solution was applied to porcine coronary artery strips. As a control, 10 nM ET-1 was added to Krebs-Ringer solution and left for 5 min without being subjected to EFS, and then the solution was applied to porcine coronary artery strips. The contractile response of porcine coronary artery strips is expressed as a percentage of the maximum tension induced by 50 mM KCl. Mean values ± s.e. ($n = 4–5$) are shown. *Significantly different from values with EFS-applied ET-1 ($P < 0.05$, ANOVA with Bonferoni correction).

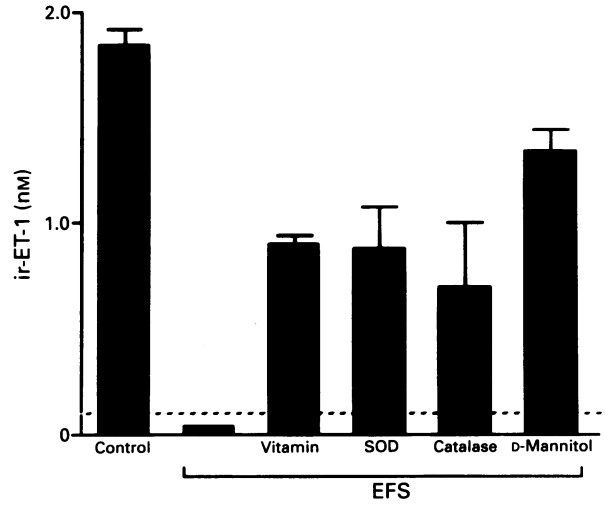

Figure 3 Effect of prolonged EFS on immunoreactive endothelin-1 (ir-ET-1). EFS (10 V, 10 Hz, 2 ms, 5 min) was applied to Krebs-Ringer solution in the absence or presence of each free radical scavenger superoxide-dismutase (SOD (40 u ml^{-1}), vitamin C (3 mM), catalase (1200 u ml^{-1}) or D-mannitol (80 mM)) which was added just after the addition of 10 nM ET-1. Then, ir-ET-1 in each solution was measured by EIA. As a control, 10 nM ET-1 was added to Krebs-Ringer solution, and the solution was subjected to EIA after 5 min. Mean values ± s.e. ($n = 4–6$) are shown. The dotted line represents the limit of detection by EIA.

hypoxic condition. As shown in Figure 4, the EFS-induced loss of release of ir-ET-1 was completely inhibited by hypoxic condition, indicating that oxygen-derived free radicals were generated in the bath by the EFS. To confirm radical species leading to the suppression of contractile activity of ET-1, we investigated the effect of oxygen-derived free radicals, chemically generated or exogenously added, on ir-ET-1. We first investigated the effect of superoxide anions generated by 10 mM xanthine plus 0.1 u ml^{-1} xanthine oxidase on ir-ET-1. As shown in Figure 5a, ir-ET-1 did not alter despite significant generation of superoxide anions in the bath. Secondly, the effect of hydrogen peroxide on ir-ET-1 was examined. As shown in Figure 5b, hydrogen peroxide (1 or 10 μM) did not affect ir-ET-1. We finally investigated the participation of hydroxyl radicals in the suppression of contractile activity of ET-1. As shown in Figure 6, EFS-induced generation of hydroxyl radicals was detected by *p*-NMA assay, and was dependent on the period of stimulation and O_2-bubbling. Significant generation of hydroxyl radicals was detected where EFS was delivered for more than 5 min. Moreover, hydroxyl radicals generated by 0.1 mM H_2O_2 plus 0.2 mM $FeSO_4$ (Fenton reaction, Freeman & Carpo, 1982) decreased ir-ET-1, and this decrease was significantly inhibited by 10^{-4} M deferoxamine, a ferrous chelator, and 1200 u ml^{-1} catalase (Figure 7).

Effect of EFS on contractile activities of other vasoactive agents

To investigate whether prolonged EFS induces suppression of the contractile activity of other vasoactive agents or not, we studied the effect of EFS on the contractile activities of the vasoactive agents, arginine[8]-vasopressin (AVP) and angiotensin-II (AII), since each is a peptide vasonconstrictor like ET-1, and $PGF_{2\alpha}$ which is frequently used for the investigation of EFS-induced relaxation of blood vessels (Rooke *et al.*, 1982; Cohen *et al.*, 1983; Feletou & Vanhoutte, 1989). After applying EFS to Krebs-Ringer solution containing each vasoconstrictor (1 μM AVP, 1 μM AII and 2 μM $PGF_{2\alpha}$), the contractile activity of each vasoconstrictor was investigated on porcine coronary artery strips for $PGF_{2\alpha}$ and rat aorta strips for AVP and AII. As shown in Figure 8a, the contractile activities of AII and AVP were not significantly different before and after EFS, although the contractile activity of $PGF_{2\alpha}$ was suppressed by EFS. This apparent effect of EFS on the contractile activity of $PGF_{2\alpha}$ was significantly

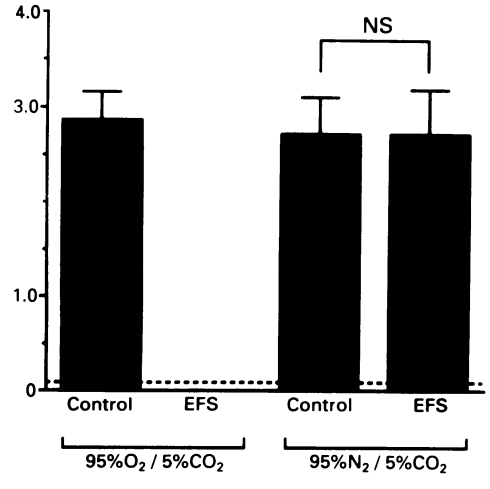

Figure 4 Effect of hypoxic condition on EFS-induced decrease of immunoreactive endothelin-1 (ir-ET-1). EFS (10 V, 10 Hz, 2 ms, 5 min) was applied to Krebs-Ringer solution during bubbling with 95% N_2/5% CO_2 or 95% O_2/5% CO_2 just after addition of 10 nM ET-1. Then, ir-ET-1 in each solution was measured by EIA. As a control, 10 nM ET-1 was added to Krebs-Ringer solution being bubbled with 95% N_2/5% CO_2 or 95% O_2/5% CO_2, and each solution was subjected to EIA after 5 min. The dotted line represents the limit of detection by EIA. Mean values ± s.e. ($n = 4-7$) are shown. NS, not significantly different (Student's *t* test for unpaired values).

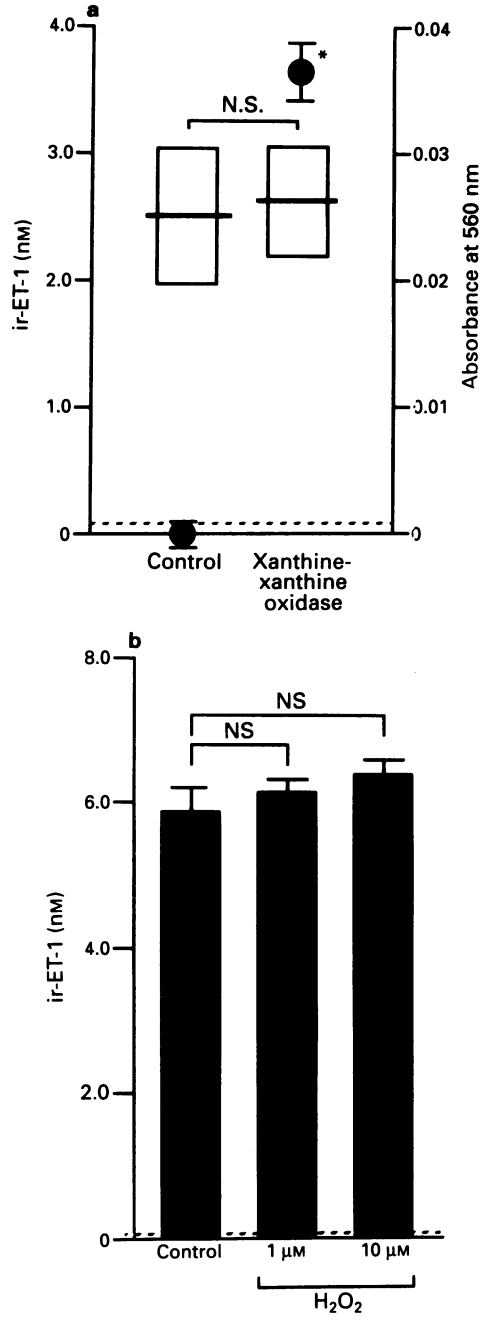

Figure 5 (a) Generation of superoxide anions by xanthine plus xanthine oxidase and its effect on immunoreactive endothelin-1 (ir-ET-1). ET-1 10 nM, xanthine 10 μM and xanthine oxidase 0.1 u ml^{-1} were added to Krebs-Ringer solution containing NBT 25 μM, and the solution was subjected to NBT assay and EIA after 20 min. As a control, 10 nM ET-1 was added to Krebs-Ringer solution containing 25 μM NBT, and the solution was subjected to NBT assay and EIA after 20 min. Histograms represent mean ± s.e. of ir-ET-1 ($n = 3$). Closed circles and bars represent mean ± s.e. of absorbance of blue formazane at 560 nm ($n = 3$). (b) Effect of incubation with H_2O_2 on ir-ET-1: 10 nM ET-1 was added to Krebs-Ringer solution containing 1 μM or 10 μM H_2O_2, and each solution was subjected to EIA after 20 min. As a control, 10 nM ET-1 was added to Krebs-Ringer solution and left for 20 min, and the solution was subjected to EIA. Mean values ± s.e. ($n = 6$). The dotted line represents the limit of detection by EIA. *Significantly different from control value with $P < 0.05$; NS, not significantly different (Student's *t* test for unpaired values).

inhibited by the free radical scavengers, 3 mM vitamin C and 40 u ml^{-1} SOD (Figure 8b).

Effect of O_2-bubbling on structure of ET-1

To investigate whether ET-1 is chemically modified by O_2 bubbling alone, were measured ir-ET-1 by sandwich EIA after incubating 10 nM ET-1 for various intervals in Krebs-Ringer bathing solution with the Po_2 level maintained above 550 mmHg. As shown in Table 1, ir-ET-1 decreased in proportion to the period of incubation and reached a plateau at 10 min. This apparent structural modification of ET-1 caused by O_2 bubbling was fully inhibited in the presence of 40 u ml^{-1} SOD, indicating that this effect may be mediated by free radicals.

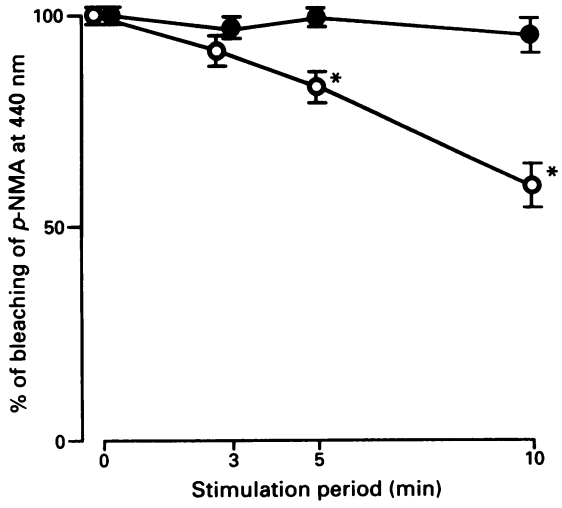

Figure 6 Time-dependent and oxygenation-dependent generation of hydroxyl radicals by EFS. EFS (10 V, 10 Hz, 2 ms) was applied to Krebs-Ringer solution containing 10 μM *p*-nitrosodimethylaniline (*p*-NMA) bubbled with 95% N_2/5% CO_2 (●) or 95% O_2/5% CO_2 (○) for various stimulation periods. Each value is expressed as a percentage of absorbance of *p*-NMA at 440 nm in Krebs-Ringer solution without bubbling. Mean ± s.e. ($n = 3$–6) are shown. *Significantly different from values in hypoxic condition with $P < 0.05$ (Student's *t* test for unpaired values).

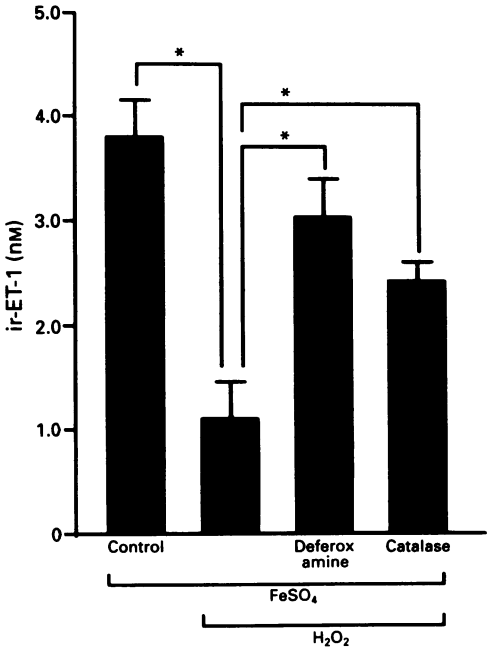

Figure 7 Effect of hydroxyl radicals generated by the Fenton reaction on immunoreactive endothelin-1 (ir-ET-1): 10 nM ET-1, 0.1 mM H_2O_2 and 0.2 mM $FeSO_4$ were added to 50 mM NaCl solution in the absence or presence of each suppressor agent for hydroxyl radicals (10^{-4}M deferoxamine or 1200 u ml^{-1} catalase) and left for 5 min, and each solution was subjected to EIA. As a control, 10 nM ET-1 was added to 50 mM NaCl solution containing 0.2 mM $FeSO_4$ and left for 5 min, and the solution was subjected to EIA. Mean values ± s.e. ($n = 4$) are shown. *Significantly different from values with Fenton reaction-applied ET-1 ($P < 0.05$, ANOVA with Bonferoni correction).

Discussion

The present study demonstrated that prolonged EFS of porcine isolated coronary artery strips precontracted with ET-1 causes a non-neurogenic and endothelium-independent response, which was biphasic with a slight contraction during EFS followed by a long-lasting relaxation after EFS. This relaxation after EFS was significantly inhibited by the free radical scavengers, SOD, catalase and D-mannitol. These results suggest that EFS-generated free radicals are involved in the relaxation response to EFS.

Free radicals show a wide spectrum of action on blood vessels. Hydrogen peroxide causes hyperpolarization and relaxation of pig coronary artery smooth muscle cells (Beny & von der Weid, 1991). Superoxide anions inactivate endoplasmic reticulum Ca^{2+} transport by lowering the activity of the phosphoenzyme which phosphorylates the 100 kDa subunit of the Ca^{2+} pump in endoplasmic reticulum (Grover & Samson, 1988). Superoxide anion and its derivatives, hydroxyl radicals, are responsible at least in part for vasodilatation of cat cerebral artery as well as for damage to the blood-brain barrier (Nelson *et al.*, 1992). Hydroxyl radicals facilitate endothelium-dependent relaxation (Rubanyi & Vanhoutte, 1986). Free radicals generated by EFS induce damage of endothelial cells in the rat tail artery (Lamb *et al.*, 1987).

However, the free radicals generated by EFS is this study are unlikely to have caused relaxation of coronary artery strips in a direct manner or to have damaged the contractile apparatus of smooth muscle cells for the following reasons: (1) the relaxation after EFS was not seen in coronary artery strips precontracted with 20 mM K^+; (2) the contractile response to 50 mM K^+ or 5 μM $PGF_{2\alpha}$ in coronary artery strips was consistent before and after EFS (Figure 1g). Thus, we hypothesized that free radicals generated by EFS might act on ET-1 and decrease its contractile activity, and we examined the effect of EFS on the contractile activity of ET-1 in cascade experiments. EFS of Krebs-Ringer solution containing ET-1 induced marked suppression of the contractile activity of ET-1 in coronary artery strips. This apparent effect of EFS was significantly inhibited by free radical scavengers (Figure 2) suggesting that EFS-generated free radicals suppress the contractile activity of ET-1. A previous study has demonstrated that the C-terminal Trp^{21} as well as the intramolecular loop structure constructed by two disulphide bonds of ET-1 are especially important for its vasoconstrictor activity (Kimura *et al.*, 1988). Thus, it is possible that EFS-derived free radicals suppress the contractile activity via structural modification of ET-1. We examined this point using an enzyme-linked immunoassay recognizing the two important domains of ET-1. As expected, EFS decreased the immunoreactivity of ET-1 (ir-ET-1) and this effect was significantly inhibited by free radical scavengers. Furthermore, the exchange of 95% O_2/5% CO_2 for 95% N_2/5% CO_2 significantly inhibited the EFS-induced decrease of ir-ET-1. These results suggest that oxygen-derived free radicals generated by EFS induce structural modifications of ET-1, thereby suppressing its contractile activity. This phenomenon is not specific for ET-1, because a similar suppression in contractile activity by EFS was recognized in the case of $PGF_{2\alpha}$, although the chemical modification of $PGF_{2\alpha}$ was not clarified in this study (Figure 8a,b). Furthermore, a previous study demonstrated the oxygen metabolites generated by pro-

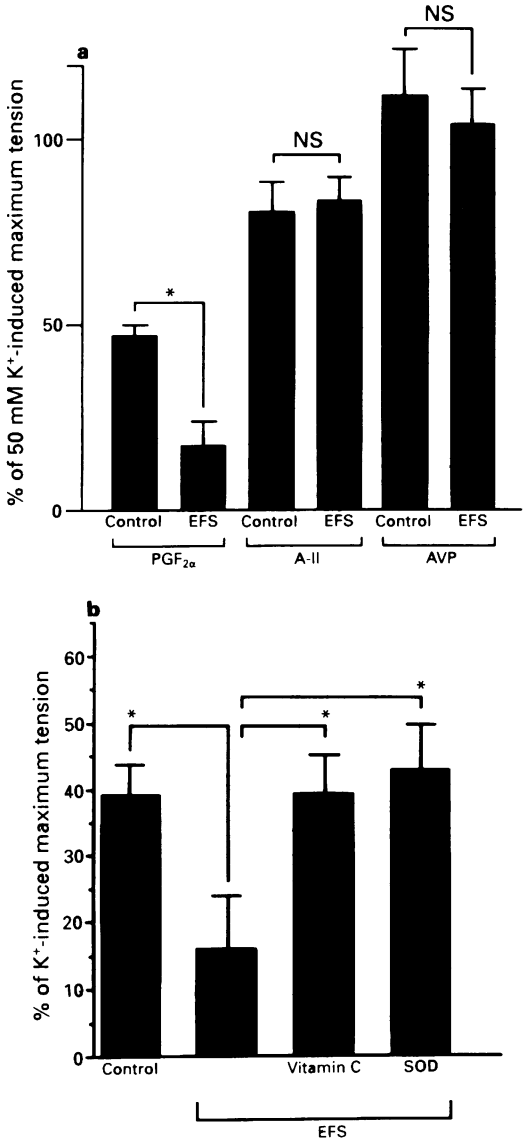

Figure 8 (a) Effect of EFS on contractile activities of prostaglandin $F_{2\alpha}$ ($PGF_{2\alpha}$), angiotensin II (AII) and Arg-vasopressin (AVP). EFS (10 V, 10 Hz, 2 ms, 5 min) was applied to each Krebs-Ringer solution containing 2 μM $PGF_{2\alpha}$, 1 μM AII or 1 μM AVP, and each solution was applied to the strips. Rat aortic strips were used for the assay of contractile activities of AII and AVP. As a control, each vasoconstrictor (2 μM $PGF_{2\alpha}$, 1 μM AII or 1 μM AVP) was added to Krebs-Ringer solution, and each solution was applied to the strips after 5 min. The contractile response of porcine coronary artery strips or rat aortic strips was expressed as percentage of maximum tension induced by 50 mM KCl. Mean values ± s.e. ($n = 6$) are shown. (b) Effect of radical scavengers on EFS-induced suppression of contractile activity of $PGF_{2\alpha}$. EFS (10 V, 10 Hz, 2 ms, 5 min) was applied to Krebs-Ringer solution in the absence or presence of each radical scavenger (vitamin C (3 mM) or SOD (40 u ml^{-1})) added just after the addition of 2 μM $PGF_{2\alpha}$. Then, each solution was applied to porcine coronary artery strips. As a control, 2 μM $PGF_{2\alpha}$ was added to Krebs-Ringer solution, and the solution was applied to the strips after 5 min. The contractile response of porcine coronary artery strips was expressed as a percentage of maximum tension induced by 50 mM KCl. Mean values ± s.e. ($n = 6$) are shown. *Significantly different from control level with $P < 0.05$; NS, not significantly different (Student's t test for unpaired values).

Table 1 Effect of O_2 bubbling on immunoreactive endothelin-1 (ir-ET-1) in the absence and presence of superoxide dismutase (SOD)

Incubation time (min)	*ir-ET-1* (nM) *Control*	*SOD*
0	6.04 ± 0.37	6.38 ± 0.57
5	3.93 ± 0.43*	6.19 ± 0.79
10	2.24 ± 0.36*	7.06 ± 0.69
20	2.13 ± 0.48*	5.73 ± 0.76

Krebs-Ringer solution was maintained at 37°C and gassed with 95% O_2/5% CO_2. The Po_2 level in Krebs-Ringer solution was maintained above 550 mmHg, which was monitored by a pH/blood gas analyser (Corning, Model 158). ET-1 (10 nM) was added to Krebs-Ringer solution in the absence or presence of SOD, and the solution was subjected to EIA after various incubation periods. Data are mean ± s.e. ($n = 4$). *Significantly different from control value with ET-1 without incubation ($P < 0.05$, ANOVA with Bonferroni correction).

longed EFS (9 V, 1 ms, 4 Hz, 5 min) oxidized noradrenaline and decreased its contractile activity (Lamb & Webb, 1984), although the degree of decrease in contractile activity of the agonist was modest in their study compared with our results.

To elucidate which free radicals are involved in the inactivation of ET-1, we examined the effect of each free radical, chemically generated or exogenously applied, on ir-ET-1. Neither superoxide anions generated by xanthine plus xanthine oxidase nor hydrogen peroxide exogenously added, affected ir-ET-1 (Figure 5a,b). In parallel with these findings, the contractile activity of ET-1 was not suppressed by these free radicals (data not shown). However, hydroxyl radicals generated by H_2O_2 plus $FeSO_4$ (Fenton reaction) significantly decreased ir-ET-1 (Figure 7). Furthermore, generation of hydroxyl radicals was detected in EFS-applied Krebs-Ringer solution, and their generation was dependent on the period of stimulation and O_2-bubbling. Significant generation of hydroxyl radicals was detectable when the stimulation period exceeded 5 min. Moreover, this generation of hydroxyl radicals was significantly inhibited in the presence of deferoxamine (data not shown). These results strongly suggest that oxygen-derived hydroxyl radicals generated by EFS mediate the suppression of the contractile activity of ET-1. In this regard, the fact that all free radical scavangers, SOD for superoxide anion, catalase for hydrogen peroxide and mannitol for hydroxyl radicals, significantly inhibited the relaxation of coronary artery strips after EFS in this study conforms with this possibility, since hydroxyl radicals are thought to be generated from superoxide anions by way of hydrogen peroxide in the presence of Fe^{2+} (Rubanyi & Vanhoutte, 1986). A possible source of Fe^{2+} in this study may be contamination from reagents comprising the Krebs-Ringer solution.

Previous studies have demonstrated that hydroxyl radicals induce conformational change of β_2 microglobulin via oxidation of tryptophan (Trp) and that hydroxyl radicals mediate glucose-induced protein damage associated with Trp fluorescence quenching (Hunt *et al.*, 1988; Capeillere-Blandin *et al.*, 1991). It has also been reported that hydroxyl radicals, as well as myeloperoxide-derived oxidants, induce inactivation of α-1-proteinase inhibitor by oxidation of the reactive site methionine (Met) (Maier *et al.*, 1989). These studies raise the possibility that Met^7 and Trp^{21} in the two important domains of ET-1 recognized by EIA are sites of oxidation by hydroxyl radicals and that the modification of each or both residues leads to the loss of both contractile activity and immunoreactivity of ET-1. However, the EIA used in the present study can detect Met sulphoxide^7 ($Met(o)^7$) ET-1 as well as ET-1 (Suzuki, personal communication). Moreover, $Met(o)^7$ ET-1 also has similar contractile activity to ET-1 (Kimura, unpublished data). It is therefore tempting to speculate that the modification of Trp^{21} of ET-1 by hydroxyl radicals is critical for EFS-induced inactivation of ET-1. On the other hand, AII and AVP are probably resistant to chemical modification by EFS since they lack both Met and

Trp (Aumelas *et al.*, 1985; Mann *et al.*, 1986). Further study is required to determine whether EFS-derived hydroxyl radicals actually oxidize Trp^{21} of ET-1.

The mechanism for the slight contraction which follows EFS of coronary artery strips is unclear. This response was insensitive to TTX and free radical scavengers. Hence, known vasoconstrictor neurotransmitters (Kalsner & Quillin, 1989) and free radicals (Auch-Schwelk *et al.*, 1989) are not likely to contribute to this response during EFS. It is most likely that activation of voltage-dependent Ca^{2+} channels secondary to EFS-induced depolarization of the smooth muscle membrane may bring about the slight contraction, because this contractile response was significantly larger in 20 mM K^+-depolarized contractions and partially inhibited in the presence of a low concentration of nicardipine. Thus (1) contractile responses during EFS were $35.9 \pm 1.7\%$ in 20 mM K^+-depolarized contractions and $22.3 \pm 2.1\%$ in ET-1-induced contractions, respectively ($n = 4$, contractile response expressed as percentage of maximum tension induced by 50 mM KCl) and (2) The contractile response during EFS in ET-1-induced contractions was reduced to $14.5 \pm 1.0\%$ in the presence of 10^{-8} M nicardipine ($n = 4$, contractile response expressed as percentage of maximum tension induced by 50 mM KCl).

Recently, it has been demonstrated that preincubation of ET-1 in oxygenated Krebs-Ringer solution results in progressive loss of its contractile activity in porcine coronary arterial rings in parallel with loss of its immunoreactivity, dependent on the period of incubation (Balwierczak *et al.*, 1992). We also confirmed this finding in the case of maintaining P_{O_2} level in Krebs-Ringer solution above 550 mmHg, and further verified that the decrease of ir-ET-1 by the incubation was fully inhibited by the free radical scavenger, SOD (Table 1). Thus, it is possible that free radicals may be generated by bubbling only with O_2/CO_2 gas, and in a free state in the solution, inactivate ET-1. However, free radicals generated by O_2-bubbling alone may be less potent in inactivating ET-1 than the hydroxyl radicals generated by EFS in this study. Since, the level of ir-ET-1 was decreased by O_2-bubbling in a time-dependent manner and reached a plateau (about 2 nM) at 10 min, although the level of ir-ET-1 was reduced to below the detection limit of EIA (1 pM) by EFS (Table 1, Figure 3). It has been demonstrated that ET-1-induced contraction of porcine coronary artery is more or less irreversible and lasts for several hours (Yanagisawa *et al.*, 1988), due to the very slow dissociation of ET-1 from its receptor once bound (Hirata *et al.*, 1988). This observation indicates that O_2-bubbling does not inactivate ET-1 bound to its receptor. On the contrary, coronary artery strips precontracted with ET-1 showed marked relaxation to near baseline values just after EFS in this study, indicating that the EFS-generated hydroxyl radicals may potently inactivate not only ET-1 in a free form in the solution but also ET-1 bound to its receptor.

This work was supported in part by grants from the Special Research Project on the Circulation Biosystem, University of Tsukuba and from the Ministry of Education, Science and Culture of Japan. We thank Dr Wendy Grey for reading our manuscript.

References

AUCH-SCHWELK, W., KATUSIC, Z.S. & VANHOUTTE, P.M. (1989). Contractions to oxygen-derived free radicals are augmented in aorta of the spontaneously hypertensive rat. *Hypertension*, **13**, 859–864.

AUMELAS, A., SAKARELLOS, C., LINTNER, K., FERMANDJIAN, S., KHOSLA, M.C., SMEBY, R.R. & BUMPUS, F.M. (1985). Studies on angiotensin II and analogs: impact of substitution in position 8 on conformation and activity. *Proc. Natl. Acad. Sci. U.S.A.*, **82**, 1881–1885.

BALWIERCZAK, J.L., HOPKINS, M.F., SAVAGE, P., MARTIN, L.L. & JENG, A.Y. (1992). Decrease in immunoreactivity and vasoactivity of endothelin-1 after exposure to oxygen. *Biochem. Int.*, **27**, 1111–1117.

BEAUCHAMP, C. & FRIDOVICH, I. (1971). Superoxide dismutase: improved assays and an assay applicable to acrylamide gels. *Anal. Biochem.*, **44**, 276–287.

BENY, J.-L. & VON DER WEID, P.-Y. (1991). Hydrogen peroxide: an endogenous smooth muscle cell hyperpolarizing factor. *Biochem. Biophys. Res. Commun.*, **176**, 378–384.

BORS, W., MICHEL, C. & SARAN, M. (1979). On the nature of biochemically generated hydroxyl radicals. *Eur. J. Biochem.*, **95**, 621–627.

BUGA, G.M. & IGNARRO, L.J. (1992). Electrical field stimulation causes endothelium-dependent and nitric oxide-mediated relaxation of pulmonary artery. *Am. J. Physiol.*, **262**, H973–H979.

CAPEILLERE-BLANDIN, C., DELAVEAU, T. & DESCAMPS-LATSCHA, B. (1991). Structural modifications of human β_2 microglobulin treated with oxygen-derived radicals. *Biochem. J.*, **277**, 175–182.

COHEN, R.A., SHEPHERD, J.T. & VANHOUTTE, P.M. (1983). Prejunctional and postjunctional actions of endogenous norepinephrine at the sympathetic neuroeffector junction in canine coronary arteries. *Circ. Res.*, **52**, 16–25.

FELETOU, M. & VANHOUTTE, P.M. (1987). Relaxation of canine coronary artery to electrical stimulation: limited role of free radicals. *Am. J. Physiol.*, **253**, H884–H889.

FELETOU, M. & VANHOUTTE, P.M. (1989). Tetrodotoxin-insensitive relaxation of coronary arterial smooth muscle to electrical stimulation: possible involvement of a dopaminergic mechanism. *Blood Vessels*, **26**, 213–227.

FREEMAN, B.A. & CARPO, J.D. (1982). Biology of disease. Free radicals and tissue injury. *Lab. Invest.*, **47**, 412–426.

FUJIMORI, A., SAITO, A., KIMURA, S., WATANABE, T., UCHIYAMA, Y., KAWASAKI, H. & GOTO, K. (1989). Neurogenic vasodilation and release of calcitonin gene-related peptide (CGRP) from perivascular nerves in the rat mesenteric artery. *Biochem. Biophys. Res. Commun.*, **165**, 1391–1398.

GREENBERG, B., RHODEN, K. & BARNES, P.J. (1986). Activated oxygen molecules generated by electrical stimulation affect vascular smooth muscle. *J. Mol. Cell. Cardiol.*, **18**, 975–981.

GROVER, A.K. & SAMSON, S.E. (1988). Effect of superoxide radical on Ca^{2+} pumps of coronary artery. *Am. J. Physiol.*, **255**, C297–C303.

HIRATA, Y., YOSHIMI, H. & TAKAICHI, S. (1988). Binding and receptor down regulation of a novel vasoconstrictor endothelin in cultured rat vascular smooth muscle cells. *FEBS Lett.*, **239**, 13–17.

HUNT, J.V., DEAN, R.T. & WOLFF, S.P. (1988). Hydroxyl radical production and autoxidative glycosylation. *Biochem. J.*, **256**, 205–212.

KALSNER, S. & QUILLIN, M. (1989). Cholinergic contraction to field stimulation in coronary arteries of cattle. *J. Pharmacol. Exp. Ther.*, **249**, 785–789.

KASUYA, Y., ISHIKAWA, T., YANAGISAWA, M., KIMURA, S., GOTO, K. & MASAKI, T. (1989). Mechanism of contraction to endothelin in isolated porcine coronary artery. *Am. J. Physiol.*, **257**, H1828–H1835.

KASUYA, Y., TAKUWA, Y., YANAGISAWA, M., MASAKI, T. & GOTO, K. (1992). A pertussis toxin-sensitive mechanism of endothelin action in porcine coronary artery smooth muscle. *Br. J. Pharmacol.*, **107**, 456–462.

KIMURA, S., KASUYA, Y., SAWAMURA, T., SHINMI, O., SUGITA, Y., YANAGISAWA, M., GOTO, K. & MASAKI, T. (1988). Structure-activity relationships of endothelin: importance of the C-terminal moiety. *Biochem. Biophys. Res. Commun.*, **156**, 1182–1186.

LAMB, F.S., KING, C.M., HARRELL, K., BURKEL, W. & WEBB, R.C. (1987). Free radical-mediated endothelial damage in blood vessels after electrical stimulation. *Am. J. Physiol.*, **252**, H1041–H1046.

LAMB, F.S. & WEBB, R.S. (1984). Vascular effects of free radicals generated by electrical stimulation. *Am. J. Physiol.*, **247**, H704–H714.

MAIER, K.L., MATEJKOVA, E., HINZE, H., LEUSCHEL, L., WEBER, H. & BECKSPEIER, I. (1989). Different selectivities of oxidants during oxidation of methionine residues in the α-1-proteinase inhibitor. *FEBS Lett.*, **250,** 221–226.

MANN, W.A., STASSEN, F., HUFFMAN, W. & KINTER, L.B. (1986). Mechanism of action and structural requirements of vasopressin analog inhibition of transepithelial water flux in toad urinary bladder. *J. Pharmacol. Exp. Ther.*, **238,** 401–406.

MCCULLOCH, J. & EDVINSSON, L. (1980). Cerebral circulatory and metabolic effects of vasoactive intestinal polypeptide. *Am. J. Physiol.*, **238,** H449–H456.

MINOTTI, G. & AUST, S.D. (1987). The requirement for iron (III) in the initiation of lipid peroxidation by iron (II) and hydrogen peroxide. *J. Biol. Chem.*, **262,** 1098–1104.

NELSON, C.W., WEI, E.P., POVLISHOCK, J.T., KONTOS, H.A. & MOSKOWITZ, M.A. (1992). Oxygen radicals in cerebral ischaemia. *Am. J. Physiol.*, **263,** H1356–H1362.

ROOKE, T., COHEN, R.A., VERBEUREN, T.J. & VANHOUTTE, P.M. (1982). Non-neurogenic inhibitory effect of electrical impulses in isolated canine coronary arteries. *Eur. J. Pharmacol.*, **80,** 251–254.

RUBANYI, G.M. & VANHOUTTE, P.M. (1986). Oxygen-derived free radicals, endothelium, and responsiveness of vascular smooth muscle. *Am. J. Physiol.*, **250,** H815–H821.

SAKURAI, T., YANAGISAWA, M. & MASAKI, T. (1992). Molecular characterization of endothelin receptors. *Trends Pharmacol Sci.*, **13,** 103–108.

SUZUKI, N., MATSUMOTO, H., KITADA, C., MASAKI, T. & FUJINO, M. (1989). A sensitive sandwich-enzyme immunoassay for human endothelin. *J. Immunol. Methods*, **118,** 245–250.

TODA, N. (1982). Relaxant responses to transmural stimulation and nicotine of dog and monkey cerebral arteries. *Am. J. Physiol.*, **243,** H145–H153.

VAN RIPER, D.A. & BEVAN, J.A. (1992). Electrical field stimulation-mediated relaxation of rabbit middle cerebral artery. *Circ. Res.*, **70,** 1104–1112.

VERMA, A., HIRSCH, D.J., GLATT, C.E., RONNETT, G.V. & SNYDER, S.H. (1993). Carbon monoxide: a putative neural messenger. *Science*, **259,** 381–384.

YANAGISAWA, M., KURIHARA, H., KIMURA, S., TOMOBE, Y., KOBAYASHI, M., MITSUI, Y., YAZAKI, Y., GOTO, K. & MASAKI, T. (1988). A novel potent vasoconstrictor peptide produced by vascular endothelial cells. *Nature*, **332,** 411–415.

(Received April 26, 1993
Revised April 25, 1994
Accepted April 28, 1994)

Br. J. Pharmacol. (1994), **113**, 29–34

Characterization and transduction mechanisms of purinoceptors in activated rat microglia

J.M. Langosch, *P.J. Gebicke-Haerter, [1]W. Nörenberg & [1]P. Illes

Department of Pharmacology, University of Freiburg, Hermann-Herder-Strasse 5, and *Department of Psychiatry, University of Freiburg, Hauptstrasse 5, D-79104 Freiburg, Germany

1 Purinoceptor agonist-induced currents in untreated (proliferating) and lipopolysaccharide- (LPS; 100 ng ml^{-1}) treated (non-proliferating) rat microglial cells were recorded by the whole-cell patch-clamp technique.

2 In non-proliferating microglia, adenosine (0.01–100 μM), 2-methylthio ATP (3-3000 nM), ATP (0.1–1000 μM), and ATP-γ-S (1–10 μM), but not α,β-methylene ATP (α,β-MeATP; 100 μM) produced a slow outward current at a holding potential of 0 mV. When K^+ was replaced in the pipette solution by an equimolar concentration of Cs^+ (150 mM), the 2-methylthio ATP- (300 nM) induced outward current disappeared. The effect of 2-methylthio ATP (300 nM) did not depend on the presence of extracellular Mg^{2+} (1 mM). The outward current response to 2-methylthio ATP (300 nM) was larger in proliferating than in non-proliferating microglia.

3 ATP (1–1000 μM) evoked a fast inward current at a holding potential of −70 mV in non-proliferating microglia, while adenosine (100–1000 μM) was inactive. When the effects of ATP were compared at 0 and −70 mV, it became evident that ATP is much more potent in evoking the outward current.

4 The 2-methylthio ATP- (300 nM) induced outward current was blocked by suramin (300 μM), but not by 8-(*p*-sulphophenyl)-theophylline (100 μM), while the adenosine- (1 μM) induced outward current had the reverse sensitivity to these antagonists.

5 The 2-methylthio ATP- (300 nM) induced outward current was inhibited by inclusion of GDP-β-S (200 μM) into the pipette solution or by preincubation of microglial cells with pertussis toxin (50 ng ml^{-1}) for 12 h. The 2-methylthio ATP- (300 μM) induced inward current was not changed by intracellular GDP-β-S (200 μM). The outward current response to adenosine (1 μM) was also abolished after pretreatment with pertussis toxin (50 ng ml^{-1}).

6 Rat microglia possess both ATP-sensitive P_{2Y}- and adenosine-sensitive P_1-purinoceptors. The ATP-evoked inward current is mediated by P_{2Y}-purinoceptors, while the ATP- and adenosine-evoked outward currents are mediated by P_{2Y}- and P_1-purinoceptors, respectively. The transduction mechanisms of the outward, but not the inward current activation involve a pertussis toxin-sensitive G protein.

Keywords: Microglia; P_2-purinoceptor; P_1-purinoceptor; ATP; adenosine; non-selective cationic channel; potassium channel

Introduction

Microglial cells play important roles in mediating immune responses in the central nervous system (Streit *et al.*, 1988; Dickson *et al.*, 1991; Thomas, 1992). Pathological conditions lead to a conversion of resting microglia to macrophages which strongly influence the regenerative process (Streit *et al.*, 1988). In tissue culture systems, cells become initially activated by the isolation procedure, and are capable of both proliferation and phagocytosis (Rieske *et al.*, 1989). They can be driven further into macrophage-like microglia by stimuli such as bacterial lipopolysaccharide (Adams & Hamilton, 1987). These cells no longer proliferate but are still capable of phagocytosis (Bignami, 1991; Dickson *et al.*, 1991). Moreover, non-proliferating microglia secrete cytokines (e.g. interleukin-1 and -6) and produce superoxide anions (oxidative burst) (Bignami, 1991; Dickson *et al.*, 1991).

While proliferating microglial cells exhibit voltage-dependent inwardly rectifying potassium channels (Kettenmann *et al.*, 1990; Banati *et al.*, 1991), LPS-treatment for > 3 h results in the expression of previously lacking outwardly rectifying potassium channels (Nörenberg *et al.*, 1992). The physiological and pharmacological properties of this conductance (Nörenberg *et al.*, 1992, 1993, 1994a) greatly resemble those of an outwardly rectifying K^+ current in peripheral lymphocytes (K_n; Gallin, 1991; Gardner, 1990). In an effort to search for signal substances inducing rapid changes in microglia, adenosine 5'-triphosphate (ATP) has been identified. ATP leads both in proliferating (Kettenmann *et al.*, 1993; Walz *et al.*, 1993) and non-proliferating microglia (Nörenberg *et al.*, 1994b) to transient activation of a cationic conductance followed by more sustained activation of an outward potassium current.

ATP is rapidly degraded by ectonucleotidases to adenosine; these two compounds stimulate different types of purinoceptors named P_2 and P_1, respectively (Burnstock & Buckley, 1985). Based on the potencies of structural analogues of ATP, P_2-receptors were classified into the P_{2X}- and P_{2Y}-subtypes (Burnstock & Kennedy, 1985; Kennedy, 1990). At the P_{2X}-purinoceptor the potency order is α,β-methylene ATP (α,β-MeATP) > ATP = 2-methylthio ATP, whereas at the P_{2Y}-purinoceptor it is 2-methylthio ATP > ATP > α,β-MeATP.

The aim of the present study was to characterize microglial purinoceptors involved in the increase of K^+ permeability, to examine their transduction mechanisms and to compare ATP effects in proliferating and non-proliferating microglia.

Methods

Cell culture

Mixed astroglial-microglial cell cultures were prepared as described previously (Keller *et al.*, 1985). In brief, newborn

[1] Authors for correspondence.

(Wistar) rat forebrains were minced and gently dissociated by trituration in Hank's balanced salt solution. Cells were collected by centrifugation at 200 *g* for 10 min, resuspended in Dulbecco's modified Eagle's medium (DMEM), supplemented with 10% heat inactivated foetal calf serum (FCS), plated onto 100 mm Falcon culture dishes (5×10^5 cells/dish) and cultured in an atmosphere of 5% CO_2 at 37°C for 2 weeks. Media were prepared taking extreme care to avoid all potential sources of LPS contamination. Floating microglial cells were harvested and reseeded into 35 mm Petri dishes to give pure microglial cultures (2×10^4 cell/dish) (Gebicke-Haerter *et al.*, 1989). Small cells (diameter, 5–8 μm) with unipolar or bipolar processes were observed under phase contrast optics immediately after reseeding. When LPS (100 ng ml^{-1}) was added to the medium for 12–24 h, many microglial cells became circular in shape with ruffled edges (diameter, 15–23 μm).

Cytochemical methods

The identity of the cell type was confirmed by the intracellular monocyte marker ED1 (Dijkstra *et al.*, 1985). Since all isolated cells were ED1-positive, it was concluded that only cells derived from the monocyte/macrophage linage were present in isolated microglial cultures. Moreover, no GFAP- and fibronectin positive cells were detectable (Nörenberg *et al.*, 1994a).

Patch-clamp experiments

Cultures were maintained on the stage of an inverted microscope at room temperature (20–24°C). They were superfused with a standard salt solution containing in mM: NaCl 160, KCl 4.5, $CaCl_2$ 2, $MgCl_2$ 1, HEPES 5, glucose 11. The pH was adjusted with NaOH to 7.4.

Whole cell currents were recorded by the patch-clamp technique (Hamill *et al.*, 1981). Recording pipettes contained in mM: KCl 150, $CaCl_2$ 1, $MgCl_2$ 2, EGTA 11 and HEPES 10. The pH was adjusted with KOH to 7.3. In some cases the pipette also contained GDP-β-S (200 μM). In other cases, intracellular KCl was replaced by CsCl (150 mM) and the pH was adjusted to 7.3 by adding CsOH. The resistance of the pipettes varied from 2 to 10 MΩ.

Compensation of capacitance and series resistance was achieved with the inbuilt circuitry of the patch amplifier (List EPC-7, Darmstadt, Germany). Data were digitized at 0.1–1 kHz (Cambridge Electronic Devices 1401, Cambridge, UK) and then stored on and analyzed with a laboratory computer (ESCOM/486, Heppenheim, Germany). Cells were held either at −70 or 0 mV. Data are non-leak subtracted.

Application of drugs and evaluation of data

In most experiments, the outward current was isolated from the early inward current by holding the cells at 0 mV which is near the reversal potential for the early inward current. Purinoceptor agonists were applied for 10 s by means of separate, wide-bore, pressurized (10 kPa) puffer pipettes, placed approximately 50 μm away from the cell under examination. Each agonist concentration was applied only once (T_1) to a cell except in some cases, when two subsequent applications (T_1, T_2) separated by 10 min intervals were made. During this interval the bath was superfused with drug-free medium or with medium containing purinoceptor antagonists at a flow rate of 2 ml min^{-1}. Puffer application of drug-free extracellular solution failed to induce a current response. When the effects of two consecutive administrations of purinoceptor agonists were compared, the current induced by T_2 was normalized with respect to the current induced by T_1.

Concentration-response curves of ATP and adenosine for the outward current were obtained by pressure applying each agonist concentration onto a single cell. The curves were fitted to the data points by using the equation:

$$I/I_{max} = 1/\{1 + (K_D/[ATP]^{n_H}\} \quad (1)$$

where K_D is the apparent dissociation constant which equals the concentration evoking a half-maximal current (EC_{50}), and n_H is the Hill coefficient. Concentration-response relationships of ATP for the inward current were determined at a holding potential of −70 mV, close to the reversal potential of the late outward current. These data were replotted from a previous paper (Nörenberg *et al.*, 1994b) by using equation (1).

Materials

The following materials and drugs were used: suramin hexasodium salt (Bayer, Leverkusen, Germany); Dulbecco's modified Eagle's medium (DMEM), Hank's balanced salt solution, foetal calf serum (FCS) (Gibco, Eggenstein, Germany); pertussis toxin (List, Campbell, CA, U.S.A.); 2-methylthioadenosine 5′-triphosphate tetrasodium salt, 8-(*p*-sulphophenyl)-theophylline (RBI, Natick, MA, U.S.A.); lipopolysaccharide from *Salmonella typhimurium* (Sebak, Aidenbach, Germany); adenosine, adenosine 5′-triphosphate disodium salt (ATP), adenosine 5′-O-(3-thio)-triphosphate tetralithium salt (ATP-γ-S), guanosine 5′-O-(2-thiodiphosphate) tetralithium salt (GDP-β-S), α,β-methyleneadenosine 5′-triphosphate lithium salt (α,β-MeATP) (Sigma, Deisenhofen, Germany).

Pertussis toxin was dissolved in sterile water (100 μg ml^{-1}) and aliquots were stored at −20°C. Pertussis toxin (50 ng ml^{-1}) was added to the culture dishes under aseptic conditions for 12 h at 37°C, prior to the start of the experiments. LPS, dissolved in distilled water (1 mg ml^{-1}), was further diluted into DMEM. Stock solutions (10–100 mM) of all other drugs were prepared with distilled water and aliquots were stored at −20°C. Further dilutions were made in saline at respective experimental days.

Statistics

Means ± s.e.mean of *n* trials are shown. Student's paired or unpaired *t* test was used to compare means as appropriate. A probability level of 0.05 or less was considered to be statistically significant.

Results

Characterization of purinoceptors by agonists

Concentration-response relationships of different ATP analogues and adenosine for the outward current were determined in order to identify the purinoceptor subtype involved. At a holding potential of 0 mV both 2-methylthio ATP (300 nM; Figure 1a) and adenosine (1 μM; Figure 1b) produced non-desensitizing outward currents with slow onsets and offsets. The time-courses of these currents showed some variability between individual microglial cells (for 2-methylthio ATP compare Figures 1a and 3b), but were basically similar for equipotent concentrations of the two agonists. 2-methylthio ATP (3–3000 nM), adenosine (0.01–100 μM), ATP (0.1–1000 μM), and ATP-γ-S (1–10 μM), but not α,β-MeATP (100 μM) produced concentration-dependent responses (Figure 1c). Maximal currents were evoked by concentrations of 2-methylthio ATP (88.8 ± 17.4 pA at 300 nM; $n = 5$), adenosine (114.9 ± 10.2 pA at 10 μM; $n = 8$) and ATP (143.5 ± 25.4 pA at 100 μM; $n = 6$). When K^+ was replaced in the pipette solution by an equimolar concentration of Cs^+ (150 mM), the 2-methylthio ATP- (300 nM) induced response disappeared (0.9 ± 0.3 pA; $n = 5$; $P < 0.01$). Finally, the effect of 2-methylthio ATP (300 nM) did not depend on the

presence of extracellular Mg^{2+} (1 mM) in the bath medium (Figure 1c, inset).

Subsequently, EC_{50} values and Hill coefficients were calculated from the concentration-response curves of ATP and adenosine for the outward current. They were 1.4 μM and 0.7 for ATP, and 320.0 nM and 0.6 for adenosine. Concentration-response curves of ATP for the inward current were replotted from a previous publication (Nörenberg *et al.*, 1994b), where measurements were made at a holding potential of − 70 mV, close to the reversal potential of the outward current. The EC_{50} value and the Hill coefficient were 37.0 μM and 1.0, respectively. Adenosine (100–1000 μM) failed to initiate an inward current.

Comparison of the EC_{50} values showed that ATP is much more potent in evoking an outward than an inward current. It is noteworthy that adenosine evokes an outward current only. In further experiments 2-methylthio ATP (EC_{50} = 39.0 nM; n_H = 1.5) was used instead of ATP because of its higher potency and its relatively greater stability.

All previous experiments were carried out in non-proliferating microglia. Outward current responses upon application of 2-methylthio ATP (300 nM) were considerably larger in proliferating (247.7 ± 39.7 pA; $n = 8$; $P < 0.01$) than in non-proliferating (96.4 ± 14.3 pA, $n = 7$) cells.

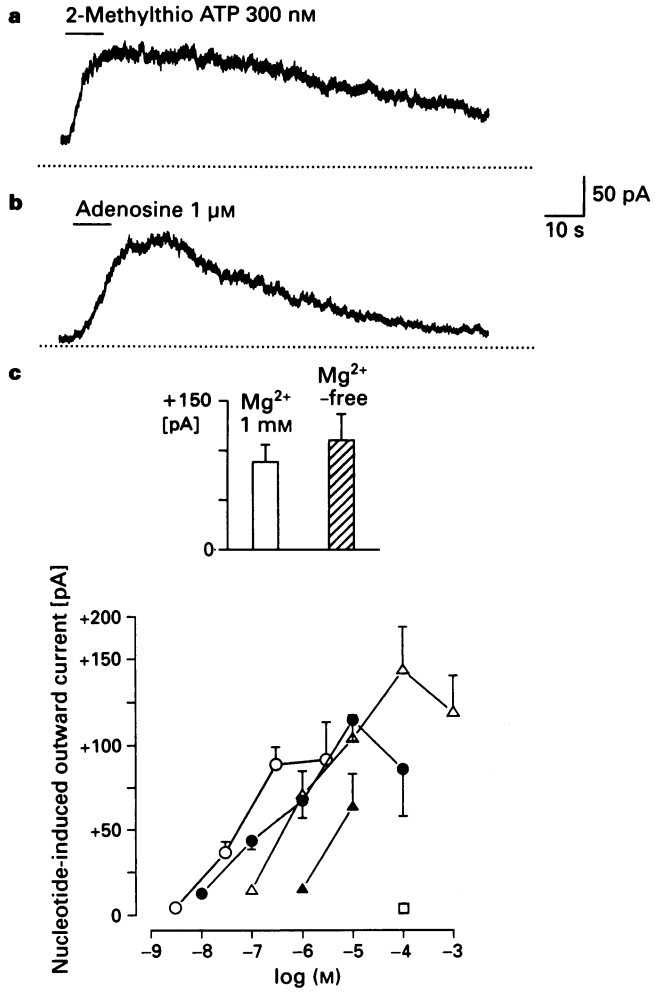

Figure 1 Outward currents activated by purinoceptor agonists in rat microglia. Holding potential was 0 mV. Each concentration was pressure applied for 10 s, only once and to different cells. (a) Current induced by 2-methylthio ATP (300 nM). (b) Current induced by adenosine (1 μM). The dotted lines indicate the zero current level. Recordings from two different cells are shown. (c) Concentration-response curves of 2-methylthio ATP (○; $n = 4–7$), adenosine (●; $n = 5–13$), ATP (△; $n = 5–11$), ATP-γ-S (▲; $n = 7–8$) and α,β-MeATP (□; $n = 4$). The current induced by 2-methylthio ATP (300 nM) was the same both in the presence (open column; $n = 5$) and absence of Mg^{2+} (1 mM) (hatched column; $n = 7$; $P > 0.05$) (inset). Means ± s.e.mean from n experiments.

Characterization of purinoceptors by antagonists

Since the same outward current could be elicited by 2-methylthio ATP and adenosine, further pharmacological studies were undertaken to discriminate between P_1- and P_2-purinoceptor-mediated effects. When 2-methylthio ATP (300 nM) was applied twice with a 10 min interval, stable amplitudes of outward currents were obtained (Figure 2a). Suramin (300 μM), a P_2-purinoceptor blocker, markedly inhibited the effect of 2-methylthio ATP (300 nM), whereas 8-(*p*-sulphophenyl)-theophylline (100 μM), a P_1-purinoceptor blocker, was inactive (Figure 2a). By contrast, after a control

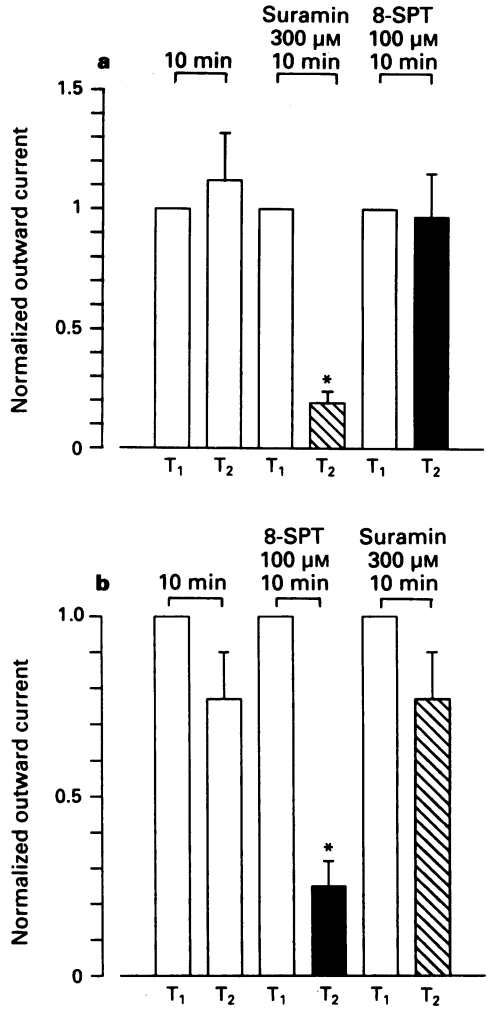

Figure 2 Interaction between purinoceptor agonists and antagonists in rat microglia. Holding potential was 0 mV. Purinoceptor agonists were pressure applied twice for 10 s with 10 min interval (T_1–T_2). The effects of T_2 were normalized with respect to the effect of T_1. (a) Antagonism of the 2-methylthio ATP- (300 nM) induced outward current by suramin (300 μM) (hatched column; $n = 6$), but not 8-(*p*-sulphophenyl)-theophylline (8-SPT, 100 μM) (solid column; $n = 5$). 2-Methylthio ATP (300 nM) was applied the second time either in the absence (open column; $n = 10$) or presence of the antagonists. $^*P < 0.01$; significant difference between T_1 and T_2 in the 2nd set of columns. (b) Antagonism of the adenosine- (1 μM) induced current by 8-(*p*-sulphophenyl)-theophylline (100 μM) (solid column; $n = 7$), but not suramin (300 μM) (hatched column, $n = 6$). Adenosine (1 μM) was applied the second time either in the absence (open column; $n = 7$) or presence of the antagonists. $^*P < 0.01$; significant differences between T_1 and T_2 in the 2nd set of columns. Means ± s.e.mean from n experiments.

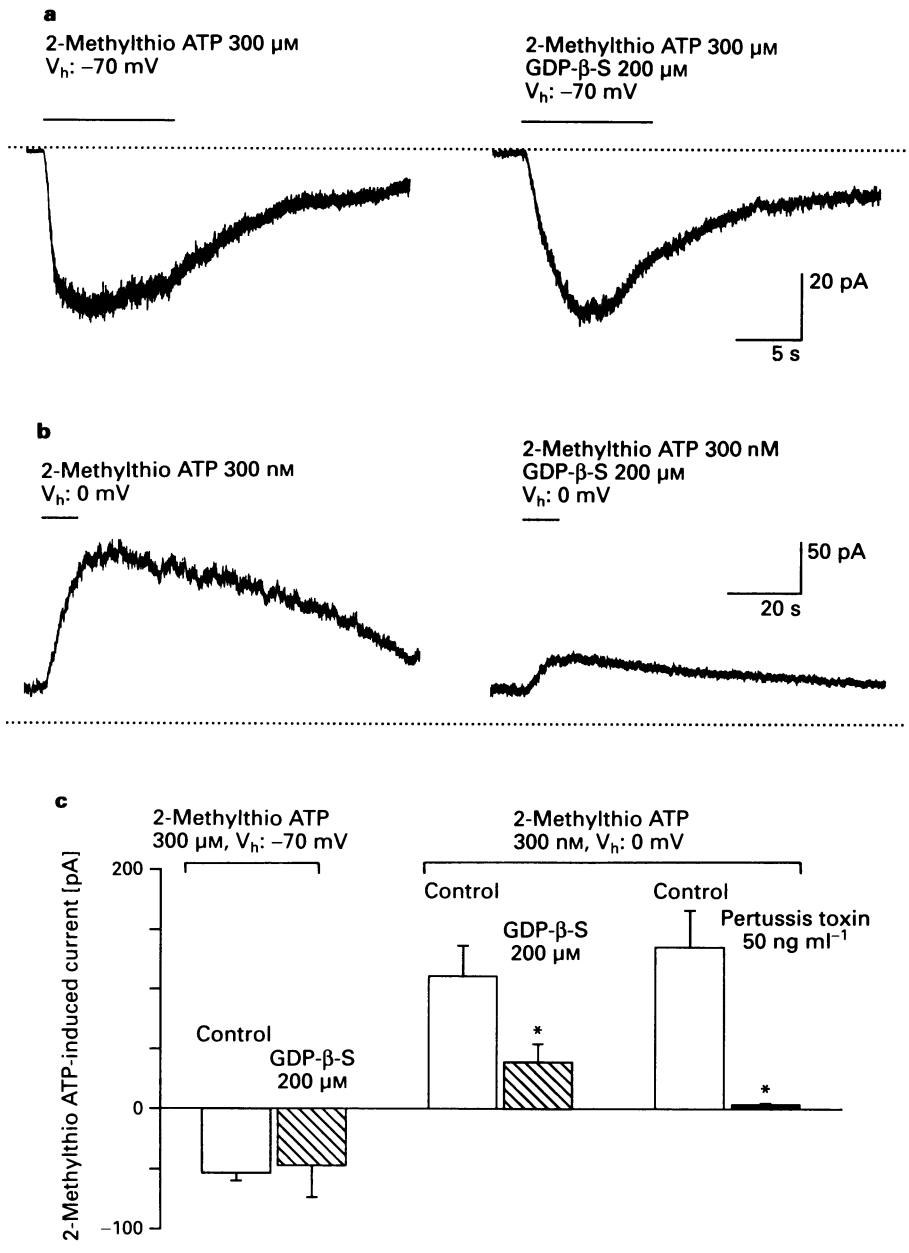

Figure 3 Inhibition of 2-methylthio ATP-induced currents by intracellular GDP-β-S or preincubation with pertussis toxin in rat microglia. Each agonist concentration was pressure applied for 10 s only once and to different cells. (a) Inward current evoked by 2-methylthio ATP (300 μM) at a holding potential of − 70 mV. Either a standard pipette solution was used (left panel) or a solution which also contained GDP-β-S (200 μM) (right panel). (b) Outward current evoked by 2-methylthio ATP (300 nM) at a holding potential of 0 mV. Either a standard pipette solution was used (left panel) or a solution which contained also GDP-β-S (200 μM) (right panel). Representative tracings are shown in (a) and (b). The dotted lines indicate the zero current level. (c) Inward currents recorded with a standard pipette solution (open column; $n = 6$) are not altered when the solution contains also GDP-β-S (200 μM) (hatched column; $n = 6$). Outward currents recorded with a standard pipette solution (open column; $n = 11$) are inhibited when the solution contains also GDP-β-S (200 μM) (hatched column; $n = 12$). Incubation of the cells for 12 h with pertussis toxin (50 ng ml^{-1}) (solid column; $n = 7$) also depressed the current obtained in control cells (open column; $n = 6$). *$P < 0.01$; significant differences from the corresponding control values. Means ± s.e.mean from n experiments are shown.

application of adenosine (1 μM), 8-(*p*-sulphophenyl)-theophylline (100 μM) markedly inhibited a second adenosine- (1 μM) induced current, when compared to two consecutive control applications, while suramin (300 μM) did not alter it (Figure 2b).

Transduction mechanisms of purinoceptors

As shown earlier, 2-methylthio ATP caused an inward current at a potential of − 70 mV (Nörenberg *et al.*, 1994b), and an outward current at a potential of 0 mV (Figure 1). The possible involvement of G proteins in mediating these two response components was investigated in further detail. Since sensitivities of the ATP-induced inward and outward currents were different, a 300 μM concentration of 2-methylthio ATP was chosen to elicit an inward current at a membrane potential of − 70 mV and 300 nM to elicit an outward current at 0 mV.

When GDP-β-S (200 μM) was included in the patch pipette, an inward current similar to that measured under control conditions was obtained in response to 2-methylthio ATP (Figures 3a and c). In contrast, the outward current was markedly decreased in the presence of intracellular GDP-β-S (200 μM) (Figures 3b and c), suggesting an involvement of G

proteins in the activation of outward but not inward currents evoked by 2-methylthio ATP. Pretreatment of microglial cells with pertussis toxin (50 ng ml^{-1}) for 12 h abolished the outward current response to 2-methylthio-ATP (300 nM) (Figure 3c). In addition, the adenosine- (1 μM) evoked current was also abolished after pretreatment with pertussis toxin (50 ng ml^{-1}) for 12 h (4.7 ± 1.0 pA; $n = 7$; $P < 0.01$).

Discussion

The present results confirm previous findings that ATP activates a rapidly desensitizing non-selective cationic conductance followed by a non-desensitizing K^+ conductance in rat microglia (Kettenmann *et al.*, 1993; Walz *et al.*, 1993; Nörenberg *et al.*, 1994b). The two current components could be studied separately, by holding the cells at − 70 mV close to the reversal potential of the outward current or at 0 mV near the reversal potential of the inward current. In accordance with previous results (Nörenberg *et al.*, 1994b), replacement of intracellular K^+ by Cs^+ abolished the outward current.

ATP and some of its structural analogues (2-methylthio ATP, ATP-γ-S) evoked outward currents. These compounds appear to increase the permeability of the membrane by receptor stimulation, rather than by phosphorylation of extracellular proteins. ATP-induced phosphorylation depends on extracellular Mg^{2+} (see e.g. Christie *et al.*, 1992) and, therefore, the similar current amplitudes induced by 2-methylthio ATP both in the presence and absence of extracellular Mg^{2+} (1 mM) suggest a receptor-mediated effect. Microglial cells appear to possess two classes of purinoceptor, a P_2-type activated by ATP and a P_1-type activated by adenosine. Suramin is a P_2-purinoceptor antagonist, without any preference for the P_{2X}- or P_{2Y}-subtypes (Kennedy, 1990). 8-(*p*-Sulphophenyl)-theophylline is a P_1-purinoceptor antagonist; it is a polar compound which penetrates cells only to a limited extent and, therefore, does not inhibit the cellular enzyme phosphodiesterase (Bruns *et al.*, 1980). 8-(*p*-Sulphophenyl)-theophylline also fails to differentiate between further subtypes of P_1-purinoceptors named A_1 and A_2 (Burnstock & Buckley, 1985). The antagonism of the 2-methylthio ATP effect by suramin, but not 8-(*p*-sulphophenyl)-theophylline strongly suggests that 2-methylthio ATP activates P_2-purinoceptors only. The rank order of agonist potencies (2-methylthio ATP > ATP >> α,β-MeATP) classifies this receptor as a P_{2Y}-purinoceptor (Burnstock & Kennedy, 1985; Kennedy, 1990). On the other hand, the antagonism of the adenosine effect by 8-(*p*-sulphophenyl)-theophylline, but not by suramine documents the additional presence of a P_1-purinoceptor in microglia.

Hence, P_{2Y}-purinoceptors may be involved both in inward current-activation at a holding potential of − 70 mV (Nörenberg *et al.*, 1994b) and outward current-activation at a holding potential of 0 mV (present study). It is important to note that much lower concentrations of ATP were needed to activate the outward conductance. This may be due to the presence of two different subtypes of P_{2Y}-purinoceptor. It is suggested that one subtype ($P_{2Y\alpha}$) is a ligand-activated cation channel, while the other ($P_{2Y\beta}$) is a G protein-coupled receptor (Illes & Nörenberg, 1993). In both cases Hill coefficients of about 1 were obtained indicating that one agonist molecule was required to open both non-selective cationic channels and potassium channels. In sensory neurones (Bean, 1990) and smooth muscle cells (Friel, 1988) the Hill coefficient was larger than 1 suggesting a 3:1 or 2:1 stoichiometry, respectively (Bean, 1992). We do not know the reason for this discrepancy. Finally, in contrast to ATP and its analogues, adenosine evoked an outward, but not an inward current.

It is interesting to note that 2-methylthio ATP at 0 mV induced a larger outward current in proliferating than in non-proliferating microglial cells. This is in contradiction to the similar inward current amplitudes evoked by 2-methylthio ATP in proliferating and non-proliferating cells at − 70 mV (Nörenberg *et al.*, 1994b).

In search for a possible coupling of P_{2Y}-purinoceptors to G proteins, the cells were microdialysed with an enzymatically stable GDP analogue. GDP-β-S is known to block G protein-mediated effects of agonists (Dunlap *et al.*, 1987). In fact, GDP-β-S markedly decreased the outward current evoked by 2-methylthio ATP, while leaving the inward current uninfluenced. Another means of proving the involvement of G proteins in receptor-coupling is the use of pertussis toxin which selectively ADP-ribosylates α-subunits of G proteins (Dolphin, 1987). Incubation of microglial cells with pertussis toxin abolished the 2-methylthio ATP- and adenosine-induced outward currents. Hence, both P_{2Y}- and P_1-purinoceptors are probably coupled to a G protein which mediates opening of K^+ channels with or without the involvement of further protein kinases (Pfaffinger & Siegelbaum, 1990).

ATP has been reported to cause a long-lasting depolarization in proliferating rat microglia (Kettenmann *et al.*, 1993). In these cells the outwardly rectifying K^+ conductance activated by ATP apparently is not able to repolarize the membrane efficiently. Cellular damage may both activate microglia (Dickson *et al.*, 1991) and allow leakage of ATP from neurones and glia cells into the extracellular space (White & Hoehn, 1991). ATP has been shown to produce a much shorter depolarization in non-proliferating microglia than in their proliferating counterparts (Nörenberg *et al.*, 1994b). This is due to the LPS-induced expression of outwardly rectifying K^+ channels.

In conclusion, rat microglia possess both ATP-sensitive P_{2Y}- and adenosine-sensitive P_1-purinoceptors. Early inward currents are mediated by P_{2Y}-purinoceptors, while late outward currents are mediated either by P_{2Y}- or P_1-purinoceptors. Microglial cells have two suitable membrane potentials, one at − 70 mV and another at − 35 mV (Nörenberg *et al.*, 1994a). Hence, ATP may cause depolarization at the higher and hyperpolarization at the lower membrane potential, whereas adenosine elicits hyperpolarization only.

Note added in proof

Our classification of P_2-purinoceptors into $P_{2Y\alpha}$- and $P_{2Y\beta}$-subtypes is based on the rank order of agonist potencies (Illes & Nörenberg, 1993). Recently, it was proposed to name all P_2-purinoceptors utilizing ligand-gated cation channels P_{2X}-, and all P_2-purinoceptors utilizing G proteins P_{2Y}-, irrespective of their sensitivities to the presently known agonist (Abbracchio *et al.*, 1993; *Drug Develop. Res.*, **28**, 207–213).

The authors are grateful to Dr H. Kettenmann for initiating this study and for further stimulating discussions. This work was supported by grants of the Deutsche Forschungsgemeinschaft to P.I. (SFB 325, A2) and P.J.G.-H. (Ge 486/6-1).

References

ADAMS, D.O. & HAMILTON, T.A. (1987). Molecular transduction mechanisms by which IFNγ and other signals regulate macrophage development. *Immunol. Rev.*, **97**, 5–27.

BANATI, R.B., HOPPE, D., GOTTMANN, K., KREUTZBERG, G.W. & KETTENMANN, H. (1991). A subpopulation of bone marrow-derived macrophage-like cells share a unique ion channel pattern with microglia. *J. Neurosci. Res.*, **30**, 593–600.

BEAN, B.P. (1990). ATP-activated channels in rat and bullfrog sensory neurons: concentration-dependence and kinetics. *J. Neurosci.*, **10**, 1–10.

BEAN, B.P. (1992). Pharmacology and electrophysiology of ATP-activated ion channels. *Trends Pharmacol. Sci.*, **13**, 87–90.

BIGNAMI, A. (1991). Glial cells in the central nervous system. *Disc. Neurosci.*, **8**, 11–45.

BRUNS, R.F., DALY, J.W. & SNYDER, S.H. (1980). Adenosine receptors in brain membranes: binding of N^6-cyclohexyl-[^{3}H]adenosine and 1,3-diethyl-8-[^{3}H]phenylxanthine. *Proc. Natl. Acad. Sci. U.S.A.*, **77**, 5547–5551.

BURNSTOCK, G. & BUCKLEY, N.J. (1985). The classification of receptors for adenosine and adenine nucleotides. In *Methods in Pharmacology*, vol. 6. ed. Paton, D.M. pp. 193–212. New York: Plenum Press.

BURNSTOCK, G. & KENNEDY, C. (1985). Is there a basis for distinguishing two types of P_2-purinoceptor? *Gen. Pharmacol.*, **5**, 433–440.

CHRISTIE, A., SHARMA, V.K. & SHEU, S.-S. (1992). Mechanism of extracellular ATP-induced increase of cytosolic Ca^{2+} concentration in isolated rat ventricular myocytes. *J. Physiol.*, **445**, 369–388.

DICKSON, D.W., MATTIACE, L.A., KURE, K., HUTCHINS, K., LYMAN, W.D. & BROSNAN, C.F. (1991). Biology of disease. Microglia in human disease, with an emphasis on acquired immune deficiency syndrome. *Lab. Invest.*, **64**, 135–156.

DIJKSTRA, C.D., DÖPP, E.A., JOLING, P. & KRAAL, G. (1985). The heterogeneity of mononuclear phagocytes in lymphoid organs: distinct macrophage subpopulations in the rat recognized by monoclonal antibodies ED1, ED2 and ED3. *Immunology*, **54**, 589–599.

DOLPHIN, A.C. (1987). Nucleotide binding proteins in signal transduction and disease. *Trends Neurosci.*, **10**, 53–57.

DUNLAP, K., HOLZ, G.G. & RANE, S.G. (1987). G proteins as regulators of ion channel function. *Trends Neurosci.*, **10**, 241–244.

FRIEL, D.D. (1988). An ATP-sensitive conductance in single smooth muscle cells from the rat vas deferens. *J. Physiol.*, **401**, 361–380.

GALLIN, E.K. (1991). Ion channels in leukocytes. *Physiol. Rev.*, **71**, 775–811.

GARDNER, P. (1990). Potassium channels in immunoresponsive cells. In *Potassium Channels, Structure, Classification, Function and Therapeutic Potential.* ed. Cook, N.S. pp. 382–399. Chichester: Ellis Horwood.

GEBICKE-HAERTER, P.J., BAUER, J., SCHOBERT, A. & NORTHOFF, H. (1989). Lipopolysaccharide-free conditions in primary astrocyte cultures allow growth and isolation of microglial cells. *J. Neurosci.*, **9**, 183–194.

HAMILL, O.P., MARTY, E., NEHER, E., SAKMANN, B. & SIGWORTH, F.J. (1981). Improved patch-clamp techniques for high resolution current recording from cells and cell-free membrane patches. *Pflügers Arch.*, **391**, 85–100.

ILLES, P. & NÖRENBERG, W. (1993). Neuronal ATP receptors and their mechanism of action. *Trends Pharmacol. Sci.*, **14**, 50–54.

KELLER, M., JACKISCH, R., SEREGI, A. & HERTTING, G. (1985). Comparison of prostanoid forming capacity of neuronal and astroglial cells in primary culture. *Neurochem. Int.*, **7**, 655–665.

KENNEDY, C. (1990). P_1- and P_2-purinoceptor subtypes – an update. *Arch. Int. Pharmacodyn. Ther.*, **303**, 30–50.

KETTENMANN, H., BANATI, R. & WALZ, W. (1993). Electrophysiological behaviour of microglia. *Glia*, **7**, 93–101.

KETTENMANN, H., HOPPE, D., GOTTMANN, K., BANATI, R. & KREUTZBERG, G. (1990). Cultured microglial cells have a distinct pattern of membrane channels different from peritoneal macrophages. *J. Neurosci. Res.*, **26**, 278–287.

NÖRENBERG, W., APPEL, K., BAUER, J., GEBICKE-HAERTER, P.J. & ILLES, P. (1993). Expression of an outwardly rectifying K^+ channel in rat microglia cultivated on teflon. *Neurosci. Lett.*, **160**, 69–72.

NÖRENBERG, W., GEBICKE-HAERTER, P.J. & ILLES, P. (1992). Inflammatory stimuli induce a new K^+ outward current in cultured rat microglia. *Neurosci. Lett.*, **147**, 171–174.

NÖRENBERG, W., GEBICKE-HAERTER, P.J. & ILLES, P. (1994a). Voltage-dependent potassium channels in activated rat microglia. *J. Physiol.*, **475**, 15–32.

NÖRENBERG, W., LANGOSCH, J.M., GEBICKE-HAERTER, P.J. & ILLES, P. (1994b). Characterization and possible function of adenosine 5′-triphosphate receptors in activated rat microglia. *Br. J. Pharmacol.*, **111**, 942–950.

PFAFFINGER, P.J. & SIEGELBAUM, S.A. (1990). K^+ channel modulation by G proteins and second messengers. In *Potassium Channels. Structure, Classification, Function and Therapeutic Potential.* ed. Cook, N.S. pp. 117–153. Chichester: Ellis Horwood.

RIESKE, E., GRAEBER, M.B., TETZLAFF, W., CZLONKOWSKA, A., STREIT, W.J. & KREUTZBERG, G.W. (1989). Microglia and microglia-derived brain macrophages in culture: generation from axotomized rat facial nuclei, identification and characterization in vitro. *Brain Res.*, **492**, 1–14.

STREIT, W.J., GRAEBER, M.B. & KREUTZBERG, G.W. (1988). Functional plasticitity of microglia: a review. *Glia*, **1**, 301–307.

THOMAS, W.E. (1992). Brain macrophages: evaluation of microglia and their functions. *Brain Res. Rev.*, **17**, 61–74.

WALZ, W., ILSCHNER, S., OHLEMEYER, C., BANATI, R. & KETTENMANN, H. (1993). Extracellular ATP activates a cation conductance and a K^+ conductance in cultured microglial cells from mouse brain. *J. Neurosci.*, **13**, 4403–4411.

WHITE, T.D. & HOEHN, K. (1991). Release of adenosine and ATP from nervous tissue. In *Adenosine in the Nervous System.* ed. Stone, T.W. pp. 173–195. London: Academic Press.

(Received January 20, 1994
Revised April 5, 1994
Accepted May 4, 1994)

Br. J. Pharmacol. (1994), **113**, 35–42

Investigation of the endogenous chemoattractants involved in ^{111}In-eosinophil accumulation in passive cutaneous anaphylactic reactions in the guinea-pig

[1]Vivian B. Weg, [2]Malcolm L. Watson, [3]Lucia H. Faccioli & Timothy J. Williams

Department of Applied Pharmacology, National Heart & Lung Institute, Dovehouse Street, London SW3 6LY

1 Eosinophil accumulation and plasma extravasation are features of type I allergic responses. In an attempt to characterize the mediators of these responses, we have examined the local accumulation of ^{111}In-eosinophils and leakage of ^{125}I-human serum albumin (^{125}I-HSA) during passive cutaneous anaphylaxis (PCA) reactions and in response to defined inflammatory mediators in the guinea-pig. Animals were passively sensitized by intradermal injection of anti-bovine gamma globulin antibody (50 µl, 1/50 dilution). After 20–24 h, animals were injected intravenously with ^{111}In-eosinophils and ^{125}I-HSA for the measurement of cell accumulation and plasma leakage, respectively.

2 When injected into sensitized sites, antigen caused a dose-related increase in the accumulation of ^{111}In-eosinophils and plasma leakage in guinea-pig skin. Time course experiments over 24 h revealed that the maximal rate of ^{111}In-eosinophil accumulation occurred over the first 90 min, with little accumulation at later time points. Plasma leakage was completed within the first 30 min after challenge. Responses to the mast cell degranulator, compound 48/80, exhibited very similar responses to the PCA reaction.

3 Co-injection of antigen with the PAF antagonist, WEB 2086 (10^{-7} mol/site) or the 5-lipoxygenase inhibitor, PF 5901 (10^{-7} mol/site) did not significantly alter the accumulation of ^{111}In-eosinophils or plasma leakage, whereas these drug doses abolished responses to exogenous PAF (10^{-9} mol/site) and arachidonic acid (AA, 3×10^{-8} mol/site), respectively. The H_1 receptor antagonist chlorpheniramine (2.5×10^{-8} mol/site) did not reduce antigen-induced ^{111}In-eosinophil accumulation. Drug combinations were also injected with antigen into sensitized sites, but were unable to reduce ^{111}In-eosinophil accumulation.

4 These results indicate that anaphylactic eosinophil accumulation in this model involves mediators other than histamine, PAF or lipoxygenase products. This is in contrast to plasma leakage in this reaction, which can be abolished by a combination of antagonists blocking these mediators.

Keywords: Passive cutaneous anaphylaxis (PCA); compound 48/80; eosinophils; PAF; leukotriene B_4 (LTB_4); histamine

Introduction

Type I hypersensitivity responses are conveniently studied in the form of the passive cutaneous anaphylaxis (PCA) reaction, as coined by Ovary in 1950 (Ovary, 1950). In the guinea-pig, both IgE and IgG_1 antibodies are capable of evoking anaphylactic reactions (Perini & Mota, 1972; Ovary *et al.*, 1976). Upon challenge with specific antigen the release of inflammatory mediators from sensitized mast cells leads to an increase in vascular permeability and consequently plasma extravasation into tissues. Infiltration of inflammatory cells such as neutrophils and eosinophils is also observed at PCA sites in different species (Kay, 1970; Nourshargh *et al.*, 1989; Wershil *et al.*, 1991). This type of response contributes to the pathology of several diseases such as extrinsic asthma, atopic eczema and allergic rhinitis (reviewed in Samter, 1978).

Eosinophil accumulation is a hallmark of the inflammation associated with infection with helminthic parasites and allergic disorders. Allergic patients have elevated levels of circulating eosinophils and these cells accumulate after antigenic challenge in the skin and airways (de Monchy *et al.*, 1985; Henocq & Vargaftig, 1988; Lozewicz *et al.*, 1991). There is now considerable evidence implicating the eosinophil in the pathophysiology of asthma. Following activation, eosinophils release a variety of preformed and newly synthesized mediators (reviewed in Kay & Corrigan, 1992) which are thought to contribute to the development of this disease. Indeed, several studies show the presence of eosinophils and their products in bronchoalveolar fluid from asthmatics (de Monchy *et al.*, 1985; Kay *et al.*, 1986; Diaz *et al.*, 1989). In addition, it has been shown recently in an *Ascaris*-challenge primate model that an antibody to intercellular adhesion molecule 1 that inhibited lung eosinophil accumulation also reduced bronchial hyper-reactivity (Wegner *et al.*, 1990).

An increased understanding of the basic mechanisms underlying the recruitment of eosinophils *in vivo* may therefore have important therapeutic consequences. Nevertheless, despite much progress, the mechanisms that mediate and regulate the accumulation of this cell type in sites of allergic inflammation remain unclear. Several mediators such as platelet activating factor (PAF) (Wardlaw *et al.*, 1986), leukotriene B_4 (LTB_4) (Czarnetzki & Mertensmeier, 1985) and C5a (Ogawa *et al.*, 1981) have been described as chemotactic for eosinophils *in vitro*. However, results obtained with *in vitro* chemotaxis cannot be safely extrapolated in the *in vivo* situation since such test systems do not mimic all the requirements for cell adhesion and transmigration across the endothelial cell barrier. For this reason, it was important to establish an animal model that allowed detailed investigation of eosinophil accumulation in defined allergic inflammatory reactions. In a previous study, we developed a system for measuring the accumulation of ^{111}In-eosinophils *in vivo* and showed that guinea-pig C5a des Arg, human recombinant C5a, PAF and LTB_4 are able to induce eosinophil accumulation in guinea-pig skin (Faccioli *et al.*, 1991). Subsequently, we demonstrated that a monoclonal antibody to very late

[1] Author for correspondence.
Present address: [2] Dept. Pharmacology, University of Bath, Claverton Down, Bath BA2 7AY and [3]Fac Medicina de Ribeirao Preto, Departamento de Parasitologia, Microbiologia e Imunologia, Av. Bandeirantes, No 3900, Monte Alegre, 14049-900 Ribeirao Preto-SP, Brazil.

activation antigen-4 inhibits the accumulation of ^{111}In-eosinophils in response to inflammatory mediators and during a PCA reaction (Weg *et al.*, 1993). In the present study, in order to elucidate further the nature of the inflammatory mediators involved in eosinophil accumulation *in vivo*, we have used this method to examine eosinophil infiltration during PCA reactions in the guinea-pig. In addition, compound 48/80, was used in comparison to study non-immunological activation and degranulation of mast cells.

Methods

Animals

Ex-breeder Dunkin-Hartley cell donor guinea-pigs (800–900 g) and Dunkin-Hartley test guinea-pigs (300–500 g) of either sex were purchased from Harlan-Olac, Oxon.

Preparation of guinea-pig PCA serum

Guinea-pigs were immunised by subcutaneous injection of 0.2 mg BGG in 0.2 ml Freund's complete adjuvant, divided between the rear footpads and the nape of the neck. Animals were boosted by similar injections of antigen in incomplete adjuvant on day 21. Animals were exsanguinated and serum prepared on day 30. Aliquots were stored frozen at −20°C. The fixation time course and heat stability of this antibody are consistent with IgG_1-like activity (Weg *et al.*, 1991).

Separation and ^{111}In-labelling of peritoneal guinea-pig eosinophils

This technique has been described previously in detail by Faccioli *et al.* (1991). Briefly, ex-breeder guinea-pigs received 4 injections of horse serum at 2–3 days intervals. Peritoneal cells were collected by lavage 24 h after the last injection and purified over a discontinuous Percoll gradient. The cell population was used only when the eosinophil purity was above 90%. The predominant contaminating cell type was mononuclear and a major exclusion criterion was the presence of neutrophils. The cells were then incubated with $^{111}InCl_3$ (approximately 100 μCi in 10 μl) chelated with 2-mercaptopyridine-*N*-oxide (40 μg in 0.1 ml of 50 mM PBS, pH 7.4) for 15 min at room temperature. The labelled eosinophils were washed twice and resuspended in Hanks' solution (10^7 eosinophils ml^{-1}) pH 7.3 containing cell-free citrated guinea-pig plasma to a final concentration of 10%.

Induction and measurement of plasma leakage and eosinophil accumulation in guinea-pig skin

Eosinophil infiltration and plasma leakage in the guinea-pig skin were simultaneously measured using the local accumulation of i.v. injected ^{111}In-labelled eosinophils and ^{125}I-HSA (Faccioli *et al.*, 1991).

PCA was prepared as previously described (Weg *et al.*, 1991). Guinea-pigs were sedated with Hypnorm and their dorsal skin shaved. Diluted antiserum (1/50) or purified IgG_1 (2 μg) were then injected i.d. in 50 μl volumes into the dorsal skin. After a fixation period of 20–24 h 1 ml of Hanks' solution containing 1×10^7 eosinophils mixed with ^{125}I-HSA (2.5 μCi/animal) was injected i.v. via an ear vein. Five minutes later antigen (BGG or OA) was injected i.d. into serum-pretreated sites. This protocol was modified in time course experiments so that sites were challenged at specified time points prior to the injection of ^{111}In-eosinophils and ^{125}I-HSA.

In experiments performed to determine mediator involvement in the PCA response, antigen was injected locally in a mixture with antagonists. In each of these experiments exogenous agonists (histamine, PAF and AA) were injected into naive sites in the presence and absence of their respective antagonist or in the case of AA, inhibitor of 5-lipoxygenase metabolism. Each test was performed in duplicate sites according to a balanced site injection plan with an injection volume of 100 μl/site. Except in certain time course experiments, a cardiac blood sample was collected after 2 h and animals were killed by an overdose of sodium pentobarbitone. The dorsal skin was then removed, skin sites were punched out with a 17 mm diameter punch and samples were counted together with plasma samples in an automatic gamma counter (Canberra, Berks.). The ^{111}In counts per eosinophil were determined and used to express eosinophil accumulation in each skin site in terms of number of labelled leukocytes. Leakage at each site was expressed as μl of plasma by dividing skin sample ^{125}I counts by ^{125}I counts in 1 μl of plasma.

Materials

Pentobarbitone sodium (Sagatal, 60 mg ml^{-1}) was purchased from May and Baker, Dagenham, Essex. Hypnorm (0.315 mg ml^{-1} fentanyl citrate and 10 mg ml^{-1} fluanisone) was purchased from Janssen Pharmaceutical Ltd, Grove, Oxford, ^{111}Indium chloride ($^{111}InCl_3$; 10 mCi ml^{-1} in pyrogen-free 0.04 N hydrochloric acid) and ^{125}I-human serum albumin (^{125}I-HSA; 20 mg albumin per ml of sterile isotonic saline, 50 μCi ml) were purchased from Amersham International, Amersham, Bucks. Histamine, bovine gamma globulin

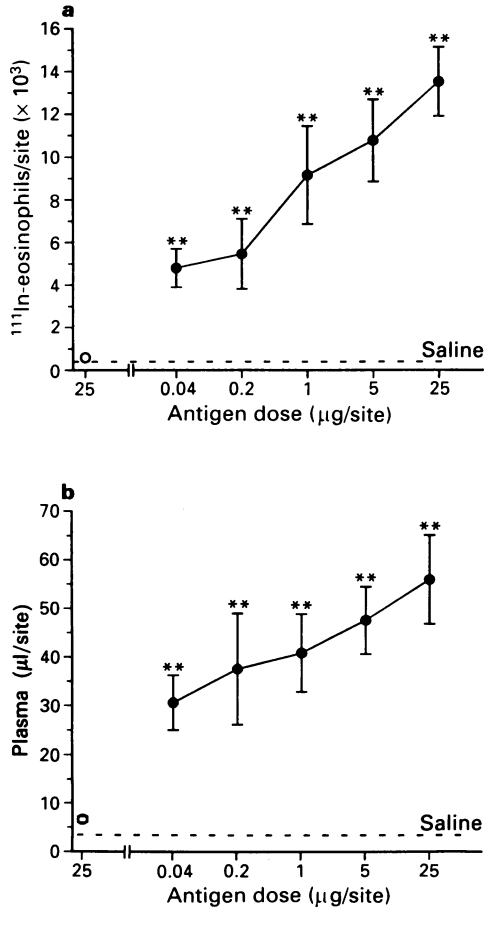

Figure 1 Effect of antigen dose on ^{111}In-eosinophil accumulation (a) and plasma leakage (b) during passive cutaneous anaphylaxis responses in guinea-pig skin. Skin sites were sensitized by i.d. injection of a fixed dose of antiserum (1/50 dilution, 50 μl/site) and challenged with the indicated dose of BGG 24 h later. The open symbols represent responses detected at naive sites injected with the highest dose (25 μg) of BGG. Dashed lines indicate control responses to saline. Points indicate mean ± s.e.mean for $n = 6$ animals. Asterisks indicate a significant difference from the BGG responses: $^{**}P < 0.01$.

(BGG), bovine serum albumin (BSA), ovalbumin (OA), 2-mercaptopyridine-*N*-oxide, dimethyl sulphoxide (DMSO), arachidonic acid (AA), were purchased from Sigma Chemical Company, Dorset. Horse serum, sterile Hanks' Balanced Salt solution (Hanks' solution 10 ×) and HEPES (1 M) were purchased from Gibco Limited, Paisley, Renfrewshire. Percoll was purchased from Pharmacia Fine Chemicals, Uppsala, Sweden. Pyrogen- and preservative-free heparin sodium (5000 u ml^{-1}) was purchased from Pabyrn Laboratories, Greenford, Middlesex. Chlorpheniramine maleate (Piriton 10 mg ml^{-1}) was purchased from Allen and Hanburys Ltd., Middlesex. PAF (1-O-hexadecyl-2-acetyl-sn-glycero-3-phosphorylcholine) was purchased from Bachem, Bubendorf, Switzerland. Stock solutions of PAF (3.6×10^{-3} M) and AA (3.3×10^{-2} M) in ethanol were stored at − 20°C and diluted in saline containing 0.1% bovine serum albumin (BSA) immediately before injection. The following substances were obtained as gifts: WEB 2086 (3-[4-(2-chlorphenyl)-9-methyl-6H-thieno [3,2-f] [1,-2,4]-triazolo-[4,3,a] [1,4]-diazepin-2yl]-1-(4-morpholinyl)-1-propanone) from Boeringher-Ingelheim AG, Ingelheim am Rhein, Germany; and PF 5901 (α-Pentyl-3-(2-quinolinylmethoxy) benzenemethanol) from Purdue Frederick, CT, U.S.A. WEB 2086 and chlorpheniramine were dissolved in saline. PF 5901 was dissolved in DMSO before dilution in saline. The final DMSO concentration injected was 3% v/v. Purified guinea-pig anti-ovalbumin IgG_1 was a gift from Dr H.J. Showell, Pfizer Central Research, CT, U.S.A.

Statistical analysis

Results are expressed as the means ± s.e.mean for *n* animals where each datum unit is the average of responses in duplicate sites. Data were analyzed by two-way analysis of variance (ANOVA) of log transformed data and statistical significance determined with the Neuman-Keuls procedure for repeated comparisons (Snedecor & Cochran, 1967).

Results

Antigen-induced plasma leakage and eosinophil accumulation during PCA reactions

Injection of antigen into guinea-pig skin sites previously sensitized with 1/50 dilution of anti-BGG antiserum led to a marked and dose-dependent eosinophil accumulation measured over 2 h (Figure 1a). Even at the lowest antigen dose tested (0.04 μg/site) there was a 10 fold increase in ^{111}In-eosinophil accumulation compared with control sites. Oedema formation was also dose-related, although with a flatter dose-response curve (Figure 1b). In the same experiments the

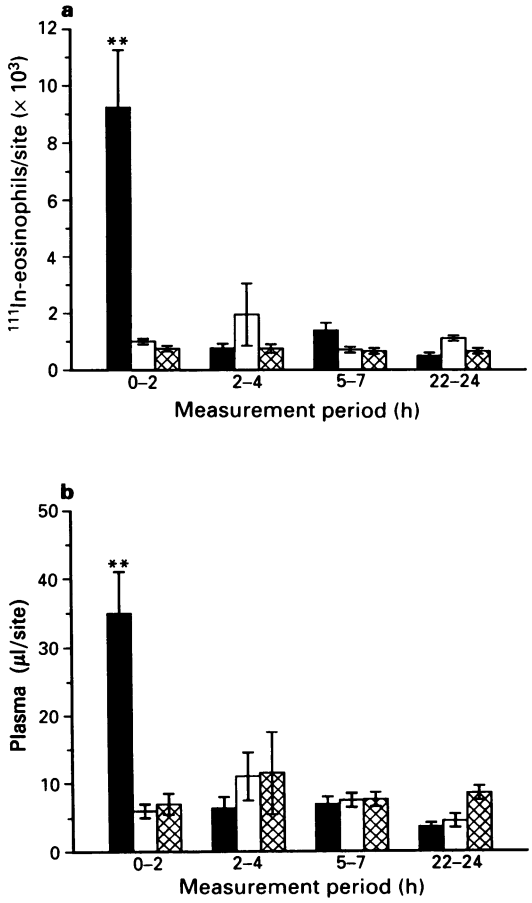

Figure 2 Long time course of ^{111}In-eosinophil accumulation (a) and plasma leakage (b) during passive cutaneous anaphylaxis responses in guinea-pig skin. Sites were injected with antisera (1/50 dilution, 50 μl/site) before injection of BGG (1 μg/site, solid columns) or saline (open columns). Responses obtained in sites pretreated with saline before injection of BGG are also shown (cross-hatched columns). BGG or saline was injected at intervals (as shown on the abscissa scale). ^{111}In-eosinophils and ^{125}I-HSA were injected i.v. and responses measured over a period of 2 h. Results are the mean ± s.e.mean for $n = 6-11$ animals. Asterisks indicate a significant difference from the BGG responses: $^{**}P < 0.01$.

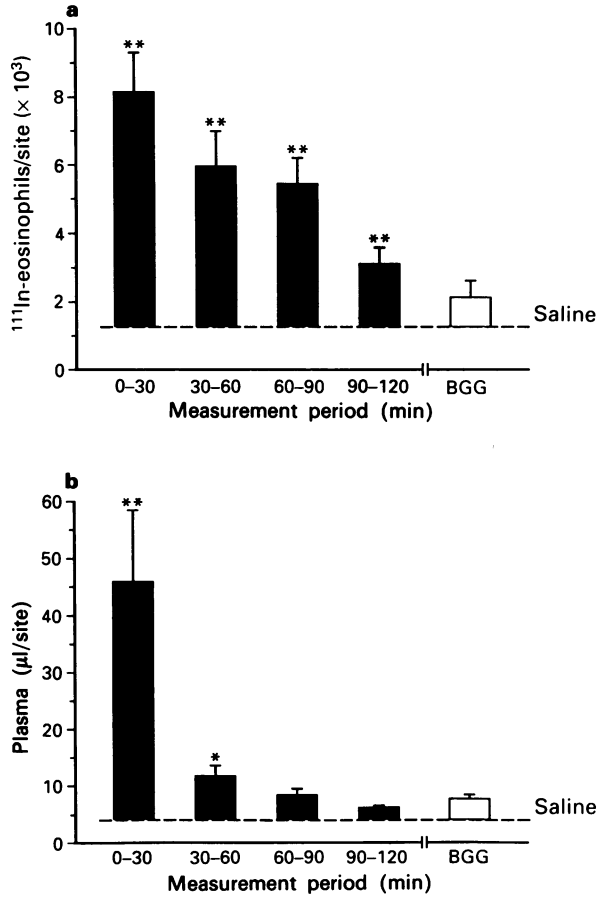

Figure 3 Short time course of ^{111}In-eosinophil accumulation (a) and plasma leakage (b) during passive cutaneous anaphylaxis responses in guinea-pig skin. Sites were injected with antisera (1/50 dilution, 50 μl/site) 24 h before injection of BGG (1 μg/site, solid columns). BGG was injected at intervals (as shown on the abscissa scale). Responses obtained in sites pretreated with saline before injection of BGG are also shown (open columns). Dashed lines indicate control responses to saline. ^{111}In-eosinophils and ^{125}I-HSA were injected i.v. and responses measured over a period of 30 min. Results are the mean ± s.e.mean for $n = 5$ animals. Asterisks indicate a significant difference from the BGG responses: $^{*}P < 0.05$; $^{**}P < 0.01$.

highest dose of antigen (25 μg) did not cause exudation or cell accumulation at naive sites. The submaximal dose of 1 μg of BGG was used for subsequent experiments.

The temporal development of the PCA response was then studied in two stages, using a long and a short time course (Figures 2 and 3, respectively). For the long time course sensitized sites were challenged at different time points (22, 5, 2 and 0 h) prior to i.v. administration of ^{111}In-eosinophils and ^{125}I-HSA and the reaction was then measured over a period of 2 h. Using this technique, eosinophil accumulation was detected only during the period after injection of radiolabelled cells, allowing the examination of rates of accumulation at different periods during the reaction. A pronounced eosinophil accumulation was observed at sites challenged at the time of ^{111}In-eosinophil injection ($t = 0-2$ h, Figure 2a). In contrast, no accumulation of ^{111}In-eosinophils was observed at sites challenged 2, 5 or 22 h before injection of radiolabel. Increased plasma leakage was also only apparent during the first measurement period ($t = 0-2$ h, Figure 2b). In short time course experiments we modified this protocol to examine ^{111}In-eosinophil and plasma leakage over 30 min time intervals during the first 2 h of the PCA reaction. Sensitized sites were challenged at 90, 60, 30 or 0 min prior to the i.v. injection of ^{111}In-eosinophils and ^{125}I-HSA. Figure 3 shows that while the leakage of plasma was almost complete during the first 30 min (Figure 3b), ^{111}In-eosinophil continued to accumulate throughout the 2 h period (Figure 3a). Therefore, in subsequent experiments measurements were made over the first 2 h of the reaction.

Study of the mediators involved in the PCA reaction

The effects of chlorpheniramine (2.5×10^{-8} mol/site), an H_1-receptor antagonist; WEB 2086 (10^{-7} mol/site), a PAF receptor antagonist; and PF 5901 (10^{-7} mol/site), a 5-lipoxygenase inhibitor; were tested against cutaneous anaphylactic responses elicited by 1 μg of BGG. It was observed that none of these drugs, when given alone, was capable of significantly reducing ^{111}In-eosinophil accumulation (Figure 4a) during the PCA reaction. Plasma leakage in response to this dose of antigen was partially inhibited by chlorpheniramine, but not by WEB 2086 or PF 5901 (Figure 4b). At control sites in the same experiments PAF (10^{-9} mol/site) and AA (3×10^{-8} mol/site) caused the accumulation of ^{111}In-eosinophils and these responses were abolished by WEB 2086 or PF 5901 respectively. The inhibition of AA by PF 5901 indicates that the effect of AA is probably mediated by metabolism to chemotactic 5-lipoxygenase products such as LTB_4. Histamine (2.5×10^{-8} mol/site) was unable to induce ^{111}In-eosinophil accumulation (Figure 4c).

The effect of a combination of the three drugs (chlorpheniramine, WEB 2086 and PF 5901) was then tested against the PCA response. As shown in Figure 4b the combined treatment virtually abolished oedema formation, but

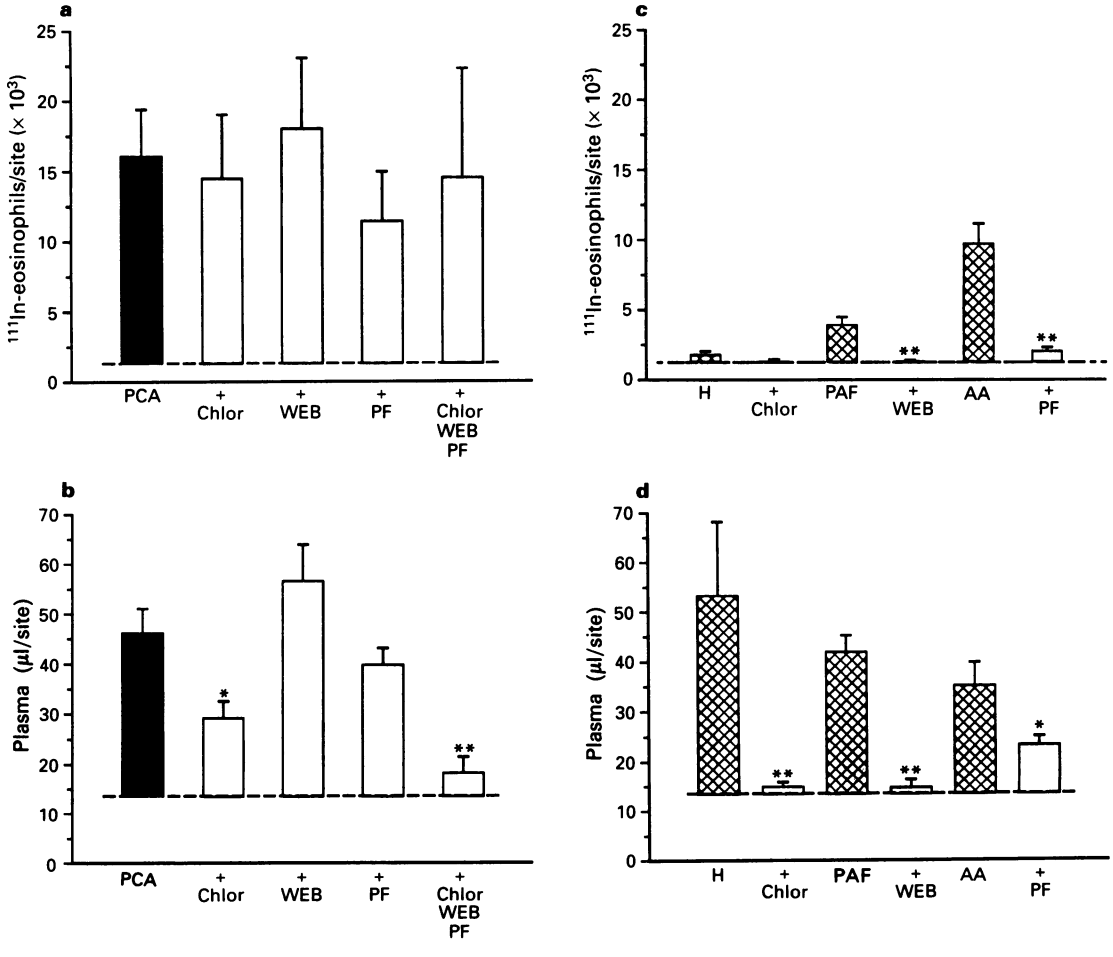

Figure 4 Effects of chlorpheniramine (Chlor, 2.5×10^{-8} mol/site); WEB 2086 (WEB, 10^{-7} mol/site) and PF 5901 (PF, 10^{-7} mol/site) on ^{111}In-eosinophil accumulation (a) and plasma leakage (b) during passive cutaneous anaphylaxis (PCA) responses in guinea-pig skin. BGG (1 μg/site) was injected without (solid columns) and with (open columns) drugs as indicated on the abscissa scale. Also shown are control responses (c and d) to histamine (H, 2.5×10^{-8} mol/site); PAF (PAF, 10^{-9} mol/site) and arachidonic acid (AA, 3×10^{-8} mol/site) in the presence (open columns) or absence (cross hatched columns) of their respective antagonists or inhibitor of metabolism. The dashed lines indicate control responses to saline. Results are the mean ± s.e. mean for $n = 4-10$ animals. $^*P < 0.05$; $^{**}P < 0.01$.

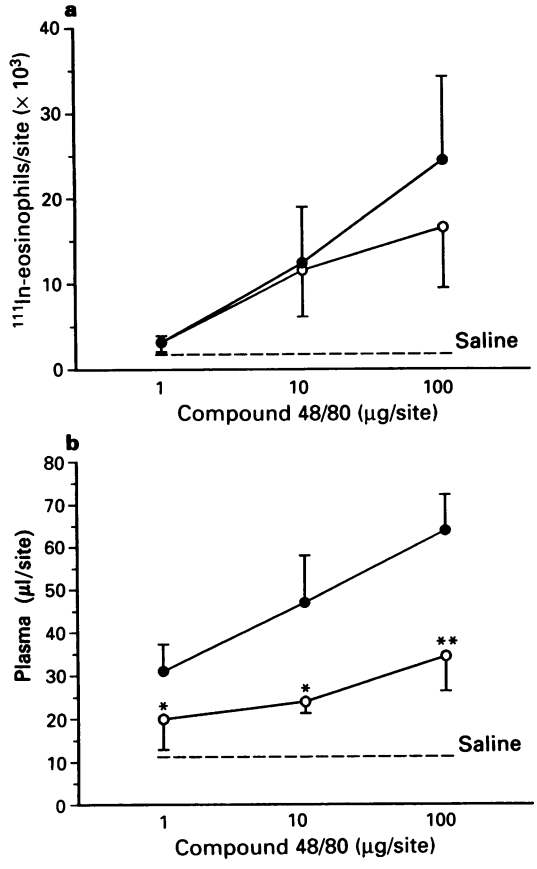

Figure 5 Effect of chlorpheniramine on ^{111}In-eosinophil accumulation (a) and plasma leakage (b) during 48/80-induced reactions. The indicated dose of 48/80 was injected without (●) or with (○) antagonist at 2.5×10^{-8} mol/site. Dashed lines indicate control responses to saline. Results are the mean ± s.e.mean for $n = 4$ animals. $^*P < 0.05$; $^{**}P < 0.01$.

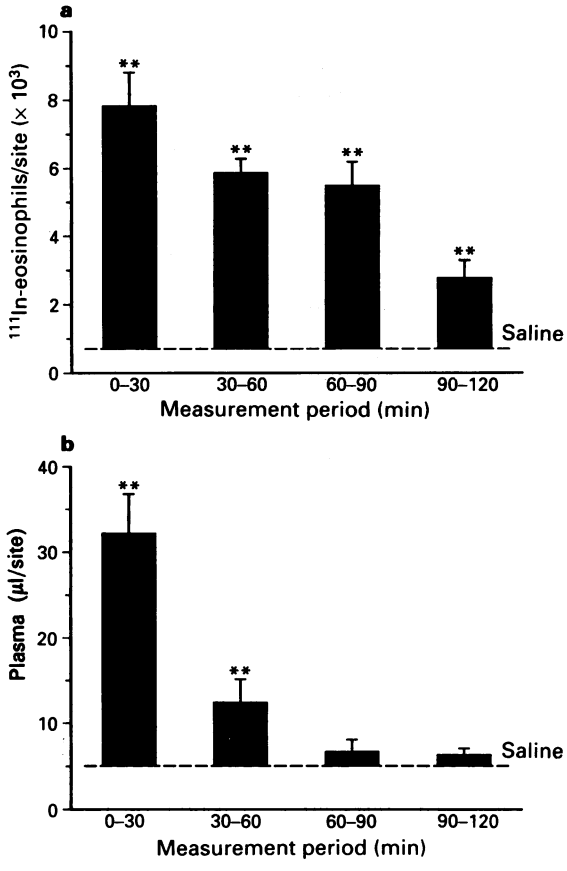

Figure 6 Time course of ^{111}In-eosinophil accumulation (a) and plasma leakage (b) induced by 48/80 in guinea-pig skin. Compound 48/80 (100 μg/site) was injected at intervals (as shown on the abscissa scale). Dashed lines indicate control responses to saline. ^{111}In-eosinophils and ^{125}I-HSA were injected i.v. and responses measured over a period of 30 min. Results are the mean ± s.e.mean for $n = 4$ animals. Asterisks indicate a significant difference from the saline responses: $P < 0.01$.

had no significant effect on cell accumulation (Figure 4a). In further experiments, purified anti-ovalbumin IgG_1 (2 μg/site) was used to sensitize the guinea-pig skin. Challenge of sites sensitized with IgG_1 elicited similar ^{111}In-eosinophil responses to those occurring at sites sensitized with unfractionated sera. Again a combination of chlorpheniramine, WEB 2086 and PF 5901 had no effect on the accumulation of ^{111}In-eosinophils, i.e. PCA = 21.45 ± 6.27 × 10^3 ^{111}In-eosinophils/site and PCA + drug combination = 17.02 ± 7.80 × 10^3 ^{111}In-eosinophils/site, for $n = 5$ animals.

^{111}In-eosinophil accumulation and oedema formation induced by compound 48/80 in the guinea-pig skin

Figure 5 shows that the local injection of compound 48/80 (1–100 μg/site) led to a dose-related increase in ^{111}In-eosinophil accumulation (Figure 5a) and oedema formation (Figure 5b) over 2 h in guinea-pig skin. The kinetics of this reaction are illustrated in Figure 6. As with the responses observed during the PCA reaction, the plasma leakage induced by 100 μg of compound 48/80 was almost complete during the first 30 min (Figure 6b) while ^{111}In-eosinophils continued to accumulate throughout the 2 h period (Figure 6a). Since compound 48/80 is a potent mast cell degranulating agent, one likely mediator to be involved in these reactions is histamine. The role of histamine was investigated by co-injecting different doses of compound 48/80 with the H_1 antagonist, chlorpheniramine. It was observed that chlorpheniramine significantly inhibited the oedema formation (Figure 5b) without significantly reducing cell accumulation in all 48/80 doses used (Figure 5a). In addition, as observed with the PCA reaction, the combination of these drugs failed to inhibit significantly eosinophil accumulation induced by 100 μg of compound 48/80, i.e. 48/80 = 27 ± 13.68 × 10^3 ^{111}In-eosinophils/site and 48/80 + drug combination = 16.85 ± 5.79 ^{111}In-eosinophils/site, for $n = 5$ animals.

Discussion

The present results show that antigen challenge at sensitized sites induced a dose-dependent ^{111}In-eosinophil accumulation and oedema formation in guinea-pig skin. Time course experiments over 24 h revealed that the maximal rate of ^{111}In-eosinophil accumulation occurred over the first 90 min while odema formation was mainly completed within the first 30 min after antigen challenge. Thus, no evidence of a late response was found as far as these parameters were concerned. Although eosinophil accumulation is often considered a feature of the late phase response to antigen in both the skin and the airways, several investigators have also observed eosinophil infiltration within an hour of antigen challenge. Atkins *et al.* (1973) noted perivascular eosinophils in skin biopsies following ragweed challenge of sensitive patients which began at about 20 min and continued to increase over 4 h. Extracellular deposition of eosinophil granule contents such as eosinophil derived neurotoxin and major basic protein, can be detected within 15 min of challenge and are deposited throughout the dermis by 3 h (Leiferman *et al.*, 1990). An early phase influx of eosinophils (30 min after

challenge) was also observed in the nasal mucous membrane of patients with allergic rhinitis (Lozewicz *et al.*, 1991). It is also possible that in the present study the sensitization procedure employed accounts for the absence of a more prolonged ^{111}In-eosinophil accumulation. In models of actively, as opposed to passively sensitized guinea-pigs, two peaks of eosinophil recruitment were observed in the lungs and conjunctiva (Chan *et al.*, 1990; Makino *et al.*, 1991).

Although some attempts have been made to determine the chemical mediators involved in tissue eosinophilia in cutaneous anaphylaxis (Kay, 1970; Hirashima *et al.*, 1983) this reaction has not yet been fully characterized. Histamine is a well-established mediator of mast cell-dependent responses and is partly responsible for the oedema formation observed in the PCA reactions in the guinea-pigs (Weg *et al.*, 1991). Since histamine was reported to be chemotactic for human eosinophils *in vitro* (Clark *et al.*, 1975) we investigated the potential role of this mediator in causing eosinophil accumulation in the PCA response. We observed that the intradermal administration of histamine while inducing plasma leakage caused little cell accumulation and that treatment of PCA sites with the H_1 antagonist, chlorpheniramine, failed to affect ^{111}In-eosinophil infiltration in this reaction. It is therefore unlikely that endogenous histamine can account for the ^{111}In-eosinophil accumulation in guinea-pig PCA reactions.

Other possible contributors to the accumulation of ^{111}In-eosinophils in the present model may include lipid mediators such as LTB_4 and PAF. LTB_4, in addition to its potent effects on neutrophils (Ford-Hutchinson *et al.*, 1980), is also chemotactic for eosinophils *in vitro* (Czarnetzki & Mertensmeier, 1985). The intradermal injection of LTB_4 is also potent in inducing the accumulation of ^{111}In-eosinophils in the guinea-pig (Faccioli *et al.*, 1991). The eosinophil chemoattractant activity produced by challenged-sensitized guinea-pig lung fragments, formerly thought to reside in small peptides, was later identified as LTB_4 and 8,15-di-HETE (Sehmi *et al.*, 1991). Further, aerosolized LTB_4 administered by inhalation to guinea-pigs was shown to induce eosinophil accumulation (Silbaugh *et al.*, 1987) and a selective LTB_4 antagonist to inhibit eosinophil accumulation induced by antigen challenge (Richards *et al.*, 1989). PAF has been shown to be a potent mediator in stimulating human eosinophil chemotaxis *in vitro* (Wardlaw *et al.*, 1986) and induces the accumulation of eosinophils when administered to a skin window chamber in man (Henocq & Vargaftig, 1988). Furthermore, the ability of PAF to mimic several aspects of antigen challenge including bronchoconstriction, increased bronchial reactivity and tissue oedema formation (reviewed in Braquet *et al.*, 1987) suggests a potential role for PAF in the mediation of allergic responses.

In the present study, the local administration of a PAF antagonist, WEB 2086, had no significant effect on local eosinophil accumulation in the PCA suggesting that endogenous PAF is unlikely to be involved in attracting eosinophils. There was no evidence for the generation of chemotactic 5-lipoxygenase products since PF 5901 was without effect. However, PF 5901 is not a potent inhibitor and it is possible that other 5-lipoxygenase inhibitors may be active in this model. In addition, contrary to the effect on oedema formation, the combination of WEB 2086, PF 5901 and chlorpheniramine did not significantly affect the accumulation of radiolabelled eosinophils. Experiments were also performed with purified IgG_1. Results from such experiments gave very similar results to those obtained with unfractionated sera, further indicating that IgG_1 is likely to be the predominant antibody type responsible for the anaphylactic reactions investigated in these experiments. The apparent lack of involvement of PAF and LTB_4 in the present system differs from other reports where these mediators appear to be implicated in the eosinophil accumulation observed in models of lung anaphylaxis in the guinea-pig (Silbaugh *et al.*, 1987; Lellough-Tubiana *et al.*, 1988; Richards *et al.*, 1989; Gulbenkian *et al.*, 1990). Several factors could account for differences between cutaneous and lung anaphylaxis. Among those is the fact that subpopulations of mast cells show functional heterogeneity in their ability to respond to immunological (IgE/IgG_1-dependent) or non-immunological (e.g. substance P, compound 48/80) stimuli (Church *et al.*, 1991).

Mast cells from guinea-pig lung and mesentery are almost totally unresponsive to non-cytotoxic concentrations of 48/80 (Ennis & Pearce, 1980; Barrett *et al.*, 1982). Similarly, dispersed human lung mast cells (Ennis, 1982), failed to release histamine on incubation with low doses of 48/80. In contrast, 48/80 injected intradermally in the guinea-pig liberates local histamine which is accompanied by mast cell degranulation (Kay, 1970). In the same way human skin mast cells are able to respond to non-immunological stimuli such as compound 48/80 (Atkins *et al.*, 1973; Dor *et al.*, 1983). Thus guinea-pig lung and cutaneous mast cells appear to respond similarly to the corresponding human cells when challenged with 48/80. Furthermore, the fact that guinea-pig skin, but not lung mast cells, respond to 48/80 indicates functional heterogeneity between mast cell populations within this species. These observations were further extended in this study. The local administration of 48/80 in guinea-pig skin led to a dose-related oedema formation which was accompanied by the accumulation of radiolabelled-eosinophils at doses ranging from $1-100\,\mu g$/skin site of the secretagogue. Furthermore, the co-injection of 48/80 with the H_1 antagonist chlorpheniramine markedly inhibited the oedema formation induced by all doses of 48/80. In addition, like the results observed with the PCA responses, the PAF antagonist WEB 2086 and the 5-lipoxygenase inhibitor PF5901 alone or in combination failed to inhibit the local infiltration of ^{111}In-eosinophils.

Taken together these results suggest that mast cell products can be chemotactic for eosinophils and that these mediators can be released after immunological and non-immunological stimulation. From the results presented in this paper it seems unlikely that PAF, LTB_4 or histamine account for the eosinophil accumulation observed during guinea-pig PCA. Recently, it has been demonstrated that mast cells are able to produce a group of cytokines including interleukin-3 (IL-3), IL-4, IL-5 and GM-CSF (Plaut *et al.*, 1989; Wodnar-Filipowicz *et al.*, 1989), all of which have been implicated in the process of leukocyte accumulation (reviewed in Noursharghi, 1993). Furthermore, normal mast cells contain substantial stores of preformed tumour necrosis factor-α (TNFα) that are available for immediate release upon appropriate stimulation of the cell (Gordon *et al.*, 1990). Some evidence suggests that TNF (Watson *et al.*, 1993) may play a role in eosinophil accumulation, perhaps because of its action in inducing adhesion molecule expression on the endothelium, or alternatively it may be an intermediate in triggering the release of eosinophil chemoattractants. Recently, two members of the C-C chemokine family, namely RANTES and MIP-1α, have been shown to induce the migration and activation of eosinophils *in vitro* (Kameyoshi *et al.*, 1992; Rot *et al.*, 1992). Neither RANTES nor MIP-1α exhibit neutrophil activating properties (Rot *et al.*, 1992; Kameyoshi *et al.*, 1992). Furthermore, intradermal injection of IL-8 in the guinea-pig caused significant accumulation of radiolabelled eosinophils *in vivo* (Collins *et al.*, 1993). It is possible that these and/or other unidentified factors are contributing for the eosinophil accumulation observed in the present study and the generation and activity of such mediators are currently under investigation.

In summary, the present study indicates that eosinophil accumulation in this model of allergic inflammation involves mediators other than histamine, PAF or 5-lipoxygenase products. This is in contrast with the plasma leakage in this reaction, which can be abolished by a combination of antagonists blocking the effects of these mediators (Weg *et al.*, 1991). The characterization of novel eosinophil attractants may allow the development of anti-inflammatory drugs

which inhibit eosinophil-mediated tissue damage in allergic disease.

This work was supported by the National Asthma Campaign, British Biotechnology Ltd and CAPES, Brazil.

References

ATKINS, P., GREEN, G.R. & ZWEIMAN, B. (1973). Histologic studies of human skin test responses to ragweed, compound 48/80, and histamine. *J. Allergy Clin. Immunol.*, **51**, 263–273.

BARRETT, K.E., ENNIS, M. & PEARCE, F.L. (1982). Mast cells from guinea-pig lung: isolation and properties. *Br. J. Pharmacol.*, **75**, 1P.

BRAQUET, P., TOUQUI, L., SHEN, T.Y. & VARGAFTIG, B.B. (1987). Perspectives in platelet-activating factor research. *Pharmacol. Rev.*, **39**, 97–145.

CHAN, C.-C., MCKEE, K., TAGARI, P., CHEE, P. & FORD-HUTCHINSON, A. (1990). Eosinophil-eicosanoid interactions: inhibition of eosinophil chemotaxis in vivo by a LTD_4-receptor antagonist. *Eur. J. Pharmacol.*, **191**, 273–280.

CHURCH, M.K., EL-LATI, S. & OKAYAMA, Y. (1991). Biological properties of human skin mast cells. *Clin. Exp. Allergy*, **21**, 1–9.

CLARK, R.A.F., GALLIN, J.I. & KAPLAN, A.P. (1975) The selective eosinophil chemotactic activity of histamine. *J. Exp. Med.*, **142**, 1462–1476.

COLLINS, P.D., WEG, V.B., FACCIOLI, L.H., WATSON, M.L., MOQBEL, R. & WILLIAMS, T.J. (1993). Eosinophil accumulation induced by human interleukin-8 in the guinea-pig in vivo. *Immunology*, **79**, 312–318.

CZARNETZKI, B.M. & MERTENSMEIER, R. (1985). In vitro and in vivo chemotaxis of guinea pig leukocytes toward leukotriene B_4 and its w-oxidation products. *Prostaglandins*, **30**, 5–11.

DE MONCHY, J.G.R., KAUFFMAN, H.F., VENGE, P., KOETER, G.H., JANSEN, H.M., SLUITER, H.J. & DE VRIES, K. (1985). Bronchoalveolar eosinophilia during allergen-induced late asthmatic reactions. *Am. Rev. Respir. Dis.*, **131**, 373–376.

DIAZ, P., GONZALEZ, M.C., GALLEGUILLOS, F.R., ANCIC, P., CROMWELL, O., SHEPHERD, D., DURHAM, S.R., GLEICH, G.J. & KAY, A.B. (1989). Leukocytes and mediators in bronchoalveolar lavage during allergen-induced late-phase asthmatic reactions. *Am. J. Respir. Dis.*, **139**, 1383–1389.

DOR, P.J., VERVLOET, D., SAPENE, M., ANDRAC, L., BONERANDI, J.J. & CHARPIN, J. (1983). Induction of late cutaneous reaction by kallikrein injection: comparison with allergic-like late response to compound 48/80. *J. Allergy Clin. Immunol.*, **71**, 363–370.

ENNIS, M. (1982). 3. Histamine release. Histamine release from human pulmonary mast cells. *Agents Actions*, **12**, 60–63.

ENNIS, M. & PEARCE, F.L. (1980). Differential reactivity of isolated mast-cells from the rat and guinea pig. *Eur. J. Pharmacol.*, **66**, 339–345.

FACCIOLI, L.H., NOURSHARGH, S., MOQBEL, R., WILLIAMS, F.M,. SEHMI, R., KAY, A.B. & WILLIAMS, T.J. (1991). The accumulation of ^{111}In-eosinophils induced by inflammatory mediators in vivo. *Immunology*, **73**, 222–227.

FORD-HUTCHINSON, A.W., BRAY, M.A., DOIG, M.V., SHIPLEY, M.E. & SMITH, M.J.H. (1980). Leukotriene B, a potent chemokinetic and aggregating substance released from polymorphonuclear leukocytes. *Nature*, **286**, 264–265.

GORDON, J.R., BURD, P.R. & GALLI, S.J. (1990). Mast cells as a source of multifunctional cytokines. *Immunology Today*, **11**, 458–464.

GULBENKIAN, A.R., FERNANDEZ, X., KREUTNER, W., MINNICOZZI, M., WATNICK, A.S., KUNG, T. & EGAN, R.W. (1990). Anaphylactic challenge causes eosinophil accumulation in bronchoalveolar lavage fluid of guinea pigs. Modulation by Betamethasone, Phenidone, Indomethacin, WEB 2086, and a novel anti-allergy agent, SCH 37224. *Am. Rev. Respir. Dis.*, **142**, 680–685.

HENOCQ, E. & VARGAFTIG, B.B. (1988). Skin eosinophilia in atopic patients. *J. Allergy Clin. Immunol.*, **81**, 691–695.

HIRASHIMA, M., TASHIRO, K., HIROTSU, Y. & HAYASHI, H. (1983). The mediation of tissue eosinophilia in hypersensitivity reactions. Comparative study of tissue eosinophilia in the skin lesions of local and systemic passive cutaneous anaphylactic reactions. *Immunology*, **50**, 85–91.

KAMEYOSHI, Y., DORSCHNER, A., MALLET, A.I., CHRISTOPHERS, E. & SCHRODER, J.-M. (1992). Cytokine RANTES released by thrombin-stimulated platelets is a potent attractant for human eosinophils. *J. Exp. Med.*, **176**, 587–592.

KAY, A.B. (1970). Studies of eosinophil leucocyte migration. I. Eosinophil and neutrophil accumulation following antigen-antibody reactions in guinea-pig skin. *Clin. Exp. Immunol.*, **6**, 75–86.

KAY, A.B. & CORRIGAN, C.J. (1992). Eosinophils and neutrophils. *Br. Med. Bull.*, **48**, 51–64.

KAY, A.B., WARDLAW, A.J., COLLINS, J.V,. DUNNETTE, S. & GLEICH, G.J. (1986). Eosinophil and major basic protein in broncho alveolar lavage in asthma: Relationship to non-specific hyperreactivity. *J. Allergy Clin. Imunol.*, **77**, 236.

LEIFERMAN, K.M., FUJISAWA, T., GRAY, B.H. & GLEICH, G.J. (1990). Extracellular deposition of eosinophil and neutrophil granule proteins in the IgE-mediated cutaneous late phase reaction. *Lab. Invest.*, **62**, 579–589.

LELLOUCH-TUBIANA, A., LEFORT, J., SIMON, M.-T., PFISTER, A. & VARGAFTIG, B.B. (1988). Eosinophil recruitment into guinea pig lungs after PAF-acether and allergen administration. Modulation by prostacyclin, platelet depletion, and selective antagonists. *Am. Rev. Respir. Dis.*, **137**, 948–954.

LOZEWICZ, S., GOMEZ, E., CHALSTREY, S., GATLAND, D. & DAVIES, R.J. (1991). Time course of cellular infiltration in the nasal mucosa during the immediate allergic reaction. *Int. Archs. Allergy Appl. Immunol.*, **95**, 273–277.

MAKINO, S., FUKUDA, T., MOTOJIMA, S. & YUKAWA, T. (1991). Eosinophils in airway hyperresponsiveness. In *Inflammatory Cells and Mediators in Bronchial Asthma*. ed. Agrawal, D.K. & Townley, R.G. pp. 115–132. Florida: CRC Press Inc.

NOURSHARGH, S. (1993). Mechanisms of neutrophil and eosinophil accumulation in vivo. *Am. Rev. Respir. Dis.*, **148**, S60–S64.

NOURSHARGH, S., RAMPART M., HELLEWELL, P.G., JOSE, P.J., HARLAN, J.M., EDWARDS, A.J. & WILLIAMS, T.J. (1989). Accumulation of ^{111}In-neutrophils in rabbit skin in allergic and non-allergic inflammatory reactions in vivo: inhibition by neutrophil pretreatment in vitro with a monoclonal antibody recognising the CD18 antigen. *J. Immunol.*, **142**, 3193–3198.

OGAWA, H., KUNKEL, S.L., FANTONE, J.C. & WARD, P.A. (1981). Comparative study of eosinophil and neutrophil chemotaxis and enzyme release. *Am. J. Pathol.*, **105**, 149–155.

OVARY, Z. (1950). Recherches sur l'anaphylaxie passive cutanee locale du cobaye; influence de la procaine et de l'adrenaline en infiltrations locales dans l'anaphylaxie passive cutanee locale due cobaye. *Rev. Immunol.*, **14**, 375–378.

OVARY, Z., KAPLAN, B. & KOJIMA, S. (1976). Characteristics of guinea pig IgE. *Int. Archs. Allergy Appl. Immunol.*, **51**, 416–428.

PERINI, A. & MOTA, I. (1972). Heterogeneity of guinea-pig homocytotropic antibodies. *Immunology*, **22**, 915–923.

PLAUT, M., PIERCE, J.H., WATSON, C.J., HANLEY-HYDE, J., NORDAN, R.P. & PAUL, W.E. (1989). Mast cell lines produce lymphokines in response to cross-linkage of Fc epsilon RI or to calcium ionophores. *Nature*, **339**, 64–67.

RICHARDS, I.M., GRIFFIN, R.L., OOSTVEEN, J.A., MORRIS, J., WISHKA, D.G. & DUNN, C.J. (1989). Effect of the selective leukotriene B_4 antagonist U-75302 on antigen-induced bronchopulmonary eosinophilia in sensitized guinea pigs. *Am. Rev. Respir. Dis.*, **140**, 1712–1716.

ROT, A., KRIEGER, M., BRUNNER, T., BISCHOFF, S.C., SCHALL, T.J. & DAHINDEN, C.A. (1992). RANTES and macrophage inflammatory protein 1α induce the migration and activation of normal human eosinophil granulocytes. *J. Exp. Med.*, **176**, 1489–1495.

SAMTER, M. (1978). *Immunological Diseases*. Volume II. New York, USA: Little, Brown & Co.

SEHMI, R., CROMWELL, O., TAYLOR, G.W. & KAY, A.B. (1991). Identification of guinea pig eosinophil chemotactic factor of anaphylaxis as leukotriene B_4 and 8(S)-Dihydroxy-5,9,11,13 (Z,E,Z,E)-Eicosatetraenoic acid. *J. Immunol.*, **147**, 2276–2283.

SILBAUGH, S.A., STENGEL, P.W., WILLIAMS, G.D., HERRON, D.K, GALLAGHER, P. & BAKER, S.R. (1987). Effects of leukotriene B_4 inhalation. Airway sensitization and lung granulocyte infiltration in the guinea pig. *Am. Rev. Respir. Dis.*, **136**, 930–934.

SNEDECOR, G.W. & COCHRAN, W.G. (1967). *Statistical Methods*. Iowa: Iowa State UP.

WARDLAW, A.J., MOQBEL, R., CROMWELL, O. & KAY, A.B. (1986). Platelet-activating factor. A potent chemotactic and chemokinetic factor for human eosinophils. *J. Clin. Invest.*, **78**, 1701–1706.

WATSON, M.L., SMITH, D., BOURNE, A.D., THOMPSON, R.C. & WESTWICK, J. (1993). Cytokines contribute to airway dysfunction in antigen-challenged guinea pigs: Inhibition of airway hyperreactivity, pulmonary eosinophil accumulation and tumor necrosis factor generation by pretreatment with an interleukin-1 receptor antagonist. *Am. J. Respir. Cell Mol. Biol.*, **8**, 365–369.

WEG, V.B., WATSON, M.L., CORDEIRO, R.S.B. & WILLIAMS, T.J. (1991). Histamine, leukotriene D_4 and platelet activating factor in guinea-pig passive cutaneous anaphylaxis. *Eur. J. Pharmacol.*, **204**, 157–163.

WEG, V.B., WILLIAMS, T.J., LOBB, R.R. & NOURSHARGH, S. (1993). A monoclonal antibody recognising very late activation antigen-4 (VLA-4) inhibits eosinophil accumulation in vivo. *J. Exp. Med.*, **177**, 561–566.

WEGNER, C.D., GUNDEL, R.H., REILLY, P., HAYNES, N., LETTS, L.G. & ROTHLEIN, R. (1990). Intercellular adhesion molecule-1 (ICAM-1) in the pathogenesis of asthma. *Science*, **247**, 456–459.

WERSHIL, B.K., WANG, Z.-S., GORDON, J.R. & GALLI, S.J. (1991). Recruitment of neutrophils during IgE-dependent cutaneous late phase reactions in the mouse is mast cell-dependent. Partial inhibition of the reaction with antiserum against tumor necrosis factor-alpha. *J. Clin. Invest.*, **87**, 446–453.

WODNAR-FILIPOWICZ, A., HEUSSER, H. & MORONI, C. (1989). Production of the haemopoietic growth factors GM-CSF and interleukin-3 by mast cells in response to IgE receptor-mediated activation. *Nature*, **339**, 150–152.

(Received October 21, 1993
Revised April 14, 1994
Accepted May 4, 1994)

Br. J. Pharmacol. (1994), **113**, 43–48

Inhibition by KF17837 of adenosine A_{2A} receptor-mediated modulation of striatal GABA and ACh release

*†Masako Kurokawa, *Ian P. Kirk, *Karen A. Kirkpatrick, †Hiroshi Kase & [1]*Peter J. Richardson

*Department of Pharmacology, University of Cambridge, Tennis Court Road, Cambridge CB2 1QJ and †Pharmaceutical Research Laboratories, Kyowa Hakko Kogyo Co. Ltd., 1188 Shimotogari, Nagaizumi-cho, Sunto-gun, Shizuoka-ken 411, Japan

1 The effect of the A_{2A} adenosine receptor agonist, 2-*p*-(-2-carboxyethyl)phenethyl-amino-5'-N-ethylcarboxamidoadenosine (CGS 21680) on the potassium evoked release of [^{3}H]-γ-aminobutyric acid ([^{3}H]-GABA) from nerve terminals derived from the caudate-putamen and the globus pallidus of the rat was compared. In both preparations CGS 21680 (1 nM) inhibited the [^{3}H]-GABA release evoked by 15 mM KCl but had no effect on that evoked by 30 mM KCl.

2 The ability of CGS 21680 (1 nM) to inhibit the release of [^{3}H]-GABA from striatal nerve terminals was unaffected by the presence of the GABA receptor antagonists, bicuculline (10 μM), phaclofen (100 μM) and 2-hydroxysaclofen (100 μM). Similarly the opioid receptor antagonist, naloxone (10 μM), the adenosine A_1 receptor antagonist, 8-cyclopentyl-1,3-dipropylxanthine (DPCPX, 40 nM), and the cholinoceptor antagonists, mecamylamine (10 μM) and atropine (100 nM) had no effect on this inhibition.

3 The ability of CGS 21680 (0.1 nM) to stimulate the release of [^{3}H]-acetylcholine ([^{3}H]-ACh) from striatal nerve terminals was unaffected by the presence of bicuculline (10 μM), 2-hydroxysaclofen (100 μM), phaclofen (100 μM), naloxone (10 μM) and DPCPX (4 nM).

4 The novel A_{2A} receptor antagonist, (E)-8-(3,4-dimethoxystyryl)-1,3-dipropyl-7-methylxanthine (KF 17837), blocked the CGS 21680 (1 nM)-induced inhibition of [^{3}H]-GABA efflux with an EC_{50} of approximately 30 nM and also antagonized the CGS 21680 (0.1 nM)-induced stimulation of [^{3}H]-ACh release with an EC_{50} of approximately 0.3 nM.

5 It is concluded that the A_{2A} adenosine receptor is present on both GABAergic and cholinergic nerve terminals of the rat striatum and that in both the caudate-putamen and the globus pallidus this receptor inhibits [^{3}H]-GABA release. No evidence was seen for a difference in the ligand binding sites of this receptor in the two groups of nerve terminals.

Keywords: Acetylcholine release; GABA release; CGS 21680; A_{2A} adenosine receptor; rat striatum; globus pallidus; KF17837

Introduction

The adenosine A_{2A} receptor has been reported to have a number of effects in the CNS, including the modulation of transmitter release (Simpson *et al.*, 1992; Kirkpatrick & Richardson, 1993; Kirk & Richardson, 1994), the regulation of dopamine D_2 receptor affinity (Ferre *et al.*, 1991a) and the control of motor behaviour (Green *et al.*, 1982; Brown *et al.*, 1991; Barraco *et al.*, 1993; Vellucci *et al.*, 1993). This receptor, whose mRNA has been localised by *in situ* hybridisation to the GABAergic striato-pallidal medium-spiny neurones (Schiffman *et al.*, 1991), has been shown to inhibit γ-amino butyric acid (GABA) release from striatal nerve terminals (Kirk & Richardson, 1993; 1994). There is also considerable evidence for the presence of A_{2A} receptors on striatal cholinergic nerve terminals (Brown *et al.*, 1990; James & Richardson, 1993; Kirk & Richardson, 1993; 1994; Kirkpatrick & Richardson, 1993), despite the fact that *in situ* hybridisation, using probes derived from the cloned A_{2A} receptor sequence (Maenhaut *et al.*, 1990) failed to detect any expression of A_{2A} receptor mRNA in striatal cholinergic neurones (Schiffman *et al.*, 1991). Although this may have been because the levels of mRNA expression in these cells was below the limit of detection, it is also possible that the receptors present on the two nerve terminal populations are significantly different in their primary sequences.

The density of the A_{2A} receptor is between 4 and 10 fold greater in the striatum than other regions of the CNS (Bruns *et al.*, 1987), even though some A_{2A} like receptor effects have been observed in other areas of the brain (Barraco & Phillis; 1991; Simpson *et al.*, 1992; Sebastião & Ribeiro, 1992). Since the A_{2A} receptor is present on the striato-pallidal neurones which are overactive in Parkinson's disease (Mitchell *et al.*, 1990), and because the A_{2A} receptor tends to oppose the influence of dopamine D_2 receptors *in vitro* and *in vivo*, (Brown *et al.*, 1990; Ferre *et al.*, 1991b; 1993; Vellucci *et al.*, 1993; Schiffman & Vanderhaghen, 1993) there has been some interest in the use of A_{2A} receptor antagonists as therapies for Parkinsons disease (e.g. Ferre & Fuxe, 1992). It is therefore important to characterize fully the effects of A_{2A} receptor stimulation. In this context it is interesting to note that in contrast to our results describing an inhibition of [^{3}H]-GABA release by the A_{2A} receptor, it has been reported that this receptor stimulates GABA release from slices of the globus pallidus (Mayfield *et al.*, 1993). There are a number of possible explanations for these conflicting results, including the possibility that the effects of A_{2A} receptor stimulation may differ in the caudate-putamen and the globus pallidus. We therefore set out to determine whether any significant difference can be observed in the effect of the A_{2A} receptor on GABA release in these two areas of the striatum. Since there is also a discrepancy between the localization of the A_{2A} receptor mRNA and its observed effects on the striatal cholinergic nerve terminal, we have also further characterized the effects on acetylcholine (ACh) release. In particular we have checked that they were not simply a consequence of an inhibition of endogenous GABA release, which could have reduced the inhibitory action of endogenous GABA on labelled ACh release.

[1] Author for correspondence.

Recently a novel A_{2A} receptor antagonist, (E)-8-(3,4-dimethoxystyryl)-1,3-dipropyl-7-methylxanthine (KF17837), has been synthesized which shows much greater selectivity for this receptor than those previously available (Nonaka *et al.*, 1994). This therefore could provide an opportunity for determining whether the adenosine receptor(s) responsible for modulating both ACh and GABA release are of the A_{2A} subtype, and whether or not they can be distinguished by this ligand.

Methods

Subcellular fractionation

Nerve terminals were prepared from the striatum of adult Wistar rats of either sex. In most experiments the whole striatum, including both caudate-putamen and globus pallidus, was used but in experiments where the differences between the two areas of the striatum were being investigated, great care was taken to dissect each area free of the other. After dissection the tissue was homogenized in 0.32 M sucrose, 10 mM HEPES (pH 7.4) with a motor driven (640 r.p.m.), loose fitting Teflon-glass homogenizer. After centrifugation (1,000 *g*, 10 min, 4°C) the terminals were purified on a Percoll gradient (Verhage *et al.*, 1989) and resuspended in a balanced salt solution (pH 7.4) of the following composition (mM): NaCl 126.4, KCl 3.6, NaH_2PO_4 0.4, $NaHCO_3$ 5, HEPES 20, $MgCl_2$ 1, glucose 10 and $CaCl_2$ 2. After centrifugation (15,000 *g*, 20 min, 4°C) the nerve terminals were stored on ice for up to 3 h prior to use.

[^{3}H]-GABA release assays

The nerve terminals were resuspended in the balanced salt solution containing 0.1 mM aminoxyacetic acid to give a final protein concentration of 0.5–1.5 mg ml^{-1} and then incubated at 37°C for 10 min, after which [^{3}H]-GABA was added to give a final concentration of 0.014 μM (1 μCi ml^{-1}) in the presence of 0.1 μM unlabelled GABA. After incubation at 37°C for 60 min the nerve terminals were diluted 1:4 with perfusion buffer of the following composition (mM): NaCl 125, KCl 3, NaH_2PO_4 1, $NaHCO_3$ 22, $MgCl_2$ 1.3, glucose 10, $CaCl_2$ 1.3 containing 0.05 mM aminooxyacetic acid; 1 u ml^{-1} adenosine deaminase and 1 μM nipecotic acid. The terminals were then drawn into perfusion chambers containing Whatman GF/B filters where they were superfused at 37°C at a rate between 0.4 and 0.5 ml min^{-1} and constantly aerated with 95% O_2/5% CO_2. A series of 8 parallel perfusion chambers were used. Control and test conditions were performed in duplicate, thereby allowing a maximum of three drug concentrations plus controls to be tested with any one set of stimuli. After an equilibration period of 36 min, samples were collected at 2 min intervals and counted for radioactivity. Release of [^{3}H]-GABA was evoked by inclusion of elevated KCl (15 mM) for 90 s in the perfusion buffer. Isotonicity was maintained by a corresponding reduction in the NaCl concentration. The evoked release for each stimulus was expressed as a percentage of the total amount of radiolabel present in the synaptosomes at the point at which release was evoked. Evoked release was calculated by subtracting basal release from total release for each stimulus.

Modulation of release was assessed by changes in the ratio of the ^{3}H-label released between two stimuli spaced 12 min apart (i.e. S2/S1 ratio). The individual test ratios were then expressed as a percentage of the mean ratio in the control perfusions in order to normalize the data. Experimental controls were run in parallel, i.e. both stimuli contained elevated KCl alone, while test experiments included putative modulators in the second stimulation. Agonists were added during the depolarizing stimulus only, whereas antagonists were perfused 6 min prior to, and during depolarization. Using this system it was possible to carry out a total of four stimuli on any one run, thus enabling a second set of release ratios to be calculated.

[^{3}H]-acetylcholine release assays

Two methods were used to assess the effect of A_{2A} receptor stimulation on the release of [^{3}H]-ACh. In the perfusion method a similar system to that described above was used except 1.0 μM [^{3}H]-choline was used to label the terminals and physostigmine (100 μM) was included in the loading buffer (pH 7.4) which had the following composition (mM): NaCl 125, KCl 4.75, $MgCl_2$ 1.4, $CaCl_2$ 2.0, HEPES 20.0 and glucose 10.0 and the synaptosomes incubated for 30 min at 37°C. The identity of the ^{3}H label released by elevated KCl concentrations in this system has been shown to be greater than 75% ACh (Kirk & Richardson, 1994). In the second method, after a 2 min preincubation at 37°C the release of ACh was evoked from the nerve terminals by the addition of 75 μM veratridine in the presence of 100 μM physostigmine. After a further 2 min the reaction was stopped by centrifugation at 10,000 *g* for 2 min at 0°C. The release of [^{3}H]-ACh into the supernatant was then measured by the choline kinase extraction method (Pittel *et al.*, 1990), as modified by Kirkpatrick & Richardson (1993).

Drugs and chemicals

[^{3}H]-GABA (60 Ci mmol^{-1}) and [^{3}H]-choline (75 Ci mmol^{-1}) were obtained from Amersham International. Phaclofen, 2-hydroxysaclofen, naloxone, physostigmine, bicuculline, atropine, mecamylamine, nipecotic acid, Percoll, amino-oxyacetic acid and adenosine deaminase were all from Sigma Chemicals. 2-*p*-(-2-Carboxyethyl)phenethylamino 5'-*N*-ethylcarboxamidoadenosine (CGS 21680) and 8-cyclopentyl-1,3-dipropylxanthine (DPCPX) were from Research Biochemicals Incorporated. (E)-1,3-dipropyl-7-methyl-8-(3,4-dimethoxystyryl) xanthine (KF17837) was from Kyowa Hakko Kogyo Co. Ltd., Shinzuoka-Ken, Japan. DPCPX and KF17837 were dissolved in dimethylsulphoxide, the final concentration of this solvent being 0.02%. KF17837 is stereoselective, the E isomer exhibiting a higher affinity for the A_{2A} receptor than the Z isomer. Exposure of the E isomer to visible light results in a photo-isomerization which finally results in a stable mixture of the two isomers. Such a mixture was used in these experiments, in which the ratio of the E to Z isomers was 2:8 (Nonaka *et al.*, 1994). All other chemicals were of the highest available purity and were obtained from BDH Chemicals.

Statistics

Statistical analysis of the normalized data (derived from each individual determination) was evaluated using either a one way analysis of variance (ANOVA) followed by a Dunnett's test, when making multiple comparisons from the same set of data with control values. Alternatively, Student's *t* test was used for comparing individual treatments with their respective controls. In both cases a probability of $P<0.05$ was accepted as denoting a statistically significant difference.

Results

In order to determine if there was a difference in the effect of adenosine A_{2A} receptor stimulation in two areas of the striatum, the effect of the A_{2A} selective agonist, CGS 21680 (Jarvis *et al.*, 1989; Lupica *et al.*, 1990) on [^{3}H]-GABA release was measured separately in nerve terminals derived from the caudate-putamen and the globus pallidus. CGS 21680, 1 nM, was used as this concentration of the A_{2A} agonist has previously been shown to have a maximal effect on [^{3}H]-GABA release from nerve terminals derived from the whole striatum (Kirk & Richardson, 1994). Figure 1 shows that CGS 21680 (1 nM) inhibited the release of [^{3}H]-GABA

from both areas of the rat striatum when the stimulus was 15 mM KCl but not when the efflux of [^{3}H]-GABA was evoked by 30 mM KCl (Figure 1a,b). In the globus pallidus the inhibition of [^{3}H]-GABA release was 22.2 ± 3.8% (n = 4, Figure 1a) while the same concentration of CGS 21680 reduced the efflux of tritiated GABA from the caudate-putamen by 23.1 ± 3.2% (n = 11, Figure 1b). Figure 1 also shows that the selective A_{2A} antagonist, KF17837, greatly impaired the CGS 21680-mediated inhibition of [^{3}H]-GABA release. In the presence of KF17387 (100 nM), CGS 21680 (1 nM) inhibited the efflux of [^{3}H]-GABA by only 8.9 ± 2.0% (n = 4) in the globus pallidus (Figure 1a) and by 8.0 ± 0.5% (n = 3) in the caudate-putamen (Figure 1b). Since A_{2A} receptor stimulation had similar effects in both areas of the striatum subsequent experiments were performed using nerve terminals derived from the whole striatum.

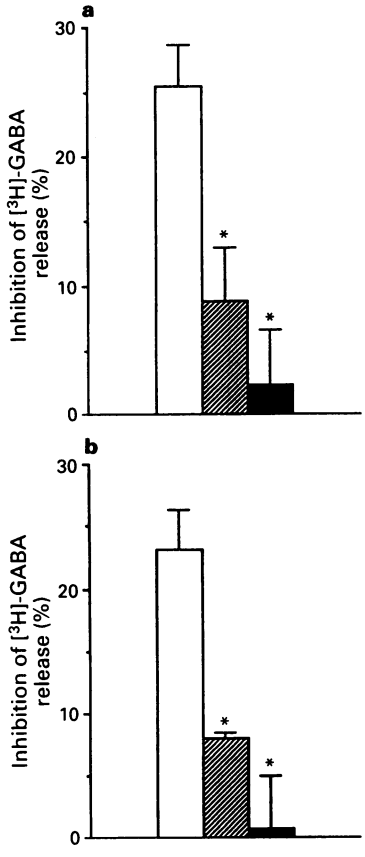

Figure 1 A_{2A} receptor-mediated inhibition of [^{3}H]-GABA release from nerve terminals of either (a) the globus pallidus or (b) caudate-putamen. Nerve terminals were perfused as described and the release of [^{3}H]-GABA evoked by 15 mM KCl (open columns), 15 mM KCl with 100 nM KF17837, (hatched columns) or 30 mM KCl (solid columns); all in the presence of 1 nM CGS 21680. The results are expressed as % inhibition of the control release of [^{3}H]-GABA, i.e. that evoked by elevated KCl in the absence of CGS 21680, and are means ± s.e.mean of 3 experiments, each experiment containing triplicate determinations. *Indicates significantly different from the inhibition of release induced in the presence of 15 mM KCl (P<0.05).

Table 1 illustrates that neither the $GABA_A$ antagonist, bicuculline (10 μM) nor the $GABA_B$ antagonist, 2-hydroxysaclofen (100 μM), had any effect on the potassium-evoked release, nor on the ability of CGS 21680 (1 nM) to inhibit evoked [^{3}H]-GABA release. Similarly, the potassium-evoked release of [^{3}H]-GABA, and its inhibition by CGS 21680, were unaffected by the presence of the cholinoceptor (muscarinic and nicotinic) antagonists atropine (100 nM) and mecamylamine (10 μM). Since the striato-pallidal neurone bearing A_{2A} receptors also express Met-enkephalin (Schiffman *et al.*, 1991), the effect of the opioid receptor antagonist, naloxone (10 μM), on the inhibition of [^{3}H]-GABA release was also assessed, as was the A_1 receptor antagonist, DPCPX (40 nM). Once again no effect was observed. None of the antagonists used had a significant effect on the basal efflux of [^{3}H]-GABA (data not shown).

Table 2 demonstrates that the ability of CGS 21680 (0.1 nM) to enhance the release of [^{3}H]-ACh from rat striatal synaptosomes is also unimpaired by the presence of GABA, opioid or A_1 adenosine receptor antagonists. The concentration of CGS 21680 (0.1 nM) was chosen because it was previously shown to affect the evoked efflux of [^{3}H]-ACh maximally (Kirkpatrick & Richardson, 1993). The antagonists used were: bicuculline (10 μM), 2-hydroxysaclofen (100 μM), phaclofen (100 μM) and DPCPX (4 nM). None of the antagonists used had any effect on the evoked release of [^{3}H]-ACh (see Table 2) nor on the basal efflux (data not shown).

In a previous study, we reported that increasing concentrations of CGS 21680 enhanced the veratridine-evoked efflux of [^{3}H]-ACh (Kirkpatrick & Richardson, 1993) but in these experiments [^{3}H]-ACh release was measured by a batch analysis method. When using this particular method it is more likely that the continued presence of endogenous released neurotransmitter(s) could affect the release of other (labelled) transmitters. Therefore, we investigated the effect of GABA receptor antagonists and naloxone on the ability of CGS 21680 to increase the veratridine (75 μM)-evoked release of [^{3}H]-ACh. Table 2 shows that under these conditions CGS 21680 (0.1 nM) enhanced the release of [^{3}H]-ACh by 22.7 ± 6.4% (n = 3). This augmentation was unaffected by the presence of the GABA receptor antagonists, bicuculline (10 μM) and phaclofen (100 μM), and naloxone (10 μM). No effects on either the veratridine-evoked release of [^{3}H]-ACh (see Table 2) nor the basal efflux were seen with any of the antagonists used.

Having established that there are adenosine A_{2A}-like receptors on both cholinergic and GABAergic nerve terminals, we assessed further the ability of the novel A_{2A} antagonist, KF17837, to inhibit the modulation of transmitter release.

Table 1 The effects of various antagonists on the evoked release of [^{3}H]-GABA from rat striatal synaptosomes in the presence and absence of CGS 21680 (1 nM)

	Antagonists alone	*Antagonists plus CGS 21680*
None	100.0 ± 3.0 (14)	75.5 ± 3.2 (14)
Bicuculline (10 μM) plus 2-hydroxysaclofen (100 nM)	100.0 ± 4.0 (4)	75.9 ± 7.2 (4)*
Atropine (100 nM) plus mecamylamine (10 μM)	97.4 ± 8.3 (3)	73.0 ± 3.7 (3)*
Naloxone (10 μM)	93.6 ± 6.6 (4)	79.8 ± 5.0 (4)*
DPCPX (40 nM)	92.1 ± 1.3 (3)	67.7 ± 6.4 (3)*

Results are expressed as a percentage of the release observed in the controls (i.e. 15 mM KCl alone) and are means ± s.e.mean from the number of experiments indicated in parentheses, each experiment containing duplicate determinations. In the control experiment the S2/S1 ratios were 1.180 ± 0.033. *Indicates significantly different from antagonists alone.

Table 2 The effect of various antagonists on the 15 mM KCl-evoked[a] and veratridine (75 μM)-evoked[b] release of [^{3}H]-ACh from rat striatal synaptosomes, in the presence and absence of CGS 21680 (0.1 nM)

	Antagonists alone	*Antagonists plus CGS 21680*
None[a]	100.0 ± 2.7 (6)	155 ± 8.1 (6)
Bicuculline (10 μM) plus 2-hydroxysaclofen (100 μM)[a]	113.3 ± 7.8 (3)	146.7 ± 0.3 (3)*
DPCPX (4 nM)[a]	98.2 ± 4.6 (3)	153.4 ± 6.2 (3)*
None[b]	100.0 ± 3.3 (3)	122.7 ± 6.4 (3)
Bicuculline (10 μM) plus phaclofen (100 μM)[b]	100.0 ± 11.8 (3)	121.9 ± 0.3 (3)*
Naloxone (10 μM)[b]	100.0 ± 2.6 (3)	118.7 ± 6.3 (3)*

Results are expressed as a percentage of the release observed in the controls (i.e. 15 mM KCl alone or veratridine alone) and are means ± s.e.mean from the number of experiments indicated in parentheses, each experiment containing duplicate determinations. In the perfusion experiments the S2/S1 ratios were 1.090 ± 0.036. *Indicates significantly different from antagonists alone ($P<0.05$).

Figure 2 demonstrates that increasing concentrations of KF17837 (0.1–100 nM) inhibited A_{2A} receptor-mediated modulation of [^{3}H]-ACh and [^{3}H]-GABA release. Figure 2a illustrates that in these experiments CGS 21680 (1 nM) alone decreased the release of [^{3}H]-GABA by 30.1 ± 3.2% ($n = 8$) and that this effect was antagonized in a dose-dependent manner by increasing concentrations of KF17837; the IC_{50} being approximately 30 nM with a maximal inhibition of the effect of CGS 21680 occurring at 100 nM. This maximal concentration of KF17837 alone had no significant effect on either the evoked (an inhibition of 5.7 ± 8.2%, $n = 4$) or basal release of [^{3}H]-GABA. The effects of increasing concentrations of KF17837 on [^{3}H]-ACh release, evoked by 15 mM potassium in perfusion experiments, are shown in Figure 2b. In the absence of KF17837, CGS 21680 (0.1 nM) increased the efflux of [^{3}H]-ACh by 55.5 ± 6.9% ($n = 4$). KF17837 (0.1–10 nM) inhibited the action of CGS 21680 in a dose-dependent manner with an apparent IC_{50} of approximately 0.3 nM and its effects appeared maximal at 1 nM (Figure 2b). In the absence of CGS 21680, KF17837 (10 nM) had no effect on the evoked (an inhibition of 5.8 ± 2.7%, $n = 3$) or basal (data not shown) release of [^{3}H]-ACh.

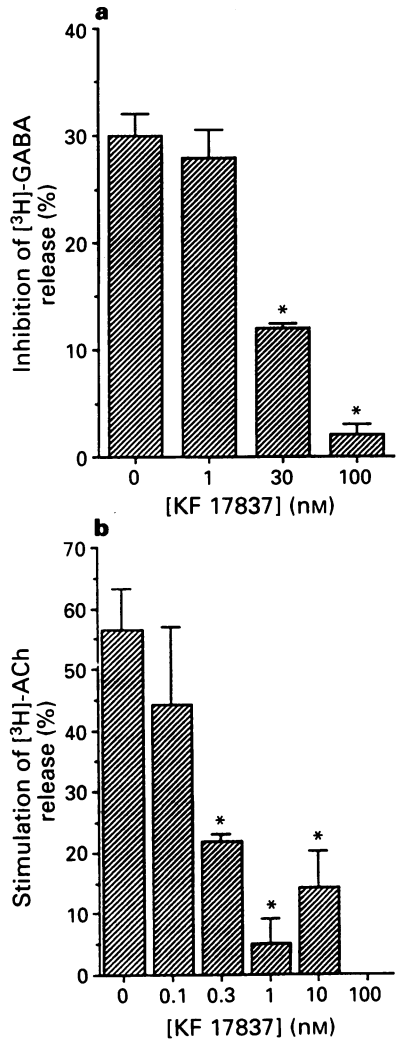

Figure 2 A_{2A} receptor-mediated inhibition of striatal [^{3}H]-GABA and [^{3}H]-ACh release by KF17837. Striatal nerve terminals were perfused as described, and the release of [^{3}H]-GABA (a) or [^{3}H]-ACh (b) evoked by 15 mM KCl, in the presence of either 1 nM (a) or 0.1 nM (b) CGS 21680 and various concentrations of KF17837. The results are expressed as % inhibition (GABA) or % stimulation (ACh) of the control release (i.e. that evoked by 15 mM KCl alone) and are means ± s.e.mean of experiments each containing duplicate determinations. *Indicates significantly different from the modulation of release observed in the absence of KF17837 ($P<0.05$).

Discussion

The A_{2A} receptor-mediated inhibition of labelled GABA release from striatal nerve terminals has already been described, and shown to be due to a reduction in calcium-dependent release (Kirk & Richardson, 1993; 1994). The experiments described in this paper were undertaken in order to clarify the effects of the adenosine A_{2A} receptor on transmitter release in the striatum. The recent report that this receptor stimulated the release of GABA from globus pallidus slices (Mayfield *et al.*, 1993), contradicted our previous observations that stimulation of A_{2A} receptors inhibited the release of [^{3}H]-GABA (Kirk & Richardson, 1993; 1994). This could have been because the overwhelming majority of the terminals in our preparation were derived from the caudate-putamen and were not derived from the striato-pallidal neurones, or that this receptor stimulated release at the axonal terminals of these neurones in the globus pallidus but inhibited release at the recurrent collaterals in the caudate-putamen. The results in Figure 1 clearly demonstrate that A_{2A} receptor stimulation inhibits [^{3}H]-GABA release from nerve terminals derived from both the caudate-putamen and the globus pallidus, and that this inhibition is antagonized in both regions by the novel A_{2A} antagonist, KF17837. There are a number of differences between our methodology and that of Mayfield *et al.* (1993) including the use of high potassium concentrations rather than electrical stimulation. Although it is possible that their results are a consequence of an inhibition of GABA release by the A_{2A} receptor, resulting in a reduction of an endogenous tonic (GABA mediated) inhibition of [^{3}H]-GABA release, the methodology used by Mayfield *et al.* (1993) permitted the observation of two A_{2A} receptor mediated effects, inhibition as well as stimulation. Since, under the stimulation conditions used in this paper

(i.e. elevated potassium concentrations), any effect arising from receptor-mediated modulation of potassium channels would be negated (McMahon & Nicholls, 1991), it may be that the stimulation of GABA release observed by Mayfield *et al.* (1993) was a consequence of A_{2A} receptor-mediated inhibition of such a channel.

The results in this paper provide yet more evidence that the A_{2A} receptor is present on striatal cholinergic nerve terminals. The inability of the GABA receptor and cholinoceptor (and other) antagonists to affect A_{2A} receptor-mediated modulation of transmitter release clearly demonstrates that the effect of adenosine agonists on acetylcholine release is not a consequence of a secondary effect mediated by changes in GABA release in our experimental system. Given the absence of detectable A_{2A} receptor mRNA in cholinergic neurones and since A_{2A} agonists inhibit the release of GABA but stimulate that of ACh (Kirkpatrick & Richardson, 1993; Kirk & Richardson, 1994), it is possible that more than one type of A_{2A} receptor exits. Indeed, two A_{2A}-like binding sites have been reported in human brain (James *et al.*, 1992) and rat brain (Johansson *et al.*, 1993). It is not however possible to determine from the data presented whether the ligand binding sites of the receptors on these two nerve terminals are the same or different. The concentrations of the antagonists and agonists affecting the release of ACh and GABA are different in the two systems, while the relative potencies of the agonists CGS 21680, N-ethylcarboxamidoadenosine and R-phenylisopropyladenosine are similar. Interestingly the antagonist KF17837 appeared to be more effective in blocking the modulation of ACh release than that of GABA, although it would be necessary to determine the pA_2 value of KF17837 at the A_{2A} receptor on the two nerve terminals in order to determine whether or not these are indeed two different receptors.

In summary KF17837, the most A_{2A}-selective antagonist synthesized to date, is a potent inhibitor of CGS 21680-mediated modulation of both striatal GABA and ACh release. Under the conditions described in this paper the A_{2A} receptor inhibits potassium-evoked release of GABA in both the caudate-putamen and globus pallidus, while stimulating the release of ACh.

This work was funded by the Medical Research Council and the Sir Jules Thorne Charitable Trust. I.P.K. is the recipient of a Glaxo Group Research Training Award. We are grateful to Kyowa Hakko Kogyo Co. Ltd. for the supply of KF17837.

References

BARRACO, R.A., MARTENS, K.A., PARIZON, M. & NORMILE, H.J. (1993). Adenosine A_{2A} receptors in the nucleus accumbens mediate locomotor depression. *Br. Res. Bull.*, **31**, 397–404.

BARRACO, R.A. & PHILLIS, J.W. (1991). Subtypes of adenosine receptors in the brainstem mediate opposite blood pressure responses. *Neuropharmacol.*, **30**, 403–407.

BRUNS, R.F., LU, G.H. & PUGSLEY, T.A. (1987). Adenosine receptor subtypes: binding studies. In *Topics and Perspectives in Adenosine Research*. ed. Gerlach, E. & Becker, B.F. pp. 59–73. Berlin: Springer Verlag.

BROWN, S.J., GILL, R., EVENDEN, J., IVERSEN, S.D. & RICHARDSON, P.J. (1991). Purine mediated inhibition of apomorphine induced rotation in rats with unilateral nigrostriatal lesions. *Psychopharmacol.*, **103**, 78–82.

BROWN, S.J, JAMES, S., REDDINGTON, M. & RICHARDSON, P.J. (1990). Both A_1 and A_{2A} purine receptors regulate striatal ACh release. *J. Neurochem.*, **55**, 31–38.

FERRE, S. & FUXE, K. (1992). Dopamine denervation leads to an increase in the intramembrane interaction between adenosine A_2 and dopamine D_2 receptors in the neostriatum. *Brain Res.*, **594**, 124–130.

FERRE, S., VON EULER, G., JOHANSSON, B., FREDHOLM, B.B. & FUXE, K. (1991a). Stimulation of high affinity adenosine A2 receptors decreases the affinity of dopamine D2 receptors in rat striatal membranes. *Proc. Natl. Acad. Sci. U.S.A.*, **88**, 7238–7241.

FERRE, S., RUBIO, A. & FUXE, K. (1991b). Stimulation of adenosine A2 receptors induces catalepsy. *Neurosci. Lett.*, **130**, 162–164.

FERRE, S., SNAPRUD, P. & FUXE, K. (1993). Opposing actions of an adenosine A2 receptor agonist and a GTP analogue on the regulation of dopamine D2 receptors in rat neostriatal membranes. *Eur. J. Pharmacol.*, **244**, 311–315.

GREEN, R.D., PROUDFIT, H.K. & YEUNG, S.-M.H. (1982). Modulation of striatal dopaminergic function by local injection of 5'-N-ethylcarboxamidoadenosine. *Science*, **218**, 58–60.

JAMES, S., ASKALAN, R., XUEREB, J. & RICHARDSON, P.J. (1992). Adenosine receptors in post mortem human brain. *Br. J. Pharmacol.*, **105**, 238–244.

JAMES, S. & RICHARDSON, P.J. (1993). The subcellular distribution of the [^{3}H]-CGS 21680 binding sites in the rat striatum: copurification with cholinergic nerve terminals. *Neurochem. Int.*, **23**, 115–122.

JARVIS, M.F., SCHUTZ, R., HUTCHISON, A.J., DO, E., SILLS, M.A. & WILLIAMS, M. (1989). [^{3}H]-CGS 21680, an A_2 selective adenosine receptor agonist directly labels A_2 receptors in rat brain tissue. *J. Pharmacol. Exp. Ther.*, **251**, 888–893.

JOHANSSON, B., GEORGIEV, V., PARKINSON, P.E. & FREDHOLM, B.B. (1993). The binding characteristics of the adenosine A2 receptor selective agonist [^{3}H]-CGS 21680 to rat cortex differs from its binding to rat striatium. *Eur. J. Pharmacol.*, **247**, 103–110.

KIRK, I.P. & RICHARDSON, P.J. (1993). Adenosine A2 receptor modulation of striatal ACh and GABA release. *Br. J. Pharmacol.*, **108**, 45P.

KIRK, I.P. & RICHARDSON, P.J. (1994). Adenosine A_{2A} receptor mediated modulation of striatal [^{3}H]-GABA and [^{3}H]-ACh release. *J. Neurochem.*, **62**, 960–966.

KIRKPATRICK, K.A. & RICHARDSON, P.J. (1993). Adenosine receptor mediated modulation of ACh release from rat striatal synaptosomes. *Br. J. Pharmacol.*, **110**, 949–954.

LUPICA, C.R., CASS, W.A., ZAHNISER, N.R. & DUNWIDDIE, T.V. (1990). Effects of the selective adenosine A_2 receptor agonist CGS 21680 on in vitro electrophysiology, cAMP formation and dopamine release in rat hippocampus and striatum. *J. Pharmacol. Exp. Ther.*, **252**, 1134–1141.

MAENHAUT, C., VAN SANDE, J., LIBERT, F., PARMENTIER, M., VANDERHAEGEN, J.J., DUMONT, J.E., VASSART, G. & SCHIFFMAN, S. (1990). RDC8 codes for an adenosine A_2 receptor with physiological constitutive activity. *Biochem. Biophys. Res. Commun.*, **173**, 1169–1178.

MAYFIELD, R.D, SUZUKI, F. & ZAHNISER, N.R. (1993). Adenosine A_{2A} receptor modulation of electrically evoked endogenous GABA release from slices or rat globus pallidus. *J. Neurochem.*, **60**, 2334–2337.

MCMAHON, H.T. & NICHOLLS, D.G. (1991). The bioenergetics of neurotransmitter release. *Biochim. Biophys. Acta.*, **1059**, 243–264.

MITCHELL, I.J., CLARKE, C.E., BOYCE, S., ROBERTSON, R.G., PEGGS, D., SAMBROOK, M.A. & CROSSMAN, A.R. (1990). Neural mechanisms underlying parkinsonian symptoms based on regional uptake of 2-deoxyglucose in monkeys exposed to MPTP. *Neurosci.*, **32**, 213–226.

NONAKA, H., ICHIMURA, M., TAKEDA, M., NONAKA, Y., SHIMADA, J., SUZUKI, F., YAMAGUCHI, K. & KASE, H. (1994). KF 17837 ((E)-8-(3,4-dimethoxystyryl)-1,3-dipropylxanthine), a potent and selective adenosine A_2 receptor antagonist. *Eur. J. Pharmacol.*, (in press).

PITTEL, Z., HELDMAN, E., RUBINSTEIN, R. & COHEN, S. (1990). Distinct muscarinic receptor subtypes differentially modulate release from corticocerebral synaptosomes. *J. Neurochem.*, **55**, 665–672.

SCHIFFMAN, S.N., JACOBS, O. & VANDERHAEGEN, J.J. (1991). Striatal restricted adenosine A_2 receptor (RDC8) is expressed by enkephalin, but not by substance P neurons: An *in situ* hybridisation histochemistry study. *J. Neurochem.*, **57**, 1062–1067.

SCHIFFMAN, S.N. & VANDERHAEGHEN, J.-J. (1993). Adenosine A_2 receptors regulate the gene expression of striatopallidal and striatonigral neurons. *J. Neurosci.*, **13**, 1080–1087.

SEBASTIÃO, A.M. & RIBEIRO, J.A. (1992). Evidence for the presence of excitatory A_2 adenosine receptors in the rat hippocampus. *Neurosci. Lett.*, **138**, 41–44.

SIMPSON, R.E., O'REGAN, M.H., PERKINS, L.M. & PHILLIS, J.W. (1992). Excitatory transmitter amino acid release from the ischaemic rat cerebral cortex: Effects of adenosine receptor agonists and antagonists. *J. Neurochem.*, **58**, 1683–1690.

VELLUCCI, S.V., SIRINATHSINGHJI, D.J.S. & RICHARDSON, P.J. (1993). Adenosine A2 receptor regulation of apomorphine-induced turning in rats with unilateral striatal dopamine denervation. *Psychopharmacol.*, **111**, 383–389.

VERHAGE, M., BESSELSEN, E., LOPES, DA SILVA, F.H. & GHIJSEN, W.E.J.M. (1989). Ca^{2+} dependent regulation of presynaptic stimulus-secretion coupling. *J. Neurochem.*, **47**, 1188–1194.

(Received January 12, 1994
Revised April 29, 1994
Accepted May 5, 1994)

Br. J. Pharmacol. (1994), **113**, 49–54

Vasoconstrictor endothelin receptors characterized in human renal artery and vein *in vitro*

[1]Janet J. Maguire, Rhoda E. Kuc, Gillian O'Reilly & Anthony P. Davenport

Clinical Pharmacology Unit, University of Cambridge, Box 110, Addenbrooke's Hospital, Cambridge CB2 2QQ

1 We have identified the endothelin receptors present in the media of human main stem renal artery and vein and characterized the subtypes mediating vasoconstriction in these blood vessels *in vitro*.

2 Messenger RNA encoding both ET_A and ET_B receptors was identified in the smooth muscle layer of human renal artery and vein by reverse transcriptase-polymerase chain reaction assay. In cryostat-cut cross-sections of both vessels autoradiographical visualisation suggested a majority of ET_A receptors. Intense binding was obtained to the non-selective ligand [^{125}I]-ET-1 and the ET_A-selective [^{125}I]-PD151242 but only weak labelling of sites by the ET_B-selective [^{125}I]-BQ3020.

3 ET-1 potently constricted renal artery and vein preparations with EC_{50} values of 4.06 nM and 1.00 nM, respectively. Sarafotoxin 6b was approximately ten times less potent than ET-1 with EC_{50} values of 36.3 nM and 13.8 nM respectively. In the renal artery, ET-3 and sarafotoxin 6c showed little or no activity up to 300 nM. Responses to these peptides were more variable in the renal vein. Preparations from three individuals did not respond to ET-3 but in three further cases, although ET-3 was much less potent than ET-1, full dose-response curves were obtained. S6c elicited dose-related contractions in vein preparations from 5/6 individuals and although more potent than ET-1, the maximum response was 30–60% of that obtained to ET-1.

4 ET-1-induced vasoconstriction of renal artery and vein was antagonized by the ET_A-selective, BQ123 (3–10 μM). The dose-response curves to ET-1 were displaced in a parallel rightward fashion with no attenuation of the maximum responses. pA_2 values were estimated to be 6.8 ± 0.1 and 6.8 ± 0.4 for artery and vein respectively.

5 These data suggest that mRNA encoding both ET_A and ET_B receptors is present in the media of human main stem renal artery and vein. However, autoradiographical studies indicate that the majority of ET receptors expressed are of the ET_A subtype. The relative potencies of ET-1 and ET-3 as vasoconstrictors of renal blood vessels *in vitro* is consistent with this being an ET_A-mediated response, and therefore whilst responses to S6c indicate that constrictor ET_B receptors may be present in renal veins from some individuals these are likely to be of less importance in these blood vessels.

Keywords: Endothelin; ET_A receptor; ET_B receptor; human renal artery; human renal vein; vasoconstriction; mRNA detection; *in vitro* pharmacology

Introduction

The precise role of the endothelin (ET) peptides in human renal vascular disease remains to be elucidated, but elevated plasma ET levels have been reported in conditions of acute renal failure (Tomita *et al.*, 1989), chronic renal failure (Stockenhuber *et al.*, 1992), cyclosporine-induced nephrotoxicity (DeRay *et al.*, 1991) and following haemodialysis of uraemic patients (Koyama *et al.*, 1989; Totsune *et al.*, 1989; Suzuki *et al.*, 1990). Cyclosporine treatment in rats is also associated with an increase in the density of renal endothelin binding sites (Nambi *et al.*, 1990).

Subtypes of endothelin receptors have been proposed, characterized according to the relative potencies of the three endogenous endothelin isoforms. ET-1 and ET-2 are more potent than ET-3 at the ET_A receptor whereas all three have equal affinity for the ET_B receptors (Sakurai *et al.*, 1992; Watson & Girdlestone, 1993). The endothelin receptors which mediate the pathophysiological effects of ET in the human kidney have not yet been defined; indeed the physiological role of the endothelins and their receptors in the kidney remains to be clarified. In human kidney, subtype-selective ligands have identified the presence of both ET_A and ET_B receptors. Although ET_B receptors comprise 70% of the total ET receptor population, microautoradiographical studies indicate that it is the ET_A receptors which localize to the media of the renal resistance vessels (Karet *et al.*, 1993). This contrasts with findings in the rat, in which renal vasoconstriction *in vivo* may be mediated via activation of both receptor subtypes. This has been determined not only by the profound pressor effects of selective ET_B agonists (Davis *et al.*, 1991; Clozel *et al.*, 1992; Gardiner *et al.*, 1993) but also by the inability of selective ET_A antagonists to antagonize completely the vasoconstrictor response to ET-1 (Bigaud & Pelton, 1992; Cristol *et al.*, 1993; Pollock & Opgenorth, 1993). Similar data have been obtained in the rat isolated perfused kidney (Battistini *et al.*, 1993; Wellings *et al.*, 1994).

The relative density of vasoconstrictor ET_A to ET_B receptors appears to be dependent on both the vascular bed and the species studied (Davenport & Maguire, 1994), therefore it is important to determine the relative contribution made by each receptor subtype to the regulation of blood flow through the human kidney. We have obtained segments of human main stem renal artery and vein and as an initial step to characterizing vasoconstrictor ET receptors in the human kidney, we have identified those endothelin receptors present in these vessels using reverse transcriptase polymerase chain reaction (RT-PCR) assays and autoradiographical visualisation. Endothelin-induced vasoconstriction in rings of isolated renal artery and vein was characterized by use of the non-selective agonists, ET-1 and sarafotoxin 6B (S6b), the ET_B-selective agonists, ET-3 and sarafotoxin 6c (S6c) and the ET_A-selective antagonist, BQ123 (cyclo-(D-Trp-D-Asp-L-Pro-D-Val-L-Leu)).

[1] Author for correspondence.

Methods

Tissue collection

Histologically normal sections of main branch renal artery and vein were obtained from nine individuals (6 male and 3 female aged 29–73 years) undergoing nephrectomy for non-obstructive carcinoma, and were immediately transferred to cold oxygenated Krebs solution. Excised kidneys were functional and of normal size. Biochemical functions were normal and renal ultrasound showed no evidence of hydronephrosis.

Reverse-transcriptase polymerase chain reaction assays

The media of renal arteries and veins from three individuals was separated from the intima and the endothelial layer removed by scraping. Extraction of total RNA, cDNA synthesis and RT-PCR assays were carried out using previously described methods (O'Reilly *et al.*, 1992; 1993a,b; Davenport *et al.*, 1993; Molenaar *et al.*, 1993). Briefly, RNA was extracted by the guanidinium isothiocyanate method and cDNA synthesized using avian myoblastosis virus reverse transcriptase enzyme. The following nested oligonucleotide primers were designed from published nucleotide sequences:

(A) ET_A, ET_B forward TATCACAGAAACTGAAAGTGCTATG (Bases 379–396)
(B) ET_A, ET_B reverse CAAGCAAGCAAGCAACGTAAGAGCA (Bases 1214–1198)
(C) ET_A forward CCTTTTGATCACAATGACTTT (Bases 439–459)
(D) ET_A reverse TTTGATGTGGCATTGAGCATACAG (Bases 737–714)
(E) ET_B forward ACTGGCCATTTGGAGCTGAGAT (Bases 497–519)
(F) ET_B reverse CTGCATGCCACTTTTCTTTCTCAA (Bases 924–901)

PCR amplification was carried out using 1 μl cDNA, 5 μl reaction buffer (100 mM Tris-HCl, pH 8.3 at 25°C, 500 mM KCl and 15 mM $MgCl_2$), 5 μl deoxyNTPs (2 mM), 5 μl of each oligonucleotide primer A and B (10 μM) and 2.5 u Taq polymerase in a Techne PHC-3 programmable thermocycler (Techne, Cambridge). One μl of this reaction mixture was used in the second round of amplification using the internal primer pairs C and D and E and F. PCR products were separated by agarose gel electrophoresis and the bands stained with ethidium bromide. These PCR products have been previously cloned and sequenced and show 100% homology with published sequences for ET_A and ET_B receptor mRNA respectively.

Autoradiography

ET_A and ET_B receptors were visualized using published autoradiographical techniques (Molenaar *et al.*, 1992). Consecutive 10 μm thick cross-sections of renal artery and vein from three individuals were cut on a cryostat microtome (Bright Instruments, Huntingdon) and thaw mounted onto gelatine subbed slides. Sections were pre-incubated for 15 min at room temperature (23°C) in incubation buffer (50 mM HEPES containing 5 mM $MgCl_2$, bovine serum albumin, 0.3% w/v). The sections were then incubated in the same buffer for 2 h containing either 0.1 nM [^{125}I]-ET-1 (~2000 Ci mmol^{-1}) to detect all ET receptors or the ET_A-selective [^{125}I]-PD151242 (~2000 Ci mmol^{-1}) (Davenport *et al.*, 1994) or ET_B-selective [^{125}I]-BQ3020 (~2000 Ci mmol^{-1}) (Molenaar *et al.*, 1992). Non-specific binding was determined by incubating adjacent sections in the presence of 1 μM of the corresponding unlabelled peptide. At the end of the incubation period, sections were rinsed in three successive 5 min washes of ice cold Tris buffer (pH 7.4) and dried under a stream of cold air. Sections were exposed to radiation sensitive film (Hyperfilm βmax).

In vitro pharmacology experiments

Segments of vessels ($n = 9$) were cut into rings, 2 mm in width, and the endothelium removed by gently rubbing with a metal seeker. Verification of this procedure was made histologically (see Figure 1). Rings were attached to isometric transducers (Swema, Stockholm, Sweden) and mounted under an initial resting tension of 1–2 g in 25 ml organ baths containing Krebs solution. The bathing medium was continuously gassed with 95% O_2:5% CO_2 and maintained at 37°C. Contractile responses were recorded on a Graphtec chart recorder (Linton Instruments, Diss, Norfolk). The preparations were allowed to equilibrate for 90 minutes before control responses were obtained to a maximal concentration of KCl (50 mM). After washing, cumulative dose-response curves (DRCs) were constructed to ET-1, ET-3, S6b and S6c (10^{-10} M–3×10^{-7} M) with only one agonist tested per preparation. The experiments were terminated by addition of 50 mM KCl to the organ bath to determine the maximum contractile response possible, and agonist contractions were subsequently expressed as a percentage of this. In a further series of experiments the effect of BQ123 (3 and 10 μM) on ET-1-mediated contractions was determined. ET-1 DRCs were constructed in the absence (control) and presence of BQ123 added to the bathing medium 30 min prior to ET-1.

Materials

Reagents for RT-PCR were purchased from Pharmacia Biotech (St. Albans, Herts.) and H.T. Biotechnology Ltd. (Cambridge). [^{125}I]-ET-1, [^{125}I]-PD151242 and [^{125}I]-BQ3020 were from Amersham International (Amersham, Bucks.), BQ3020 ([Ala^{11,15}]Ac-ET-$1_{(6-21)}$), BQ123 (Davenport *et al.*, 1993) and PD151242 (N-[(hexahydro-1-azepinyl) carbonyl])L-Leu(1-me)D-Trp-D-Tyr; Davenport *et al.*, 1994) were synthesized using solid phase t-Boc chemistry. ET-1, ET-3, S6b, S6c and BQ123 were purchased from Novabiochem, (Nottingham). Stock solutions (10^{-4} M) of ET-1, ET-3, S6b and S6c were dissolved in 0.1% acetic acid; BQ123 (10^{-3} M) was dissolved in dimethylsulphoxide (DMSO) and used directly or diluted in distilled water. The concentration of unlabelled peptides was determined by u.v. spectrophotometry. All other reagents were purchased from Sigma Chemical Co. (Poole, Dorset) or BDH (Lutterworth, Leics.), and were of analar grade or better. Krebs solution had the following composition (mM): NaCl 90, KCl 5, $MgSO_4.7H_2O$ 0.5, Na_2HPO_4 1, $NaCO_3$ 45, $CaCl_2$ 2.25, glucose 10, Na pyruvate 5, fumarate 5.

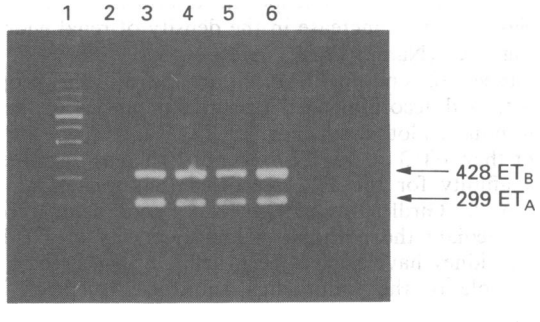

Figure 1 Agarose gel showing cDNA from the media of renal arteries and veins amplified with ET_A and ET_B specific primers. In lane 1, the marker is a 100 base pair ladder: in lane 2, the DNA template has been omitted as the negative control. The results show the presence of bands corresponding to size predicted for ET_A (299 base pairs) and ET_B (428 base pairs) in lanes 3 and 4 (renal arteries from two individuals) and 5 and 6 (renal veins from two individuals). These results are typical of arteries and veins from four individuals.

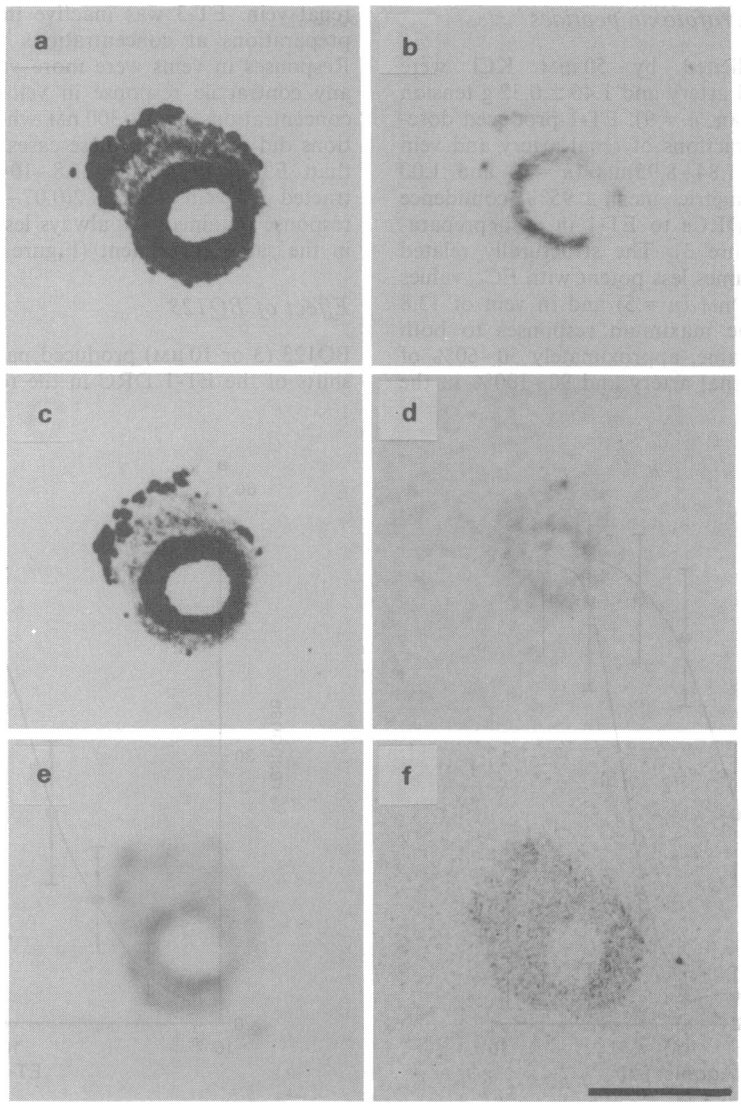

Figure 2 Autoradiographical localization of ET receptors in cross-sections of human renal artery following incubation with ligands for 2 h, washing and apposition to radiation sensitive film. (a) Total [^{125}I]-ET-1 binding showing the distribution of all ET receptors. (c) ET_A receptors localized using [^{125}I]-PD151242. (e) ET_B receptors localised with [^{125}I]-BQ3020. Non-specific binding determined by incubating adjacent sections in the presence of 1 μM of unlabelled ET-1 (b), PD151242 (d), or BQ3020 (f). Scale bar = 2 mm.

Results

Detection of ET_A and ET_B receptor mRNA

The amplified products of cDNA from the media of human renal artery and vein taken from four individuals, separated on an agarose gel (Figure 1), were of the size predicted for ET_A (299 base pairs) and ET_B (428 base pairs) receptors.

Localization of ET_A and ET_B receptors

In sections of renal artery and vein from three individuals, intense staining was obtained to both [^{125}I]-ET-1, binding to both receptor subtypes, and the ET_A-selective [^{125}I]-PD151242. In contrast lower levels of binding were detected with the ET_B agonist, [^{125}I]-BQ3020 (Figure 2).

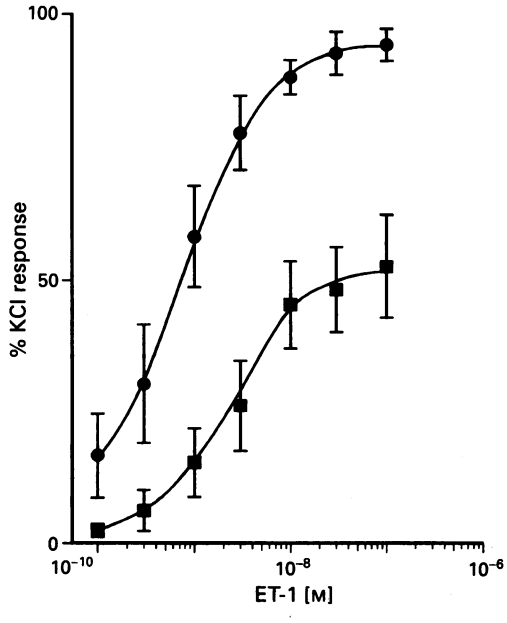

Figure 3 Dose-response curves to ET-1 in rings of human isolated renal artery (■) and vein (●). Cumulative dose-response curves were constructed to ET-1 (10^{-10} M–3×10^{-7} M) with each response expressed as a % of the maximal contraction elicited by 50 mM KCl. Data are the mean ± s.e.mean from 8–10 experiments.

Relative potencies of ET/sarafotoxin peptides

Maximum contractions elicited by 50 mM KCl were 1.36 ± 0.25 g tension in renal artery and 1.46 ± 0.32 g tension in renal vein (mean ± s.e.mean, $n = 9$). ET-1 produced dose-dependent long lasting contractions of renal artery and vein with EC_{50} values of 4.06 (1.84–8.95)nM ($n = 9$) and 1.00 (0.56–2.04)nM ($n = 8$, geometric mean ± 95% confidence interval), respectively. The DRCs to ET-1 in each preparation were monophasic (Figure 3). The structurally related S6b was approximately ten times less potent with EC_{50} values in artery of 36.3 (18.8–70.3)nM ($n = 5$) and in vein of 13.8 (2.36–81.07)nM ($n = 3$). The maximum responses to both ET-1 and S6b were comparable, approximately 50–60% of that to 50 mM KCl in the renal artery and 90–100% in the renal vein. ET-3 was inactive in 6/6 and S6c in 5/6 artery preparations at concentrations up to 300 nM (Figure 4a). Responses in veins were more variable. ET-3 failed to elicit any contractile response in veins from three individuals at concentrations up to 300 nM whereas three further preparations did respond. In these cases ET-3 was much less potent than ET-1 (EC_{50} 51.9 (25.8–104.5)nM). S6c potently contracted 3/4 veins (EC_{50} 0.2(0.07–0.54)nM) but the maximum response obtained was always less than 60% of that to ET-1 in the same experiment (Figure 4b).

Effect of BQ123

BQ123 (3 or 10 μM) produced parallel dose-related rightward shifts of the ET-1 DRC in the renal artery (Figure 5a). The

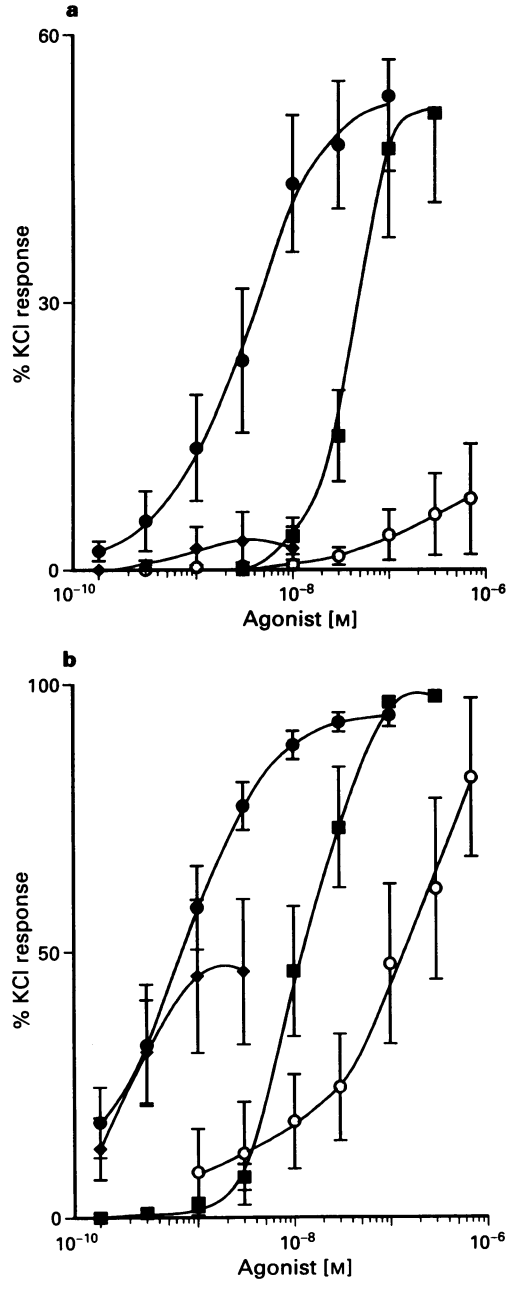

Figure 4 Cumulative dose-response curves to ET-1 (●), S6b (■), ET-3 (○) and S6c (◆) in (a) renal artery and (b) renal vein *in vitro*. Agonist responses were expressed as a % of the maximal contraction to 50 mM KCl. Only one agonist dose-response curve was constructed per preparation and data are the mean ± s.e.mean from 3–10 experiments per agonist. For ET-3 and S6c in renal vein only data from those preparations which responded are included.

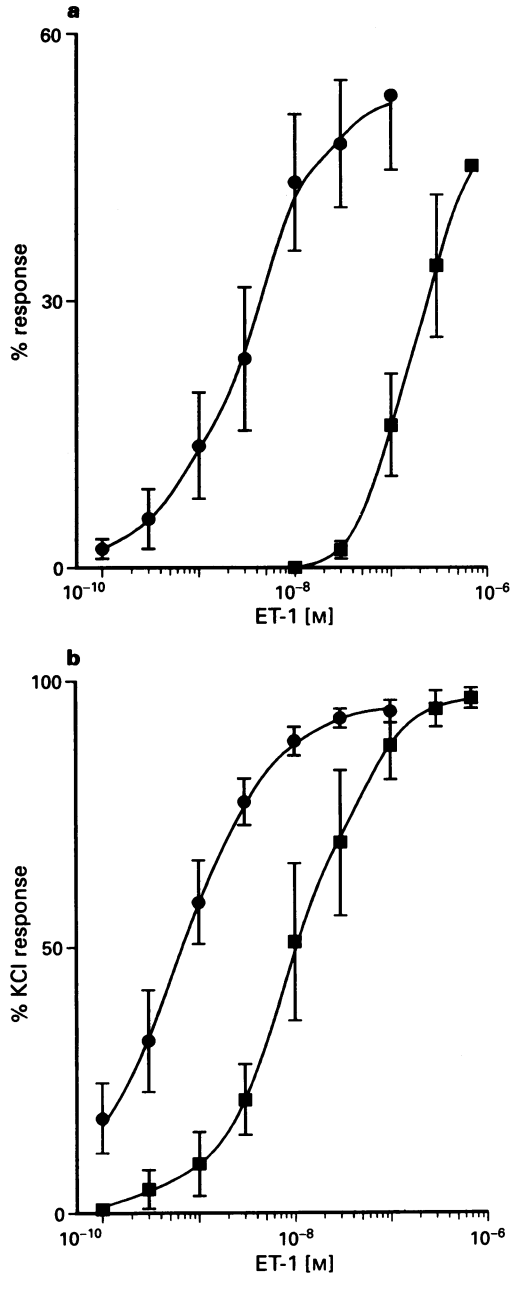

Figure 5 The effect of 3 μM BQ123 on the vasoconstrictor responses to ET-1 in human renal artery (a) and vein (b) *in vitro*. ET-1 dose-response curves were constructed in the absence (●) and presence (■) of 3 μM BQ123 added to the bathing medium 30 min prior to ET-1. ET-1 responses are expressed as a % of the maximal contraction to 50 mM KCl. Data are the mean ± s.e.mean from 3–10 experiments.

pA_2 value estimated from the Gaddum-Schild equation was 6.8 ± 0.1 ($n = 6$). Similar results were obtained using 3 μM BQ123 against ET-1 in renal vein with the pA_2 estimated as 6.8 ± 0.4 ($n = 3$) (Figure 5b). In all cases no attenuation of the maximum response to ET-1 was observed.

Discussion

We have shown that ET_A and ET_B mRNA can be detected in the media of renal arteries and veins in concordance with previous results in other human blood vessels including aorta, pulmonary and coronary arteries (Davenport *et al.*, 1993; Davenport & Maguire, 1994). *In situ* hybridization has confirmed the localization of mRNA encoding both receptors to the media of these vessels (Davenport *et al.*, 1993).

Autoradiography using [^{125}I]-ET-1 identified ET receptors localized to the media and intima of renal vessels. Use of the ET_A-selective [^{125}I]-PD151242 confirmed the presence of the ET_A sub-type, with a lower density of ET_B receptors detected using the ET_B-selective [^{125}I]-BQ3020. These results are in agreement with previous studies which showed that ET_A and ET_B selective compounds competed for iodinated ET-1 in a biphasic manner, suggesting the expression of both endothelin receptor sub-types, for example in the media of coronary arteries (Davenport *et al.*, 1993), with ET_A receptors comprising more than 80% of the total. The relative potency of the endogenous endothelins, ET-1 and ET-3, in both artery and vein are consistent with the presence of constrictor ET_A receptors. This was particularly striking in the renal artery in which ET-3 was without effect. As expected the non-selective compound S6b produced similar responses to ET-1 although it was ten times less potent. In agreement with these observations was the lack of effect of the ET_B-selective agonist, S6c in the renal artery confirming that vasoconstriction in this blood vessel, at least *in vitro*, is exclusively an ET_A-mediated phenomena. In common with other human blood vessels such as the coronary artery, mammary artery and saphenous vein (Maguire & Davenport, 1993) S6c did, on occasion, elicit small responses in the renal vein. These were variable and the magnitude of the responses were always considerably less than those to ET-1. However, these data do suggest that constrictor ET_B receptors are present in human renal vein although vasoconstriction by the endothelin peptides appears to be via ET_A receptors. BQ123 antagonized the effect of ET-1 in both preparations with estimated pA_2 values comparable with those obtained for blockade of ET-1 responses in the rat aorta (exclusively ET_A). This serves to confirm the involvement of ET_A receptors in ET-1-mediated vasoconstriction of human renal vascular smooth muscle. The apparent lack of ET_B response to either ET-1 or ET-3 may reflect the relatively small number of ET_B receptors in these vessels and suggests that the snake venom toxin S6c exhibits higher efficacy for this receptor subtype than either of the naturally occurring mammalian ET peptides. As far as is possible to determine in this limited study, there was no obvious correlation between the age or sex of an individual and whether or not responses to S6c were obtained.

A recent study of ET-1 and ET-3 vasoconstriction in rat main branch artery *in vitro* reported ET-3 to be 12 times less potent than ET-1 (Pierre & Clark, 1994). In agreement with our own findings this suggests the presence of vasoconstrictor ET_A receptors in large diameter renal blood vessels. In contrast to our own observations, the effect of ET-1 could not be antagonized by 3 μM BQ123, although they were able to antagonize responses to ET-3 with a low concentration (0.3 μM) of this peptide. The authors suggested the additional presence of a vasoconstrictor BQ123-insensitive receptor for which we have no supporting evidence in human renal blood vessels.

Regulation of blood flow through the normal and diseased human kidney is determined by the small resistance blood vessels rather than the large capacitance vessels used in this study. It is possible that these smaller diameter vessels express both ET_A and ET_B receptors as predicted, for example, from *in vivo* experiments in rats. Further experiments on human renal resistance vessels are required to confirm or refute this. However, microautoradiographical visualisation of sections of human kidney using the ET_A-selective [^{125}I]-BQ123 and the ET_B-selective [^{125}I]-BQ3020 clearly indicate that intrarenal vascular endothelin receptors are labelled only by the ET_A-selective [^{125}I]-BQ123 but not by the ET_B-selective [^{125}I]-BQ3020 (Karet *et al.*, 1993). Whilst data obtained for one vascular bed cannot be extrapolated to another, it is interesting that experiments carried out using human small resistance arteries and veins *in vitro* suggest that endothelin-induced vasoconstriction in the resistance vessels of the heart (Godfraind, 1993) and omentum (Riezebos *et al.*, 1994), as in the larger human blood vessels, is mediated via the ET_A receptor.

If human renal vasoconstriction is an ET_A-mediated event then antagonism of this receptor may provide a novel therapeutic target in a number of pathophysiological conditions. Even if some of the constrictor effects of endothelin intrarenally are mediated via ET_B receptors, ET_A-selective compounds have already proved effective not only in antagonizing the haemodynamic responses in rats to infused ET-1 and big ET-1 (Pollock & Opgenorth, 1994) but also in limiting tissue necrosis and biochemical changes in at least two rat models; a cyclosporine-induced model of nephrotoxicity (Fogo *et al.*, 1992) and a model of chronic renal failure associated with reduced renal mass (Benigni *et al.*, 1993). This is despite reports that, in rats at least, some part of renal vasoconstriction is ET_B-mediated. It would be very interesting to know whether non-selective endothelin antagonists are more effective than ET_A-selective antagonists such as BQ123 in either of these models. If not, selective blockade of ET_A receptors in the kidney would have the beneficial 'side effects' of leaving unapposed ET_B-mediated vasodilatation and those non-vascular ET_B receptors whose function remains to be determined.

In summary we have demonstrated the presence of both ET_A and ET_B receptors in the media of human renal artery and vein but endothelin-mediated vasoconstriction *in vitro* is due to ET_A receptor activation.

We thank the staff of Addenbrooke's and Hinchingbrooke Hospitals and Dr Fiona Karet for their co-operation in collecting renal tissue and Dr A.M. Doherty (Parke-Davis Pharmaceutical Research Division) for synthesizing PD151242. Supported by grants from British Heart Foundation, Wellcome Trust, Royal Society and Newton Trust.

References

BATTISTINI, B., ALLCOCK, G.H., WARNER, T.D. & VANE, J.R. (1993). ET_A and ET_B receptors mediate the release of eicosanoids from the rat kidney induced by endothelin/sarafotoxin peptides. *Br. J. Pharmacol.*, **110**, 46P.

BENIGNI, A., ZOJA, C., CORNA, D., ORISIO, S., LONGARETTI, L., BERTANI, T. & REMUZZI, G. (1993). A specific endothelin subtype A receptor antagonist protects against injury in renal disease progression. *Kidney Int.*, **44**, 440–445.

BIGAUD, M. & PELTON, J.T. (1992). Discrimination between ET_A- and ET_B-receptor mediated effects of endothelin-1 and [$Ala^{1,3,11,15}$] endothelin-1 by BQ123 in the anaesthetised rat. *Br. J. Pharmacol.*, **107**, 912–917.

CLOZEL, M., GRAY, G.A., BREU, V., LÖFFLER, B.-M. & OSTERWALDER, R. (1992). The endothelin ET_B receptor mediates both vasodilation and vasoconstriction *in vivo*. *Biochem. Biophys. Res. Commun.*, **186**, 867–873.

CRISTOL, J.-P., WARNER, T.D., THIEMERMANN, C. & VANE, J.R. (1993). Mediation via different receptors of the vasoconstrictor effects of endothelins and sarafotoxins in the systemic circulation and renal vasculature of the anaesthetised rat. *Br. J. Pharmacol.*, **108**, 776–779.

DAVENPORT, A.P., KUC, R.E., FITZGERALD, F., MAGUIRE, J.J., BERRYMAN, K. & DOHERTY, A.M. (1994). [^{125}I]-PD151242: a selective radioligand for human ET_A receptors. *Br. J. Pharmacol.*, **111**, 4–6.

DAVENPORT, A.P. & MAGUIRE, J.J. (1994). Is endothelin-induced vasoconstriction mediated only by ET_A receptors in humans? *Trends Pharmacol. Sci.*, **15**, 9–11.

DAVENPORT, A.P., O'REILLY, G., MOLENAAR, P., MAGUIRE, J.J., KUC, R.E., SHARKEY, A., BACON, C.R. & FERRO, A. (1993). Human endothelin receptors characterised using reverse transcriptase-polymerase chain reaction, *in situ* hybridization and sub-type selective ligands BQ123 and BQ3020: evidence for expression of ET_B receptors in human vascular smooth muscle. *J. Cardiovasc. Pharmacol.*, **22(S8)**, 22–25.

DAVIS, L.S., LADOUCEUR, D.M., KEISER, J.A. & HALEEN, S.J. (1991). Relative vasodilator and vasoconstrictor activity of endothelin-1 (ET-1), endothelin-3 (ET-3) and sarafotoxin 6c (SFTX-6c) on regional arterial beds of the anaesthetized rat: relationship to ET_A and ET_B receptor agonist activity. *FASEB*, **6**, 391.

DERAY, G., CARAYON, A. & LEHOANG, P. (1991). Increased endothelin level after cyclosporine therapy. *Ann. Intern. Med.*, **114**, 809.

FOGO, A., HELLINGS, S.E., INAGAMI, T. & KON, V. (1992). Endothelin receptor antagonism is protective in rats with cyclosporine A-induced nephrotoxicity. *Kidney Int.*, **42**, 770–774.

GARDINER, S.M., KEMP, P.A., BENNETT, T. & DAVENPORT, A.P. (1993). Regional haemodynamic responses to the ET_B-receptor-selective agonist, BQ3020, in conscious rats. *Br. J. Pharmacol.*, **109**, 131P.

GODFRAIND, T. (1993). Evidence for heterogeneity of endothelin receptor distribution in human coronary artery. *Br. J. Pharmacol.*, **110**, 1201–1205.

KARET, F., KUC, R.E. & DAVENPORT, A.P. (1993). Novel ligands BQ123 and BQ3020 characterize endothelin receptor subtypes ET_A and ET_B in human kidney. *Kidney Int.*, **44**, 36–42.

KOYAMA, H., NISHZAWA, Y., MORII, H., TABATA, T., INOUE, T. & YAMAJI, T. (1989). Plasma endothelin levels in patients with uraemia. *Lancet*, **i**, 991–992.

MAGUIRE, J.J. & DAVENPORT, A.P. (1993). Endothelin-induced vasoconstriction in human isolated vasculature is mediated predominantly via activation of ET_A receptors. *Br. J. Pharmacol.*, **110**, 47P.

MOLENAAR, P., KUC, R.E. & DAVENPORT, A.P. (1992). Characterization of two new ET_B selective radioligands, [^{125}I]-BQ3020 and [^{125}I]- [Ala^{1,3,11,15}]ET-1 in human heart. *Br. J. Pharmacol.*, **107**, 637–639.

MOLENAAR, P., O'REILLY, G., SHARKEY, A., KUC, R.E., HARDING, D.P., PLUMPTON, P., GRESHAM, G.A. & DAVENPORT, A.P. (1993). Characterization and localization of endothelin receptor sub-types in the human atrioventricular conducting system and myocardium. *Circ. Res.*, **72**, 526–538.

NAMBI, P., PULLEN, M., CONTINO, L.C. & BROOKS, D.P. (1990). Upregulation of renal endothelin receptors in rats with cyclosporine A-induced nephrotoxicity. *Eur. J. Pharmacol.*, **187**, 113–116.

O'REILLY, G., CHARNOCK-JONES, D.S., DAVENPORT, A.P., CAMERON, I.T. & SMITH, S.K. (1992). Presence of mRNA for endothelin-1, endothelin-2, and endothelin-3 in human endometrium, and a change in the ratio of ET_A and ET_B receptor subtype across the menstrual cycle. *J. Clin. Endocrinol. Metab.*, **75**, 1545–1549.

O'REILLY, G., CHARNOCK-JONES, D.S., CAMERON, I.T., SMITH, S.K. & DAVENPORT, A.P. (1993a). Endothelin-2 mRNA splice variants detected by RT-PCR in cultured human vascular smooth muscle and endothelial cells. *J. Cardiovasc. Pharmacol.*, **22(S8)**, 18–21.

O'REILLY, G., CHARNOCK-JONES, D.S., MORRISON, J.J., CAMERON, I.T., DAVENPORT, A.P. & SMITH, S.K. (1993b). Alternatively spliced mRNAs for human endothelin-2 and their tissue distribution. *Biochem. Biophys. Res. Commun.*, **193**, 834–840.

PIERRE, L. & CLARK, K.L. (1994). Characteristics of endothelin receptors in rat main branch renal artery. *Br. J. Pharmacol.*, **112**, 163P.

POLLOCK, D.M. & OPGENORTH, J. (1993). Evidence for endothelin-induced renal vasoconstriction independent of ET_A receptor activation. *Am. J. Physiol.*, **264**, R222–R226.

POLLOCK, D.M. & OPGENORTH, J. (1994). ET_A receptor-mediated responses to endothelin-1 and big endothelin-1 in the rat kidney. *Br. J. Pharmacol.*, **111**, 729–732.

RIEZEBOS, J., WATTS, I.S. & VALLANCE, P.J.T. (1994). Endothelin receptors mediating functional responses in human small arteries and veins. *Br. J. Pharmacol.*, **111**, 609–615.

SAKURAI, T., YANAGISAWA, A. & MASAKI, T. (1992). Molecular characterisation of endothelin receptors. *Trends Pharmacol. Sci.*, **13**, 103–108.

STOCKENHUBER, F., GOTTSAUNER-WOLF, M., MAROSI, L., LIEBISCH, B., KURZ, R.W. & BLACKE, P. (1992). Plasma levels of endothelin in chronic renal failure and after renal transplantation: impact on hypertension and cyclosporine A-associated nephrotoxicity. *Clinical Sci.*, **82**, 255–258.

SUZUKI, N., MATSUMOTO, H., MIYAUCHI, T., GOTO, K., MASAKI, T., TSUDA, M. & FUJINO, M. (1990). Endothelin-3 concentration in human plasma: the increased concentrations in patients undergoing haemodialysis. *Biochem. Biophys. Res. Commun.*, **169**, 809–815.

TOMITA, K., UJIIE, K., NAKANISHI, T., TOMITA, S., MATSUDA, O., ANDO, K., SHICHIRI, M., HIRATA, Y. & MARUMO, F. (1989). Plasma endothelin levels in patients with acute renal failure. *New Engl. J. Med.*, **324**, 1127.

TOTSUNE, K., MOURI, T., TAKAHASHI, K., OHNEDA, M., SONE, M., SAITO, T. & YOSHINAGA, K. (1989). Detection of immunoreactive endothelin in plasma of haemodialysis patients. *FEBS Lett.*, **249**, 239–242.

WATSON, S. & GIRDLESTONE, D. (1993). *Trends Pharmacol. Sci. Receptor Nomenclature Supplement*, 14.

WELLINGS, R.P., CORDER, R., WARNER, T.D., CRISTOL, J.-P., THIEMERMANN, C. & VANE, J.R. (1994). Evidence from receptor antagonists for an important role for ET_B-mediated vasoconstrictor effects of endothelin-1 in the rat kidney. *Br. J. Pharmacol.*, **111**, 515–520.

(Received March 4, 1994
Revised May 9, 1994
Accepted May 10, 1994)

Br. J. Pharmacol. (1994), **113**, 55–62

Phorbol ester-induced M-current suppression in bull-frog sympathetic ganglion cells: insensitivity to kinase inhibitors

[1]Hsinyo Chen, Balvinder S. Jassar, [2]Dmitry E. Kurenny & [3]Peter A. Smith

Department of Pharmacology, University of Alberta, Edmonton, Alberta, Canada T6G 2H7

1 The effects of 1-oleoyl-2-acetyl-sn-glycerol (OAG), phorbol 12-myristate 13-acetate (PMA), 4-α-phorbol and muscarine on B-neurones from bull-frog sympathetic ganglion were studied by means of whole-cell patch-clamp recording. With the exception of 4-α-phorbol, all of these agonists reduced the steady-state outward current recorded at −30 mV as a result of suppression of a voltage-dependent, non-inactivating K^+-current, the M-current, (I_M).

2 Of the cells tested, 34% displayed *bona fide* responses to OAG (20 μM). The chance of recording a response was not decreased when the protein kinase inhibitor, 1-(5-isoquinolinylsulphonyl)-2-methyl-piperazine (H-7; 50 or 75 μM) was included simultaneously in the extracellular solution and in the pipette solution.

3 The presence of 50 μM H-7 on both sides of the membrane or 500 nM staurosporine in the pipette solution did not prevent responses to brief (1–2 min) or prolonged (>20 min) applications of PMA.

4 Brief (1–2 min) extracellular application of H-7 (300 μM) suppressed I_M by about 29%.

5 The most likely explanation of these data is that PMA and OAG modulate I_M via a mechanism that is independent of protein kinase C (PKC). The availability of such a mechanism poses new questions as to the mechanism of muscarine-induced I_M suppression.

Keywords: Potassium channel; muscarinic receptor; autonomic ganglia; M-current; protein kinase; G-protein; phorbol ester

Introduction

Many types of autonomic ganglion cells, including the B-cells in bull-frog sympathetic ganglia (BFSG), are depolarized following activation of muscarinic and/or peptide receptors (for review see Smith, 1993). This effect is attributed, at least in part, to suppression of a voltage-dependent, non-activating K^+-current termed the M-currrent (I_M; Brown & Adams, 1980, Adams *et al.*, 1982a,b). Although it is well-established that the response of both mammalian and amphibian sympathetic ganglia to muscarinic receptor stimulation is effected by a G-protein (Pfaffinger, 1988; Brown *et al.*, 1989; Lopez, 1992), it remains to be established whether other second messengers are involved in the transduction mechanism (Smith *et al.*, 1992; Selyanko *et al.*, 1992; Marrion, 1993). In amphibian paravertebral sympathetic ganglia, responses to G-protein-coupled agonists, such as muscarinic and luteinizing hormone releasing hormone (LHRH), are insensitive to protein kinase inhibitors such as staurosporine, H-7 (1-(5-isoquinolinylsulphonyl)-2-methyl-piperazine), gold sodium thiomalate, or protein kinase C pseudosubstrate peptide (Bosma & Hille, 1989; Selyanko *et al.*, 1990). This observation, as well as the probable lack of involvement of phosphorylation/dephosphorylation processes (Chen & Smith, 1992) argues against a role for protein kinases in agonist-induced I_M suppression.

Unlike muscarine and peptides, it has been suggested that phorbol esters exert an effect on I_M which is mediated via activation of protein kinase C (PKC). This idea is supported by the observation that phorbol esters suppress I_M in both mammalian (Brown & Adams, 1987; Brown *et al.*, 1989) and amphibian sympathetic ganglia and that these responses, as well as those to the DAG analogue, dioctanoylglycerol, are antagonized by PKC inhibitors such as H-7 or staurosporine (Bosma & Hille, 1989; Grove *et al.*, 1990). Experiments in our laboratory, however, failed to demonstrate antagonism of phorbol ester responses by H-7 (Selyanko *et al.*, 1990). The present paper therefore describes our re-examination of the effect of H-7 on the response of BFSG neurones to phorbol 12-myristate 13-acetate (PMA). We have also examined the effect of H-7 on responses to the DAG analogue, 1-oleoyl-2-acetyl-sn-glycerol (OAG) as well as the effect of staurosporine on PMA responses. A preliminary account of some of this work has appeared (Chen *et al.*, 1992).

Methods

Small bull-frogs (*Rana catesbeiana*, body-length <10 cm) were purchased from a biological supply house and stored in running water at room temperature (20°C). Each animal was killed by pithing. Neurones in the VIth to Xth paravertebral sympathetic ganglia were dissociated with trypsin and collagenase and their electrophysiological properties examined by whole-cell patch-clamp recording as described previously (Selyanko *et al.*, 1990). All experiments were carried out at room temperature (20°C). Recordings were made using an Axopatch 1B amplifier, a Labmaster TMA interface connected to an IBM-compatible computer. Data were acquired and analysed with 'Pclamp' software (Axon Instruments, Foster City, CA, U.S.A.) and stored on a hard disk prior to off-line analysis. Permanent records were obtained from an *x-y* plotter or a d.c. rectilinear pen recorder (Gould-Brush 2400; pen rise time <8 ms). The corner frequency of the filter on the Axopatch amplifier was set to 200 Hz for voltage-ramp experiments and to 500 Hz for voltage-jumps. Current was set to zero at resting membrane potential (r.m.p.) which was usually −50 to −55 mV. The holding potential for all experiments was −30 mV. An estimate of the cell size was obtained from the input capacitance (C_{in}) and experiments were only done on the 'large' cells (C_{in} > 30 pF) in which muscarine suppressed steady-state outward current at −30 mV ($[K^+]_o$ = 6 mM). Since the currents to be recorded were usually <0.5 nA, no corrections were made for the voltage-drop across the series resistance, which

[1] Present address: National Research Institute of Chinese Medicine, Taipei 23177, Taiwan.
[2] Present address: Division of Medical Physiology, University of Calgary Medical School, Calgary, Ab. T2N 1N4, Canada.
[3] Author for correspondence.

varied between 10 and 20 MΩ. Although this means that the maximum possible voltage error due to series resistance could be as much as 10 mV, errors of this magnitude would only have been encountered in the few cells which exhibited exceptionally large currents whilst being studied with relatively high resistance pipettes. Whole-cell M-channel conductance (G_M) was examined using a 5 s ramp command from the holding potential of −30 mV to −110 mV (16 mV s^{-1} see Figures 2 and 5). The high conductance part of the resulting *I-V* relationship (i.e. above −75 mV) represents current through M-channels plus leak current (Selyanko *et al.*, 1990). Total I_M at −30 mV was estimated after digitally-subtracting the leak current predicted by the slope between −75 mV and −90 mV. The percentage suppression of I_M induced by agonists was calculated using the equation

$$\%\ I_M \text{ suppression} = \frac{I_{M,c} - I_{M,a}}{I_{M,c}} \times \frac{100}{1}$$

where $I_{M,c}$ = control, leak-subtracted I_M at −30 mV prior to the application of agonist and $I_{M,a}$ is the leak-subtracted I_M at −30 mV recorded in the presence of the agonist. This procedure allowed separation of agonist-induced changes in I_M from changes in voltage-independent leak current which occurred in a few cells.

The physiological salt solution contained (in mM): NaCl 113, KCl 6, $MgCl_2$ 2, $CaCl_2$ 2, HEPES/NaOH (pH 7.2) and D-glucose 10. Patch pipettes were prepared with tip diameters that yielded d.c resistances of about 10 MΩ (range 7–15 MΩ). Pipette tips were coated with Sylgard elastomer. The solution used to fill the pipettes contained (in mM): KCl 110, NaCl 10, $MgCl_2$ 2, $CaCl_2$ 0.4, EGTA 4.4, HEPES/KOH (pH 6.7) 5, D-glucose 10, cyclic AMP Na^+ salt 0.1. The pCa of this solution, measured with a Ca^{2+}-electrode, was about 7. In some experiments, staurosporine (500 nM) or H-7 (50 μM) was added to the solution in the patch-pipette. The time constant (τ) for diffusion of H-7 into an averaged-sized BFSG B-cell (C_{in} = 40 pF) is about 45 min and that for staurosporine is 53 min. These values were obtained using the empirical equations of Pusch & Neher (1988) assuming an access resistance of 20 MΩ, which corresponds to the maximum value read from the amplifier series resistance compensation control. The values of τ have therefore been calculated to reflect the minimum rates of diffusion of drugs into BFSG B-cells. The theoretical change in intracellular concentration of H-7 and staurosporine with time can be read from the graphs in Figure 1a and b, which are plots of the equation

$$[D]_{i,t} = [D]_p\ (1 - \exp^{-t/\tau})$$

where $[D]_{i,t}$ = intracellular concentration of drug D at time t, $[D]_p$ = concentration of drug D in the pipette (50 μM for H-7, 500 nM for staurosporine), t = time in min and τ is the time constant for equilibration of drug D in the pipette with the intracellular fluid (= 45 min for H-7 and 53 min for staurosporine). The horizontal lines on the graphs represent the K_i value for inhibition of PKC by H-7 (6 μM; Hidaka *et al.*, 1984) and the IC_{50} value for staurosporine inhibition (2.7 nM; Tamaoki *et al.*, 1986). The graphs show that these concentrations should be attained after about 6 min with 50 μM H-7 and in less than 1 min with 500 nM staurosporine.

Drugs were applied to the extracellular surface of the membrane by bath superfusion or by using the U-tube technique (Selyanko *et al.*, 1990). The fluid exchange time for the U-tube was about 0.2 s. Experiments involving phorbol esters or staurosporine were carried out under subdued lighting conditions. 1-oleoyl-2-acetyl-sn-glycerol (OAG), phorbol 12-myristate 13-acetate (PMA) and 4-α-phorbol were prepared as 10 mM stock solutions in ethanol and diluted in external solution as required. Appropriate control experiments were done to verify the lack of effect of the vehicle on I_M. All drugs and chemicals were purchased from Sigma, St. Louis, MO, U.S.A. except for staurosporine which was from Calbiochem, LaJolla, CA, U.S.A. H-7 from Sigma was from lot Nos 62H5810 or 122H5805.

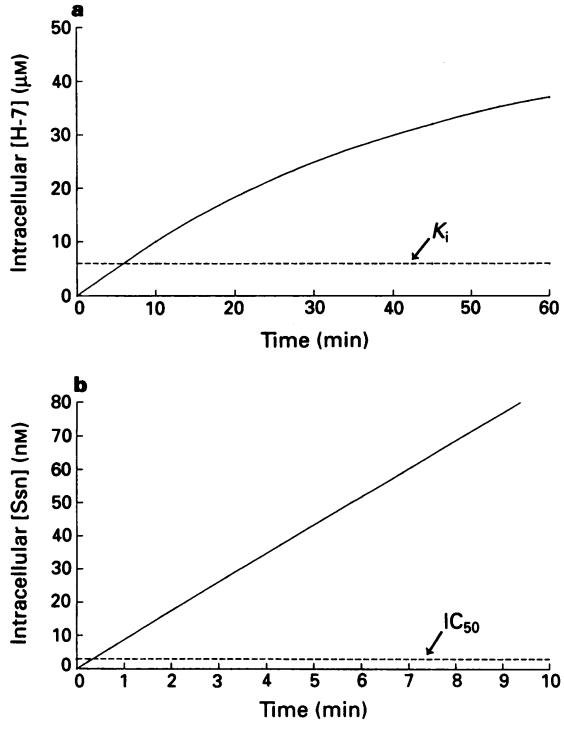

Figure 1 Graphs showing the theoretical rate of change of intracellular concentration of (a) H-7 and (b) staurosporine (Ssn) in a 40 pF cell during recording with a patch-pipette containing 50 μM H-7 or 500 nM staurosporine. The dotted horizontal lines represent the K_i for protein kinase C (PKC) inhibition by H-7 and the IC_{50} value for PKC inhibition by staurosporine.

Data are expressed as mean ± s.e.mean and significance of differences estimated by Student's two-tailed, unpaired *t* test.

Results

Responses to the DAG analogue, 1-oleoyl-2-acetyl-sn-glycerol (OAG)

Eight out of 23 control cells (34.1%) exhibited obvious responses to 20 μM OAG in which steady-state outward current at −30 mV (I_M) was depressed by more than 10%. In these cells, the response was small and slow in onset. Most of the cells exhibited a rapid decline in sensitivity to OAG such that it was not possible to elicit a response to a second application of agonist. Another 24 cells were studied using an internal solution containing 50 or 75 μM H-7; 50 μM H-7 was also present in the extracellular solution. Despite the likely inhibition of most isoforms of PKC under these conditions, 8 out of these 24 cells (33.3%) still responded to 20 μM OAG. Although OAG was applied at various time intervals (2.5–40 min) following initiation of recording with H-7-filled pipettes, there was no obvious correlation between the time of application and the presence or absence of a response. Thus, the presence of H-7 did not decrease the chance of recording an OAG response.

An experiment in which the patch pipette contained 50 μM H-7 for 40 min prior to the application of OAG is illlustrated in Figure 2. The steady-state current-voltage characteristics of the cell were determined by using a slow, hyperpolarizing voltage-ramp command from the holding potential of −30 mV to −110 mV (Selyanko *et al.*, 1990). Application of 20 μM OAG with 50 μM H-7 in the extracellular solution suppresses steady-state outward current at −30 mV (Figure

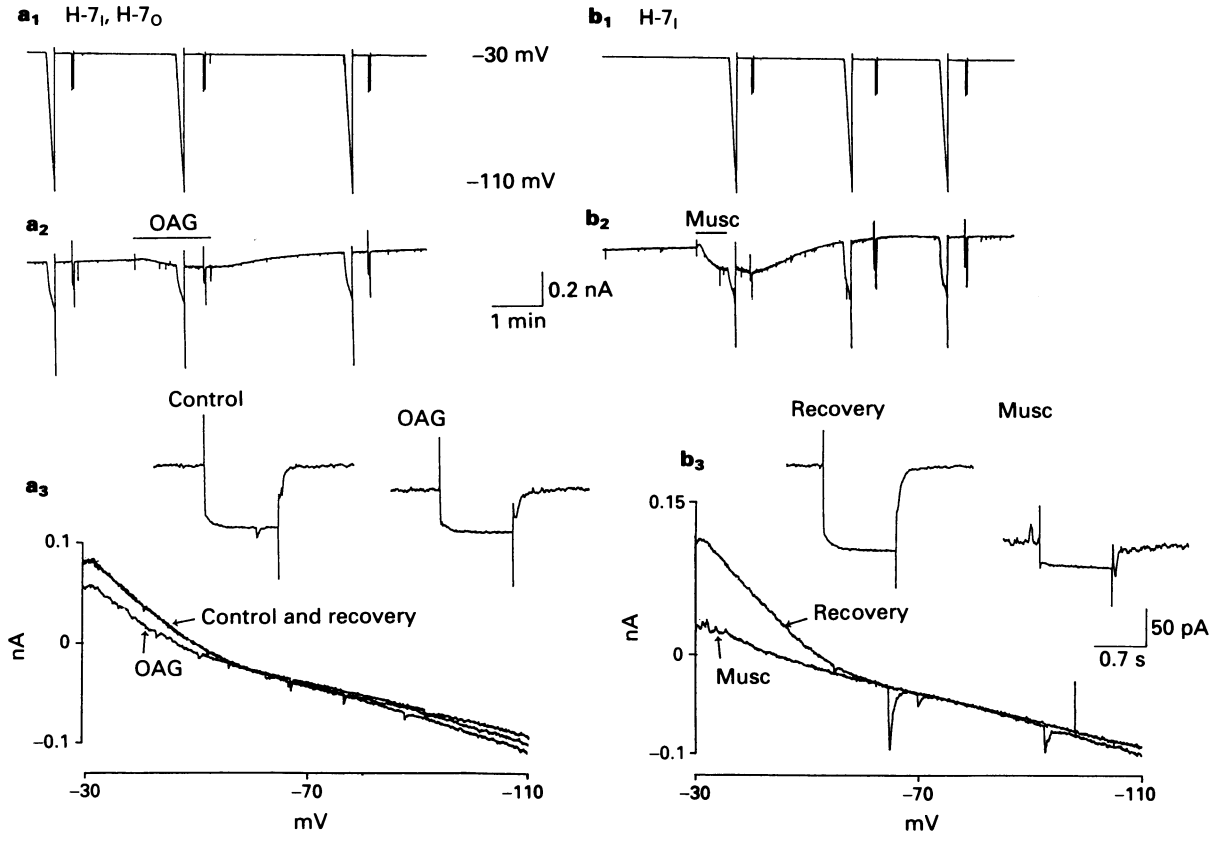

Figure 2 Effects of (a) OAG (20 μM) and (b) muscarine (Musc, 1 μM) on M-current. Pipette contained 50 μM H-7. All records from the same cell. Extracellular solution contained 50 μM H-7 for 10 min prior to application of OAG from a U-tube. This was washed out before application of muscarine (also from a U-tube). (a_1 and b_1) Voltage protocols: 5 s ramp command from holding potential of −30 mV to −110 mV followed by single step to −50 mV. (a_2 and b_2) Suppression of steady-state outward current by OAG and muscarine. OAG was applied 40 min after initiation of recording with an H-7 filled pipette. (a_3 and b_3) Steady-state current-voltage plots obtained from current response to voltage ramps before, during and after application of OAG and during and after muscarine. Note that both agonists decrease conductance above about −70 mV, i.e. in the I_M range with some slight increase in leak conductance. Insets in (a_3) and (b_3) are current responses to voltage steps (from −30 to −50 mV). The characteristic I_M relaxations which are evident at the start and end of each trace are suppressed by OAG and almost eliminated by muscarine. The traces are aligned to show the reduction in steady-state outward current produced by each agonist. 50 pA, 0.7 s calibration refers to insets in both (a_3) and (b_3). Calibrations 0.2 nA, 1 min refer to records in (a_2) and (b_2). Records in (a_2) and (b_2) from rectilinear pen recorder and records in (a_3) and (b_3) from *x-y* plotter. For abbreviations, see text.

$2a_2$) and decreases conductance at potentials positive to about −70 mV as would be expected for I_M suppression (Figure $2a_3$). I_M relaxations recorded following a step from −30 mV to −50 mV are also reduced by OAG (see Brown & Adams, 1980; Adams *et al.*, 1982a). In the same cell, muscarine (1 μM) produces a robust response (Figure $2b_2$) which is associated with obvious I_M suppression (Figure $2b_3$).

Responses to brief applications of phorbol 12-myristate 13-acetate (PMA)

Because phorbol esters consistently produce I_M suppression in amphibian sympathetic ganglion cells (Bosma & Hille, 1989; Selyanko *et al.*, 1990), we studied the effects of H-7 on responses to PMA. Since it produces irreversible I_M suppression, it was necessary to study responses to PMA in one group of cells and responses to PMA in the presence of kinase inhibitors in another group of cells. A log concentration-response curve was constructed by averaging the response of several cells to three different concentrations of PMA with 50 μM H-7 on both sides of the membrane. So as to allow the intracellular concentration of H-7 to reach a level which would be expected to inhibit protein kinase activity (see Figure 1), responses to the phorbol ester were evoked at least 30 min after initiating recording with an H-7 filled pipette. All cells were also exposed to extracellular H-7 for at least 10 min before the effects of PMA were examined. The data are shown in Figure 3a. The figure also illustrates the log concentration-response curve to muscarine (obtained by averaging data from several cells for each concentration) and a single point which represents the mean amplitude of the response to five control cells to 200 nM PMA. Since the response to 200 nM PMA in the presence of the kinase inhibitor is larger that in its absence, H-7 does not antagonize phorbol ester responses. These data also confirm that the maximal I_M suppression which can be attained following *brief* (1–2 min) applications of PMA is less than that which can be attained with muscarine (Bosma & Hille, 1989; Selyanko *et al.*, 1990).

Responses to long-term application of phorbol 12-myristate 13-acetate (PMA)

By contrast with the effects of *brief* applications of PMA, *long-term* applications were at least as effective as muscarine in promoting I_M suppression. In these experiments, PMA was ejected from the U-tube for 20 min or more until I_M reached a steady-state value. Little or no response to muscarine could be evoked after the full effect of PMA had developed. A typical experiment in the presence of H-7 is illustrated in Figure 4a. Muscarine (1 μM) produces a marked suppression of steady-state outward current (at −30 mV) followed by an

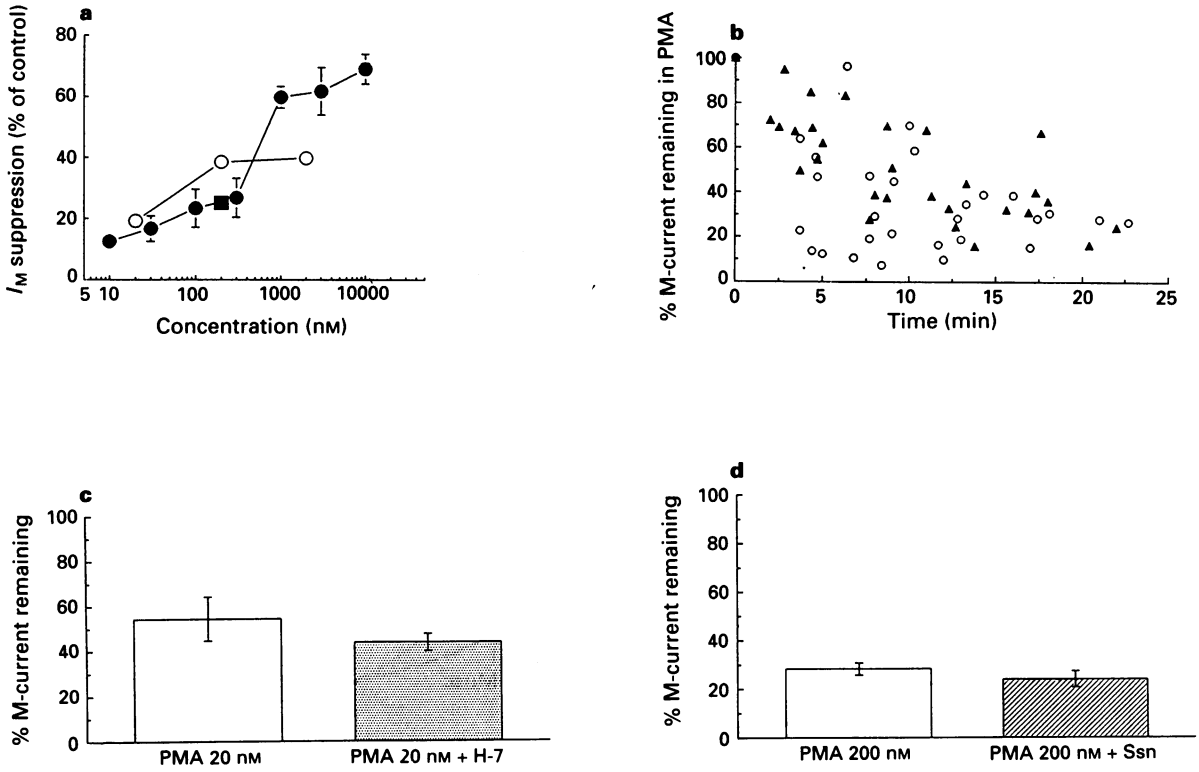

Figure 3 (a) Log-concentration response relationships for acute (1–2 min) applications of muscarine (●) and PMA + H-7 (○, 50 μM H-7 in pipette, 50 μM H-7 in extracellular solution). In some cases, error bars (for s.e.mean) are smaller than the symbols to designate the data points. Data are mean suppression of control I_M from different cells for different concentrations of agonists. For muscarine; 10 nM $n = 8$, 20 nM $n = 8$, 100 nM $n = 9$, 200 nM $n = 6$, 1 μM $n = 38$, 2 μM $n = 7$, 10 μM $n = 6$. For PMA/H-7; 20 nM $n = 5$, 200 nM $n = 6$, 2 μM $n = 4$. (■) Designates mean amplitude of response of 5 control cells to 200 nM PMA. (b) Time course of effects of (▲) 2 nM and (○) 200 nM PMA on I_M. Individual data points were collected at various time intervals from 7 cells for 2 nM and 8 cells for 200 nM PMA and normalized to the initial (100%) value of I_M obtained before exposure to phorbol ester. Note that both 2 and 200 nM PMA suppress I_M to about 20% of its initial value. (c) Normalized, mean value of I_M (± s.e.mean) recorded after 10–20 min in 20 nM PMA in the absence (6 measurements on 6 cells) and presence of H-7 (50 μM on both sides of the membrane, 6 measurements on 4 cells). (d) Normalized, mean value of I_M during 10–20 min exposure to 200 nM PMA in the absence (11 measurements on 8 cells) and presence (11 measurements on 5 cells) of 500 nM staurosporine (Ssn). Note that PMA-induced I_M suppression is neither prevented by staurosporine ($P > 0.3$) nor by H-7 ($P > 0.4$). For abbreviations, see text.

obvious 'over-recovery' (Pfaffinger, 1988; Chen *et al.*, 1993). Long-term application of 20 nM PMA slowly suppresses I_M to almost the same level as seen with muscarine. Subsequent application of muscarine is almost without effect. Some normalized I_M values recorded from 7 cells studied for 20 min or more in the presence of 2 nM PMA and from 8 cells studied in the presence of 200 nM PMA are plotted against time in Figure 3b. Two points clearly emerge from these data; the effect of PMA is quite variable and both 2 and 200 nM suppress I_M to about 20% of its initial value after about 25 min. Although it was not possible to fit lines to these data points and thereby derive rate constants for the change in I_M, PMA clearly produces more suppression of I_M than would be predicted by 'run-down'. This is because under the conditions of experiments, I_M usually retains about 70% of its initial value after 25 min of recording (see Figure 2d Chen *et al.*, 1985). A possible explanation for the absence of a clear-cut concentration-dependence may be that the partition coefficient for PMA for cell membranes compared to aqueous solutions is so large that the concentration achieved within the membrane exceeds that in the external solution. Thus, the concentration of PMA achieved in the membrane following extracellular application of a 2 nM solution may eventually equal that achieved in a shorter time period with 200 nM.

As with acute responses, the presence of 50 μM H-7 on both sides of the membrane had no obvious effect on the response to the long-term application of PMA. Figure 3c compares the amount of I_M remaining after 10–20 min in 20 nM PMA (data points were collected from 6 cells) with that remaining in the presence of PMA plus H-7 (data from 4 cells; 50 μM H-7 on both sides of the membrane). This treatment failed to protect I_M from suppression by PMA. In another 4 cells, H-7 failed to attenuate the effect of a long-term exposure to 200 nM PMA (data not shown).

Figure 3d shows that similar results were obtained in cells that were studied after 20–28 min recording with 500 nM staurosporine in the pipette. Data for this figure were collected from 8 control cells exposed for 10–20 min to 200 nM PMA and from 5 other cells exposed to PMA but studied with pipettes which contained staurosporine. A typical experiment is illustrated in Figure 4b. Even after 21 min of recording using a pipette containing 500 nM staurosporine, PMA reduced the steady-state outward current at −30 mV as a result of I_M suppression. The full effect of PMA, which took at least 20 min to develop, was comparable to that produced by 1 μM muscarine.

Lack of effect of 4-α-phorbol

There are two possible explanations for the insensitivity of PMA responses to H-7 and staurosporine. Either these responses are mediated by isoforms of PKC which are resistant to inhibition by these compounds or the responses are mediated by a mechanism which is completely independent of PKC. In an attempt to distinguish between these possibilities, we examined the effect of 4-α-phorbol which is unable to stimulate protein kinases (Higashida & Brown, 1986). Prolonged application of this substance (> 20 min; 200 nM) had

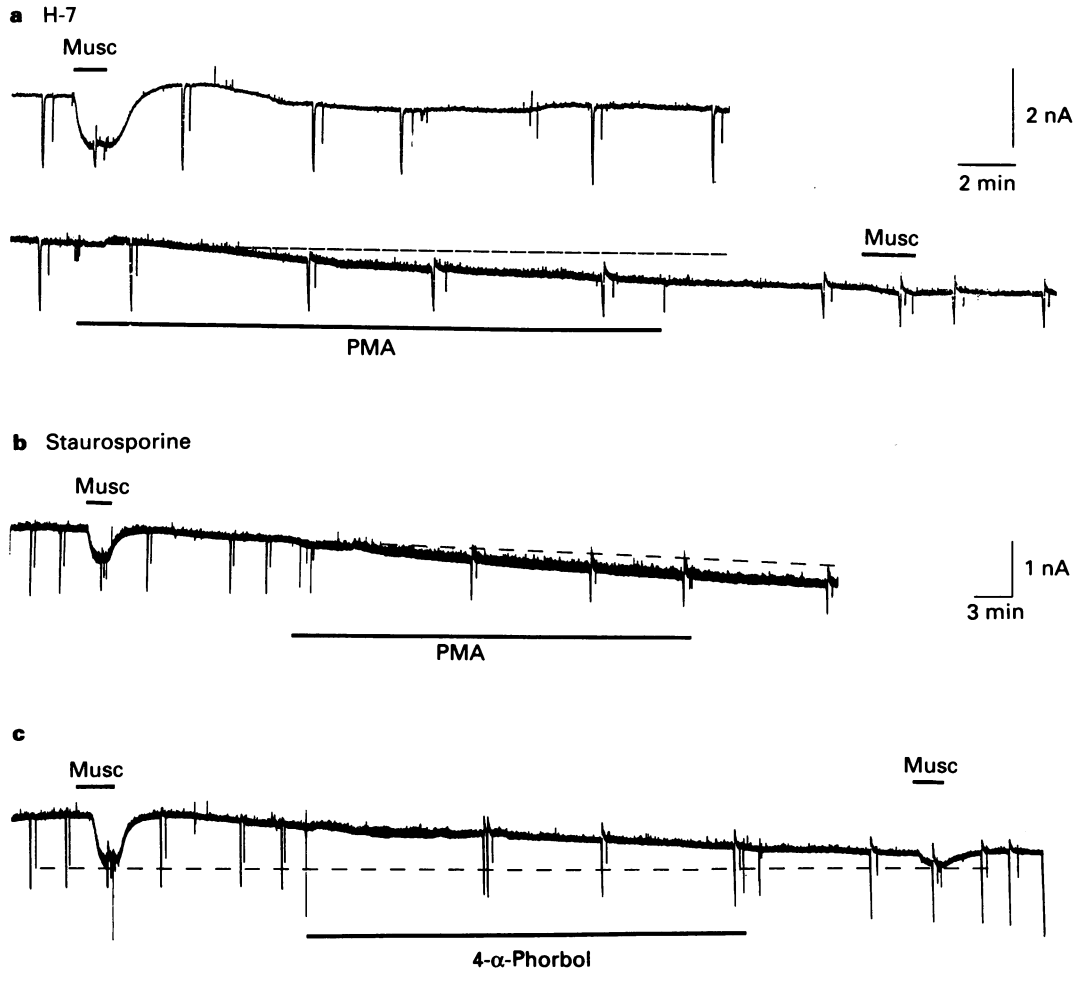

Figure 4 Pen recorder tracings showing acute effect of 1 μM muscarine and effect of long-term exposure to PMA or 4-α-phorbol on steady-state current recorded at −30 mV. Voltage command traces omitted for clarity. (a) Initial response to muscarine (Musc) obtained 4 min after initiating recording with a pipette containing 50 μM H-7. PMA, 20 nM, was applied 10 min after initiating extracellular superfusion with 50 μM H-7 and 23 min after initiating recording with H-7 in the pipette. Note slow decrease in steady-state outward current produced by the phorbol ester and very small response to muscarine following removal of PMA. Dashed lines depict predicted amount of steady-state outward current expected to remain had PMA not been applied. About 1 min of recording is omitted between the end of the upper trace and the start of the lower trace. (b) Effect of 1 μM muscarine and 200 nM PMA on a cell which was studied with a pipette that contained 500 nM staurosporine. PMA was applied 21 min after initiation of recording. Note slow time course of effect of PMA. Dotted line reflects predicted 'run-down' of I_M had PMA not been applied. (c) Data from another experiment showing the lack of effect of long-term exposure to 4-α-phorbol. Steady decline in outward current presumably reflects I_M 'run-down'. Note that 1 μM muscarine reduces I_M to the same absolute level prior to and after exposure to 4-α-phorbol. Downward deflections on traces reflect current responses to voltage steps and ramps which were applied from the holding potential of −30 mV to measure I_M during the course of the experiment (see Figures 2 and 5). Calibration 1 nA/3 min refers to records in (b) and (c). Note very slow time scale for these records and difference in time scale for the experiment shown in (a).

no obvious effect on I_M in any of 4 cells treated. Application of muscarine after 4-α-phorbol was able to suppress I_M to the same level seen with muscarine alone. A typical experiment is illustrated in Figure 4c; 20 min superfusion of 200 nM 4-α-phorbol failed to produce any more I_M suppression than might have been predicted by I_M 'run-down' (see Selyanko *et al.*, 1990). After removal of 4-α-phorbol, 1 μM muscarine suppressed I_M to the same level as was seen at the start of the experiment.

Agonist effects of H-7

Whereas our experiments, in which 50 μM H-7 was applied to both sides of the membrane, failed to demonstrate antagonism of phorbol ester responses, Bosma & Hille (1989) reported antagonism of PMA responses following extracellular application of 300 μM H-7. Since H-7 is structurally-related to adenosine nucleotides and substances such as ATP are able to promote I_M suppression by interaction with an extracellular receptor (Groul *et al.*, 1981; Adams *et al.*, 1982b), it is possible that H-7 may suppress I_M and thereby occlude responses to phorbol esters. H-7 (300 μM) was therefore tested on 9 cells and was found to suppress I_M by 29.1 ± 4.4%. A typical experiment illustrating the response to a brief application of H-7 is shown in Figure 5. I_M recorded following the action of H-7 is almost identical to control whereas an obvious over-recovery is observed following the removal of muscarine (Pfaffinger, 1988; Chen *et al.*, 1993). The effect of H-7 is associated with a marked increase in noise which may reflect activation of 'spontaneous miniature outward currents' as a result of activation of Ca^{2+}-dependent K^+-currents (Satin & Adams, 1987; Selyanko *et al.*, 1990).

Any alteration of steady-state I_M following long-term exposure to 50 or 75 μM H-7, as used in the present experiments, was difficult to distinguish from 'run-down' of I_M.

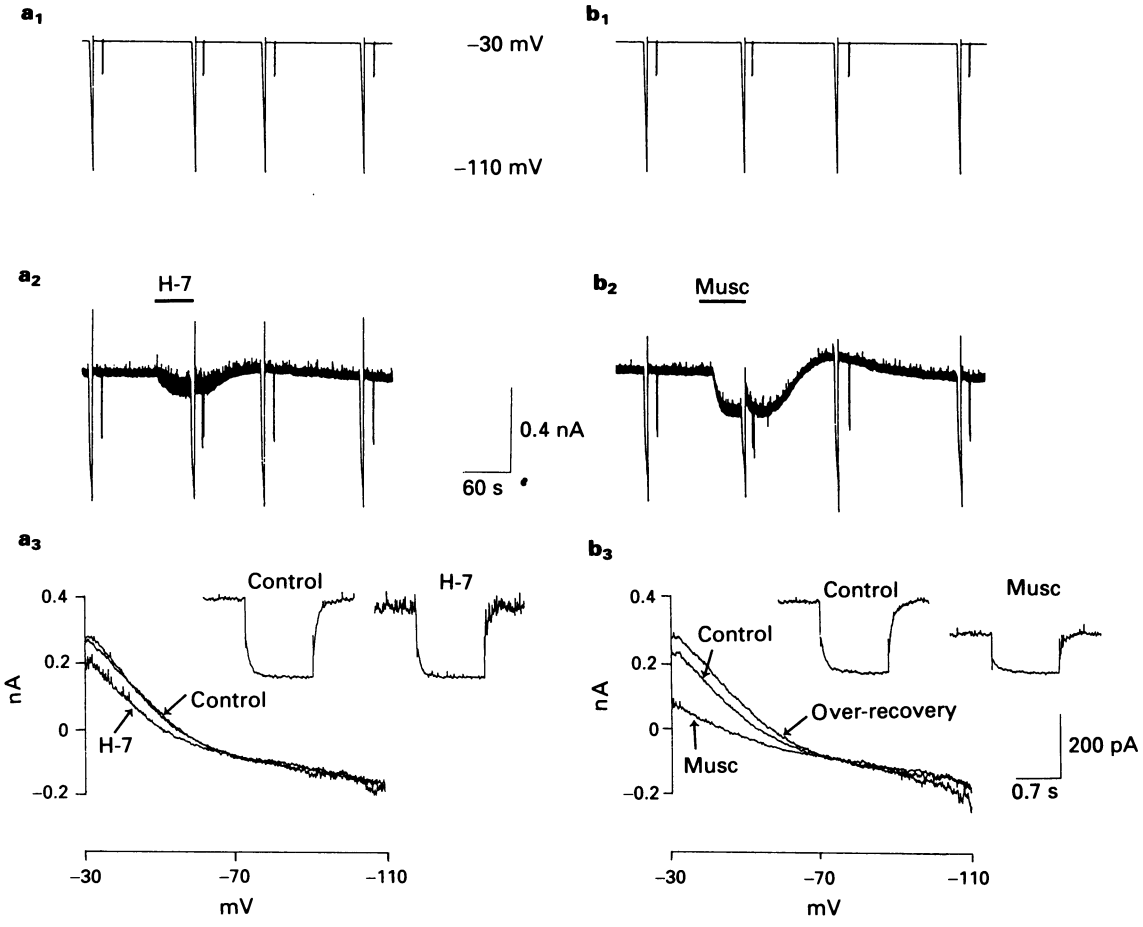

Figure 5 Effect of brief extracellular application of 300 μM H-7 on I_M: comparison with the action of muscarine (Musc). (a_1 and b_1) Voltage protocols; (a_2 and b_2) suppression of steady-state outward current by application of H-7 (300 μM) or muscarine (1 μM); (a_3 and b_3) steady-state current-voltage plots obtained from current responses to voltage ramps before during and after application of H-7 and muscarine. Insets are current responses to voltage steps (from −30 to −50 mV) recorded before and during the action of drugs. Note suppression of I_M by both drugs. Calibration 200 pA, 0.7 s refers to insets in both (a_3) and (b_3). Records in (a_2) and (b_2) from rectilinear pen recorder and records in (a_3) and (b_3) from *x-y* plotter. Calibration 0.4 nA, 60 s refers to records in (a_2) and (b_2).

Discussion

Like the inhibition of neuronal Ca^{2+} currents (I_{Ca}) by phorbol esters (Hockberger *et al.*, 1989; Plummer *et al.*, 1991; Abrahams & Scholfield, 1992), inhibition of I_M in BFSG by OAG and PMA seems resistant to the action of PKC inhibitors. This finding confirms and extends our previous data (Selyanko *et al.*, 1990) yet differs from the results of Bosma & Hille (1989) who reported that suppression of I_M in frog sympathetic ganglion by phorbol esters or dioctanoylglycerol could be prevented by H-7 or staurosporine. A similar type of result was obtained by Grove *et al.* (1990) who used extracellular recording to study phorbol ester responses in rat superior cervical ganglion. The differences between our data and those of Bosma & Hille (1989) may be attributable to (*i*) the inconsistency and lack of reproducibility of responses to DAG analogues such as OAG which was used in our experiments and perhaps to dioctanoylglycerol which was used in their experiments, (*ii*) the slow rate of onset and the irreversible nature of responses to phorbol esters and (*iii*) differences between the effects of intracellularly and extracellularly applied H-7.

The concentration of H-7 (50 or 75 μM) used in our experiments is about 10 times the K_i for inhibition of PKC (6 μM; Hidaka *et al.*, 1984) and that of staurosporine (500 nM) is almost 200 times the IC_{50} (2.7 nM; Tamaoki *et al.*, 1986). Since the intracellular concentration of either substance should, in theory, exceed these values in less than 5 min of whole-cell recording (see Figure 1), it is likely that PKC is exposed to potentially effective concentrations of inhibitors during the time course of our experiments. This conclusion is supported by the observation that substances such as staurosporine, ATP-γ-S (adenosine-5'-O-[3-thiotriphosphate]) and GTP-γ-S (guanosine-5'-O-[3-thiotriphosphate]), which have similar molecular weights to H-7, diffuse readily from patch pipettes and evoke obvious pharmacological responses in BFSG cells (Pfaffinger, 1988; Selyanko *et al.*, 1990; Simmons *et al.*, 1990; Chen & Smith, 1992; Werz *et al.*, 1993). Furthermore, because H-7 acts competitively at the ATP binding site on protein kinase (Hidaka *et al.*, 1984), the *intracellular* method of application used in our experiments should have been effective in delivering the inhibitor to its site of action. Bosma & Hille (1989) did not examine the effect of intracellularly-applied H-7 but reported that *extracellularly* applied H-7 (300 μM) effectively antagonized responses to dioctanoglycerol and PMA. It is possible that this effect resulted from occlusion of the responses as a result of the direct suppression of I_M by 300 μM H-7 (see Figure 4). Also, because responses to DAG analogues such as OAG are weak and inconsistent and only occur in 34% of the cells tested, the absence of a response in the presence of H-7 does not necessarily imply that blockade has occurred.

One explanation for the lack of effect of PKC inhibitors on PMA- and OAG-induced I_M suppression is that those isoforms of PKC which might be involved in I_M suppression

of BFSG may be resistant to H-7 and staurosporine. This would seem unlikely because Werz *et al.* (1993) recently demonstrated that 1 μM staurosporine, applied simultaneously to both the outer and inner surface of the membrane, can attenuate okadaic acid-induced enhancement of I_{Ca} inactivation in this tissue, suggesting that at least some of the isoforms of the enzyme present in BFSG are staurosporine-sensitive. Another possibility is that the effects of phorbol esters are generated by a kinase-independent mechanism. For example, they may interact *directly* with the M-channel or a closely related structure. This possibility has been discussed by Clapp *et al.* (1992) for phorbol ester-induced I_M suppression in smooth muscle cells. If this mechanism were available, a novel transduction mechanism for muscarinic agonists might be proposed whereby DAG, which is produced in amphibian sympathetic neurones following activation of muscarinic receptors (Pfaffinger *et al.*, 1988), suppresses I_M via *direct* interaction with the M-channel. Kinase-independent actions of phorbol esters and OAG would then reflect their interaction with the site which is normally activated by DAG. Our data suggest that this site would not be activated by 4-α-phorbol.

The observation that phosphorylation/dephosphorylation reactions do not seem to be involved agonist-induced I_M suppression (Chen & Smith, 1992) is consistent with the possible involvement of a direct DAG-M-channel pathway. Furthermore, the opening probability of putative M-channels, recorded in the cell-attached mode, is reduced when muscarine is applied *outside* the recording pipette (Selyanko *et al.*, 1992; Marrion, 1993). This effect requires the production of a second messenger which is capable of diffusion from the site of G-protein activation to the M-channels which are under the recording pipette. According to our speculation, DAG could play the role of diffusible yet membrane-delimited second messenger. Additional support for this possibility comes from the observation that, at least in rat superior cervical ganglion neurones, the α- subunit of G_q, the G-protein responsible for phospholipase C activation and DAG production, seems to play a role in the transduction mechanism for oxotremorine-M-induced I_M suppression (Jones *et al.*, 1993).

Although the idea that ion channels may be controlled by membrane lipids is not without precedent (Ordway *et al.*, 1989), preliminary attempts to test the 'direct-DAG' hypothesis by limiting DAG catabolism have yielded inconclusive results (Chen *et al.*, 1992). Also 'kinase-independent' actions of phorbol esters on Ca^{2+} channel currents seem to involve different effects on activation kinetics from those produced by G-protein-coupled agonists (Plummer *et al.*, 1991; Abrahams & Schofield, 1992). This implies that the transduction mechanism used by agonists to alter I_{Ca} does not involve the site which is activated by phorbol esters. If a similar situation obtains for agonist-induced I_M suppression, this would argue against the 'direct DAG' hypothesis.

Supported by grants from the Medical Research Council of Canada and the University of Alberta Central Research Fund. Certain items of major equipment were provided by the Alberta Heritage Foundation for Medical Research. P.A.S. was an Alberta Heritage Medical Scholar. We thank Dr W.F. Dryden for his comments on an early version of this manuscript.

References

ABRAHAMS, T.P. & SCHOLFIELD, G.G. (1992). Norepinephrine-induced Ca^{2+} current inhibition in adult rat sympathetic neurons does not require protein kinase C activation. *Eur. J. Pharmacol.*, **227**, 189–197.

ADAMS, P.R., BROWN, D.A. & CONSTANTI, A. (1982a). M-currents and other potassium currents in bullfrog sympathetic neurones. *J. Physiol.*, **330**, 537–572.

ADAMS, P.R., BROWN, D.A. & CONSTANTI, A. (1982b). Pharmacological inhibition of the M-current. *J. Physiol.*, **332**, 232–262.

BOSMA, M.M. & HILLE, B. (1989). Protein kinase C is not necessary for peptide-induced suppression of M-current or for desensitization of the peptide receptors. *Proc. Natl. Acad. Sci. U.S.A.*, **86**, 2943–2947.

BROWN, D.A. & ADAMS, P.R. (1980). Muscarinic suppression of a novel voltage-sensitive K^+-current in a vertebrate neurone. *Nature*, **283**, 673–676.

BROWN, D.A. & ADAMS, P.R. (1987). Effects of phorbol dibutyrate on M-currents and M-current inhibition in bullfrog sympathetic neurones. *Cell. Mol. Neurobiol.*, **7**, 255–269.

BROWN, D.A., MARRION, N.V. & SMART, T.G. (1989). On the transduction mechanism for muscarine-induced suppression of the M-current in cultures of rat sympathetic ganglion neurones. *J. Physiol.*, **413**, 469–488.

CHEN, H., KURENNY, D.E. & SMITH, P.A. (1992). Is diacylglycerol involved in the effect of muscarine on sympathetic ganglion cells? *Soc. Neurosci. Abstr.*, **18**, 1341.

CHEN, H., KURENNY, D.E. & SMITH, P.A. (1993). Heparin prevents M-current over-recovery but not M-current suppression in bullfrog sympathetic ganglion cells. *Brain Res.*, **625**, 323–327.

CHEN, H. & SMITH, P.A. (1992). M-current suppression in frog sympathetic ganglion following manipulation of membrane phosphorylation. *Br. J. Pharmacol.*, **105**, 329–334.

CLAPP, L.H., SIMS, S.M. & WALSH, J.V. (1992). Role of diacylglycerol in mediating the actions of ACh on M-current in gastric smooth muscle cells. *Am. J. Physiol. (Cell Physiol.)*, **321**, C1274–C1281.

GROVE, E.A., CAULFIELD, M.P. & EVANS, F.J. (1990). Inhibition of protein kinase C prevents phorbol ester- but not muscarine-induced depolarizations in the rat superior cervical ganglion. *Neurosci. Lett.*, **110**, 162–166.

GROUL, D.L., SIGGINS, G.R., PADJEN, A. & FORMAN, D.S. (1981). Explant cultures of adult amphibian sympathetic ganglia: electrophysiological and pharmacological investigation of neurotransmitter and nucleotide action. *Brain Res.*, **223**, 81–106.

HIDAKA, H., INAGAKI, M., KAWAMOTO, S. & SASAKI, Y. (1984). Isoquinoline sulphonamides, novel and potent inhibitors of cyclic nucleotide dependent protein kinase and protein kinase C. *Biochemistry*, **23**, 5036–5041.

HIGASHIDA, H. & BROWN, D.A. (1986). Two polyphosphatidylinositol metabolites control two K^+ currents in a neuronal cell. *Nature*, **323**, 332–335.

HOCKBERGER, P., TOSSELLI, M., SWANDULLA, H. & LUX, H.D. (1989). A diacylglycerol analogue reduces neuronal calcium currents independently of protein kinase C activation. *Nature*, **338**, 340–342.

JONES, S., CAULFIELD, M.P., BROWN, D.A. & BUCKLEY, N.J. (1993). Gα11 and Gαq antisense oligonucleotides reduce muscarinic receptor mediated inhibition of M-current in rat sympathetic neurones. *Soc. Neurosci. Abstr.*, **19**, 710.

LOPEZ, H.S. (1992). Kinetics of G-protein mediated modulation of the potassium M-current in bullfrog sympathetic neurons. *Neuron*, **8**, 725–736.

MARRION, N.V. (1993). Selective reduction of one mode of M-channel gating by muscarine in sympathetic neurones. *Neuron*, **11**, 77–84.

ORDWAY, R.W., WALSH, J.V. & SINGER, J.J. (1989). Arachidonic acid and other fatty acids directly activate potassium channels in smooth muscle cells. *Science*, **244**, 1176–1179.

PFAFFINGER, P.J. (1988). Muscarine and LHRH suppress M-current by activating an IAP-insensitive G-protein. *J. Neurosci.*, **8**, 3343–3353.

PFAFFINGER, P.J., LEIBOWITZ, M.D., SUBERS, E.M., NATHANSON, N.M., ALMERS, W. & HILLE, B. (1988). Agonists that suppress M-current elicit phosphoinositide turnover and Ca^{2+} transients, but these events do not explain M-current suppression. *Neuron*, **1**, 477–484.

PLUMMER, M.R., RITTENHOUSE, A., KANAEVSKY, M. & HESS, P. (1991). Neurotransmitter modulation of calcium channels in rat sympathetic neurons. *J. Neurosci.*, **11**, 2339–2348.

PUSCH, M. & NEHER, E. (1988). Rates of diffusional exchange between small cells and a measuring patch pipette. *Pflüger's Arch.*, **411**, 204–211.

SATIN, L.S. & ADAMS, P.R. (1987). Spontaneous miniature outward currents in cultured bullfrog neurons. *Brain Res.*, **401**, 331–339.

SELYANKO, A.A., SMITH, P.A. & ZIDICHOUSKI, J.A. (1990). Effects of muscarine and adrenaline on neurones from *Rana pipiens* sympathetic ganglion. *J. Physiol.*, **425**, 471–500.

SELYANKO, A.A., STANSFIELD, C.E. & BROWN, D.A. (1992). Closure of potassium M-channels by muscarinic acetylcholine-receptor stimulants requires a diffusible messenger. *Proc. Soc. B*, **250**, 119–125.

SIMMONS, M.A., BECKER, J.B. & MATHER, R.J. (1990). Desensitization of the M-current in sympathetic neurones; effect of ATP analogs, polyanions and multiple agonist applications. *Neuron*, **4**, 557–562.

SMITH, P.A. (1993). The autonomic ganglia and the modulation of ganglionic transmission. In *Advances in Structural Biology*, Vol. 2. ed. Malhotra, S.K. pp. 245–316. Greenwich: JAI press.

SMITH, P.A., CHEN, H., KURENNY, D.E., SELYANKO, A.A. & ZIDICHOUSKI, J.A. (1992). Regulation of the M-current: transduction mechanism and role in ganglionic transmission. *Can. J. Physiol. Pharmacol. (Suppl).*, **70**, S12–S18.

TAMAOKI, T., NOMOTO, H., TAKAHASHI, I., KATO, Y., MORIMOTO, M. & TOMITA, F. (1986). Staurosporine, a potent inhibitor of phospholipid/Ca^{2+} dependent protein kinase. *Biochem. Biophys. Res. Commun.*, **135**, 397–402.

WERZ, M.A., ELMSLIE, K.S. & JONES, S.W. (1993). Phosphorylation enhances inactivation of N-type calcium channel current in bullfrog sympathetic neurones. *Pflüger's Arch.*, **424**, 538–545.

(Received December 23, 1993
Revised April 19, 1994
Accepted May 11, 1994)

Br. J. Pharmacol. (1994), **113**, 63–68

The involvement of bradykinin B_1 and B_2 receptor mechanisms in cytokine-induced mechanical hyperalgesia in the rat

A.J. Davis & [1]M.N. Perkins

Sandoz Institute for Medical Research, 5 Gower Place, London WC1E 6BN

1 Interleukin-1β (IL-1β), IL-2 and IL-8 induced a mechanical hyperalgesia following intra-articular (i.artic.) injection into rat knee joints, whereas IL-6 and tumour necrosis factor α (TNF-α) were without effect.

2 Co-administration of IL-1 receptor antagonist (0.1 μg) with IL-1β (1 u), IL-2 (10 u) or IL-8 (0.1 u) prevented the subsequent development of the hyperalgesia.

3 Co-administration of desArg^{9}Leu^{8}BK (0.5–5 nmol) with IL-1β (1 u), IL-2 (10 u) or IL-8 (0.1 u) reduced the level of hyperalgesia at 1, 4 and 6 h post administration, whereas Hoe 140 (5 pmol) antagonized the hyperalgesia only at the 1 h time point.

4 Intravenous administration of desArg^{9}Leu^{8}BK (10 nmol kg^{-1}) or Hoe 140 (100 pmol kg^{-1}) following IL-1β (1 u), IL-2 (10 u), or IL-8 (0.1 u) reversed the subsequent hyperalgesia.

5 Administration of desArg^{9}BK into joints 24 h after pre-treatment with IL-1β (1 u) produced analgesia at low doses (50 pmol) and hyperalgesia at a higher dose (0.5 nmol). Both these effects were blocked by desArg^{9}Leu^{8}BK (0.5 nmol).

6 Administration of desArg^{9}BK (0.5 nmol i.artic.) to animals 24 h after pre-treatment with IL-2 (1–100 u) or IL-8 (0.1–10 u) had no effect on the load tolerated by the treated joint.

7 Administration of indomethacin (1 mg kg^{-1}, s.c.) prior to IL-1β (1 u i.artic.) prevented the development of hyperalgesia. Administration of desArg^{9}BK (5 pmol–0.5 nmol, i.artic.) to animals 24 h after indomethacin and IL-1β pretreatment had no effect on the load tolerated by the treated joint.

8 These data suggest that both bradykinin B_1 and B_2 receptors are involved in the induction and maintenance of cytokine-induced hyperalgesia. They also show that the induction of B_1 receptor-mediated hyperalgesia requires both cyclo-oxygenase products and IL-1 *in vivo*.

Keywords: Cytokines; hyperalgesia; interleukin-1 receptor antagonist; bradykinin; desArg^9 bradykinin; prostaglandins

Introduction

Cytokines have been implicated in the mechanisms of both inflammation and hyperalgesia. In inflammatory diseases such as rheumatoid arthritis increased levels of interleukin-1 (IL-1) tumour necrosis factor α (TNF-α), IL-6 and IL-8 have been measured in the joint (Hirano *et al.*, 1988; Yocum *et al.*, 1989; Brennan *et al.*, 1990; Remick *et al.*, 1992). These cytokines have also been shown, to varying degrees, to cause cellular infiltration and plasma extravasation in several animal models of inflammation (Colditz & Watson, 1992; Cooper *et al.*, 1992; Forrest *et al.*, 1992). Additionally IL-1, IL-6, IL-8 and TNF-α may contribute to the hyperalgesia accompanying inflammation since they can induce mechanical hyperalgesia following local administration in rats (Ferreira *et al.*, 1988; Follenfant *et al.*, 1989; Cunha *et al.*, 1992).

The role of kinins in inflammation and hyperalgesia has been extensively studied. Bradykinin is known to excite nociceptors via activation of B_2 receptors (Steranka *et al.*, 1988; Haley *et al.*, 1989; Dray *et al.*, 1992; Heapy *et al.*, 1993) and can cause inflammation, extravasation and cellular migration (McFadden & Vickers, 1989; Damas & Remacle-Volon, 1992; Green *et al.*, 1993). Recently we have shown that, subsequent to an inflammatory insult, the B_1 receptor plays an important role in mechanisms of mechanical (Perkins *et al.*, 1992; 1993; Davis & Perkins, 1994) and thermal (Perkins & Kelly, 1993) hyperalgesia.

Interactions between cytokines and kinins have been shown in several systems. IL-1 and IL-2 have been shown to induce bradykinin B_1 receptors *in vitro* (Deblois *et al.*, 1988), and synergistic interactions have been demonstrated in human fibroblasts between bradykinin, desArg^{9}BK and IL-1 (Lerner & Modeer, 1991; Bathon *et al.*, 1992; Lerner *et al.*, 1992).

In this study we have investigated the hyperalgesic action of inflammatory cytokines after intra-articular injection into rat knee joint and the possible involvement of B_1 and B_2 receptors.

Methods

The method used in this study for assessment of mechanical hyperalgesia has been described previously (Perkins *et al.*, 1992; 1993; Davis & Perkins, 1993; 1994) and entailed intra-articular (i.artic.) injections of inflammatory or hyperalgesic agents into one knee joint of female Sprague-Dawley rats (80–100 g Charles-Rivers, kept at 21 ± 2°C, 12 h light/dark, food and water *ad libitum*) and subsequently measuring the load tolerated by the injected leg. For assessment of the load tolerated by the treated leg, animals were placed with their hind paws on separate balanced force transducers and a downward force applied such that the load tolerated by the untreated joint was 100 g. At this point the injected leg would tolerate less load and this reduction in load was used as a measure of hyperalgesia (Perkins *et al.*, 1992). The load of 100 g was chosen as it gave a sufficient reduction in tolerated load subsequent to intra-articular injections of inflammatory or hyperalgesic agents such that the dose-response relationships to test compounds could be properly assessed. All injections into the joint were made under brief enflurane anaesthesia.

Time course of cytokine-induced hyperalgesia

Animals received unilateral intra-articular injections (100 μl, phosphate buffered saline vehicle) of either IL-1β (0.1–100 u), IL-2 (1–100 u), IL-6 (1–100 u), IL-8 (0.01–10 u) or

[1] Author for correspondence.

TNF-α (1–500 u). The load tolerated by the treated joint was then assessed at 1, 4, 6 and 24 h post injection. Control animals received cytokines which had been heated to above 50°C for 60 min, the highest dose of each cytokine being used for this control. ANOVA and MANOVA followed by *post hoc* analysis of means was used to establish a reduction in tolerated load over the time course and to compare groups with their heat-treated control at each time point.

Antagonism of cytokine-induced hyperalgesia

Animals were administered a sub-maximal dose of cytokine (100 μl, i.artic.) either alone or in combination with IL-1 receptor antagonist(ra) (0.1 μg), desArg^{9}Leu^{8}BK (0.5–5 nmol), desArg^{10}[Hoe 140] (5 pmol) or Hoe 140 (5 pmol). The load tolerated by the treated leg was then assessed at 1, 4 and 6 h after administration. MANOVA followed by *post hoc* analysis of means was used to compare treatments at each time point.

Reversal of cytokine-induced hyperalgesia

Animals were injected with a sub-maximal dose of cytokine (100 μl, i.artic.) and the load tolerated by the treated joint was assessed 4 h later. Animals were injected with either desArg^{9}Leu^{8}BK (10 nmol kg^{-1}), Hoe 140 (100 pmol kg^{-1}) or saline via their tail vein, under brief enflurane anaesthesia, 30 min before assessing the level of hyperalgesia. ANOVA followed by *post hoc* analysis of means was used to compare the saline and antagonist-treated groups.

Induction of B_1 receptor

Animals received unilateral intra-articular injections (100 μl) of cytokine and then 24 h later the load tolerated by the injected leg was assessed. Control readings were taken to establish the baseline level of hyperalgesia, then 50 μl of desArg^{9}BK (5 pmol–1 nmol) was subsequently injected into the cytokine-treated joint. The level of hyperalgesia was then assessed at 30 min intervals for 2 h. Antagonists were co-administered with desArg^{9}BK. ANOVA followed by *post hoc* analysis of mean was used to study the time course of desArg^{9}BK-induced hyperalgesia for each dose administered.

Separate groups of animals were injected with indomethacin 0.1–10 mg kg^{-1}, s.c. or 2% Na_2CO_3 vehicle (buffered to pH 7 with NaH_2PO_4) 30 min before administration of IL-1β (1 u, i.artic.). The load tolerated by the treated leg was assessed at 1, 4 and 24 h after administration of IL-1β. DesArg^{9}BK (5 pmol–0.5 nmol, i.artic.) was also administered, as described above, 24 h after indomethacin and IL-1β pre-treatment.

Drugs

All cytokines used in this study were human recombinant type. IL-1β, IL-6, IL-8 (72 amino acids) and TNF-α were obtained from The National Institute for Biological Standards and Controls (NIBSC), with specific activities of 1×10^8 (IL-1β), 5×10^6 (IL-6), 1×10^6 (IL-8) and 4×10^7 u mg^{-1} (TNF-α) and code numbers 86/552, 88/514, 89/520 and 87/650 respectively. IL-2 was obtained from Sandoz Basel, with a specific activity of 2×10^6 u mg^{-1}. DesArg^{9}Leu^{8}BK and IL-1ra were obtained from Bachem A.G. and Hoe 140 (D-Arg [Hyp^3, Thi^5,D-Tic^7,Oic^8]BK) and desArg^{10}[Hoe 140] were synthesized by Dr A. Hallett, Sandoz Institute for Medical Research. Indomethacin was obtained from Sigma.

Results

IL-1β (1–100 u, i.artic.) induced a reduction in tolerated load when injected into naive joints. This hyperalgesia was significant at 1, 4, 6 and 24 h post-injection with 1–100 u, whereas 0.1 u and heat treated IL-1β (100 u) had no effect (Figure 1). The highest dose of IL-1β tested was 100 u which caused a reduction in tolerated load from 94 ± 1 g to 49 ± 5 g at 6 h ($n = 8$, $P < 0.05$). By 24 h post administration only the animals which received 10 and 100 u IL-1β showed a reduction in tolerated load when compared to the heat-treated control (60 ± 3 g and 75 ± 3 g, $n = 8$ respectively, vs 90 ± 4 g $n = 16$, $P < 0.05$); however, the animals which received 1 u IL-1β were still significantly hyperalgesic compared to their pretreatment levels (82 ± 2 g vs 94 ± 1 g, $n = 8$, $P < 0.05$).

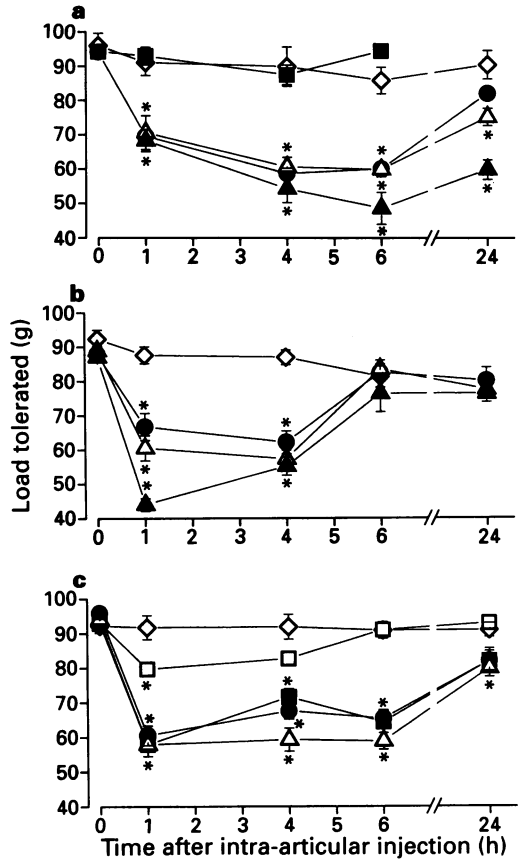

Figure 1 Load (g) tolerated by the ipsilateral leg after intra-articular administration of interleukin-1β (IL-1β) (a) IL-2 (b) or IL-8 (c) into naive joints, all injections were made after the first (0 h) reading: (a) shows the time course of hyperalgesia after IL-1β 0.1 u (■), 1 u (●), 10 u (△), 100 u (▲) and heat-treated 100 u (◇, $n = 16$). (b) Shows the time course of hyperalgesia after IL-2 1 u (●), 10 u (△), 100 u (▲) and heat-treated 100 u (◇). (c) Shows the time course of hyperalgesia after IL-8 0.01 u (□), 0.1 u (■), 1 u (●), 10 u (△) and heat-treated 10 u (◇). All results are expressed as mean ± s.e.mean ($n = 8$ animals per group, unless stated otherwise). *$P < 0.05$ compared to heat-treated control at each time point.

IL-2 (1–100 u, i.artic.) produced a reduction in tolerated load when injected into naive joints. The hyperalgesia was significant at 1 and 4 h post-injection with 1–100 u, whereas heat treated IL-2 (100 u) had no effect over the time course (Figure 1). The maximum reduction in hyperalgesia occurred 1 h post-injection at all doses tested. With 100 u IL-2, the tolerated load fell from 87 ± 1 g pre-treatment level, to 44 ± 2 g at 1 h ($n = 8$, $P < 0.05$). By 6 h after all doses the level of hyperalgesia was no longer significantly different from the control group.

IL-8 (0.01–10 u) caused a reduction in tolerated load when injected into naive joints, whereas heat-treated IL-8 (10 u) had no effect (Figure 1). After 0.1–10 u IL-8 the hyperalgesia was significant at 1, 4 and 6 h post-injection. By 24 h post-injection only the group which received 10 u IL-8 were

hyperalgesic, with a tolerated load of 80 ± 2 g compared to their pretreatment level of 94 ± 1 g ($n = 8$, $P < 0.05$).

IL-6 (1–100 u, i.artic.) and TNF-α (1–500 u, i.artic.) did not induce hyperalgesia at 1, 4, 6 or 24 h (data not shown).

Antagonism of cytokine-induced hyperalgesia

Co-administration of desArg^{9}Leu^{8}BK (0.5 nmol) with IL-1β (1 u) reduced the hyperalgesia over the entire time course (Figure 2). After 1 h the load tolerated was 89 ± 2 g ($n = 16$) compared to 67 ± 2 g ($n = 24$, $P < 0.05$) in animals which received IL-1β alone. The hyperalgesia was still reduced at 6 h with a tolerated load of 75 ± 3 g compared to 65 ± 2 g ($P < 0.05$) with IL-1β alone. Hoe 140 (5 pmol) only blocked IL-1β-induced hyperalgesia at 1 h; animals tolerated 86 ± 5 g ($n = 8$, $P < 0.05$) at this time point. By 4 h post administration the hyperalgesia was the same as in animals which received IL-1β alone (59 ± 3 g with Hoe 140 vs 60 ± 2 g with IL-1β alone).

Co-administration of desArg^{9}Leu^{8}BK (5 nmol) with IL-2 (10 u) prevented the development of hyperalgesia at all time points studied (Figure 2); animals tolerated 86 ± 2 g and 91 ± 2 g ($n = 8$) compared to 66 ± 2 g and 63 ± 2 g ($n = 32$, $P < 0.05$) in control animals at 1 and 4 h post injection. A lower dose of desArg^{9}Leu^{8}BK (0.5 nmol) prevented the hyperalgesia only at the 1 h time point, however desArg^{10} [Hoe 140] 5 pmol prevented development of hyperalgesia over the entire time course (Figure 2). Hoe 140 (5 pmol) blocked the development of IL-2-induced hyperalgesia only at the 1 h time point, when the tolerated load was 92 ± 3 g ($n = 8$) compared to 66 ± 2 g ($n = 32$, $P < 0.05$) in animals which received IL-2 alone; by 4 h post injection the load tolerated fell to 60 ± 3 g in animals which received Hoe 140 compared to 63 ± 2 g in animals which received IL-2.

Co-administration of desArg^{9}Leu^{8}BK (0.5 nmol) with IL-8 (0.1 u) blocked the development of hyperalgesia over the entire time course (Figure 2). After 1 h the load tolerated was 94 ± 1 g ($n = 8$) compared to 63 ± 2 g ($n = 16$, $P < 0.05$) in animals which received IL-8 alone. The hyperalgesia was still reduced at 6 h with a tolerated load of 94 ± 2 g compared to 70 ± 3 g ($P < 0.05$) with IL-8 alone. Hoe 140 (5 pmol) blocked IL-8-induced hyperalgesia only at 1 h; animals tolerating 92 ± 2 g ($n = 8$, $P < 0.05$) at this time point. By 4 h post administration the hyperalgesia was the same as in

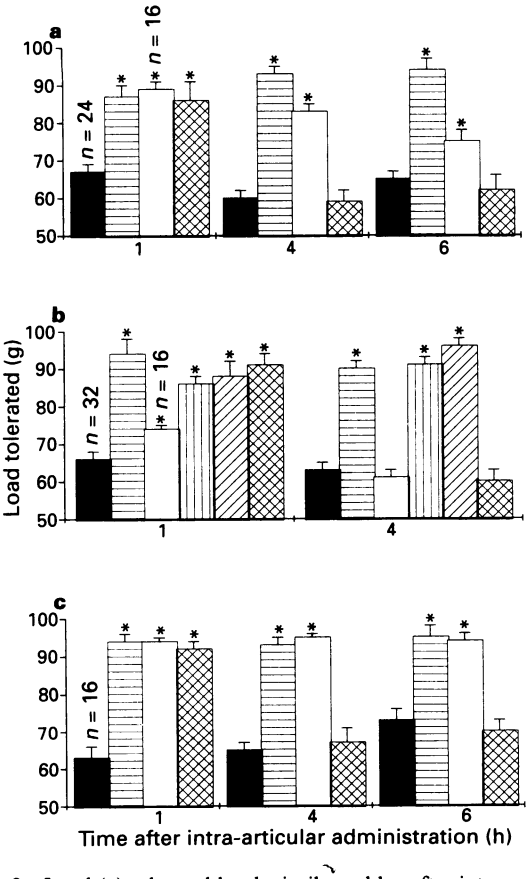

Figure 2 Load (g) tolerated by the ipsilateral leg after intra-articular administration of interleukin-1β (IL-1β) 1 u (a). IL-2 10 u (b) and IL-8 0.1 u (c). Animals either received cytokine alone (solid columns) or co-administered with IL-1 receptor antagonist (horizontally hatched columns) desArg^{9}Leu^{8}BK 0.5 nmol (open columns) or 5 nmol (vertically hatched columns), desArg^{10}[Hoe 140] 5 pmol (right hatched columns) or Hoe 140 (cross hatched columns). All results are expressed as mean ± s.e.mean ($n = 8$, unless stated otherwise). *$P <$ 0.05 compared to control at each time point.

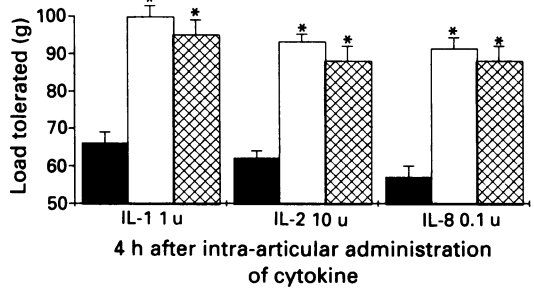

Figure 3 Load (g) tolerated by the ipsilateral leg 4 h after intra-articular administration of interleukin-1β (IL-1β) 1 u, IL-2 10 u or IL-8 0.1 u into naive joints. Saline (closed columns, $n = 16$), desArg^{9}Leu^{8}BK 10 nmol kg^{-1} (open columns) or Hoe 140 100 pmol kg^{-1} (cross hatched columns) were administered i.v. 3.5 h after each cytokine. All results are expressed as mean ± s.e.mean ($n = 8$, unless stated otherwise). *$P < 0.05$ compared to saline group.

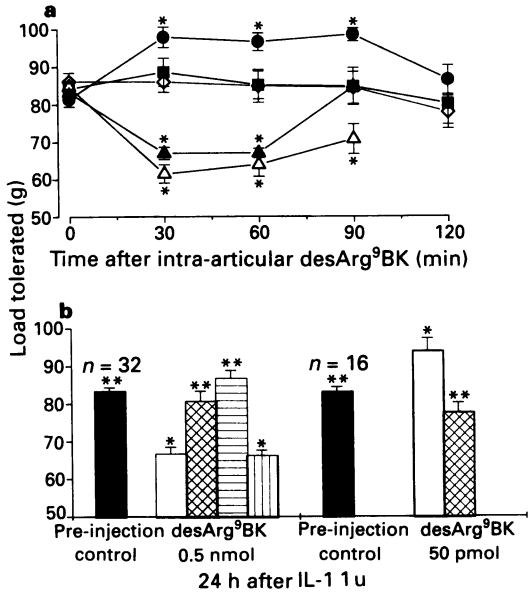

Figure 4 Load (g) tolerated by the ipsilateral leg 24 h after intra-articular administration of interleukin-1β (IL-1β) 1 u (a). desArg^{9}BK was injected into the IL-1β pretreated joint after the first reading at 5 pmol (■), 50 pmol (●), 0.5 nmol (▲) and 1 nmol (△). Control joints (◇) were injected with PBS (50 μl). (b) After control readings (solid columns), desArg^{9}BK was either administered alone (open columns) co-administered with desArg^{9}Leu^{8}BK 0.5 nmol (cross hatched columns), desArg^{10}[Hoe 140] 5 pmol (horizontally hatched columns) or Hoe 140 (vertically hatched columns). All results are expressed as mean ± s.e.mean ($n = 8$, unless stated otherwise). *$P < 0.05$ compared to pre-injection reading. **$P < 0.05$ compared to desArg^{9}BK-treated group.

animals which received IL-8 alone (67 ± 4 g with Hoe 140 vs 66 ± 2 g with IL-8 alone).

Co-administration of IL-1ra (0.1 μg) with IL-1β (1 u), IL-2 (10 u) or IL-8 (0.1 u) blocked the development of hyperalgesia over the entire time course (Figure 2). A lower dose of IL-1ra (0.01 μg) only partially blocked IL-1β-induced hyperalgesia (data not shown) so 0.1 μg was used to antagonize IL-2 and IL-8-induced hyperalgesia.

None of the doses of antagonists used had any effect when administered alone to the naive joint over the dose-ranges used in these experiments (data not shown).

Reversal of cytokine-induced hyperalgesia

When desArg^{9}Leu^{8}BK (10 nmol kg^{-1}) or Hoe 140 (100 pmol kg^{-1}) were administered i.v. to animals 3.5 h after intra-articular injection of IL-1β, IL-2 or IL-8 the hyperalgesia was reversed when measured 30 min later (Figure 3). The load tolerated after desArg^{9}Leu^{8}BK and Hoe 140 was 100 ± 3 g (n = 8) and 95 ± 4 g (n = 8) respectively compared to 66 ± 3 g after saline (n = 16, $P<0.05$) in IL-1β-treated animals; 93 ± 2 g (n = 8) and 88 ± 4 g (n = 8) respectively compared to 62 ± 2 g after saline (n = 16, $P<0.05$) in IL-2-treated animals; 91 ± 3 g (n = 8) and 88 ± 4 g (n = 8) compared to 57 ± 3 g after saline (n = 16, $P<0.05$) in IL-8-treated animals (Figure 3).

Induction of B_1 receptors

When desArg^{9}BK (1–100 nmol, i.artic.) was administered to naive rats there was no effect on tolerated load. After 1 and 100 nmol the loads tolerated by the treated leg at 1 h post injection were 94 ± 3 g and 92 ± 5 g respectively, compared to pretreatment values of 93 ± 2 g and 93 ± 1 g respectively (n = 8). Twenty four hours after administration of IL-1β (1 u) into the knee joint, injection of desArg^{9}BK into the same joint produced opposite effects depending on the dose used. With a low dose of desArg^{9}BK (50 pmol) the load tolerated increased from 83 ± 3 g to 96 ± 2 g (n = 8, $P<0.05$) after 1 h, whereas at higher doses (0.5 and 1 nmol) there was a reduction in load tolerated (Figure 4). After 0.5 nmol desArg^{9}BK, the mean tolerated load fell from 82 ± 2 g to 66 ± 4 g at 1 h (n = 8, $P<0.05$); this reduction was blocked when desArg^{9}BK was co-administered with desArg^{9}Leu^{8}BK (0.5 nmol) or desArg^{10}[Hoe 140] (5 pmol), but Hoe 140 (5 pmol) had no effect (Figure 4).

There was no change in load tolerated when desArg^{9}BK (0.5 nmol) was injected into joints pretreated with IL-2 (1–100 u), IL-6 (1–100 u), IL-8 (0.1–10 u) or TNF-α (1–500 u), 24 h previously (data not shown).

Following indomethacin pretreatment (1 mg kg^{-1}, s.c.) 30 min before intra-articular injection of IL-1β (1 u) there was no reduction in tolerated load when assessed 1, 4 or 24 h later (Figure 5). At 24 h, the load tolerated by the treated joint was 91 ± 1 g (n = 24) in animals which received indomethacin and IL-1β, compared to 85 ± 2 g (n = 8, $P<0.05$) in animals which received vehicle and IL-1β. Intra-articular administration of desArg^{9}BK (5 pmol–1 nmol) to animals 24 h after indomethacin and IL-1β pretreatment had no significant effect on the tolerated load (Figure 5).

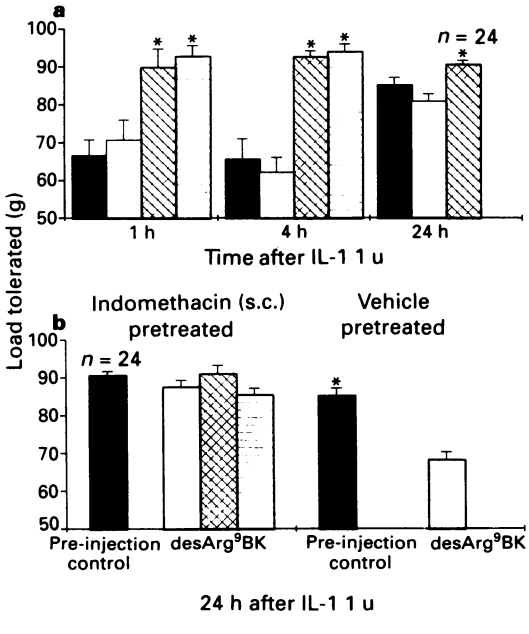

Figure 5 Load (g) tolerated by ipsilateral leg after intra-articular administration of interleukin-1β (IL-1β) 1 u. (a) Time course of hyperalgesia in animals pretreated with indomethacin 0.1 mg kg^{-1} (open columns), 1 mg kg^{-1} (cross hatched columns), 10 mg kg^{-1} (horizontally hatched columns) or vehicle (solid columns) s.c., 30 min prior to IL-1β. (b) DesArg^{9}BK was administered into the ipsilateral joint 24 h after IL1β. After pre-injection readings (solid columns), desArg^{9}BK was administered at 0.5 nmol (open columns), 50 pmol (cross hatched columns), or 5 pmol (horizontally hatched columns). All results are expressed as mean ± s.e.mean (n = 8, unless stated otherwise). *$P<0.05$ compared to pre-injection reading.

Discussion

These data show that the cytokines IL-1β, IL-2 and IL-8 all induce mechanical hyperalgesia when injected into the rat knee joint, whereas IL-6 and TNF-α were without effect. The blockade of IL-1β, IL-2 and IL-8-induced hyperalgesia by the IL-1 receptor antagonist, IL-1ra, (Eisenberg *et al.*, 1990) suggests the involvement of IL-1 in the induction of hyperalgesia by these cytokines. Furthermore, the antagonism of the cytokine-induced hyperalgesia by desArg^{9}Leu^{8}BK and Hoe 140 also implicates bradykinin B_1 and B_2 receptor systems in this hyperalgesia. These data therefore further suggests a possible role of IL-1β in hyperalgesia, and supports evidence *in vitro* (Deblois *et al.*, 1989) and *in vivo* (Perkins & Kelly, 1993) for a link between B_1 receptor expression and IL-1β.

The time course experiments did not show a clear dose-response relationship for IL-1β, IL-2 or IL-8. However, increasing the dose of IL-1β and IL-8 did prolong the duration of hyperalgesia. At the doses of cytokines used for the antagonist work, there was no significant difference in the magnitude of hyperalgesia.

When B_1 and B_2 receptor antagonists, at doses previously shown to be specific for their respective agonists (Davis & Perkins, 1994), were co-administered with IL-1β, IL-2 or IL-8, the B_1 receptor antagonist, desArg^{9}Leu^{8}BK, caused significant antagonism of hyperalgesia over the time course of study, whereas a B_2 receptor antagonist, Hoe 140, antagonized the hyperalgesia only at the 1 h time point. With IL-2, higher doses of desArg^{9}Leu^{8}BK were required to block the development of hyperalgesia, compared to the IL-1β or IL-8 experiments. The reason for this reduced potency is unclear; however, IL-2-induced hyperalgesia was blocked by IL-1ra which suggests that IL-2 causes hyperalgesia via production of IL-1. Any delay therefore in the endogenous production of IL-1 following IL-2 administration would allow time for desArg^{9}Leu^{8}BK to be metabolically degraded thereby reducing its effective concentration. This possibility is supported by the blockade of IL-2-induced hyperalgesia by desArg^{10}[Hoe 140], a metabolically protected B_1 receptor antagonist (Wirth *et al.*, 1992).

The shorter duration of Hoe 140-induced antagonism of cytokine-induced hyperalgesia, compared to desArg^{9}Leu^{8}BK seen in these experiments, was also observed in a previous study where the hyperalgesia was induced by Freund's complete adjuvant (Davis & Perkins, 1994). Since Hoe 140 has been shown to be metabolically stable in synovial fluid (Bond

et al., 1992) it is unlikely that the shorter duration of action, compared to the B_1 antagonist desArg^{9}Leu^{8}BK, is due to more rapid metabolism. When administered systemically, Hoe 140 has been shown to have a very long duration of action with respect to antagonism of BK (Wirth *et al.*, 1991) so it is unlikely that kinetics favour desArg^{9}Leu^{8}BK in this regard, particularly as desArg^{9}Leu^{8}BK is not metabolically stable and would be expected to have a relatively short half life. In addition, the fact that desArg^{10}[Hoe 140] another B_1 receptor antagonist (Wirth *et al.*, 1992) antagonized IL-2-induced hyperalgesia with a duration of action similar to desArg^{9}Leu^{8}BK supports the conclusion that B_1 but not B_2 receptor blockade prevents the development of hyperalgesia.

Although the data presented here suggest a more important role of B_1 receptors in the initial development of cytokine- induced hyperalgesia, both desArg^{9}Leu^{8}BK and Hoe 140 were equally effective in reversing the hyperalgesia after it had developed. We chose the 4 h time point to study the role of the kinin system in maintenance of hyperalgesia since IL-1β, IL-2 and IL-8 all induced a similar level of hyperalgesia at this time point. Administration of antagonists 30 min prior to testing was chosen since we have previously shown that desArg^{9}Leu^{8}BK and Hoe 140 are most effective at this time (Perkins *et al.*, 1993; Davis & Perkins, 1994).

Since both B_1 and B_2 receptor antagonists almost completely reverse the cytokine-induced hyperalgesia seen in this model, this suggests a complex interaction between B_1 and B_2 receptors in the development and maintenance of this type of hyperalgesia. There are several ways in which such interactions could occur. Recently it has been shown that bradykinin and desArg^{9}BK can up-regulate the expression of cell specific receptors for high and low molecular weight kininogen possibly leading to an enhanced production of bradykinin (Zini *et al.*, 1993). Interestingly, this effect of bradykinin was not via a B_2 receptor but was partially blocked by desArg^{9}Leu^{8}BK. A B_2 receptor antagonist would, therefore, be expected to antagonize the action of BK but not affect any such increase in its production. DesArg^{9}Leu^{8}BK, however, would not only antagonize the action of desArg^{9}BK but may also reduce an increase in production of BK (Zini *et al.*, 1993). If this up-regulation of kininogen receptors underlies to any significant extent the development of hyperalgesia in this model, then this may explain the prevention of the hyperalgesia by B_1 antagonists at the later time points. Another possibility could be that desArg^{9}BK may act at B_1 receptors to produce co-factors, such as prostaglandins (Cahill *et al.*, 1988; Tiffany & Burch, 1989; Lerner & Modeer, 1991) which may be necessary to maintain the inflammatory cascade leading to further BK production and sensitization of the nociceptor to BK. In either case blockade of either B_1 or B_2 receptors would antagonize the hyperalgesia.

The initial antagonist studies suggested an involvement of B_1 receptors in both the development and maintenance of hyperalgesia; thus the latter set of experiments looked at the effect of the B_1 receptor agonist desArg^{9}BK when administered to cytokine pretreated joints. These experiments were conducted 24 h after administration of IL-1β, IL-2 or IL-8 since the load tolerated by the cytokine pre-treated joint was similar with all three cytokines at this time point. Mechanical hyperalgesia was only induced by desArg^{9}BK in joints pretreated with IL-1β, whereas desArg^{9}BK has no effect when administered alone into naive joints. A previous study from this laboratory has also shown the induction of thermal hyperalgesia following IL-1β administration (Perkins & Kelly, 1993). The paradoxical increase in tolerated load seen with low doses of desArg^{9}BK is interesting but at present we do not have an explanation for this, although it appears to be a specific B_1 receptor-mediated effect since it was antagonized by co-administration of desArg^{9}Leu^{8}BK. Experiments are in progress to investigate further the pharmacology of desArg^{9}BK in IL-1β pretreated joints. The lack of effect of desArg^{9}BK in joints pre-treated with IL-2 or IL-8 suggests that B_1 receptors are not present 24 h after administration of these two cytokines. However, IL-2 and IL-8 showed different time courses of action and dose-response relationships from IL-1β, thus it is possible that functional expression of the B_1 receptor has a finite life, requiring the continued presence of inflammatory mediators such as IL-1β to remain functional. Since our interest was mechanisms underlying the induction of B_1 receptors, further experiments were not performed with IL-2 and IL-8.

The effect of indomethacin on the induction of B_1-mediated hyperalgesia suggests prostanoid production mediates this response. Conflicting data exist in the literature concerning the role of prostaglandins in IL-1β-induced hyperalgesia (Ferreira *et al.*, 1988; Follenfant *et al.*, 1989). Our experiments show that, at least in the knee joint, the hyperalgesia induced by IL-1β is dependent on prostaglandins, since indomethacin blocked the development of hyperalgesia at a systemic dose sufficient to inhibit prostaglandin biosynthesis completely (Salmon *et al.*, 1983; Follenfant *et al.*, 1989). Furthermore, the lack of effect of desArg^{9}BK when administered to animals 24 h after indomethacin and IL-1β pretreatment, suggests that prostaglandins are also involved in the induction of the B_1 responses. This is interesting since the spontaneous induction of B_1 receptors *in vitro* is not inhibited by continuous exposure to indomethacin (Regoli *et al.*, 1978) or IL-1ra (Petitclerc *et al.*, 1992). However IL-1ra does prevent the enhanced B_1 responses induced by incubation with IL-1β, suggesting that the spontaneous induction of B_1 receptors in isolated tissues and the IL-1-induced B_1 responses could possibly occur via different mechanisms (Petitclerc *et al.*, 1992).

Although B_2 receptors are known to be present on sensory neurones (Sterenka *et al.*, 1988), the location of B_1 receptors in these studies is not known. It is possible that the cytokines induce or up-regulate B_1 receptors on the sensory neurone as seen in smooth muscle studies (Bouthillier *et al.*, 1987; Deblois *et al.*, 1988; 1989; Siebeck *et al.*, 1989) but there is, as yet, no evidence to support this. DesArg^{9}BK has been shown to increase the synthesis and release of inflammatory mediators such as IL-1 and PGI_2 from other cell types (Cahill *et al.*, 1988; Tiffany & Burch, 1989; Lerner & Modeer, 1991) and such actions of desArg^{9}BK could indirectly increase the excitability of the nociceptor. Whatever the site of the B_1 receptor, B_1 receptor antagonists are not only effective in preventing the development of hyperalgesia, but, along with B_2 receptors they can also reverse the hyperalgesia once established.

In conclusion, the present paper suggests that subsequent to a challenge of IL-1β desArg^{9}BK can induce a B_1 receptor-mediated mechanical hyperalgesia. In addition the data indicate that the cytokines IL-1β, IL-2 and IL-8 can induce mechanical hyperalgesia in a rat knee joint model and this involves both B_1 and B_2 receptors. B_1 receptors, however, seem to have a greater role than B_2 receptors in the development of cytokine-induced mechanical hyperalgesia. There could, therefore be potential therapeutic uses of both B_1 and B_2 receptor antagonists in conditions of inflammatory hyperalgesia.

References

BATHON, J.M, CROGHAN, J.E., GOLDMAN, D.W., MACGLASHAN, D.W. & PROUD, D. (1992). Modulation of kinin responses in human synovium by interleukin-1. *Agents Actions Suppl.*, **38,** 16–22.

BOND, A.P., BREIPOHL, G., WORTHY, K,. CAMPION, G., DIEPPE, P.A. & BHOOLA, K.D. (1992). Metabolism and characterisation of kinins and Hoe 140 (kinin antagonist) in the synovial fluid of patients with inflammatory joint diseases. *Agents Actions Suppl.*, **38,** 582–589.

BOUTHILLIER, J., DEBLOIS, D. & MARCEAU, F. (1987). Studies on the induction of pharmacological responses to des-Arg^9-BK *in vitro* and *in vivo*. *Br. J. Pharmacol.*, **92,** 257–264.

BRENNAN, F.M., ZACHARIAE, C.O., CHANTRY, D., LARSEN, C.G., TURNER, M., MAINI, R.N., MATSUSHIMA, K. & FELDMANN, M. (1990). Detection of interleukin 8 biological activity in synovial fluids from patients with rheumatoid arthritis and production of interleukin 8 mRNA by isolated cells. *Eur. J. Pharmacol.*, **20,** 2141–2144.

CAHILL, M., FISHMAN, J.B. & POLGAR, P. (1988). Effect of desArg9-BK and other bradykinin fragments on the synthesis of prostacyclin and the binding of bradykinin by vascular cells in culture. *Agents Actions*, **24,** 224–231.

COLDITZ, I.G. & WATSON, D.L. (1992). The effect of cytokines and chemotactic agonists on the migration of T lymphocytes into skin. *Immunology*, **76,** 272–278.

COOPER, W.O., FAVA, R.A., GATES, C.A., CREMER, M.A. & TOWNES, A.S. (1992). Acceleration of onset of collagen-induced arthritis by intra-articular injection of tumour necrosis factor or transforming growth factor-beta. *Clin. Exp. Immunol.*, **89,** 244–250.

CUNHA, F.Q., POOLE, S., LORENZETTI, B.B. & FERREIRA, S.H. (1992). The pivotal role of tumour necrosis factor α in the development of inflammatory hyperalgesia. *Br. J. Pharmacol.*, **107,** 660–664.

DAMAS, J.D. & REMACLE-VOLON, G. (1992). Influence of a long-acting bradykinin antagonist, Hoe 140, on some acute inflammatory reactions in the rat. *Eur. J. Pharmacol.*, **211,** 81–86.

DAVIS, A. & PERKINS, M.N. (1993). The effect of capsaicin and conventional analgesics on two models of monoarthritis in the rat. *Agents Actions*, **38,** C10–C12.

DAVIS, A.J. & PERKINS, M.N. (1994). Induction of B1 receptors in vivo in a model of persistent inflammatory mechanical hyperalgesia in the rat. *Neuropharmacol.*, **33,** 127–133.

DEBLOIS, D., BOUTHILLIER, J. & MARCEAU, F. (1988). Effects of glucocorticoids, monomines and growth factors on the spontaneously developing responses of the rabbit aorta to desArg^9-BK. *Br. J. Pharmacol.*, **93,** 969–977.

DEBLOIS, D., BOUTHILLIER, J. & MARCEAU, F. (1989). Pharmacological modulation of the up-regulated responses to des-Arg^9-BK in vivo and in vitro. *Immunopharmacology*, **17,** 187–198.

DRAY, A., PATEL, I.A., PERKINS, M.N. & RUEFF, A. (1992). Bradykinin-induced activation of nociceptors: receptor and mechanistic studies on the neonatal rat spinal cord-tail preparation *in vitro*. *Br. J. Pharmacol.*, **107,** 1129–1134.

EISENBERG, S.P., EVANS, R.J., AREND, W.P., VERDERBER, E., BREWER, M.T., HANNUM, C.H. & THOMPSON, R.C. (1990). Primary structure and functional expression from complementary DNA of a human interleukin-1 receptor antagonist. *Nature*, **343,** 341–346.

FERREIRA, S.H., LORENZETTI, B.B., BRISTOW, A.F. & POOLE, S. (1988). Interleukin-1β as a potent hyperalgesic agent antagonized by a tripeptide analogue. *Nature*, **334,** 698–700.

FOLLENFANT, R.L., NAKAMURA-CRAIG, M., HENDERSON, B. & HIGGS, G.A. (1989). Inhibition by neuropeptides of interleukin-1β-induced, prostaglandin-independent hyperalgesia. *Br. J. Pharmacol.*, **98,** 41–43.

FORREST, M.J., EIERMANN, G.J., MEURER, R., WALAKOVITS, L.A. & MACINTYRE, D.E. (1992). The role of CD18 in IL-8 induced dermal and synovial inflammation. *Br. J. Pharmacol.*, **106,** 287–294.

GREEN, P.G., LUO, J., HELLER, P. & LEVINE, J.D. (1993). Modulation of Bradykinin-induced extravasation in the rat knee joint by sympathetic co-transmitters. *Neuroscience*, **52,** 451–458.

HALEY, J.E., DICKENSON, A.H. & SCHACHTER, M. (1989). Electrophysiological evidence for a role of bradykinin in chemical nociception in the rat. *Neuroscience Lett.*, **97,** 198–202.

HEAPY, C.G., SHAW, J.S. & FARMER, S.C. (1993). Differential sensitivity of antinociceptive assays to the bradykinin antagonist Hoe 140. *Br. J. Pharmacol.*, **108,** 209–213.

HIRANO, T., MATSUDA, T., TURNER, M., MIYASAKA, N., BUCHAN, G., TANG, B., SATO, K., SHIMIZU, M., MAINI, R., FELDMANN, M. & KISHIMOTO, T. (1988). Excessive production of interleukin 6/b cell stimulatory factor in rheumatoid arthritis. *Eur. J. Pharmacol.*, **18,** 1797–1801.

LERNER, U.H, BRUNIUS, G. & MODEER, T. (1992). On the signal transducing mechanisms involved in the synergistic interaction between Interleukin-1 and bradykinin on prostaglandin biosynthesis in human gingival Fibroblasts. *Bioscience Reports*, **12,** 263–271.

LERNER, U.H. & MODEER, T. (1991). Bradykinin B1 and B2 receptor agonists synergistically potentiate interleukin-1-induced prostaglandin biosynthesis in human gingival fibroblasts. *Inflammation*, **15,** 427–436.

MCFADDEN, R.G. & VICKERS, K.E. (1989). Bradykinin augments the in vitro migration of nonsensitized lymphocytes. *Clin. Investig. Med.*, **12,** 247–253.

PERKINS, M.N., CAMPBELL, E.A., DAVIS, A. & DRAY, A. (1992). Antinociceptive activity of bradykinin B_1 and B_2 antagonists in two models of persistent hyperalgesia in the rat. *Br. J. Pharmacol.*, **107,** 237P.

PERKINS, M.N., CAMPBELL, E.A. & DRAY, A. (1993). Anti-nociceptive activity of the bradykinin B1 and B2 receptor antagonists, desArg9,leu8-BK and Hoe 140, in two models of persistent hyperalgesia in the rat. *Pain*, **53,** 191–197.

PERKINS, M.N. & KELLY, D. (1993). Interleukin-1β (IL-1β) but not tumour necrosis factor-alpha (TNF-α), can induce bradykinin B_1 receptor-mediated thermal hyperalgesia in the rat. *Br. J. Pharmacol.*, **108,** 18P.

PETITCLERC, E., ABEL, S., DEBLOIS, D., POUBELLE, P.E. & MARCEAU, F. (1992). Effects of interleukin-1 receptor antagonist on three types of responses to interleukin-1 in rabbit isolated blood vessels. *J. Cardiovasc. Pharmacol.*, **19,** 821–829.

REGOLI, D., MARCEAU, F. & BARABE, J. (1978). *De novo* formation of vascular receptors for kinins. *Can. J. Physiol. Pharmacol.*, **56,** 674–677.

REMICK, D.G., DEFORGE, L.E., SULLIVAN, J.F. & SHOWELL, H.J. (1992). Profile of cytokines in synovial fluid specimens from patients with arthritis. Interleukin 8 and IL-6 correlate with inflammatory arthritides. *Immunol. Invest.*, **21,** 321–327.

SALMON, J.A., SIMMONS, P.M. & MONCADA, S. (1983). The effects of BW755C and other anti-inflammatory drugs on eicosanoid concentrations and leucocyte accumulation in experimentally-induced acute inflammation. *J. Pharm. Pharmacol.*, **35,** 808–813.

SIEBECK, M., WHALLEY, E.T., HOFFMANN, H., WEIPERT, J. & FRITZ, H. (1989). The hypotensive response to desArg^9-BK increases during E. coli septicemia in the pig. *Adv. Exp. Med. Biol.*, **247b,** 389–393.

STERANKA, L.R., MANNING, D.C., DEHAAS, C.J., FERKANY, S.A., BOROSKY, S.A., CONNOR, J.R., VAVREK, R.J., STEWART, J.M. & SNYDER, S.H. (1988). Bradykinin as a pain mediator: receptors are localized to sensory neurons, and antagonists have analgesic actions. *Proc. Natl. Acad. Sci. U.S.A.*, **85,** 3245–3249.

TIFFANY, C.W. & BURCH, R.M. (1989). Bradykinin stimulates tumor necrosis factor and interleukin-1 release from macrophages. *FEBS Lett.*, **247,** 189–192.

WIRTH, K., HOCK, F.J., ALBUS, U., LINZ, W., ALPERMANN, H.G., ANAGNOSTOPOULOS, H., HENKE, S.T., BREIPOHL, G., KONIG, W., KNOLLE, J. & SCHOLKENS, B.A. (1991). Hoe 140 a new potent and long acting bradykinin-antagonist: *in vivo* studies. *Br. J. Pharmacol.*, **102,** 774–777.

WIRTH, K.J., WIEMER, G. & SCHOLKENS, B.A. (1992). DesArg10 [Hoe 140] is a potent B1 bradykinin antagonist. *Agents Actions Suppl.*, **38,** 406–413.

YOCUM, D.E., ESPARZA, L., DUBRY, S., BENJAMIN, J.B., VOLZ, R. & SCUDERI, P. (1989). Characteristics of tumor necrosis factor production in rheumatoid arthritis. *Cell Immunol.*, **122,** 131–145.

ZINI, J.M., SCHMAIER, A.H. & CINES, D.B. (1993). Bradykinin regulates the expression of kininogen binding sites on endothelial cells. *Blood*, **81,** 2936–2946.

(Received January 10, 1994
Revised May 9, 1994
Accepted May 16, 1994)

Br. J. Pharmacol. (1994), **113**, 69–76

The electrophysiological effects of dicentrine on the conduction system of rabbit heart

Ming-Lon Young, [1],*Ming-Jai Su, **Mei-Hwan Wu & †Chien-Chih Chen

Department of Pediatrics, University of Miami, *Department of Pharmacology and **Department of Pediatrics, National Tawain University and †National Institute of Chinese Medicine, Taipei, Taiwan

1 The electrophysiological effects of dicentrine, an aporphine alkaloid isolated from the root of *Lindera megaphylla*, were examined in the Langendorff perfused rabbit heart and rabbit isolated cardiac cells.

2 Standard electrophysiological characters were measured in the Langendorff perfused rabbit heart (control study) and after 5 min exposure to 1, 3 and 9 μM of dicentrine and during the subsequent recovery phase sequentially ($n = 7$). The same study protocols were performed in 0.5 to 4.5 μM quinidine ($n = 7$), 18 to 162 μM procainamide and N-acetylprocainamide ($n = 7$) for comparison.

3 The results showed that the spontaneously beating heart rate and the sinoatrial (SA) and atrioventricular nodal (AH) conduction time were not significantly affected by dicentrine but were significantly suppressed by the higher doses of quinidine (4.5 μM) and procainamide (162 μM).

4 The His-Purkinje conduction time was significantly increased by the higher dose of dicentrine, quinidine and procainamide.

5 The ventricular repolarization time and its effective refractory period were significantly increased by the higher dose of dicentrine and the other agents.

6 The effective refractory period of the atrium, AV node and His-Purkinje system were also significantly increased by dicentrine and the other agents.

7 A voltage clamp study revealed that the prolongation of atrial action potential duration by dicentrine (9 μM) was associated with a significant inhibition of the transient potassium outward current. As well as inhibition of the transient outward current, a significant inhibition of the sodium inward current by dicentrine was found.

8 We conclude that (1) dicentrine is potentially a useful antiarrhythmic agent with type I_a and type III antiarrhythmic action; (2) the relative potency of dicentrine on the electrophysiological function of cardiac tissue is 10–20 times more than that of procainamide.

Keywords: Dicentrine; quinidine; procainamide; conduction time; refractory period; transient outward current; sodium inward current; myocytes

Introduction

Medicinal plants have been used as traditional remedies in Taiwan for over hundreds of years. Among them, several aporphine alkaloids were isolated and reported to cause bradycardia and exert antiarrhythmic activity (Li *et al.*, 1984; 1989).

Dicentrine, a chemical principle isolated from the root of *Lindera megaphylla*, is an aporphine alkaloid found to have some antithrombotic activity and strong α-adrenoceptor blocking activity (Chen *et al.*, 1991; Teng *et al.*, 1991). In a study of the hypotensive effect on dogs, dicentrine when injected at 1 mg kg^{-1} could effectively reverse the heart beats to normal sinus rhythm in dogs with recurrent ventricular tachycardia. In rat isolated ventricular cells, dicentrine prolongs the action potential duration (APD_{50}), and reduces the rate of action potential upstroke (Su *et al.*, 1994). These results indicate that dicentrine may possess antiarrhythmic activity. The effects of dicentrine on the conduction system of the rabbit heart were studied and compared with its effect on membrane currents of rabbit cardiac cells. We conclude that dicentrine is potentially a useful type I and type III antiarrhythmic agent.

Methods

Electrophysiological study of conduction in rabbit hearts

Hearts were removed from New Zealand white rabbits (≥ 2 kg) and retrogradely perfused with Tyrode solution at a rate of 4 ml min^{-1} g^{-1} tissue. Tyrode solution was used, composition (mM): NaCl 120.3, NaH_2PO_4 1.2, $NaHCO_3$ 24.2, KCl 5, $MgCl_2$ 1.3, $CaCl_2$ 1.2, and dextrose 5.5, which was saturated with 95% O_2 and 5% CO_2 to give a pH of 7.4 and warmed to 37°C.

For His bundle electrogram recording, a silver electrode connected to a tungsten spring was placed on the endocardium near the apex of the triangle of Koch. In order to obtain a recognizable T wave and a ventricular depolarization wave simultaneously on the ventricular electrogram, the tips of the ventricular recording electrode were separate and placed on the opposite sides of the ventricular epicaridum near the ventricular apex.

High right atrial and ventricular pacing electrodes were placed near the junction of the superior vena cava and right atrium and on the epicardium near the right ventricular apex respectively. Pacing studies were performed utilizing a programmable stimulator (Bloom Ltd. DTU 215). A pacing stimulus of 1 ms in duration and twice the diastolic threshold voltage was applied to the preparation through the bipolar atrial or ventricular electrodes. The signals were continuously monitored on an oscilloscope (Hewlett Packard, 54503A) and pertinent data recorded on a two-channel physiological recorder (Gould, RS 3200) with a paper speed of 100 mm s^{-1}.

Electrophysiological studies were performed according to standard methods described previously (Josephson & Seides, 1979; Klitzner & Roberts, 1983; Young *et al.*, 1989).

The right atrium was paced at a constant rate that was slightly faster than the spontaneous heart rate and the following electrophysiological measurements made:

Intra-atrial conduction time (SA): the conduction interval

[1] Author for correspondence at: Department of Pharmacology, College of Medicine, National Taiwan University, Taipei, Taiwan.

measured from the beginning of the stimulation artifact to the first rapid deflection of the atrial depolarization wave. AV nodal conduction time (AH): the conduction interval measured from the first rapid deflection of the atrial depolarization wave to the beginning of the His bundle depolarization wave. His-Purkinje conduction time (HV): the conduction interval measured from the beginning of the His bundle depolarization to the earliest ventricular depolarization wave. Corrected ventricular repolarization time (QTc): the Q-T interval was defined as the interval measured from the beginning of the ventricular depolarization to the end of the T wave and corrected (QTc) by dividing the Q-T interval by the square root of the pacing cycle length.

The atrial pacing cycle length was then decrementally decreased (every 5–10 s) in steps of 10 or 20 ms, until a stable 1:1 AV nodal conduction pattern was lost. The longest pacing cycle length at which a 1:1 AV conduction pattern could not be maintained (either 2:1 conduction or Wenckebach cycle) was defined as the Wenckebach periodicity.

Refractory periods were determined using continuous premature stimulation techniques. Refractory periods were defined as follows: Atrial effective refractory period: the longest S_1-S_2 interval that could not evoke an atrial depolarization (A_2) wave. AV nodal effective refractory period: the longest S_1-S_2 interval in which the evoked A_2 failed to evoke a His bundle depolarization wave (H_2). His-Purkinje effective refractory period: the longest H_1H_2 interval (measured from the His bundle spike of the last beat of constant rate pacing to the premature His bundle spike evoked by the conducted S_2 beat) that fails to evoke a premature ventricular depolarization (V_2).

The ventricular extrastimulation study protocol was similar to the atrial extrastimulation study. The ventricular effective refractory period was defined as the longest S_1-S_2 interval in which the S_2 stimulation failed to evoke a premature ventricular depolarization (V_2).

Isolation of myocytes

Hearts were quickly removed from adult New Zealand white rabbits ($\geqslant 2$ kg) under anaesthesia (sodium pentobarbitone), 30 mg kg^{-1} and systemic heparinization (300 iu kg^{-1}, i.v.). The hearts were retrogradely perfused with a Langendorff apparatus by using prewarmed (37°C) calcium-free Tyrode solution for 3 min, followed by perfusing with the same solution containing 0.5 mg ml^{-1} collagenase (Type 1, Sigma Chemical Co., St. Louis, MO, U.S.A.) and 0.075 mg ml^{-1} protease (Type VII, Sigma). The calcium paradox was prevented by perfusion with Kraftbruhe (KB) medium for 5 min after the enzymatic digestion (Isenberg & Klockner, 1981). Thereafter, the left and right ventricles were separated from the atria, dispersed and stored in KB medium at room temperature (25–27°C) for later use.

Whole-cell recording

Ionic currents were studied by a whole cell voltage clamp method (Hamill *et al.*, 1981) and pipette electrodes with a tip resistance of 2–5 MΩ. A Dagon 8900 patch/whole cell clamp amplifier fitted with a 100 MΩ feedback resistor in the headstage was used to voltage clamp the myocyte. The formation of a high resistance seal was monitored by applying a 1 nA current from a digital pulse generator. A high resistance seal (5 to 10 gigaohm) was obtained before the disruption of the membrane patch. The cells were dialyzed with the electrode solution for 3–5 min to reach a state of equilibrium after disruption of the membrane patch. The total series resistance for the pathway between pipette interior and cell membrane was estimated from the cell capacitance and capacitance decay time constant. It was possible to compensate electronically for 60% of the voltage drop across the electode produced by the current. The maximal sodium inward current elicited from adult myocytes in normal Tyrode solution was usually higher than 20 nA and would escape effective voltage clamps. Therefore, Na currents were studied in low Na^+ Tyrode solution (80 mM NaCl was substituted with choline chloride) dialysis of the cell with Na containing (10 mM) Cs^+ pipette solution to reduce the membrane Na^+ concentration gradient and to prevent the contamination of potassium outward current.

During measurement of the potassium outward current, contamination by the calcium inward current (I_{Ca}) was prevented by adding 0.5 to 1.0 mM Co^{2+} to the bathing medium. In this condition, 400 ms depolarization of the membrane potential results in a generation of a fast inward current followed by a transient outward current (I_{to}). Since most of the I_{Na} inactivates within 5 to 10 ms after the start of depolarizing pulses, the contamination of I_{to} by this current could be reduced if the magnitude of I_{to} was measured at 10 ms after the start of the depolarizing pulse.

The effective refractory period (ERP) of rabbit ventricular cells was determined by twin stimulation at 0.2 Hz. The interval between the twin stimulation was decrementally decreased in 20 ms steps until the action potential could not be elicited by the second stimulation.

Solutions

Five basic solutions were used with the following composition in mM: (1) Ca^{2+}-Tyrode: NaCl 137, KCl 5.4, $MgCl_2$ 1.1, $CaCl_2$ 1.8, HEPES 12, titrated with NaOH to pH 7.4; (2) Calcium-free Tyrode: Tyrode solution without $CaCl_2$; (3) Cobalt containing Tyrode solution: Tyrode solution containing $CoCl_2$ 1 mM: (4) Internal solution for filling the suction

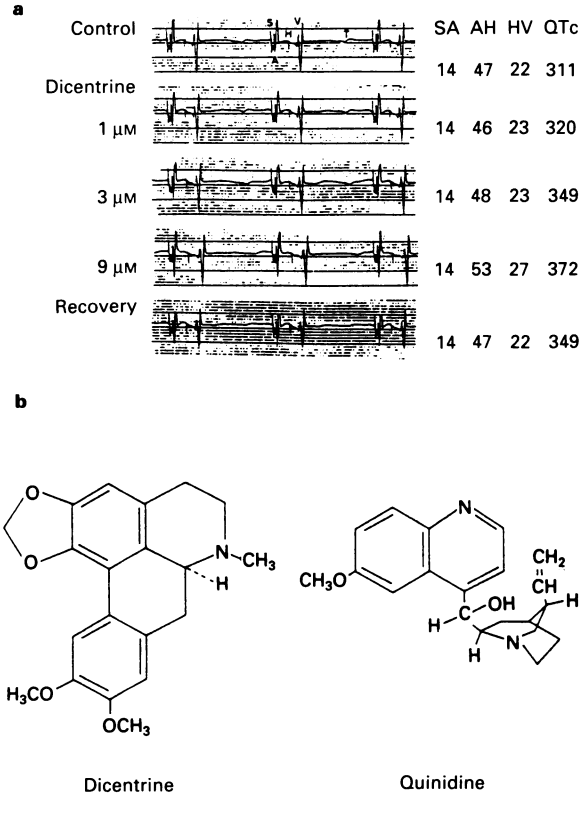

Figure 1 (a) His bundle electrograms showing effects of 1, 3 and 9 μM dicentrine on the electrophysiological function of an adult rabbit heart. The right atrium near the superior vena cava was paced at a constant rate with a pacing cycle length of 350 ms. A: atrial depolarization. H: His bundle depolarization. S: stimulation artifact. T: ventricular repolarization. V: ventricular depolarization. Paper speed: 100 mm s^{-1}. Calibration line: 10 ms. The measurements of SA, AH, HV and QTc (see Text for definitions) are in ms. (b) Chemical structures of dicentrine and quinidine.

pipettes: KCl 120, NaCl 10, MgATP 5, K_2EGTA 11, $CaCl_2$, HEPES 10, titrated with KOH to pH 7.4. Internal solution containing 120 mM Cs^+ instead of K^+ was used for I_{Na} and I_{Ca} studies; (5) KB medium: taurine 10, glutamic acid 70, KCl 25, KH_2PO_4 10, dextrose 22, EGTA 0.5, titrated with KOH to pH 7.3

Drugs

Quinidine, procainamide and N-acetylprocainamide were purchased from Sigma Chemical Company (St. Louis, MO, U.S.A.). Dicentrine ((±)-form, 99% purity) was isolated by column chromatography of the ethanol extract of the roots of *Lindera megaphylla* on silica gel columns (Chen *et al.*, 1991). Both quinidine and dicentrine were dissolved in dimethylsulphoxide (DMSO) as a 10 mM stock solution and further dilutions made in Tyrode solution. Procainamide (18, 55 and 165 μM) and N-acetylprocainamide (18, 55 and 165 μM) were dissolved in Tyrode solution.

In each of the Langendorff preparations the entire electrophysiological study protocol was performed before and after each drug addition.

In order to test the stability of the preparations and the reversibility of the agent, the same electrophysiological study protocol was repeated after the heart was again perfused in Tyrode solution for a period of at least 50 min. If the control data suggested a dysfunction of the conduction system of the preparation, or the recovery data deviated from that of the control by 20% or more, the data were discarded.

Figure 1 shows example tracing of His bundle electrograms taken from one experiment in which the atrium of an adult rabbit heart was paced at a pacing cycle length of 350 ms.

The results obtained were expressed as mean ± s.e. for each parameter. Student's *t* test was used for the comparison of control data among drugs. A repeated-measures analysis of variance was used for data comparison of different drugs and doses. A value of $P<0.05$ was taken to indicate statistical significance.

Results

Forty adult rabbit hearts divided into four groups (ten in each group) were sequentially exposed to increasing concentrations of dicentrine, quinidine, procainamide and N-acetylprocainamide respectively.

The control values for all parameters except the ventricular effective refractory period were not significantly different among drug testing groups. The recovery values for all parameters were not significantly different from the control values.

Basic cycle length

The results showed that there was a significant dose-dependent increase ($P<0.001$) in the basic cycle length for quinidine, procainamide and N-acetylprocainamide. Dicentrine exerted no significant effect on this parameter.

Atrial function

Quinidine and procainamide both caused a significant degree of lengthening ($P<0.01$) of the intra-atrial conduction time (Figure 2). At the highest dose tested, the latter caused a significantly higher degree of prolongation of the SA interval (29%) than the former (13%) ($P<0.01$). On the other hand, dicentrine and N-acetylprocainamide exerted no significant effect on this parameter.

All 4 drugs produced a significant lengthening of the atrial effective refractory period ($P<0.01$) (Figure 2). At the highest dose tested, the lengthening of the atrial effective refractory period for procainamide (54%) and quinidine (43%) was much more than that for N-acetylprocainamide (26%) and dicentrine (15%).

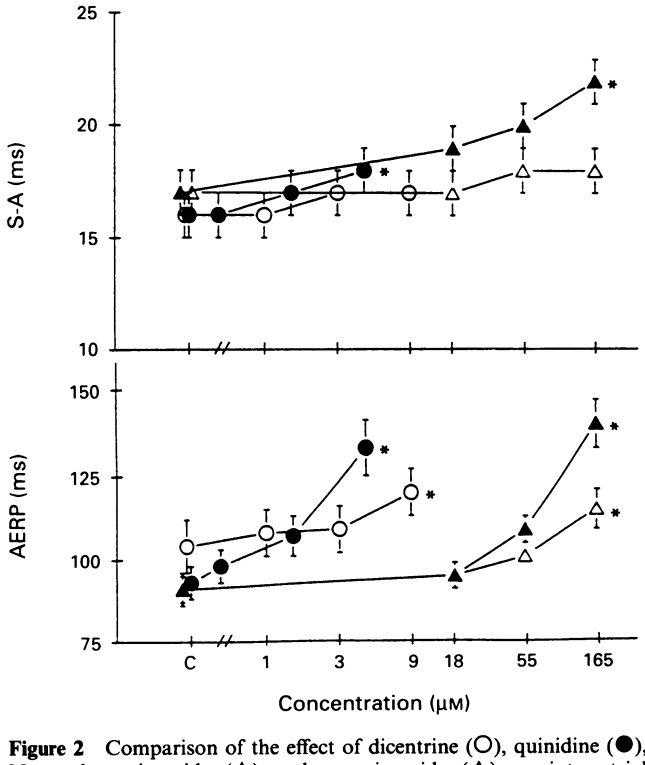

Figure 2 Comparison of the effect of dicentrine (○), quinidine (●), N-acetylprocainamide (△) and procainamide (▲) on intra-atrial conduction (S-A interval) and effective refractory period of atrial tissue. The method for the measurement of S-A interval and AERP was described in the text. *$P<0.001$.

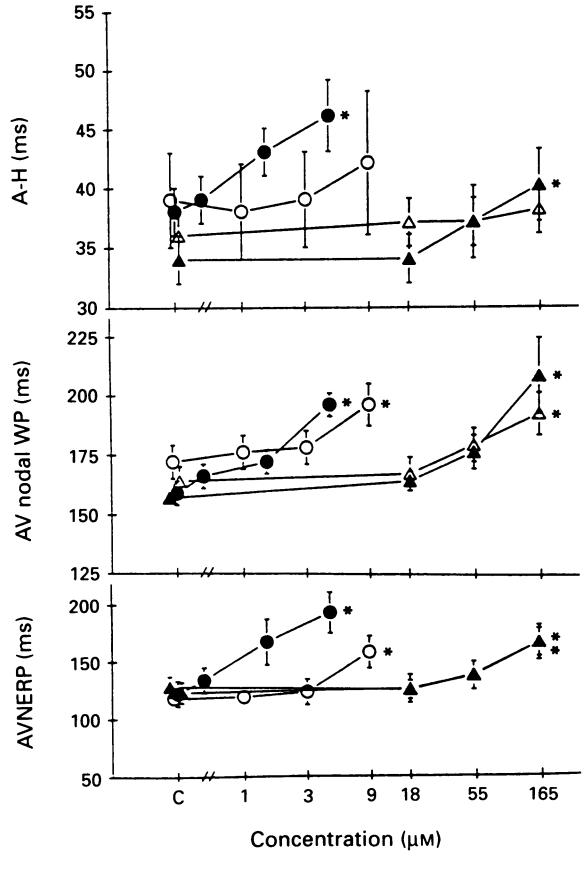

Figure 3 Comparison of the effect of dicentrine (○), quinidine (●), N-acetylprocainamide (△) and procainamide (▲) on rabbit AV nodal function. *$P<0.001$.

AV nodal function

Quinidine and procainamide both caused a significant degree of lengthening ($P<0.01$) of the AV nodal conduction time (Figure 3). At the highest dose tested, the former exerted more effect (21%) than the latter (18%) ($P=0.01$). Dicentrine and N-acetylprocainamide exerted no significant effect on the AV nodal conduction.

All 4 drugs caused a significant lengthening of the Wenckebach periodicity ($P<0.001$) (Figure 3). Significant lengthening of the Wenckebach periodicity over the control values was observed at all doses of quinidine and procainamide, at medium and high doses of N-acetylprocainamide and at high dose dicentrine only.

The reason for the missing data in the AV nodal effective refractory period measurement was that, in some experiments, the atrial tissue became refractory to premature atrial stimulation prior to the AV nodal tissue becoming refractory, thus the AV nodal effective refractory period could not be measured directly. In those experiments in which this parameter could be measured, all drugs caused a significant lengthening of the AV nodal effective refractory period ($P<0.001$) (Figure 3). Significant lengthening of the AV nodal effective refractory period was seen at all doses of quinidine and at the 'high' dose of dicentrine, procainamide and N-acetylprocainamide only. At the highest dose tested, the degree of lengthening of the AV nodal effective refractory period was significantly more with quinidine (59%) than with N-acetylprocainamide (38%), dicentrine (36%) or procainamide (33%).

His-Purkinje function

Dicentrine, quinidine and procainamide all exerted a significant lengthening effect on the His-Purkinje conduction time in the highest doses tested ($P<0.01$) (Figure 4). At these doses the degree of lengthening of this parameter with procainamide (33%) was more than that with dicentrine (13%) or quinidine (15%). N-acetylprocainamide exerted no effect on the His-Purkinje conduction time.

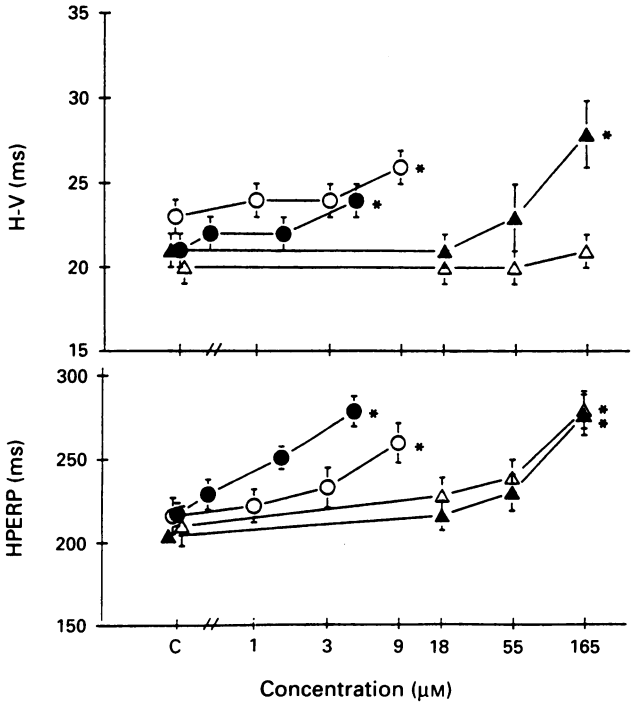

Figure 4 Comparison of the effect of dicentrine (○), quinidine (●), N-acetylprocainamide (△) and procainamide (▲) on rabbit His-Purkinje function. *$P<0.001$.

All 4 drugs caused a significant dose-dependent increase in the His-Purkinje effective refractory period ($P=0.001$) (Figure 4). At the highest dose tested the degree of lengthening of this parameter with procainamide (36%) was more

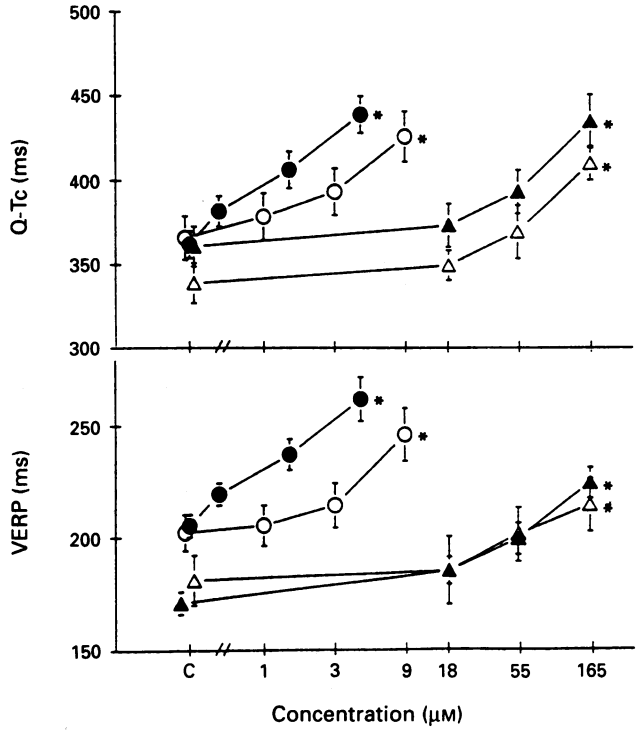

Figure 5 Comparison of the effect of dicentrine (○), quinidine (●), N-acetylprocainamide (△) and procainamide (▲) on rabbit ventricular function. *$P<0.001$.

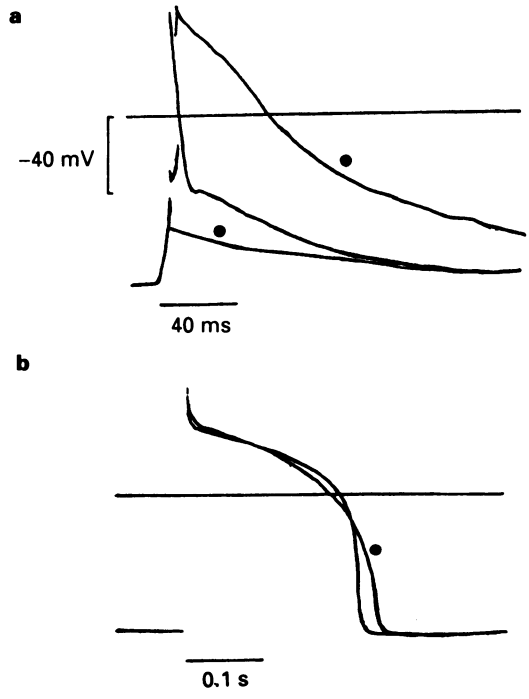

Figure 6 Effect of dicentrine on action potential of the rabbit atrial (a) and ventricular (b) cells. The cells were bathed in Ca^{2+}-Tyrode solution and stimulated at a frequency of 0.2 Hz. Superimposed action potentials obtained before and 4 min after treatment (●) with 9 μM dicentrine are shown. Note the atrial cells became inexcitable after treatment with 9 μM dicentrine. Therefore, the stimulation current should be increased to elicit the action potential of the atrial cell.

than that with N-acetylprocainamide (33%), quinidine (29%) or dicentrine (20%).

Ventricular function

All 4 drugs produced a significant dose-dependent increase in the corrected QT interval and in the ventricular effective refractory period ($P = 0.001$) (Figure 5). The degree of lengthening of the QTc interval with all 4 drugs was similar and their dose-response curves were parallel. At the highest dose tested the degree of prolongation of the ventricular effective refractory period with procainamide (31%) was more than that with quinidine (27%), dicentrine (22%) or N-acetylprocainamide (18%).

Effects of dicentrine on action potential of rabbit cardiac myocytes

In rabbit atrial cells driven at 0.2 Hz, the action potential duration measured at 50% and 90% repolarization was 9.7 ± 1.6 ms and 69.3 ± 7.8 ms ($n = 7$), respectively. After treatment with 9 μM dicentrine, these values increased to 66.0 ± 5.1 ms and 137.2 ± 9.8 ms, respectively (Figure 6). In rabbit ventricular cells exposed to 9 μM dicentrine, the APD_{50} was unchanged but the APD_{90} was lengthened by $13.2 \pm 1.4\%$ ($n = 6$). It is noteworthy that the spontaneous shortening of APD_{50} and APD_{90} due to the 'rundown' of L-type Ca^{2+} current with time (Belles *et al.*, 1988) was observed in rabbit ventricular cells in the absence of dicentrine. In our control study, APD_{50} and APD_{90} measured at 8 min after disruption of the membrane patch was shortened to $72.3 \pm 2.7\%$ (from 315.0 ± 6.1 ms to 227.5 ± 8.5 ms) and $78.4 \pm 5.2\%$ (from 337.5 ± 6.0 ms to 265.0 ± 17.5 ms) of that measured at 4 min after disruption of the membrane patch. When spontaneous shortening of APD was corrected, APD_{50} and APD_{90} after exposure to 9 μM dicentrine were lengthened by $14.1 \pm 1.8\%$ and $16.8 \pm 1.8\%$, respectively.

In the absence of drugs, the effective refractory period obtained at 8 min after disruption of the membrane patch was shortened to 82.5% of (from 385 to 318 ms) that measured at 4 min after disruption of the membrane patch. When the spontaneous shortening of ERP was corrected, ERP after exposure to 4.5 μM was lengthened by $45.7 \pm 2.3\%$ ($n = 6$, Figure 7). In cells treated with the same concentration of quinidine, ERP was lengthened by $97.9 \pm 4.8\%$ ($n = 6$, Figure 7).

Effect of dicentrine on sodium current and potassium current of rabbit cardiac myocytes

Figure 8a shows the transient potassium outward current (I_{to}) elicited by depolarization from a holding potential of

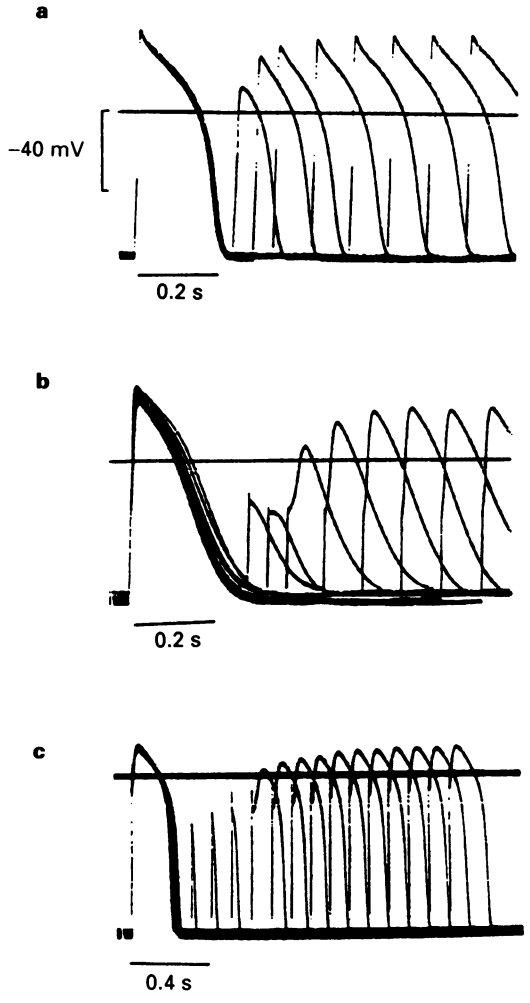

Figure 7 Effects of dicentrine and quinidine on recovery of membrane excitability of rabbit ventricular cells. Following a conditioning stimulation (TS, 4 ms, 1 nA), the premature action potential was elicited by test stimulation (TS, 4 ms, 1 nA) at different time interval. Each twin stimulation was applied at 0.2 Hz. (a) Typical action potentials in the absence of drug. (b) Action potentials obtained from the cell after exposure to 4.5 μM dicentrine. (c) Action potentials obtained from the cell treated with 4.5 μM quinidine.

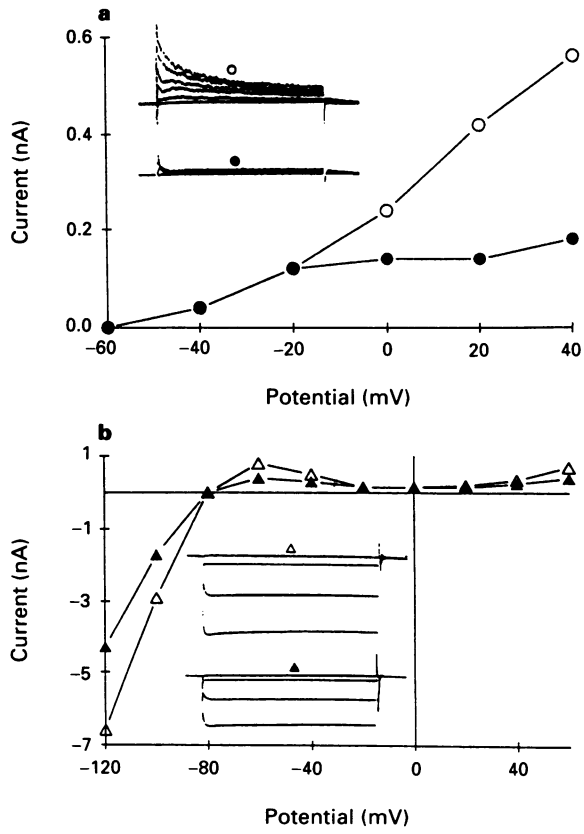

Figure 8 Effect of dicentrine on potassium outward current of the rabbit atrial cell and ventricular cell. (a) Effect of 9 μM dicentrine on transient outward current of the rabbit atrial cell. The cell was bathed in Tyrode solution containing 0.5 μM nifedipine. Transient outward currents were elicited by ms depolarization of membrane potentials to −40, −20, 0, 20, 40 and 60 mV. Transient outward current was defined as the peak outward current measured at 5 to 10 ms after the start of depolarizing step. Insets are typical current obtained before and after exposure to dicentrine. (b) Effect of 9 μM dicentrine on potassium current of rabbit ventricular cells. The cells were bathed in Tyrode solution containing 0.5 μM nifedipine. Insets are typical inwardly rectifying current obtained before and after exposure to 9 μM dicentrine.

– 80 mV to different potentials between – 40 to + 60 mV in atrial and ventricular cells. Four minutes treatment with 9 μM dicentrine reduced the amplitude of I_{to} by 67.7%. If the integral of potassium outward current from the start of depolarization to the end of the depolarization step was measured, 86.6% reduction of potassium outward current was obtained. I_{to} is less prominent in rabbit ventricular cells than in rabbit atrial cells (Giles & Imaizumi, 1988) but the magnitude of inward rectifying current is larger in ventricular cells than in atrial cells. In Figure 8b, the relative amplitude of outward current through K_1 channels was decreased to nearly 40% after 4 min exposure to 9 μM dicentrine but a 62.5% inward current through K_1-channels remained. Figure 9a shows the effects of dicentrine on the current voltage relationship for I_{Na}. I_{Na} was elicited by 15 ms depolarization from – 80 mV to various potentials ranging between – 60 and 0 mV. Under control conditions (in the presence of 0.5 μM nifedidipine), I_{Na} was activated at a threshold potential of around – 60 mV and attained a maximum value at – 30 to – 20 mV. Dicentrine (9 μM) blocked I_{Na} completely. If the holding potential was changed from – 80 mV to – 90 mV, a partial recovery of I_{Na} was obtained.

The effect of dicentrine on the steady state inactivation of I_{Na} was studied by using a double pulse protocol. The suppressive effect of dicentrine was accompanied by a shift of the I_{Na} availability ($h_\infty - V$) curve. The $h_\infty - V$ curves were obtained by normalizing the I_{Na} (induced by a test pulse to – 20 mV) by taking the maximum value as unity. The curves were fitted by the Boltzmann equation:

$$h_\infty = 1/[1 + \exp (E\text{-}V_h)/s]$$

Where E denotes the first conditioning potential, V_h the potential at which h_∞ is equal to 0.5, and s, the slope factor. Dicentrine at 1.5, 4.5 and 15 μM altered V_h from – 81.7 mV to – 89 mV, – 99.4 mV and – 115.9 mV, respectively (Figure 9). The maximal I_{Na} induced by a test pulse to – 20 mV from a holding potential of – 140 mV was reduced from – 5.6 nA to – 5.0 nA, – 3.2 nA and – 1.3 nA, respectively. In rabbit ventricular cells, similar exposure to 3 μM dicentrine resulted in a change of V_h from – 82.6 ± 2.9 mV to – 87.1 ± 3.5 mV (Figure 9). The maximal I_{Na} induced by test pulse to – 20 mV from a holding potential of – 140 mV was reduced from – 7.9 ± 1.2 nA to – 5.6 ± 1.2 nA ($n = 5$). This result indicates that the sensitivity of rabbit ventricular cells to dicentrine is similar to that of atrial cells.

Discussion

Several new antiarrhythmic drugs, previously available only for investigative purposes have been approved for general use, such as tocainide, mexiletine, flecainide, encainide and

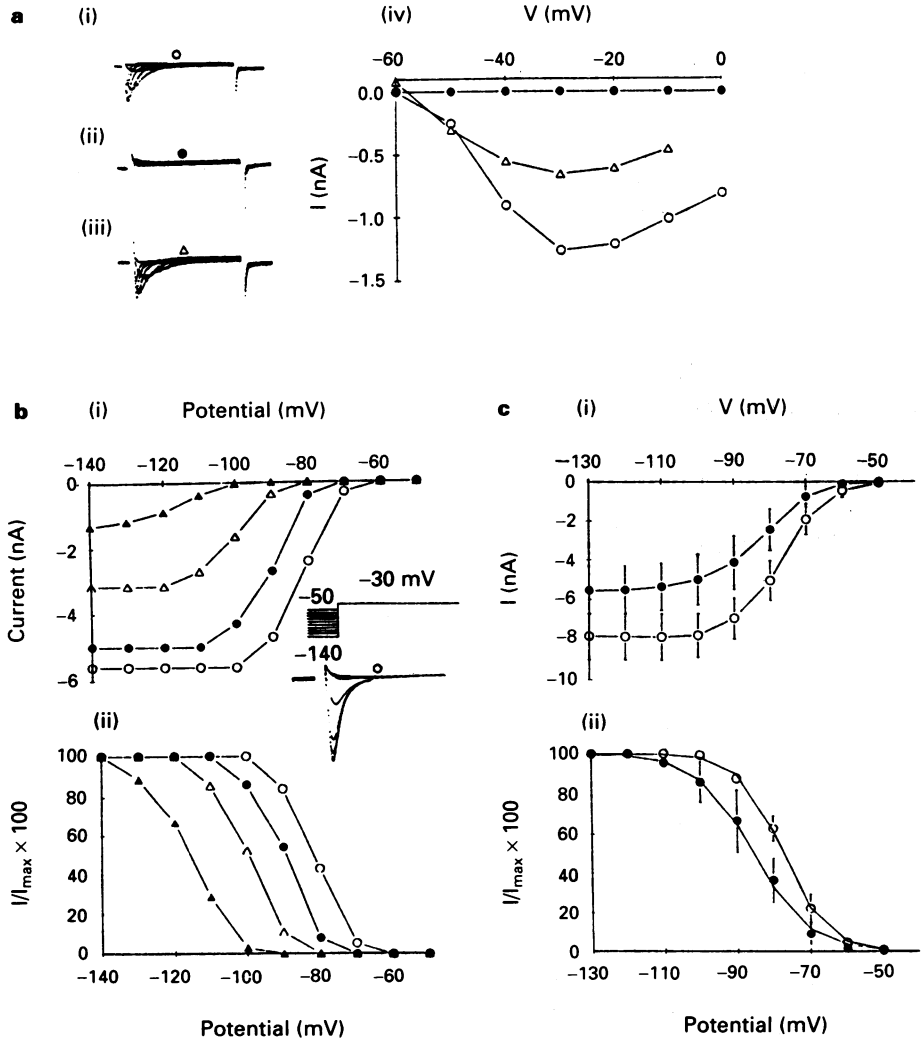

Figure 9 Effect of dicentrine on sodium inward current of rabbit atrial and ventricular cell. (a) Effect of 9 μM dicentrine on potential dependent activation of I_{Na} in the atrial cell. (b) Effect of 1.5, 4.5 and 15 μM dicentrine on voltage-dependent inactivation curves of I_{Na} in a rabbit atrial cell. (c) Effect of 9 μM dicentrine on voltage-dependent inactivation curves of I_{Na} in ventricular cells ($n = 6$).

amiodarone. However, prompted by the need for more effective and less toxic drugs, considerable interest in the search for new antiarrhythmic agents exists.

In 1969, Vaughan Williams proposed a classification for antiarrhythmic agents that has subsequently become widely accepted (Vaughan Williams, 1972; Singh *et al.*, 1972; Harrison, 1985; Hondeghen & Katzung, 1984). His classification, based on the effect of such agents on cardiac action potentials or intracardiac conduction intervals categorizes the drugs into 4 classes (Hoffman, 1985; Vaughan Williams, 1984; Weld *et al.*, 1982; Wettrel & Andersson, 1986).

In this study, dicentrine was found to inhibit action potential upstroke and prolong action potential duration. In a perfused heart model, dicentrine was found to inhibit H-V conduction but without significant inhibition of A-H conduction.

The inhibition of action potential upstroke and suppression of H-V conduction is correlated well with the inhibition of sodium current. Use-dependent inhibition of I_{Na}, retardation of the recovery of Na^+ channels from their inactivated state and negative shift of the voltage-dependent inactivation curve of I_{Na} are major mechanisms responsible for the action of most group I antiarrhythmic agents (Chen *et al.*, 1975; Lee *et al.*, 1981; Carmeliet & Saikawa, 1982; Sanchez-Chapula *et al.*, 1983; Clarkson & Hondeghem, 1985; Clarkson *et al.*, 1988; Su & Morad, 1987; Su *et al.*, 1990). Since the inhibition of I_{Na} by dicentrine is associated with a prominent leftward shift of the voltage-dependent inactivation curve of I_{Na}, the Na^+ channels available for activation may be markedly decreased after treatment with dicentrine.

Our voltage clamp study proved that the prolongation of rabbit atrial action potential duration by dicentrine is due to its inhibition of the transient outward current. In rabbit ventricular cells, the suppression of the transient outward current and the suppression of the potassium outward current through the inward rectifier both contributed to the prolongation of action potential duration. Our data from the voltage clamp study correlated well with the data obtained from the perfused heart model.

Early afterdepolarizations (EADs) and associated triggered arrhythmias can be induced by interventions that either depress outward (repolarizing) current or augment inward (depolarizing) current. These include caesium and class III antiarrhythmic agents which block potassium channels (Isenberg 1976; Roden & Hoffman 1985; Quantz & Nattel 1986; Hondeghem & Snyder, 1990); the calcium channel activator Bay K 8644 (January *et al.*, 1988); and agents that interfere with sodium channel inactivation such as aconitine and anthopleurin-A (Craelius *et al.*, 1988). EADs and associated triggered activity occurring during APD prolongation can be blocked by sodium channel blockers such as tocainide or mexiletine (Valois & Sasyniuk 1987; Roden & Hoffman, 1987) or potassium channel openers such as cromakalim and pinacidil (Fish *et al.*, 1990).

In the present study, we found that dicentrine blocks both Na^+ and K^+ channels like procainamide, quinidine and amiodarone (Carmeliet & Saikawa, 1982; Colatsky, 1982; Sanchez-Chapula *et al.*, 1983; Clarkson & Hondeghem, 1985; Nattel 1986; Clarkson *et al.*, 1988), which are broadly used in treating supraventricular as well as ventricular arrhythmias. The I_{Na} blocking action can antagonize the generation of EADs which occur after inhibition of potassium outward currents. Furthermore, a lesser degree of L-type calcium current inhibition by dicentrine as compared to quinidine (Su *et al.*, 1994), along with its rapid onset in action in perfused heart preparations and isolated cardiac myocytes, will make dicentrine useful in treating acute cardiac arrhythmias.

This work was supported partially by a research grant of the National Science Council of the Republic of China (NSC83-0425-B002-001) and partially by a research grant of National Tawian University Hospital (NTUH-78-032-A12).

References

BELLES, B., MALECOT, C.O., HESCHELER, J. & TRAUTWEIN, W. (1988). 'Rundown' of the Ca current during long whole-cell recordings in guinea pig heart cells: role of phosphorylation and intracellular calcium. *Pflügers Arch.*, **411**, 353–360.

CARMELIET, E. & SAIKAWA, T. (1982). Shortening of the action potential and reduction of pacemaker activity by lidocaine, quinidine and procainamide in sheep cardiac Purkinje fibers: an effect on Na or K currents? *Circ. Res.*, **50**, 257–272.

CHEN, C.M., GETTES, L.S. & KATZUNG, B.G. (1975). Effect of lidocaine and quinidine on steady state characteristics and recovery kinetics of (dV/dt)max in guinea pig ventricular myocardium. *Circ. Res.*, **37**, 20–29.

CHEN, C.C., HUANG, Y.H., OU, J.C., SU, M.J., YU, S.M. & TENG, C.M. (1991). Bioactive principles from the roots of *Lindera Megaphylla*. *Planta Medica*, **57**, 406–408.

CLARKSON, C.W., FOLLMEN, C.H., TEN EICK, R.E., HONDEGHEM, L.M. & YEH, J.Z. (1988). Evidence for two components of sodium channel block by lidocaine in isolated cardiac myocytes. *Circ. Res.*, **63**, 869–878.

CLARKSON, C.W. & HONDEGHEM, L.M. (1985). Evidence for a specific receptor site for lidocaine, quinidine and bupivacaine associated with cardiac sodium channel in guinea pig ventricular myocardium. *Circ. Res.*, **56**, 496–506.

COLATSKY, T.J. (1982). Mechanism of action of lidocaine and quinidine on action potential duration in rabbit cardiac Purkinje fibers. An effect on steady state sodium currents? *Circ. Res.*, **50**, 17–27.

CRAELIUS, W., CHEN, V.K.H. & EL-SHERIF, N. (1988). Sodium current modifications by anthopleurin-A and their role in early afterdepolarizations (abstract). *J. Am. Coll. Cardiol.*, **11** (Suppl A), 253a.

FISH, F.A., PRAKASH, C. & RODEN, D.M. (1990). Suppression of repolarization-related arrhythmics in vitro and in vivo by low-dose potassium channel activators. *Circulation*, **82**, 1362–1369.

GILES, W.R. & IMAIZUMI, Y. (1988). Comparison of potassium currents in rabbit atrial and ventricular cells. *J. Physiol.*, **405**, 123–145.

HAMILL, O.P., MARTY, A., NEHER, E., SAKMANN, B. & SIGWORTH, F.J. (1981). Improved patch clamp technique for high resolution current recording from cells and cell free membrane patches. *Pflügers Arch.*, **381**, 85–100.

HARRISON, D.C. (1988). Antiarrhythmic drug classification: new science and practical applications. *Am. J. Cardiol.*, **56**, 185–187.

HOFFMAN, B.F. (1985). *Mechanisms of Antiarrhythmias*. ed. Zipes, D.P. pp. 193–197. New York: Grune and Stratton Inc.

HONDEGHEM, L.M. & KATZUNG, B.G. (1984). Antiarrhythmic agents: The modulated receptor mechanism of action of sodium and calcium channel blocking drugs. *Annu. Rev. Pharmacol. Toxicol.*, **24**, 387–423.

HONDEGHEM, L.M. & SNYDER, D.J. (1990). Class III antiarrhythmic agents have a lot of potential but a long way to go: reduced effectiveness and dangers of reverse use-dependence. *Circulation*, **81**, 687–689.

ISENBERG, G. (1976). Cardiac Purkinje fibers: cesium as tool to block inward rectifying potassium currents. *Pflügers Arch.*, **365**, 99–106.

ISENBERG, G. & KLOCKNER, U. (1982). Calcium tolerant ventricular myocytes prepared by preincubation in a 'KB medium'. *Pflügers Arch.*, **395**, 6–18.

JANUARY, C.T., RIDDLE, J.M. & SALATA, J.J. (1988). A model for early afterdepolarizations: induction with calcium channel agonist Bay K 8644. *Circ. Res.*, **62**, 563–571.

JOSEPHSON, M.E. & SEIDES, S.F. (1979). *Clinical Cardiac Electrophysiology. Techniques and Interpretations*. pp. 41–65. Philadelphia: Lea & Febiger.

KLITZNER, T. & ROBERTS, N.K. (1983). The investigation of an arrhythmia: the invasive approach. In *Cardiac Arrhythmias in the Neonate, Infant and Child.* ed. Roberts, N.K. & Gelband, H. Norwald: Appleton-Century-Crofts.

LEE, K.S., HUME, J.R., GILES, W. & BROWN, A.M. (1981). Sodium current depression by lidocaine and quinidine in isolated ventricular cells. *Nature*, **291**, 325–327.

LI, G.R., HU, C.J. & JU, F.H. (1984b). Antagonistic effect of dauricine on experimental arrhythmia. *J. Chin. Trad. Med.*, **4**, 25–28.

LI, G.R., LI, X.G. & LU, F.H. (1989). Effect of neferine on transmembrane potentials of guinea pig myocardium. *Acta Pharm. Sin.*, **10**, 406–410.

MITRA, R. & MORAD, M. (1985). A reliable method for dissociation of myocytes from heart and stomach of vertebrates. *Am. J. Physiol.*, **249**, H1056–H1060.

NATTEL, S. (1986). Pharmacodynamics studies of amidarone and its active N-desmethyl metabolite. *J. Cardiovasc. Pharmacol.*, **8**, 771–777.

QUANTZ, M.A. & NATTEL, S. (1986). The ionic mechanism for quinidine induced early afterdepolarization (abstract). *Circulation*, **74** (Suppl II), II-420.

RODEN, D.M. & HOFFMAN, B.F. (1985). Action potential prolongation and induction of abnormal automaticity by low quinidine concentrations in canine Purkinje fibers: relationship to potassium and cycle length. *Circ. Res.*, **56**, 856–867.

SINGH, B.N. & VAUGHAN WILLIAMS, E.M. (1972). A fourth class of antidysrhythmic action? Effect of verapamil on ouabain toxicity, on atrial and ventricular intracellular potentials, and on other features of cardiac function. *Cardiovasc. Res.*, **6**, 109–119.

SANCHEZ-CHAPULA, J., TSUDA, Y. & JOSEPHSON, I.R. (1983). Voltage and use-dependent effect of lidocaine on sodium current in rat single ventricular cells. *Circ. Res.*, **52**, 557 –565.

SU, M.J., LIN, S.O., WANG, C.H., TSENG, Y.Z. & TSENG, C.D. (1990). Comparison of the electrophysiological effect of amidoarone, lidocaine and quinidine on rat ventricular cells. *Proc. Natl. Acad. Sci. (ROC)*, **14**, 105–113.

SU, M.J. & MORAD, M. (1987). Effect of quinidine and lidocaine on action potential and membrane current of frog ventricles. *Proc. Natl. Acad. Sci. (ROC)*, **11**, 362–369.

SU, M.J., NIEH, Y.C., HUANG, H.W. & CHEN, C.C. (1994). Dicentrine, an α-adrenoceptor antagonist with sodium and potassium channel blocking activities. *Naunyn-Schmied. Arch. Pharmacol.*, **349**, 42–49.

TENG, C.M., YU, S.M., KO, K.N., CHEN, C.C., HUANG, Y.L. & HUANG, T.F. (1991). Dicentrine, a natural vascular α_1 adrenoceptor antagonist isolated from *Lindera magephylla*. *Br. J. Pharmacol.*, **104**, 651–656.

VALOIS, M. & SASYNIUK, B.I. (1987). Modification of the frequency- and voltage-dependent effects of quinidine when administered in combination with tocainide in canine Purkinje fibers. *J. Pharmacol. Exp. Ther.*, **76**, 427–441.

VAUGHAN WILLIAMS, E.M. (1972). Classification of antiarrhythmic drugs. In *Symposium on Cardiac Arrhythmias.* ed. Sandoe, E., Flensted-Jansen, E. & Olesen, K.H. pp. 449–472. Sodertalje, Sweden: AB Astra.

VAUGHAN WILLIAMS, E.M. (1984). A classification of antiarrhythmic actions reassessed after a decade of new drugs. *J. Clin. Pharmacol.*, **24**, 129–147.

WELD, F.M., COROMILAS, J., ROTTMAN, J. & BIGGER, J.T. Jr. (1982). Mechanisms of quinidine-induced depression of maximum upstroke velocity in bovine cardiac Purkinje fibers. *Circ. Res.*, **50**, 369–376.

WETTREL, G. & ANDERSSON, K.E. (1986). Cardiovascular drugs I: antidysrhythmic drugs. *Ther. Drug. Monit.*, **8**, 59–77.

YOUNG, M.L., TAN, R.C., RAMZA, B.M. & JOYNER, R.W. (1989). Effects of hypoxia on atrioventricular node of adult and neonatal rabbit heart. *Am. J. Physiol.*, **256**, H1337–1343.

(Received September 21, 1993
Revised April 22, 1994
Accepted May 16, 1994)

Br. J. Pharmacol. (1994), **113**, 77–80

On the nature of the 5-HT receptor subtype inhibiting acetylcholine release in the guinea-pig ileum

M.J. Ramírez, [1]*J. Del Río, E. Cenarruzabeitia & B. Lasheras

Department of Pharmacology, Schools of Pharmacy and *Medicine, University of Navarra, 31080 Pamplona, Spain.

1 The nature of the 5-hydroxytryptamine (5-HT) receptor subtype controlling acetylcholine release and contraction induced by stimulation of the neurokinin NK_3 receptor has been studied in the longitudinal muscle-myenteric plexus preparation from guinea-pig ileum.

2 In preparations preloaded with [^{3}H]-choline, the selective NK_3 agonist, senktide, produced a concentration-dependent increase in tritium overflow, an index of [^{3}H]-acetylcholine release. Low concentrations of neurokinin B, also markedly increased tritium efflux.

3 The senktide-induced acetylcholine release was markedly increased by the same concentration of methysergide and mesulergine. The 5-$HT_{2A/2C}$ agonist DOI (1 μM) inhibited the tritium overflow while 8-OH-DPAT, sumatriptan and ketanserin (1 μM each) were without effect on the senktide-induced tritium efflux.

4 The contractile response to senktide in the guinea-pig ileum was attenuated by atropine, 0.1 μM. Methysergide, a 5-$HT_{1/2}$ receptor antagonist, and mesulergine, a 5-$HT_{2A/2B/2C}$ receptor antagonist, (1 μM each), enhanced the contractile effect of the NK_3 receptor agonist.

5 It is concluded that the acetylcholine release induced by a NK_3 receptor agonist is inhibited by stimulation of a 5-HT receptor, possibly of the 5-HT_{2C} or 5-HT_{2B} subtype.

Keywords: 5-HT_2 receptors; 5-HT_4 receptors; acetylcholine release; neurokinins; senktide

Introduction

Acetylcholine release is considered as the final event in the action of many neurotransmitters, such as 5-hydroxytryptamine (5-HT) and neurokinins in guinea-pig ileum (Yau & Yougher, 1982; Featherstone *et al.*, 1986; Fox & Morton, 1990; Eglen *et al.*, 1990). The 5-HT agonist, 5-methoxytryptamine, has been suggested to facilitate (via 5-HT_4 receptors) and to inhibit (via 5-HT_1 receptors) the release of acetylcholine from guinea-pig ileum (Kilbinger & Wolf, 1992). In the absence of 5-HT_1 receptor antagonists, the inhibitory effect of 5-methoxytryptamine on the electrically evoked acetylcholine release predominates (Kilbinger & Wolf, 1992). The nature of the 5-HT_1 receptor subtype mediating the inhibition of acetylcholine release is uncertain and it has been proposed that different 5-HT receptor subtypes, in particular the 5-HT_{1A} receptor (Kilbinger & Pfeuffer-Friederich, 1985; Fozard & Kilbinger, 1985) are involved in this inhibitory effect.

It has also been reported that 5-methoxytryptamine is not able to enhance basal acetylcholine release from guinea-pig myenteric neurones (Fox & Morton, 1990). However, the contraction elicited by 5-methoxytryptamine in the guinea-pig ileum is atropine-sensitive and it has been consequently suggested that 5-HT_4 receptor stimulation causes release of acetylcholine (Craig & Clarke, 1990). We have recently presented evidence suggesting the involvement of neurokinin NK_3 receptors in the acetylcholine release after 5-methoxytryptamine (Ramírez *et al.*, 1994). Selective NK_3 receptor agonists, such as senktide, release acetylcholine from tissues preloaded with choline (Guard *et al.*, 1991; Yau *et al.*, 1991; 1992). Accordingly, we considered that senktide-induced acetylcholine release might be a valid approach to analyse the nature of the 5-HT receptor subtype inhibiting acetylcholine release. Agonists and antagonists at different 5-HT receptor subtypes were used to study their influence on the contractile response to senktide in the longitudinal muscle-myenteric plexus preparation from guinea-pig ileum and also on acetylcholine release from the same preparation.

[1] Author for correspondence at: Department of Pharmacology, School of Medicine, University of Navarra, 31080 Pamplona, Spain.

Methods

Guinea-pigs of either sex weighing 300–400 g were killed by cervical dislocation and exsanguinated. The ileum was excised approximately 10 cm from the ileo-caecal junction and longitudinal muscle strips with the myenteric plexus attached (LMMP) were prepared as described by Paton & Vizi (1969).

Contractility studies

LMMP strips were suspended in a 10 ml organ bath containing Tyrode solution (composition in mM: NaCl 136, KCl 2.7, $CaCl_2$ 1.8, $MgCl_2$ 1.05, NaH_2PO_4 0.42, $NaHCO_3$ 11.9, glucose 5.5) aerated with 95% O_2/5% CO_2 and maintained at 37°C. Contractile responses were recorded isometrically with a resting tension of 0.5 g. Before the experiments were started, tissues were equilibrated for 30 min.

Concentration-response curves were constructed in a non-cumulative fashion with an agonist exposure period of 30 s during a 10 min dose-cycle. In studies with antagonists, each strip was used to record two concentration-response curves: the first for the agonist alone and the second for the agonist in the presence of the antagonist, each strip serving as its own control. Antagonists were allowed to pre-equilibrate for 15 min prior to the addition of the agonists.

Characterization of the concentration-response curves

Responses were measured as an increase in the isometric tension and expressed as a percentage of the maximum response. In the presence of an antagonist, results were expressed as a percentage of the maximal response obtained with the agonist alone in the same tissue. Agonist potency was expressed as the agonist concentration yielding a half-maximal effect, EC_{50}.

Release experiments

The method employed to measure the release of acetylcholine was a modification of that described by Kilbinger & Wessler (1980). Briefly, LMMP strips weighing approximately 30 mg were suspended isometrically under a tension of 0.5 g in a

5 ml organ bath and superfused with Tyrode solution containing 1 μM choline. After 30 min incubation with [methyl-^{3}H]-choline (8 μCi ml^{-1}) and continuous stimulation during this time through platinum electrodes with square wave pulses (0.2 Hz, 1 ms, 13.5 V), the strips were superfused with Tyrode solution containing 10 μM hemicholinium-3 to prevent reuptake of choline. After a washout period of 60 min, aliquots were collected in 3 min fractions. Strips were stimulated twice (S_1, S_2) by field stimulation (1 Hz, 1 ms, 13.5 V), the two pulses being spaced 21 min apart. Neurokinins or synthetic agonists were added to the superfusion fluid 21 min after S_2. 5-HT agents were left in contact with the tissue for 15 min before the addition of senktide. The spontaneous outflow was calculated by fitting a linear regression line based on the samples taken before and during S_1 stimulation.

The tritium content of the superfused samples was measured by liquid scintillation spectrometry. Under the present experimental conditions, the validity of assuming total tritium as a measure of [^{3}H]-acetylcholine released has been extensively documented (Szerb, 1976; Wikberg, 1977; Yau *et al.*, 1991).

The effect of the drugs (D) studied on the outflow of ^{3}H label was expressed as a percentage of the increase in the output of ^{3}H label evoked by the second electrical stimulation (S_2). The increase in the output of ^{3}H label in response to either the drug or the second electrical stimulation was calculated by subtracting the output during the preceding resting period of 3 min from the output during the stimulation.

Data analysis

The significance of the difference between two groups was assessed using Student's *t* test. To characterize the agonist potency the log EC_{50} was calculated with GraphPAD, ISI Software.

Drugs used

The following drugs were purchased from the suppliers indicated: substance P acetate, atropine sulphate, choline bromide, hemicholinium-3 bromide (Sigma, U.S.A.); neurokinin B (Bachem, Switzerland); 8-hydroxy-2-(di-n-propylamino) tetralin (8-OH-DPAT), (2,5-dimethoxy-1-iodophenyl)-2-aminopropane (DOI), [Sar^9,Met(O$_2$)^{11}]SP, mesulergine chloride, senktide (RBI, U.S.A.); choline chloride[methyl-^{3}H] (NEN-Du Pont, Boston, MA, U.S.A.). Methysergide maleate, ketanserin and sumatriptan were kindly provided by Sandoz, Janssen and Glaxo respectively. Peptides were made up in a stock of 0.1 mM concentration in 0.1 N acetic acid; aliquots were stored frozen and diluted before use. Ketanserin was dissolved in 50 mM ascorbic acid. All other drugs were dissolved in distilled water.

Results

Contractility studies

The selective NK_3 agonist, senktide, yielded a shallow monophasic concentration-response curve ($-\log EC_{50} = 8.3 \pm 0.1$). Atropine 0.1 μM markedly inhibited the response to senktide, while methysergide, a 5-$HT_{1/2}$ receptor antagonist and mesulergine, a 5-$HT_{2A/2B/2C}$ receptor antagonist, both at a 1 μM concentration, enhanced the contractile effect of this NK_3 receptor agonist (Figure 1). The concentration-response curve to the NK_3 receptor agonist was shifted to the left and the maximum response was also augmented with both 5-HT receptor antagonists. To study the specificity of this effect, the selective NK_1 receptor agonist, [Sar^9,met(O$_2$)^{11}]SP, was also used. The concentration-response curve to [Sar^9,met(O$_2$)^{11}]SP was also monophasic ($-\log EC_{50} = 8.2 \pm 0.1$). Neither atropine, 0.1 μM, nor methysergide, 1 μM, was able

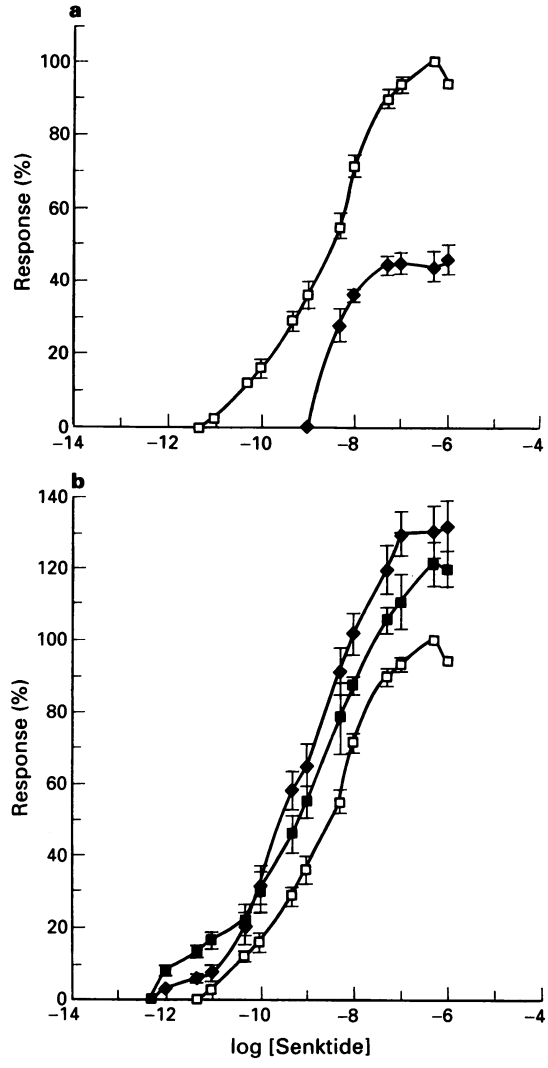

Figure 1 Concentration-response curve to senktide (□) and the effects of (a) atropine, 0.1 μM (◆); (b) methysergide, 1 μM (◆) and mesulergine, 1 μM (■). Values are means ± s.e.mean from 10–12 preparations and are expressed as percentage of the maximum response obtained with senktide.

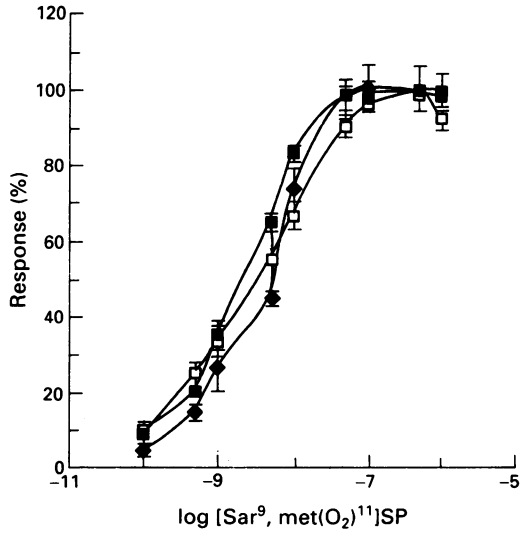

Figure 2 Concentration-response curve to [Sar^9,met(O$_2$)^{11}]SP (□) and the effects of atropine, 0.1 μM (◆) and methysergide, 1 μM (■). Values are means ± s.e.mean from 10–12 preparations and are expressed as percentage of the maximum response obtained with [Sar^9,met(O$_2$)^{11}]SP.

to modify the contractile response to [Sar^9,met(O$_2$)^{11}]SP (Figure 2).

Stimulation of [^{3}H]-acetylcholine release by physiological neurokinins, senktide and [Sar^9, met(O$_2$)^{11}]SP

The contractile response to NKB in the LMMP preparation yielded a biphasic concentration-response curve (not shown). At low concentrations, corresponding to the first phase of its concentration-response curve, neurokinin B (NKB) was able to promote a marked ^{3}H-overflow from the LMMP preparation preloaded with [^{3}H]-choline. Substance P (SP) produced a concentration-dependent increase in ^{3}H-efflux, while an inverse relationship was found with NKB. Senktide increased in a concentration-dependent manner the ^{3}H-overflow. The $-\log EC_{50}$, relative to the efflux evoked by senktide, 0.1 μM, obtained by interpolation was 9.1 ± 0.5 ($n = 10$). [Sar^9,met(O$_2$)^{11}]SP, 0.1 μM, slightly increased (30.8%) the tritium efflux, lower concentrations being ineffective (Figure 3).

Effect of different agents acting at 5-HT receptors on the senktide-induced [^{3}H]-acetylcholine release

The spontaneous outflow of tritium from preparations preloaded with [^{3}H]-choline was not modified in the presence of methysergide or mesulergine (1 μM each). A 0.5 nM concentration of senktide, approximately the mean effective concentration for [^{3}H]-acetylcholine release, was used to investigate the effect of different agents acting on 5-HT receptors. As shown in Table 1, methysergide, 1 μM, and mesulergine, 1 μM, were able to increase markedly the ^{3}H-efflux evoked by senktide. 8-OH-DPAT, a 5-HT$_{1A}$ receptor agonist, and sumatriptan, a 5-HT$_{1D}$ receptor agonist, also at a 1 μM concentration, had no effect on the tritium overflow. The 5-HT$_{2A/2C}$ receptor agonist, DOI, was able to reduce the senktide-induced ^{3}H-overflow. Ketanserin, 1 μM, a specific 5-HT$_{2A}$ antagonist, was without effect on the ^{3}H-efflux.

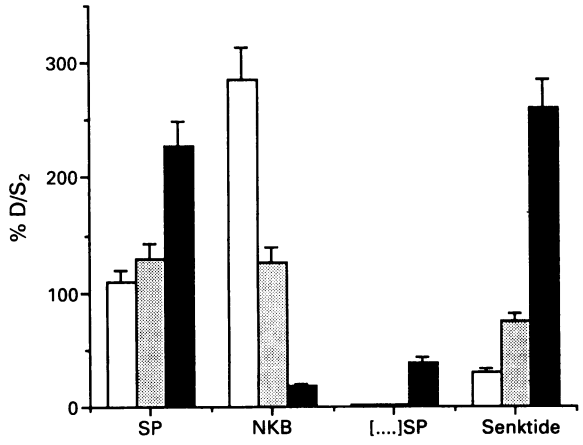

Figure 3 Effect of different concentrations of substance P (SP), neurokinin B (NKB), senktide and [Sar^9,met(O$_2$)^{11}]SP ([....]SP) on ^{3}H-overflow from LMMP preparations preloaded with [^{3}H]-choline: open columns 0.5 nM; stippled columns 5 nM, solid columns, 0.1 μM. The effect is expressed as a percentage of the increase in the output of ^{3}H-label evoked by S_2; D, drugs. Values are means ± s.e.mean from ten preparations.

Table 1 Effect of different 5-HT agents on the ^{3}H outflow induced by senktide from longitudinal muscle-myenteric plexus preparations of guinea-pig ileum

	Acetylcholine release (% S_2)
Senktide 0.5 nM	108.8 ± 9.3
+ Methysergide 1 μM	242.5 ± 20.1*
+ Mesulergine 1 μM	269.9 ± 24.9*
+ 8-OH-DPAT 1 μM	106.8 ± 15.2
+ Sumatriptan 1 μM	99.4 ± 10.4
+ DOI 1 μM	54.7 ± 8.2*
+ Ketanserin 1 μM	94.3 ± 15.3

After preincubation with [^{3}H]-choline the preparations were electrically stimulated (S_2: 1 Hz, 1 ms, 13.5 V) 27 min after the washout period. Superfusion with senktide started 21 min after S_2. 5-HT agents were present in the superfusate from 15 min before the stimulation with senktide until the end of the experiment. Results are expressed as a percentage of the tritium release induced by electrical stimulation (S_2) (mean ± s.e.mean of 6–8 determinations). (*$P < 0.05$).

Discussion

The results of the present work suggest that the senktide-induced guinea-pig ileum contraction and acetylcholine release are regulated by a 5-HT receptor, presumably of the 5-HT$_{2C}$, previously called 5-HT$_{1C}$, (Humphrey *et al.*, 1993), or 5-HT$_{2B}$ subtype.

NK$_3$ receptor stimulation elicits acetylcholine release from the myenteric plexus of guinea-pig ileum (Featherstone *et al.*, 1986; Yau *et al.*, 1991; 1992). In this study we evaluated the ability of substance P (SP), neurokinin B (NKB), senktide and [Sar^9,met(O$_2$)^{11}]SP to induce ^{3}H-overflow from tissues preloaded with [^{3}H]-choline as an index of [^{3}H]-acetylcholine release (Wikberg, 1977; Yau *et al.*, 1991). At low concentrations of the physiological neurokinins, corresponding to the selective activation of NK$_1$ receptors by SP and NK$_3$ receptors by NKB (Ramírez *et al.*, 1994), a marked increase in ^{3}H-overflow was observed only with NKB. Higher concentrations of SP can also activate the NK$_3$ receptor and promote the subsequent acetylcholine release. Conversely, higher concentrations of NKB activate the muscular NK$_1$ receptor and produce a much lower ^{3}H-overflow. Senktide, a selective NK$_3$ receptor agonist, produces in turn a concentration-dependent increase in ^{3}H-overflow as might be expected. In previous studies (Ramírez *et al.*, 1994) we reported that the concentration-response curve to NKB was biphasic, the first phase corresponding to the activation of NK$_3$ receptors and the second phase, after higher concentrations of NKB, would result from the stimulation of both NK$_1$ and NK$_3$ receptors. Interestingly, the $-\log EC_{50}$ value of the first phase of the concentration-response curve to NKB (Ramírez *et al.*, 1994) was approximately identical to the $-\log EC_{50}$ for senktide-induced acetylcholine release reported here. Contractility studies in which atropine markedly attenuated the response to senktide confirmed the cholinergic nature of the response to senktide. [Sar^9,met(O$_2$)^{11}]SP (0.1 μM) increased the ^{3}H-efflux only slightly as already reported by other authors (Guard *et al.*, 1991). NK$_1$ receptors may be located on cholinergic neurones of the guinea-pig myenteric plexus (Guard *et al.*, 1991), but these receptors seem to play a minor role in acetylcholine release. On the other hand contractility studies showed the lack of effect of atropine (0.1 μM) on the response to [Sar^9,met(O$_2$)^{11}]SP. All of these experiments suggest that cholinergic stimulation is not of much importance in the response to the NK$_1$ agonist [Sar^9,met(O$_2$)^{11}]SP.

The presence of a hypothetical 5-HT receptor subtype inhibiting acetylcholine release from myenteric neurones was previously suggested (see references in Introduction). In contractility studies we found that methysergide as well as mesulergine, a 5-HT$_{2C}$ antagonist (Pazos *et al.*, 1985), enhanced the response to senktide. These results suggest the involvement of the 5-HT$_{2C}$ or 5-HT$_{2B}$ receptors controlling the senktide-induced acetylcholine release.

To characterize fully the nature of the 5-HT receptor involved in this effect, different 5-HT agents were tested for their ability to modify senktide-induced acetylcholine release. The 5-HT$_{1/2}$ receptor antagonist methysergide (1 μM) enhanced ^{3}H-efflux, as did the 5-HT$_{2A/2B/2C}$ antagonist, mesulergine.

This enhancement in senktide-evoked acetylcholine release cannot be explained through the blockade of a hypothetical autoreceptor, as neither methysergide nor mesulergine had any intrinsic effect on acetylcholine release in this preparation. Neither the 5-HT_{1A} receptor agonist, 8-OH-DPAT (Gozlan *et al.*, 1983; Dompert *et al.*, 1985; Hoyer & Schoeffter, 1991), nor the 5-HT_{1D} receptor agonist, sumatriptan (Bruinvels *et al.*, 1991) modified the ^{3}H-overflow. In some species, 5-HT_{1B} receptors are presynaptic receptors controlling neurotransmitter release. However, this receptor subtype has not been found in the guinea-pig ileum (Heuring *et al.*, 1987), so 5-HT_{1B} receptor ligands were not investigated in this study.

To assess further the possible involvement of 5-HT_{2C} or 5-HT_{2B} receptors in the modulation of acetylcholine release, the 5-$HT_{2A/2C}$ agonist, DOI (McKenna & Peroutka, 1989; Lyon & Titeler, 1988) was also used and a marked blockade of ^{3}H-overflow was obtained. In addition, ketanserin (1 μM) one of the few available selective 5-HT_{2A} receptor antagonists, had no effect on the senktide-evoked tritium efflux. Admittedly, the location of the non-5-HT_{2C} receptors in the LM-MP preparation is muscular so it is possible to hypothesize on the presence of a 5-HT_{2C} or 5-HT_{2B} receptor inhibiting senktide-induced acetylcholine release. In the absence of better selective antagonists for other 5-HT receptor subtypes which could perhaps be expressed in the guinea-pig ileum, the more reasonable interpretation of the present findings is to suppose that 5-HT_{2C} or 5-HT_{2B} receptors could inhibit acetylcholine release. It has been speculated that these two receptors are the central and peripheral counterparts of one another (Schmuck *et al.*, 1994). It is possible that the high affinity of yohimbine for the 5-HT_{2B} receptors (Foguet *et al.*, 1992) could help to clarify the 5-HT_2 receptor subtype involved in the control of acetylcholine release.

In conclusion, the results of the present study suggest that 5-HT_{2C} or 5-HT_{2B} receptors may control senktide-induced acetylcholine release. Previous studies (see Introduction) have shown the implication of the NK_3 receptor in acetylcholine release after stimulation of the 5-HT_4 receptor (Ramírez *et al.*, 1994). Since the prokinetic effect of benzamides, such as cisapride seems to involve an activation of 5-HT_4 receptors, the present results are of interest in the analysis of other possible pharmacological influences in the prokinetic action of this class of drugs.

We thank S.Lizaso for technical help. M.J.R. is a fellow from Gobierno de Navarra (Spain).

References

BRUINVELS, A.T., LANDWEHRMEYER, B., WAEBER, C., PALACIOS, J.M. & HOYER, D. (1991). Homogeneous 5-HT_{1D} recognition sites in the human substancia nigra identified with a new iodinated radioligand. *Eur. J. Pharmacol.*, **202**, 89–91.

CRAIG, D.A. & CLARKE, D.E. (1990). Pharmacological characterization of a neuronal receptor to serotonin in guinea-pig ileum with properties similar to the 5-HT4 receptor. *J. Pharmacol. Exp. Ther.*, **252**, 1378–1386.

DOMPERT, W.U., GLASER, T. & TRABER, J. (1985). [^{3}H]-TVX Q 7821: identification of 5-HT_1 binding sites as target for a novel putative anxiolitic. *Naunyn Schmied. Arch. Pharmacol.*, **328**, 883–892.

EGLEN, R.M., SWANK, S.R., WALSH, L.K.M. & WHITING, R.L. (1990). Characterization of 5-HT_3 and 'atipical' 5-HT receptors mediating guinea-pig ileal contractions *in vitro*. *Br. J. Pharmacol.*, **101**, 513–520.

FEATHERSTONE, R.L., FOSBRAEY, P. & MORTON, I.K.M. (1986). A comparison of the effects of three substance P antagonists on the [^{3}H]-acetylcholine release in the guinea-pig ileum. *Br. J. Pharmacol.*, **87**, 73–78.

FOGUET, M., HOYER, D., PARDO, L.A., PAREKH, A., KLUXEN, F.W., KALKMAN, H.O., STÜHMER, W. & LÜBBERT, H. (1992). Cloning and functional characterization of the rat stomach fundus serotonin receptor. *EMBO J.*, **11**, 3487–3491.

FOX, A.J. & MORTON, I.K.M. (1990). An examination of the 5-HT_3 receptor mediating contraction and evoked [^{3}H]-acetylcholine release in the guinea-pig ileum. *Br. J. Pharmacol.*, **101**, 553–556.

FOZARD, J.R. & KILBINGER, H. (1985). 8-OH-DPAT inhibits transmitter release from guinea-pig enteric cholinergic neurones by activating 5-HT_{1A} receptors. *Br. J. Pharmacol.*, **85**, 601P.

GOZLAN, H., EL MESTIKAKAWY, S., PICHAT, A., GLOWINSKI, J. & HAMON, M. (1983). Identification of presynaptic serotonin autoreceptors using a new ligand ^{3}H-PAT. *Nature*, **305**, 140–142.

GUARD, S., MCKNIGHT, A.T., WATLING, K.J. & WATSON, S.P. (1991). Evidence for two types of tachykinin receptors on cholinergic neurons of guinea pig ileum myenteric plexus. *Ann. N.Y. Acad. Sci.*, **632**, 400–403.

HEURING, R.E., SCHLEGEL, R.J. & PEROUTKA, S.J. (1987). Species variations in Ru 24969 interactions with non-5-HT_{1A} binding sites. *Eur. J. Pharmacol.*, **122**, 279–282.

HOYER, D. & SCHOEFFTER, P. (1991). 5-HT receptors: subtypes and second messengers. *J. Recept. Res.*, **11**, 197–214.

HUMPHREY, P.P.A., HARTING, P. & HOYER, D. (1993). A proposed nomenclature for 5-HT receptors. *Trends Pharmacol. Sci.*, **14**, 233– 236.

KILBINGER, H. & PFEUFFER-FRIEDERICH, I. (1985). Two types of receptors for 5-hydroxytryptamine on the cholinergic nerves of the guinea-pig myenteric plexus. *Br. J. Pharmacol.*, **85**, 529–539.

KILBINGER, H. & WESSLER, I. (1980). Inhibition by acetylcholine of the stimulation-evoked release of [^{3}H]-acetylcholine from guinea-pig myenteric plexus. *Neuroscience*, **5**, 1331–1340.

KILBINGER, H. & WOLF, D. (1992). Effects of 5-HT4 receptor stimulation on basal and electrically evoked release of acetylcholine from guinea-pig myenteric plexus. *Naunyn Schmied. Arch. Pharmacol.*, **345**, 27–275.

LYON, R.A. & TITELER, M. (1988). Pharmacology and biochemistry of the 5-HT_2 receptor. In *The Serotonin Receptors*. ed. Sanders-Bush, E. pp. 59–88. Clifton, N.J.: The Humana Press.

MCKENNA, D.J. & PEROUTKA, S.J. (1989). Differentiation of 5-HT_2 receptor subtypes using [^{125}I]-(R)-DOI and [^{3}H]-ketanserin. *J. Neurosci.*, **9**, 3482–3490.

PATON, V.D. & VIZI, E.S. (1969). The inhibitory action of noradrenaline and adrenaline on acetylcholine output by guinea-pig ileum longitudinal muscle strip. *Br. J. Pharmacol.*, **35**, 10–28.

PAZOS, A., HOYER, D. & PALACIOS, J.M. (1985). The binding of serotonergic ligands to the porcine choroid plexus: characterization of a new type of serotonin recognition site. *Eur. J. Pharmacol.*, **106**, 539–546.

RAMIREZ, M.J., CENARRUZABEITIA, E., DEL RIO, J. & LASHERAS, B. (1994). Involvement of neurokinins in the non-cholinergic response to activation of 5-HT_3 and 5-HT_4 receptors in the guinea-pig ileum. *Br. J. Pharmacol.*, **111**, 419–424.

SCHMUCK, K., ULLMER, C., ENGELS, P. & LÜBBERT, H. (1994). Cloning and functional characterization of the human 5-HT_{2B} serotonin receptor. *FEBS Lett.*, **342**, 85–90.

SZERB, J.C. (1976). Storage and release of labelled acetylcholine in the myenteric plexus of guinea-pig ileum. *Can. J. Physiol. Pharmacol.*, **54**, 12–22.

WIKBERG, J. (1977). Release of [^{3}H]-acetylcholine from isolated guinea-pig ileum. A radiochemical method for studying the release of the cholinergic neurotransmitter in the intestine. *Acta Physiol. Scand.*, **101**, 302–317.

YAU, W.M., BOWEN, D.J. & YOUTHER, M.L. (1991). Evidence for an involvement of eicosanoids in neurokinin$_3$-receptor mediated acetylcholine release from myenteric neurons. *Neurosci. Lett.*, **129**, 259–261.

YAU, W.M., MANDEL, K.G., DORSETT, J.A. & YOUTHER, M.L. (1992). Neurokinin$_3$ receptor regulation of acetylcholine release from myenteric plexus. *Am. J. Physiol.*, **263**, G659–G664.

YAU, W.M. & YOUTHER, M.L. (1982). Direct evidence for a release of acetylcholine from the myenteric plexus of guinea-pig small intestine by substance P. *Eur. J. Pharmacol.*, **81**, 665–668.

(Received March 16, 1994
Revised May 4, 1994
Accepted May 16, 1994)

Br. J. Pharmacol. (1994), **113**, 81–86

Pharmacological characterization of rabbit corpus cavernosum relaxation mediated by the tissue kallikrein-kinin system

Rodrigo A.B. Lopes-Martins, [1]Edson Antunes, *Maria Luiza V. Oliva, *Cláudio A.M. Sampaio, **James Burton & Gilberto de Nucci

Department of Pharmacology, Faculty of Medical Sciences, UNICAMP, PO Box 6111, 13081-970 Campinas (SP), Brazil; *Department of Biochemistry, Escola Paulista de Medicina, São Paulo (SP), Brazil and **Boston University Hospital, Boston (MA), U.S.A.

1 The roles of the tissue kallikrein-kinin system and nitric oxide (NO) release in *Phoneutria nigriventer* venom-induced relaxations of rabbit corpus cavernosum (RbCC) smooth muscle have been investigated by use of a bioassay cascade.

2 *Phoneutria nigriventer* venom (10–30 μg), porcine pancreatic kallikrein (100 mu), rabbit urinary kallikrein (10 mu), bradykinin (BK, 0.3–3 nmol), acetylcholine (ACh, 0.3–30 nmol) and glyceryl trinitrate (GTN, 0.5–10 nmol) caused relaxations of the RbCC strips. Captopril (1 μM) substantially potentiated *Phoneutria nigriventer* venom- and BK-induced RbCC relaxations without affecting those elicited by GTN.

3 The bradykinin B_2 receptor antagonist, Hoe 140 (D-Arg-[Hyp^3,Thi^5,D-Tic^7,Oic^8]-BK, 50 nM), aprotinin (10 μg ml^{-1}) and the tissue kallikrein inhibitor, Pro-Phe-Aph-Ser-Val-Gln-NH_2 (KIZD-06, 1.3 μM) significantly inhibited *Phoneutria nigriventer* venom-induced RbCC relaxations, without affecting those provoked by GTN and ACh. The B_1 receptor antagonist, [Leu^9]des Arg^{10}BK (0.5 μM) and soybean trypsin inhibitor (SBTI, 10 μg ml^{-1}) had no effect on *Phoneutria nigriventer* venom-induced RbCC relaxations.

4 The relaxations induced by *Phoneutria nigriventer* venom, porcine pancreas kallikrein, BK and ACh were significantly inhibited by N$^{\omega}$-nitro-L-arginine methyl ester (L-NAME, 10 μM) but not by D-NAME (10 μM). L-NAME did not affect GTN-induced relaxations. L-Arginine (300 μM), but not D-arginine (300 μM), significantly reversed the inhibitory effect of L-NAME.

5 Our results indicate that *Phoneutria nigriventer* venom activates the tissue kallikrein-kininogen-kinin system in RbCC strips leading to NO release and suggest a functional role for this system in penile erection.

Keywords: Kinin receptors; penile erection; priapism; Hoe 140; aprotinin; prokallikreins; KIZD-06; *Phoneutria nigriventer* venom

Introduction

Tissue kallikreins are a subgroup of serine protease glycoproteins (mol. wt. 24–45 kD) encoded by a multigene family and are found in a wide variety of tissues (for reviews see Margolius, 1989; and Bhoola *et al.*, 1992) including the pancreas, salivary glands (Proud *et al.*, 1977), kidneys (Proud & Kaplan, 1988), gut (Schachter *et al.*, 1983), prostate (Lazure *et al.*, 1984) and pituitary gland (Powers & Nasjletti, 1982; 1983; Fuller *et al.*, 1985). In all tissues examined to date, these kallikreins are synthesized in the form of a preproenzyme, termed prokallikrein. Tissue prokallikreins have been characterized from both human (Corthon *et al.*, 1979; Spragg, 1983; Takada *et al.*, 1985) and rat (Takaoka *et al.*, 1984) urine. Although trypsin, thermolysin (Takada *et al.*, 1985), rat submandibular gland arginine esterase (Kamada *et al.*, 1990), plasmin and plasma kallikrein can activate prokallikrein, the mechanism of endogenous tissue kallikrein activation is unknown.

The venom of the armed spider *Phoneutria nigriventer* causes local oedema formation in both rat and rabbit skin *in vivo* (Antunes *et al.*, 1992) by activation of the tissue kallikrein-kinin system leading subsequently to local kinin formation (Marangoni *et al.*, 1993). Severe *Phoneutria nigriventer* envenomation in man causes intense and radiating local pain, cardiac disturbances, and in children is often accompanied by priapism, a disorder characterized by a prolonged and painful penile erection. Subcutaneous injection of *Phoneutria nigriventer* venom in mice and dogs also causes intermittent and long-lasting priapism accompanied by local oedema formation in the distal portion of the penis (Schenberg & Pereira-Lima, 1978). Since relaxation of the corpus cavernosum plays an essential role in penile erection, we have investigated the involvement of the tissue kallikrein-kinin system in this response.

[1] Author for correspondence.

Methods

Rabbit corpus cavernosum (RbCC) preparation

Male New Zealand white rabbits (1.5–2.5 kg, provided by CEMIB-UNICAMP) were anaesthetized with sodium pentobarbitone (Sagatal, 30–40 mg kg^{-1}, i.v.) and exsanguinated via the carotid artery. Following penectomy, the rabbit corpus cavernosum (RbCC) was dissected in Krebs solution and cleared of the tunica albuginea and surrounding tissues. Strips of RbCC were superfused in a cascade system (Vane, 1964) with warmed (37°C) and oxygenated (95% O_2 + 5% CO_2) Krebs solution at a flow rate of 5 ml min^{-1}. The tissue responses (tension of 1.5 g) were detected with auxotonic levers attached to Harvard heart/smooth muscle transducers and displayed on a Watanabe multichannel pen recorder (model WTR 381). After a 60–90 min period of equilibration, RbCC strips were precontracted with noradrenaline (3 μM) in order to increase the basal tone. The agonists *Phoneutria nigriventer* venom, acetylcholine (ACh), bradykinin (BK), glyceryl trinitrate (GTN), porcine pancreas kallikrein and rabbit urinary kallikrein were administered as

single bolus injection (10–50 µl). N^{ω}-nitro-L-arginine methyl ester (L-NAME), D-NAME, L-arginine, D-arginine, aprotinin (Trasylol), soybean trypsin inhibitor (SBTI), captopril, Hoe 140 (D-Arg-[Hyp^3,Thi^5,D-Tic^7,Oic^8]-BK), the bradykinin B_1 receptor antagonist [Leu^9]des Arg^{10} BK and the tissue kallikrein inhibitor KIZD-06 (Pro-Phe-Aph-Ser-Val-Gln-NH_2) were infused (0.1 ml min^{-1}) over the tissues 15 min before and during bolus injection of the appropriate agonists.

Purification of rabbit urinary kallikrein

Rabbit urinary kallikrein was partially purified by a modified procedure (Stella *et al.*, 1989) from 650 ml of rabbit urine. The urine was dialysed against distilled water, lyophilized and the crude powder suspended in 100 ml of sodium phosphate buffer (0.05 M, pH 7.0). This material was applied to a DEAE-Sephadex A-50 resin column (100 ml) previously equilibrated with 0.05 M sodium phosphate buffer. The resin was extensively washed with the equilibration buffer and with 300 ml of this same buffer containing 0.05 M NaCl. The active material (see below) was eluted by washing the column with 100 ml of phosphate buffer containing 0.3 M NaCl. This active pool was dialysed and lyophilized. Urinary kallikrein was then submitted to gel filtration on a Superose 12 column equilibrated with 0.05 M phosphate buffer. This procedure was repeated several times. The final preparation was purified 23 fold with a 12% yield and contained 80% of the active enzyme, as determined by titration against a previously titrated aprotinin solution. Rabbit urinary kallikrein activity was followed by the hydrolysis of 0.86 mM S-2266 in 0.05 M Tris-HCl, pH 8.0 at 37°C, in a final volume of 0.5 ml. The reaction was stopped by adding 0.5 ml of 15% acetic acid and the amount of product formed was determined by measuring the absorbance at 405 nm (Oliva *et al.*, 1988).

Dialysis of Phoneutria nigriventer *venom*

Since *Phoneutria nigriventer* venom contains small amounts of histamine (0.06–1.0%) and 5-hydroxytryptamine (5-HT, 0.03–0.25%; Schenberg & Pereira-Lima, 1978), we have routinely used dialysed *Phoneutria nigriventer* venom throughout this study in order to avoid the interference of these substances in the bioassay. *Phoneutria nigriventer* venom [5 ml of a 2 mg ml^{-1} 0.9% (w/v) saline solution] was dialysed for up to 48 h at 4–6°C against 2 l of 0.9% saline. The dialysing solution was changed four times during this period (Antunes *et al.*, 1992).

Venom and reagents

Phoneutria nigriventer venom was obtained by electrical stimulation of spiders maintained by the Arthropods Section, Instituto Butantan, São Paulo (Brazil) and desiccated in a vacuum desiccator containing sodium hydroxide pellets at room temperature.

Bradykinin (BK), [Leu^9]desArg^{10}-BK, acetylcholine (ACh), noradrenaline, porcine pancreas kallikrein, aprotinin, soybean trypsin inhibitor (SBTI), N^{ω}-nitro-L-arginine methyl ester (L-NAME), L-arginine and D-arginine were purchased from Sigma Co (St. Louis, U.S.A.). Glyceryl trinitrate (GTN, ampoules containing 1 mg ml^{-1} in isotonic saline), captopril and D-NAME were obtained from Lipha Pharmaceuticals (London, U.K.), Squibb Inc. (U.S.A.) and Bachem (London, U.K.), respectively. Pentobarbitone sodium (Sagatal) was purchased from May & Baker (Dagenham, Essex, U.K.). Hoe 140 (D-Arg-[Hyp^3,Thi^5,D-Tic^7,Oic^8]-BK) was obtained from Hoechst AG (Frankfurt, Germany). KIZD-06 (Pro-Phe-Aph-Ser-Val-Gln-NH_2) was synthesized by Dr J. Burton (Boston University, U.S.A.). Dialysis tubing (mol. wt. cutoff 12,000–14,000) was bought from Sigma Chem. Co., Inc. (St Louis, MO, U.S.A.).

The composition of the Krebs solution was (mM): NaCl 118, $NaHCO_3$ 25, glucose 5.6, KCl 4.7, KH_2PO_4 1.2, $MgSO_4 7H_2O$ 1.17 and $CaCl_2 6H_2O$ 2.5.

Statistical analysis

The relaxations induced by *Phoneutria nigriventer* venom, ACh, BK, porcine pancreas kallikrein and rabbit urinary kallikrein were expressed relative to the sub-maximal relaxation induced by GTN which was taken to be 100%. The results are shown as the mean ± s.e.mean of n experiments. Analysis of variance and Student's unpaired t test were employed to evaluate the data. A P value <0.05 was considered to be significant.

Results

Involvement of the tissue kallikrein-kinin system in Phoneutria nigriventer *venom-induced RbCC relaxations*

Single bolus injections of *Phoneutria nigriventer* venom (1–30 µg) caused dose-dependent relaxations of the RbCC strips (not shown). An infusion of captopril (1 µM) significantly ($P<0.01$) potentiated the relaxations induced by both BK (42 ± 8% relaxation before vs. 66 ± 9% relaxation during infusion of captopril, $n=8$) and *Phoneutria nigriventer* venom (40 ± 4% relaxation before vs. 62 ± 7% relaxation during infusion of captopril, $n=9$) but had no effect on those elicited by GTN (Figure 1, $n=7$).

The stable bradykinin B_2 receptor antagonist, Hoe-140 (50 nM), abolished the relaxations induced by BK and *Phoneutria nigriventer* venom without affecting those caused by ACh (76 ± 6% relaxation before vs. 74 ± 6% relaxation during infusion of Hoe-140, $n=6$) and GTN (Figure 2, $n=6$). In contrast, the bradykinin B_1 receptor antagonist, [Leu^9]des Arg^{10} BK (0.5 µM), did not affect either BK- or *Phoneutria nigriventer* venom-induced relaxations (45 ± 12% and 55 ± 16% relaxation before vs. 49 ± 9% and 59 ± 20% relaxation during infusion of this antagonist in the presence of BK and *Phoneutria nigriventer* venom, respectively, $n=6$).

The infusion of the protease inhibitor, aprotinin

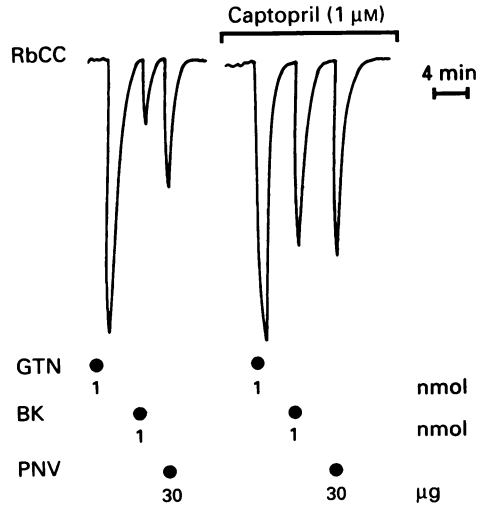

Figure 1 Captopril (1 µM) significantly potentiates the rabbit corpus cavernosum (RbCC) relaxation induced by bradykinin (BK, 1 nmol) and *Phoneutria nigriventer* venom (PNV, 30 µg) without affecting that induced by glyceryl trinitrate (GTN, 1 nmol). RbCC strips were superfused in cascade and previously contracted with noradrenaline as described in the Methods. This is a representative tracing of seven experiments (auxotonic lever).

(10 μg ml^{-1}) virtually abolished the RbCC relaxations induced by both porcine pancreas kallikrein (100 mu, $n = 4$) and *Phoneutria nigriventer* venom (3 μg, $n = 6$; Figure 3). At this concentration, aprotinin did not affect relaxations induced by BK (47 ± 7% relaxation before vs. 49 ± 9% relaxation during infusion of aprotinin, $n = 5$) and GTN (Figure 3). Infusion of the tissue kallikrein inhibitor KIZD-06 (1.3 μM) abolished the relaxations induced by rabbit urinary kallikrein and *Phoneutria nigriventer* venom (Figure 4) without affecting those induced by ACh (90 ± 9% relaxation before vs. 86% ± 2% relaxation during KIZD-06 infusion, $n = 3$) and GTN (Figure 4, $n = 3$). The plasma kallikrein inhibitor SBTI (10 μg ml^{-1}) failed to affect significantly *Phoneutria nigriventer* venom-, BK-, ACh- and porcine pancreas kallikrein-induced relaxations (55 ± 12, 54 ± 17, 85 ± 26 and 35 ± 6% relaxation before vs. 67 ± 20, 54 ± 8, 98 ± 8 and 33 ± 8% relaxation during SBTI infusion, respectively, $n = 4$).

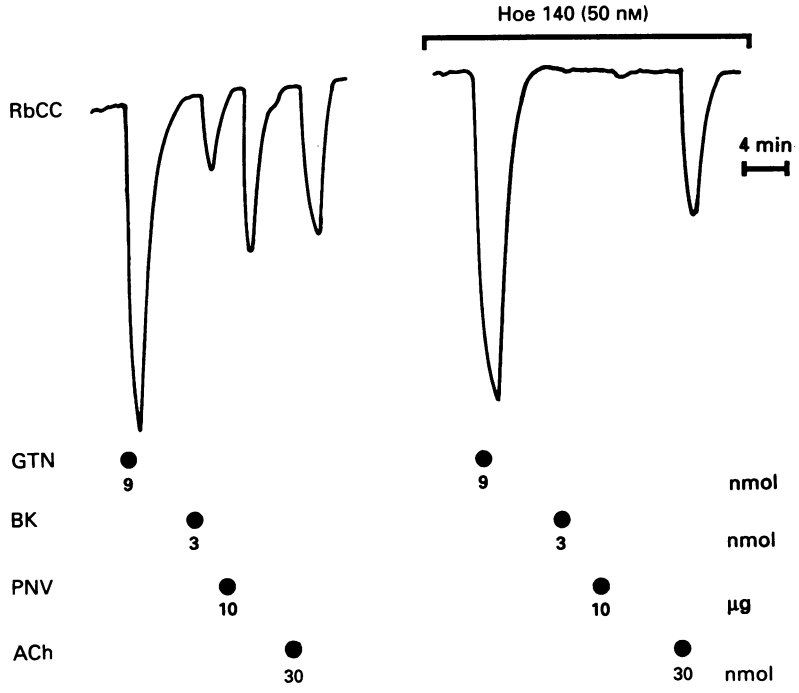

Figure 2 The bradykinin (BK) B_2 antagonist Hoe-140 (50 nM) abolished the rabbit corpus cavernosum (RbCC) relaxation induced by BK (3 nmol) and *Phoneutria nigriventer* venom (PNV, 10 μg). The relaxations induced by both glyceryl trinitrate (GTN, 9 nmol) and acetylcholine (ACh, 30 nmol) were not significantly affected by the infusion of Hoe-140. This is a representative tracing of six experiments (auxotonic lever).

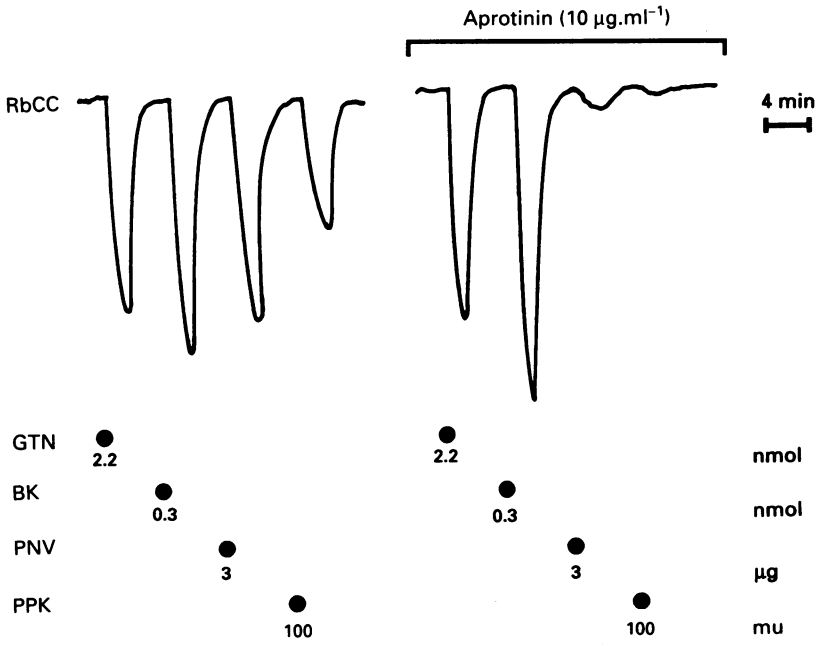

Figure 3 Infusion of aprotinin (10 μg ml^{-1}) abolished the rabbit corpus cavernosum (RbCC) relaxations induced by *Phoneutria nigriventer* venom (PNV, 3 μg) and by porcine pancreas kallikrein (PPK, 100 mu). The relaxations induced by glyceryl trinitrate (GTN, 2.2 nmol) and bradykinin (BK, 0.3 nmol) were not significantly affected by the infusion of aprotinin. This is a representative tracing of four experiments (auxotonic lever).

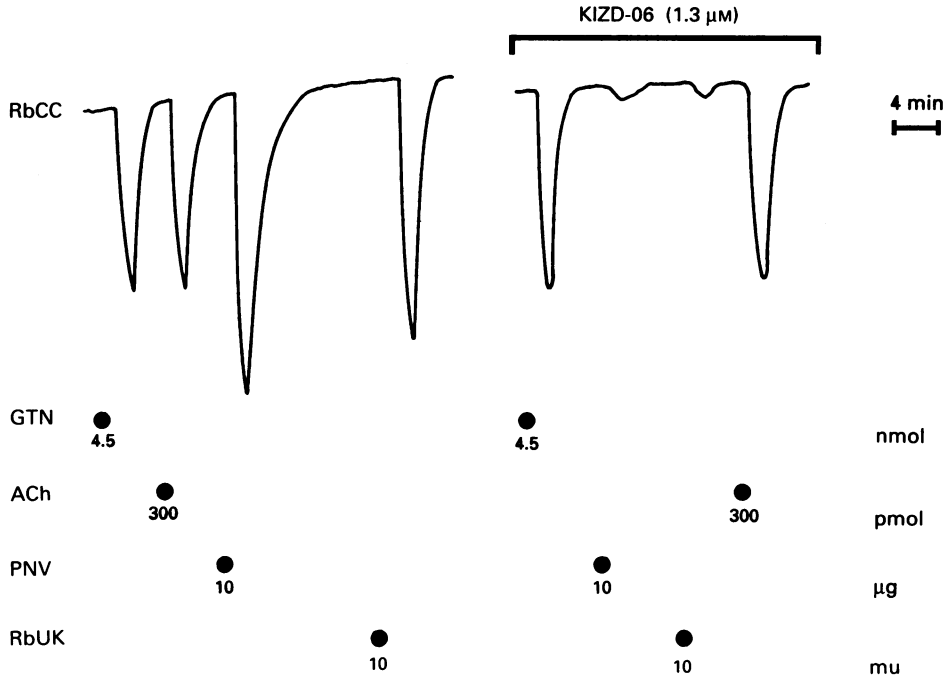

Figure 4 The specific tissue kallikrein inhibitor Pro-Phe-Aph-Ser-Val-Gln-NH_2 (KIZD-06, 1.3 μM) abolished the rabbit corpus cavernosum (RbCC) relaxations induced by both *Phoneutria nigriventer* venom (PNV, 10 μg) and rabbit urinary kallikrein (RbUK, 10 mu) without significantly affecting those evoked by glyceryl trinitrate (GTN, 4.5 nmol) and acetylcholine (ACh, 300 pmol). This is a representative tracing of three experiments (auxotonic lever).

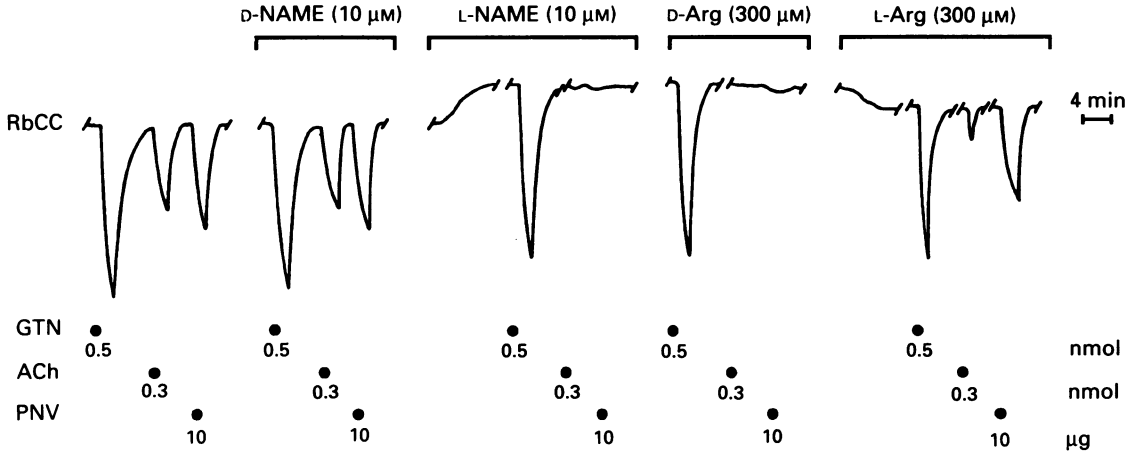

Figure 5 Effects of N^{ω}-nitro-L-arginine methyl ester (L-NAME, 10 μM), D-NAME (10 μM), L-arginine (L-Arg, 300 μM) and D-Arg (300 μM) on rabbit corpus cavernosum (RbCC) strips. The infusion of L-NAME (but not D-NAME) further increased the RbCC tone and abolished the relaxation induced by both acetylcholine (ACh, 0.3 nmol) and *Phoneutria nigriventer* venom (PNV, 10 μg). The relaxations induced by glyceryl trinitrate (GTN, 0.5 nmol) were not significantly affected by L-NAME infusion. Subsequent infusion of L-Arg (but not D-Arg) partially reversed the increased RbCC tone and also partially restored the relaxations induced by ACh and PNV. This is a representative tracing of six experiments (auxotonic lever).

Involvement of NO in the RbCC relaxations induced by Phoneutria nigriventer *venom*

Figure 5 shows that GTN (0.5 nmol), ACh (0.3 nmol) and *Phoneutria nigriventer* venom (10 μg) relaxed RbCC strips ($n = 6$). The infusion of nitro-D-arginine methyl ester (D-NAME, 10 μM) did not significantly affect either the basal tone of the RbCC strips or the relaxations induced by the above substances. In contrast, an infusion of L-NAME (10 μM) increased the tone of the tissues by 59 ± 9% ($P < 0.05$) and abolished the *Phoneutria nigriventer* venom- and ACh-induced relaxations without affecting those evoked by GTN. An infusion of L-arginine (300 μM), but not of D-arginine (300 μM), significantly reversed the increased tone and restored the relaxations induced by *Phoneutria nigriventer* venom and ACh (Figure 5).

Discussion

Our results show that tissue kallikrein causes RbCC relaxation by a mechanism dependent on the release of NO since the relaxations were significantly inhibited by the NO synthase inhibitor L-NAME (Moore *et al.*, 1989) but not by its inactive enantiomer D-NAME. The reversal of the inhibitory effect of L-NAME by L-arginine (but not by D-arginine) further confirms the involvement of NO in this response. In erectile tissues, NO has been implicated recently as an essen-

tial mediator involved in the nonadrenergic, noncholinergic neurotransmission that induces the relaxation of the corpus cavernosum and triggers penile erection (Ignarro *et al.*, 1990; Burnett *et al.*, 1992; Anderson, 1993).

Activation of the tissue kallikrein-kinin system leads to kallidin release (for review see Bhoola *et al.*, 1992) which can in turn act on bradykinin B_2 receptors (Regoli & Barabé, 1980) to release NO from endothelial cells (De Nucci *et al.*, 1988; D'Orleans-Juste *et al.*, 1989). Since corpus cavernosum tissues are characterized by a rich network of sinusoidal capillaries containing endothelial cells (De Groot & Steers, 1988), it is possible that a similar mechanism for NO release may be also operative in this tissue.

The involvement of the tissue kallikrein-kinin system in the RbCC relaxations induced by *Phoneutria nigriventer* venom is supported by several observations. First, the protease inhibitor aprotinin (Vogel & Werle, 1970) and the tissue kallikrein inhibitor KIZD-06, selectively inhibited both the tissue kallikrein- and *Phoneutria nigriventer* venom-indued RbCC relaxations. As expected, the plasma kallikrein inhibitor SBTI (Vogel & Werle, 1970) had no effect on either the porcine pancreas kallikrein- or the *Phoneutria nigriventer* venom-induced relaxations indicating that plasma kallikrein activation is not involved. Second, the kinase II inhibitor, captopril, significantly potentiated the RbCC relaxations induced by BK and *Phoneutria nigriventer* venom. Third, a specific bradykinin B_2 receptor antagonist (Hoe-140; Wirth *et al.*, 1991) selectively abolished the relaxing effects of BK and *Phoneutria nigriventer* venom. The failure of the bradykinin B_1 receptor antagonist, [Leu^9]des Arg^{10} BK, to block these relaxations eliminated the involvement of B_1 receptors.

The observation that porcine pancreas kallikrein and rabbit urinary kallikrein relaxed the RbCC strips by a kinin-dependent mechanism as discussed above indicates that RbCC contains low molecular weight kininogen which is the substrate for tissue kallikreins. Although high molecular weight kininogen is restricted to plasma, kininogens have also been detected in some organs such as brain (Shikimi *et al.*, 1973), kidney (Figueroa *et al.*, 1988), uterus (Figueiredo *et al.*, 1990), sweat and sexual glands and psoriatic skin (Poblete *et al.*, 1991).

While there are no reports on the existence of tissue kallikrein in corpus cavernosum smooth muscle, these enzymes have been detected in vascular smooth muscle tissues including rat aorta (Oza *et al.*, 1990), rat mesenteric artery (Nolly & Lama, 1982) and rat tail vein and artery (Nolly *et al.*, 1985). It seems plausible to suggest, therefore, that *Phoneutria nigriventer* venom causes RbCC relaxation by activating and/or stimulating the secretion of tissue kallikrein localized in the RbCC thereby resulting in the release of kallidin. Alternatively, *Phoneutria nigriventer* venom could function as an activator of tissue prokallikreins. An additional possibility is that *Phoneutria nigriventer* venom may itself contain tissue kallikrein. Although *Phoneutria nigriventer* venom contains histamine, 5-HT and some enzymes (Schenberg & Pereira-Lima, 1978), there are no reports on the existence of kallikreins in spider venoms. The active fraction of *Phoneutria nigriventer* venom responsible for activation of the tissue kallikrein-kinin system in rabbit skin has been partially purified (Antunes *et al.*, 1993) but further biochemical studies are necessary to elucidate the mechanisms involved.

It is interesting to note that tissue kallikreins are believed to play a functional role in spermatogenesis since they are reported to increase sperm motility, to cause sperm maturation and to increase blood flow in the testis (Saitoh & Kumamoto, 1988; Clements *et al.*, 1988). In addition, testosterone enhances tissue kallikrein gene expression in sex glands (Clements *et al.*, 1988). While our results have indicated that tissue kallikrein activation may be important in penile erection, the precise role of the tissue kallikrein-kinin system in this phenomenon remains to be established.

R.A.B.L.M. is supported by Fundação de Amparo à Pesquisa do Estado de São Paulo (FAPESP).

References

ANDERSON, K.-E. (1993). Pharmacology of lower urinary tract smooth muscles and penile erectile tissues. *Pharmacol. Rev.*, **45**, 253–308.

ANTUNES, E., MARANGONI, R.A., BRAIN, S.D. & DE NUCCI, G. (1992). *Phoneutria nigriventer* (armed spider) venom induces increased vascular permeability in rat and rabbit skin *in vivo*. *Toxicon*, **30**, 1011–1016.

ANTUNES, E., MARANGONI, R.A., BRAIN, S.D. & DE NUCCI, G. (1993). Activation of tissue kallikrein-kininogen-kinin system by a component present in the *Phoneutria nigriventer* venom. *Toxicon*, **31**, 1385–1391.

BHOOLA, K.D., FIGUEROA, C.D. & WORTHY, K. (1992). Bioregulation of kinins: kallikreins, kininogens and kininases. *Pharmacol. Rev.*, **44**, 4–80.

BURNETT, A.L., LOWENSTEIN, C.J., BREDT, D.S., CHANG, T.S.K. & SNYDER, S.H. (1992). Nitric oxide: a physiologic mediator of penile erection. *Science*, **257**, 401–403.

CLEMENTS, J.A., MATHESON, B.A., WINES, D.R., BRADY, J.M., MACDONALD, R.J. & FUNDER, J.W. (1988). Androgen dependence of specific kallikrein gene family members expressed in rat prostate. *J. Biol. Chem.*, **31**, 16132–16137.

CORTHON, J., IMANARI, T., YOSHIDA, H., KAIZU, T., PIERCE, J.V. & PISANO, J.J. (1979). Isolation of prokallikrein from human urine. *Adv. Exp. Med. Biol.*, **120B**, 575–579.

DE GROOT, W.C. & STEERS, W.D. (1988). Neuroanatomy and neurophysiology of penile erection. In *Contemporary Management of Impotence and Infertility*. ed. Tanagho, E.A., Lue, T.F. & McClure, R.D. pp. 39–50. Baltimore: Williams & Wilkins.

DE NUCCI, G., GRYGLEWSKI, R.J., WARNER, T.D. & VANE, J.R. (1988). Receptor-mediated release of endothelium derived relaxing factor and prostacyclin from bovine aortic endothelial cells is coupled. *Proc. Natl. Acad. Sci. U.S.A.*, **85**, 2334–2338.

D'ORLEANS-JUSTE, P., DE NUCCI, G. & VANE, J.R. (1989). Kinins act on B_1 or B_2 receptors to release conjointly endothelium derived relaxing factor and prostacyclin from bovine aortic endothelial cells. *Br. J. Pharmacol.*, **96**, 920–926.

FIGUEIREDO, A.F.S., SALGADO, A.H.I., SIQUEIRA, G.R.T., VELLOSO, C.R. & BERALDO, W.T. (1990). Rat uterine contraction by kallikrein and its dependence on uterine kininogen. *Biochem. Pharmacol.*, **39**, 763–767.

FIGUEROA, C.D., MACIVER, A.G., MACKENZIE, J.C. & BHOOLA, K.D. (1988). Localisation of immunoreactive kininogen and tissue kallikrein in the human nephron. *Histochemistry*, **89**, 437–442.

FULLER, P.F., CLEMENTS, J.A., WHITFIELD, P.L. & FUNDER, J.W. (1985). Kallikrein gene expression in the rat anterior pituitary. *Mol. Cell. Endocrinol.*, **39**, 99–105.

IGNARRO, L.J., BUSH, P.A., BUGA, G.M., WOOD, K.S., FUKUTO, J.M. & RAJFER, J. (1990). Nitric oxide and cyclic GMP formation upon electrical field stimulation cause relaxation of corpus cavernosum smooth muscle. *Biochem. Biophys. Res. Commun.*, **170**, 843–850.

KAMADA, M., FURUHATA, N., YAMAGUSHI, T., IKAKITA, M., KIZUKI, K. & MORIYA, H. (1990). Observation of tissue prokallikrein activation by some serine proteases, arginine esterases in rat submandilar gland. *Biochem. Biophys. Res. Commun.*, **166**, 231–237.

LAZURE, C., LEDUC, R., SEIDAH, N.G., CHRETIEN, M., DUBE, J.Y., CHAPDELAINE, P., FRENETTE, G., PAQUIN, R. & TREMBLAY, R.R. (1984). The major androgen-dependent protease in dog prostate belongs to the kallikrein family: confirmation by partial amino acid sequencing. *FEBS Lett.*, **175**, 1–7.

MARANGONI, R.A., ANTUNES, E., BRAIN, S.D. & DE NUCCI, G. (1993). Activation by *Phoneutria nigriventer* (armed spider) venom of tissue-kallikrein-kinin system in rabbit skin *in vivo*. *Br. J. Pharmacol.*, **109**, 539–543.

MARGOLIUS, H.S. (1989). Tissue kallikrein and kinins: regulation and roles in hypotensive and diabetic diseases. *Annu. Rev. Pharmacol. Toxicol.*, **29**, 343–364.

MOORE, P.K., AL-SWAYEH, O.A., CHONG, N.W.S., EVANS, R.A. & GIBSON, A. (1989). L-N^G-nitro arginine (L-NOARG) a novel, L-arginine-reversible inhibitor of endothelium-dependent vasodilatation *in vitro*. *Br. J. Pharmacol.*, **99**, 408–412.

NOLLY, H. & LAMA, M.C. (1982). 'Vascular kallikrein': a kallikrein-like enzyme present in vascular tissue of rat. *Clin. Sci.*, **63**, 249–251.

NOLLY, H., SCICLI, A.G., SCICLI, G. & CARRETERO, O. (1985). Characterization of a kininogenase from rat vascular tissue resembling tissue kallikrein. *Circ. Res.*, **56**, 816–821.

OLIVA, M.L.V., SAMPAIO, M.U. & SAMPAIO, C.A.M. (1988). Purification and partial characterization of a thiol proteinase inhibitor from *Enterolobium contortisiliquum* beans. *Biol. Chem. Hoppe-Seyler*, **369**, 229–232.

OZA, N.B., SCHWARTZ, J.H., GOUD, M.D. & LEVINSKY, N.G. (1990). Rat aortic smooth muscle cells in culture express kallikrein, kininogen and bradykinase activity. *J. Clin. Invest.*, **85**, 597–600.

POBLETE, M.T., REYNOLDS, N.J., FIGUEROA, C.D., BURTON, J.L., MULLER-ESTERL, W. & BHOOLA, K.D. (1991). Tissue kallikrein and kininogen in human sweat glands and psoriatic skin. *Br. J. Dermatol.*, **124**, 236–241.

POWERS, C.A. & NASJLETTI, A. (1982). A novel kinin-generating protease (kininogenase) in the porcine anterior pituitary. *J. Biol. Chem.*, **257**, 5594–5600.

POWERS, C.A. & NASJLETTI, A. (1983). A kininogenase resembling glandular kallikrein in the rat pituitary pars intermedia. *Endocrinology*, **112**, 1194–1200.

PROUD, D., BAILEY, G.S., NUSTAD, K. & GAUTVIK, K.M. (1977). The immunological similarity of rat glandular kallikreins. *Biochem. J.*, **167**, 835–838.

PROUD, D. & KAPLAN, A.P. (1988). Kinin formation: mechanisms and role in inflammatory disorders. *Annu. Rev. Immunol.*, **6**, 49–83.

REGOLI, D. & BARABÉ, J. (1980). Pharmacology of bradykinin and related kinins. *Pharmacol. Rev.*, **32**, 1–46.

SAITOH, S. & KUMAMOTO, Y. (1988). Effect of a kallikrein on testicular blood circulation. *Arch. Androl.*, **20**, 51–65.

SCHACHTER, M., PERET, M.W., BILLING, A.G., WHEELER, G.D. & LONGRIDGE, D.J. (1983). Immunolocalization of the protease kallikrein in the colon. *J. Histochem. Cytochem.*, **31**, 1255–1260.

SCHENBERG, S. & PEREIRA-LIMA, F.A. (1978). Arthropod venoms: venoms of Ctenidae In *Handbook of Experimental Pharmacology*. ed. Bettini, S., Vol. 48. pp. 217–245. Berling: Springer-Verlag.

SHIKIMI, T., KEMA, R., MATSUMOTO, M., YAMAHATA, Y. & MIYATA, S. (1973). Studies on kinin-like substances in brain. *Biochem. Pharmacol.*, **22**, 567–573.

SPRAGG, J. (1983). Characterization of purified human latent kallikrein. *Adv. Exp. Med. Biol.*, **156A**, 393–398.

STELLA, R.C.R., DUARTE, P.C., ARAUJO-VIEL, M.S., SAMPAIO, M.U. & SAMPAIO, C.A.M. (1989). Isolation and partial characterization of rabbit urinary kallikrein. *Adv. Med. Exp. Biol.*, **247B**, 195–200.

TAKADA, Y., SKIDGEL, R.A. & ERDOS, E.G. (1985). Purification of human urinary prokallikrein. Identification of the site of activation by the metalloproteinase thermolysin. *Biochem. J.*, **232**, 851–858.

TAKAOKA, M., OKAMURA, H., IWAMOTO, T., IKAMOTO, C., MIURA, C. & MORIMOTO, S. (1984). Purification to apparent homogeneity of inactive kallikrein from rat urine. *Biochem. Biophys. Res. Commun.*, **122**, 1282–1288.

VANE, J.R. (1964). The use of isolated organs for detecting active substances in the circulating blood. *Br. J. Pharmacol. Chemother.*, **23**, 360–373.

VOGEL, R. & WERLE, E. (1970). Kallikrein inhibitors. In *Handbook of Experimental Pharmacology*. Vol. 25. ed. Erdos, E.G. pp. 213–249. New York: Springer Verlag.

WIRTH, K., HOCK, F.J, ALBUS, U., LINZ, W., ALPERMANN H.G., ANAGNOSTOPOULOS, H., HENKE, ST., BREIPOHL, G., KONIG, W., KNOLLE, J. & SCHOLKENS, B.A. (1991). Hoe 140, a new potent and long-acting bradykinin antagonist: *in vivo* studies. *Br. J. Pharmacol.*, **102**, 774–777.

(Received March 4, 1994
Revised May 9, 1994
Accepted May 17, 1994)

Br. J. Pharmacol. (1994), **113**, 87–94

Photon pharmacology of an iron-sulphur cluster nitrosyl compound acting on smooth muscle

[1]E.K. Matthews, E.D. Seaton, M.J. Forsyth & *P.P.A. Humphrey

Department of Pharmacology and *Glaxo Institute of Applied Pharmacology, University of Cambridge, Tennis Court Road, Cambridge CB2 1QJ

1 The mechanisms of action on smooth muscle of the iron-sulphur cluster nitrosyl compound, heptanitrosyl-tri-μ3-thioxotetraferrate (1-), (RBS), a photosensitive nitric oxide donor, have been investigated in the guinea-pig taenia caeci (coli) *in vitro*.

2 After exposure to RBS (50 μM) for 30 min, and subsequent washout, a sustained contraction was recorded in the absence of light to either the agonist carbachol (50 μM) or a depolarizing concentration of KCl (23.5 mM). Photon irradiation (>400 nm) caused a prompt relaxation of precontracted RBS-treated muscle, the magnitude of which depended upon the intensity (1.1×10^3 to 1.1×10^5 lux), duration (30 s to 20 min) and wavelength (400 to 800 nm), of the incident illumination.

3 Repeated periods of illumination at 1.1×10^4 lux produced a reversible relaxation of both carbachol and KCl-evoked tone in muscle pretreated with RBS (50 μM). These photorelaxations were reproducible at 10 min intervals for several hours with a maximal relaxation amounting to 80 to 90% that of the tone produced by carbachol (50 μM).

4 The nitric oxide synthase inhibitor, N^G-nitro-L-arginine (60 μM), caused no inhibition of the photon-induced relaxation of RBS-treated muscle. In contrast, N-methylhydroxylamine (2 mM), L-cysteine (10 mM), DL-dithiothreitol (2 mM), methylene blue (30 μM), and haemoglobin (20 μM), all reversibly but significantly inhibited ($P<0.001$) the photorelaxation response. However, neither the aminothiol *N*-acetyl-L-cysteine (10 mM) nor the tripeptide glutathione (10 mM) blocked the RBS-induced photorelaxation.

5 The photolytic cleavage of RBS depended on the intensity and duration of illumination; it was accompanied by a corresponding decrease in absorbance and by the liberation of NO as measured by the Griess diazo reaction with sulphanilic acid. L-Cysteine (10 mM) prevented the decrease in absorbance and the photolytic liberation of NO.

6 It is concluded that (i) sequestered or bound RBS, when photon-activated, liberates NO by a process which can be controlled by the wavelength, intensity and duration of the incident light, (ii) the photon-released NO rapidly relaxes the smooth muscle cells of the taenia coli primarily via cyclic GMP-dependent pathways which can be blocked by use of appropriate inhibitors, and (iii) the RBS-induced photorelaxation effect does not involve the activation of NO synthase. RBS is therefore a valuable photosensitive NO donor for establishing the functional and pharmacological significance of NO.

Keywords: Photosensitive nitric oxide donor; nitric oxide measurement; smooth muscle; guinea-pig taenia caeci (coli); NO synthase; thiol inhibitors; heptanitrosyl-tri-μ3-thioxotetraferrate (1-); Roussin's Black Salt

Introduction

Iron-sulphur cluster compounds are common in nature and form an integral part of many enzymes (Prince & Grossman, 1993). They also present an important molecular framework for the synthesis of caged nitric oxide derivatives (Butler *et al.*, 1988; 1990). Such cluster nitrosyl compounds have been shown to accumulate in endothelial cells and to produce a vasodilator action (Flitney *et al.*, 1992). More importantly, it is now evident that these compounds can be photon-activated (Matthews *et al.*, 1994) and in response to light are capable of liberating large amounts of NO very rapidly, but little work has been done to assess either the molecular mechanisms involved or the pharmacological consequences of such photon-induced effects.

In the present study the iron-sulphur cluster nitrosyl compound, heptanitrosyl-tri-μ3-thioxotetraferrate (1-), has been investigated as a potential photosensitive nitric oxide donor. This compound, also known as Roussin's Black Salt (RBS), contains seven NO groups; it is one of several closely related cluster nitrosyls but differs from them in possessing an unusually high aqueous solubility (Flitney *et al.*, 1992). We have previously employed the guinea-pig taenia coli (caeci) as a model system for analysing the mechanisms of photodynamic drug action since it is composed of a relatively transparent syncytium of smooth muscle cells which produce a well-defined calcium-dependent contraction, free from the complicating presence of endothelial cells (Matthews *et al.*, 1993a,b). Furthermore, nitrovasodilator compounds, have been shown to activate guanylyl cyclase and to increase intracellular guanosine 3':5'-cyclic monophosphate (cyclic GMP) levels in the taenia causing its relaxation (Katsuki *et al.*, 1977). This preparation is therefore ideally suited for exploring the mechanism of action of RBS and for establishing the quantitative relationship between RBS photolysis, NO production, and smooth muscle relaxation. In addition, the use of inhibitors and measurement of photon-released NO has enabled further definition to be given to the photon pharmacology of RBS. The results of some of this work were communicated to the London meeting of the British Pharmacological Society in January, 1994 (Matthews *et al.*, 1994).

Methods

Superfusion of taenia coli

Male guinea-pigs (250–300 g) were killed by cervical dislocation and exsanguination. Strips of taenia muscle were dis-

[1] Author for correspondence.

sected from the caecum and superfused in a system similar to that described by Brading & Sneddon (1980). Matthews & Messler (1984) and Matthews *et al.* (1993a,b). Pieces of taenia 1 to 2 cm in length were secured by one end to the base of glass superfusion chambers (volume 1 ml) and by the other end to transducers (tension 1 g) located directly over the chambers, for the isotonic recording of contraction. The superfusate was pumped from glass reservoirs via polythene tubing (internal diameter 0.73 mm) placed in a water bath (Harvard) maintained at 32°C (to reduce spontaneous contractile activity) before entering the base of the glass chambers; the effluent superfusate was discarded. Flow rates were set at approximately 2 ml min^{-1} per channel, with four superfusion systems being run in parallel. Signal output from the four Harvard transducers was amplified and contractions recorded with Kipp & Zohnen BD40 chart recorders.

Solutions

In the majority of experiments, a modified Krebs-Henseleit solution was used of the following ionic composition (mM): NaCl 118, $CaCl_2$ 2.56, KCl 4.7, $MgCl_2$ 1.13, NaH_2PO_4 1.15, $NaHCO_3$ 25 supplemented with D-glucose 11.2. The solution was bubbled with 95% O_2 and 5% CO_2 to give a final pH of 7.4. When a five fold increase in potassium concentration was used to depolarize the tissue, the solution contained KCl 23.5 mM and the NaCl concentration was decreased to 99.12 mM to maintain isotonicity.

Light intensity

All experiments were performed in a light-sealed chamber. Controlled illumination of the tissue was provided by a Schott KL 150 quartz-halogen light source equipped with a heat filter (KG1), via two fibre-optic probes. The two probes provided a 60° illumination field of uniform intensity; each probe simultaneously illuminated two tissue preparations. Absolute light intensities were determined to a high accuracy (± 3%) using a Minolta Illuminance 1H meter. No heating of the superfusion baths by illumination was measurable.

For determination of the wavelength action spectrum, a series of sharp-cut filters of defined transmission characteristics were interposed between the optic probes and the muscle preparations. The wavelength range from 400 to 570 nm was scanned using the bandwidth limits set by five different filters, namely 400 nm sharp-cut (Schott glass filter GG-400), 457 nm sharp-cut (Schott glass filter GG-475), 515 nm sharp-cut (Schott glass filter 2A-15), 535 nm sharp-cut (Wratten glass filter type 16) and 570 nm sharp-cut (Schott glass filter OG-570). These filters permitted over 90% transmission and were each 2 mm thick. The absorption spectra of aqueous solutions of RBS (in 3 ml stoppered cuvettes), were determined with a Pye-Unicam SP8-200 UV/Vis spectrophotometer.

Experimental procedures

In the majority of experiments, preparations were first allowed to equilibrate for 30–40 min and the contractile response assessed by exposure to repeated doses of carbachol (50 μM) for 10 s at 10 or 15 min intervals. Reproducible responses to this dose could usually be obtained and provided a standard contraction against which drug action could be determined, but any preparation incapable of a consistent response was discarded.

Following equilibration, a standard experimental protocol was established as follows: incubation of the tissues with RBS (50 μM) for 30 min (during which time superfusion was suspended); wash out with superfused Krebs-Henseleit solution for 2 to 10 min; superfusion of carbachol (50 μM) for 30 to 40 min before commencing; 10 min cycles of illumination of the preparations at a controlled intensity, involving irradiation of 3 min duration at 7 min intervals. Superfusion with carbachol (50 μM) was maintained throughout these successive periods of illumination.

The effects of application of the redox agents L-cysteine, DL-dithiothreitol (DTT), reduced glutathione (GSH) and methylene blue were tested after at least three cycles of illumination. Superfusion with the agent under test was continued for a further six illumination cycles before replacement with a solution containing carbachol alone (50 μM).

Haemoglobin

Oxyhaemoglobin was freshly prepared by treatment of bovine haemoglobin with a ten fold excess of sodium dithionite followed by dialysis as described by Gibson *et al.* (1992) and Gao & Vanhoutte (1993).

Measurement of nitric oxide liberation

The amount of nitric oxide generated by the photolysis of RBS was determined by the Griess reaction for the detection of NO and NO_2^- in which sulphanilic acid is diazotized at acid pH by nitric oxide. The reaction product is subsequently coupled stoichiometrically with N-(1-naphthyl) ethylene-diamine to yield a coloured azo compound which is measured spectrophotometrically at a peak absorbance of 548 nm (Ignarro *et al.*, 1987).

Statistical analysis

Results are expressed as the mean ± s.e.mean. Statistical significance was determined by application of Student's *t* test.

Materials

All standard chemicals were of Analar or comparable purity. Other agents used were from Sigma, i.e. L-cysteine, haemoglobin (bovine), reduced glutathione (GSH), N^G-nitro-L-arginine, N-methylhydroxylamine *N*-acetyl-L-cysteine, or carbachol (Koch-Light Laboratories Ltd.) sodium nitroprusside (Fisons), S-nitroso-*N*-acetyl-DL-penicillamine (SNAP) (Cookson Chemicals, Southampton, UK), ruthenium (III) nitrosyl chloride ($Ru(NO)Cl_3$) (Johnson-Matthey, Royston, UK). Heptanitrosoyltri-μ3-thioxotetraferrate (RBS) was kindly provided by Dr A.R. Butler, Department of Chemistry, University of St Andrew's.

Results

Photorelaxation of RBS-treated smooth muscle contracted with carbachol or KCl

Photon irradiation (light intensity; 1.1×10^4 lux) of muscle precontracted with carbachol, (50 μM), or KCl (23.5 mM), invariably produced an immediate relaxation in muscle preparations pre-incubated with RBS, (50 μM) (Figure 1) but had no effect on tone in the preparations which had not been exposed to RBS (Figure 2). The relaxations were reversible, restoration of the carbachol-induced tone occurring within 10 to 20 s of the termination of illumination. In one series of experiments the relaxation response represented a 92 ± 2% ($n = 17$) inhibition of carbachol-induced tone at the first illumination period and the effect was remarkably reproducible since 120 min later a 3 min period of photo-illumination still produced an 87 ± 2% ($n = 20$) inhibition of carbachol-induced tone (e.g. Figure 1a). Short periods of light exposure, e.g., 15 to 30 s produced monophasic relaxations of smaller magnitude but with longer periods of light exposure a second, smaller, phase of relaxation often became evident 2 to 3 min after the start of illumination (see Figure 1b). The magnitude of this small but more sustained secondary relaxation amounted to 13 ± 2% ($n = 20$) that of the first relaxation phase. Photon-irradiation of tissue previously exposed to

RBS and precontracted with an increased potassium concentration of 23.5 mM also produced an inhibition of induced tone. The secondary phase of relaxation in response to RBS photon-activation was, however, more pronounced in the K^+-depolarized muscle, although the reason for this is not known.

Effect of light intensity on the photorelaxation of RBS-treated muscle

Sequential illumination of the RBS-treated taenia with light of different intensities allowed the relationship to be defined between light intensity and the magnitude of the first phase of the photo-relaxation response. The tissues were irradiated at a standard intensity of 1.1×10^4 lux for three timed periods before irradiation at any other test intensity. Some inhibition of carbachol-induced tone was evident in RBS-treated muscle even below 2×10^3 lux, i.e., at intensities approaching common ambient laboratory light levels (400–1000 lux) which emphasizes the need for adequate light shielding throughout an experiment. Photon-irradiation of RBS pretreated tissue at an intensity of 1.1×10^3 lux inhibited carbachol-induced tone by $13 \pm 1\%$ ($n = 6$). However, the magnitude of the relaxation was clearly intensity-dependent and increased progressively with light intensity up to a maximal value of $83 \pm 1\%$ ($n = 21$) at 1.1×10^4 lux in this series of experiments (Figure 3).

At intensities well in excess of 1.1×10^4 lux, a marked

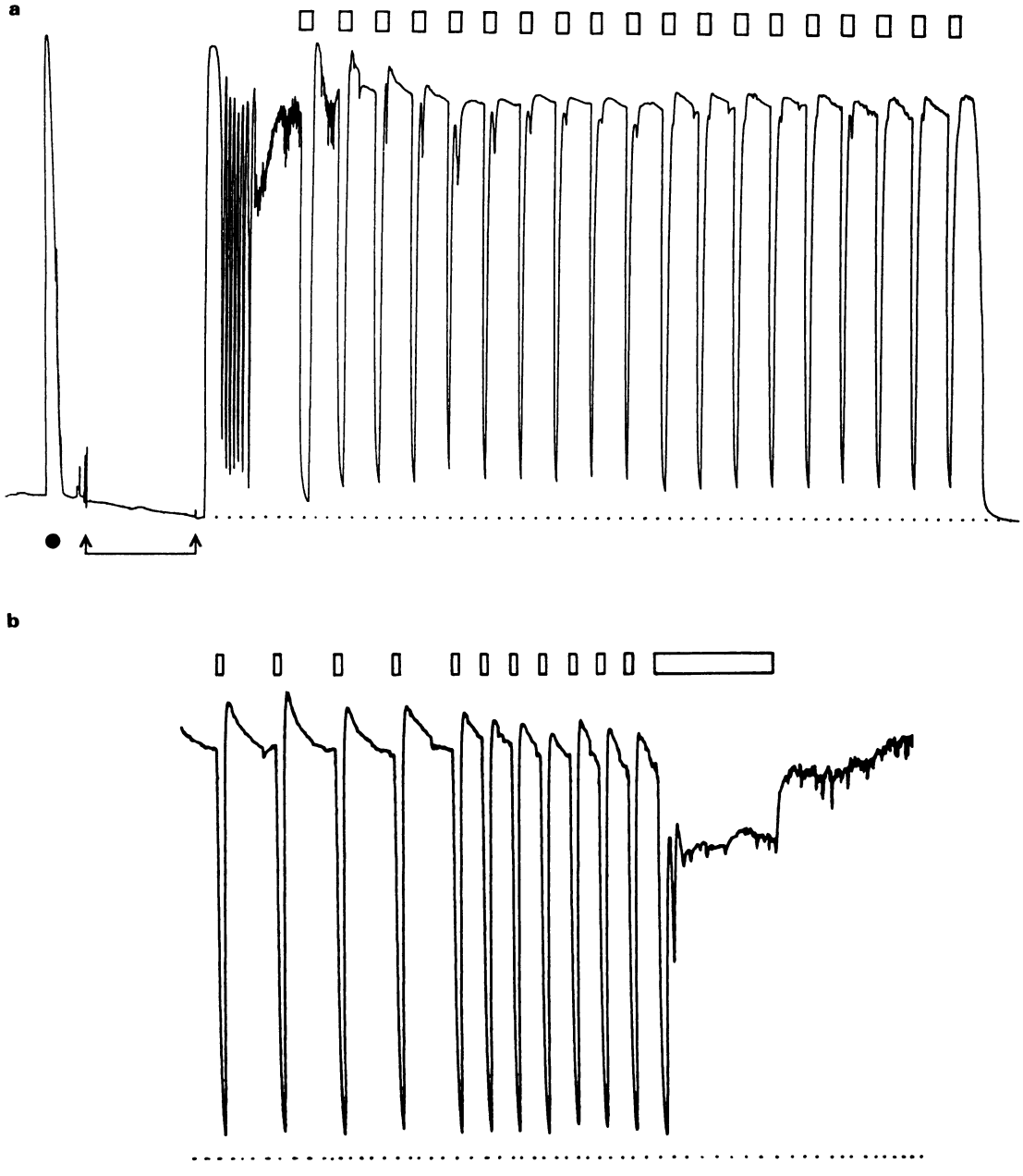

Figure 1 Photorelaxation in smooth muscle induced by RBS treatment. (a) Effect of light following RBS-pretreatment. Exposure to RBS (50 μM) for 30 min (between the arrows) was preceded by a test dose of carbachol (50 μM) for 10 s (●). After washout of RBS for 2 min, a sustained contraction was evoked by continuous exposure to carbachol (50 μM) and light at 1.1×10^3 lux applied for 3 min (□) of every 10 min commencing 30 min after initiating the sustained carbachol contraction. Baseline relaxation was re-established on removal of carbachol at the end of the experiment. (b) Effect of photon-irradiation at differing intervals and of different duration following RBS pretreatment (50 μM) and precontraction with carbachol (50 μM). Light was applied at 1.1×10^3 lux for 1 min (□) first at 10 min, then at 5 min intervals and finally the RBS-treated muscle was irradiated continuously for 20 min (open horizontal bar). Resting tone in the absence of carbachol is indicated by the dotted line.

time-dependent alteration in the level of inhibition of induced tone became more conspicuous (Figure 4). In a preparation exposed to a ten fold increase of intensity, i.e. to 1.1×10^5 lux, the inhibition of carbachol-evoked tone was 90% in the first illumination period but a rapid decline occurred in the magnitude of the first phase of the response, i.e., to 40% after 60 min and to 58% after 170 min. In contrast, exposure to light of 1.1×10^4 lux produced a well-sustained inhibitory response i.e., an inhibition of 94% after 60 min and 89% after 170 min (Figure 4). A similar time-dependent decrease in relaxation magnitude at a high intensity of illumination was observed with K^+-depolarized muscle. At 1.1×10^5 lux the relaxation in one experiment decreased to only 15% within 40 min and was followed by some recovery with a relaxation of 35% after 100 min. Again, this contrasts with the more pronounced and reproducible photorelaxation evident at lower intensities.

Wavelength-dependence of the photorelaxation in RBS-treated muscle

If local photon-activation of RBS is responsible for inhibition of the carbachol-induced contraction then both events should depend upon a similar and specific region of the radiation spectrum. By confining the radiation incident upon the superfused tissue successively to localized spectral regions with sharp-cut filters of known band-pass and transmission characteristics (see Methods) an action spectrum was established between 400 nm and 570 nm (Figure 5). Since this spectrum represents photorelaxation in response to illumination at wavelengths above the specific filtration wavelengths (400 nm, 515 nm, 535 nm, 570 nm) the action spectrum cannot be compared directly with the spectrum of RBS absorbance (Figure 9) at each wavelength. Under these circumstances it is more appropriate to compare the action spectrum with the total area under the absorbance curve at wavelengths defined by the filter cut-off values so that absorbance at and above the filtered wavelength is taken into account. If this is done then the curve depicting absorbance of RBS as restricted by the individual filters closely parallels the measured action spectrum of the tissue (Figure 5). The relative importance of the reduction in total intensity that occurs when filters are interposed between the light source and the tissue upon the shape of the action spectrum may be similarly assessed by determining the proportion of the area under the emission spectrum of the light source excluded by specific filters (Figure 5). In fact, light emission in the filtered range (400–570 nm) accounts for only some 18% of the total energy output of the halogen-light source.

Effects of redox and other agents on the photorelaxation in RBS-treated muscle

The effects of various redox agent on the RBS-dependent photorelaxation of carbachol-induced tone were investigated

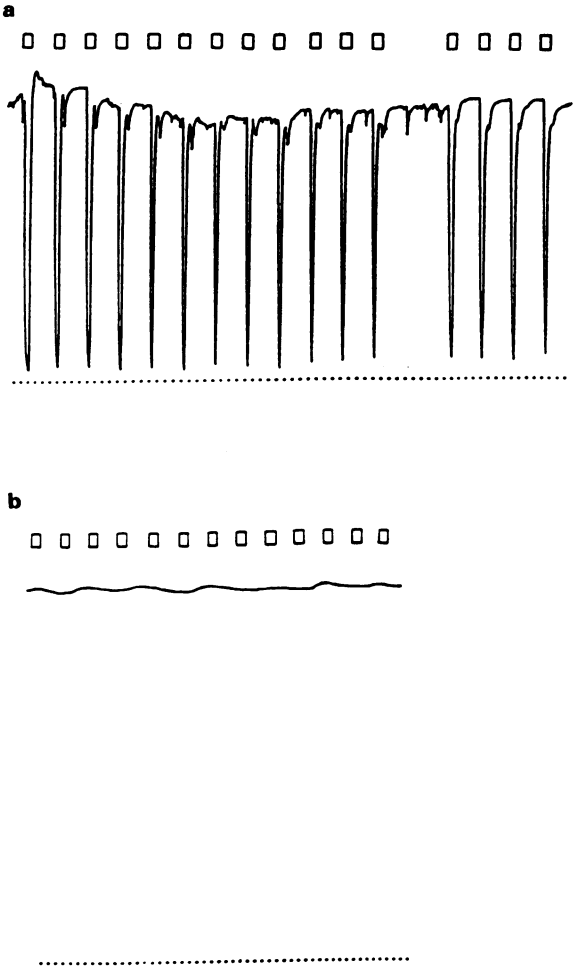

Figure 2 Effects of photon-irradiation on two smooth muscle preparations precontracted with carbachol (50 μM), both illuminated for 3 min (□) every 10 min (1.1×10^3 lux) in parallel, one pretreated with RBS (50 μM) (a), the other (b) receiving no RBS pretreatment. Resting tone in the absence of carbachol is indicated by the dotted line.

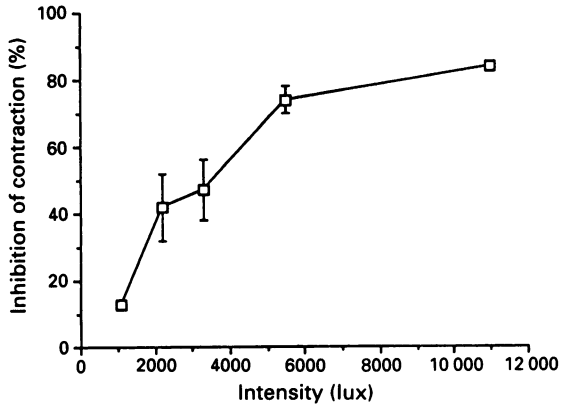

Figure 3 Intensity dependence of the photorelaxation in RBS-treated muscle. Plotted values (□) are means ± s.e.mean ($n = 6$ to 21).

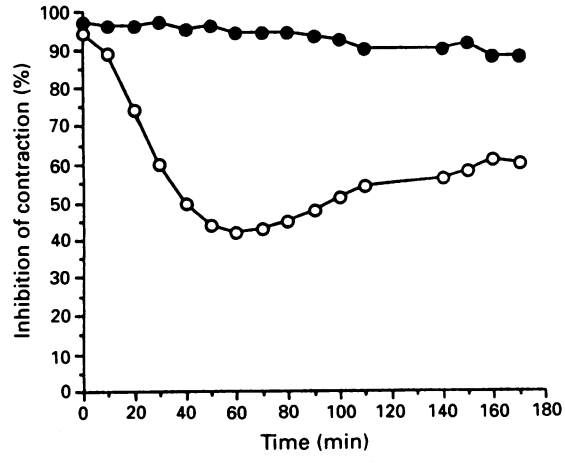

Figure 4 Time-dependent change in the RBS-induced photorelaxation at high intensity illumination. Two muscle preparations pretreated in parallel with RBS (50 μM) and illuminated for 3 min every 10 min, one at 1.1×10^4 lux (●) and the other at 1.1×10^5 lux (○).

by adding them to the superfusion solution following at least three 10 min cycles of illumination of the RBS-pretreated tissue at an intensity of 1.1×10^4 lux. Six cycles of illumination were subsequently completed during redox agent superfusion and seven to nine cycles after its removal.

L-Cysteine caused a substantial decrease in the RBS-dependent photorelaxations which was both time- and concentration-dependent. The inhibition by L-cysteine (10 mM) of the RBS-dependent response was evident within 10 min and maximal after 60 to 70 min (Figure 6). The L-cysteine inhibition was concentration-dependent with effects occurring at concentrations as low as 100 μM (Figure 7). Recovery of the photorelaxations to their original level occurred within 20 min of removal to L-cysteine from the superfusion solution (Figures 6 and 7). In contrast to L-cysteine, and to DTT (2 mM), which was also a potent inhibitor of photorelaxation (Table 1), the aminothiols N-acetyl-L-cysteine (1 to 10 mM) and GSH (1 to 10 mM) had no inhibitory effect on the photorelaxation in RBS-treated muscle. In fact, N-acetyl-L-cysteine and GSH caused a small enhancement of photorelaxation magnitude (Figure 8 and Table 1). Of the other agents tested N^G-nitro-L-arginine (60 μM), an inhibitor of nitric oxide synthase had no effect, but N-methylhydroxylamine (2 mM), methylene blue (30 μM) and haemoglobin (20 μM), all caused a reversible inhibition of the RBS-induced photorelaxation, the effect of methylene blue being the most persistent (Table 1).

Relaxation of smooth muscle by other nitric oxide donors

Illumination at 1.1×10^4 lux of carbachol pre-contracted preparations during infusion of the nitric oxide donors ruthenium nitrosyl chloride (0.5 mM), sodium nitroprusside (1 mM) or SNAP (0.5 mM) was without effect. Increasing the light intensity to 1.1×10^5 lux in the presence of these agents produced at most small or variable, photorelaxations with only sodium nitroprusside (1 mM) producing *per se* a small persistent relaxation of 15% in the absence of light. Thus, in three separate experiments with ruthenium nitrosyl chloride photo-irradiation at the higher intensity of 1.1×10^5 lux caused a $5 \pm 0.5\%$ ($n = 12$), $12 \pm 4\%$ ($n = 9$) and $57 \pm 0.5\%$ ($n = 8$) inhibition, respectively, of carbachol-induced tone. Illumination at 1.1×10^5 lux during infusion of sodium nitroprusside (1 mM) produced a $17 \pm 1\%$ ($n = 5$) inhibition of a carbachol contraction in one experiment and had no effect in another.

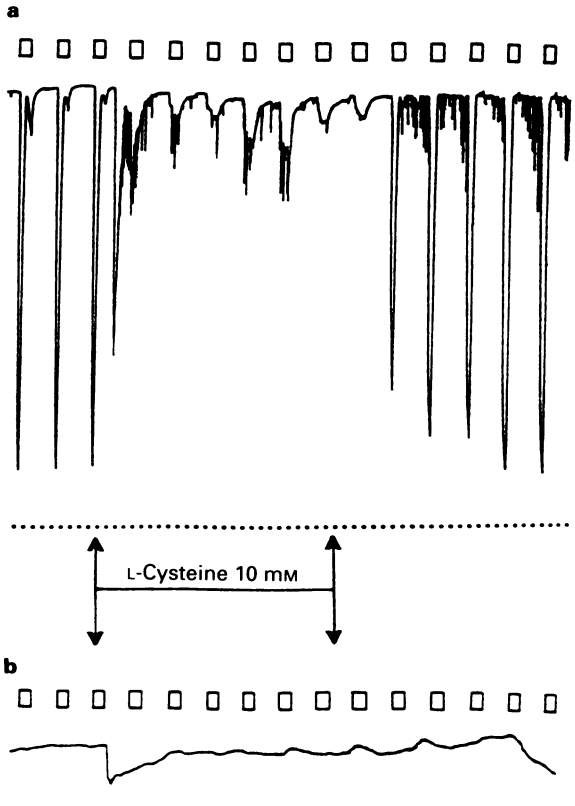

Figure 6 Effect of L-cysteine on the phororelaxation in RBS-treated muscle. Two muscle preparations were precontracted with carbachol (50 μM) and photon-irradiated in parallel at 1.1×10^4 lux for 3 min (□) every 10 min. One preparation was pretreated with RBS (50 μM) (a), the other was not (b). Resting tone in the absence of carbachol is indicated by the dotted line.

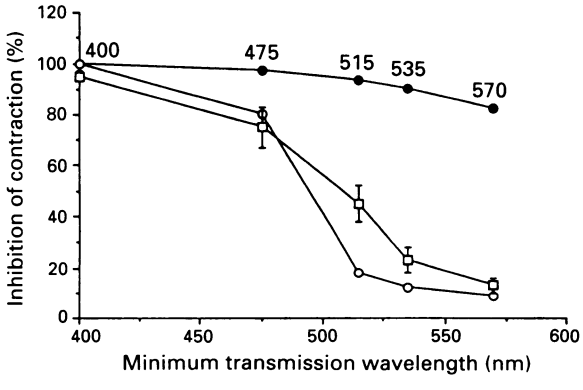

Figure 5 Wavelength-dependence of the photorelaxation in RBS-treated muscle. Photo-inhibition (%) of carbachol contraction in muscle pre-incubated with RBS (50 μM) upon illumination at 1.1×10^4 lux through sharp-cut filters. The minimum transmission wavelength of each filter is indicated. Plotted values (□) are the means ± s.e.mean ($n = 6$). Plotted also (○) is the % area of the RBS absorbance spectrum (derived from Figure 9) above the minimum transmission wavelength for each filter. The light energy incident on the preparation as a % of the total spectral emission of the light source excluded by specific filters is also indicated (●).

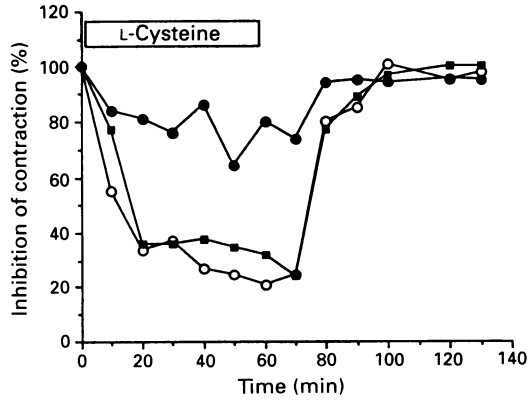

Figure 7 Concentration- and time-dependence of the L-cysteine inhibition of photorelaxation in RBS-treated muscle. Each of three preparations was pre-incubated in parallel with RBS (50 μM) and precontracted with carbachol (50 μM) before illumination at 1.1×10^4 lux for 3 min every 10 min. Each preparation was then exposed to L-cysteine for 1 h (horizontal bar) at a concentration of 100 μM (●), 5 mM (■) or 10 mM (○). The plotted values are expressed as a percentage of the mean of three photorelaxations induced in each preparation immediately before exposure to L-cysteine.

Absorbance spectra of RBS and measurement of photon-induced NO liberation

In aqueous solution RBS displays three characteristic absorbance maxima extending from the u.v. to the visible region, i.e., at 260, 350 and 560 nm. Following illumination there was an overall decrease in absorbance with no red or blue spectral shift evident (Figure 9); this suggests a photolytic cleavage of the RBS molecule with the liberation of NO. Free NO (or nitrite to which it may be converted) should therefore be detectable by the well-defined diazo reaction (see Methods). In these experiments a solution of RBS (50 μM) was illuminated at 1.1×10^5 lux for a total of 60 min and the absorbance spectrum measured before and at 30 and 60 min of illumination. Samples from both this solution and from a non-illuminated control solution were taken for analysis of NO liberation.

The absorption spectrum of non-illuminated RBS solutions remained stable over 60 min. However, when compared to the pre-illumination spectrum there was a highly significant ($P<0.001$) decrease of $33.4 \pm 0.6\%$ ($n=4$) and $52.6 \pm 0.1\%$ ($n=4$) in the absorbance at 350 nm of RBS (50 μM) after illumination (1.1×10^5 lux) for 30 and 60 min, respectively. These changes in absorbance corresponded to the photolytic generation in the same RBS samples of 256 ± 7 nmol ($n=4$) and 414 ± 11 nmol ($n=4$) of NO measured by the diazo reaction after 30 and 60 min of illumination. In the presence of L-cysteine (10 mM) the decrease in absorbance at 350 nm was markedly attenuated, amounting to only $8.0 \pm 0.5\%$ ($n=4$), and $9.6 \pm 0.7\%$ ($n=4$) after 30 and 60 min of

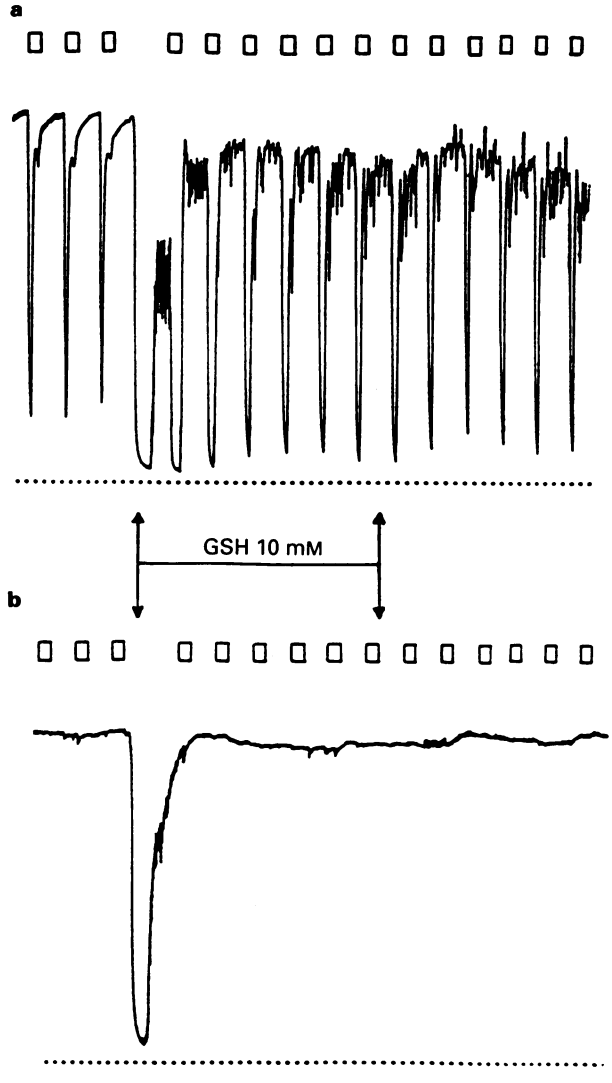

Figure 8 Effects of glutathione (GSH) on the photorelaxation in RBS-treated muscle. Two muscle preparations were precontracted with carbachol (50 μM) and photon-irradiated in parallel at 1.1×10^4 lux for 3 min (□) every 10 min. One preparation was pretreated with RBS (50 μM) (a), the other was not (b). Resting tone in the absence of carbachol is indicated by the dotted line.

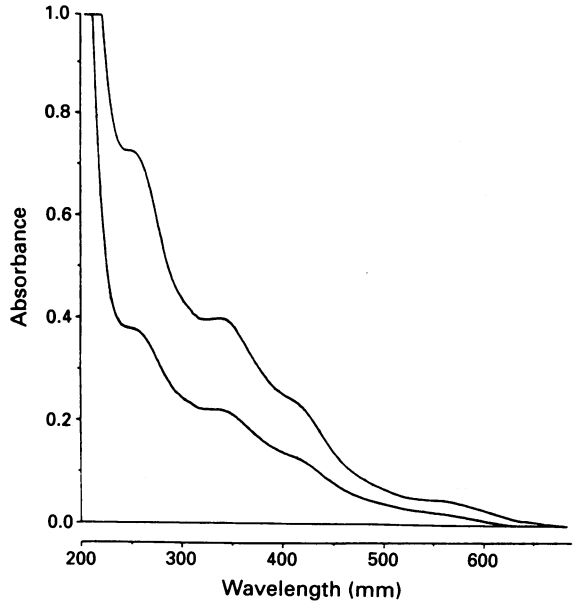

Figure 9 Absorbance spectrum of RBS (50 μM) in the absence of illumination (upper curve) and after illumination at 1.1×10^5 lux for 60 min (lower curve).

Table 1 Effects of redox and other agents on RBS-induced photorelaxations

Drug	*Concentration*	*Photorelaxation magnitude (%) Before*	*During*	*After*	n
None		93.3 ± 1.8	90.6 ± 2.4	88.4 ± 2.6	4
L-cysteine	10 mM	80.7 ± 8.9	9.7 ± 0.7***	58.1 ± 4.9	5
Dithiothreitol	2 mM	84.1 ± 2.4	14.4 ± 1.1***	74.0 ± 2.3	4
N-acetyl-L-cysteine	10 mM	80.9 ± 3.7	85.9 ± 6.5	69.3 ± 1.7	3
N-methylhydroxylamine	2 mM	88.1 ± 1.2	34.0 ± 1.7***	68.8 ± 1.5	4
N^G-nitro-L-arginine	60 μM	90.9 ± 2.5	85.1 ± 1.5	84.4 ± 1.7	3
Methylene blue	30 μM	84.0 ± 1.3	26.2 ± 2.2***	36.2 ± 6.1	7
Haemoglobin	20 μM	90.3 ± 1.5	20.3 ± 2.2***	55.6 ± 6.5	4

All results are expressed as the mean percentage magnitude ± s.e.mean of the sustained contractile response evoked by carbachol (50 μM). Photorelaxations to light (1.1×10^3 lux) of 3 min duration were elicited every 10 min. In each of three to seven separate experiments, three responses were measured immediately before drug exposure, three in the presence of drug measured during the last three of six responses in the presence of drug, and three responses after removal of the drug measured during the last three of six responses following drug removal. ***$P<0.001$.

illumination. NO production in the same samples was also significantly less ($P<0.001$) in the presence of L-cysteine, i.e., 9.6 ± 3.8 nmol ($n = 4$) and 18.3 ± 5.7 nmol, respectively.

Discussion

Iron-sulphur cluster nitrosyl compounds taken up by endothelial cells have been shown to produce a vasodilator action by the spontaneous liberation of nitric oxide (Flitney *et al.*, 1992). However, the present study establishes that the cluster compound RBS has little or no effect on the smooth muscle cells of the taenia coli in the absence of light yet causes a marked photorelaxation of muscle precontracted with either carbachol or KCl. To produce a contraction, KCl depolarizes the muscle directly; it also depolarizes nerve-endings within the muscle, so minimizing the intervention of any subsequent nerve-mediated effects. In contrast, activation of muscarinic receptors by carbachol leads to the generation of inositol trisphosphate, mobilization of stored calcium, an increase in $[Ca^{2+}]_i$, and muscle contraction. These experiments suggest that illumination of the muscle pre-incubated with RBS facilitates the production of a labile relaxant factor because photon-irradiation initiates a reversible inhibition of contraction whether produced by either of two alternative routes. It seems reasonable to assume therefore that retention and photolysis of RBS underlies these photorelaxations, the liberation of free NO then presumably activating guanylyl cyclase and generating cyclic GMP.

The RBS-induced photorelaxations demonstrated an intensity-dependence below 1.1×10^4 lux, a decrease in illumination intensity causing a corresponding decrease in the relaxation effect. It is likely therefore that below the maximal inhibitory intensity of 1.1×10^4 lux, liberation of NO by RBS photolysis and the rate of reaction with its target enzyme, guanylyl cyclase, is submaximal. As the intensity maximum is approached, sufficient NO may be produced to saturate the enzyme so that either a stage further downstream in the cyclic GMP-mediated pathway then becomes rate-limiting or some negative feed-back mechanism is activated. Photon-irradiation at the higher intensity of 1.1×10^5 lux will cause a substantial local release of nitric oxide from RBS (see below). It is known that at high concentrations the reaction of NO with oxygen becomes significant and can yield appreciable quantities of dinitrogen tri-oxide, tetra-oxide and nitrous acid (Wolfe & Swinehart, 1975; Feelisch, 1991). A decrease in intracellular pH and the generation of a highly nitrosating environment affecting cellular metabolism could well account for the decreased photorelaxation observed at higher light intensities.

Use of sharp-cut filters to eliminate progressively discrete regions of the visible spectrum defined the wavelength-action spectrum for RBS acting on smooth muscle cells and provided further convincing evidence that a wavelength-dependent absorbance of RBS is responsible for the observed photorelaxant effect on smooth muscle. The spectrum of the RBS molecule itself is characterized by three absorbance maxima at 260, 350 and 560 nm. Illumination caused a uniform decrease of the absorbance spectrum and a proportional diminution of these maxima with no discernible red or blue shift, a pattern consistent with photolytic degradation of the iron-sulphur cluster framework. The precise molecular mechanism by which NO is released from the cluster or caged state by photon irradiation has yet to be determined. Extended Hückel molecular orbital calculations have demonstrated that RBS is electron precise (Sung *et al.*, 1985) which means that either the addition or removal of an electron from the structure will weaken the cage bonding and cause the iron-sulphur framework to disintegrate, releasing free NO (Flitney *et al.*, 1992). In the present experiments just such a molecular effect will occur with the absorption of photon energy. In addition, interconversion between closely related iron-sulphur nitrosyl compounds is possible by a process of extensive fragmentation and reassembly involving dissociation to a paramagnetic species containing a single iron atom (Sung *et al.*, 1985). This raises the important question as to whether illumination and photolysis of RBS affects the equilibrium between the RBS molecule and its two closely related derivatives i.e., $[Fe_2S_2(NO_4)]^2 \rightleftharpoons [Fe_4S_3(NO_7)]^- \rightleftharpoons Fe_4S_4(NO)_4$. This factor is particularly important in the cellular environment where the structural components would be retained and able to participate in any such molecular transformation or interconversion. A fragmentation-reassembly process controlled by alternate light-dark periods could well explain the remarkable persistence of RBS action, but whatever the kinetics of the events involved there is little doubt that photon-activation of the RBS molecule does liberate nitric oxide as detected by the diazo reaction.

N-methyl-hydroxylamine and methylene blue reversibly blocked the photorelaxation effect of RBS. Both agents are known to prevent NO-induced relaxation of smooth muscle by inhibiting the activation of guanylyl cyclase (Gibson & Mirzazadeh, 1989). Although methylene blue can also inhibit NO synthase (Mayer *et al.*, 1993), it is unlikely that this action contributes to an attenuation of the RBS photorelaxation because the more selective NO synthase inhibitor N^G-methyl-L-arginine (Hobbs & Gibson, 1990) was itself completely without effect. Haemoglobin was also found to block RBS photorelaxation. It is generally assumed that because Hb is a large molecule it is unable to penetrate intracellularly and therefore acts solely as a scavenger of extracellular nitric oxide which binds to the haem site with high affinity. Haemoglobin may however also sequester NO diffusing between muscle cells (Matsunaga & Furchgott, 1989) when free nitric oxide is liberated, as it would be on photon activation of a bound localised source of RBS.

L-Cysteine is a natural amino acid which is neutral at physiological pH and has been shown to be actively transported into cells (Bannai, 1984). As a thiol containing reductant it is capable of influencing a number of events in the process of RBS-dependent photorelaxation, including interaction with the RBS molecule itself, interaction with nitric oxide and its redox-activated forms and/or interaction with guanylyl cyclase. Our spectrophotometric analysis showed that L-cysteine attenuated RBS photolysis thereby decreasing NO production upon photon-activation. However, the fact that the biological effect of L-cysteine on the RBS-dependent photorelaxation was fully reversible suggests that direct chemical reaction of L-cysteine with the RBS molecule does not occur. It is more likely that L-cysteine provides a high density of SH groups in close proximity to the RBS molecule thus stabilizing the electronic configuration of the cluster compound. Under physiological conditions free NO may be interconverted among different redox forms, each with a different preference for various target functional groups (Stamler *et al.*, 1992). This can result in the S-nitrosation of tissue bound thiol groups and the formation of thionitrates (Feelisch, 1991). These are very effective activators of guanylyl cyclase, S-nitrosocysteine being approximately 80 times more potent than nitric oxide itself (Myers *et al.*, 1990). On the other hand, agents which oxidize or reduce sulphydryl groups also markedly alter basal and stimulated guanylyl cyclase activity (Waldman & Murad, 1987). Thiol-containing reductants of high redox potential can cause a concentration-dependent reversal of nitric oxide activation of guanylyl cyclase despite an increase in the rate of formation of nitrosyl-haem (Braughler, 1983). This is due to the ability of the reductant to maintain the haem of guanylyl cyclase in the Fe^{2+} state (Waldman & Murad, 1987). On this basis, L-cysteine and other highly potent thiol reductants, e.g., DTT, would be expected to decrease the magnitude of the RBS photorelaxation, as was indeed observed. The failure of N-acetyl-L-cysteine and GSH to produce an inhibitory effect similar to that of L-cysteine and DTT is probably a consequence of their poor uptake into the intracellular compartment of the smooth muscle cells of the taenia (see Matthews

et al., 1993b). These cells may also lack the deacetylation enzymes required to convert the N-acetylated derivative to active L-cysteine. We suggest therefore that the reversible inhibition of the RBS-dependent photorelaxation by L-cysteine is attributable to (i) an interaction of the L-cysteine with RBS to diminish its rate of photolysis, and (ii) an action to decrease the NO activation of guanylyl cyclase, both effects together outweighing any potential stimulation of guanylyl cyclase by the production of S-nitrosocysteine.

In conclusion, our results can be explained by the following scheme. On exposure to RBS there is a binding or sequestration of the molecule within the tissue. After removal of RBS from the extracellular space the retained RBS liberates NO in response to light by a process which can be precisely controlled by varying the wavelength, intensity, and duration of the incident light. Nitric oxide then causes a relaxation of the smooth muscle by activation of guanylyl cyclase and the generation of cyclic GMP. This effect can be prevented by the appropriate inhibitors but does not involve the activation of NO synthase. However, we cannot yet rule out the participation of some additional cyclic GMP-independent pathway. Further experiments are therefore required to define more fully the molecular basis of the effects we have observed. Nonetheless, this investigation has demonstrated that RBS is a valuable photosensitive NO donor for probing the functional, physiological, and pharmacological significance of NO itself. The ability to control precisely the rapid local liberation of NO by photon activation suggests that RBS can be used not only in smooth muscle cells but also to generate NO for a wide variety of biological actions e.g., the modulation of CNS neurotransmission (Black *et al.*, 1994) or for investigation of its potential anti-tumour action (Matthews & Forsyth, 1994).

We are very grateful to Dr A.R. Butler for the supply of RBS.

References

BANNAI, S. (1984). Transport of cystine and cysteine in mammalian cells. *Biochem. Biophys. Acta*, **779**, 289–306.

BLACK, M.D., MATTHEWS, E.K., BUTLER, A.R. & HUMPHREY, P.P.A. (1994). The effects of a photosensitive nitric oxide donor on dopamine efflux measured by fast cyclic voltammetry in the rat striatum. *Br. J. Pharmacol.* (in press).

BRADING, A.F. & SNEDDON, P. (1980). Evidence for multiple sources of calcium for activation of the contractile mechanism of the guinea-pig taenia coli on stimulation with carbachol. *Br. J. Pharmacol.*, **70**, 229–240.

BRAUGHLER, J.M., Jr. (1983). Soluble guanylyl cyclase activation by nitric oxide and its reversal: involvement of sulfhydryl group oxidation and reduction. *Biochem. Pharmacol.*, **32**, 811–818.

BUTLER, A.R., GLIDEWELL, C. & GLIDEWELL, S.M. (1990). Formation of the heptanitrosyltri-μ3-thioxotetraferrate 1- anion, $[Fe_4S_3(NO)_7]^-$ by capture of biological sulphur in reactions with iron (II) and nitrite. *Polyhedron*, **9**, 2399–2405.

BUTLER, A.R., GLIDEWELL, C. & MIN-SHIN, L. (1988). Nitrosyl complexes of iron-sulfur clusters. *Adv. Inorg. Chem.*, **32**, 335–392.

FEELISCH, M. (1991). The biochemical pathways of nitric oxide formation from nitro vasodilators: appropriate choice of exogenous NO donors and aspects of preparation and handling of aqueous NO solutions. *J. Cardiovasc. Pharmacol. Suppl.*, **31**, 525–533.

FLITNEY, F.W., MEGSON, I.L., FLITNEY, D.E. & BUTLER, A.R. (1992). Iron-sulphur cluster nitrosyls, a novel class of nitric oxide generator: mechanism of vasodilator action on rat isolated tail artery. *Br. J. Pharmacol.*, **107**, 842–848.

GAO, Y. & VANHOUTTE, P.M. (1993). Attenuation of contractions to acetylcholine in canine bronchi by an endogenous nitric-oxide like substance. *Br. J. Pharmacol.*, **109**, 887–891.

GIBSON, A., BABBEDGE, R., BRAVE, S.R., HART, S.L., HOBBS, A.J., TUCKER, J.F., WALLACE, P. & MOORE, P.K. (1992). An investigation of some s-nitrosothiols, and of hydroxy-arginine, on the mouse anococcygeus. *Br. J. Pharmacol.*, **107**, 715–721.

GIBSON, A. & MIRZAZADEH, S. (1989). N-methylhydroxylamine inhibits and M&B 22948 potentiates relaxations of the mouse anococcygeus to non-adrenergic, non-cholinergic field stimulation and to nitrovasodilator drugs. *Br. J. Pharmacol.*, **96**, 637–644.

HOBBS, A.J & GIBSON, A. (1990). L-N^G-nitro-arginine and its methylester are potent inhibitors of non-adrenergic, non-cholinergic transmission in the rat anococcygeus. *Br. J. Pharmacol.*, **100**, 749–752.

IGNARRO, L.J., BUGA, G.M., WOOD, K.S., BYRNS, R.E. & CHAUDHURI, G. (1987). Endothelium-derived relaxing factor produced and released from artery and vein is nitric oxide. *Proc. Natl. Acad. Sci. U.S.A.*, **84**, 9265–9269.

KATSUKI, S., ARNOLD, W.P. & MURAD, F. (1977). Effects of sodium nitroprusside, nitroglycerine, and sodium azide on levels of cyclic nucleotides and mechanical activity of various tissues. *J. Cyclic Nucleotide Res.*, **3**, 239–247.

MATSUNAGA, K. & FURCHGOTT, R.F. (1989). Interactions of light and sodium nitrite in producing relaxation of rabbit aorta. *J. Pharmacol. Exp. Ther.*, **248**, 687–695.

MATTHEWS, E.K. & FORSYTH, M.J. (1994). Photosensitive nitric oxide donor action on rat pancreatoma cells. *Can. J. Physiol. Pharmacol.*, (in press).

MATTHEWS, E.K., FLAHERTY, C. & SMITH, W. (1993a). Effect of thiols on the photodynamic action of sulphonated aluminium phthalocyanine on guinea-pig taenia coli. *Br. J. Pharmacol.*, **108**, 42P.

MATTHEWS, E.K., FLAHERTY, C. & SMITH, W.H.T. (1993b). Photodynamic action of aluminium phthalocyanine tetrasulphonate ($ALPcS_4$) on smooth muscle: effects of thiols and a cyclic GMP analogue. *Br. J. Pharmacol.*, **110**, 1248–1254.

MATTHEWS, E.K. & MESSLER, D.E. (1984). Photodynamic effects of erythrosine on the smooth muscle cells of guinea-pig taenia coli. *Br. J. Pharmacol.*, **83**, 555–566.

MATTHEWS, E.K., SEATON, E., FORSYTH, M.J. & HUMPHREY, P.P.A. (1994). Effects of a photosensitive nitric oxide donor on isolated guinea-pig taenia coli. *Br. J. Pharmacol.*, **112**, 63P.

MAYER, B., BRUNNER, F. & SCHMIDT, K. (1993). Inhibition of nitric oxide synthesis by methylene blue. *Biochem. Pharmacol.*, **45**, 367–374.

MYERS, P.R., MINOR, Jr., R.L., GUERRA, Jr., R., BATES, J.N. & HARRISON, D.G. (1990). Vasorelaxant properties of the endothelium-derived relaxing factor more closely resemble S-nitrocysteine than nitric oxide. *Nature*, **345**, 161–163.

PRINCE, R.C. & GROSSMAN, M.J. (1993). Novel iron-sulfur clusters. *Trends Biochem. Sci.*, **18**, 153–154.

STAMLER, J.S., SINGEL, D.J. & LOSCALZO, J. (1992). Biochemistry of nitric oxide and its redox-activated forms. *Science*, **258**, 1898–1902.

SUNG, S.-S., GLIDEWELL, C., BUTLER, A.R. & HOFFMANN, R. (1985). Bonding in nitrosylated iron-sulphur clusters. *Inorg. Chem.*, **24**, 3856–3859.

WALDMAN, S.K. & MURAD, F. (1987). Cyclic GMP synthesis and function. *Pharmacol. Rev.*, **39**, 163–196.

WOLFE, S.K. & SWINEHART, J.H. (1975). Photochemistry of pentacyanonitrosylferrate(2-), nitroprusside. *Inorg. Chem.*, **14**, 1049–1053.

(Received March 25, 1994
Revised May 11, 1994
Accepted May 17, 1994)

Br. J. Pharmacol (1994), **113**, 95–102

Neuropeptide Y in rat detrusor and its effect on nerve-mediated and acetylcholine-evoked contractions

[1]M.M. Iravani & [2]M.A. Zar

The Department of Pharmacological Sciences, The Medical School, Framlington Place, Newcastle upon Tyne, NE2 4HH

1 Immunohistochemical and isolated organ bath techniques were used to detect the presence of neuropeptide Y (NPY) in the rat urinary bladder and to determine its effect on tone, spontaneous activity and contractile responses of the detrusor muscle to electrical field stimulation, acetylcholine and α,β-methylene ATP (α,β-MeATP).

2 A very rich presence of NPY-immunoreactive nerve fibres was found mainly within the bundles of detrusor muscle cells. Chronic treatment with 6-hydroxydopamine did not affect the density of NPY-positive nerve fibres.

3 NPY (>1 nM) enhanced the force and frequency of spontaneous contractions and generated a rise in the resting tone of the detrusor. These effects of NPY on the tone and the spontaneous activity remained unaffected by atropine (3 μM), indomethacin (10 μM) and aspirin (100 μM) but were abolished by Ca^{2+}-withdrawal from the bathing medium.

4 The enhancing effects of NPY on the spontaneous contractions and the resting tone were not prevented by the induction of purinoceptor desensitization.

5 NPY (1–250 nM) potentiated electrical field stimulation (EFS, 1–64 Hz, 0.1 ms pulses duration, 10s train duration)-evoked, tetrodotoxin (0.5 μM)-sensitive contractions. The atropine (3 μM)-resistant component of EFS-evoked contractions was also potentiated by NPY. By contrast, the nifedipine (1 μM)-resistant but atropine-sensitive component of EFS-evoked contraction was inhibited by NPY.

6 NPY (250 nM) did not affect acetylcholine-evoked contractions, but potentiated α,β-MeATP-evoked contractions.

7 It is concluded that NPY-innervation of rat urinary bladder is largely confined to the detrusor muscle and is abundant and mainly non-adrenergic. It is further concluded that the enhancing effect of NPY on detrusor spontaneous activity and tone is caused by Ca^{2+} influx through nifedipine-sensitive Ca^{2+} channels and is not mediated through acetylcholine or cyclo-oxygenase-sensitive eicosanoids or ATP.

8 The results are consistent with the hypothesis that intrinsic NPY in the rat detrusor innervation contributes to the motor transmission in two ways: by promoting non-cholinergic motor transmission and by inhibiting prejunctionally the cholinergic transmission.

Keywords: Detrusor muscle; urinary bladder; neuropeptide Y; cholinergic neurotransmission; non-cholinergic neurotransmission; nifedipine

Introduction

Neuropeptide Y (NPY), a 36 amino acid peptide is present in the autonomic nerve supply of many organs including the urinary bladder of man and rat (Gu *et al.*, 1984; Mattiasson *et al.*, 1985). NPY-containing nerve fibres originate mainly in the non-adrenergic cell bodies of the pelvic ganglia and are richly distributed in the detrusor muscle (Mattiasson *et al.*, 1985). The physiological role of NPY-containing fibres in the detrusor and the potential pharmacological significance due to their presence is not known. The present investigation was undertaken with the object of firstly confirming its presence in rat detrusor and secondly to determine its effect on detrusor tone, contractility and spontaneous mechanical activity. A preliminary account of some of the results reported here has been presented at a meeting of the physiological Society (Iravani & Zar, 1988).

Methods

All experiments were performed on isolated strip preparations of rat detrusor prepared from the urinary bladder of adult male Wistar rats (200–250 g). The strips were prepared according to the method previously described by Zar *et al.* (1990). Rats were killed by concussion and decapitation. The lower abdomen was opened and the bladder was exposed. The bladder was held at its apex, slightly stretched and the investing layers of serosal coat, connective tissue and accompanying blood vessels were cut away as close as possible from the outer surface of the bladder wall. The bladder was excised by a cut above the trigone; any residual urine was absorbed on filter paper and the bladder was washed in a Petri dish with several changes of Krebs-Henseleit solution. The bladder was then opened by two lateral incisions and unfolded to give a rectangular sheet of tissue approximately 15 mm long and 6 mm wide. The unfolded tissue was laid on Krebs-soaked filter paper and the mucosal layer was carefully separated and removed. Strips of bladder, 10–15 mm long and 2 mm wide were then cut with the aid of a pair of fine scissors.

Detrusor strips were either processed for detection of NPY-immunoreactivity or set up in an organ bath for investigation of the effect of exogenously applied NPY on the spontaneous contractions or contractions evoked by electrical pulses and by acetylcholine (ACh).

Immunohistochemistry

For immunohistochemical detection of NPY-containing nerve fibres, small pieces of the detrusor strip (not larger

[1]Present address: Department of Pharmacology, Basic Medical Sciences, Queen Mary & Westfield College, Mile End Road, London E1 4NS.
[2]Author for correspondence.

than 2 × 2 × 2 mm) were cleaned of connective tissue. The strips were fixed by immersion in 0.01 M phosphate buffered saline (PBS) containing 0.4% *p*-benzoquinone for 2 h at 4°C. Following washing in several changes of PBS containing 10% sucrose for 24 h, strips were suspended in Tissue-Tec (Miles) and frozen in liquid nitrogen prior to sectioning. Cryostat sections (10 μm thick) were mounted onto poly-L-lysine coated slides and were processed for indirect immunofluorescence staining according to standard techniques (Polak & Van Noorden, 1986). First layer antibody was rabbit anti-NPY IgG (Peninsula Europe Ltd.) and it was used at a dilution of 1:400 with PBS containing 0.1% bovine serum albumin (BSA) and 0.01% NaN_3, incubated for 16 h at room temperature. After washing with PBS (3 × 5 min) the second layer antibody, goat anti-rabbit IgG, conjugated with fluorescein isothiocyanate (FITC) was applied at a dilution of 1:50 in PBS containing 0.1% BSA and 0.01% NaN_3 for 2 h at room temperature. Slide mounted sections were further washed in PBS (3 × 5 min) and coverslipped with phosphate buffered glycerol (Sigma) mountant. For control experiments the primary antibody was pre-absorbed with excess (10 μg) synthetic porcine NPY, before being applied as the first layer. The sections were visualised under a Leitz Ortholux II microscope with excitation filter KP 490, and TK 510 dichroic mirror and a barrier filter K 515. Photomicrographs were taken with Kodak T-MAX p3200.

6-Hydroxydopamine pretreatment

Four animals were pretreated with 6-hydroxydopamine (6-OHDA). Four doses of 50 mg kg^{-1} were injected i.p. on days 1, 2, 4 and 6. The animals were killed one week after the last injection.

Organ bath study

The detrusor strip preparation was suspended in a 1 ml organ bath between built-in vertical platinum electrodes, at a resting tension of 0.5 g force, at 37°C in Krebs-Henseleit solution (composition mM: NaCl 118, KCl 4.7, $CaCl_2$ 2.5, $MgSO_4$ 1.2, $NaHCO_3$ 25, KH_2PO_4 1.2, glucose 11) gassed with 95% O_2 and 5% CO_2. The resting tension was kept constant at 0.5 g force throughout the experiment by appropriate adjustments whenever needed (except after application of drugs to the organ bath). An equilibration period of at least 30 min was allowed before starting each experiment; during this period the preparation was repeatedly washed with Krebs-Henseleit solution. For recording tension of the detrusor muscle, the preparation was connected to an isometric transducer and the changes in the tension were recorded on either a potentiometric chart recorder or a storage oscilloscope.

Spontaneous rhythmic activity of the detrusor strip was assessed by calculating the amplitude and frequency of spontaneous contractions. The amplitude was estimated by adding together the tension of individual contractions occurring during a period of 1 min, and dividing this sum by the number of contractions during this period. The value for the frequency of spontaneous activity (rate min^{-1}) was given by the total number of contractions occurring during this period.

Desensitization to the contractile action of α-β-methylene ATP (α,β-MeATP) was obatined by exposing the detrusor preparation, pretreated with indomethacin (10 μM) to α,β-MeATP (10 μM) and repeating this dose twice at 10 min intervals without washing out the drug present in the bath from preceding doses. Exposure to the initial application of α,β-MeATP caused a large contraction which subsided fully in about 5 min and subsequent applications of the drug did not evoke any contractile response.

When desired, the detrusor preparation was contracted either directly by addition of ACh or indirectly by electrical field stimulation (EFS) delivered through a Grass S-88 electronic stimulator and 2 platinum electrodes lying on either side of the muscle in the organ bath. In preliminary experiments, it was established that trains of pulses at 1–64 Hz and pulse duration of 0.1 ms at supramaximal voltage (80–90 V) produced motor responses which were fully abolished by tetrodotoxin (TTX) 0.5 μM; such responses were therefore deemed to be fully neurogenic. Further experimental details are provided in the appropriate results section.

Drugs

The drugs used and their sources were: acetylcholine chloride, acetyl salicylic acid (aspirin), atropine sulphate, 6-hydroxydopamine hydrochloride, indomethacin and α,β-methylene ATP (Sigma); tetrodotoxin (Sankyo); nifedipine (Bayer); neuropeptide Y (Cambridge Research Biochemicals). Solutions of drugs were made fresh on the day of their use except tetrodotoxin which was stored in form of stock solution, frozen at −20°C. All drugs were dissolved in distilled water except indomethacin and nifedipine which were dissolved in absolute alcohol to make solutions of 10^{-2} M and 10^{-3} M strengths respectively. NPY was first dissolved in distilled water containing 200 μg ml^{-1} bovine serum albumin (Sigma) aliquoted out into smaller volumes and then freeze dried and stored at −20°C until the day of experiment, when the aliquot was reconstituted with distilled water. All experiments involving the use of nifedipine were carried out in a laboratory illuminated solely with sodium light.

Statistics

All values are expressed as mean ± s.e. mean and the differences between means were calculated by Student's *t* test. Values of $P<0.05$ were considered as statistically significant.

Results

Immunohistochemistry

A very rich presence of NPY-immunoreactive nerve fibres were detected in the sections of the urinary bladder. Most of these fibres were seen within the bundles of detrusor muscle cells (Figure 1) and gave distinct impression of being varicose. Sub-epithelial layers of the bladder was virtually devoid of NPY-immunoreactive fibres and only an occasional NPY-immunoreactive fibre could be seen in this layer (Figure 1). 6-OHDA pretreatment had no apparent effect on the intensity of NPY-immunofluoresence or the number of NPY-positive nerve fibres, in the detrusor.

Organ bath studies

Spontaneous activity Isolated strips of rat detrusor exhibited spontaneous rhythmic activity. The rate and amplitude of the spontaneous activity varied from one preparation to another and even in different strips from the same bladder. Concentrations of NPY in excess of 1 nM produced an increase in both the rate and the amplitude of spontaneous contractions. The facilitating effect of NPY (100 nM) on spontaneous contractions is shown in a typical experiment in Figure 2a, and the results from 5 such experiments are summarised in Figure 2b. The effect of NPY was more marked on the amplitude compared to the frequency of contraction. Thus during the final 60 s of a 10 min exposure to NPY (100 nM), compared with the control values for 60 s immediately before NPY exposure the amplitude was increased by 220 ± 42% (mean ± s.e. mean; $n = 5$; $P<0.05$) while the rate increased by 37 ± 15% (mean ± s.e. mean; $n = 5$; $P<0.05$).

In order to ascertain whether the potentiating effect of NPY on spontaneous activity was mediated through prostaglandins, some experiments were conducted in the presence of indomethacin, or aspirin. Indothemacin (10 μM) caused a

gradual inhibition of spontaneous activity almost to the point of extinction (Figure 3a). Addition of NPY (50–100 nM) led to an almost immediate appearance of spontaneous activity in the indomethacin-treated preparations, suggesting that prostaglandins were not the mediator of NPY effect on spontaneous activity. In 3 experiments, aspirin (100 μM), an irreversible cyclo-oxygenase inhibitor was substituted for indomethacin. The results with aspirin were indistinguishable from those using indomethacin. Aspirin (100 μM) was effective in abolishing the spontaneous activity but it did not prevent the initiation of spontaneous activity by NPY (100 nM).

We have also examined the effect of NPY on spontaneous activity after desensitization of the purinoceptors induced by α,β-MeATP. The experiments were performed in the presence of indomethacin (10 μM). It was invariably noted that the spontaneous activity, which had been abolished by indomethacin (10 μM), reappeared in a distinctly potentiated form after induction of purinoceptor desensitization by α,β-MeATP. Nevertheless, addition of NPY (100 nM) to the 'purinoceptor-desensitized' preparation induced a further increase in both amplitude and rate of spontaneous contractions (mean % increase ± s.e. mean: amplitude = 78 ± 12; rate = 25 ± 4; $n = 3$; $P < 0.05$).

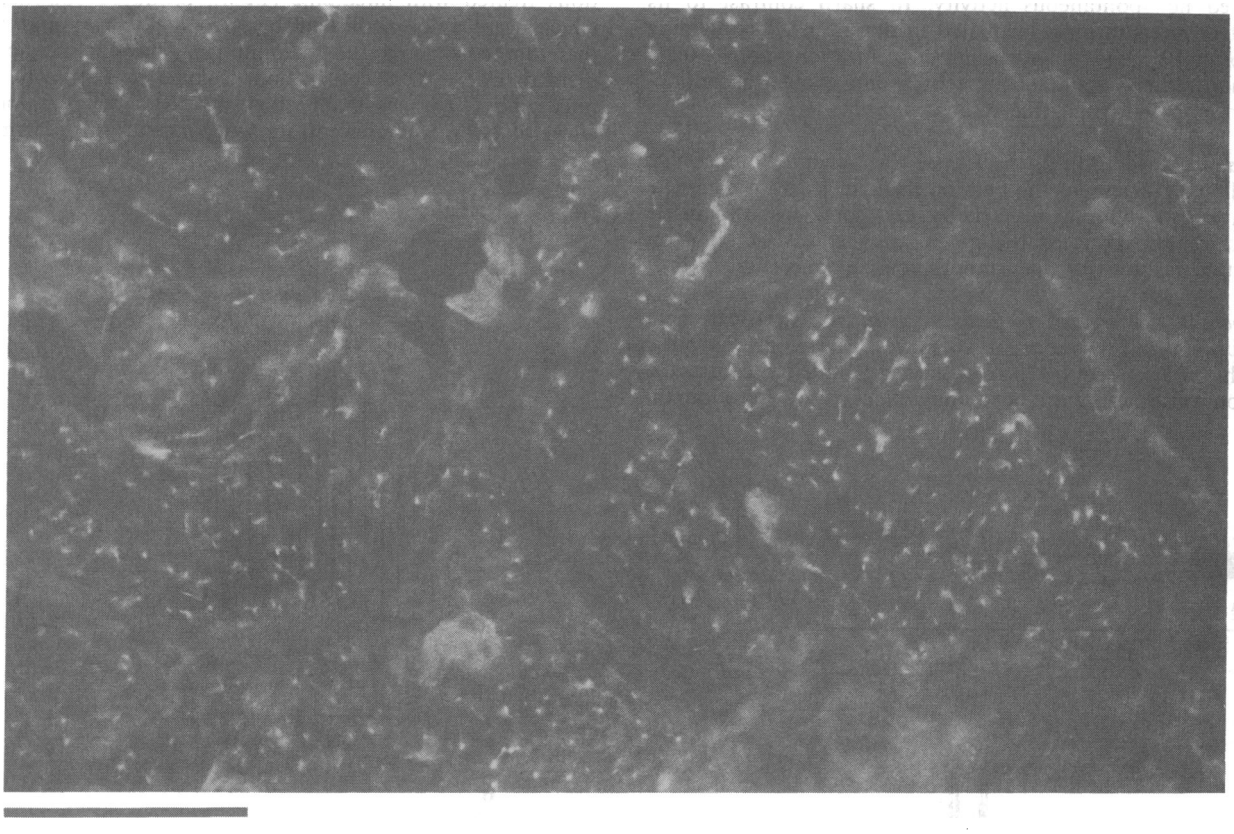

Figure 1 Neuropeptide Y (NPY) – immunofluorescence micrograph of the rat urinary bladder. NPY-immunoreactive nerve fibres and nerve endings are numerous and are mainly concentrated in the bundles of detrusor muscle cells. Scale bar = 50 μm.

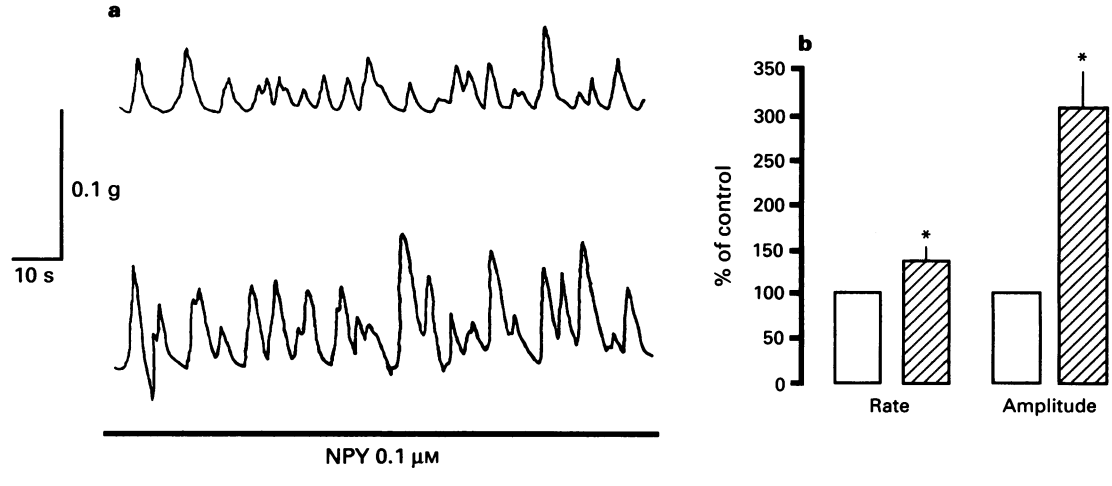

Figure 2 Effect of neuropeptide Y (NPY) on spontaneous activity of rat isolated detrusor muscle strip. (a) Record of spontaneous activity of a strip in the absence of NPY (upper panel) and after 10 min exposure to NPY 100 nM (lower panel). NPY potentiated both amplitude and frequency of spontaneous contractions. In (b) spontaneous activity is presented as histograms (open column = control; hatched column = NPY-treated) and quantified as % of control spontaneous activity prior to NPY exposure (mean ± s.e. mean; $*P < 0.05$; $n = 5$). The vertical scale shows tension in g force. The horizontal scale shows time.

Detrusor tone Addition of NPY to the bathing fluid caused a sustained rise in the smooth muscle tone accompanied with enhanced spontaneous activity. Elevation of tone by NPY was quantified by calculating the difference between stable resting tension before application of NPY and the maximum tension obtained after addition of NPY. Treatment with indomethacin (10 μM) alone (Figure 3b) or in combination with atropine (3 μM) did not prevent this effect of NPY. Tension generated by NPY 250 nM, in the presence and absence of indomethacin + atropine was respectively 0.23 ± 0.04 g force and 0.27 ± 0.05 g force (mean ± s.e. mean; $n = 5$, $P > 0.05$ Student's paired t test).

Absence of Ca^{2+} Detrusor incubated in Ca^{2+}-free Krebs, showed no spontaneous activity. In sharp contrast to its effect on preparations, incubated in normal Ca^{2+}-containing Krebs, NPY used in increasing concentrations upto 1.0 μM neither initiated spontaneous activity nor evoked a contractile response in Ca^{2+}-free Krebs.

Nifedipine Addition of the L-type Ca^{2+} channel antagonist, nifedipine (1.0 μM) to the bathing medium led to a complete cessation of spontaneous activity and some loss of muscle tone. It also abolished the potentiating effects of NPY on spontaneous activity and smooth muscle tone (Figure 3c).

Responses to electrical field stimulation Electrical field stimulation (EFS, trains of 20 pulses, 10 Hz, 0.1 ms pulse width, 30 V, 1 every 120 s) evoked reproducible contractile responses which could be readily blocked by tetrodotoxin (0.5 μM). NPY (0.25 μM) potentiated the contractile response to EFS. Tension generated by EFS was 1.6 ± 0.2 g force and 2.4 ± 0.4 g force (mean ± s.e. mean, $n = 7$, $P < 0.05$ Student's paired t test) respectively in the absence and presence of NPY. For studying the effect of NPY on cholinergic and non-cholinergic components of the contractile responses to EFS, each component was isolated by the use of selective blockers, atropine (3 μM) for blocking cholinergic component and nifedipine (1 μM) for blocking the non-cholinergic component (Iravani *et al.*, 1988; Bo & Burnstock, 1990; Zar *et al.*, 1990). The non-cholinergic component of the response to EFS, isolated by atropinisation was potentiated by NPY (Figure 4b). The degree of potentiation was not influenced by pulse frequency within the stimulus-trains. EFS of preparations treated with nifedipine (1 μM), produced contractions which were fully abolished by atropine (3 μM) and were therefore considered fully cholinergic. The cholinergic element in EFS-evoked contraction, isolated by treatment with nifedipine (1 μM), was inhibited by NPY. The inhibitory effect of NPY was concentration-dependent. An experiment

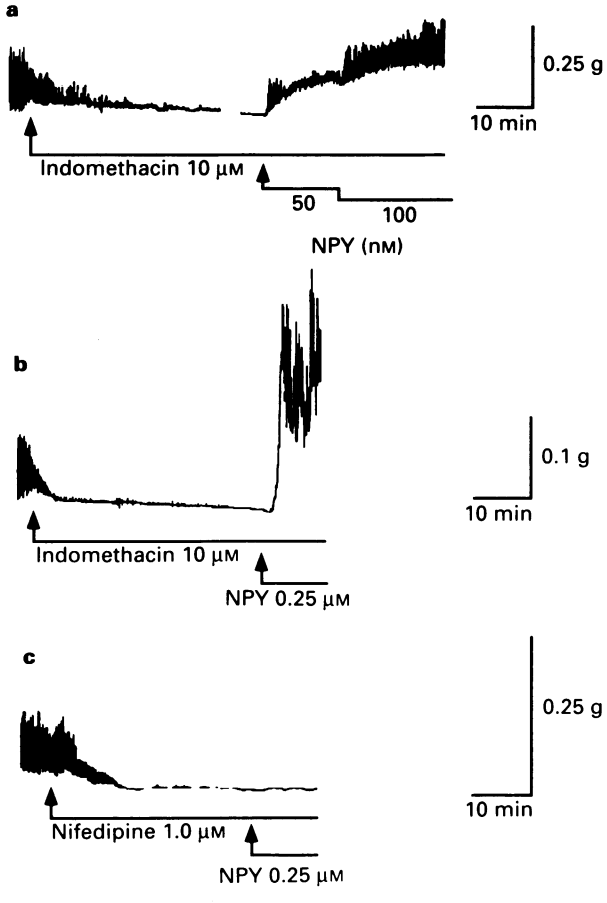

Figure 3 Rat isolated detrusor strip: The effect of indomethacin (a, b) and nifedipine (c) on the potentiation of detrusor muscle tone and spontaneous activity by neuropeptide Y (NPY). Note that although both indomethacin and nifedipine reduced or abolished spontaneous activity, only the latter prevented the effects of NPY on tone and spontaneous activity. The vertical scales show tension in g force. The horizontal scales show time.

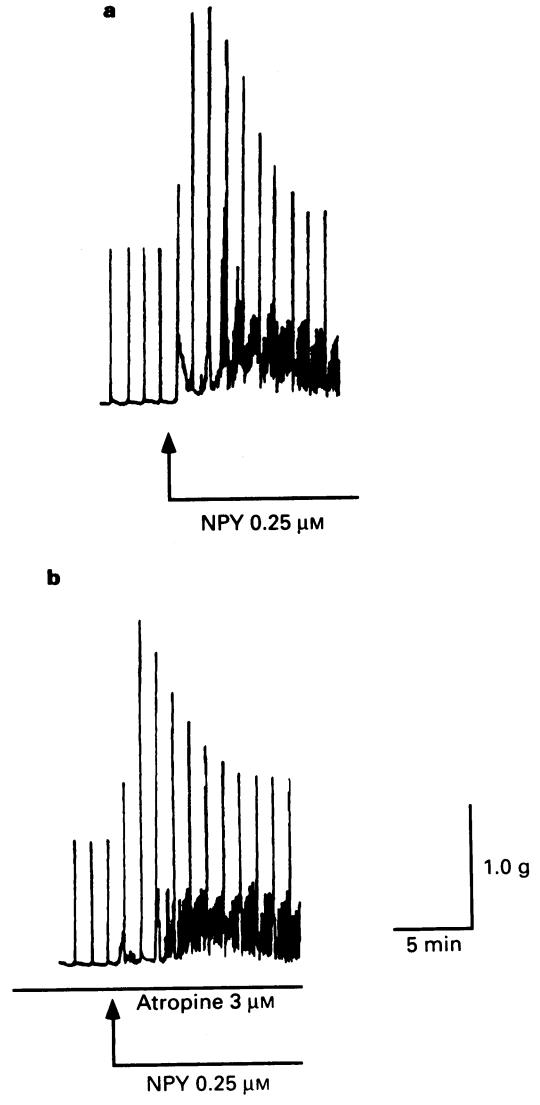

Figure 4 Rat isolated detrusor muscle strip: effect of neuropeptide Y (NPY) on contractions evoked by electrical field stimulation (EFS, train of 20 pulses, 0.1 ms pulses-duration, 2 Hz, 1 every min) in the absence (a) or presence (b) of atropine. In (b), the isolated preparation had been exposed to atropine, 3 μM for 30 min prior to the application of NPY. Note the potentiating effect of NPY on electrically-evoked contractions and its insensitivity to atropine. The vertical scale shows tension in g force. The horizontal scale shows time.

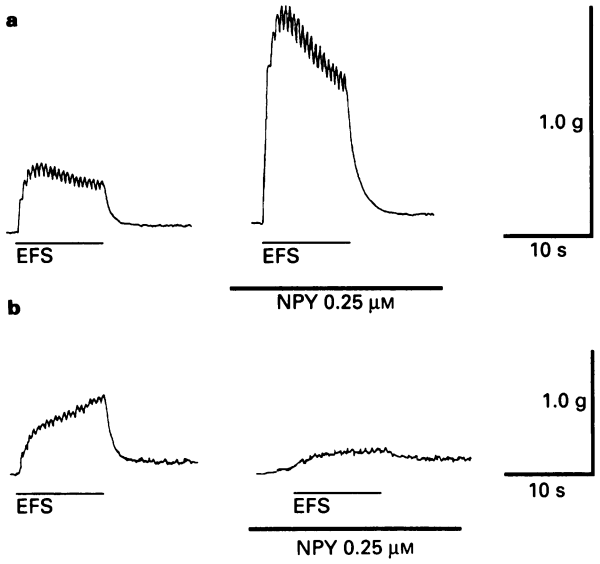

Figure 5 Rat isolated detrusor muscle strips: effect of neuropeptide Y (NPY) on contractions evoked by electrical field stimulation (EFS, train of 20 pulses at 2 Hz) and recorded on a fast time base using a storage oscilloscope. The contractions on the left in both (a) and (b) were evoked after 30 min exposure to atropine, 3 μM (a) or nifedipine, 1 μM (b) and represent stable, reproducible responses to EFS. Contractions on the right, in both panels were evoked by EFS after 5 min pretreatment with NPY (0.25 μM) in the continued presence of atropine (a) or nifedipine (b). Note the contrasting effects of NPY on electrically-evoked responses in the presence of atropine or nifedipine. The vertical scale shows tension in g force. The horizontal scale shows time.

showing the contrasting effects of NPY (0.25 μM), inhibitory on cholinergic and potentiating on non-cholinergic motor transmission is presented in Figure 5. The effect of NPY (0.25 μM) was also ascertained on cholinergic responses to different frequencies of EFS (10 s bursts of pulses at 1, 4, 8, 16, 32 and 64 Hz all at 0.1 ms pulse width). The cholinergic response to EFS, as earlier demonstrated (Zar *et al.*, 1990), was biphasic and both phases of the response were reduced by NPY (Figure 6a). The reduction was greatest at the lowest frequency (1 Hz) and declined with increasing stimulus frequency, being least at 64 Hz (Figure 7).

Acetylcholine- and α,β-MeATP-evoked contractions Submaximal contractions of the detrusor were evoked by ACh (10 μM) before and during exposure to NPY (0.5 μM). The presence of NPY had no obvious effect on the tension generated by ACh (Figure 8a). Identical results were obtained on repeating the experiment in the concurrent presence of nifedipine (1 μM) (Figure 8b).

Submaximal contractions of the detrusor were evoked by α,β-MeATP (1 μM; 45 s exposure-duration). The contractions were reproducible if 10 min or longer intervals were allowed between successive exposures. Pretreatment for 5 min with NPY (0.25 μM) potentiated the α,β-MeATP contraction by 110 ± 15% (mean ± s.e. mean; $n = 3$; $P < 0.05$).

Discussion

The present finding of a rich presence of NPY-containing fibres in rat detrusor confirms an earlier similar report by

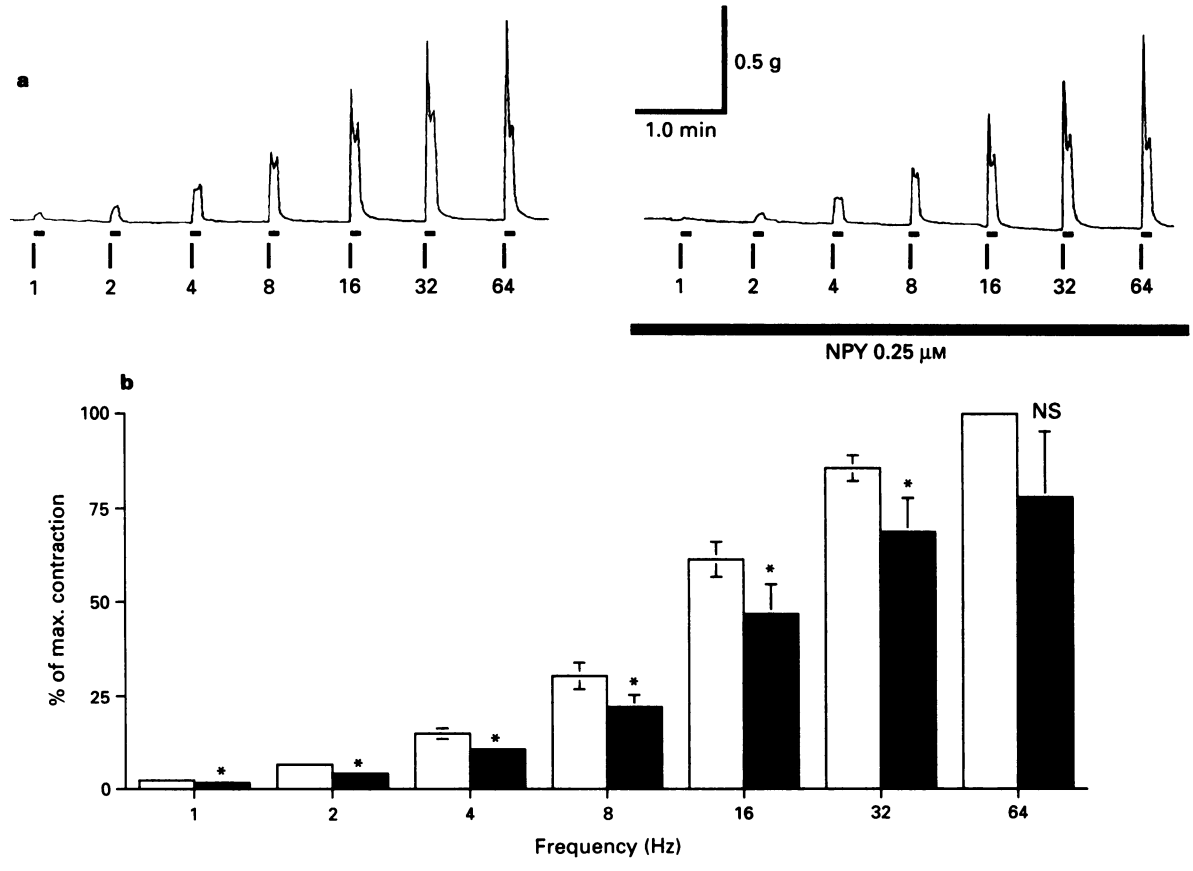

Figure 6 Rat isolated detrusor muscle: cholinergic contractile responses to different frequencies of electrical field stimulation (EFS, 1, 2, 4, 8, 16, 32 and 64 Hz; 10 s every min) in the absence (a: left panel; b: open columns) or presence of neuropeptide Y (NPY) 0.25 μM (a: right panel; b: solid columns). Bathing medium contained nifedipine (1 μM) throughout the duration of experiment. In (a), the actual contractile responses of a single experiment is shown. In (b), the contractions are expressed as a percentage of the maximal contractile response at 64 Hz in the absence of NPY (mean ± s.e. mean; $n = 7$). The response in the presence of NPY has been compared with its corresponding control response at each frequency and the level of significant difference from the control response has been expressed as $^*P < 0.05$; NS = not significant, Student's t test. The vertical scale shows tension in g force. The horizontal scale shows time.

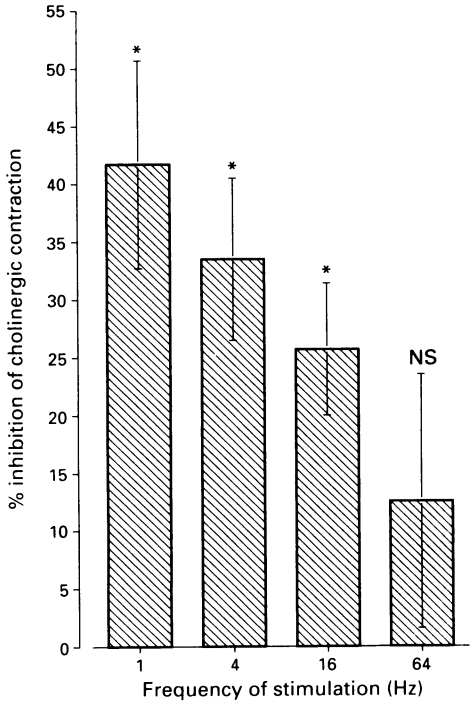

Figure 7 Rat isolated detrusor muscle preparation: histograms showing frequency-dependent inhibition of cholinergic responses to electrical field stimulation (EFS, 1, 2, 4, 16 and 64 Hz, 10 s, at 1 min intervals) by neuropeptide Y (NPY, 0.25 μM). Bathing fluid contained nifedipine (1 μM) throughout the duration of the experiment. Each histogram represents mean % inhibition of the response to EFS by NPY (0.25 μM) at a given frequency (indicated by the subscript) and the vertical bars indicate s.e. mean ($n = 7$). $^*P < 0.05$ vs. control; NS = not significant; Student's t test.

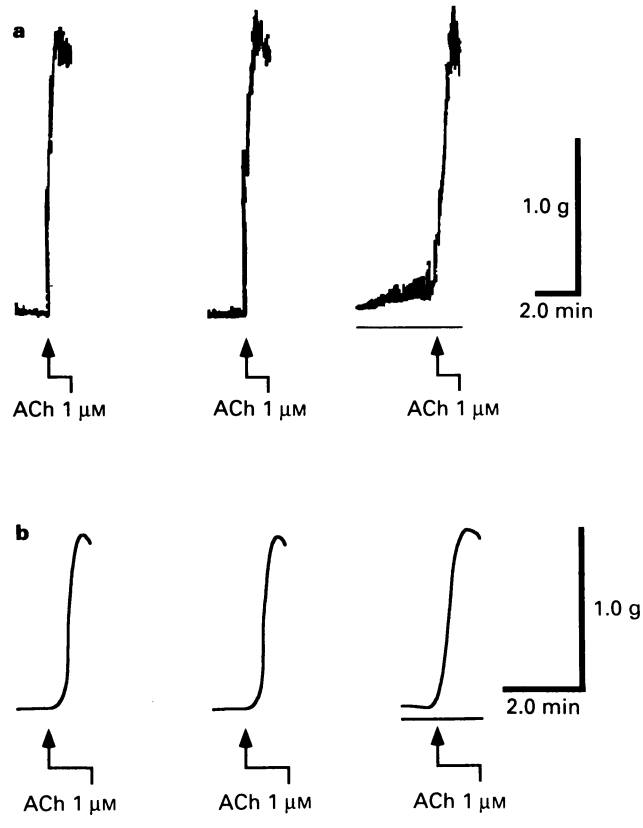

Figure 8 Effect of neuropeptide Y (NPY) on acetylcholine (ACh)-evoked contractions of rat isolated detrusor, in the absence (a) or in the presence (b) of nifedipine, 1 μM. The preparations were exposed to ACh, 1 μM (at arrows) for 1 min at 5 min interval and 4 min before the last response to ACh, NPY 0.25 μM (indicated by the thick line) was added to the bathing fluid. The vertical scale shows tension in g force. The horizontal scale shows time.

Mattiasson *et al.* (1985). In agreement with Mattiasson *et al.* (1985), we have also noticed no decrease in the number of NPY-immunoreactive fibres of rat detrusor after 6-OHDA treatment. Insensitivity of NPY-immunoreactive fibres to 6-OHDA implies that the vast majority of these fibres are not adrenergic. This conclusion is in keeping with the knowledge that in the rat bladder, the adrenergic nerve supply is concentrated in the trigone and the rest of the detrusor has a sparse adrenergic innervation (El-Badawi & Schenk, 1966; Alm & Elmer, 1975), since the combination of sparseness of adrenergic innervation and the abundance of NPY-innervation is obviously inconsistent with the presence of NA in all NPY-containing nerve fibres. The findings of Nagata *et al.* (1987) showing a failure of 6-OHDA treatment to reduce substantially the NPY content of the bladder also points towards a similar conclusion. It appears therefore that autonomic innervation of the rat detrusor is atypical, although not unique, from other peripheral organs, in having an NPY-innervation largely independent of adrenergic innervation. It remains to be established whether NPY is present in the detrusor nerve terminals on its own or in the company of some other neurotransmitters. In the mammalian detrusor, nerves containing ACh, ATP, substance P (SP), and vasoactive intestinal polypeptide (VIP) are known to be present. It is unlikely that NPY is co-localised with SP since complete disappearance of SP innervation by chronic capsaicin treatment has been reported to have no effect on NPY-innervation (Mattiasson *et al.*, 1985). Its possible co-localization with ACh, ATP or VIP remains to be investigated.

The presence of NPY-innervation in the detrusor raises the obvious question of its physiological role in this tissue. In our experiments NPY increased the level of spontaneous activity of the detrusor. In concentrations greater than 0.25 μM, it contracted the detrusor. We do not know whether the concentration of endogenously released NPY following its release reaches this level in the vicinity of its smooth muscle activating sites. Samson & Harris (1992) have calculated that a synaptic neurotransmitter concentration of 1000 μM is a reasonable estimate. If Samson & Harris's estimate of synaptic neurotransmitter concentration applies to NPY in the rat detrusor, our results indicate that NPY would be a powerful physiological contractile agent in this tissue.

It is now generally agreed that the detrusor of the rat, in common with many other mammalian species, has a dual motor transmission system comprising a cholinergic and a non-cholinergic component (Ambache & Zar, 1970; Burnstock *et al.*, 1972; Brading & Williams, 1990). In the present investigation, nifedipine a blocker of L-type Ca^{2+} channels abolished the contractile action of NPY as well as its potentiating action on spontaneous activity. It indicates that NPY, presumably through the induction of some membrane depolarization, activated voltage-sensitive Ca^{2+} channels and evoked contraction and potentiation of spontaneous activity through Ca^{2+} influx. This interpretation is supported by the loss of the NPY effect in Ca^{2+}-free medium. Nifedipine has been shown to block preferentially the non-cholinergic component of motor transmission in rat detrusor (Iravani *et al.*, 1988; Bo & Burnstock, 1990; Zar *et al.*, 1990). It has been observed that the contractions of guinea-pig and rat detrusor by ATP are also dependent upon the presence of extracellular Ca^{2+} (Iacovou *et al.*, 1988) and are antagonized by nifedipine (Katsuragi *et al.*, 1990; Bo & Burnstock, 1990). Evidently, both ATP and NPY share the property of acting through a nifedipine-sensitive, Ca^{2+}-transferring mechanism to evoke

their effects on the detrusor and it is, therefore, not surprising that NPY potentiated the contractions evoked by stimulation of purinoceptors. There is already strong evidence for ATP as the non-cholinergic motor transmitter in the rodent detrusor (Brown *et al.*, 1979; Kasakov & Burnstock, 1983; Hoyle & Burnstock, 1985; Fujii, 1988; Brading & Mostwin, 1989; Brading & Williams, 1990). On the other hand the possibility that ATP might not be the sole non-cholinergic motor transmitter is supported by partial persistence of tetrodotoxin (TTX)-sensitive contractile response after atropinisation and ATP-desensitization (Choo & Mitchelson, 1980; Luheshi & Zar, 1990; Creed *et al.*, 1991; Maggi, 1991; Parija *et al.*, 1991). The results also show that exogenous NPY potentiated the non-cholinergic motor transmission. The potentiation of non-cholinergic motor transmission by NPY appeared to be selective since it did not affect ACh-evoked contractions. Our observations that NPY contracts detrusor, potentiates non-cholinergic motor transmission and is present in abundance in the nerve-supply to the detrusor together with the finding that its effect is mediated by Ca^{2+} influx through nifedipine-sensitive channels, as is the effect of non-cholinergic motor transmitter(s), lead us to propose that NPY serves as a motor transmitter in addition to ATP in the rat detrusor. This proposal also explains why nifedipine, unlike purinoceptor-desensitization, invariably and readily blocks completely the non-cholinergic motor transmission since both ATP and NPY evoke contractions by activating voltage-operated Ca^{2+}-channels.

NPY exerted an inhibitory influence on cholinergic motor transmission. This effect of NPY is evidently prejunctional since ACh-evoked contractions were not inhibited by NPY. Prejunctional inhibition of neurotransmitter release by NPY is a very well documented phenomenon (Wahlestedt *et al.*, 1986; Edvinsson *et al.*, 1987; Westfall *et al.*, 1990; Michel, 1991) and its inhibitory effect on the cholinergic motor transmission in rat detrusor provides another example of this action.

The effect of NPY on spontaneous mechanical activity also deserves some discussion. Isolated detrusor strips from mammalian species, so far investigated, all exhibit a varying degree of spontaneous mechanical contractions (Sibley, 1984; Brading, 1987). The spontaneous activity is not inhibited by exposure to atropine, TTX and hexamethonium or by purinoceptor desensitization, giving rise to the suspicion that it is likely to be myogenic and not nerve-mediated. In our experiments, the spontaneous mechanical activity was abolished by nifedipine or withdrawal of Ca^{2+} from the bathing medium, suggesting that entry of extracellular Ca^{2+} across the cell membrane through voltage-sensitive Ca^{2+} channels is needed. NPY potentiated the frequency and amplitude of spontaneous activity through a prostaglandin- and acetylcholine-independent mechanism. The failure of NPY to initiate spontaneous activity after nifedipine-exposure or in Ca^{2+}-free medium makes it tempting to speculate that spontaneous release of intrinsic NPY from nerves may be involved in the genesis of spontaneous mechanical activity. In our experiments, the potentiation of spontaneous activity by NPY was not prevented by purinoceptor-desensitization suggesting that the effect of NPY on spontaneous activity is not mediated by ATP. An enhancing effect of α,β-MeATP on spontaneous activity in rat detrusor has been known (Luheshi & Zar, 1990). This effect of α,β-MeATP is resistant to purinoceptor-desensitization and treatment with atropine and indomethacin (Luheshi & Zar, 1990). The potentiation of spontaneous activity by NPY, also through a mechanism independent of purinoceptor-desensitization raises the possibility that the enhancing effect of α,β-MeATP on spontaneous activity might be mediated through the release of endogenous NPY.

In conclusion, the present investigation has demonstrated a rich presence of NPY-innervation in the rat urinary bladder. NPY-innervation is non-adrenergic and is almost exclusively localized within detrusor muscle bundles. The results are consistent with the proposal that NPY-containing innervation is involved in the motor transmission of the detrusor muscle, NPY acting as a non-cholinergic motor transmitter. The results also raise the possibility that spontaneous release of intrinsic NPY is responsible for spontaneous mechanical activity of the detrusor muscle.

References

ALM, P. & ELMER, M. (1975). Adrenergic and cholinergic innervation of the rat urinary bladder. *Acta Physiol. Scand.*, **94**, 36–45.

AMBACHE, N. & ZAR, M.A. (1970). Non-cholinergic transmission by postganglionic motor neurons in the mammalian bladder. *J. Physiol.*, **210**, 761–783.

BO, X. & BURNSTOCK, G. (1990). The effect of Bay K8644 and nifedipine on the responses of rat urinary bladder to electrical field stimulation, β,γ-methylene ATP and acetylchoine. *Br. J. Pharmacol.*, **101**, 494–498.

BRADING, A.E. (1987). The physiology of bladder smooth muscle. In *The Physiology of The Lower Urinary Tract*. ed. Torrens, M. & Morrison, J. pp. 161–191. Berlin: Springer-Verlaag.

BRADING, A.F. & MOSTWIN, J.L. (1989). Electrical and mechanical responses of guinea-pig bladder muscle to nerve stimulation. *Br. J. Pharmacol.*, **98**, 1083–1090.

BRADING, A.F. & WILLIAMS, J.F. (1990). Contractile responses of smooth muscle strips from rat and guinea-pig urinary bladder to transmural stimulation: effects of atropine and α,β-methylene ATP. *Br. J. Pharmacol.*, **99**, 493–498.

BROWN, C., BURNSTOCK, G & COCKS, T. (1979). Effects of adenosine 5′-triphosphate (ATP) and β-γ-methylene ATP on the rat urinary bladder. *Br. J. Pharmacol.*, **65**, 97–102.

BURNSTOCK, G., DUMSDAY, B. & SMYTHE, A. (1972). Atropine resistant excitation of the urinary bladder: the possibility of transmission via nerves releasing a purine nucleotide. *Br. J. Pharmacol.*, **44**, 457–461.

CHOO, L.K. & MITCHELSON, F. (1980). The effect of indomethacin and adenosine 5′-triphosphate on excitatory innervation of the rat urinary bladder. *Can. J. Pharmacol.*, **58**, 1042–1048.

CREED, K.E., ITO, Y. & KATSUYAMA, H. (1991). Neuorotransmission in the urinary bladder of rabbits and guinea pigs. *Am. J. Physiol.*, **261**, C271–C277.

EDVINSSON, L., HAKANSSON, R., WAHLESTEDT, C. & UDDMANN, R. (1987). Effects of neuropeptide Y on the cardiovascular system. *Trends Pharmacol. Sci.*, **8**, 231–235.

EL-BADAWAI, A. & SCHENK, E.A. (1966). Dual innervation of the mammalian urinary bladder. A histochemical study of the distribution of cholinergic and adrenergic nerves. *Am. J. Anat.*, **119**, 405–428.

FUJII, K. (1988). Evidence for adenosine triphosphate as an excitatory transmitter in guinea-pig, rabbit and pig urinary bladder. *J. Physiol.*, **404**, 39–52.

GU, J., BLANK, M.A., HUANG, W.M., ISLAM, K.N., MCGREGOR, G.P., CHRISTOFIDES, N., ALLEN, J.M., BLOOM, S.R. & POLAK, J.M. (1984). Peptide containing nerves in human urinary bladder. *Urology*, **24**, 353–357.

HOYLE, C.H.V. & BURNSTOCK, G. (1985). Atropine resistant excitatory junction potentials in rabbit bladder are blocked by α,β-methyl ATP. *Eur. J. Pharmacol.*, **114**, 239–240.

IACOVOU, J.W., HILL, S.J. & BIRMINGHAM, A.T. (1988). Involvement of extracellular calcium in agonist-induced contraction of the guinea-pig detrusor. *Br. J. Pharmacol.*, **95**, 484P.

IRAVANI, M.M., LUHESHI, G.N. & ZAR, M.A. (1988). Inhibition of non-cholinergic motor transmission in isolated rat urinary bladder by nifedipine. *J. Physiol.*, **410**, 69P.

IRAVANI, M.M. & ZAR, M.A. (1988). Evidence for neuropeptide Y (NPY) as the probable non-cholinergic motor transmitter in rat urinary bladder *in vitro*. *J. Physiol.*, **403**, 61P.

KASAKOV, L. & BURNSTOCK, G. (1983). The use of slowly degradable analog, α,β-methylene ATP, to produce desensitisation of the P_2-purinoceptors: effect on non-adrenergic, non-cholinergic responses of the guinea-pig urinary bladder. *Eur. J. Pharmacol.*, **86**, 291–294.

KATSURAGI, T., USUNE, S. & FURUKAWA, T. (1990). Antagonism by nifedipine of contraction and Ca^{2+}-influx evoked by ATP in guinea-pig urinary bladder. *Br. J. Pharmacol.*, **185,** 203–208.

LUHESHI, G.N. & ZAR, M.A. (1990). Purinoceptor desensitisation impairs but does not abolish the non-cholinergic motor transmission in rat isolated urinary bladder. *Eur. J. Pharmacol.*, **185,** 203–208.

MAGGI, C.A. (1991). Omega conotoxin and prejunctional modulation of the biphasic responses of the rat isolated urinary bladder to single pulse electrical field stimulation. *J. Autonom. Pharmacol.*, **11,** 295–304.

MATTIASSON, A., EKBLAAD, E., SUNDLER, F. & UVELIUS, B. (1985). Origin and distribution of neuropeptide Y-, vasoactive intestinal polypeptide- and substance P-containing nerve fibres in the urinary bladder of the cat. *Cell Tissue Res.*, **239,** 141–146.

MICHEL, M.C. (1991). Receptors for neuropeptide Y: multiple subtypes and multiple second messengers. *Trends Pharmacol. Sci.*, **12,** 389–394.

NAGATA, M., FRANCO-CERECEDA, A., SARIA, A., AMANN, R. & LUNDBERG, J.M. (1987). Reserpine induced depletion of neuropeptide Y in the guinea-pig: tissue-specific effects and mechanism of action. *J. Auton. Nerv. Syst.*, **20,** 257–263.

PARIJA, S.C., RAVIPRAKASH, V. & MISHRA, S.K. (1991). Adenosine- and α,β-methylene ATP-induced differential inhibition of cholinergic and non-cholinergic neurogenic responses in rat urinary bladder. *Br. J. Pharmacol.*, **102,** 396–400.

POLAK, J.M. & VAN NOORDEN, S. (1986). *Immunocytochemistry.* London: John Wright.

SAMSON, H.H. & HARRIS, R.A. (1992). Neurobiology of alcohol abuse. *Trends Pharmacol. Sci.*, **13,** 206–211.

SIBLEY, G.N.A. (1984). A comparison of spontaneous and nerve-mediated activity in bladder muscle from man, pig, and rabbit. *J. Physiol.*, **354,** 431–443.

WAHLESTEDT, C., YANAIHARA, N. & HAKANSON, R. (1986). Evidence for different pre- and postjunctional receptors for neuropeptide Y and related peptides. *Regul. Peptides*, **13,** 307–318.

WESTFALL, T.C., CHEN, X., CIARLEGLIO, A., HENDERSON, K., DEL VALLE, K., CURFMAN-FALVEY, M. & NAES, L. (1990). In vitro effects of neuropeptide Y at vascular neuro-effector junction. *Ann. N.Y. Acad. Sci.*, **611,** 145–155.

ZAR, M.A., IRAVANI, M.M. & LUHESHI, G.N. (1990). Effect of nifedipine on the contractile responses of the isolated rat bladder. *J. Urol.*, **143,** 835–839.

(Received February 24, 1994
Revised May 14, 1994
Accepted May 18, 1994)

Br. J. Pharmacol (1994), **113**, 103–110

The effect of caffeine on prostaglandin output from the guinea-pig uterus

E.K. Naderali & [1]N.L. Poyser

Department of Pharmacology, University of Edinburgh Medical School, 1 George Square, Edinburgh EH8 9JZ

1 Caffeine increased the outputs of prostaglandin $F_{2\alpha}$ ($PGF_{2\alpha}$), PGE_2 and 6-keto-$PGF_{1\alpha}$ from the guinea-pig uterus on days 7 and 15 of the oestrous cycle. The effect on PGE_2 output depended on the age of the animals and was absent in younger guinea-pigs (<4 months). Theophylline also stimulated the outputs of $PGF_{2\alpha}$ and 6-keto-$PGF_{1\alpha}$, but not the output of PGE_2, from the day 7 guinea-pig uterus.

2 The stimulatory effects of caffeine on the outputs of $PGF_{2\alpha}$, PGE_2 and 6-keto-$PGF_{1\alpha}$ from the guinea-pig uterus were not prevented by lack of extracellular calcium, ryanodine or ruthenium red (both inhibitors of calcium release via the ryanodine receptor), although the increase in $PGF_{2\alpha}$ output tended to be slower when extracellular calcium was absent. Also, ryanodine flattened and broadened the peak of increased $PGF_{2\alpha}$ release.

3 The calmodulin antagonists, W-7 and trifluoperazine, had no inhibitory effect on the caffeine-stimulated increases in uterine prostaglandin output. In fact, W-7 (but not trifluoperazine) greatly potentiated the action of caffeine on uterine $PGF_{2\alpha}$ output, but had little or no potentiating effect on the action of caffeine on uterine PGE_2 and 6-keto-$PGF_{1\alpha}$ outputs.

4 TMB-8, an intracellular calcium antagonist, inhibited the increase in $PGF_{2\alpha}$ output produced by caffeine without preventing the increases in outputs of PGE_2 and 6-keto-$PGF_{1\alpha}$.

5 These studies suggest that caffeine stimulates uterine $PGF_{2\alpha}$ synthesis and release by a mechanism dependent upon intracellular calcium, but this mechanism is not mediated by activation of any of the three well-characterized ryanodine receptors or by calmodulin. Furthermore, the increases in the synthesis and release of PGE_2 and 6-keto-$PGF_{1\alpha}$ in the guinea-pig uterus induced by caffeine appear to involve mechanism(s) different from that which stimulates $PGF_{2\alpha}$ production.

Keywords: Caffeine; prostaglandins; uterus; ryanodine; ruthenium red; TMB-8; trifluoperazine, W-7; theophylline

Introduction

Prostaglandins produced by the uterus are involved in several reproductive processes. In many non-primate mammalian species, increased prostaglandin $F_{2\alpha}$ ($PGF_{2\alpha}$) production by the endometrium is responsible for terminating the life-span of the corpus luteum and thereby regulating the length of an oestrous cycle or a pseudopregnancy and, in some species, a pregnancy (see Horton & Poyser, 1976; Poyser, 1981). In women, there is an increase in the amounts of $PGF_{2\alpha}$ and, to a lesser extent, PGE_2 produced by the endometrium at menstruation (see Poyser, 1981). Since prostaglandins contract the uterus and affect the vasculature, it is assumed that they have a role in the menstrual process. An overproduction of $PGF_{2\alpha}$ by the endometrium is the probable cause of dysmenorrhoea (Lundström *et al.*, 1976), whereas an imbalance of uterine prostaglandin production in favour of prostacyclin (PGI_2) may be the cause of menorrhagia (Smith *et al.*, 1981). The reasons for these disorders of menstruation are unknown, but may be due to intrinsic factors, such as the higher than normal production of endogenous hormones which affect uterine prostaglandin synthesis (e.g. vasopressin; Åkerlund *et al.*, 1979), or to extrinsic factors (e.g. dietary substances).

Previous experiments in the rat, guinea-pig and man have shown that increased endometrial prostaglandin synthesis is associated with increased activity of phospholipase A_2, a calcium-dependent enzyme (Dey *et al.*, 1982; Downing & Poyser, 1983; Bonney, 1985). In the guinea-pig, it was considered that the activation of phospholipase A_2 by calcium (Downing & Poyser, 1983) leads to the release of arachidonic acid from phosphatidylcholine and phosphatidylethanolamine (Ning & Poyser, 1984) which, in turn, results in increased $PGF_{2\alpha}$ synthesis by and release from the endometrium. Subsequent studies in the guinea-pig indicated that increased uterine prostaglandin production is dependent upon the release of intracellular calcium (Riley & Poyser, 1987a; Leckie & Poyser, 1990; Johnson & Poyser, 1991). However, there is no increase in inositol turnover in the guinea-pig endometrium at the end of the oestrous cycle when $PGF_{2\alpha}$ synthesis is high (Ning & Poyser, 1984). This finding indicates that the stimulation of endometrial $PGF_{2\alpha}$ synthesis is not dependent on the generation of inositol-1,4,5-trisphosphate (IP_3) and, therefore, does not involve the release of calcium from an IP_3-sensitive store.

Studies on several cell types have indicated that only part of the calcium stored in the endoplasmic reticulum is IP_3-sensitive and there is another store of calcium which can be released by caffeine. This latter pool of calcium was first described in skeletal and cardiac muscle. The release of calcium from this pool is modulated by ryanodine, and the receptors involved are called ryanodine receptors. Initial studies indicated that there were two types of the receptor; Types 1 and 2 are found in skeletal and cardiac muscle, respectively. Ryanodine can cause an initial release of calcium and then blocks the action of caffeine. Ruthenium red inhibits the calcium-releasing action of caffeine at the level of the ryanodine receptor. Ryanodine receptor Types 1 and 2 are not exclusively confined to skeletal and cardiac muscle and are present in other tissues. In addition, it is now clear that there are more than two types of ryanodine receptor (see Sorrentino & Volpe, 1993). Consequently, since caffeine (a dietary substance) releases calcium from various cell types and since uterine prostaglandin production is calcium-dependent, the effect of caffeine on uterine prostaglandin production in the guinea-pig has been investigated. As the initial experiments showed that caffeine does stimulate uterine pro-

[1] Author for correspondence.

staglandin synthesis and release, further experiments were performed to investigate some of the mechanisms by which caffeine may exert this stimulatory effect.

Methods

Procedures

Fifty-two virgin, Dunkin-Hartley guinea-pigs (600–900 g) were examined daily and a vaginal smear was taken when the vagina was open. Day 1 of the cycle was taken as the day preceding the post-ovulatory influx of leucocytes when cornification was at a maximum. All guinea-pigs had exhibited at least two cycles of normal length (about 16–17 days) before being killed (by stunning and incising the neck) on day 7 or day 15 of the cycle. Each uterus was removed and separated into its two uterine horns. The uterine horns were weighed, 'opened' by cutting longitudinally and suspended in an organ bath with one end attached to a lever so that isometric contractions of the uterus were observed. Each uterine horn was superfused with Krebs solution (5 ml min^{-1}) at 37°C, as described by Poyser & Brydon (1983), and was superfused initially for a settling period of 60 min. Samples of superfusate were then collected for 10-min periods over the next 80 min (i.e. 8 samples per uterine horn) in experiments 1, 2 and 8, and over 100 min (i.e. 10 samples per uterine horn) in experiments 3 to 7. The uterine horns in each experiment were treated as described below.

Treatments

In expt 1, caffeine (10 mmol l^{-1}) was present in the Krebs solution superfusing one uterine horn from each of five animals on day 7 of the oestrous cycle and from five animals on day 15 of the cycle during the collection of samples 4 and 5. The other uterine horn from each animal was untreated. In expt 2, one uterine horn from each of five animals on day 7 of the cycle was superfused with normal Krebs solution and the other uterine horn was superfused with Krebs solution from which the calcium chloride had been omitted (calcium-depleted Krebs solution). Caffeine (10 mmol l^{-1}) was present in both types of Krebs solution during the collection of samples 4 and 5.

In experiments 3 to 7, both uterine horns from 4 or 5 guinea-pigs on day 7 of the cycle were superfused with normal Krebs solution, and caffeine (10 mmol l^{-1}) was present in the solution superfusing both uterine horns during the collection of samples 6 and 7. The following additions were made to the Krebs solution superfusing one uterine horn from each animal during the collection of samples 4 to 7: Expt 3: 8-(N,N-diethylamino)octyl-3,4,5-trimethoxybenzoate hydrochloride (TMB-8; an intracellular calcium antagonist, Malagodi & Chiou, 1974; 150 μmol l^{-1}; $n = 5$); Expt 4: Ryanodine (2, 20 or 200 μmol l^{-1}; $n = 4$); Expt 5: Ruthenium red (10 or 100 μmol l^{-1}; $n = 4$); Expt 6: N-(6-aminohexyl)-5-chloro-1-naphthalene-sulphonamide (W-7; a calmodulin antagonist, Hidaka *et al.*, 1978; 150 μmol l^{-1}; $n = 4$). Expt 7: Trifluoperazine (a calmodulin antagonist, Levin & Weiss, 1977; 100 μmol l^{-1}; $n = 4$).

In experiments 6 and 7, the concentrations of W-7 and trifluoperazine used had previously been shown to be sufficient to inhibit the increase in $PGF_{2\alpha}$ output induced by A23187 from the guinea-pig uterus (Poyser, 1985a,b).

In expt 8, both uterine horns from each of four animals on day 7 of the cycle were superfused with normal Krebs solution, and theophylline (10 mmol l^{-1}) was present in the Krebs solution superfusing one uterine horn from each animal during the collection of samples 4 and 5.

Solutions of each compound were freshly made up in Krebs solution before use, except for ryanodine. A concentrated solution of ryanodine was prepared in ethanol and stored at −20°C. The appropriate concentration of ryanodine in Krebs solution was prepared by adding up 0.25 ml of the ethanolic solution to 250 ml Krebs solution. Krebs solution superfusing the control uterine horn during the same time period contained an equivalent concentration of ethanol.

Assays

After collection, the pH of each sample was lowered to 4.0 with 1 M HCl and the prostaglandins were extracted by shaking twice with 50 ml ethyl acetate. The two ethyl acetate fractions were combined and evaporated to dryness on a rotary evaporator. The recoveries of $PGF_{2\alpha}$ and PGE_2 by this method are >90% and the recovery of 6-keto-$PGF_{1\alpha}$ by this method is >80% (Poyser & Scott, 1980; Swan & Poyser, 1983). Each dried extract was re-dissolved in 10 ml ethyl acetate and stored at −20°C. The amounts of $PGF_{2\alpha}$, PGE_2 and 6-keto-$PGF_{1\alpha}$ present in each sample were measured by radioimmunoassay using antibodies raised in this laboratory; the cross-reactivities have been reported elsewhere (Poyser, 1987). The intra-assay coefficients of variation were <12% for all three assays. The inter-assay coefficients of variation were 19.9%, 11.5% and 18.8% for the $PGF_{2\alpha}$, PGE_2 and 6-keto-$PGF_{1\alpha}$ assays, respectively. The detection limit was 20–40 pg per assay tube. Since prostaglandins are not stored in the guinea-pig uterus (Poyser, 1972), prostaglandin release into the superfusing fluid reflects fresh prostaglandin synthesis particularly as their release is inhibited by indomethacin (Poyser, 1985b).

Sources of material

Caffeine, ruthenium red, TMB-8, W-7, trifluoperazine and theophylline were purchased from Sigma Chemical Co., Poole, Dorset; ryanodine was purchased from Calbiochem-Novabiochem, Nottingham.

Statistical tests

Changes in the output of prostaglandins with time were analysed by Duncan's multiple range test. Other comparisons were made using Student's t test, or if the variances of the two groups were significantly different by the Variance ratio F test, by a modified t test for unequal variances (see Steel & Torrie, 1980).

Results

Caffeine significantly ($P < 0.05$) increased the outputs of $PGF_{2\alpha}$ and 6-keto-$PGF_{1\alpha}$ from the day 7 and day 15 guinea-pig uterus, and of PGE_2 from the day 15 uterus (Figure 1). Caffeine significantly ($P < 0.05$) increased the outputs of $PGF_{2\alpha}$, PGE_2 and 6-keto-$PGF_{1\alpha}$ from day 7 guinea-pig uterine horns superfused with calcium-containing or calcium-depleted Krebs solution. However, the stimulatory effect of caffeine on $PGF_{2\alpha}$ output tended to be reduced during the first 10 min period of treatment in calcium-depleted Krebs solution compared to normal Krebs solution (Figure 2). TMB-8 caused small, but significant ($P < 0.05$) increases in the outputs of $PGF_{2\alpha}$, PGE_2 and 6-keto-$PGF_{1\alpha}$ from the day 7 guinea-pig uterus, an effect reported previously (Poyser, 1985a). However, TMB-8 prevented the increase in $PGF_{2\alpha}$ output produced by caffeine without preventing the increases in outputs of PGE_2 and 6-keto-$PGF_{1\alpha}$ induced by caffeine (Figure 3).

Ryanodine alone had no effects on the outputs of $PGF_{2\alpha}$ and PGE_2 from the day 7 guinea-pig uterus, although ryanodine (20 and 200 μmol l^{-1}) significantly ($P < 0.05$) increased the output of 6-keto-$PGF_{1\alpha}$. Ryanodine (2 to 200 μmol l^{-1}) did not inhibit the increase in outputs of $PGF_{2\alpha}$ and 6-keto-$PGF_{1\alpha}$ induced by caffeine from the day 7 guinea-pig uterus (Figure 4). However, ryanodine (20 and 200 μmol l^{-1})

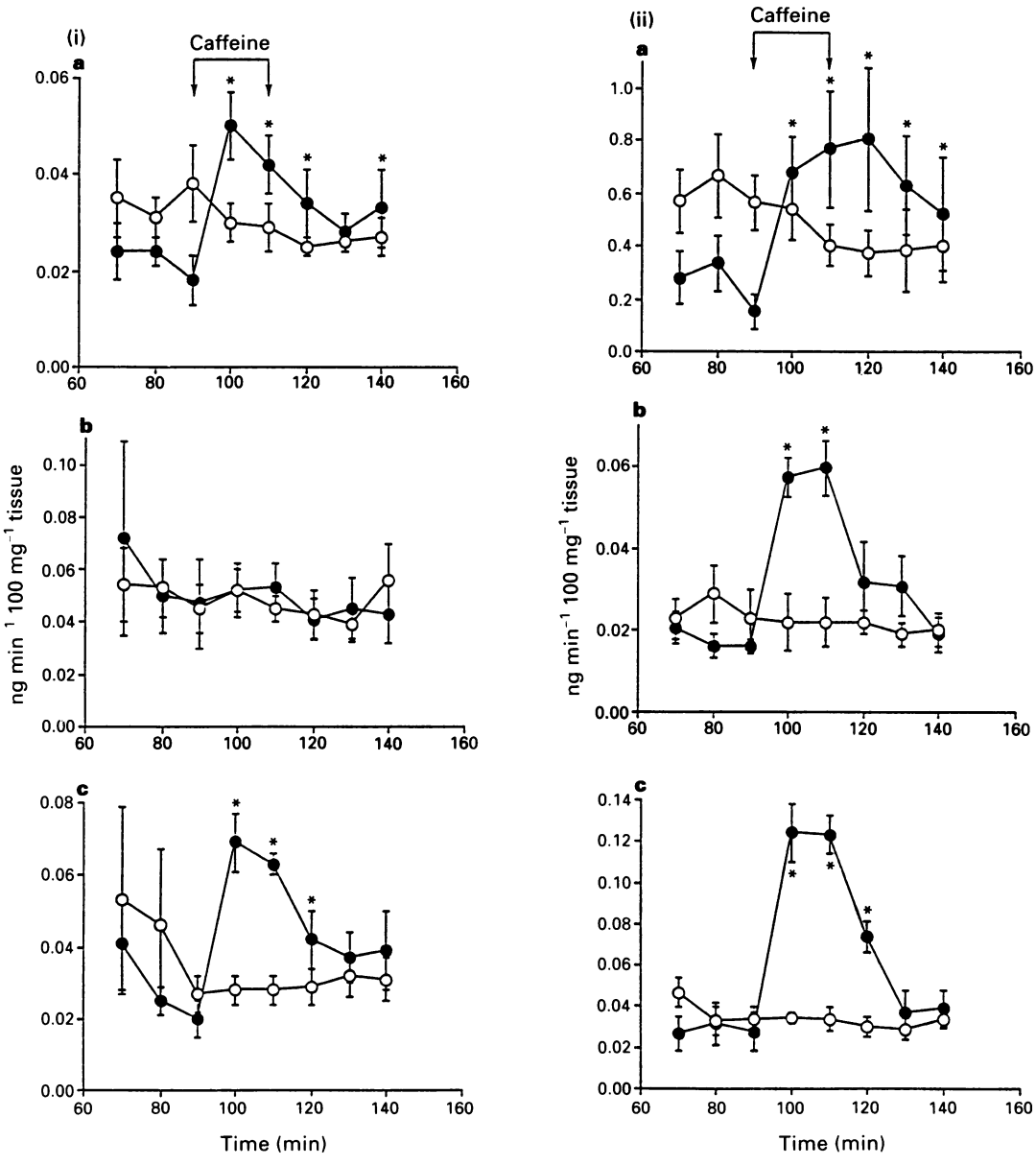

Figure 1 Mean (± s.e. mean, $n = 5$) outputs of (a) prostaglandin $F_{2\alpha}$ ($PGF_{2\alpha}$), (b) PGE_2 and (c) 6-keto-$PGF_{1\alpha}$ from the (i) day 7 and (ii) day 15 guinea-pig uterus superfused *in vitro* in the presence (●) and absence (○) of caffeine. *Significantly ($P<0.05$) higher than before caffeine treatment.

delayed both the increase and subsequent decrease in $PGF_{2\alpha}$ output produced by caffeine such that the 'peak of increased $PGF_{2\alpha}$ release' was flatter and broader. PGE_2 output was not affected by caffeine or ryanodine in this experiment (Figure 4).

In the absence of ruthenium red, caffeine increased the outputs of $PGF_{2\alpha}$, PGE_2 and 6-keto-$PGF_{1\alpha}$ from the day 7 guinea-pig uterus 2.3, 2.1 and 3.8 fold, respectively. In the presence of ruthenium red (10 μmol l^{-1}), caffeine increased the outputs of $PGF_{2\alpha}$, PGE_2 and 6-keto-$PGF_{1\alpha}$ by 2.5, 1.9 and 3.8 fold, respectively. In the presence of ruthenium red (100 μmol l^{-1}), caffeine increased the outputs of $PGF_{2\alpha}$, PGE_2 and 6-keto-$PGF_{1\alpha}$ 2.1, 2.3 and 3.9 fold, respectively. Therefore, ruthenium red at both concentrations used had no significant effect on the increases in outputs of $PGF_{2\alpha}$, PGE_2 and 6-keto-$PGF_{1\alpha}$ produced by caffeine from the day 7 guinea-pig uterus.

W-7 had no inhibitory effect on the increases in output of $PGF_{2\alpha}$, PGE_2 and 6-keto-$PGF_{1\alpha}$ produced by caffeine from the day 7 guinea-pig uterus. In fact, W-7 caused a 3 fold potentiation of the increase in $PGF_{2\alpha}$ output induced by caffeine. W-7 also caused a much smaller potentiation of the increase in PGE_2 output and had no effect on the increase in 6-keto-$PGF_{1\alpha}$ output produced by caffeine from the day 7 guinea-pig uterus (Figure 5). Trifluoperazine produced small increases in the outputs of $PGF_{2\alpha}$ and 6-keto-$PGF_{1\alpha}$ from the day 7 guinea-pig uterus, an effect noted previously (Poyser, 1985b). However, trifluoperazine had no effect on the increases in $PGF_{2\alpha}$ and 6-keto-$PGF_{1\alpha}$ produced by caffeine from the day 7 guinea-pig uterus. In this experiment, PGE_2 output from the uterus increased after the caffeine treatment had finished in both the control and trifluoperazine-treated uterine horns (Figure 5). Theophylline significantly ($P<0.05$) increased the outputs of $PGF_{2\alpha}$ and 6-keto-$PGF_{1\alpha}$ from the day 7 guinea-pig uterus 3.6 and 4.3 fold, respectively. Theophylline had no significant effect on uterine PGE_2 output.

Caffeine, ryanodine (2, 20 or 200 μmol l^{-1}), ruthenium red (100 but not 10 μmol l^{-1}) and theophylline relaxed the superfused uterine horns and abolished any occasional spontaneous contractions. W-7 and TMB-8 caused an initial contraction of the uterus which lasted about 3 min. Following the

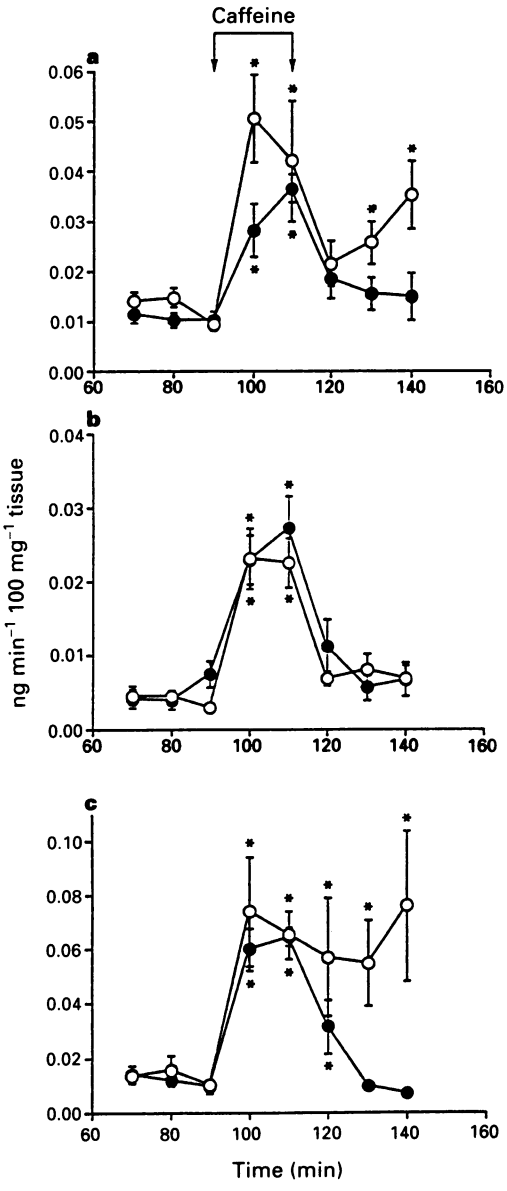

Figure 2 Effect of caffeine on the mean (± s.e. mean, $n = 5$) outputs of (a) prostaglandin $F_{2\alpha}$ ($PGF_{2\alpha}$), (b) PGE_2 and (c) 6-keto-$PGF_{1\alpha}$ from the day 7 guinea-pig uterus superfused *in vitro* in the presence of normal Krebs solution (○) and calcium-depleted Krebs solution (●). *Significantly ($P<0.05$) higher than before caffeine treatment.

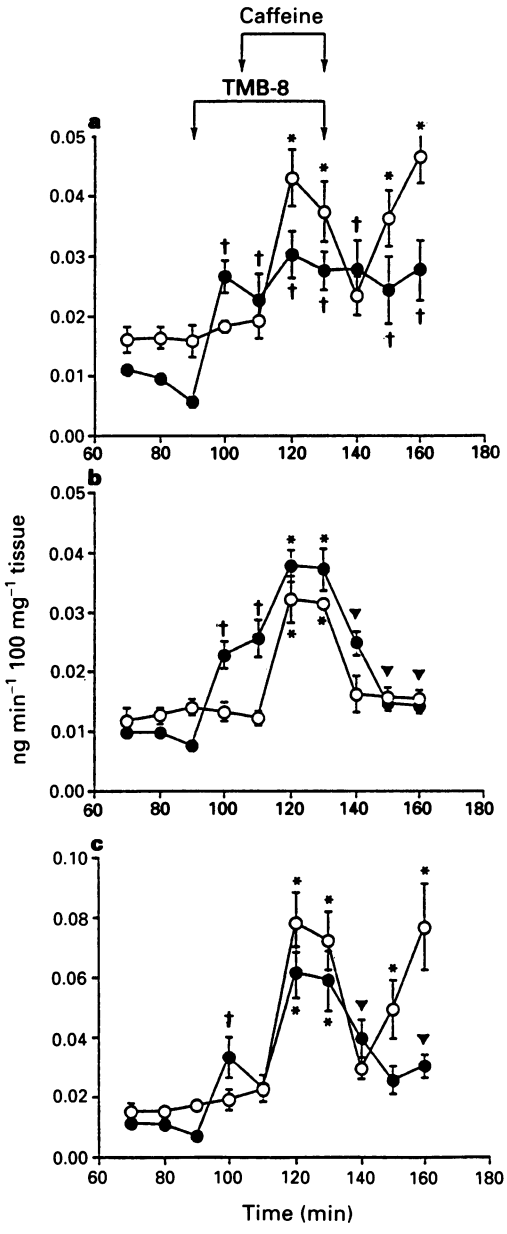

Figure 3 Effect of caffeine on the mean (± s.e. mean, $n = 5$) outputs of (a) prostaglandin $F_{2\alpha}$ ($PGF_{2\alpha}$), (b) PGE_2 and (c) 6-keto-$PGF_{1\alpha}$ from the day 7 guinea-pig uterus superfused *in vitro* in the presence (●) and absence (○) of TMB-8. †Significantly ($P<0.05$) higher than before TMB-8 treatment alone. *Significantly ($P<0.05$) increased by caffeine treatment. ▼Significantly ($P<0.05$) lower following the end of caffeine treatment but significantly higher than before TMB-8 treatment.

subsequent relaxation, the uterine horns continued to exhibit the occasional spontaneous contraction. Trifluoperazine had no effect on the contractile state of the uterus.

Discussion

The basal outputs of $PGF_{2\alpha}$, PGE_2 and 6-keto-$PGF_{1\alpha}$ from the day 7 guinea-pig uterus were typically low. However, by day 15 the output of $PGF_{2\alpha}$ from the uterus had increased approximately 20 fold whereas the outputs of PGE_2 and 6-keto-$PGF_{1\alpha}$ showed little change. This is in agreement with previous findings (Poyser & Brydon, 1983). Studies in ovariectomized guinea-pigs have shown that oestradiol acting on a uterus which has been primed with progesterone for 10 days is the optimum stimulus for this selective increase in uterine $PGF_{2\alpha}$ synthesis and release (Poyser, 1983a). During the oestrous cycle, progesterone output from the ovary is increased after day 3 and oestradiol output from the ovary increases after day 10 (Joshi *et al.*, 1973). This increase in oestradiol output from the ovary precedes an increase in $PGF_{2\alpha}$ output from the uterus by 24 h (Blatchley *et al.*, 1972; Earthy *et al.*, 1975; Antonini *et al.*, 1976). Oestradiol acting on a progesterone-primed uterus appears to be the physiological stimulus for increased $PGF_{2\alpha}$ production by the guinea-pig uterus towards the end of the cycle, especially as treatment of guinea-pigs with a progesterone receptor antagonist or an oestrogen receptor antagonist from days 11 to 14 of the cycle prevents the increase in uterine $PGF_{2\alpha}$ output seen on day 15 (Poyser, 1993). Oxytocin has no stimulatory effect on uterine $PGF_{2\alpha}$ output in guinea-pigs (Poyser & Brydon, 1983; Riley & Poyser, 1987b). The guinea-pig uterus is a good animal model for the human uterus when studying the factors controlling prostaglandin production since oestradiol acting

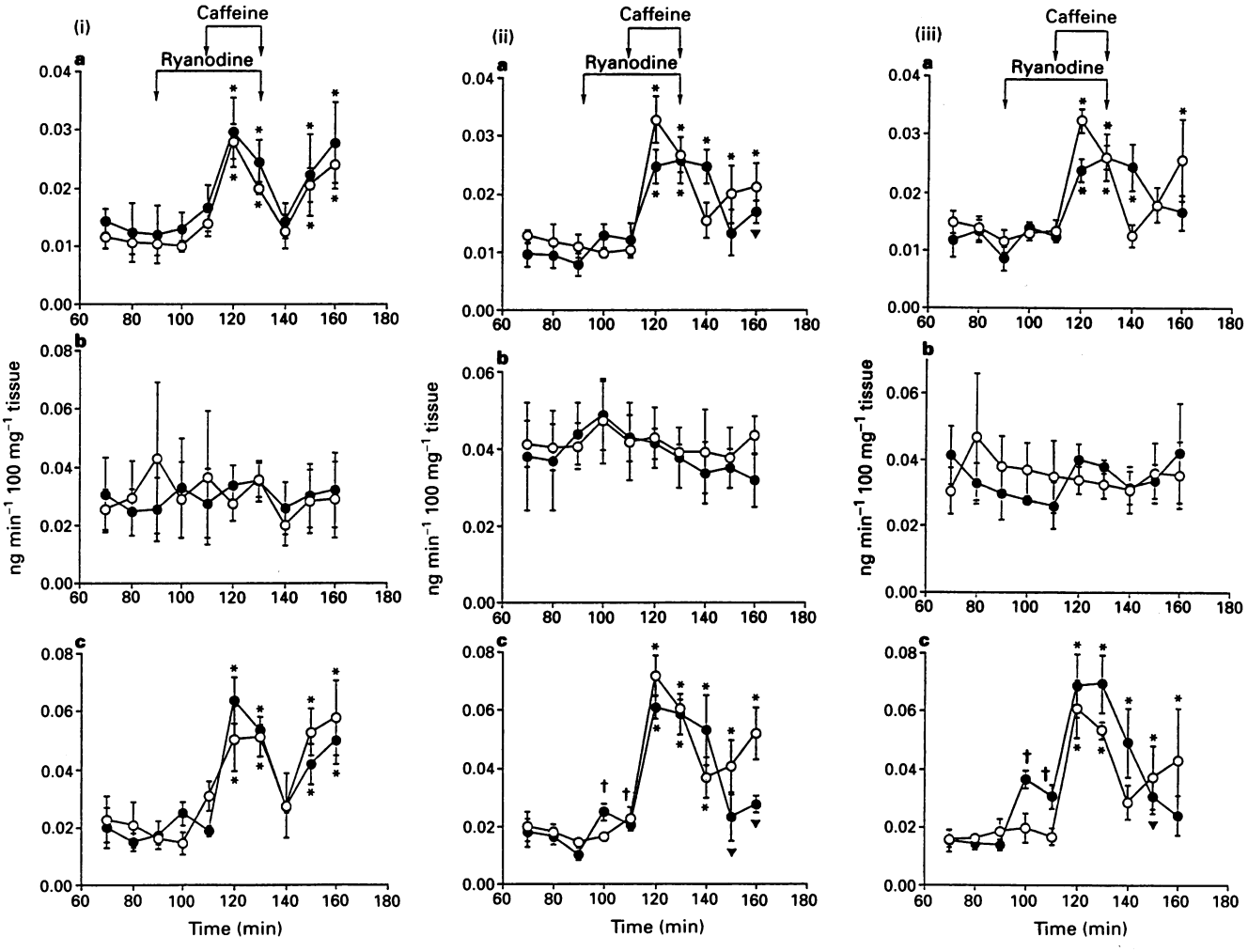

Figure 4 Effect of caffeine on the mean (± s.e. mean, $n = 4$) outputs of (a) prostaglandin $F_{2\alpha}$ ($PGF_{2\alpha}$), (b) PGE_2 and (c) 6-keto-$PGF_{1\alpha}$ from the day 7 guinea-pig uterus superfused *in vitro* in the absence (○) and presence of ryanodine (●) at concentrations of (i) 2 μmol l^{-1}, (ii) 20 μmol l^{-1} and (iii) 200 μmol l^{-1}. †Significantly ($P < 0.05$) higher than before ryanodine treatment. *Significantly ($P < 0.05$) higher than before caffeine treatment. ▼Significantly ($P < 0.05$) lower following the end of caffeine treatment but significantly higher than before ryanodine treatment.

on a progesterone-primed uterus is the optimum stimulus for increased $PGF_{2\alpha}$ production by the human uterus (Smith *et al.*, 1984), and oxytocin has only a weak stimulatory effect on $PGF_{2\alpha}$ production by the nonpregnant human uterus (Leaver & Richmond, 1984).

Caffeine caused 3 to 4 fold increases in the outputs of $PGF_{2\alpha}$ and 6-keto-$PGF_{1\alpha}$ from the guinea-pig uterus on days 7 and 15 of the oestrous cycle. $PGF_{2\alpha}$ and 6-keto-$PGF_{1\alpha}$ are the major prostaglandins synthesized by the endometrium and myometrium, respectively (Poyser, 1983b), although the endometrium synthesizes and secretes 6-keto-$PGF_{1\alpha}$ also (Riley & Poyser, 1987a,b). The effects of caffeine on uterine PGE_2 output were variable. Sometimes caffeine increased PGE_2 output whereas other times it had no effect. In one instance, the stimulatory effect of caffeine on PGE_2 output was delayed. Subsequent analysis of the guinea-pig ages showed that caffeine had no effect on uterine PGE_2 output in younger animals (<4 months) in which basal PGE_2 tended to be higher, but stimulated uterine PGE_2 output in older animals (>4 months) in which basal PGE_2 output tended to be lower. Basal PGE_2 output, but not basal $PGF_{2\alpha}$ output, from the rat uterus also decreases with age and this appears to be due to a reduced response of the ageing uterus to oestradiol and progesterone (Brown *et al.*, 1984). A similar phenomenon in guinea-pigs may explain the reduced basal output of PGE_2 in older animals. However, why the older guinea-pigs should be responsive to caffeine is not clear, except that a lower basal output allows any increase in output to be seen more easily. There is more variability in the output of $PGF_{2\alpha}$ and, to a lesser extent, of the other two prostaglandins on day 15 since output increases progressively at the end of the cycle. Since the cycle may last from 15 to 18 days, day 15 in one animal may not be exactly equivalent to day 15 in another animal which may account for the greater variability in output. This does not apply to day 7 since prostaglandin output from the uterus is consistently low between days 3 and 10 of the cycle. For these reasons, guinea-pig uteri on day 7 of the cycle rather than on day 15 of the cycle were used since the outputs of $PGF_{2\alpha}$, PGE_2 and 6-keto-$PGF_{1\alpha}$ are lower and show less variability. The guinea-pigs used on day 7 in any one experiment were approximately of the same age.

Caffeine increased the outputs of $PGF_{2\alpha}$, PGE_2 and 6-keto-$PGF_{1\alpha}$ from the day 7 guinea-pig uterus when superfused with calcium-depleted Krebs solution. However, the increase in $PGF_{2\alpha}$ output but not the increases in PGE_2 and 6-keto-$PGF_{1\alpha}$ outputs tended to be slower than when calcium-containing Krebs solution was used. Thus the action of caffeine on $PGF_{2\alpha}$ output, but not on PGE_2 and 6-keto-$PGF_{1\alpha}$ outputs, may depend to a small extent on the presence of extracellular calcium. Therefore, the mechanism by which caffeine stimulates $PGF_{2\alpha}$ synthesis and release may be

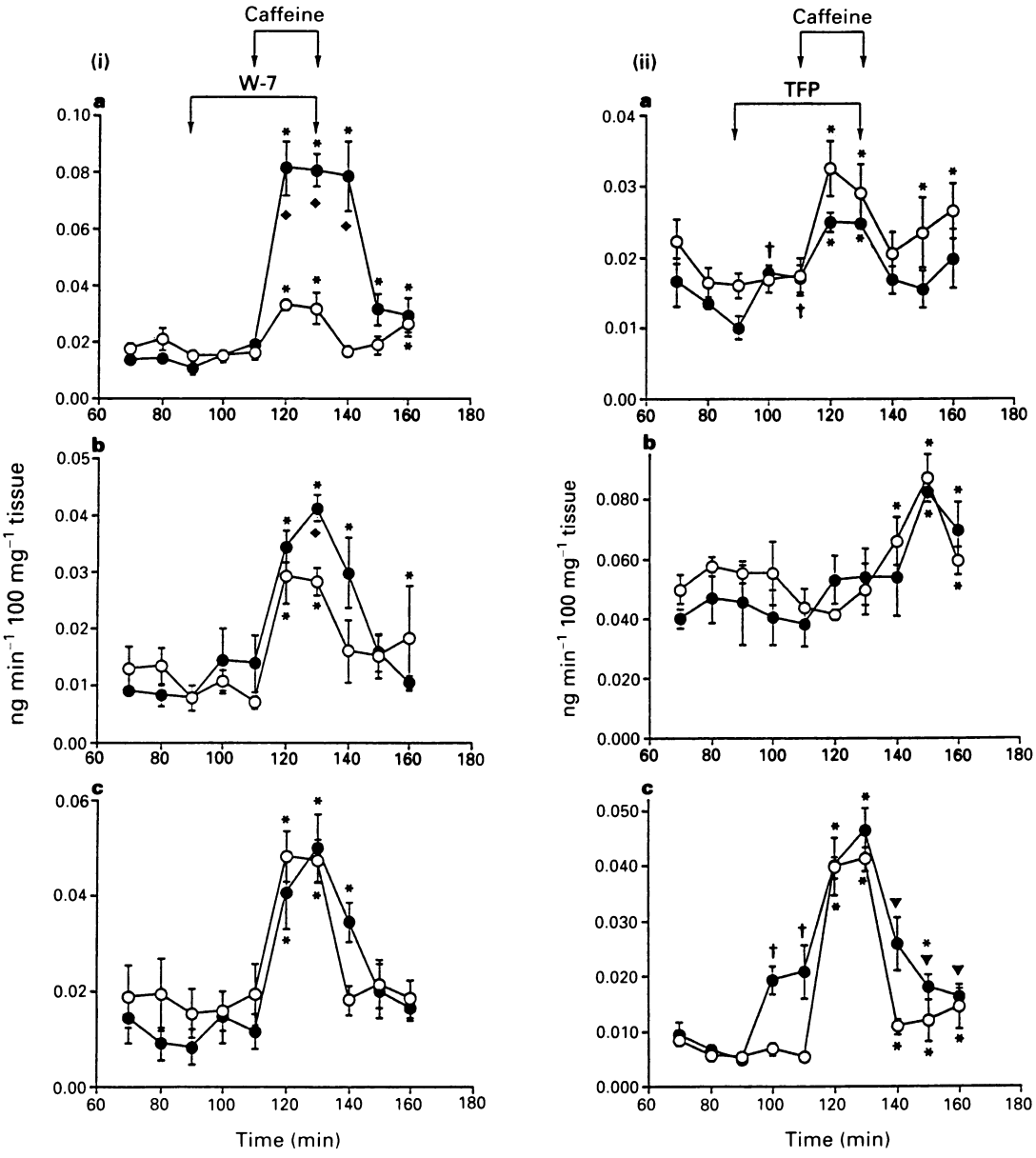

Figure 5 Effect of caffeine on the mean (± s.e. mean, $n = 4$) outputs of (a) prostaglandin $F_{2\alpha}$ ($PGF_{2\alpha}$), (b) PGE_2 and (c) 6-keto-$PGF_{1\alpha}$ from the day 7 guinea-pig uterus superfused *in vitro* in the absence (○) and presence (●) of (i) 100 μmol l^{-1} W-7 and (ii) 150 μmol l^{-1} trifluoperazine (TFP). †Significantly ($P<0.05$) higher than before trifluoperazine treatment alone. *Significantly ($P<0.05$) higher than before caffeine treatment. ▼Significantly ($P<0.05$) lower following the end of caffeine treatment but significantly higher than before trifluoperazine treatment. ◆Significantly ($P<0.05$) higher than corresponding control value (i.e. without W-7 treatment) for the same prostaglandin.

different from the mechanisms by which caffeine stimulates the synthesis and release of PGE_2 and PGI_2 (measured as 6-keto-$PGF_{1\alpha}$). TMB-8 (an intracellular calcium antagonist) completely prevented the stimulatory effect of caffeine on uterine $PGF_{2\alpha}$ output without affecting the stimulatory effect of caffeine on the outputs of PGE_2 and 6-keto-$PGF_{1\alpha}$. This finding suggests that the stimulation of uterine $PGF_{2\alpha}$ synthesis and release by caffeine is dependent on intracellular calcium, but the stimulation of uterine PGE_2 and PGI_2 synthesis by caffeine is independent of intracellular calcium or is dependent on a pool of intracellular calcium not affected by TMB-8. Therefore these results provide further evidence that the mechanism by which caffeine stimulates uterine $PGF_{2\alpha}$ synthesis and release is different from the mechanisms by which caffeine stimulates the synthesis and release of PGE_2 and PGI_2 in the uterus. The stimulatory action of caffeine on uterine prostaglandin output was not prevented by the calmodulin antagonists, W-7 and trifluoperazine, indicating that calmodulin does not mediate this action of caffeine. In fact, W-7 greatly potentiated the stimulatory effect of caffeine on $PGF_{2\alpha}$ output. However, W-7 only weakly potentiated the stimulatory effect of caffeine on PGE_2 output and had no effect on the stimulatory effect of caffeine on 6-keto-$PGF_{1\alpha}$ output. Also, trifluoperazine did not potentiate these actions of caffeine. Therefore, W-7 was probably not producing its potentiating effect by inhibiting calmodulin and, since W-7 affected the stimulation of $PGF_{2\alpha}$ output to a much greater extent than the stimulation of PGE_2 and 6-keto-$PGF_{1\alpha}$ outputs, the mechanism by which caffeine stimulates uterine $PGF_{2\alpha}$ synthesis and release again appears to be different from the mechanisms by which caffeine stimulates the synthesis and release of PGE_2 and PGI_2 in the uterus. The reason why W-7 should potentiate the stimulatory action of caffeine on uterine $PGF_{2\alpha}$ synthesis and release is not clear. Oestradiol

acting on a progesterone-primed uterus can selectively 'switch on' $PGF_{2\alpha}$ synthesis by the guinea-pig uterus (Poyser, 1983a), so perhaps W-7 is promoting the 'switching on' by caffeine of this steroid-dependent pathway of $PGF_{2\alpha}$ synthesis.

Caffeine acts on ryanodine receptors Types 1 and 2 to release intracellular calcium, an effect blocked by ruthenium red and high concentrations of ryanodine (see Sorrentino & Volpe, 1993). Ruthenium red and ryanodine had no inhibitory effect on the increase in output of $PGF_{2\alpha}$, PGE_2 and 6-keto-$PGF_{1\alpha}$ induced by caffeine from the day 7 guinea-pig uterus. Thus caffeine appears to stimulate uterine prostaglandin synthesis by mechanisms which are not dependent upon the activation of Type 1 or Type 2 ryanodine receptors. However, the fact that ruthenium red and ryanodine caused the uterus to relax and abolished spontaneous contractile activity suggests that these two compounds are possibly preventing the release of calcium from an intracellular calcium pool. Ryanodine at the two higher concentrations (20 and 200 $\mu mol\,l^{-1}$) altered the time course of the increase in $PGF_{2\alpha}$ output produced by caffeine. The 'peak of increased release' was flatter and broader in the presence of ryanodine. In addition, ryanodine alone at the two higher concentrations increased the output of 6-keto-$PGF_{1\alpha}$. Why ryanodine should have these two actions is not apparent.

A third type of ryanodine receptor has been described in mink lung epithelial cells (see Sorrentino & Volpe, 1993). This receptor is also present in rat brain and smooth muscle (McPherson & Campbell, 1993). However, this receptor, although binding ryanodine, is not activated by caffeine. Thus it is unlikely that caffeine is stimulating uterine prostaglandin synthesis by acting on a ryanodine Type 3 receptor. Caffeine-sensitive calcium stores have been reported as being present in adrenal chromaffin cells (Burgoyne *et al.*, 1989), liver (Shoshan-Barmatz, 1990) and pancreas (Schmid *et al.*, 1990). The receptor type involved in the chromaffin cells and liver may be one of the three main ryanodine types. However, the receptor type involved in the pancreas is not one of these three ryanodine types since it is not sensitive to ryanodine, but it is blocked by ruthenium red (Dehlinger-Kremer *et al.*, 1991). Consequently, since in the present study the effects of caffeine are not prevented by ryanodine or ruthenium red, caffeine does not appear to be stimulating $PGF_{2\alpha}$ synthesis in the guinea-pig uterus by acting on any of the caffeine and/or ryanodine intracellular calcium pools described so far. Recently, an intracellular calcium pool has been described in hepatocytes which is caffeine-sensitive and ryanodine-insensitive. Additionally, the effect of caffeine in hepatocytes is not blocked by ruthenium red (McNulty & Taylor, 1993). This stimulation by caffeine and lack of inhibition by ryanodine and ruthenium red in hepatocytes is exactly the same profile as that seen in the stimulation of $PGF_{2\alpha}$ output by caffeine in the guinea-pig uterus. Thus, it is possible that caffeine-sensitive calcium pool present in hepatocytes is also present in the uterus and is involved in the stimulation of uterine $PGF_{2\alpha}$ synthesis by caffeine. However, theophylline also stimulated uterine prostaglandin synthesis yet theophylline does not release calcium in hepatocytes (McNulty & Taylor, 1993). Theophylline may be acting to stimulate uterine prostaglandin synthesis by a mechanism different from that of caffeine or, if caffeine and theophylline are acting through the same mechanism, then caffeine may be stimulating calcium release in hepatocytes and $PGF_{2\alpha}$ synthesis in the uterus by different mechanisms.

Since caffeine and theophylline are phosphodiesterase inhibitors, they may be acting to increase adenosine 3':5'-cyclic monophosphate (cyclic AMP) concentrations in the uterus. This may be the mechanism by which caffeine and theophylline relaxed the uterus and abolished spontaneous uterine contractions. However, a previous study has shown that increasing cyclic AMP concentrations in the guinea-pig uterus (by using forskolin) does not lead to an increase in the outputs of $PGF_{2\alpha}$, PGE_2 and 6-keto-$PGF_{1\alpha}$ from the uterus (Poyser, 1987). Thus, it is unlikely that caffeine and theophylline increased uterine prostaglandin output by elevating the cyclic AMP concentration. The effects of caffeine and theophylline on the intracellular calcium concentration of uterine cells in the presence and absence of extracellular calcium merit further study to investigate whether the actions of caffeine and theophylline on uterine prostaglandin synthesis involve the release of intracellular calcium and/or the influx of extracellular calcium.

In conclusion, caffeine stimulated the synthesis and release of $PGF_{2\alpha}$ from the guinea-pig uterus by an action which may be dependent on the release of intracellular calcium since TMB-8 (an intracellular calcium antagonist) prevented the action of caffeine. However, the action of caffeine does not appear to be mediated by any of the three ryanodine receptors identified so far. Caffeine also stimulated the synthesis and release of PGE_2 and 6-keto-$PGF_{1\alpha}$ from the uterus, apparently by mechanisms different from the one by which it stimulated $PGF_{2\alpha}$ production. The mechanism controlling PGE_2 production by the uterus is age-dependent since it was not present in young guinea-pigs. The results of this study showing that caffeine stimulates uterine prostaglandin production raise the possibility that caffeine, which is consumed in beverages by many women each day, may be one of the extrinsic factors responsible for or contributing to menstrual disorders in some women. A high concentration of caffeine was used in the present studies since this is the optimum concentration found in other tissues to release intracellular calcium. However, other studies have shown that concentrations of caffeine as low as $1\,\mu g\,ml^{-1}$ stimulate prostaglandin output from rat blood vessels (Naderali & Poyser, unpublished observations). The average cup of coffee contains about 100 mg caffeine and, after drinking 300 ml of a beverage containing 250 mg caffeine, the plasma concentration obtained 1 h later is between 4.2 and $26\,\mu g\,ml^{-1}$ (Robertson *et al.*, 1978). Therefore, there is some evidence that caffeine can release prostaglandin from tissues in concentrations that are obtained after drinking 1 or 2 cups of coffee. Consequently the present findings in guinea-pigs suggest that similar studies should now be performed on human uterine tissues. In one study, ryanodine increased the free intracellular calcium concentration in human cultured myometrial smooth muscle cells in the presence and absence of extracellular calcium, which indicates that a ryanodine receptor is present in human myometrium. However, caffeine had no such stimulatory effect on calcium release (Lynn *et al.*, 1993), which suggests that caffeine may not stimulate prostaglandin production by human myometrial smooth muscle cells. The endometrium is the main source of prostaglandin during the cycle (see Poyser, 1981), so an investigation of the effect of caffeine on human endometrium is merited.

This study was supported by a MRC student research scholarship to E.K.N. The technical assistance of Mrs Lorna Turnbull is much appreciated.

References

ÅKERLUND, M., STRÖMBERG, P. & FORSLING, M. (1979). Primary dysmenorrhoea and vasopressin. *Br. J. Obstet. Gynaecol.*, **86**, 484–487.

ANTONINI, R., TURNER, T.T. & PAUERSTEIN, C.J. (1976). The hormonal control of the guinea-pig corpus luteum during early pregnancy. *Fertil. Steril.*, **27**, 1322–1325.

BLATCHLEY, F.R., DONOVAN, B.T., HORTON, E.W. & POYSER, N.L. (1972). The release of prostaglandins and progestin into the utero-ovarian venous blood of guinea-pigs during the oestrous cycle and following oestrogen treatment. *J. Physiol.*, **222**, 69–88.

BONNEY, R.C. (1985). Measurement of phospholipase A_2 activity in human endometrium during the menstrual cycle. *J. Endocrinol.*, **107**, 183–189.

BROWN, C., GOSDEN, R.G. & POYSER, N.L. (1984). Effects of age and steroid treatment on prostaglandin production by the rat uterus in relation to implantation. *J. Reprod. Fertil.*, **70**, 649–656.

BURGOYNE, R.D., CHEEK, T.R., MORGAN, A., O'SULLIVAN, A.J., MORETON, R.B., BERRIDGE, M.J., COLYER, J., LEE, A.G. & EAST, J.M. (1989). Distribution of two distinct Ca^{2+}-ATPase-like proteins and their relationships to the agonist-sensitive calcium store in chromaffin cells. *Nature*, **342**, 72–74.

DEHLINGER-KREMER, M., ZEUZEM, S. & SCHULZ, I. (1991). Interaction of caffeine-, IP_3- and vandate-sensitive Ca^{2+} pools in acinar cells of the exocrine pancreas. *J. Membr. Biol.*, **119**, 85–100.

DEY, S.K., HOVERSLAND, R.C. & JOHNSON, D.C. (1982). Phospholipase A_2 activity in the rat uterus – Modulation by steroid hormones. *Prostaglandins*, **23**, 619–630.

DOWNING, I. & POYSER, N.L. (1983). Estimation of phospholipase A_2 activity in guinea-pig endometrium on days 7 and 16 of the oestrous cycle. *Prostaglandins, Leukot. Med.*, **12**, 107–117.

EARTHY, M., BISHOP, C. & FLACK, J.D. (1975). Progesterone and prostaglandin F concentrations in utero-ovarian venous blood of cyclic guinea-pigs. *J. Endocrinol.*, **64**, 11P–12P.

HIDAKA, H., ASANO, M., IWADARE, S., MUSUMOTO, I., TOTSUKA, T. & AOKI, N. (1978). A novel vascular relaxing agent N-(6-aminohexyl)-5-chloro-1-naphthalene-sulphonamide. *J. Pharmacol. Exp. Ther.*, **207**, 8–15.

HORTON, E.W. & POYSER, N.L. (1976). Uterine luteolytic hormone: a physiological role for prostaglandin $F_{2\alpha}$. *Physiol. Rev.*, **56**, 595–651.

JOHNSON, F.A. & POYSER, N.L. (1991). Effect of melittin on prostaglandin production by guinea-pig uterus. *J. Reprod. Fertil.*, **93**, 577–583.

JOSHI, H.S., WATSON, D.J. & LABHSETWAR, A.P. (1973). Ovarian secretion of oestradiol, oestrone, 20-dihydroprogesterone and progesterone during the oestrous cycle of the guinea-pig. *J. Reprod. Fertil.*, **35**, 177–182.

LEAVER, H.A. & RICHMOND, D.H. (1984). The effect of oxytocin, estrogen, calcium ionophore A23187 and hydrocortisone on prostaglandin $F_{2\alpha}$ and 6-oxo-prostaglandin $F_{1\alpha}$ production by cultured human endometrial and myometrial explants. *Prostaglandins, Leukot. Med.*, **13**, 179–196.

LECKIE, C.M. & POYSER, N.L. (1990). Investigation into the mechanisms by which sodium fluoride stimulates prostaglandin production in guinea-pig uterus. *J. Reprod. Fertil.*, **89**, 753–759.

LEVIN, R.M. & WEISS, B. (1977). Binding of trifluoperazine to the calcium activator of cyclic nucleotide phosphodiesterase. *Mol. Pharmacol.*, **13**, 690–697.

LUNDSTRÖM, V., GRÉEN, K. & WIQVIST, N. (1976). Prostaglandins, indomethacin, and dysmennorhoea. *Prostaglandins*, **11**, 893–904.

LYNN, S., MORGAN, J.M., GILLESPIE, J.M. & GREENWELL, J.R. (1993). A novel ryanodine sensitive calcium release mechanism in cultured human myometrial smooth muscle cells. *FEBS Lett.*, **330**, 227–230.

MALAGODI, M.H. & CHIOU, C.Y. (1974). Pharmacological evaluation of a new Ca^{2+} antagonist, 8-(N,N-diethylamino)-octyl-3,4,5-trimethoxybenzoate hydrochloride (TMB-8): studies in smooth muscle. *Eur. J. Pharmacol.*, **27**, 25–33.

MCNULTY, T.J. & TAYLOR, C.W. (1993). Caffeine-stimulated Ca^{2+} release from the intracellular stores of hepatocytes is not mediated by ryanodine receptors. *Biochem. J.*, **291**, 799–803.

MCPHERSON, P.S. & CAMPBELL, K.P. (1993). The ryanodine receptor/Ca^{2+} release channel. *J. Biol. Chem.*, **268**, 13765–13768.

NING, A.C.W.S. & POYSER, N.L. (1984). Further studies on the control of arachidonic acid turnover in guinea-pig endometrium in relation to prostaglandin production. *Prostaglandins, Leukot. Med.*, **16**, 285–302.

POYSER, N.L. (1972). Production of prostaglandins by the guinea-pig uterus. *J. Endocrinol.*, **54**, 147–159.

POYSER, N.L. (1981). *Prostaglandins in Reproduction.* Chichester: John Wiley and Sons Ltd.

POYSER, N.L. (1983a). Effect of treating ovariectomized guinea-pigs with estradiol and progesterone on basal and A23187-stimulated release of prostaglandins superfused *in vitro*. *Prostaglandins, Leukot. Med.*, **11**, 345–360.

POYSER, N.L. (1983b). Differential stimulation of prostaglandin and thromboxane synthesizing capacities in the guinea-pig uterus and ovary. *Prostaglandins, Leukot. Med.*, **10**, 162–177.

POYSER, N.L. (1985a). Effects of TMB-8, an intracellular calcium antagonist, and W-7, a calmodulin antagonist, on prostaglandin output from the guinea-pig uterus. *J. Reprod. Fertil.*, **75**, 223–230.

POYSER, N.L. (1985b). Effect of trifluoperazine, a calmodulin antagonist, on prostaglandin output from the guinea-pig uterus. *J. Reprod. Fertil.*, **73**, 295–303.

POYSER, N.L. (1987). Effects of various factors on prostaglandin synthesis by guinea-pig uterus. *J. Reprod. Fertil.*, **81**, 269–276.

POYSER, N.L. (1993). Effects of onapristone, tamoxifen and ICI 182780 on uterine prostaglandin production and luteal function in nonpregnant guinea-pigs. *J. Reprod. Fertil.*, **98**, 307–312.

POYSER, N.L. & BRYDON, L.J. (1983). Prostaglandin release from the guinea-pig uterus superfused *in vitro*. Effect of stage of estrous cycle, progesterone, oxytocin and A23187. *Prostaglandins*, **25**, 443–456.

POYSER, N.L. & SCOTT, F.M. (1980). Prostaglandin and thromboxane production by the rat uterus and ovary during the oestrous cycle. *J. Reprod. Fertil.*, **60**, 33–40.

RILEY, S.C. & POYSER, N.L. (1987a). Prostaglandin production by the guinea-pig endometrium: is calcium necessary? *J. Endocrinol.*, **113**, 463–471.

RILEY, S.C. & POYSER, N.L. (1987b). Effects of oestradiol, progesterone, hydrocortisone and oxytocin on prostaglandin output from the guinea-pig endometrium maintained in tissue culture. *Prostaglandins*, **34**, 535–552.

ROBERTSON, D., FROLICH, J.C., CARR, R.K., WATSON, J.T., HOLLIFIELD, J.W., SHAND, D.G. & OATES, J. (1978). Effects of caffeine on plasma renin activity, catecholamines and blood pressure. *New Engl. J. Med.*, **298**, 181–186.

SCHMID, A., DEHLINGER-KREMER, M., SHULZ, I. & GOGELEIN, H. (1990). Voltage-dependent $InsP_3$-insensitive calcium channels in membranes of pancreatic endoplasmic reticulum vesicles. *Nature*, **346**, 374–376.

SHOSHAN-BARMATZ, V. (1990) High affinity ryanodine binding sites in rat liver endoplasmic reticulum. *FEBS Lett.*, **263**, 317–320.

SMITH, S.K., ABEL, M.H. & BAIRD, D.T. (1984). Effects of 17β-estradiol and progesterone on the levels of prostaglandin $F_{2\alpha}$ and prostaglandin E_2 in human endometrium. *Prostaglandins*, **27**, 591–598.

SMITH, S.K., ABEL, M.H., KELLY, R.W. & BAIRD, D.T. (1981). A role of prostacyclin (PGI_2) in excessive menstrual bleeding. *Lancet*, **i**, 522–524.

SORRENTINO, V. & VOLPE, V. (1993). Ryanodine receptors: how many, where and why? *Trends Pharmacol. Sci.*, **13**, 98–103.

STEEL, R.B.D. & TORRIE, J.H. (1980). *Principles and Procedures of Statistics – A Biometrical Approach.* (2nd Edn), pp. 106–107. Tokyo: McGraw-Hill Kogakusha Ltd.

SWAN, C.G. & POYSER, N.L. (1983). Prostaglandin synthesis by, and the effects of prostaglandins and prostaglandin analogues on, the vas deferens of the rabbit and rat *in vitro*. *J. Reprod. Fertil.*, **69**, 91–99.

(Received January 31, 1994
Revised May 16, 1994
Accepted May 18, 1994)

Br. J. Pharmacol (1994), **113**, 111–116

Role of intrathecal tachykinins for micturition in unanaesthetized rats with and without bladder outlet obstruction

#,†Osamu Ishizuka, #,†Yasuhiko Igawa, **Alessandro Lecci, **Carlo Alberto Maggi, #‡Anders Mattiasson & [1]*Karl-Erik Andersson

#Departments of Urology and *Clinical Pharmacology, Lund University Hospital, Lund, Sweden; †Department of Urology, Shinshu University School of Medicine, Matsumoto, Japan, and **Pharmacology Department, A. Menarini Pharmaceuticals, Florence, Italy.

1 The effects on micturition of RP 67,580, a selective NK_1 receptor antagonist, and SR 48,968, a highly potent antagonist at NK_2 receptor sites, given intrathecally (i.t.) or intra-arterially (i.a.) near the bladder, were investigated in unanaesthetized rats with and without bladder outlet obstruction.

2 In normal rats, RP 67,580, given i.t. in doses of 2 and 20 nmol per rat, decreased micturition pressure, but did not change other cystometric parameters. After 20 nmol of RP 67,580, dribbling incontinence due to retention was observed in 1 out of 7 animals. This effect was reversible. I.t. RP 67,580 in a dose of 2 nmol, had no effect on hyperactivity induced by intravesically instilled capsaicin.

3 In animals with bladder hypertrophy secondary to outflow obstruction, RP 67,580, given i.t. in a dose of 2 nmol per rat, decreased the micturiton pressure, but had no effect on other cystometric parameters. After 20 nmol, dribbling incontinence due to retention was observed in 5 out of 7 animals.

4 RP 67,580, given i.a. in a dose of 4 nmol, had little effect on the cystometric parameters investigated, both in normal animals and rats with bladder hypertrophy.

5 SR 48,968, given i.t. in doses of 2 and 20 nmol per rat, had no clear-cut effects on the micturition pattern in normal rats, or rats with bladder hypertrophy. However, the drug reduced capsaicin-induced bladder hyperactivity. When given i.a. in a dose of 4 nmol, SR 48,968 had no effect on cystometric parameters in normal rats or rats with bladder hypertrophy.

6 The effects of both RP 67,580 and SR 48,968 were stereoselective, their enantiomers (RP 68,651 and SR 48,965) being inactive.

7 These results thus suggest that at the spinal level there is a tachykinin involvement (via NK_1 receptors) in the micturition reflex induced by bladder filling, both in normal rats, and, more clearly, in animals with bladder hypertrophy secondary to outflow obstruction. The bladder response to filling was not influenced by blockade of vesical NK_1 and NK_2 receptors. On the other hand, the bladder hyperactivity evoked by intravesical capsaicin seems to involve NK_2 receptors both at the bladder and spinal levels.

Keywords: Bladder outlet obstruction; unanaesthetized rat; cystometry; tachykinins; NK_1 receptor; NK_2 receptor

Introduction

Several peptides have been found in the central and peripheral nervous systems innervating the lower urinary tract. Among them, tachykinins (substance P and neurokinin A) and calcitonin gene-related peptide (CGRP) have been implicated as mediators and/or modulators of capsaicin-sensitive primary afferents (Maggi & Meli, 1986; Maggi, 1991). It is known that both tachykinins and CGRP are released from central endings of capsaicin-sensitive primary afferent neurones in the rat and cat spinal cords (Saria *et al.*, 1986; Duggan *et al.*, 1987; Go & Yaksh, 1987), and previous functional studies support the view that the capsaicin-sensitive bladder afferents are involved in regulating the micturition reflex in the rat (Maggi *et al.*, 1984; Holzer-Petsche & Lembeck, 1984). Sharkey *et al.* (1983) demonstrated with double staining technique that 10–16% of rat dorsal root ganglionic neurones, receiving afferents from the bladder, contain substance P (SP). The authors also showed that SP-positive neurones were not observed in the dorsal root ganglia of capsaicin-pretreated animals. It has been postulated that capsaicin-sensitive fibres arising from the rat bladder may use SP as excitatory neurotransmitter to activate the second neurone in the micturition reflex pathway (Maggi *et al.*, 1984).

In the rat urinary bladder, three receptor types, classified as NK_1, NK_2, and NK_3 have been demonstrated, as evidenced by radioligand binding, autoradiographic, and functional experiments (Maggi *et al.*, 1991). Both NK_1 and NK_2 receptors seem to be involved in the contractile response of the rat isolated bladder to tachykinins (Maggi *et al.*, 1987; Hall *et al.*, 1992). This seems to be the case also *in vivo*. Thus, Palea *et al.* (1993a) showed that the selective NK_1 receptor agonist GR 73632 and the selective NK_2 receptor agonist GR 64349, given intravenously, were equipotent in activating micturition reflexes in the urethane-anaesthetized rat.

Rats subjected to bladder outlet obstruction show bladder hypertrophy and 'hyperactivity' (Malmgren *et al.*, 1987) or 'premicturition contractions' (Igawa *et al.*, 1994). Even if such bladder 'hyperactivity' observed in rats with outlet obstruction and bladder hypertrophy may be of myogenic origin (Igawa *et al.*, 1994), these animals show facilitation of bladder reflex mechanisms (Steers & de Groat, 1988) and several neural changes, including hypertrophy of the dorsal root ganglionic neurones innervating the bladder (Steers *et al.*, 1991). If bladder outlet obstruction leads to an increase in the afferent input from the bladder to the dorsal gangli-

[1] Author for correspondence.

onic neurones, and the input is conveyed, at least partly, via primary capsaicin-sensitive afferents, spinal tachykinins may have an important role for micturition in rats with outlet obstruction.

Recently, several potent and selective non-peptide antagonists of SP (NK_1) and neurokinin A (NK_2) receptors have been developed (Garret *et al.*, 1991; Emonds-Alt *et al.*, 1992; Maggi *et al.*, 1993a). These drugs, given i.t., appear to be helpful tools for assessment of the functional importance of tachykinins for modulation of micturition at the spinal level. In the present study we wanted: (1) to examine the effects of RP 67,580, which is selective for NK_1 receptors (Garret *et al.*, 1991), and SR 48,968, which is a highly potent antagonist at NK_2 receptor sites (Emonds-Alt *et al.*, 1992; Maggi *et al.*, 1993a), given intrathecally or intra-arterially near the bladder, on micturition in unanaesthetized rats with and without bladder outlet obstruction; (2) to investigate whether intrathecal administration of the antagonists influenced the bladder hyperactivity induced in normal animals by intravesical capsaicin (Ishizuka *et al.*, 1994).

Methods

Animals

Female Sprague-Dawley rats (weighing 185–245 g) with and without previous outflow obstruction were used. The experimental protocol was accepted by the Animal Ethics Committee, University of Lund.

Procedures

Outlet obstruction procedure The methods used for establishing infravesical outflow obstruction and the technique of cystometry in conscious rats have been described in detail previously (Malmgren *et al.*, 1987). Six weeks after partial ligature of the urethra, the animals were subjected to cystometrical evaluation. Within two days after removal of the ligature, when the animals of this study were investigated, the bladder still exhibited a significant degree of hypertrophy and hyperactivity (Malmgren *et al.*, 1990). For simplicity, the previously obstructed rats are referred to as rats with bladder hypertrophy.

Bladder catheter implantation Rats were anaesthetized with ketamine (75 mg kg^{-1}, i.m.) and xylazine (15 mg kg^{-1}, i.m.). Thereafter, the abdomen was opened through a midline incision, and a polyethylene catheter (Clay-Adams PE-50, NJ, U.S.A.) was implanted into the bladder through the dome as described previously (Malmgren *et al.*, 1987). In the animals subjected to outlet obstruction, the urethral ligature was removed at the same time. The catheters were tunnelled subcutaneously and orifices were made on the back of the animal. After implantation of the catheters, rats were housed individually in cages on a 12 h/12 h light/dark photo cycle.

Intrathecal catheter implantation An i.t. catheter was implanted at the same time as the bladder catheter. A polyethylene catheter (Clay-Adams PE-10, NJ, U.S.A.) was inserted into the subarachnoid space at the level of L_6-S_1 spinal cord segments for i.t. administration of drugs as described in detail previously (Igawa *et al.*, 1993). The injection sites in the spinal cord and the extent of dye distribution were confirmed by injection of dye (methylene blue) in every animal at the end of the experiment.

Intra-arterial cathether implantation The day before cystometric investigations, the rats were again anaesthetized, a femoral artery was exposed through an inguinal incision, and a polyethylene catheter (Clay-Adams PE-10, NJ, U.S.A.) filled with heparinized saline (30 iu ml^{-1}) was inserted into the vessel and advanced proximally until the tip of the catheter reached the abdominal aortic bifurcation. In order to increase the amount of drug reaching the bladder, both femoral arteries were tied. The catheter was tunnelled subcutaneously and an orifice was made on the back of the rat.

Cystometrical investigations Cystometrical investigations were performed without any anaesthesia one day and three days after the bladder catheterization in animals with bladder hypertrophy and in control animals, respectively. The bladder catheter was connected via a T-tube to a pressure transducer (P23 DC, Statham Instrument Inc., CA, U.S.A.) and an infusion pump (CMA 100, Carnegie Medicine AB, Solna, Sweden). The conscious rat was placed, without any restraint, in a metabolic cage which also enabled measurements of micturition volumes by means of a fluid collector connected to a Grass force displacement transducer (FT 03 C, Grass Instrument Co., Quincy, Mass, U.S.A.). Saline or capsaicin at room temperature were infused into the bladder at a rate of 10 ml h^{-1} and 20 ml h^{-1} in control animals and in animals with bladder hypertrophy, respectively. Intravesical pressure and micturition volumes were recorded continuously on a Grass polygraph (Model 7E, Grass Instrument Co., Quincy, Mass, U.S.A.). Three reproducible micturition cycles, corresponding to a 20 min period, were recorded before drug administration and used as baseline values. After each drug administration, recording was continued for another 60 min. In case the micturition reflex was abolished, recording was continued until it was restored. The following urodynamic parameters were investigated: micturition pressure, micturition and residual volumes, and bladder capacity (Malmgren *et al.*, 1987). Analysis was performed for a 20 min period before drug administration. Drug effects on cystometrical parameters were assessed for 60 min and the three micturition cycles showing the most pronounced changes in the parameters measured (increase or decrease) were subjected to analysis.

Administration of drugs The following drugs were used for i.t. or i.a. administration: RP 67,580 [(3a**R**, 7a**R**)-7,7-diphenyl-2-[1-imino-2(2-methoxyphenyl)ethyl] perthdroisoindol-4-one], RP68,651 (the inactive enantiomer of RP 67,580), SR 48,968 [(**S**)-N-methyl-*N*[4-(acetylamino-4-phenyl piperidino)-2-(3,4-dichlorophenyl) butyl] benzamide and SR 48,965 (the inactive enantiomer of SR 49,968). RP 67,580 and RP 68,651 were obtained from Rhone-Poulenc Rorer (Vitry, France), and SR 48,968 and SR 48,965 from Sanofi (Montpellier, France). RP 67,580 and RP 68,651 were dissolved in acidic redistilled water. SR 48,968 and SR 48,965 were dissolved in saline. The drugs were then stored at −70°C, and subsequent dilutions of the drugs were made in saline on the day of experiments.

A 100 mM stock solution of capsaicin (LabKemi, Lund, Sweden) was made in absolute ethanol and then diluted in saline, just before use, to give a concentration of 30 μM. The syringe used for saline instillation was exchanged for a syringe containing capsaicin solution, and capsaicin was instilled intravesically by a microinjection pump for a period of 28 min. With the tubing of the system used, capsaicin reached the bladder within 8 min. The doses of the drugs used were chosen on the basis of pilot experiments, and previously published data (Lecci *et al.*, 1993; Palea *et al.*, 1993a,b; Ishizuka *et al.*, 1994).

Statistical analysis

The results are given as mean values ± s.e. mean. Student's paired *t* test was used for comparison between treatments within the control group and the group with bladder hypertrophy. One way factorial ANOVA was used for comparisons between groups with regard to bladder weight, baseline

(pretreatment) cystometric parameters, and the drug effects (the difference between pre- and post-treatment in each cystometric parameter). It was followed by Scheffe's F-test. A probability level of $<5\%$ was accepted as significant.

Results

Partial obstruction of the urethra led to a significant increase in bladder weight (from 150 ± 5 mg, $n = 12$ to 930 ± 12 mg, $n = 14$; $P < 0.001$). Repeated cystometries gave reproducible results in both control animals and animals with bladder hypertrophy. In control animals, the bladder pressure was low and almost devoid of spontaneous fluctuations during the cystometry. On the other hand, cystometry in animals with bladder hypertrophy revealed spontaneous contractile activity during filling (Figure 1).

Effects of RP 67,580

Normal animals RP 67,580, given i.t. in doses of 2 nmol ($n = 5$) and 20 nmol ($n = 6$) per rat, decreased the micturition pressure significantly from 61.4 ± 9.0 to 50.7 ± 5.6 cmH_2O ($n = 5$; $P < 0.05$) from 62.1 ± 9.8 to 43.9 ± 11.3 ($n = 6$; $P < 0.001$), respectively. There was no change in other cystometric parameters (bladder capacity, micturition volume and residual volume). After 20 nmol of RP 67,580, dribbling incontinence due to retention was observed in 1 out of 7 rats. In this rat, bladder capacity before administration of RP 67,580 was 0.80 ml, and at the time of dribbling 1.70 ml. The effect was reversible.

Intravesical capsaicin, at a concentration of 30 μM, increased micturition pressure ($P < 0.001$), and decreased bladder capacity ($P < 0.001$) and micturition volume ($P < 0.001$), (Table 1). The animals showed no signs of distress and behaved normally, except for occasional licking of the lower abdomen. Intrathecal RP 67,580, 2 nmol, had no effect on capsaicin-induced hyperactivity (Table 1).

RP 67,580, given i.a. in doses of 4 nmol ($n = 7$) had no effect on the cystometric parameters investigated, except a significant ($P < 0.001$) suppression of the micturition pressure from 63.6 ± 2.9 to 55.0 ± 2.6 cmH_2O.

Animals with bladder hypertrophy RP 67,580, given i.t. in a dose of 2 nmol ($n = 6$), decreased the micturition pressure from 149.0 ± 34.1 to 134.6 ± 33.8 cmH_2O ($P < 0.05$), but had no effect on other cystometric parameters. After 20 nmol ($n = 7$), dribbling incontinence due to retention was observed in 5 out of 7 animals (Figure 2). The effect was reversible. Before administration of RP 67,580, the mean bladder capacity was 3.04 ± 0.36 ml, and at the start of dribbling, it was 5.73 ± 0.37 ml. This difference was statistically significant ($P < 0.01$).

RP 67,580, given i.a. in doses of 4 nmol ($n = 5$) had no effect on the cystometric parameters investigated.

Effects of RP 68,651

RP 68,651, the inactive enantiomer of RP 67,580, given i.t. in a dose of 20 nmol, had no effects on the micturition pattern, in normal animals ($n = 6$), or in animals with bladder hypertrophy ($n = 6$).

Effects of SR 48,968

Normal animals SR 48,968, given i.t. in a dose of 2 nmol ($n = 5$) and 20 nmol ($n = 6$) had no clear-cut effects on the micturition pattern. After 2 nmol i.t., capsaicin-induced hyperactivity was significantly reduced, but not abolished (Table 1).

When given i.a. in doses of 4 nmol ($n = 8$), SR 48,968 had no effect on the cystometric parameters.

Animals with bladder hypertrophy SR 48,968 given i.t. in a dose of 2 nmol ($n = 5$) and 20 nmol ($n = 6$) had no clear-cut effects on the micturition pattern. When given i.a. in doses of 4 nmol ($n = 5$), SR 48,968 had no effect on the cystometric parameters.

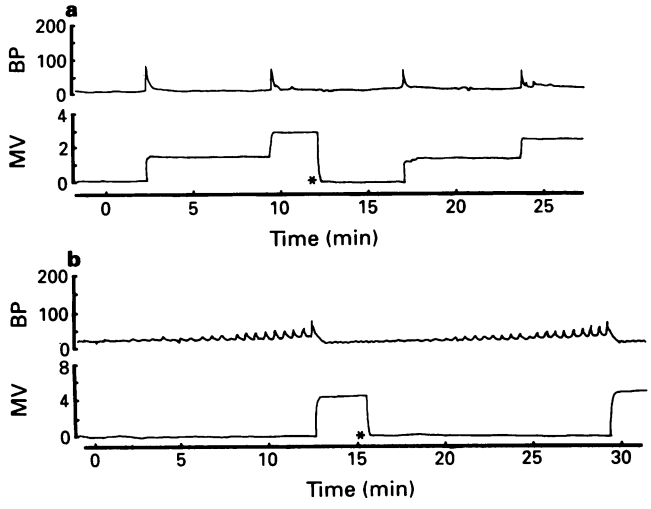

Figure 1 Micturition patterns in a normal rat (a) and in a rat with bladder outflow obstruction (b). Note the variations in bladder pressure before the micturition contractions in the rat with bladder outflow obstruction. BP = bladder pressure (cmH_2O); MV = micturition volume (ml). Asterisk (*) denotes adjustment to baseline position.

Table 1 Effect of intrathecal administration of RP 67,580 and SR 48,968 on capsaicin-induced hyperactivity in unanaesthetized, normal rats

		MP	*BC*	*MV*	*RV*
Capsaicin (30 μM)					
($n = 10$)	Before	68.0 ± 7.2	0.98 ± 0.09	0.84 ± 0.09	0.15 ± 0.01
	After	107.8 ± 10.6**	0.44 ± 0.08***	0.36 ± 0.07***	0.08 ± 0.02*
Capsaicin (30 μM) *in the presence of RP 67,580* (2 nmol) *i.t.*					
($n = 8$)	Before	68.8 ± 9.6	0.79 ± 0.04	0.72 ± 0.04	0.07 ± 0.01
	After	91.5 ± 10.6*	0.35 ± 0.06***	0.30 ± 0.06***	0.04 ± 0.01
Capsaicin (30 μM) *in the presence of SR 48,968* (2 nmol) *i.t.*					
($n = 8$)	Before	61.5 ± 8.8	0.84 ± 0.11	0.78 ± 0.11	0.10 ± 0.03
	After	75.8 ± 11.5**††	0.58 ± 0.06*†	0.53 ± 0.07*†	0.08 ± 0.03

MP: micturition pressure (cmH_2O), BC: bladder capacity (ml), MV: micturition volume (ml), RV: residual volume (ml).
Results are expressed as mean ± s.e. mean.
Before vs. after administration *$P<0.05$; **$P<0.01$; ***$P<0.001$ (Student's paired two tailed t test)
Capsaicin vs. capsaicin in the presence of RP 67,580 or SR 48,968. †$P<0.05$; ††$P<0.01$, (ANOVA followed by Scheffe's F-test).

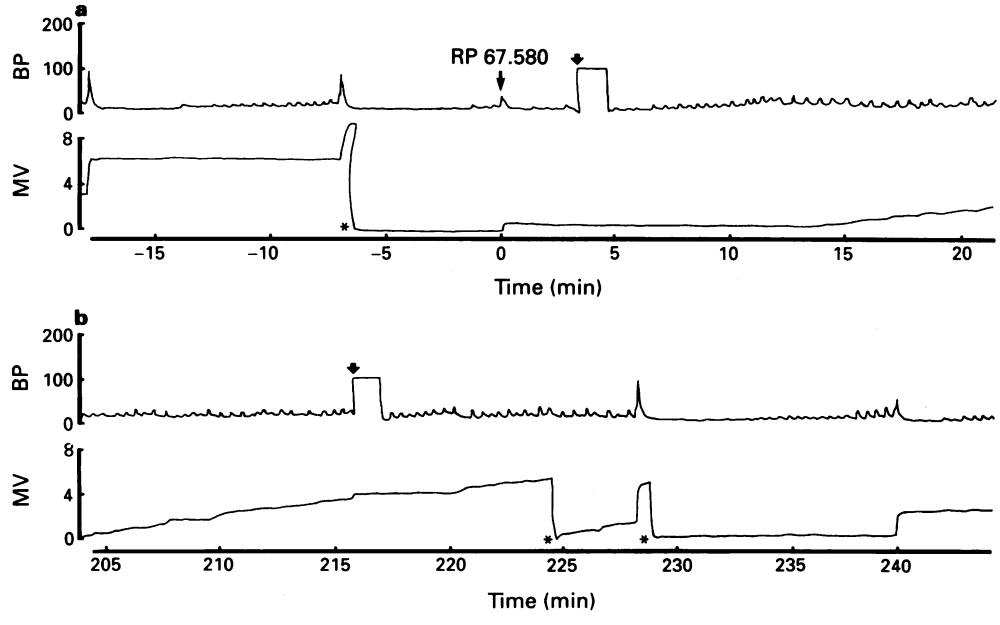

Figure 2 Effect of intrathecal RP 67,580, 20 nmol, on micturition in a rat with bladder outflow obstruction. Starting from minute 15 (a) to and lasting for more than 200 min (b), a dribbling incontinence, due to urinary retention, was induced. Micturition contractions, leading to emptying of the bladder, then reappeared. BP = bladder pressure (cmH_2O); MV = micturition volume (ml). Asterisk (*) denotes adjustment to baseline position, and short arrow (↓) change of the syringe of the infusion pump.

Effects of SR 48,965

SR 48,965, the inactive enantiomer of SR 49,968, given i.t. in a dose of 2 nmol ($n = 4$) had no effects on the capsaicin-induced hyperactivity.

Discussion

In the present investigation, we used the non-peptide tachykinin antagonists RP 67,580 (Garret *et al.*, 1991), which is a selective antagonist of NK_1 receptors, and SR 48,968, which is a potent and competitive antagonist of NK_2 receptors (Maggi *et al.*, 1993a). RP 67,580 is inactive on NK_2 and NK_3 receptors, and SR 48,968 is inactive on NK_1 and NK_3 receptors (Maggi *et al.*, 1993b). The drugs were administered i.t. to reveal whether any of these receptor subtypes at the spinal level may be involved in the micturition reflex induced by bladder filling in conscious, normal rats and/or in rats with bladder hypertrophy secondary to outflow obstruction. The doses of the drugs were selected based on our own pilot experiments, and on previously published data (Lecci *et al.*, 1993; Palea *et al.*, 1993a,b). In addition, we tested the effects of the antagonists on the bladder hyperactivity induced by intravesically administered capsaicin in normal rats (Ishizuka *et al.*, 1994).

In previous investigations performed in normal, urethane-anaesthetized animals (Lecci *et al.*, 1993), different types of micturition-related reflexes have been elicited: (1) a supraspinal chemonociceptive vesico-vesical reflex produced by topical application of capsaicin to the dome of the urinary bladder, (2) a supraspinal mechanoreceptive reflex evoked by saline filling of the urinary bladder, and (3) a spinal somatovesical mechanonociceptive reflex evoked by perineal pinching. These studies, using several NK_1 receptor selective antagonists, including RP 67,580, provided evidence for the involvement of spinal NK_1 receptors, in the activation of reflexes produced by topical application of capsaicin to the bladder, and a modulatory influence on bladder capacity elicited by distension. Magnan *et al.* (1993), studying the effects of i.t. administered NK_1 and NK_2 antagonists on xylene-induced hyperactivity in urethane-anaesthetized animals, arrived at a similar conclusion, suggesting that NK_1 receptors at a spinal level are involved in the bladder response to chemonociceptive stimuli.

Our findings in unanaesthetized rats, showed that RP 67,580, when given intrathecally to normal animals, reduced micturition pressure, and in one animal out of seven produced dribbling incontinence due to urinary retention. In this animal, the effect was reversible. Since dribbling incontinence was not produced by i.t. saline, or by RP 68,651, the inactive enantiomer of RP 67,580, the finding may be interpreted as an effect of the NK_1 antagonist. The failure of the highly potent non-peptide NK_2 receptor antagonist, SR 48,968, to affect normal micturition when given i.t., seems to exclude spinal involvement of NK_2 receptors in the micturition reflexes induced by filling. This interpretation is in line with the findings of Lecci *et al.* (1993), suggesting that spinal NK_1 receptors, at least to some extent, may be involved in the micturition reflex induced by bladder filling in normal animals, but at variance with those of Magnan *et al.* (1993), who found no evidence in support of involvement of spinal NK_1 (or NK_2) receptors in regulation of normal micturition.

In animals with bladder hypertrophy, the effect of RP 67,580, given i.t., was more convincing, producing not only a decrease in micturition pressure at a low dose (2 nmol), but also dribbling incontinence, due to urinary retention, in five out of seven animals at a high dose (20 nmol). That this in fact was due to urinary retention and not to relaxation of the outflow region, making filling of the bladder impossible, was indicated by the finding that there was an increase of the bladder volume (twice bladder capacity before drug administration) before leakage started. No effect was obtained with the inactive isomer RP 68,651, supporting the view that the urinary retention was caused by NK_1 receptor blockade. It may therefore be speculated that the changes of obstruction were associated with an increased afferent activity involving spinal NK_1 receptors. However, the present results do not exclude an additional supraspinal action of the NK_1 antagonist.

I.a. administration of the NK_1 receptor antagonists near

the bladder had no effect either in normal animals (except for a decrease in micturition pressure), or in rats with bladder hypertrophy. This suggests that afferent activity induced by bladder filling, also in rats with bladder hypertrophy, does not involve release of bladder tachykinins.

I.t. RP 67,580 had no effect on the hyperactivity induced by intravesical capsaicin. However, this activity was reduced, but not abolished by i.t. SR 48,968. It has previously been shown (Ishizuka *et al.*, 1994) that intravesical capsaicin evokes a concentration-dependent, reversible and repeatable bladder hyperactivity. This hyperactivity could be abolished by intravenous hexamethonium or i.t. administered morphine, suggesting that it was reflex-mediated and not secondary to a direct contractile effect on bladder smooth muscle. I.a. administration of SR 48,968, and the nonselective NK receptor antagonist spantide, which by themselves did not affect cystometric parameters, both counteracted this capsaicin-induced hyperactivity, whereas RP 67,580 failed to do so. Thus, it seemed that intravesical capsaicin released tachykinins from sensory nerves, and that these tachykinins via stimulation of NK_2 receptors provoked bladder hyperactivity.

Maggi *et al.* (1991) and Pietra *et al.* (1992) have previously shown that NK_2 receptors can be involved at the peripheral level in detrusor hyperactivity induced by irritants. Thus, selective antagonists of NK_2, but not antagonists of NK_1 receptors, counteracted hyperactivity associated with xylene-induced cystitis in the rat (Pietra *et al.*, 1992; Magnan *et al.*, 1993). The findings of the present study suggest that the bladder hyperactivity induced by intravesical capsaicin may involve spinal NK_2 receptors. Such receptors have been demonstrated in the dorsal horns of the rat spinal cord (Yashpal *et al.*, 1990), and have been implicated in the processing of nociceptive inputs in rats (Fleetwood-Walker *et al.*, 1990; 1991; Xu *et al.*, 1991). However, as in the case of the effects of RP 67,580, the present results do not exclude an additional supraspinal action of the NK_2 antagonist.

These results thus suggest that at the spinal level, there is a tachykinin-mediated (via NK_1 receptors) involvement in the micturition reflex induced by bladder filling, both in normal rats, and, more clearly, in animals with bladder hypertrophy secondary to outflow obstruction. The bladder response to filling was not influenced by blockage of vesical NK_1 and NK_2 receptors. The bladder hyperactivity evoked by intravesical capsaicin in normal rats, however, seems to involve NK_2 receptors both at the bladder and spinal levels.

This project was supported by the Swedish Medical Research Council (No 6837 and No 10399), and by the Medical Faculty of Lund, Sweden.

References

DUGGAN, A.W., MORTON, C.R., ZHAO, Z.Q. & HENDRY, I.A. (1987). Noxious heating of the skin releases immunoreactive substance P in the substantia gelatinosa of the cat: a study with antibody microprobes. *Brain Res.*, **403**, 345–349.

EMONDS-ALT, X., VILAIN, P., GOULAOUIC, P., PROIETTO, V., VAN BROECK, D., ADVENIER, C., NALINE, E., NELIAT, G., LE FUR, G. & BRELIÈRE, J.C. (1992). A potent and selective non-peptide antagonist of the neurokinin A (NK_2) receptor. *Life Sci.*, **50**, PL101–PL106.

FLEETWOOD-WALKER, S.M., MITCHELL, R., HOPE, P.J., EL-YASSIR, N., MOLONY, V. & BLADON, C.M. (1990). The involvement of neurokinin receptor subtypes in somatosensory processing in the superficial dorsal horn of the cat. *Brain Res.*, **519**, 169–182.

FLEETWOOD-WALKER, S.M., HOPE, P.J., PARKER, R.M.C. & MITCHELL, R. (1991). Effects of antagonists selective for neurokinin-1 and neurokinin-2 receptors on somatosensory responses of rat dorsal horn neurones. *Br. J. Pharmacol.*, **104**, 472P.

GARRET, C., CARRUETTE, A., FARDIN, V., MOUSSAOUI, S., PEYRONEL, J.-F., BLANCHARD, J.-C. & LADURON, P.M. (1991). Pharmacological properties of a potent and selective nonpeptide substance P antagonist. *Proc. Natl. Acad. Sci. USA*, **88**, 10208–10212.

GO, V.L.W. & YAKSH, T.L. (1987). Release of substance P from the cat spinal cord. *J. Physiol.*, **391**, 141–167.

HALL, J.M., FLOWERS, J.M. & MORTON, I.K.M. (1992). A pharmacological study of NK_1 and NK_2 tachykinin receptor characteristics in the rat isolated urinary bladder. *Br. J. Pharmacol.*, **107**, 777–784.

HOLZER-PETSCHE, U. & LEMBECK, F. (1984). Systemic capsaicin treatment impairs the micturition reflex in the rat. *Br. J. Pharmacol.*, **83**, 935–941.

IGAWA, Y., ANDERSSON, K.-E., POST, C., UVELIUS, B. & MATTIASSON, A. (1993). A rat model for investigation of spinal mechanisms in detrusor instability associated with infravesical outflow obstruction. *Urol. Res.*, **21**, 239–244.

IGAWA, Y., MATTIASSON, A. & ANDERSSON, K.-E. (1994). Micturition and premicturition contractions in unanaethetized rats with bladder outlet obstruction. *J. Urol.*, **151**, 244–249.

ISHIZUKA, O., IGAWA, A.Y., MATTIASSON, A. & ANDERSSON, K.-E. (1994). Capsaicin-induced bladder hyperactivity in normal conscious rats. *J. Urol.*, (in press).

LECCI, A., GIULIANI, S., GARRET, C. & MAGGI, C.A. (1993). Evidence for a role of tachykinins as sensory transmitters in the activation of micturition reflex. *Neuroscience*, **54**, 827–837.

MAGGI, C.A. (1991). The role of peptides in the regulation of the micturition reflex: an update. *Gen. Pharmacol.*, **22**, 1–24.

MAGGI, C.A., GUILIANI, S., SANTICIOLI, P., ABELLI, L., REGOLI, D. & MELI, A. (1987). Further studies on the mechanisms of the tachykinin-induced activation of micturition reflex in rats: evidence for the involvement of the capsaicin-sensitive bladder mechanoreceptors. *Eur. J. Pharmacol.*, **136**, 189–205.

MAGGI, C.A. & MELI, A. (1986). The role of neuropeptides in the regulation of the micturition reflex. *J. Auton. Pharmacol.*, **6**, 133–162.

MAGGI, C.A., PATACCHINI, R., GIULIANI, S. & GIACHETTI, A. (1993a). In vivo and in vitro pharmacology of SR 48, 968, a non-peptide tachykinin NK_2 receptor antagonist. *Eur. J. Pharmacol.*, **234**, 83–90.

MAGGI, C.A., PATACCHINI, R., ROVERO, P. & GIACHETTI, A. (1993b). Tachykinin receptors and tachykinin receptor antagonists. *J. Auton. Pharmacol.*, **13**, 23–93.

MAGGI, C.A., PATACCHINI, R., SANTICIOLO, P. & GIULIANI, S. (1991). Tachykinin antagonists and capsaicin-induced contraction of the rat isolated urinary bladder: evidence for tachykinin-mediated cotransmission. *Br. J. Pharmacol.*, **103**, 1535–1541.

MAGGI, C.A., SANTICIOLI, P. & MELI, A. (1984). The effects of topical capsaicin on rat urinary bladder motility in vivo. *Eur. J. Pharmacol.*, **103**, 41–50.

MAGNAN, A., BETTELINI, L., HAGAN, R.M. & PIETRA, C. (1993). Effects of intrathecal NK-1 and NK-2 antagonists on xylene-induced cystitis in rat. *Neuropeptides*, **24**, 199–200 (abstract P31).

MALMGREN, A., SJÖGREN, C., UVELIUS, B., MATTIASSON, A., ANDERSSON, K.-E. & ANDERSSON, P.O. (1987). Cystometrical evaluation of bladder instability in rats with infravesical outflow obstruction. *J. Urol.*, **137**, 1291–1294.

MALMGREN, A., UVELIUS, B., ANDERSSON, K.-E. & ANDERSSON, P.O. (1990). On the reversibility of functional bladder changes induced by infravesical outflow obstruction in the rat. *J. Urol.*, **143**, 1026–1031.

PALEA, S., DALFORNO, G., GAVIRAGHI, G., HAGAN, R.M., TRIST, D.G. & PIETRA, C. (1993a). Further studies on the effects of selective neurokinin agonists upon the activation of micturition reflex in rats. Evidence for a dual NK-1 receptor mediated excitatory and inhibitory activity. *Neuropeptides*, **24**, 285–291.

PALEA, S., ZIVIANI, L. & PIETRA, C. (1993b). Characterization of the inhibitory response to intravesical capsaicin during cystometry in guinea-pig with spinal cord transection. *Neuropeptides*, **24**, 199 (abstract P30).

PIETRA, C., BETTELINI, L., HAGAN, R.M., WARD, P., MCELROY, A. & TRIST, D.G. (1992). Effect of selective antagonists at tachykinin NK-1 and NK-2 receptors on xylene-induced cystitis in rats. *Neuropeptides, (Suppl.)*, **22,** 52.

SARIA, A., GAMSE, R., PETERMANN, J., FISCHER, J.A., THEODORSSON-NORHEIM, E. & LUNDBERG, J.M. (1986). Simultaneous release of several tachykinins and calcitonin gene-related peptide from rat spinal cord slices. *Neurosci. Lett.*, **63,** 310–314.

SHARKEY, K.A., WILLIAMS, R.G., SCHULTZBERG, M. & DOCKRAY, G.J. (1983). Sensory substance P-innervation of the urinary bladder: possible site of action of capsaicin in causing urine retention in rats. *Neuroscience*, **10,** 861–868.

STEERS, W.D. & DE GROAT, W.C. (1988). Effect of bladder outlet obstruction on micturition reflex pathways in the rat. *J. Urol.*, **140,** 864–871.

STEERS, W.D., CIAMBOTTI, J., ETZEL, B., ERDMAN, S. & DE GROAT, W.C. (1991). Alterations in afferent pathways from the urinary bladder of the rat in response to partial urethral obstruction. *J. Comp. Neurol.*, **310,** 401–410.

XU, X.-J., MAGGI, C.A. & WIESENFELD-HALLIN, Z. (1991). On the role of NK-2 tachykinin receptors in the mediation of spinal reflex excitability in the rat. *Neuroscience*, **44,** 483–490.

YASHPAL, K., DAM, T.-V. & QUIRION, R. (1990). Quantitative autoradiographic distribution of multiple neurokinin binding sites in rat spinal cord. *Brain Res.*, **506,** 259–266.

(Received December 2, 1993
Revised May 6, 1994
Accepted May 19, 1994)

Br. J. Pharmacol (1994), **113**, 117–120

Effect of *in vivo* desensitization to leukotriene B_4 on eosinophil infiltration in response to C5a in guinea-pig skin

[1]E.R. Pettipher, E.D. Salter & H.J. Showell

Department of Immunology and Infectious Diseases, Central Research Division, Pfizer Inc., Groton, CT 06340, U.S.A.

1 The effect of *in vivo* desensitization to leukotriene B_4 (LTB_4) on eosinophil infiltration in response to recombinant C5a was examined in guinea-pig skin.

2 LTB_4 (10–300 ng) and C5a (1–10 μg) caused a dose-dependent increase in the levels of eosinophil peroxidase activity (a measure of eosinophil infiltration) 4 h after injection into guinea-pig skin. Leukotriene B_4 and C5a were approximately equipotent on a molar basis. Platelet activating factor (0.01–10 μg) also caused eosinophil accumulation but was much less active than LTB_4 or C5a.

3 20-Hydroxy-LTB_4 caused a dose-dependent desensitization of eosinophil responses to LTB_4 (ED_{50} = 1.6 μg kg^{-1}, s.c.) and partially reduced responses to C5a. At a dose of 20-hydroxy-LTB_4 (10 μg) which inhibited responses to LTB_4 completely, responses to C5a were reduced by 56.5 ± 1.8% (n = 5). The structurally related metabolite of 20-hydroxy-LTB_4, 20-carboxy-LTB_4, which does not cause desensitization to the effects of LTB_4, did not inhibit eosinophil infiltration in response to C5a.

4 The LTB_4 receptor antagonist, SC-41,930 (10 mg kg^{-1}, p.o.), also inhibited eosinophil accumulation in response to C5a by 63.0 ± 3.9% (n = 5) at a dose which inhibited responses to LTB_4 by 86.5 ± 1.9% (n = 5).

5 These data indicate that eosinophil infiltration in response to C5a may, in part, be mediated by the generation of secondary chemotactic factors such as LTB_4.

Keywords: Leukotriene B_4; neutrophils; eosinophils; inflammation; asthma; C5a

Introduction

Eosinophils infiltrate the lungs of asthmatic patients and are thought to contribute to disease pathology by releasing granule constituents which are cytotoxic to bronchial epithelium (Gleich, 1990). While the mediators responsible for attracting eosinophils to the lungs of asthmatics have not been clearly identified, several mediators are capable of stimulating eosinophil chemotaxis *in vitro*. These include non-selective chemoattractants such as leukotriene B_4 (LTB_4), platelet activating factor (PAF) and C5a (Wardlaw *et al.*, 1986; Hakansson *et al.*, 1987; Sehmi *et al.*, 1992) which have activity on a wide variety of leukocyte types and have been demonstrated to cause eosinophil accumulation *in vivo* (Faccioli *et al.*, 1991). In contrast, RANTES, a β-chemokine, is chemotactic for eosinophils, monocytes and lymphocytes but does not affect neutrophils directly (Schall *et al.*, 1991; Kameyoshi *et al.*, 1992) while the α-chemokine, interleukin-8, is active on neutrophils but not eosinophils or monocytes (Baggiolini *et al.*, 1989).

Although the *in vitro* chemotactic effects of these mediators are due to direct actions on leukocytes, secondary mediators may be generated *in vivo* which contribute to the pattern of leukocyte infiltration observed in inflamed tissues. An example of this is the ability of interleukin-8, which lacks direct chemotactic activity for eosinophils, to stimulate eosinophil emigration *in vivo* through an indirect mechanism (Collins *et al.*, 1993). We have compared the ability of LTB_4, PAF and C5a to induce an eosinophilic infiltrate in guinea-pig skin *in vivo* over a 4 h period. As LTB_4 may be produced from resident macrophages and migrating leukocytes in response to other mediators, we have investigated the contribution of endogenously produced LTB_4 to eosinophil emigration induced by C5a by treating guinea-pigs with 20-hydroxy-LTB_4, an agent which causes specific desensitization to effects of LTB_4 *in vitro* and *in vivo* (Pettipher *et al.*, 1993). We have also used the selective LTB_4 receptor antagonist, SC-41930 (Fretland *et al.*, 1990), to investigate the role of LTB_4 receptor stimulation in eosinophil infiltration in these responses.

[1] Author for correspondence.

Methods

Induction of eosinophil infiltration in guinea-pig skin

Male Hartley guinea-pigs (400–450 g) were anaesthetized in an atmosphere of Metofane (methoxyflurane) and their backs shaved. LTB_4, PAF, human recombinant C5a were dissolved in saline containing 0.25% bovine serum albumin. Duplicate intradermal injections of saline or mediators were given in a volume of 0.1 ml such that there were a maximum of 6 sites per guinea-pig. Four hours after injection animals were killed, skin removed and sites punched out with a 13 mm gasket punch. Skin homogenates were prepared for assay as previously described (Pettipher *et al.*, 1993).

Animals were predosed with vehicle or 20-hydroxy-LTB_4 subcutaneously in 0.5 ml saline immediately prior to intradermal challenge. Animals were dosed orally with the LTB_4 antagonist, SC-41930 (7-[3-{4-acetyl-3-methoxy-2-propylphenoxy}-propoxy]-3, 4-dihydro-8-propyl-2H-1-benzopyran-2-carboxylic acid) in 0.5% carboxymethylcellulose vehicle (10 ml kg^{-1} body weight) 1 h prior to intradermal challenge.

Assay of eosinophil peroxidase

Eosinophil peroxidase (EPO) was assayed in diluted skin homogenates as previously described (Strath *et al.*, 1985; Cheng *et al.*, 1993). Diluted sample (50 μl) was incubated with 0.6 mg ml^{-1} *o*-phenylenediamine dihydrochloride in 50 mM Tris HCl (pH 8.0) containing 0.02% hydrogen peroxide for 5 min at room temperature and the reaction termination by the addition of 4 M sulphuric acid (100 μl). The absorbance was read at 490 nm using a microtitre plate

reader (Molecular Devices, Menlo Park, CA, U.S.A.). Guinea-pig eosinophils were isolated on a Percoll gradient after harvest from the peritoneal cavities of animals which had been repeatedly injected with human serum. These preparations contained 100% eosinophils and 0.06×10^3 – 3.0×10^4 cells per ml were included in each assay as a calibration curve. Neutrophils were harvested from the peritoneal cavities of guinea-pigs injected with casein and these preparations contained 92% neutrophils, 7% monocytes and 1% eosinophils.

Materials

Platelet activating factor (C-16), LTB_4 and 20-hydroxy-LTB_4 were purchased from Biomol, Plymouth Meeting, PA., U.S.A.; *o*-phenylenediamine dihydrochloride was from Eastman Kodak Co., Rochester, NY, U.S.A. SC-41930 was synthesized by Dr. Lawrence Reiter in the department of Medicinal Chemistry, Pfizer Inc., Groton, CT., U.S.A. All other reagents were purchased from the Sigma Chemical Company, St. Louis, MO, U.S.A.

Statistical analysis

The differences between drug-treated and control groups were analysed by ANOVA and considered significant when $P < 0.05$.

Results

Eosinophil peroxidase activities in guinea-pig eosinophils and neutrophils

The eosinophil peroxidase levels in guinea-pig eosinophils and neutrophils is shown in Figure 1. Guinea-pig eosinophils contain 34.8 times more eosinophil peroxidase activity than guinea-pig neutrophils. As the neutrophil preparation contained 1% contaminating eosinophils this is probably even a slight underestimate of the specificity of the enzyme for eosinophils versus neutrophils.

Effect of 3-amino-1,2,4-triazole on eosinophil peroxidase activity in guinea-pig skin sites injected with LTB_4

Eosinophil peroxidase activity was increased in guinea-pig skin sites injected with LTB_4 and this activity was reduced by 88.9% in the presence of 3-amino-1,2,4-triazole, a selective inhibitor of eosinophil peroxidase (Cramer *et al.*, 1984) (Figure 2).

Eosinophil peroxidase activity in guinea-pig skin sites after injection of LTB_4, C5a and PAF

LTB_4 (10–300 ng) and recombinant C5a (1–10 μg) caused a dose-dependent increase in the levels of eosinophil peroxidase activity in skin sites after injection into guinea-pig skin (Figure 3). LTB_4 and C5a were approximately equipotent on a molar basis and both induced an approximately 50 fold increase in the levels of eosinophil peroxidase over the saline control at the highest doses tested. In contrast, PAF caused a relatively low level of eosinophil infiltration compared to LTB_4 and C5a (5.7 × saline response at the highest dose tested, Figure 3).

Effects of 20-hydroxy-LTB_4 and SC41930 on eosinophil infiltration in response to LTB_4 and C5a

For inhibition studies with 20-hydroxy-LTB_4, doses of LTB_4 (100 ng) and C5a (2 μg) were chosen. Systemic treatment of guinea-pigs with 20-hydroxy LTB_4 inhibited eosinophil emigration in response to LTB_4 (100 ng) with an ED_{50} of 1.6 μg kg^{-1} (Figure 4). 20-Hydroxy-LTB_4 also dose-depen-

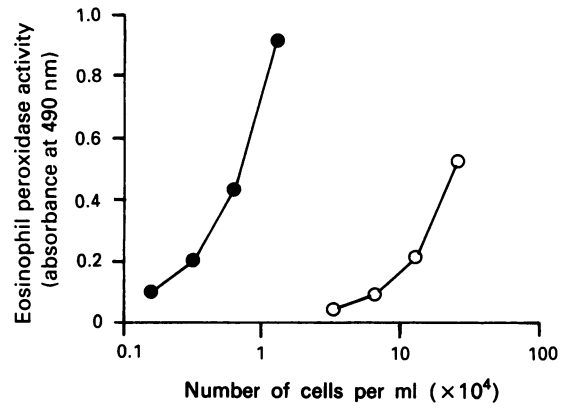

Figure 1 Eosinophil peroxidase activity in guinea-pig eosinophils (●) and neutrophils (○).

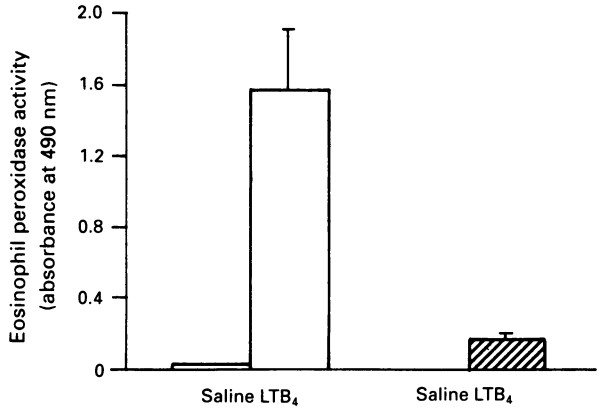

Figure 2 Effect of 3-amino-1,2,4-triazole on eosinophil peroxidase activity in guinea-pig skin sites. Skin sites were removed 4 h after injection of LTB_4 (100 ng) or saline and homogenized in 8 ml phosphate-buffered saline (pH 7.2) containing 0.5% hexadecyltrimethylammonium bromide and assayed for eosinophil peroxidase as described in the Methods. Activity in untreated samples is shown by open columns and activity in the presence of 3-amino-1,2,4-triazole (10 mM) is shown by hatched columns. Data are presented as mean ± s.e. mean ($n = 5$).

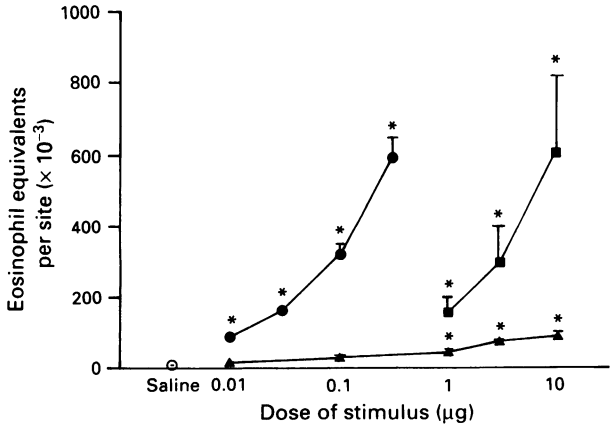

Figure 3 Eosinophil infiltration (as measured by eosinophil peroxidase activity) 4 h after intradermal injection of LTB_4 (●), human recombinant C5a (■) or PAF (▲) into guinea-pig skin. Each point represents the mean ± s.e. mean of data derived from 5–10 animals (*$P < 0.05$ vs saline control).

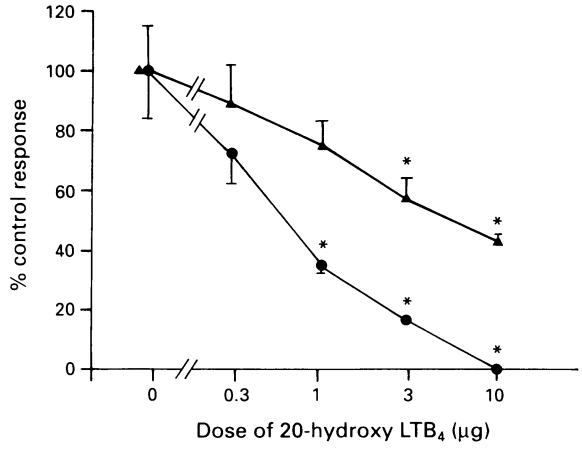

Figure 4 Effect of systemic treatment with 20-hydroxy-LTB_4 (given subcutaneously in 0.5 ml saline containing 0.25% bovine serum albumin) on eosinophil infiltration in response to LTB_4 (100 ng) (●) or human recombinant C5a (2 μg) (▲) at 4 h after intradermal injection. Results are expressed as a % of the untreated control responses which in absolute numbers were $412.0 \pm 65.8 \times 10^{-3}$ ($n = 10$) eosinophil equivalents for LTB_4 and $154.9 \pm 25.8 \times 10^{-3}$ ($n = 10$) eosinophil equivalents for C5a. Saline-injected sites contained $10.9 \pm 7.3 \times 10^{-3}$ ($n = 10$) eosinophil equivalents. Each point is the mean ± s.e. mean of data derived from 5–10 animals (*$P < 0.05$ versus vehicle-treated control animals).

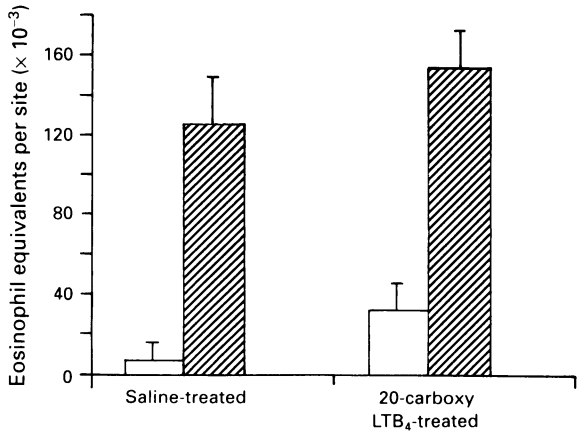

Figure 5 Effect of systemic treatment with 20-carboxy-LTB_4 (10 μg s.c.) on eosinophil infiltration measured 4 h after intradermal injection of human recombinant C5a (2 μg). Data are the mean ± s.e. mean of values from 5 animals. Responses to saline are depicted by open columns and responses to LTB_4 are shown by hatched columns (*$P < 0.05$ versus control).

dently inhibited eosinophil responses to C5a (Figure 4). At a dose of 20-hydroxy-LTB_4 which completely inhibited responses to 100 ng LTB_4, responses to C5a were reduced by 56.5 ± 1.8% ($n = 5$). 20-Carboxy LTB_4 did not affect eosinophil responses to C5a (Figure 5).

The LTB_4 receptor antagonist, SC-41930, also reduced eosinophil infiltration in response to C5a (Figure 6). At the highest dose tested (10 mg kg^{-1}, p.o.) which caused 86.5 ± 1.9% inhibition of responses to 100 ng LTB_4, eosinophil infiltration in response to C5a was inhibited by 63.0 ± 3.9% ($n = 5$).

Discussion

We have confirmed the observations of Cheng *et al.* (1993) that eosinophil peroxidase is a selective marker for the

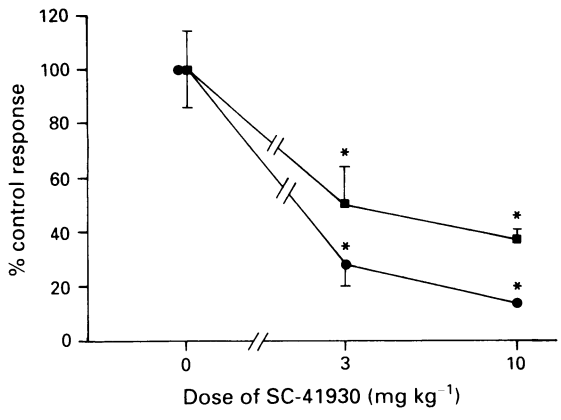

Figure 6 Effect of oral administration of the LTB_4 receptor antagonist, SC-41930, on eosinophil infiltration in response to LTB_4 (100 ng) (●) or C5a (2 μg) (■) in guinea-pig skin. Each point is the mean ± s.e. mean of data from 5 animals (*$P < 0.05$ versus responses in vehicle-treated animals).

presence of eosinophils in inflamed tissues and using this enzyme marker, we have compared the ability of various chemotactic factors to induce eosinophil infiltration after intradermal injection in guinea-pigs. The inflammatory mediators, LTB_4, C5a and PAF all elicited an increase in eosinophil peroxidase activity after intradermal injection in guinea-pigs. The peroxidase activity detected in this assay is likely to be predominantly due to the presence of eosinophils as reflected by the ability of a selective inhibitor of eosinophil peroxidase, 3-amino-1,2,4-triazole (Cramer *et al.*, 1984), to reduce peroxidase activity in skin sites by approximately 90%. However, based on data presented in this paper, neutrophils may contain low levels of eosinophil peroxidase-like activity and since these cells accumulate in skin sites in much higher numbers than eosinophils, a small contribution of neutrophil-derived peroxidase to the activity detected in skin sites cannot be excluded. LTB_4 and C5a were approximately equipotent on a molar basis, while PAF was much less active in this assay, confirming previous observations with these mediators in guinea-pig skin (Czarnetzki & Mertensmeier, 1985; Faccioli *et al.*, 1991) which suggests that the oedema producing activity of PAF may predominate over its effects on leukocyte activation at sites of inflammation. Invading neutrophils in inflamed tissues are a rich source of LTB_4 (Simmons *et al.*, 1983) which, in addition to its effects on neutrophils, is chemotactic for eosinophils and may therefore amplify neutrophil and eosinophil recruitment into skin sites injected with other chemotactic factors, particularly at late time points. In order to investigate the contribution of LTB_4 to eosinophil infiltration in response to C5a we have treated guinea-pigs with 20-hydroxy-LTB_4 which causes *in vivo* desensitization to the effects of LTB_4 (Pettipher *et al.*, 1993).

20-Hydroxy-LTB_4 reduced eosinophil infiltration in response to LTB_4 with a potency similar to its effect on neutrophil accumulation (Pettipher *et al.*, 1993). 20-Hydroxy-LTB_4 also caused a dose-related inhibition of eosinophil accumulation measured 4 h after injection of C5a. Doses of 20-hydroxy-LTB_4 which cause maximal desensitization to LTB_4 inhibited responses to C5a by over 50%. These data indicate that endogenously generated LTB_4 may contribute to eosinophil accumulation after injection of C5a, although other mediators which interact with the LTB_4 receptor such as 12(**R**)-HETE may be responsible for the observed effects. In terms of specificity controls, we have previously shown that 20-hydroxy-LTB_4 does not affect neutrophil infiltration in response to C5a (Pettipher *et al.*, 1993) and the structurally related metabolite of 20-hydroxy-LTB_4, 20-carboxy-LTB_4, did not inhibit eosinophil infiltration in response to

C5a. Furthermore, the LTB_4 receptor antagonist, SC-41930, also inhibited eosinophil infiltration in response to C5a and to much the same extent as 20-hydroxy-LTB_4. Taken together these data suggest that the observed effects of 20-hydroxy-LTB_4 can be interpreted as an effect involving LTB_4 receptors and is not due to general toxicity or some other nonspecific effect. The fact that 20-hydroxy-LTB_4 does not significantly affect the levels of myeloperoxidase in skin sites injected with C5a (Pettipher *et al.*, 1993) suggests neutrophils do not contribute significantly to the eosinophil peroxidase activity present in these inflamed skin sites.

It is uncertain which chemotactic factors are of primary importance in mediating eosinophil infiltration in allergic disease but the results from the present study suggest that LTB_4 may serve a key role in amplifying eosinophil infiltration in response to other mediators such as C5a. This view is supported by the findings that eosinophil infiltration into the airways of allergic guinea-pigs can be reduced by LTB_4 receptor antagonists (Richards *et al.*, 1989) or 5-lipoxygenase inhibitors (Yeadon *et al.*, 1993).

References

BAGGIOLINI, M., WALZ, A. & KUNKEL, S.L. (1989). Neutrophil-activating peptide-1/interleukin 8, a novel that activates neutrophils. *J. Clin. Invest.*, **84**, 1045–1049.

CHENG, J.B., PILLAR, J.S., SHIRLEY, J.T., SHOWELL, H.J., WATSON, J.W. & COHAN, V.L. (1993). Antigen-mediated pulmonary eosinophilia in immunoglobulin G1-sensitized guinea-pigs: Eosinophil peroxidase as a simple specific marker for detecting eosinophils in bronchoalveolar lavage fluid. *J. Pharmacol. Exp. Ther.*, **264**, 922–929.

COLLINS, P.D., WEG, V.B., FACCIOLI, L.H., WATSON, M.L., MOQBEL, R. & WILLIAMS, T.J. (1993). Eosinophil accumulation induced by human interleukin 8 in the guinea-pig *in vivo*. *Immunology*, **79**, 312–318.

CRAMER, R., SORANZO, M.R., DRI, P., MENEGAZZI, R., PITOTTI, A., ZABUCCHI, G. & PATRIARCA, P. (1984). A simple reliable assay for myeloperoxidase in mixed neutrophil-eosinophil cell suspensions: Application to detection of myeloperoxidase deficiency. *J. Immunol. Methods*, **70**, 119–125.

CZARNETZKI, B.M. & MERTENSMEIER, R. (1985). *In vitro* and *in vivo* chemotaxis of guinea pig leukocytes toward leukotriene B_4 and its ω-oxidation products. *Prostaglandins*, **30**, 5–11.

FACCIOLI, L.H., NOURSHARGH, S., MOQBEL, R., WILLIAMS, F.M., SEHMI, R., KAY, A.B. & WILLIAMS, T.J. (1991). The accumulation of ^{111}In-eosinophils induced by inflammatory mediators, *in vivo*. *Immunology*, **73**, 222–227.

FRETLAND, D.J., WIDOMSKI, D.L., ZEMAITIS, J.M., WALSH, R.E., LEVIN, S., DJURIC, S.W., SHONE, R.L., TSAI, B.S. & GAGINELLA, T.S. (1990). Inflammation of guinea pig dermis. Effects of leukotriene B_4 receptor antagonist, SC-41930. *Inflammation*, **14**, 727–739.

GLEICH, G.J. (1990). The eosinophil and bronchial asthma: current understanding. *J. Allergy Clin. Immunol.*, **85**, 422–436.

HAKANSSON, L., WESTERLUND, D. & VENGE, P. (1987). New method for the measurement of eosinophil migration. *J. Leukocyte Biol.*, **42**, 689–696.

KAMEYOSHI, Y., DORSCHER, A., MALLET, A.I., CHRISTOPHERS, E. & J.-M. SCHRODER. (1992). Cytokine RANTES released from thrombin-stimulated platelets is a potent attractant for human eosinophils. *J. Exp. Med.*, **176**, 587–592.

PETTIPHER, E.R., SALTER, E.D., BRESLOW, R., RAYCROFT, L. & SHOWELL, H.J. (1993). Specific inhibition of leukotriene B_4 (LTB_4)-induced neutrophil emigration by 20-hydroxy LTB_4: implications for the regulation of inflammatory repsonses. *Br. J. Pharmacol.*, **110**, 423–427.

RICHARDS, I.M., GRIFFIN, R.L., OOSTVEEN, J.A., MORRIS, J., WISHKA, D.G. & DUNN, C.J. (1989). Effect of the selective leukotriene B_4 antagonist U-75302 on antigen-induced bronchopulmonary eosinophilia in sensitized guinea pigs. *Am. Rev. Respir. Dis.*, **140**, 1712–1716.

SCHALL, T.J. (1991). Biology of the RANTES/SIS cytokine family. *Cytokine*, **3**, 165–183.

SEHMI, R., ROSSI, A.G., KAY, A.B. & CROMWELL, O. (1992). Identification of receptors for leukotriene B_4 expressed on guinea pig peritoneal eosinophils. *Immunology*, **77**, 129–135.

SIMMONS, P.M., SALMON, J.A. & MONCADA, S. (1983). The release of leukotriene B_4 during experimental inflammation. *Biochem. Pharmacol.*, **32**, 1353–1359.

STRATH, M., WARREN, D.J. & SANDERSON, C.J. (1985). Detection of eosinophils using an eosinophil peroxidase assay. Its use as an assay for eosinophil differentiation factors. *J. Immunol. Methods*, **83**, 209–215.

WARDLAW, A.J., MOQBEL, R., CROMWELL, O. & KAY, A.B. (1986). Platelet-activating factor. A potent chemotactic and chemokinetic factor for human eosinophils. *J. Clin. Invest.*, **78**, 1701–1706.

YEADON, M., DOUGAN, F.L., PETROVIC, A., BEESLEY, J.E. & PAYNE, A.N. (1993). Effect of BW B70C, a novel inhibitor of arachidonic acid 5-lipoxygenase, on allergen-induced bronchoconstriction and late-phase lung eosinophil accumulation in sensitised guinea-pigs. *Agents Actions*, **38**, 8–18.

(Received March 31, 1994
Accepted May 19, 1994)

Br. J. Pharmacol (1994), **113**, 121–128

Hyperpolarization by opioids acting on μ-receptors of a sub-population of rat periaqueductal gray neurones *in vitro*

[1]B. Chieng & M.J. Christie

Department of Pharmacology, The University of Sydney, NSW 2006, Australia

1 The actions of opioids on membrane properties of rat periaqueductal gray neurones were investigated using intracellular recordings from single neurones in brain slices. Morphological properties and anatomical location of each impaled neurone were characterized by use of intracellular staining with biocytin. The present paper primarily considers neurones which were directly hyperpolarized by opioids. The accompanying paper considers inhibition of synaptic transmission by opioids.

2 Met-enkephalin (10–30 μM) hyperpolarized 29% (38/130) of neurones. The hyperpolarization was fully antagonised by naloxone (1 μM, $n = 3$). The response to Met-enkephalin was not affected by agents which block synaptic neurotransmission (1 μM tetrodotoxin, and 0.1 μM tetrodotoxin + 4 mM Co^{2+}, $n = 3$).

3 The specific μ-receptor agonist, D-ala-met-enkephalin-glyol (3 μM, $n = 17$) produced hyperpolarizations of similar amplitude to those produced by Met-enkephalin (10–30 μM). The EC_{50} of D-ala-met-enkephalin-glyol was 80 nM and the maximum response was achieved at 1–3 μM. The δ-receptor (D-Pen-D-Pen-enkephalin, 3 μM, $n = 7$) and κ-receptor (U50488H, 3 μM, $n = 5$) agonists had no effect on the membrane properties of these neurones.

4 The opioid-induced hyperpolarization was associated with an increased potassium conductance. Hyperpolarizations were accompanied by a significant decrease in membrane resistance between −70 and −80 mV, and a significantly greater decrease between −110 and −140 mV ($n = 16$). Hyperpolarizations reversed polarity at -111 ± 3 mV ($n = 16$), close to the expected equilibrium potential for potassium ions. The reversal potential of outward currents increased by 24 mV when the extracellular potassium concentration was raised from 2.5 to 6.5 mM, which is close to the value predicted by the Nernst equation (25 mV) for a potassium conductance.

5 Resting inward rectification (reduced input resistance at potentials more negative than −100 mV in the absence of opioids) was significantly greater in neurones which were hyperpolarized by opioids than in those which were not hyperpolarized. The amplitude of action potential after hyperpolarizations was significantly smaller in neurones which were hyperpolarized by opioids. Other membrane properties did not differ significantly between opioid-sensitive and -insensitive neurones.

6 Neurones hyperpolarized by opioids were multipolar (58%), triangular (21%) or fusiform (5%) in shape with a soma diameter of 22 ± 1 μm ($n = 19$, longest axis). Dendritic spread was in a large radiating pattern, usually in all directions, with axons usually originating from primary dendrites. The axons were usually branched and projected in several directions. Morphological properties did not differ significantly between opioid-sensitive and -insensitive neurones.

7 Neurones hyperpolarized by opioids were located predominantly in the lateral periaqueductal gray, as well as in the more dorsal areas of the ventrolateral periaqueductal gray, whereas neurones not hyperpolarized by opioids were located in the more ventral areas of the ventrolateral periaqueductal gray.

8 These studies demonstrate that opioids acting on μ-receptors increase potassium conductance in a sub-population of large neurones located predominantly in the lateral column of the periaqueductal gray. The neurones hyperpolarized by opioids could be involved in the antinociceptive actions of opioids, but might also be involved in other functions because a large proportion lie outside of the main 'antinociceptive zone' of the periaqueductal gray. It is also unlikely that these neurones are GABAergic, suggesting that they might not participate in the postulated antinociceptive action of opioids mediated via disinhibition of neurones which project to the ventral medulla.

Keywords: Periaqueductal gray; opioid; enkephalin; μ-receptor; δ-receptor; κ-receptor; intracellular recording; potassium conductance; analgesia

Introduction

The periaqueductal gray (PAG) is an important site for the antinociceptive actions of opioids. Direct microinjections of morphine into PAG have been reported to produce antinociception, via an effect of neurones located in the rostral ventromedial medulla which participate in descending antinociceptive mechanisms (Yaksh *et al.*, 1988; Fields *et al.*, 1991). The rat PAG is rich in nerve terminals and fibres containing endogenous opioids (see Reichling *et al.*, 1988) and electrical stimulation in PAG has been reported to produce antinociception which can be antagonized by naloxone (Adams, 1976; Akil *et al.*, 1976). The PAG is also thought to be involved in the expression of opioid withdrawal signs in morphine-dependent animals (Laschka *et al.*, 1976; Bozarth & Wise, 1984; Maldonado *et al.*, 1992).

Opioid-mediated antinociception was most pronounced when micro-injections or electrical stimulation were directed at the caudal part of ventrolateral PAG (Yaksh *et al.*, 1988). This is consistent with the notion that the PAG is organised into anatomically and functionally distinct columns of neurones extending along the rostrocaudal axis (see Bandler *et al.*, 1991). However, little is known of the actions of

[1] Author for correspondence.

opioids on membrane properties of PAG neurones, or actions on neurones in different functional subdivisions of the PAG.

From a study of extracellular recordings from brain slices, opioids were reported to excite, inhibit or have no effect on neurones distributed throughout the PAG (Behbehani *et al.*, 1990). By use of intracellular electrodes, neurones located in the dorsolateral PAG were shown to be inhibited by opioids (ibid). The present study used intracellular recordings from neurones in the lateral and ventrolateral PAG in brain slices to characterize the effects of opioids on membrane properties in subdivisions which are thought to be involved in antinociception. The accompanying paper considers the effects of opioids on synaptic transmission in PAG.

Disinhibition of neurones which project to the ventral medulla, mediated via inhibition of GABAergic interneurones by opioids, has been proposed as the mechanism by which opioids act in PAG to induce antinociception (Basbaum & Field, 1984). Similar mechanisms appear to account for excitatory effects of opioids elsewhere in the central nervous system. In many of these cases distinct morphological and/or physiological properties of opioid-sensitive (presumably GABAergic) and -insensitive neurones have been described (Madison & Nicoll, 1988; Lacey *et al.*, 1989; Pan *et al.*, 1990; Johnson & North, 1992). In the present study physiological properties of opioid-sensitive and -insensitive neurones in PAG were also characterized and morphological properties defined by use of intracellular labelling with biocytin.

Methods

Preparation of tissue and solutions

Male Sprague-Dawley rats (150–250 g) were anaesthetized with halothane, decapitated, and horizontal brain slices containing PAG (300 μm) were cut and maintained in physiological saline at 35°C. Slices containing PAG lateral or ventral to the aqueduct were transferred to a tissue bath. Submerged slices were superfused with physiological saline at 35°C (1.5 ml min^{-1}). The physiological saline solution contained (in mM): NaCl 126, KCl 2.5, NaH_2PO_4 1.2, $MgCl_2$ 1.2, $CaCl_2$ 2.4, glucose 11 and $NaHCO_3$ 24 and was gassed with 95% O_2 + 5% CO_2. Drugs were applied to the slice by changing the solution to one that differed only in its content of the drug.

Electrophysiological recording

Intracellular recordings of membrane potential were made with microelectrodes (70–120 MΩ, filled with 2 M KCl + 2% biocytin buffered with 50 mM Tris HCl, pH 7.4) using a single electrode current- and voltage-clamp amplifier (Axoclamp-2A). The approximate locations of impaled neurones were plotted on an atlas of the rat PAG (Paxinos & Watson, 1986). Recordings of membrane potential and applied current were plotted directly on chart recorder paper as well as being digitized for later analyses (PCLAMP and AXOTAPE software, Axon Instruments). Electrode resistance was monitored and balanced throughout experiments. For measurement of the amplitude of hyperpolarizations, membrane potential was held between −65 and −75 mV by application of constant current through the recording electrode. Input resistance was determined throughout with brief (250 ms) hyperpolarizing current pulses (0.3 Hz, −40 to −200 pA). The same currents were applied throughout drug applications. For determination of voltage-current relationships, membrane potential was monitored over a range (usually −50 to −150 mV) by applying an incremental series of current pulses of 200 ms duration. In these cases, the basal membrane potential was adjusted to control values during drug application by application of constant current. The total applied current was used to determine voltage-current relationships. In several cases stable recordings were achieved with sufficiently low resistance electrodes (70–80 MΩ) to permit the use of discontinuous voltage-clamp at switching frequencies of 2–3 kHz while continuously monitoring the potential at the headstage with a separate oscilloscope. All data are expressed as mean ± s.e. mean.

Histochemistry

After recording, slices were fixed for at least 12 h in 10% formalin/phosphate buffer solution at 4°C. Slices were then rinsed in phosphate buffer and incubated in 0.3% H_2O_2/phosphate buffer (0.1 M pH 7.2) solution for 30 min. A further rinse was performed before incubating the slice in 0.3% Triton X-100/phosphate buffer solution for four days at 4°C. Slices were then rinsed and incubated in a solution containing 1:200 dilution of Extravidin peroxidase (Sigma, St Louis), and phosphate buffer for 2 h at room temperature with gentle rotations. This was followed by a rinse in 0.04% nickel/phosphate buffer solution for 1 h. The final incubation was in a solution containing 3,3'-diaminobenzidine (0.05%), nickel (0.04%), H_2O_2 (0.005%) and phosphate buffer. The reaction was stopped by rinsing the slice several times in phosphate buffer, when background staining started to become prominent. Slices were then mounted on gelatinised slides, dried, dehydrated in a graded series of alcohol and histolene, and coverslipped in D.P.X. mounting medium (BDH, UK). The coordinates of each stained section were identified from a rat brain atlas (Paxinos & Watson, 1986) and morphological properties were characterized as described in the results section. All morphological data are expressed as mean ± s.e. mean.

Drugs and reagents

Biocytin, Met-enkephalin and tetrodotoxin were obtained from Sigma (St Louis, U.S.A.), Tyr-D-Ala-Gly-MePhe-Glyol (DAMGO) and Tyr-D-Pen-Gly-Phe-D-Pen (Pen = penicillamine, DPDPE) from National Institute on Drug Abuse (U.S.A.), *trans*-(+)-3,4-dichloro-*N*-methyl-*N*-[2-(1-pyrro-

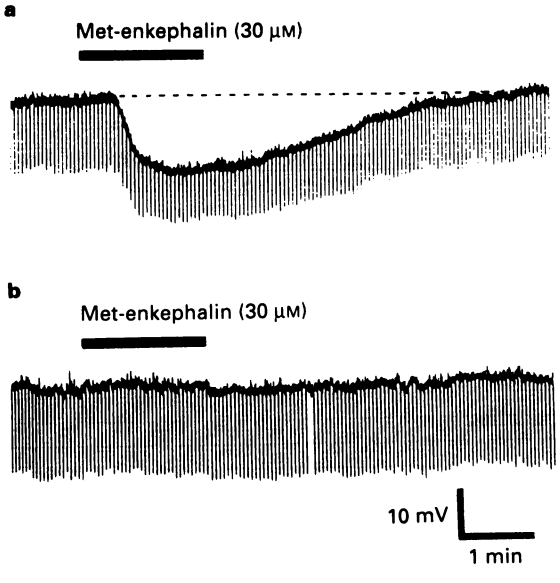

Figure 1 Responses of PAG neurones to Met-enkephalin (30 μM). (a) Example of a neurone hyperpolarized by Met-enkephalin. The hyperpolarization was associated with decreased input resistance (decreased amplitude of downward deflections). (b) Example of lack of effect of Met-enkephalin on membrane potential or input resistance. Downward deflections are membrane potential responses to constant current pulses passed through the recording electrode (−120 pA, 250 ms in a, −50 pA, 250 ms in b).

lidinyl)-cyclohexyl]benzeneacetamide methane sulphonate (U50488H) from Upjohn and naloxone hydrochloride from Research Biochemicals Inc (Natick, MA, U.S.A.).

Results

Opioids acting on μ-receptors directly hyperpolarize a sub-population of PAG neurones

Superfusion of Met-enkephalin (10–30 μM) produced a hyperpolarization in 29% of PAG neurones (38/130). Hyperpolarizations were associated with a decrease in membrane resistance (Figure 1a, Figure 4). Met-enkephalin did not affect the membrane properties of the other 92 neurones tested (Figure 1b). The hyperpolarization induced by Met-enkephalin persisted in the presence of agents which block synaptic transmission ($n = 3$, 1 μM tetrodotoxin or tetrodotoxin + 4 mM Co^{2+}), suggesting a direct action on impaled neurones. These agents completely abolished electrically-evoked postsynaptic potentials (see Chieng & Christie, 1994).

Neurones which were hyperpolarized by Met-enkephalin were also hyperpolarized by the selective μ-receptor agonist, DAMGO (e.g. Figure 2a, $n = 17$). The effects of DAMGO were completely reversed by the opioid antagonist, naloxone (1 μM, $n = 3$, e.g. Figure 2b). Figure 3 depicts the concentration-response relationship of DAMGO. The EC_{50} was approximately 80 nM, and maximum response was achieved at approximately 3 μM. When tested in the same neurones, the maximum amplitudes of the hyperpolarizations produced by DAMGO (8.5 ± 1.2 mV, $n = 17$) and Met-enkephalin (Figure 3, 7.7 ± 1.2 mV, $n = 17$) were similar (paired-$t = 2.0$, $P > 0.05$).

The membrane properties of neurones which were hyperpolarized by Met-enkephalin were not affected by selective δ- (DPDPE, 3 μM, $n = 7$, Figure 2c) or κ-receptor (U50488H, 3 μM, $n = 5$, Figure 2d) agonists. The solutions of DPDPE and U50488H used in these experiments were subsequently found to be pharmacologically active at appropriate concentrations on δ- and κ-receptors in mouse vas deferens (N. Lavidis, personal communication) and guinea-pig ileum preparations (data not shown) respectively.

Opioids increase an inwardly rectifying potassium conductance

Opioids decreased input resistance at all potentials tested (Figures 4 and 5). For determination of voltage-current relationships (Figure 4), an incremental series of current pulses was applied through the recording electrode. The membrane potential during the application of Met-enkephalin or DAMGO was adjusted to the pre-drug level by application of constant current and the same series of current pulses was then applied. The hyperpolarization produced by opioids

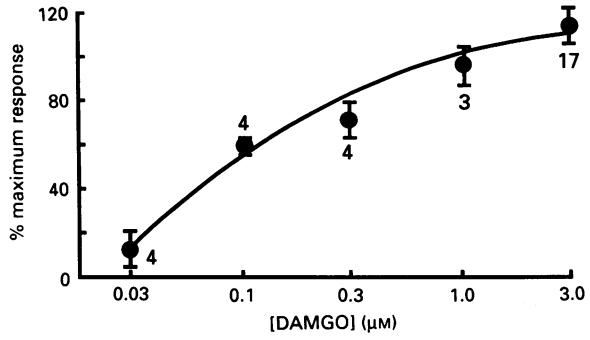

Figure 3 Concentration-response curve of DAMGO in neurones which were hyperpolarized by Met-enkephalin. The effect of DAMGO is expressed on the ordinate scale as a percentage of the hyperpolarization produced by Met-enkephalin (10 or 30 μM) in the same neurone. The EC_{50} for DAMGO was approximately 80 nM.

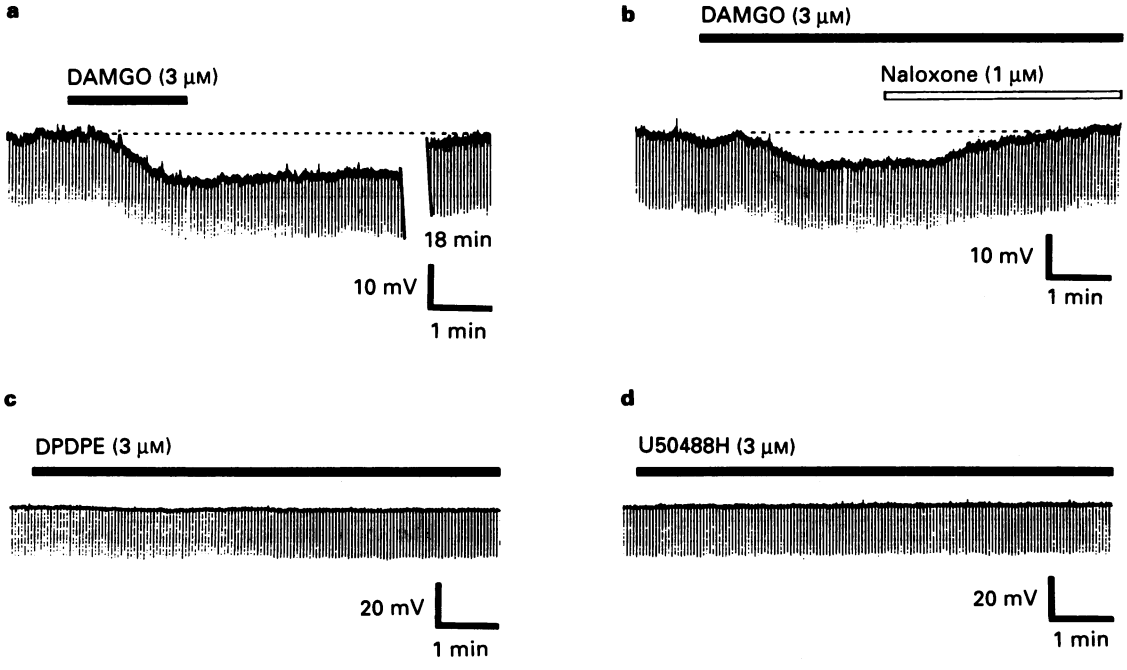

Figure 2 Hyperpolarizations induced by selective μ-, but not δ- or κ-receptor agonists. (a) DAMGO (3 μM) induced a reversible hyperpolarization and decreased input resistance. (b) The hyperpolarization induced by DAMGO was completely antagonized by naloxone (1 μM). The selecitve δ-receptor agonist DPDPE (3 μM, c) and κ-receptor agonist U50488H (3 μM, d) had no effect. These recordings (c and d) are from a single neurone which were hyperpolarized by Met-enkephalin (−5 mV at −71 mV). Drugs were superfused during periods indicated by solid bars. Resting membrane potentials of neurones were maintained at −71 mV. Downward deflections are membrane potential responses to constant current pulses passed through the recording electrode (−70 pA, 250 ms in a and b; −300 pA, 250 ms in c and d). Periods of superfusion of drugs are shown by bars. For abbreviations, see text.

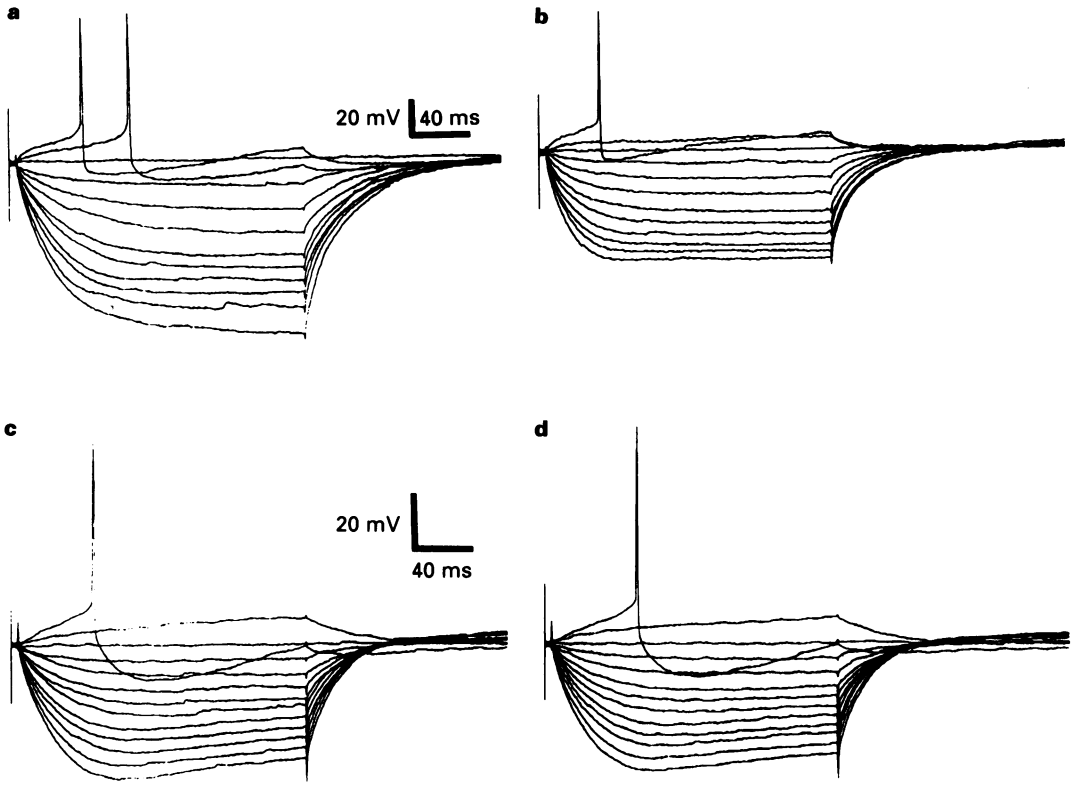

Figure 4 Voltage-current relationships (raw data) of two neurones (one neurone in a and b, another in c and d) to opioids. Left figures (a and c) were sampled just prior to superfusion of opioids, and right figures (b and d) during opioid superfusion. Incremental step current pulses (60 pA increments from −270 pA, 200 ms in a and b, 70 pA from −350 pA in c and d) were applied for 200 ms (current record not shown). Resting membrane potential was maintained at −70 mV in each example by applying a constant current to the recording electrode (a = −10 pA, b = 80 pA, c = −70 pA, d = −50 pA). Resting (i.e., without superfusion of opioids) inward rectification (decreased membrane resistance at very negative membrane potentials) was evident in both neurones. DAMGO (3 μM, b) and Met-enkephalin (30 μM, d) hyperpolarized (compensated by application of constant current in record, see above) and decreased input resistance of each neurone at all potentials tested. The second neurone (c and d) displayed a slowly developing depolarization during large hyperpolarizing current pulses, which slowly relaxed on repolarization. Met-enkephalin had no effect on this slowly developing depolarization. Met-enkephalin and DAMGO did not substantially affect action potentials or afterhyperpolarizations in either neurone.

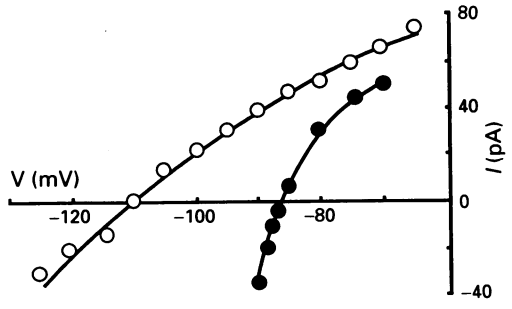

Figure 5 Effects of Met-enkephalin (30 μM) on subtracted steady-state current-voltage relationship of a single neurone in two extracellular potassium concentrations (control current subtracted from current in the presence of Met-enkephalin): (○) 2.5 mM, (●) 6.5 mM potassium.

(10–30 μM Met-enkephalin, $n = 10$, or 3 μM DAMGO, $n = 6$) reversed polarity at −111 ± 3 mV ($n = 16$, Figures 4 and 5). Using voltage-clamp, the reversal potential shifted from −110 mV to −86 mV when the extracellular potassium concentration was raised from 2.5 mM to 6.5 mM (Figure 5). This 24 mV shift is in close agreement with the value predicted by the Nernst equation (25 mV) for a potassium conductance. In this experiment, the slope conductance of the opioid-induced current showed inward rectification both in 2.5 mM (1.1 nS at −70 mV and 2.3 nS at −120 mV) and 6.5 mM extracellular potassium (1.8 nS at −70 mV and 10.7 nS at −90 mV). Complementary results were obtained from recordings of membrane potential. The opioid-induced decrease in input resistance was smaller when determined between −70 and −80 mV (17 ± 4%, $n = 16$) than between −110 and −140 mV (37 ± 6%, $n = 16$, difference = 20 ± 6%, paired $t = 3.37$, $P < 0.005$). Other membrane properties including amplitude and duration of action potentials and afterhyperpolarizations, and the slowly developing depolarization at negative potentials were not affected (Figure 4).

Other membrane properties of opioid-sensitive and -insensitive neurones

In the absence of applied opioids, opioid-sensitive neurones displayed more resting inward rectification than -insensitive neurones. The input resistance of opioid-sensitive neurones was significantly smaller at more negative membrane potentials (−110 to −140 mV, 147 ± 18 MΩ, $n = 19$) than between −70 and −80 mV (288 ± 36 MΩ, difference = 140 ± 31 MΩ, paired $t = 4.59$, $P < 0.001$). Input resistance of opioid-insensitive neurones was also smaller at negative membrane potentials (−110 to −140 mV, 248 ± 13 MΩ, $n = 67$) than between −70 and −80 mV (289 ± 13, difference = 47 ± 5 MΩ, paired $t = 6.00$, $P < 0.0001$). However, the decrease in input resistance at negative potentials was significantly larger in opioid-sensitive than -insensitive neurones (40 ± 6%, $n = 19$ versus 17 ± 2%, $n = 67$, unpaired $t = 4.9$, $P < 0.001$).

With the exception of the amplitude of afterhyperpolariza-

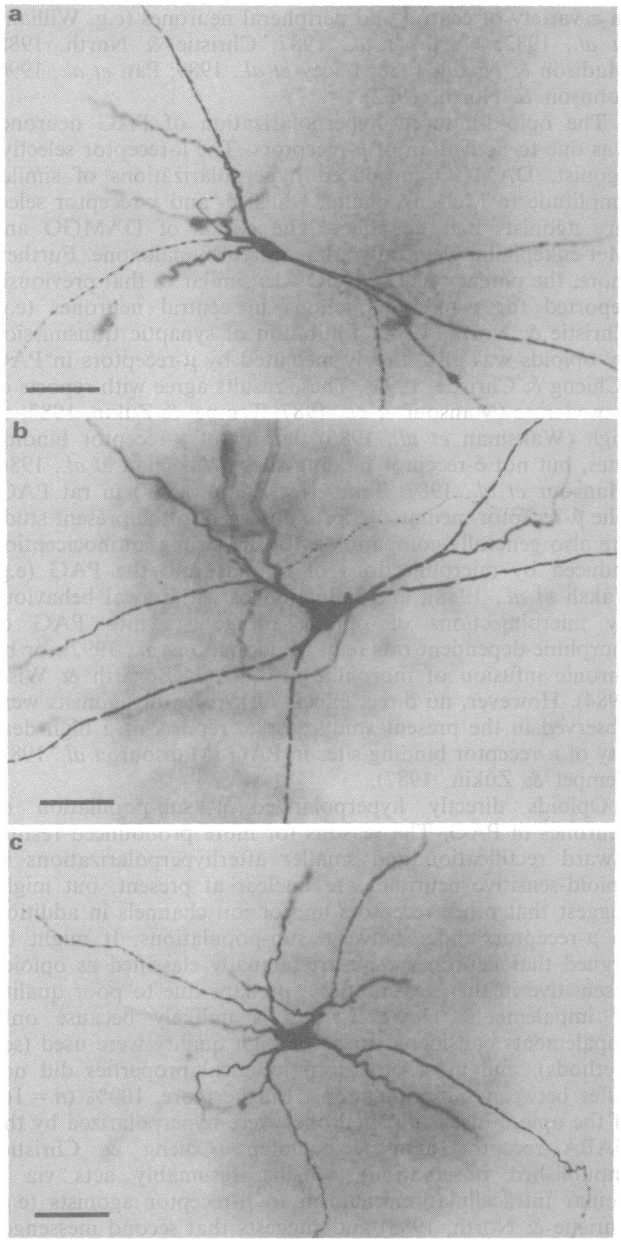

Figure 6 Examples of three morphological types of biocytin-filled PAG neurones. (a) Fusiform, (b) triangular and (c) multipolar, from horizontal midbrain sections. The somata are ovoid shaped and primary dendrites arise from thick extensions of somata. Dendrites branch out in a radiating pattern. Note varicosities, as well as isolated and sparse dendritic spines. Scale bar = 50 μm.

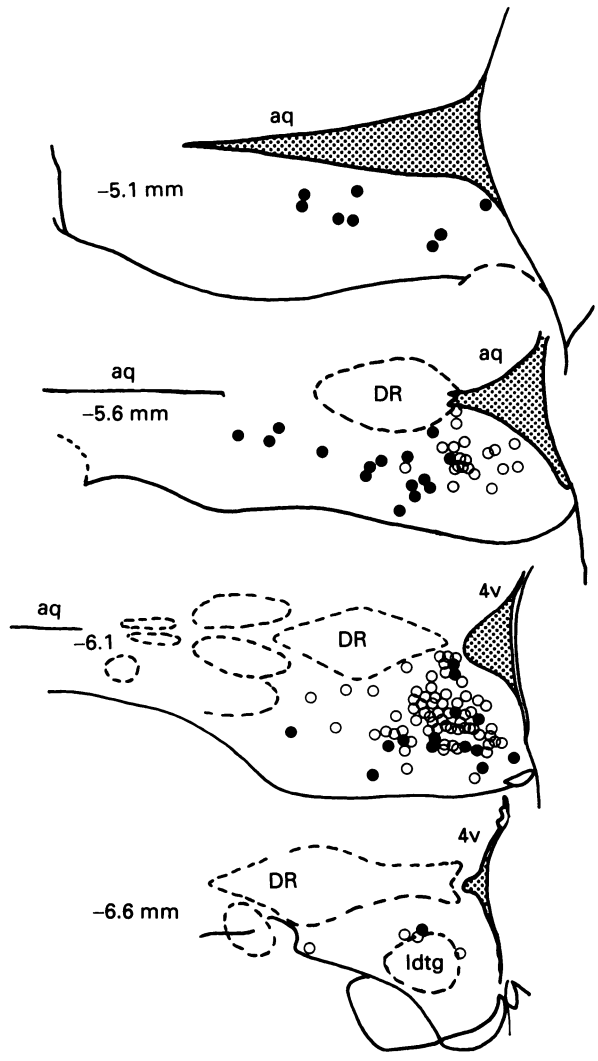

Figure 7 Anatomical locations of opioid-sensitive (●) and -insensitive (○) neurones in four dorso-ventral levels of horizontal PAG sections (5.1, 5.6, 6.1 mm and 6.6 mm ventral to bregma). The precise locations of neurones were determined by visualization of biocytin staining and plotted on diagrams prepared from a stereotaxic atlas of the rat brain (Paxinos & Watson, 1986). Abbreviations: 4v, fourth ventricle; aq, aqueduct; DR, dorsal raphe nucleus; ldtg, laterodorsal tegmental necleus.

tions, other membrane properties of opioid-sensitive and -insensitive neurones did not differ signficantly. The amplitude of afterhyperpolarization was 20 ± 2 mV ($n = 16$) in opioid-sensitive and 25 ± 1 mV ($n = 58$, unpaired $t = 2.45$, $P < 0.02$). Sixty-three percent (12/19) of opioid-sensitive neurones fired spontaneous action potentials at 10 ± 4 Hz (range 0.2 to 50 Hz) in the absence of applied current, versus 50% (34/68) of opioid-insensitive neurones (4 ± 1 Hz, range 0.2 to 14 Hz). Resting membrane potential was -66 ± 4 mV ($n = 7$) in quiescent opioid-sensitive neurones (versus -71 ± 2 mV in opioid-insensitive neurones, $n = 32$). Action potentials had a threshold of -56 ± 1 mV ($n = 16$) in opioid-sensitive neurones, versus -54 ± 1 mV ($n = 58$) in opioid-insensitive neurones, amplitude of 62 ± 2 mV (versus 63 ± 1 mV), duration at threshold of 1.1 ± 0.1 ms (versus 1.4 ± 0.1 ms) and 10–90% rise-time 0.27 ± 0.02 ms (versus 0.31 ± 0.01 ms). During large hyperpolarizing current pulses, a slowly developing depolarization which slowly relaxed on repolarization occurred in 21% (4/19) of opioid-sensitive neurones and 8% (5/65) of opioid-insensitive neurones (e.g. Figure 4c,d). The membrane time constant of opioid-sensitive neurones was 22 ± 2 ms ($n = 19$) between -60 and -80 mV (versus 26 ± 1 ms, $n = 67$ for opioid-insensitive neurones).

Morphology of opioid-sensitive and -insensitive neurones

No significant morphological differences were observed between opioid-sensitive and -insensitive neurones (Figure 6). Soma diameters (measured along the longest axis) of opioid-sensitive neurones (22 ± 1 μm, range 13 to 30 μm, $n = 20$) were nearly identical to opioid-insensitive neurones (22 ± 1 μm, range 10 to 33 μm, $n = 48$). Of the opioid-sensitive neurones, 58% were multipolar (11/19) with ovoid shaped soma (versus 49% [21/43] of opioid-insensitive neurones); 37% were triangular (versus 30% of opioid-insensitive neurones) and 5% fusiform (versus 21% of opioid-insensitive neurones). Orientations of the somata were mostly in the horizontal plane (16/21 versus 37/40 opioid-insensitive neurones). Dendritic spread was usually in a radiating pat-

tern in all directions. Primary dendrites of opioid-sensitive and -insensitive neurones arose from thick extensions of the soma and formed a number of branches (mode = 4 for opioid-sensitive and 3 for -insensitive neurones). Of opioid-sensitive neurones, 29% (6/21) had spines on the primary dendrites (versus 56% [23/41] of opioid-insensitive neurones) and 10% had varicosities (versus 26% of opioid-insensitive neurones). The length of the primary dendrites was 33 ± 10 μm ($n = 21$) with a diameter 2.5 ± 0.2 μm ($n = 21$) (versus 45 ± 8, and 2.7 ± 0.1, $n = 47$ respectively for opioid-insensitive neurones). Secondary dendrites were usually very long (155 ± 26 μm, $n = 21$) and thin (1.3 ± 0.1 μm, $n = 21$) (versus 113 ± 15 μm and 1.4 ± 0.1 μm, $n = 44$ respectively for opioid-insensitive neurones). Spines were visible on 71% of secondary dendrites, and 67% had varicosities (versus 72% and 49% respectively for opioid-insensitive neurones). In all cases spines and varicosities were isolated and sparse (Figure 6). Tertiary dendrites usually appeared to have been damaged during slice preparation. Where they could be identified, axons (<0.5 μm diameter) were usually branched with aborisations oriented in many directions. Axons appeared to originate from the soma in 38% of opioid-sensitive neurones (3/8 versus 73% [24/33] for opioid-insensitive neurones), and from primary dendrites in others.

Anatomical location of opioid-sensitive and -insensitive neurones

Figure 7 depicts the anatomical location of opioid-sensitive and -insensitive neurones in horizontal sections of PAG. The proportions of neurones hyperpolarized by opioids significantly differed among the three main dorso-ventral levels categorized (5.1, 5.6 and 6.1 mm ventral to bregma, $\chi^2 = 29$, 2 d.f., $P < 0.001$). All neurones impaled in the most dorsal slices (lateral PAG, approximately 5.1 mm ventral to bregma) were hyperpolarized by opioids (9/9). In intermediate slices 50% of neurones (15/30) were hyperpolarized by opioids. At this dorso-ventral location the majority of opioid-sensitive neurones appeared to lie adjacent to the dorsal raphe nucleus. In more ventral slices (ventrolateral PAG, approximately 6.1 mm ventral to bregma), only 19% (14/75) of neurones scattered throughout the region were hyperpolarized by opioids. Although 20% (1/5) of neurones in the most ventral section (6.6 mm ventral to bregma) were also hyperpolarized by opioids, too few neurones were impaled for reliable comparisons to be made with other sections.

Discussion

The present study demonstrated that opioid agonists selective for μ-receptors directly hyperpolarized a sub-population of PAG neurones by increasing an inwardly rectifying potassium conductance. Opioid-sensitive neurones were impaled more frequently in lateral than in ventrolateral PAG. With the exception of greater resting inward rectification and smaller amplitude of afterhyperpolarizations in opioid-sensitive neurones, other membrane and morphological properties did not discriminate the sub-populations.

Opioids directly hyperpolarized PAG neurones by increasing an inwardly rectifying potassium conductance. The hyperpolarization reversed polarity at the expected equilibrium potential for potassium ions (E_K), assuming an intracellular potassium concentration of 165 mM. The reversal potential became less negative in close agreement with the Nernst equation when the external potassium concentration was increased, strongly suggesting that the hyperpolarization was due to increased potassium conductance. The opioid-induced potassium conductance displayed inward rectification at hyperpolarized potentials, i.e. the change in input resistance (or conductance using voltage-clamp) was greater at potentials negative to E_K than at more positive potentials. A similar mechanism of action of opioids has been described in a variety of central and peripheral neurones (e.g. Williams *et al.*, 1982; North *et al.*, 1987; Christie & North, 1988; Madison & Nicoll, 1988; Lacey *et al.*, 1989; Pan *et al.*, 1990; Johnson & North, 1992).

The opioid-induced hyperpolarization of PAG neurones was due to activation of μ-receptors. The μ-receptor selective agonist, DAMGO, produced hyperpolarizations of similar amplitude to Met-enkephalin, whilst δ- and κ-receptor selective agonists had no effect. The effects of DAMGO and Met-enkephalin were fully antagonized by naloxone. Furthermore, the potency of DAMGO was similar to that previously reported for μ-receptor actions in central neurones (e.g. Christie & North, 1988). Inhibition of synaptic transmission by opioids was also largely mediated by μ-receptors in PAG (Chieng & Christie, 1994). These results agree with reports of a moderate (Mansour *et al.*, 1987; Tempel & Zukin, 1987) to high (Waksman *et al.*, 1986) density of μ-receptor binding sites, but not δ-receptor binding sites (Waksman *et al.*, 1986; Mansour *et al.*, 1987; Tempel & Zukin, 1987) in rat PAG. The μ-receptor-mediated effects observed in the present study are also generally compatible with the strong antinociception induced by microinjections of opioids into the PAG (e.g. Yaksh *et al.*, 1988), and induction of withdrawal behaviour by microinjections of opioid antagonists into PAG of morphine-dependent rats (e.g. Maldonado *et al.*, 1992), or by chronic infusion of morphine into PAG (Bozarth & Wise, 1984). However, no direct effects of κ-receptor agonists were observed in the present study despite reports of a high density of κ-receptor binding sites in PAG (Mansour *et al.*, 1987; Tempel & Zukin, 1987).

Opioids directly hyperpolarized a sub-population of neurones in PAG. The reasons for more pronounced resting inward rectification and smaller afterhyperpolarizations in opioid-sensitive neurones are unclear at present, but might suggest that other receptors and/or ion channels in addition to μ-receptors differ between sub-populations. It might be argued that neurones were artefactually classified as opioid-insensitive in the present study, perhaps due to poor quality of impalements. However, this is unlikely because only impalements considered to be of high quality were used (see methods), and most other physiological properties did not differ between sub-populations. Furthermore, 100% ($n = 16$) of the opioid-insensitive neurones were hyperpolarized by the $GABA_B$-receptor agonist, baclofen (Chieng & Christie, unpublished observation), which presumably acts via a similar intracellular mechanism to μ-receptor agonists (e.g. Christie & North, 1988) and suggests that second messenger systems were functional in opioid-insensitive neurones.

Populations of opioid-sensitive and -insensitive neurones studied in other brain regions were easily discriminated on the basis of physiological and/or morphological properties, e.g. in the hippocampus (Madison & Nicoll, 1988), substantia nigria (Lacey *et al.*, 1989), ventral tegmental area (Johnson & North, 1992) and nucleus raphe magnus (Pan *et al.*, 1990). However, with the exception of significantly greater resting inward rectification and smaller afterhyperpolarizations in opioid-sensitive neurones, other physiological and morphological features of PAG neurones failed to distinguish separate sub-populations. Glutamatergic and GABAergic components of spontaneous and electrically-evoked synaptic potentials also failed to discriminate the two sub-populations (Chieng & Christie, 1994). Membrane properties of neurones were similar to those previously described for guinea-pig PAG neurones (Sanchez & Ribas, 1991).

It is not clear whether the relatively uniform properties of opioid-sensitive and -insensitive neurones observed in the present study suggest a novel organisation of opioid-sensitive and -insensitive neurones in PAG, or are perhaps due to biased sampling of large cells by intracellular recording techniques. The mean soma diameter of impaled neurones were 22 μm and very few small (<15 μm diameter) neurones were sampled. In contrast, the mean diameter was reported to be 14 μm in Nissl and Golgi staining studies of rat lateral and

ventrolateral PAG (Beitz, 1985; Beitz & Shepard, 1985). Only 33% of Golgi-stained neurones correspond the large fusiform, triangular, and multipolar types impaled in the present study (Beitz & Shepard, 1985). Barbaresi & Manfrini (1988) also reported that most glutamate decarboxylase immunoreactive interneurones in lateral and ventrolateral PAG were small (mean diameter of 10 μm calculated from reported area). It is therefore possible that opioids also act on physiologically distinct small neurones. It is also possible that δ- and κ-receptors on small neurones mediate some actions of opioids in PAG.

The anatomical locations of the two types of PAG neurones found in the present study support the concept that PAG is organised into functional columns extending along the rostrocaudal axis (see Bandler *et al.*, 1991). Opioids hyperpolarized a greater proportion of neurones located in the lateral column (100% of neurones) and dorsal parts of the ventrolateral column (50% of neurones) than in the ventrolateral PAG (19% of neurones, Figure 7). Behbehani *et al.* (1990) also reported that Met-enkephalin hyperpolarized 95% of neurones located in dorsolateral PAG. In contrast, the main antinociceptive zone identified by microinjections of opioids or electrical stimulation was reported to lie within the caudal ventrolateral region of PAG (Yaksh *et al.*, 1988). The somata of neurones which were hyperpolarised by opioids therefore appear to lie outside of the main antinociceptive zone of PAG. However, this discrepancy should not be viewed as critical. Firstly, it is possible that most of the opioid-sensitive neurones sampled in this study have nothing to do with eliciting antinociception, i.e. they might not interact with projection neurones which are parts of the descending antinociceptive pathway. Our physiological roles of PAG influenced by opioids might include organisation of autonomic and somatic components of defence and escape behaviours, or perhaps cardio-respiratory functions (see Bandler *et al.*, 1991). Second, it is conceivable that the abundant small neurones which were not sampled in the ventrolateral PAG (see above) do respond to opioids and are involved in antinociception. Finally, it should be noted that inhibition of synaptic transmission by opioids occurred throughout the lateral and ventrolateral PAG and could be important for the antinociceptive actions of opioids (Chieng & Christie, 1994).

Disinhibition of neurones which project to the ventral medulla was proposed as the mechanism by which opioids act in PAG to induce antinociception (Basbaum & Fields, 1984). This has been postulated to occur via opioid inhibition of tonically active GABAergic interneurones, thereby disinhibiting PAG output neurones projecting to the ventral medulla. Although neurones which were hyperpolarized by opioids in the present study could conceivably participate in this kind of disinhibition, it is unlikely that they were GABAergic because neurones in PAG reported to be immunoreactive for glutamate decarboxylase (Barbaresi & Manfrini, 1988) were much smaller than the neurones sampled in the present study. The neurotransmitters present and anatomical organisation of opioid-sensitive and -insensitive neurones in the PAG have yet to be directly established.

The authors thank Drs N. Lavidis and P.B. Osborne for their helpful comments. Donations of opioid peptides by the National Institute on Drug Abuse (U.S.A.) is gratefully acknowledged. This work was supported by the National Health and Medical Research Council of Australia (910831), National Heart Foundation and the Clive and Vera Ramaciotti Foundation.

References

ADAMS, J.E. (1976). Naloxone reversal of analgesia produced by brain stimulation in the human. *Pain*, **2**, 161–166.

AKIL, H., MAYER, D.J. & LIEBESKIND, J.C. (1976). Antagonism of stimulation-produced analgesia by naloxone, a narcotic antagonist. *Science*, **191**, 961–962.

BANDLER, R., CARRIVE, P. & DEPAULIS, A. (1991). Introduction: Emerging principles of organization of the midbrain periaqueductal gray matter. In *The Midbrain Periaqueductal Gray Matter*. ed. Depaulis, A. & Bandler, R., pp. 1–8. New York: Plenum Press.

BARBARESI, P. & MANFRINI, E. (1988). Glutamate decarboxylase-immunoreactive neurons and terminals in the periaqueductal gray of the rat. *Neurosci.*, **27**, 183–191.

BASBAUM, A.I. & FIELDS, H.L. (1984). Endogenous pain control systems: brainstem spinal pathways and endorphin circuitry. *Annu. Rev. Neurosci.*, **7**, 309–338.

BEHBEHANI, M.M., JIANG, M. & CHANDLER, S.D. (1990). The effect of [Met]enkephalin on the periaqueductal gray neurons of the rat: an *in vitro* study. *Neurosci.*, **38**, 373–380.

BEITZ, A.J. (1985). The midbrain periaqueductal gray in the rat. I. Nuclear volume, cell number, density, orientation and regional subdivisions. *J. Comp. Neurol.*, **237**, 445–459.

BEITZ, A.J. & SHEPARD, R.D. (1985). The midbrain periaqueductal gray in the rat. II. A Golgi analysis. *J. Comp. Neurol.*, **237**, 460–475.

BOZARTH, M.A. & WISE, R.A. (1984). Anatomically distinct opiate receptor fields mediated reward and physical dependence. *Science*, **224**, 516–517.

CHIENG, B. & CHRISTIE, M.J. (1994). Inhibition by opioids acting on μ-receptors of GABAergic and glutamatergic postsynaptic potentials in single rat periaqueductal gray neurones *in vitro*. *Br. J. Pharmacol.*, **113**, 303–309.

CHRISTIE, M.J. & NORTH, R.A. (1988). Agonists at μ-opioid, M_2-muscarinic and $GABA_B$-receptors increase the same potassium conductance in rat lateral parabrachial neurones. *Br. J. Pharmacol.*, **95**, 896–902.

FIELDS, H.L., HEINRICHER, M.M. & MASON, P. (1991). Neurotransmitters in nociceptive modulatory circuits. *Annu. Rev. Neurosci.*, **14**, 219–245.

JOHNSON, S.W. & NORTH, R.A. (1992). Opioids excite dopamine neurons by hyperpolarization of local interneurons. *J. Neurosci.*, **12**, 483–488.

LACEY, M.G., MERCURI, N.B. & NORTH, R.A. (1989). Two cell types in rat substantia nigra zone compacta distinguished by membrane properties and the actions of dopamine and opioids. *J. Neurosci.*, **9**, 1233–1241.

LASCHKA, E., TESCHEMACHER, H.J., MEHRAEIN, P. & HERZ, A. (1976). Sites of action of morphine involved in the development of physical dependence in rats. II. Morphine withdrawal precipitated by application of morphine antagonists into restricted parts of the ventricular system and by microinjection into various brain areas. *Psychopharmacol. (Berl.)*, **46**, 141–147.

MADISON, D.V. & NICOLL, R.A. (1988). Enkephalin hyperpolarizes interneurones in rat hippocampus. *J. Physiol.*, **398**, 123–130.

MALDONADO, R., STINUS, L., GOLD, L.H. & KOOB, G.F. (1992). Role of different brain structures in the expression of the physical morphine withdrawal syndrome. *J. Pharmacol. Exp. Ther.*, **261**, 669–677.

MANSOUR, A., KHACHATURIAN, H., LEWIS, M.E., AKIL, H. & WATSON, S.J. (1987). Autoradiographic differentiation of mu, delta and kappa opioid receptors in the rat forebrain and midbrain. *J. Neurosci.*, **7**, 2445–2464.

NORTH, R.A., WILLIAMS, J.T., SUPRENANT, A. & CHRISTIE, M.J. (1987). μ and δ receptors belong to a family of receptors that are coupled to potassium channels. *Proc. Natl. Acad. Sci. USA*, **84**, 5487–5491.

PAN, Z.Z., WILLIAMS, J.T. & OSBORNE, P.O. (1990). Opioid actions on single nucleus raphe magnus neurons from rat and guinea-pig *in vitro*. *J. Physiol.*, **427**, 519–532.

PAXINOS, G. & WATSON, C. (1986). *The Rat Brain in Stereotaxic Coordinates*. Second edition. Sydney, Australia: Academic Press.

REICHLING, D.B., KWIAT, G.C. & BASBAUM, A.I. (1988). Anatomy, physiology and pharmacology of the periaqueductal gray contribution to antinociceptive controls. *Prog. Brain Res.*, **77**, 31–46.

SANCHEZ, D. & RIBAS, J. (1991). Properties and ionic basis of the action potentials in the periaqueductal grey neurones of the guinea-pig. *J. Physiol.*, **440**, 167–187.

TEMPEL, A. & ZUKIN, R.S. (1987). Neuroanatomical patterns of the μ, δ and κ opioid receptors of rat brain as determined by quantitative *in vitro* autoradiography. *Proc. Natl. Acad. Sci. USA*, **84**, 4308–4312.

WAKSMAN, G., HAMEL, E., FOURNIE-ZALUSKI, M.-C. & ROQUES, B.P. (1986). Autoradiographic comparison of the distribution of the neutral endopeptidase 'enkephalinase' and of μ and δ opioid receptors in rat brain. *Proc. Natl. Acad. Sci. USA*, **83**, 1523–1527.

WILLIAMS, J.T., EGAN, T.M. & NORTH, R.A. (1982). Enkephalin opens potassium channels on mammalian central neurones. *Nature*, **299**, 74–77.

YAKSH, T.L., AL-RODHAN, N.R.F. & JENSEN, T.S. (1988). Sites of action of opiates in production of analgesia. *Prog. Brain Res.*, **77**, 371–394.

(Received January 4, 1994
Revised April 18, 1994
Accepted May 19, 1994)

Br. J. Pharmacol. (1994), **113**, 129–136

Effects of chronic infusions of α-trinositol on regional and cardiac haemodynamics in conscious rats

[1]S.M. Gardiner, P.A. Kemp, *B. Fallgren & T. Bennett

Department of Physiology & Pharmacology, University of Nottingham Medical School, Queen's Medical Centre, Nottingham NG7 2UH, England and *Perstorp Pharma, Science Park, Ideon, S-223 70 Lund, Sweden

1 Male, Long Evans rats (350–450 g) were chronically instrumented for the measurement of renal, mesenteric and hindquarters haemodynamics, and were given three consecutive, 24 h infusions of vehicle (sterile saline at 0.3 ml h^{-1}; $n = 8$) or α-trinositol (D-*myo*-inositol-1,2,6-triphosphate) at 5, 20 and 80 mg kg^{-1} h^{-1} (0.3 ml h^{-1}; $n = 9$). During infusion of α-trinositol at 5 or 20 mg kg^{-1} h^{-1}, cardiovascular changes were little different from those seen during saline infusion. However, during infusion of α-trinositol at 80 mg kg^{-1} h^{-1} there were increases in hindquarters vascular conductance, renal flow and vascular conductance, that were all significantly different from the changes seen in the saline group. Infusion of α-trinositol at the high dose in naive rats ($n = 8$) had even more marked vasodilator effects.

2 Two groups of rats ($n = 8$ in each), chronically instrumented for the measurement of cardiac haemodynamics, were given 48 h infusions of saline (0.3 ml h^{-1}) or α-trinositol (2 mg kg^{-1} bolus, 80 mg kg^{-1} h^{-1} infusion at 0.3 ml h^{-1}). During the infusion of saline, there were slight reductions in heart rate, cardiac index, peak aortic flow, dF/dt_{max} and central venous pressure. In the animals receiving α-trinositol, with the exception of central venous pressure, all the above variables, together with total peripheral conductance, increased.

3 These results, collectively, indicate that incremental infusions of α-trinositol do not reveal its full vasodilator potential, possibly due to concurrent activation of counter-regulatory vasoconstrictor mechanisms. However, infusion of α-trinositol at a high dose causes substantial increases in renal, mesenteric and hindquarters flows and vascular conductances, supported by significant increases in indices of cardiac inotropism. Such effects, in the absence of significant hypotension, tachycardia or signs of desensitization, give α-trinositol a unique cardiovascular profile.

Keywords: α-Trinositol; regional vasodilatation; cardiac inotropism

Introduction

There is increasing evidence that D-*myo*-inositol-1,2,6-triphosphate (α-trinositol, previously known as PP56) has unusual pharmacological attributes. For example, α-trinositol appears to act as an antagonist of the effects of exogenous neuropeptide Y (NPY), both *in vivo* and *in vitro* (Edvinsson *et al.*, 1990; Adamsson & Edvinsson, 1991; Edvinsson & Adamsson, 1992; Sun *et al.*, 1991a,b; 1992; 1993; Potter *et al.*, 1992; Donoso *et al.*, 1993; Schweiler & Hjemdahl, 1993), although this finding is not unanimous (Pernow *et al.*, 1992; Feth *et al.*, 1993). However, in the study of Pernow *et al.* (1992) only a single bolus injection of α-trinositol was given and Feth *et al.* (1993) performed only few experiments. Moreover, while recent findings indicate that α-trinositol may also act as an antagonist of the vasoconstrictor effects of exogenous ATP on the basilar artery of the guinea-pig (Wahlestedt *et al.*, 1992), this effect required higher doses of α-trinositol than those needed to antagonize the actions of NPY.

It has been shown that α-trinositol normalizes platelet aggregation to ADP and thrombin in rats with streptozotocin (STZ)-induced diabetes mellitus (Ruf *et al.*, 1991), and, in the same experimental model, α-trinositol has been found to prevent the reduction in sciatic motor nerve conduction velocity and to suppress partly the increased resistance to hypoxic conduction block (Carrington *et al.*, 1993). It is not known if these actions of α-trinositol in STZ-treated rats are due to inhibition of an effect mediated by endogenous NPY and/or ATP, although Carrington *et al.* (1993) suggested that the beneficial effects of α-trinositol on sciatic neuronal function may have been due to a vascular action. However, the *in vivo* haemodynamic effects of α-trinositol are not known in detail, because previous studies in conscious animals involved measurements of blood pressure and heart rate only.

Therefore, the first objective of the present work was to assess the regional haemodynamic effects of incremental, 24 h infusion of vehicle or α-trinositol in conscious rats. From this experiment we obtained evidence (see Results) that infusion of α-trinositol at 80 mg kg^{-1} h^{-1} exerted vasodilator actions, particularly in the hindquarters vascular bed. Thus, our second objective was to investigate the regional haemodynamic effects of a primed infusion of α-trinositol (2 mg kg^{-1} bolus, 80 mg kg^{-1} h^{-1}) over 72 h. From this experiment it became clear (see Results) that α-trinositol caused substantial increases in renal, mesenteric and, particularly, hindquarters flows and vascular conductances. These findings indicated that marked changes in cardiac haemodynamics were probably occurring. So, our final objective was, in a third experiment, to assess cardiac haemodynamics during primed infusion of vehicle or α-trinositol (as above).

Methods

Experiments were carried out on male, Long Evans rats (350–450 g) bred in the Biomedical Services Unit, Nottingham University Medical School. All surgery was carried out under sodium methohexitone anaesthesia (Brietal, Lilly; 40–60 mg kg^{-1}, i.p., supplemented as required). All details of pulsed Doppler probe implantation, aortic electromagnetic flow probe placement, and intravascular catheter implantation have been published (Gardiner *et al.*, 1990a,b; 1991a, b,c). At least 24 h after the final surgical intervention (catheter implantation) the following experiments were performed:-

[1] Author for correspondence.

Regional haemodynamic effects of infusion of vehicle (saline) or incremental doses of α-trinositol

One group of animals ($n = 8$), instrumented for measurement of regional haemodynamics was monitored for 30 min (06 h 30 min–07 h 00 min) before an infusion of sterile isotonic saline (154 mmol l^{-1} NaCl) was begun (at 0.3 ml h^{-1}) and maintained for 3 days. Recordings (see below) were also made up to 24 h after the end of the saline infusions.

In another group of rats ($n = 9$), instrumented for meas-

Table 1 Resting cardiovascular variables before infusion of saline or α-trinositol in three separate groups of conscious, Long Evans rats, instrumented for the measurement of regional haemodynamics

	Pre-saline (n = 8)	*Pre-α-trinositol (incremental;* n = 9)	*Pre-α-trinositol (high dose;* n = 8)
Heart rate (beats min^{-1})	328 ± 5	329 ± 7	323 ± 8
Mean arterial blood pressure (mmHg)	101 ± 2	105 ± 2	104 ± 1
Renal flow (kHz)	8.0 ± 0.8	8.1 ± 1.0	7.2 ± 0.5
Mesenteric flow (kHz)	8.2 ± 0.5	8.7 ± 0.8	6.6 ± 0.5*
Hindquarters flow (kHz)	3.9 ± 0.1	4.5 ± 0.4	4.6 ± 0.5
Renal conductance ([kHz $mmHg^{-1}$]10^3)	79 ± 7	77 ± 8	70 ± 5
Mesenteric conductance ([kHz $mmHg^{-1}$]10^3)	82 ± 6	84 ± 8	64 ± 5*
Hindquarters conductance ([kHz $mmHg^{-1}$]10^3)	39 ± 2	43 ± 4	45 ± 6

Values are mean ± s.e.mean.
*$P < 0.05$ versus pre-α-trinositol (incremental).

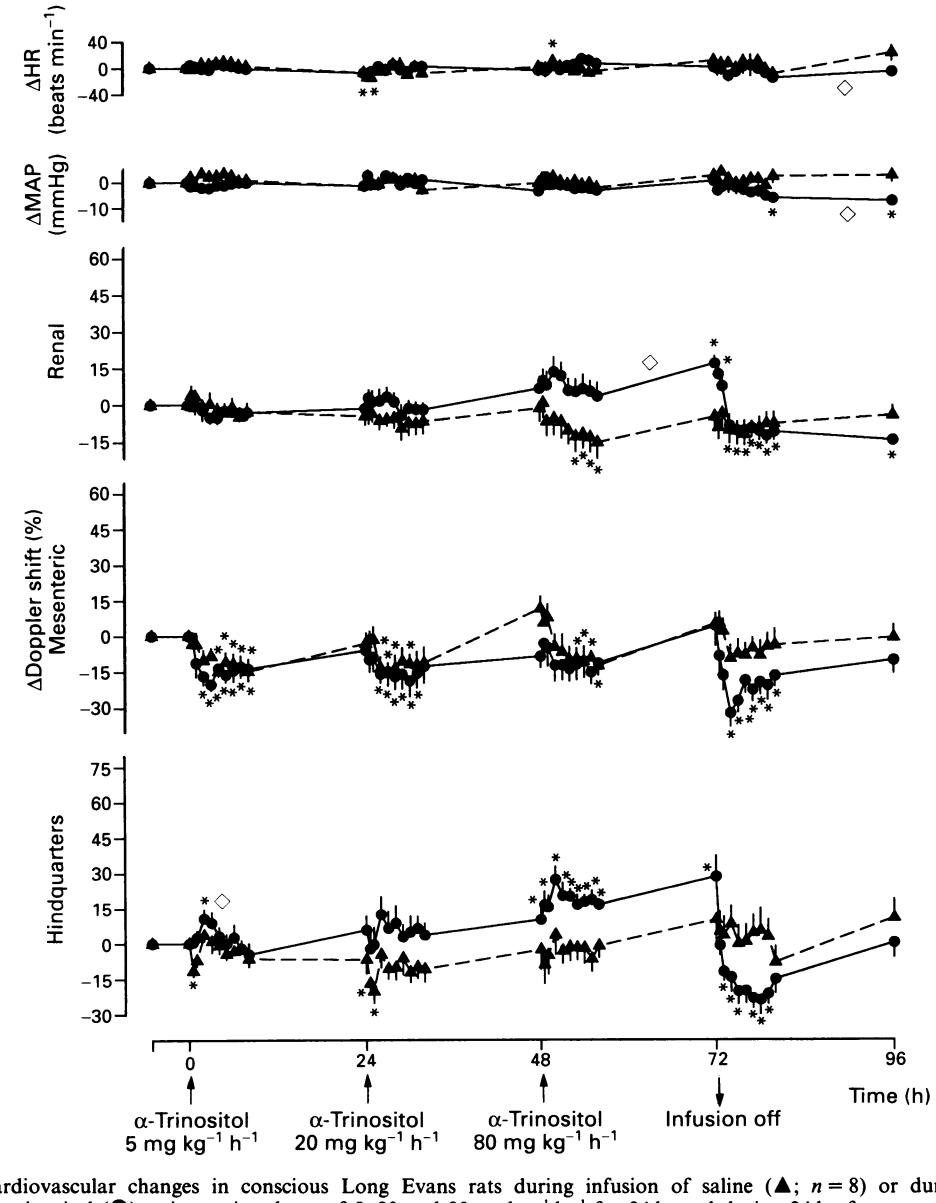

Figure 1 Cardiovascular changes in conscious Long Evans rats during infusion of saline (▲; $n = 8$) or during consecutive infusions of α-trinositol (●) at increasing doses of 5, 20 and 80 mg kg^{-1} h^{-1} for 24 h, and during 24 h after cessation of the latter dose ($n = 9$). HR = heart rate; MAP = mean arterial blood pressure. Values are mean ± s.e.mean; *$P < 0.05$ versus first pre-infusion baseline; ◇$P < 0.05$ versus corresponding integrated change during saline infusion.

urement of regional haemodynamics, 3 consecutive, 24 h infusions of α-trinositol were administered at doses of 5, 20 and 80 mg kg^{-1} h^{-1}. On the first experimental day, following a pre-infusion baseline recording period of 30 min (06 h 30 min–07 h 00 min), α-trinositol infusion (0.3 ml h^{-1}) at 5 mg kg^{-1} h^{-1} was begun, and continued until 07 h 00 min the following day, when the infusion was changed to 20 mg kg^{-1} h^{-1}. On the following day at 07 h 00 min the infusion was changed to 80 mg kg^{-1} h^{-1}, and was maintained for 24 h; the experiment was continued for 24 h after the end of infusion. Recordings were made for 10 min across the time points 0.5, 1, 2, 3, 4, 5, 6, 7, 8 and 24 h on each day during, and for the day after, infusion of saline or α-trinositol.

Regional haemodynamic effects of primed infusion of α-trinositol

On the basis of the first experiment (see Results), we investigated the regional haemodynamic changes in a group ($n = 8$) of rats during primed infusion (2 mg kg^{-1} bolus, 80 mg kg^{-1} h^{-1}) of α-trinositol for 72 h, and for 24 h after the infusion had been stopped. Measurements were made at the same time points as above on the first and last experimental day, but only at 4, 8 and 24 h on the second and third experimental days.

Cardiac haemodynamic effects of primed infusion of saline or α-trinositol

From the second experiment it seemed that the cardiovascular effects of α-trinositol had reached a steady state by 48 h into the infusion (see Results). Therefore, in another 2 groups ($n = 8$ in each) of rats, instrumented for measurement of cardiac haemodynamics (Gardiner *et al.*, 1990a,b; 1991a), we gave infusions of vehicle (isotonic saline) or α-trinositol (2 mg kg^{-1} bolus, 80 mg kg^{-1} h^{-1}). Measurements were made at 1, 2, 3, 4, 5, 6, 7, 8, 24 and 48 h during infusion, and at the same time intervals after infusion.

Data analysis

The pulsed Doppler system does not provide an absolute measure of volume flow, but under conditions of chronic probe implantation, changes in the mean pulsed Doppler shift signal provide a good index of changes in volume flow (Gardiner *et al.*, 1990b). Since, under this condition, the changes in mean Doppler shift signal are determined by the behaviour of the downstream resistance vessels, rather than the vessel under the probe, then calculation of % changes in vascular conductance from % changes in mean Doppler shift and mean systemic arterial blood pressure provides a useful index of changes in regional haemodynamics (e.g., Gardiner *et al.*, 1991a).

Since the system used for monitoring cardiac haemodynamics gives absolute values for thoracic aortic flow (Gardiner *et al.*, 1990a,b; 1991a), then changes in cardiac haemodynamic variables were not expressed as percentages. Within-group analysis of responses during or after infusion of saline or α-trinositol was by Friedman's test (Theodorsson-Norheim, 1987). Comparison of responses during or after infusion of saline or α-trinositol was by Wilcoxon's

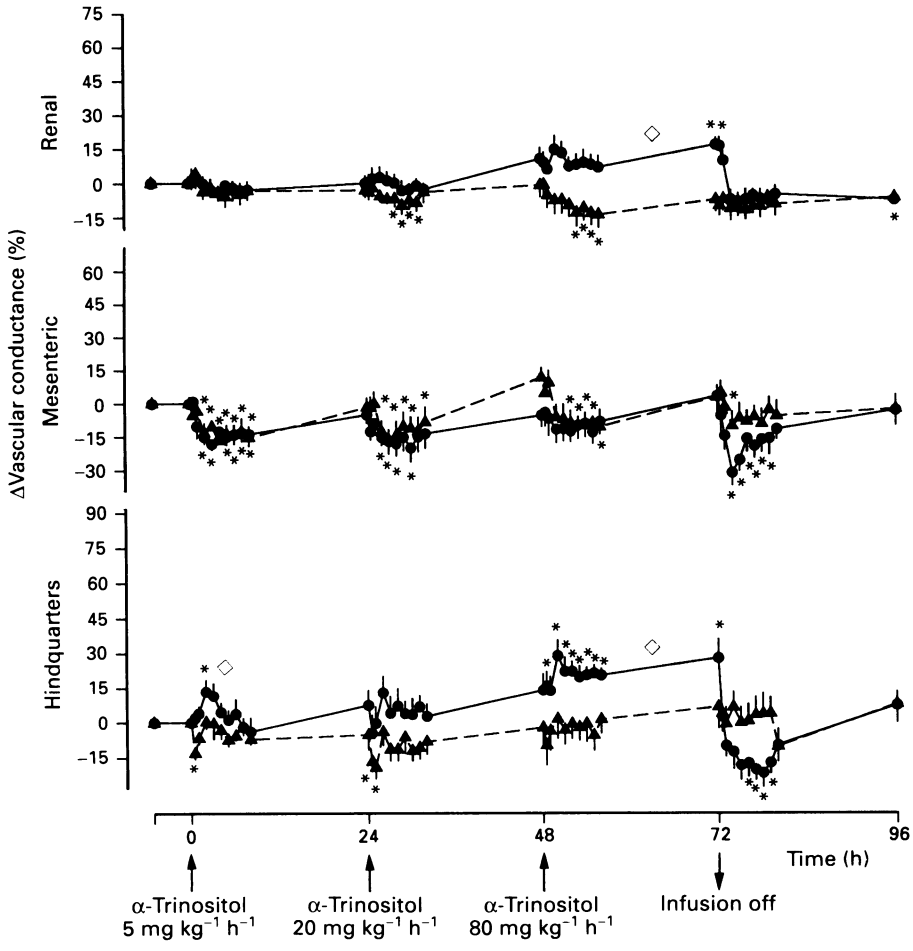

Figure 2 Cardiovascular changes in conscious Long Evans rats during infusion of saline (▲; $n = 8$) or during consecutive infusions of α-trinositol (●) at increasing doses of 5, 20 and 80 mg kg^{-1} h^{-1} for 24 h, and during 24 h after cessation of the latter dose ($n = 9$). Values are mean ± s.e.mean; $^*P < 0.05$ versus first pre-infusion baseline; ◇ $P < 0.05$ versus corresponding integrated change during saline infusion.

ranks sums test or the Mann-Whitney U test (as appropriate) applied to integrated responses (i.e. areas under or over curves) measured over each experimental day. A P value <0.05 was taken as significant.

Drugs

α-Trinositol (Na^+ salt) was supplied by Perstorp Pharma as a freeze-dried powder in sealed vials. This was reconstituted in sterile water immediately before use to give a stock solution of 200 mM; this stock solution was diluted with sterile isotonic saline to give lower concentrations of α-trinositol. This procedure allowed reasonable matching of the tonicity of the saline and α-trinositol infusions, within the constraint of keeping the infusion rate constant.

Results

Resting cardiovascular variables in the 3 groups of animals instrumented for the measurement of regional haemodynamics are shown in Table 1.

Regional haemodynamic effects of saline or incremental infusions of α-trinositol

Cardiovascular changes during and after infusion of saline During and after infusion of saline, mesenteric flow and conductance showed some circadian variation, but other variables showed little change (Figures 1 and 2).

Cardiovascular changes during and after infusion of α-trinositol With infusion of α-trinositol at 5 or 20 mg kg^{-1} h^{-1} cardiovascular changes were generally similar to those seen during saline infusion (Figures 1 and 2). However, during infusion of α-trinositol at 80 mg kg^{-1} h^{-1} there were increases in renal flow and conductance and in hindquarters conductance that were significantly different from those during saline infusion (Figures 1 and 2). Following infusion of α-trinositol, changes in cardiovascular variables were generally similar to those following saline infusion (Figures 1 and 2).

Regional haemodynamic effects of primed infusion of α-trinositol

There was a slight, progressive tachycardia which became significant 6–8 h after onset of α-trinositol infusion (Figure

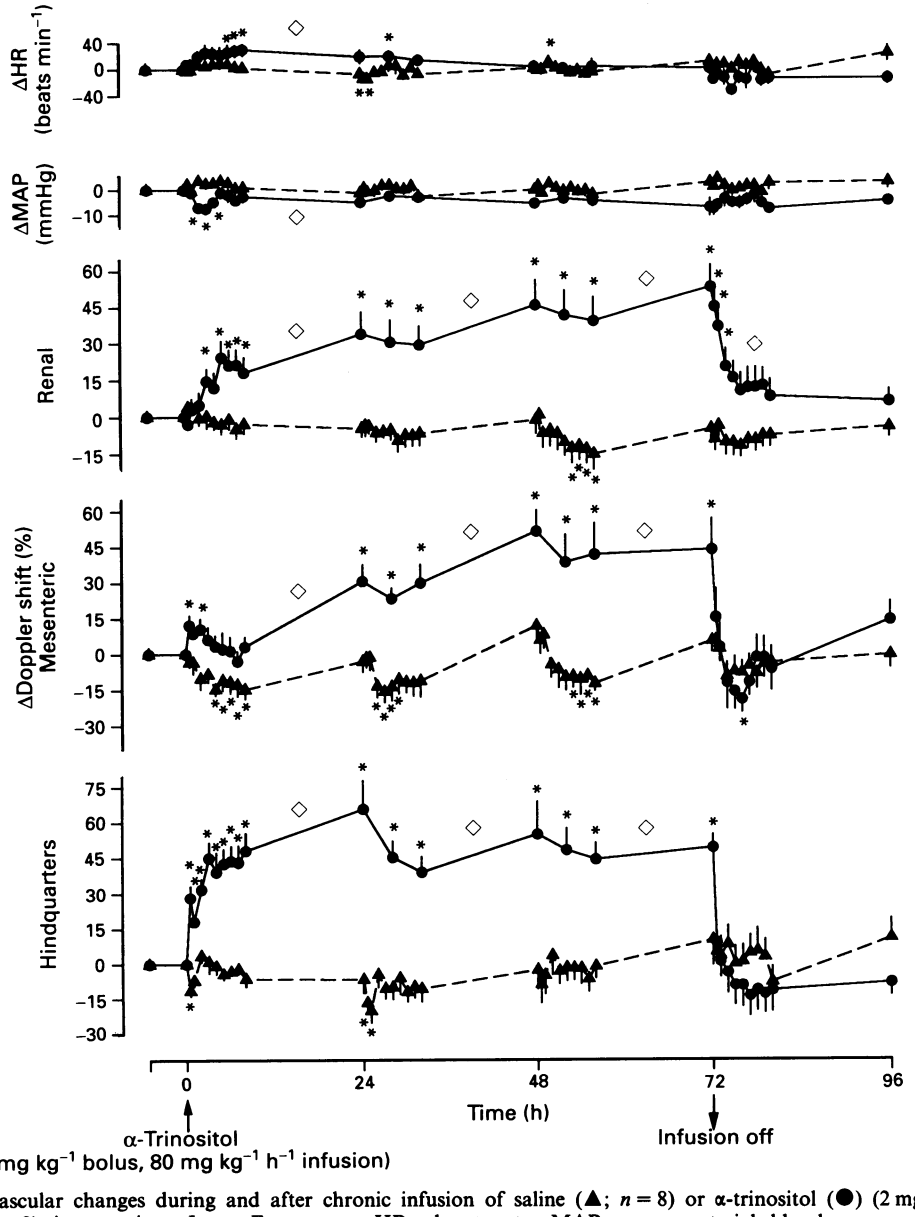

Figure 3 Cardiovascular changes during and after chronic infusion of saline (▲; $n = 8$) or α-trinositol (●) (2 mg kg^{-1} bolus, 80 mg kg^{-1} h^{-1}; $n = 8$) in conscious Long Evans rats. HR = heart rate; MAP = mean arterial blood pressure. Values are mean ± s.e.mean; $*P<0.05$ versus original baseline; $\diamond P<0.05$ versus corresponding integrated change during saline infusion.

3), but thereafter (except at 28 h) heart rate was not significantly different from baseline (Figure 3). The initial tachycardia was significantly different from the change seen during infusion of saline (Figure 3).

Over the first 1 h after the onset of the α-trinositol infusion, there was no significant change in mean arterial blood pressure (Figure 3). However from 3–5 h after the onset of α-trinositol infusion there was a small, but significant, hypotension and this was significantly different from the change seen during saline infusion (Figure 3).

By 3 h after the onset of α-trinositol infusion, renal blood flow and vascular conductance were increased significantly, and these variables rose progressively throughout the infusion period. Although there was some circadian variation, renal flow and vascular conductance were significantly higher than they were during infusion of saline (Figures 3 and 4). After the infusion of α-trinositol was stopped, renal blood flow and vascular conductance fell, but they remained significantly above baseline levels for up to 4 h. During this time, the elevations in renal flow and vascular conductance were significantly different from the changes seen following saline infusion (Figures 3 and 4).

Within the first 1 h after the onset of α-trinositol infusion, mesenteric blood flow and vascular conductance showed small, but significant, increases (Figures 3 and 4) and by 24 h after the onset of α-trinositol infusion, there were substantial increases in mesenteric flow and vascular conductance that were significantly greater than those during infusion of saline (Figures 3 and 4). Within 30 min of the end of the α-trinositol infusion, mesenteric flow and vascular conductance fell towards the baseline level.

During the first 30 min after the onset of α-trinositol

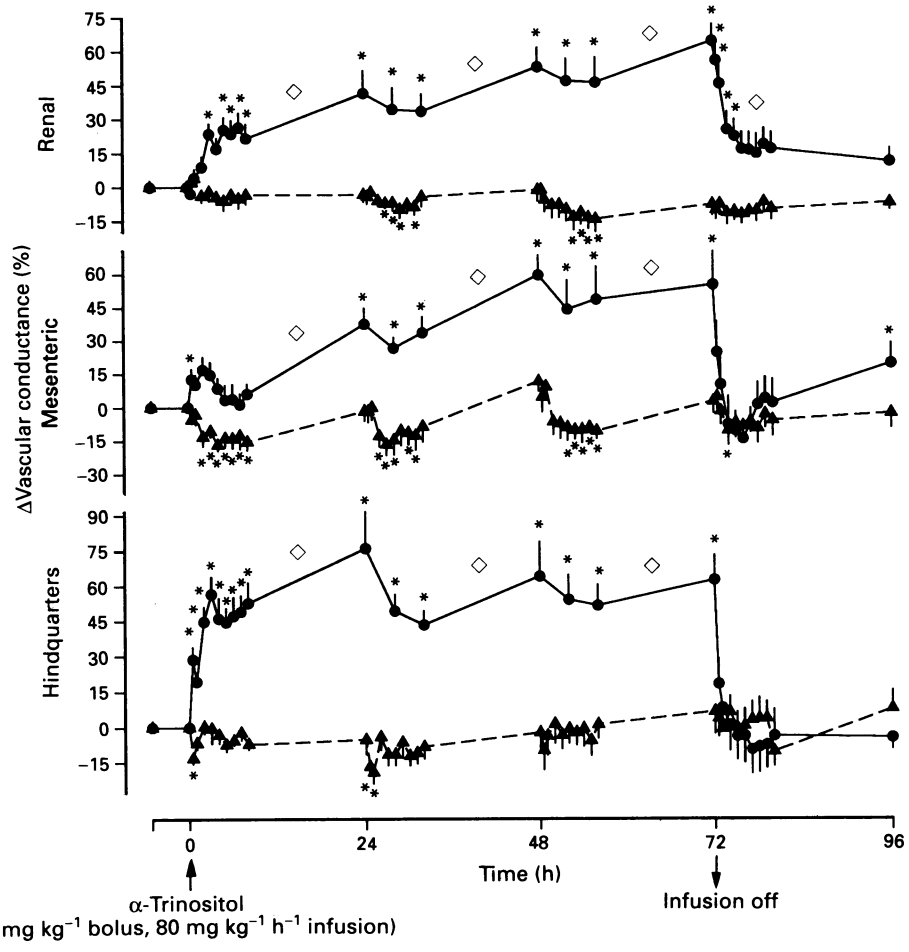

Figure 4 Cardiovascular changes during and after chronic infusion of saline (▲; $n = 8$) or α-trinositol (●) (2 mg kg^{-1} bolus, 80 mg kg^{-1} h^{-1}; $n = 8$) in conscious Long Evans rats. Values are mean ± s.e.mean; *$P < 0.05$ versus original baseline; ◇$P < 0.05$ versus corresponding integrated change during saline infusion.

Table 2 Resting cardiovascular variables before infusion of saline or α-trinositol in two separate groups ($n = 8$ in each) of conscious, Long Evans rats instrumented for the measurement of cardiac haemodynamics

	Pre-saline	*Pre-α-trinositol*
Mean arterial blood pressure (mmHg)	100 ± 2	96 ± 2
Heart rate (beats min^{-1})	373 ± 10	370 ± 14
Cardiac index (ml min^{-1} 100 g^{-1})	24.9 ± 1.4	25.4 ± 1.5
Stroke index (μl min^{-1} 100 g^{-1})	67 ± 4	69 ± 5
Peak aortic flow (ml min^{-1} 100 g^{-1})	101 ± 5	105 ± 4
dF/dt_{max} (1 min^{-2} 100 g^{-1})	433 ± 23	443 ± 20
Total peripheral conductance (μl min^{-1} mmHg^{-1} 100 g^{-1})	252 ± 18	266 ± 19
Central venous pressure (cmH_2O)	3.3 ± 0.4	3.9 ± 0.2

Values are mean ± s.e.mean.

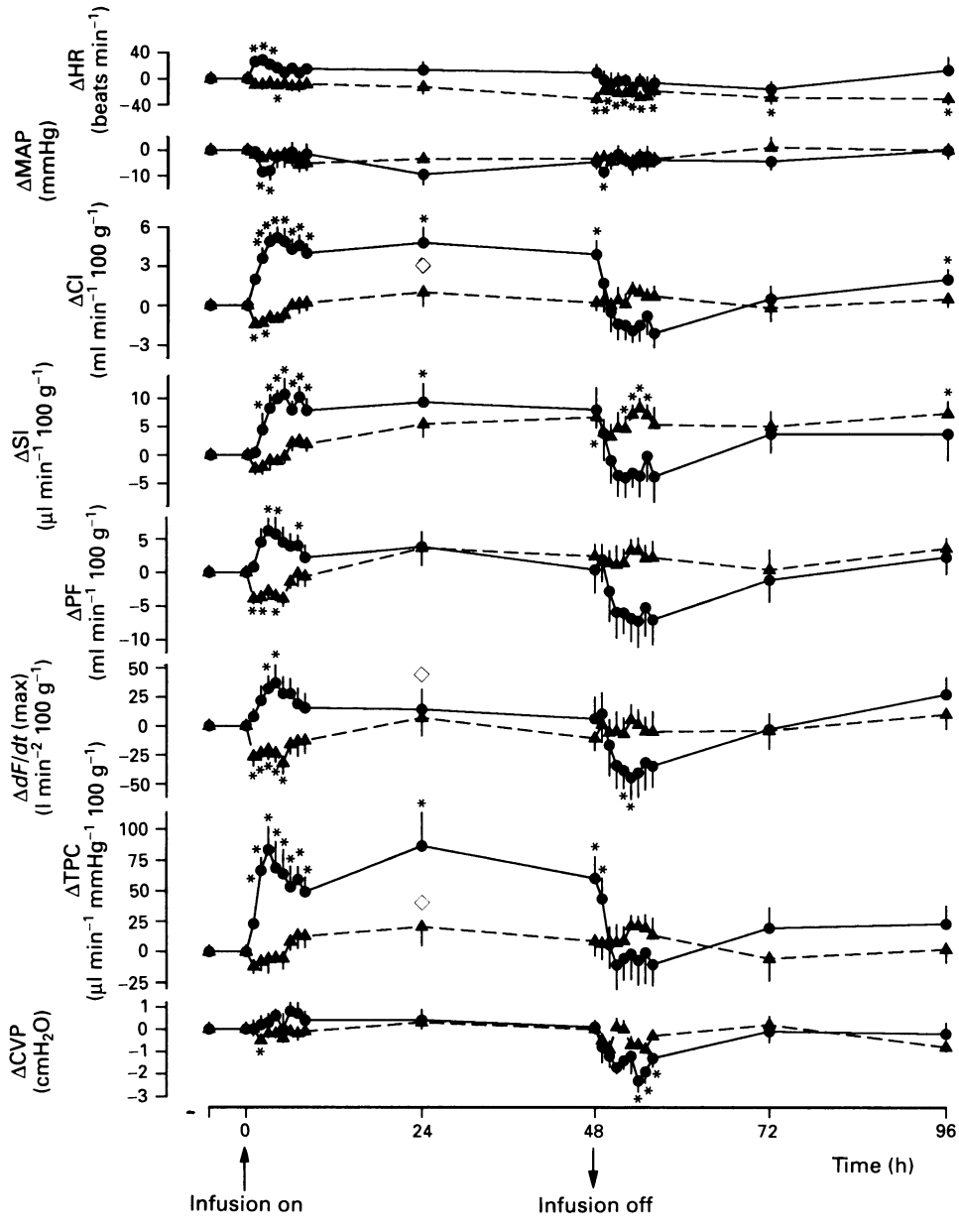

Figure 5 Cardiovascular changes during and after infusion of saline (▲) or α-trinositol (●, 2 mg kg^{-1}, 80 mg kg^{-1} h^{-1}) in separate groups of conscious Long Evans rats ($n = 8$ in each group). HR = heart rate; MAP = mean arterial blood pressure; CI = cardiac index; SI = stroke index; PF = peak aortic flow; dF/dt_{max} = maximum rate of rise of aortic flow; TPC = total peripheral conductance; CVP = central venous pressure. Values are mean ± s.e.mean; *$P < 0.05$ versus original baseline; ◇$P < 0.05$ versus corresponding integrated change during saline infusion.

Table 3 Integrated cardiovascular responses (areas under or over curves, AUC or AOC, respectively) during 48 h infusion of saline or α-trinositol (2 mg kg^{-1} bolus, 80 mg kg^{-1} h^{-1}), and for 7 h following infusion in separate groups ($n = 8$ in each) of conscious, Long Evans rats

	During infusion		*After infusion*	
	Saline	*α-Trinositol*	*Saline*	*α-Trinositol*
Heart rate	− 993 ± 177	945 ± 305*	− 164 ± 31	− 123 ± 57
Mean blood pressure	− 271 ± 55	− 393 ± 81	− 39 ± 14	− 37 ± 16
Cardiac index	58 ± 20	205 ± 41*	8 ± 3	− 15 ± 5
Stroke index	251 ± 61	428 ± 128	44 ± 10	− 153 ± 60
Peak aortic flow	195 ± 56	207 ± 86	24 ± 10	− 55 ± 18*
dF/dt_{max}	− 864 ± 300	1290 ± 623*	− 128 ± 40	− 315 ± 96
Total peripheral conductance	1015 ± 241	3366 ± 745*	155 ± 48	− 170 ± 55
Central venous pressure	15.9 ± 7.8	33.1 ± 10.2	− 5.3 ± 1.3	− 12.1 ± 1.9

During and after infusion of α-trinositol, the preinfusion baseline values were used as the reference level for the integrated changes. Following infusion, the latter were calculated starting 2 h and ending 8 h after the offset of the infusion. Values are mean ± s.e.mean in arbitrary units.
*$P < 0.05$ versus the corresponding value in the saline group.

infusion, hindquarters blood flow and vascular conductance were increased significantly above baseline and above the saline control, and they remained so throughout the period of α-trinositol infusion (Figures 3 and 4). By 30 min after the end of the α-trinositol infusion, hindquarters blood flow and vascular conductance were not significantly different from baseline levels (Figures 3 and 4). There were no differences, under these conditions, between hindquarters haemodynamics following infusion of α-trinositol or saline (Figures 3 and 4).

Cardiac haemodynamic effects of primed infusion of saline or α-trinositol

Prior to infusion of saline or α-trinositol, there were no significant differences in resting cardiovascular variables in the two groups studied (Table 2).

Cardiovascular changes during and after infusion of saline There were only slight changes in cardiac haemodynamic variables during and after infusion of saline (Figure 5).

Cardiovascular changes during and after infusion of α-trinositol The notable difference between changes during saline and α-trinositol infusion was that the latter caused significantly greater increases in cardiac index and total peripheral conductance (Figure 5, Table 3).

Discussion

In the present work, during infusion of saline, although mean arterial blood pressure and heart rate were relatively stable, there were circadian variations, particularly in mesenteric haemodynamics, with the highest values being noted at the beginning of the recording period (i.e. 06 h 30 min–07 h 00 min). Since rats are nocturnal feeders, and since the animals were kept on a 12 h light/dark cycle, with the light period beginning at 06 h 00 min, it is likely the rats were in a post-prandial state when recordings began. Thus, throughout the day, the mesenteric hyperaemic vasodilator effects of feeding were probably waning. Against this background, incremental infusions (5 and 20 mg kg^{-1} h^{-1} over 24 h) of α-trinositol had only small regional haemodynamic effects, and, although subsequent infusion at 80 mg kg^{-1} h^{-1} did increase renal and hindquarters flows and vascular conductances, these effects were modest, and there were no increases in mesenteric haemodynamics. While this picture could indicate that α-trinositol is relatively inert, when the infusion was stopped there were substantial falls in renal, mesenteric and hindquarters flows. This finding is consistent with activation of counter-regulatory vasoconstrictor mechanisms during administration of α-trinositol. Since the infusion of the high dose of α-trinositol (2 mg kg^{-1} bolus, 80 mg kg^{-1} h^{-1} infusion) in naive rats caused substantial increases in renal, mesenteric, and, particularly, hindquarters flows and vascular conductances over a period of 3 days, and because these effects appeared well within the first 24 h of infusion, then it seems that incremental infusion of α-trinositol may not reveal its full vasodilator potential.

With the high dose infusion of α-trinositol in naive rats, there were significant rises in blood flow, and vascular conductance, in the renal, mesenteric and hindquarters vascular beds, although the patterns of change differed. Thus, the increases in hindquarters flow and vascular conductance were almost maximal within 3 h of the onset of α-trinositol infusion, whereas the effects in the renal and mesenteric vascular beds developed much more slowly. While it is feasible that the mechanisms of the α-trinositol-induced vasodilatation were different in the different vascular beds, we cannot discount the possibility that the slower onset of the renal and mesenteric vasodilator effects of α-trinositol was due to more effective autoregulation in these vascular beds, than in the hindquarters. However, if this were the case, it appears that such mechanisms were not capable of suppressing the effects of α-trinositol during chronic administration, because, at the end of the 3 day infusion period, the increases in renal, mesenteric and hindquarters flows and vascular conductances were similar, and all substantial. The fact that there was no significant hypotension or tachycardia at this stage indicates that the increases in regional blood flow must have been met by an increase in cardiac output, or by substantial steal from other vascular territories. However, in the final experiment we demonstrated a sustained increase in cardiac output during chronic infusion of α-trinositol, so it is likely that this effect provided for the observed increases in regional blood flows.

In the experiment in which cardiac haemodynamics were measured, we found that during infusion of saline there was a slight, slowly developing, bradycardia accompanied by earlier, transient reductions in cardiac index, peak aortic flow, dF/dt_{max} and central venous pressure. It is likely the bradycardia represented the animals becoming acclimatized to the experimental conditions, whereas the initial changes in cardiac haemodynamics may well have been due to diminution of feeding-induced myocardial stimulation (see above). Whatever the explanation, it is notable that the changes were directionally opposite to those seen in the animals infused with α-trinositol. Chronic infusion of α-trinositol caused sustained increases in cardiac index and total peripheral conductance, with no accompanying change in mean systemic arterial blood pressure or central venous pressure. It is feasible that the increase in cardiac index caused by α-trinositol was due to a preferential reduction in afterload (i.e., a rise in total peripheral conductance in the absence of a reduction in central venous pressure) (Bhatia & Frohlich, 1973; Tarazi *et al.*, 1976; Tarazi, 1978; Trapani *et al.*, 1991). However, the increase in cardiac index caused by a reduction in afterload is not accompanied by any significant change in dF/dt_{max} (de Wildt & Sangster, 1983), whereas, compared to saline, α-trinositol caused a significant increase in dF/dt_{max}. There is evidence that, in the absence of a change in heart rate, a relative increase in dF/dt_{max} is a reliable index of a positive inotropic effect (de Wildt & Sangster, 1983). Thus, overall, it is feasible that α-trinositol has a positive inotropic action, in addition to its vasodilator effect, although there are no *in vitro* data supporting this proposition.

At first sight this haemodynamic profile of α-trinositol does not appear to be unique since, for example, (±)-dobutamine has similar attributes (Gardiner *et al.*, 1991a). However, α-trinositol differs in several fundamental ways from any compounds we have studied previously. Thus, without causing hypotension or tachycardia, α-trinositol (2 mg kg^{-1} bolus, 80 mg kg^{-1} h^{-1} infusion) evoked sustained increases in renal, mesenteric and hindquarters flow. In contrast, although (±)-dobutamine elicited sustained (over 1 h) increases in cardiac function and hindquarters blood flow, these effects were accompanied by substantial tachycardia and hypotension, with no increase in mesenteric flow, and a reduction in renal blood flow (Gardiner *et al.*, 1991a). Likewise, during the infusion of human α-CGRP, although hindquarters flow was increased, renal and mesenteric blood flows were reduced, and significant hypotension and tachycardia occurred (Gardiner *et al.*, 1989; 1991a,b).

Another notable difference between α-trinositol and human α-CGRP is that during chronic (3 day) infusion of the latter, marked desensitization occurred (Gardiner *et al.*, 1991b), whereas in the present work we found that the hindquarters hyperaemic effect of α-trinositol was sustained, and the renal and mesenteric haemodynamic actions of α-trinositol progressively increased during the 3 day infusion period. A further remarkable feature of the pharmacodynamic profile of α-trinositol was that, following the offset of the 3 day infusion, there was little evidence of undershoot (i.e., reduction below pre-infusion baseline) in the variables measured. Hence, it appeared that there may not have been sustained

activation of counter-regulatory vasoconstrictor mechanisms during infusion of α-trinositol. This picture contrasts starkly with that seen with (±)-dobutamine, where, following the end of infusion, there was rebound hypertension and depression of cardiac function accompanied by impairment of renal and mesenteric blood flow (Gardiner *et al.*, 1991a). A similar change in renal haemodynamics was seen after infusion of human α-CGRP, if desensitization had not occurred (Gardiner *et al.*, 1989; 1991b). A likely explanation of the ability of α-trinositol to cause marked increases in renal, mesenteric and hindquarters vascular conductances, without triggering counter-regulatory vasoconstrictor mechanisms, is the absence of a hypotensive stimulus for activation of the latter, due to the concurrent increase in cardiac output. However, we cannot preclude the possibility that there was adaptation of the counter-regulatory mechanisms during the 3 day infusion of α-trinositol; this would be consistent with the more marked undershoot in haemodynamic variables following the infusion of the high dose of α-trinositol for only 24 h. The present results cannot be compared with previous reports of the cardiovascular effects of α-trinositol (see Introduction) since those studies involved relatively short duration administration of the drug, and only heart rate and blood pressure were measured. It remains to be determined what accounts for the remarkable haemodynamic profile of α-trinositol during chronic infusion.

In summary, α-trinositol possesses a unique cardiovascular profile that may make it useful in a variety of clinical conditions, including the critically ill patient (Kulka & Tryba, 1993).

We are grateful to J.E. March for technical assistance. This work was supported by a donation from Perstorp Pharma.

References

ADAMSSON, M. & EDVINSSON, L. (1991). Blockade of neuropeptide Y-induced potentiation of noradrenaline-evoked vasoconstriction by d-myo-inositol-1,2,6-trisphosphate (PP56) in rabbit femoral arteries. *Neuropeptides*, **19**, 13–16.

BHATIA, S.K. & FROHLICH, E.D. (1973). Hemodynamic comparison of agents useful in hypertensive emergencies. *Am. Heart J.*, **85**, 367–373.

CARRINGTON, A.L., CALCUTT, N.A., ETTLINGER, C.B., GUSTAFSSON, T. & TOMLINSON, D.R. (1993). Effects of treatment with myo-inositol or its 1,2,6-trisphosphate (PP56) on nerve conduction in streptozotocin-diabetes. *Eur. J. Pharmacol.*, **237**, 257–263.

DE WILDT, D.J. & SANGSTER, B. (1983). An evaluation of derived aortic flow parameters as indices of myocardial contractility in rats. *J. Pharmacol. Methods*, **10**, 55–64.

DONOSO, M.V., BORIC, M., PRADO, M., FOURNIER, A., ST. PIERRE, S., EDVINSSON, L. & HUIDOBRO-TORO, J.P. (1993). D-myo-inositol 1,2,6-trisphosphate blocks neuropeptide Y-induced facilitation of noradrenaline-evoked vasoconstriction of the mesenteric bed. *Eur. J. Pharmacol.*, **240**, 93–97.

EDVINSSON, L. & ADAMSSON, M. (1992). Neuropeptide Y inhibits relaxation of guinea pig cerebral, coronary and uterine arteries: blockade by d-myo-inositol-1,2,6-triphosphate. *J. Cardiovasc. Pharmacol.*, **20**, 466–472.

EDVINSSON, L., ADAMSSON, M. & JANSEN, L. (1990). Neuropeptide Y antagonistic properties of d-myo-inositol-1,2,6-trisphosphate in guinea pig basilar arteries. *Neuropeptides*, **17**, 99–105.

FETH, F., ERDBRÜGGER, W., RASCHER, W. & MICHEL, M.C. (1993). Is PP56 (D-myo-inositol-1,2,6-trisphosphate) an antagonist at neuropeptide Y receptors? *Life Sci.*, **52**, 1835–1844.

GARDINER, S.M., COMPTON, A.M. & BENNETT, T. (1989). Regional hemodynamic effects of calcitonin gene-related peptide. *Am. J. Physiol.*, **256**, R332–R338.

GARDINER, S.M., COMPTON, A.M., BENNETT, T. & HARTLEY, C.J. (1990a). Can pulsed Doppler technique measure changes in aortic blood flow in conscious rats? *Am. J. Physiol.*, **259**, H448–H456.

GARDINER, S.M., COMPTON, A.M., KEMP, P.A. & BENNETT, T. (1990b). Regional and cardiac haemodynamic responses to glyceryl trinitrate, acetylcholine, bradykinin and endothelin-1 in conscious rats: effects of N^G-nitro-L-arginine methyl ester. *Br. J. Pharmacol.*, **101**, 632–639.

GARDINER, S.M., COMPTON, A.M., KEMP, P.A., BENNETT, T., HUGHES, B. & FOULKES, R. (1991a). Differential effects of (±)-dobutamine and human α-CGRP on cardiac and on regional haemodynamics in conscious Long Evans rats. *Br. J. Pharmacol.*, **103**, 1500–1508.

GARDINER, S.M., COMPTON, A.M., KEMP, P.A., BENNETT, T., HUGHES, B. & FOULKES, R. (1991b). Regional haemodynamic effects of prolonged infusions of human α-calcitonin gene-related peptide in conscious, Long Evans rats. *Br. J. Pharmacol.*, **103**, 1509–1514.

GARDINER, S.M., KEMP, P.A. & BENNETT, T. (1991c). Effects of N^G-nitro-L-arginine methyl ester on vasodilator responses to adrenaline or BRL 38227 in conscious rats. *Br. J. Pharmacol.*, **104**, 731–737.

KULKA, P.J. & TRYBA, M. (1993). Inotropic support of the critically ill patient: a review of the agents. *Drugs*, **45**, 654–667.

PERNOW, J., MODIN, A. & LUNDBERG, J.M. (1992). No effect of D-myo-inositol-1,2,6-triphosphate on vasoconstriction evoked by neuropeptide Y and non-adrenergic sympathetic nerve stimulation. *Eur. J. Pharmacol.*, **222**, 171–174.

POTTER, E.K., EDVINSSON, L. & GUSTAFSSON, T. (1992). Antagonism of pre- and postjunctional responses to neuropeptide Y and sympathetic stimulation by D-myo-inositol-1,2,6-trisphosphate in the anaesthetised dog. *Eur. J. Pharmacol.*, **221**, 307–314.

RUF, J.C., CIAVATTI, M., GUSTAFSSON, T. & RENAUD, S. (1991). Effects of PP-56 and vitamin E on platelet hyperaggregability, fatty acid abnormalities, and clinical manifestations in streptozocin-induced diabetic rats. *Diabetes*, **40**, 233–239.

SCHWIELER, J.H & HJEMDAHL, P. (1993). D-myo-inositol-1,2,6-trisphosphate (PP56) antagonizes nonadrenergic sympathetic vasocontriction: possible involvement of neuropeptide Y. *J. Cardiovasc. Pharmacol.*, **21**, 347–352.

SUN, X.Y., DAHLÖF, C., EDVINSSON, L. & HEDNER, T. (1991a). D-myo-inositol-1-2-6-trisphosphate is a selective antagonist of neuropeptide Y-induced pressor responses in the pithed rat. *Eur. J. Pharmacol.*, **204**, 281–286.

SUN, X.Y., EDVINSSON, L. & HEDNER, T. (1991b). Neuropeptide Y-induced pressor responses in spontaneously hypertensive and Wistar-Kyoto rats antagonized by D-myo-inositol-1,2,6-trisphosphate (PP56). *J. Hypertens.*, **9**, S344–S345.

SUN, X.Y., EDVINSSON, L. & HEDNER, T. (1992). Effects of d-myo-inositol-1,2,6-trisphosphate on neuropeptide Y-induced potentiation of various vasoconstrictor agents in the rat. *J. Pharmacol. Exp. Ther.*, **261**, 1147–1152.

SUN, X.Y., EDVINSSON, L. & HEDNER, T. (1993). Cardiovascular effects of alpha-trinositol in spontaneously hypertensive and normotensive Wistar-Kyoto rats. *J. Hypertens.*, **11**, 935–943.

TARAZI, R.C. (1978). Vasodilators in hypertension: spectrum of actions and counteractions. *Cardiovasc. Med.*, **3**, 1125–1131.

TARAZI, R.C., DUSTAN, H.P., BRAVO, E.L. & NIARCHOS, A.P. (1976). Vasodilating drugs: contrasting haemodynamic effects. *Clin. Sci. Mol. Med.*, **51**, 575s–578s.

THEODORSSON-NORHEIM, E. (1978). Friedman and Quade test: BASIC computer program to perform non-parametric two-way analysis of variance and multiple comparisons on ranks of several related samples. *Comput. Biol. Med.*, **17**, 85–99.

TRAPANI, A.J., SMITS, G.J., MCGRAW, D.E., MCMAHON, E.G. & BLAINE, E.H. (1991). Hemodynamic basis for the depressor activity of zaprinast, a selective cyclic GMP phosphodiesterase inhibitor. *J. Pharmacol. Exp. Ther.*, **258**, 269–274.

WAHLESTEDT, C., REIS, D.J., YOO, H., ADAMSSON, M., ANDERSSON, D. & EDVINSSON, L. (1992). A novel inositol phosphate selectively inhibits vasoconstriction evoked by the sympathetic co-transmitters neuropeptide Y (NPY) and adenosine triphosphate (ATP). *Neurosci. Lett.*, **143**, 123–126.

(Received January 13, 1994
Revised May 6, 1994
Accepted May 24, 1994)

Br. J. Pharmacol. (1994), **113**, 137–142

Generation by the phosphoramidon-sensitive peptidases, endopeptidase-24.11 and thermolysin, of endothelin-1 and C-terminal fragment from big endothelin-1

Leonard J. Murphy, *Roger Corder, †Anthony I. Mallet & [1]Anthony J. Turner

Department of Biochemistry & Molecular Biology, University of Leeds, Leeds LS2 9JT; *The William Harvey Research Institute, St Bartholomew's Hospital Medical College, Charterhouse Square, London EC1M 6BQ and †Mass Spectrometry Facility, St. John's Institute of Dermatology, St. Thomas' Hospital, Lambeth Palace Road, London SE1 7EH.

1 Phosphoramidon, a potent inhibitor of endopeptidase-24.11 (E-24.11) and thermolysin, has been shown to reduce the hypertensive effect of exogenous big endothelin-1 (big ET-1) in rats. To examine whether E-24.11 or thermolysin convert big ET-1 to endothelin-1 (ET-1) and C-terminal fragment (CTF), the effects on porcine and human big ET-1 of each of the purified enzymes were compared *in vitro*.

2 For E-24.11, the relative rates of hydrolysis were ET-1 > CTF >> big ET-1. The relative half-lives for hydrolysis of 3 nmol of each peptide by 200 ng enzyme were: big ET-1 > 24 h; ET-1, 37 min; CTF, 57 min. For comparison, the half-life for hydrolysis of substance P under similar conditions was 2.1 min.

3 For thermolysin the relative rates of hydrolysis were found to be big ET-1 > CTF > ET-1. The relative half-lives for hydrolysis of 3 nmol peptide by 50 ng enzyme were: big ET-1, 25 min; ET-1, 56 min; CTF, 47 min.

4 Because the low rate of conversion of big ET-1 to ET-1 by E-24.11 did not yield sufficient ET-1 for h.p.l.c. quantification a RIA specific for ET-1(16-21) was used to study further the hydrolysis of big ET-1 by E-24.11. Incubation of big ET-1 (0.2–2 nmol) with E-24.11 (4–400 ng) generated ET-1 levels of between 1.7 and 33 pmol measured by RIA. Incubation of big ET-1 (2 nmol) with E-24.11 (40 ng) for 8 h showed that steady state levels of ET-1 were achieved after 4 h indicating that the rate of ET-1 degradation was then equal to the formation of new ET-1. Characterization of the immunoreactivity by h.p.l.c. and RIA confirmed that authentic ET-1 had been produced, but the yield was insufficient for verification by mass spectrometry.

5 Both ET-1-like and CTF-like peaks were detected at 214 nm when the products of big ET-1 hydrolysis by thermolysin were resolved by h.p.l.c. RIA and mass spectrometry confirmed the production of ET-1 with amounts in the range 120–160 pmol.

6 The hydrolysis profile of ET-1 by E-24.11 and thermolysin shows that both enzymes have some common cleavage sites consistent with their similar specificities hydrolysing on the amino side of a hydrophobic residue.

7 Thermolysin, for which 3D structural information is available, may represent a better model for endothelin converting enzyme (ECE) action than E-24.11 and could be useful for the design of ECE inhibitors. Since E-24.11 can both synthesize and hydrolyse ET-1, the presence of E-24.11 in membrane fractions or in partially purified ECE preparations may produce misleading estimates of ECE activity.

Keywords: Endopeptidase-24.11; endothelin converting enzyme; thermolysin; phosphoramidon; thiorphan

Introduction

Endothelin-1, a 21 amino acid, potent vasoconstrictor peptide, is produced by cleavage of its precursor 'big endothelin' at the Trp^{21}-Val^{22} bond by a putative endothelin converting enzyme (ECE) (Yanagisawa *et al.*, 1988). Several lines of study have recently implicated a phosphoramidon-sensitive metalloendopeptidase in the physiological conversion of big endothelin-1 to endothelin-1 and its C-terminal fragment (big ET-1(22-39)) (Ikegawa *et al.*, 1990; Matsumura *et al.*, 1990; 1991; McMahon *et al.*, 1991; Pollock & Opgenorth, 1991). For example, phosphoramidon was found to reduce the hypertensive effect of exogenous big ET-1, but not that of ET-1, in rats (McMahon *et al.*, 1991; Pollock & Opgenorth, 1991).

The fungal metabolite, phosphoramidon, was first recognised as an inhibitor of certain bacterial neutral metalloproteases such as thermolysin (EC 3.4.24.4) (K_i = 28 nM; Suda *et al.*, 1973). Subsequently, phosphoramidon was shown to be a highly selective and potent (K_i = 2 nM) inhibitor of mammalian endopeptidase-24.11 (EC 3.4.24.11; E-24.11) (Kenny, 1977; Turner, 1987). Endopeptidase-24.11 is a membrane glycoprotein existing as an ectoenzyme (M_r approx 90 kDa). It exhibits a broad tissue distribution and substrate specificity, hydrolysing a wide range of biologically active peptides by cleaving on the amino side of a hydrophobic residue (Turner *et al.*, 1987; Roques *et al.*, 1993). This would suggest the enzyme to be a possible candidate for cleavage of the Trp^{21}-Val^{22} bond of big ET-1. However E-24.11 also hydrolyses ET-1 *in vitro* (Vijayaraghavan *et al.*, 1990; Fagny *et al.*, 1991) and has been implicated in the physiological inactivation of endothelin (Abassi *et al.*, 1992). For this reason E-24.11 seems unlikely to serve as the principal ECE activity in cells. Furthermore, Abassi *et al.* (1993) have recently suggested that recombinant E-24.11 is unable to generate ET-1 and C-terminal fragment from big ET-1.

The substrate specificity of E-24.11 is similar to that of thermolysin. Thus, thermolysin also hydrolyses peptide bonds involving the amino groups of hydrophobic amino acid residues with bulky side chains (Monzingo & Matthews, 1984). The active site of E-24.11 has been explored by chemical modification (Beaumont & Roques, 1986; Jackson & Hersh, 1986), site-directed mutagenesis (Bateman & Hersh, 1987; Devault *et al.*, 1988) and by hydrophobic cluster analysis of the primary sequence (Benchetrit *et al.*, 1988).

[1] Author for correspondence.

These studies have revealed that the Zn^{2+}-binding and catalytic residues present in thermolysin are conserved in E-24.11. Although E-24.11 and thermolysin are sensitive to phosphoramidon in the nanomolar range, they differ substantially in their sensitivity to thiorphan (Fulcher *et al.*, 1982). In this respect thermolysin more closely resembles ECE which is relatively insensitive to thiorphan (Ohnaka *et al.*, 1993).

As yet, no data have been reported comparing the actions of these two enzymes on big ET-1. We have re-evaluated the potential of E-24.11 to function as an endothelin converting enzyme and have studied its ability to degrade ET-1 and CTF. These actions have been compared with those of thermolysin to determine if the bacterial phosphoramidon-sensitive metalloprotease may represent a more useful model for metallopeptidase ECE, especially since the 3D structure of thermolysin has been solved both in the absence and presence of inhibitors (Weaver *et al.*, 1977; Monzingo & Matthews, 1982; 1984).

Methods

Hydrolysis of peptides by E-24.11 and thermolysin

Time courses of hydrolysis of ET-1, big ET-1 (1-39), pCTF and substance-P by E-24.11 Endopeptidase-24.11 (200 ng protein) in 0.1 M Tris/HCl at pH 7.4 was incubated with ET-1, big ET-1 (1-39), pCTF or substance P (3 nmol of each) at 37°C (final volume 100 µl) for up to 180 min. Reactions were stopped either by acidification with 50 µl 9% v/v trifluoroacetic acid (TFA) or by addition of 50 µl of phosphoramidon (150 µM). The hydrolysis of each of the peptides was monitored by reverse phase high performance liquid chromatography (r.p.-h.p.l.c.) analysis as described below. The above procedure was also repeated for big ET-1 but using 4 µg E-24.11 protein instead of 200 ng.

Time courses of hydrolysis of ET-1, big ET-1 and pCTF by thermolysin Thermolysin (50 ng) in 0.1 M Tris/HCl, 3 mM $CaCl_2$ at pH 7.4 was incubated with either ET-1, big ET-1 (1-39) or pCTF (3 nmol of each) at 37°C (final volume 100 µl) for up to 80 min. All reactions were stopped by acidification with 50 µl 30% v/v acetic acid. The hydrolysis of each of the peptides was monitored by r.p.-h.p.l.c. analysis as described below. Hydrolysis was completely inhibited by 10 µM phosphoramidon.

R.p.-h.p.l.c. methods for time course studies

(a) Endothelin peptides – big ET-1 (1-39), ET-1 and pCTF were resolved by r.p.-h.p.l.c. on a µBondapak C18 column (3.9 × 300 mm, Millipore Corporation, Milford, MA, U.S.A.) using a Waters h.p.l.c. system. Elution was performed by using 0.02% TFA in water (solvent A) and 0.02% TFA in acetonitrile (solvent B). The gradient was linear from 10 to 36.5 %v/v solvent B in 15 min, followed by a further gradient up to 43% v/v solvent B over the next 20 min. The flow rate was 1 ml min^{-1} and detection was at 214 nm. pCTF, big ET-1 (1-39) and ET-1 typically eluted with retention times of 17.2 min, 23.5 min and 25.3 min respectively. Samples from reactions were centrifuged and a known volume of the supernatant analysed by r.p.-h.p.l.c.

(b) Substance P – substance P was resolved using the same column as above but under different conditions. Solvent A was 0.08% H_3PO_4 while solvent B consisted of 45% acetonitrile/0.08% H_3PO_4. The gradient was linear from 9% to 100% v/v solvent B in 20 min followed by 5 min at final conditions. Substance P typically eluted with a retention time of 16.9 min.

Characterization by radioimmunoassay, h.p.l.c. and mass spectrometry of the products of human big ET-1 incubation with E-24.11 or thermolysin

The studies described above used porcine big ET-1. However, to facilitate the identification of ET-1 and CTF by radioimmunoassay, human big ET-1 was employed because a specific RIA for human big ET-1(22-38) (hCTF) was available (Corder *et al.*, 1993).

Incubations with E-24.11 and thermolysin: E-24.11 To define the most appropriate enzyme to substrate ratio for E-24.11, either 1 µM (0.2 nmol) or 10 µM (2 nmol) human big ET-1 was incubated with a range of concentrations of E-24.11 (20 ng ml^{-1}–2 µg ml^{-1}) for 2 h at 37°C in a total volume of 200 µl. The reaction was terminated by 10 min of heat treatment at 80°C. Samples were centrifuged at 10,000 *g* and, after appropriate dilutions in RIA buffer, the ET-1 generated in each sample was assayed by RIA. The time course for ET-1 formation by E-24.11 was investigated by incubating 2 nmol human big ET-1 with 40 ng E-24.11 in a total volume of 200 µl, and samples were taken for RIA at 1, 2, 4 and 8 h. All incubations were performed in triplicate.

Thermolysin 10 µM (2 nmol) big ET-1 was incubated with thermolysin at 40 or 400 ng for 2 h at 37°C in a total volume of 200 µl. At the end of the incubation the samples were processed as described above and subjected to RIA for ET-1 immunoreactivity.

RIA of ET-1 and hCTF ET-1 was measured using a RIA specific for the C-terminal ET-1(16-21) sequence (crossreactivity with big ET-1 $<0.015\%$) (Corder *et al.*, 1993). This antibody was raised by injecting rabbits with His-Leu-Asp-Ile-Ile-Trp conjugated to bovine thyroglobulin with glutaraldehyde. [^{125}I]-ET-1 was used as tracer and dilutions of ET-1 were used as standard. Samples from incubations with big ET-1 or h.p.l.c. fractions were measured for ET-1(16-21)-immunoreactivity after appropriate dilution. Identification of hCTF in h.p.l.c. fractions was performed using a RIA specific for the C-terminal 22-38 sequence of human big ET-1. This antibody was raised by injecting rabbits with hCTF (Val-Asn-Thr-Pro-Glu-His-Val-Val-Pro-Tyr-Gly-Leu-Gly-Ser-Pro-Arg-Ser) conjugated to bovine serum albumin with glutaraldehyde (Corder *et al.*, 1993). [^{125}I]-human big ET-1 was used as tracer and dilutions of human big ET-1 were used as standard.

Both RIAs were performed as follows: standards or unknowns (200 µl) in RIA buffer (50 mM sodium phosphate buffer, pH 7.4, containing 0.15% bovine serum albumin, 0.005% Triton X-100 and 0.01% sodium azide) were incubated overnight at 4°C with 50 µl antibody and 50 µl tracer (7500 c.p.m.). The following day, 100 µl sheep anti-(rabbit IgG Fc region) serum and 100 µl normal rabbit serum were added to each tube and left to incubate for 3 h. At the end of the incubation period, 500 µl of 4% polyethylene glycol was added to each tube and bound ligand was separated from free by centrifugation at 2000 *g* for 30 min.

Identification by h.p.l.c. of ET-1, big ET-1 and big ET-1(22-38) This was performed using a column of 5 µm TSK gel ODS-120T, (4.6 × 250 mm; TOSOH Corporation, Japan from Anachem, Luton, Beds). Samples were first acidified and extracted using TechElut SPE C_{18} columns, eluted with 1 ml 80% acetonitrile containing 0.1% TFA, concentrated to 0.2 ml under a stream of N_2, and injected onto the h.p.l.c. system. The h.p.l.c. column was eluted at a flow rate of 1 ml min^{-1} with a gradient of acetonitrile in 0.1% TFA using a Pharmacia LKB model 2249 gradient pump and 0.5 min fractions were collected. The acetonitrile gradient used was 0–20% over 3 min, 20–32% over 12 min, 32–40% over 15 min, 40–48% over 8 min. The column effluent was monitored at 280 nm using a Pharmacia LKB model 2141

variable wavelength monitor. Using this system, elution times for standard peptides were hCTF 15.1 min, big ET-1 27.5 min and ET-1 30.1 min.

Mass spectrometry To verify the identity of the immunoreactivity measured in h.p.l.c. fractions, samples were subjected to continuous flow FAB mass spectrometry using a VG-analytical 70 VSEQ mass spectrometer (Fisons Instruments, Manchester).

Materials

Porcine big ET-1 (1-39), human big ET-1 (1-38) and ET-1 were purchased from the Peptide Institute Inc., Osaka, Japan. Porcine big ET-1 (22-39) (porcine C-terminal fragment; pCTF) and phosphoramidon were obtained from Peninsula Laboratories Europe Ltd., St. Helens, Lancs. ET-1(19-21) Ile-Ile-Trp (IIW) was from Zinsser Analytic (UK) Ltd, Maidenhead, Berks. Human big ET-1 (22-38) (human C-terminal fragment; hCTF) was synthesized by Prof. Ramage and Dr A. Stewart, Department of Chemistry, University of Edinburgh. Substance P and recrystallized thermolysin (type X protease) were from the Sigma Chemical Company, Poole, Dorset. Porcine endopeptidase-24.11 was isolated by immunoaffinity chromatography as described by Gee *et al.* (1983), except that the monoclonal antibody used was GK4A9 (Gee & Kenny, 1985). The purified enzyme was homogeneous as assessed by polyacrylamide gel electrophoresis in the presence of sodium dodecylsulphate. [^{125}I]-ET-1 and [^{125}I]-big ET-1 were from Amersham International plc, Amersham, Bucks.

Results

ET-1 and pCTF were efficiently hydrolysed by E-24.11. The respective half-lives for hydrolysis of 3 nmol of ET-1 and CTF by 200 ng E-24.11 were 37 and 57 min respectively (Figure 1) which compares with a $t_{\frac{1}{2}}$ of 2 min for substance P, one of the best substrates identified to date for this enzyme (Turner *et al.*, 1987). In contrast, less than 5% of porcine big ET-1 at a similar concentration was degraded by 200 ng E-24.11 in 3 h (Figure 1). Using as much as 4 μg E-24.11, a $t_{\frac{1}{2}}$ of 150 min was calculated. No such marked differences in half-lives were seen when the peptides were hydrolysed by thermolysin. The respective half-lives under comparable conditions were estimated as porcine big ET-1 (25 min), ET-1 (56 min) and pCTF (47 min) (Figure 2).

When porcine big ET-1 (3 nmol) was incubated with either 200 ng or 4 μg E-24.11 and the products were resolved by reverse phase h.p.l.c. there was insufficient yield of product with the retention time of ET-1 for quantification by h.p.l.c. However, radioimmunoassay confirmed that under certain conditions of substrate/enzyme ratio, ET-1 immunoreactivity was a detectable product (Table 1). In a subsequent experiment, evaluation of the time course of ET-1 production by E-24.11 (40 ng) from big ET-1 (2 nmol) showed levels of immunoreactivity of 16.1 ± 0.6, 22.8 ± 1.1, 30.8 ± 1.8 and 34.0 ± 3.8 pmol 200 μl^{-1} incubation volume at 1, 2, 4 and 8 h, compared to control values of $<$0.06 pmol 200 μl^{-1}, illustrating the rapid rise in immunoreactivity during 1 h and approximately steady state levels by 4 h.

Characterization of the products by h.p.l.c. combined with RIA showed the presence of authentic ET-1 and hCTF

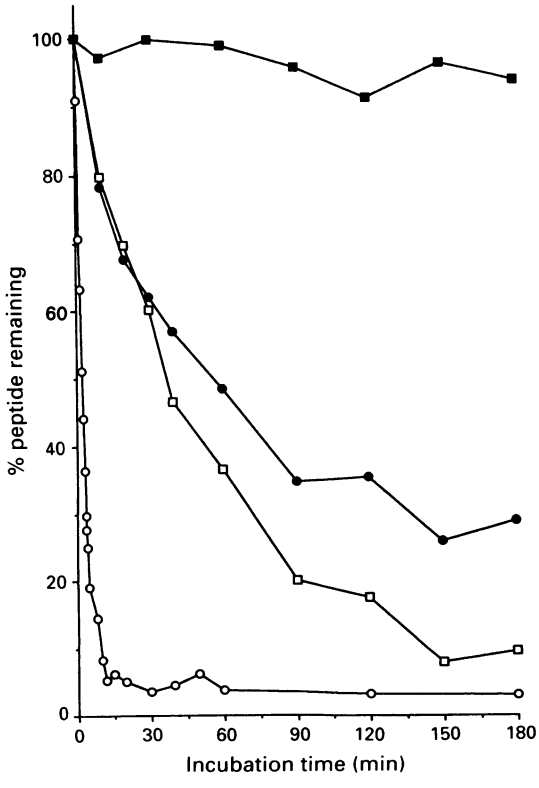

Figure 1 Hydrolysis of big endothelin-1 (big ET-1), ET-1, C-terminal fragment and substance P by purified porcine E-24.11. Peptide (3 nmol) was incubated at 37°C, pH 7.4 with E-24.11 (200 ng protein) for up to 180 min. Products were separated and analysed by reverse phase h.p.l.c. and depletion of substrate was quantified by A_{214}. The symbols correspond to: (□) ET-1; (○) substance P; (■) big ET-1; (●) C-terminal fragment. The experiment was repeated twice, with similar results.

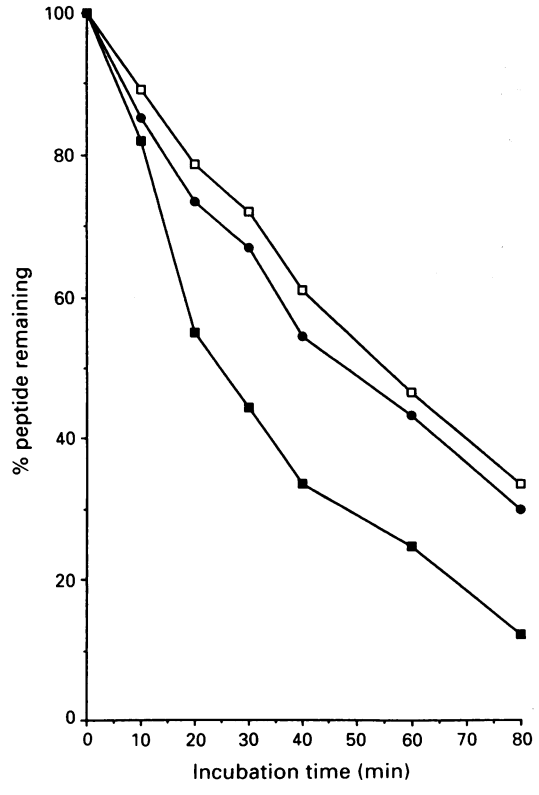

Figure 2 Hydrolysis of big endothelin-1 (big ET-1), ET-1 and C-terminal fragment by thermolysin. Peptide (3 nmol) was incubated at 37°C, pH 7.4 with thermolysin (50 ng protein) for up to 80 min. All incubations were in the presence of 3 mM $CaCl_2$. Products were separated and analysed by reverse phase h.p.l.c. and depletion of substrate was quantified by A_{214}. The symbols correspond to: (□) ET-1; (■) big ET-1; (●) C-terminal fragment. The experiment was repeated twice, with similar results.

(Figure 3). Although insufficient ET-1 was generated for unequivocal identification by mass spectrometry, the identity of hCTF was confirmed ($MH^+ = 1809$) hence demonstrating that E-24.11 is able to cleave the Trp^{21}-Val^{22} bond of big endothelin-1. In addition to ET-1 a second peak of ET-1(16-21) immunoreactivity was observed. This was identified by mass spectrometry to be ET(17-21) ($MH^+ = 659$, LDIIW). The major product of E-24.11 incubations with big ET-1, in terms of A_{280}, eluted in the position of the ET(19-21) standard (IIW) (Figure 3), and this product was also confirmed by mass spectrometry. In agreement with studies using porcine big ET-1, the majority of human big ET-1 remained undigested at the end of the incubation period.

When thermolysin was incubated with big ET-1, both ET-1-like and CTF-like products were detected at 214 nm by h.p.l.c. The formation of ET-1 was confirmed by RIA in amounts approximately 5 fold greater than seen with E-24.11 (Figure 4 and Table 1). As with E-24.11, h.p.l.c. characterization of the products from human big ET-1 demonstrated ET-1 and a second immunoreactive product corresponding to ET-1 (17-21). Mass spectrometry confirmed the identity of ET-1, ET-1(17-21) and hCTF (MH^+ of 2493, 659, 1809 respectively). Like E-24.11 the major peak in terms of u.v. absorbance from thermolysin incubations eluted in the position of ET-1(19-21) standard (Figure 4).

Table 1 RIA values for endothelin-1 (ET-1) production from big ET-1 catalysed by E-24.11 and thermolysin

	Endothelin-1 like immunoreactivity (pmol 200 μl^{-1})		
	20 ng ml^{-1}	200 ng ml^{-1}	2 μg ml^{-1}
E-24.11			
big ET-1 (1 μM)	1.7 ± 0.1	6.1 ± 0.1	2.3 ± 0.1
big ET-1 (10 μM)	7.5 ± 0.1	27.6 ± 0.3	33.4 ± 0.4
Thermolysin			
big ET-1 (10 μM)		161 ± 4	121 ± 4

Values are mean ± s.e.mean; $n = 3$ for each 2 h incubation.

Discussion

The nature and identity of the physiological ECE has generated considerable controversy in the literature (Opgenorth *et al.*, 1992; Turner, 1993). The consensus is that a phosphoramidon-sensitive membrane metallopeptidase effects this conversion. However, the cellular and subcellular location of this activity is still unclear as is the cell biology of endothelin processing itself (Harrison *et al.*, 1993). The sensitivity of ECE to phosphoramidon suggests a similarity with the well characterized metallopeptidases E-24.11 and thermolysin. However, Abassi *et al.* (1993) failed to detect production of ET-1 from big ET-1 by recombinant E-24.11. The ability of thermolysin to generate ET-1 from its precursor has not previously been examined. A possible candidate for the physiological ECE has recently been isolated from rat lung and porcine aortic endothelial cells and is characterized by sensitivity to phosphoramidon (IC_{50} in the range 0.1–1 μM) but not by another E-24.11 inhibitor, thiorphan (Takahashi *et al.*, 1993; Ohnaka *et al.*, 1993).

In the present study, a marked difference was seen in the abilities of E-24.11 and thermolysin to metabolize big ET-1. Thermolysin degraded big ET-1, ET-1 and CTF at broadly similar rates. When big ET-1 was the substrate, both ET-1 and CTF were detected by RIA and h.p.l.c. as intermediates and their production was confirmed by mass spectrometry. In contrast, E-24.11 degraded big ET-1 approximately two orders of magnitude more slowly than the product peptides.

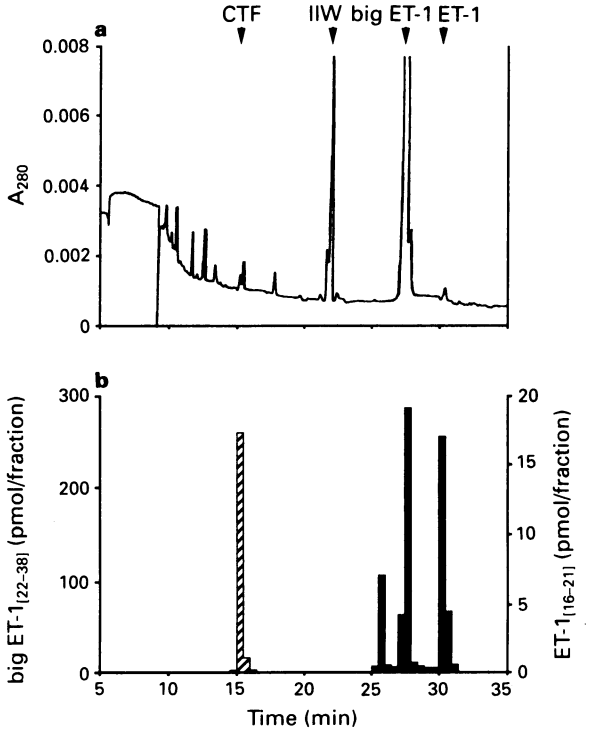

Figure 3 High performance liquid chromatography (h.p.l.c.) characterization of products of E24.11 incubation with human big endothelin-1 (big ET-1). H.p.l.c. was performed on the pooled material obtained after 8 h incubation of E.24.11 and human big ET-1; equivalent to 100 ng enzyme and 5 nmol peptide. (a) u.v. absorption at 280 nm; (b) hatched columns = hCTF immunoreactivity; solid columns = ET-1(16-21) immunoreactivity. The elution positions of the standard peptides, hCTF, IIW, human big ET-1 and ET-1 are indicated.

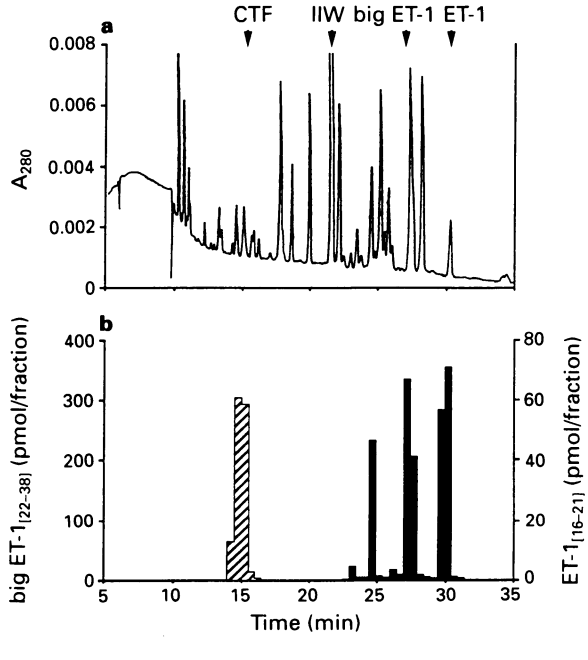

Figure 4 High performance liquid chromatography (h.p.l.c.) characterization of products of thermolysin incubation with human big endothelin-1 (big ET-1). H.p.l.c. was performed on the pooled material obtained after 2 h incubation of thermolysin and human big ET-1; equivalent to 120 ng enzyme and 6 nmol peptide. (a) u.v. absorption at 280 nm; (b) hatched columns = hCTF immunoreactivity; solid columns = ET-1(16-21) immunoreactivity. The elution positions of the standard peptides, hCTF, IIW, human big ET-1 and ET-1 are indicated.

Nevertheless, low, steady state levels of ET-1 were clearly detected by RIA and confirmed by h.p.l.c. In addition, confirmation of the Trp^{21}-Val^{22} cleavage was obtained by the production of ET-1 and CTF, with the identity of the latter being verified by mass spectrometery. However, the levels of detectable ET-1 depend critically on the enzyme-big ET-1 ratio as the generated ET-1 is degraded rapidly to the 17-21 and 19-21 fragments. The failure of Abassi *et al.* (1993) to detect ET-1 production from big ET-1 by recombinant E-24.11 may reflect not only the lack of sensitivity of their assay system and relatively poor resolution of substrate and product peptides by h.p.l.c., but also the ratio of enzyme to substrate used, which would have favoured degradation of any ET-1 generated. Earlier reports of the hydrolysis of ET-1 by E-24.11 described the formation of ET-1(17-21) (LDIIW) and ET-1(19-21) (IIW), with the latter being the predominant fragment obtained from metabolism of the C-terminal hexapeptide sequence of ET-1 (Vijayaraghavan *et al.*, 1990; Fagny *et al.*, 1991). Under our conditions, the major product in terms of A_{280} from thermolysin or E-24.11 incubations eluted in the position of ET-1(19-21) (Figures 3 and 4). The identification of this fragment, and the observations from the time course of ET-1 production by E-24.11 suggest that ET-1 reaches a critical concentration, and then degradation matches the formation of fresh ET-1, hence the large peak of IIW compared to the ET-1 peak. We predict that the formation of this fragment required the initial cleavage of big ET-1 at Trp^{21}-Val^{22} to form ET-1, which then underwent hydrolysis in the manner described for ET-1.

The marked differences in the relative rates of metabolism of big ET-1 and ET-1 by E-24.11 and thermolysin can be rationalised in terms of their individual specificity requirements. Both Hersh & Morihara (1986) and Poszgay *et al.* (1986) have compared some of the properties of E-24.11 and thermolysin in detail. In summary, a major difference was seen between the active site of E-24.11 and thermolysin in terms of hydrophobicity. Thermolysin appears to utilise hydrophobic interactions as a major binding force whereas E-24.11 utilises weaker hydrophobic binding interactions but also make use of an ionic interaction with the C-terminal carboxylate of its substrates. Thus, E-24.11 prefers small peptide substrates and exhibits some of the characteristics of a carboxydipeptidase as in the cleavage of the Gly^3-Phe^4 bond in [Leu^5]-enkephalin. In addition, thermolysin prefers a bulky hydrophobic residue in the P_1 position and a small hydrophobic residue in the P_2 position (Poszgay *et al.*, 1986). Big ET-1 fits these requirements for thermolysin with the presence of Trp at the P_1 position and Ile at the P_2 position. Thus, although thermolysin further degrades ET-1 and cannot be regarded as an endothelin converting enzyme in the strict sense of the term, it may represent a more useful model for ECE than E-24.11. In particular, it is readily available in homogeneous form and X-ray crystal structures of inhibitor-thermolysin complexes are available (Weaver *et al.*, 1977; Monzingo & Matthews, 1982; 1984). In the case of the phosphoramidon-thermolysin complex, the inhibitor is bound with its phosphoramide function mimicking the proposed tetrahedral transition state for peptide bound hydrolysis (Weaver *et al.*, 1977). Unlike E-24.11, which is equally sensitive to phosphoramidon and thiorphan, thermolysin is much less sensitive to inhibition by thiorphan ($I_{50} = 60\,\mu M$; Fulcher *et al.*, 1982), reinforcing the similarity with ECE.

The relative stability of big ET-1 in the presence of E-24.11 compared to ET-1 and CTF is consistent with the known preference of the enzyme for oligopeptides. The present studies provide little evidence of metabolism of big ET-1 at the cleavage sites of ET-1 without first undergoing the initial cleavage at the Trp^{21}-Val^{22} bond. This indicates that the conformation of big ET-1 under these conditions favours this particular cleavage, and protects against hydrolysis of other bonds.

An enzyme-linked immunoadsorbent assay has been used to demonstrate that E-24.11 is widely distributed on mammalian cells and tissues although the enzyme is predominantly localized to the brush border epithelial cells of intestine and kidney (Howell *et al.*, 1991). Low levels of the enzyme have, however, been detected on endothelial cells of venous or arterial origin (Llorens-Cortes *et al.*, 1992). Thus, E-24.11 has the required specificity, cellular localization and topology to function in the processing and metabolism of big ET-1. The kinetics of metabolism of big ET-1 and ET-1 by E-24.11 (Figure 1) would tend to favour a role for the enzyme in ET-1 inactivation rather than the processing of big ET-1. Nevertheless, the presence of E-24.11 in endothelial plasma membranes or in partially purified preparations of ECE may lead to erroneous estimates of endothelin converting activity. E-24.11 activity can be eliminated either by immunoabsorption (Murphy *et al.*, 1993) or by the routine inclusion of thiorphan in assays of ECE.

We thank the British Heart Foundation (A.J.T., L.J.M.) and Parke-Davis Pharmaceutical Research Division of Warner Lambert Co. (R.C.) for their financial support. We are grateful for the assistance of Dr Ian Kay with the mass spectrometry, and indebted to Miss Noorafza Khan for her technical assistance.

References

ABASSI, Z.A., GOLOMB, E., BRIDENBAUGH, R. & KEISER, H.R. (1993). Metabolism of endothelin-1 and big endothelin-1 by recombinant neutral endopeptidase EC 3.4.24.11. *Br. J. Pharmacol.*, **109**, 1024–1028.

ABASSI, Z.A., TATE, J.E., GOLOMB, E. & KEISER, H.R. (1992). Role of neutral endopeptidase in the metabolism of endothelin. *Hypertension*, **20**, 89–95.

BATEMAN, R.C. & HERSH, L.B. (1987). Evidence for an essential histidine in neutral endopeptidase-24.11. *Biochemistry*, **26**, 4237–4242.

BEAUMONT, A. & ROQUES, B.P. (1986). Presence of a histidine at the active site of the neutral endopeptidase-24.11. *Biochem. Biophys. Res. Commun.*, **139**, 733–739.

BENCHETRIT, T., BISSRY, V., MORNON, J.P., DEVAULT, A., CRINE, P. & ROQUES, B.P. (1988). Primary structure homologies between two zinc metallopeptidases, the neutral endopeptidase-24.11 (enkephalinase) and thermolysin, through clustering analysis. *Biochemistry*, **27**, 592–596.

CORDER, R., HARRISON, V., KHAN, N., ANGGARD, E.E. & VANE, J.R. (1993). Effects of phosphoramidon in endothelial cell cultures on the endogenous synthesis of endothelin-1 and on conversion of exogenous big endothelin-1 to endothelin-1. *J. Cardiovasc. Pharmacol.*, **22** (Suppl. 8), S73–S76.

DEVAULT, A., SALES, V., NAULT, C., BEAUMONT, A., ROQUES, B., CRINE, P. & BOILEAU, G. (1988). Exploration of the catalytic site of endopeptidase-24.11 by site-directed mutagenesis. Histidine residues 583 and 587 are essential for catalysis. *FEBS Lett.*, **231**, 54–58.

FAGNY, C., MICHEL, A., LEONARD, I., BERKENBOOM, G., FONTAINE, J. & DESCHODT-LANCKMANN, M. (1991). In vitro degradation of endothelin-1 by endopeptidase-24.11 (enkephalinase). *Peptides*, **12**, 773–778.

FULCHER, I.S., MATSAS, R., TURNER, A.J. & KENNY, A.J. (1982). Kidney neutral endopeptidase and the hydrolysis of enkephalin by synaptic membranes show similar sensitivity to inhibitors. *Biochem. J.*, **203**, 519–522.

GEE, N.S. & KENNY, A.J. (1985). Dissection of renal brush border membranes with monoclonal antibodies. *Biochem. Soc. Trans.*, **13**, 101–102.

GEE, N.S., MATSAS, R. & KENNY, A.J. (1993). A monoclonal antibody to kidney endopeptidase-24.11. Its application in immunoadsorbent purification of the enzyme and immunofluorescent microscopy of kidney and intestine. *Biochem. J.*, **214**, 377–386.

HARRISON, V., CORDER, R., ANGGARD, E.E. & VANE, J.R. (1993). Evidence for vesicles that transport endothelin-1 in bovine aortic endothelial cells. *J. Cardiovasc. Pharmacol.*, **22** (Suppl. 8), S57–S60.

HERSH, L.B. & MORIHARA, K. (1986). Comparison of the sub-site specificity of the mammalian neutral endopeptidase-24.11 (enkephalinase) to the bacterial neutral endopeptidase thermolysin. *J. Biol. Chem.*, **261**, 6433–6437.

HOWELL, S., MURRAY, H., TURNER, A.J. & KENNY, A.J. (1991). A highly sensitive elisa for endopeptidase-24.11, the common acute lymphoblastic leukaemia antigen (CALLA, CD-10), applicable to material of porcine and human origin. *Biochem. J.*, **278**, 417–421.

IKEGAWA, R., MATSUMURA, Y., TSUKAHARA, Y., TAKAOKA, M. & MORIMOTO, S. (1990). Phosphoramidon, a metalloproteinase inhibitor, suppresses the secretion of endothelin-1 from cultured endothelial cells by inhibiting a big endothelin-1 converting enzyme. *Biochem. Biophys. Res. Commun.*, **171**, 669–675.

JACKSON, D.G. & HERSH, L.B. (1986). Reaction of neutral endopeptidase-24.11 with arginine reagents. *J. Biol. Chem.*, **261**, 8649–8654.

KENNY, A.J. (1977). Proteinases associated with cell membranes. In *Proteinases in Mammalian Cells and Tissues*. ed. Barrett, A.J. pp. 393–444. Amsterdam: Elsevier/North-Holland Biomedical Press.

LLORENS-CORTES, C., HUANG, H., VICART, P., GASC, J.M., PAULIN, D. & CORVOL, P. (1992). Identification and characterization of neutral endopeptidase in endothelial cells from venous or arterial origins. *J. Biol. Chem.*, **267**, 14012–14018.

MATSUMURA, Y., IKEGAWA, R., HISAKI, K., TSUKUHARA, Y., TAKAOKA, M. & MORIMOTO, S. (1991). Conversion of big endothelin-1 to endothelin-1 by phosphoramidon-sensitive metalloproteinase derived from aortic endothelial cells. *J. Cardiovasc. Pharmacol.*, **17** (Suppl. 7), S65–S67.

MATSUMURA, Y., IKEGAWA, R., TSUKUHARA, Y., TAKAOKA, M. & MORIMOTO, S. (1990). Phosphoramidon-sensitive endothelin-converting enzyme in vascular endothelial cells converts big endothelin-1 and big endothelin-3 to their mature form. *FEBS Lett.*, **272**, 166–170.

MCMAHON, E., PALOMO, M., MOORE, W., MCDONALD, T. & STERN, M. (1991). Phosphoramidon blocks the pressor activity of porcine big endothelin-1(1-39) in vivo and conversion of big endothelin-1-(1-39) to endothelin-1-(1-21) in vitro. *Proc. Natl. Acad. Sci. U.S.A.*, **88**, 703–707.

MONZINGO, A.F. & MATTHEWS, B.W. (1982). Structure of a mercaptan-thermolysin complex illustrates mode of inhibition of zinc proteases by substrate-analogue mercaptans. *Biochemistry*, **21**, 3390–3394.

MONZINGO, A.F. & MATTHEWS, B.W. (1984). Binding of N-carboxymethyl dipeptide inhibitors to thermolysin determined by X-ray crystallography: a novel class of transition-state analogues for zinc peptidases. *Biochemistry*, **23**, 5724–5729.

MURPHY, L.J., GREENHOUGH, K.J. & TURNER, A.J. (1993). Processing and metabolism of endothelin peptides by porcine lung membranes. *J. Cardiovasc. Pharmacol.*, **22** (Suppl. 8), S94–S97.

OHNAKA, K., TAKAYANAGI, R., NISHIKAWA, M., HAJI, M. & NAWATA, H. (1993). Purification and characterisation of a phosphoramidon-sensitive endothelin-converting enzyme in porcine aortic endothelin. *J. Biol. Chem.*, **268**, 26759–26766.

OPGENORTH, T.J., WU-WONG, J.R. & SHIOSAKI, K. (1992). Endothelin-converting enzymes. *FASEB J.*, **6**, 2653–2659.

POLLOCK, D. & OPGENORTH, T. (1991). Evidence for metalloprotease involvement in the in vivo effects of big endothelin-1. *Am. J. Physiol.*, **261**, R257–R263.

POSZGAY, M., MICHAUD, C. LIEBMAN, M. & ORLOWSKI, M. (1986). Substrate and inhibitor studies of thermolysin-like neutral metalloendopeptidase from kidney membrane fractions. Comparison with bacterial thermolysin. *Biochemistry*, **25**, 1292– 1299.

ROQUES, B.P., NOBLE, F., DAUGÉ, V., FOURNIÉ-ZALUSKI, M.-C. & BEAUMONT, A. (1993). Neutral endopeptidase 24.11: structure, inhibition and experimental and clinical pharmacology. *Pharmacol. Rev.*, **45**, 87–146.

SUDA, H., AOYAGI, T., TAKEUCHI, T. & UMEZAWA, H. (1973). A thermolysin inhibitor produced by actinomycetes: phosphoramidon. *J. Antibiotics*, **26**, 621–623.

TAKAHASHI, M., MATSUSHITA, Y., IIJIMA, Y. & TANZAWA, K. (1993). Purification and characterization of endothelin-converting enzyme from rat lung. *J. Biol. Chem.*, **268**, 21394–21398.

TURNER, A.J. (1987). *Neuropeptides and their Peptidases*. ed. Turner, A.J. pp. 183–201. Chichester, Sussex: Ellis Horwood.

TURNER, A.J. (1993). Endothelin converting enzyme and other families of metalloendopeptidases. *Biochem. Soc. Trans.*, **21**, 697–701.

TURNER, A.J., HOOPER, N.M. & KENNY, A.J. (1987). Metabolism of neuropeptides. In *Mammalian Ectoenzymes* ed. Kenny, A.J. & Turner, A.J. pp. 211–248. Amsterdam: Elsevier.

VIJAYARAGHAVAN, J., SCICLI, A., CARRETERO, O., SLAUGHTER, C., MOOMAW, C. & HERSH, L.B. (1990). The hydrolysis of endothelins by neutral endopeptidase-24.11 (enkephalinase). *J. Biol. Chem.*, **265**, 14150–14155.

WEAVER, L.H., KESTER, W.R. & MATTHEWS, B.W. (1977). A crystallographic study of the complex of phosphoramidon with thermolysin. A model for the presumed catalytic transition state and for the binding of extended substrates. *J. Mol. Biol.*, **114**, 119–132.

YANAGISAWA, M., KURIHARA, H., KIMURA, S., TOMOBE, Y., KOBAYASHI, M., MITSUI, Y., YAZAKI, Y., GOTO, K. & MASAKI, T. (1988). A novel potent vasoconstrictor peptide produced by vascular endothelial cells. *Nature*, **332**, 411–415.

(Received February 1, 1994
Revised May 3, 1994
Accepted May 24, 1994)

Br. J. Pharmacol. (1994), **113**, 143–150

Characterization of the 5-hydroxytryptamine receptor type involved in inhibition of spontaneous activity of human isolated colonic circular muscle

F.S.-F. Tam, [1]K. Hillier & *K.T. Bunce

Clinical Pharmacology Group, Faculty of Medicine, University of Southampton, Southampton SO9 3TU and *Department of Gastrointestinal Pharmacology, Glaxo Group Research, Ware, Herts

1 Experiments were carried out to characterize pharmacologically the 5-hydroxytryptamine (5-HT) receptor types which mediate inhibition of spontaneous contractions of the intertaenial circular muscle in human isolated colon.

2 5-HT caused a reproducible concentration-dependent inhibition of spontaneous contractions of the circular muscle of human colon *in vitro* with a mean EC_{50} value of 0.2 μM and 95% confidence limits of 0.1–0.5 μM. No evidence for a contractile action of 5-HT was found. Tetrodotoxin (TTX, 1.5 μM) caused a rightward shift of the concentration-response curve of 5-HT with a concentration-ratio of 2.9.

3 The inhibitory response to 5-HT was mimicked by several indoles with the rank order of potency 5-HT > 5-methoxytryptamine = α-methyl-5-HT > 5-carboxamidotryptamine >> 2-methyl-5-HT. 5-Hydroxyindalpine was inactive.

4 The substituted benzamides were agonists with the following rank order of potency, 5-HT > renzapride > zacopride > metoclopramide > cisapride.

5 The inhibitory responses to 5-HT were not inhibited by methysergide (10 μM) or methiothepin (1 μM), which are antagonists selective for 5-HT_1-like and 5-HT_2 receptors, nor by ondansetron (10 μM) which is an antagonist at 5-HT_3 receptors.

6 The inhibitory responses induced by 5-HT and 5-methoxytryptamine were competitively antagonized by a weak 5-HT_4 receptor antagonist, tropisetron, with pK_B values of approximately 6. Tropisetron had no significant effect on the inhibitory response curve produced by isoprenaline (0.01–100 μM).

7 The pharmacological profile of the 5-HT-evoked relaxations of human colon circular muscle are consistent with activation of a 5-HT_4-like receptor.

Keywords: 5-Hydroxytryptamine; human colon; 5-HT_4-like receptors; prokinetic benzamides; tropisetron

Introduction

5-HT_4 receptors were first characterized in mouse embryonic colliculi neurones and guinea-pig hippocampus (Dumuis *et al.*, 1988a,b; Bockaert *et al.*, 1990). They are also present in porcine heart (Villalon *et al.*, 1990) and human atria (Kaumann *et al.*, 1990; 1991) and were the subject of a recent review (Bockaert *et al.*, 1992).

In the gastrointestinal tract, the 5-HT_4 receptor has been identified at neuronal sites of the guinea-pig ileum (Craig & Clarke, 1990) and colon (Elswood *et al.*, 1991; Wardle & Sanger, 1993) and at non-neuronal sites in rat oesophagus (Reeves *et al.*, 1991; Baxter *et al.*, 1991) and terminal ileum (Tuladhar *et al.*, 1991a). In preparations from the guinea-pig, activation of these receptors results in a contractile response while in those from the rat, relaxation.

The pharmacological profile of the 5-HT_4 receptor can be characterized and differentiated from other 5-HT receptor subclasses by a particular rank order of potency of 5-HT indoles in which 5-HT, 5-methoxytryptamine and α-methyl-5-HT are the most potent. Additionally, substituted benzamides, including renzapride, cisapride, zacopride and metoclopramide, which are 5-HT_3 receptor antagonists, are agonists at the 5-HT_4 receptor. Further characterization of 5-HT_4 receptors is by the weak antagonistic effect of tropisetron with pK_B 5.8–6.7 (Baxter *et al.*, 1991; Reeves *et al.*, 1991), although this compound is a potent 5-HT_3 receptor antagonist, pK_B 7.8–10.6 (Richardson *et al.*, 1985). The 5-HT_4 receptor is also antagonized by SDZ 205-557, DAU 6285 (Bockaert *et al.*, 1992) and GR 113808 (Grossman *et al.*, 1993) with pA_2 values of 7.5, 6.8 and 9.2–9.5 respectively.

In human colon smooth muscle, the reported *in vitro* effects of 5-HT have been variable. Longitudinal muscle strips prepared from taenia coli either not precontracted (Couture *et al.*, 1980) or precontracted by carbachol (Burleigh, 1977) relaxed in response to 5-HT. However, with non precontracted muscle strips prepared from the intertaenial circular region, either contraction (Couture *et al.*, 1980) or relaxation (Fishlock & Parks, 1963) has been reported, while relaxation has been observed when the strips were precontracted with carbachol (Burleigh, 1977). Investigation of the types of receptors upon which 5-HT acts have not been pursued with rigour. In the present study, we have characterized the 5-HT receptor in the intertaenial circular muscle of human colon by using a series of 5-HT receptor agonists and antagonists. A preliminary account of these studies has been published in abstract form (Tam *et al.*, 1992).

Methods

Tissues preparation and concentration-response curves

Macroscopically normal human colon was obtained from regions away from the tumour in patients having resection of ascending, descending or sigmoid colon for colo-rectal carcinoma. Muscle strips from 33 patients were used in this study of which 24 were from the sigmoid colon. No regional difference in the response to 5-HT was seen and data from

[1] Author for correspondence.

the different regions were combined. The specimens were immediately transferred to ice-cold, oxygenated (95% O_2 and 5% CO_2) Krebs solution (pH 7.2). Mucosa and serosa were blunt dissected from the muscle. Experiments were performed on either fresh or stored specimens kept at 4°C for up to 12 h. In practice no differences were seen between fresh or stored specimens.

Full thickness pieces of circular muscle strips from between the three prominent bands of taenia coli were prepared with dimensions 2–3 mm wide and 10–15 mm long and suspended vertically under a load of 15 mN in 10 ml jacketed organ baths containing Krebs solution (mM: NaCl 121.5, KCl 4.7, $MgSO_4$ 1.2, $CaCl_2$ 2.5, KH_2PO_4 1.2, $NaHCO_3$ 25.0 and glucose 11.0) gassed with 95% O_2 and 5% CO_2 at 37°C. No further adjustment in tension was made. Isometric tension was recorded by means of a transducer and displayed on a pen recorder. Tissue was allowed to equilibrate for 1 h with washing at 15 min intervals, during which time the basal tension decayed to less than 1 mN and rapid spontaneous activity of up to 15.0 mN amplitude developed. About 20% of strips set up developed little spontaneous activity after equilibration and were discarded.

Construction of concentration-response curves to agonists within the range of 0.01–100 μM was made by adding each agonist concentration cumulatively in a volume of 0.1 ml and with a contact time of 2 min. Two series of experiments were performed. In the first, each experiment involved setting up 4–6 strips and after equilibration, single cumulative concentration-response curves to 5-HT, indoles or substituted benzamides were made on individual tissues. This cautious procedure was followed because of the concern that tachyphylaxis might develop to repeated concentration-response curves, obscuring the responsiveness to agonists added in second and subsequent concentration-response curves. In every experiment using tissue strips from one patient, at least one 5-HT concentration-response curve was constructed.

In further studies, evaluation of two cumulative concentration-response curves to 5-HT or to 5-methoxytryptamine with 30 min between them showed that they were superimposable (Figure 4a,b). The results of each curve were calculated by expressing the total spontaneous activity in the 2 min during which each concentration of drug was present as a percentage of control activity. The control activity was that displayed by the tissue in the 2 min period immediately before construction of each curve. Between the first and second concentration-response curves, with frequent washing spontaneous activity did not fully recover to the level seen before construction of the first curve. Thus in Figure 4a the spontaneous activity in the 2 min period prior to construction of the second concentration-response curve was 51.7 ± 10.7% less than that in the 2 min period immediately before the first concentration-response curve. In Figure 4b where the effect of 5-methoxytryptamine was studied, the activity prior to the second curve was reduced by 31.6 ± 11.1%. Despite the lower spontaneous activity the curves were superimposable when the appropriate control activity was used in calculating the results. The consistency of the effect of 5-HT in repeated concentration-response curves is further demonstrated in Figure 6, where despite some expected variability in each set of experiments the curves are superimposable.

Cocaine (30 μM) and pargyline (100 μM) incubated in the tissue bath for 30 min did not shift the 5-HT cumulative concentration-response curve to the left but resulted in a reduction in the maximum inhibition achieved with 10 μM 5-HT from 90.4 ± 3.8 to 72.7 ± 16 ($n = 4$). Cocaine and pargyline were not included in subsequent experiments.

Expression of results and statistical analysis

EC values were normally obtained from each preparation at the level of 50% inhibition of the control spontaneous activity. However, when the less effective 2-methyl-5-HT, zacopride, metoclopramide and cisapride were investigated, EC values at either 20% or 30% inhibition were used. Data obtained for each agonist were then combined and expressed as geometric means with 95% confidence limits. In the first series of experiments, concentration ratios and equipotent molar ratios (e.p.m.rs) for agonists were determined by calculating the ratio of the mean EC value for all preparations studied to that of the relevant mean EC value for 5-HT. In the second series of experiments where 5-HT and agonists were used on the same preparation, concentration ratios and e.p.m.rs were determined from each individual preparation.

pK_B values for antagonists were calculated using the Schild equation $pK_B = \log_{10}$ (concentration ratio − 1) − $\log_{10}$ (molar concentration of antagonist) and expressed as arithmetic means with s.e.means; n represents the number of patients studied. Statistical analysis was performed with Student's unpaired t test.

Drugs

Tetrodotoxin, 5-hydroxytryptamine maleate, 5-methoxytryptamine hydrochloride, metoclopramide monohydrochloride and isoprenaline hydrochloride were obtained from Sigma Chemicals (UK). α-Methyl-5-hydroxytryptamine maleate, carboxamidotryptamine maleate and 2-methyl-5-hydroxytryptamine maleate were obtained from Research Biochemicals Inc. (U.S.A.). 5-Hydroxyindalpine, zacopride, ondansetron hydrochloride dihydrate were synthesized at Glaxo Group Research. Cisapride base was purchased from Janssen and prepared as the tartrate salt at Glaxo. Tropisetron (ICS 205-930; (3α-tropanyl)-1H-indole-3-carboxylic acid ester) and methysergide maleate were gifts from Sandoz (UK). Renzapride was a gift from SmithKline Beecham, ketanserin a gift from Janssen (UK) and methiothepin maleate a gift from Roche Products (UK).

All drugs were dissolved in water at stock concentrations of 10^{-2} M. They were further diluted to the required concentration with Krebs solution.

Results

Receptor agonists

All agonists used caused inhibition of spontaneous contractions and no evidence was seen of a contractile response in any preparation. Figure 1 shows a representative tracing of the effect of 5-HT. Subsequent figures show the percentage inhibition of spontaneous activity following addition of each drug concentration. Figures 2 and 3 show the effect of the agonists from a series of experiments in which only one agonist concentration-response curve was carried out on each strip set up. At least one 5-HT curve was always constructed on the tissue strips set up from each patient.

Figure 2 shows that 5-HT caused concentration-related inhibition of spontaneous contractions over a range of 0.01–5 μM with a mean EC_{50} value of 0.2 (0.1–0.5) μM. The maximum inhibition of spontaneous contractions achieved with 5-HT was 85.2 ± 5.2% (s.e.mean, $n = 12$).

Concentration-response curves to a range of indoles ($n = 5$–6) gave a rank order of potency 5-HT > 5-methoxytryptamine = α-methyl-5-HT > 5-carboxamidotryptamine ≫ 2-methyl-5-HT (Figure 2, Table 1A) and the curves (except 2-methyl-5HT) were approximately parallel over the concentration range 0.01–10 μM. Maximum inhibition of the spontaneous contractions by the indoles was similar except for 2-methyl-5-HT which was only 37.80 ± 12.2% of the control (Table 1A) and the e.p.m.r. was, therefore, calculated at the EC_{20} level.

Figure 3 and Table 1A show the agonist activity of 5-HT and four substituted benzamides ($n = 5$–6). The response curves to 5-HT, renzapride, zacopride, metoclopramide and

cisapride were constructed within the concentration range 0.1–100 μM. The rank order of potency was 5-HT > renzapride > zacopride > metoclopramide ≥ cisapride. The response curve to metoclopramide was very shallow and with the highest concentration (100 μM) caused only 46.4 ± 12.1% inhibition. Because of the shallow nature of its response and that higher concentrations were not applied it is equivocal whether metoclopramide is a partial agonist.

The rank orders of potency of the indoles and substituted benzamides was confirmed in later experiments ($n = 3$) where a 5-HT concentration-response curve was followed by a second concentration-response curve to one of these agonists in the same strip. This method was used after showing that the two 5-HT concentration-response curves were reproducible when made at 30 min intervals (Figure 4a). The e.p.m.rs of these agonists were determined from their relevant EC values (as in Table 1**B** with EC_{20} values for 2-methyl-5-HT, metoclopramide and cisapride, EC_{30} value for zacopride and EC_{50} values for other compounds) in each strip set up. The relevant EC value, e.p.m.r. and percentage of maximum inhibition of the agonists are shown in Table 1**B**. Although the values of e.p.m.r. using this alternative method were, for some agents, somewhat higher than those in Table 1**A**, similar rank orders of potency as well as maximum responses of both indoles and substituted benzamides were observed.

5-Hydroxyindalpine, a 5-HT_{1P} agonist, had relatively little effect. The mean maximum response was 24.1 ± 9.82% at 1 μM ($n = 5$, results not shown).

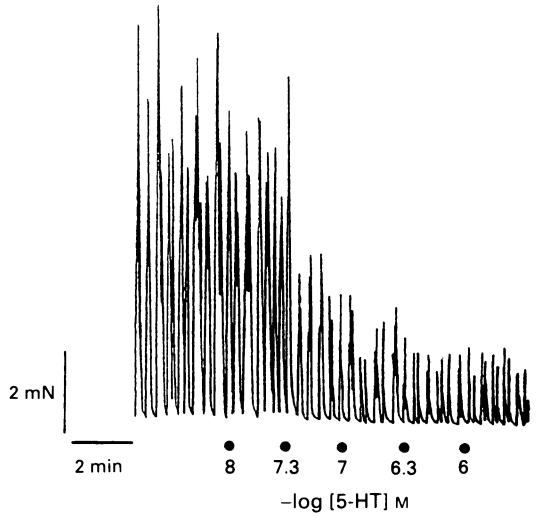

Figure 1 Representative tracing showing the effect of 5-hydroxytryptamine (5-HT) on the spontaneous contractions of the intertaenial circular muscle of human colon. 5-HT was added cumulatively (0.1–1 μM) with 2 min contact time for each concentration.

5-HT receptor antagonists

A concentration-response curve to 5-HT or 5-methoxytryptamine was first constructed and the agonist removed by washing. The antagonist was then incubated for 30 min and a second concentration-response curve constructed. As previously described the spontaneous contractility was lower prior to the second response curve but the reduction of spontaneous activity in the presence of antagonists did not differ significantly when compared to that in the absence of an antagonist. Following 30 min incubation with tropisetron (10 μM $n = 5$), methiothepin (1 μM $n = 4$), methysergide (10 μM $n = 5$) and ondansetron (10 μM $n = 4$), the spontaneous activity measured prior to the second response curve was 57.4 ± 8.8%, 67.7 ± 12.7%, 23.7 ± 16.7% and 18.25 ± 8.5%, less respectively than the activity measured before the first response curve.

Tropisetron at concentrations of 5 and 10 μM produced parallel and rightward shifts of the concentration-response curves to 5-HT yielding estimated pK_B values of 5.9 ± 0.4 ($n = 4$) and 5.8 ± 0.3 ($n = 5$) respectively. The maximum response to 5-HT was not altered (Figure 5a). Tropisetron (10 μM) also caused a rightward shift of the 5-methoxytry-

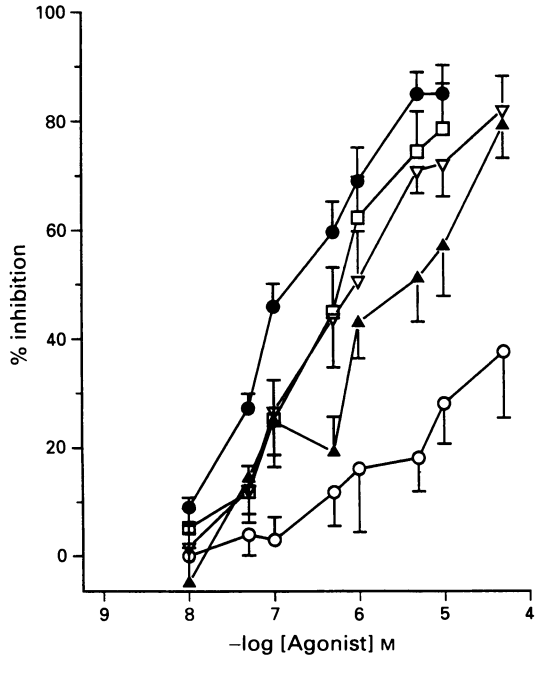

Figure 2 The effect of 5-hydroxytrypamine (5-HT) and related indoles on the spontaneous contractions of intertaenial circular muscle of human colon. Values are calculated as the percentage inhibition of control spontaneous contractions. (●) 5-HT ($n = 12$); (□) α-methyl-5-HT ($n = 6$); (▽) 5-methoxytryptamine ($n = 6$); (▲) 5-carboxamidotryptamine ($n = 5$); (○) 2-methyl-5-HT ($n = 5$). Each point is the mean value ± s.e.mean.

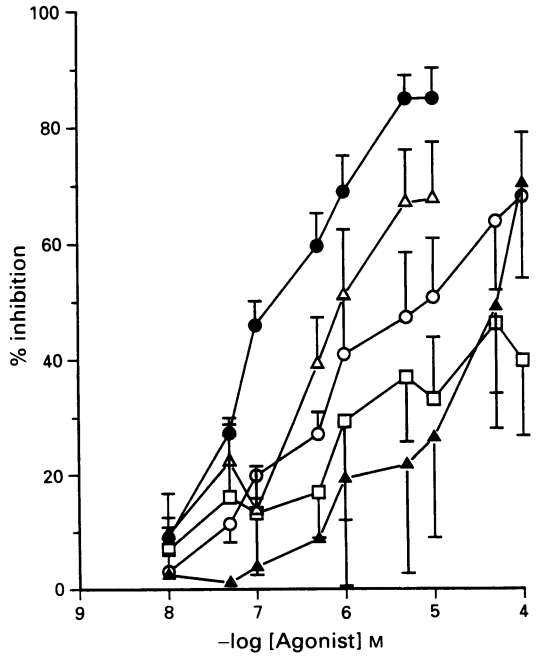

Figure 3 The effect of benzamides and 5-hydroxytryptamine (5-HT) on the spontaneous contractions of intertaenial circular muscle of human colon., (●) 5-HT ($n = 12$); (△) renzapride ($n = 6$); (○) zacopride ($n = 5$); (□) metoclopramide ($n = 6$); (▲) cisapride ($n = 5$). Other details as in Figure 2.

Table 1 Inhibitory effect of indoles and substituted benzamides on spontaneous contractions of human colon circular muscle

Compound	*EC value* (μM)[1]	*e.p.m.r.*	*% maximum inhibition of spontaneous contractility*
A			
5-HT	0.2 (0.1–0.5)	1	85.2 ± 5.2
5-Methoxytryptamine	0.7 (0.2–3.2)	3	82.3 ± 6.2
α-Methyl-5-HT	0.6 (0.2–2.0)	3	80.3 ± 19.8
5-Carboxamidotryptamine	3.9 (0.8–18.4)	18	79.4 ± 6.0
2-Methyl-5-HT	0.9 (0.1–13.7)†	30	37.8 ± 12.2
Renzapride	1.5 (0.2–12.8)	7	73.4 ± 4.7
Zacopride	0.9 (0.2–4.1)*	13	68.3 ± 11.0
Metoclopramide	1.1 (0.0–34.1)†	37	46.4 ± 12.1
Cisapride	3.2 (0.4–27.0)†	107	70.5 ± 16.3
B			
5-HT	0.14	1	87.5
5-Methoxytryptamine	2.92	15	86.6
α-Methyl-5-HT	1.33	8	82.2
5-Carboxamidotryptamine	5.07	28	86.5
2-Methyl-5-HT	1.64†	63	31.6
Renzapride	1.03	9	86.5
Zacopride	1.86*	23	64.1
Metoclopramide	2.50†	110	24.0
Cisapride	2.37†	113	70.9

Data in (**A**) show values from experiments ($n = 5-12$) where concentration-response curves were constructed for the inhibitory responses to one agonist on each strip.
In (**B**) data were derived from experiments ($n = 3$) in which a concentration-response curve to 5-HT was obtained and then response-curves to a second agonist were constructed after 30 min. Full details are given in Methods.
[1]Values are mean EC_{50} (95% confidence limits) μM except for † which is EC_{20} and * which is EC_{30}. The mean EC_{20} and EC_{30} values for 5-HT were 0.03 (0.02–0.05) and 0.07 (0.04–0.12) μM respectively.
e.p.m.r. is equipotent molar ratio. Other values are mean ± s.e.mean.

ptamine concentration-response curve (Figure 5b) yielding a pK_B value of 5.7 ± 0.2 ($n = 5$). Tropisetron (10 μM) had no effect on isoprenaline (0.01–100 μM)-induced inhibition with a concentration-ratio of 1.0 ($n = 3$, data not shown).

Figure 6a,b,c shows that inhibition of spontaneous activity by 5-HT was not prevented by the 5-HT_1-like and 5-HT_2 receptor antagonists, methysergide (10 μM, $n = 5$) and methiothepin (1 μM, $n = 4$) and the 5-HT_3 receptor antagonist, ondansetron (10 μM, $n = 4$) which yielded concentration-ratios of 0.6 (0.2–1.7), 1.0 (0.8–1.3) and 1.0 (0.7–1.4) respectively. Neither the slopes nor the maxima of the 5-HT response curves were affected by these concentrations of antagonists.

Metoclopramide, was also tested as an antagonist. At a concentration of 10 μM ($n = 6$) it caused no significant shift of the 5-HT-induced response with a concentration ratio of 1.1 (1.0–1.3). The maximum response was not altered (results not shown).

Tetrodotoxin (1.5 μM) incubated for 15 min caused a statistically non-significant rightward shift of the 5-HT concentration-response curve ($n = 6$) yielding a concentration-ratio of 2.9 (1.0–4.3) without affecting the maximum response. Tetrodotoxin at the same concentration also inhibited the response to isoprenaline by shifting the isoprenaline concentration-response curve to the right and its maximum response was reduced by 26.6% of the control ($n = 4$, data not shown).

Discussion

We do not have a clear picture of the place of 5-HT in the control of gastrointestinal smooth muscle contractility. In part, this is because investigations have revealed a wide heterogeneity in the 5-HT receptor type, distribution and function, in different parts of the gastrointestinal tract and between species. A clearer picture may emerge following the identification of a 5-HT receptor type now designated 5-HT_4 at neuronal and non-neuronal sites in the gastrointestinal tracts of several laboratory species.

In the guinea-pig ileum, ascending colon and the distal colon the 5-HT_4 receptor mediated contraction is tetrodotoxin-sensitive (Craig & Clarke, 1990; Eglen *et al.*, 1990; Hill *et al.*, 1990; Elswood *et al.*, 1991; Wardle & Sanger, 1993) whereas in the rat oesophagus (Baxter *et al.*, 1991; Reeves *et al.*, 1991) and terminal ileum (Tuladhar *et al.*, 1991b) 5-HT_4-mediated relaxation is unaffected by tetrodotoxin.

In the colon of other laboratory animal species, different 5-HT receptor types exist. In circular muscle preparations from rabbit colon, 5-HT increased contractions and these were abolished by methysergide but not by ketanserin or tropisetron indicating a 5-HT_1-like receptor (Ng *et al.*, 1991). In guinea-pig ascending colon, 5-HT induced relaxation through 5-HT_1-like receptors (Elswood & Bunce, 1992). In smooth muscle cells from the circular muscle of dog colon 5-HT reduced carbachol-induced contractions but the receptor subtype was not identified (Zhang *et al.*, 1992).

The effects of 5-HT on human colon have not been extensively studied. *In vitro* 5-HT causes a relaxation of basal or spasmogen-elevated tone (Fishlock & Parks, 1963; Burleigh, 1977) but in one study using circular muscle, 5-HT caused increased contractions (Couture *et al.*, 1980). Interestingly, Burleigh (1977) showed that the 5-HT-induced relaxation in the longitudinal muscle layer but not the circular layer was antagonized by methysergide, but receptor types were not further characterized.

In the present study only a concentration-dependent inhibitory effect of 5-HT on spontaneous contractions of circular muscle strips was observed. When expressed as a percentage of the spontaneous activity measured immediately before constructing the response curve, the inhibition could be quantitated and two consecutive response curves prepared 30 min apart shown to be superimposable. This was true despite the fact that spontaneous activity tended to be lower at the time of constructing the second response curve. Some

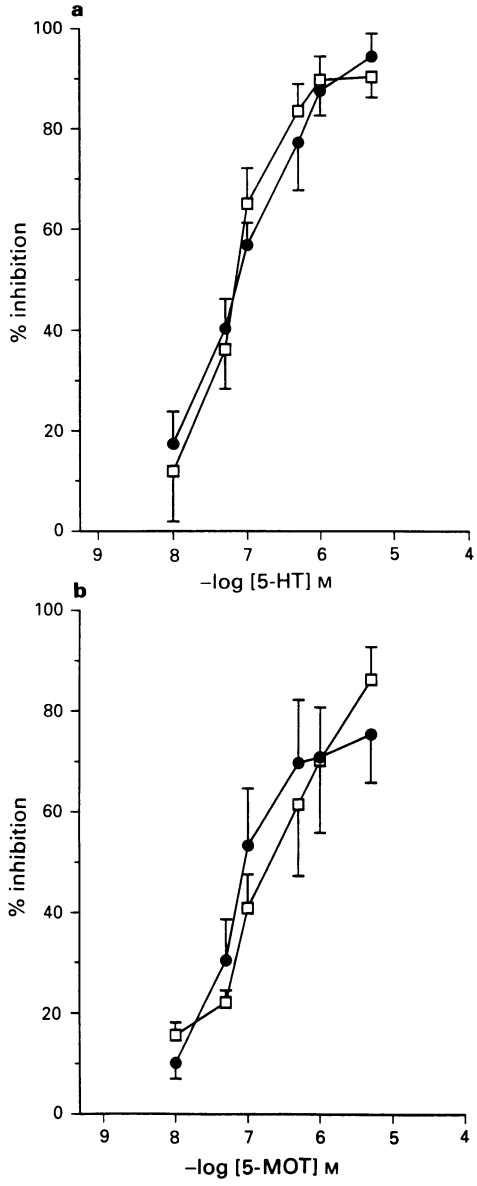

Figure 4 The inhibitory effect of two concentration-response curves in the same isolated strip to 5-hydroxytryptamine (5-HT) (a) and 5-methoxytryptamine (b) in intertaenial circular muscle of human colon. The interval between the first curve (●) and the second curve (□) was 30 min. Each point is the mean value obtained with tissues from 4 patients (other details as in Figure 2).

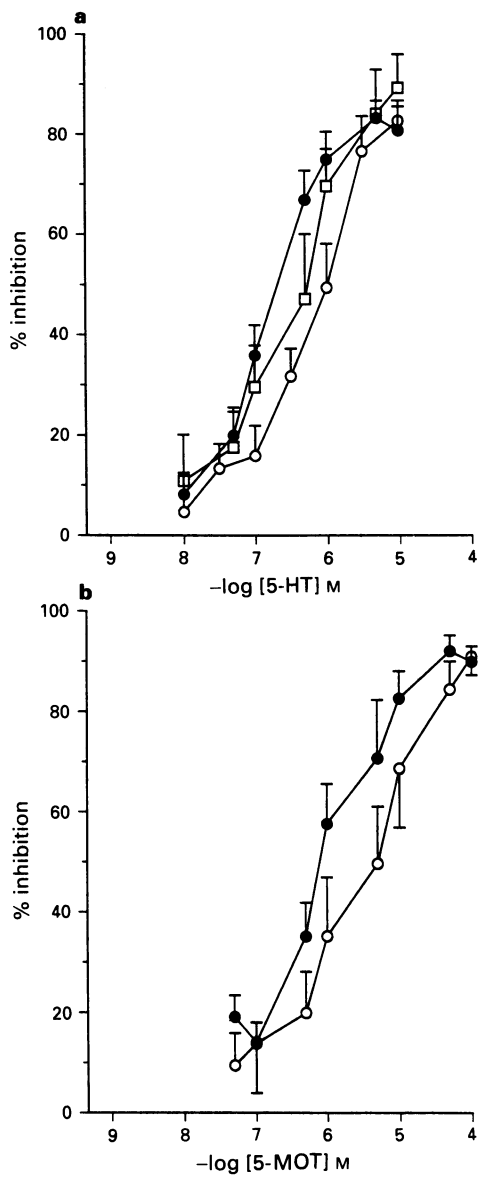

Figure 5 The effect of tropisetron on the responses to 5-hydroxytryptamine (5-HT) (a) and to 5-methoxytryptamine (5-MOT) (b). Agonist response curves are shown in the absence (●) and in the presence of tropisetron 5 μM (□) and 10 μM (○). For each point $n = 4-5$. Other details as in Figure 2.

variability in concentration-response curves between tissues was noted as might be expected from a very heterogeneous supply of human tissue. However, the linear range of response to 5-HT was generally between 10 nM and 5 μM and the response curves showed no evidence of being biphasic. Tetrodotoxin in a concentration (1.5 μM) known to abolish neuronal transmission in this preparation (unpublished data) caused a small shift to the right of the response curve and no suppression of the maximum response. It is, therefore, possible that a small component of the 5-HT response may be neuronally-mediated but its effects appear predominantly to be at a non-neuronal site.

The receptor type present was investigated using a range of agonists. The effectiveness of the agonists was initially tested utilising only one drug on each preparation but latterly a series of experiments were performed where a 5-HT concentration-response curve was constructed followed 30 min later by another agonist on the same preparation. We proved that, with the latter procedure, no tachyphylaxis developed to 5-HT. The data obtained from the two procedures did not differ in any major respect although when both 5-HT and another agonist were tested on the same strip, rather than a single agonist, moderately different values for the equipotent molar ratios of some of the agonists were obtained.

The present study demonstrates that the receptor that mediates 5-HT-induced inhibition of the circular muscle of human colon spontaneous contractions appears to be 5-HT_4-like. Our evidence is that the inhibitory effect of 5-HT was mimicked by several indoles and substituted benzamides. The rank order of inhibitory potency of the indoles was 5-HT > 5-methoxytryptamine = α-methyl-5-HT > 5-carboxamidotryptamine >> 2-methyl-5-HT. This order is consistent with that determined for 5-HT_4 receptor activation reported in the literature in a variety of guinea-pig and rat tissues where the receptor is either neuronally or non-neuronally sited (Craig & Clarke, 1990; Eglen *et al.*, 1990; Baxter *et al.*, 1991; Elswood *et al.*, 1991; Costall *et al.*, 1993; Wardle & Sanger, 1993). With 5-methoxytryptamine, α-methyl-5-HT and 5-carbox-

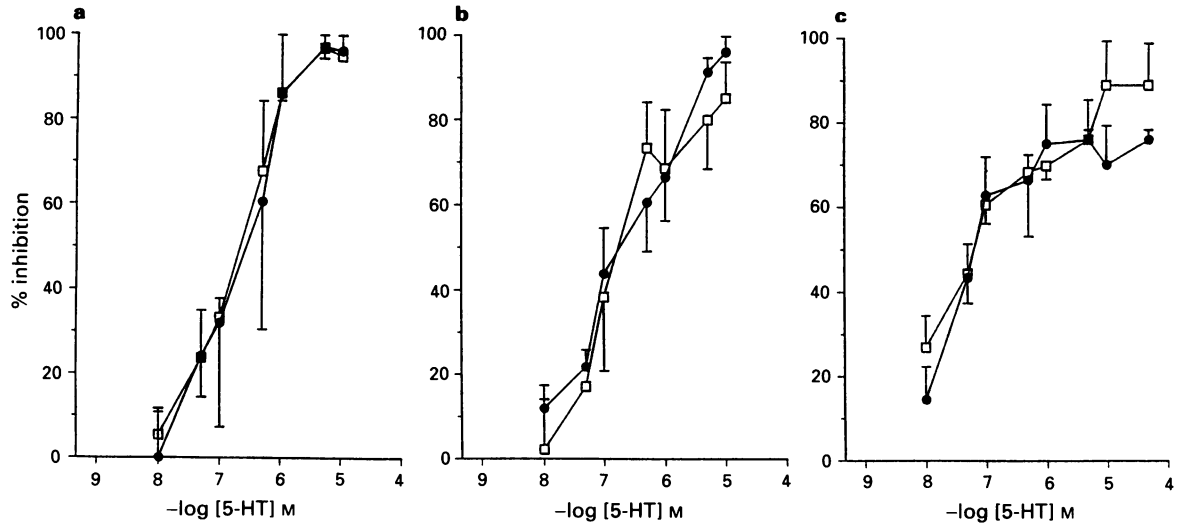

Figure 6 The effect of 5-HT_1, 5-HT_2 and 5-HT_3 receptor antagonists on the responses to 5-HT. 5-HT response curves are shown in the absence (●) and presence (□) of antagonist to 5-HT before and following 30 min incubation with (a) 10 μM ondansetron ($n = 4$), (b) 10 μM methysergide ($n = 5$), (c) 1 μM methiothepin ($n = 4$). Other details as in Figure 2.

amidotryptamine it was possible to construct a full concentration-response curve whereas with the highest concentrations of 2-methyl-5-HT (50 μM) only approximately 38% inhibition of control spontaneous contractility was reached. Although the ranking data are largely consistent with other tissues some differences in the magnitude of the rank differences do exist when compared with other tissues. Baxter *et al.* (1991) and Wardle & Sanger (1993) point out that variable factors such as uptake and metabolism of the analogues may contribute to these differences.

The rank order of the indoles was not that seen at 5-HT_1-like or 5-HT_3-like receptors which is 5-CT > 5-HT > 2-methyl-5-HT = α-methyl-5-HT and 5-HT = 2-methyl-5-HT > α-methyl-5-HT > 5-CT respectively (Humphrey, 1984).

Th order of potency is actually fairly similar to the 5-HT_2 receptors identified by Humphrey (1984); 5-HT = α-methyl-5-HT > 5-CT > 2-methyl-5-HT. However, methysergide and methiothepin which are antagonists at 5-HT_2 receptor sites did not alter the concentration-response curves to 5-HT indicating the absence of a significant effect of 5-HT at a 5-HT_2 type receptor.

The lack of effect of 5-hydroxyindalpine also indicated the absence of a putative 5-HT_{1P} type receptor.

Evidence for 5-HT_4 receptor involvement was also obtained by investigating the effects of substituted benzamides. These are antagonists at 5-HT_3 receptors but have agonist activity at the 5-HT_4 receptor (see Bockaert *et al.*, 1992). We found that they were agonists in this preparation and the rank order was 5-HT > renzapride > zacopride > metoclopramide ≥ cisapride. Renzapride had approximately equal activity to 5-methoxytryptamine and α-methyl-5-HT and the response to cisapride was very variable. The maximum responses to renzapride, zacopride and cisapride were not significantly different from 5-HT. The potency profile again is similar to that reported for 5-HT_4 receptors by other investigators (Craig & Clarke, 1990; Baxter *et al.*, 1991; Costall *et al.*, 1993). However, as with the indoles, some differences are apparent; thus Wardle & Sanger (1993) investigating the distal colon longitudinal muscle myenteric-plexus preparation found that cisapride was more potent than zacopride or metoclopramide. Because of the weak nature of the agonist effect of metoclopramide we feel that it is equivocal whether it is a partial agonist. At 100 μM (the greatest concentration tried in any experiment) spontaneous contractility was inhibited by only 46.4 ± 12.1%. However in subsequent investigations, metoclopramide (10 μM) had no antagonistic effect against 5-HT and did not affect the maximum response. Metoclopramide has variable actions in different preparations where receptors are purported to be 5-HT_4-like. In the guinea-pig distal colon longitudinal muscle-myenteric plexus preparation (Wardle & Sanger, 1993) and in the rat oesophagus (Baxter *et al.*, 1991) it has been reported to be a full agonist whereas in rat oesophagus (Reeves *et al.*, 1989), guinea-pig ascending colon (Elswood *et al.*, 1991) and guinea-pig ileum (Hill *et al.*, 1990) and in studies of short-circuit current in guinea-pig ileal mucosa (Scott *et al.*, 1992) it was a partial agonist. However, the antagonist effect of metoclopramide against 5-HT appears very weak with a pK_B value of 4.8 (Scott *et al.*, 1992) or pD_2 value of 5.0 (Hill *et al.*, 1990). It is worth noting that besides having agonist activity at 5-HT_4 receptors and antagonist activity at 5-HT_3 receptors, metoclopramide is also an antagonist at dopamine D_2 receptors (Jenner & Marsden, 1979). Renzapride and zacopride have been shown to exhibit full agonist activity at the 5-HT_4 receptors in the guinea-pig ileum (Eglen *et al.*, 1990) although, in the same preparation, Hill *et al.* (1990) reported that they are partial agonists. Cisapride has also been shown to be a partial agonist in the guinea-pig ileum (Hill *et al.*, 1990) and ascending colon (Elswood *et al.*, 1991). It has also been tested as an antagonist in these preparations and shown to produce inhibition of the 5-HT-induced responses (Hill *et al.*, 1990; Elswood *et al.*, 1991). Full agonist activity at 5-HT_4 receptors of these benzamides has also been observed in the mouse embryo colliculi neurones (Bockaert *et al.*, 1990); however, they are partial agonists in the guinea-pig hippocampus (Dumuis *et al.*, 1989). Cisapride has also been shown to have antagonist activity at 5-HT_2 receptors (Moriarty *et al.*, 1987).

Ondansetron, a tetrahydrocarbazolone, having 5-HT_3 antagonist activity but no 5-HT_4 stimulant activity (Dumuis *et al.*, 1989) did not modify 5-HT-induced response curves.

Tropisetron is a potent 5-HT_3 antagonist with weak 5-HT_4 receptor antagonist activity. The low pK_B values found in the circular muscle of human colon using 5-HT (pK_B 5.8–5.9) or 5-methoxytryptamine (pK_B 5.7) as the agonist are within the range of values found for antagonism of 5-HT responses at the 5-HT_4 receptor in other tissues. Tropisetron was selective as it was without effect on isoprenaline-induced inhibition of spontaneous contractions.

The 'prokinetic' benzamides, cisapride and metoclopramide, which antagonize 5-HT_3 receptors but stimulate 5-HT_4 receptors enhance gastric emptying and small bowel intestinal transit and lower oesophageal sphincter pressure in man (see Farthing, 1991). However, there is no evidence in man that

their actions are through 5-HT_3 receptors nor is there evidence that 5-HT_3 receptors are present in the upper gastrointestinal tract in man. An alternative explanation for the 'prokinetic' effect of the benzamides is that their stimulant effect upon 5-HT_4 receptors causes increased motility in man as it does in some laboratory animal species (Costall & Naylor, 1990). For this explanation to be tenable, 5-HT_4 receptors need to be shown to be present in the upper gastrointestinal tract in man. Only preliminary evidence for 5-HT_4 receptors that induce contraction in human stomach has been obtained *in vitro* by Schuurkes *et al.* (1991). They showed in circular cut strips of human stomach that electrical field stimulation (EFS) induced twitch contractions could be enhanced by cisapride, 5-HT and the 5-HT_4 receptor agonist, 5-methoxytryptamine. Both EFS-induced twitches and agonist-induced enhancement of twitches could be reduced by the weak 5-HT_4 receptor antagonist, tropisetron. Desensitization experiments also indicated the presence of a 5-HT_4 receptor. These data, although preliminary, indicated that unlike the 5-HT_4 receptor in the human colon the gastric 5-HT_4 receptor is neuronally-sited and activation induces contraction.

Although in this study we have produced evidence for a 5-HT_4-like receptor on the circular muscle of human colon, we have preliminary evidence that the longitudinal muscle of the taenia coli possesses a 5-HT_1-like receptor which is tetrodotoxin insensitive and work to confirm this is being carried out. Stimulation of this receptor also causes inhibition of basal tone.

In summary we conclude that the heterogeneity of 5-HT receptors seen in laboratory animals is also present within the human intestine. Using a range of indoles, substituted benzamides and tropisetron, criteria that have been widely accepted in the literature as indicating the presence of a 5-HT_4-like receptor, we have established the presence of a receptor type present in the circular muscle of the human colon that is 5-HT_4-like.

We thank Glaxo Group Research for financial assistance of a research student, ORS for partial support of F.S.-F.T., and Messrs F. McGinn, H. Steer, R. Lane, R. Rainsbury and I. Taylor for surgical samples.

References

BAXTER, G.S., CRAIG, D.A. & CLARKE, D.E. (1991). 5-Hydroxytryptamine$_4$ receptors mediate relaxation of the rat oesophageal tunica muscularis mucosae. *Naunyn-Schmied. Arch. Pharmacol.*, **343,** 439–446.

BOCKAERT, J., FOZARD, J.R., DUMUIS, A. & CLARKE, D.E. (1992). The 5-HT_4 receptor: a place in the sun. *Trends Pharmacol. Sci.*, **13,** 141–145.

BOCKAERT, J., SEBBEN, M. & DUMUIS, A. (1990). Pharmacological characterisation of 5-hydroxytryptamine$_4$ (5-HT_4) receptors positively coupled to adenylate cyclase in adult guinea pig hippocampal membranes: effect of substituted benzamide derivatives. *Mol. Pharmacol.*, **37,** 408–441.

BURLEIGH, D.E. (1977). Evidence for more than one type of 5-hydroxytryptamine receptor in the human colon., *J. Pharm. Pharmacol.*, **29,** 538–541.

COSTALL, B. & NAYLOR, R.J. (1990). 5-Hydroxytryptamine: new receptors and novel drugs for gastrointestinal motor disorders. *Scand. J. Gastroenterol.*, **25,** 769–787.

COSTALL, B., NAYLOR, R.J. & TULADHAR, B.R. (1993). 5-HT_4 receptor-mediated facilitation of the emptying phase of the peristaltic reflex in the guinea-pig isolated ileum. *Br. J. Pharmacol.*, **110,** 1572–1578.

COUTURE, R., MIZRAHI, J. & REGOLI, D. (1980). Peptides and the human colon: an *in vitro* pharmacological study. *Can. J. Physiol. Pharmacol.*, **59,** 957–964.

CRAIG, D.A. & CLARKE, D.E. (1990). Pharmacological characterisation of a neuronal receptor for 5-hydroxytryptamine in guinea-pig ileum with properties similar to the 5-hydroxytryptamine$_4$ receptor. *J. Pharmacol. Exp. Ther.*, **252,** 1378–1386.

DUMUIS, A., BOUHELAL, R., SEBBEN, M. & BOCKAERT, J. (1988a). A 5-HT receptor in the central nervous system positively coupled with adenylate cyclase is antagonized by ICS 205-930. *Eur. J. Pharmacol.*, **146,** 187–188.

DUMUIS, A., BOUHELAL, R., SEBBEN, M., CORY, R. & BOCKAERT, J. (1988b). A non-classical 5-hydroxytryptamine receptor positively coupled with adenylate cyclase in the central nervous system. *Mol. Pharmacol.*, **34,** 880–887.

DUMUIS, A., SEBBEN, M. & BOCKAERT, J. (1989). The gastrointestinal prokinetic benzamide derivatives are agonists at the non-classical 5-HT receptor (5-HT_4) positively coupled to adenylate cyclase in neurons. *Naunyn-Schmied. Arch. Pharmacol.*, **340,** 403–410.

EGLEN, R.M., SWANK, S.R., WALSH, L.K.M. & WHITING, R.L. (1990). Characterization of 5-HT_3 and 'atypical' 5-HT receptors mediating guinea-pig ileal contractions *in vitro*. *Br. J. Pharmacol.*, **101,** 513–520.

ELSWOOD, C.J. & BUNCE, K.T. (1992). Investigation of the 5-HT receptor mediating relaxation in guinea-pig proximal colon. *J. Pharm. Pharmacol.*, **44,** 264–266.

ELSWOOD, C.J., BUNCE, K.T. & HUMPHREY, P.P.A. (1991). Identification of putative 5-HT_4 receptors in guinea-pig ascending colon. *Eur. J. Pharmacol.*, **196,** 149–155.

FARTHING, M.J.C. (1991). 5-Hydroxytryptamine and 5-hydroxytryptamine-3 receptor antagonists. *Scand. J. Gastroenterol.*, **26** Suppl. 188, 92–100.

FISHLOCK, D.J. & PARKS, A.G. (1963). A study of human colonic muscle *in vitro*. *Br. Med. J.*, **ii,** 666–667.

GROSSMAN, C.J., KILPATRICK, G.J. & BUNCE, K.T. (1993). Development of a radioligand binding assay for the 5-HT_4 receptor: use of a novel antagonist. *Br. J. Pharmacol.*, **108,** 106P.

HILL, J.M., BUNCE, K.T. & HUMPHREY, P.P.A. (1990). Investigation of the neuronal non-5-HT_3 receptor mediating contraction of guinea-pig ileum. *Br. J. Pharmacol.*, **99,** 182P.

HUMPHREY, P.P.A. (1984). Peripheral 5-hydroxytryptamine receptors and their classification. *Neuropharmacology*, **23,** 1503–1510.

JENNER, C. & MARSDEN, C.D. (1979). The substituted benzamides: a novel class of dopamine antagonists. *Life Sci.*, **25,** 479–486.

KAUMANN, A.J., SANDERS, L., BROWN, A.M., MURRAY, K.J. & BROWN, M.J. (1990). A 5-hydroxytryptamine receptor in human atrium. *Br. J. Pharmacol.*, **100,** 879–885.

KAUMANN, A.J., SANDERS, L., BROWN, A.M., MURRAY, K.J. & BROWN, M.J. (1991). A 5-HT_4-like receptor in human right atrium. *Naunyn-Schmied. Arch. Pharmacol.*, **344,** 150–159.

MORIARTY, K.J., HIGGS, N.B., WOODFORD, M., WARHURST, G. & TURNBERG, L.A. (1987). Inhibition of the effect of serotonin on rat ileal transport by cisapride: evidence in favour of the involvement of 5-HT_2 receptors. *Gut*, **28,** 844–848.

NG, W.W., JING, J., HYMAN, P.E. & SNAPE, Jr. W.J. (1991). Effect of 5-hydroxytryptamine and its antagonists on colonic smooth muscle of the rabbit. *Dig. Dis. Sci.*, **36,** 168–173.

REEVES, J., BUNCE, K.T. & HUMPHREY, P.P.A. (1991). Investigation into the 5-hydroxytryptamine receptor mediating smooth muscle relaxation in the rat oesophagus. *Br. J. Pharmacol.*, **103,** 1067–1072.

REEVES, J., BUNCE, K.T., HUMPHREY, P.P.A. & GUNNING, S.J. (1989). Further characterisation of the 5-HT receptor mediating smooth muscle relaxation in the rat oesophagus. *Br. J. Pharmacol.*, **98,** 800P.

RICHARDSON, B.P., ENGEL, G., DONATSCH, P. & STADLER, P.A. (1985). Identification of serotonin M-receptor subtypes and their specific blockade by a new class of drugs. *Nature*, **316,** 126–131.

SCOTT, C.M., BUNCE, K.T. & SPRAGGS, C.F. (1992). Investigation of the 5-hydroxytryptamine receptor mediating the 'maintained' short-circuit response in guinea-pig ileal mucosa. *Br. J. Pharmacol.*, **106,** 877–882.

SCHUURKES, J.A.J., MEULEMANS, A.L., OBERTOP, H. & AKKERMANS, L.M.A. (1991). 5-HT_4 receptors on the human stomach. *J. Gastrointest. Motility*, **3,** 199.

TAM, F.S.-F., HILLIER, K. & BUNCE, K. (1992). Investigation of the 5-HT receptor type involved in inhibition of spontaneous activity of human colonic circular muscle. *Br. J. Pharmacol.*, **106,** 25P.

TULADHAR, B.R., COSTALL, B. & NAYLOR, R.J. (1991a). Putative 5HT_4 receptor involvement in the relaxations induced by 5-HT in the rat ileum. *Br. J. Pharmacol.*, **104,** 151P.

TULADHAR, B.R., COSTALL, B. & NAYLOR, R.J. (1991b). Investigation of the 5-HT_4 receptor mediating relaxation of the rat ileum. In *The 10th Iranian Congress of Physiology and Pharmacology*, Ahwaz, Iran. Abstract 89.

VILLALON, C.M., DEN BOER, M.O., HEILIGERS, J.P.C. & SAXENA, P.R. (1990). Mediation of 5-hydroxytryptamine-induced tachycardia in the pig by the putative 5-HT_4 receptor. *Br. J. Pharmacol.*, **100**, 665–667.

WARDLE, K.A. & SANGER, G.J. (1993). The guinea-pig distal colon – a sensitive preparation for the investigation of 5-HT_4 receptor mediated contractions. *Br. J. Pharmacol.*, **110**, 1593–1599.

ZHANG, L., GERTHOFFER, W.T. & BUXTON, I.L.O. (1992). Inhibition of canine colonic motility by 5-hydroxytryptamine. In *International Symposium on Serotonin: from Cell Biology to Pharmacology and Therapeutics*. Houston, Texas. Abstract 80.

(Received March 11, 1994
Revised May 12, 1994
Accepted May 25, 1994)

Br. J. Pharmacol. (1994), **113**, 151–158

Infection by HIV-1 blocked by binding of dextrin 2-sulphate to the cell surface of activated human peripheral blood mononuclear cells and cultured T-cells

[1]Sunil Shaunak, *Nigel J. Gooderham, *Robert J. Edwards, Nassrin Payvandi, Caroline M. Javan, ‡Neil Baggett, *John MacDermot, †Jonathan N. Weber & *Donald S. Davies

Department of Infectious Diseases, Royal Postgraduate Medical School, London; *Department of Clinical Pharmacology, Royal Postgraduate Medical School, London; ‡Department of Chemistry, University of Birmingham, Birmingham and †Department of Communicable Diseases, St Mary's Hospital Medical School, London

1 Structural analogues of a sulphated polysaccharide, dextrin sulphate, were synthesized and tested for their ability to block infection by HIV-1. Using the T-cell lines, C8166 and HPB-ALL, and the laboratory adapted strains of HIV-1.MN, HIV-1.IIIb and HIV-1.RF, dextrin 2-sulphate (D2S) combined the best combination of high anti-HIV-1 activity (95% inhibitory concentration (IC_{95}) = 230 nM) and low anticoagulant activity. It also blocked infection of activated peripheral blood mononuclear (PBMN) cells by five primary viral isolates at an IC_{95} of 230–3700 nM depending upon the primary viral isolate tested.

2 In saturation binding studies, [^{3}H]-D2S bound to a cell surface protein on HPB-ALL cells in a specific and saturable manner with a K_d of 82 ± 14 nM and a B_{max} of 4.8 ± 0.3 pmol/10^6 cells. It bound to other human T-cell lines in a similar manner.

3 There was very little binding of [^{3}H]-D2S to freshly isolated PBMN cells (B_{max} 0.18 ± 0.03 pmol/10^6 cells) and these cells could not be infected by HIV-1. Culture of PBMN cells in lymphocyte growth medium (LGM) containing IL-2 did not significantly change the B_{max} of [^{3}H]-D2S. In contrast, PBMN cells which had been cultured with phytohaemagglutinin (PHA; 5 μg ml^{-1}) for 72 h had a B_{max} of [^{3}H]-D2S binding of 7.2 ± 0.1 pmol/10^6 cells and these cells could be infected by HIV-1. Removal of the PHA and further culture of the PBMN cells in LGM containing IL-2 resulted in a fall in the B_{max} to 2.0 ± 0.1 pmol/10^6 cells. The K_d of binding did not change significantly during the course of these experiments.

4 [^{3}H]-D2S did not bind to freshly isolated erythrocytes or to erythrocytes which had been cultured in PHA for 72 h.

5 These results suggest that there is a relationship between the expression of the [^{3}H]-D2S binding protein on the plasma membrane of PBMN cells and the susceptibility of these cells to infection by HIV-1.

Keywords: HIV-1; laboratory adapted isolates of HIV-1; primary viral isolates of HIV-1; sulphated polysaccharides; chemical synthesis and characterization of sulphated polysaccharides; dextrin 2-sulphate; human cultured T-cells; human peripheral blood mononuclear cells

Introduction

Infection by the Human Immunodeficiency Virus-1 (HIV-1) is a prerequisite for the development of the Acquired Immune Deficiency Syndrome (AIDS) which is characterized by a progressive loss of CD4 positive T-cells. Infection of these cells is initiated by the binding of the viral envelope glycoprotein gp120 to the cell surface protein CD4, following which there is a temperature-dependent dissociation of gp120 from the viral envelope (Dalgleish *et al.*, 1984; Klatzmann *et al.*, 1984; Maddon *et al.*, 1986; Hart *et al.*, 1991; Dimitrov *et al.*, 1992; Klasse & Moore, 1992). This exposes gp41 which is believed to be involved in the fusion of the virion with the cell membrane (Brasseur *et al.*, 1988). The mechanism of viral entry however remains obscure.

Endogenous sulphated polysaccharides have a role in cell adhesion and cell recognition (Rossignol *et al.*, 1984; Yamaguchi *et al.*, 1985; Cole *et al.*, 1986; Coombe *et al.*, 1987) and have been implicated in the binding of lymphocytes to endothelial venules (Stoolman & Rosen, 1983; Brenan & Parish, 1986; Coombe & Rider, 1989). More recently, sulphated polysaccharides have become the focus of renewed interest because they block infection of T-cell lines by laboratory adapted strains of HIV-1 *in vitro*. A variety of compounds have been studied; fucoidan, dextran sulphate, pentosan polysulphate, mannan sulphate, lentinan sulphate, sulphated bacterial glycosaminoglycan, dextrin 2-sulphate, heparin and fragmented derivatives of heparin (Ito *et al.*, 1987; Ueno & Kuno, 1987; Baba *et al.*, 1988b; Bagasra & Lischner, 1988; McClure *et al.*, 1991; 1992; Beddows *et al.*, 1993). In previous studies, D2S was shown to block infection of human T-cell lines by a variety of laboratory adapted cell-free isolates of HIV-1 (McClure *et al.*, 1991; 1992; Beddows *et al.*, 1993).

It remains to be established whether the large family of sulphated polysaccharides which block HIV-1 infection share a common mechanism of action or whether several different mechanisms are responsible for their anti-HIV-1 activity. In the case of D2S, fucoidan and dextran sulphate, previous studies have suggested that they block HIV-1 infection by acting at the level of the cell surface but they did not characterize this binding (Mitsuya *et al.*, 1988; Baba *et al.*, 1988a; 1990; McClure *et al.*, 1991; 1992; Beddows *et al.*, 1993).

The identification and characterization of a cell surface receptor to which D2S binds and blocks HIV-1 infection has important implications for therapy. In this paper, we have synthesized structural variants of dextrin sulphate and used them to study the binding of these compounds to T-cells.

[1] Author for correspondence.

Methods

Synthesis of D2S and its analogues

Limit dextrin (ML Labs, Waverley, Liverpool) was produced by enzymatic hydrolysis of starch and purified by ultra filtration and passage through absorptive filters. The product complies with the British Pharmacopoeia monograph for dextrin and consists predominantly of α-1, 4 linked glucan units. D2S was synthesized by sulphation of a solution of dextrin (40 g in 40 ml water) at room temperature using sulphur trioxide-trimethylamine complex (60 g) in the presence of sodium hydroxide (16.8 g). The stirred mixture was maintained alkaline over 12 h with 5 M sodium hydroxide. Excess reagent was removed by dialysis against water and the product recovered after freeze-drying. Dextrin 2,3,6-trisulphate was prepared in the same way as D2S but with a large excess of the sulphating agent.

Dextrin 3-sulphate was prepared from dextrin (16.2 g) after being acetylated over 2 d with acetic anhydride (20.4 g) and triethylamine (10 g) in dimethylformamide (150 ml). The product (12.3 g), predominantly the 2,6-diacetyl derivative, was collected by precipitation after the addition of water, dissolved in dimethylformamide (75 ml) and sulphated with trimethylamine-sulphur trioxide complex (25 g) over 24 h. The mixture was poured into acetone (500 ml) to yield a sticky residue and the supernatant decanted. The residue was dissolved in water (150 ml) and saponified with sodium hydroxide (5 g) to remove the acetyl groups. The dextrin 3-sulphate mixture was finally dialysed against water and freeze-dried.

Dextrin 6-sulphate was prepared by sulphation of dextrin (10 g) in dimethylformamide (100 ml) with cyclamic acid (22.5 g) at 78°C over 1.5 h. The mixture was made alkaline with sodium hydroxide in aqueous ethanol (10%; 50 ml) and then poured into diethyl ether (400 ml). The resultant solid was washed with ether, dissolved in sodium acetate solution (50%; 100 ml), dialysed against water and freeze-dried.

Dextrin 2-(2-hydroxypropyl-3-trimethylammonium salt) was prepared by stirring dextrin (81 g) in 5% sodium hydroxide (240 ml) with glycidyltrimethylammonium chloride (120 g) for 12 h at 20°C. The resulting solution was dialysed against water and freeze-dried. Dextrin 2-(2-hydroxypropyl-3-triethylammonium salt) was prepared in the same way except that glycidyltriethylammonium chloride was used in place of glycidyltrimethylammonium chloride.

Dextrin and its sulphated derivatives were characterized by sulphate analysis, Fourier transformed infra red spectra recorded in KBr discs and ^{13}C n.m.r.

Synthesis of radiolabelled D2S

[^{3}H]-D2S was prepared by partial alkylation of D2S with [^{3}H]-methyl iodide in dimethylformamide in the presence of a silver (I) oxide catalyst. A stirred solution of D2S (27.7 mg) and silver (I) oxide (10 mg) in dimethylformamide (2 ml) was treated dropwise with [^{3}H]-methyl iodide (3.74 mg in 1 ml of toluene; specific activity 80 Ci mmol^{-1}, Amersham, Bucks) over 4 h at room temperature. Distilled water (5 ml) was then added with vigorous stirring before the mixture was allowed to separate into aqueous and organic layers. The organic layer was removed. The residual aqueous phase was dialysed against distilled water (8 × 10 l) followed by gel filtration (Sephadex G-25) to yield D2S in which it was estimated that 1 in 500–1000 glucan units was [^{3}H]-methylated (specific activity 70–200 mCi mmol^{-1}). This degree of methylation did not affect its anti-HIV-1 activity.

Cell lines and primary cells

The human T-cell lines studied were HPB-ALL (Morikawa *et al.*, 1978), CEM (Foley *et al.*, 1965), C8166 (Salahuddin *et al.*, 1983) and H9 (Popovic *et al.*, 1984). The human epithelial-like cell line HeLa (Scherer *et al.*, 1953) and the HeLa cell line transfected with the gene for human CD4 (Chesebro & Wehrly, 1988) were also studied. HPB-ALL cells were maintained in Iscove's modified Dulbecco's medium and C8166 cells, H9 cells, HeLa cells and HeLa CD4 cells were maintained in RPMI 1640 medium. The culture medium was supplemented with 10% (v/v) foetal calf serum (FCS), 2 mM glutamine, 250 iu ml^{-1} penicillin and 250 μg ml^{-1} streptomycin. Cell lines were obtained from the MRC AIDS Directed Programme.

PBMN cells were isolated from whole blood using Ficoll-Paque (Pharmacia). The cells were suspended at 2 × 10^6 cells ml^{-1} in lymphocyte growth medium (LGM) which contains RPMI 1640, 2 mM L-glutamine, 15% (v/v) FCS, 250 iu penicillin ml^{-1} and 250 μg streptomycin ml^{-1}. In some experiments, cells were cultured with 5 μg ml^{-1} phytohaemagglutinin (PHA; Sigma) for up to 72 h, washed with phosphate buffered saline (PBS)/5% (v/v) FCS, and then resuspended in fresh LGM containing 20 iu recombinant IL-2 ml^{-1} (MRC AIDS Directed Programme). In other experiments, cells were cultured with 5 μg PHA ml^{-1} for up to 96 h, washed with PBS/5% (v/v) FCS and then resuspended in fresh lymphocyte growth medium containing 20 iu recombinant IL-2 ml^{-1} for up to 96 h.

Freshly isolated PBMN cells were also incubated with LGM containing 1.0 μg ml^{-1} of the monoclonal antibody OKT3 (anti-CD3, a T-cell specific activator antibody) (Roosnek *et al.*, 1990) or with LGM containing 20 iu recombinant IL-2 ml^{-1} and one of several cytokines (Schrier *et al.*, 1993) (1 ng ml^{-1} human recombinant IL-1α, 1 ng ml^{-1} human recombinant IL-1β, 50 ng ml^{-1} human recombinant IL-4 and 50 ng ml^{-1} human recombinant IL-6; Genzyme Diagnostics, Kent) for up to 72 h prior to being washed with PBS/2% (v/v) FCS and binding studies being performed.

Infectivity assays

The HIV-1 isolates HIV-1.MN, HIV-1.IIIb and HIV-1.RF were obtained through the MRC AIDS Directed Programme and were propagated in H9 cells. Cell free supernatants containing HIV-1 were prepared by lysis of acutely infected H9 cells and centrifugation of the cellular debris at 400 *g* for 5 min. The titre of virus was determined by endpoint dilution of the viral supernatant on C8166 cells (Lifson *et al.*, 1986; McClure *et al.*, 1991). Productive infection resulted in the formation of syncytia in the C8166 cells and the result was recorded as the tissue culture infectious dose (TCID). Syncytial assays and/or measurement of the major core protein of HIV-1 (p24) were used to determine the anti-HIV-1 activity of D2S and its analogues. Cells were incubated with the test compound for 1 h at 37°C prior to the addition of HIV-1. The cultures were then assessed by light microscopy on a daily basis for 5 days for the formation of syncytia and/or cell free culture supernatants collected for measurement of p24 (EIA, Coulter, Luton, Beds).

The ability of D2S to block infection of PBMN cells by primary viral isolates of HIV-1 was also determined. These isolates were grown from HIV-1 positive patients by culturing their PBMN cells (2 × 10^6 ml^{-1}) with an equal number of PHA activated PBMN cells from seronegative donors (Hollinger *et al.*, 1992). The co-culture was fed every 4 days with fresh LGM containing IL-2 and fresh PHA activated PBMN cells (0.5 × 10^6 cells ml^{-1}). Cell free supernatants were collected 10 days after the start of the co-culture and stored in liquid nitrogen until use. The titre of the primary viral isolate was determined by endpoint dilution of the viral supernatant on PHA stimulated PBMN cells. Productive infection was determined by measurement of p24 in cell free culture supernatants and the result recorded as the TCID.

The anti-HIV-1 activity of the compounds studied was determined using PHA stimulated PBMN cells which, after washing, had been resuspended in fresh LGM containing IL-2 (20 iu ml^{-1}). They were then incubated with D2S

($20-100\ \mu g\ ml^{-1}$) for 1 h at 37°C. Following this, either HIV-1.MN (10^2 TCID) or one of 5 primary viral isolates of HIV-1 (10^1-10^2 TCID) was added to the culture. After 24 h, the cells were washed with PBS/2% (v/v) FCS and cultured in LGM containing IL-2 ($20\ iu\ ml^{-1}$) for a further 4 days. Cell free culture supernatants were then collected, filtered and p24 measured. The inhibitory concentration (IC_{95}) of each compound was defined as the concentration which reduced the level of p24 in cell free supernatants by 95% as compared to the positive control. The IC_{95} was measured in preference to the IC_{50} because studies with recombinant soluble CD4 have suggested that its inhibitory effect on plasma viraemia correlates with the *in vitro* IC_{95} of the viral isolate and not its IC_{50} (Schacker *et al.*, 1994).

Anticoagulant assays

Thrombin mediated fibrin formation was measured in pooled human plasma. Compounds were diluted in plasma/veronal buffer (2/1, pH 7.35) and incubated at 37°C for 30 min. Fractions of each solution ($200\ \mu l$) were then mixed with bovine thrombin (7 u) and the time to clot formation recorded. The normal thrombin time was 17 s.

Receptor-ligand binding studies

C8166 cells were used to determine the anti-HIV-1 activity of the compounds synthesized. However, although they are an ideal T-cell line for infection screening assays, they were not used for the binding assays because they grow in clumps which are difficult to separate into individual cells. HPB-ALL cells (which are also very sensitive to infection by HIV-1) were used for the binding studies because they grow predominantly as single cells and the small percentage of cells which grow in clumps can be easily separated. For the purpose for which these cell lines were used, there was no difference between them; the K_d and B_{max} values of the two cell types were similar and D2S blocked infection of both C8166 and HPB-ALL cells at the same concentration (see results).

All binding studies were performed at 4°C. Competition binding studies were performed in triplicate using HPB-ALL cells at a concentration of $2 \times 10^6\ ml^{-1}$ (Coulter ZM counter) and $0.2\ \mu M$ [^{3}H]-D2S. Dextran sulphate (8 kDa), fucoidan, pentosan polysulphate, auran tricarboxylic acid, sodium sulphate and glucose 6 phosphate were purchased from Sigma, UK. The total reaction volume was $250\ \mu l$. After 1 h at 4°C, the cells were washed with PBS containing 9 mM calcium chloride and 4.9 mM magnesium chloride and collected on Whatman GF/C filters using a Brandel cell harvester. The [^{3}H]-D2S bound to cells was measured in a Tricarb 2000A (Packard, UK) liquid scintillation counter.

The saturation binding curves for [^{3}H]-D2S were established using at least 8 different concentrations and tested in triplicate. Adherent cells were removed in PBS containing 2 mM EDTA/2% (v/v) FCS, counted and resuspended in RPMI 1640 at a concentration of 2×10^6 cells ml^{-1}. Non-specific binding was determined using at least a 100 fold excess of unlabelled D2S. After 1 h at 4°C, the cells were washed, collected and counted as described above.

In several experiments, HPB-ALL cells were preincubated with the antibody Leu 3a (an anti-CD4 monoclonal antibody which blocks the interaction of the HIV-1 envelope glycoprotein gp120 with CD4) for 1 h. Anti-CD 14 and anti-CD 26 monoclonal antibodies were used as control antibodies. In other experiments, HPB-ALL cells were incubated with 0.05% (w/v) trypsin for 15 min at 37°C or 1.25 units neuraminidase ml^{-1} for 30 min at 37°C prior to the binding studies.

Binding curves were modelled by computer using an iterative non-linear least squares regression (Graphpad, Inplot, U.S.A.) from which the dissociation constant (K_d) and the B_{max} were determined. A 1:1 receptor-ligand stoichiometry and no co-operativity between receptors were assumed. The ED_{50} (concentration of the competing drug which displaced 50% of the [^{3}H]-D2S bound) was determined from the competition binding curves. The inhibitory constant (K_i) was calculated from $K_i = ED_{50}/\{1 + (*L/K_d)\}$ where *L is the concentration of [^{3}H]-D2S in the reaction and K_d is the dissociation constant of [^{3}H]-D2S.

Statistical analysis

This was performed with Student's unpaired *t* test.

Results

Synthesis of modified dextrins

Since dextrin is a polymer comprising repeat units, chemical modification such as sulphation yields a product which is predominantly (but not exclusively) modified at the same site of each repeating unit. Elemental and spectroscopic analysis provide evidence for, and distinguished between, the various sites of modification. The mol. wt. of D2S was calculated as 27 kDa on the basis of the incorporation of 1 sulphate per glucan unit (see below).

The sulphate content of the dextrin 2-, 3-, and 6-sulphates was determined by elemental analysis as 37%, being equivalent to one sulphate per glucan moiety. In the case of dextrin 2,3,6-trisulphate, the sulphate content was determined as 70%, this being equivalent to complete hydroxyl substitution (three sulphate groups per glucan).

Sulphated dextrins all yielded infrared specta with a band at about $1220\ cm^{-1}$ characteristic of the presence of sulphate and another band between $820\ cm^{-1}$ and $840\ cm^{-1}$. Neither of these bands were present in the infrared spectrum of dextrin itself. A peak at $820\ cm^{-1}$ has been reported as typical for primary sulphates of sugars, i.e. for 6-substitution, whereas equatorial secondary sulphate gives a peak at $835\ cm^{-1}$ (Turvey, 1965).

By comparison to authentic reference sugars, the ^{13}C n.m.r. spectrum of dextrin was assigned as follows; the C-1 acetal carbon is to lowest field, 100.3 p.p.m. and the primary C-6 is to the highest field near 61 p.p.m. Between these two are C-4 (77.6 p.p.m.), C-3 (73.9 p.p.m.), C-2 (72.2 p.p.m.) and C-5 (71.8 p.p.m.).

The structure of D2S was confirmed by comparison with dextrin. A major signal for unsubstituted C-6-OH at 61.1 p.p.m. was present and a C-4 signal at 78.1 p.p.m. The major C-1 peak moved upfield to 99.8 p.p.m. (100.3 p.p.m. for dextrin) due to the 2-O-sulphation. The spectrum of dextrin 3-sulphate had a strong signal at 61.1 p.p.m. characteristic of unmodified C-6-OH. Prominent new signals were present at 82.2 and 82.5 p.p.m. and are assigned to C-3 (a shift of 8.3 and 8.6 p.p.m. downfield compared to dextrin). These are close to the chemical shifts for C-3 in glucose 3-sulphate (8.5 and 9.5 p.p.m. downfield compared to glucose). The assignment is supported by the virtual disappearance of the C-4 signal (77.6 p.p.m. in dextrin) since substitution at C-3 would be expected to cause an upfield shift (eg. 2.2 p.p.m. upfield shift in glucose 3-sulphate relative to glucose), taking it under the envelope of other signals. The C-2 and C-5 peaks shifted upfield to 70.2 and 70.8 p.p.m., respectively (from 72.2 or 71.8 p.p.m. in dextrin). This is similar to the 1.1 p.p.m. upfield shift for C-2 in glucose 3-sulphate compared to glucose. The C-1 region showed six closely spaced lines between 100.1 to 98.3 p.p.m. slightly upfield from that in dextrin (100.3 p.p.m.).

In the spectrum of dextrin 6-sulphate the original C-6 peak at 61.1 p.p.m. was greatly diminished and a new signal was present at 67.5 p.p.m., a 6.4 p.p.m. downfield shift from C-6 in dextrin. This is similar to the reported 6.2 p.p.m. downfield shift seen in glucose 6-sulphate compared to glucose. The signal for C-5 was shifted upfield (2.5 p.p.m.) to

69.3 p.p.m. A similar upfield shift of 1.7 p.p.m. has been reported for the 6-O-sulphation of glucose (Bock & Pedersen, 1983).

In the ^{13}C n.m.r. spectrum of dextrin 2-(2-hydroxypropyl-3-trimethylammonium salt), the sharp singlet at 54.8 p.p.m. confirmed the pendent trimethylammonium group. The hydroxypropyl bridge gave signals at 65.6 and 68.5 p.p.m. and the C-1 signal was shifted 3.3 p.p.m. upfield to 97 p.p.m. (from 100.3 p.p.m. in dextrin) confirming C-2 substitution. The spectrum of dextrin 2-(2-hydroxypropyl-3-triethylammonium salt) contained signals at 7.9 and 54.2 p.p.m. demonstrating the presence of the methyl and methylene groups in the triethylammonium moiety. The hydroxypropyl bridge gave signals at 59.2 and 64.8 p.p.m. The unsubstituted C-6 gave a peak at 60.9 p.p.m. (dextrin C-6, 61.1 p.p.m.). The C-1 signal was shifted 3 p.p.m. upfield to 97.3 p.p.m. (100.3 p.p.m. in dextrin) confirming C-2 substitution.

Infectivity and anticoagulent measurement

The anti-HIV-1 activity (as determined in C8166 cells and 3 laboratory adapted strains of HIV-1) and the anticoagulant activity of dextrin sulphate were affected by the number and position of the sulphate groups present. D2S, dextrin 6-sulphate and dextrin 2,3,6-trisulphate were potent anti-HIV-1 compounds with similar IC_{95} values (Table 1). Amongst the compounds tested, D2S had the shortest thrombin time and dextrin 2,3,6-trisulphate the longest (Table 1). The 3-sulphated derivative had poor anti-HIV-1 activity (Table 1) although its thrombin time was similar to that for dextrin 6-sulphate (D6S) (Table 1). Dextrin 2-(2-hydroxypropyl-3-trimethylammonium salt) and dextrin 2-(2-hydroxypropyl-3-triethylammonium salt) had no anti-HIV-1 activity (Table 1). The inhibition of infection by HIV-1 was confirmed by measurement of HIV-1 p24 in cell free culture supernatants. Amongst the sulphated derivatives of dextrin, D2S combined high anti-HIV-1 activity with low anticoagulant activity. Neither D2S nor [^{3}H]-D2S was toxic to C8166 or to HPB-ALL cells (as determined by cell viability) at a concentration of 7.4 μM, even after several weeks of culture.

Freshly isolated PBMN cells can only be infected by HIV-1 (as determined by p24) after they have been activated by culturing the cells in LGM containing PHA for 24–72 h. Gowda *et al.* (1989) have also shown, using PCR for HIV-1 proviral DNA, that activated but not resting PBMN cells can be infected by HIV-1. The susceptibility of these cells to infection by HIV-1 following activation is not due to an increased cell surface expression of CD4 (Gowda *et al.*, 1989). Dextrin 2-sulphate was found to block infection of PHA activated PBMN cells by 5 primary viral isolates with an IC_{95} of 230–3700 nM depending upon the primary viral isolate tested as determined by the measurement of p24 in cell free culture supernatants.

Receptor-ligand binding studies

Competition binding studies In competition binding studies using HPB-ALL cells, dextrin 6-sulphate, dextrin 3-sulphate and dextrin 2,3,6-trisulphate were all effective inhibitors of [^{3}H]-D2S binding (Table 1; Figure 1). The positively charged molecules, dextrin 2-(2-hydroxypropyl-3-trimethylamine) and dextrin 2-(2-hydroxypropyl-3-triethylamine), did not inhibit [^{3}H]-D2S binding and had no anti-HIV-1 activity. Similarly, dextrin, glucose 6-phosphate and sodium sulphate had no anti-HIV-1 activity and did not displace [^{3}H]-D2S (Table 1).

Competition binding studies were also performed using several naturally occurring sulphated polysaccharides and polyanionic compounds which have anti-HIV-1 activity. Of those tested, fucoidan was the most effective competitor (Table 1). Dextran sulphate (8 kDa) was less effective than the sulphated derivatives of dextrin. Pentosan polysulphate did not compete at all whilst auran tricarboxylic acid competed very poorly.

Saturation binding studies on T-cell lines [^{3}H]-D2S bound to HPB-ALL cells in a specific and saturable manner (Figure 2). The dissociation constant (K_d) for HPB-ALL cells was 82 ± 14 nM with a B_{max} of 4.8 ± 0.3 pmol per 10^6 cells. CEM, C8166 and H9 cells had similar K_d values for the binding of [^{3}H]-D2S (Table 2).

Pre-treatment of HPB-ALL cells with trypsin reduced the saturable component of [^{3}H]-D2S binding by 91%, in contrast to pretreatment with neuraminidase which did not reduce the binding of [^{3}H]-D2S as compared to PBS-treated control cells. Exposure of HPB-ALL cells to an antibody against CD4 (Leu 3a) or with the control antibodies (anti-CD14 and anti-CD26) at a concentration of 2 μg ml^{-1} for 1 h prior to performing the binding studies made no difference to either the B_{max} or the K_d of [^{3}H]-D2S binding. Recombinant gp120 also failed to displace [^{3}H]-D2S in competition binding studies.

The binding of [^{3}H]-D2S to HeLa cells was also compared

Table 1 The anti-HIV-1 activity, anticoagulant activity and inhibition of [^{3}H]-dextrin 2-sulphate ([^{3}H]-D2S) binding

	Thrombin time (s) {$n = 3$}	*anti-HIV-1 activity* (IC_{95}, nM) {$n = 9$}	*[^{3}H]-D2S binding* (K_i, nM) {$n = 6$}
Dextrin 2-sulphate	32 ± 1	230 ± 15	66 ± 10
Dextrin 6-sulphate	56 ± 2	230 ± 15	55 ± 12
Dextrin 3-sulphate	63 ± 2	1850 ± 67	198 ± 6
Dextrin 2,3,6 trisulphate	> 180	300 ± 14	50 ± 3
Dextrin 2-(2-hydroxypropyl-3-trimethylamine)	ND	Not active	No competition
Dextrin 2-(2-hydroxypropyl-3-triethylamine)	ND	Not active	No competition
Dextrin	17 ± 1	Not active	No competition
Glucose 6-phosphate	ND	Not active	No competition
Sodium sulphate	ND	Not active	No competition
Fucoidan	80 ± 2	80 ± 6	190 ± 8
Dextran sulphate (8 kDa)	27 ± 1	780 ± 49	410 ± 14
Pentosan polysulphate	ND	2000 ± 128	No competition
Aurin tricarboxylic acid	ND	3700 ± 196	29000 ± 970

The inhibitory concentration (IC_{95}) is the mean concentration of the compound which blocked infection by HIV-1.MN, HIV-1.IIIb and HIV-1.1.RF of C8166 cells by 95% as measured by syncytia formation and HIV-1 p24. The thrombin time was measured using the concentration of each compound which corresponded to the IC_{95} for its anti-HIV-1 activity. Competition binding studies were performed with HPB-ALL cells. The inhibitory constant (K_i) was determined from these experiments using the concentration of the competing compound which inhibited the binding of [^{3}H]-D2S by 50%.
Results are shown as the mean ± s.e.mean. ND = not done.

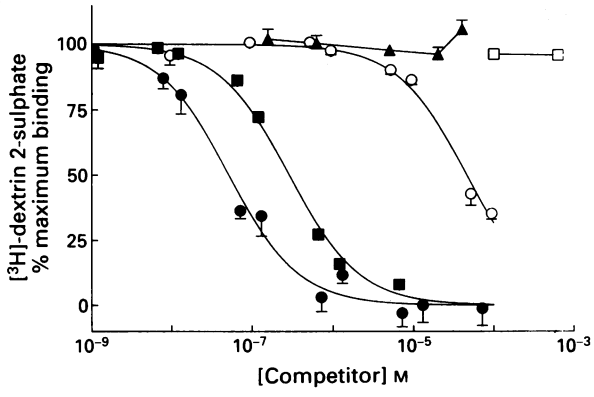

Figure 1 Inhibition of the binding of 0.2 μM [^{3}H]-D2S to HPB-ALL cells. Competition curves of specific binding of dextrin 2-sulphate (●), fucoidan (■), aurin tricarboxylic acid (○), pentosan polysulphate (▲) and glucose 6-phosphate (□).

with that to HeLa cells transfected with the gene for human CD4. Although the K_d for [^{3}H]-D2S binding did not change, the B_{max} value for HeLa cells was 4.1 ± 0.2 pmol/10^6 cells compared to HeLa cells transfected with CD4 for which it was 2.2 ± 0.1 pmol/10^6 cells; $n = 9$, $P < 0.05$.

Saturation binding studies on PBMN cells There was little binding of [^{3}H]-D2S to freshly isolated PBMN cells (B_{max} = 0.18 ± 0.03 pmol/10^6 cells; Figure 3). Binding increased 2–3 fold after 4 h of culture in LGM containing IL-2 (B_{max} = 0.5 ± 0.1 pmol/10^6 cells; K_d 134 ± 59 nM), but no further increase in binding was seen even where the cells were maintained in culture with IL-2 for up to 72 h (Figure 3). In contrast, when PBMN cells were cultured in the presence of PHA, the B_{max} increased over 72 h to a maximum of 7.2 ± 0.1 pmol/10^6 cells (K_d 198 ± 18 nM). The binding of [^{3}H]-D2S to PHA-activated PBMN cells was specific and saturable within the concentration range studied. Culture of PBMN cells in PHA beyond 72 h to 96 h resulted in a small reduction in cell viability (as measured by Trypan blue exclusion) and in the B_{max} to 6.0 ± 0.4 pmol/10^6 cells. The K_d did not change during the course of these cultures. There was no difference in the binding constants of [^{3}H]-D2S to PBMN cells from men as compared to women with no variation seen during the menstrual cycle (data not shown).

The binding of [^{3}H]-D2S to activated PBMN cells fell following removal of PHS, washing with PBS/5% (v/v) FCS and resuspension in LGM containing IL-2 (Figure 3). Twenty-four hours after the change in the culture medium, the B_{max} had fallen to 2.0 ± 0.1 pmol/10^6 cells and it then remained at this level with further culture. Cell viability was >90% at all times except where indicated in Figure 3.

In order to determine whether the PHA-dependent increase in the binding of [^{3}H]-D2S to activated PBMN cells could have been mediated by the adherence of cellular products in the culture medium to the surface of PBMN cells, freshly isolated PBMN cells were incubated for 1 h at 4°C with cell free culture media from 96 h old cultures of HPB-ALL cells, washed with PBS/2% (v/v) FCS and binding studies performed. The B_{max} of binding (0.18 ± 0.03 pmol/10^6 cells) did not change as compared to control cells (0.18 ± 0.03 pmol/10^6 cells) despite the high B_{max} of [^{3}H]-D2S binding to the HPB-ALL cells (4.8 ± 0.3 pmol/10^6 cells). Addition of cell free supernatants from 96 h old cultures of PBMN cells in LGM containing PHA also failed to increase the binding of [^{3}H]-D2S to freshly isolated PBMN cells under similar conditions. The same result was obtained with supernatants from PBMN cells cultured without PHA.

Culture of freshly isolated PBMN cells with anti-CD3 for 72 h increased the B_{max} of [^{3}H]-D2S to 2.0 ± 0.2 pmol/10^6 cells (K_d = 138 ± 26 nM; $n = 6$) and made these cells susceptible to infection by HIV-1 as measured by p24 and as previously shown by Gowda *et al.* (1989). In contrast, incubating PBMN cells in LGM containing the cytokines IL-1α, IL-1β, IL-4 or IL-6 for 72 h did not change the B_{max} of [^{3}H]-D2S as compared to PBMN cells which had been cultured in LGM containing IL-2 only. These cells could not be infected by HIV-1.

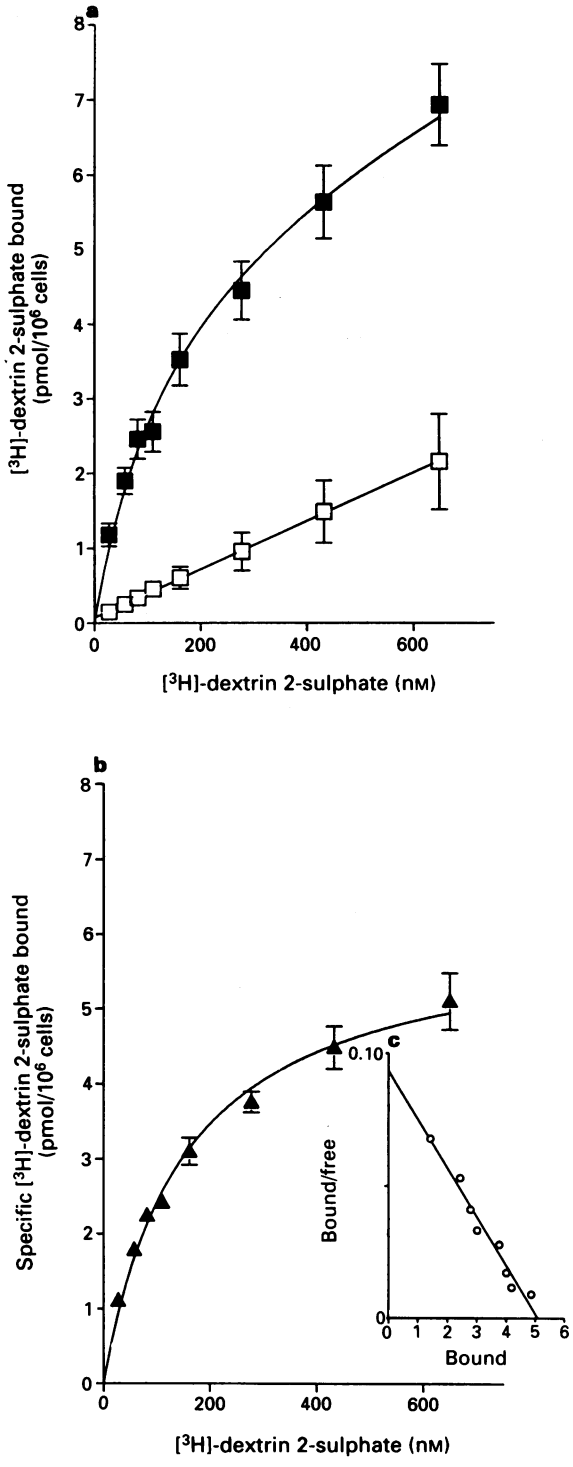

Figure 2 The binding of [^{3}H]-D2S to HPB-ALL cells. (a) Total binding (■) and non-specific binding (□), (b) the specific component of binding of [^{3}H]-D2S. The specific binding (○) is shown as a Scatchard plot in (c), where bound = pmol [^{3}H]-D2S/10^6 cells and free = free ligand (nM).

[^{3}H]-D2S did not bind to fresh human erythrocytes, nor to erythrocytes after 72 h of culture in LGM with PHA. Furthermore, [^{3}H]-D2S did not bind to erythrocytes even when

Table 2 Binding constants for [^{3}H]-dextrin 2-sulphate to human T-cells

Cell line	Dissociation constant K_d (nM)	B_{max} (pmol/10^6 cells)	
HPB-ALL	82 ± 14	4.8 ± 0.3	$n = 7$
CEM	163 ± 56	5.3 ± 1.2	$n = 3$
C8166	190 ± 11	4.2 ± 0.2	$n = 3$
H9	137 ± 18	2.2 ± 0.1	$n = 3$

These cell lines are all susceptible to infection by HIV-1. Infection of these cells is blocked by D2S (McClure *et al.*, 1991; 1992; Shaunak, 1993). The saturation binding curves were determined with at least 8 different concentrations and tested in triplicate. The results are given as the mean ± s.e.mean. The mean K_d of these T-cell lines is 143 ± 23 nM with a mean B_{max} of 4.1 ± 0.7 pmol/10^6 cells.

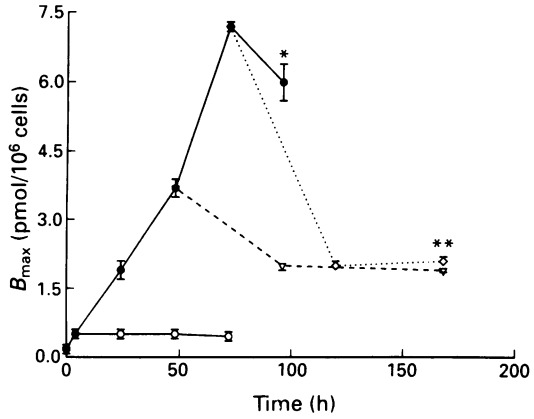

Figure 3 The binding of [^{3}H]-D2S to PBMN cells. Following isolation from whole blood, PBMN cells were cultured in either LGM with PHA (5 μg ml^{-1}) (●) or in LGM with IL-2 (20 iu ml^{-1}) (○) for up to 96 h. In some experiments, PBMN cells were first cultured in LGM with PHA for 48 h (▽) or 72 h (◇), washed with PBS/2% (v/v) FCS and then resuspended in LGM with IL-2 (20 iu ml^{-1}) and cultured. Cell viability was 90–99% at all times except as shown; *(77%) and **(80%). All points are shown as the mean ± s.e.mean ($n = 12$).

their isolation from PBMN cells was performed after whole blood had first been cultured in LGM containing PHA for 48 h.

Discussion

In this study, the relationship between the structure of sulphated dextrins and their ability to block infection of T-cells by HIV-1 was examined. The position of the sulphate group on the glucan moiety was found to be important for their anti-HIV-1 activity. Sulphation at the 2-position or 6-position of dextrin resulted in considerably better anti-HIV-1 activity compared to sulphation at the 3-position. Increasing the number of sulphate groups per glucan molecule (dextrin 2,3,6-trisulphate) resulted in a considerable increase in the anticoagulant activity of the molecule. Neither dextrin nor 2-substituted quaternary ammonium dextrin had any anti-HIV-1 activity. Thus the cell surface binding of these compounds and their anti-HIV-1 activity is dependent upon the spatial arrangement of the negatively charged sulphate groups.

Competition binding experiments were used to compare [^{3}H]-D2S with other sulphated polysaccharides and polyanionic compounds which have anti-HIV-1 activity. Fucoidan was a good competitor of [^{3}H]-D2S in contrast to pentosan polysulphate which did not compete at all. Fucoidan is thought to share a similar mechanism of action to D2S for its anti-HIV-1 activity (McClure *et al.*, 1992) in contrast to pentosan polysulphate which binds to CD4 (Parish *et al.*, 1990). Aurin tricarboxylic acid, which also blocks HIV-1 infection by binding to CD4 (Schols *et al.*, 1989; Szabo *et al.*, 1992), was a very poor competitor of [^{3}H]-D2S.

The results of saturation and competition binding studies suggest that [^{3}H]-D2S is binding to a cell surface molecule with a K_d in the range of 82–198 nM and a B_{max} of 0.18–7.2 pmol/10^6 cells. The B_{max} was affected by the state of activation of the cells. The reduction in the binding of [^{3}H]-D2S to the cell surface following treatment with trypsin indicates that the cell surface molecule is a protein. Furthermore, competition experiments with the anti-CD4 monoclonal antibody, Leu 3a, and with gp120, together with the binding observed to HeLa and HeLa CD4 cells suggests that this binding is independent of CD4.

D2S blocked infection of several human T-cell lines by a variety of cell free, laboratory adapted isolates of HIV-1 at an IC_{95} of 230 nM as judged by the inhibition of syncytia formation in C8166 cells and HIV-1 p24 levels. We have also shown that HIV-1 proviral DNA cannot be detected by PCR in cells incubated with D2S and then exposed to HIV-1 (Bieniasz *et al.*, 1991; Shaunak, 1993), providing evidence that D2S prevents HIV-1 infection by blocking viral entry into cells. In view of the recent observation that the concentration of recombinant soluble CD4 which blocks infection of PBMN cells by primary viral isolates of HIV-1 is 200–2700 times greater than that required to block infection of T-cell lines by laboratory adapted isolates of HIV-1 (Daar *et al.*, 1990), the activity of D2S against primary viral isolates of HIV-1 was also tested. D2S blocked infection of PHA activated PBMN cells by several different primary viral isolates at concentrations that were up to 16 times higher than those required to block laboratory adapted isolates. D2S therefore has potential as a clinically useful compound.

All the T-cell lines examined bound [^{3}H]-D2S and the addition of PHA or IL-2 to the culture media did not alter the B_{max} of binding (data not shown). In contrast, the binding of [^{3}H]-D2S to freshly isolated PBMN cells increased when the cells were cultured in LGM with PHA to a B_{max} that was almost double that for the T-cell lines that we studied (Table 2). When the cells were then transferred to LGM containing IL-2, the B_{max} fell to 2.0 ± 0.1 pmol/10^6 cells and it remained at this level with further culture. Several experiments were performed to ensure that the binding of [^{3}H]-D2S to the cell surface was not an artifact of *in vitro* culture, for example, with intracellular material from disrupted PBMN cells being adsorbed onto the surface of intact PBMN cells. Freshly isolated PBMN cells did not bind [^{3}H]-D2S following addition of conditioned media either from 96 h old cultures of HPB-ALL cells or from 96 h old cultures of PBMN cells. Furthermore, erythrocytes did not bind [^{3}H]-D2S under any of the experimental conditions tested.

PBMN cells which have been activated by culturing them either in LGM containing PHA or with an anti-CD3 antibody were susceptible to infection by HIV-1. Infectivity correlated with an increased expression of the binding [^{3}H]-D2S. In contrast, culture of fresh PBMN cells with LGM and each of the cytokines interleukin-1α (IL-1α), IL-1β, IL-2, IL-4 and IL-6 for up to 72 h failed to increase the expression of the [^{3}H]-D2S binding protein significantly or to make the cells susceptible to infection by HIV-1. These results suggest a relationship between the expression of the [^{3}H]-D2S binding protein and the susceptibility of PBMN cells to infection by HIV-1.

In conclusion, we have synthesized several structural analogues of sulphated dextrin. Of these, D2S combines high anti-HIV-1 activity against both laboratory-adapted and primary viral isolates of HIV-1 with low anticoagulant activity. Our experiments with trypsin suggest that it binds to a cell surface protein which is expressed on T-cell lines. D2S

blocks infection of these cells by both laboratory-adapted isolates of HIV-1 and primary viral isolates of HIV-1. Unstimulated PBMN cells, which cannot be infected by HIV-1, bound little [^{3}H]-D2S. However, after activation by PHA or anti-CD3 antibody, these cells could be infected by HIV-1 and they bound [^{3}H]-D2S. Infection of these cells was blocked by D2S. These results suggest that there is a relationship between the expression of the [^{3}H]-D2S binding protein on the plasma membrane of PBMN cells and their susceptibility to infection by HIV-1.

We are grateful to Koya Ariyoshi, Simon Beddows and Paul Bieniasz for technical help and to Ann Bradshaw for performing the thrombin time assays. This work was supported by the MRC AIDS Directed Programme, UK, and ML Laboratories plc (UK).

References

BABA, M., DE CLERCQ, E., SCHOLS, D., PAUWELS, R., SNOECK, R., VAN BOECKEL, C., VAN DEDEM, G., KRAAIJEVELD, N., HOBBELEN, P., OTTENHEIJM, H. (1990). Novel sulfated polysaccharides: dissociation of anti-human immunodeficiency virus activity from antithrombin activity. *J. Infect. Dis.*, **161,** 208–213.

BABA, M., NAKAJIMA, M., SCHOLS, D., PAUWELS, R., BALZARINI, J. & DE CLERCQ, E. (1988a). Pentosan polysulfate, a sulfated oligosaccharide, is a potent and selective anti-HIV agent in vitro. *Antiviral Res.*, **9,** 335–343.

BABA, M., PAUWELS, R., BALZARINI, J., ARNOUT, J., DESMYTER, J. & DE CLERCQ, E. (1988b). Mechanism of inhibitory effect of dextran sulfate and heparin on replication of human immunodeficiency virus *in vitro*. *Proc. Natl. Acad. Sci. U.S.A.*, **85,** 6132–6136.

BAGASRA, O. & LISCHNER, H.W. (1988). Activity of dextran sulfate and other polyanionic polysaccharides against human immunodeficiency virus. *J. Infect. Dis.*, **158,** 1084–1087.

BEDDOWS, S., BIENIASZ, P., SHAUNAK, S. & WEBER, J.N. (1993). HIV replication in CD4-negative cell lines: effect of cloning, CD4 expression and inhibition by dextrin sulphate. *Antiviral Chem. Chemother.*, **4,** 173–177.

BIENIASZ, P.D., BEDDOWS, S.A. & WEBER, J.N. (1991). Quantitative assessment of CD4 independent HIV-1 infection *in vitro*. *MRC AIDS Directed Programme Workshop*. University of Warwick. Abstract Number 28.

BOCK, K. & PEDERSEN, C. (1983). C-13 nuclear magnetic-resonance spectroscopy of monosaccharides. *Adv. Carbohydr. Chem. Biochem.*, **41,** 27–66.

BRASSEUR, R., CORNET, B., BURNY, A., VANDENBRANDEN, M. & RUYSSCHAERT, J.M. (1988). Mole of insertion into a lipid membrane of the N-terminal HIV gp41 peptide segment. *AIDS Res. Hum. Retroviruses*, **4,** 83–90.

BRENAN, M. & PARISH, C.R. (1986). Modification of lymphocyte migration by sulfated polysaccharides. *Eur. J. Immunol.*, **16,** 423–430.

CHESEBRO, B. & WEHRLY, K. (1988). Development of a sensitive quantitative focal assay for human immunodeficiency virus infectivity. *J. Virol.*, **62,** 3779–3788.

COLE, G.J., LOEWY, A. & GLASER, L. (1986). Neuronal cell-cell adhesion depends on interactions of N-CAM with heparin-like molecules. *Nature*, **320,** 445–447.

COOMBE, D.R., JAKOBSEN, K.B. & PARISH, C.R. (1987). A role for sulfated polysaccharide recognition in sponge cell aggregation. *Exp. Cell Res.*, **170,** 381–401.

COOMBE, D.R. & RIDER, C.C. (1989). Lymphocyte homing receptors cloned – a role for anionic polysaccharides in lymphocyte adhesion. *Immunol. Today*, **10,** 289–291.

DAAR, E.S., LI, X.L., MOUDGIL, T. & HO, D.D. (1990). High concentrations of recombinant soluble CD4 are required to neutralize primary human immunodeficiency virus type 1 isolates. *Proc. Natl. Acad. Sci. U.S.A.*, **87,** 6574–6578.

DALGLEISH, A.G., BEVERLEY, P.C., CLAPHAM, P.R., CRAWFORD, D.H., GREAVES, M.F. & WEISS, R.A. (1984). The CD4 (T4) antigen is an essential component of the receptor for the AIDS retrovirus. *Nature*, **312,** 763–767.

DIMITROV, D.S., HILLMAN, K., MANISCHEWITZ, J., BLUMENTHAL, R. & GOLDING, H. (1992). Correlation between kinetics of soluble CD4 interactions with HIV-1-Env-expressing cells and inhibition of syncytia formation: implications for mechanisms of cell fusion and therapy for AIDS. *AIDS*, **6,** 249–256.

FOLEY, G.E., LAZARUS, H. & FARBER, S. (1965). Continuous culture of human lymphoblasts from peripheral blood of a child with acute leukaemia. *Cancer*, **18,** 522–529.

GOWDA, S.D., STEIN, B.S., MOHAGHEGHPOUR, N., BENIKE, C.J. & ENGLEMAN, E.G. (1989). Evidence that T-cell activation is required for HIV-1 entry in CD4+ lymphocytes. *J. Immunol.*, **142,** 773–780.

HART, T.K., KIRSH, R., ELLENS, H., SWEET, R.W., LAMBERT, D.M., PETTEWAY, S.R. Jr., LEARY, J. & BUGELSKI, P.J. (1991). Binding of soluble CD4 proteins to human immunodeficiency virus type 1 and infected cells induces release of envelope glycoprotein gp120. *Proc. Natl. Acad. Sci. U.S.A.*, **88,** 2189–2193.

HOLLINGER, F.B., BREMER, J.W., MYERS, L.E., GOLD, J.W. & MCQUAY, L. (1992). Standardization of sensitive human immunodeficiency virus coculture procedures and establishment of a multicenter quality assurance program for the AIDS Clinical Trials Group. The NIH/NIAID/DAIDS/ACTG Virology Laboratories. *J. Clin. Microbiol.*, **30,** 1787–1794.

ITO, M., BABA, M., SATO, A., PAUWELS, R., DE CLERCQ, E. & SHIGETA, S. (1987). Inhibitory effect of dextran sulfate and heparin on the replication of human immunodeficiency virus (HIV) in vitro. *Antiviral Res.*, **7,** 361–367.

KLASSE, P.J. & MOORE, J.P. (1992). Kinetics of the HIV-CD4 interactions and virus-cell fusion. *AIDS*, **6,** 325–327.

KLATZMANN, D., CHAMPAGNE, E., CHAMARET, S., GRUEST, J., GUETARD, D., HERCEND, T., GLUCKMAN, J.C. & MONTAGNIER, L. (1984). T-lymphocyte T4 molecule behaves as the receptor for human retrovirus LAV. *Nature*, **312,** 767–768.

LIFSON, J.D., FEINBERG, M.B., REYES, G.R., RABIN, L., BANAPOUR, B., CHAKRABARTI, S., MOSS, B., WONG-STAAL, F., STEIMER, K.S. & ENGLEMAN, E.G. (1986). Induction of CD4-dependent cell fusion by the HTLV-III/LAV envelope glycoprotein. *Nature*, **323,** 725–728.

MADDON, P.J., DALGLEISH, A.G., MCDOUGAL, J.S., CLAPHAM, P.R., WEISS, R.A. & AXEL, R. (1986). The T4 gene encodes the AIDS virus receptor and is expressed in the immune system and the brain. *Cell*, **47,** 333–348.

MCCLURE, M.O., MOORE, J.P., BLANC, D.F., SCOTTING, P., COOK, G.M., KEYNES, R.J., WEBER, J.N., DAVIES, D. & WEISS, R.A. (1992). Investigations into the mechanism by which sulfated polysaccharides inhibit HIV infection in vitro. *AIDS Res. Hum. Retroviruses*, **8,** 19–26.

MCCLURE, M.O., WHITBY, D., PATIENCE, C., GOODERHAM, N.J., BRADSHAW, A., CHEINGSONG-POPOV, R., WEBER, J.N., DAVIES, D.S., COOK, G.M.W., KEYNES, R.J. & WEISS, R.A. (1991). Dextrin sulphate and fucoidan are potent inhibitors of HIV infection in vitro. *Antiviral Chem. Chemother.*; **2,** 149–156.

MITSUYA, H., LOONEY, D.J., KUNO, S., UENO, R., WONG-STAAL, F. & BRODER, S. (1988). Dextran sulfate suppression of viruses in the HIV family: inhibition of virion binding to CD4+ cells. *Science*, **240,** 646–649.

MORIKAWA, S., TATSUMI, E., BABA, M., HARADA, T. & YASUHIRA, K. (1978). Two E-rosette-forming lymphoid cell lines. *Int. J. Cancer*, **21,** 166–170.

PARISH, C.R., LOW, L., WARREN, H.S. & CUNNINGHAM, A.L. (1990). A polyanion binding site on the CD4 molecule. Proximity to the HIV-gp120 binding region. *J. Immunol.*, **145,** 1188–1195.

POPOVIC, M., SARNGADHARAN, M.G., READ, E. & GALLO, R.C. (1984). Detection, isolation, and continuous production of cytopathic retroviruses (HTLV-III) from patients with AIDS and pre-AIDS. *Science*, **224,** 497–500.

ROOSNEK, E., TUNNACLIFFE, A. & LANZAVECCHIA, A. (1990). T-cell activation by a bispecific anti-CD3/anti-major histocompatibility complex class I antibody. *Eur. J. Immunol.*, **20,** 1393–1396.

ROSSIGNOL, D.P., EARLES, B.J., DECKER, G.L. & LENNARZ, W.J. (1984). Characterization of the sperm receptor on the surface of eggs of Stronglyocentrotus purpuratus. *Dev. Biol.*, **104,** 308–321.

SALAHUDDIN, S.Z., MARKHAM, P.D., WONG-STAAL, F., FRANCHINI, G., KALYANARAMAN, V.S. & GALLO, R.C. (1983). Restricted expression of human T-cell leukemia-lymphoma virus (HTLV) in transformed human umbilical cord blood lymphocytes. *Virology*, **129,** 51–64.

SCHACKER, T., COOMBS, R.W., COLLIER, A.C., ZEH, J.E., FOX, I., ALAM, J., NELSON, K., EGGERT, E. & COREY, L. (1994). The effects of high-dose recombinant soluble CD4 on HIV-1 viraemia. *J. Infect. Dis.*, **169,** 37–40.

SCHERER, W.F., SYVERTON, J.T. & GEY, G.O. (1953). Studies on propogation *in vitro* of poliomyelitis viruses. *J. Exp. Med.*, **97,** 695–710.

SCHOLS, D., BABA, M., PAUWELS, R., DESMYTER, J. & DE CLERCQ, E. (1989). Specific interaction of aurin tricarboxylic acid with the human immunodeficiency virus/CD4 cell receptor. *Proc. Natl. Acad. Sci. U.S.A.*, **86,** 3322–3326.

SCHRIER, R.D., MCCUTCHAN, J.A. & WILEY, C.A. (1993). Mechanisms of immune activation of human immunodeficiency virus in monocytes/macrophages. *J. Virol.*, **67,** 5713–5720.

SHAUNAK, S. (1993). Cell surface receptors for HIV-1. *PhD thesis. University of London.*

STOOLMAN, L.M. & ROSEN, S.D. (1983). Possible role for cell-surface carbohydrate-binding molecules in lymphocyte recirculation. *J. Cell Biol.*, **96,** 722–729.

SZABO, G. Jr., PINE, P.S., WEAVER, J.L., RAO, P.E. & ASZALOS, A. (1992). CD4 changes conformation upon ligand binding. *J. Immunol.*, **149,** 3596–3604.

TURVEY, J.R. (1965). Sulfates of the simple sugars. *Adv. Carbohydr. Chem. Biochem.*, **20,** 183–212.

UENO, R. & KUNO, S. (1987). Dextran sulphate, a potent anti-HIV agent *in vitro* having synergism with zidovudine. *Lancet*, **i,** 1379.

YAMAGUCHI, M. & KINOSHITA, S. (1985). Polysaccharides sulfated at the time of gastrulation in embryos of the sea urchin *Clypeaster japonicus*. *Exp. Cell Res.*, **159,** 353–365.

(Received March 2, 1994
Revised May 18, 1994
Accepted May 26, 1994)

Br. J. Pharmacol. (1994), **113**, 159–164

Action of adenosine receptor antagonists on the cardiovascular response to defence area stimulation in the rat

J.H. St Lambert, [1]M.S. Dawid-Milner, [2]L. Silva-Carvalho & [3]K.M. Spyer

Department of Physiology, Royal Free Hospital School of Medicine, Rowland Hill St, Hampstead, London NW3 2PF

1 The action of adenosine in the mediation of the cardiovascular changes associated with the defence reaction has been investigated in the rat using two A_1 receptor antagonists.

2 Cumulative doses of 1,3 dipropyl-cyclopentylxanthine (DPCPX) (0.3–3 mg kg^{-1}) and ethanol (0.03–0.25 ml) and bolus doses of DPCPX (3 mg kg^{-1}) and 8-sulphophenyltheophylline (8-SPT) (20 mg kg^{-1}) were given into α-chloralose, paralysed and artificially ventilated rats. Recordings were made of arterial blood pressure and heart rate.

3 Ethanol, the vehicle for DPCPX, failed to modify the magnitude of the defence response; however, cumulative doses of DPCPX produced a dose-dependent decrease in the HDA (hypothalamic defence area)-evoked increase in arterial blood pressure, accompanied by a similar fall in the magnitude of the evoked heart rate response.

4 The evoked rise in arterial blood pressure was reduced significantly by intravenous injection of DPCPX (3 mg kg^{-1}) but not 8-SPT (20 mg kg^{-1}), a purely peripherally acting adenosine antagonist.

5 These results suggest that adenosine acting at A_1 receptors located in the central nervous system, is involved in the HDA-evoked pressor response. Whilst the site of action of the A_1 receptors is not known, possible locations are discussed.

Keywords: Adenosine A_1 receptors; hypothalamic defence area; 1,3 dipropyl-cyclopentylxanthine (DPCPX); 8-sulphophenyltheophylline (8-SPT); blood pressure; heart rate

Introduction

Adenosine, in addition to its function in intermediary metabolism, is, one of the major neuromodulators in the mammalian brain (see Stone, 1991, for review). It is locally and rapidly metabolized (Mudumbi *et al.*, 1993) and has numerous effects within the CNS and peripheral nervous system (see Contreras, 1990, for review). There is evidence suggesting a possible role of adenosine in the control of the cardiovascular system, often through its ability to modify the neural pathways related to the chemoreceptor and baroreceptor reflex responses (Mullane & Williams, 1990). A particular effect is the attenuation of the baroreceptor reflex (Hintze *et al.*, 1985). Further, there is evidence of an involvement of adenosine release in both the respiratory (hypoxic apnoea) and cardiovascular effects (secondary bradycardia and peripheral vasodilatation) observed during systemic hypoxia (Neylon & Marshall, 1991; Richter *et al.*, 1992).

Stimulation within the hypothalamic defence area in the cat produces circulatory changes which are partially mediated by the facilitation of the chemoreceptor reflex (Silva-Carvalho *et al.*, 1993) and an inhibition of the baroreceptor reflex, involving a GABAergic mechanism in the nucleus tractus solitarius (NTS) (Jordan *et al.*, 1988). These changes in baroreceptor and chemoreceptor reflex function resemble the effects of adenosine on these reflexes (see Silva-Carvalho *et al.*, 1993). Accordingly, it seemed reasonable to suggest that adenosine release might play a role in the cardiovascular and respiratory components of the defence response. Indeed, preliminary observations have indicated the involvement of adenosine in the pressor response to electrical stimulation within the hypothalamic defence area in the cat (Dawid-Milner *et al.*, 1993) and rat (St Lambert *et al.*, 1993).

Two major subclasses of adenosine receptors have been distinguished, A_1 and A_2 (Schwabe *et al.*, 1991), which are coupled to G-proteins and regulate several effector systems including adenylate cyclase, inositol phosphate and glucose transport (Merkel *et al.*, 1993). The object of this present study was to examine the potential role of adenosine A_1 receptors in the hypothalamic defence response. To examine the effect of adenosine on the defence response, two adenosine A_1 receptor antagonists were used. These are 1,3 dipropyl-cyclopentylxanthine (DPCPX), which acts both at a central and peripheral level (Williams, 1991), and 8-sulphophenyltheophylline (8-SPT), a purely peripherally acting non-specific adenosine antagonist (Daly, 1982).

Methods

Experiments were performed on 24 male Sprague Dawley rats (300–350 g). Anaesthesia was induced with sodium pentobarbitone (40 mg kg^{-1}, i.p.) and supplemented as necessary with α-chloralose (5 mg kg^{-1}, i.v.).

Surgical procedures

Catheters were inserted into a femoral artery for the measurement of arterial blood pressure and a femoral vein for the administration of drugs. The trachea was cannulated below the larynx and the animals breathed spontaneously until positioned in a stereotaxic frame, after which they were paralysed with gallamine triethiodide (4 mg kg^{-1}, i.v. supplemented with 3 mg kg^{-1} h^{-1}) and artificially ventilated with O_2-enriched air. End tidal CO_2, recorded with a fast response CO_2 analyser (Analytical Development Company Ltd), was maintained in the range of 4–5 vol% by adjusting respiratory frequency. The ECG was recorded via a preamplifier and filter (Neurolog), from which heart rate was derived. Rectal temperature was maintained at 37–38°C by a

[1] Present address: Dpto de Fisiologia, Faculatd de Medicina, Universidad de Malaga, Malaga, Spain.
[2] Present address: Instituto de Fisiologia, Faculdade de Medicina de Lisboa, Ava Egas Maniz, 1600 Lisboa, Portugal.
[3] Author for correspondence.

servo-controlled heating pad. The depth of anaesthesia was assessed by observing the absence of changes in arterial blood pressure, heart rate and phrenic nerve activity to a paw pinch and supplementary doses of α-chloralose were given as required. In three cases blood flow to the hindlimb was assessed with an electromagnetic flow probe (Carolina Medical Electronics) placed around the femoral artery after ligation of the paw. The hypothalamus was stimulated (1 ms pulses, 50–200 μA at 100 Hz for 5 s) with a concentric electrode (SNE 100, Rhodes Medical Electrodes). The hypothalamic defence area was located on the basis of the characteristic cardio-respiratory response observed in the rat (Yardley & Hilton, 1986).

Experimental protocol

Dose-related effects of DPCPX on the evoked blood pressure and heart rate response to hypothalamic stimulation were assessed. The effects of the A_1 antagonist, DPCPX (0.3–3.0 mg kg^{-1}) on the hypothalamic defence area evoked cardiovascular response was assessed by constructing a cumulative dose-response curve to the drug. DPCPX was administered cumulatively at 0.3, 0.7 and 2 mg kg^{-1} doses in each rat. The drug was administered over a period of 5 min at intervals sufficient to allow blood pressure to a return to pre-stimulus resting values. Since DPCPX was dissolved in absolute ethanol, cumulative vehicle dose-response curves to ethanol (0.03–0.25 ml) were also constructed. The volume of absolute ethanol injected was the same as the volumes required to dissolve the various doses of DPCPX.

In the second part of the study, the effects of DPCPX and 8-SPT on the responses evoked on hypothalamic stimulation were compared. A single bolus dose of 8-SPT (20 mg kg^{-1}), ($n = 6$), or DPCPX (3 mg kg^{-1}), ($n = 6$), was administered intravenously 10 min before stimulating the hypothalamic defence area. In three of the animals in which a bolus dose of DPCPX (3 mg kg^{-1}) was administered, femoral blood flow was also measured in addition to the blood pressure and heart rate.

Histology

Stimulation sites were marked at the end of the experiment by passing 500 μA d.c. current through the electrode for 10–20 s. Frozen sections of 100 μm were cut at the level of the hypothalamus, counter stained with neutral red and examined under a light microscope for localization of stimulation sites. It should be noted that analysis was undertaken only after histological data had been obtained.

Analysis of data

In all experiments baseline values for mean arterial blood pressure and heart rate were measured immediately prior to hypothalamic defence area stimulation. As stimulation of the hypothalamic sites, corresponding to the defence area, resulted in a biphasic pressor response, changes in mean arterial blood pressure were divided into two categories, the primary and secondary phase. The primary response was assessed by measuring the peak rise in blood pressure observed during the 5 s stimulation of the hypothalamus. The secondary response was measured 5–10 s after the cessation of hypothalamic stimulation. Stimulus-evoked changes in heart rate were measured as the peak response observed during the 5 s stimulation of the defence area.

The effects of cumulative doses of DPCPX (0.3, 0.7 and 2 mg kg^{-1}) on baseline blood pressure and heart rate were compared with the response to the appropriate vehicle control (absolute ethanol, 0.03, 0.1 and 0.25 ml) at matched time intervals by two way analysis of variance and least significance difference for comparison between the means (Sokal & Rohlf, 1969). In addition, the effect of a bolus dose of DPCPX (3 mg kg^{-1}), ethanol (0.25 ml) and 8-SPT (20 mg kg^{-1}) on baseline blood pressure and heart rate were analysed statistically by Student's paired t test. The effects of cumulative doses of DPCPX (0.1, 1 and 3 mg kg^{-1}) on the response to hypothalamic stimulation were then compared with the effects of the appropriate vehicle control at matched time intervals by two way analysis of variance and least significance difference for comparison between the means (Sokal & Rohlf, 1969). The effects of a bolus dose of DPCPX (3 mg kg^{-1}), ethanol (0.25 ml) and 8-SPT (20 mg kg^{-1}) on the blood pressure and heart rate responses were analysed statistically by Student's paired t test. All data are given as the means ± s.e.mean. Differences were considered significant when $P < 0.05$.

Drugs and solutions

The following compounds were used: gallamine triethiodide (Flaxedil) and sodium pentobarbitone (Sagatal) (May and Baker Ltd, Dagenham); 8-cyclopentyl-1,3,-dipropylxanthine (DPCPX) dissolved in 100% ethanol and 8-(*p*-sulphophenyl)theophylline (8-SPT), dissolved (20 mg) in 0.2 ml of 0.4 N NaOH then diluted in distilled water (Research Biochemicals Incorporated Natick); α-chloralose and di-sodium tetraborate 10-hydrate (BDH Ltd. Poole).

Results

The i.v. administration of ethanol ($n = 6$) and DPCPX ($n = 6$), caused only small and insignificant changes in baseline mean arterial blood pressure. Following administration of ethanol alone (0.03, 0.1 and 0.25 ml) small and insignificant changes from control values of heart rate were noted. However, DPCPX (0.3–3 mg kg^{-1}) caused a significant fall in heart rate at both 1 mg kg^{-1} (− 9 ± 5 beats min^{-1}) and 3 mg kg^{-1} (− 10 ± 3 beats min^{-1}) doses ($P < 0.01$).

Hypothalamic stimulation elicited a biphasic increase in blood pressure consisting of an initial increase in mean arterial blood pressure (Figure 2a and b), which was followed by a secondary elevation in pressure (Figure 2c and d) which continued for approximately 10–30 s after the cessation of stimulation (Figure 1). When applied cumulatively, DPCPX (0.3–3 mg kg^{-1}), induced a dose dependent reduction in the hypothalamic defence area-evoked increase in mean arterial blood pressure. A significant reduction occurred in both the primary (− 12 ± 2 mmHg) and secondary phase (− 22 ± 9 mmHg) of the response (Figures 1 and 2) at the highest dose ($P < 0.01$ and $P < 0.05$ respectively). In contrast, DPCPX had no significant effect on the magnitude of the tachycardia observed during hypothalamic stimulation at any dose. When applied alone, ethanol caused small yet statistically insignificant changes in the primary and secondary component of the pressor response (Figure 2) and in the heart rate response to hypothalamic defence area stimulation.

The i.v. bolus administration of DPCPX (3 mg kg^{-1}), ethanol (0.25 ml) and 8-SPT (20 mg kg^{-1}) failed to alter the resting values of mean arterial blood pressure (Figure 3). The bolus doses of ethanol and 8-SPT also failed to cause changes in baseline heart rate, whilst DPCPX (3 mg kg^{-1}) produced a significant increase (from 408.5 ± 30.1 to 428 ± 44.6 b.p.m., $P < 0.05$). A bolus injection of 8-SPT ($n = 6$) failed to alter the magnitude of the blood pressure and heart rate changes elicited on hypothalamic stimulation, whilst a subsequent bolus injection of DPCPX (3 mg kg^{-1}) ($n = 6$), caused a decrease in the primary phase of the evoked pressor response (from 58.1 ± 10.3 to 35.1 ± 10.8 mmHg, $P < 0.02$) but left the heart rate response unaffected (Figures 3 and 4). In the three experiments in which blood flow was measured, stimulation in this area of the hypothalamus elicited a marked increase (1.3 to 2.9 ml min^{-1}) in femoral blood flow. The administration of a bolus dose of DPCPX (3 mg kg^{-1})

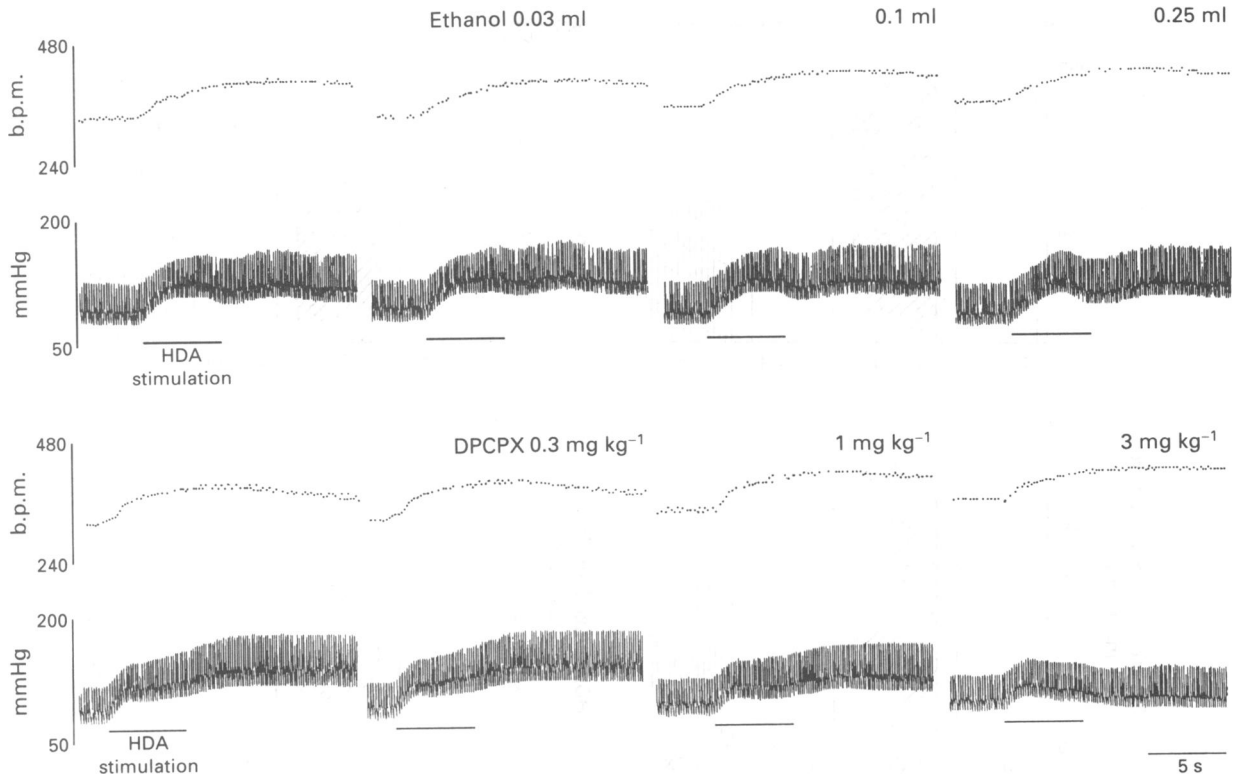

Figure 1 Typical recordings of arterial blood pressure and heart rate in an anaesthetized rat. The figure shows the effect of cumulative i.v. doses of ethanol (0.03–0.25 ml) and 1,3 dipropyl-cyclopentylxanthine (DPCPX, 0.3–3 mg kg^{-1}) on the pressor and heart rate responses evoked by 5 s hypothalamic defence area (HDA) stimulation.

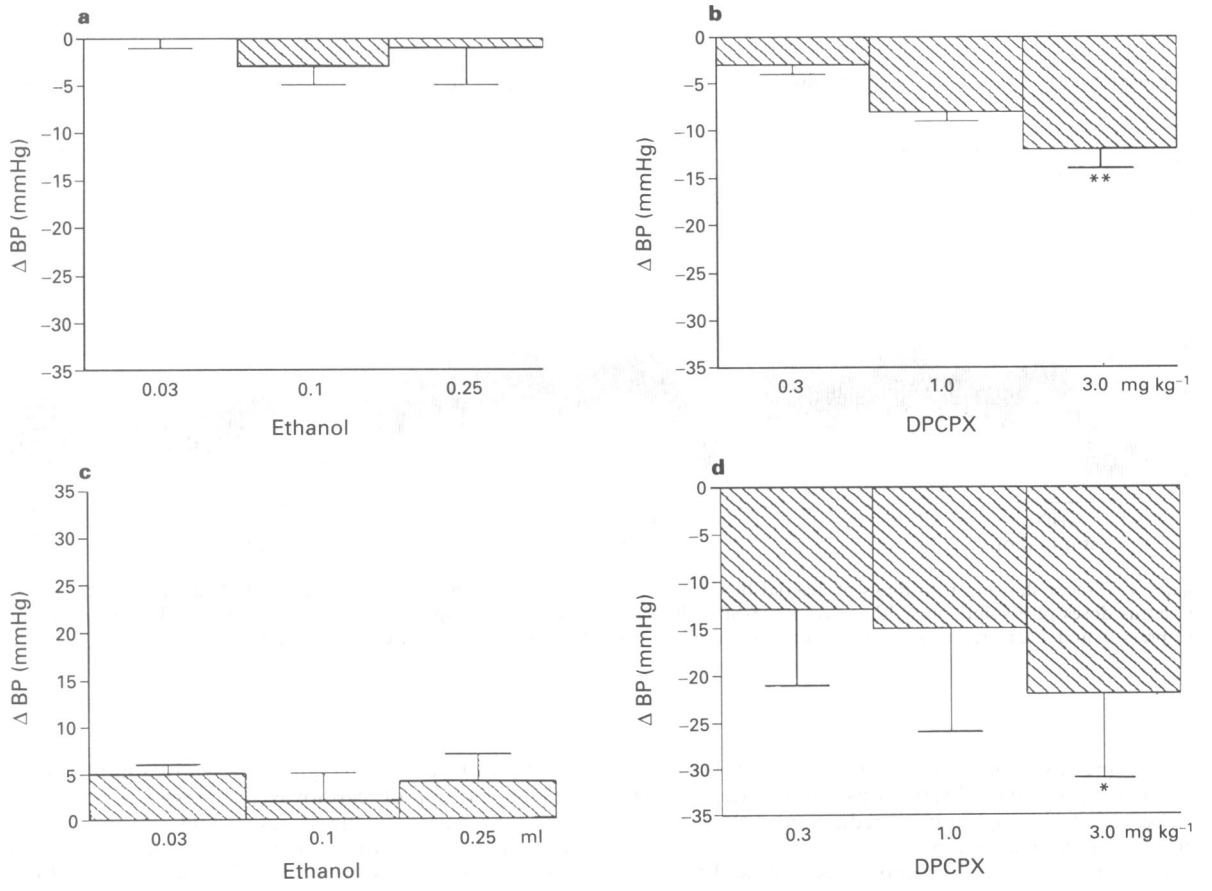

Figure 2 Anaesthetized rats: the effect of cumulative i.v. doses of 1,3-dipropyl-cyclopentylxanthine (DPCPX) (0.3–3.0 mg kg^{-1}) and absolute ethanol (0.03–0.25 ml) on the absolute changes (Δ) (mmHg) in mean arterial blood pressure (BP) with respect to both the primary (1°), (a and b), and secondary (2°), (c and d), phases of the defence response. Each column shows the mean value ($n = 6$) with s.e.mean. These changes are compared with those changes caused by the vehicle, ethanol, by two way analysis of variance and the least significant difference test to compare the means. $*P < 0.05$; $**P < 0.01$.

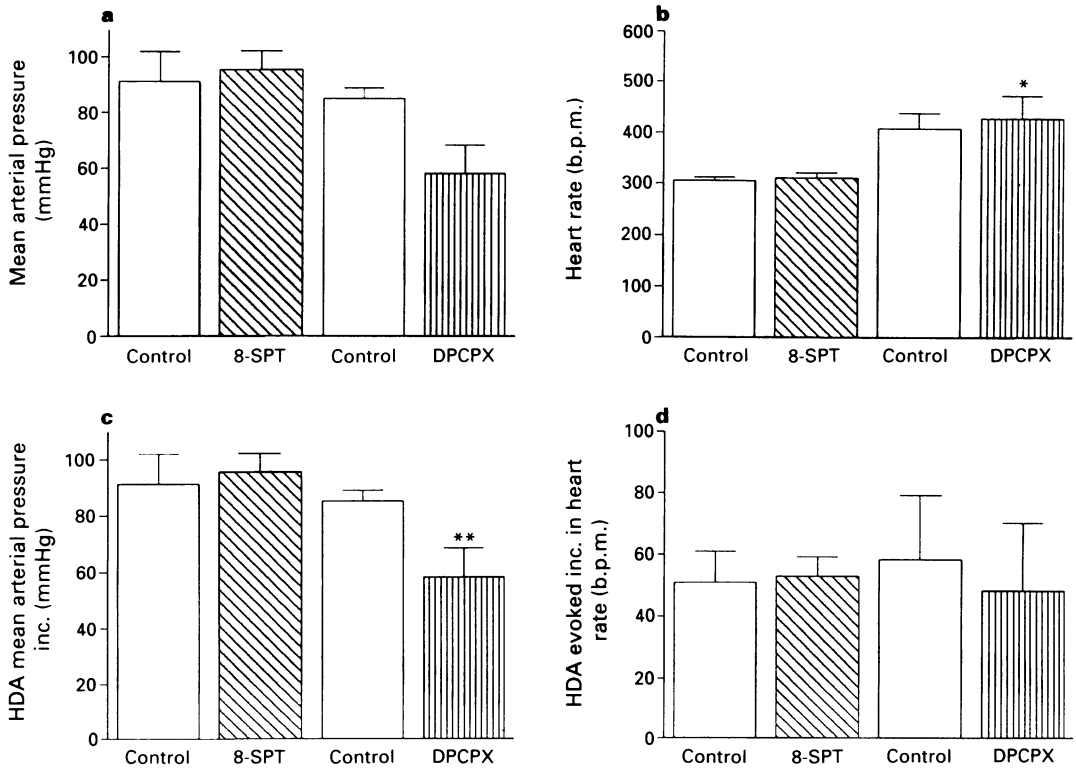

Figure 3 Anaesthetized rat: the effect of i.v. bolus doses of 8-sulphophenyltheophylline (8-SPT, 20 mg kg^{-1}) and 1,3 dipropyl-cyclopentylxanthine (DPCPX, 3 mg kg^{-1}) on baseline values of mean arterial blood pressure and heart rate and changes in mean arterial blood pressure and heart rate associated with the primary phase, evoked by hypothalamic defence area (HDA) stimulation. Each column shows the mean value ($n = 6$) with s.e.mean. $*P < 0.05$, $**P < 0.02$.

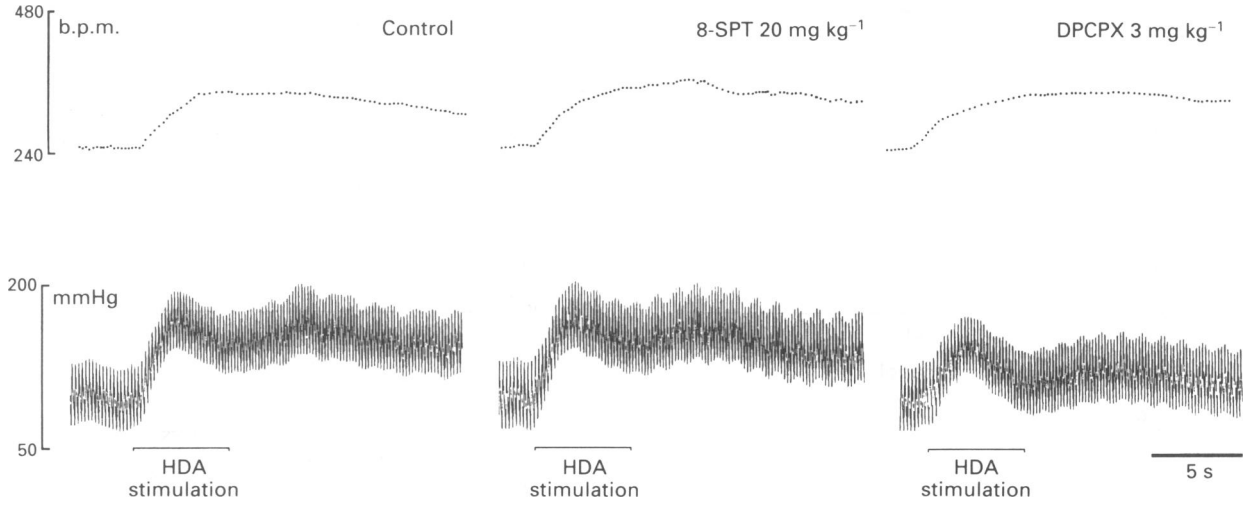

Figure 4 Traces showing recordings of arterial blood pressure and heart rate in anaesthetized rat. The figure shows the effect of i.v. bolus doses of 8-sulphophenyltheophylline (8-SPT, 20 mg kg^{-1}) and 1,3 dipropyl-cyclopentylxanthine (DPCPX, 3 mg kg^{-1}) on the pressor and heart rate responses evoked by stimulation of the hypothalamic defence area (HDA) for 5 s.

reduced this increase somewhat (1.0–2.5 ml min^{-1}). However, we have insufficient observations to provide a quantitative assessment although a clear reduction in flow is seen in Figure 5 (compare a and b).

Histological analysis of all the above cases showed that the stimulation sites were in the region of the paraventricular nucleus of the hypothalamus (PVH) and the anterior hypothalamic area (AHA), 6.4 to 6.8 mm rostral to interaural level (Pellegrino *et al.*, 1979) (Figure 5c), overlapping the hypothalamic defence area as defined by Yardley & Hilton (1986). In three cases (Figure 5c), whilst stimulation elicited a similar pattern of cardiovascular response (a rise in both blood pressure and heart rate), DPCPX was ineffective in reducing the magnitude of the evoked responses (increase in mean arterial pressure; from 49 to 48 mmHg). In all three cases the stimulation sites were ventral to the hypothalamic defence area (Figure 5c). These results were not included in the statistical evaluation of the action of adenosine antagonists on the responses induced by the stimulation of the hypothalamic defence area.

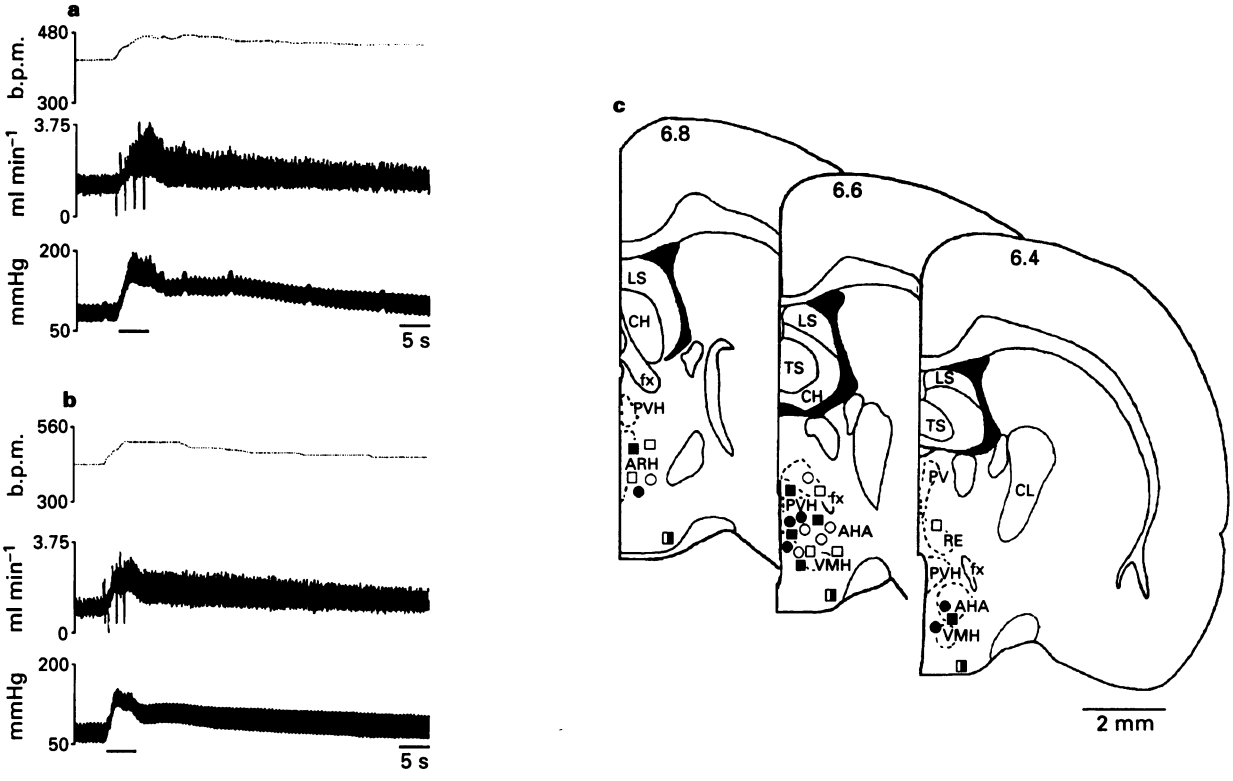

Figure 5 Traces showing a control recording (a) and the effect of an i.v. bolus dose of 1,3 dipropyl-cyclopentylxanthine (DPCPX, 3 mg kg^{-1}) (b) on heart rate, femoral blood flow and arterial blood pressure following the stimulation of the hypothalamic defence area. The distribution of histologically determined sites from which cardiovascular responses were elicited are illustrated in (c). The sections were taken from a level 6.8 mm rostral from interaural line. Stimulation sites where the evoked responses were antagonized by: (○) bolus dose of DPCPX (3 mg kg^{-1}); (□) 8-sulphonyltheophylline (20 mg kg^{-1}); (●) cumulative doses of DPCPX (0.3–3 mg kg^{-1}) and (■) cumulative doses of ethanol (0.03–0.25 ml) and stimulation sites where the evoked responses were unaffected by DPCPX (□).

Discussion

The present study has indicated that adenosine A_1 receptors, located in the central nervous system, are activated during the defence reaction that is evoked by electrical stimulation at restricted sites within the hypothalamus (Yardley & Hilton, 1986). The evoked cardiovascular response, which includes an increase in blood pressure and heart rate, was found to be reduced by the intravenous application of an DPCPX which is a highly potent and selective A_1 antagonist (Lohse *et al.*, 1987). It is known to act both peripherally and within the central nervous system (Williams, 1991). Conversely, the application of 8-SPT, an A_1/A_2 receptor antagonist, with a solely peripheral site of action (Daly, 1982), was ineffective in modifying the cardiovascular component of the hypothalamic defence response. Although 8-SPT is a broad spectrum adenosine antagonist, its K_i values indicate its higher affinity for the A_1 than A_2 receptor (K_i 2630 nM and 15,300 nM, respectively; RBI Handbook 1993). Our present observations on the dose-related effect of DPCPX required careful control as it was dissolved in ethanol, which on its own could cause changes in cardiovascular parameters. Sun & Reis (1992), and many other workers have suggested that ethanol decreases baroreceptor sensitivity. In the present study ethanol, in equivalent doses to those used as a vehicle, had no effect on resting levels of either mean arterial blood pressure or heart rate.

Stimulation of the hypothalamic defence area elicits a biphasic pressor response. It has been proposed that the two phases are mediated by different mechanisms, the primary phase being due to an increase in sympathetic tone, whilst the secondary phase is due to the release of catecholamines from the adrenal medulla (Eferakeya & Bunag, 1974). Whilst 8-SPT and ethanol failed to alter the magnitude of either component of the blood pressure response, DPCPX caused a dose-dependent decrease in both phases. Furthermore, its effect on the secondary phase was more prominent than on the primary phase. DPCPX was found ineffective in modulating the effects of stimulation at hypothalamic sites located ventral to the hypothalamic defence area. However stimulation at these sites had elicited similar changes in blood pressure and heart rate to those evoked on stimulating in the hypothalamic defence area. This implies, but does not prove, that the effects of DPCPX observed are linked specifically to the pathways descending from the hypothalamic defence area.

As yet, little is known of the neuropharmacology of the synaptic interactions that underlie the expression of the hypothalamic-induced defence response. There are indications, that the evoked cardiovascular response involves a centrally mediated attenuation of the baroreceptor reflex (see Coote *et al.*, 1972). This involves the activation of a GABAergic mechanism within the NTS that is directed to those NTS neurones that receive an excitatory baroreceptor input (Jordan *et al.*, 1988; Mifflin *et al.*, 1988b). Recent studies have also shown that the chemoreceptor reflex is facilitated during the defence reaction and this again involves an interaction between inputs at the level of the NTS (Silva-Carvalho *et al.*, 1993).

There is a growing literature indicating that adenosine, acting both peripherally and within the central nervous system, is involved in the control of respiration (Monteiro & Ribeiro, 1987; 1989; Wessberg *et al.*, 1988; Barraco & Jańusz, 1989) and cardiovascular activity (de Burgh Daly, 1986; Tseng *et al.*, 1988). The present data indicate that adenosine A_1 receptors located in the central nervous system are

involved in the hypothalamic defence area-evoked pressor response. As yet the sites of adenosine action within the central nervous system are not resolved. Preliminary studies in the cat have shown that the magnitude of the cardiovascular response to baroreceptor and chemoreceptor stimulation may be modulated by the central action of DPCPX (Silva-Carvalho *et al.*, 1993). This A_1 antagonist appears to cause a facilitation of the baroreceptor reflex and a reduction in the chemoreceptor-evoked pressor response. Therefore it is attractive to speculate that this action of DPCPX involves effects at A_1 receptors located in the NTS since this nucleus plays a major role in the processing of both respiratory and cardiovascular reflexes (Jordan & Spyer, 1986) and is also involved in the expression of centrally evoked cardiovascular and respiratory responses (Mifflin *et al.*, 1988a). Another possible site of action is the rostroventrolateral medulla since its sympatho-excitatory neurones are excited by stimulation within the hypothalamic defence area (McAllen, 1986a,b). This suggestion is strengthened by the fact that DPCPX produces a more profound effect on the pressor response observed during the defence response than on the accompanying tachycardia. The absence of an obvious effect of DPCPX and ethanol on respiratory evoked responses is also significant as it may well indicate that the site of A_1 receptors is at a point in the reflex pathways after which they have split into cardiovascular and respiratory components such as the rostroventrolateral medulla. Further experiments will be needed to resolve these issues.

This work was undertaken with financial support from the Wellcome Trust. J. St L. is an M.R.C. student.

References

BARRACO, R.A. & JANUSZ, C.A. (1989). Respiratory effects of 5-ethylcarboxamidoadenosine, an analog of adenosine, following microinjections into the nucleus tractus solitarius. *Brain Res.*, **480**, 360–364.

CONTRERAS, E. (1990). Adenosine: physiological and pharmacological actions. *Arch. Biol. Med. Exp.*, **23**, 1–12.

COOTE, J.H. & MACLEOD, V.H. (1972). The possibility that noradrenaline is a sympatho-inhibitory transmitter in the spinal cord. *J. Physiol.*, **225**, 44–46P.

DALY, J.W. (1982). Adenosine receptors: targets for future drugs. *J. Med. Chem.*, **25**, 197–207.

DAWID-MILNER, M.S., SILVA-CARVALHO, L., GOLDSMITH, G.E. & SPYER, K.M. (1994). A potential role of central adenosine A_1 receptors in the responses to hypothalamic stimulation in the anaesthetized cat. *J. Autonom. Nerv. Sys.*, (in press).

DE BURGH DALY, M. (1986). In *Handbook of Physiology*, Section 3, *The Respiratory System*. Control of breathing, Part II, ed. Cherniack, N.S. & Widdicombe, J.G. pp. 529–594. American Physiological Society. Bethesda.

EFERAKEYA, A. & BUNAG, R.D. (1974). Adrenomedullary pressor responses during posterior hypothalamic stimulation. *Am. J. Physiol.*, **227**, 114–118.

HINTZE, T.H., BELLONI, F.L., HARRISON, J.E. & SHAPIRO, G.C. (1985). Apparent reduction in baroreceptor sensitivity to adenosine in conscious dogs. *Am. J. Physiol.*, **249** (3 pt 2), H554–559.

JORDAN, D., MIFFLIN, S.W. & SPYER, K.M. (1988). Hypothalamic inhibition of neurones in the nucleus tractus solitarius of the cat is GABA mediated. *J. Physiol.*, **399**, 389–404.

JORDAN, D. & SPYER, K.M. (1986). Brainstem integration of cardiovascular and pulmonary afferent activity. *Prog. Brain Res.*, **67**, 295–314.

LOHSE, M.J., KLOTZ, K.N., LINDENBORN-FOTINOS, J., REDDINGTON, M., SCHWABE, U. & OLSSON, R.A. (1987). 8-Cyclopentyl-1,3-dipropylxanthine (DPCPX) – a selective high affinity antagonist radioligand for A_1 adenosine receptors. *Naunyn-Schmied. Arch. Pharmacol.*, **336**, 204–210.

MCALLEN, R.M. (1986a). Identification and properties of subretrofacial bulbospinal neurones, a descending cardiovascular pathway in the cat. *J. Auton. Nerv. Sys.*, **17**, 151–164.

MCALLEN, R.M. (1986b). Location of neurones with cardiovascular and respiratory function at the ventral surface of the cat's medulla. *Neurosciences*, (Oxford), **18**, 43–49.

MERKEL, L.A., RIVERA, L.M., COLUSSI, D.J., PERRONE, M.H., SMITS, G.J. & COX, B.F. (1993). In vitro and in vivo characterization of an A_1 selective adenosine agonist, RG14202. *J. Pharmacol. Exp. Ther.*, **265**, 699–706.

MIFFLIN, S.W., SPYER, K.M. & WITHINGTON-WRAY, D.J. (1988a). Baroreceptor inputs to the nucleus tractus solitarius in the cat: postsynaptic actions and the influence of respiration. *J. Physiol.*, **399**, 339–367.

MIFFLIN, S.W., SPYER, K.M & WITHINGTON-WRAY, D.J. (1988b). Baroreceptor inputs to the nucleus tractus solitarius in the cat: modulation by hypothalamus. *J. Physiol.*, **399**, 369–387.

MONTEIRO, E.C. & RIBEIRO, J.A. (1987). Ventilatory effects of adenosine mediated by carotid body chemoreceptors in the rat. *Naunyn-Schmied. Arch. Pharmacol.*, **335**, 143–148.

MONTEIRO, E.C. & RIBEIRO, J.A. (1989). Adenosine deaminase and adenosine uptake inhibitors facilitate ventilation in rats. *Naunyn Schmied. Arch. Pharmacol.*, **340**, 230–238.

MUDUMBI, R.V., MONTAMAT, S.C., BRUNS, R.F. & VESTAL, R.E. (1993). Cardiac functional responses to adenosine by PD81, 723, an allosteric enhancer of the adenosine A_1 receptor. *Am. J. Physiol.*, **264** (3 pt 2), H1017–H1022.

MULLANE, K.M. & WILLIAMS, M. (1990). Adenosine and cardiovascular function. In *Adenosine and Adenosine Receptors*. ed. Williams, M. pp. 289–333. N.J., U.S.A.: The Humana Press.

NEYLON, M. & MARSHALL, J.M. (1991). The role of adenosine in the respiratory and cardiovascular response to systemic hypoxia in the rat. *J. Physiol.*, **440**, 529–549.

PELLEGRINO, L.J., PELLEGRINO, A.S. & CUSHMAN, A.J. (1979). *A Stereotaxic Atlas of the Rat Brain*. 2nd Edition. New York and London: Plenum Press.

RICHTER, D.W., BELLINGHAM, M. & SCHMIDT, C. (1992). Maintenance of the respiratory rhythm during normoxia and hypoxia. In *Control of Breathing and its Modelling Perspectives*. ed. Honda, Y.L., Miyamoto, Y., Konno, K. & Widdicombe, J.G. New York: Plenum Press.

RESEARCH BIOCHEMICALS INCORPORATED. (1993). *Catolog/Handbook*.

SCHWABE, U., LORENZEN, A. & GRUN, S. (1991). Adenosine receptors in the central nervous system. *J. Neural Transm. Suppl.*, **34**, 149–155.

SILVA-CARVALHO, L., DAWID-MILNER, M.S., GOLDSMITH, G.E. & SPYER, K.M. (1993). Hypothalamic evoked effects in cats nucleus tractus solitarius facilitating chemoreceptor reflex. *Exp. Physiol.*, **78**, 425–428.

SOKAL, R.R. & ROHLF, F.J. (1969). *Biometry: The Principles and Practice of Statistics in Biological Research*. New York: W.H. Freeman & Company.

ST LAMBERT, J.H., DAWID-MILNER, M.S., SILVA-CARVALHO, L., GOLDSMITH, G.E. & SPYER, K.M. (1993). Action of an A_1 adenosine receptor antagonist on the cardiovascular response to defence area stimulation in cat and rat. *J. Physiol.*, **473**, 69P.

STONE, T.W. (1991). *Adenosine in the Nervous System*. London: Academic Press.

SUN, M.K. & REIS, D.J. (1992). Effects of systemic ethanol on medullary vasomotor neurons and baroreflexes. *Neurosci. Lett.*, **137**, 232–236.

TSENG, C.J., BIAGGIONI, I., APPALSAMY, M. & ROBERTSON, D. (1988). Purinergic receptors in the brainstem mediate hypertension and bradycardia. *Hypertension*, **11**, 191–197.

WESSBERG, P., HEDNER, J., HEDNER, T., PERSSON, B. & JONASON, J. (1988). Adenosine mechanisms in the regulation of breathing in the rat. *Eur. J. Pharmacol.*, **106**, 59–67.

WILLIAMS, M. (1991). Adenosine receptor agonists and antagonists. In *Adenosine in the Nervous System*. ed. Stone, T.W. pp. 137–171. London: Academic Press.

YARDLEY, C.P. & HILTON, S.M. (1986). The hypothalamic and brainstem areas from which the cardiovascular and behavioural components of the defence response are elicited in the rat. *J. Autonom. Nerv. Sys.*, **15**, 227–244.

(Received December 23, 1993
Revised April 28, 1994
Accepted May 26, 1994)

Br. J. Pharmacol. (1994), **113**, 165–170

A novel antagonist, phenylbenzene ω-phosphono-α-amino acid, for strychnine-sensitive glycine receptors in the rat spinal cord

T. Saitoh, M. Ishida, *M. Maruyama & [1]H. Shinozaki

Department of Pharmacology, The Tokyo Metropolitan Institute of Medical Science, 3-18-22, Honkomagome, Bunkyo-ku, Tokyo 113 and *Mitsubishi Kasei Institute of Life Science, 11 Minamiooya, Machida, Tokyo 194, Japan

1 3-[2′-Phosphonomethyl[1,1′-biphenyl]-3-yl]alanine (PMBA) is a novel glycine antagonist at strychnine-sensitive receptors. The chemical structure of PMBA, possessing both a glycine moiety and a phosphono group, is quite different from that of strychnine.

2 In the spinal motoneurone of newborn rats, glycine (100 μM–1 mM) induced depolarizing responses in a concentration-dependent manner. PMBA effectively inhibited depolarizing responses to glycine and other agonists, such as taurine and β-alanine. The dose-response curves for glycine were shifted to the right in an almost parallel manner (pA_2 value: 5.30 ± 0.23, $n = 5$) by PMBA which was about 60 times less potent than strychnine (pA_2 value: 7.08 ± 0.21, $n = 5$) as a glycine antagonist.

3 PMBA (1–100 μM) did not interact with modulatory glycine sites on N-methyl-D-aspartate (NMDA) receptors, which suggests a high selectivity of PMBA for strychnine-sensitive glycine receptors. At considerably high concentrations (0.1 mM–1 mM), PMBA depressed responses to GABA (pA_2 value: 3.57 ± 0.24, $n = 3$).

4 PMBA inhibited the binding of [^{3}H]-strychnine to synaptosomes from adult rat spinal cords; the IC_{50} values of PMBA, glycine and strychnine were 8 ± 2, 9 ± 3 and 0.08 ± 0.04 μM, respectively ($n = 5$) for [^{3}H]-strychnine (4.8 nM).

5 PMBA is a central excitant drug with relatively high potency and selectivity and should be useful as a pharmacological probe for analysing the mechanisms underlying physiological functions of glycine receptors.

Keywords: Glycine; glycine antagonist; strychnine; newborn rat spinal cord

Introduction

Glycine has been proposed as an inhibitory neurotransmitter in the mammalian central nervous system (CNS), most notably the spinal cord (Werman *et al.*, 1967; Ottersen & Storm-Mathisen, 1990), and strychnine effectively blocks both the inhibitory action of glycine on the anterior horn cells of the spinal cord and that of the endogenous transmitter released from Renshaw cells (Curtis *et al.*, 1968a,b; 1971). Furthermore, at concentrations lower than 0.1 μM, glycine potentiates depolarizing responses to N-methyl-D-aspartate (NMDA) in mammalian cultured central neurones in a strychnine-insensitive manner (Johnson & Ascher, 1987), and some potent antagonists for the glycine modulatory site on NMDA receptors have recently been discovered (Kemp *et al.*, 1988; Foster & Kemp, 1989), which are useful probes for elucidating the function of NMDA receptors. Thus, glycine functions as an inhibitory transmitter and as a modulator of excitatory amino acid transmission mediated by NMDA receptors (Ottersen & Storm-Mathisen, 1990). In the case of strychnine-sensitive glycine receptors, a few antagonists including strychnine have been discovered which block selectively the actions of glycine on neurones of the mammalian CNS (Curtis *et al.*, 1971; Krogsgaard-Larsen *et al.*, 1982; Curtis & Malik, 1985; Simmonds & Turner, 1985; Brehm *et al.*, 1986; Braestrup *et al.*, 1986).

In the course of studies on structure-activity relationships with a view to designing new potent glutamate antagonists, we incidentally found that 3-[2′-phosphonomethyl[1,1′-biphenyl]-3-yl]alanine (PMBA) (Patent No. JP 4-275265) (Figure 1) effectively inhibited strychnine-sensitive responses to glycine without affecting depolarizing responses to excitatory amino acids. This compound, a derivative of phenylbenzene amino acids containing both a glycine moiety and an ω-phosphono group, would be expected to be a source of new strychnine-sensitive glycine receptor antagonists whose chemical structure is considerably different from that of strychnine. In the present paper, we examined the pharmacological profile of PMBA in the rat spinal cord. One of the purposes of this paper is to encourage the utilization of this new and valuable compound.

Methods

Electrophysiological studies in isolated spinal cords

The methods used for electrophysiological experiments on the isolated spinal cord of newborn rats (1–7 day-old Wistar rats, $n = 141$) were similar to those described previously by Shinozaki *et al.* (1989). Under ether anaesthesia, the lumbar-sacral spinal cord was isolated, hemisected sagitally and placed in a 0.15 ml bath perfused at a fixed flow rate of 5–6 ml min^{-1} with artificial cerebrospinal fluid (ACSF) (in mM: NaCl 138.6, KCl 3.4, $CaCl_2$ 1.3, $MgCl_2$ 1.2, $NaHCO_3$ 20.9, NaH_2PO_4 0.58 and glucose 10.0; pH 7.4), which was

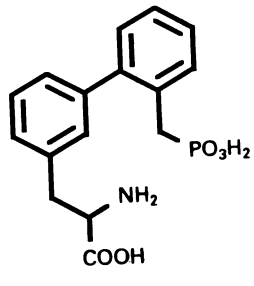

Figure 1 Chemical structure of 3-[2′-phosphonomethyl[1,1′-biphenyl]-3-yl]alanine (PMBA)

[1] Author for correspondence.

oxygenated with a gas mixture of 95% O_2 and 5% CO_2. Tetrodotoxin (TTX, 0.5 μM) was added to the bathing fluid in order to block spontaneous depolarization and indirect drug effects. For examining the depolarizing responses to NMDA, Mg^{2+}-free perfusing fluid was used. The potential changes generated in the spinal motoneurones were recorded extracellularly from the L_4 or L_5 ventral roots with a suction electrode through d.c. amplifiers connected to a pen-writer. Glycine, other transmitter agonists and test compounds were applied to the preparation either by continuous perfusion or by brief pulse injection into the perfusion system for a constant duration. The temperature of the perfusing fluid was kept at 27 ± 0.2°C.

Binding studies

Spinal cord synaptosomes from male Wistar rats (150–200 g) were used for the binding experiments. Synaptosomes were purified according to the method of Hajos (1975) and frozen (ca. 30 mg protein ml^{-1}) at − 70°C until use. Protein concentrations were determined by the method of Peterson (1977).

The detailed procedures of the binding experiments have been described previously (Maruyama & Takeda, 1989). Briefly, the binding capacities were measured by the centrifugation method in which the incubation for the binding assay was carried out in centrifugation tubes. For routine procedures, an aliquot (100 μl) containing Triton X-100 (0.01%)-treated synaptosomes (5–25 μg protein) was incubated in quadruplicate with approximately 5 nM of [^{3}H]-strychnine for 10 min at 25°C (Young & Snyder, 1973). Non-specific binding was measured in the presence of 0.1 mM strychnine. Receptor-ligand complexes were isolated by centrifugation at approximately 210,000 *g* (70,000 r.p.m.) for 5 min at 4°C, after which supernatants were rapidly aspirated and the pellets rapidly washed with 3 × 250 μl aliquots of ice cold HEPES-KOH buffer (pH 7.5). The resultant pellets were solubilized in 50 μl of 1 M NaOH, neutralized with 1 M HCl and the radiaoctivity was counted in a Beckman liquid scintillation spectrophotometer (efficiency 51%).

Drugs

3-[2′-Phosphonomethyl[1,1′-biphenyl[-3-yl]alanine (PMBA) and its derivatives were generous gifts from Nippon Chemiphar. The following compounds were commercially obtained from the following sources: β-alanine, L-α-alanine, D-α-alanine, L-serine and taurine from Nacalai tesque; (1S,3R)-1-aminocyclopentane-1,3-dicarboxylic acid (ACPD), α-3-hydroxy-5-methyl-4-isoxazolepropionic acid (AMPA), 7-chlorokynurenic acid and L-quisqualic acid from Tocris; γ-aminobutyric acid (GABA), L-glutamic acid, glycine, L-α-kainic acid, noradrenaline from Wako Pure Chemicals; baclofen, histamine, 3-hydroxytyramine (dopamine), N-methyl-D-aspartic acid (NMDA), muscimol, 5-hydroxytryptamine (5-HT), strychnine hydrochloride, substance P, tetrodotoxin (TTX) from Sigma; acetylcholine (ACh, Ovisot) from Daiichiseiyaku; [benzene ring-^{3}H]strychnine (24.5 Ci $mmol^{-1}$), [butyl-2,3-^{3}H]-SR95531 (2-(3′-carboxy-2′-propyl)-3-amino-6-*p*-methoxyphenylpyridazinium) (51.6 Ci $mmol^{-1}$) and [^{3}H]-MK-801 ((+)-5-methyl-10,11-dihydro-5H-dibenzo[a,d]cyclohepten-5,10-imine maleate) (24.0 Ci $mmol^{-1}$) from NEW England Nuclear.

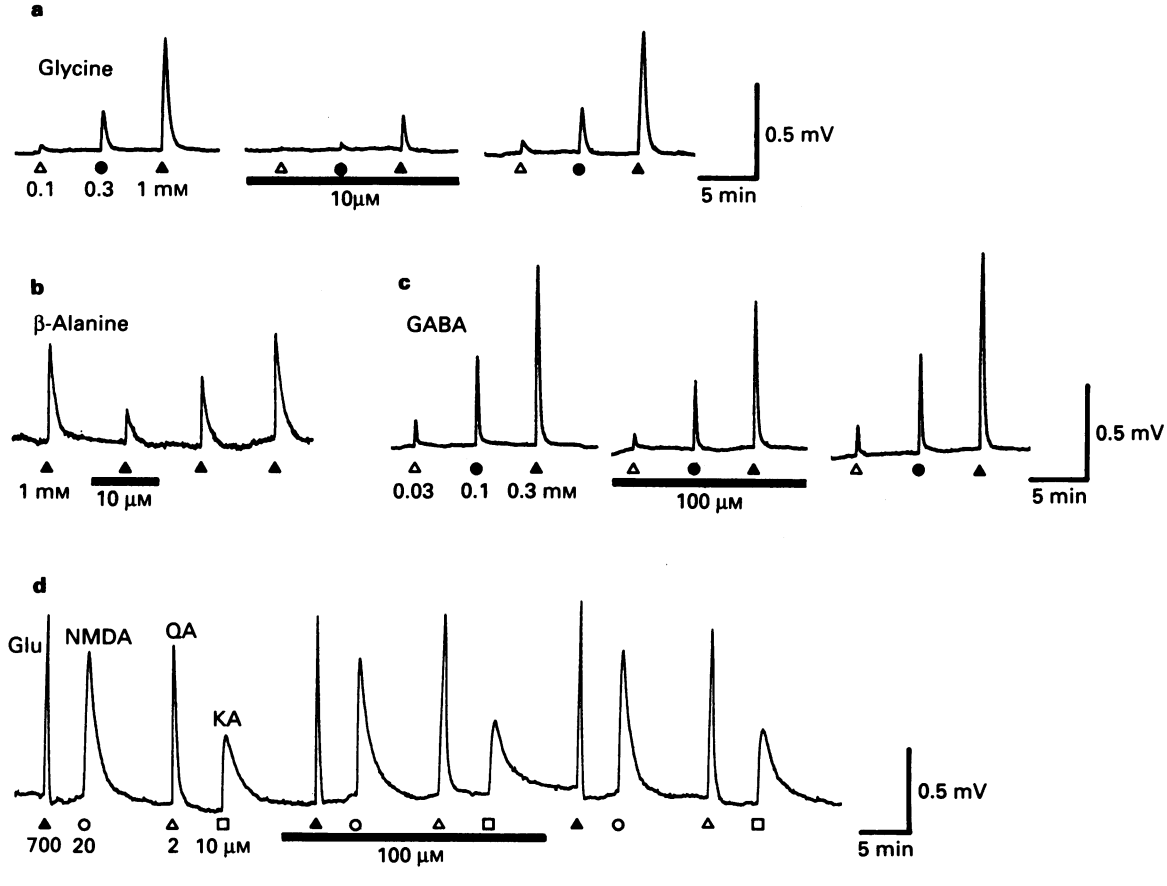

Figure 2 Sample records of depolarizing responses to glycine and other transmitter agonists in the absence and presence of 3-[2′-phosphomethyl[1,1′-biphenyl]-3-yl]alanine (PMBA). Agonists were added to the tetrodotoxin containing (0.5 μM) perfusing fluid for 10 s. In (d),Mg^{2+}-free solution was perfused. PMBA was applied for the period shown by horizontal bars. Numerals under each trace represent concentrations of agonists. GABA: γ-aminobutyric acid, Glu: L-glutamic acid, NMDA: N-methyl-D-aspartic acid, QA: quisqualic acid, KA: kainic acid.

Results

Effect of PMBA on various transmitter/receptor systems

In the isolated spinal cord of newborn rats, almost all neurotransmitters cause potential changes of motoneurones with differing effectiveness in TTX-containing ACSF. Thus, this preparation is useful for investigating effects on responses to various neurotransmitters in terms of potential changes (Konishi & Otsuka, 1974; Yanagisawa *et al.*, 1982; Shinozaki *et al.*, 1989).

Addition of L-glutamate (0.1–1 mM), GABA (0.03–1 mM), glycine (100 μM–1 mM), dopamine (30–300 μM), ACh (10–300 μM), noradrenaline (3–30 μM), 5-HT (1–30 μM), substance P (0.3–3 μM) and histamine (0.03–1 mM) to the TTX-containing (0.5 μM) perfusing fluid (ACSF) for a period of 10 s caused depolarization of spinal motoneurones of newborn rats in a concentration-dependent manner. PMBA (1–100 μM) did not affect the peak amplitude of depolarization induced by these agonists, except for the depolarization induced by glycine and GABA (n at least 3 at each concentration) (Figure 2) (see below).

No effect on NMDA-induced depolarization

As mentioned above, depolarization induced by L-glutamate was not affected by PMBA; however, it is known that some ω-phosphono-α-amino acids reduce depolarizing responses to NMDA in a competitive manner. Therefore, PMBA, an ω-phosphono-α-amino acid, would be expected to reduce depolarizing responses to NMDA. However PMBA (100 μM) did not affect the depolarization induced by NMDA (10–50 μM) in the spinal motoneurones of newborn rats. In addition, depolarizing responses to kainic acid (3–10 μM), AMPA (2–5 μM), quisqualic acid (1–5 μM) and a metabotropic glutamate receptor agonist, (1S,3R)-ACPD (10–100 μM), were also not affected by PMBA (100 μM).

7-Chlorokynurenate (10 μM), a blocker of glycine binding sites on NMDA receptors (Kemp *et al.*, 1988), depressed the depolarizing responses to NMDA (20 μM) to about 30% of the control ($n = 4$) in TTX-containing and Mg^{2+}-free ACSF, while PMBA (10–100 μM) neither affected the NMDA-induced depolarization nor reduced the inhibitory action of 7-chlorokynurenate on responses to NMDA. This result suggests that PMBA does not act on the glycine binding site on NMDA receptors.

Dose-dependent glycine antagonism by PMBA

In general, glycine induces hyperpolarization in mammalian spinal motoneurones (Curtis *et al.*, 1968b). In newborn rats, however, glycine causes depolarizing responses (Yanagisawa *et al.*, 1982), which is probably due to the difference of the equilibrium potential of chloride ions (Takahashi, 1984), and responses to GABA also very closely resemble those to glycine. Glycine (100 μM–1 mM) and other agonists such as L-α-alanine, L-serine, β-alanine, taurine and D-α-alanine (Curtis *et al.*, 1968b, Aprison, 1990) caused dose-dependent depolarization of motoneurones in newborn rats, although the depolarizing activities of these glycine agonists were considerably less than that of glycine itself on a molar basis. The rank order of their depolarizing activities in the motoneurones was as follows: glycine (1) > β-alanine (0.85) > taurine (0.2) = L-α-alanine (0.2) > L-serine (0.15) = D-α-alanine (0.15) (the values in parentheses represent the approximate potency relative to 1 mM glycine, at least $n = 4$). The depolarization induced by glycine (100 μM–1 mM) still did not attain a maximum level even when 1 mM glycine was applied, and it was quite difficult to obtain the maximal level of the depolarizing responses, which hindered the analysis of agonist-receptor characteristics. Furthermore, at concentrations higher than 1 mM glycine, it was difficult to obtain reproducible responses.

When PMBA (1–100 μM) or strychnine (0.1–1 μM) was added to the TTX-containing perfusing fluid (ACSF) for a fixed period of 3–10 min, these agents reversibly and effectively depressed depolarizing responses to glycine and other agonists in a concentration-dependent manner (Figure 3). Dose-response curves to glycine were shifted to the right in an almost parallel manner. The minimum effective (threshold) concentrations of PMBA and strychnine were less than 0.5 μM and 0.01 μM, respectively. The time course of recovery from PMBA actions was about 3 times faster than

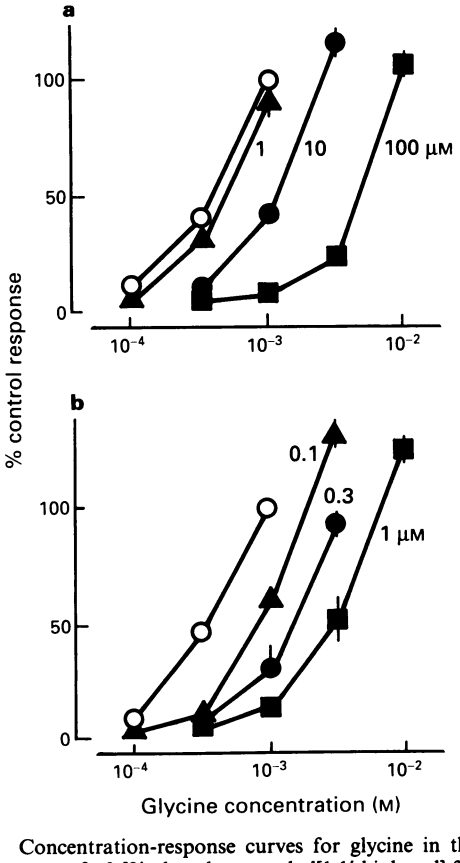

Figure 3 Concentration-response curves for glycine in the absence and presence of 3-[2′-phosphonomethyl[1,1′-biphenyl]-3-yl]alanine (PMBA) and strychnine. Glycine was added to the tetrodotoxin containing (0.5 μM) fluid for 10 s. Peak amplitudes of depolarizing responses to glycine were plotted against concentration (results were normalized to that of glycine 1 mM). Values are means ± s.e.mean ($n = 5$). Numerals represent concentrations of PMBA (a) and strychnine (b). (○) control.

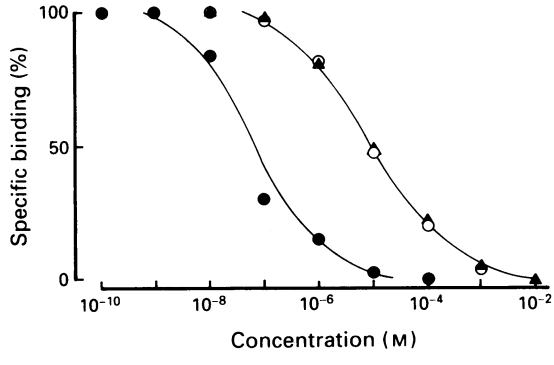

Figure 4 Inhibition curves for specific binding of [^{3}H]-strychnine (4.8 nM) to Triton-treated synaptosomes from rat spinal cords by unlabelled strychnine (●), glycine (▲) and 3-[2′-phosphonomethyl[1,1′-biphenyl]-3-yl]alanine (PMBA, ○).

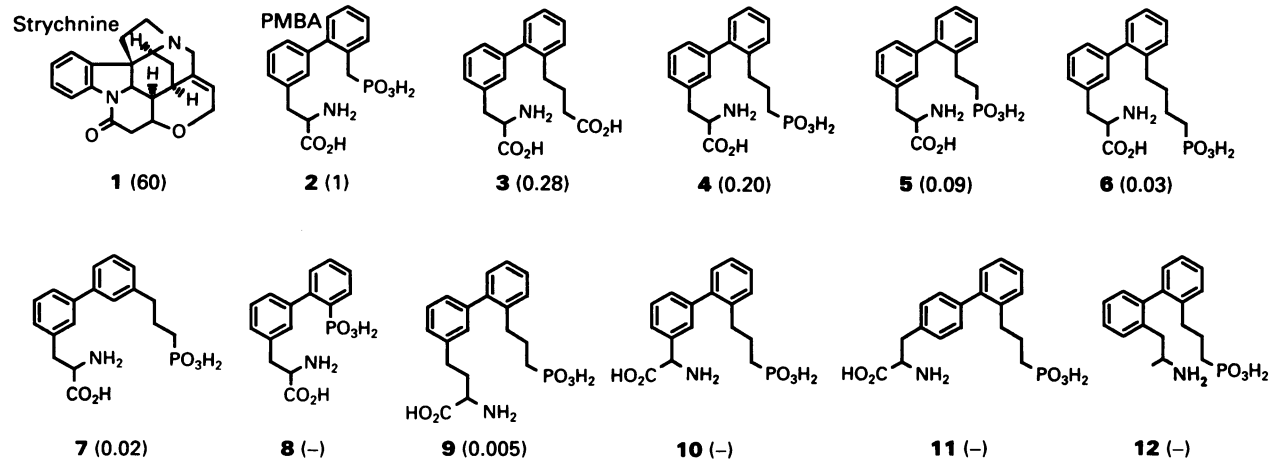

Figure 5 Chemical structures of some phenylbenzene derivatives tested and their relative potencies (PMBA = 1) in depressing glycine-induced depolarization ($n = 4$). Numerals under each chemical structure represent the compound number, and the values in parentheses show the relative potency. A minus sign, represents no response at a concentration of 0.1 mM.

that of strychnine, when they were compared at equipotent doses. Schild plots of PMBA actions demonstrated almost straight lines with a slope of 0.79 ($n = 5$, $\gamma = 0.98$), and strychnine gave a slope of 0.85 ($n = 5$, $\gamma = 0.98$). The pA_2 values were tentatively obtained, demonstrating that PMBA (5.30 ± 0.23) was approximately 60 times less potent than strychnine (7.08 ± 0.21) as a glycine antagonist in the newborn rat spinal cord.

Inhibitory effect of PMBA on GABA responses

Depolarizing responses to GABA (0.03–1 mM) and the potent $GABA_A$ agonist, muscimol (1–10 μM), were dose-dependently reduced by PMBA only when high concentrations (100 μM– 1 mM) of PMBA were applied. The dose-response curves for GABA were also shifted by PMBA (100 μM and 1 mM) to the right in an almost parallel manner. The threshold concentration seemed to be less than 30 μM. Schild plots demonstrated almost straight lines with a slope of 0.88 ($n = 3$, $\gamma = 0.96$) and a tentative pA_2 value of 3.57 ± 0.24, showing that PMBA was about 55 times less effective in reducing responses to GABA than those to glycine. Strychnine (10 μM) also reduced the depolarizing responses to GABA (0.03–1 mM), but was less active than PMBA (1 mM). Baclofen, a potent $GABA_B$ receptor agonist, did not cause any detectable potential change in spinal motoneurones up to concentrations of 1 mM, while it effectively depressed the spinal reflexes at concentrations lower than 1 μM in the newborn rat, probably due to inhibition of transmitter release from presynaptic terminals (Ishida *et al.*, 1993). There was no interaction between PMBA and baclofen. Thus, PMBA has some actions on $GABA_A$ receptors, but its effective dose is much higher than that usually used for experimental purposes *in vitro*.

Binding experiments

Saturation binding experiments in the spinal cord synaptosomes revealed a single binding site with an apparent dissociation constant (K_d) of 3.2 ± 0.8 nM (mean ± s.d., $n = 3$) and an apparent number of maximum binding (B_{max}) of 1.4 ± 0.3 pmol mg^{-1} of protein ($n = 3$) for [^{3}H]-strychnine. PMBA effectively inhibited the binding of [^{3}H]-strychnine, giving a slope of inhibition curves quite similar to that of strychnine. The IC_{50} values for PMBA, glycine and strychnine for inhibiting the binding of [^{3}H]-strychnine (4.8 nM) were 8 ± 2 μM, 9 ± 3 μM and 0.08 ± 0.04 μM, respectively ($n = 5$). Thus, PMBA was as effective as glycine in displacing [^{3}H]-strychnine bindings, but was 100 fold less active than strychnine (Figure 4).

The binding of [^{3}H]-SR95531, a selective $GABA_A$ receptor ligand, to rat spinal cord synaptosomes was markedly inhibited by GABA or muscimol, but PMBA was more than 1000 times less active in producing inhibition. The IC_{50} values of PMBA, GABA and muscimol for inhibition of the binding of [^{3}H]-SR95531 (3.7 nM) were about 0.4 mM, 0.3 μM and 0.3 μM, respectively ($n = 3$). The slope of inhibition curves for specific binding of [^{3}H]-SR95531 in the presence of PMBA was apparently different from that of GABA or muscimol (data not shown).

The binding of [^{3}H]-MK-801 (9.8 nM) to spinal cord synaptosomes was stimulated by L-glutamate (100 μM) up to 198 ± 28% ($n = 3$) of the basal binding. Combined treatment with L-glutamate (100 μM) and glycine (10 μM) further enhanced the binding of [^{3}H]-MK-801 up to 309 ± 25% ($n = 3$), probably due to an increase in the probability of opening of ion-channels. PMBA (100 μM) did not affect this enhancement of binding (294 ± 27%, $n = 3$).

Structure-activity relationships

In order to find more active compounds, inhibitory actions of some phenylbenzene derivatives with both a glycine moiety and a phosphonyl group on glycine-induced depolarization were tested in the newborn rat spinal cord. Figure 5 represents their chemical structures and relative potencies (PMBA = 1.0) ($n = 4$) in causing inhibition of glycine responses (maximum concentration used: 0.1 mM). Among these biphenyl compounds, only the compound **11** demonstrated slight inhibitory actions on depolarizing responses to NMDA, while its inhibitory action on glycine responses was markedly less potent than the others. In the presence of the compound **11** (100 μM), the amplitude of depolarizing responses to NMDA (20 μM) decreased to about half of the control values. Among all the ω-phosphonobiphenyl derivatives tested, PMBA showed the most potent inhibitory actions on glycine responses.

Discussion

PMBA, whose chemical structure is quite different from that of strychnine, is suggested to be a new type of strychnine-sensitive glycine receptor antagonist. PMBA is reasonably selective for strychnine-sensitive glycine receptors, although it has some actions on $GABA_A$ receptors at high concentrations, but is inactive on all the other neurotransmitter/

receptor systems we studied. PMBA and strychnine seemed to bind to the same binding site, judging from the similar slope of their inhibition curves for binding (Figure 4). PMBA was about 60 times less potent than strychnine in the spinal cord of newborn rats, and similar inhibitory ratios of PMBA to strychnine have been obtained in other *in vitro* electrophysiological experiments. *Xenopus* oocytes injected with cRNA encoding rat glyR responded to glycine (Akagi *et al.*, 1991), and the inward current induced by glycine was effectively blocked by PMBA (IC_{50}: 0.5 μM) and strychnine (IC_{50}: 0.01 μM) (personal communication from Dr H. Akagi). PMBA was 100 fold less active than strychnine in displacing [^{3}H]-strychnine binding in synaptosomes from the adult rat spinal cord. However, when PMBA was systemically administered to rats or mice in order to induce characteristic tonic convulsions, the animals required higher doses than those calculated from the IC_{50} values for PMBA and strychnine in electrophysiological experiments *in vitro*. The time course of recovery from actions of PMBA was much faster than that of strychnine, which probably reflected the relative water solubility or lipid/water partition coefficients. It is quite reasonable to consider that PMBA penetrates the blood brain barrier with greater difficulty than strychnine, because PMBA is an ω-phosphono-α-amino acid which is very water soluble.

In the present study, the pA_2 values were determined, although detailed quantitative analysis of agonist-receptor kinetics seemed unreasonable in the present preparation, because the voltage change recorded extracellularly from ventral roots did not always reflect the conductance change of motoneurones, which is a more suitable parameter for analysis. The slopes of the Schild plots obtained were less than unity in the presence of PMBA and strychnine, being 0.79 and 0.85, respectively. Therefore, it is possible that the interaction is non-competitive; for example, blockade of chloride channels and unknown modulatory sites. Also it is possible that the glycine moiety plays a key role in the competitive inhibition. In any case, it seems plausible that PMBA and strychnine bind to the same receptor sites.

A new class of antagonists for strychnine-sensitive glycine receptor antagonists would provide a new opportunity for researchers to examine the mechanism underlying spinal regulation of motor functions and inhibitory transmitter systems. PMBA possess both a glycine moiety and an ω-phosphono group and therefore it seems reasonable to assume that these functional groups of PMBA have some role in blocking glycine receptors because the inhibitory activities of PMBA analogues depended to a considerable extent on both the position of substitution and the length between the α-amino acid and phosphonic acid part. PMBA is an ω-phosphono-α-amino acid which sometimes acts as a competitive NMDA antagonist in the mammalian CNS. However, PMBA had no inhibitory action on NMDA receptors or on the glycine binding sites on the receptors. It is of great interest that, among PMBA derivatives tested, only compound **11** demonstrated any inhibitory effect on NMDA-induced depolarization with no activity on strychnine-sensitive glycine inhibitory receptors, because conformational analysis of these compounds would provide a hint for resolving the difference in binding activities between strychnine-sensitive glycine receptors and glycine sites on NMDA receptors. We do not know whether it acts on the same site or a different site from other strychnine-sensitive glycine receptor antagonists. With further structure-activity studies, improved strychnine-sensitive glycine receptor antagonists may be developed, and once the site of action has been established, further insight into the interaction of ligand-receptor binding at the glycine receptor may be achieved.

The authors wish to thank all our colleagues and researchers in Nippon Chemiphar for their creative input and whose collaborative efforts are so crucial to our progress. This work was supported in part by Grant-in-Aids for Scientific Research from the Ministry of Education, Science and Culture of Japan to M.I. and H.S.

References

AKAGI, H., HIRAI, K. & HISHINUMA, F. (1991). Cloning of a glycine receptor subtype expressed in rat brain and spinal cord during a specific period of neuronal development. *FEBS Lett.*, **281**, 160–166.

APRISON, M.H. (1990). The discovery of the neurotransmitter role of glycine. In *Glycine Neurotransmission*. ed. Ottersen, O.P. & Storm-Mathisen, J. pp. 1–23. Chichester: John Wiley & Sons.

BRAESTRUP, C., NIELSEN, M. & KROGSGAARD-LARSEN, P. (1986). Glycine antagonists structurally related to 4,5,6,7-tetrahydroisoxazolo-[5,4-c]pyridin-3-ol inhibit binding of [^{3}H]strychnine to rat brain membranes. *J. Neurochem.*, **47**, 691–696.

BREHM, L., KROGSGAARD-LARSEN, P., SCHAUMBURG, K., JOHANSEN, J.S., FALCH, E. & CURTIS, D.R. (1986). Glycine antagonists. Synthesis, structure, and biological effects of some bicyclic 5-isoxazolol zwitterions. *J. Med. Chem.*, **29**, 224–229.

CURTIS, D.R., DUGGAN, A.W. & JOHNSTON, G.A.R. (1971). The specificity of strychnine as a glycine antagonist in the mammalian spinal cord. *Exp. Brain Res.*, **12**, 547–565.

CURTIS, D.R., HÖSLI, L. & JOHNSTON, G.A.R. (1968a). A pharmacological study of the depression of spinal neurones by glycine and related amino acids. *Exp. Brain Res.*, **6**, 1–18.

CURTIS, D.R., HÖSLI, L., JOHNSTON, G.A.R. & JOHNSTON, I.H. (1968b). The hyperpolarization of spinal motoneurones by glycine and related amino acids. *Exp. Brain Res.*, **5**, 238–262.

CURTIS, D.R. & MALIK, R. (1985). Glycine antagonism by RU 5135. *Eur. J. Pharmacol.*, **110**, 383–384.

FOSTER, A.C. & KEMP, J.A. (1989). HA-966 antagonizes NMDA receptors through a selective interaction with the glycine modulatory site. *J. Neurosci.*, **9**, 2191–2196.

HAJOS, F. (1975). An improved method for the preparation of synaptosomal fractions in high purity. *Brain Res.*, **93**, 485–489.

ISHIDA, M., SAITOH, T., SHIMAMOTO, K., OHFUNE, Y. & SHINOZAKI, H. (1993). A novel metabotropic glutamate receptor agonist: marked depression of monosynaptic excitation in the newborn rat isolated spinal cord. *Br. J. Pharmacol.*, **109**, 1169–1177.

JOHNSON, J.W. & ASCHER, P. (1987). Glycine potentiates the NMDA response in cultured mouse brain neurons. *Nature*, **325**, 529–531.

KEMP, J.A., FOSTER, A.C., LEESON, P.D., PRIESTLEY, T., TRIDGETT, R., IVERSEN, L.L. & WOODRUFF, G.N. (1988). 7-Chlorokynurenic acid is a selective antagonist of the glycine modulatory site of the NMDA receptor complex. *Proc. Natl. Acad. Sci. U.S.A.*, **85**, 6547–6550.

KONISHI, S. & OTSUKA, M. (1974). Excitatory actions of hypothalamic substance P on spinal motoneurones of newborn rats. *Nature*, **252**, 734–735.

KROGSGAARD-LARSEN, P., HJEDS, H., CURTIS, D.R., LEAH, J.D. & PEET, M.J. (1982). Glycine antagonists structurally related to muscimol, THIP, or isoguvacine. *J. Neurochem.*, **39**, 1319–1324.

MARUYAMA, M. & TAKEDA, K. (1989). Effects of acromelic acid A on the binding of [^{3}H]glutamic acid and [^{3}H]kainic acid to synaptic membranes and on the depolarization at the frog spinal cord. *Brain Res.*, **504**, 328–331.

OTTERSEN, O.P. & STORM-MATHISEN, J. (ed.) (1990). *Glycine Neurotransmission*. Chichester: John Wiley & Sons.

PETERSON, G.L. (1977). A simplication of the protein assay method of Lowry et al. which is more generally applicable. *Anal. Biochem.*, **83**, 346–356.

SIMMONDS, M.A. & TURNER, J.P. (1985). Antagonism of inhibitory amino acids by the steroid derivative RU5135. *Br. J. Pharmacol.*, **84**, 631–635.

SHINOZAKI, H., ISHIDA, M., SHIMAMOTO, K. & OHFUNE, Y. (1989). Potent NMDA-like actions and potentiation of glutamate responses by conformational variants of a glutamate analogue in the rat spinal cord. *Br. J. Pharmacol.*, **98**, 1213–1224.

TAKAHASHI, T. (1984). Inhibitory miniature synaptic potentials in rat motoneurones. *Proc. R. Soc. B.*, **221**, 103–109.

WERMAN, R., DAVIDOFF, R.A. & APRISON, M.H. (1967). Inhibition of motoneurons by iontophoresis of glycine. *Nature*, **214**, 681–683.

YANAGISAWA, M., OTSUKA, M., KONISHI, S., AKAGI, H. FOLKERS, K. & ROSELL, S. (1982). A substance P antagonist inhibits a slow reflex response in the spinal cord of the newborn rat. *Acta Physiol. Scand.*, **116**, 109–112.

YOUNG, A.B. & SYNDER, S.H. (1973). Strychnine binding associated with glycine receptors of the central nervous system. *Proc. Natl. Acad. Sci. U.S.A.* **70**, 2832–2836.

(Received June 14, 1993
Revised March 14, 1994
Accepted May 26, 1994)

Br. J. Pharmacol. (1994), **113**, 171–178

Effects of protein kinase C activators upon the late stages of the ACTH secretory pathway of AtT-20 cells

Brian W. McFerran & [1]Simon B. Guild

Molecular Endocrinology Group, School of Biological and Medical Sciences, University of St. Andrews, St. Andrews KY16 9TS

1 The mouse AtT-20/D16-16 anterior pituitary tumour cell line was used as a model system for the study of phorbol 12-myristate 13-acetate (PMA)-mediated enhancement of calcium-evoked adrenocorticotrophin (ACTH) secretion.

2 PMA stimulated ACTH secretion from intact cells in a concentration-dependent manner. Other phorbol esters; phorbol 12,13-dibutyrate (PDBu) and phorbol 12,13-didecanoate (PDD) and diacylglycerol analogues; 1-oleoyl-2-acetyl-sn-glycerol (OAG) and 1,2-dioctanoyl-sn-glycerol (DOG) also stimulated ACTH release from intact AtT-20 cells. This would suggest that activation of protein kinase C (PKC) stimulates ACTH secretion from AtT-20 cells.

3 Calcium stimulated ACTH secretion from electrically-permeabilized cells over the concentration-range of 10^{-7} M to 10^{-5} M. PMA (10^{-7} M) enhanced the amount of ACTH secreted at every concentration of calcium investigated. The PKC inhibitor, chelerythrine (10^{-5} M) blocked the PMA (10^{-7} M)-evoked enhancement of calcium (10^{-5} M)-stimulated ACTH secretion but did not alter significantly the calcium (10^{-5} M)-evoked secretion itself. This suggests that PKC modulates the secretory response to increases in intracellular calcium but does not mediate the effects of calcium.

4 Guanosine 5'-O-(3-thiotriphosphate) (GTP-γ-S, 10^{-5} M) stimulated ACTH secretion from permeabilized cells in the absence of calcium and was additive with calcium-evoked ACTH secretion up to a maximum value which could be achieved by calcium acting alone. This suggests that a GTP-binding protein mediates the secretory response to increases in the intracellular calcium. PMA (10^{-7} M) enhanced ACTH secretion stimulated by the combination of calcium and GTP-γ-S (10^{-5} M).

5 GTP-γ-S stimulated ACTH secretion from permeabilized cells in a concentration-dependent manner with a threshold of 10^{-6} M. PMA (10^{-7} M) increased the amount of ACTH secretion evoked by every concentration of GTP-γ-S investigated. Chelerythrine (10^{-5} M) blocked the PMA (10^{-7} M)-evoked enhancement of GTP-γ-S (10^{-4} M)-stimulated ACTH secretion but did not significantly alter GTP-γ-S (10^{-4} M)-evoked secretion itself. This suggests that PKC modulates the secretory response to GTP-γ-S but does not mediate the effects of GTP-γ-S.

6 GTP-γ-S (10^{-8}–10^{-4} M) stimulated ACTH secretion from permeabilized cells either in the presence or absence of ATP (5 mM) indicating that its effects on secretion are ATP-independent.

7 The results of the present study support the hypothesis that, in AtT-20 cells, PMA is acting at some site distal to calcium entry which modulates the ability of an increase in cytosolic calcium concentration to stimulate ACTH secretion. This site of action is either at the level of or at some stage distal to a GTP-binding protein which mediates the effects of calcium upon secretion.

8 PMA, unlike adenosine 3':5'-cyclic monophosphate (cyclic AMP) (Guild, 1991), can stimulate ACTH secretion from permeabilized cells in the absence of added calcium and guanine nucleotides which suggests that PMA and cyclic AMP are acting through distinct mechanisms at this post calcium site of action.

Keywords: PMA; protein kinase C; calcium; G-protein; anterior pituitary cell line; adrenocorticotrophin (ACTH)

Introduction

Calcium has long been established as a trigger to hormone secretion (Douglas, 1968) and supporting evidence for this comes from the use of permeabilized cells in which the cytosolic free calcium concentration can be controlled. Calcium has been shown to stimulate secretion from a variety of permeabilized cell types (for review see Knight & Scrutton, 1986) including adrenocorticotrophin (ACTH) secretion from the mouse AtT-20/D16-16 anterior pituitary cell line, a model system for the normal corticotroph (Luini & De Matteis, 1988; Guild, 1991). The ability of a particular concentration of calcium to stimulate hormone secretion can however be influenced by various factors including other second messengers.

The adenosine 3':5'-cyclic monophosphate (cyclic AMP)-dependent protein kinase A (PKA), which mediates the effects of changes in cellular cyclic AMP content (for review see Taylor *et al.*, 1990), stimulates ACTH secretion from AtT-20 cells and from rat anterior pituitary corticotrophs (Aguilera *et al.*, 1983; Axelrod & Reisine, 1984; Heisler & Reisine, 1984; Miyazaki *et al.*, 1984). The action of this enzyme upon the secretory pathway in AtT-20 cells is thought to be due, at least partly, to an interaction with the calcium messenger system on at least two levels. Cyclic AMP enhances calcium entry via voltage-dependent calcium channels, thus raising intracellular calcium levels (Luini *et al.*, 1985; Guild & Reisine, 1987). In addition cyclic AMP potentiates the ability of a particular increase in cytosolic calcium levels to stimulate ACTH secretion (Guild *et al.*, 1986; Guild, 1991). These results suggest two points of regulation for PKA including a post calcium site of action (Guild, 1991).

Calcium stimulates hormone secretion in AtT-20 cells via stimulation of a guanosine 5'-triphosphate (GTP)-binding protein and therefore intracellular concentrations of GTP

[1] Author for correspondence.

analogues such as guanosine 5'-O-(3-thiotriphosphate) (GTP-γ-S) can stimulate ACTH secretion from AtT-20 cells in the absence of calcium (Luini & De Matteis, 1988; 1990; Guild, 1991). This GTP-binding protein involved in the late stages of the secretory pathway, termed G_E by Gomperts and co-workers, is present in a variety of secretory cells (for review see Gomperts, 1990). Cyclic AMP enhances GTP-γ-S stimulated ACTH secretion from AtT-20 cells suggesting this post calcium site of action is either at the level of G_E or at some stage distal to this protein (Guild, 1991).

Protein kinase C (PKC) is a kinase which is also regulated by second messenger action (for review, see Hug & Sarre, 1993). This enzyme also plays an important role in ACTH secretion from AtT-20 cells (Reisine & Guild, 1987) and in the normal corticotroph (Abou-Samra *et al.*, 1986). The ability of PKC to stimulate ACTH secretion from AtT-20 cells is again due, at least partly, to an interaction with the calcium messenger system. Phorbol esters such as phorbol 12-myristate 13-acetate (PMA), activators of PKC (for review, see Hug & Sarre, 1993), stimulate a rapid increase in intracellular free calcium levels in this cell line (Reisine & Guild, 1987; Reisine, 1989) and thus stimulate hormone secretion. This increase in cytosolic calcium levels induced by PMA in AtT-20 cells is however transient but the induced ACTH secretion is sustained (Reisine & Guild, 1987) suggesting that the rise in cytosolic calcium cannot account completely for the triggered hormone secretion. This study, therefore, investigated the possibility that PKC has a similar post calcium site of action to that of PKA.

The results of the present study suggest that, in AtT-20 cells, PMA is acting at some stage distal to changes in free calcium concentrations to modulate calcium-evoked ACTH secretion. In addition, such an action may be at the level of, or at some stage distal to G_E, suggesting that PKC does have a similar post calcium site of action to that of PKA. However PMA stimulated ACTH secretion in the absence of calcium and guanine nucleotides which was not the case for cyclic AMP (Guild, 1991) suggesting that PKA and PKC may be acting through distinct mechanisms. PKC acts to modulate the regulation of ACTH secretion by the calcium/G_E system but is not essential to the stimulation of secretion by this system. Preliminary accounts of this study have been communicated to the British Pharmacological Society (McFerran *et al.*, 1994).

Methods

Culture of AtT-20 cells

Cells of the mouse AtT-20/D16-16 pituitary tumour cell line were grown and subcultured in Dulbecco's modified Eagle's medium (DMEM) (4500 mg glucose l^{-1}) supplemented with 10% (w/v) foetal calf serum as previously described (Reisine, 1984). Cells to be used in ACTH release experiments from intact cells were plated in 24-well (16 mm diameter) multiwell plates (Costar, U.S.A.) at an initial density of 10^5 cells/well and were used 5–7 days after subculturing (80–90% confluency). Cells to be used in experiments involving electrically permeabilized cells were plated in 75 cm^2 flasks (Nunc, Gibco, UK) at an initial density of 2×10^6 cells/flask and were used 7–9 days after subculturing (80–90% confluency).

Preparation of AtT-20 cells

Intact cell preparations The culture medium was removed, cells adhering to the substrate in each well were washed 3 times with 1 ml of DMEM supplemented with 0.1% (w/v) bovine serum albumin (DMEM/BSA) and then incubated for 1 h in 1 ml of fresh DMEM/BSA at 37°C in a humidified atmosphere of 10% CO_2 in air. The DMEM/BSA was then decanted and replaced with 1 ml of fresh DMEM/BSA.

Permeabilized cell preparations The culture medium was removed, cells adhering to the substrate were liberated by trypsin (0.05% w/v)/EDTA (1 mM). The cells were washed twice by centrifugation (200 *g*, 5 min)/resuspension in a balanced salt solution of the following composition (mM): NaCl 145, KCl 5.6, $CaCl_2$ 2, $MgCl_2$ 0.5, glucose 5.6, HEPES 5, sodium ascorbate 0.5, BSA 0.1% (w/v); pH 7.4. After washing, the cells were suspended at a density of 10^6 cells ml^{-1} in this buffer and incubated for a further 30 min at 37°C. The cell suspension was then centrifuged (200 *g*, 5 min) and the cell pellet washed twice by resuspension/centrifugation (200 *g*, 5 min) in the standard permeabilization buffer of the following composition (mM): potassium glutamate 129, PIPES (potassium salt) 20; glucose 5; ATP 5; EGTA 5; BSA 0.1% (w/v); pH 6.6. The cells were finally resuspended in this buffer at a density of 4×10^7 cells ml^{-1} and electrically permeabilized by subjection to intense electric fields of brief duration (Knight & Baker, 1982). Optimum permeabilization parameters were determined as previously described (Guild, 1991) and were found to be 10 discharges each of 2500 V cm^{-1}. These parameters were adopted in these experiments.

Measurement of stimulated ACTH secretion from intact cells

The ability of phorbol esters and diacylglycerol analogues to stimulate ACTH secretion from intact AtT-20 cells remaining attached to the culture dishes was measured as previously described (Hook *et al.*, 1982). Drugs were added to the 1 ml of DMEM/BSA bathing the cells in the wells of the culture dishes. Zero time samples were taken at this point and the remaining cells incubated for 1 h at 37°C in a humidified atmosphere of 10% CO_2 in air. In each experiment sextuplicate samples were run for each condition. Incubations were terminated by removing the DMEM/BSA bathing the cells, centrifugation (10,000 *g*, 20 s) of this sample and the removal of the supernatant. The ACTH content of the supernatant was measured by radioimmunoassay.

Measurement of stimulated ACTH secretion from permeabilized AtT-20 cells

Calcium-stimulated ACTH secretion Permeabilized cells were suspended at a density of 10^5 cells ml^{-1} in a series of calcium-EGTA buffers chosen to give free calcium concentrations over the range of 10^{-9}–10^{-5} M as previously described (Guild, 1991). At this point the zero time samples were centrifuged (200 *g*, 5 min) and samples of the supernatant stored for subsequent measurement of ACTH content. The cell suspensions were incubated at 37°C for 30 min at which point incubations were terminated by centrifugation (200 *g*, 5 min, 4°C) and samples of the supernatant stored for subsequent measurement of ACTH content. In experiments investigating the effects of phorbol esters, diacylglycerol analogues and GTP-γ-S upon calcium-evoked ACTH secretion, the calcium-EGTA buffers were supplemented by PMA, PDD, PDBu, DOG, OAG or GTP-γ-S as indicated in the legends to the figures. In each experiment sextuplicate samples of the supernatant were removed from each condition and the ACTH content measured by radioimmunoassay.

Guanine nucleotide-stimulated ACTH secretion Permeabilized cells were suspended at a density of 10^5 cells ml^{-1} in a calcium-EGTA buffer (10^{-9} M) supplemented with GTP-γ-S (10^{-8}–10^{-4} M) as previously described (Guild, 1991). The effect of PMA upon GTP-γ-S (10^{-8}–10^{-4} M)-evoked ACTH secretion were investigated by co-incubation of PMA with GTP-γ-S (10^{-8}–10^{-4} M). At this point the zero time samples were centrifuged (200 *g*, 5 min) and samples of the supernatant stored for subsequent measurement of ACTH content. The cell suspensions were incubated at 37°C for 30 min at which point incubations were terminated by centrifugation

(200 g, 5 min, 4°C) and samples of the supernatant stored for subsequent measurement of ACTH content. In each experiment sextuplicate samples of the supernatant were removed from each condition and the ACTH content measured by radioimmunoassay.

The effect of inhibiting PKC upon calcium- and guanine nucleotide-stimulated ACTH secretion

The PKC inhibitor, chelerythrine (Herbert *et al.*, 1990), was used to investigate whether calcium and GTP-γ-S stimulated PKC to evoke ACTH secretion. This possibility of an indirect regulation of ACTH secretion, mediated by PKC, by these agents was tested by measuring calcium- and guanine nucleotide-stimulated ACTH secretion (as described above) in the presence and absence of chelerythrine (10^{-5} M). In addition, the effect of omitting ATP from the permeabilization media, and hence depriving protein kinases of ATP for their actions, upon guanine nucleotide-stimulated ACTH secretion was investigated.

Radioimmunoassay

The radioimmunoassay for ACTH was performed as previously described (Reisine, 1984). [^{125}I]-ACTH for radioimmunoassay use was produced using the lodogen reagent (1,3,4,6-tetrachloro-3α,6α-diphenylglycoluril) which was first described as a reagent for iodination by Fraker & Speck (1978). The amount of ACTH released was expressed as the amount present at the end of the specified incubation period less the amount present at zero time.

Statistics

A two-sided, 0.05 level, paired *t* test was used to determine if the effect of a treatment was significant.

Materials

The following substances (with their sources) were used: ATP, bovine serum albumin (BSA) (fraction V), 4α phorbol, phorbol 12,13-dibutyrate (PDBu), phorbol 12,13-didecanoate (PDD), phorbol 12-myristate 13-acetate (PMA) from Sigma, UK; 1-oleoyl-2-acetyl-sn-glycerol (OAG), 1,2-dioctanoyl-sn-glycerol (DOG) and chelerythrine chloride from Calbiochem-NovaBiochem, UK; guanosine 5'-O-(3-thiotriphosphate) (GTP-γ-S) from Boehringer Mannheim, UK; DMEM, foetal calf serum and trypsin EDTA from GIBCO, UK; human ACTH antiserum and human ACTH standards were a gift of the National Hormone and Pituitary programme, Baltimore, MD, U.S.A.; Iodogen iodination reagent from Pierce & Warriner. All other chemicals were of Analar grade and readily commercially available.

Results

The effect of PKC activators upon ACTH secretion from intact AtT-20 cells

PMA (10^{-12}–10^{-7} M) stimulated a concentration-dependent increase in ACTH secretion (Figure 1) as previously shown (Reisine & Guild, 1987). ACTH secretion in response to PMA was significantly greater than control at concentrations of 10^{-10} M and above with a 4 fold increase over basal obtained at maximum. A supramaximal concentration of 10^{-7} M was chosen for subsequent use of PMA in the following experiments. The phorbol esters phorbol 12,13 didecanoate (PDD) and phorbol 12,13 dibutyrate (PDBu) (Table 1) and the diacylglycerol analogues 1-oleoyl-2-acetyl-sn-glycerol (OAG) and 1,2-dioctanoyl-sn-glycerol (DOG) (Table 2), at concentrations of 10^{-7} M and 10^{-4} M respectively, produced a similar significant increase in ACTH secretion (4–5 fold over basal). However, the inactive 4 α-phorbol did not stimulate secretion to the same extent (Table 1).

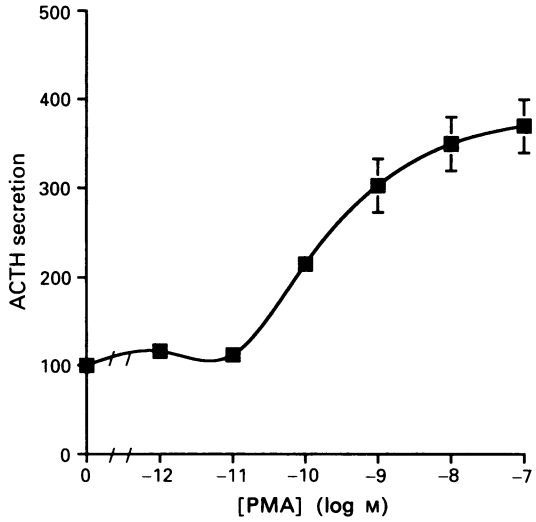

Figure 1 Effect of phorbol 12-myristate 13-acetate (PMA) on adrenocorticotrophin (ACTH) secretion from intact AtT-20 cells. Intact cells were incubated for 1 h in Dulbecco's Modified Eagles Medium with 0.1% bovine serum albumin (DMEM/BSA) supplemented with the indicated concentration of PMA. The hormone release results were standardized and expressed as % of the control responses, the control responses being that obtained in the absence of PMA. The results are expressed as the mean ± s.e.mean from 3 separate experiments. Absence of error bars indicate that they lie within the symbol used.

Table 1 Effects of phorbol 12,13-dibutyrate (PDBu), phorbol 12,13-dideconoate (PDD) and 4 α phorbol on adrenocorticotrophin (ACTH) secretion from intact AtT-20 cells

Phorbol ester (10^{-7} M)	*ACTH secretion* (% of control)
PDBu	413 ± 26
PDD	437 ± 64
4 α phorbol	148 ± 28

Intact cells were incubated for 1 h in Dulbecco's Modified Eagles Medium with 0.1% bovine serum albumin (DMEM/BSA) in the absence of phorbol ester or in the presence of 10^{-7} M phorbol ester. The hormone release results were standardized and expressed as % of the control responses, the control responses being that obtained in the absence of phorbol ester. The results are expressed as the mean ± s.e.mean from 3 separate experiments.

Table 2 Effects of 1-oleoyl-2-acetyl-sn-glycerol (OAG) and 1,2-dioctanoyl-sn-glycerol (DOG) on adrenocorticotrophin (ACTH) secretion from intact AtT-20 cells

Diacylglycerol analogue (10^{-4} M)	*ACTH secretion* (% of control)
OAG	398 ± 31
DOG	456 ± 75

Intact cells were incubated for 1 h in Dulbecco's Modified Eagles Medium with 0.1% bovine serum albumin (DMEM/BSA) in the absence of diacylglycerol analogue or in the presence of 10^{-4} M diacylglycerol analogue. The hormone release results were standardized and expressed as % of the control responses, the control responses being those obtained in the absence of diacylglycerol analogue. The results are expressed as the mean ± s.e.mean from 3 separate experiments.

The effect of PMA and chelerythrine upon calcium-evoked ACTH secretion from permeabilized AtT-20 cells

Calcium-evoked ACTH secretion from permeabilized AtT-20 cells was dependent upon the concentration of free calcium in the permeabilization medium (Figure 2). Calcium stimulated ACTH secretion in a concentration-dependent manner between 10^{-7} and 10^{-5} M as previously shown (Guild, 1991). ACTH secretion in response to free calcium concentrations of 10^{-6} M and above were significantly greater than the 10^{-9} M calcium control. PMA (10^{-7} M) significantly enhanced calcium evoked ACTH secretion from permeabilized AtT-20 cells at all concentrations of calcium investigated (Figure 2). Importantly, PMA significantly enhanced ACTH secretion in the effective absence of calcium (free calcium concentration of 10^{-9} M). The protein kinase c inhibitor, chelerythrine (10^{-5} M), did not significantly alter the ACTH secretion obtained at either 10^{-9} M (cont.) or 10^{-5} M (Ca^{2+}) calcium (Figure 3a) but inhibited the PMA (10^{-7} M)-evoked enhancement of ACTH secretion at both of these calcium concentrations (Figure 3a). This suggests that PKC modulates the secretory response to increases in intracellular calcium but does not mediate the effects of calcium.

The effect of guanine nucleotides and PMA upon calcium-evoked ACTH secretion from permeabilized AtT-20 cells

GTP-γ-S (10^{-5} M), a non-hydrolysable GTP analogue which persistently activates GTP-binding proteins, significantly stimulated ACTH secretion in the absence of calcium (free calcium concentration of 10^{-9} M, Figure 4). When co-incubated with a range of free calcium concentrations this effect of GTP-γ-S (10^{-5} M) was additive with that of calcium up to a maximum value which could be produced by calcium acting alone, obtained at 10^{-5} M calcium, at which point there was no significant difference between ACTH secretion obtained in the presence or absence of GTP-γ-S (10^{-5} M) (Figure 4). This is consistent with the concept that a GTP-binding protein mediates the effect of calcium upon ACTH secretion in AtT-20 cells. Co-incubation of PMA (10^{-7} M) with either a range of free calcium concentrations alone or with a range of free calcium concentrations supplemented with GTP-γ-S (10^{-5} M) resulted in a significant enhancement of both calcium (10^{-9}–10^{-5} M)-evoked ACTH secretion and ACTH secretion in response to the combination of calcium (10^{-9}–10^{-5} M) and GTP-γ-S (10^{-5} M) (Figure 4). The potentiation of calcium (10^{-9}–10^{-5} M)-evoked ACTH secretion by PMA (10^{-7} M) remained significant at all concentrations of calcium investigated. The enhancement by PMA (10^{-7} M) of the calcium (10^{-9}–10^{-5} M)/GTP-γ-S (10^{-5} M) combination was significant at all calcium concentrations except 10^{-8} M calcium. There was no significant difference between ACTH secretion obtained in response to the combination of calcium

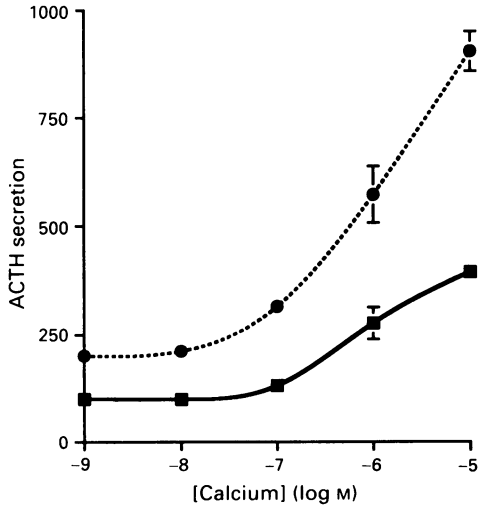

Figure 2 Effect of phorbol 12-myristate 13-acetate (PMA) on calcium-dependent adrenocorticotrophin (ACTH) secretion from permeabilized AtT-20 cells. Permeabilized cells were incubated in standard permeabilization medium containing various proportions of calcium and EGTA, such that the indicated concentrations of free calcium resulted, either in the presence (●) or absence (■) of PMA (10^{-7} M). The hormone release results were standardized and expressed as % of the control responses, the control responses being those obtained in the absence of calcium (10^{-9} M). The results are expressed as the mean ± s.e.mean from 3 separate experiments. Absence of error bars indicate that they lie within the symbol used.

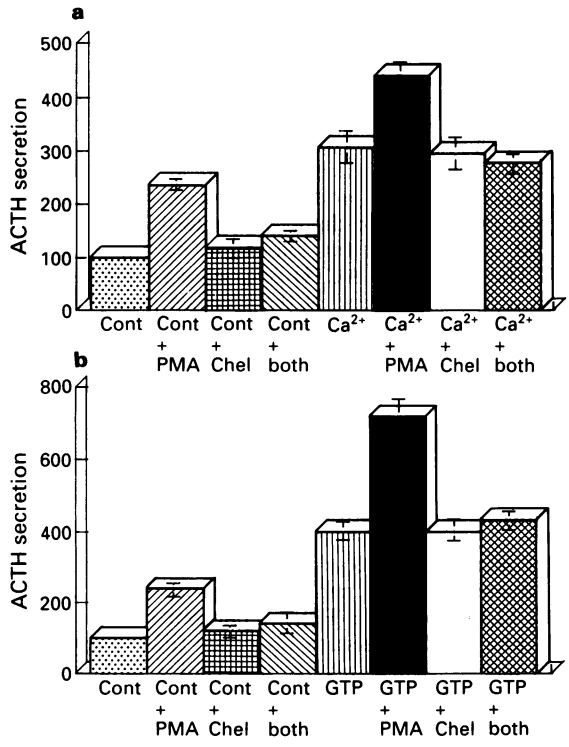

Figure 3 Effect of chelerythrine upon calcium- and guanosine 5'-O-(3-thiotriphosphate) (GTP-γ-S)-dependent adrenocorticotrophin (ACTH) secretion from permeabilized AtT-20 cells and the ability of phorbol 12-myristate 13-acetate (PMA) to potentiate their effects. (a) Permeabilized cells were incubated in standard permeabilization medium containing calcium-EGTA buffers designed to give 10^{-9} M free calcium (Cont) or 10^{-5} M free calcium (Ca^{2+}) either in the presence (Cont + PMA, Ca^{2+} + PMA) or absence (Cont, Ca^{2+}) of PMA (10^{-7} M). The effects of chelerythrine (10^{-5} M) at 10^{-9} M free calcium (Cont + Chel) and at 10^{-5} M free calcium (Ca^{2+} + Chel) and upon combination of 10^{-9} M free calcium plus PMA (10^{-7} M) (Cont + both) and 10^{-5} M free calcium plus PMA (10^{-7} M) (Ca^{2+} + both) were measured. The hormone release results were standardized and expressed as % of the control responses, the control responses being those obtained in the absence of calcium (10^{-9} M). The results are expressed as the mean ± s.e.mean from 3 separate experiments. (b) Permeabilized cells were incubated in standard permeabilization medium containing calcium-EGTA buffers designed to give 10^{-9} M free calcium (Cont) alone or supplemented with GTP-γ-S (10^{-4} M) (GTP) either in the presence (Cont + PMA, GTP + PMA) or absence (Cont, GTP) of PMA (10^{-7} M). The effects of chelerythrine (10^{-5} M) at 10^{-9} M free calcium (Cont + Chel) and GTP-γ-S (10^{-4} M) (GTP + Chel) and upon combination of 10^{-9} M free calcium plus PMA (10^{-7} M) (Cont + both) and GTP-γ-S (10^{-4} M) plus PMA (10^{-7} M) (GTP + both) were measured. The hormone release results were standardized and expressed as % of the control responses, the control responses being those obtained in the absence of calcium (10^{-9} M). The results are expressed as the mean ± s.e.mean from 3 separate experiments.

(10^{-5} M) and PMA (10^{-7} M) with that of the combination of calcium (10^{-5} M, PMA 10^{-7} M) and GTP-γ-S (10^{-5} M). A maximum ACTH secretion could be achieved by calcium and PMA together at which point there was no significant difference between ACTH secretion obtained in response to calcium and PMA (10^{-7} M) in the presence or absence of GTP-γ-S (10^{-5} M) (Figure 4).

The effect of PMA upon guanine nucleotide-evoked ACTH secretion from permeabilized AtT-20 cells

GTP-γ-S stimulated ACTH secretion, in the absence of calcium, in a concentration-dependent manner with a threshold of 10^{-6} M and which became significant at concentrations of GTP-γ-S above 10^{-5} M (Figure 5). PMA (10^{-7} M) significantly stimulated ACTH secretion in the absence of GTP-γ-S and significantly enhanced the stimulated ACTH secretion at every concentration of the nucleotide investigated. Thus PMA enhanced both calcium and guanine nucleotide-evoked ACTH secretion. The protein kinase c inhibitor, chelerythrine (10^{-5} M), did not significantly alter the ACTH secretion obtained either in the absence (cont) or presence of 10^{-4} M GTP-γ-S (GTP) (Figure 3b) but inhibited the PMA (10^{-7} M)-evoked enhancement of ACTH secretion at both of these conditions (Figure 3b). This suggests that PKC modulates the secretory response to GTP-γ-S but does not mediate the effects of the nucleotide nor presumably the GTP-binding protein(s) activated by this agent.

Guanine nucleotide-evoked ACTH secretion in the presence and absence of ATP

GTP-γ-S (10^{-8}–10^{-4} M) stimulated ACTH secretion from permeabilized AtT-20 cells both in the presence and absence of ATP (5 mM) (Figure 6). The omission of ATP from the permeabilization medium significantly reduced the ACTH secretion obtained in the absence of GTP-γ-S and had the effect of reducing the base line from which GTP-γ-S stimulated ACTH secretion from permeabilized cells. Importantly, GTP-γ-S stimulated ACTH secretion to a similar degree at 10^{-4} M either in the presence or absence of ATP (5 mM). Thus GTP-γ-S-stimulated ACTH secretion in AtT-20 cells, unlike calcium-stimulated ACTH secretion (Guild,

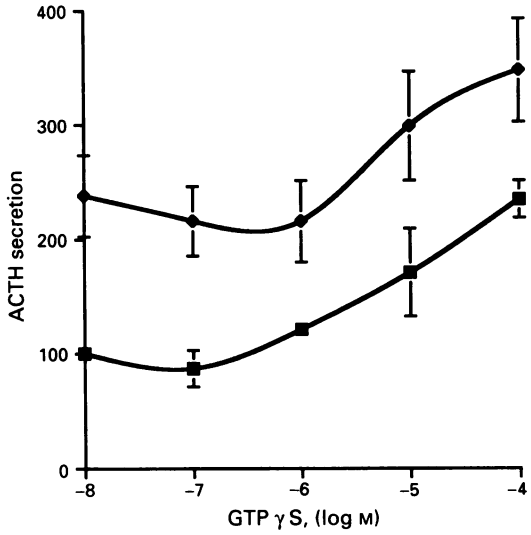

Figure 5 Effect of phorbol 12-myristate 13-acetate (PMA) on guanosine 5'-O-(3-thiotriphosphate) (GTP-γ-S)-stimulated adrenocorticotrophin (ACTH) secretion from permeabilized AtT-20 cells. Permeabilized cells were incubated in standard permeabilization medium supplemented with the indicated concentration of GTP-γ-S either in the presence (◆) or absence (■) of PMA (10^{-7} M). The hormone release results were standardized and expressed as % of the control responses, the control responses being those obtained in the presence of GTP-γ-S (10^{-8} M). The results are expressed as the mean ± s.e.mean from 3 separate experiments. Absence of error bars indicate that they lie within the symbol used.

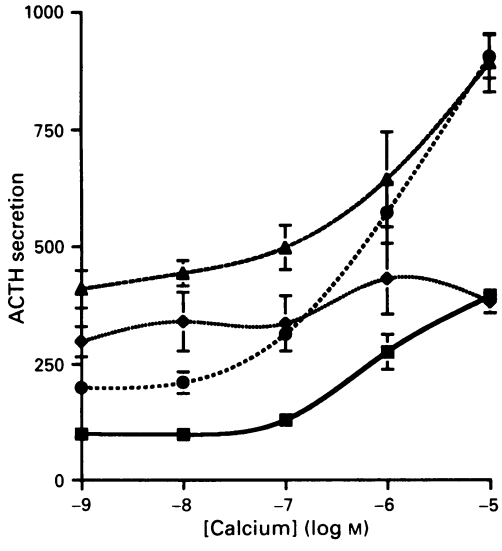

Figure 4 Effects of phorbol 12-myristate 13-acetate (PMA) and guanosine 5'-O-(3-thiotriphosphate) (GTP-γ-S) on calcium-dependent adrenocorticotrophin (ACTH) secretion from permeabilized AtT-20 cells. Permeabilized cells were incubated in standard permeabilization medium containing various amounts of calcium and EGTA, such that the indicated concentrations of free calcium resulted, in the presence of 10^{-7} M PMA (●), 10^{-5} M GTP-γ-S (◆), both 10^{-7} M PMA and 10^{-5} M GTP-γ-S (▲) or in the absence of both PMA and GTP-γ-S (■). The hormone release results were standardized and expressed as % of the control responses, the control responses being that obtained in the absence of calcium (10^{-9} M). The results are expressed as the mean ± s.e.mean from 3 separate experiments. Absence of error bars indicate that they lie within the symbol used.

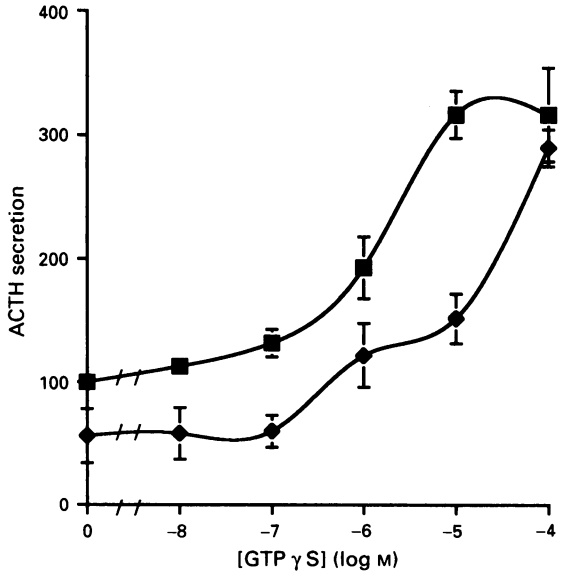

Figure 6 Guanosine 5'-O-(3-thiotriphosphate) (GTP-γ-S)-dependent ACTH secretion from permeabilized AtT-20 cells in the presence and absence of ATP. Permeabilized cells were incubated in standard permeabilization medium supplemented with the indicated concentration of GTP-γ-S either in the presence (■) or absence (◆) of 5 mM ATP. The hormone release results were standardized and expressed as % of the control responses, the control responses being those obtained in the absence of GTP-γ-S in the presence of 5 mM ATP. The results are expressed as the mean ± s.e.mean from 3 separate experiments. Absence of error bars indicate that they lie within the symbol used.

1991), is not dependent upon the presence of ATP in the incubation medium. ATP could provide a source of GTP, via the enzyme nucleoside diphosphate kinase (Gomperts, 1990), and so result in a 'basal' stimulation of secretion via the G_E system upon which added GTP-γ-S exerted its effect.

Discussion

PMA, PDBu and PDD all stimulated ACTH secretion from intact AtT-20 cells. The ability of analogues of diacylglycerol; the physiological activator of PKC (Hug & Sarre, 1993), OAG and DOG, to stimulate a similar secretory response coupled with the inability of 4 α-phorbol, an inactive phorbol ester, to produce such a response suggest that the effects of PMA upon ACTH secretion from AtT-20 cells are mediated by PKC and are not due to a simple biophysical effect. The ability of PMA to stimulate ACTH secretion from AtT-20 cells is consistent with studies using the normal corticotroph (Abou-Samra *et al.*, 1986). PMA was chosen as a representative phorbol ester for further experiments to complement these studies in the normal corticotroph and previous studies in AtT-20 cells (Reisine & Guild, 1987; Reisine, 1989).

In order to determine if PMA was acting at a late stage in the secretory pathway, a more direct manipulation of the intracellular environment was required. This was provided by the use of electrically permeabilized cells, a technique which has been used previously to gain access to the cytosol in AtT-20 cells (Guild, 1991). The ability of calcium over the physiological range of 10^{-7} to 10^{-5} M to stimulate ACTH secretion from permeabilized AtT-20 cells is entirely consistent with previous studies using digitonin- (Luini & De Matteis, 1988) and electrically (Guild, 1991)-permeabilized AtT-20 cells and in a variety of other permeabilized cell types (for review, see Knight & Scrutton, 1986). In these studies a free calcium concentration of 10^{-5} M produced maximal stimulation.

PMA enhanced calcium-dependent ACTH secretion from permeabilized AtT-20 cells. This suggests that, in permeabilized AtT-20 cells, PMA does not enhance ACTH secretion by increasing the cytosolic calcium concentration, since any change in calcium concentration would be buffered by the calcium-EGTA buffers which are designed for this purpose. Therefore PMA, in addition to stimulating calcium entry into the cell across the plasma membrane (Reisine & Guild, 1987; Reisine, 1989), may enhance ACTH secretion from AtT-20 cells by an action distal to changes in the cytosolic calcium concentration. Previous studies show PMA induced a transient rise in the cytosolic calcium concentration in AtT-20 cells however the resultant ACTH secretion is sustained (Reisine & Guild, 1987). This additional post calcium site of action, therefore, may be responsible for the more sustained nature of the ACTH secretion induced by PMA.

It is difficult to interpret apparent additivity of secretory responses in studies of this sort and caution should be exercised when making claims about physiological mechanisms underlying these observations. Notwithstanding these limitations, in this study there was an apparent interaction between calcium and PMA which was additive at lower calcium concentrations and which become synergistic at higher calcium concentrations. Whilst acknowledging the dangers, a possible explanation for this can be put forward. PKC is now known to consist of a group of at least nine different PKC isoenzymes (for review, see Hug & Sarre, 1993). This family of isozymes can be divided into two main groups, the calcium-dependent or conventional PKCs (cPKCs) and the calcium-independent or novel PKCs (nPKCs) (Ohno *et al.*, 1991). PMA is able to stimulate both cPKCs and nPKCs although calcium is required for maximal stimulation of cPKCs by PMA (Ryves *et al.*, 1991). Therefore the additive enhancement by PMA of calcium-stimulated secretion seen at lower calcium concentrations may be due to stimulation of nPKCs which are active in the absence of calcium and partial stimulation of cPKCs. The synergistic interaction between calcium and PMA seen at higher calcium concentrations could therefore be due to stimulation of both nPKCs and cPKCs which become fully stimulated by PMA at higher calcium concentrations (Ryves *et al.*, 1991).

The ability of GTP-γ-S to enhance calcium-stimulated secretion confirms a previous report from this lab suggesting a GTP-binding mediates the effects of calcium upon ACTH secretion from AtT-20 cells (Guild, 1991). The ability of PMA to potentiate the calcium/GTP-binding protein system suggests that, in AtT-20 cells, the post-calcium site of interaction between calcium and PMA is either at the level of, or at some stage distal to, G_E. Cyclic AMP has been shown to have a similar post-calcium site of action (Guild, 1991), but cyclic AMP requires the stimulation of ACTH secretion by either calcium or guanine nucleotides in order for this post-calcium potentiation of ACTH secretion from AtT-20 cells to be manifest (Guild, 1991). In contrast, this study shows that PMA is able to stimulate ACTH secretion from permeabilized AtT-20 cells in the absence of both calcium and guanine nucleotides. Therefore both PMA and cyclic AMP enhance the calcium/GTP-binding protein system; however, PMA has the additional action of enhancing secretion in the absence of calcium or GTP-γ-S. This important difference may suggest that although cyclic AMP and PMA both have similar post-calcium sites of action they are acting through distinct mechanisms to enhance calcium-stimulated ACTH secretion. This has already been shown to be the case at an earlier stage in the stimulus-secretion coupling pathway. PMA and cyclic AMP both stimulate ACTH secretion from AtT-20 cells by enhancing calcium entry into the cell across the plasma membrane but do so through distinct mechanisms (Reisine & Guild, 1987, Reisine, 1989).

The ability of PMA to stimulate ACTH secretion from permeabilized cells in the absence of calcium and added GTP-γ-S raises the possibility that PKC may mediate the effects of the calcium-G_E system upon secretion. This argument was used to support the idea that a GTP binding protein mediated the effects of calcium upon the secretory apparatus of AtT-20 cells (this study and Guild, 1991) as added guanine nucleotides stimulated a step distal to that regulated by calcium. The data in this study, however, do not support the hypothesis that PKC mediates the effect of calcium-G_E system upon secretion. Firstly, PMA potentiates calcium-evoked ACTH secretion and the combination of the two evoked much greater ACTH secretion than could be obtained by calcium alone. If PKC mediated calcium-evoked ACTH secretion then addition of PMA and activation of PKC would show the same pattern of interaction upon hormone secretion as seen with GTP-γ-S and calcium. Secondly, the PKC inhibitor, chelerythrine, did not inhibit calcium- or GTP-γ-S-evoked ACTH secretion from AtT-20 cells. This agent did, however, inhibit the PMA-evoked potentiation of both calcium- and GTP-γ-S-evoked ACTH secretion from AtT-20 cells indicating that it did indeed inhibit PKC in AtT-20 cells but that this did not result in any significant attenuation of the secretory response to activation of the calcium-G_E system. Another possibility for the actions of PMA in the absence of calcium and added GTP-γ-S is that PKC, in addition to an action at a late stage (i.e. post G_E) in the secretory pathway, may also stimulate a parallel pathway to promote ACTH secretion. From the data presented in this study, it would appear that PKC plays a modulatory role in regulating secretion and is not necessary for secretion. In this sense AtT-20 cells are similar to adrenal chromaffin, PC12 cells, neuroendocrine and mast cells (for review, see Burgoyne & Morgan, 1993).

GTP-γ-S is able to stimulate ACTH secretion from permeabilized AtT-20 cells, under the present conditions, in the absence of ATP to a similar degree to that obtained in the presence of ATP. This argues against the involvement of a protein kinase in mediating the effect of G_E upon secretion

and leads us to believe that ATP in this system serves mainly as a modulator as suggested for rat mast cells (Gomperts, 1990). We have previously demonstrated that calcium-evoked secretion from permeabilized AtT-20 cells is dependent upon the presence of ATP in the permeabilization media (Guild, 1991). We believe that ATP in this case provides a source of GTP via the enzyme nucleoside diphosphate kinase (Gomperts, 1990) and so permits the stimulation of secretion via the calcium/G_E system when activated by calcium. These results are similar to those obtained in permeabilized rat mast cells (Lillie & Gomperts, 1992; Koffer & Churcher, 1993) and in adrenal chromaffin cells (reviewed in Burgoyne & Morgan, 1993).

The nature of the GTP-binding protein (G_E) controlling the late stage of ACTH secretion in AtT-20 cells is as yet unclear. Synaptic vesicles and secretory granules possess both monomeric ras-like (Burgoyne & Morgan, 1989; Darchen *et al.*, 1990; Fischer von Mollard *et al.*, 1991) and trimeric (Toutant *et al.*, 1987) GTP-binding proteins. Rab 3 proteins (monomeric ras-like GTP-binding proteins) have been shown in AtT-20 cells to be important for localisation, sequestration and storage of secretory vesicles (Ngsee *et al.*, 1993). An inhibitory form of G_E (G_{Ei}), thought to be a trimeric protein, is responsible for inhibition of secretion in AtT-20 cells (Luini & DeMatteis, 1988) and in chromaffin cells (Vitale *et al.*, 1993). Whether the stimulatory form of G_E (G_{Es}) in AtT-20 cells is similarly a trimeric GTP-binding protein has yet to be determined.

The results of this and a previous study (Guild, 1991) suggest that not only does a G-protein directly regulate exocytosis but its action is regulated by second messenger systems perhaps by increasing the readily releasable pool of stored hormone (Dannies, 1982). It is clear that calcium alone cannot stimulate the maximal possible hormone secretion and that co-operation with PKC and PKA increases the amount of hormone secreted in response to a particular concentration of calcium. Interestingly, in mast cells GTP-γ-S-stimulated secretion requires a phosphorylated 'primed' state but no MgATP needs to be utilized during the process of exocytosis (Koffer & Churcher, 1993). It is tempting to speculate that in AtT-20 pituitary cells the protein kinases modulate the secretory response by maintaining a 'primed' state and the size of the readily-releasable pool of hormone but the exocytotic machinery is directly controlled by the calcium/G_E system (Gomperts, 1990).

The authors would like to acknowledge gratefully the financial support of the Wellcome Trust, the Royal Society and the Nuffield Foundation. B.W.M. is supported by a Maitland-Ramsay scholarship.

References

ABOU-SAMRA, A., CATT, K.J. & AGUILERA, G. (1986). Involvement of protein kinase C in the regulation of adrenocorticotrophin release from rat anterior pituitary cells. *Endocrinology*, **118**, 212–217.

AGUILERA, G., HARWOOD, J., WILSON, J., BROWN, J. & CATT, K. (1983). Mechanism of action of corticotrophin-releasing factor and other regulators of corticotrophin release in rat pituitary cells. *J. Biol. Chem.*, **258**, 8039–8045.

AXELROD, J. & REISINE, T. (1984). Stress hormones: their interaction and regulation. *Science*, **224**, 452–459.

BURGOYNE, R.D. & MORGAN, A. (1989). Low molecular mass GTP-binding proteins of adrenal chromaffin cells are present on secretory granule. *FEBS Lett.*, **245**, 122–126.

BURGOYNE, R.D. & MORGAN, A. (1993). Regulated exocytosis. *Biochem. J.*, **293**, 305–316.

DANNIES, P.S. (1982). Prolactin: multiple intracellular processing routes plus several potential mechanisms for regulation. *Biochem. Pharmacol.*, **31**, 2845–2849.

DARCHEN, F., ZAHRAOUI, A., HAMMEL, F., MONTEILS, M.P., TAVITIAN, A. & SCHERMAN, D. (1990). Association of the GTP-binding protein rab 3A with bovine adrenal chromaffin granules. *Proc. Natl. Acad. Sci. U.S.A.*, **87**, 5692–5696.

DOUGLAS, W. (1968). Stimulus-secretion coupling: the concept and clues from chromaffin and other cells. *Br. J. Pharmacol.*, **34**, 451–474.

FISCHER VON MOLLARD, G., SUDHOF, T.C. & JAHN, R. (1991). A small GTP-binding protein dissociates from synaptic vesicles during exocytosis. *Nature*, **349**, 79–81.

FRAKER, P. & SPECK, J. (1978). Protein and cell membrane iodination's with a sparingly soluble chloramide. 1,3,4,6-tetrachloro-3α,6α-diphenylglycoluril. *Biochem. Biophys. Res. Commun.*, **80**, 849–857.

GOMPERTS, B.D. (1990). G_E: GTP-binding protein mediating exocytosis. *Annu. Rev. Physiol.*, **52**, 591–606.

GUILD, S. (1991). Effects of adenosine 3':5'-cyclic monophosphate and guanine nucleotides on calcium-evoked ACTH release from electrically-permeabilised AtT-20 cells. *Br. J. Pharmacol.*, **109**, 117–122.

GUILD, S., ITOH, Y., KEBABIAN, J.W., LUINI, A. & REISINE, T. (1986). Forskolin enhances basal and potassium-evoked hormone release from normal and malignant pituitary tissue. The role of calcium. *Endocrinology*, **118**, 268–279.

GUILD, S. & REISINE, T. (1987). Molecular mechanisms of corticotrophin-releasing factor stimulation of calcium mobilization and adrenocorticotrophin release from anterior pituitary tumour cells. *J. Pharmacol. Exp. Ther.*, **241**, 125–130.

HEISLER, S. & REISINE, T. (1984). Forskolin stimulates adenylate cyclase activity, cAMP accumulation and ACTH secretion from mouse pituitary tumours. *J. Neurochem.*, **42**, 1659–1665.

HERBERT, J.M., AUGEREAU, J.M., GLEYE, J. & MAFFRAND, J.P. (1990). Chelerythrine is a potent and specific inhibitor of protein kinase-C. *Biochem. Biophys. Res. Commun.*, **172**, 993–999.

HOOK, V.Y.H., HEISLER, S., SABOL, S.L. & AXELROD, J. (1982). Corticotrophin releasing factor stimulates adrenocorticotrophin and β-endorphin release from AtT-20 mouse pituitary tumour cells. *Biochem. Biophys. Res. Commun.*, **106**, 1364–1371.

HUG, H. & SARRE, T.F. (1993). Protein kinase C isozymes: divergence in signal transduction? *Biochem. J.*, **291**, 329–343.

KNIGHT, D.E. & BAKER, P.F. (1982). Calcium-dependence of catecholamine release from adrenal medulary cells after exposure to intense electric fields. *J. Memb. Biol.*, **68**, 107–140.

KNIGHT, D.E. & SCRUTTON, M.C. (1986). Gaining access to the cytosol: the technique and some applications of electropermeabilization. *Biochem. J.*, **234**, 497–450.

KOFFER, A. & CHURCHER, Y. (1993). Calcium and GTP-γ-S as single effectors of secretion from permeabilised rat mast cells: requirements for ATP. *Biochem. Biophys. Res. Commun.*, **1176**, 222–230.

LILLIE, T.H.W. & GOMPERTS, B.D. (1992). Nucleotides and divalent cations as effectors of exocytosis in permeabilised rat mast cells. *Phil. Trans. R. Soc. B*, **336**, 25–34.

LUINI, A. & DE MATTEIS, M.A. (1988). Dual regulation of ACTH secretion by guanine nucleotides in permeabilised AtT-20 cells. *Cell. Mol. Biol.*, **8**, 129–138.

LUINI, A. & DE MATTEIS, M.A. (1990). Evidence that receptor-linked G-protein inhibits exocytosis by post-second messenger mechanism in AtT-20 cells. *J. Neurochem.*, **54**, 30–38.

LUINI, A., LEWIS, D., GUILD, S., CORDA, D. & AXELROD, J. (1985). Hormone secretagogues elevate cytosolic calcium by increasing cAMP in corticotrophin-secreting cells. *Proc. Natl. Acad. Sci. U.S.A.*, **82**, 8034–8038.

MCFERRAN, B.W., SEMPLE, S.E. & GUILD, S.B. (1994). Phorbol ester potentiates calcium- but not guanine nucleotide-evoked ACTH secretion from electrically-permeabilised AtT-20 cells. *Br. J. Pharmacol.*, **111**, 112P.

MIYAZAKI, K., REISINE, T. & KEBABIAN, J.W. (1984). Cyclic AMP-dependent protein kinase activity in rodent pituitary tissue: possible role in cAMP-dependent hormone secretion. *Endocrinology*, **115**, 1933–1945.

NGSEE, J.K., FLEMING, A.M. & SCHELLER, R.H. (1993). A rab protein regulates the localisation of secretory granules in AtT-20 cells. *Mol. Biol. Cell.*, **4**, 747–756.

OHNO, S., AKITA, Y., HATA, A., OSADA, S., KUBO, K., KONNO, Y., AKIMOTO, K., MIZUNO, K., SAIDO, T., KUROKI, T. & SUZUKI, K. (1991). Structural and functional diversities of a family of signal transducing protein-kinases, protein-kinase-C family - 2 distinct classes of PKC, conventional cPKC and novel nPKC. *Adv. Enzyme Regul.*, **31**, 287–303.

RYVES, W.J., EVANS, A.T., OLIVIER, A.R., PARKER, P.J. & EVANS, F.J. (1991). Activation of the PKC-isotypes α, β_1, γ, δ and ε by phorbol esters of different biological activities. *FEBS Lett.*, **228**, 5–9.

REISINE, T. (1984). Somatostatin desensitisation: loss of the ability of somatostatin to inhibit cAMP accumulation and ACTH release. *J. Pharmacol. Exp. Ther.*, **229**, 14–20.

REISINE, T. (1989). Phorbol esters and corticotrophin-releasing factor stimulate calcium influx in the anterior pituitary tumour cell line, AtT-20, through different intracellular sites of action. *Mol. Pharmacol.*, **248**, 984–990.

REISINE, T. & GUILD, S. (1987). Activators of protein kinase C and cyclic AMP-dependent protein kinase regulate intracellular calcium levels through distinct mechanisms in mouse anterior pituitary tumour cells. *Mol. Pharmacol.*, **32**, 488–496.

TAYLOR, S.S., BUECHLER, J.A. & YONEMOTO, W. (1990). cAMP-dependent protein kinase: framework for a diverse family of regulatory enzymes. *Annu. Rev. Biochem.*, **59**, 971–1005.

TOUTANT, M., AUNIS, D., BOCKAERT, J., HOMBURGER, V. & ROUOT, B. (1987). Presence of three pertussis toxin substrates and $G_o\alpha$ immunoreactivity in both plasma and granule membranes of chromaffin cells. *FEBS Lett.*, **215**, 339–344.

VITALE, N., MUKAI, H., ROUOT, B., THIERSE, D., AUNIS, D. & BADER, M. (1993). Exocytosis in chromaffin cells: possible involvement of the heterotrimeric GTP-binding protein G_o. *J. Biol. Chem.*, **268**, 14715–14723.

(Received March 21, 1994
Revised May 4, 1994
Accepted June 1, 1994)

Br. J. Pharmacol. (1994), **113**, 179–189

BMS-180560, an insurmountable inhibitor of angiotensin II-stimulated responses: comparison with losartan and EXP3174

[1]K.E.J. Dickinson, R.B. Cohen, S. Skwish, C.L. Delaney, R.P. Serafino, M.A. Poss, Z. Gu., D.E. Ryono, S. Moreland & J.R. Powell

Departments of Cardiovascular Biochemistry, Pharmacology, and Chemistry, Bristol-Myers Squibb Pharmaceutical Research Institute, P.O. Box 4000, Princeton, NJ 08543-4000, U.S.A.

1 This study compares the activity of BMS-180560 (2-butyl-4-chloro-1-[[1-[2-(2H-tetrazol-5-yl)phenyl]-1H-indol-4-yl]methyl]-1H-imidazole-5-carboxylic acid), an insurmountable angiotensin II (AII) receptor antagonist, with that of losartan and EXP3174 in functional and biochemical models of AII-receptor activation.

2 BMS-180560 selectively inhibited [^{125}I]-Sar^{1}Ile^{8}AII ([^{125}I]SI-AII) binding to rat aortic smooth muscle (RASM) cell and rat adrenal cortical AT_1 receptors ($K_i = 7.6 \pm 1.2$ and 18.4 ± 3.9 nM respectively) compared to adrenal cortical AT_2 receptors ($K_i = 37.6 \pm 1.3$ μM). The K_i values of BMS-180560 and EXP3174, but not losartan, varied as a function of the BSA concentration used in the assays, indicating that the diacid drugs bound to albumin.

3 BMS-180560 (3–300 nM) increased the K_D of SI-AII for RASM cell AT_1 receptors. Only at high concentrations of BMS-180560 (300 nM) were B_{max} values decreased.

4 BMS-180560 inhibited AII-stimulated contraction of rabbit aorta with a calculated $K_B = 0.068 \pm 0.048$ nM and decreased maximal AII-stimulated contraction at 1 nM BMS-180560 by 75%. In the presence of 0.1% BSA, a higher K_B value (5.2 ± 0.92 nM) was obtained. Losartan behaved as a competitive antagonist with a $K_B = 2.6 \pm 0.13$ nM. Contraction stimulated by endothelin-1, noradrenaline, KCl, or the TXA_2 receptor agonist U-46619 were unaffected by BMS-180560 (1 nM).

5 AII stimulated the acidification rates of RASM cells as measured by a Cytosensor microphysiometer with an EC_{50} of 18 nM. Losartan (30 nM) shifted the AII concentration-effect curves in a competitive manner whereas BMS-180560 (0.01 and 0.1 nM) decreased the maximum responses by 60 and 75% respectively. Inhibition by losartan and BMS-180560 could be reversed following washout although recovery took longer for BMS-180560.

6 In [^{3}H]-myoinositol-labelled RASM cells, losartan (30 and 200 nM), shifted the EC_{50} for AII-stimulated [^{3}H]-inositol monophosphate formation to higher values, with no change in the maximal response. By contrast, EXP3174 (0.1 to 1 nM) decreased the maximal response in a concentration-dependent manner (17–55%). BMS-180560 (3 and 10 nM) increased the EC_{50} for AII and decreased the maximum response by 30 and 80% respectively. The inhibition by EXP3174 and BMS-180560 could be reversed by inclusion of losartan (200 nM) indicating that the inhibition was not irreversible.

7 In conclusion, BMS-180560 is a potent, specific, predominantly competitive, reversible AII receptor antagonist, which displays insurmountable receptor antagonism. At concentrations of BMS-180560 which have no effect on receptor number, BMS-180560 produced insurmountable antagonism of AII-stimulated second messenger formation, extracellular acidification, and smooth muscle contraction.

Keywords: Angiotensin II receptor; vascular smooth muscle; [^{125}I]-Sar^{1}Ile^8 binding; adrenal cortex; insurmountable antagonism; losartan; BMS-180560

Introduction

The antiotensin II (AII) receptor contributes significantly to hypertension in man and therefore represents a key target for the design of anti-hypertensive agents. Recently a number of non-peptidic AII receptor antagonists have been described which provide a new class of anti-hypertensive agents (Timmermans *et al.*, 1991), and indicate the potential for small molecules to mimic the binding of an octapeptide to its receptor. The use of these non-peptide antagonists has provided evidence for subtypes of AII receptors (Chiu *et al.*, 1989; Whitebread *et al.*, 1989; Chang & Lotti, 1990). Thus, AII receptors which exhibit high affinity for losartan are designated AT_1 receptors, the classical AII receptors which modulate vascular tone and adrenal aldosterone secretion. The AT_1 receptor is coupled in most tissues via a G protein to phospholipase C activation, inositol phospholipid breakdown, and Ca^{2+} mobilization (Smith *et al.*, 1984; Griendling *et al.*, 1987; 1991). This receptor therefore represents the target site for potential anti-hypertensive and anti-hypertrophic agents. AT_2 receptors exhibit low affinity for losartan but high affinity for PD 123,177 (Wong *et al.*, 1990a; Dudley *et al.*, 1990). Both AT_1 and AT_2 receptors are present in different proportions on membranes derived from rat adrenal cortex and medulla (Chang & Lotti, 1990), whereas rat phaeochromocytoma PC-12W cells contain a homogeneous population of AT_2 receptors (Speth & Kim, 1990). The function of AT_2 receptors on PC12W cells (Webb *et al.*, 1992b) or other cells (Pucell *et al.*, 1991; Dudley *et al.*, 1991) is unknown.

Peptide analogues of AII have been described which function as antagonists of AII-mediated responses. Thus, Phe^4,Tyr^{8}AII exhibits classical competitive receptor antagonism and produces parallel shifts of the AII-stimulated

[1] Author for correspondence at Dept. of Cardiovascular Biochemistry.

concentration-response curves of smooth muscle preparations without suppressing the maximum response (Pendleton *et al.*, 1989). By contrast, sarcosyl substituted AII peptides including Sar^1,Leu^8AII inhibit AII-mediated contraction of rabbit aorta in an insurmountable manner; the maximum AII-stimulated contraction cannot be overcome by increasing concentrations of AII (Pendleton *et al.*, 1989; Liu *et al.*, 1992). The basis of this activity has been attributed to slow dissociation of these peptides from the AII receptor which results in a pseudo-irreversible inhibition (Pendleton *et al.*, 1989) or to ligand-mediated decreases in available AII receptors (Liu *et al.*, 1992).

A number of nonpeptidic AII receptor antagonists exhibit classical receptor antagonism. These include the earliest known examples of nonpeptide antagonists such as S-8307 (Wong *et al.*, 1988), and more recent disclosures such as losartan (Wong *et al.*, 1990a,c), SC 51366 (Olins *et al.*, 1992) and SKF 108566 (Edwards *et al.*, 1992). Schild slopes of antagonists such as losartan are close to unity (Wong *et al.*, 1990a), which indicates that the interaction of losartan with the AT_1 receptor represents a reversible, competitive reaction. Nonpeptidic AII receptor antagonists have also been described which display insurmountable inhibition of AII-stimulated contraction of vascular preparations. These include EXP3174, the di-acidic metabolite of DuP 753 (Wong *et al.*, 1990b), EXP3892 (Wong & Timmermans, 1991), DuP 532 (Wong *et al.*, 1991), L-158,809 (Chang *et al.*, 1992), SR 47436 (Cazaubon *et al.*, 1993) and GR 117289 (Robertson *et al.*, 1992). It is unlikely that the insurmountable behaviour relates to irreversible binding of antagonists since losartan has been shown to attenuate the EXP3174-induced decrease in maximum AII-stimulated contractions (Wong & Timmermans, 1991). The basis of this activity is currently unknown but it may contribute to the long duration of action of these compounds *in vivo*. No direct evidence for the location of the sites responsible for insurmountable antagonism have so far been presented although most models implicate the AII receptor. The present paper characterizes the pharmacological properties of BMS-180560, a di-acidic AII receptor antagonist which produces long-lasting anti-hypertensive effects in Na^+-depleted SHR, and potently antagonizes AII pressor responses in conscious Sprague Dawley rats (Poss *et al.*, 1993). The present study compares the interaction of BMS-180560, losartan and EXP3174 with AT_1 receptors using functional contraction measurements, binding techniques, and biochemical determinations of AII-receptor activation. A preliminary account of these findings was presented to the British Pharmacological Society (Dickinson *et al.*, 1992).

Methods

Membrane preparation

Rat adrenal cortex Rats were killed by CO_2 asphyxiation, the adrenals were removed, and the cortex separated from the medulla at 4°C. The cortices were placed in ice-cold buffer A (0.2 M sucrose, 1 mM EDTA, 10 mM Tris-HCl pH 7.4), and homogenized in 10-volumes of buffer A at 4°C with a Brinkman Polytron homogenizer (setting 9.3 × 8 s). The homogenate was centrifuged at 1000 *g* for 10 min at 4°C, the supernatant was re-centrifuged at 100,000 *g* for 1 h at 4°C. The pellet was suspended in 50 mM Tris-HCl pH 7.4, 5 mM $MgCl_2$ (2.5 vol of buffer/original wet weight), by gentle homogenization in a Potter-Elvehjem glass/teflon homogenizer. Aliquots (5 ml) of the membrane preparation were frozen at a protein concentration of 0.1 mg protein ml^{-1} and stored at −80°C until use.

Rat aortic smooth muscle cells RASM cells were cultured at 37°C in T-75 flasks under humidified 95% air/5% CO_2 in HEPES-buffered Dulbecco's modified Eagle's medium (DMEM) containing 10% foetal calf serum, 50 u ml^{-1} penicillin, 50 μg ml^{-1} streptomycin (Gibco Labs). Following the attainment of confluence (5–7 days), cells were trypsinized with 2 ml 0.25% trypsin/1 mM EDTA and cells collected into buffer (0.1 mM phenylmethylsulphonyl fluoride, 10 μg ml^{-1} soy bean trypsin inhibitor, 20 mM HEPES pH 7.4, dissolved in DMEM) at a concentration of $3–4 \times 10^5$ cells ml^{-1}. The cell suspension was washed with this buffer, and homogenized in 50 mM Tris HCl pH 7.4, 1 mM EGTA, 10 mM $MgCl_2$, 0.24 TI units ml^{-1} aprotinin, and 0.1 mg ml^{-1} 1,10-phenanthroline with a Brinkmann Polytron homogenizer (setting 7, 3 × 6 s). The homogenate was passed through 2 layers of cheesecloth, and centrifuged at 40,000 *g* for 20 min at 4°C. The supernatant was discarded, and the membranes resuspended in buffer and washed three times. The pellet was resuspended in this buffer at a concentration of 0.2–0.8 mg protein ml^{-1}. The cell homogenate was stored in 1 ml aliquots at −80°C until use.

[^{125}I]-Sar^1,Ile^8 angiotensin II binding

Assays were conducted in a total volume of 250 μl in tubes arranged in microtitre plate format (Marsh Biomed Corp). The incubation mixture contained 50 μl [^{125}I]-SI-AII (80–200 pM, 70,000–180,000 c.p.m.); 25 μl displacing drug, or AII to define non-specific binding (1 μM); and incubation buffer. Binding to RASM cell membranes was conducted in the following assay buffer: 50 mM Tris-HCl pH 7.4, 5 mM $MgCl_2$, 0.1% bovine serum albumin, 1 mM PMSF, 0.24 TI units ml^{-1} aprotinin, and 0.1 mg ml^{-1}, 10-phenanthroline (Cohen *et al.*, 1993). Binding to rat adrenal cortex (RAC) membranes was routinely conducted in the following assay buffer: 50 mM Tris-HCl pH 7.4, 5 mM $MgCl_2$, and 0.22% BSA. In some cases the concentration of BSA was changed to 0.07%, or 0.01%. The binding reaction was initiated by the addition of 100 μl membranes (7–12 μg protein) diluted in incubation buffer. The tubes were incubated at 37°C (RASM cell membranes) or 22°C (RAC membranes) for 2 h with continuous shaking (Easyshaker, SLT-Labinstruments, A-5082 Grodig, Austria). Bound and free radioligand were separated by simultaneous filtration on a Tomtec cell harvester in combination with a filtermat B which had been pre-soaked for 1 h in 0.1% polyethyleneimine (PEI) in order to reduce non-specific binding. The filtermat was rinsed of excess PEI during a pre-wash cycle, and the membranes were filtered and washed with 150 mM NaCl, 5 mM Tris-HCl, pH 7.4 at 4°C. The filtermat was removed and microwaved, membrane-side up, at full power for 3 × 2 min in a microwave oven. The dried filtermat was placed in a sample bag, a sheet of Meltilex solid scintillant wax placed on the filtermat and the Meltilex sheet melted into the mat using a T-Tray Heat-Sealer (Wallac, Pharmacia). The impregnated sheet was counted in a Betaplate liquid scintillation counter (L.K.B. Pharmacia, T-tray compatible Model 1205) at 60% efficiency. Protein assays were performed on the membrane preparation using B.C.A. reagent (Pierce, Rockford, IL) with BSA as standard.

Measurements of cell activation using Cytosensor microphysiometer

The Cytosensor microphysiometer (Molecular Devices, Menlo Park, CA, U.S.A.) measures extracellular acidification rates of cells with silicon pH-sensitive sensors (Owicki *et al.*, 1990). Upon activation of cells with agonists, the extracellular acidification rate increases in a time and concentration-dependent manner. RASM cells were cultured for 8 h in the presence of foetal bovine serum (10%), the serum was removed and after a further 16 h cells were placed in the microphysiometer and perfused with media (Dulbeccos MEM without $NaHCO_3$) at 37°C for 1 h prior to drug addition. Acidification rates were monitored for 30 s every min and rates plotted continuously against time. RASM cells

were stimulated with the stated concentrations of AII for 10 s followed by a change of perfusate to media. Short periods of AII application were necessary because longer stimulation protocols resulted in desensitized responses. Using this protocol, peak increases in acidification rates were obtained in response to AII. AII was added every 15 min to a maximum concentration of 10 μM. Antagonists BMS-180560 and losartan were preincubated with cells for 15–30 min prior to AII addition. Peak height was used as a measure of the cellular activation. Maximum responses to AII routinely represented 130% of basal acidification rate (normalized to be 100%). Results reported are the means (± s.e.mean) of at least three determinations with different passage numbers.

Measurement of phosphoinositide turnover

RASM cells were cultured in 35 mm wells, and labelled to isotopic equilibrium with [^{3}H]-myoinositol (2 μCi ml^{-1}) in inositol-free medium for 48 h. Cell monolayers (approximately 90% confluent) were washed, and incubated for 15 min at 37°C in a medium containing 10 mM LiCl in the absence or presence of AII antagonist. The cells were stimulated with agonist for 30 min, the media removed, and 2 mM EDTA at 100°C was added to the cell monolayer to disrupt cell integrity and release soluble inositol phosphates (IP). The cells and supernatant were removed, re-boiled, and centrifuged. The supernatant was applied to a Dowex AG-1X8 anion exchange column, the labelled inositol, glycerophosphoinositol, and inositol 1-, 2-, and 3-phosphates fractionated essentially as described by Berridge (1983) and aliquots counted in a liquid scintillation counter using Packard Ultima Gold XR scintillation fluid (Packard Inst. Co., Meriden, CT, U.S.A.).

Force determinations in vascular smooth muscle

Male New Zealand white rabbits (2–3 kg) were killed by i.v. injection of Nembutal and the thoracic aorta was removed and cleaned of connective tissue. Circumferential strips (3.5–5.0 mm wide) were mounted for isometric force recording as described in detail elsewhere (Webb *et al.*, 1992a). In brief, cumulative concentration-response curves were elicited by agonists (AII, ET-1, KCl, noradrenaline, and U-46619) in the presence and absence of test compound. Antagonists were preincubated with the tissue for 20 min prior to addition of agonists. The data are plotted as the mean (± s.e.mean) of at least 4 tissues from different animals. EC_{50} values were calculated by linear regression analysis. K_B values for competitive antagonists were calculated from the following equation: $K_B = BMS/[EC_{50}'/EC_{50})-1]$, where BMS represents the concentration of compound tested, EC_{50}' is the EC_{50} value determined in the presence of BMS, and EC_{50} is the EC_{50} value determined in response to AII alone. For insurmountable antagonists, the $K_{B\ app}$ values were calculated by double-reciprocal regression analysis: $K_{B\ app} = BMS/(slope-1)$ where the slope is obtained by regression analysis of 1/[A] versus 1/[A'] with [A] and [A'] denoting the equiactive agonist concentrations in the absence and presence of BMS, respectively (Tallarida & Jacob, 1979).

Drugs

[^{125}I]-Sarcosine^{1}Ile^{8}angiotensin II ([^{125}I]-SI-AII, 2200 Ci mmol^{-1}) was obtained from NEN Research Products (Boston, MA, U.S.A.), and [^{3}H]-myoinositol (94 Ci mol^{-1}) was from Amersham (Arlington Hts, IL, U.S.A.). Angiotensin II and SI-AII were from Peninsula Labs (Belmont, CA, U.S.A.), and cell culture reagents from Gibco (Rockville, MD, U.S.A.). Bovine serum albumin, lithium, sodium, magnesium and potassium chlorides, noradrenaline, sucrose, EDTA, EGTA, phenylmethylsulphonylfluoride (PMSF), polyethyleneimine, aprotinin, 1,10-phenanthroline, HEPES, and Tris were from Sigma Chemical Co (St. Louis, MO, U.S.A.). Dowex AG-1X8 was from Biorad (Richmond, CA, U.S.A.). U-46619 (11α, 9α-epoxymethano-PGH$_2$) was purchased from Cayman Chemical Co. (Ann Arbor, MI, U.S.A.) and endothelin-1 from Peptides International (Louisville, KY, U.S.A.). All other chemicals were from Fisher (Pittsburgh, PA, U.S.A.) and were reagent grade. Losartan, EXP3174 and BMS-180560 were synthesized in Department of Chemistry, Bristol-Myers Squibb Pharmaceutical Research Institute.

Results

Figure 1 shows the structures of losartan, its metabolite EXP3174 and BMS–180560 which differs from the biphenyl compounds losartan and EXP3174 in having an indole linker between the imidazole and phenyl tetrazole moieties. The chemical synthesis of BMS-180560 and the *in vivo* pharmacological activity of BMS-180560 and its prodrugs are described elsewhere (Poss *et al.*, 1994).

Binding studies

The ability of losartan and BMS-180560 to inhibit [^{125}I]-SI-AII binding to rat adrenal cortical, and aortic smooth muscle cell membranes was compared. Figure 2 shows the competition curves, and Table 1 shows the K_i values obtained under standard assay conditions. Competition curves for losartan and BMS-180560 binding to adrenal AII receptors were biphasic and indicative of binding to two populations of sites (Figure 2a). A high affinity population (AT_1 receptors), and a low affinity population (AT_2 receptors) represented 75% and 25% of the labelled sites respectively. Both losartan and BMS-180560 were selective for the AT_1 receptors relative to the AT_2 receptors (9,000 and 2,000 fold respectively). Both antagonists generated competition curves with RASM cell membranes which were monophasic, with slope factors which were close to unity indicating a homogeneous, high affinity, population of AT_1 receptors (Figure 2b, Table 1). The K_i values obtained for losartan and BMS-180560 for vascular

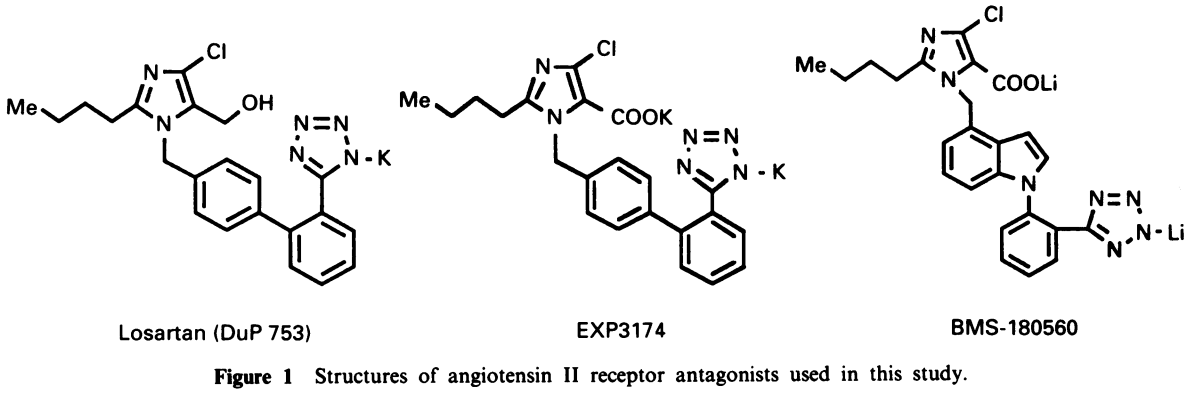

Figure 1 Structures of angiotensin II receptor antagonists used in this study.

Table 1 Inhibition constants (K_i) of losartan and BMS-180560 for rat adrenal and smooth muscle cell AII receptors

Compound	K_i values (nM) Adrenal AT_1	Adrenal AT_2	RASM cell AT_1	n_H
Losartan	9.0 ± 3.2*	85,800 ± 8.700*	16.2 ± 4.6	0.91 ± 0.03
BMS 180560	18.4 ± 3.9	37,600 ± 13,000	7.6 ± 1.2	0.99 ± 0.17

n_H = slope factor of competition curves for RASM cell binding. *Slope factor constrained to $n_H = 1$ for two-site analysis, which yielded the proportions of AT_1 and AT_2 sites of 75 ± 1, and 25 ± 1% respectively. K_i values were computed from IC_{50} values using the equation of Cheng & Prusoff (1973). Results show mean (±s.e.mean) for 3–10 experiments.

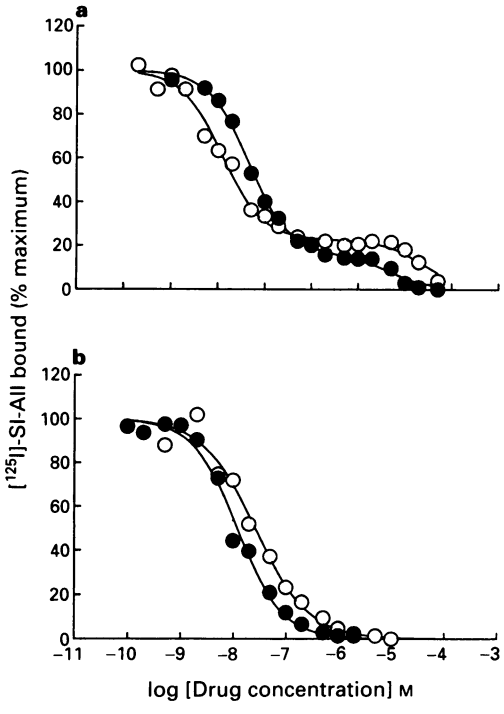

Figure 2 Competition curves of losartan (○) and BMS-180560 (●) binding to rat adrenal cortical (a) and RASM cell (b) membranes. Membranes were incubated with [^{125}I]-SI-AII (0.2 nM) in the presence of the shown concentrations of antagonists. Specific binding, calculated as % maximum, has been plotted against antagonist concentration. The lines are computer generated best fit to a one or two site analysis where slope factors for both sites are constrained to unity. The curves are representative of experiments performed 3–10 times.

AII receptors (16 and 18 nM) were similar to those obtained for adrenal cortical receptors (9 and 18 nM).

Recent reports indicate diacid AII receptor antagonists bind avidly to serum proteins, whereas losartan show less activity in this regard (Chiu *et al.*, 1991). Since this property reduces the free drug able to interact with the AII receptor, we have investigated the influence of BSA concentration on the calculated K_i of BMS-180560. Table 2 shows that reduction of BSA in the assay buffer from 0.22 to 0.07% decreased the K_i of BMS-180560 for adrenal AT_1 receptors by 3.4 fold. Decreasing the BSA to lower values (0.01%) decreased the K_i by a further 6.8 fold to a value of 0.8 nM. Similar results were obtained for EXP3174 which exhibited a K_i of 11.4 ± 2.6 nM in 0.22% BSA and 1.9 ± 1.4 nM in 0.07% BSA ($n = 4$). Losartan was insensitive to the BSA concentration in the assay over the concentration-range tested, and K_i values obtained with 0.01% BSA were not significantly different from those determined in 0.22% BSA (Table 2). Similar findings were observed with RASM membranes, where the K_i for losartan was 17 ± 1.4 nM ($n = 3$) in 0.01% BSA, and 16.2 ± 4.6 nM ($n = 3$) in 0.1% BSA.

The characteristics of losartan and BMS-180560 binding to the rat vascular smooth muscle cell AT_1 receptors were compared. Saturation binding isotherms were conducted in the absence or presence of increasing concentrations of losartan or BMS-180560, and K_D and binding site maxima (B_{max}) values calculated in order to define shifts in affinity (competitive inhibition) or decreases in B_{max} values, with no change in K_D (non-competitive inhibition). Time course studies indicated that equilibrium binding of [^{125}I]-SI-AII was reached within 120 min either in the absence or presence of 3–30 nM BMS-180560 (data not shown). In order to obtain accurate assessment of the B_{max} values we have used tracer concentrations of radioligand and saturated the binding sites with unlabelled SI-AII. Data analysis assumed that tracer radioligand and SI-AII bind to the same population of sites with similar affinities. This assumption is valid since K_D and B_{max} values using exclusively [^{125}I]-SI-AII ($K_D = 0.3 \pm 0.04$ nM, $B_{max} = 2{,}860 \pm 700$ fmol mg^{-1} protein, $n = 4$) were similar to values reported in Table 3.

Table 2 Effect of BSA concentration on the inhibition constants of BMS-180560 and losartan for rat adrenal cortical AT_1 receptors

Drug	K_i values (nM) 0.01% BSA	0.07% BSA	0.22% BSA
BMS-180560 AT_1	0.8 ± 0.1	5.4 ± 2.0	18.4 ± 3.9
Losartan AT_1	9.8 ± 0.1	NT	9.0 ± 3.2

K_i values (nM) were calculated from competition curves determined in the presence of the stated concentration of BSA. Results show mean ± s.e.mean K_i values of drugs for AT_1 receptors derived from 3–6 experiments.

The presence of losartan resulted in shifts to the right of the SI-AII saturation binding isotherms with progressive increases in K_D values (see Table 3), but no decreases in the maximum number of binding sites. Figure 3a shows the Scatchard plots of representative data where losartan caused successive decreases in the slopes (indicative of increased K_D values for SI-AII), with no decreases in the binding site maxima (defined by the lines' intercept with the abscissa). These data are consistent with reversible competitive interaction of losartan with the AT_1 receptor. These data were analysed by the method of Arunlakshana & Schild (1959) in order to define a binding K_B value for losartan. The calculated Schild slope was 1.07 ± 0.06 and the K_B was 10 ± 2.9 nM, which is in good agreement with the K_i of 16.2 nM determined from competition curves.

BMS-180560 (3–100 nM) also shifted the SI-AII saturation binding isotherms to the right and increased the K_D of SI-AII. This is shown in Figure 3b as a successive decrease in the slopes of the Scatchard plots. At low concentrations of BMS-180560 (3–30 nM), there was no significant depression of the B_{max} values (Table 3), which indicated that the drug acted as a competitive inhibitor of SI-AII binding. Similar results were obtained with membranes either pre-incubated with BMS-180560 for 30 min or co-incubated with the antagonist (data not shown). At a higher concentration of BMS-180560 (100–300 nM), there was a 10 to 20 fold in-

crease in the K_D for SI-AII, and a decrease in the B_{max} value at the highest BMS-180560 concentration. Similar results were obtained using exclusively [^{125}I]-SI-AII to saturate the binding sites (data not shown). These data suggest that BMS-180560 interacts competitively at low concentrations but may exhibit mixed (competitive and non-competitive) inhibition at higher concentrations. The Schild slope of these binding data which also incorporates the higher drug concentrations was 0.89 ± 0.06, and the calculated K_B value from this plot was 9.0 ± 4.6 nM, which is in good agreement with the K_i of 7.6 nM calculated from competition curves.

Table 3 Effect of losartan and BMS-180560 on SI-AII binding to RASM cell membranes

Drug	*Conc.* (nM)	B_{max} (% control)	n	K_D (nM)	n
Losartan	0	100		0.20 ± 0.04	4
	5	110 ± 12	3	0.28 ± 0.04	3
	20	119 ± 10	4	0.84 ± 0.33	4
	50	121 ± 9	3	1.06 ± 0.27	3
BMS-180560	0	100		0.20 ± 0.04	4
	3	91	2	0.32	2
	10	97 ± 3	3	0.39 ± 0.05	3
	30	91 ± 3	5	0.86 ± 0.05	5
	100	88 ± 7	3	2.13 ± 0.25	3
	300	53 ± 8	3	4.0 ± 0.10	3

RASM membranes were pre-incubated for 15 min at 37°C with the stated concentrations of antagonists, and incubated with ligand [^{125}I]-SI-AII (0.2 nM) in the presence of increasing concentrations of SI-AII. Specific binding was calculated and analysed by computer assisted iterative curve fitting to obtain B_{max} and K_D values. B_{max} values have been normalized to % control which was $2,840 \pm 430$ fmol mg^{-1} protein. Results show mean ± s.e.mean of the stated number of experiments.

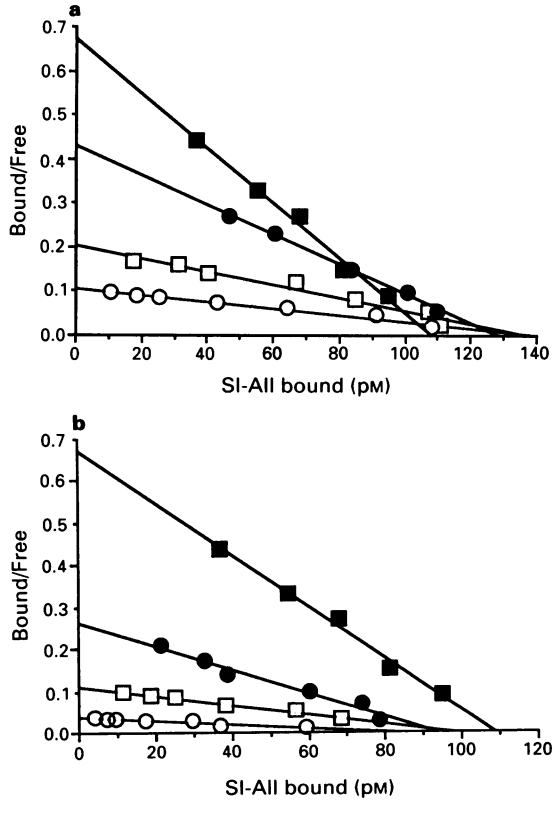

Figure 3 Scatchard plots of SI-AII binding to RASM cell membranes in the absence (■) or presence of 5 (●), 10 (□), or 50 (○) nM losartan (a) and 10 (●), 30 (□), or 100 (○) nM BMS-180560 (b). RASM membranes were pre-incubated for 15 min at 37°C with antagonists and incubated with radioligand [^{125}I]-SI-AII (0.1 nM) in the presence of increasing concentrations of SI-AII. Specific binding was determined using computer assisted LIGAND software program (Munson & Rodbard, 1980) and the data has been graphically displayed according to Scatchard. Results show representative data from experiments presented in Table 3.

Vascular smooth muscle contraction

The effects of losartan and BMS-180560 on AII-stimulated contractile responses in rabbit aortic rings are shown in Figure 4. Losartan (3 to 100 nM) produced parallel shifts to the right of the AII dose-response curve and did not affect maximum contractile responses (Figure 4a). The calculated K_B was 2.6 ± 0.13 nM. Data were also generated in the presence of 0.1% BSA in order to reproduce conditions used for the binding studies and phosphoinositide turnover measurements (see below). The Schild slope of these data was -0.9, and the calculated K_B was 6.7 ± 1.6 nM which was little different from that determined in the absence of BSA. BMS-180560 (0.1 to 1 nM) produced progressive shifts in the AII dose-response curve, and decreased the maximum AII-stimulated response by 25–75% (Figure 4c). Since AII was unable to overcome the inhibition by BMS-180560 the antagonism can be defined as insurmountable. The calculated apparent K_B was 0.068 ± 0.048 nM in the absence of BSA (Figure 4c) which was similar to the apparent K_B of 0.058 ± 0.016 nM calculated for EXP3174 (data not shown). By contrast, the K_B generated for BMS-180560 in the presence of BSA (5.2 ± 0.92 nM) was 76 fold greater (Figure 4d) and the insurmountable behaviour was maintained.

Figure 5 shows the specificity of BMS-180560 for AII receptors on rabbit aortic rings. At 1 nM, a concentration producing profound inhibition of AII-mediated contractions, BMS-180560 produced no effect on contractions elicited by KCl, noradrenaline, or the thromboxane A_2 receptor agonist, U-46619. The slight effect of BMS-180560 on endothelin-mediated contractions was attributed to differences in tissue sensitivity to ET. These data suggest BMS-180560 is a specific AII receptor antagonist.

Vascular smooth muscle cell activation determined with a Cytosensor microphysiometer

Exposure of RASM cells to AII produced a time and concentration-dependent increase in the extracellular acidification rates which reflects cellular activation (Owicki *et al.*, 1990). Since prolonged stimulation of cells (15 min) with AII desensitized the cells to subsequent stimulation, cumulative concentration-response curves were obtained with short application times. Stimulation of cells with AII for 10 s increased the extracellular acidification rates to a peak level (130% of basal rates after 2 min) which declined to basal rates during the next 12 min. This protocol provided reproducible responses to AII and allowed concentration-response curves to be obtained. Figure 6 shows the AII-stimulated increase in RASM extracellular acidification rates. The EC_{50} for AII was 18 ± 13 nM ($n = 10$) in control cells and in the presence of losartan (30 nM) the EC_{50} was increased 8 fold with no significant change in the maximum response, indicating simple competitive interaction. Assuming a Schild slope of unity (see above), the calculated K_B for losartan was 2.5 ± 1.0 nM, $n = 3$, which correlated with its potency as an inhibitor of rabbit aortic smooth muscle contraction ($K_B = 2.6$ nM). BMS-180560 at 0.01 nM had little effect on the EC_{50} for AII ($EC_{50} = 22$ nM) whereas 0.1 nM BMS-180560 increased the EC_{50} to 940 nM. The maximum responses to AII were decreased by 60% and 75% for both concentrations of BMS-180560 indicating insurmountable receptor antagonism. In these experiments BMS-180560 was more potent as an inhibitor of AII-stimulated cellular acidification than of contractile responses or phosphoinositide turnover (see below). These findings may relate to

the short AII stimulation protocol which was used for the cell based studies.

In order to compare the rates of dissociation of losartan and BMS-180560 from the RASM cells, cells were stimulated with AII in the absence of antagonist, and following exposure and washout of losartan and BMS-180560. Figure 7 shows the acidification rate of cells stimulated for 10 s initially, stimulated in the presence of losartan or BMS-180560, and stimulated after washout of drugs for 5 and 38 min. In the presence of losartan (50 nM) AII responses were decreased by 40% relative to control AII stimulation performed at the same time. BMS-180560 (0.1 and 1 nM) decreased AII responses by 22% and 100% respectively. Following washout of drugs for 5 min, AII responses to losartan had recovered to greater than control levels, probably reflecting protection of the AII receptors from desen-

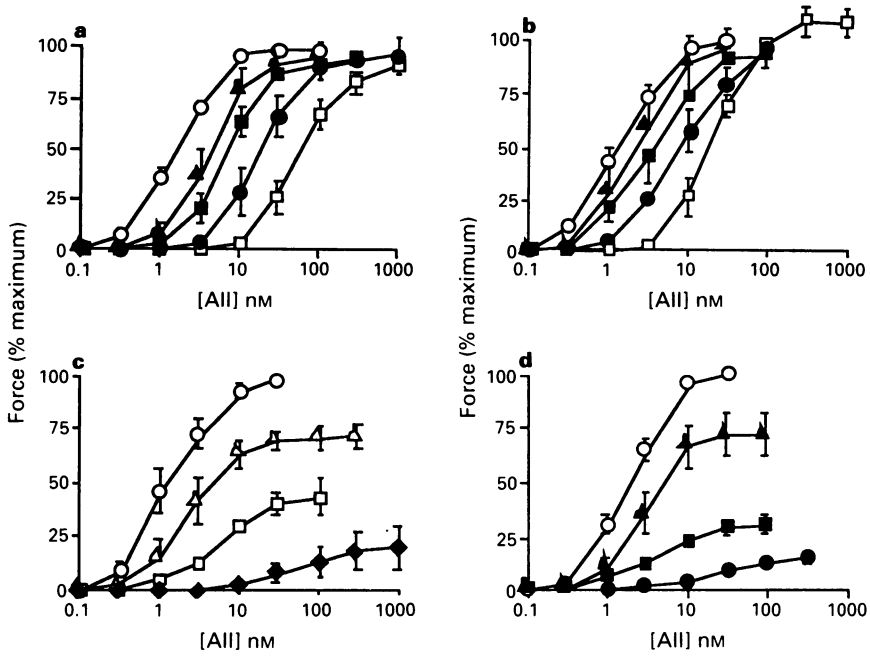

Figure 4 Effect of losartan and BMS-180560 on AII-stimulated contractile responses in rabbit aortic rings. Cumulative concentration-response curves elicited by AII were determined in the absence (○) or presence of: 3 (▲), 10 (■), 30 (●), or 100 (□) nM losartan (a,b). AII concentration-response curves were also obtained in the absence (○) or presence of 0.1 (△), 0.3 (□), 1 (◆), 3 (▲), 10 (■), or 30 (●) nM BMS-180560 (c,d). Experiments were conducted in the absence (a,c) or presence (b,d) of 0.1% BSA. Data shown are mean ± s.e.mean of at least 4 aortae from different rabbits.

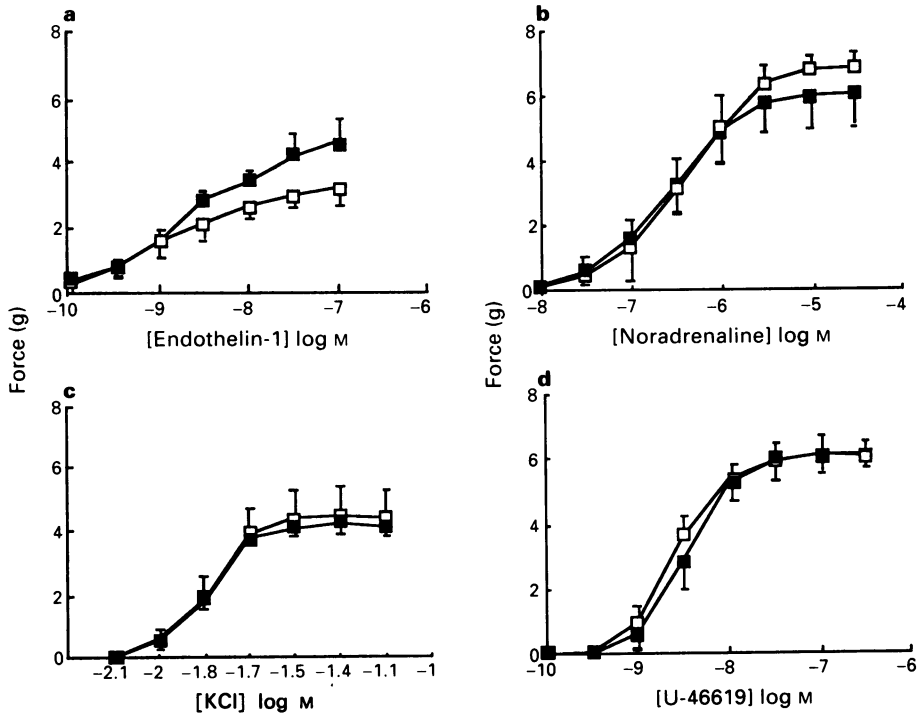

Figure 5 Effect of BMS-180560 on contractions elicited by endothelin-1 (a), noradrenaline (b), KCl (c), and U-46619 (d) in rabbit aortic rings. Aortic rings were exposed to the stated concentration of agonist in the absence (□) or presence (■) of 1 nM BMS-180560. Results are plotted as mean ± s.e.mean of 4 determinations.

sitization. Thus, AII-stimulated responses of control cells were decreased 40–45% during the course of this experiment. The inhibition of AII-stimulated responses by BMS-180560 (0.1 and 1 nM) were maintained following 5 min washout. More prolonged washing (38 min) was necessary in order to recover AII-stimulated responses following BMS-180560 treatment. This recovery was complete for cells exposed to 0.1 nM BMS-180560 and partial (70%) for cells treated with 1 nM BMS-180560. These findings indicate that losartan dissociates more rapidly from RASM cell AII receptors than the insurmountable antagonist BMS-180560 but both drugs can be considered reversible antagonists of AII-mediated responses.

Phosphoinositide metabolism

The ability of losartan and BMS-180560 to inhibit AII-stimulated phosphoinositide turnover was examined in RASM cells labelled to isotopic equilibrium with [^{3}H]-myoinositol. In the presence of LiCl (to inhibit inositol monophosphatase), AII (1 μM) produced a time-, and concentration-dependent increase in inositol mono-, bis-, and tris-phosphate which was linear for 0–40 min (data not shown). The IP_2/IP_3 fraction was 35–45% of the IP_1 fraction.

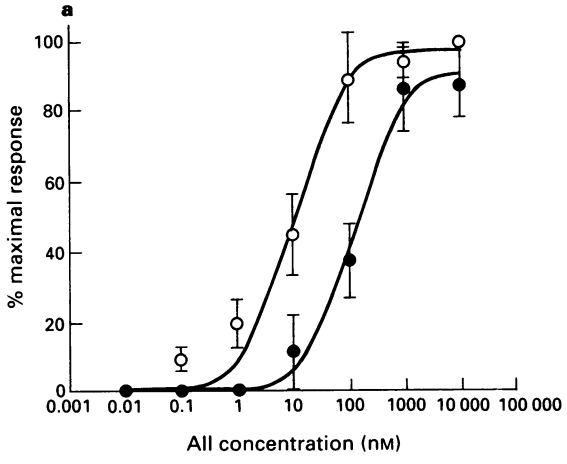

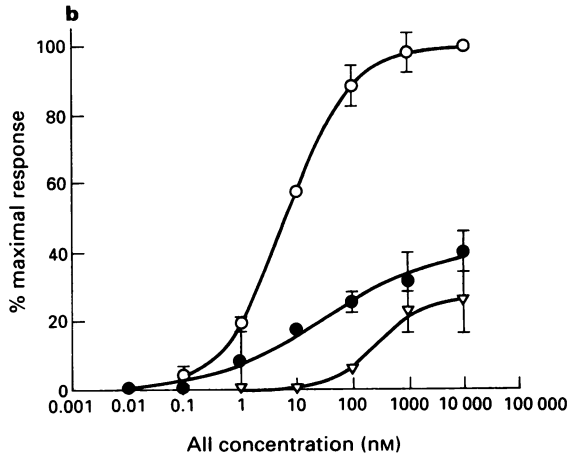

Figure 6 Effects of losartan and BMS-180560 on AII-stimulated increase in extracellular acidification rates of RASM cells. (a) RASM cells were preincubated for 20 min with media (○) or 30 nM losartan (●) and stimulated with the stated concentration of AII for 10 s. (b) Cells were preincubated with media (○), 0.01 nM (●), or 0.1 nM (▽) BMS-180560 followed by AII. Rates of extracellular acidification were measured with a Cytosensor microphysiometer. Peak increases in rates were computed, normalized to the maximum AII-stimulated increase in acidification rates, and plotted against the AII concentration. Results show mean ± s.e.mean of duplicate experiments which were performed three times.

The EC_{50} for AII-stimulated IP_1 response was 27 ± 6.9 nM ($n = 6$) and similar values were obtained for the increases in IP_2/IP_3 (data not shown). The maximum stimulation by AII varied somewhat with passage number, but routinely represented a 10 to 40 fold stimulation above basal IP_1 levels. The effect of losartan on AII-stimulated IP_1 formation in RASM cells is shown in Figure 8a. Losartan (30 and 200 nM) shifted the AII concentration-effect curve to the right and increased the EC_{50} for AII by 3 and 7 fold respectively. The effect of losartan was surmountable since higher concentrations of AII were able to overcome the inhibition by losartan, and the maximum AII-stimulated increase in IP_1 was similar in the absence or presence of antagonist. In marked contrast to the data obtained with losartan, its acid metabolite EXP3174 decreased the maximal AII-stimulated IP_1 formation in a concentration-dependent manner (Figure 8b). At a concentration of 1 nM EXP3174, and in the absence of BSA, maximal AII-stimulated responses were decreased by 50–60%. Thus, the insurmountable activity of EXP3174 (Wong & Timmermans, 1991) can be monitored at the level of second messanger formation.

The effects of BMS-180560 on AII-stimulated IP_1 formation is shown in Figure 8c. At a concentration of 3 nM and in the presence of 0.1% BSA, BMS-180560 produced somewhat variable effects on the AII concentration-response curve. Mean data demonstrated a small rightward shift of the curve and a 30% decrease in the maximum response. A higher concentration of BMS-180560 (10 nM) decreased the maximum IP_1 response by 80%. Losartan (100 nM) and BMS-180560 (10 nM) were used for these studies at equi-effective inhibitory concentrations such that at 10 nM AII, there was 85–90% inhibition of IP_1 formation. Increasing the AII concentration overcame the inhibition by losartan, but it was unable to overcome the inhibition by BMS-180560. Thus the inhibitory activity of BMS-180560 on IP_1 formation may be classified as insurmountable. The BMS-180560-induced decrease in maximal AII-stimulated IP_1 formation in RASM cells was quantitatively similar to that observed for AII-stimulated contraction of rabbit aortic smooth muscle (compare Figures 4d and 8c). Thus, in the presence of BSA, 3 and 10 nM BMS-180560 decreased maximum contractile force by 30 and 70% respectively, compared to 30 and 80% decreases in IP formation.

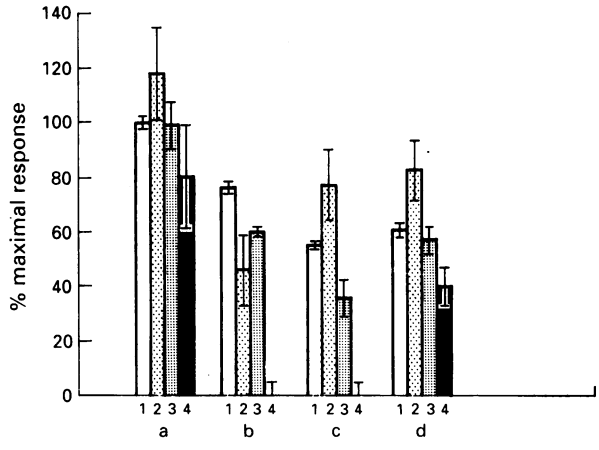

Figure 7 Reversal of losartan and BMS-180560 mediated inhibition of AII-stimulated RASM cell acidification. RASM cells were stimulated for 10 s with 100 nM AII in the absence (1) or presence of: 50 nM losartan (2), 0.1 nM BMS-180560 (3), or 1 nM BMS-180560 (4). (a) Initial responses to AII; (b) cells preincubated with drugs for 30 min and restimulated with AII; (c) drugs removed from the perfusate cells washed for 5 min and restimulated with AII; (d) cells washed for 38 min and restimulated with AII. Acidification rates were measured and normalized to rates obtained initially. Results are the mean ± s.e.mean of duplicate experiments which were performed 4 times.

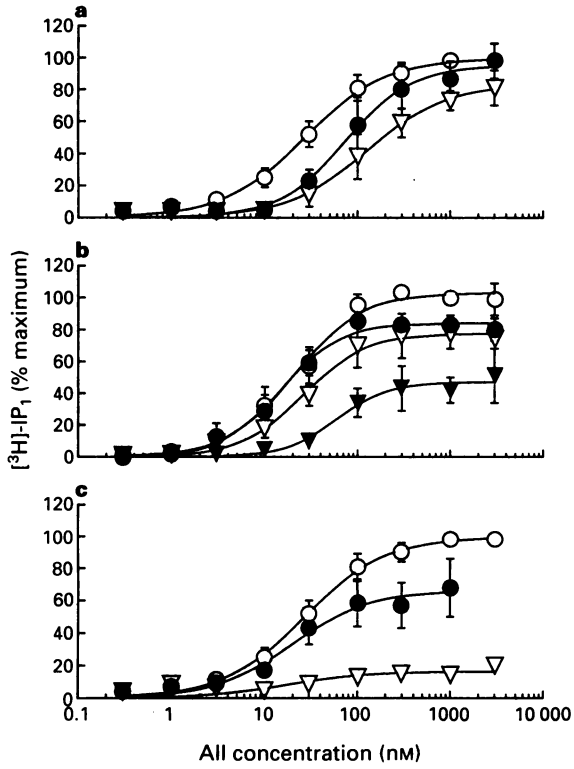

Figure 8 Effect of losartan, EXP3174, and BMS-180560 on AII-stimulated IP_1 formation in RASM cells. [^{3}H]-myoinositol-labelled RASM cell monolayers were incubated in the absence (○) or presence of 30 (●), and 200 (▽) nM losartan (a), or 0.1 (●), 0.3 (▽), or 1 (▼) nM EXP3174 (b) or 3 (●) and 10 (▽) nM BMS-180560 (c) for 15 min at 37°C, and stimulated for 30 min with increasing concentrations of AII. BSA (0.1%) was included in the experiments performed with losartan and BMS-180560. [^{3}H]-IP_1 was extracted as described in Methods and separated by anion exchange chromatography. IP_1 levels were normalized to % maximal stimulation produced by 1 μM AII. Results show mean curves ± s.e.mean of 4–6 determinations obtained with cells from different passage numbers.

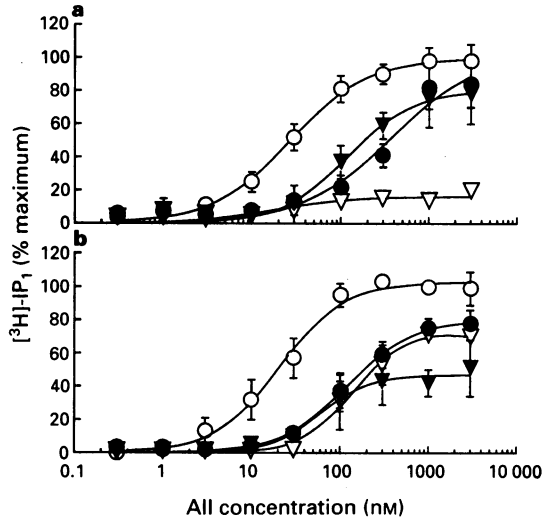

Figure 9 Reversal of BMS-180560 and EXP3174-mediated insurmountable inhibition of AII-stimulated IP_1 formation in RASM cells by losartan. [^{3}H]-myoinositol-labelled RASM cell monolayers were incubated in the absence (○) or presence of: 10 nM BMS-180560 (▽), 200 nM losartan (▼) and 200 nM losartan + 10 nM BMS-180560 (●) (a); or 200 nM losartan (●), 1 nM EXP3174 (▼), and 200 nM losartan + 1 nM EXP3174 (▽) (b) for 15 min at 37°C. For the combination experiment, cells were incubated with losartan for 15 min at 37°C, followed by BMS-180560 for 15 min. Cells were then stimulated with the stated concentrations of AII. [^{3}H]-IP_1 was extracted as described in Methods and separated by anion exchange chromatography. IP_1 levels were normalized to % maximal stimulation produced by 1 μM AII. Results show mean curves ± s.e.mean of 4–6 determinations obtained with cells from different passage numbers.

We have examined whether the inhibition by EXP3174 and BMS-180560 was irreversible by attempting to attenuate the antagonist-mediated inhibition by co-administration of losartan. Figure 9 shows that losartan was able to reverse the insurmountable inhibition by BMS-180560 and EXP3174. Thus, the maximum AII-stimulated IP_1 response was 20% of control in the presence of 10 nM BMS-180560, and 80% of control in the presence of 200 nM losartan (Figure 9a). The combination increased the AII-stimulated response to values not significantly different from those of losartan alone. Similarly, losartan reversed the EXP3174-mediated inhibition of AII-stimulated IP_1 formation to values not different from losartan alone.

Discussion

This study compared the interactions of the competitive AII receptor antagonist, losartan and the insurmountable antagonists, BMS-180560 and EXP3174 with the AT_1 receptor. Losartan and BMS-180560 were potent inhibitors of [^{125}I]-SI-AII binding to rat adrenal cortex and vascular AT_1 receptors with K_i values of 9 and 16 nM for losartan, and 18 and 7 nM for BMS-180560 respectively. The value obtained for BMS-180560 was dependent on the concentration of BSA in the assay buffer since lowering the BSA concentration to 0.01% decreased the K_i by 23 fold. By contrast, the K_i of losartan was little affected by lowering the BSA concentration whereas its structurally related acid analogue EXP3174, exhibited an 8 fold decrease in K_i in low (0.07%) BSA. These findings were quantitatively similar to those reported by Chiu *et al.* (1991). This property probably relates to the physicochemical characteristics of these molecules. Thus, it has been suggested that the presence of a di-acidic function in the AII receptor antagonist molecule may be responsible for protein binding. Chiu *et al.* (1991) demonstrated that 99% of the diacid DuP 532 bound to BSA, compared to 60% for losartan, which contains a mono-acidic function. We have also examined the protein binding activities of a series of mono and diacid AII antagonists and the protein binding activity was related to, but was not totally dependent upon, the presence of a diacid function (data not shown). From the possible binding sites on BSA (Kragh-Hansen, 1981) it is likely that AII receptor antagonists bind at the bilirubin site 3, or the common drug binding site 6. Our results with BMS-180560 indicate that a substantial amount of drug (>90%) was bound to BSA, thereby reducing the concentration of free drug able to interact with the AT_1 receptor. Thus, BMS-180560 exhibited a K_B for rabbit aortic smooth muscle AII receptors of 0.068 nM in the absence and 5.2 nM in the presence of 0.1% BSA, indicating >95% binding of drug to BSA. The recently described Glaxo antagonist, GR 117,289, is a diacid which also shows significant binding to BSA (Robertson *et al.*, 1992). The pronounced binding of these drugs to plasma and tissue proteins may provide an explanation, in part, for the long duration of action of these diacid AII receptor antagonists.

Saturation binding experiments conducted in the presence of losartan indicated that the interaction of losartan with the vascular AT_1 receptor was competitive. Thus, in the presence of losartan, the K_D of SI-AII was increased to higher values, with no change in the B_{max}. Moreover, Schild slopes of the saturation binding data were close to unity suggesting a competitive interaction of losartan with the AT_1 receptor.

The interaction of BMS-180560 with the AT_1 receptor appeared competitive at low concentrations of BMS-180560, since the K_D for SI-AII was increased with no change in B_{max} value. Similar results have been reported for the insurmountable antagonists L-159,809 and CV-11974. Thus, L-158,809 and CV-11974 at concentrations similar to their K_i values increased the K_D of [^{125}I]-SI-AII but had no effect on B_{max} (Chang *et al.*, 1992; Shibouta *et al.*, 1993). However, at high concentrations of BMS-180560 (10 to 30 fold greater than its K_i for vascular AII receptors) the K_D for SI-AII was increased 10 to 20 fold and the B_{max} value was decreased by 12–45%. These findings suggest that BMS-180560 may exhibit mixed (competitive and non-competitive) inhibitory activity at high concentrations. The structurally similar insurmountable antagonist, GR 117,289 has also been reported to produce both decreases in B_{max} and increases in K_D for [^{3}H]-AII binding to rat liver membranes (Robertson *et al.*, 1992). Similar results were also reported for EXP3174 which decreased the B_{max} and increased the K_D for [^{125}I]-AII binding to rat lung membranes (Wienen *et al.*, 1992). However in contrast to our findings, inhibition was obtained at concentrations of EXP3174 which were close to its K_i value for the AII receptor. These discrepancies could result from differences in the AT_1 receptor subtypes in liver compared to the smooth muscle (Widdowson *et al.*, 1993) although both liver and lung are reported to contain predominantly the AT_{1a} receptor subtype (Kakar *et al.*, 1992; Widdowson *et al.*, 1993). Alternatively, slow kinetics of antagonist binding may have contributed to the degree of inhibition obtained. Thus, Pendleton *et al.* (1989) showed that the insurmountable peptide antagonist, Sar^{1}Leu^{8}AII reduced the B_{max} of [^{125}I]-AII binding sites on rabbit adrenal membranes only if membranes were preincubated with antagonist, whereas coincubation resulted in competitive inhibition. Decreases in B_{max} values were therefore attributed to slow dissociation of the peptide antagonist from the receptor. In our study the radioligand reached equilibrium during the course of the 2 h incubation in the absence or presence of BMS-180560 (3–30 nM) and preincubation of membranes with BMS-180560 did not change the competitive nature of the inhibition. These data suggest that BMS-180560 had reached equilibrium with the vascular AII receptor and at concentrations similar to its K_i value, BMS-180560 functioned as a competitive inhibitor. Concentrations of BMS-180560 which decreased B_{max} values (100–300 nM) were greatly in excess of those required to depress AII-stimulated contraction of rabbit aorta (3–30 nM) when measured in the presence of BSA. Liu *et al.* (1992) proposed that insurmountable antagonism of a series of AII receptor analogues was related to peptide-dependent internalization of AII receptors thereby decreasing receptor concentration. However, our data do not support the concept that BMS-180560 decreased receptor number at concentrations of BMS-180560 which produced insurmountable antagonism.

Losartan functioned as a classical competitive antagonist of AII-mediated smooth muscle contraction. Thus, AII concentration-response curves were shifted to the right with no depression of maximum response. These findings confirm reports of others who demonstrated losartan was a competitive inhibitor of AII-stimulated rabbit aortic contraction (Wong *et al.*, 1990a,c; Liu *et al.*, 1992; Wienen *et al.*, 1992; Robertson *et al.*, 1992; Cazaubon *et al.*, 1993; Shibouta *et al.*, 1993). In contrast BMS-180560 decreased the maximum AII-stimulated contraction of rabbit aorta in a concentration dependent manner and at 1 nM BMS-180560 (in the absence of BSA) maximum contractile responses were inhibited by 75%. Similar results have been reported for L-158,809 (Chang *et al.*, 1992), GR 117,289 (Robertson *et al.*, 1992) and EXP3174 (Wong & Timmermans, 1991; Wienen *et al.*, 1992), although the maximum reduction observed for EXP3174 was only 24% (Wienen *et al.*, 1992). Liu *et al.* (1992) demonstrated concentration-dependent saturable inhibition of maximum AII-stimulated contraction of rabbit aorta by a series of peptide AII analogues and the depression of AII contraction maxima correlated with the pA_2 values of the antagonists for the AII receptor. However, in the case of the nonpeptide antagonists, the ability of these drugs to decrease AII contraction maxima appears not to correlate with potency. Thus, BMS-180560 produced substantially greater decreases than EXP3174 although the antagonists had similar apparent K_B and K_i values for AII receptors.

This study also examined the effects of AII antagonists on smooth muscle cells using extracellular acidification as a monitor of cellular activation. AII stimulated the acidification rates of smooth muscle cells in a concentration-dependent manner and with an EC_{50} of 18 nM which correlated with the EC_{50} for AII-stimulated phosphoinositide turnover (27 nM) suggesting that phospholipase C (PLC) stimulation may be correlated with cellular activation. Losartan shifted the AII concentration-response curve in a manner commensurate with competitive inhibition and with a potency which was similar to its interaction with AII receptors on rabbit aortic rings. By contrast, BMS-180560 produced insurmountable inhibition of AII-stimulated cellular activation with increases in EC_{50} values and depression of AII maximal responses. The magnitude of this inhibition was similar to that observed for inhibition of AII-stimulated contraction of rabbit aortic rings and phosphoinositide turnover although these effects were observed at lower concentrations of BMS-180560. Robertson *et al.* (1992) reported differences in the potency of GR 117,289 in functional studies compared to its affinity for AII binding sites; these parameters may be influenced by pretreatment time, protein binding, drug lipophilicity, or receptor concentration. It is also possible that the short stimulation protocol used for the microphysiometer experiments did not allow AII to compete effectively with AII receptors which were occupied with BMS-180560 especially if BMS-180560 dissociated slowly. Indeed, washout studies indicated that BMS-180560 did dissociate from the RASM cells slower than losartan but that functional responses to AII could be restored following more extensive washing. These observations indicate that BMS-180560 binding to the RASM cell AII receptor was reversible.

AT_1 receptors on RASM cells transduce their signal in part by activation of a PLC (Smith *et al.*, 1984; Griendling *et al.*, 1987; 1991). Phosphoinositide turnover is enhanced with production of diacylglycerol, and inositol trisphosphate. The elevation of intracellular Ca^{2+} is thought to be ultimately responsible for the increased contractile state of smooth muscle. In order to define the site at which BMS-180560 exerted its insurmountable action, IP_1 formation was determined as a measure of PLC activation. Losartan shifted the AII-mediated IP_1 formation to the right with no change in the maximal response. Thus, losartan behaved as a competitive antagonist of AII-mediated responses whether the determinations were made at the level of receptor binding, IP_1 formation, smooth muscle contraction, or cellular activation (measured as extracellular acidification). Others have reported the ability of losartan to inhibit AII-mediated second messenger formation such as Ca^{2+} transients (Chiu *et al.*, 1990), phosphoinositide turnover (Pfeilschifter, 1990), aldosterone secretion (Balla *et al.*, 1991) but demonstration of the competitive nature of this inhibition has been lacking. By contrast BMS-180560 functioned as an insurmountable antagonist of AII-mediated vascular contractile responses, extracellular acidification and IP_1 formation. Both BMS-180560 and EXP3174 decreased maximal AII-stimulated IP_1 formation in an insurmountable manner. Chang *et al.* (1992) have also reported that L-158,809 shifted the AII-stimulated [^{3}H]-IP accumulation in RASM cells to the right and significantly decreased the maximal response. Inhibition of AII-stimulated phosphoinositide turnover by BMS-180560 was quantitatively similar to that for AII-stimulated contraction of rabbit vascular smooth muscle, when measurements were made under the same conditions of BSA concentration.

Our IP measurements were made after 30 min of cell stimulation. Wojcikiewicz et al. (1993) have recently reviewed the problems of measuring IP formation in Li-containing assays after long time intervals (>5 min) of cell stimulation. Moreover, our measured [^{3}H]-IP_1 may have derived from both PIP_2 and PI hydrolysis. Griendling et al. (1991) have described two isoforms of PLC in RASM cells with different Ca^{2+}, pH and substrate specificities. Thus, it was possible that the measured [^{3}H]-IP_1 pool derived from activation of two PLCs. Since IP_2 and IP_3 are thought to be generated in RASM cells as a result of rapid PLC-mediated PIP_2 hydrolysis (Griendling et al., 1991), it was important to establish that the insurmountable activity was also demonstrable at short time intervals using IP_3 formation as a monitor of PIP_2 hydrolysis. We have demonstrated that EXP3174 and BMS-180560 (at 1 nM) produced insurmountable antagonism of AII-stimulated IP_2/IP_3 formation at 4 min (data not shown). Since the insurmountable activity was detected at this level, it follows that the insurmountable target site for these antagonists lies proximal to PLC-mediated PIP_2 hydrolysis.

The interaction of insurmountable antagonist and receptor is not irreversible since losartan reversed the insurmountable inhibition of AII-stimulated phosphoinositide turnover caused by EXP3174 and BMS-180560 and inhibition of AII-stimulated increase in RASM extracellular acidification rates by BMS-180560 was irreversible following washout. These data confirm previous reports showing losartan was able to attenuate EXP3174-induced decrease in maximum AII contraction of vascular smooth muscle (Wong & Timmermans, 1991). Moreover, these findings suggest that the reversible antagonist losartan but not AII was able to access the BMS-180560 binding site which was responsible for insurmountable inhibition.

The molecular basis for insurmountable inhibition remains to be established although a number of theories have been proposed. Receptor heterogeneity could explain this phenomenon although available evidence suggest that the AII receptors on RASM cells represent a homogeneous population (Kakar et al., 1992; Cohen et al., 1993). Pseudoirreversible antagonism and allosteric modulation of AII receptors have also been proposed as the basis for insurmountable antagonism although our studies were unable to discriminate between these alternatives. Pseudoirreversible antagonism, which decreases the available receptors for effector coupling, could be produced by slow dissociation of the antagonist from the receptor. Our studies indicated that BMS-180560 dissociated slower than losartan and slow dissociation rates have also been reported for EXP3174 (Chiu et al., 1991). Thus, replacement of receptor-bound BMS-180560 or EXP-3174 by the rapidly dissociating antagonist losartan would allow AII to compete more effectively. This mechanism could explain the reversibility by losartan of BMS-180560- or EXP3174-induced insurmountable inhibition.

An allosteric model has also been proposed to explain insurmountable antagonism at AII receptors (Timmermans et al., 1991). Two binding sites are postulated, one which binds AII BMS-180560, and losartan and a second site which could allosterically decrease receptor-effector coupling thereby producing depression of the maximal AII-stimulated responses. The first site is demonstrable with AII radioligands and AII and nonpeptides compete for binding to this site. The second site is not available to AII whereas BMS-180560, EXP3174, and losartan can all bind. However, only BMS-180560 and EXP3174 can allosterically decrease receptor-effector coupling and cause insurmountable inhibition, perhaps by stabilizing a receptor conformation which had reduced ability to couple to G proteins. Binding of losartan (but not AII) to this site would be predicted to reverse BMS-180560- or EXP3174-mediated insurmountable inhibition. These two sites may have similar molecular characteristics since insurmountable and surmountable antagonists differ only slightly in their structure. Thus, insurmountable activity is associated with the presence of a -COOH group whereas the parent $-CH_2OH$ containing drug generally exhibits surmountable antagonism. Perhaps more convincing are data for a series of imidazol-2-one AII receptor antagonists, where modest changes in alkyl substitution changed the nature of the antagonism (Reitz et al., 1993). Thus, methyl and isopropyl containing drugs were surmountable whereas ethyl substitution resulted in an insurmountable antagonist. Whether this behaviour is due to differential dissociation rates of the compounds or their abilities to bind to secondary allosteric sites remains to be established.

References

ARUNLAKSHANA, O. & SCHILD, H.O. (1959). Some quantitative uses of drug antagonists. *Br. J. Pharmacol. Chemother.*, **14**, 48–58.

BALLA, T., BAUKAL, A.J., ENG, S. & CATT, K.J. (1991). Angiotensin II receptor subtypes and biological responses in the adrenal cortex and medulla. *Mol. Pharmacol.*, **40**, 401–406.

BERRIDGE, M.J. (1983). Rapid accumulation of inositol trisphosphate reveals that agonists hydrolyse polyphosphoinositides instead of phosphatidylinositol. *Biochem. J.*, **212**, 849–858.

CAZAUBON, C., GOUGAT, J., BOUSQUET, F., GUIRAUDOU, P., GAYRAUD, R., LACOUR, C., ROCCON, A., GALINDO, G., BARTHELEMY, G., GAUTRET, B., BERNHART, C., PERREAUT, P., BRELIERE, J.-C., LE FUR, G. & NISATO, D. (1993). Pharmacological characterization of SR 47436, a new nonpeptide AT_1 subtype angiotensin II receptor antagonist. *J. Pharmacol. Exp. Ther.*, **265**, 826–834.

CHANG, R.S.L. & LOTTI, V.J. (1990). Two distinct angiotensin II receptor binding sites in rat adrenal revealed by new selective nonpeptide ligands. *Mol. Pharmacol.*, **29**, 347–350.

CHANG, R.S.L., SIEGL, P.K.S., CLINESCHMIDT, B.V., MANTLO, N.B., CHAKRAVARTY, P.K., GREENLEE, W.J., PATCHETT, A.A. & LOTTI, V.J. (1992). In vitro pharmacology of L-158,809, a new highly potent and selective angiotensin II receptor antagonist. *J. Pharmacol. Exp. Ther.*, **262**, 133–138.

CHENG, Y.C. & PRUSOFF, W.H. (1973). Relationship between the inhibition constant (K_i) and the concentration of the inhibitor which causes 50 per cent inhibition (I_{50}) of an enzymatic reaction. *Biochem. Pharmacol.*, **22**, 3099–3108.

CHIU, A.T., CARINI, D.J., DUNCIA, J.V., LEUNG, K.H., MCCALL, D.E., PRICE, W.A., WONG, P.C., SMITH, R.D., WEXLER, R.R. & TIMMERMANS, P.B.M.W.M. (1991). DuP 532: a second generation of nonpeptide angiotensin II receptor antagonists. *Biochem. Biophys. Res. Commun.*, **177**, 209–217.

CHIU, A.T., HERBLIN, W.F., MCCALL, D.E., ARDECKY, R.J., CARINI, D.J., DUNCIA, J.V., PEASE, L.J., WONG, P.C., WEXLER, R.R., JOHNSON, A.L. & TIMMERMANS, P.B.M.W.M. (1989). Identification of angiotensin II receptor subtypes. *Biochem. Biophys. Res. Commun.*, **165**, 196–203.

CHIU, A.T., MCCALL, D.E., PRICE, W.A., WONG, P.C., CARINI, D.J., DUNCIA, J.V., WEXLER, R.R., YOO, S.E., JOHNSON, A.L. & TIMMERMANS, P.B.M.W.M. (1990). Nonpeptide angiotensin II receptor antagonists. VII. Cellular and biochemical pharmacology of DuP 753, an orally active antihypertensive agent. *J. Pharmacol. Exp. Ther.*, **252**, 711–718.

COHEN, R.B., WEBB, M.L. & DICKINSON, K.E.J. (1993). Peptidases and smooth muscle cell angiotensin II receptor pharmacology. *Peptides*, **14**, 345–352.

DICKINSON, K.E.J., COHEN, R.B., BIRD, J.E., WALDRON, T.L., SCHAEFFER, T.R., MORELAND, S., DELANEY, C.L., SERAFINO, R., POSS, M.A., GU, Z., RYONO, D.E. & POWELL, J.R. (1992). Pharmacological properties of BMS 180,560: an insurmountable angiotensin II receptor antagonist. *Br. J. Pharmacol.*, **107**, P465.

DUDLEY, D.T., HUBBELL, S.E. & SUMMERFELT, R.M. (1991). Characterization of angiotensin II (AT_2) binding sites in R3T3 cells. *Mol. Pharmacol.*, **40**, 360–367.

DUDLEY, D.T., PANEK, R.L., MAJOR, T.C., LU, G.H., BRUNS, R.F., KLINKEFUS, B.A., HODGES, J.C. & WEISHAAR, R.E. (1990). Subclasses of angiotensin II binding sites and their functional significance. *Mol. Pharmacol.*, **38,** 370–377.

EDWARDS, R.M., AIYAR, N., OHLSTEIN, E.H., WEIDLEY, E.F., GRIFFIN, E., EZEKIEL, M., KEENAN, R.M., RUFFOLO, R.R. & WEINSTOCK, J. (1992). Pharmacological characterization of the nonpeptide angiotensin II receptor antagonist SK&F 108566. *J. Pharmacol. Exp. Ther.*, **260,** 175–181.

GRIENDLIJNG, K.K., BERK, B.C., GANZ, P., GIMBRONE, M.A. & ALEXANDER, R.W. (1987). Angiotensin II stimulation of vascular smooth muscle phosphoinositide metabolism. *Hypertension*, **SIII 9,** 181–185.

GRIENDLING, K.K., TAUBMAN, M.B., AKERS, M., MENDLOWITZ, M. & ALEXANDER, R.W. (1991). Characterization of phosphatidylinositol-specific phospholipase C from cultured vascular smooth muscle cells. *J. Biol. Chem.*, **266,** 15,498–15,504.

KAKAR, S.S., SELLERS, J.C., DEVOR, D.C., MUSGROVE, L.C. & NEIL, J.D. (1992). Angiotensin II type-1 receptor subtype cDNAS: differential tissue expression and hormonal regulation. *Biochem. Biophys. Res. Commun.*, **183,** 1090–1096.

KRAGH-HANSEN, U. (1981). Molecular aspects of ligand binding to serum albumin. *Pharmacol. Rev.*, **33,** 17–53.

LIU, Y.J., SHANKLEY, N.P., WELSH, N.J. & BLACK, J.W. (1992). Evidence that the apparent complexity of receptor antagonism by angiotensin II analogues is due to a reversible and syntopic action. *Br. J. Pharmacol.*, **106,** 233–241.

MUNSON, P.J. & RODBARD, D. (1980). LIGAND: a versatile computerized approach for characterization of ligand-binding systems. *Anal. Biochem.*, **107,** 220–239.

OLINS, G.M., CORPUS, V.M., MCMAHON, E.G., PALOMO, M.A., SCHUH, J.R., BLEHM, D.J., HUANG, H.-C., REITZ, D.B., MANNING, R.E. & BLAINE, E.H. (1992). In vitro pharmacology of a nonpeptide angiotensin II receptor antagonist, SC-51316. *J. Pharmacol. Exp. Ther.*, **261,** 1037–1043.

OWICKI, J.C., PARCE, J.W., KERSO, K.M., SIGAL, G.B., MUIR, V.C., VENTER, J.C., FRASER, C.M. & MCCONNELL, H.M. (1990). Continuous monitoring of receptor-mediated changes in the metabolic rates of living cells. *Proc. Natl. Acad. Sci. U.S.A.*, **87,** 4007–4011.

PENDLETON, R.G., GESSNER, G. & HORNER, E. (1989). Studies on inhibition of angiotensin II receptors in rabbit adrenal and aorta. *J. Pharmacol. Exp. Ther.*, **248,** 637–643.

PFEILSCHIFTER, J. (1990). Angiotensin II B-type receptor mediates phosphoinositide hydrolysis in mesangial cells. *Eur. J. Pharmacol.*, **184,** 201–202.

POSS, M.A., GU, Z., RYONO, D.E., REID, J.A., SIEBER-MCMASTER, E., SPITZMILLER, E.R., DEJNEKA, T., DICKINSON, K.E.J., MORELAND, S., DELANEY, C.L., BIRD, J.E., WALDRON, T.L., SCHAEFFER, T.R., KIM, K.S., QIAN, L., HEDBERG, S.A. & PETRILLO, E.W. (1994). 1,4-substituted indoles: a potent and selective class of angiotensin II receptor antagonists. *Bioorg. Med. Chem. Lett.*, **4,** 145–150.

PUCELL, A.G., HODGES, J.C., SEN, I., BUMPUS, F.M. & HUSAIN, A. (1991). Biochemical properties of the ovarian granulosa cell type 2-angiotensin II receptor. *Endocrinology*, **128,** 1947–1959.

REITZ, D.B., GARLAND, D.J., NORTON, M.B., COLLINS, J.T., REINHARD, E.J., MANNING, R.E., OLINS, G.M., CHEN, S.T., PALOMO, M.A., MCMAHON, E.G. & KOEHLER, K.F. (1993). N1-sterically hindered 2H-imidazol-2-one angiotensin II receptor antagonists: the conversion of surmountable antagonists to insurmountable antagonists. *Bioorg. Med. Chem. Lett.*, **3,** 1055–1060.

ROBERTSON, M.J., BARNES, J.C., DREW, G.M., CLARK, K.L., MARSHALL, F.H., MICHEL, A., MIDDLEMISS, D., ROSS, B.C., SCOPES, D. & DOWLE, M.D. (1992). Pharmacological profile of GR 117289 in vitro: a novel, potent and specific non-peptide angiotensin AT_1 receptor antagonist. *Br. J. Pharmacol.*, **107,** 1173–1180.

SHIBOUTA, Y., INADA, Y., OJIMA, M., WADA, T., NODA, M., SANADA, T., KUBO, K., KOHARA, Y., NAKA, T. & NISHIKAWA, K. (1993). Pharmacological profile of a highly potent and long-acting angiotensin II receptor antagonist, 2-ethoxy-1-[[2'-(1H-tetrazol-5-yl)biphenyl-4-yl]methyl]-1H-benzimidazole-7-carboxylic acid (CV-11974), and its prodrug, (±)-1-(cyclohexyloxycarbonyloxy)-ethyl-2-ethoxy-1-[[2'-(1H-tetrazol-5yl)byphenyl-4-yl]methyl]-1H-benximidazole-7-carboxylate (TCV-116). *J. Pharmacol. Exp. Ther.*, **266,** 114–120.

SMITH, B.J., SMITH, L., BROWN, E.R., BARNES, D., SABIR, M.A., DAVIS, J.S. & FARESE, R.V. (1984). Angiotensin II rapidly increases phosphatidate-phosphoinositide hydrolysis and mobilizes intracellular calcium in cultured arterial muscle cells. *Proc. Natl. Acad. Sci. U.S.A.*, **81,** 7812–7816.

SPETH, R.C. & KIM, K.H. (1990). Discrimination of two angiotensin II receptor subtypes with a selective analogue of angiotensin II, p aminophenylalanine^6 angtiotensin II. *Biochem. Biophys. Res. Commun.*, **169,** 997–1006.

TALLARIDA, R.J. & JACOB, L.S. (1979). *The Dose-Response Relation in Pharmacology*. New York: Springer-Verlag.

TIMMERMANS, P.B.M.W.M., WONG, P.C., CHIU, A.T. & HERBLIN, W.F. (1991). Nonpeptide angiotensin II receptor antagonists. *Trends Pharmacol. Sci.*, **12,** 55–62.

WEBB, M.L., DICKINSON, K.E.J., DELANEY, C.L., LIU, E.C.-K., SERAFINO, R., COHEN, R.B., MONSHIZADEGAN, H. & MORELAND, S. (1992a). The endothelin receptor antagonist, BQ-123, inhibits angiotensin II-induced contractions in rabbit aorta. *Biochem. Biophys. Res. Commun.*, **185,** 887–892.

WEBB, M.L., LIU, E.C.-K., COHEN, R.B., HEDBERG, A., BOGOSIAN, E.A., MONSHIZADEGAN, H., MOLLOY, C., SERAFINO, R., MORELAND, S., MURPHY, T.J. & DICKINSON, K.E.J. (1992b). Molecular characterization of angiotensin II type 2 (AT_2) receptors in rat pheochromocytoma cells: evidence for functional and structural diversity in the angiotensin II receptors. *Peptides*, **13,** 499–508.

WHITEBREAD, S., MELE, M., KAMBER, B. & DE GASPARO, M. (1989). Preliminary biochemical characterization of two angiotensin II receptor subtypes. *Biochem. Biophys. Res. Commun.*, **163,** 284–291.

WIDDOWSON, P.S., RENOUARD, A. & VILAINE, J.-P. (1993). Binding of [^{3}H]angiotensin II and [^{3}H]DuP 753 (Losartan) to rat liver homogenates reveals multiple sites. Relationship to AT_{1a}- and AT_{1b}-type angiotensin receptors and novel nonangiotensin binding sites. *Peptides*, **14,** 829–837.

WIENEN, W., MAUZ, A.B.M., VAN MEEL, J.C.A. & ENTZEROTH, M. (1992). Different types of receptor interaction of peptide and nonpeptide angiotensin II antagonists revealed by receptor binding and functional studies. *Mol. Pharmacol.*, **41,** 1081–1088.

WOJCIKIEWICZ, R.J.H., TOBIN, A.B. & NAHORSKI, S.R. (1993). Desensitization of cell signalling mediated by phosphoinositidase C. *Trends Pharmacol. Sci.*, **14,** 279–285.

WONG, P.C., CHIU, A.T., PRICE, W.A., THOOLEN, M.J.M.C., CARINI, D.J., JOHNSON, A.L., TABER, R.I. & TIMMERMANS, P.B.M.W.M. (1988). Nonpeptide angiotensin receptor antagonists. I. Pharmacological characterization of 2-n-butyl-1-(2-chlorobenzyl)imidazole-5-acetic acid, sodium salt (S-8307). *J. Pharmacol. Exp. Ther.*, **247,** 1–7.

WONG, P.C., HART, S.D., CHIU, A.T., HERBLIN, W.F., CARINI, D.J., SMITH, R.D., WEXLER, R.R. & TIMMERMANS, P.B.M.W.M. (1991). Pharmacology of DuP 532, a selective and noncompetitive T1 receptor antagonist. *J. Pharmacol. Exp. Ther.*, **259,** 861–870.

WONG, P.C., HART, S.D., ZASPEL, A.M., CHIU, A.T., ARDECKY, R.J., SMITH, R.D. & TIMMERMANS, P.B.M.W.M. (1990a). Functional studies of nonpeptide angiotensin II receptor subtype-specific ligands: DuP 753 (AII-1) and PD123177 (AII-2). *J. Pharmacol. Exp. Ther.*, **255,** 584–592.

WONG, P.C., PRICE, W.A., CHIU, A.T., DUNCIA, J.V., CARINI, D.J., WEXLER, R.R., JOHNSON, A.L. & TIMMERMANS, P.B.M.W.M. (1990b). Nonpeptide angiotensin II receptor antagonists. XI. Pharmacology of EXP3174: an active metabolite of DuP 753, an orally active antihypertensive agent. *J. Pharmacol. Exp. Ther.*, **255,** 211–217.

WONG, P.C., PRICE, W.A., CHIU, A.T., DUNCIA, J.V., CARINI, D.J., WEXLER, R.R., JOHNSON, A.L. & TIMMERMANS, P.B.M.W.M. (1990c). Nonpeptide angiotensin II receptor antagonists. VIII. Characterization of functional antagonism displayed by DuP 753, an orally active antihypertensive agent. *J. Pharmacol. Exp. Ther.*, **252,** 719–725.

WONG, P.C. & TIMMERMANS, P.B.M.W.M. (1991). Non-peptide angiotensin II receptor antagonists: insurmountable angiotensin II antagonism of EXP3892 is reversed by the surmountable antagonist DuP 753. *J. Pharmacol. Exp. Ther.*, **258,** 49–57.

(Received December 23, 1993
Revised May 2, 1994
Accepted May 17, 1994)

Br. J. Pharmacol. (1994), **113**, 190–194

Abolition of flow-dependent EDRF release before that evoked by agonists in hypercholesterolaemic rabbits

Iain R. Hutcheson, *Jerry A. Smith & [1]Tudor M. Griffith

Departments of Diagnostic Radiology and *Cardiology, University of Wales College of Medicine, Heath Park, Cardiff CF4 4XN

1 We have used a pulsatile cascade bioassay system to investigate the effects of dietary-induced hypercholesterolaemia on EDRF release evoked by acetylcholine and by the oscillatory and time-averaged components of flow, in isolated segments of rabbit abdominal aorta.

2 Flow pulsatility (frequency range 0.1–10 Hz) was studied with constant flow (9 ml min^{-1}) at a pulse pressure amplitude of 2 mmHg. Frequency-related EDRF release, maximal at 6 Hz, was slightly attenuated after 4 weeks and abolished after 8 weeks of cholesterol feeding.

3 Time-averaged shear stress was manipulated with dextran (1–4% w/v, 80000 mol. wt.), to increase perfusate viscosity. EDRF release induced by increased perfusate viscosity was unaffected after 4 weeks but abolished after 8 weeks of cholesterol feeding.

4 Endothelium-dependent relaxations to acetylcholine (0.1–10 μM) were not influenced after 4 weeks and only partially attenuated (by 60% of the maximal response, EC_{50} unchanged at 6.45 ± 0.04 vs. 6.4 ± 0.1 μM) after 8 weeks of cholesterol feeding.

5 Blood cholesterol levels were significantly ($P<0.001$) increased after 4 weeks (26 ± 3.6 vs 2.6 ± 0.6 mmol l^{-1}) and 8 weeks (56.2 ± 3.8 vs 1.3 ± 0.1 mmol l^{-1}) of cholesterol feeding but after 8 weeks plasma L-arginine levels were not significantly different from the age-matched controls (0.2 ± 0.05 vs. 0.19 ± 0.04 mmol l^{-1}).

6 We conclude that hypercholesterolaemia impairs flow-related (pulsatile- and time-averaged shear-induced) EDRF release earlier than acetylcholine-induced relaxation in rabbit aorta. This is consistent with the view that different transduction mechanisms mediate EDRF release in response to agonists and flow.

Keywords: Rabbit aorta; pulsatile flow; hypercholesterolaemia; endothelium-derived relaxing factor (EDRF)

Introduction

Atherosclerosis is a major inflammatory disorder of the arterial wall that is characterized by recruitment of monocytes and their transformation into lipid-rich foam cells, smooth muscle proliferation, intimal thickening and deposition of extracellular matrix to form fibrous plaques. It has been proposed that injury to the endothelium is the initiating event in atherogenesis and progression of the disease occurs as a result of an excessive inflammatory-fibroproliferative response to this insult (Ross, 1993). A major risk factor in this disease process is hypercholesterolaemia which is associated with raised levels of low density lipoprotein (LDL), the principal carrier of cholesterol in the blood. Recently, oxidized LDL (OxLDL), a modified form of LDL, has been implicated both as a key factor in endothelial injury and a potential promoter of atheroma formation (Ross, 1993; Witztum, 1993).

A reduced level of EDRF activity could promote the atherogenesis by making the arterial wall a more thrombogenic and adherent surface for platelets and monocytes and by enhancing smooth muscle proliferation (Moncada *et al.*, 1988; Garg & Hassid, 1990; Bath *et al.*, 1991). Indeed, regions of blood vessel prone to atherosclerosis are associated with areas of low longitudinal endothelial shear stress and thus presumably a low degree of mechanical stimulus for EDRF synthesis (Ku *et al.*, 1985). An early manifestation of hypercholesterolaemia is an impairment in endothelium-dependent responses to specific agonists in both animals and human subjects (Verbeuren *et al.*, 1986; Bossaller *et al.*, 1987; Forstermann *et al.*, 1988; Flavahan, 1992). This dysfunction displays regional differences in conduit arteries, with the most severe impairment occurring at bifurcations and in the proximal aorta (Ragazzi *et al.*, 1989, McLenachan *et al.*, 1990) and is not a consequence of decreased vascular smooth muscle responsiveness since relaxations to exogenous donors of nitric oxide are unaffected (Bossaller *et al.*, 1987; Flavahan, 1992). The abnormality also extends to the microcirculation, so that the effects of hypercholesterolaemia cannot simply be attributed to a diffusion barrier to EDRF resulting from intimal thickening or plaque formation as resistance vessels do not show these pathological features (Yamamoto *et al.*, 1988; Kuo *et al.*, 1992).

Flow-dependent dilatation is compromised in human conduit arteries by hypercholesterolaemia (Cox *et al.*, 1989) and flow-related EDRF activity is attenuated in resistance arteries from the porcine coronary circulation in an experimental model of atheroma (Kuo *et al.*, 1993). Recently Randall *et al.* (1993) have demonstrated that a 4 week dietary supplement of 1% cholesterol has little effect on agonist-dependent EDRF release but severely depresses the EDRF-dependent opening of pre-existing collateral vessels following arterial ligation in the rabbit ear. However, after 8 weeks dietary supplementation both collateral perfusion and agonist-induced responses are significantly impaired. These observations may reflect a greater susceptibility of basal and flow-induced EDRF activity to the deleterious effects of hypercholesterolaemia than agonist-evoked responses and represent a further example of differences in the transduction mechanisms for flow- and agonist-induced EDRF release (Griffith *et al.*, 1987; Macarthur *et al.*, 1993; Hutcheson & Griffith, 1994). In the present study, a pulsatile flow cascade bioassay system was used to compare the effect of 4 and 8 weeks dietary-induced hypercholesterolaemia on flow- (both

[1] Author for correspondence.

the oscillatory and time-averaged components) and agonist-induced EDRF release.

Methods

Feeding protocol

Male New Zealand White rabbits matched by age and weight (2–2.5 kg) were divided into two groups, one being fed a cholesterol-supplemented (1%) diet (Special Diet Services, Witham, Essex), the other kept on standard chow.

Experimental protocol

Half the rabbits in each group were killed by cervical dislocation after 4 weeks, the remainder after 8 weeks. Abdominal aortae were removed and placed into pre-gassed (95% O_2–5% CO_2, pH 7.4) Holman's Solution of the following composition (mM): NaCl 120, KCl 5, NaH_2PO_4 1.3, $NaHCO_3$ 25, $CaCl_2$ 2.5 glucose 11, sucrose 10, containing indomethacin (10 μM). N^G-nitro-L-arginine methyl ester (L-NAME) was used as a specific inhibitor of EDRF formation from L-arginine. Plasma L-arginine levels were determined by gas chromatography as described by Williams *et al.* (1993).

The bioassay system used to quantify EDRF release in response to changes in flow pulsatility has been previously described (Hutcheson & Griffith, 1991). Briefly, segments (3–5 cm) of endothelium-intact abdominal aorta from either the cholesterol or control group (the donor) were placed horizontally in an organ chamber filled with oxygenated buffer at 37°C. The preparations were perfused at a mean flow rate of 9 ml min^{-1} by a Watson-Marlow peristaltic pump (Type 503U), and an air-filled compliance chamber was connected immediately proximal to the infusion cannula. EDRF activity in the effluent from the donor vessel was assayed by relaxation of a preconstricted (phenylephrine; 300 nM) ring of endothelium-denuded thoracic aorta (the recipient) which was positioned directly below the organ bath outlet. Its tension was measured by an isometric force transducer (Dynamometer UFI) and the transit time between the donor and recipient was ca. 2 s. The recipient ring was taken from young control rabbits to eliminate the effects of aging on its ability to respond to EDRF.

The pulse frequency of perfusion was varied by employing silastic tubing (Watson-Marlow) of three different internal diameters (3.2 mm, 1.6 mm and 0.8 mm). The narrower the diameter of the tubing, the higher the frequency of the oscillatory flow required to perfuse the donor aorta at a mean flow rate of 9 ml min^{-1}. Technical details have been provided elsewhere (Hutcheson & Griffith, 1991). Flow rate was calibrated against pump speed for each diameter of tubing before each experiment. Maximum damping of the perfusion circuit was introduced by a 70 ml compliance chamber when studying pulse frequency-related effects (from 0.15 to 9.75 Hz), the amplitude of the pressure pulse then remaining at 2 mmHg. Dextran (80,000 mol wt; 1–4% w/v) was added to the perfusate to study changes in viscosity and thus time-averaged shear stress. Relaxations to the endothelium-dependent vasodilator, acetylcholine were also assessed. When constructing cumulative concentration-response curves to acetylcholine, atropine (3 μM) was superfused over the recipient ring to eliminate direct vasoconstriction. The presence or absence of endothelium was also confirmed histologically by *en face* silver staining of the donor vessel at the end of each experiment.

Drugs

Acetylcholine, phenylephrine, dextran 80, indomethacin, atropine and N^G-nitro-L-arginine methyl ester were obtained from Sigma Limited, Poole, Dorset. All drugs were dissolved in Holman buffer with the exception of indomethacin (5% w/v $NaHCO_3$ in distilled water).

Statistics

All data are given as mean ± s.e.mean, where n denotes the number of animals studied for each data point. Statistical analysis was assessed by Student's t test for paired and unpaired data as appropriate, $P<0.05$ being considered as significant. EC_{50} values for vasodilator responses were obtained from individual concentration-response curves as the concentration at which half maximal reduction in recipient tone occurred.

Results

Effects of cholesterol diet on plasma cholesterol and L-arginine levels

Plasma cholesterol levels in animals receiving a 1% cholesterol diet were 26 ± 3.6 mmol l^{-1} after 4 weeks, (n = 10) and 56.2 ± 3.8 mmol l^{-1} after 8 weeks (n = 10) both being significantly ($P<0.001$) elevated above their corresponding controls (2.6 ± 0.6 mmol l^{-1}, and 1.3 ± 0.1 mmol l^{-1}, n = 10 respectively). Plasma L-arginine levels were 0.2 ± 0.05 mmol l^{-1} after 8 weeks of cholesterol supplementa-

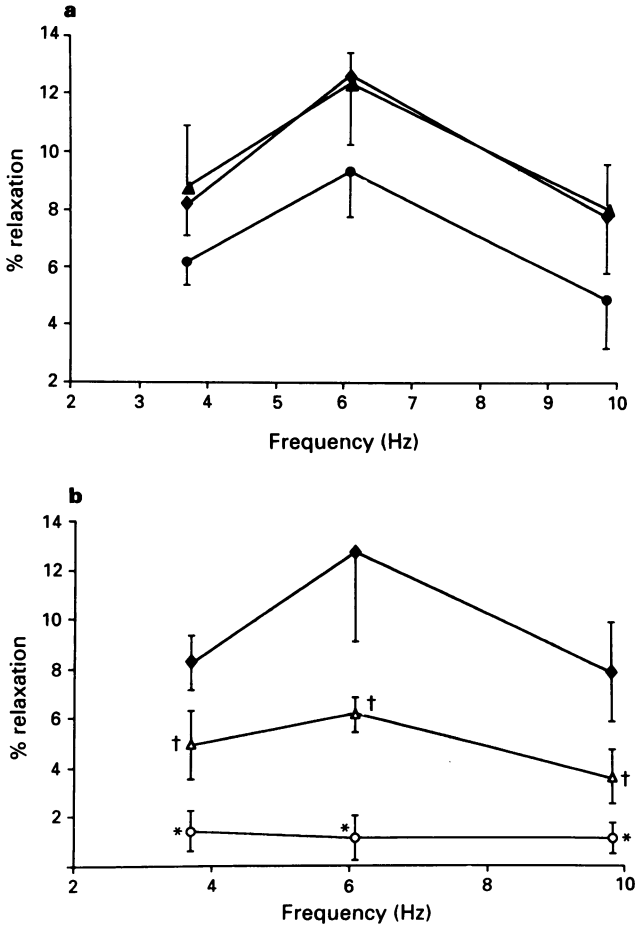

Figure 1 Effects of age and hypercholesterolaemia on frequency-related release of EDRF. This was significantly depressed after 8 but not 4 weeks in control animals. Hypercholesterolaemia abolished EDRF release after 8 weeks, but the slight reduction after 4 weeks was not statistically significant (†$P<0.05$ cf. 4 week control; *$P<0.05$ cf. 8 week control). (◆) Control 0–1 week; (▲) control 4 weeks; (△) control 8 weeks; (●) cholesterol-fed 4 weeks; (○) cholesterol-fed 8 weeks.

tion ($n = 8$) and were not significantly different from the age-matched control value of 0.19 ± 0.04 mmol l^{-1} ($n = 7$).

Frequency-dependent responses

Increasing the pulse frequency of the perfusate through segments of abdominal aorta from rabbits receiving a normal diet evoked relaxation of the recipient ring with a peak response at 6 Hz (Figure 1). However, the amplitudes of the responses at 6 Hz were significantly ($P < 0.05$) smaller in the 8 week ($7.1 \pm 0.8\%$) compared to the 4 week ($12.2 \pm 1.1\%$) control group ($n = 8$ and 4 respectively, Figure 1). Aortae from rabbits receiving a high cholesterol diet for 4 weeks produced smaller frequency-dependent relaxations of $9.2 \pm 1.6\%$ relative to control, but this did not achieve statistical significance (Figure 1a). In contrast, frequency-dependent relaxations were absent in aortae from the 8 week cholesterol-supplemented group ($P < 0.05$; $n = 8$; Figure 1b). No frequency-dependent relaxations were observed in the 4 and 8 week control groups following pre-incubation of the donor with L-NAME ($n = 4$ in each case).

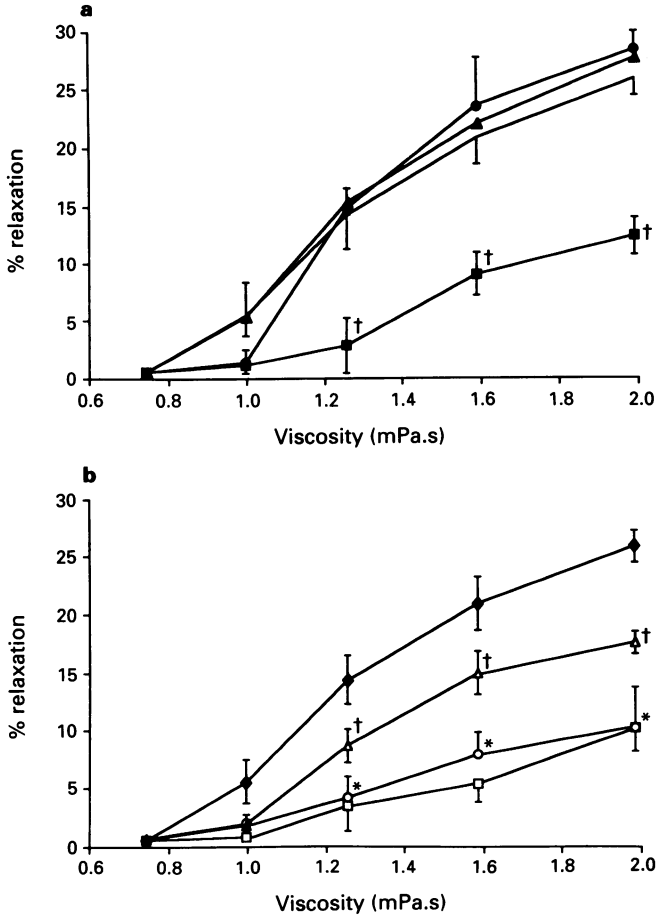

Figure 2 Viscosity-related EDRF release was abolished by 8 but not by 4 weeks of high cholesterol feeding. Control responses were again significantly depressed in the older animals. Note the small residual relaxation in the presence of 100 μM N^G-nitro-L-arginine methyl ester (L-NAME) in both groups which represents a direct effect of dextran on the recipient. †$P < 0.05$ cf. 4 week control; (*$P < 0.05$ cf. 8 week control). (◆) Control 0–1 week; (▲) control 4 weeks; (△) control 8 weeks; (●) cholesterol-fed 4 weeks; (○) cholesterol-fed 8 weeks; (■) control 4 weeks + L-NAME; (□) control 8 weeks + L-NAME.

Viscosity-dependent responses

Dextran elicited concentration-dependent relaxations of the detector tissue when introduced into the aortic perfusate of both the 4 and 8 week control groups, although the absolute responses were significantly smaller ($P < 0.05$) in the older animals ($n = 4$ and 8 respectively; Figure 2). There was no significant loss of viscosity-related relaxations after 4 weeks of the cholesterol rich diet (Figure 2a) but those of the 8 week cholesterol-fed group were significantly ($P < 0.05$) reduced compared to their age-matched controls ($n = 4$, Figure 2b). The responses in the 4 week group were significantly attenuated by pre-incubation of the donor with L-NAME (Figure 2a), although a minor degree of relaxation to dextran was still evident which represents a direct effect of dextran on the recipient ring (Hutcheson & Griffith, 1994). In contast, L-NAME did not significantly decrease relaxation to dextran after 8 weeks of hypercholesterolaemia ($n = 4$, not shown). The effects of L-NAME in control vessels and those of 8 weeks of hypercholesterolaemia were similar in terms of their impairment of viscosity-related relaxations (Figure 2b).

Acetylcholine-induced responses

In the 4 week control group, acetylcholine evoked concentration-dependent, L-NAME-sensitive relaxations of the detector tissue in the cascade bioassay which were similar in terms of EC_{50} values and maximum reduction in tone to those obtained with donor aortae from 4 week cholesterol-fed rabbits (Table 1, Figure 3a). The maximum relaxation of control preparations from the 8 week group of animals was significantly lower than in the 4 week group (Table 1; Figure 3a and b), and was further depressed in animals fed a cholesterol-rich diet for 8 weeks (Table 1, Figure 3b).

Discussion

The object of the present series of experiments was to determine the degree to which EDRF release evoked by receptor stimulation, increased time-averaged shear stress and changes in the frequency of pulsatile flow is compromised in a model of dietary-induced hypercholesterolaemia. A previously described cascade bioassay system (Hutcheson & Griffith, 1991) was used to quantify EDRF release and the specificity of responses confirmed with L-NAME. The involvement of prostanoids was excluded by addition of indomethacin to the perfusate in all experiments.

Hypercholesterolaemia impaired EDRF release to both acetylcholine and flow, to an extent that was directly related to the duration of the dietary supplementation. After 8 weeks of hypercholesterolaemia, both viscosity- and frequency-

Table 1 Effect of age and cholesterol feeding on the EC_{50} values and maximum relaxations of the recipient ring to acetylcholine

	EC_{50} (−logM)	*Maximal response* (%)		EC_{50} (−logM)	*Maximal response* (%)
4-week group			*8-week group*		
Control	6.25 ± 0.06	57.2 ± 3.5 ($n = 4$)	Control	6.45 ± 0.04	34.5 ± 1.7 ($n = 4$)†
Cholesterol-fed	6.25 ± 0.02	57 ± 1 ($n = 4$)	Cholesterol-fed	6.1 ± 0.11	23.5 ± 7.7 ($n = 4$)*

Responses of endothelium-denuded aortic rings constricted by phenylephrine to EDRF released by aortae from rabbits fed a high-cholesterol diet for 4 and 8 weeks and that observed with the appropriate controls. Maximum responses were depressed both by age and dietary supplementation for 8 but not 4 weeks (†$P < 0.05$ cf. 4 week control: *$P < 0.05$ cf. 8 week control). EC_{50} values were similar in all groups.

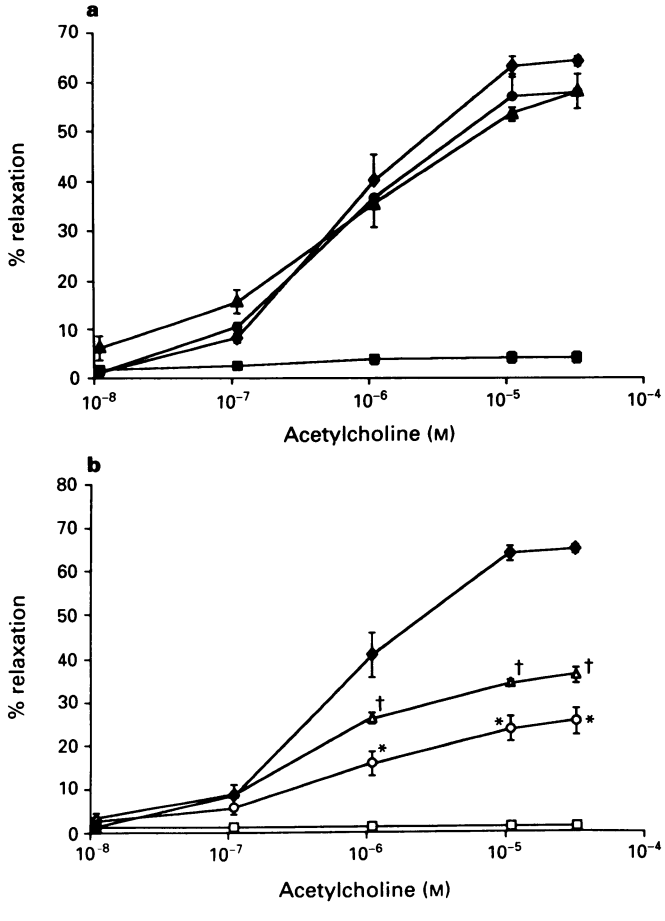

Figure 3 EDRF release evoked by acetylcholine was abolished by 100 μM N^G-nitro-L-arginine methyl ester (L-NAME) and significantly depressed by 8 weeks of high cholesterol diet. As in Figures 1 and 2, control responses were significantly smaller in the older animals. (†$P<0.05$ cf. 4 week control; *$P<0.05$ cf. 8 week control). (◆) Control 0–1 week; (▲) control 4 weeks; (△) control 8 weeks; (●) cholesterol-fed 4 weeks; (○) cholesterol-fed 8 weeks; (■) control 4 weeks + L-NAME; (□) control 8 weeks + L-NAME.

related EDRF release were abolished (i.e. attenuated to the same extent as with 100 μM L-NAME) consistent with previous evidence that EDRF-mediated flow-dependent dilatation is impaired in hypercholesterolaemia (Kuo *et al.*, 1993; Randall *et al.*, 1993). The response to acetylcholine, however, was normal after 4 weeks of dietary supplementation and partially retained even after 8 weeks. This suggests that the response to acetylcholine is less susceptible to the deleterious effects of hypercholesterolaemia. It is possible that this may simply reflect varying strengths of stimulus on the same mechanistic pathway; however, it is also consistent with evidence from a number of groups that flow- and agonist-induced EDRF release involve distinct signal transduction mechanisms (Griffith *et al.*, 1987; Macarthur *et al.*, 1993; Hutcheson & Griffith, 1994). There was also a progressive decrease in both agonist- and flow-induced EDRF release over the 8 week period in the rabbits fed standard chow. This is consistent with previous reports of an age-related reduction in endothelium-dependent relaxation that does not simply reflect a reduced capacity of vascular smooth muscle to respond to nitrovasodilators (Shirasaki *et al.*, 1986).

The endothelium of atherosclerotic arteries becomes refractory to acetylcholine, ATP and 5-hydroxytryptamine, whereas responses to bradykinin and the receptor-independent calcium ionophore A23187 are preserved until a relatively late stage of the disease when there may be non-specific effects (Bossaller *et al.*, 1987; Shimokawa *et al.*, 1991; Flavahan, 1992). A similar pattern of impaired endothelial function follows administration of pertussis toxin to normal vessels, suggesting that hypercholesterolaemia selectively inhibits a pertussis toxin-sensitive G_i protein and/or its coupling to phospholipase C (Shimokawa *et al.*, 1991; Flavahan, 1992). Both the EDRF response to acute changes in shear and its upregulation by prolonged increases in flow are also reportedly sensitive to inhibition by pertussis toxin, which may reflect direct G_i protein–K_{Ca} channel coupling (Miller & Burnett, 1992; Ohno *et al.*, 1993). Interestingly, the endothelium which regenerates following balloon angioplasty exhibits prolonged functional impairment to agonists at the level of G_i protein subtype (Shimokawa *et al.*, 1990), but flow-dependent dilatation reportedly returns to normal after one week (Hayashi *et al.*, 1988). This raises the possibility that G_i proteins may be coupled to more than one transduction pathway.

Oxidized LDL may contribute to the dysfunction in hypercholesterolaemia as it is a potent and rapidly acting inhibitor of endothelium-dependent relaxation (Jacobs *et al.*, 1990; Flavahan, 1992), that may chemically inactivate EDRF (Jacobs *et al.*, 1990) and directly inhibit NO synthase (Mitchell *et al.*, 1992). It also contains lysophosphatidylcholine (LPC) which can impair endothelium-dependent relaxation (Kugiyama *et al.*, 1990; Yokoyama *et al.*, 1990). This may result from transient activation of protein kinase C (Kugiyama *et al.*, 1992) which attenuates agonist-mediated endothelium-dependent relaxation by inhibiting a G_i protein (Flavahan *et al.*, 1991), depletion of internal Ca^{2+} stores (Inoue *et al.*, 1992), and direct disruption of receptor-G protein coupling (Flavahan, 1993). Lysophospholipids are also capable of rapid incorporation into the endothelial plasma membrane (Kugiyama *et al.*, 1990) potentially affecting transmembrane ion transport kinetics (Karli *et al.*, 1979). Such an action could specifically impair the flow response since in rabbit aorta, EDRF release induced by flow but not agonists involves the activation of K_{Ca} and K_{ATP} channels (Hutcheson & Griffith, 1994).

There is accumulating evidence that *in vivo* administration of L-arginine can improve impaired EDRF activity in conduit vessels from both animals and man, although this has not been a universal finding *in vitro* (Cooke *et al.*, 1991; Drexler & Zeiher, 1991; Mugge & Harrison, 1991). Complete restoration of 5-HT, histamine and ADP responses has nevertheless been reported in isolated coronary resistance arterioles from hypercholesterolaemic pigs (Kuo *et al.*, 1993). It has been suggested that the availability of L-arginine for NOS becomes a rate-limiting step for NO synthesis in hypercholesterolaemia, even though pathways exist to recycle L-citrulline to L-arginine at the expense of other amino acids (Mitchell *et al.*, 1990). However, plasma L-arginine levels were found to be normal in our hypercholesterolaemic rabbits. Similarly, enhanced formation of vasoconstrictor prostaglandins, which has also been proposed as an explanation for reduced endothelium-dependent relaxation in hypercholesterolaemic pigs (Shimokawa & Vanhoutte, 1989), cannot account for the impairment of flow- and agonist-induced reponses in the present study since the cyclo-oxygenase inhibitor indomethacin was present throughout.

In conclusion, this study confirms previous findings that short term hypercholesterolaemia impairs agonist- and flow-induced EDRF release in rabbit aorta. Both the pulsatile- and shear-related components of flow-induced EDRF release are abolished at an early stage in the disease process whereas acetylcholine-induced relaxations are still present reinforcing the suggestion that basal/flow-induced EDRF release is more susceptible to the deleterious actions of hypercholesterolaemia in conduit vessels. This greater susceptibility also provides further evidence that the mechanisms of pulsatile flow-induced EDRF release differ from those of agonist-induced release in this artery type.

This work was funded by a grant from the British Heart Foundation. The authors are grateful to Mrs R. Maylin for secretarial assistance and thank Professor G.M. Roberts of the University of Wales College of Medicine for his support and interest.

References

BATH, P.M.W., HASSELL, D.G., GLADWIN, A.M., PALMER, R.M.J. & MARTIN, J.F. (1991). Nitric oxide and prostacyclin: divergence of inhibitory effects on monocyte chemotaxis and adhesion to endothelium in vitro. *Arterioscler. Thromb.* **11,** 254–260.

BOSSALLER, C., HABIB, G.B., YAMAMOTO, H., WILLIAMS, C., WELLS, S. & HENRY, P.D. (1987). Impaired muscarinic endothelium-dependent relaxation and cyclic guanosine 5-monophosphate formation in atherosclerotic human coronary artery and rabbit aorta. *J. Clin. Invest.*, **79,** 170–174.

COOKE, J.P., ANDON, N.A., GIRERD, X.J., HIRSCH, A.T. & CREAGER. M.A. (1991). Arginine restores cholinergic relaxations by hypercholesterolemic rabbit aorta. *Circulation*, **83,** 1057–1062.

COX, D.A., VITA, J.A., TREASURE, C.B., FISH, R.D., ALEXANDER, R.W., GANZ, P. & SELWYN, A.P. (1989). Atherosclerosis impairs flow-mediated dilation of coronary arteries in humans. *Circ. Res.*, **80,** 458–465.

DREXLER, H. & ZEIHER, A.M. (1991). L-arginine improves endothelial function in the coronary microcirculation of patients with hypercholesterolaemia. *Circulation*, **84** (Suppl. 11), 11–14.

FLAVAHAN, N.A. (1992). Atherosclerosis or lipoprotein-induced endothelial dysfunction. Potential mechanisms underlying reduction in EDRF nitric oxide activity. *Circulation*, **85,** 1927–1938.

FLAVAHAN, N.A. (1993). Lysophosphatidylcholine modified G protein-dependent signalling in porcine endothelial cells. *Am. J. Physiol.*, **264,** H722–H727.

FLAVAHAN, N.A., SHIMOKAWA, H. & VANHOUTTE, P.M. (1991). Inhibition of endothelium-dependent relaxation by phorbol myristate acetate: role of a pertussis toxin-sensitive G-protein. *J. Pharmacol. Exp. Ther.*, **264,** 50–55.

FÖSTERMANN, U., MÜGGE, A., ALHEID, U., HAVERICH, A. & FRÖLICH, J.C. (1988). Selective attenuation of endothelium-mediated vasodilation in atherosclerotic human coronary arteties. *Circ. Res.*, **62,** 185–190.

GARG, U.C. & HASSID, A. (1990). Nitric oxide generating vasodilators and 8-bromo-cyclic GMP inhibit mitogenesis and proliferation of cultured rat vascular smooth muscle cells. *J. Clin. Invest.*, **83,** 1774–1777.

GRIFFITH, T.M., EDWARDS, D.H. & HENDERSON, A.H. (1987). Unstimulated release of endothelium-derived relaxing factor is independent of mitochondrial ATP generation. *Cardiovasc. Res.*, **21,** 565–568.

HAYASHI, Y., TOMOIKE, H., NAGASAWA, K., YAMADA, A., NISHIJIMA, H., ADACHI, H. & NAKAMURA, M. (1988). Functional and anatomical recovery of endothelium denudation of coronary artery. *Am. J. Physiol.*, **254,** H1081–H1090.

HUTCHESON, I.R. & GRIFFITH, T.M. (1991). Release of endothelium-derived relaxing factor is modulated both by frequency and amplitude of pulsatile flow. *Am. J. Physiol.*, **261,** H257–H262.

HUTCHESON, I.R. & GRIFFITH, T.M. (1994). Heterogeneous populations of K^+ channels mediate EDRF release to pulsatile flow but not agonists in rabbit aorta. *Am. J. Physiol.*, **266,** H590–596.

INOUE, N., HIRATA, K.-I., YAMADA, M., HAMAMORI, Y., MATSUDA, Y., AKITA, H. & YOKOYAMA, M. (1992). Lysophosphatidylcholine inhibits bradykinin-induced phosphoinositide hydrolysis and calcium transients in cultured bovine aortic endothelial cells. *Circ. Res.*, **71,** 1410–1421.

JACOBS, M., PLANE, F. & BRUCKDORFER, K.R. (1990). Native and oxidized low-density lipoproteins have different inhibitory effects on endothelium-derived relaxing factor in the rabbit aorta. *Br. J. Pharmacol.*, **100,** 21–26.

KARLI, J.N., KARIKAS, G.A., HATZIPAVLOU, P.K., LEVIS, G.M. & MOULOPOULOS, S.N. (1979). The inhibition of Na+ and K+ stimulated ATPase activity of rabbit and dog heart sarcolemma by lysophosphatidyl choline. *Life Sci.*, **24,** 1869–1876.

KUGIYAMA, K., KERNS, S.A., MORRISETT, J.D., ROBERTS, R. & HENRY, P.D. (1990). Impairment of endothelium-dependent relaxation by lysolecithin in modified low-density lipoproteins. *Nature*, **344,** 160–162.

KUGIYAMA, K., OHGUSHI, M., SUGIYAMA, S., MUROHARA, T., FUKUNAGA, K., MIYAMOTO, E. & YASSUE, H. (1992). Lysophosphatidylcholine inhibits surface receptor-mediated intracellular signals in endothelial cells by a pathway involving protein kinase C activation. *Circ. Res.*, **71,** 1422–1428.

KU, D.N., GIDDENS, D.P., ZARINS, C.K. & GLAGOV, S. (1985). Pulsatile flow and atherosclerosis in human and carotid bifurcation: positive correlation between plaque location and low and oscillating shear stress. *Arteriosclerosis*, **5,** 293–302.

KUO, L., DAVIES, M.J., CANNON, S. & CHILIAN, W.M. (1992). Pathophysiological consequences of atherosclerosis extend into the coronary microcirculation. *Circ. Res.*, **70,** 465–476.

MACARTHUR, H., HECKER, M., BUSSE, R. & VANE, J.R. (1993). Selective inhibition of agonist induced but not shear stress-dependent release of endothelial autocoids by thapsigargin. *Br. J. Pharmacol.*, **108,** 100–105.

McLENACHAN, J.M., VITA, J., FISH, R.D., TREASURE, C.B., COX, D.A., GANZ, P. & SELWYN, A.P. (1990). Early evidence of endothelial vasodilator dysfunction at coronary branch points. *Circulation*, **82,** 1169–1173.

MILLER, V.M. & BURNETT, J.C. (1992). Modulation of NO and endothelin by chronic increases in blood flow in canine femoral arteries. *Am. J. Physiol.*, **263,** H103–H108.

MITCHELL, J.A., HECKER, M., ANGGARD, E.E. & VANE, J.R. (1990). Cultured endothelial cells maintain their L-arginine level despite the continuous release of EDRF. *Eur. J. Pharmacol.*, **182,** 573–576.

MITCHELL, J.A., WARNER, T.D., HUANG, Z.-J., FORSTERMANN, U. & MURAD, F. (1992). Native LDL inhibits the release of endothelial derived relaxing factor by reducing the activity of endothelial nitric oxide synthase. *J. Vasc. Res.*, **29,** 169.

MONCADA, S., RADOMSKI, M.W. & PALMER, R.M.J. (1988). Endothelium-derived relaxing factor: identification as nitric oxide and role in the control of vascular tone and platelet function. *Biochem. Pharmacol.*, **37,** 2495–2501.

MUGGE, A. & HARRISON, D.G. (1991). L-arginine does not restore endothelial dysfunction in atherosclerotic rabbit arota *in vitro*. *Blood Vessels*, **28,** 354–357.

OHNO, M., GIBBONS, G.H., DZAU, V.J. & COOKE, J.P. (1993). Shear stress elevates endothelial cGMP-role of a potassium channel and G protein coupling. *Circulation*, **88,** 193–197.

RAGAZZI, E., FROLDI, G., PANDOLFO, L., CHINELATTO, A., DE BIASI, M., PROSDOCIMI, M., CAPARROTTA, L. & FASSINA, G. (1989). Segmental impairment of endothelium-mediated relaxation in thoracic aortas from atherosclerotic rabbits. Comparison to cholesterol infiltration and energy metabolism. *Artery*, **16,** 327–345.

RANDALL, M.D., SMITH, J.A. & GRIFFITH, T.M. (1993). Hypercholesterolaemia severely impairs EDRF-dependent collateral perfusion following acute arterial occlusion in rabbit isolated ear. *Br. J. Pharmacol.*, **109,** 838–844.

ROSS, R. (1993). The pathogenesis of athersclerosis: a perspective for the 1990s. *Nature*, **362,** 801–809.

SHIMOKAWA, H., FLAVAHAN, N.A. & VANHOUTTE, P.M. (1990). Natural course of the impairment of endothelium-dependent relaxations in regenerating porcine endothelial cells. Possible dysfunction of a pertussis-toxin-sensitive G-protein. *Circ. Res.*, **65,** 740–753.

SHIMOKAWA, H., FLAVAHAN, N.A. & VANHOUTTE, P.M. (1991). Loss of endothelial pertussis toxin-sensitive G-protein function in atherosclerotic porcine coronary arteries. *Circulation*, **83,** 652–660.

SHIMOKAWA, H. & VANHOUTTE, P.M. (1989). Impaired endothelium-dependent relaxation to aggregating platelets and related vasoactive substances in porcine coronary arteries in hypercholesterolaemia and atherosclerosis. *Circ. Res.*, **61,** 256–270.

SHIRASAKI, Y., SU, C., LEE, T.J.-F., KOLM, P., CLINE, W.H. & NICHOLS, G.A. (1986). Endothelial modulation of vascular relaxation to nitrovasodilators in ageing and hypertension. *J. Pharmacol. Exp. Ther.*, **239,** 861–866.

VERBEUREN, T.J., JORDAENS, F.H., ZONNEKEYN, L.L., VAN HOVE, C.E., COENE, M.C. & HERMAN, A.G. (1986). Effects of hypercholesterolaemia on vascular reactivity in the rabbit. *Circ. Res.*, **58,** 552–554.

WILLIAMS, J., LANG, D., SMITH, J.A. & LEWIS, M.J. (1993). Plasma L-arginine levels in a rabbit model of hypercholesterolaemia. *Biochem. Pharmacol.*, (in press).

WITZTUM, J.F. (1993). Role of oxidised low density lipoprotein in atherogenesis. *Br. Heart J.*, **69** (suppl), S12–S18.

YAMAMOTO, H., BOSSALLER, C., CARTWRIGHT, J. & HENRY, P.D. (1988). Videomacroscopic demonstration of defective cholinergic arteriolar vasodilatation in atherosclerotic rabbit. *J. Clin. Invest.*, **81,** 1752–1758.

YOKOYAMA, M., HIRATA, K., MIYAKA, R., AKITA, H., ISHIKAWA, Y. & FUKUZAKI, H. (1990). Lysophosphatidylcholines: essential role in the inhibition of endothelium-dependent vasorelaxation by oxidised low-density lipoprotein. *Biochem. Biophys. Res. Commun.*, **168,** 301–308.

(Received February 14, 1994
Revised April 19, 1994
Accepted April 27, 1994)

Br. J. Pharmacol. (1994), **113**, 195–203

Factors underlying the increased sensitivity to field stimulation of urinary bladder strips from streptozotocin-induced diabetic rats

[1]Teuvo L.J. Tammela, Janice A.K. Briscoe, Robert M. Levin & [2]Penelope A. Longhurst

Division of Urology, Hospital of the University of Pennsylvania, 3400 Spruce Street, Philadelphia, Pennsylvania 19104, U.S.A.

1 The responses of bladder strips from control, streptozotocin-diabetic, and sucrose-drinking rats to electrical field stimulation were investigated. Sucrose-drinking rats were included as additional controls because they have enlarged bladders as a result of non-diabetic diuresis.

2 Bladder strips from diabetic rats developed more spontaneous activity than those from the two control groups. Indomethacin reduced the amplitude and frequency of spontaneous contractions suggesting that they resulted from endogenous prostaglandin formation. Tetrodotoxin (TTX) had little effect, while α,β-methylene ATP caused increases in spontaneous activity.

3 Bladder strips from diabetic rats responded to field stimulation with greater contractions than controls in the absence of antagonists as well as in the presence of atropine and α,β-methylene ATP. Increasing TTX concentrations caused a step-wise depression of the contractile response to electrical stimulation which was not affected by preincubation with either atropine or α,β-methylene ATP.

4 Atropine and indomethacin had no effect on stength-duration curves constructed to measure threshold contractile responses to five pulses stimulation. The curves were shifted to the right by both TTX and α,β-methylene ATP, indicating that the responses were neurogenic in nature and at least partially, the result of stimulation of P_2-purinoceptors. In the absence of drugs, bladder strips from diabetics responded at lower voltages and pulse widths than those of control and sucrose-drinking rats, suggesting that they were more excitable.

5 The response curve of bladder strips from diabetics to field stimulation at increasing voltage was shifted upwards and to the left compared to strips from control or sucrose-drinking rats.

6 Bladder strips from diabetics responded to stimulation at increasing pulse width with greater responses than those from control or sucrose-drinking rats. At 1.0 ms pulse width, the TTX-resistant response of strips from diabetic rats was still greater than that of the other groups, indicating that a myogenic component was also involved.

7 The data suggest that bladder strips from diabetic rats are more excitable than those of control or sucrose-drinking rats. This may result from diabetes-induced decreases in bladder lipid or other membrane changes, and/or be a result of partial depolarization, perhaps related to diabetic neuropathy.

Keywords: Diabetes mellitus; sucrose; rat bladder; muscle contraction; electric stimulation

Introduction

The autonomic neuropathy associated with diabetes mellitus results in bladder dysfunction, characterized by a large capacity, atonic bladder (Frimodt-Møller, 1976). Although asymptomatic urodynamic changes have been found in diabetic children with or without neuropathy (Faerman *et al.*, 1971; Barkai & Szabo, 1993), the symptoms of diabetic cystopathy are more likely to present problems in older patients.

The urodynamic changes associated with experimental diabetes mellitus are similar to those found in diabetic patients. Micturition frequency and volume are increased; intravesical pressure upon filling remains low, and the amplitude of filling-induced intravesical contractions is reduced (Santicioli *et al.*, 1987; Andersson *et al.*, 1988; Longhurst *et al.*, 1991). However, there are some differences between the characteristics of human and experimental diabetes. Neurophysiological studies on insulin-treated spontaneously diabetic BB rats at 4 and 6 months, and 2 month streptozotocin-diabetic rats show changes in sensory innervation, but only modest changes in motor innervation (Paro *et al.*, 1990; Steers *et al.*, 1990; Nadelhaft & Vera, 1992). Furthermore, electrical field stimulation of strips from diabetic rat bladders fails to show any evidence of neuropathy; decreases in responsiveness have not been observed (Carpenter, 1983; Lincoln *et al.*, 1984; Luheshi & Zar, 1990; 1991; Paro *et al.*, 1990; Longhurst *et al.*, 1991). Some markers of innervation include acetylcholinesterase, choline acetyltransferase, and nerve growth factor (NGF). Decreased acetylcholinesterase and choline acetyltransferase staining has been noted in bladders from human and experimental diabetics when expressed as concentration, suggesting that cholinergic innervation is altered by diabetes (Faerman *et al.*, 1973; Lincoln *et al.*, 1984). Buttyan and co-workers found increased bladder NGF mRNA 4 weeks after streptozotocin (STZ) treatment, but a steady decrease in NGF protein up to 8 weeks, suggesting a decreased efficiency of NGF mRNA translation (Te *et al.*, 1992). More recently, the same group found decreases in NGF expression 6 weeks after induction of diabetes (Koo *et al.*, 1993).

The response of urinary bladder strips to electrical field stimulation is thought to be at least partially the result of stimulation of cholinergic and purinergic nerves. The relative contributions of cholinergic and non-adrenergic, non-cholinergic (NANC) innervation to the contractile response appear to be species and stimulus-dependent (Sibley, 1984; Brading & Williams, 1990). It is generally agreed that the rapid phasic portion of the response to field stimulation, which is relatively unchanged after atropine treatment but lost after

[1] Present address: Division of Urology and Department of Clinical Medicine, University of Tampere, Tampere, Finland.
[2] Author for correspondence.

desensitization of P_2-purinoceptors with α,β-methylene ATP, results from stimulation of purinergic nerves. Conversely, the tonic portion, which is reduced after atropine treatment but unaltered by P_2-purinoceptor desensitization, is thought to result from stimulation of cholinergic nerves (Brading & Williams, 1990). A series of studies by Luheshi & Zar suggested that bladder strips from diabetic rats had a reduced NANC response and increased cholinergic response to field stimulation, as a result of increased acetylcholine release and reduced NANC transmitter release (Luheshi & Zar, 1990; 1991). Previous studies from this laboratory showed that bladder strips from diabetic rats responded to electrical field stimulation with significantly greater responses than those from control or sucrose-drinking rats (Longhurst *et al.*, 1991).

In the present paper we have investigated the possibility that differences in excitability of diabetic rat bladders were responsible for the changes in response to electrical stimulation, by altering stimulation parameters, and using compounds which altered resting membrane potential or nerve conduction. We also examined further the effects of diuresis induced by sucrose consumption on the contractile responses to electrical stimulation to evaluate whether the observed changes in bladders from diabetics resulted from the diabetic state or increases in bladder mass *per se*.

Methods

Animals

Male Sprague-Dawley rats (300–325 g) obtained from Ace Animals Inc. (Boyertown, PA, U.S.A.) were used throughout the study. All animals received food and water *ad libitum*, except when indicated.

Induction of diabetes

Rats were fasted for 18–24 h. Diabetes was induced in approximately one-third of the rats with a single injection of STZ (60 mg kg^{-1}, i.p.) in ice-cold 0.02 M citrate saline. The remainder of the rats were injected with vehicle. Rats were used 9–12 weeks after the induction of diabetes.

Sucrose treatment

After injection of the vehicle, one-half of the control rats was given 5% sucrose in tap water to drink instead of water. This was continued until the day of experimentation. Sucrose consumption causes polyuria and increases in bladder mass (Longhurst *et al.*, 1990b). For this reason this group was included as non-diabetic controls. Rats were used 9–12 weeks after onset of sucrose treatment. The remaining group of control rats was given tap water to drink.

Tissue preparation

Before anaesthesia, blood samples were collected from the tail artery and the serum separated and analyzed for serum glucose by use of the ABTS method of Bergmeyer & Bernt (1974). The rats were then anaesthetized with pentobarbitone (50 mg kg^{-1}, i.p.). The urinary bladder was removed from each rat and placed in ice-cold Krebs-Henseleit buffer of the following composition (mM): NaCl 113, KCl 4.8, $CaCl_2$ 2.5, KH_2PO_4 1.2, $MgSO_4.7H_2O$ 1.2, $NaHCO_3$ 25 and dextrose 5.6 The bladder was separated into bladder body and base at the level of the ureters. Three or four equally sized longitudinal strips of approximately 2 mm × 10 mm were cut from the bladder body, suspended on 000 sutures between a pair of platinum ring electrodes 8 mm apart, and placed in 30 ml organ baths containing Krebs-Henseleit solution equilibrated with 95% O_2, 5% CO_2, and maintained at 32°C (to reduce spontaneous activity). The tissues were connected to Grass force displacement transducers (FT03) and adjusted to 2 g resting tension. Previously it was determined in our laboratory that maximal active tension was generated at 2 g resting tension in all groups (Longhurst *et al.*, 1990a). Responses were recorded on a Grass Model 7E polygraph. All tissues were then given a 30 min equilibration period during which they were washed and the resting tension was adjusted every 10 min. Electrical stimuli were delivered using a Grass S88 stimulator. Rate of tension development was measured using a LS-14 logging analyzer (Buxco Electronics, Inc., Troy, NY, U.S.A.).

Influence of antagonists on response to field stimulation

Frequency-response curves were elicited by stimulating the tissues for 15 s with pulses of 0.05 ms width at 100 V every 2 min. Subsequently after resting periods of 15 min, frequency-response curves were repeated in the presence of different antagonists as described in the results sections.

Construction of strength-duration curves

Using separate strips, the voltage required at each pulse width to produce a just noticeable contractile response to five stimuli at 1 Hz was recorded. After construction of a control (no drug) curve, antagonists were added, and a second curve recorded after an appropriate period of time (see drugs). One strip from each bladder was exposed to each antagonist. Preliminary experiments showed that repetitive contractile responses to stimulation were not altered by time.

Measurement of voltage and pulse width dependence

Using separate strips, the contractile response to 10 pulses at 32 Hz stimulation was measured at increasing voltage using 0.05 ms width, or at increasing pulse width using 100 V stimulus.

Drugs

The following drugs were obtained from Sigma Chemical Company (time of exposure and dose in parentheses): atropine (15 min, 1 μM), α,β-methyleneadenosine 5'-triphosphate (α,β-methylene ATP) (15 min, 100 μM), indomethacin (60 min, 10 μM), and tetrodotoxin (TTX) (15 min, 1 μM). Indomethacin was dissolved in 0.5 ml dimethylsulphoxide (DMSO) and made up to 100 ml with Krebs. This was then added to the organ bath in a 1:10 dilution.

Statistical analysis

Data are presented as means ± s.e.mean or as a percentage of maximal control (no drug) response. To avoid confusion between references to control (no drug) contractile responses and those to control (not diabetic) animals or tissues, control contractile responses will be referred to in the results section as 'no drug'. Differences between the response of a single strip to field stimulation before and after drug treatment during construction of strength-duration curves were compared by the paired t test. Comparisons between groups were done using the Bonferroni test. A probability of $P < 0.05$ was taken as the criterion of significance. In all instances N = number of animals and n = number of strips.

Results

Rat weight, bladder weight, and serum glucose concentration

Diabetes caused the usual decreases in body weight, and increases in serum glucose concentration and bladder weight compared to control and sucrose-drinking rats (Table 1).

Table 1 Effect of streptozotocin (STZ)-induced diabetes and sucrose-consumption on rat weight, bladder and strip weights, and serum glucose concentration

	Control	*STZ*	*Sucrose*
Rat weight (g)	549 ± 14	276 ± 12†	564 ± 19
Bladder weight (mg)	143.5 ± 4.5	243.2 ± 9.2†	187.0 ± 8.3*
Serum glucose (mmol/l)	5.9 ± 0.2	24.5 ± 1.2†	6.0 ± 0.3

Values indicate the mean ± s.e.mean ($N = n = 32-48$). *Significant difference compared to controls; †significant difference compared to both controls and the sucrose group ($P < 0.05$).

Bladder weights were significantly increased in sucrose-drinking rats compared to controls, but there were no differences in rat weight or serum glucose concentration between the control and sucrose group (Table 1).

General observations of the contractile responses of bladder strips

There was a great deal of spontaneous activity generated by the bladder strips, particularly those from diabetic rats. To reduce this as much as possible, the studies were done at 32°C. Addition of indomethacin decreased the amplitude of spontaneous activity. TTX had little or no effect on spontaneous activity, while α,β-methylene ATP increased the amplitude, particularly in strips from diabetics (Figure 1). On several occasions after α,β-methylene ATP treatment it was difficult to distinguish the response to low frequencies of field stimulation from the spontaneous activity, which in some instances was 1–3 g in amplitude.

The mean contractile response of bladder strips from diabetic rats to α,β-methylene ATP was significantly greater than that of controls (Figure 2). Bladder strips appeared to be fully desensitized with one dose of α,β-methylene ATP, because administration of a second dose was without effect. After treatment with indomethacin the contractile response to α,β-methylene ATP was slightly reduced in the control group (Figure 2). In both the STZ and sucrose-drinking group, the response to α,β-methylene ATP was significantly reduced by indomethacin pretreatment to control levels, indicating that the increased tension observed in response to α,β-methylene ATP was probably mediated by prostaglandin release.

Non-cholinergic, non-adrenergic component of the response to field stimulation

There was a difference in the general shape of the response to field stimulation in the absence of drugs between strips from diabetic rats and those from control and sucrose-drinking rats (Figure 3). In particular, strips from diabetic rats had less distinction between the phasic (within 5 s) and tonic

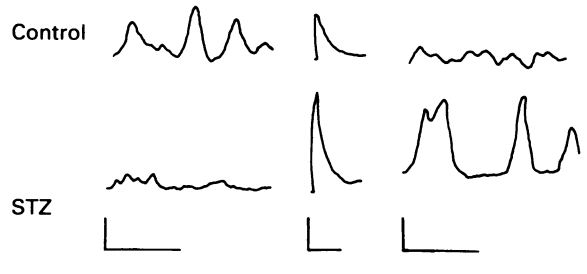

Figure 1 Influence of α,β-methylene ATP (100 μM) on spontaneous activity in bladder strips from control (top) and diabetic (STZ) (bottom) rats. Left panel, spontaneous activity before α,β-methylene ATP; centre panel, response to α,β-methylene ATP; right panel, spontaneous activity after α,β-methylene ATP. Left and right panels, vertical line represents 0.5 g, horizontal line represents 1 min. Centre panel, vertical line represents 2 g, horizontal line represents 4 min.

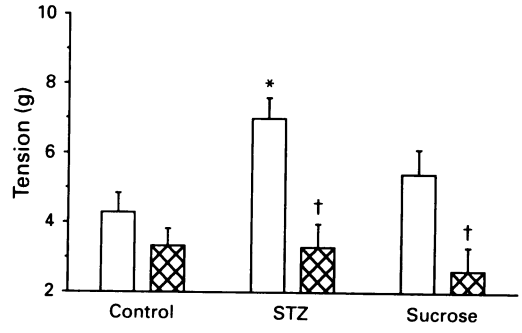

Figure 2 Contractile response of bladder body strips from control, diabetic (STZ), and sucrose-drinking rats to α,β-methylene ATP (100 μM) in the absence (open columns) and presence (cross-hatched columns) of indomethacin (10 μM, 60 min). Each column represents the mean ± s.e.mean ($N = n = 6-9$). *Significantly different from response of control bladder strips; †significantly different from α,β-methylene ATP alone ($P < 0.05$).

Figure 3 Representative responses of bladder strips from control (Con), diabetic (STZ), and sucrose-drinking (Suc) rats to 4 Hz stimulation. Parameters were 100 V, 0.05 ms pulse width, 15 s stimulation.

(after 15 s of stimulation) portion of the response, while in control and sucrose-drinking rats the phasic portion was usually easily distinguishable, and larger than the tonic portion. At all frequencies, the phasic:tonic component of the contractile response of strips from diabetic rats was significantly less than that of control and sucrose-drinking rats. Values at 2 and 32 Hz are shown in Table 2. In general, after treatment with α,β-methylene ATP the phasic component of the response to field stimulation was lost and the contraction appeared more like that shown for the bladder from the diabetic rat in Figure 3. In separate experiments, we calculated the rate of tension development in response to stimulation at low and high rates of frequency. Tension and maximal rate of tension development in response to electrical stimulation at 2 and 32 Hz were significantly greater in strips from sucrose-drinking rats than controls, and greater than controls at 32 Hz for strips from diabetic rats (Table 2).

Frequency-response curves for bladder strips in the absence and presence of atropine, α,β-methylene ATP, and TTX are shown in Figure 4. Because of the difficulty in distinguishing phasic and tonic responses, the data are presented as maximal responses. Strips from diabetics responded to stimulation in the absence of antagonists with significantly

Table 2 Effect of streptozotocin (STZ)-induced diabetes and sucrose-consumption on phasic and tonic components and maximal rate of tension development after 2 and 32 Hz field stimulation

	Control	*STZ*	*Sucrose*
Relative proportion of phasic:tonic component (phasic response (g)/tonic response (g))			
2 Hz	2.53 ± 0.32	1.15 ± 0.10*	2.03 ± 0.23
32 Hz	2.27 ± 0.27	1.35 ± 0.12*	1.59 ± 0.11
Maximal rate of tension development ($g\ s^{-1}$)			
2 Hz	1.49 ± 0.17	2.35 ± 0.42	2.39 ± 0.23*
32 Hz	4.30 ± 0.38	6.58 ± 0.80*	6.87 ± 0.58*

Parameters used were 0.05 ms width, 0.01 ms delay, 100 V, stimulation for 15 s. Values indicate the mean ± s.e.mean (for phasic:tonic experiments, $N = n = 17-20$; for rate experiments, $N = 6-9$, $n = 12-18$). *Significant difference compared to controls ($P < 0.05$).

greater contractions than those of control or sucrose-drinking rats. Incubation with atropine caused a 46% decrease in the response of control bladder strips to 32 Hz field stimulation. The responses of strips from diabetic and sucrose-drinking rats were decreased to a slightly greater extent, by 54% and 50% respectively (Figure 4). The effects of atropine were most noticeable at higher frequencies. Addition of α,β-methylene ATP caused a further decrease in the response to 32 Hz to 27% of the no drug maximum in controls and 16% and 27% in diabetic and sucrose-drinking rats. TTX reduced the contractile response to 32 Hz to 10% of the no drug maximum in controls and 5 and 6% in strips from diabetic and sucrose-drinking rats. In the presence of atropine the absolute responses of strips from diabetic rats were significantly greater than those of the control groups, but there were no significant differences in the degree of antagonist-induced suppression between groups.

Incubation with indomethacin had greater effects on the responses of bladder strips to low frequency stimulation than high frequency (Figure 5). Responses of strips from controls to low frequencies of stimulation were reduced by pretreatment with indomethacin ($P = 0.040$); the decrease was less at higher frequencies. In contrast, strips from diabetic and sucrose-drinking rats were less affected by indomethacin pretreatment. Cumulative addition of atropine and α,β-methylene ATP with indomethacin, or TTX alone caused significant decreases in contractile response of a similar magnitude to those shown in Figure 4.

To try to identify the relative importance of cholinergic vs. purinergic transmitter release in the response to field stimulation, the effects of increasing TTX concentrations were monitored in the presence or absence of atropine or α,β-methylene ATP. Three separate strips from each rat were used. All strips were stimulated first in the absence of drugs (no drug curves). Subsequently one strip was incubated in normal Krebs to establish a time-effect, one with atropine, and one with α,β-methylene ATP before repeating the frequency-response curve (time; atropine; α,β-methylene ATP curves). Then each strip was incubated with increasing concentrations of TTX, 15 min before stimulation. Bladder strips from diabetic rats responded to field stimulation with significantly greater responses than the two control groups, both in the absence and presence of atropine and α,β-methylene ATP. In all groups, TTX caused a sequential decrease in contractile response, which was not altered by the presence of atropine or α,β-methylene ATP. Inhibition was first seen at 20–40 nM TTX. Maximal inhibition was seen with 320 nM TTX. Increasing the concentration of TTX to 640 nM did not reduce the response further (data not shown). There were no differences between the responses of strips from control (Figure 6), diabetic (not shown), or sucrose-drinking rats (not shown) in the absence and presence of atropine and α,β-

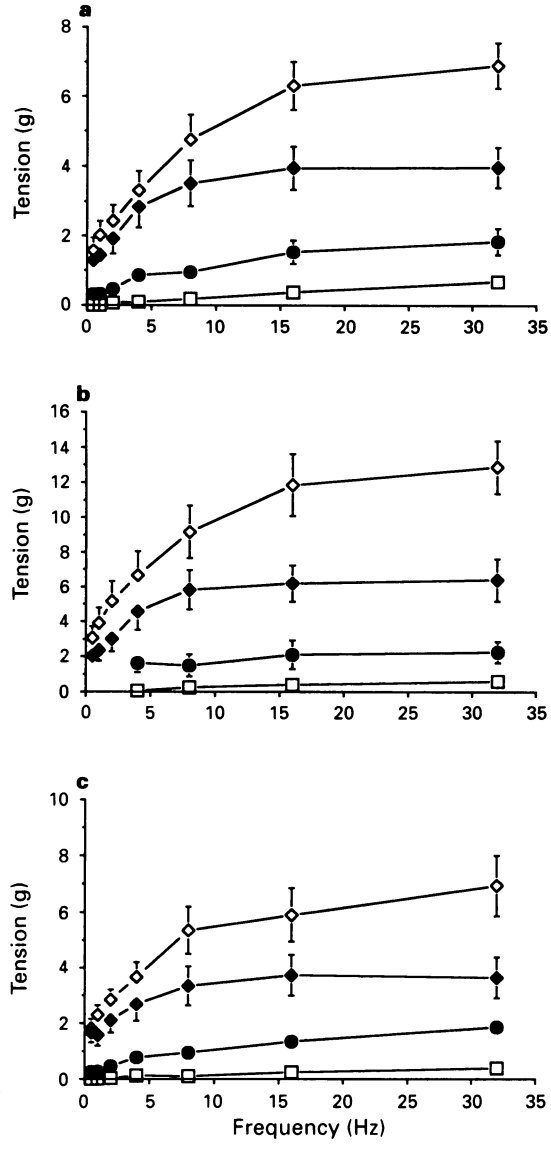

Figure 4 Influence of diabetes mellitus (b) and sucrose-consumption (c) on frequency-response curves of rat bladder body strips after cumulative addition of different antagonists; (a) control: (◇) no drug; (◆) atropine 1 μM, 15 min; (●) atropine + α,β-methylene ATP 100 μM, 15 min; (□) tetrodotoxin 1 μM 15 min. Each point represents the mean ± s.e.mean ($N = n = 7$ or 8).

methylene ATP, and there were no differences in the IC_{50} values for TTX, whether used in the absence or presence of antagonists. Nor were there any differences in TTX IC_{50} values between strips from control, diabetic, or sucrose-drinking rats.

Strength-duration curves

Bladder strips from diabetic rats responded to five pulses of field stimulation at significantly lower voltages and pulse widths than did those of control or sucrose-drinking rats (Figure 7). At 0.1 ms width, 43.2 ± 2.6 V were required to elicit a contraction in strips from control rats ($N = 12$, $n = 36$), 31.5 ± 2.8 V for diabetics ($N = 13$, $n = 39$; $P = 0.003$ vs. controls, $P = 0.058$ vs. sucrose), and 39.4 ± 3.1 V for sucrose-drinking rats ($N = 12$, $n = 36$; $P = 0.35$ vs. controls). Addition of α,β-methylene ATP and TTX caused significant shifts of rat bladder strength-duration curves to the right, while atropine and indomethacin had no effects on the strength-duration curves (Figure 7). No differences were

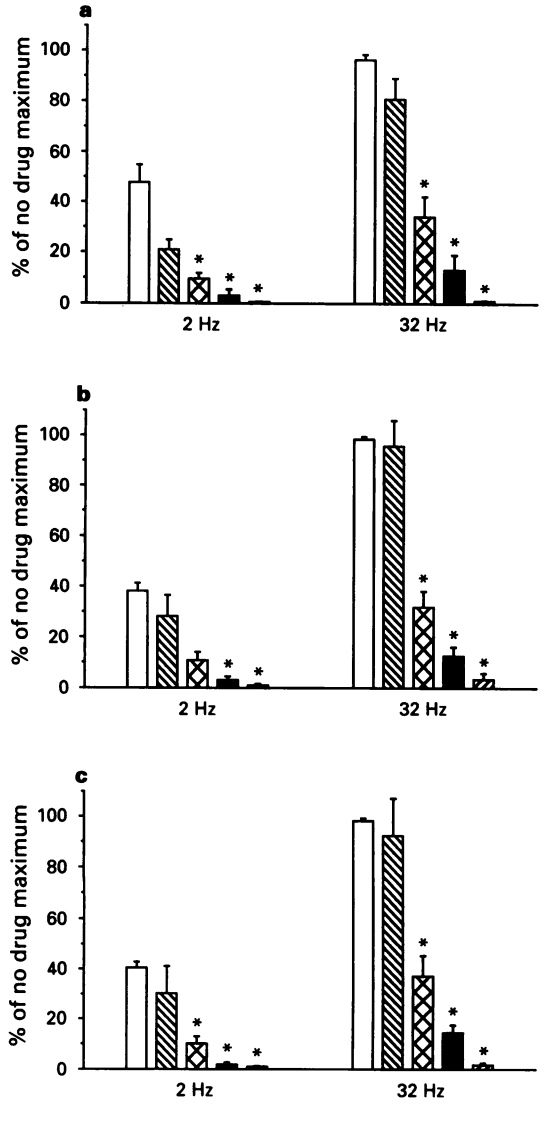

Figure 5 Influence of diabetes mellitus (b) and sucrose-consumption (c) on responses of rat urinary bladder strips to electrical stimulation after cumulative addition of different antagonists; (a) control: no drug (open columns); indomethacin 10 μM, 60 min (left hatched-columns); indomethacin + atropine 1 μM, 15 min (cross-hatched columns); indomethacin + atropine + α,β-methylene ATP 100 μM, 15 min (solid columns); TTX 1 μM, 15 min (right hatched columns). Data are expressed as percentage of no drug maximum. Each bar represents the mean ± s.e.mean ($N = n = 6$–9). *Significantly different from the no drug response ($P < 0.05$).

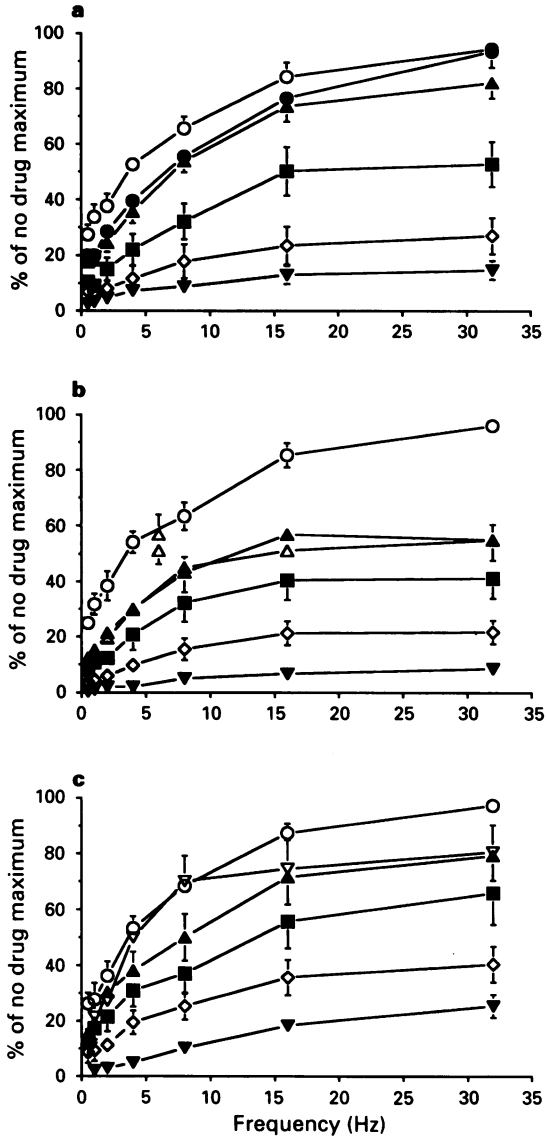

Figure 6 Effects of increasing tetrodotoxin (TTX) concentrations on the frequency-response curves of control rat bladder body strips. Data are expressed as percentage of the maximum no drug response. Each point represents the mean ± s.e.mean ($N = n = 5$–9). (a) (○) No drug; (●) time curve; (▲) TTX 20 nM; (■) TTX 80 nM; (◇) TTX 160 nM; (▼) TTX 320 nM. (b) (○) No drug; (△) atropine 1 μM, 15 min; (▲) atropine + TTX 20 nM; (■) atropine + TTX 80 nM; (◇) atropine + TTX 160 nM; (▼) atropine + TTX 320 nM. (c) (○) No drug; (▽) α,β-methylene ATP 100 μM, 15 min; (▲) α,β-methylene ATP + TTX 20 nM; (■) α,β-methylene ATP + TTX 80 nM; (◇) α,β-methylene ATP + TTX 160 nM; (▼) α,β-methylene ATP + TTX 320 nM. Curves generated in the presence of 10, 40 and 640 nM TTX have been omitted for clarity.

noted in the responses of bladders strip from control, diabetic, or sucrose-drinking rats in the sensitivity of the strength-duration curves to antagonists.

Responses to increasing voltage or pulse width

The increased spontaneous activity and increased sensitivity to electrical stimulation of the strips from diabetic rats during construction of the voltage-duration curves led us to investigate the responses to increasing voltage and pulse width more closely. Diabetes caused a significant shift of the voltage-response curve upwards and to the left compared to the two control groups, indicating that the strips were more excitable (Figure 8). The responses of the strips from diabetics were significantly greater than those of controls at all voltages studied. There were no differences between the responses of strips from sucrose-drinking and control rats.

The effects of increasing pulse width while stimulating at 32 Hz and 100 V were also determined. At 0.05 and 0.1 ms pulse width the contractile responses of strips from diabetics were significantly greater than those from control or sucrose-drinking rats (Figure 9). At all pulse widths the contractile responses of strips from sucrose-drinking rats were the same as those of controls. Incubation with TTX almost completely suppressed the response to stimulation at widths less than 0.2 ms, and at these widths there were no differences in response between the three groups. Increasing the pulse width to 1.0 ms duration in the presence of TTX caused significantly greater responses of strips from diabetics (4.18 ± 0.60 g, $N = n = 8$) than those from control (2.40 ±

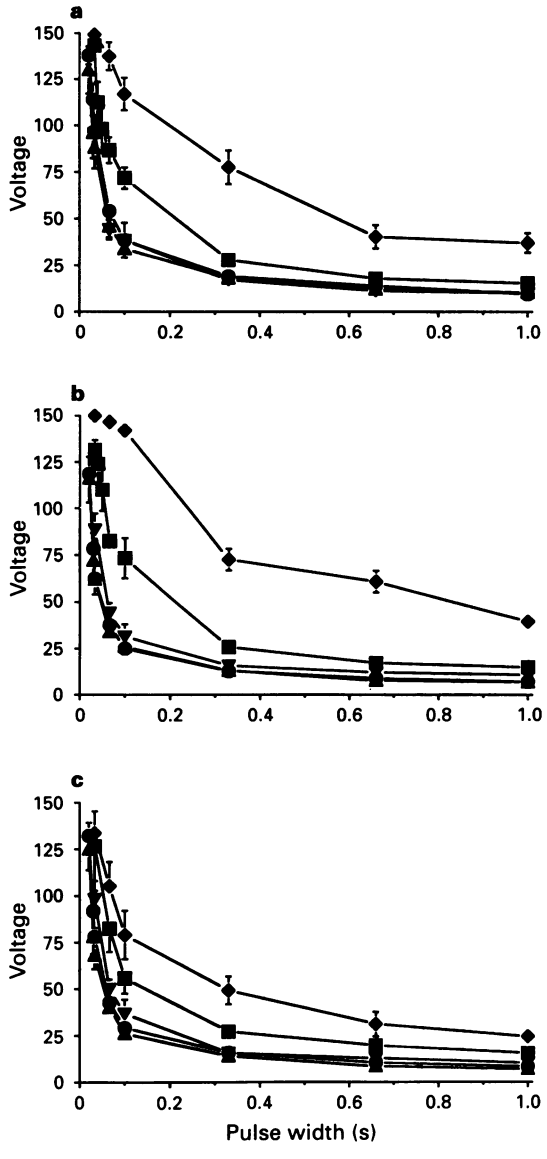

Figure 7 Influence of diabetes mellitus (b) and sucrose-consumption (c) on strength-duration curves of rat urinary bladder body strips; (a) control: (●) no drug; (■) α,β-methylene ATP 100 μM, 15 min; (▲) indomethacin 10 μM, 60 min; (◆) tetrodotoxin 1 μM, 15 min; (▼) atropine 1 μM, 15 min. Each point represents the mean ± s.e.mean of response to five stimuli at 1 Hz ($N = n = 5-15$).

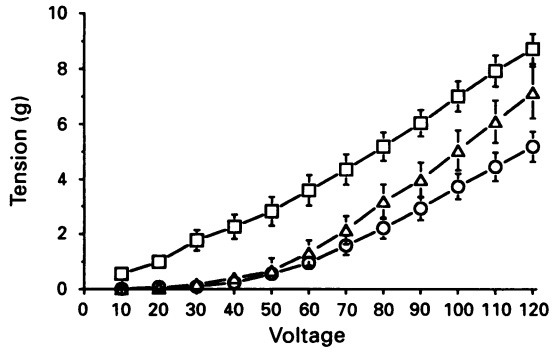

Figure 8 Influence of diabetes mellitus and sucrose-consumption on the contractile response of rat bladder body strips to ten pulses at increasing voltage during stimulation at 32 Hz and 0.05 ms width: (○) control; (□) diabetic; (△) sucrose. Each point represents the mean ± s.e.mean ($N = n = 5-12$). Responses of strips from diabetic rats were significantly greater than those of controls at all voltages studied ($P < 0.05$).

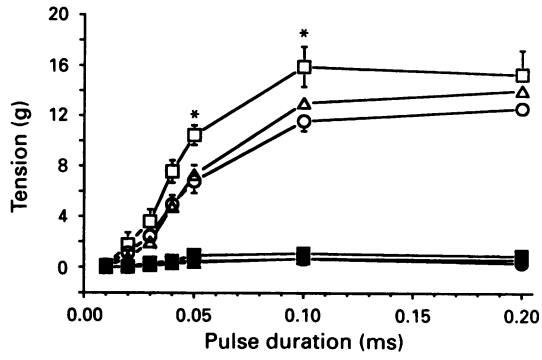

Figure 9 Influence of diabetes mellitus and sucrose-consumption on the contractile response of rat bladder body strips to ten pulses with increasing width at 32 Hz and 100 V. Open symbols are in the absence, and closed symbols in the presence of tetrodotoxin TTX (1 μM, 15 min): (○, ●) control; (□, ■) diabetic; (△, ▲) sucrose. Each point represents the mean ± s.e.mean ($N = n = 8$). *Significantly different from response of control bladder strips ($P < 0.05$).

0.32 g, $N = n = 8$) or sucrose-drinking rats (2.88 ± 0.19 g, $N = n = 8$).

Discussion

Several laboratories have shown that bladders from diabetic rats respond to field stimulation and contractile agents with greater responses than those of controls (Latifpour *et al.*, 1989; Longhurst *et al.*, 1991). The non-specificity of this increased responsiveness implies that the mechanism is unlikely to be the result of changes in specific receptors, but rather, could result from increases in bladder excitability or post-receptor events. The findings of the current study suggest that bladders from diabetic rats are more excitable and therefore more sensitive to membrane depolarization than are bladders from control or sucrose-drinking rats.

Previous studies from this laboratory found that bladder strips from diabetic rats responded to electrical field stimulation with significantly greater responses than those of control or sucrose-drinking rats, and this finding was confirmed in the present study. The shape of the response to field stimulation was different between groups: the phasic component, which is thought to result from ATP release, was smaller in relation to the tonic portion in bladder strips from diabetic compared to control and sucrose-drinking rats, and resembled the response obtained with control strips in the presence of the acetylcholinesterase inhibitor, physostigmine (Longhurst & Tammela, unpublished observation), suggestive of an increase in the cholinergic component. This indirect quantitative evidence supports the finding of Luheshi & Zar who found that in the presence of atropine, the non-cholinergic response was significantly smaller in diabetics than controls (Luheshi & Zar, 1990), while in the presence of 1 μM nifedipine, the cholinergic response was significantly larger (Luheshi & Zar, 1991). They postulated that this might result from early degenerative cholinergic nerve changes resulting in loss of normal control over quantal transmitter release, or alternatively a compensatory overactivity of the cholinergic component, resulting in increases in release of the cholinergic transmitter and decreases in release of the NANC transmitter(s).

Bladder strips from diabetic rats exhibited an increased amplitude of spontaneous activity and had an increased sensitivity to increasing voltage and pulse width compared to those from control and sucrose-drinking rats. The spontaneous activity was probably partially the result of prostaglandin release, as previously suggested by Maggi *et al.* (1984), since the amplitude was substantially reduced by

indomethacin. Anderson & Kohn (1978) found a non-competitive antagonism of the calcium dose-response curve in 80 mM K^+ depolarized rabbit bladder strips, and suggested that indomethacin had effects on calcium channels as well as on prostaglandin synthesis. However, other studies have shown only minor suppressant effects of 10 μM indomethacin on bladder strip responses to acetylcholine (Maggi *et al.*, 1984), carbachol (Anderson, 1982), or palytoxin (Posangi *et al.*, 1992). Additionally, indomethacin had no effects on carbachol-induced calcium uptake by rabbit bladder strips (Anderson, 1982). Bladders from diabetic rats have an increased basal prostacyclin release (Jeremy *et al.*, 1986) and bradykinin-stimulated prostaglandin $F_{2\alpha}$ release (Pinna *et al.*, 1992) compared to controls. Increased prostaglandin release could therefore account, at least in part, for the greater spontaneous activity observed in bladders from diabetic rats. However, the lack of effect of indomethacin on strength-duration and frequency-response curves indicates that increases in prostaglandin release cannot explain the increased responsiveness to electrical stimulation.

In our experiments, incubation with α,β-methylene ATP caused contraction followed by a considerable degree of spontaneous activity. This was particularly noticeable with the strips from diabetic rats, was long-lasting, and presumably the result of generation of spontaneous action potentials. Previous studies have shown that the contractile response of the urinary bladder to ATP is partially dependent on prostaglandin synthesis (Dean & Downie, 1978; Andersson *et al.*, 1980; Choo & Mitchelson, 1980). Although incubation with indomethacin had little effect on the contractile response of control bladder strips to α,β-methylene ATP, the responses of strips from diabetic and sucrose-drinking rats were significantly reduced, suggesting that the response was at least partially the result of prostaglandin synthesis. Increased prostaglandin synthesis in bladders from diabetic rats could therefore explain the changes in activity after α,β-methylene ATP treatment, as well as basal spontaneous activity.

Increases in spontaneous activity are frequently associated with changes in membrane excitability. In the vas deferens and other smooth muscles, spontaneous activity increases after denervation, and this is associated with significant decreases in the contractile response to field stimulation and non-specific increases in responses to agonists (Fleming *et al.*, 1973). This postjunctional supersensitivity is thought to be due to a reduction in the resting membrane potential (Fleming & Westfall, 1975). One explanation for the apparent increase in excitability in bladders from diabetic rats is that it could result from depolarization, causing the Em to be closer to the threshold voltage required to generate action potentials or excitatory junction potentials, similar to the mechanism proposed in the vas deferens to explain postjunctional supersensitivity (Fleming & Westfall, 1975). Electrophysiological studies have not been done on bladders from diabetics rats, therefore the presence of depolarization has not been established.

Removal of the pelvic ganglion or chemical sympathectomy causes increases in spontaneous activity of rat bladder strips, which are insensitive to TTX, but no difference in the response to field stimulation between denervated and control bladder strips (Ekström & Uvelius, 1981), and supersensitivity to autonomic agonists (Ekström, 1981; Ekström & Malmberg, 1984), which may be related to bladder distension and hypertropy. Studies of the influence of denervation or decentralization on choline acetyltransferase, which is used as a marker for cholinergic innervation, found that although initially decreased, levels increased rapidly after surgery and returned to control levels 10 to 25 days after surgery (Ekström, 1981). This suggests that measurement of choline acetyltransferase and other enzymes modulating acetylcholine synthesis, as well as evaluation of the contractile response to field stimulation, may not be very specific tests for denervation in the bladder. The possibility that diabetic neuropathy-induced changes could cause a postjunctional supersensitivity in bladders from two month-diabetic rats has seemed unlikely because of the findings of increases (Longhurst *et al.*, 1991) or no changes (Carpenter, 1983; Lincoln *et al.*, 1984; Luheshi & Zar, 1990; 1991; Paro *et al.*, 1990) in responses to electrical stimulation, and increases in the total activities of acetylchlinesterase and choline acetyltransferase per bladder (Lincoln *et al.*, 1984). However, acetylcholinestserase activity was unchanged in a study by Kudlacz *et al.* (1989). Luheshi & Zar concluded that possible mechanisms contributing to the relative increase in the cholinergic component of the response of diabetic bladder strips to electrical field stimulation were increased transmitter release, decreased inactivation, or degenerative nerve changes. They could find no difference in responses to acetylcholine in the presence of 1 μM nifedipine, and this in conjunction with the findings of increased cholinesterase activity of Lincoln *et al.* (1984), led them to conclude that decreased inactivation was unlikely to be a factor. However, if we consider that removal of the pelvic ganglia fails to affect the contractile responses of bladder strips to nerve stimulation (Ekström & Uvelius, 1981), and produces only temporary changes in choline acetyltransferase activity (Ekström, 1981), the findings of increases or no change in contractile response of bladder strips from diabetic rats to electrical stimulation, associated with variable levels of acetylcholinesterase and choline acetyltransferase, cannot be used as circumstantial evidence that two months after induction of diabetes with streptozotocin, there is no evidence of neuropathy in the bladder. The possibility remains that the increased responsiveness of bladder strips from diabetic rats to agonists could therefore result from some form of denervation supersensitivity, maybe related to diabetic neuropathy.

Strength-duration curves provide information about the general excitability of tissues. Similar to the findings of Brading & Williams (1990), atropine had little effect on the strength-duration curves of bladder strips from any group, implying that acetylcholine is not the predominant transmitter involved in the response to field stimulation. Similarly, indomethacin had little effect on the strength-duration curves. However, both atropine and indomethacin had quite significant depressant effects on the frequency-response curve. The explanation for this apparent discrepancy is probably related to the difference between transmitter release stimulated by five pulses (strength-duration) vs. 15 s stimulation in the frequency-response curves (ranging from seven pulses to 0.5 Hz to 960 pulses at 64 Hz). The amount of acetylcholine released by a small number of pulses (as seen in the strength-duration curves at at low frequencies of stimulation) is probably too low to stimulate influx of extracellular calcium or initiate pharmacomechanical coupling and cause a contraction. Apparently ATP can be released by low numbers of pulses, because the strength-duration curve is shifted to the right by α,β-methylene ATP, and the response to low frequencies of stimulation in frequency-response curves is more sensitive to α,β-methylene ATP than to atropine.

The experiments using increasing concentrations of TTX were done to determine whether acetylcholine and ATP, the presumed major transmitters responsible for field stimulation-induced contraction in the rat bladder, were released from the same nerve terminals, or whether separate cholinergic and purinergic nerves were present. Our rationale was that if the transmitters were released from the same nerve, the sensitivity to TTX blockade would be the same. Whether the strips were incubated with no drug, atropine to block muscarinic receptors and the responses to cholinergic stimulation, or α,β-methylene ATP to block the response to ATP release, the sensitivity to TTX was the same, and there were no differences between diabetics and controls. However, we cannot exclude the possibility that separate nerves releasing acetylcholine and ATP are present (different nerves with the same sensitivity to TTX could be present).

In separate experiments we looked at the influence of TTX on the contractile response to increasing pulse width. In the

absence of TTX, the response of strips from diabetics were significantly greater than those of the two control groups at 0.05 and 0.1 ms, widths at which the response was subsequently shown to be of neural origin. At 1.0 ms width in the presence of TTX, where the response was elicited by direct muscle stimulation, the response was also significantly greater in the strips from diabetics. This indicates that some of the diabetes-induced alterations in contractile responsiveness of the urinary bladder may result from myogenic changes, presumably related to alterations in calcium homeostasis, or second messenger systems. Previous studies from this laboratory examined the sensitivity of bladder strips from diabetics to calcium, and could find no differences in responsiveness (Longhurst *et al.*, 1992). However, studies by Belis *et al.* (1992) found changes in calcium channel activity in bladders from diabetic rats. Additionally, the non-specificity of the increased responses makes alterations in specific receptors an unlikely explanation.

Changes in membrane lipid content or type could alter the membrane properties of the bladder cells, and cause alterations in excitability as well as responsiveness to agonists. We previously showed that bladders from diabetic rats had a significantly lower lipid content than those of controls (Eika *et al.*, 1992). We could not distinguish between nerve-associated lipids or those associated with smooth muscle membranes, but theoretically alterations in neural lipids could alter nervous transmission and excitability. Additionally, synthesis and metabolism of phosphatidylinositol is known to be altered in diabetes (Greene *et al.*, 1988), which could have implications both for neural transmission and as a second messenger system for a number of agonists. To our knowledge, the influence of diabetes on either bladder phosphatidylinositol hydrolysis or lipid metabolism has not been investigated.

The experiments described in this paper included sucrose-drinking rats as controls for the effects of diuresis on bladder contractility. The bladders from these rats were significantly larger than those of controls, although smaller than those of the diabetics. In general, the responses of strips from sucrose-drinking rats were similar to those of the controls, rather than the diabetics. The shape of the response, and sensitivity to antagonists resembled the control response, as did the sensitivity to increasing voltage and pulse width. The data lead us to conclude that the increased responsiveness of bladders from diabetic rats to electrical stimulation results from the diabetic state rather than from the effects of diuresis-induced increases in bladder mass.

In conclusion, the present study suggests that bladders from diabetic rats are more excitable than those of control or sucrose-drinking rats, resulting in increased contractile responses to field stimulation. These effects on responsiveness to electrical stimulation do not seem to result from diuresis-induced effects on the bladder. The increased excitability could be the result of decreased nerve or bladder membrane lipids associated with diabetes mellitus, resulting in changes in resting membrane potential or other membrane effects. Additional possibilities include a diabetes-induced partial denervation which results in a form of postjunctional supersensitivity.

This work was supported in parts by grants from the Veteran's Administration, NIH grants DK 26508, DK 33559, and DK 41610, and also by the Finnish Academy of Sciences and the Paulo Foundation, Finland.

References

ANDERSON, G.F. (1982). Evidence for a prostaglandin link in the purinergic activation of rabbit bladder smooth muscle. *J. Pharmacol. Exp. Ther.*, **220**, 347–352.

ANDERSON, G.F. & KOHN, K.I. (1978). Interactions of calcium, prostaglandins and indomethacin on the smooth muscle of the bladder. *Pharmacology*, **16**, 306–313.

ANDERSSON, K.-E., HUSTED, S. & SJÖGREN, C. (1980). Contribution of prostaglandins to the adenosine triphosphate-induced contraction of rabbit urinary bladder. *Br. J. Pharmacol.*, **70**, 443–452.

ANDERSSON, P.O., MALMGREN, A. & UVELIUS, B. (1988). Cystometrical and in vitro evaluation of urinary bladder function in rats with streptozotocin-induced diabetes. *J. Urol.*, **139**, 1359–1362.

BARKAI, L. & SZABO, L. (1993). Urinary bladder dysfunction in diabetic children with and without subclinical cardiovascular autonomic neuropathy. *Eur. J. Pediatr.*, **152**, 190–192.

BELIS, J.A., CURLEY, R.M., MURTY, V.N., WAGNER, C.H., WINTER, S.J. & ROHNER, T.J.Jr. (1992). Calcium channel agonist/antagonist effects on cholinergic stimulation of the diabetic rat bladder. *Pharmacology*, **44**, 81–91.

BERGMEYER, H.U. & BERNT, E. (1974). D-glucose determination with glucose oxidase and peroxidase. In *Methods of Enzymatic Analysis*, 3rd edn, vol. 3 (ed. Bergmeyer, H.U. & Bernt, E.). pp. 1205–1215. New York: Academic Press, 2nd English Edition.

BRADING, A.F. & WILLIAMS, J.H. (1990). Contractile responses of smooth muscle strips from rat and guinea-pig urinary bladder to transmural stimulation: effects of atropine and α,β-methylene ATP. *Br. J. Pharmacol.*, **99**, 493–498.

CARPENTER, F.C. (1983). Impairment and restoration of rat urinary bladder responsiveness following distension. *Am. J. Physiol., (Regulatory Integrative Comp. Physiol., 13)*, **244**, R106–R113.

CHOO, L.K. & MITCHELSON, F. (1980). The effect of indomethacin and adenosine 5'-triphosphate on the excitatory innervation of the rat urinary bladder. *Can. J. Physiol. Pharmacol.*, **58**, 1042–1048.

DEAN, D.M. & DOWNIE, J.W. (1978). Interaction of prostaglandins and adenosine 5'-triphosphate in the noncholinergic neurotransmission in rabbit detrusor. *Prostaglandins*, **16**, 245–251.

EIKA, B., LEVIN, R.M. & LONGHURST, P.A. (1992). Collagen and bladder function in streptozotocin-diabetic rats: effects of insulin and aminoguanidine. *J. Urol.*, **148**, 167–172.

EKSTRÖM, J. (1981). Increase in choline acetyltransferase activity in surgically isolated postganglionic neurones of the urinary bladder of adult rats. *Acta Physiol. Scand.*, **111**, 81–86.

EKSTRÖM, J. & MALMBERG, L. (1984). Development of supersensitivity to methacholine in the rat detrusor following either parasympathetic denervation or decentralization. *Acta Physiol. Scand.*, **122**, 175–179.

EKSTRÖM, J. & UVELIUS, B. (1981). Length-tension relations of smooth muscle from normal and denervated rat urinary bladders. *Acta Physiol. Scand.*, **112**, 443–447.

FAERMAN, I., GLOCER, L., CELENER, D., JADZINSKY, M., FOX, D., MALER, M. & ALVAREZ. E. (1973). Autonomic nervous system and diabetes. Histological and histochemical study of the autonomic nerve fibers of the urinary bladder in diabetic patients. *Diabetes*, **22**, 225–237.

FAERMAN, I., MALER, M., JADZINSKY, M., ALVAREZ, E., FOX, D., ZILBERVARG, J., CIBEIRA, J.B. & COLINAS, R. (1971). Asymptomatic neurogenic bladder in juvenile diabetics. *Diabetologia*, **7**, 168–172.

FLEMING, W.W., MCPHILLIPS, J.J. & WESTFALL, D.P. (1973). Postjunctional supersensitivity and subsensitivity of excitable tissue to drugs. *Ergeb. Physiol. Biol. Chem. Exp. Pharmacol.*, **68**, 56–119.

FLEMING, W.W. & WESTFALL, D.P. (1975). Altered resting membrane potential in the supersensitive vas deferens of the guinea pig. *J. Pharmacol. Exp. Ther.*, **192**, 381–389.

FRIMODT-MØLLER, C. (1976). Diabetic cystopathy I: a clinical study of the frequency of bladder dysfunction in diabetics. *Dan. Med. Bull.*, **23**, 267–278.

GREENE, D.A., LATTIMER, S.A. & SIMA, A.A.F. (1988). Are disturbances of sorbitol, phosphoinositide, and Na^+-K^+-ATPase regulation involved in pathogenesis of diabetic neuropathy. *Diabetes*, **37**, 688–693.

JEREMY, J.Y., MIKHAILIDIS, D.P., THOMPSON, C.S. & DANDONA, P. (1986). The effect of streptozotocin-induced diabetes on PGI_2 synthesis by the rat bladder. *J. Urol.*, **135**, 1290–1292.

KOO, H.P., SANTAROSA, R.P., BUTTYAN, R., SHABSIGH, R., OLSSON, C.A. & KAPLAN, S.A. (1993). Comparison of gene expression in streptozotocin induced diabetic cystopathy and osmotic diuresis in rat bladders. *J. Urol.*, **149**, 267A.

KUDLACZ, E.M., GERALD, M.C. & WALLACE, L.J. (1989). Effects of diabetes and diuresis on contraction and relaxation mechanisms in rat urinary bladder. *Diabetes*, **38**, 278–284.

LATIFPOUR, J., GOUSSE, A., KONDO, S., MORITA, T. & WEISS, R.M. (1989). Effects of experimental diabetes on biochemical and functional characteristics of bladder muscarinic receptors. *J. Pharmacol. Exp. Ther.*, **248**, 81–88.

LINCOLN, J., CROCKETT, M., HAVEN, A.J. & BURNSTOCK, G. (1984). Rat bladder in the early stages of streptozotocin-induced diabetes: adrenergic and cholinergic innervation. *Diabetologia*, **26**, 81–87.

LONGHURST, P.A., BROTCKE, T.P., LEGGETT, R.E. & LEVIN, R.M. (1992). The influence of streptozotocin-induced diabetes mellitus on the sensitivity of rat urinary bladder body and base strips to changes in extracellular calcium. *Gen. Pharmacol.*, **23**, 83–88.

LONGHURST, P.A., KANG, J., WEIN, A.J. & LEVIN, R.M. (1990a). Length-tension relationship of urinary bladder strips from streptozotocin-diabetic rats. *Pharmacology*, **40**, 110–121.

LONGHURST, P.A., KAUER, J. & LEVIN, R.M. (1991). The ability of insulin treatment to reverse or prevent the changes in urinary bladder function caused by streptozotocin-induced diabetes mellitus. *Gen. Pharmacol.*, **22**, 305–311.

LONGHURST, P.A., WEIN, A.J. & LEVIN, R.M. (1990b). In-vivo urinary bladder function in rats following prolonged diabetic and non-diabetic diuresis. *Neurourol. Urodynam.*, **9**, 171–178.

LUHESHI, G.N. & ZAR, M.A. (1990). Inhibitory effect of streptozotocin-induced diabetes on non-cholinergic motor transmission in rat detrusor and its prevention by sorbinil. *Br. J. Pharmacol.*, **101**, 411–417.

LUHESHI, G.N. & ZAR, M.A. (1991). The effect of streptozotocin-induced diabetes on cholinergic motor transmission in the rat urinary bladder. *Br. J. Pharmacol.*, **103**, 1657–1662.

MAGGI, C.A., EVANGELISTA, S., GRIMALDI, G., SANTICIOLI, P., GIOLITTI, A. & MELI, A. (1984). Evidence for the involvement of arachidonic acid metabolites in spontaneous and drug-induced contractions of rat urinary bladder. *J. Pharmacol. Exp. Ther.*, **230**, 500–513.

NADELHAFT, I. & VERA, P.L. (1992). Reduced urinary bladder afferent conduction velocities in streptozotocin diabetic rats. *Neurosci. Lett.*, **135**, 276–278.

PARO, M., ITALIANO, G., TRAVAGLI, R.A., PETRELLI, L., ZANONI, R., PROSDOCIMI, M. & FIORI, M.G. (1990). Cystometric changes in alloxan diabetic rats: evidence for functional and structural correlates of diabetic autonomic neuropathy. *J. Auton. Nerve. Syst.*, **30**, 1–11.

PINNA, C., CARATOZZOLO, O. & PUGLISI, L. (1992). A possible role for urinary bladder epithelium in bradykinin-induced contraction in diabetic rats. *Eur. J. Pharmacol.*, **214**, 143–148.

POSANGI, J., ZAR, M.A. & HARRIS, J.B. (1992). The actions of palytoxin on the isolated detrusor muscle of the rat. *Br. J. Pharmacol.*, **106**, 307–314.

SANTICIOLI, P., GAMSE, R., MAGGI, C.A. & MELI, A. (1987). Cystometric changes in the early phase of streptozotocin-induced diabetes in rats: evidence for sensory changes not correlated to diabetic neuropathy. *Naunyn. Schmied. Arch. Pharmacol.*, **335**, 580–587.

SIBLEY, G.N.A. (1984). A comparison of spontaneous and nerve-mediated activity in bladder muscle from man, pig and rabbit. *J. Physiol.*, **354**, 431–443.

STEERS, W.D., MACKWAY, A.M., CIAMBOTTI, J. & DE GROAT, W.C. (1990). Effects of streptozotocin-induced diabetes on bladder function in the rat. *J. Urol.*, **143**, 1032–1036.

TE, A.E., BUTTYAN, R., KOO, H.P., SHABSIGH, R., OLSSON, C.A. & KAPLAN, S.A. (1992). Nerve growth factor in diabetic cystopathy. *J. Urol.*, **147**, 350A.

(Received November 15, 1993
Revised April 20, 1994
Accepted April 26, 1994)

Br. J. Pharmacol. (1994), **113**, 204–208

Hydrolysis of iodine labelled urodilatin and ANP by recombinant neutral endopeptidase EC. 3.4.24.11

*,[1]Zaid A. Abassi, *Eliahu Golomb, †Riad Agbaria, †Peter P. Roller, *John Tate & *Harry R. Keiser

*Hypertension-Endocrine Branch, National Heart, Lung and Blood Institute, and †Laboratory of Medicinal Chemistry, DTP, DCT, National Cancer Institute, National Institutes of Health, Bethesda, Maryland 20892, U.S.A.

1 Urodilatin is a 32 amino-acid peptide of similar sequence to atrial natriuretic peptide (ANP), with four additional amino-acids at the N-terminus. Although ANP and urodilatin bind to the same receptors with similar affinities, urodilatin is more active than ANP as a natriuretic agent. Previous studies, using neutral endopeptidase EC 3.4.24.11 (NEP) derived from crude membrane preparations, were inconclusive, but suggested that urodilatin was more resistant than ANP to degradation by this enzyme. In the present study, we compared the degradation rates of [^{125}I]-urodilatin and [^{125}I]-ANP by pure recombinant NEP (rNEP).

2 Incubation of radioactively labelled ANP with rNEP resulted in a much more rapid degradation of the peptide than that for labelled urodilatin.

3 Both phosphoramidon and SQ-28,603, potent inhibitors of NEP, completely protected both peptides from metabolism by rNEP.

4 The circular dichroism spectra of the two peptides indicate that they are very similar and exist largely in unordered or flexible conformations.

5 These results support the relative resistance of urodilatin to NEP, and indicate that urodilatin may be of use as a therapeutic agent, in conditions in which ANP is ineffective.

Keywords: Atrial natriuretic peptide; urodilatin; neutral endopeptidase; h.p.l.c.; phosphoramidon; SQ-28,603

Introduction

Urodilatin (URO) is a 32 amino-acid peptide, first isolated from human urine (Schulz-Knappe *et al.*, 1988). It has the same amino-acid sequence as atrial natriuretic peptide (ANP_{99-126}) with four additional amino-acids at the amino-terminus. These amino-acids are the same ones that immediately precede ANP in its precursor molecule, suggesting that URO is derived from pre-pro-ANP. Like ANP, URO has a 17 amino-acids loop structure closed by a disulphide bridge between cysteine-105 and cysteine-121. While ANP is abundant in cardiac atria and the circulation, URO is found only in human urine, and has not been detected in blood (Schulz-Knappe *et al.*, 1988; Goetz, 1992; Abassi *et al.*, 1992a; Valentin & Humphreys, 1993).

URO and ANP exert similar renal and cardiovascular effects. In general, both peptides increase sodium excretion and urine flow (Goetz *et al.*, 1990; Abassi *et al.*, 1992b; Valentin & Humphreys, 1993). Infusion of either ANP or URO into experimental animals (Villarreal *et al.*, 1991; Abassi *et al.*, 1992b; Hildebrandt *et al.*, 1992) and man (Saxenhofer *et al.*, 1990; Kentsch *et al.*, 1992) induces significant natriuresis, diuresis and a reduction of blood pressure. In some studies, URO was found to be more potent than ANP (Riegger *et al.*, 1990; Saxenhofer *et al.*, 1990; Abassi *et al.*, 1992b; Hildebrandt *et al.*, 1992; Bestle & Bie, 1993). In normal subjects, bolus injections of URO induced natriuresis and diuresis, which were twice as large as those obtained with similar doses of ANP (Saxenhofer *et al.*, 1990). Similar findings were documented in rats (Abassi *et al.*, 1992b) and dogs (Riegger *et al.*, 1990; Villarreal *et al.*, 1991) with experimental congestive heart failure (CHF).

Since ANP and URO exert their effect by binding to the same receptors, with similar affinities *in vitro* (Heim *et al.*, 1989; Saxenhofer *et al.*, 1993; Valentin *et al.*, 1993; Koike *et al.*, 1993), the difference in potency between these peptides is either due to different conformations of the peptides *in vivo*, or, more likely, due to higher availability of URO at the medullary collecting duct, resulting from its resistance to proteolytic degradation. URO was found to be less susceptible to biological inactivation by neutral endopeptidase EC 3.4.24.11 (NEP) in renal membrane preparations (Gagelmann *et al.*, 1988; Kenny *et al.*, 1993) and *in vivo* (Abassi *et al.*, 1992c). NEP is a zinc-containing metalloendopeptidase widely distributed in brain, lung and in the brush border of the kidney and intestines (Booth & Kenny, 1974; Johnson *et al.*, 1985). Several studies demonstrated that NEP is the main enzyme that degrades ANP, through a single cleavage between cysteine-105 and phenylalanine-106 (Olins *et al.*, 1987; Stephenson & Kenny, 1987). The product of the initial proteolytic attack is subject to further cleavage within the loop, and at the amino- and carboxy-termini (Olins *et al.*, 1986; Stephenson & Kenny, 1987; Vanneste *et al.*, 1988). The different stability of ANP and URO to degradation may account for the differences in the intensity of their renal effects. Data concerning the relative resistance of URO to degradation are based on work in crude membrane preparations. These preparations probably contain other enzymes, besides NEP 24.11. The present study was designed to assess directly the relative stability of [^{125}I]-ANP and [^{125}I]-URO to pure recombinant NEP 24.11 (rNEP).

Methods

Recombinant human neutral endopeptidase EC.3.4.24.11 was produced by Genentech. Inc. (San Francisco, CA, U.S.A.). The full length cDNA coding for human neutral endopeptidase EC.3.4.24.11 was cloned originally from a human placental cDNA library (Malfroy *et al.*, 1988) and transfection of mammalian cells with an expression plasmid containing this cDNA resulted in the production of the enzymatically active protein (Gorman *et al.*, 1989), which was purified by a modification of a standard procedure and quantified in terms of protein catalytic activity. The active enzyme is a glycoprotein, of approximately 90 kilodaltons.

[1] Author for correspondence.

One ng of either [^{125}I]-Tyr$_{126}$-human α-ANP$_{99-126}$ or [^{125}I]-Tyr$_{126}$-URO$_{95-126}$ (both 2000 Ci mmol^{-1}, NEN, Boston, MA, U.S.A.), were incubated with either 1 or 10 μg of the rNEP at 37°C, in 1 ml solution of 50 mM HEPES, pH = 7.4, 50 mM NaCl, 10% acetonitrile, for different times (0.5–120 min). This concentration of acetonitrile was necessary to obtain a homogeneous solution of [^{125}I]-URO and prevent its adherence to the reaction tubes, because [^{125}I]-URO is less water-soluble than [^{125}I]-ANP. It had been confirmed in preliminary experiments that this concentration of acetonitrile did not interfere with NEP activity upon either [^{125}I]-ANP or [^{125}I]-URO. In some experiments either phosphoramidon (Peptides International, Louisville, KY, U.S.A.) or SQ-28,603 (N-[2-(mercaptomethyl)-1-o × o-3-phenylpropyl]-< b-alanine; Bristol-Myers Squib Pharmaceuticals, Princeton, NJ, U.S.A.) was added to the solution at a final concentration of 10 μM prior to the addition of the enzyme. Each reaction was terminated by the addition of 50 μl of 70% acetic acid, followed by heating at 60°C for 3 min. Fifty microliters of each reaction mixture were analysed by reverse phase high performance liquid chromatography (h.p.l.c.) (C_{18}μ Bondapak, 3.9 × 300 mm column, Waters, Milford, MA, U.S.A.), using a linear gradient of 10–60% acetonitrile in 0.1% trifluoroacetic acid over 35 min, at a flow rate of 1 ml min^{-1}. The h.p.l.c. system was calibrated with ^{125}I-labelled ANF or ^{125}I-labelled URO. Radioactivity eluting from the column was continuously monitored with a gamma-counter (Beckman Instruments, Irvine, CA, U.S.A.). In addition, 50 μl of each reaction mixture ($n = 6$ for each time period) were treated with 250 μl of 10% trichloroacetic acid (TCA) at 0°C and centrifuged at 2200 g. The pellets were resuspended in 250 μl of TCA at 0°C and recentrifuged. The radioactivity in either the combined supernatants (TCA-soluble) or in the pellet (TCA-precipitate) was determined. The TCA-precipitable ^{125}I-radioactivity was shown by h.p.l.c. to be mainly intact [^{125}I]-ANF or [^{125}I]-URO, while the soluble ^{125}I-radioactivity represents mainly free ^{125}I and some hydrolytic products. This agrees with previous reports in the literature (Almeida *et al.*, 1989; Chiu *et al.*, 1991; Abassi *et al.*, 1992c).

Circular dichroism (CD) spectra were measured on a JASCO model J-500A/DP-501N spectropolarimeter using 1 mm path Hellma quartz cells. Spectra were scanned from 190 to 260 nm, and the spectral amplitudes are expressed as mean residue ellipticities [θ]. Spectra were measured on 16 μM solutions in pH 7.4, 50 mM phosphate buffer containing 10% acetonitrile, as well as in the same buffer containing 10% acetonitrile and 40% trifluoroethanol.

The disappearance rate of [^{125}I]-ANP was compared to that of [^{125}I]-urodilatin by using two-way analysis of variance (ANOVA), followed by an unpaired t test; a value of $P < 0.05$ was considered significant.

Results

Radioactively labelled URO and ANP eluted from the h.p.l.c. with retention times of 23 and 24 min, respectively. Incubation of [^{125}I]-ANP with 1 μg ml^{-1} rNEP at 37°C resulted in rapid degradation of the peptide (Figure 1). After a short incubation with the enzyme, most of the radioactivity eluted at 22 min, whereas increasing the incubation time to more than 30 min resulted in the appearance of an additional major peak at 16 min (Figure 2a). Increasing the concentration of rNEP to 10 μg ml^{-1}, resulted in total degradation of the ^{125}I-ANP within 2 min (Figure 2a).

Incubation of [^{125}I]-URO with rNEP, at the same concentration as [^{125}I]-ANP, resulted in a much slower degradation of this peptide. After incubation with rNEP 1 μg ml^{-1}, degradation of [^{125}I]-URO was first detected at 5 min of incubation (Figure 1a). Even after incubation of labelled URO with rNEP at a concentration of 10 μg ml^{-1}, about half of the radioactivity in the reaction mixture eluted as intact [^{125}I]-URO after 15 min (Figure 1b and Figure 2b).

These results are further confirmed by the use of TCA precipitation. The rate of disappearance of the TCA precipitable (TCA-ppt) radioactivity, which represents the intact peptide, is shown in Figure 3. The disappearance of [^{125}I]-URO was significantly slower than that of [^{125}I]-ANP, at both concentrations of rNEP. Addition of either of the NEP inhibitors, SQ-28,603 or phosphoramidon, completely inhibited the degradation of both [^{125}I]-ANP and [^{125}I]-URO by rNEP (data not shown).

The CD spectral features of the two peptides are very similar in buffered solutions (pH 7.4) containing 10% acetonitrile, i.e., showing single negative ellipticity maxima at 197 nm, with mean residue ellipticity values of − 7300 deg × cm^2 × dmol^{-1} for ANP and − 8700 deg × cm^2 × dmol^{-1} for urodilatin. On addition of 40% trifluoroethanol to solutions of the peptides the spectra became identical with negative ellipticity maximum shifted to 205 nm, [θ] = − 8000 deg × cm^2 × dmol^{-1} and the appearance of a broad shoulder in the 217–222 nm region [θ] = − (3799 to 3200) deg × cm^2 × dmol^{-1}. The concentrations of ANP and URO in the solutions were confirmed by u.v. absorption maximum at 275 nm with extinction coefficient, ε = 2000 for both peptides.

Discussion

The present study confirms that [^{125}I]-URO is relatively resistant to degradation by NEP. This finding is in agreement with previous *in vitro* studies. Gagelmann *et al.* (1988) demonstrated that ANP, but not URO, was proteolytically deg-

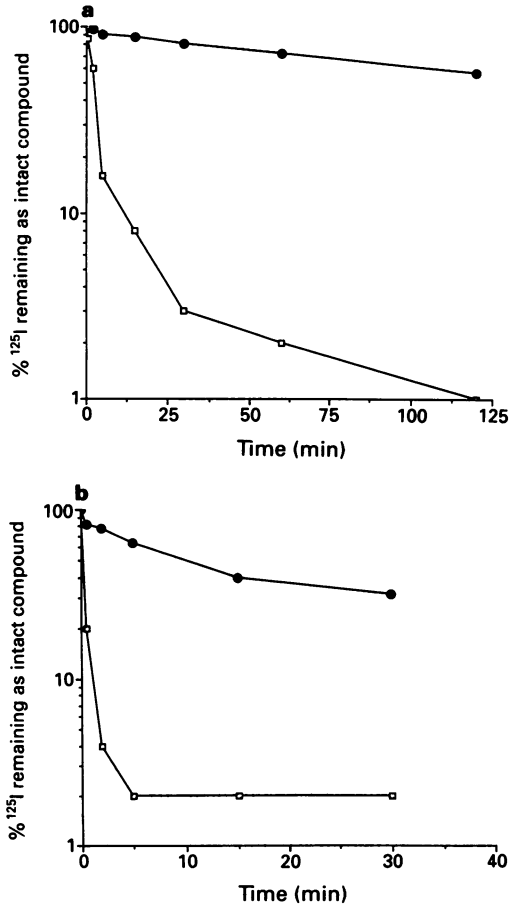

Figure 1 Disappearance of intact [^{125}I]-atrial natriuetic peptide (□) and [^{125}I]-urodilatin (●) incubated with recombinant neutral endopeptidase EC.3.4.24.11, (1 μg (a) and 10 μg (b)) for different time periods (0.5–120 min). The intact [^{125}I]-atrial natriuretic peptide and [^{125}I]-urodilatin were separated from their hydrolytic products by h.p.l.c. (see Figure 2).

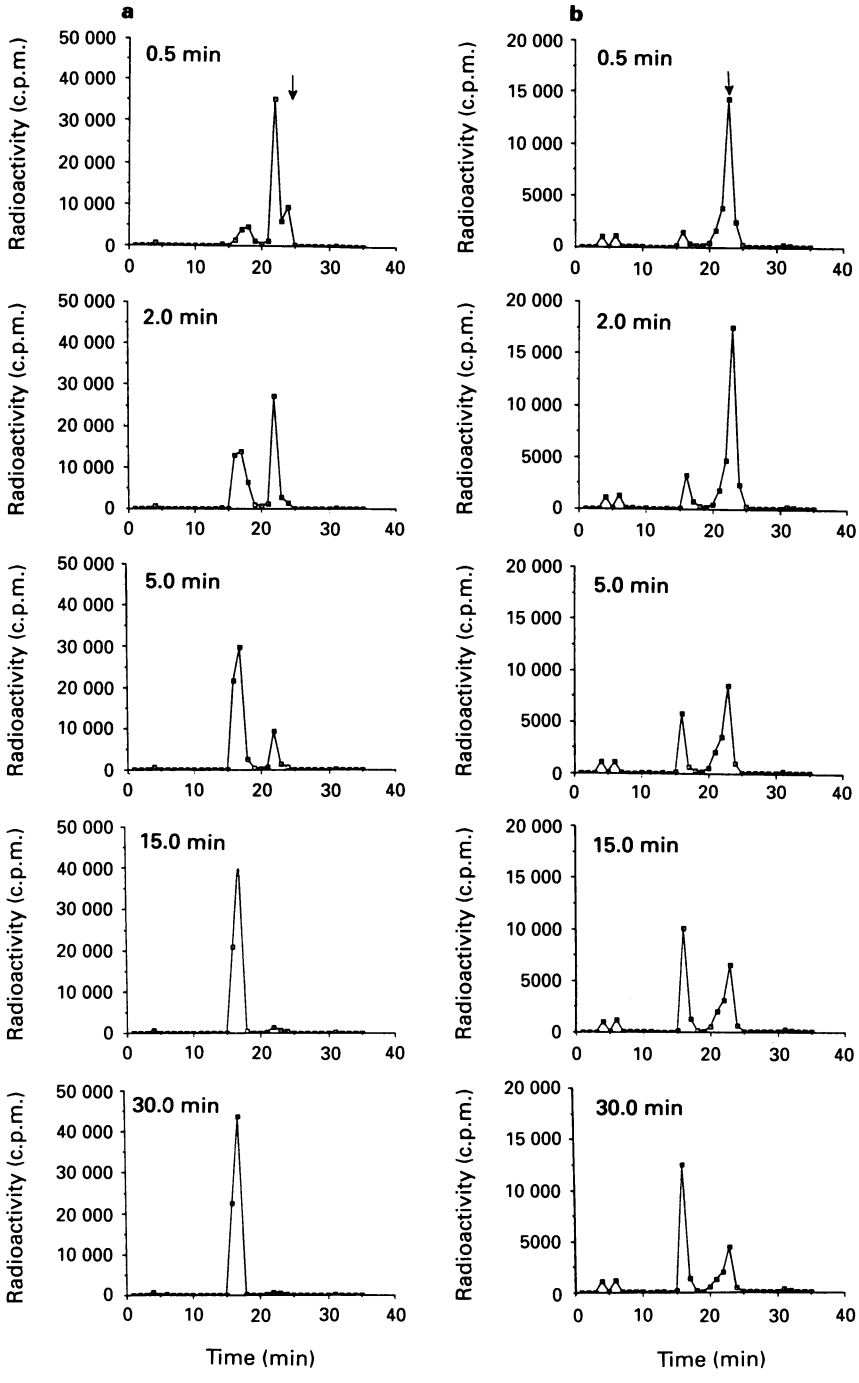

Figure 2 Reversed-phase h.p.l.c. radioactive flow monitoring analysis of the fragmentation of (a) [^{125}I]-atrial natriuretic peptide ([^{125}I]-ANP) and (b) [^{125}I]-urodilatin ([^{125}I]-URO) by human recombinant neutral endopeptidase. The figure depicts typical radiochromatograms of reaction mixture of 1 ng of [^{125}I]-ANP or [^{125}I]-URO with 10 μg ml^{-1} of recombinant neutral endopeptidase incubated for different time periods (0.5–30 min). The arrow indicates the elution times of intact [^{125}I]-ANF (a) and [^{125}I]-URO (b).

raded within 5 min by crude preparations of dog kidney cortex. Similarly, Kenny *et al.* (1993), reported that URO was relatively resistant to metabolism by NEP derived from porcine choroid plexus membranes, whereas other members of the natriuretic peptide family, namely, ANP, brain natriuretic peptide (BNP) and C-type natriuretic peptide (CNP), were degraded rapidly by the enzyme. In these studies, enzymes were extracted from membranes that are rich in NEP 24.11, as well as other enzymes. Use of the recombinant enzyme enabled us to determine specifically the metabolism of ANP and URO by a pure preparation. However, a reservation should be pointed out, that the iodine labelling of URO and ANP might cause steric changes in these peptides, that might interfere with their interactions with the enzyme. Even though the site of labelling (Tyr 126) is far from the site of hydrolysis (Cys105-Phe106), the possibility of such interference cannot be ruled out.

It should be emphasized, that the resistance of URO to NEP is not absolute and URO is degraded by high concentrations of the enzyme, or by exposure to low concentrations for long periods, as indicated by Kenny *et al.* (1993). In addition, these investigators noted, that the relative resistance of URO to NEP is not merely due to its larger size, since BNP, which is also a 32 amino acids peptide, is susceptible to degradation by NEP. The large difference between the sensitivity of ANP and URO in the present study supports this

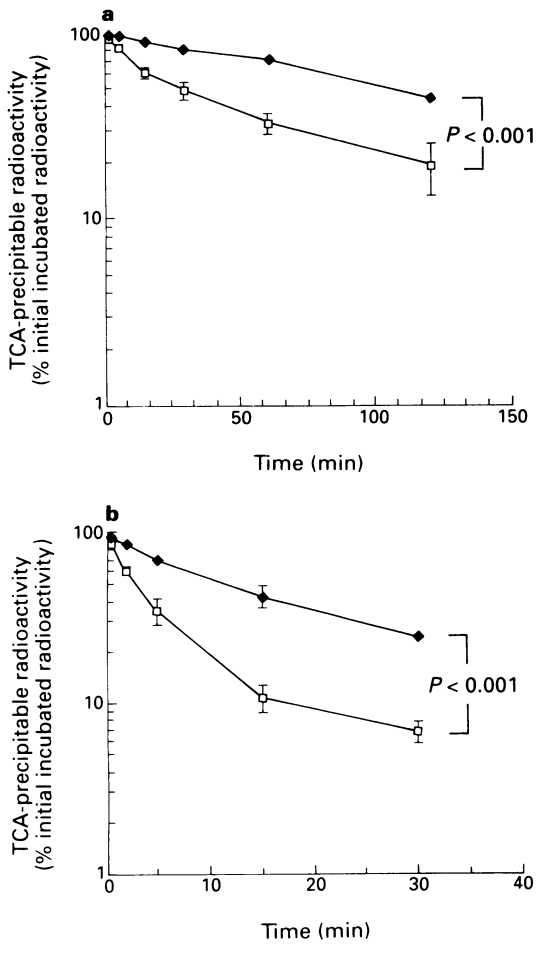

Figure 3 Disappearance of trichloroacetic acid-precipitable (TCA-ppt) radioactivity, i.e., intact [^{125}I]-atrial natriuretic peptide ([^{125}I]-ANP) (□) or intact [^{125}I]-urodilatin ([^{125}I]-urodilatin) (●) in the presence of 1 μg ml^{-1} (a) or 10 μg ml^{-1} (b) of recombinant neutral endopeptidase. Radioactivity in intact peptide is expressed as counts per min (c.p.m.) in 50 μl of reaction mixture. Results are means ± s.e.; $n = 5-6$ in each group. The degradation of ANP by neutral endopeptidase was much faster than that of urodilatin; $P < 0.001$ by analysis of variance (ANOVA).

view. It is therefore suggested, that the four N-terminal amino acids of URO (Thr-Ala-Pro-Arg) make a specific contribution to the relative resistance of URO to NEP. On the other hand, when shorter natriuretic peptides, such as: CNP, ANP_{4-23} and ANP_{5-28}, were incubated with NEP, their degradation was faster than that of ANP_{1-28} (Kenny *et al.*, 1993). In addition, incubation of $ANP_{103-126}$ (atriopeptin III) with NEP resulted in rapid inactivation due to attacks on several cleavage sites, compared to ANP, in which the initial attack is restricted to a single site between Cys_{105} and Phe_{106} (Olins *et al.*, 1986). These findings led to the controversial assumption, that the susceptibility of natriuretic peptides to NEP depends primarily on their length, so that elongated peptides are relatively more resistant to NEP inactivation than shorter forms or fragments of the peptides. Our findings that the circular dichroism spectra of ANP and URO are very similar, tends to exclude the possibility that differences in configuration contribute to the relative resistance of URO to NEP. The spectral features of ANP and URO indicate that both peptides have random or flexible conformations, with a notable lack of α-helical or β-sheet conformation components (Woody *et al.*, 1985). The structure of ANP in dimethylsulphoxide was examined earlier with n.m.r. by others, and was shown to have a very flexible N-terminal segment (Kobayashi *et al.*, 1988). It appears that elongation of the N-terminal region of ANP by four amino acids (URO) does not fix the conformation of that region to any extent measurable by CD spectroscopy. Addition of a model lipophylic solvent, such as trifluoroethanol, induces an increased order in the structure, as evidenced by the red-shift of the 197 nm spectral band, and by the appearance of the board shoulder in the 217–222 nm spectral region. However, these solvents induced parallel conformational changes in both peptides.

The relative resistance of URO, compared with ANP, to NEP is of special interest, since it suggests a potential clinical application of URO in pathophysiological conditions, in which beneficial effects of ANP are still doubtful. For instance, the renal response to infusion of pharmacological doses of ANP into patients (Cody *et al.*, 1986) or experimental animals (Riegger *et al.*, 1988; Hoffman *et al.*, 1988; Abassi *et al.*, 1990; 1991) with congestive heart failure (CHF) is attenuated, and even blunted in severe stages of the disease. In contrast, infusion of equimolar doses of URO into rats with CHF (Abassi *et al.*, 1992b) or dogs with CHF (Riegger *et al.*, 1990; Villarreal *et al.*, 1991), and into healthy individuals and animals (Saxenhofer *et al.*, 1990; Hildebrandt *et al.*, 1992; Bestle & Bie, 1993), increased sodium excretion more than ANP. These differences in the potency of URO and ANP at the renal level may be explained partially by the relative resistance of URO to NEP, so that it reaches its target, namely, the distal segment of the nephron, in greater amounts, and thereby induces greater sodium excretion. Support for this view comes from several studies, in which inhibition of NEP increased longevity and augmented the natriuretic and diuretic effects of exogenous and endogenous ANP in animals (Koepke *et al.*, 1989; Wilkins *et al.*, 1990) and in man (Jardine *et al.*, 1989; Northridge *et al.*, 1989), possibly due to protection of ANP from NEP inactivation (see review by Roques *et al.*, 1993). However, we found that the specific NEP inhibitor SQ-28,603 also potentiated the renal effects of URO in rats with CHF (Abassi *et al.*, 1992b). The finding that URO is not completely resistant to NEP, may explain the stimulatory influence of SQ-28,603 on the renal effects of the peptide. But, we cannot exclude other possibilities, such as protection of other peptides with natriuretic activity, e.g., bradykinin (Ura *et al.*, 1987) and BNP (Kirk & Wilkins, 1993; Mark Richards *et al.*, 1993) and the inhibitory effects of the drug on sodium reabsorption in the proximal tubule (Cavero *et al.*, 1990).

In summary, using purified recombinant NEP the present study confirms previous reports that suggested that URO was less susceptible than ANP to degradation by NEP. This advantage of URO over ANP may make the former a better potential candidate for the treatment of a variety of diseases characterized by attenuated or blunted renal response to ANP.

We thank Dr Robert Bridenbaugh, from the Genentech Corp., for the gift of the recombinant enzyme

References

ABASSI, Z.A., BURNETT, J.C., GRUSHKA, E., HOFFMAN, A., HARAMATI, A. & WINAVER, J. (1991). Atrial natriuretic factor and renal cGMP in rats with experimental heart failure. *Am. J. Physiol.*, **261**, R858–R864.

ABASSI, Z.A., GOLOMB, E., KLEIN, H. & KEISER, H.R. (1992a). Urodilatin: a natriuretic peptide of renal origin. *Cardiovasc. Drug Rev.*, **10**, 199–210.

ABASSI, Z.A., HARAMATI, A., HOFFMAN, A., BURNETT, J.C. & WINAVER, J. (1990). Effect of converting enzyme inhibition on renal response to ANF in rats with experimental heart failure. *Am. J. Physiol.*, **259,** R84–R89.

ABASSI, Z.A., POWELL, J.R., GOLOMB, E. & KEISER, H.R. (1992b). Renal and systemic effects of urodilatin in rats with high-output heart failure. *Am. J. Physiol.*, **262,** F615–F621.

ABASSI, Z.A., TATE, J., HUNSBERGER, S., KLEIN, H., TRACHEWSKY, D. & KEISER, H.R. (1992c). Pharmacokinetics of ANF and urodilatin during cANF receptor blockade and neutral endopeptidase inhibition. *Am. J. Physiol.*, **263,** E870–E876.

ALMEIDA, F.A., SUZUKI, M., SCARBOROUGH, R.M., LEWICKI, J.A. & MAACK, T. (1989). Clearance function of type C receptors of atrial natriuretic factor in rats. *Am. J. Physiol.*, **256,** R469–R475.

BESTLE, M.H. & BIE, P. (1993). Renal effects of urodilatin and atrial natriuretic peptide in volume expanded conscious dogs. *Acta. Physiol. Scand.*, **149,** 77–83.

BOOTH, A.G. & KENNY, A.J. (1974). A rapid method for the preparation of microvilli from rabbit kidney. *Biochem. J.*, **142,** 575–581.

CAVERO, P.G., MARGULIES, K.B., WINAVER, J., SEYMOUR, A.A., DELANEY, N.G. & BURNETT, J.C. (1990). Cardiorenal actions of neutral endopeptidase inhibition in experimental congestive heart failure. *Circulation*, **82,** 196–201.

CHIU, P.J.S., TETZLOFF, G., ROMANO, M.T., FOSTER, C.J. & SYBERTZ, E.J. (1991). Influence of cANF receptor and neutral endopeptidase on pharmacokinetics of ANF in rat. *Am. J. Physiol.*, **260,** R208–R216.

CODY, R.J., ATLAS, S.A., LARAGH, J.H., KUBO, S.H., COVIT, A.B., RYMAN, K.S., SHAKNOVICH, A., PONDOLFINO, K., CLARK, M, CAMARGO, M.J., SCARBOROUGH, R.M. & LEWICKI, J.A. (1986). Atrial natriuretic factor in normal subjects and heart failure patients. Plasma levels and renal, horomonal and hemodynamic responses to peptide infusion. *J. Clin. Invest.*, **78,** 1362–1374.

GAGELMANN, M., HOCK, D. & FORSSMANN, W.-G. (1988). Urodilatin (CDD/ANP-95–126) is not biologically inactivated by a peptidase from dog kidney cortex membranes in contrast to atrial natriuretic peptide/cardiodilatin (a-hANP/CDD-99-126). *FEBS Lett.*, **233,** 249–254.

GOETZ, K.L., DRUMMER, C., ZHU, J.L., LEADLEY, R., FIEDLER, F. & GERZER, R. (1990). Evidence that urodilatin rather than ANP, regulates renal sodium excretion. *J. Am. Soc. Nephrol.*, **1,** 867–874.

GOETZ, K.L. (1992). Renal natriuretic peptide (urodilatin) and atriopeptin: evolving concept. *Am. J. Physiol.*, **261,** F921–F932.

GORMAN, C., GIESS, D., SCHOFIELD, P., KADU-FONG, H. & MALFROY, B. (1989). Expression of enzymatically active enkephalinase (neutral endopeptidase) in mammalian cells. *J. Cell Biochem.*, **39,** 277–284.

HEIM, J.M., KIEFERSAUER, S., FULLER, H.J. & GERZER, R. (1989). Urodilatin and b-ANF: binding properties and activation of particulate guanylate cyclase. *Biochem. Biophys. Res. Commun.*, **163,** 37–41.

HILDEBRANDT, D.A., MIZELLE, H.L., BRANDS, M.W. & HALL, J.E. (1992). Comparison of renal actions of urodilatin and atrial natriuretic peptide. *Am. J. Physiol.*, **262,** R395–R399.

HOFFMAN, A., BURNETT, J.C., HARAMATI, A. & WINAVER, J. (1988). Effects of atrial natriuretic factor in rats with experimental high-output heart failure. *Kidney Int.*, **33,** 656–661.

JARDINE, A.G., CONNEL, J.M.C., DILLY, S.G., CUSSANS, N.J., NORTHRIDGE, D.B., LECKIE, B.J. & LEVER, A.F. (1989). Inhibition of ANP degradation by the atriopeptin inhibitor UK 69,578 in man. *Clin. Sci.*, **74** (Suppl. 20), 21P.

JOHNSON, A.R., ASHTON, J., SCHULZ, W.W. & ERDOS, E.G. (1985). Neutral metalloendopeptidase in human lung tissue and cultured cells. *Annu. Rev. Respir.*, **132,** 564–568.

KENNY, A.J., BOURNE, A. & INGRAM, J. (1993). Hydrolysis of human and pig brain natriuretic peptides, urodilatin, C-type natriuretic peptide and some C-receptor ligands by endopeptidase. *Biochem. J.*, **291,** 83–88.

KENTSCH, M., LUDWIG, D., DRUMMER, C., GERZER, R. & MULLER-ESCH, G. (1992). Haemodynamic and renal effects of urodilatin in healthy volunteers. *Eur. J. Clin. Invest.*, **22,** 319–325.

KIRK, J.E. & WILKINS, M.R. (1993). Effect of endopeptidase-24.11 inhibition and of atrial natriuretic peptide clearance receptor ligand on the response to rat brain natriuretic peptide in the conscious rat. *Br. J. Pharmacol.*, **110,** 350–354.

KOBAYASHI, Y., OHKUBO, T., KYOGOKU, Y., KOYAMA, S., KOBAYASHI, M. & GO, N. (1987). In *Peptide Chemistry* ed. Shiba, T. & Sakakibara, S. pp. 81–84. Osaka: Protein Research Foundation.

KOEPKE, J.P., TYLER, L.D., TRAPANI, A.J., BOVY, P.R., SPEAR, K.L., OLINS, G.M. & BLAIN, E.H. (1989). Interaction of non-guanylate cyclase-linked atriopeptin receptor ligand and endopeptidase inhibitors in conscious rats. *J. Pharmacol. Exp. Ther.*, **249,** 172–176.

KOIKE, J., NONOGUCHI, H., TERADA, Y., TOMITA, K. & MARUMO, F. (1993). Effect of urodilatin on cGMP accumulation in the kidney. *J. Am. Soc. Nephrol.*, **3,** 1705–1709.

MALFROY, B., KUANG, W.-J., SEEBURG, P., MASON, A. & SCHOFIELD, P. (1988). Molecular cloning and amino acid sequence of human enkephalinase (neutral endopeptidase). *FEBS Lett.*, **229,** 206–210.

MARK RICHARDS, A., CROZIER, I.G., ESPINER, E.A., YANDLE, T.G. & NICHOLLS, G. (1993). Plasma brain natriuretic peptide and endopeptidase 24.11 inhibition in hypertension. *Hypertension*, **22,** 231–236.

NORTHRIDGE, D.B., JARDINE, A.J., ALABASTER, C.T., BARCLAY, P.L., CONNEL, J.M.C., DARGIE, H.J., DILLY, S.G., LEVER, A.F., FINDLAY, I.N. & SAMUELS, G.M.R. (1989). Preliminary studies with a novel atriopeptidase inhibitor (UK 69,578) in animals, normal volunteers and heart failure patients. *Lancet*, **ii,** 591–593.

OLINS, G.M., SPEAR, K.L., SIEGEL, N.R. & ZURCHER-NEELY, H.A. (1987). Inactivation of atrial natriuretic factor by the renal brush border. *Biochem. Biophys. Acta.*, **901,** 97–100.

OLINS, G.M., SPEAR, K.L., SIEGEL, N.R., ZURCHER-NEELY, H.A. & SMITH, C.E. (1986). Proteolytic degradation by Atriopeptin III by kidney brush border membranes. *Fed. Proc.*, **45,** 427A.

RIEGGER, G.A.J., ELSNER, D., FORSSMANN, W.-G. & KROMER, E.P. (1990). Effects of ANP-(95-126) in dogs before and after induction of heart failure. *Am. J. Physiol.*, **259,** H1643–H1648.

RIEGGER, A.E.G., ELSNER, D., KROMER, E.P., DAFFNER, C., FORSSMANN, W.-G., MUDRES, F., PASCHER, E.W. & KOCHSIEK, K. (1988). Atrial natriuretic peptide in congestive heart failure in the dog: plasma levels, cyclic guanosine monophosphate, ultrastructure of atrial myoendocrine cells and hemodynamic, hormonal and renal effects. *Circulation*, **77,** 398–406.

ROQUES, B.P., NOBLE, F., DAUGE, V., FOURNIE-ZALUSKI, M.-C. & BEAUMONT, A. (1993). Neutral endopeptidase 24.11: Structure, Inhibition, and Experimental and clinical pharmacology. *Pharmacol. Rev.*, **45,** 87–146.

SAXENHOFER, H., FITZGIBBON, W.R. & PAUL, R.V. (1993). Urodilatin: binding properties and stimulation of cGMP generation in rat kidney cells. *Am. J. Physiol.*, **264,** F267–F273.

SAXENHOFER, H., RASELLI, A., WEIDMANN, P., FORSSMANN, W.-G., BUB, A., FERRARI, P. & SHAW, S.G. (1990). Urodilatin, a natriuretic factor from kidneys, can modify renal and cardiovascular function in man. *Am. J. Physiol.*, **259,** F832–F838.

SCHULZ-KNAPPE, P., FORSSMANN, K., HERBST, F., HOCK, D. & FORSSMANN, W.-G. (1988). Isolation and structural analysis of 'urodilatin', a new peptide of the cardiolatin-(ANP)-family, extracted from human urine. *Klin. Wochenschrift*, **66,** 752–759.

STEPHENSON, S.L. & KENNY, A.J. (1987). The hydrolysis of a-human natriuretic peptide by pig kidney microvillar membranes is initiated by neutral endopeptidase 24.11. *Biochem. J.*, **243,** 183–187.

URA, N., CARRETERO, O.A. & ERDOS, E.G. (1987). Role of endopeptidase 24.11 in kinin metabolism in vitro and in vivo. *Kidney Int.*, **32,** 507–513.

VALENTIN, J.P. & HUMPHREYS, M.H. (1993). Urodilatin: a paracrine renal natriuretic peptide. *Sem. Nephrol.*, **13,** 61–70.

VALENTIN, J.P., SECHI, L.A., QIU, C., SCHAMBELAN, M. & HUMPHREYS, M.H. (1993). Urodilatin binds to and activates renal receptors for atrial natriuretic peptide. *Hypertension*, **21,** 432–438.

VANNESTE, Y., MICHEL, A., DIMALINE, R., NAJDOVSKI, T. & DESCHODT-LANCKMAN, M. (1988). Hydrolysis of α-human natriuretic peptide in vitro by human kidney membranes and purified endopeptidase-24.11. *Biochem. J.*, **254,** 531–537.

VILLARREAL, D., FREEMAN, R.H. & JOHNSON, R.A. (1991). Renal effects of ANF (95-126), a new atrial analogue, in dogs with experimental heart failure. *Am. J. Hypertens.*, **4,** 508–515.

WILKINS, M.R., SETTLE, S.L., STOCKMAN, P. & NEEDLEMAN, P. (1990). Maximizing the natriuretic effect of endogenous atriopeptin in a rat model of heart failure. *Proc. Natl. Acad. Sci. U.S.A.*, **87,** 6465–6469.

WOODY, R.W. (1985). Circular dichroism of peptides. In *The Peptides: Analysis Synthesis, Biology.* ed. Hruby, V.J. pp. 113–114. New York: Academic Press.

(Received February 4, 1994
Revised April 20, 1994
Accepted April 28, 1994)

Br. J. Pharmacol. (1994), **113**, 209–215

Antifibrillatory effects of clofilium in the rabbit isolated heart

Gregory S. Friedrichs, Liguo Chi, Alysia L. Green & [1]Benedict R. Lucchesi

University of Michigan Medical School, Department of Pharmacology, M6322 Medical Science Building I, Ann Arbor, Michigan 48109-0626 U.S.A.

1 This study was designed to determine whether clofilium exhibits antifibrillatory activity in a pinacidil + hypoxia-induced model of ventricular fibrillation (VF) in Langendorff-perfused hearts.

2 Ten minutes after exposure to vehicle or clofilium (0.1, 1.0 and 10.0 μM), hearts were exposed to pinacidil (1.25 μM), then subjected to 12 min of hypoxia and reoxygenated. Onset to VF was recorded. Additional groups of hearts were pretreated with UK-68,798 (1.0, 3.0 and 10.0 μM), a delayed rectifier channel blocker, and 5-hydroxydecanoate (10 μM), a known ATP-dependent K^+ channel blocker, and subjected to an identical protocol.

3 Clofilium decreased the incidence of VF in a concentration-dependent manner; 7/9 control hearts developed VF *vs* 1/9 hearts ($P = 0.007$, Fisher's Exact) treated with 10.0 μM clofilium. In addition, 5-hydroxydecanoate protected hearts from VF, while UK-68,798 pretreatment did not.

4 In a separate group of hearts, electrically-induced VF was converted to sinus rhythm in 10/11 hearts after clofilium was introduced as a bolus.

5 Clofilium is capable of preventing VF in the rabbit isolated heart in a concentration-dependent manner. We have data to suggest that the ability of clofilium to attenuate the effects of pinacidil + hypoxia in our model may include blockade of metabolically active K^+ channels, i.e., K_{ATP} (glibenclamide-sensitive) channel.

Keywords: Class III antiarrhythmic drugs; clofilium; UK-68,798; 5-hydroxydecanoate; ATP-dependent K^+ channels; rabbit isolated heart; chemical defibrillation; ventricular fibrillation

Introduction

In view of the inefficacy of Class I agents to prevent sudden cardiac death, there is a renewed effort in the development of antiarrhythmic drugs with selected cardiac electrophysiological properties. Agents with demonstrated experimental efficacy against ventricular arrhythmias include: UK-68,798 (Black *et al.*, 1991), CK3579 and sematilide (Chi *et al.*, 1990a), E-4031 (Lynch *et al.*, 1989), (±)-sotalol (Lynch *et al.*, 1984), and amiodarone (Patterson *et al.*, 1983). In each of the examples cited, the incidence of ventricular fibrillation (VF), or sudden cardiac death in the conscious dog, was reduced significantly when compared to vehicle-treated controls. Another promising investigational agent is WAY-123,398, purported to prolong ventricular refractoriness and increase the ventricular fibrillation threshold without affecting impulse conduction (Spinelli *et al.*, 1992).

The antiarrhythmic compound clofilium, is a bretylium congener devoid of sympathomimetic or sympatholytic effects (Steinberg & Molley, 1975; Steinberg *et al.*, 1981; Lindstrom *et al.*, 1982). Clofilium has been shown to prolong the effective refractory period or action potential duration in a number of animal models (Steinberg & Molley, 1975; Steinberg *et al.*, 1981; Kowey *et al.*, 1985; Wu *et al.*, 1989; Li *et al.*, 1990) as well as to increase the refractory period in the human ventricular myocardium without affecting conduction time or haemodynamics (Greene *et al.*, 1983). An additional potential benefit of clofilium derives from its ability to decrease the electrical energy requirement for ventricular defibrillation (Kopia *et al.*, 1985; Dorian *et al.*, 1991). However, its reported mechanism of action varies with species and model employed. For example, clofilium is capable of inducing closed states in batrachotoxin-actived Na^+ channels from rabbit skeletal muscle (Nettleton *et al.*, 1991). Others report a decrease in outward potassium (delayed rectifier) current of guinea-pig ventricular myocytes after clofilium treatment (Snyders & Katzung, 1985), a finding repeated in ischaemic Purkinje fibres of the dog (Gough *et al.*, 1988). It has been reported that the delayed rectifier, but not the inward rectifier current, is blocked by quaternary clofilium in guinea-pig ventricular cells (Arena & Kass, 1988). Moreover, clofilium and its tertiary homologue LY 97119 have been shown to block the transient outward potassium current (I_{to}) in rat ventricular myocytes (Castle, 1991). Most recently, clofilium was shown to inhibit glibenclamide-sensitive K^+ channels in voltage-clamped *Xenopus* oocytes (Sakuta *et al.*, 1993).

It is clear the clofilium may have the capacity to affect a number of potassium channels in the normal or ischaemic myocardium. To define further its antifibrillatory actions, we studied clofilium in a Langendorff-perfused rabbit isolated heart model in which K_{ATP} channels have been implicated in the genesis of VF (Chi *et al.*, 1993). The primary objective of our study was to determine whether clofilium was capable of antagonizing the effects of pinacidil, a known K_{ATP} channel opener in ventricular myocardium, especially when applied in the presence of hypoxia and an associated decrease in tissue ATP content (Chi *et al.*, 1993). The conditions for perfusion, low extracellular K^+, pinacidil and hypoxia, favoured the induction of ventricular fibrillation through activation of the K_{ATP}-dependent or glibenclamide-sensitive K^+ channel (Chi *et al.*, 1993). We postulated that clofilium may owe its antifibrillatory effect to the blockade of the metabolically active K_{ATP} channel or glibenclamide-sensitive K^+ channel. We examined this hypothesis in the rabbit perfused isolated heart.

Methods

Guidelines for animal research

The procedures followed in this study are in accordance with the guidelines of the University of Michigan Committee on the Use and Care of Animals. Veterinary care was provided by the University of Michigan Unit for Laboratory Animal Medicine. The University of Michigan is accredited by the American Association of Accreditation of Laboratory Animal Care. The animal care and use programme conforms

[1] Author for correspondence.

to the standards in *The Guide for the Care and Use of Laboratory Animals*, DHEW Publ. No. (NIH) 86-23.

Isolated heart preparation

New Zealand, white rabbits (1.8–2.0 kg) were rendered unconscious by cervical dislocation. A median sternotomy was performed immediately therafter and the heart removed. The aorta was cannulated (Langendorff preparation) and perfused with a buffer solution at a constant rate of 18–20 ml min^{-1}. The time taken to complete the isolation of the heart and initiate perfusion was less than 10 s. The isolated heart was allowed to stabilize for approximately 20 min during which time, flow rate (Master Flex Roller Pump, Cole Parmer, Chicago, IL, U.S.A.) was adjusted to produce a coronary artery perfusion pressure of 50 ± 5 mmHg. Once a steady state had been established, pump settings remained constant throughout the protocol. The buffered perfusion medium (pH 7.4) was composed of (in mM): NaCl 117, KCl 1.41, $CaCl_2$ 2.4, $MgCl_2$ 1.2, $NaHCO_3$ 25, KH_2PO_4 1.1, glucose 5.0, L-glutamate (Na^+ salt) 5.0 and sodium pyruvate 2.0. The final K^+ concentration in the perfusate was 2.5 mM.

The perfusion medium was passed through an 'artificial lung' that consisted of 6 m of medical grade gas permeable tubing (Silastic, Dow Corning Corp, Midland, MI, U.S.A.) placed in a double-walled, water-heated chamber. Changing the oxygen mixture in the lung chamber caused the perfusion medium to equilibrate with the introduced gas mixture within 60 s.

During normoxia, the chamber was gassed continuously with 95% O_2/5% CO_2. Hypoxia was produced by gassing the chamber with 95% N_2/5% CO_2. The temperature of the perfusion medium and isolated heart were maintained at 37°C using a temperature controlled circulating water bath. The hearts were paced electrically from the right atrium at a frequency of 20–30% above the intrinsic sinus rate. Electrical pacing was maintained for the duration of each protocol.

A latex balloon was advanced into the left ventricle through an incision in the left atrial appendage and connected *via* a rigid cannula to a pressure transducer positioned at the level of the heart. The intraventricular balloon was expanded with distilled water to establish a ventricular end-diastolic pressure of 5 mmHg. Continuous measurement of left ventricular isovolumic developed pressure and end-diastolic pressure were made with the intraventricular balloon. A polyethylene cannula was placed in the left ventricle to vent the chamber of fluid entering the left ventricle *via* the Thebesian vessels. A thermistor probe (Tele-thermometer, Yellow Springs Instrument Co., Yellow Springs, OH, U.S.A.) was inserted in the left ventricle to monitor the temperature of the heart. A pressure transducer was attached to a side arm of the aortic cannula and was zeroed at the level of the heart. The rate of coronary artery flow was maintained constant by the roller pump. Therefore, changes in perfusion pressure in the aortic cannula reflected changes in coronary artery resistance.

Oxygen tension (P_{O_2}) of the perfusion buffer was monitored continuously by an in-line Clark type oxygen electrode (Instech dual oxygen electrode amplifier model 203, Instech Laboratories, Plymouth Meeting, PA, U.S.A.) placed immediately proximal to the aortic cannula. The electrogram was recorded from leads placed on the aorta and at the cardiac apex.

The following parameters were recorded with a Model 7 Grass Polygraph (Grass Instrument Co. Quincy, MA, U.S.A.): electrogram, monophasic action potential, coronary perfusion pressure, left ventricular pressure and its first derivative ± dP/dt.

Experimental protocol

Hearts were randomized by blind selection of preassigned treatments. Ten experimental groups, consisting of Langendorff perfused hearts were used in this study: Group I: Vehicle + pinacidil (1.25 μM) + hypoxia + reoxygenation (n = 9); Group II: clofilium (0.1 μM) + pinacidil (1.25 μM) + hypoxia + reoxygenation (n = 7); Group III: clofilium (1.0 μM) + pinacidil (1.25 μM) + hypoxia + reoxygenation (n = 7); Group IV: clofilium (10.0 μM) + pinacidil (1.25 μM) + hypoxia + reoxygenation (n = 9); Group V: electrophysiological studies (n = 8); Group VI: electrically induced ventricular fibrillation, treatment with clofilium (n = 11); Group VII: UK-68,798 (1.0 μM) + pinacidil (1.25 μM) + hypoxia + reoxygenation (n = 5); Group VIII: UK-68,798 (3.0 μM) + pinacidil (1.25 μM) + hypoxia + reoxygenation (n = 4); Group IX: UK-68,798 (10.0 μM) + pinacidil (1.25 μM) + hypoxia + reoxygenation (n = 5); Group X: 5-hydroxydecanoate (10.0 μM) + pinacidil (1.25 μM) + hypoxia + reoxygenation (n = 9).

A drug-free equilibration period of 20 min elapsed before the start of each protocol (Figure 1). In groups I–IV, clofilium or drug-free buffer, perfused the hearts for 10 min. In groups VII-X either UK-68,798 or 5-hydroxydecanoate was added to the buffer and perfused the hearts for 10 min. Pinacidil was added to the buffer to achieve a final concentration of 1.25 μM. Five minutes after pinacidil was added to the perfusion medium, global hypoxic perfusion was initiated by changing the gas mixture in the 'artificial lung' to 95% N_2 5% CO_2. The state of global hypoxic perfusion was maintained for 12 min (hypoxic period). Normoxic perfusion was re-established by returning the gas mixture in the 'artificial lung' to 95% O_2, 5% CO_2 (reoxygenation) for the remaining 40 min of the experimental protocol. The period of time to onset of spontaneous, sustained ventricular fibrillation (30 s minimum) was recorded. Groups I–IV and VII–X were studied under conditions of a reduced potassium concentration (2.5 mM) in the perfusion medium. Under these conditions, during global hypoxic perfusion, myocardial ATP content decreases approximately 50%. We have shown in the past that under conditions of 2.5 mM K^+ and reduced ATP, the heart becomes susceptible to the development of ventricular fibrillation in the presence of pinacidil (Chi *et al.*, 1993).

Electrophysiological effects of clofilium

In Group V hearts, a miniature bipolar plunge electrode (INAPRES, Norwich, NY, U.S.A.) was sutured over the right ventricular outflow tract (RVOT) for delivery of the S2 ventricular stimulus from a Grass S8800 square wave stimulator and stimulus isolation unit (SIU5; Grass Instrument Co., Quincy, MA, U.S.A.). The S2 stimulus duration was 4 ms and was triggered 250 ms after the R wave of the ECG. The threshold current was defined as the minimum current required to elicit a propagated ventricular impulse. To determine effective refractory period (ERP), stimulation (S2) to the RVOT (at 1.5 times threshold current) was initiated at a 250 ms delay. The S2 delay stimulation was decreased repeatedly by 10 ms until the refractory period was reached. The refractory period determined in the region of the RVOT is defined as the longest R-wave stimulus interval that fails to elicit a propagated ventricular complex.

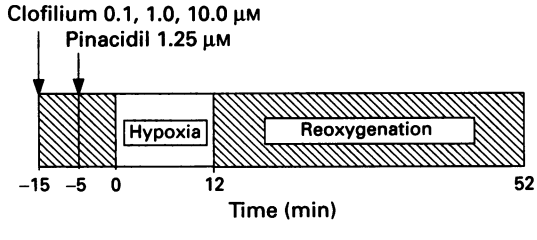

Figure 1 Experimental protocol for Groups I–IV and VII–X; hatched areas, 95% O_2/5% CO_2; open areas, 95% N_2/5% CO_2.

Determination of the ventricular effective refractory period under conditions of low K^+ (2.5 mM) invariably resulted in the induction of ventricular fibrillation. Therefore, Group IV hearts were perfused with perfusion medium containing a potassium concentration of 5.1 mM. Refractory periods were determined at 5, 15 and 30 min after clofilium was added to the perfusion medium.

A Ag-AgCl electrode was used to record the endocardial monophasic action potential duration. Action potential durations (APD) at 90% repolarization were determined at baseline, 10 min after addition of clofilium, and 5 min after pinacidil plus clofilium in groups II–IV.

Group VI hearts received a train of stimuli delivered to the region of the RVOT (S2, S3, S4-instead of a single impulse) until ventricular fibrillation occurred. After 30 s of sustained ventricular fibrillation, a volume of drug diluent (perfusion medium) was administered immediately proximal to the cannulated aorta. Time for injection to reversion of normal sinus rhythm was recorded. If 30 s had elapsed and reversion was not evident, clofilium (0.35 or 0.6 ml of 10.0 mM), dissolved in perfusion medium, was administered rapidly, and time to return of normal rhythm was recorded.

Drugs

Pinacidil and clofilium were gifts from the Eli Lilly Co. (Indianapolis, IN, U.S.A.). A stock solution of pinacidil was prepared daily, by dissolving the drug in acidified perfusate (pH 2.0–2.5). The stock solution was added to the perfusion buffer to yield a final concentration of 1.25 μM. Clofilium was dissolved in the perfusate buffer and prepared just before use in each experiment. UK-68,798 (dofetilide) was a gift from Pfizer Central Research (Sandwich, U.K.) and 5-hydroxydecanoate was a gift from Parke-Davis (Ann Arbor, MI, U.S.A.). Analytical grade chemicals used for preparation of the buffer solution were obtained from commercial sources.

Statistical analysis

The data are expressed as mean ± s.e.mean. The difference between groups (fibrillation occurrence) was analysed by Fisher's Exact test. A one-way ANOVA was used for comparisons between groups (factorial) at specific time points, as well as within groups (repeated measures). Differences were considered significant at $P<0.05$.

Results

Antifibrillatory effects of clofilium

The antifibrillatory effect of clofilium was examined in a Langendorff-perfused rabbit isolated heart model in which ventricular fibrillation was induced by the combined introduction of pinacidil (1.25 μM) to the perfusion medium with the subsequent induction of global hypoxia for 12 min followed by reoxygenation for 40 min. Exposure of the heart to pinacidil (1.25 μM) during normoxic perfusion, did not result in the development of cardiac arrhythmias. However, when pinacidil-treated hearts were subjected to 12 min of hypoxia followed by reoxygenation, there was a 78% (7 of 9 hearts) incidence of ventricular fibrillation in the control group (Group I). Most of the hearts in Group I developed ventricular fibrillation during hypoxia or within the first 20 min of reoxygenation (Figure 2). Clofilium pretreatment was associated with a concentration-related suppression in the incidence of ventricular fibrillation. At a concentration of 10.0 μM, 1 of 9 (11%) hearts developed ventricular fibrillation during the period of reoxygenation ($P<0.05$ *vs* vehicle-treated hearts; Figure 2). Clofilium concentrations of 0.1 and 1.0 μM did not confer a significant protective effect against the induction of ventricular fibrillation upon exposure to the combined effects of pinacidil and hypoxia/reoxygenation.

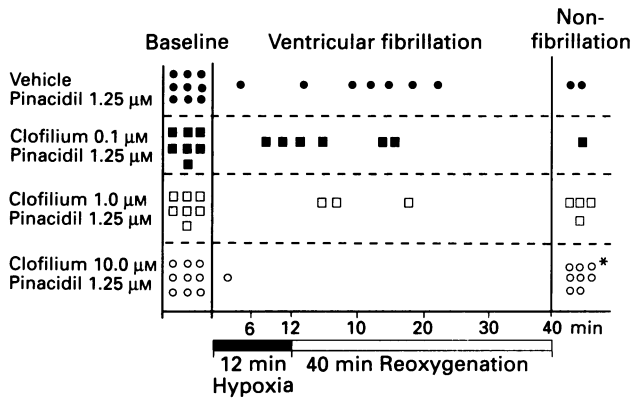

Figure 2 Incidence of ventricular fibrillation in the presence of vehicle or clofilium. Each symbol represents an individual isolated heart. *$P<0.05$ vs vehicle, Fisher's exact test.

Effects of UK-68,798 and 5-hydroxydecanoate on ventricular fibrillation

Groups VII–IX were added to our study to determine if another putative Class III antiarrhythmic agent, devoid of ATP-dependent/glibenclamide-sensitive K^+ channel blocking activity, was able to prevent the induction of ventricular fibrillation by exposing the perfused heart to the combined effects of pinacidil and hypoxia. The selective inhibitor of the rapid component of the delayed rectifier channel, UK-68,798 was used to test this hypothesis. Finally, Group X was included to examine a specific ATP-dependent/glibenclamide-sensitive K^+ channel blocker, 5-hydroxydecanoate, in the isolated heart model of ventricular fibrillation.

UK-68,798 pretreatment was not associated with a concentration-related suppression in the incidence of ventricular fibrillation. At a concentration of 10.0 μM, 3 of 5 (60%) hearts developed ventricular fibrillation during the period of reoxygenation (Figure 3). UK-68,798 concentrations of 1.0 μM (80% VF) and 3.0 μM (100% VF) did not confer a significant protective effect against the induction of ventricular fibrillation upon exposure to the combined effects of pinacidil and hypoxia-reoxygenation. However, at a concentration of 10 μM, 5-hydroxydecanoate, reduced the incidence of ventricular fibrillation to 2 of 9 (22%) hearts during the period of reoxygenation ($P<0.05$ *vs* vehicle treated hearts).

Effects of clofilium on cardiac function

Coronary perfusion pressure (Table I) did not differ between Groups I–IV at baseline. The highest concentration of

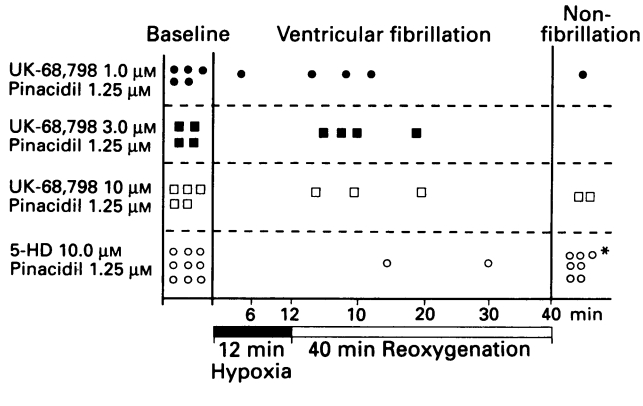

Figure 3 Incidence of ventricular fibrillation in the presence of UK-68,798 and 5-hydroxydecanoate (5-HD). Each symbol represents an individual isolated heart. *$P<0.05$ vs vehicle, Fisher's Exact test.

Table 1 Coronary perfusion pressure (mmHg) in the rabbit isolated heart treated with vehicle or clofilium

	Vehicle	0.1 μM	1.0 μM	10.0 μM
Baseline	52 ± 3 (9)	52 ± 1 (7)	61 ± 4 (7)	58 ± 3(9)
Clofilium (10 min)	-	57 ± 2 (7)[a]	66 ± 6 (7)[a]	50 ± 2 (9)[ac]
Pinacidil (5 min)	37 ± 2 (9)[a]	45 ± 2 (7)[ab]	50 ± 4 (7)[ab]	48 ± 2 (9)[ab]
Hypoxia (5 min)	31 ± 4 (7)[a]	38 ± 4 (7)[a]	42 ± 4 (7)[a]	38 ± 3 (8)[a]
Hypoxia (12 min)	40 ± 4 (7)[a]	45 ± 3 (6)[a]	55 ± 6 (7)	53 ± 4 (8)
Reoxygen (10 min)	48 ± 3 (5)	57 ± 9 (3)	59 ± 6 (5)	55 ± 4 (8)
Reoxygen (40 min)	-	-	82 ± 18 (4)	75 ± 6 (8)[a]

Data are expressed as mean ± s.e.mean, *n* in parentheses.
[a]$P<0.05$ vs. corresponding baseline; [b]$P<0.05$ vs. respective clofilium (10 min); [c]$P<0.05$ vs 1.0 μM clofilium

clofilium (10.0 μM) produced a reduction in coronary perfusion pressure from baseline, 58 ± 3 mmHg to 50 ± 2 mmHg after 10 min of exposure ($P<0.05$). More striking was the coronary perfusion pressure (CPP) response upon the subsequent administration of pinacidil (1.25 μM). For hearts treated with 0.1 and 1.0 μM clofilium, CPP decreased in the presence of pinacidil. In contrast, hearts treated with 10.0 μM clofilium exhibited a modest reduction of CPP. Clearly, at a concentration of 10.0 μM clofilium attenuates the vasodilator effects of pinacidil. Hypoxia further decreased CPP in each group and there were no differences in coronary artery perfusion pressure among groups during hypoxia or reoxygenation.

Clofilium produced minimal effects upon myocardial contractile performance when added to the perfusion medium (10.0 μM) compared to the control group of hearts. In hearts exposed to clofilium followed by pinacidil (1.25 μM), $+dP/dt$ was 475 ± 6 mmHg s^{-1}, compared to 470 ± 9 mmHg s^{-1} before pinacidil treatment. Vehicle-treated hearts typically exhibit a 10% reduction in $+dP/dt$ upon the addition of pinacidil (1.25 μM), clofilium attenuated this response. During hypoxia, ($t = 12$ min) $+dP/dt$ was 355 ± 14 mmHg s^{-1} in the clofilium-treated group. Lower concentrations of clofilium failed to show significant haemodynamic changes compared to vehicle-treated hearts throughout the experimental protocol.

Electrophysiological effects of clofilium

As shown in Table 2, a group of hearts was used for the characterization of the ventricular effective refractory period (ERP) determinations in the absence and presence of cumulative concentrations of clofilium (0.3, 1.0 and 3.0 μM). In the presence of the lowest concentration of clofilium (0.3 μM), ERP increased 17 ± 5% above baseline after 30 min of exposure ($P<0.05$). At a concentration of 1.0 μM, clofilium progressively increased ERP 25 ± 9% above baseline after 30 min of exposure to the drug in the perfusion medium. An additional prolongation to 213 ± 16 ms was found after 30 min of exposure to 3.0 μM clofilium ($P<0.05$ vs baseline). The total increase in ERP was 37 ± 18% compared to baseline values. Stepwise increases above 3.0 μM clofilium decreased atrioventricular conduction velocity and interfered with the ability to maintain atrial pacing. Therefore the electrophysiological effects of clofilium at concentrations greater than 3.0 μM were not studied.

Table 2 Ventricular effective refractory periods (ms) of paced rabbit isolated hearts in the presence of graded concentrations of clofilium

Concentration	*Predrug*	*5 min*	*15 min*	*30 min*
0.3 μM ($n = 8$)	156 ± 13	173 ± 16	175 ± 17[a]	170 ± 9[a]
1.0 μM ($n = 6$)	-	177 ± 15	184 ± 15	189 ± 9[a]
3.0 μM ($n = 6$)	-	190 ± 15	203 ± 13[a]	213 ± 16[a]

Data are mean ± s.e.mean. [a]$P<0.05$ relative to predrug value.

Action potential durations (APD) at 90% repolarization were determined at baseline, 10 min after addition of clofilium, and 5 min after pinacidil plus clofilium in groups II–IV. Table 3 summarizes the results. The changes in APD were not as profound in our preparation as were the changes in measured refractory period after clofilium exposure. An important result was obtained in this portion of the study. While we measured only slight increases in APD after clofilium alone, there was a significant change in APD after pinacidil had been administered. After the lowest 2 concentrations of clofilium had been administed (0.1 and 1.0 μM), pinacidil reduced APD ($P<0.05$ vs corresponding baseline). In the presence of 10.0 μM clofilium, there was no reduction in APD compared to baseline. These findings indicate that the prevention of APD shortening by 10.0 μM clofilium may contribute to its antifibrillatory action.

Chemical defibrillatory effects of clofilium

Hearts in Group VI were used to explore the ability of clofilium to achieve chemical defibrillation in the isolated perfused heart. Ventricular fibrillation was induced by direct current pulses applied to the RVOT of the isolated heart while coronary flow was maintained constant. Ventricular fibrillation was permitted to persist for a period of 30 s to ensure the presence of a persistent state of fibrillation after which a volume of vehicle buffer was administered just proximal to the aorta. Repeated administration of the drug diluent did not influence the fibrillation status of the isolated heart. Isolated perfused hearts, while in ventricular fibrillation, were given a single dose of clofilium (0.35 or 0.60 ml of a 10 mM solution) rapidly, immediately above the aorta. Conversion of the electrically-induced VF to normal sinus rhythm occurred in 10 of 11 hearts (Figure 4). The mean time to conversion was 14 ± 2 s in 5/5 hearts ($P<0.05$ vs vehicle), using 0.35 ml of 10.0 mM clofilium. Time to conversion after 0.60 ml of 10.0 mM clofilium was 42 ± 13 s in 5/6 hearts ($P<0.05$ vs vehicle). The longer time to conversion in the latter group was related to sinus arrest associated with exposure to 0.6 ml of

Table 3 Action potential duration (ms) on paced rabbit isolated hearts during baseline, and in the presence of clofilium and pinacidil

Concentration	*Baseline*	*Clofilium* (10 min)	*Clofilium + pinacidil*
0.1 μM ($n = 6$)	139 ± 6	143 ± 6 (3 ± 2)	123 ± 8[a] (−9 ± 5)
1.0 μM ($n = 7$)	141 ± 9	150 ± 9 (7 ± 3)	134 ± 8[a] (−4 ± 5)
10.0 μM ($n = 5$)	143 ± 13	150 ± 12 (5 ± 2)	142 ± 11 (+4 ± 2[b])

Data are mean ± s.e.mean at 90% repolarization (ms). Values in parentheses represent % change from baseline. [a]$P<0.05$ vs corresponding clofilium (10 min) value. [b]$P<0.05$ relative to 0.1 μM clofilium + pinacidil (1.25 μM) % change.

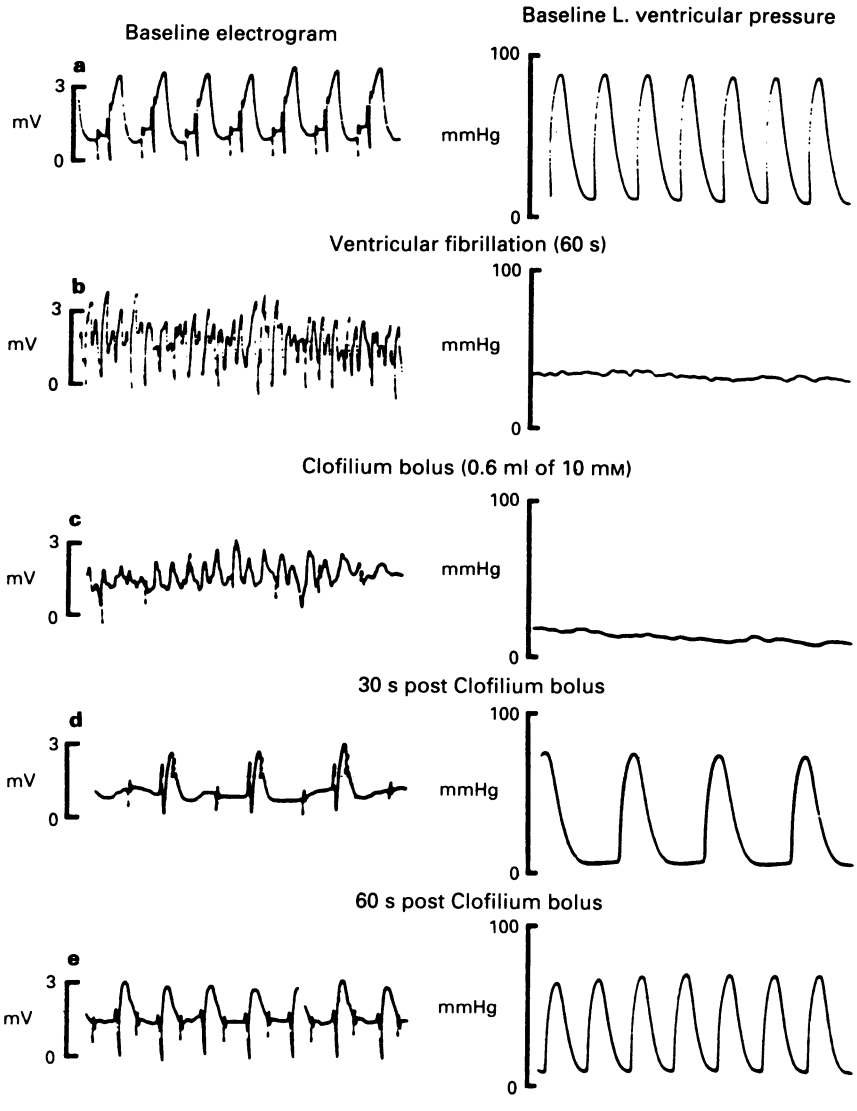

Figure 4 (a) Electrogram (left), and corresponding left ventricular pressure (right); under baseline conditions. (b) Electrogram after 60 s of sustained ventricular fibrillation (L) and left ventricular function (R). (c) Electrogram after induction of clofilium bolus (0.6 ml of 10 mM) to the heart (L) and left ventricular function (R). (d) Electrogram 30 s post administration of clofilium (L) and left ventricular function (R). (e) Electrogram 60 s post administration of clofilium (L) and left ventricular function (R).

10 mM clofilium. The administration of a non-drug containing volume of perfusion buffer was used as a vehicle control. Introduction of the placebo buffer never resulted in the conversion of ventricular fibrillation to sinus rhythm.

Discussion and conclusions

The inefficacy of many Class I agents for the prevention of sudden cardiac death has prompted a renewed effort in the development of antiarrhythmic drugs. Class III antiarrhythmic therapy targeting lethal arrhythmias is receiving much attention. Several Class III agents in various stages of development have been reported to be efficacious in animal models characterized by the development of ventricular fibrillation (Lynch *et al.*, 1984; Chi *et al.*, 1990a; Black *et al.*, 1991). It is novel however to find an agent that possesses not only an antiarrhythmic/antifibrillatory capacity, but a defibrillatory capacity. Reports in the past have ascribed this effect to bretylium (Bacaner, 1968; Sanna & Arcidiacono, 1973), but the effects of bretylium on the sympathetic nervous system, i.e., release of catecholamines from sympathetic nerve terminals (Boura & Green, 1959) and side effects of hypotension contributed to its lack of widespread use. Clofilium, another quaternary antiarrhythmic agent has been shown to prolong the effective refractory period or action potential duration in animal models (Steinberg & Molloy, 1975; Steinberg *et al.*, 1981; Kowey *et al.*, 1985; Wu *et al.*, 1989; Li *et al.*, 1990) as well as increase the refractory period in man without affecting conduction time or haemodynamics (Greene *et al.*, 1983). The role of clofilium as an antifibrillatory agent has been shown to be beneficial by lowering defibrillation requirements (Kopia *et al.*, 1985; Dorian *et al.*, 1991). To date, there has not been a report that systematically describes the chemical defibrillatory ability of clofilium. We have evidence that clofilium, which up to now has been considered to be a I_{to}/I_K (Arena & Kass, 1988; Castle, 1991) channel blocker is not only efficacious as an antifibrillatory agent, but as a defibrillatory agent as well.

While it is generally understood that ATP-dependent potassium channels (glibenclamide-sensitive channels) are closed under normal conditions (Noma, 1983), blockade of channels that are closed would be expected to produce few measurable effects. Under normal conditions, the rabbit isolated heart treated with graded concentrations of clofilium responds by a progressive increase in the ventricular effective refractory period (Table 2). We observed slight increases in the duration of the monophasic action potential after

clofilium administration (Table 3). If the mechanism of action of clofilium were K_{ATP} channel blockade, we would expect to find very little change in either measure. This was not the case, which implies that clofilium does not block the ATP dependent K^+ channel under normal conditions during which the intracellular ATP concentration is not perturbed. Blockade of delayed rectifier current by clofilium in ischaemic Purkinje fibres has been reported by several investigators (Gough *et al.*, 1988; Reeve, 1992). In the present study, clofilium produced a dose-dependent increase in the effective refractory period, whereas changes in the monophasic action potential duration (90% repolarization) failed to reach statistical significance after 10 min of exposure. This is not surprising since it has been reported that clofilium causes substantial prolongation of action potential duration in the Purkinje fibre, but the duration was unchanged in the ventricular muscle cell (Carlsson *et al.*, 1992).

Addition of pinacidil before induction of hypoxia unmasked effects of clofilium not associated with blockade of channels associated with the transient outward (I_{to}) or delayed rectifier currents. In the presence of lower concentrations of clofilium (0.1 and 1.0 μM), pinacidil exposure produced a reduction in the monophasic action potential duration. The highest dose of clofilium (10.0 μM), however, prevented the pinacidil-induced reduction in the monophasic action potential duration. Therefore the functional data implicate clofilium in the blockade of ATP-dependent potassium channels in the presence of the K_{ATP} channel opener, pinacidil (Arena & Kass, 1989; Martin & Chinn, 1990). In support of our functional data is a recent report in which clofilium was capable of inhibiting glibenclamide-sensitive K^+ channels in voltage-clamped *Xenopus* oocytes (Sakuta *et al.*, 1993). However, we cannot exclude the possibility of a functional antagonism by clofilium. The action potential duration shortening by pinacidil may be counteracted by blockade by clofilium of transient outward and/or delayed rectifier currents, the net result being little change in the duration of the monophasic action potential.

Membrane channel activity becomes more complex as the biochemical cascade of events associated with hypoxia ensues. In our experimental model, control hearts subjected to hypoxia in the absence of pinacidil had a 20% incidence of ventricular fibrillation as compared to the significant increase when pinacidil was present in the perfusion medium. The results indicate that opening of the K_{ATP} channel by pinacidil, together with a previous hypoxic insult and decrease in intracellular ATP content, is pivotal in the promotion of ventricular fibrillation (Chi *et al.*, 1993). Clofilium (10.0 μM) consistently prevented the development of ventricular fibrillation under the same experimental conditions that otherwise proved to be arrhythmogenic. Moreover, administration of two additional agents possessing known pharmacological activity on myocardial potassium channels add support to our findings. UK-68,798 which has been shown to block selectively the delayed rectifier current (Gwilt *et al.*, 1989; Rasmussen *et al.*, 1992; Carmeliet, 1992) was not effective in reducing the incidence of ventricular fibrillation in response to pinacidil plus hypoxia. In contrast, the administration of 5-hydroxydecanoate, a well characterized inhibitor of the ATP-dependent K^+ channel (Niho *et al.*, 1987; Notsu *et al.*, 1992; Notsuto *et al.*, 1992) was equally as effective as clofilium in preventing the development of ventricular fibrillation.

It is reasonable to believe that clofilium is able to block not only the transient outward and/or the delayed rectifier potassium currents, but the metabolically active ATP-dependent potassium channel under conditions of decreased intracellular ATP that would promote its opening. In the present experimental model, pinacidil administration in the presence of a reduced intracellular ATP content, would be expected to facilitate opening of the ATP-dependent potassium channel. The increase in the outward potassium current *via* the ATP-dependent potassium channel most likely accounts for the initiation of ventricular fibrillation; an event that can be prevented by glibenclamide (Chi *et al.*, 1993), and 5-hydroxydecanoate. It follows that clofilium may owe *part* or *all* of its antifibrillatory action to the prevention of action potential shortening *via* blockade of ATP-dependent K^+ channels. The prevention of ventricular fibrillation in the present experimental model may be dependent upon a very specific electrophysiological derangement initiated by opening of the ATP-dependent potassium of glibenclamide-sensitive channel. This specific action of clofilium may not occur under conditions in which the initiation of ventricular fibrillation is not associated with opening of the ATP-dependent potassium channel. Hypoxia-induced decrease in myocardial ATP content increases the responsiveness of the ATP-dependent K^+ channel to the opening effects of pinacidil. The experimental model, therefore, utilizes the vulnerability of the heart under a specific set of conditions to explore the role of the ATP-dependent K^+ channel in the genesis of ventricular fibrillation. Using this approach, it becomes possible to identify those pharmacological interventions capable of preventing ventricular fibrillation arising from opening of the ATP-dependent potassium channel. Clofilium, in addition to its other potential effects on myocardial membrane potassium channels, appears to have a salutary effect similar to that of glibenclamide and 5-hydroxydecanoate, and radically different from that of dofetilide (UK68,798) in terms of preventing ventricular fibrillation. These observations support the concept that clofilium has the potential to modulate the ATP-dependent potassium channel and to prevent those electrophysiological changes leading to ventricular fibrillation associated with decreases in myocardial tissue ATP content.

It is noteworthy that clofilium is capable of reverting electrically induced sustained ventricular fibrillation to sinus rhythm. This group of hearts was an addendum to our primary study after we had noted that 4/9 hearts in the 10.0 μM clofilium group reverted to sinus rhythm after transient episodes of spontaneous ventricular flutter during the 40 min reperfusion period, a phenomenon that has not been observed in vehicle-treated rabbit hearts. A bolus of clofilium (0.35 ml of 10 mM) slowed the rate of fibrillation, until the heart resumed normal sino-atrioventricular conduction within 14 ± 2 s. This event was observed in 5 isolated hearts. A larger quantity of administered clofilium ($n = 5$, 0.6 ml of 10 mM) to the fibrillating heart, not only slowed the frequency of fibrillatory waves, but elicited sinoatrial arrest. Since coronary perfusion was maintained constant in our preparation, and oxygen delivery uncompromised, the heart was capable of resuming normal sinus rhythm in 42 ± 16 s.

The ability of clofilium to antagonize the coronary vasodilator action of pinacidil should not be overlooked. Before induction of hypoxia, pinacidil alone produced vasodilatation and a negative inotropic effect on the rabbit isolated perfused heart. The first derivative of left ventricular pressure, $+dP/dt$ is reduced approximately 10% within 5 min after pinacidil was added to the perfusion medium. The presence of clofilium in the perfusate attenuated this effect (see Table 1). It is well known that pinacidil is capable of specific K_{ATP} channel activation (Arena & Kass, 1989), while others report a profibrillatory effect of pinacidil (Chi *et al.*, 1990a, 1993). This evidence suggests that pinacidil will promote ventricular fibrillation given the proper substrate or altered physiological conditions. Clofilium prevents these responses, thereby leading us to suggest that clofilium (10.0 μM) may, in part, block the metabolically activated ATP-dependent potassium channel. This conclusion is supported by the observation that UK-68,798 (specific delayed rectifier current antagonist) was not effective, while 5-hydroxydecanoate (specific ATP-dependent K^+ current antagonist) was effective in attenuating the development of ventricular fibrillation. It may be that clofilium has been overlooked as a potentially efficacious antifibrillatory agent.

This work was supported in part by a grant from the National Institutes of Health, Heart Lung and Blood Institute, HL-05806-34. G.S.F. was the recipient of a Merck Postdoctoral Fellowship during the conduct of the study. We thank Lilly Research Laboratories (Indianapolis, Indiana U.S.A.) for the generous supply of clofilium.

References

ARENA, J.P. & KASS, R.A. (1988). Block of heart potassium channels by clofilium and its tertiary analogs: relationship between drug structure and type of channel blocked. *Mol. Pharmacol.*, **34,** 60–66.

ARENA, J.P. & KASS, R.S. (1989). Activation of ATP sensitive K channels in heart cells by pinaicidil: dependence on ATP. *Am. J. Physiol.*, **257** (Heart Circ Physiol 26), H2092–H2096.

BACANER, M. (1968). Treatment of ventricular fibrillation and other acute arrhythmias with bretylium tosylate. *Am. J. Cardiol.*, **21,** 530–543.

BLACK, S.C., CHI., L., MU, D.-X. & LUCCESHI, B.R. (1991). The antifibrillatory actions of UK-68,798, a Class III antiarrhythmic agent. *J. Pharmacol. Exp. Ther.*, **258,** 416–423.

BOURA, A.L.A. & GREEN, A.F. (1959). The action of bretylium: adrenergic neuron blocking and other effects. *Br. J. Pharmacol. Chemother.*, **14,** 536–548.

CARLSSON, L., ABRAHAMSSON, C., DREWS, L. & DUKER, G. (1992). Antiarrhythmic effects of potassium channel openers in rhythm abnormalities related to delayed repolarization. *Circulation*, **85,** 1491–1500.

CARMELIET, E. (1992). Voltage- and time-dependent block of the delayed K+ current in cardiac myocytes by dofetilide. *J. Pharmacol. Exp. Ther.*, **262,** 809–817.

CASTLE, N.A. (1991). Selective inhibition of potassium currents in rat ventricle by clofilium and its tertiary homology. *J. Pharmacol. Exp. Ther.*, **257,** 342–350.

CHI, L., BLACK, S.C., KUO, P.I., FAGBEMI, S.O. & LUCCHESI, B.R. (1993). Actions of pinacidil at a reduced potassium concentration: a direct cardiac effect possibly involving the ATP-dependent potassium channel. *J. Cardiovasc. Pharmacol.*, **21,** 179–190.

CHI, L., MU, D.-X., DRISCOLL, E.M. & LUCCHESI, B.R. (1990a). Antiarrhythmic and electrophysiologic actions of CK-3579 and sematilide in a conscious canine model of sudden coronary death. *J. Cardiovasc. Pharmacol.*, **16,** 312–324.

CHI, L., U'PRICHARD, A.C.G. & LUCCHESI, B.R. (1990b). Profibrillatory actions of pinacidil in a conscious canine model of sudden coronary death. *J. Cardiovasc. Pharmacol.*, **15,** 452–464.

DORIAN, P., WANG, M., DAVID, I & FEINDEL, C. (1991). Oral clofilium produces sustained lowering of defibrillation energy requirements in a canine model. *Circulation*, **83,** 614–621.

GOUGH, W.B., HU, D. & EL-SHERIF, N. (1988). Effects of clofilium on ischemic subendocardial Purkinje fibers 1 day post-infarction. *J. Am. Coll. Cardiol.*, **11,** 431–437.

GREENE, H.L., WERNER, J.A., GROSS, B.W., SEARS, G.K., TROBAUGH, G.B. & COBB, L.A. (1993). Prolongation of cardiac refractory times in man by clofilium phosphate, a new antiarrhythmic agent. *Am. Heart J.*, **106,** 492–500.

GWILT, M., DALRYMPLE, H.W., BURGES, R.A., BLACKBURN, K.J., ARROWSMITH, J.E., CROSS, P.E. & HIGGINS, A.J. (1989). UK-68,798 is a novel, potent and selective class III antiarrhythmic agent. *J. Mol. Cell. Cardiol.*, **21,** S11.

KOPIA, G.A., ELLER, B.T., PATTERSON, E., SHEA, M.J. & LUCCHESI, B.R. (1985). Antiarrhythmic and electrophysiologic actions of clofilium in experimental canine models. *Eur. J. Pharmacol.*, **116,** 49–61.

KOWEY, P.R., FRIEHLING, T.D., O'CONNER, K.M., WETSTEIN, L. & KELLIHER, G.J. (1985). The effect of bretylium and clofilium on dispersion of refractoriness and vulnerability to ventricular fibrillation in the ischemic feline heart. *Am. Heart J.*, **110,** 363–370.

LI, T., CARR, A.A. & DAGE, R.C. (1990). Effects of MDL 11,939 on action potential and contractile force in cardiac tissues: a comparison with bretylium, clofilium, and sotalol. *J. Cardiovasc. Pharmacol.*, **16,** 917–923.

LINDSTROM, T.D., MURPHY, P.J., SMALLWOOD, J.K., WIEST, S.A. & STEINBERG, M.I. (1982). Correlation between the disposition of [14C] clofilium and its cardiac electrophysiological effects. *J. Pharmacol. Exp. Ther.*, **221,** 584–589.

LYNCH, J.J., WILBER, D.J., MONTGOMERY, D.G., HSIEH, T.M., PATTERSON, E. & LUCCHESHI, B.R. (1984). Antiarrhythmic and antifibrillatory actions of the levo- and dextro-rotary isomers of sotalol. *J. Cardiovasc. Pharmacol.*, **6,** 1132–1141.

LYNCH, J.J., WILBER, D., MONTGOMERY, D.G., HSIEH, T.M., PATTERSON, E. & LUCCHESHI, B.R. (1989). Suppression of lethal ischemic ventricular arrhythmias by the class III agent E4031 in a canine model of previous myocardial infarction (abstr). *J. Mol. Cell. Cardiol.*, **21** (Suppl II), S154.

MARTIN, C.L. & CHINN, K. (1990). Pinacidil opens ATP-dependent K^+ channels in cardiac myocytes in an ATP and temperature dependent manner. *J. Cardiovasc. Pharmacol.*, **15,** 510–514.

NETTLETON, J., CASTLE, N.A. & WANG, G.K. (1991). Block of single batrachotoxin-activated Na^+ channels by clofilium. *Mol. Pharmacol.*, **39,** 352–358.

NIHO, T., NOTSU, T., ISHIKAWA, H., FUNATO, H., YAMAZAKI, M., TAKAHASHI, H., TANAKA, I., KAYAMOTO, M., DABASKI, F., SHINKAWA, T., UEMURA, A. & MIZOTA, M. (1987). Study of mechanisms and effects of sodium 5-hydroxydecanoate on experimental ischemic ventricular arrhythmia. *Folia Pharmacol. (Japan)*, **89,** 155–167.

NOMA, A. (1983). ATP-regulated K^+ channels in cardiac muscle. *Nature*, **305,** 147–148.

NOTSU, T., OHHASHI, K., TANAKA, I., ISHIKAWA, H., NIHO, T., FUKUTAKE, K. & MIZOTA, M. (1992). 5-Hydroxydecanoate inhibits ATP-sensitive K+ channel currents in guinea-pig single ventricular myocytes. *Eur. J. Pharmacol.*, **220,** 35–41.

NOTSUTO, T., TANAKA, I., TAKANO, M. & NOMA, A. (1992). Blockade of the ATP-sensitive K+ channel by 5-hydroxydecanoate in guinea pig ventricular myocytes. *J. Pharmacol. Exp. Ther.*, **260,** 702–708.

PATTERSON, E., ELLER, B.T., ABRAMS, G.D., VASILIADES, J. & LUCCHESI, B.R. (1983). Ventricular fibrillation in a conscious canine preparation of sudden coronary death. Prevention by short and long-term amiodarone administration. *Circulation*, **68,** 857–864.

RASMUSSEN, H.S., ALLEN, M.J., BLACKBURN, K.J., BUTROUS, G.S. & DALRYMPLE, H.W. (1992). Dofetilide, a novel class III antiarrhythmic agent. *J. Cardiovasc. Pharmacol.*, **20** (Suppl 2), S96–S1051.

REEVE, H.L. & PEERS, C. (1992). Blockade of delayed rectifier K^+ currents in neuroblastoma × glioma hybrid (NG 108-15) cells by clofilium, a class III antidysrhythmic agent. *Br. J. Pharmacol.*, **105,** 458–462.

SAKUTA, H., OKAMOTO, K. & WATANABE, Y. (1993). Antiarrhythmic drugs, clofilium and cibenzoline are potent inhibitors of glibenclamide-sensitive K+ currents in *Xenopus* oocytes. *Br. J. Pharmacol.*, **109,** 866–872.

SANNA, G. & ARCIDIACONO, R. (1973). Chemical ventricular defibrillation of the human heart with bretylium tosylate *Am. J. Cardiol.*, **32,** 982–987.

SYNDERS, D.J. & KATZUNG, B.G. (1985). Clofilium reduces the plateau potassium current in isolated cardiac myocytes. *Circulation*, **72** (Suppl III), 233.

SPINELLI, W., PARSONS, R.W. & COLATSKY, T.J. (1992). Effects of WAY-123,398, a new Class III antiarrhythmic agent, on cardiac refractoriness and ventricular fibrillation threshold in anesthetized dogs: a comparison with UK-68798, E-4031, and dl-Sotalol. *J. Cardiovasc. Pharmacol.*, **20,** 913–922.

STEINBERG, M.I. & MOLLOY, B.B. (1975). Clofilium–a new antifibrillatory agent that selectively increases cellular refractoriness. *Life Sci.*, **25,** 1397–1406.

STEINBERG, M.I., SULLIVAN, M.E., WIEST, S.A., ROCKHOLD, F.W. & MOLLOY, B.B. (1981). Cellular electrophysiology of clofilium, a new antifibrillatory agent, in normal and ischemic canine Purkinje fibers. *J. Cardiovasc. Pharmacol.*, **3,** 881–895.

WU, K.-M., ROSS, S. & HOFFMAN, B.F. (1989). Monophasic action potentials during reentrant atrial flutter in the dog: effects of clofilium and acetylcholine. *J. Cardiovasc. Pharmacol.*, **13,** 908–914.

(Received January 18, 1994
Revised March 29, 1994
Accepted April 11, 1994)

Br. J. Pharmacol. (1994), **113**, 216–220

Natriuretic peptide-induced cyclic GMP accumulation in adult guinea-pig cerebellar slices

[1]Félix Hernández, [2]Stephen P.H. Alexander & David A. Kendall

Department of Physiology & Pharmacology, Medical School, Queen's Medical Centre, Nottingham NG7 2UH

1 Second messenger responses to natriuretic peptides were studied in guinea-pig cerebellar slices by use of radioactive precursors.

2 The rank order of potency of the different natriuretic peptides in generating [^{3}H]-guanosine 3':5'-cyclic monophosphate (cyclic GMP) was atrial natriuretic peptide (ANP) > brain natriuretic peptide (BNP) >>C-type natriuretic peptide (CNP) with EC_{50} values of 19.5 ± 8.8 nM for ANP and 169 ± 41 nM for BNP. CNP induced [^{3}H]-cyclic GMP accumulation only at concentrations greater than 1 μM.

3 An additive response to ANP (1 μM) was observed in the presence of the adenosine receptor agonist, 5'-N-ethylcarboxamidoadenosine (NECA, 10 μM) or the soluble guanylyl cyclase activator, sodium nitroprusside (SNP, 100 μM) for [^{3}H]-cyclic GMP accumulation.

4 ANP, BNP and CNP (all at 1 μM) failed to alter significantly either basal-, forskolin- (10 μM), isoprenaline- (100 μM), or NECA- (10 μM) induced [^{3}H]-cyclic AMP generation. Natriuretic peptides also did not change the [^{3}H]-cyclic AMP steady-state reached after 10 min of treatment with 10 μM forskolin.

5 Natriuretic peptides failed to elicit significant accumulation of [^{3}H]-inositol phosphates at concentrations up to 10 μM.

6 These data are consistent with the presence of ANP_A, rather than ANP_B or clearance receptors (C-receptors), linked to second messenger cascades in guinea-pig cerebellar slices.

Keywords: ANP_A receptor; cyclic GMP; guinea-pig cerebellum; natriuretic peptides

Introduction

The natriuretic peptide family are considered to play a major role in cardiovascular homoeostasis. However, the role of the natriuretic peptides in the central nervous system is comparatively poorly understood. The presence of natriuretic peptides in the brain has been clearly demonstrated by immunological and molecular biological approaches, e.g. atrial natriuretic peptide (ANP)-like immunoreactivity has been reported in different brain areas (Morii *et al.*, 1985; Quirion *et al.*, 1986; Quirion, 1988) and ANP mRNA transcripts have been detected in the brain (Gardner *et al.*, 1987). ANP can be released, at least in hypothalamic slices, in a Ca^{2+}-dependent manner (Shibasaki *et al.*, 1986). Brain natriuretic peptide (BNP), the second member of the natriuretic peptide family, first isolated from porcine brain (Sudoh *et al.*, 1988), exhibits a high diversity between species in both its amino acid sequence (Ogawa *et al.*, 1990; Suga *et al.*, 1992) and sites of synthesis (Saito *et al.*, 1989; Kojima *et al.*, 1990; Ogawa *et al.*, 1990). C-type natriuretic peptide (CNP), the last member of the natriuretic peptide family discovered (Sudoh *et al.*, 1990), is found almost exclusively in the brain (Ueda *et al.*, 1991) and CNP mRNA also seems to be restricted to brain (Kojima *et al.*, 1990).

Molecular cloning studies have identified three natriuretic peptide receptor subtypes (for reviews see Maack, 1992; Garbers, 1992; Levin, 1993). ANP_A (or GC-A) and ANP_B (GC-B) are monomeric receptors with constitutive guanylyl cyclase activity. At ANP_A receptors, ANP is the most potent for displacing [^{125}I]-ANP binding, followed by BNP, while CNP is very much less potent. In contrast, CNP appears to be a specific ligand for ANP_B receptors (Koller *et al.*, 1991). The third member of the natriuretic peptide family, called the clearance receptor (C-receptor), is dimeric in nature with an unclear physiological role other than the clearance of circulating natriuretic peptides (Levin, 1993). Any signal transduction system associated with this receptor has yet to be clearly demonstrated. [^{125}I]-ANP binding to the C-receptor is most potently inhibited by ANP, while BNP and CNP appear to be equipotent (Maack, 1992). In rat brain, mRNA for both guanylyl cyclase receptors has been detected (Tallerico-Melnyk *et al.*, 1992), although there is evidence for binding of natriuretic peptides to sites resembling ANP_A and C-receptors, but not ANP_B receptors (Brown & Zuo, 1993). However, a high degree of variability exists between species. Thus, neither binding of ANP (Quirion & Dalpé, 1988) nor an increase in guanosine 3':5'-cyclic monophosphate (cyclic GMP) (Takayanagi *et al.*, 1986) could be observed in rat cerebellum, while a high density of binding sites was apparent in guinea-pig cerebellum (Quirion *et al.*, 1986).

It has been proposed that natriuretic peptides can signal through transduction systems other than cyclic GMP generation. Thus, a decrease in adenosine 3':5'-cyclic monophosphate (cyclic AMP) levels has been observed either through an inhibition of adenylyl cyclase activity (Pandey *et al.*, 1985; Resink *et al.*, 1988; Anand-Srivastava *et al.*, 1990; Tseng *et al.*, 1990) or through activation of cyclic GMP-stimulated phosphodiesterases (MacFarland *et al.*, 1991). Activation of phosphoinositide turnover has been reported in vascular smooth muscle cells (Resink *et al.*, 1988; Hirata *et al.*, 1989) and in inner medullary collecting tubule cells (Berl *et al.*, 1991).

The purpose of this study was to use guinea-pig cerebellum, an area which exhibits high density of [^{125}I]-ANP binding sites (Quirion & Dalpé, 1988), to investigate functional receptors to natriuretic peptides using second messenger cascades as an assay for receptor function.

[1] Present Address: Departamento de Biología Molecular, Centro de Biología Molecular 'Severo Ochoa' (CSIC-UAM), Universidad Autónoma de Madrid, E-28049 Madrid, Spain.

[2] Author for correspondence.

Methods

Tissue preparation and cyclic nucleotides accumulation

Preparation and incubation of slices were essentially the same as described previously (Hernández *et al.*, 1993). Briefly, cross-chopped cerebellar slices (350 × 350 μm) were prepared from guinea-pigs (Dunkin-Hartley, either sex, weighing 200–300 g) and incubated in a shaking water bath for 60 min at 37°C in Krebs-bicarbonate medium (mM): NaCl 118, KCl 4.7, $MgSO_4$ 1.2, KH_2PO_4 1.2, glucose 11.7, $NaHCO_3$ 25, $CaCl_2$ 1.2, equilibrated with 95% O_2:5% CO_2 to pH 7.4. The slices were then suspended in fresh Krebs medium and either [^{3}H]-guanine or [^{3}H]-adenine was added to a final concentration of 74 kBq ml^{-1}. After an additional 60 min of incubation, the slices were washed and aliquots (25 μl–ca. 1 mg protein) transferred into flat-bottomed plastic vials containing Krebs buffer to give a final volume of 300 μl. Slices were allowed to equilibrate for 15 min prior to addition of agents in 10 μl; the tubes were resealed under 95% O_2:5% CO_2 after each addition. Unless otherwise stated, peptidase inhibitors were not included in the assays of natriuretic peptide receptor function. Incubations were terminated at the indicated times by addition of 200 μl of HCl (1 M), followed by 750 μl of ice-cold water. [^{3}H]-cyclic GMP and [^{3}H]-cyclic AMP were extracted by the Dowex-alumina method of Salomon *et al.* (1974), monitoring recovery of cyclic nucleotides through the addition of [^{14}C]-cyclic AMP and [^{14}C]-cyclic GMP (ca. 30 Bq/tube) to the samples. Data are expressed as d.p.m. per 25 μl slices.

Inositol phosphates accumulation

Slices were equilibrated with Krebs-bicarbonate buffer for 60 min and distributed as 25 μl aliquots into flat-bottomed vials in the presence of [^{3}H]-inositol (40 kBq ml^{-1}) and LiCl (5 mM) to a final volume of 300 μl, as previously described (Alexander *et al.*, 1989). After 40 min, histamine or natriuretic peptides was added in 10 μl aliquots and the incubation continued for 45 min, before termination with 100 μl of 7.5% perchloric acid. After neutralization, [^{3}H]-inositol phosphates were resolved by chromatography on Dowex-1 (chloride form) columns. Data are expressed as d.p.m. per 25 μl slices.

Chemicals

[8-^{3}H]-guanine (324 GBq mmol^{-1}) was purchased from Rotem Industries Ltd., Beer-Sheva, Israel. [8-^{3}H]-adenine (962 GBq mmol^{-1}) and [adenine-U-^{14}C]-adenosine 3',5'-cyclic phosphate (11.4 GBq mmol^{-1}) were obtained from Amersham International, plc, UK. [8-^{14}C]-guanosine 3':5'-cyclic phosphate (1.9 GBq mmol^{-1}) was from Moravek Biochemicals Inc., California, U.S.A. [^{3}H]-inositol (455.1 GBq mmol^{-1}) was purchased from DuPont NEN, 5'-N-ethylcarboxamidoadenosine (NECA) was from RBI SEMAT, Herts. 3-Isobutyl-1-methylxanthine (IBMX), sodium nitroprusside (SNP), thiorphan, histamine, synthetic rat ANP (A2288), BNP (B9901) and CNP (N8768) were all from Sigma. All other compounds were from standard commercial sources. The natriuretic peptides were dissolved to 300 μM in purified water (Waters Milli-Q system) and stored as aliquots at − 20°C for up to 2 weeks.

Calculations and statistical analysis

In the text, values represent means ± s.e.mean of n experiments conducted in triplicate. The results were analysed by Student's unpaired t test to determine the significant difference between means. The computer programme InPlot (GraphPad, California, U.S.A.) was used to generate EC_{50} values from concentration-response data.

Results

Effects of natriuretic peptides on [^{3}H]-cyclic GMP accumulation

Incubation of [^{3}H]-guanine-prelabelled adult guinea-pig cerebellar slices in the presence of ANP (1 μM) led to an increase in [^{3}H]-cyclic GMP levels. In the absence of IBMX, a significant stimulation of [^{3}H]-cyclic GMP accumulation in response to 1 μM ANP was observed within 2 min, and remained elevated for at least 20 min (Figure 1). In the presence of the phosphodiesterase inhibitor, IBMX (0.5 mM), the response to ANP was much larger and reached an elevated steady-state level within 15 min. Concentration-response curves for natriuretic peptide-stimulated [^{3}H]-cyclic GMP production at 5 min in the presence of 0.5 mM IBMX are shown in Figure 2. ANP and BNP increased [^{3}H]-cyclic GMP production in a concentration-dependent manner with EC_{50} values of 19.5 ± 8.8 nM (n = 5) and 169 ± 41 nM (n = 3), respectively. At 1 μM, [^{3}H]-cyclic GMP levels were 273 ± 15.5 (n = 7, $P<0.01$) and 208 ± 10 (n = 3, $P<0.01$) % over the control levels, respectively. CNP significantly stimulated [^{3}H]-cyclic GMP production only at concentrations greater than 10 μM in the presence of 0.5 mM IBMX (at 10 μM, 80 ± 10% over control, n = 3, $P<0.05$).

Preliminary experiments suggested that the natriuretic peptides were not subject to endopeptidase 24-11-mediated hydrolysis during the incubation period, since thiorphan (10 μM) failed to alter significantly the potency of either ANP or BNP to generate [^{3}H]-cyclic GMP when added 5 min prior to a 5 min incubation with the natriuretic peptides (data not shown).

We have recently described the cyclic GMP response elicited by activation of the soluble guanylyl cyclase activity in guinea-pig cerebellar slices by sodium nitroprusside (Hernández *et al.*, 1994), and so we compared the time course of cyclic GMP responses elicited by soluble and particulate guanylyl cyclases. Although the magnitude of the cyclic GMP response to SNP was greater than the ANP response, the two agents elicited similar time course profiles when assayed in the presence of 0.5 mM IBMX (Figure 3). When responses to ANP (Figure 1) and SNP (Hernández *et al.*, 1994) are compared in the absence of IBMX, however, it is apparent that the response to ANP is smaller, but appears to

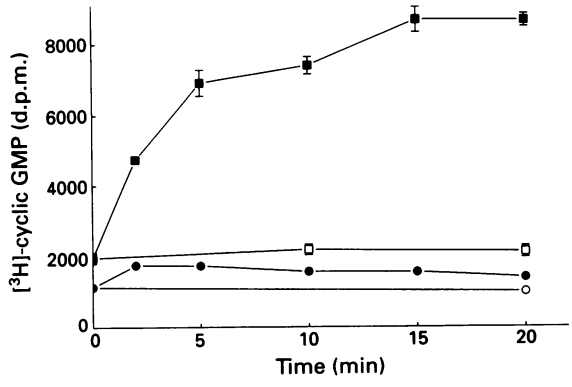

Figure 1 Time course profiles for atrial natriuretic peptide (ANP)-stimulated [^{3}H]-cyclic GMP accumulation in the presence or absence of 3-isobutyl-1-methylxanthine (IBMX), [^{3}H]-guanine prelabelled slices were preincubated in the presence (□, ■) or in the absence (○, ●) of 0.5 mM IBMX for 5 min, prior to addition of 1 μM ANP (filled symbols) or vehicle (open symbols) for varying incubation periods. Data are means ± s.e.mean of triplicate determinations from a single experiment repeated on two additional occasions with essentially identical results. In this and in subsequent figures, where error bars are not shown, they are smaller than the symbol used. Basal [^{3}H]-cyclic GMP accumulation was 1135 ± 41 d.p.m. per 25 μl aliquot.

be better maintained. The response to a combination of 1 μM ANP and 100 μM SNP appeared to be additive when assayed in the presence of 0.5 mM IBMX (Figure 3), implying compartmentalisation of soluble and particulate guanylyl cyclases in the guinea-pig cerebellum.

Adenosine and related analogues acting through A_{2b} adenosine receptors are able to potentiate the cyclic GMP response to SNP in guinea-pig cerebellar slices (Hernández et al., 1993). In the absence of IBMX (since the phosphodiesterase inhibitor is a potent adenosine receptor antagonist, Smellie et al., 1979), NECA elicited an increase in [^{3}H]-cyclic GMP levels (Figure 4), as previously noted (Hernández et al., 1994). However, NECA failed to potentiate the [^{3}H]-cyclic GMP accumulation elicited by ANP (Figure 4).

Effects of natriuretic peptides on cyclic AMP generation

We examined the potential interaction of natriuretic peptides with cyclic AMP generating systems using two approaches. Firstly, we investigated whether simultaneous application of natriuretic peptides with different adenylyl cyclase activators led to a modified cyclic AMP response. ANP, BNP and CNP (all at 1 μM) failed to alter significantly either basal-, forskolin- (10 μM), isoprenaline- (100 μM) or NECA- (10 μM) induced [^{3}H]-cyclic AMP accumulation (data not shown). Secondly, we studied the effects of natriuretic peptides on elevated levels of [^{3}H]-cyclic AMP. Forskolin (10 μM) stimulated an increase in [^{3}H]-cyclic AMP levels with a maximal response at about 10 min, stable for up to 30 min. This maintained response was unchanged by the addition of ANP, BNP, or CNP (all at 1 μM, for example at 10 min, responses were 104 ± 8, 105 ± 5 and 107 ± 7% control, respectively, $n = 3$).

Effects of natriuretic peptides on phosphoinositide turnover

Since ANP has been observed to stimulate phosphoinositide turnover in vascular smooth muscle cells (Resink et al., 1988; Hirata et al., 1989) and in inner medullary collecting tubule cells (Berl et al., 1991), we investigated whether this response might also be elicited in the guinea-pig cerebellum. All three natriuretic peptides, in the presence of 5 mM LiCl, failed to alter significantly basal levels of [^{3}H]-inositol phosphates accumulation over the range of concentrations tested (0.01 nM to 10 μM). For example, at 1 μM the response to ANP, BNP and CNP was 89 ± 19, 82 ± 22, and 122 ± 15% control, respectively ($n = 3$). In contrast, 1 mM histamine elicited a large accumulation of [^{3}H]-inositol phosphates from basal levels of 969 ± 100 d.p.m. to 5678 ± 650 d.p.m. per 25 μl aliquot.

Discussion

Cyclic GMP generation in guinea-pig cerebellum by natriuretic peptides is mediated by ANP_A receptors

In this paper, we present evidence that natriuretic peptides elicit increases in cyclic GMP accumulation in guinea-pig

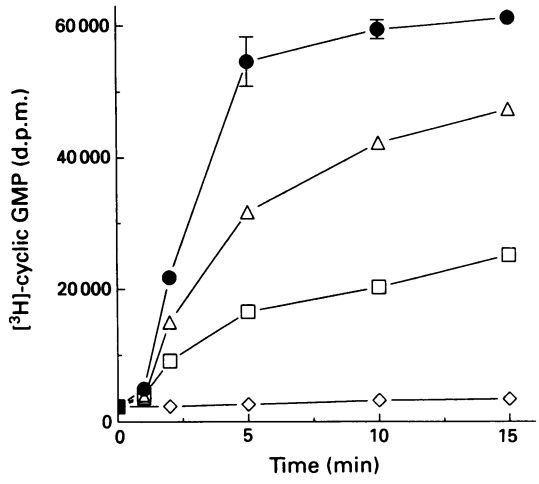

Figure 3 Time course profiles for atrial natriuretic peptide (ANP)- and sodium nitroprusside (SNP)-stimulated [^{3}H]-cyclic GMP accumulation in the presence of 3-isobutyl-1-methylxanthine (IBMX). [^{3}H]-guanine prelabelled slices were preincubated in the presence of 0.5 mM IBMX for 10 min, prior to addition of 1 μM ANP (□), 100 μM SNP (△), 1 μM ANP plus 100 μM SNP (●) or vehicle (◇) for varying incubation periods. Data are means ± s.e.mean of triplicate determinations from a single experiment repeated on two additional occasions with essentially identical results.

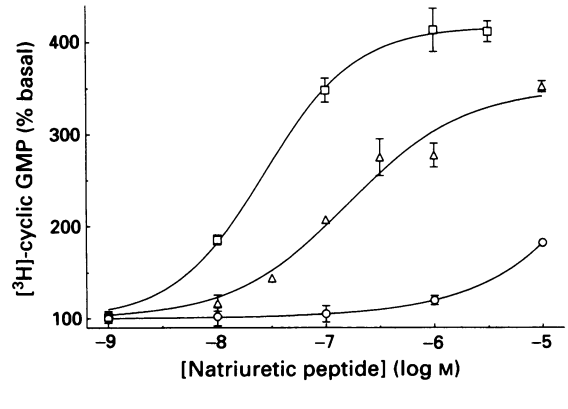

Figure 2 Concentration-response curves for stimulation of [^{3}H]-cyclic GMP induced by atrial natriuretic peptide (□), brain natriuretic peptide (△) or C-type natriuretic peptide (○). [^{3}H]-guanine prelabelled slices were preincubated in the presence of 0.5 mM 3-isobutyl-1-methylxanthine (IBMX), for 5 min, prior to addition of natriuretic peptides. The incubations were continued for an additional 5 min. Basal [^{3}H]-cyclic GMP levels in the absence and presence of 0.5 mM IBMX were 2120 ± 164 and 8137 ± 213 d.p.m., respectively. Data are means ± s.e.mean of triplicate determinations from a single experiment repeated on two additional occasions with essentially identical results.

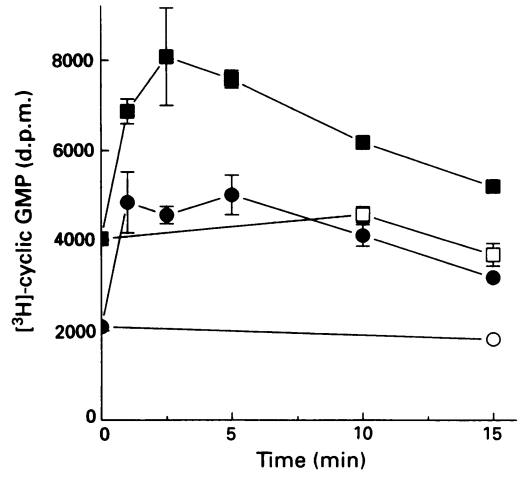

Figure 4 Time course profiles for atrial natriuretic peptide (ANP)-stimulated [^{3}H]-cyclic GMP accumulation in the presence or absence of 5'-N-ethylcarboxamidoadenosine (NECA). [^{3}H]-guanine prelabelled slices were preincubated in the presence (□, ■) or in the absence (○, ●) of 10 μM NECA for 10 min, prior to addition of 1 μM ANP (filled symbols) or vehicle (open symbols) for varying incubation periods. Data are means ± s.e.mean of triplicate determinations from a single experiment repeated on two additional occasions with essentially identical results.

cerebellar slices, without any contemporary change in cyclic AMP accumulation or phosphoinositide turnover. The rank order of agonist potency (ANP >BNP >>CNP) is indicative of the involvement of ANP_A receptors in this response (Schulz *et al.*, 1989). However, the divergence of BNP molecular weight between species, together with the variable affinity of BNP from different species, means that some caution must be exercised when viewing data regarding natriuretic peptide potency (Ogawa *et al.*, 1990; Suga *et al.*, 1992). In an homologous assay system (natriuretic peptides and receptors of the same species), the ratio of EC_{50} values (EC_{50} of rat-ANP/EC_{50} of rat-BNP) for cyclic GMP production through ANP_A receptors in PC12 cells is 0.17 (Suga *et al.*, 1992). In our experimental conditions (a heterologous system comprising synthetic rat natriuretic peptides and guinea-pig receptors), the ratio of EC_{50} values is 0.12. Taking into account the lack of effect of CNP in the present study, therefore, it is likely that ANP increases cyclic GMP through an ANP_A receptor.

Other natriuretic peptide receptors and signal transduction mechanisms

We find no evidence for the suggested routes of coupling of the C-receptor (inhibition of cyclic AMP and stimulation of phosphoinositide turnover – see Introduction), implying either the absence of C-receptors in guinea-pig cerebellum or, more likely, that the C-receptors are not coupled to these signal transduction mechanisms in this tissue. The lack of effect of CNP at concentrations up to 1 μM on cyclic GMP generation suggests that ANP_B receptors do not exist or are not functionally active in guinea-pig cerebellum. Similar results might be expected if the peptides were subject to peptidase activity or removal from the biophase by the C-receptor. The former eventuality appears unlikely since there was no effect of thiorphan (an inhibitor of endopeptidase 24–11, Trapani *et al.*, 1989) on natriuretic peptide-induced cyclic GMP generation. Similarly the latter can be effectively dismissed since the C-receptor exhibits higher affinity for ANP than for CNP (Suga *et al.*, 1992), and thus would be expected to influence the responses to both peptides. ANP_B receptors have been detected in brain microvessel endothelial cells, but not in aortic endothelial cells, which express ANP_A receptors (Vigne & Frelin, 1992). The possible role of CNP (apparently a brain-restricted peptide, Kojima *et al.*, 1990; Komatsu *et al.*, 1991) in the cerebellum and whether CNP interacts with the cerebral microvasculature require further investigation.

Although there is evidence for ANP and/or the C-receptor coupling to phosphoinositide turnover in other systems (see Introduction), we were unable to observe an increase in [^{3}H]-inositol phosphates induced by ANP, BNP or CNP in the guinea-pig cerebellum, although 1 mM histamine generated a substantial increase in phosphoinositide turnover (ca. 6 fold). We were also unable to find evidence for coupling of natriuretic peptide receptors to modulation of cyclic AMP generation in guinea-pig cerebellum. This indicates that ANP- (and SNP-, Hernández *et al.*, 1994) induced cyclic GMP elevations do not activate type II (cyclic GMP-stimulated cyclic AMP) or type III (cyclic GMP-inhibited cyclic AMP) phosphodiesterase activity, and therefore one potential route of ANP modulation of cyclic AMP accumulation in guinea-pig cerebellum can be disregarded (cf. MacFarland *et al.*, 1991).

Cellular localizations of particulate and soluble guanylyl cyclases

The particulate (ANP_A receptor) and soluble (nitric oxide-stimulated) guanylyl cyclase activities are likely to be in distinct cellular populations, since accumulations of [^{3}H]-GMP were additive in the presence of both these agents. The particulate guanylyl cyclase activity and A_{2b} adenosine receptor also appear to be in distinct cellular populations, since NECA failed to enhance ANP-evoked cyclic GMP elevations. In contrast, the NECA-induced elevation of SNP-evoked cyclic GMP accumulation suggests co-localization of these two entities to some extent (Hernández *et al.*, 1993). ANP seems to be generally associated with cerebral structures involved in fluid and cardiovascular control (Quirion *et al.*, 1986; Brown & Czarnecki, 1990), but the physiological relevance of ANP in the cerebellum is less obvious. ANP binding sites are present in guinea-pig cerebellum, but not in the rat (Quirion & Dalpé, 1988) and the potential consequences of this variability are at present unknown, as is the physiological role of natriuretic peptide-induced cyclic GMP generation.

Concluding remarks

In summary, we have observed functional receptors for natriuretic peptides in guinea-pig cerebellum, linked to cyclic GMP formation through ANP_A receptors. No activation through ANP_B receptors could be detected. In addition, we have not been able to furnish evidence for other transduction pathways (cyclic AMP or phosphoinositide systems) for natriuretic peptides in this tissue. Cyclic GMP induced by nitric oxide through activation of soluble guanylyl cyclase has been implicated in the phenomenon of long-term depression in the cerebellum (Shibuki & Okada, 1991) and the question of whether a similar role exists for the particulate guanylyl cyclases requires further investigation.

We are grateful for the financial support of the Medical Research Council and the Wellcome Trust.

References

ALEXANDER, S.P.H., KENDALL, D.A. & HILL, S.J. (1989). Differences in the adenosine receptor modulating inositol phosphates and cyclic AMP accumulation in mammalian cerebral cortex. *Br. J. Pharmacol.*, **98**, 1241–1248.

ANAND-SRIVASTAVA, M.B., SAIRAM, M.R. & CANTIN, M. (1990). Ring-deleted analogs of atrial natriuretic factor inhibit adenylate cyclase/cAMP system. *J. Biol. Chem.*, **265**, 8566–8572.

BERL, T., MANSOUR, J. & TEITELBAUM, I. (1991). ANP stimulates phospholipase C in cultured RIMCT cells: roles of protein kinases and G protein. *Am. J. Physiol.*, **260**, F590–F595.

BROWN, J. & CZARNECKI, A. (1990). Autoradiographic localisation of atrial and brain natriuretic peptide receptors in rat brain. *Am. J. Physiol.*, **258**, R57–R63.

BROWN, J. & ZUO, Z. (1993). C-type natriuretic peptide and atrial natriuretic peptide receptors of the rat brain. *Am. J. Physiol.*, **264**, R513–R523.

GARBERS, D.L. (1992). Guanylyl cyclase receptors and their endocrine, paracrine, and autocrine ligands. *Cell*, **71**, 1–4.

GARDNER, D.G., VLASUK, G.P., BAXTER, J.D., FIDDES, J.C. & LEWICKI, J.A. (1987). Identification of atrial natriuretic factor gene transcripts in the central nervous system of the rat. *Proc. Natl. Acad. Sci. U.S.A.*, **84**, 2175–2179.

HERNÁNDEZ, F., ALEXANDER, S.P.H. & KENDALL, D.A. (1994). Forskolin potentiates the effects of sodium nitroprusside on cyclic GMP levels in adult guinea-pig cerebellar slices. *J. Neurochem.*, **62**, 2212–2218.

HERNÁNDEZ, F., KENDALL, D.A. & ALEXANDER, S.P.H. (1993). Adenosine receptor-induced second messenger production in adult guinea-pig cerebellum. *Br. J. Pharmacol.*, **110**, 1085–1090.

HIRATA, M., CHANG, C.-H. & MURAD, F. (1989). Stimulatory effects of atrial natriuretic factor on phosphoinositide hydrolysis in cultured aortic smooth muscle cells. *Biochim. Biophys. Acta*, **1010**, 346–351.

KOJIMA, M., MINAMINO, N., KANGAWA, K. & MATSUO, H. (1990). Cloning and sequence analysis of a cDNA encoding a precursor for rat C-type natriuretic peptide (CNP). *FEBS Lett.*, **276**, 209–213.

KOLLER, K.J., LOWE, D.G., BENNET, G.L., MINAMINO, N., KANGAWA, K., MATSUO, H. & GOEDDEL, D.V. (1991). Selective activation of the B natriuretic peptide receptor by C-type natriuretic peptide (CNP). *Science*, **252**, 120–123.

KOMATSU, T., NAKAO, K., SUGA, S., OGAWA, Y., MUKOYAMA, M., ARAI, H., SHIRAKAMI, G., HOSODA, K., NAKAGAWA, O., HAMA, N., KISHIMOTO, I. & IMURA, H. (1991). C-type natriuretic peptide (CNP) in rats and humans. *Endocrinology*, **129**, 1104–1106.

LEVIN, E.R. (1993). Natriuretic peptide C-receptor: more than a clearance receptor. *Am. J. Physiol.*, **264**, E483–E489.

MAACK, T. (1992). Receptors of atrial natriuretic factor. *Annu. Rev. Physiol.*, **54**, 11–27.

MACFARLAND, R.T., ZELUS, B.D. & BEAVO, J.A. (1991). High concentrations of a cGMP-stimulated phosphodiesterase mediate ANP-induced decreases in cAMP and steroidogenesis in adrenal glomerulosa cells. *J. Biol. Chem.*, **266**, 136–142.

MORII, N., NAKAO, K., SUGAWARA, A., SAKAMOTO, M., SUDA, M., SHIMOKURA, M., KISO, Y., KIHARA, M, YAMORI, Y. & IMURA, H. (1985). Occurrence of atrial natriuretic polypeptide in brain. *Biochem. Biophys. Res. Commun.*, **127**, 413–419.

OGAWA, Y., NAKAO, K., MUKOYAMA, M., SHIRAKAMI, G., ITOH, H., HOSODA, K., YOSHIHIKO, S., ARAI, H,. SUGA, S.-I., JOUGASAKI, M., YAMADA, T., KAMBAYASHI, Y., INOUYE, K. & IMURA, H. (1990). Rat brain natriuretic peptide, tissue distribution and molecular form. *Endocrinology*, **126**, 2225–2227.

PANDEY, K.N., KOVACS, W.J. & INAGAMI, T. (1985). The inhibition of progesterone secretion and the regulation of cyclic nucleotides by atrial natriuretic factor in gonadotropin responsive murine Leydig tumor cells. *Biochem. Biophys. Res. Commun.*, **133**, 800–806.

QUIRION, R. (1988). Atrial natriuretic factor and the brain: an update. *Trends Neurosci.*, **11**, 58–62.

QUIRION, R. & DALPÉ, M. (1988). Characterization, distribution, and plasticity of atrial natriuretic factor binding sites in brain. *Can. J. Physiol. Pharmacol.*, **66**, 280–287.

QUIRION, R., DALPÉ, M., DAM, T.V. & DAM, T.V. (1986). Characterization and distribution of receptors for the atrial natriuretic peptides in mammalian brain. *Proc. Natl. Acad. Sci. U.S.A.*, **83**, 174–178.

RESINK, T.J., SCOTT-BURDEN, T., BAUR, U., JONES, C.R. & BÏHLER, F.R. (1988). Atrial natriuretic peptides induce breakdown of phosphatidylinositol phosphates in cultured vascular smooth-muscle cells. *Eur. J. Biochem.*, **172**, 499–505.

SAITO, Y., NAKAO, K., ITOH, H., YAMADA, T., MUKOYAMA, M., ARAI, H., HOSODA, K., SHIRAKAMI, G., SUGA, S.-I., MINAMINO, N., KANGAWA, K., MATSUO, H. & IMURA, H. (1989). Brain natriuretic peptide is a novel cardiac hormone. *Biochem. Biophys. Res. Commun.*, **158**, 360–368.

SALOMON, Y., LONDOS, C. & RODBELL, M. (1974). A highly sensitive adenylate cyclase assay. *Anal Biochem.*, **58**, 541–548.

SCHULZ, S., SINGH, S., BELLET, R.A., SINGH, G., TUBB, D.J, CHIN, H. & GARBERS, D.L. (1989). The primary structure of a plasma membrane guanylate cyclase demonstrates diversity within this new receptor family. *Cell*, **58**, 1155–1162.

SHIBASAKI, T., NARUSE, M., NARUSE, K., MASUDA, A., KIM, Y.S., IMAKI, T., YAMAUCHI, N., DEMURA, H., INAGAMI, T. & SHIZUME, K. (1986). Atrial natriuretic is released from rat hypothalamus in vitro. *Biochem. Biophys. Res. Commun.*, **136**, 590–595.

SHIBUKI, K. & OKADA, D. (1991). Endogenous nitric oxide release required for long-term synaptic depression in the cerebellum. *Nature*, **349**, 326–328.

SMELLIE, F.W., DAVIS, C.W., DALY, J.W. & WELLS, J.N. (1979). Alkylxanthines: inhibition of adenosine-elicited accumulation of cyclic AMP in brain slices and of brain phosphodiesterase activity. *Life Sci.*, **24**, 2475–2482.

SUDOH, T., KANGAWA, K., MINAMINO, N. & MATSUO, H. (1988). A new natriuretic peptide in porcine brain. *Nature*, **332**, 78–81.

SUDOH, T., MINAMINO, N, KANGAWA, K. & MATSUO, H. (1990). C-type natriuretic peptide (CNP): a new member of natriuretic peptide family identified in porcine brain. *Biochem. Biophys. Res. Commun.*, **168**, 863–870.

SUGA, S.-I., NAKAO, K., HOSODA, K., MUKOYAMA, M., OGAWA, Y., SHIRAKAMI, G., ARAI, H., SAITO, Y., KAMBAYASHI, Y., INOUYE, K. & IMURA, H. (1992). Receptor selectivity of natriuretic peptide family, atrial natriuretic peptide, brain natriuretic peptide, and C-type natriuretic peptide. *Endocrinol.*, **130**, 229–239.

TAKAYANAGI, R., GRAMMER, R.T. & INAGMI, T. (1986). Regional increase of cyclic GMP by atrial natriuretic factor in rat brain: markedly elevated response in spontaneously hypertensive rats. *Life Sci.*, **39**, 573–580.

TALLERICO-MELNYK, T., YIP, C.C. & WATT, V.M. (1992). Widespread co-localization of mRNAS encoding the guanylate cyclase-coupled natriuretic peptide receptors in rat tissues. *Biochem. Biophys. Res. Commun.*, **189**, 610–616.

TRAPANI, A.J., SMITS, G.J., MACGRAW, D.E., SPEAR, K.L., KOEPKE, J.P., OLINS, G.M. & BLAINE, E.H. (1989). Thiorphan, an inhibitor of endopeptidase 24.11, potentiates the natriuretic activity of atrial natriuretic peptide. *J. Cardiovasc. Pharmacol.*, **14**, 419–424.

TSENG, Y.-C.L., LAHIRI, S., SELLITI, D.F., BURMAN, K.D., D'AVIS, J.C. & WARTOFSKY, L. (1990). Characterization by affinity cross-linking of a receptor for atrial natriuretic peptide in cultured human thyroid cells associated with reductions in both adenosine 3′,5′-monophosphate production and thyroglobulin secretion. *J. Clin. Endocrinol. Metab.*, **70**, 528–533.

UEDA, S., MINAMINO, N., ABURAYA, M., KANGAWA, K., MATSUKURA, S. & MATSUO, H. (1991). Distribution and characterisation of immunoreactive porcine C-type natriuretic peptide. *Biochem. Biophys. Res. Commun.*, **175**, 759–767.

VIGNE, P. & FRELIN, C. (1992). C-type natriuretic peptide is a potent activator of guanylate cyclase in endothelial cells from brain microvessels. *Biochem. Biophys. Res. Commun.*, **183**, 640–644.

(Received February 3, 1994
Revised May 9, 1994
Accepted May 16, 1994)

Br. J. Pharmacol. (1994), **113**, 221–227

The electrophysiological effects of antiarrhythmic potential of a secoaporphine, N-allylsecoboldine

Mei-Hwan Wu, Ming-Jai Su, Shoei-Sheng Lee & Ming-Long Young

Department of Pediatrics and Pharmacy, and Institute of Pharmacology, National Taiwan University, Taipei, Taiwan

1 A satisfactory antiarrhythmic potential of N-allylsecoboldine, a synthetic derivative of secoaporphine, has been documented. Its effects on the ionic currents of cardiac myocytes and the influence on the electrophysiological properties of the conduction system in Langendorff perfused hearts were investigated.

2 Ionic currents were studied by voltage clamp in the whole cell configuration. N-allylsecoboldine blocked the Na channel with a leftward-shift of its half voltage-dependent inactivation and a slower rate of recovery from the inactivation state. Similarly, calcium inward currents were inhibited but to a much smaller extent.

3 N-allylsecoboldine inhibited the 4-AP-sensitive transient outward K current. Currents through the K_1 channels were also reduced.

4 As compared with quinidine, N-allylsecoboldine caused a comparable degree of block on Na and K_1 currents but blocked to a lesser extent the Ca and I_{to} currents.

5 In the perfused whole-heart model, N-allylsecoboldine caused a dose-dependent prolongation in sinoatrial, atrioventricular and His-Purkinje system conduction intervals and prolonged the effective refractory periods of the atrium, AV node, His-Purkinje system and ventricle. However, the basic cycle length was not significantly affected. As compared to quinidine, N-allylsecoboldine exerted less pronounced effects on both the basic cycle length and the atrial and AV nodal refractory periods.

6 We conclude that N-allylsecoboldine predominantly blocks Na and K_1 channels and in similar concentrations partly blocks Ca channels and I_{to}. These effects result in a modification of the electrophysiological properties of the conduction system which provides a satisfactory therapeutic potential for the treatment of cardiac arrhythmias.

Keywords: N-allylsecoboldine; Na^+, K^+ and Ca^{2+} currents; cardiac arrhythmia; cardiac myocytes; quinidine

Introduction

The natural aporphine alkaloids, such as dicentrine, have recently been shown to possess potent α_1-adrenoceptor blocking and antiarrhythmic activities (Teng *et al.*, 1991). N-allylsecoboldine (Figure 1), mol.wt. 353 g, is a secoaporphine prepared from the aporphine, boldine. This compound was therefore studied for antiarrhythmic and electrophysiological effects in our laboratory. The current study was conducted to define its effects on ionic currents of cardiac myocytes and the effects on the conduction system of Langendorff isolated perfused hearts. The antiarrhythmic efficacy was assessed against reperfusion-induced arrhythmias. We concluded that N-allylsecoboldine is a useful class Ia and III antiarrhythmic agent with a satisfactory antiarrhythmic potential.

Methods

Voltage clamp experiments on isolated myocytes

Adult (>3 months) New Zealand white rabbits were anaesthetized with intravenous injection of sodium pentobarbitone (30 mg kg^{-1}. i.v.) and given heparin (300 units kg^{-1}).

Isolation of myocytes Cardiac myocytes were isolated as previously described (Mitra & Morad, 1985). In brief, hearts were quickly removed and retrogradely perfused in a Langendorff apparatus with prewarmed (37°C) calcium-free Tyrode solution, followed by enzymatic digestion. The calcium paradox was prevented by perfusion with Kraftbruhe (KB) medium for 5 min after the enzymatic digestion (Isenberg & Klockner, 1981). Isolated ventricular myocytes were incubated in KB medium at room temperature (25–27°C) before the start of electrophysiological studies.

Electrophysiological study All the experiments were performed at room temperature (25–27°C). Ionic currents were studied using a whole-cell voltage-clamp method (Hamill *et al.*, 1981). A Dagon 8900 patch/whole cell clamp fitted with 100 MΩ feedback resistor in the headstage was used to clamp the myoctyes. The total series resistance for the pathway between the pipette interior and the cell membrane was estimated from the cell capacitance and capacitance current decay. It was possible to compensate electronically for 60–80% of the voltage drop across the electrode produced

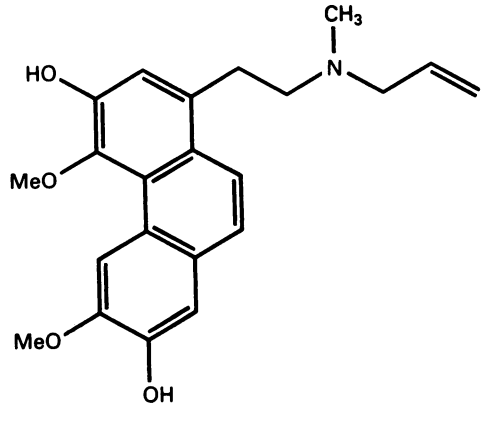

Figure 1 Chemical structure of N-allylsecoboldine.

[1] Author for correspondence at: Department of Pediatrics, National Taiwan University Hospital, No. 7 Chung-Shen South Road, Taipei, Taiwan, 100.

by the current flow. Experiments on I_{Na} were performed in a low Na^+ Tyrode solution ($[Na^+] = 54$ mM, with NaCl replaced by choline chloride). The I_{Na} elicited was lower than 5 nA, and the estimated voltage error attributed to uncompensated series resistance would be lower than 5 mV. Cells were exposed to each concentration of test drug for 7 min.

Intracardiac electrocardiogram recording experiment

Animal preparation The heart including part of the superior and inferior vena cava and the ascending aorta was quickly excised via thoracotomy. The aorta was retrogradely perfused at a rate of 4 ml min^{-1} g^{-1} cardiac tissue with Tyrode solution (continuously gassed with 95% O_2 and 5% CO_2 to give a pH of 7.4 and warmed to 37°C). The experimental protocol was not started until at least 45 min after isolation. The endocardial surface of the right atrium was exposed via a small incision along the anterolateral atrioventricular groove. Tungsten wires (3 mm in length and 0.05 mm in diameter) were soldered onto the tip of silver-wire bipolar electrodes to increase the flexibility. His bundle electrograms (HBE) were recorded from an area near the apex of the triangle of Koch. The ventricular recording electrodes were placed on the epicardium of the right ventricular apex to obtain an easily recognizable T wave.

A pacing stimulus of 1 ms in duration and three times the diastolic threshold voltage was applied to the preparation (a twisted pair of insulated silver wires with a wire diameter of 125 μm). The high right atrial pacing electrode was placed on the epicardium near the junction of the superior vena cava and right atrium. The ventricular pacing electrode was placed on the pericardium near the right ventricular apex.

Experimental protocol Electrophysiological studies were performed according to standard methods (Josephson & Seides, 1979). The average of 4 stable cycle lengths of spontaneous heart beats was taken as the parameter of the pacemaker automaticity, which could be a sinus or an atrial pacemaker. The corrected QT interval was a parameter of ventricular repolarization which was measured from the beginning of the ventricular depolarization wave to the end of the T wave and corrected by the square root of basic cycle length.

The right atrium was then paced at a constant rate that was slightly faster than the spontaneous heart rate. At this constant rate pacing, the following parameters were measured pre-, during and post-drug perfusion.

Intra-atrial conduction time (SA) was measured from the beginning of the stimulation artifact to the first rapid atrial depolarization wave recorded in the HBE. AV nodal conduction time was measured from the largest and rapid deflection of the atrial depolarization wave recorded in the HBE to the beginning of the His bundle depolarization wave recorded in the HBE. His-Purkinje conduction time was measured from the beginning of the His bundle depolarization wave to the beginning of the ventricular depolarization wave recorded in the HBE.

The atrial pacing cycle length was then decreased (every 5–10 s) in steps of 10–20 ms, until a stable 1:1 AV nodal conduction pattern was lost. The longest pacing cycle length at which a 1:1 AV conduction could not be maintained was defined as the Wenckebach cycle length.

An atrial premature extra-stimulus (S_2) was then delivered to the HRA after a train of constant rate atrial pacing (S_1S_1) for 8 beats. This atrial extra-stimulation (S_1S_2) interval was decreased in 10 ms-steps until the atrial refractory period was reached. The following data were obtained:

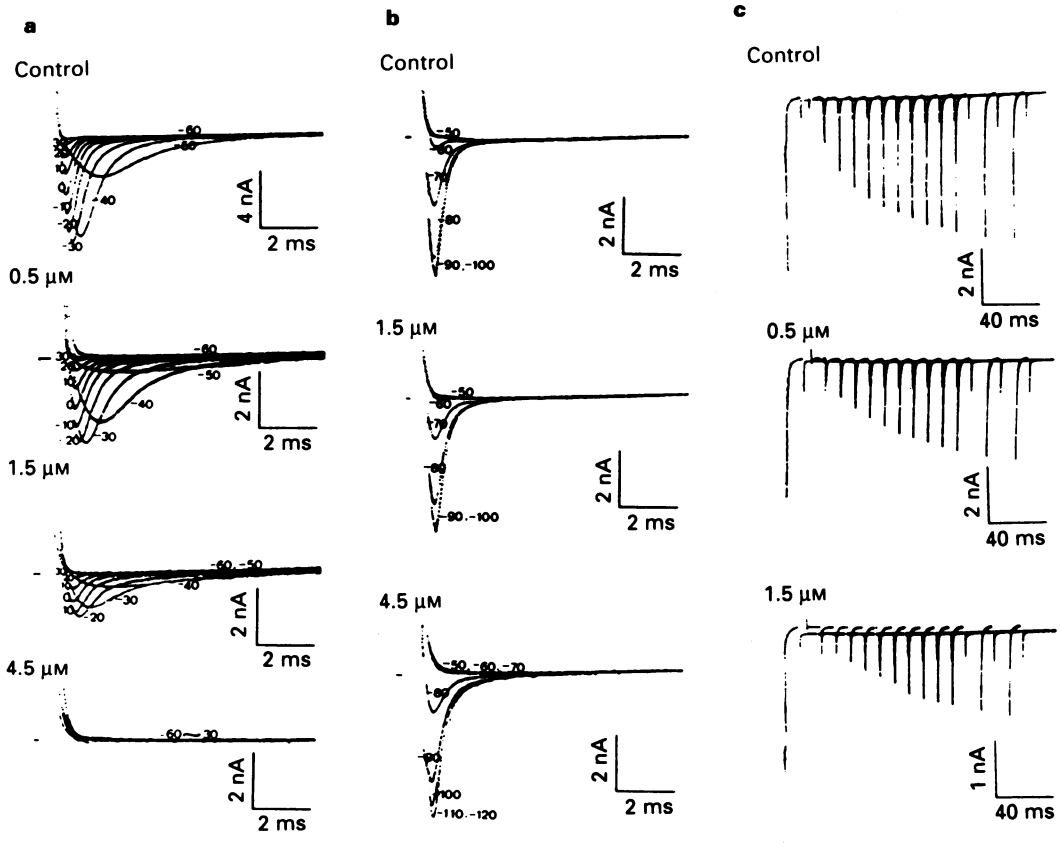

Figure 2 Changes in Na currents after N-allylsecoboldine. (a) Na currents were elicited from a holding potential of − 80 mV to − 60 mV to 30 mV in 10 mV steps. (b) Steady-state voltage-dependent inactivation of I_{Na} was studied by altering the holding potentials (− 100 mV to − 50 mV, in 10 mV steps) for 1 s and then a depolarizing pulse to − 20 mV. (c) Recovery of Na channels from their inactivation state. Na currents were elicited by twin-pulse depolarization protocol. Cells were first depolarized to − 20 mV for 10 ms from a holding potential of − 80 mV. The kinetics of recovery were then defined by a second depolarization given at various time intervals after the first pulse. Ratios of the currents elicited by the second and first pulses reflected the fractions of Na channels already recovered from inactivation.

Atrial effective refractory period (AERP) was the longest S_1S_2 interval that did not evoke an atrial depolarization wave (A_2). AV nodal effective refractory period (AVERP) was the longest S_1S_2 interval in which the evoked A_2 failed to evoke a His bundle depolarization wave (H_2). The longest H_1H_2 interval that failed to evoke a premature ventricular depolarization was defined as the His Purkinje effective refractory period (HPERP).

The ventricular extrastimulation study protocol was similar to the atrial extrastimulation study. The ventricular effective period (VERP) was defined as the longest S_1S_2 interval that failed to evoke a premature ventricular depolarization.

Ischaemia-reperfusion-induced arrhythmias

The Langendorff-perfused heart model with constant perfusion pressure instead of constant flow was used (Curtis & Hearse, 1989).

The electrograms were recorded from a low atrial and a ventricular recording electrode. The left coronary artery (left anterior descending artery) was ligated for 30 min before the release of the ligature. The establishment of ischaemia and reperfusion were ascertained by the amount of coronary effluent. The antiarrhythmic effect of the compound was tested after arrhythmias had been induced by reperfusion.

Drugs

N-allylsecoboldine was prepared from boldine by exhaustive N-alkylation (Lee *et al.*, 1992). The purity is about 99% as analysed by ^{1}H-n.m.r. and h.p.l.c. The compound (stored at − 20°C) was dissolved in dimethysulphoxide as a 50 mM stock solution from which the test solutions in concentrations of 0.5, 1.5 and 4.5 μM were prepared. Quinidine was purchased from Sigma.

Solutions

Three basic solutions were used with the following compositions in mM: (1) Ca^{2+}-Tyrode: NaCl 137, KCl 5.4, $MgCl_2$ 1.1,

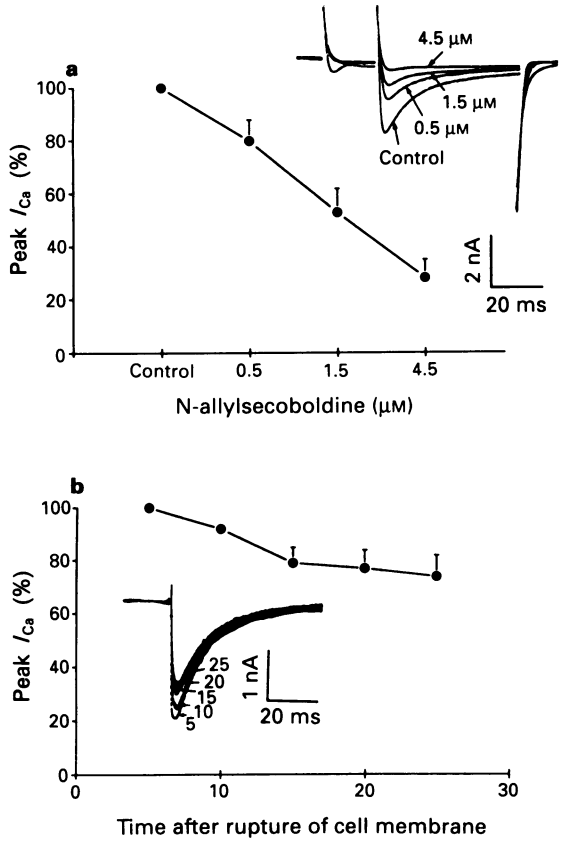

Figure 3 (a) A conditioning pulse to − 40 mV was applied to inactivate the Na channel and 'T' type Ca channels. Depolarizing pulses of 80 ms duration to 0 mV were then applied to elicit the peak Ca currents. (b) Spontaneous 'rundown' of Ca currents during the experiments. This curve was obtained from 8 cells.

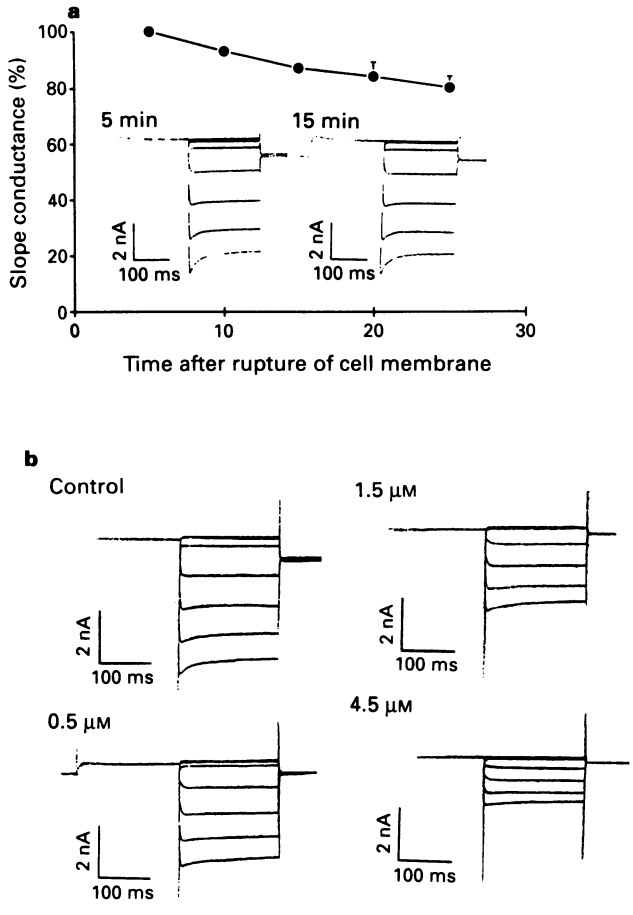

Figure 4 (a) Spontaneous 'rundown' phenomenon of I_{K1} with time. Inserts are current traces recorded 5 and 15 min after rupture of the cell membrane. From a holding potential of − 80 mV, currents were serially elicited (− 30 to − 150 mV in 20 mV steps) after a prepulse of − 20 mV for 200 ms. (b) N-allylsecoboldine suppressed the currents through K_1 channels. The voltage clamp protocol was the same as in (a).

Table 1 Changes of Na channel kinetics after N-allylsecoboldine and quinidine

	N-allylsecoboldine (μM)				*Quinidine* (μM)				P
	Control	0.5	1.5	4.5	Control	0.5	1.5	4.5	
Peak I_{Na} (%)	100 ± 0 (n = 8)	86 ± 8	42 ± 11	4 ± 2	100 ± 0 (n = 8)	83 ± 8	47 ± 17	8 ± 5	0.82
V_{mid} (− mV)	76 ± 3 (n = 6)	79 ± 4	87 ± 4	98 ± 4	81 ± 2 (n = 8)	90 ± 5	92 ± 5	103 ± 6	0.25
τ (ms)	67 ± 1 (n = 4)	88 ± 3	122 ± 4	-	64 ± 4 (n = 6)	94 ± 13	127 ± 10	-	0.86

$CaCl_2$ 1.8, HEPES 12, titrated with NaOH to pH 7.4; (2) Internal solution for filling the suction pipettes: KCl 120, NaCl 10, MgATP 5, K_2EGTA 11, $CaCl_2$ 1, HEPES 10, titrated with KOH to pH 7.4. Internal solution containing 120 mM Cs^+ instead of K^+ was used for I_{Na} and I_{Ca} studies. (3) KB medium: taurine 10, glutamic acid 70, KCl 25, KH_2PO_4 10, dextrose 22, EGTA 0.5, titrated with KOH to pH 7.3.

Statistics

The data were expressed as mean ± s.e. for each parameter. A repeated-measures analysis of variance was used for data comparison of different drugs and doses.

Results

Ionic current modification by N-allylsecoboldine

Na currents N-allylsecoboldine blocked the Na channel by causing a leftward shift of the voltage-dependent steady-state inactivation curves as well as a slower rate of recovery from inactivation (Figure 2). Dose-dependent changes in the Na channel properties are summarized in Table 1. Peak Na currents which were elicited from a holding potential of − 80 mV to − 40 mV decreased after N-allylsecoboldine, and the changes were comparable to those seen after quinidine. The V_{mid} (the membrane potential at which half of the Na channels were inactivated) was obtained by fitting the normalized inactivation curves to the Boltzmann equation (Hille, 1984). The recovery of Na channels from their inactivation state was studied using twin-pulse depolarization by step-increase of the interval duration between pulses. The time constant (τ) was obtained after fitting the recovered fraction of I_{Na} with time to a single exponential function. The magnitude of changes in V_{mid} and τ after N-allylsecoboldine was similar to that observed after quinidine (Table 1).

Ca currents L-type Ca currents were elicited after application of a prepulse to − 40 mV to inactivate the Na and 'T' type Ca channels. A noticeable reduction of Ca currents due to the 'rundown' phenomenon with time was observed in the absence of drugs (Figure 3b). This rundown phenomenon was more prominent during the initial 5–15 min access of the patch pipette to the interior of the cells. After this equilibration period, a slower rundown was observed. Therefore, experiments were performed only on those cells with stable Ca currents 15 min after cell rupture. A dose-dependent decrease in the Ca currents was observed after N-allylsecoboldine (Figure 3a). Peak Ca currents elicited at the potential of 10 mV decreased to 80 ± 8, 53 ± 9 and 28 ± 7% after 0.5, 1.5 and 4.5 μM N-allylsecoboldine ($n = 6$), and to 49 ± 8, 31 ± 10 and 7 ± 5% respectively ($n = 6$) after quinidine ($P = 0.04$, N-allylsecoboldine vs quinidine). Hence, N-allylsecoboldine suppressed the Ca currents to a much smaller extent than quinidine.

K currents Three voltage-dependent K currents (inwardly rectifying (I_{K1}), transient outward (I_{to}) and delayed outward

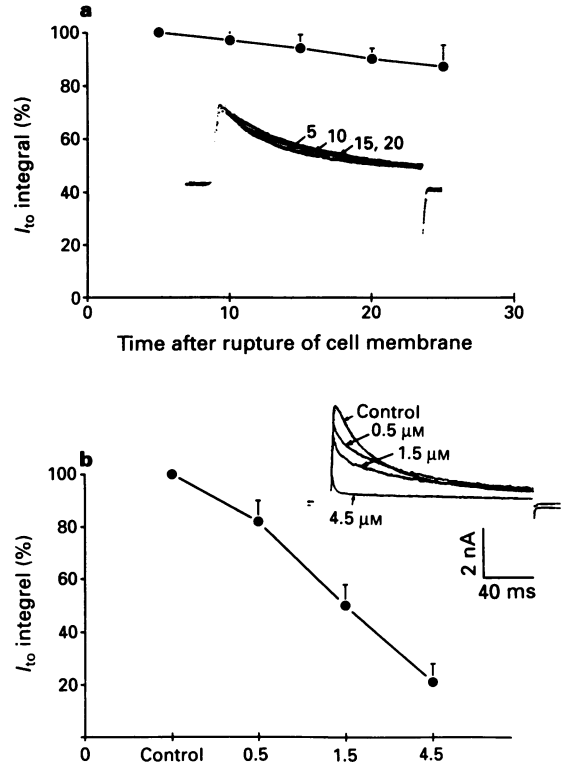

Figure 5 (a) Spontaneous 'rundown' phenomenon of I_{to} with time. Insert: current traces recorded at 5, 10, 15 and 20 min after rupture of cell membrane. Currents were elicited by a depolarizing step to 60 mV from a holding potential of − 80 mV. (b) N-allylsecoboldine reduced the I_{to} current peaks and accelerated its inactivation. The voltage-clamp protocol was the same as in (a).

Table 2 Comparative dose-related effects of quinidine and N-allylsecoboldine on the conduction system of rabbit isolated perfused hearts

	Quinidine (μM)					*N-allylsecoboldine* (μM)					P
	Control	0.5	1.5	4.5	Wash	Control	0.5	1.5	4.5	Wash	
BCL	100 ± 0 *(8)	107 ± 2	114 ± 4	118 ± 6	105 ± 7	100 ± 0 (8)	99 ± 3	104 ± 3	108 ± 3	106 ± 4	0.05
SA	100 ± 0	107 ± 7	105 ± 7	117 ± 6	106 ± 6	100 ± 0	106 ± 3	113 ± 7	132 ± 9	108 ± 5	0.85
AH	100 ± 0	103 ± 2	114 ± 5	132 ± 5	107 ± 4	100 ± 0	106 ± 2	118 ± 4	129 ± 4	108 ± 2	0.73
HV	100 ± 0	105 ± 2	118 ± 3	135 ± 5	110 ± 7	100 ± 0	102 ± 3	112 ± 4	121 ± 7	105 ± 8	0.59
QTc	100 ± 0	106 ± 4	116 ± 5	126 ± 5	100 ± 2	100 ± 0	107 ± 3	113 ± 3	123 ± 3	87 ± 11	0.72
WCL	100 ± 0	102 ± 1	116 ± 5	135 ± 5	98 ± 3	100 ± 0	100 ± 3	110 ± 4	127 ± 9	96 ± 4	0.33
AERP	100 ± 0	119 ± 6	130 ± 7	156 ± 8	103 ± 5	100 ± 0	104 ± 5	117 ± 5	134 ± 5	104 ± 7	0.03
HPERP	100 ± 0 (7)	111 ± 2	126 ± 4	148 ± 4	107 ± 2	100 ± 0 (7)	106 ± 1	120 ± 5	140 ± 7	105 ± 4	0.34
AVERP	100 ± 0 (7)	125 ± 6	156 ± 13	209 ± 16	95 ± 5	100 ± 0 (6)	108 ± 5	123 ± 3	138 ± 9	104 ± 4	0.01
VERP	100 ± 0	113 ± 3	123 ± 4	141 ± 6	101 ± 3	100 ± 0	105 ± 2	114 ± 3	124 ± 10	98 ± 3	0.12

Data were obtained from 10 experiments and were expressed as a percentage of the control values (mean ± s.e.). Numbers in the parentheses indicate the numbers of experimental measurements for the parameters (BCL, HPERP and AVERP) which sometimes were limited by the physiological properties. Abbreviations: BCL: basic cycle length; SA: sinoatrial conduction interval; AH: atrio-His bundle conduction interval; HV: His-ventricular conduction interval; QTc: corrected QT interval; WCL: Wenckebach cycle length; AERP: atrial effective refractory period; HPERP: His-Purkinje system effective refractory period; AVERP: AV nodal effective refractory period; VERP: ventricular effective refractory period.

K currents) were studied. Of these, the delayed outward K current was found to be very small in both atrial and ventricular cells, as reported by Giles & Imaizumi (1988), and has been considered to play only a minor role in the regulation of the action potential of rabbit myocytes. Thus, only the I_{K1} and I_{to} were studied further.

Currents through the I_{K1} were elicited by serial hyperpolarization after a prepulse to − 20 mV. These currents became smaller after N-allylsecoboldine (Figure 4b). The slope conductance measured between the membrane potential − 70 to − 110 mV was suppressed to 82 ± 7, 57 ± 10 and 28 ± 9% after 0.5, 1.5 and 4.5 μM of N-allylsecoboldine and 84 ± 5, 67 ± 5 and 46 ± 3% respectively after quinidine ($P = 0.34$, N-allylsecoboldine vs quinidine).

I_{to} was studied in the presence of 0.5 mM cobalt. Serial depolarization to 60 mV from a holding potential of − 80 mV at a slow stimulation frequency of 0.1 Hz was used to avoid incomplete recovery of these currents from their inactivation state. N-allylsecoboldine decreased the current peak and accelerated the inactivation of I_{to} (Figure 5). The area under the current curve elicited at 60 mV was calculated to estimate the total charge through the I_{to} channels after a baseline was obtained by rapid depolarization to fully inactivate I_{to}. The integral of the curves decreased to 76 ± 8, 41 ± 11 and 21 ± 8% ($n = 8$) after 0.5, 1.5 and 4.5 μM N-allylsecoboldine, and the corresponding values after quinidine were 42 ± 13, 24 ± 9 and 4 ± 2% ($n = 6$) respectively ($P = 0.03$).

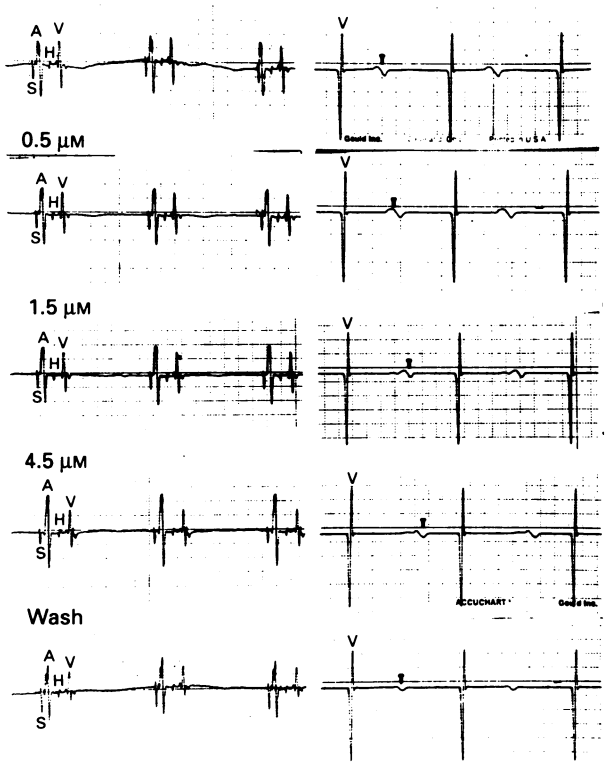

Figure 6 Representative His bundle electrograms (left panel) and ventricular electrograms after N-allylsecoboldine. A: atrial depolarization; H: His bundle depolarization; S: stimulation artifact; V: ventricular depolarization. The paper speed was 100 mm s^{-1}.

Modification of the electrophysiological properties of the conduction system

Changes in the electrophysiological properties of the cardiac conduction system after N-allylsecoboldine are summarized in Table 2. N-allylsecoboldine caused a dose-dependent prolongation in the sinoatrial, atrioventricular and His-Purkinje system conduction intervals (Figure 6) as well as prolonging the effective refractory periods of the atrium, AV node, His-Purkinje system and ventricle (Table 2). However, the basic cycle length was not significantly affected. As compared with quinidine, N-allylsecoboldine caused less significant effects on the basic cycle length, and effective refractory periods of the atrium and AV node.

Antiarrhythmic efficacy on reperfusion arrhythmias

At a concentration of 1.5 to 4.5 μM, N-allylsecoboldine was able to convert a polymorphic ventricular tachycardia induced by the ischaemia-reperfusion experiment model (Figure 7). Out of ten episodes of ventricular tachycardia induced by ischaemia-reperfusion N-allylsecoboldine at 1.5 μM converted the tachyrhythmias to normal sinus rhythm

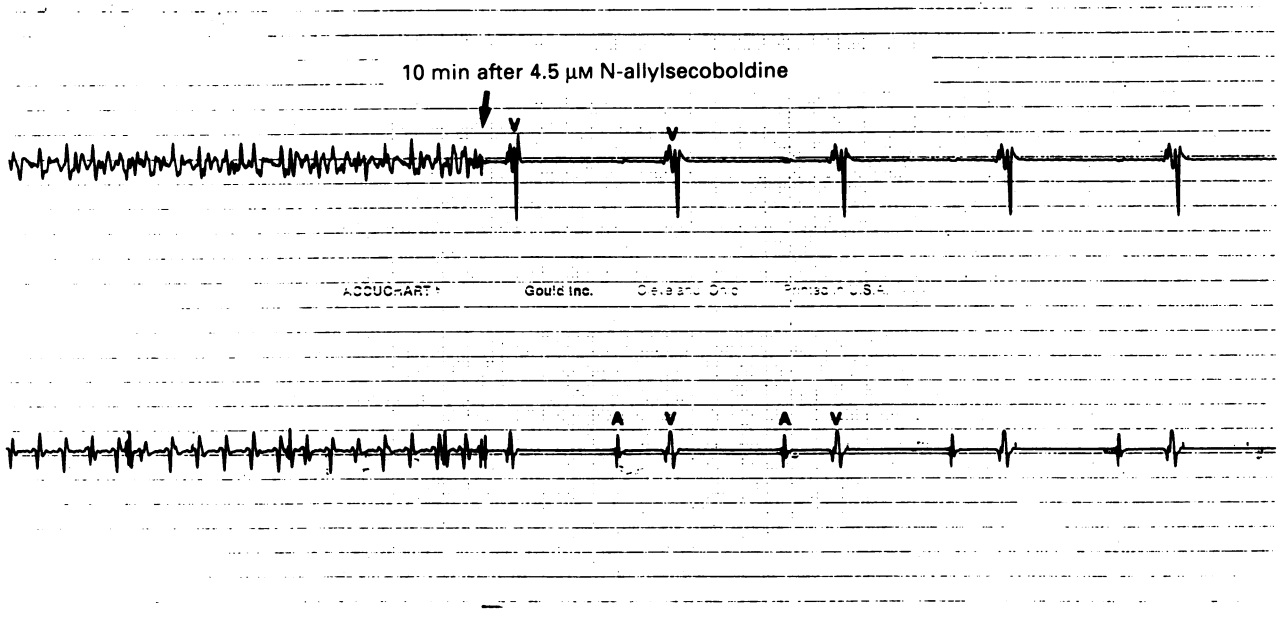

Figure 7 A polymorphic ventricular tachycardia induced by ischaemia-reperfusion was converted to normal sinus rhythm 10 min after N-allylsecoboldine. Upper panel shows the ventricular electrograms. The electrogram in the lower panel was recorded from the lower right atrium. Simultaneous recording of atrial (A) and ventricular depolarization (V) is shown. The paper speed was 100 mm s^{-1}.

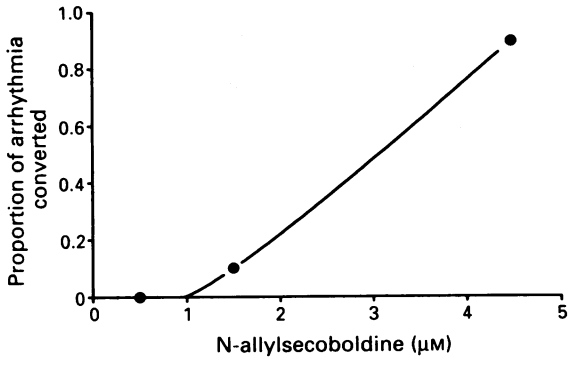

Figure 8 Antiarrhythmic efficacy of N-allylsecoboldine at various concentrations is plotted against the drug concentration.

in one instance and at 4.5 μM converted eight of the remaining nine episodes. For the one episode of refractory tachyrhythmia, when 13.5 μM of N-allylsecoboldine was applied, complete atrioventricular block occurred. The dose-response curve for arrhythmia conversion showed an ED_{50} of 3.2 μM (Figure 8). No new tachyrhythmias upon the perfusion of N-allylsecoboldine for about 2 h were observed during the experiment.

Discussion

N-allylsecoboldine was shown to have a satisfactory antiarrhythmic potential in the present study, an action which may be mediated through blockade mainly of the Na and I_{K1} channels, and partly through the I_{to} and I_{Ca} channels. Consequently, N-allylsecoboldine could prolong the conduction intervals and the refractoriness of the cardiac conduction system. The electrophysiological effects were similar to those found for quinidine, but were different from it in channel selectivity.

Use-dependent inhibition of I_{Na}, retardation of the recovery of Na channel from their inactivation state and negative shift of the voltage-dependent inactivation curve of I_{Na} are major mechanisms responsible for the action of most class I antiarrhythmic agents (Chen *et al.*, 1975; Ducouret, 1976; Lee *et al.*, 1981; Saikawa, 1982; Colatsky, 1982; Saikawa, 1982; Sanchez-Chapula *et al.*, 1983; Clarkson & Hondeghem, 1985; Su & Morad, 1987; Clarkson *et al.*, 1988). In this current study, as compared with quinidine, N-allylsecoboldine caused a similar degree of blocking action on Na channels. This action like that of other class I antiarrhythmic drugs, would explain not only prolongation of the conduction intervals of the atrial, atrioventricular, His-Purkinje system and ventricular area but also the increased refractoriness of these structures.

The class III antiarrhythmic agents exert their antiarrhythmic effects by suppressing the K outward currents to prolong the action potential duration and thereby increase the refractoriness of the conduction system (Singh & Nademanee, 1985; Hondeghem & Katzung, 1987; Imaizumi & Giles, 1987; Dukes *et al.*, 1990; Kurachi *et al.*, 1990; Su *et al.*, 1990; 1993; Gwilt *et al.*, 1991). Our results showed that N-allylsecoboldine could suppress the I_{K1} and the I_{to}, which consequently prolonged the action potential duration and increased further the refractoriness of the myocardium.

In rabbit atrial and atrioventricular nodal cells, I_{to} is responsible for the repolarization phase of the action potential (Nakayama & Irisawa, 1985). Therefore, I_{to} suppression would increase the refractoriness of the atrial and atrioventricular nodal area. The less marked prolongation of the atrial and atrioventricular refractory periods by N-allylsecoboldine than by quinidine could be attributed to a smaller suppression of I_{to} by N-allylsecoboldine. In diseased human atrial strips, the resting membrane potential of partially depolarized cells is noted to be between −40 and −50 mV, at which I_{to} is partially activated and may overlap I_{Ca} (Escande *et al.*, 1987). Therefore, it has been proposed that I_{to} plays a protective role against arrhythmias in the diseased human atrium by preventing the firing at foci of abnormal automaticity. The current data indicated that N-allylsecoboldine had a weaker effect in suppressing I_{to} than quinidine. This would imply that in the presence of a partially depolarized myocardium, the proarrhythmic potential of N-allylsecoboldine would be at least no greater than quinidine.

Drugs that block the Ca channel may preferentially prolong the conduction and refractoriness of slow response fibres (Rosen *et al.*, 1975; Harrison, 1985). However, they may also result in a negative inotropic effect which is hazardous in some situations. In this respect, the antiarrhythmic effect of N-allylsecoboldine would be expected to be associated with a less significant suppression of cardiac contractility than quinidine. Unpublished results from our laboratory have shown that N-allylsecoboldine (9 μM) causes an increase in the contractile tension, to about 160%, in rat right atrial strips. This effect may be attributed to an inhibition of K channels (an increase in the action potential duration) which is accompanied by a less significant inhibition of I_{Ca}.

In conclusion, we have identified a satisfactory antiarrhythmic potential for the newly synthesized secoaporphine, N-allylsecoboldine. This drug has both class I and class III properties. However, its channel selectivity, in comparison to quinidine, may give this agent a less negative inotropic and less proarrhythmic potential, and suggests that N-allylsecoboldine may be a promising drug for the treatment of cardiac arrhythmias.

The authors thank Ms Su-Chien Wang and Ms Li-Ting Lin for technical assistance and Ms Chiu-Yu Chen for her secretarial help. This study was supported by a grant from Institute of BioMedical Sciences, Academia Sinica (IBMS-CRC83-T16) and a grant from National Science Council, Taiwan (NSC 83-0425-B002-001).

References

CARMELIET, E. & SAIKAWA, T. (1982). Shortening of the action potential and reduction of pacemaker activity by lidocaine, quinidine and procainamide in sheep cardiac Purkinje fibers: an effect on Na or K currents? *Circ. Res.*, **50**, 257–272.

CHEN, C.M., GETTES, L.S. & KATZUNG, B.G. (1975). Effect of lidocaine and quinidine on steady state characteristics and recovery kinetics of (dV/dt) max in guinea pig ventricular myocardium. *Circ. Res.*, **37**, 20–29.

CLARKSON, C.W., FOLLMEN, C.H., TEN EICK, R.E., HONDEGHEM, L.M. & YEH, J.Z. (1988). Evidence for two components of sodium channel block by lidocaine in isolated cardiac myocytes. *Circ. Res.*, **63**, 869–878.

CLARKSON, C.W. & HONDEGHEM, L.M. (1985). Evidence for a specific receptor site for lidocaine quinidine and bupivocaine associated with cardiac sodium channel in guinea pig ventricular myocardium. *Circ. Res.*, **56**, 496–506.

COLATSKY, T.J. (1982). Mechanism of action of lidocaine and quinidine on action potential duration in rabbit cardiac Purkinje fibers. An effect on steady state sodium currents? *Circ. Res.*, **50**, 17–27.

CURTIS, M.J. & HEARSE, D.J. (1989). Ischemia-induced and reperfusion-induced arrhythmias differ in their sensitivity to potassium: implications for mechanisms of initiation and maintenance of ventricular fibrillation. *J. Mol. Cell. Cardiol.*, **21**, 21–40.

DUCOURET, P. (1976). The effect of quinidine on membrane electrical activity in frog auricular fibers studied by current and voltage clamp. *Br. J. Pharmacol.*, **57**, 163–184,

DUKES, I.D., CLEEMANN, L. & MORAD, M. (1990). Tedisamil blocks the transient and delayed rectifier K^+ currents in mammalian cardiac and glial cells. *J. Pharmacol. Exp. Ther.*, **254**, 560–569.

ESCANDE, D., COULOMBE, A., FAIVRE, J.F., DEROUBAIX, E. & CORABOERF, E. (1987). Two types of transient outward currents in adult human atrial cells. *Am. J. Physiol.*, **252**, H142–148.

GILES, W.R. & IMAIZUMI, Y. (1988). Comparison of potassium currents in rabbit atrial and ventricular cells. *J. Physiol.*, **405**, 123–145.

GWILT, M., ARROWSMITH, J.E., BLACKBURN, K.J., BURGES, R.A., CROSS, P.E., DALRYMPLE, H.W. & HIGGINS, A.J. (1991). UK-68789, a novel, potent and highly selective class III antiarrhythmic drug which blocks potassium channels in cardiac cells. *J. Pharmacol. Exp. Ther.*, **256**, 318–324.

HAMILL, O.P., MARY, A., NEHER, E., SAKMANN, B. & SIGWORTH, F.J. (1981). Improved patch clamp techniques for high resolution current recording from cells and cell-free membrane patches. *Pflügers Arch.*, **391**, 85–100.

HARRISON, D.C. (1985). Antiarrhythmic drug classification: new science and practical applications. *Am. J. Cardiol.*, **56**, 185–187.

HILLE, B. (1984). Classical biophysics of the squid giant axon. In *Ionic Channels of excitable Membranes*. ed. Hille, B. pp. 23–57. Sunderland, Mass: Sinauer Associates Inc.

HONDEGHEM, L.M. & KATZUNG, B.G. (1987). Antiarrhythmic agents: the modulated receptor mechanism of action of sodium and calcium channel blocking drugs. *Annu. Rev. Pharmacol. Toxicol.*, **24**, 387–423.

IMAIZUMI, Y. & GILES, W.R. (1987). Quinidine-induced inhibition of transient outward current in cardiac muscle. *Am. J. Physiol.*, **253**, H704–708.

ISENBERG, G. & KLOCKNER, U. (1981). Calcium tolerant ventricular myocytes prepared by preincubation in a 'KB medium'. *Pflügers Arch.*, **395**, 6–18.

JOSEPHSON, M.E. & SEIDES, S.F. (1979). *Clinical Cardiac Electrophysiology. Technique and Interpretations*. pp. 41–65. Philadelphia: Lea & Febiger.

KURACHI, K., ASANO, Y., ITO, H. & SUGIMOTO, T. (1990). Voltage-dependent inhibition of the delayed potassium current by POC-8490, a novel positive inotropic agent, in isolated atrial myocytes of guinea pig heart. *Naunyn-Schmied. Arch. Pharmacol.*, **341**, 324–330.

LEE, K.S., HUME, J.R., GILES, W. & BROWN, A.M. (1981). Sodium current depression by lidocaine and quinidine in isolated ventricular cells. *Nature*, **291**, 325–327.

LEE, S.S., LIN, Y.J., CHEN, M.Z., WU, Y.C. & CHEN, C.M. (1992). A facile semisynthesis of litebamine, a novel phenanthrene alkaloid, from boldine via a biogenetical approach. *Tetrahedron Lett.*, **33**, 6309–6310.

MITRA, R. & MORAD, M. (1985). A uniform enzymatic method for dissociation of myocytes from hearts and stomachs of vertebrates. *Am. J. Physiol.*, **249**, H1056–1060.

NAKAYAMA, T. & IRISAWA, H. (1985). Transient outward current carried by potassium and sodium in quiescent atrioventricular node cells of rabbit. *Circ. Res.*, **57**, 65–73.

ROSEN, M.R., WIT, A.L. & HOFFMAN, B.F. (1975). Electrophysiology and pharmacology of cardiac arrhythmias. VI. Cardiac effects of verapamil. *Am. J. Heart. J.*, **89**, 665–673.

SANCHEZ-CHAPULA, J., TSUDA, Y. & JOSEPHASON, I.R. (1983). Voltage and use-dependent effect of lidocaine on sodium current in rat single ventricular cells. *Circ. Res.*, **52**, 557–565.

SINGH, B.N. & NADEMANEE, K. (1985). Control of cardiac arrhythmia by selective lengthening of repolarization: theoretic considerations and clinical observations. *Am. Heart. J.*, **109**, 421–430.

SU, M.J., CHANG, G.J. & KUO, S.C. (1993). Mechanical and electrophysiological studies on the positive inotropic effect of 2-phenyl-4-oxo-hydroquinoline in rat cardiac tissues. *Br. J. Pharmacol.*, **110**, 310–316.

SU, M.J., LIN, S.O., WANG, C.H., TSENG, Y.Z. & TSENG, C.D. (1990). Comparison of the electrophysiological effect of amiodarone, lidocaine and quinidine on rat ventricular cells. *Proc. Natl. Acad. Sci. (ROC)*, **14**, 105–113.

SU, M.J. & MORAD, M. (1987). Effect of quinidine and lidocaine on action potential and membrane currents of frog ventricles. *Proc. Natl. Acad. Sci. (ROC)*, **11**, 362–369.

TENG, C.M., YU, S.M., KO, H.N., CHEN, C.C., HUANG, Y.L. & HUANG, T.F. (1991). Decentrine, a natural vascular α adrenoceptor antagonist isolated from *Lindera megaphylla*. *Br. J. Pharmacol.*, **104**, 651–656.

(Received January 13, 1994
Revised April 15, 1994
Accepted April 20, 1994)

Br. J. Pharmacol. (1994), **113**, 228–232

Nitric oxide as a mediator of the laxative action of magnesium sulphate

Angelo A. Izzo, [1]Timothy S. Gaginella, Nicola Mascolo & [2]Francesco Capasso

Department of Experimental Pharmacology, University of Naples, Federico II, via D. Montesano 49, 80131, Naples, Italy

1 Magnesium sulphate was studied for its effects on diarrhoea, fluid secretion, gastrointestinal transit and nitric oxide (NO) synthase activity in rats.

2 At a dose of 2 g kg^{-1} orally magnesium sulphate produced diarrhoea that was delayed in onset and intensity in a dose-related manner by the NO synthase inhibitor N^G-nitro-L-arginine methyl ester (L-NAME). This was prevented by the NO precursor, L-arginine and the NO donating compound, isosorbide-5-mononitrate (IMN).

3 Nitric oxide synthase activity was stimulated in gut tissue from rats given magnesium sulphate and this was inhibited by L-NAME. Dexamethasone (1 mg kg^{-1}, i.p.), an inhibitor of inducible NO synthase, had no effect on magnesium sulphate-induced diarrhoea.

4 Magnesium sulphate stimulated fluid and electrolyte accumulation in the intestinal lumen; these effects were prevented by L-NAME but not D-NAME.

5 Gastrointestinal transit of a non-absorbable marker (charcoal suspension) was increased by oral magnesium sulphate from a mean value of 54.1% to 72.9% ($P<0.01$), and this was prevented by pretreatment with L-NAME.

6 The results demonstrate that oral magnesium sulphate produces diarrhoea in rats by increasing the accumulation of fluid in the intestinal lumen and enhancing flow from the proximal to distal intestine. The mechanism involves release of NO, probably through stimulation of the constitutive form of NO synthase. Whether or not the effects of magnesium sulphate are due to an osmotic action or an intrinsic effect of the magnesium or sulphate ions cannot be determined from these experiments.

Keywords: Magnesium sulphate; laxatives; nitric oxide; intestinal secretion; gastrointestinal transit

Introduction

Pharmacological studies on the laxative action of magnesium sulphate are reported (Wood, 1908) to have been done over 100 years ago. The early studies attributed the action of this saline laxative to the osmotic activity of the constituent ions in the intestinal lumen. However, measurement of water absorption from *in situ* intestinal loops prepared in cats was impaired by an isotonic solution of magnesium sulphate (Lium & Florey, 1939), suggesting that the magnesium or sulphate ions have an action on the bowel that is independent of an osmotic effect. Harvey & Read (1973) presented arguments to support the idea that the laxative effect of magnesium sulphate is not due simply to osmotic effects, but involves the release of cholecystokinin (CCK).

Whilst the proposal that the laxative effect of magnesium sulphate could be due to the release of a hormone such as CCK is not universally accepted, perfusion of magnesium ions as part of an isosmotic solution into the duodenum of man evoked a moderate stimulatory effect on CCK release (Malagelada *et al.*, 1978). CCK is an intestinal secretagogue in rats (Hubel, 1972), guinea-pigs (Kachur *et al.*, 1991), dogs (Bussjaeger & Johnson, 1973) and man (Moritz *et al.*, 1973). In the human jejunum, isotonic magnesium sulphate induced net fluid secretion and increased transit through the small intestine (Wanitschke & Ammon, 1976). In an *in vivo* animal model, others confirmed that an isotonic magnesium sulphate solution produces secretion, possibly through changes in intracellular calcium (Reichelderfer *et al.*, 1979).

Because the laxative action of magnesium sulphate (whether isotonic or hypertonic) might be due to the release of other mediators, we considered the involvement of nitric oxide (NO). NO is an apparent mediator of the action of other laxatives (Mascolo *et al.*, 1993; 1994; Gaginella, personal communication). NO is an intestinal secretagogue (Tamai & Gaginella, 1994) and it relaxes intestinal smooth muscle (Boeckxstaens *et al.*, 1993; Grider, 1993; Stark *et al.*, 1993). This muscle relaxant effect is likely to enhance intestinal transit and contribute to a laxative/diarrhoeal effect (Gullikson & Bass, 1984).

Methods

Animals

Male Wistar (Morini) rats (150–170 g) were used after a week of acclimatization to their housing conditions (temperature 23 ± 2°C; humidity 60%). Food was withheld 18 h before experiments but there was free access to drinking water. Each rat was placed in a separate cage at the beginning of the experiment.

Laxative (diarrhoeal) test

Rats were injected intraperitoneally with N^G-nitro-L-arginine methyl ester (L-NAME, 2.5–25 mg kg^{-1}), or D-NAME (25 mg kg^{-1}) 15 min before and 3 h after oral dosing with magnesium sulphate or mannitol. L-Arginine (600 and 1500 mg kg^{-1}, i.p.) was given 15 min before, the NO donor isosorbide-5-mononitrate (IMN, 30–120 mg kg^{-1}, orally) 30 min before plus 3 h after, and the glucocorticoid, dexamethasone (1 mg kg^{-1}, i.p.) 2 h before the laxatives were given.

One hour after dosing with the laxatives and each hour for 8 h, the individual rat cages were inspected (by an observer unaware of the particular treatment) for the presence of

[1] Present address: Aphton Corporation, P.O. Box 1049, Woodland, CA 95776, U.S.A.
[2] Author for correspondence.

unformed water faecal pellets; their absence was recorded as a positive result, indicating protection from diarrhoea at that time.

Water and electrolyte secretion

Four and one-half hours after dosing with magnesium sulphate or mannitol, the rats were anaesthetized with urethane (1.3 g kg^{-1}, i.p.). The colon was rinsed carefully with sterile 0.9% (w/v) NaCl solution (37°C) to remove the bowel contents. After 30 min, the colon was ligated after filling with 2.5 ml sterile Tyrode solution consisting of (in g l^{-1}): NaCl 8.00, KCl 0.20, $NaH_2PO_4 \cdot 7H_2O$ 0.05, $MgSO_4 \cdot 7H_2O$ 0.05, D-glucose $\cdot H_2O$ 1.0, $NaHCO_3$ 1.00 and $CaCl_2 \cdot H_2O$ 0.26. One hour later, the animals were killed and the colon was quickly removed. Net water transport was calculated from the volume of the fluid content of the colon minus the 2.5 ml of the solution used to fill the colon.

Electrolyte content was analysed in the supernatant (after centrifugation) by high performance liquid chromatography (h.p.l.c.) utilizing a conductivity detector (Poole & Shuette, 1984). Net transport was calculated by difference (Van Hoestenberghe *et al.*, 1992). L-NAME (25 mg kg^{-1}, i.p.) or D-NAME (at the same dose, i.p.) was given 15 min before and 3 h after laxative challenge.

Gastrointestinal transit

Magnesium sulphate or mannitol, at the same doses used in the diarrhoea and fluid transport protocols, was administered orally 2 h before the oral administration of 1 ml of a transit marker (10% charcoal suspension in 5% gum arabic). After 30 min, the rats were killed and the gastrointestinal tract was removed. The distance travelled by the marker was measured and expressed as a percentage of the total length of the intestine from the pylorus to caecum. A dose of 25 mg kg^{-1} of L-NAME or D-NAME was administered i.p. 30 min before oral administration of laxatives. Control rats received water.

NO synthase assay

The activity of NO synthase in colonic tissue from control animals and those treated with magnesium sulphate and mannitol, some of which were treated with L-NAME or dexamethasone, was assessed. Five hours after giving the laxatives the animals were anaesthetized and killed. Full thickness segments of the colon (0.5 g) were homogenized for 20 s on ice in 2.5 ml of a buffer containing sucrose (0.32 M), dithiothreitol (1 mM), soybean trypsin inhibitor (10 $\mu g\ ml^{-1}$). The homogenates were centrifuged at 10,000 *g* for 5 min (5°C) and the supernatant processed for colorimetric determination of citrulline as described by Boyde & Rahmatullah (1980). In brief, 0.1 ml of supernatant was added to 3 ml of chromogenic solution, vortexed for 30 s and boiled at 100°C for 5 min. Colorimetric readings were made at room temperature, measuring the absorbance at 530 nm. Citrulline standard was determined simultaneously with the samples. The NO synthase activity was expressed as nmol g^{-1} tissue.

Chemicals

L-NAME hydrochloride, magnesium sulphate, mannitol, citrulline, dithiothreitol, soybean trypsin inhibitor and dexamethasone were purchased from Sigma Chemical Co. (Milan, Italy); Isosorbide-5-mononitrate, and D-NAME came from Astra and RBI respectively (Milan, Italy). These compounds were dissolved in saline before being used except for IMN, which was suspended in 1% carboxymethylcellulose. All chemicals used for the Tyrode and other solutions were of the highest purity available, from commercial sources.

Statistics

The Chi-Squared test was used to determine the significance between groups with or without diarrhoea. Intestinal fluid volume, electrolyte secretion and small intestinal transit were expressed as mean ± s.e. and compared by One-way Analysis of Variance (ANOVA) followed by Duncan's New Multiple-Range Test and Student's *t* test respectively. A *P* value less than 0.05 was considered significant.

Results

Diarrhoea

Diarrhoea occurred in the magnesium sulphate-treated group of rats from 3–8 h and from 2–8 h in the mannitol-treated group; dexamethasone (an inhibitor of inducible nitric oxide synthase) had no effect on either of these laxatives (Table 1). Four hours after administration of the laxatives and for the next 4 h, diarrhoea was evident in all the animals. L-NAME dose-dependently delayed the onset of diarrhoea to both drugs and reduced the total number of animals with diarrhoea over the time frame studied (Figure 1). The 25 mg kg^{-1} dose significantly ($P<0.05$) reduced the incidence of diarrhoea from 4–8 h after magnesium sulphate. L-Arginine (1500 mg kg^{-1}) reversed the effect of 25 mg kg^{-1} L-NAME

Table 1 Effect of dexamethasone (1 mg kg^{-1}, i.p., 2 h before laxative challenge) on the diarrhoea induced by magnesium sulphate (2 g kg^{-1}) and mannitol (10 g kg^{-1})

Laxative (oral)	*Number of rats (12) with diarrhoea at different times*							
	1	2	3	4	5	6	7	8 (h)
Magnesium sulphate	0	0	2	8	12	12	12	12
+ Dexamethasone	0	0	1	9	12	12	12	12
Mannitol	0	2	6	10	12	12	12	12
+ Dexamethasone	0	3	5	9	11	12	12	12

Results were analysed by the Chi-squared test. There were no significant effects of dexamethasone on any of the laxatives.

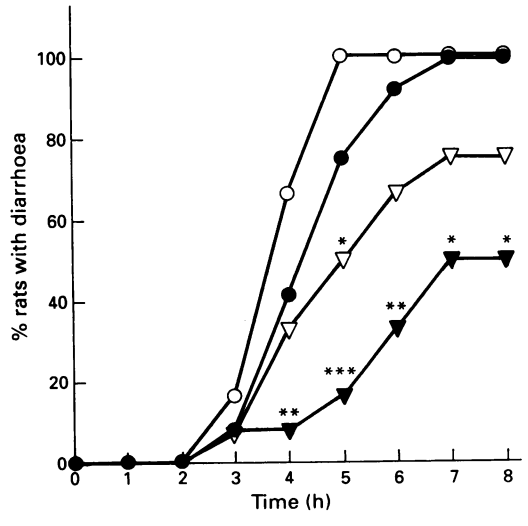

Figure 1 Inhibitory effect of N^G-nitro-L-arginine methyl ester (L-NAME) (2.5–25 mg kg^{-1}) on the percentage of rats (out of 12) with diarrhoea at various times after oral magnesium sulphate (2 mg kg^{-1}, ○). The L-NAME was given (i.p.) 15 min before and 3 h after the laxative: L-NAME, 2.5 mg kg^{-1} (●); 10 mg kg^{-1} (▽) and 25 mg kg^{-1} (▼). Asterisks indicate significance compared to control (laxative only) at $*P<0.05$, $**P<0.01$ and $***P<0.001$ by the Chi squared test.

on the magnesium sulphate-induced diarrhoea (Figure 2). L-Arginine (1500 mg kg^{-1}) itself did not modify the diarrhoeal effect nor did D-NAME (25 mg kg^{-1}), inhibit the response (data not shown). The NO donating compound IMN prevented the inhibitory effect of L-NAME in rats with magnesium sulphate-induced diarrhoea (Table 2).

Secretion

Magnesium sulphate produced fluid secretion into the intestinal loops. This was reversed by L-NAME but unaffected by D-NAME (Table 3); L-NAME and D-NAME had no effect on the mannitol response. Likewise, L-NAME inhibited the magnesium sulphate but not the mannitol-induced electrolyte secretion (Table 4).

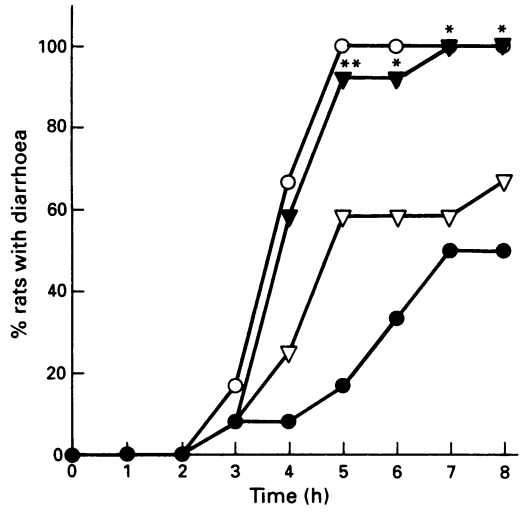

Figure 2 Reversal by L-arginine (600, ▽, and 1500 mg kg^{-1}, ▼, i.p.) of the inhibitory effect of N^{G}-nitro-L-arginine methyl ester (L-NAME, 25 mg kg^{-1}, i.p., ●) on diarrhoea in animals ($n = 12$) dosed orally with magnesium sulphate (2 mg kg^{-1}, ○). The L-NAME alone was given 15 min before and 3 h after the laxative, while L-arginine was given (i.p.) only 15 min before the laxative. *$P<0.05$ and **$P<0.01$ compared to control (laxative only) by the Chi Squared test.

Table 2 Reversal of the antidiarrhoeal effect of N^{G}-nitro-L-arginine methyl ester (L-NAME) on magnesium sulphate (2 g kg^{-1}, p.o.) by isosorbide-5-mononitrate (IMN)

Treatment	*Number of rats with diarrhoea* ($n = 12$)	*% reversion*
Magnesium sulphate	12	–
+ L-NAME	2	–
+ L-NAME + IMN	5	30
+ L-NAME + IMN	9	70
+ L-NAME + IMN	10*	80

Results were analysed by the Chi squared test.
*$P<0.05$ vs corresponding laxative + L-NAME.
Magnesium sulphate was given orally. L-NAME and IMN were given twice i.p. 15 min before and 3 h after laxative challenge. Diarrhoea was assessed at 4 h.

NO synthase activity

Magnesium sulphate significantly stimulated nitric oxide synthase activity and this was inhibited by L-NAME (25 mg kg^{-1}) (Figure 3). Mannitol was not tested for this effect because neither fluid nor electrolyte secretion were affected by L-NAME.

Gastrointestinal transit

The gastrointestinal transit of charcoal was increased from 54.1 ± 2.1% ($n = 12$) of the total length of intestine (control group) to 72.9 ± 2.0% (magnesium sulphate group) ($P<0.01$). L-NAME (25 mg kg^{-1} twice) had no effect (48.2 ± 2.2%) on the control response and prevented ($P<0.05$) the magnesium sulphate effect (58.2 ± 2.3% transit compared to to the 72.9% for the laxative).

Discussion

Our results support previous suggestions (Harvey & Read, 1973; Stewart *et al.*, 1975; Wanitschke & Ammon, 1976) that magnesium sulphate produces a laxative effect through a mechanism that is not solely due to an osmotic gradient. We used mannitol as an osmotic control for the magnesium sulphate. Assuming an animal weight of 150 g and dilution in 10 ml of gastrointestinal fluid, magnesium sulphate and mannitol at the doses used here would yield intraluminal concentrations of approximately 570 and 825 milliosmolar, respectively. Even though mannitol represented nearly 1.5 times more osmotic equivalents than magnesium sulphate and both agents produced diarrhoea, only the effects of magnesium sulphate were influenced by modulating the generation of NO. These findings suggest that NO probably serves as an intermediate in the laxative action of magnesium sulphate. This does not exclude the possibility that other, perhaps osmotic factors, also contribute to its mechanism of action.

Dexamethasone, a glucocorticoid that inhibits the inducible form of NO synthase (see Moncada *et al.*, 1991), failed to inhibit diarrhoea after dosing with magnesium sulphate or mannitol, but L-NAME (a competitive inhibitor of constitutive and inducible NO synthases) dose-dependently antagonized the diarrhoeal effect of magnesium sulphate. Assay of NO synthase confirmed that magnesium sulphate stimulated NO synthase activity in the intestine and that L-NAME can block this effect. The NO synthesis precursor, L-arginine, and the NO donating compound, IMN, both antagonized the diarrhoeal effect of magnesium sulphate, providing additional support for the involvement of NO. Taken together, the data indicate that the NO release arises from magnesium and/or sulphate activation of the constitutive, not the inducible form of NO synthase.

Table 3 Effect of N^{G}-nitro-L-arginine methyl ester (L-NAME, 25 mg kg^{-1}, i.p.) and D-NAME (25 mg kg^{-1}, i.p.) on magnesium sulphate and mannitol-induced water flux in the ligated rat colon

Treatment	*Net fluid accumulation* (ml) *Saline*	*L-NAME*	*D-NAME*
Control[a]	– 1.08 ± 0.08	– 1.00 ± 0.07	– 1.10 ± 0.07
Magnesium sulphate	0.17 ± 0.10[b]	– 0.75 ± 0.04[c]	0.14 ± 0.07
Mannitol	0.16 ± 0.07	0.17 ± 0.10	0.14 ± 0.09

[a]Results are expressed as mean ± s.e. for 6–8 experiments. The colon was rinsed with 2 ml saline solution. A negative value represents net absorption and a positive value net secretion.
[b]$P<0.01$ vs control.
[c]$P<0.001$ vs corresponding laxative + saline group.

Table 4 Effect of N^G-nitro-L-arginine methyl ester (L-NAME, 25 mg kg^{-1}, i.p.) on electrolyte movements in response to laxatives in the rat ligated colon

Treatment	*Net electrolyte transport* (μEq) *Sodium*	*Chloride*	*Potassium*
Control[a]	− 202.4 ± 14.6	− 210.0 ± 11.4	7.4 ± 1.7
Magnesium sulphate	17.5 ± 12.2[b]	12.3 ± 10.5[b]	19.2 ± 1.9[b]
+ L-NAME	− 170.2 ± 16.5[c]	− 179.1 ± 11.3[c]	10.1 ± 2.9[c]
Mannitol	− 10.2 ± 10.5[b]	− 20.1 ± 14.2[b]	12.2 ± 10.5[b]
+ L-NAME	− 5.2 ± 12.3	− 12.3 ± 16.5	9.3 ± 2.2

[a]Results are expressed as mean ± s.e. for 6–8 experiments. A negative value represents net absorption and a positive value net secretion. L-NAME was administered 15 min before and 3 h after laxatives challenge.
[b]$P<0.001$ vs control.
[c]$P<0.01$ vs magnesium sulphate.

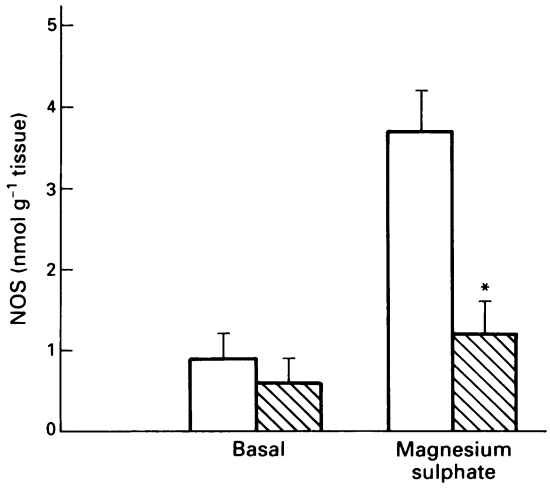

Figure 3 Effect of magnesium sulphate on nitric oxide synthase (NOS) activity under control conditions (open column) and after pretreatment (i.p.) with N^G-nitro-L-arginine methyl ester (L-NAME) (25 mg kg^{-1}, hatched column). Columns are means with s.e. (n = 6–8). *$P<0.01$ compared to control by Duncan's test.

The laxative response to magnesium sulphate results from effects on gut smooth muscle (enhancement of transit) and mucosal electrolyte transport (Gullikson & Bass, 1984; Stewart *et al.*, 1975). The inhibition of electrolyte absorption or stimulation of secretion causes the accumulation of fluid in the gut lumen, which is what we observed in the present experiments. Consistent with the results of the experiments on diarrhoea, L-NAME reversed the effect of magnesium sulphate but not mannitol on electrolyte transport and luminal fluid accumulation. Furthermore, the effect was enantiomer-specific because D-NAME was inactive.

We also found that magnesium sulphate increased the transit of a non-absorbable marker through the gut. L-NAME attenuated the enhanced transit, implicating NO in this effect. Relaxation of colonic circular smooth muscle reduces resistance to flow and promotes movement of material through the intestine (Gullikson & Bass, 1984). Such an effect would explain the reversal of the constipation due to morphine by L-arginine in the mouse (Calignano *et al.*, 1991); a reduction in the force of contraction of ileal and colonic circular muscle in dogs has been reported (Stewart *et al.*, 1975). NO also relaxes small intestinal and colonic circular smooth muscle (Boeckxstaens *et al.*, 1993; Stark *et al.*, 1993) and also seems to be involved in relaxation of the gut during the peristaltic reflex (Grider, 1993). In the latter case, vasoactive intestinal peptide (VIP) is postulated to interact with NO, whereby VIP stimulates the influx of calcium into muscle cells and activates constitutive NO synthase, liberating NO as the agonist of relaxation (Murthy *et al.*, 1993). We have no evidence for the involvement of VIP in the responses to magnesium sulphate in the present study but we cannot rule out this possibility, as VIP is not only a smooth muscle relaxant but also a potent intestinal secretatogue and diarrhoeagenic peptide (Gaginella *et al.*, 1982).

This study was supported by CNR (Rome) and Murst 60%.

References

BOECKXSTAENS, G.E., PELCKMANS, P.A., HERMAN, A.G. & VAN MAERCKE, Y.M. (1993). Involvement of nitric oxide in the inhibitory innervation of the human isolated colon. *Gastroenterology*, **104**, 690–697.

BOYDE, T.C.R. & RAHMATULLAH, M. (1980). Optimization of conditions for the colorimetric determination of citrulline, using diacetyl monoxime. *Anal. Biochem.*, **107**, 424–431.

BUSSJAEGER, L.J. & JOHNSON, L.R. (1973). Evidence for hormonal regulation of intestinal absorption by cholecystokinin. *Am. J. Physiol.*, **224**, 1276–1279.

CALIGNANO, A., MONCADA, S. & DI ROSA, M. (1991). Endogenous nitric oxide modulates morphine-induced constipation in mice. *Biochem. Biophys. Res. Commun.*, **181**, 889–893.

GAGINELLA, T.S., HUBEL, K.A. & O'DORISION, T.M. (1982). Vasoactive intestinal polypeptide and intestinal chloride secretion. In *Vasoactive Intestinal Polypeptide*. ed. Said, S. Vol. 1, pp. 211–222. New York: Raven Press.

GRIDER, J.R. (1993). Interplay of VIP and nitric oxide in regulation of the descending relaxation phase of peristalsis. *Am. J. Physiol.*, **264**, G334–G340.

GULLIKSON, G.W. & BASS, P. (1984). Mechanism of action of laxative drugs. In *Pharmacology of Intestinal Permeation* II, Chapter 28. pp. 419–459, New York: Springer-Verlag.

HARVEY, R.F. & READ, A.E. (1973). Saline purgatives act by releasing cholecystokinin. *Lancet*, July 28, 185–187.

HUBEL, K.A. (1972). Effects of pentagastrin and cholecystokinin on intestinal transport of ions and water in the rat. *Proc. Soc. Exp. Biol. Med.*, **140**, 670–672.

KACHUR, J.F., PHILLIPS, G.S. & GAGINELLA, T.S. (1991). Neuromodulation of guinea pig intestinal electrolyte transport by cholecystokinin octapeptide. *Gastroenterology*, **100**, 344–349.

LIUM, R. & FLOREY, H.W. (1939). The action of magnesium sulphate on the intestine of the cat. *Q. J. Exp. Physiol.*, **29**, 303–319.

MALAGELADA, J.R., HOLTERMULLER, K.H., MCCALL, J.T. & GO, V.L.W. (1978). Pancreatic, gallbladder and intestinal responses to intraluminal magnesium salts in man. *Dig. Dis.*, **23**, 481–485.

MASCOLO, N., IZZO, A.A., AUTORE, G., BARBATO, F. & CAPASSO, F. (1994). Nitric oxide and castor oil-induced diarrhea. *J. Pharmacol. Exp. Ther.*, **68**, 291–295.

MASCOLO, N., IZZO, A.A., BARBATO, F. & CAPASSO, F. (1993). Inhibitors of nitric oxide synthetase prevent castor oil-induced diarrhoea in the rat. *Br. J. Pharmacol.*, **108**, 861–864.

MONCADA, S., PALMER, R.M.J. & HIGGS, E.A. (1991). Nitric oxide: physiology, pathophysiology and pharmacology. *Pharmacol. Rev.*, **43**, 109–142.

MORITZ, M., FINKELSTEIN, G., MESHKINPOUR, H., FINGERHYT, J. & LORRER, H. (1973). Effect of secretin and cholecystokinin on the transport of electrolyte and water in human jejunum. *Gastroenterology*, **64**, 77–80.

MURTHY, K.S., ZHANG, K.-M., JIN, J.-G., GRIDER, J.R. & MAKHLOUF, G.M. (1993). VIP-mediated G protein-coupled Ca^{2+} influx activated a constitutive NOS in dispersed gastric muscle cells. *Am. J. Physiol.*, **265**, G660–G671.

POOLE, C.F. & SHUETTE, S.A. (1984). *Contemporary Practice of Chromatography*, pp. 313–317. Amsterdam: Elsevier.

REICHELDERFER, M., PERO, B., LORENZSON, V. & OLSEN, W.A. (1979). Is magnesium-induced intestinal secretion mediated by changes in intracellular calcium? *Gastroenterology*, **76**, 1224.

STARK, M.E., BAUER, A.J., SARR, M.G. & SRUZSZEWSKI, J.H. (1993). Nitric oxide mediates inhibitory nerve input in human and canine jejunum. *Gastroenterology*, **104**, 398–405.

STEWART, J.J., GAGINELLA, T.S., OLSEN, W.A. & BASS, P. (1975). Inhibitory actions of laxatives on motility and water and electrolyte transport in the gastrointestinal tract. *J. Pharmacol. Exp. Ther.*, **192**, 458–467.

TAMAI, H. & GAGINELLA, T.S. (1993). Direct evidence for nitric oxide stimulation of electrolyte secretion in the rat colon. *Free Rad. Res. Commun.*, **19**, 229–239.

VAN HOESTENBERGHE, A., DE WITTE, P., GEBOES, K., EYSSEN, H., NIJS, G. & LEMLI, J. (1992). The effect of rhein and rhein anthrone on intestinal fluid transport and on large intestine transit in germ-free rats. *Eur. J. Pharmacol.*, **212**, 121–123.

WANITSCHKE, R. & AMMON, H.V. (1976). Effect of magnesium sulphate on transit time and water transport in the human jejunum. *Gastroenterology*, **76**, 949.

WOOD, H.C. (1908). *Cathartics. Therapeutics. Its Principles and Practice*. pp. 497–524. Philadelphia: Lippincott.

(Received March 9, 1994
Revised May 12, 1994
Accepted May 23, 1994)

Br. J. Pharmacol. (1994), **113**, 233–239

Ca^{2+} release induced by myotoxin *a*, a radio-labellable probe having novel Ca^{2+} release properties in sarcoplasmic reticulum

[1]Ken-Ichi Furukawa, Kaori Funayama, Masamichi Ohkura, Yoshiteru Oshima, *Anthony T. Tu & Yasushi Ohizumi

Department of Pharmaceutical Molecular Biology, Pharmaceutical Institute Tohoku University, Aobayama, Sendai 980, Japan and *Department of Biochemistry, Colorado State University, Colorado 80523, U.S.A.

1 Myotoxin *a* (MYTX), a polypeptide toxin purified from the venom of prairie rattlesnakes (*Crotalus viridis viridis*) induced Ca^{2+} release from the heavy fraction (HSR) but not the light fraction of skeletal sarcoplasmic reticulum at concentrations higher than 1 μM, followed by spontaneous Ca^{2+} reuptake by measuring extravesicular Ca^{2+} concentrations using the Ca^{2+} electrode.

2 The rate of $^{45}Ca^{2+}$ release from HSR vesicles was markedly accelerated by MYTX in a concentration-dependent manner in the range of concentrations between 30 nM and 10 μM, indicating the most potent Ca^{2+} releaser in HSR.

3 The Ca^{2+} dependency of MYTX-induced $^{45}Ca^{2+}$ release has a bell-shaped profile but it was quite different from that of caffeine, an inducer of Ca^{2+}-induced Ca^{2+} release.

4 $^{45}Ca^{2+}$ release induced by MYTX was remarkable in the range of pCa between 8 and 3, whereas that by caffeine was prominent in the range of pCa, i.e., between 7 and 5.5.

5 MYTX-induced $^{45}Ca^{2+}$ release consists of both early and late components. The early component caused by MYTX at low concentrations (30–300 nM) completed within 20 s, while the late component induced by it at higher concentrations (>0.3 μM) was maintained for at least 1 min.

6 Both the components were almost completely inhibited by inhibitors of Ca^{2+} release such as Mg^{2+}, ruthenium red and spermine.

7 $^{45}Ca^{2+}$ release induced by caffeine or β,γ-methyleneadenosine 5′-triphosphate (AMP-PCP) was completely inhibited by high concentrations of procaine. Procaine abolished the early component but not the late one, suggesting that at least the early component is mediated through Ca^{2+}-induced Ca^{2+} release channels.

8 On the basis of these results, the character of Ca^{2+} release induced by MYTX was quite different from that caused by caffeine or AMP-PCP, suggesting that MYTX induces Ca^{2+} release having novel properties in HSR. MYTX is the first polypeptide Ca^{2+} inducer and has become a useful pharmacological tool for clarifying the mechanism of Ca^{2+} release from skeletal muscle SR.

Keywords: Myotoxin *a*; skeletal muscle; sarcoplasmic reticulum; Ca^{2+} release; caffeine; procaine; excitation-contraction coupling

Introduction

The contractile state of skeletal muscle is determined by the intracellular Ca^{2+} concentration ($[Ca^{2+}]_i$) (Rüegg, 1986). Muscle cells maintain a high gradient of Ca^{2+} across not only the plasma membrane but also the sarcoplasmic reticulum membrane (SR) (Endo, 1977; Martonosi, 1984). SR has an ATP-dependent Ca^{2+} pump that accumulates Ca^{2+} into its lumen to reduce $[Ca^{2+}]_i$ below 0.1 μM and to maintain the Ca^{2+} gradient (Ebashi, 1991). It has been generally accepted that excitation of the plasma membrane evokes the depolarization of the transverse tubular membrane that leads to Ca^{2+} release from SR through a putative Ca^{2+} release channel (Schneider, 1981; Block *et al.*, 1988). This is a major process in excitation-contraction coupling. One possible candidate for the machinery of the physiological process is the Ca^{2+}-induced Ca^{2+} release channels that have been recently purified by using the plant alkaloid ryanodine, as a biochemical probe and extensively characterized (Hymel *et al.*, 1988; Smith *et al.*, 1988; Lai *et al.*, 1988; Saito *et al.*, 1988; Wagenknecht *et al.*, 1989). Application of specific drugs that affect the Ca^{2+} releasing mechanism is a useful approach to achieve a better understanding of the molecular mechanism of this release. Ryanodine (McPherson & Campbell, 1993) and 9-methyl-7-bromoeudistomin D (MBED), the most powerful caffeine-like Ca^{2+} releaser (Seino *et al.*, 1991; Fang *et al.*, 1993) have provided us with useful information. However, little information has accumulated about the physiological mechanism of the signal transduction between the transverse tubular system and SR (Schneider & Chandler, 1973; Schneider, 1981).

Myotoxin *a* (MYTX) purified from the venom of prairie rattlesnakes (*Crotalus viridis*) is a muscle toxic polypeptide composed of 42 amino acids (Fox *et al.*, 1979). Electron microscopic study has revealed that MYTX causes muscle degeneration and disturbance of the endoplasmic reticulum and muscle filaments (Cameron & Tu, 1977). In the course of our survey of natural products having Ca^{2+} releasing activity in SR, we have found that MYTX is the most powerful Ca^{2+} releaser known having novel pharmacological properties; the radio-labelled compound can be synthesized. This paper reports the detailed evidence that MYTX causes Ca^{2+} release from skeletal muscle SR. MYTX may provide a pharmacologically useful tool for resolving the molecular mechanism of Ca^{2+} release from SR.

Methods

Purification of MYTX

Myotoxin *a* (MYTX) was purified as described previously (Cameron & Tu, 1977). Crude prairie rattlesnake venom (1 g)

[1] Author for correspondence.

was dissolved in 5–6 ml of an elution buffer consisting of 0.05 M Tris, pH 9.0, at 22°C, containing 0.1 M KCl. This was applied to a Sephadex G-50 gel filtration column (4 × 115 cm) equilibrated with the elution buffer. Fractions of 5 ml were collected at a flow rate of 0.5 ml min^{-1}. Absorbance of each fraction at 280 nm was monitored on a Shimazu UV-260 spectrometer. Appropriate tubes were pooled, and an aliquot of each fraction was used for protein determination by the method of Lowry *et al.* (1951). The Sephadex G-50 fractions were lyophilized. The lyophilized fraction was dissolved in about 4 ml of the Sephadex G-50 elution buffer, and was applied to a Sephadex C-25 cation-exchange column (1.6 × 15 cm) equilibrated with the same elution buffer. After washing the column, elution was then performed with a three-step KCl salt gradient in the 0.05 M Tris buffer. Five-ml fractions were collected, and the absorbance of each fraction at 280 nm was measured. Appropriate tubes were pooled and were dialyzed and lyophilized.

Preparation of SR vesicles from skeletal muscle

The heavy fraction of fragmented SR (HSR) was prepared from rabbit skeletal muscle by the method of Kim *et al.* (1983). Rabbits were stunned and exsanguinated. White muscle was homogenized in five volumes of 5 mM Tris-maleate (pH 7.0) and centrifuged at 5,000 *g* for 5 min. The supernatant was further centrifuged at 12,000 *g* for 30 min. The pellet was suspended in a solution containing 0.1 M KCl and 5 mM Tris-maleate and centrifuged at 70,000 *g* for 40 min. The HSR obtained was stored in the same solution at 0°C and used within 4 days.

Ca^{2+} electrode experiments

The concentration of extravesicular Ca^{2+} in the SR suspension was measured at 30°C with a Ca^{2+} electrode as described previously (Seino *et al.*, 1991). The Ca^{2+} electrode showed a Nernstian response (slope, 27–29 mV/pCa unit) in the calibration buffer containing Ca^{2+}-EGTA between pCa decreased from 6 to 4. The assay solution (final volume, 1 ml) contained 0.05 mM $CaCl_2$, 90 mM KCl, 0.25 mM $MgCl_2$,

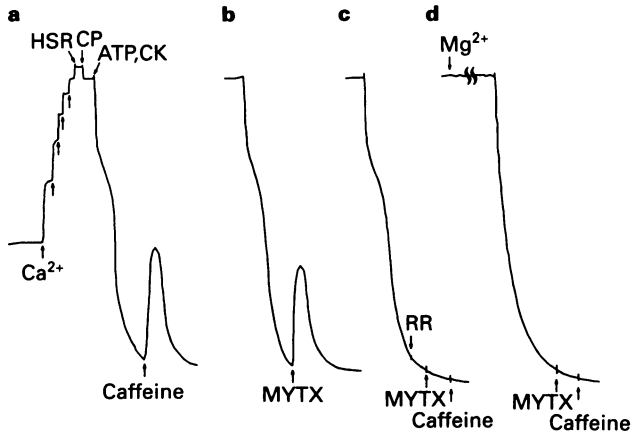

Figure 1 Ca^{2+} release induced by MYTX from skeletal muscle HSR. The concentrations of extravesicular Ca^{2+} were monitored at 30°C with a Ca^{2+} electrode in the assay solution containing 0.05 mM $CaCl_2$, 90 mM KCl, 0.25 mM $MgCl_2$, 50 mM MOPS-Tris (pH 7.0), 1 mg ml^{-1} of HSR, 5 mM creatine phosphate (CP), 0.13 mg ml^{-1} of creatine kinase (CK) and 0.5 mM (CK) and 0.5 mM ATP. At the beginning of each experiment, 0.01 mM $CaCl_2$ was added five time stepwise as the internal standard. The reaction of Ca^{2+} uptake was started by a simultaneous addition of CK and ATP. Vertical calibration bars indicate responses for voltage change (10 mV) corresponding to 0.5 pCa unit. In (b) to (d), the traces are those only after the addition of ATP; (a) 1 mM caffeine; (b) 1 μM MYTX; (c) 2 μM ruthenium red (RR) plus 10 μM MYTX and 5 mM caffeine; (d) 4 mM $MgCl_2$ plus 10 μM MYTX and 5 mM caffeine. For abbreviations in this and other legends, please see text.

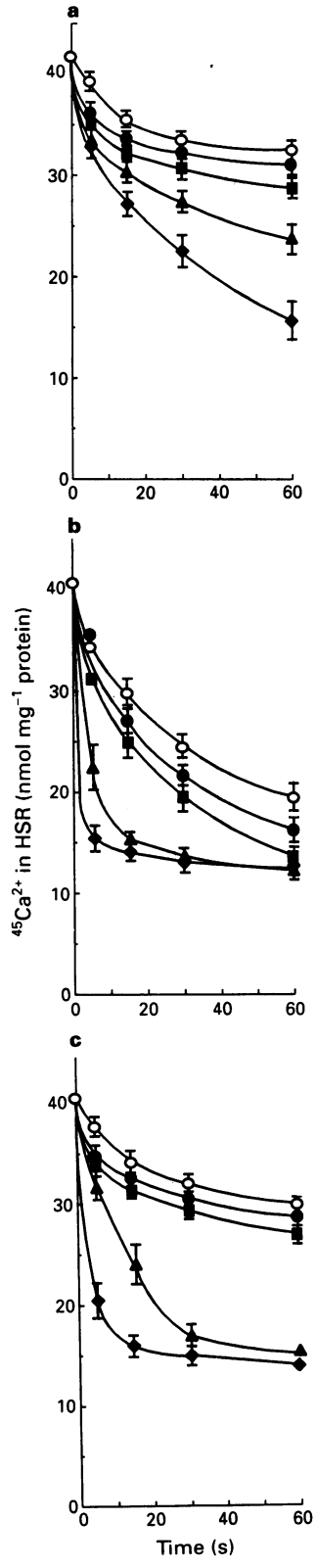

Figure 2 Stimulatory effect of MYTX on the $^{45}Ca^{2+}$ from skeletal muscle HSR at difference Ca^{2+} concentrations. The $^{45}Ca^{2+}$ content in HSR vesicles was measured at 0°C by the Millipore filtration method after 100 fold dilution of passively $^{45}Ca^{2+}$-preloaded HSR into a medium containing 90 mM KCl, 0.4 mM $CaCl_2$ with various concentrations of EGTA and 50 mM MOPS-KOH (pH 7.0) in the presence or absence of various concentrations of test substance. The initial content of $^{45}Ca^{2+}$ in HSR was obtained by adding the HSR suspension into the reaction medium containing 90 mM KCl, 5 mM $MgCl_2$, 5 mM $LaCl_3$, and 50 mM MOPS (pH 7.0). Free Ca^{2+} concentration was maintained with Ca-EGTA buffer. Values are mean with s.e.mean. ($n = 3$–4). (a) pCA 7; (b) pCa 6; (c) pCa 4. The concentrations of MYTX were 0 nM (○), 30 nM (●), 100 nM (■), 1 μM (▲), and 10 μM (◆).

50 mM MOPS-Tris (pH 7.0), 1 mg ml^{-1} of HSR, 5 mM creatine phosphate, 0.13 mg ml^{-1} of creatine kinase and 0.5 mM ATP. The reaction of Ca^{2+} uptake was started by the simultaneous addition of creatine kinase and ATP.

$^{45}Ca^{2+}$ release experiments

$^{45}Ca^{2+}$ release from HSR passively preloaded with $^{45}Ca^{2+}$ was measured at 0°C as described previously (Nakamura *et al.*, 1986; Kobayashi *et al.*, 1987) with slight modification. After 12-h preincubation of 20 mg ml^{-1} HSR with 5 mM $^{45}Ca^{2+}$ in a solution containing 90 mM KCl and 50 mM MOPS-KOH (pH 7.0) at 0°C, the HSR suspension was diluted with 100 volumes of an ice-cold reaction medium containing, 0.4 mM $CaCl_2$ with various concentrations of EGTA, 90 mM KCl and 50 mM MOPS-KOH (pH 7.0). For measurement of the amount of $^{45}Ca^{2+}$ in HSR at time 0 the HSR suspension was diluted with the reaction medium containing 5 mM $LaCl_3$. At an appropriate time, 5 mM $LaCl_3$ was added to stop $^{45}Ca^{2+}$. The reaction mixture was then filtered through Millipore filter (HAWP type, 0.45 μm pore size), and washed with 5 ml of a solution containing 5 mM $LaCl_3$, 5 mM $MgCl_2$, 90 mM KCl and 50 mM MOPS-KOH (pH 7.0). The amount of $^{45}Ca^{2+}$ remaining in the HSR vesicles was measured by counting the radioactivity on the washed filters.

[^{3}H]-ryanodine binding assay

[^{3}H]-ryanodine binding was examined as described previously (Inui *et al.*, 1987) with modification. HSR was incubated with 10 nM [^{3}H]-ryanodine at 37°C for 1 h in a solution containing 0.3 M sucrose, 1 M NaCl, 10 μM $CaCl_2$, 2 mM DTT, 0.1 mM *p*-APMSF and 20 mM Tris-HCl (pH 7.4). The amount of [^{3}H]-ryanodine bound was determined by membrane filtration through Whatman filters (GF/B). Nonspecific binding was determined in the presence of 10 μM unlabelled ryanodine.

Measurement of (Ca^{2+}-Mg^{2+})ATPase activity

(Ca^{2+}-Mg^{2+})ATPase reaction was carried out at 37°C in a medium of 0.1 M KCl, 20 mM Tris-maleate, pH 7.5, 2 mM $MgCl_2$, and 2 mM ATP. ATPase activity was determined from the amount of phosphate liberated, which was measured by the method of Chan *et al.* (1986).

Free Ca^{2+} concentration

Free Ca^{2+} concentration was maintained by using Ca^{2+}-EGTA buffer (0.2 mM $CaCl_2$ plus various concentrations of

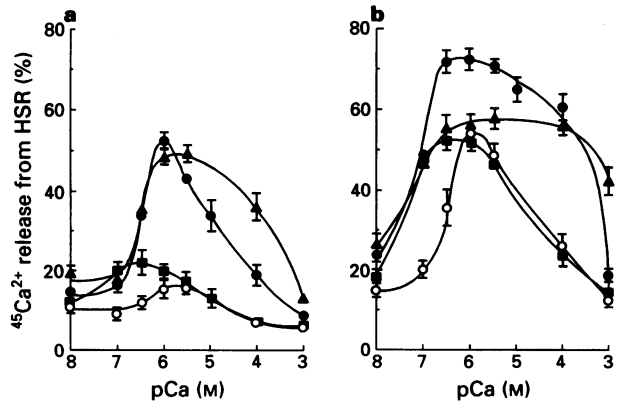

Figure 3 Effect of free Ca^{2+} concentrations on $^{45}Ca^{2+}$ release induced by several drugs from skeletal muscle HSR. $^{45}Ca^{2+}$ release from HSR for 5 s (a) and 1 min (b) was measured. Experimental protocols were similar to those described in Figure 2. Values are mean with s.e.mean. ($n = 4$). Control (○); 1 μM MYTX (●); 1 mM caffeine (■); 100 μM AMP-PCP (▲).

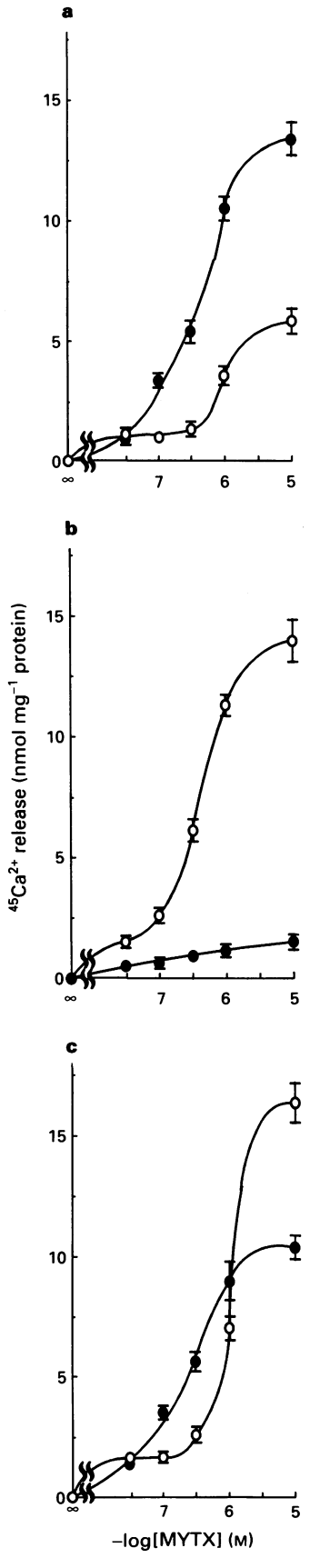

Figure 4 Concentration-dependent acceleration of $^{45}Ca^{2+}$ release from skeletal muscle HSR by MYTX. $^{45}Ca^{2+}$ release was measured at pCa 7 (a), 6 (b) and 4 (c). Experimental protocols were the same as those described in Figure 2. $^{45}Ca^{2+}$ release was carried out using HSR vesicles during 5 s (○) and 1 min (●) after dilution in the absence (control) or presence (experimental condition) of MYTX (up to 10 μM). The difference between control and experimental conditions is plotted. Values are mean with s.e.mean. ($n = 3$–4).

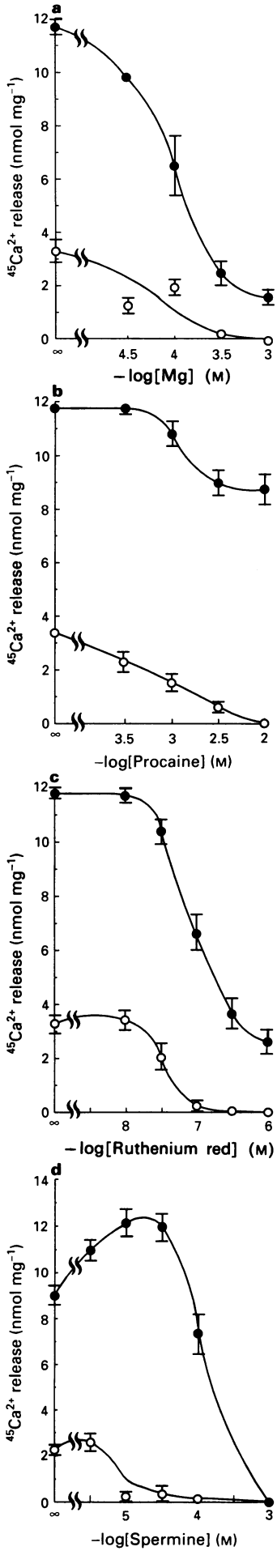

EGTA). The free Ca^{2+} was estimated using a microcomputer programme taking into account the binding constant for Ca-EGTA, pH, and the concentrations of K^+, Mg^{2+}, and nucleotides present (Sillen & Martell, 1964; 1971).

Materials

The sources of materials used in this work were as follows: crude venom of prairie rattlesnake from Miami Serpentarium Laboratories; procaine HCl and AMP-PCP from Sigma; ryanodine from S.B. Penick Company; $^{45}CaCl_2$ (0.70 Ci mmol^{-1}) and [^{3}H]-ryanodine (60 Ci mmol^{-1}) from Du-Pont New England Nuclear; MBED was prepared by the method described previously (Kobayashi *et al.*, 1988). All other chemicals were of analytical grade.

Results

Ca^{2+} release experiments with a Ca^{2+} electrode

The effect of MYTX on the Ca^{2+}-mobilizing activity of SR can be visualized clearly by monitoring extravesicular Ca^{2+} concentrations of HSR directly with a Ca^{2+} electrode (Nakamura *et al.*, 1986; Seino *et al.*, 1991). When the Ca^{2+} concentration was reduced to submicromolar levels, the apparent Ca^{2+} uptake slowed. As shown in Figure 1, the addition of 1 mM caffeine or 1 μM MYTX to Ca^{2+}-filled HSR caused an immediate Ca^{2+} release followed by a Ca^{2+} reuptake. The rate of Ca^{2+} reuptake was almost the same as that before the addition of caffeine or MYTX. Pretreatment of HSR with 2 μM ruthenium red (Figure 1c) or 4 mM $MgCl_2$ (Figure 1d) blocked the effect of 10 μM MYTX and 5 mM caffeine. In the light fraction of SR (LSR), however, neither MYTX (0.1–10 μM) nor caffeine (0.5–5 mM) caused Ca^{2+} release (data not shown).

$^{45}Ca^{2+}$ release from HSR

Effects of MYTX on $^{45}Ca^{2+}$ release from HSR were investigated by the Millipore filtration method. Figure 2 shows the time courses of change in the $^{45}Ca^{2+}$ content in HSR evoked by various concentrations of MYTX at three different free Ca^{2+} concentrations. $^{45}Ca^{2+}$ release was markedly accelerated by MYTX, in a concentration-dependent manner at any pCa used. MYTX at concentrations of 30 nM or more caused the acceleration of Ca^{2+} release and this release was completed within 20 s at pCa 7 and pCa 4. $^{45}Ca^{2+}$ release stimulated by MYTX at concentrations higher than 1 μM maintained at least for 1 min. The Ca^{2+} dependency of ^{45}Ca release induced by MYTX, caffeine and AMP-PCP has a bell-shaped profile (Figure 3). $^{45}Ca^{2+}$ release was stimulated remarkably by MYTX and AMP-PCP in the wider range of pCa between 8 and 3, whereas that induced by caffeine was accelerated in the range of pCa, i.e., between 7 and 5.5. Figure 4 shows the concentration-response curve for MYTX in $^{45}Ca^{2+}$ release during 5 s and 1 min. MYTX caused a concentration-dependent increase in $^{45}Ca^{2+}$ release at concentrations higher than 30 nM. The first saturation was observed at concentrations around 0.1 μM. When the concentration of MYTX was further increased, the $^{45}Ca^{2+}$ release activity increased again and reached the maximum response to MYTX at 10 μM. The effects of various inhibitors on $^{45}Ca^{2+}$ release induced by

Figure 5 Effects of representative inhibitors for Ca^{2+}-induced Ca^{2+} release on $^{45}Ca^{2+}$ release induced by MYTX from skeletal muscle HSR. Concentration-dependent effects of free Mg^{2+} (a), procaine (b), ruthenium red (c) and spermine (d) on MYTX-induced Ca^{2+} release was investigated. Data are expressed as difference between $^{45}Ca^{2+}$ release in the presence or absence of MYTX. Experimental protocols were the same as those described in Figure 2. Values are mean with s.e.mean. ($n = 3$–4). 100 nM MYTX (○); 10 μM MYTX (●).

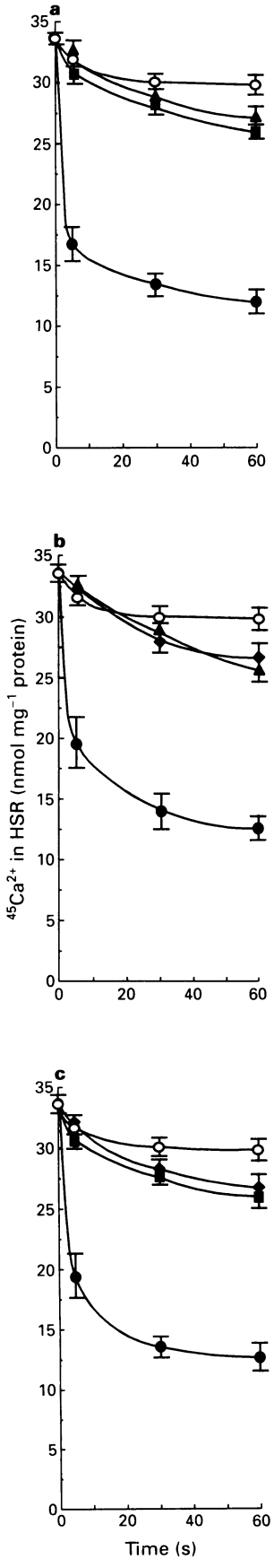

Figure 6 Interrelations among the Ca^{2+}-releasing activities of MYTX, MBED and AMP-PCP. Experimental protocols were the same as those described in Figure 2. Values are mean ($n = 4$). Control (○); 10 μM MYTX (▲); 10 μM MBED (■); 0.1 mM AMP-PCP(◆). (a), 10 μM MYTX plus 10 μM MBED (●). (b), 10 μM MYTX plus 0.1 mM AMP-PCP (●). (c), 10 μM MBED plus 0.1 mM AMP-PCP (●).

MYTX at concentrations of 100 nM and 10 μM were investigated. Figure 5a shows the effects of Mg^{2+} on $^{45}Ca^{2+}$ release triggered by MYTX. $^{45}Ca^{2+}$ release caused by MYTX at two concentrations was nearly completely inhibited by Mg^{2+} in a concentration-dependent manner. Each IC_{50} value for Mg^{2+} was approximately 100 μM. $^{45}Ca^{2+}$ release induced by caffeine or AMP-PCP from HSR was completely inhibited by procaine at a high concentration of 10 mM. As shown in Figure 5b, $^{45}Ca^{2+}$ release stimulated by 100 nM MYTX was completely inhibited by procaine (10 mM), whereas that stimulated by 10 μM MYTX was only partly inhibited. Ruthenium red caused a concentration-dependent inhibition of $^{45}Ca^{2+}$ release induced by MYTX at 100 nM and 10 μM with each IC_{50} value of about 0.1 μM (Figure 5c). $^{45}Ca^{2+}$ release caused by MYTX at 100 nM was completely inhibited by spermine at concentrations higher than 10 μM (Figure 5d). However, the effect of spermine on the release caused by 10 μM MYTX was complex. The release was potentiated by spermine at concentrations between 3 and 30 μM, whereas release was inhibited by spermine at concentrations higher than 100 μM in a concentration-dependent manner. Figure 6 shows the interrelations among the $^{45}Ca^{2+}$ releasing activities of MYTX, MBED and AMP-PCP at pCa 8. MYTX and MBED caused the maximum increase in $^{45}Ca^{2+}$ release at 10 μM. The additional application of AMP-PCP (0.1 mM) further increased the maximum response of $^{45}Ca^{2+}$ release to MYTX and MBED (Figure 6b and c). Furthermore, $^{45}Ca^{2+}$-releasing effects of MYTX and MBED are additive, suggesting that each drug potentiates $^{45}Ca^{2+}$ release from HSR through binding to the different binding sites.

[^{3}H]-ryanodine binding to HSR

[^{3}H]-ryanodine binding to the HSR membrane was examined in the presence of unlabelled ryanodine or MYTX. MYTX (up to 10 μM) did not affect [^{3}H]-ryanodine binding to HSR, although the binding of [^{3}H]-ryanodine was inhibited by unlabelled ryanodine in a concentration-dependent manner with the IC_{50} value of approximately 15 nM.

(Ca^{2+}-Mg^{2+})ATPase activity of HSR

Volpe *et al.* (1986) reported that MYTX inhibited Ca^{2+} loading and stimulated Ca^{2+}-dependent ATPase of LSR without affecting unidirectional Ca^{2+} release. But in HSR, MYTX at concentrations up to 400 μM did not exhibit significant effect on the (Ca^{2+}-Mg^{2+})ATPase activity (Figure

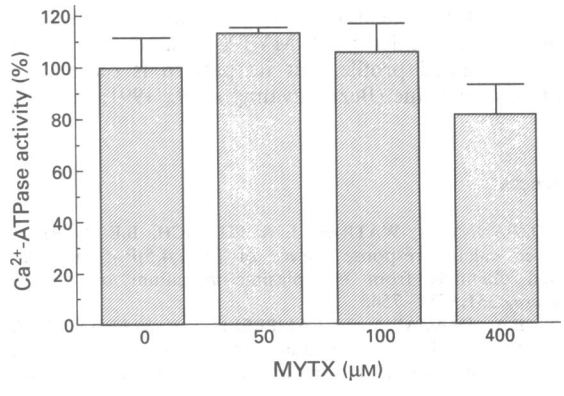

Figure 7 Effects of MYTX on Ca^{2+}-ATPase activity of skeletal muscle HSR. HSR vesicles (0.1 mg ml^{-1}) were incubated at 27°C for 5 min with varying concentrations of MYTX and A23187 (4 μM). At the end of incubation, ATPase activity was measured as described under Methods. Results are the mean ± s.e. of three experiments and are expressed as a percentage against control activity determined in the absence of MYTX (control, 1040 ± 122 nmol P_i mg^{-1} protein min^{-1}; 40 μM MYTX, 1178 ± 20 nmol P_i mg^{-1} protein min^{-1}; 100 μM MYTX, 1100 ± 118 nmol P_i mg^{-1} protein min^{-1}; 400 μM MYTX, 848.5 ± 120 nmol P_i mg^{-1} protein min^{-1}).

7). The EC_{50} value of MYTX for $^{45}Ca^{2+}$ release was about 1 μM. In addition, MYTX did not cause $^{45}Ca^{2+}$ release from LSR (data not shown). In the $^{45}Ca^{2+}$-release measurement, therefore, the effect of MYTX on the (Ca^{2+}-Mg^{2+})ATPase is excluded.

Discussion

The Ca^{2+}-induced Ca^{2+} release channels may be the machinery of the physiological process in the excitation-contraction coupling in skeletal muscle (Endo *et al.*, 1979; Ford & Podolsky, 1970; Endo, 1977). The channels have been purified using [^{3}H]-ryanodine as a specific ligand (Inui *et al.*, 1987; Hymel *et al.*, 1988; Wagenknecht *et al.*, 1989). The functions of Ca^{2+} release channels are inhibited by several inhibitors such as procaine, Mg^{2+}, ruthenium red and spermine (Palade, 1987; McPherson & Campbell, 1993). In the present study, we found that MYTX accelerated $^{45}Ca^{2+}$ release from HSR in a concentration-dependent manner at concentrations higher than 30 nM, making it the most potent inducer known of Ca^{2+} release in SR. MYTX even at high concentrations had no ionophoretic activity on the membrane of HSR because the rate of Ca^{2+} reuptake after a rapid Ca^{2+} release was almost the same as that before the addition of MYTX or caffeine. MYTX had no effect on (Ca^{2+}-Mg^{2+})ATPase even at high concentrations up to 400 μM. The Ca^{2+} mobilizing effect of MYTX were blocked by inhibitors of Ca^{2+}-release (Mg^{2+}, ruthenium red and spermine). These results suggest that MYTX induces Ca^{2+} release by affecting Ca^{2+} release channels in SR.

Procaine is a selective inhibitor (Endo, 1977) of Ca^{2+}-induced Ca^{2+} release channels with an IC_{50} value of 1 mM (Seino *et al.*, 1991). Ca^{2+} release induced by potentiators of Ca^{2+}-induced Ca^{2+} release such as caffeine and AMP-PCP was abolished in the presence of procaine (10 mM), indicating total block of Ca^{2+}-induced Ca^{2+} release channels. $^{45}Ca^{2+}$ release induced by 100 nM MYTX was completely inhibited by 10 mM procaine (IC_{50}, 0.91 mM), whereas that by 10 μM MYTX was only partially inhibited by it (IC_{50}, 1.1 mM) (Figure 5b). Therefore, $^{45}Ca^{2+}$ release evoked by MYTX at concentrations higher than 300 nM probably has two components (Figure 2). These observations suggest that the early component inhibited by procaine is due to Ca^{2+} release through the Ca^{2+}-induced Ca^{2+} release channels, while the late one resistant to procaine possibly mediated through Ca^{2+} release channels with novel pharmacological properties. However, we cannot exclude the possibility that procaine cannot completely inhibit Ca^{2+}-induced Ca^{2+} release induced by a potent Ca^{2+} releaser. This needs further consideration.

The Ca^{2+} dependency of MYTX-induced $^{45}Ca^{2+}$ release has a bell-shaped profile, but its pattern is quite different from that of caffeine (Bezprozvanny *et al.*, 1991; Seino *et al.*, 1991). The affinity of Ca^{2+} for the channels increased in the presence of caffeine (the EC_{50} values of Ca^{2+} for $^{45}Ca^{2+}$ release in the absence and presence of 1 mM caffeine were approximately 300 and 30 nM), whereas this was not changed by MYTX. Although the Ca^{2+} dependency of MYTX-induced Ca^{2+} release was rather similar to that of AMP-PCP, the pharmacological properties of MYTX, including the procaine sensitivity, were quite different from those of AMP-PCP.

It has been reported that the ryanodine receptor protein consists of several ligand-binding domains, i.e. domains for caffeine, adenine nucleotides, ryanodine and divalent cations (Pessah *et al.*, 1987). The maximum responses of $^{45}Ca^{2+}$ release to AMP-PCP and MBED increased further in the presence of MYTX. These data suggest that MYTX binds to different sites from those of AMP-PCP and MBED/caffeine. It has been reported that [^{3}H]-ryanodine binds to Ca^{2+}-induced Ca^{2+} release channels in an open state, this binding being increased by binding of several potentiators of Ca^{2+}-induced Ca^{2+}-release to the channels (Fleisher *et al.*, 1985; McPherson & Campbell, 1993). MYTX had no effect on [^{3}H]-ryanodine binding to HSR. Imperatoxins from the scorpion *Pandinus imperator* affected [^{3}H]-ryanodine binding (Valdivia *et al.*, 1992) suggesting that their binding sites are different from those of MYTX. Furthermore, the binding of [^{125}I]-MYTX to HSR was not affected by MBED/caffeine or AMP-PCP (Ohkura *et al.*, unpublished data). On the basis of these observations, it is suggested that there are three possibilities, i.e., MYTX binds to (1) a novel binding site on Ca^{2+}-induced Ca^{2+} release channels, (2) a regulatory protein of Ca^{2+}-induced Ca^{2+} release channels, or (3) a novel type of Ca^{2+} release channels.

One of the great advantages of MYTX as a pharmacological probe is that this compound is a polypeptide and ^{125}I-labelled MYTX can be synthesized. We have recently succeeded in the synthesis of ^{125}I-labelled MYTX with a high specific radioactivity (40–70 Ci mmol^{-1}) and in the demonstration of the presence of its specific binding site on HSR (Ohkura *et al.*, unpublished data). We also found that MYTX caused Ca^{2+} release from SR of chemically skinned fibres (Furukawa *et al.*, unpublished data). MYTX is the first polypeptide Ca^{2+} inducer in SR and has become a useful pharmacological tool, not only clarifying the regulatory mechanism of Ca^{2+} release channels but also purifying a novel type of Ca^{2+} release channel or its regulatory protein.

This work was partly supported by Grants-in Aid for Scientific Research on Priority Areas: 'Vascular Endothelium-Smooth Muscle Coupling' (No. 05256203) and for Scientific Research (No. 05557103) from the Ministry of Education, Science and Culture, Japan and grants from The Mitsubishi Foundation, Kowa Life Science Foundation, The Kanae Foundation, and The Naito Foundation, Japan.

References

BEZPROZBANNY, I., WATRAS, J. & EHRLICH, B.E. (1991). Bell-shaped calcium-response curves of Ins(1,4,5)P_3- and calcium-gated channels from endoplasmic reticulum of cerebellum. *Nature*, **351**, 751–754.

BLOCK, B.A., IMAGAWA, T., CAMPBELL, K.P. & FRANZINI-ARMSTRONG, C. (1988). Structural evidence for direct interaction between the molecular components of the transverse tubule/sarcoplasmic reticulum junction in skeletal muscle. *J. Cell Biol.*, **107**, 2587–2600.

CAMERON, D.L. & TU, A.T. (1977). Characterization of myotoxin *a* from the venom of prairie snake (*Crotalis viridis viridis*). *Biochemistry*, **224**, 89–96.

CHAN, K.-M., DELFERT, D. & JUNGER, K.D. (1986). A direct colourimetric assay for Ca^{2+}-stimulated ATPase ativity. *Anal. Biochem.*, **157**, 375–380.

EBASHI, S. (1991). Excitation-contraction coupling and the mechanism of muscle contraction. *Annu. Rev. Physiol.*, **53**, 1–16.

ENDO, M. (1977). Calcium release from the sarcoplasmic reticulum. *Physiol. Rev.*, **57**, 71–108.

ENDO, M., TANAKA, M. & OGAWA, Y. (1970). Calcium induced release of calcium from the sarcoplasmic reticulum of skinned skeletal muscle fibers. *Nature*, **228**, 34–36.

FANG, Y.-I., ADACHI, M., KOBAYASHI, M., KOBAYASHI, J. & OHIZUMI, Y. (1993). High affinity binding of 9-[^{3}H]methyl-7-bromoeudistomin D to the caffeine-binding site of skeletal muscle sarcoplasmic reticulum. *J. Biol. Chem.*, **268**, 18622–18625.

FLEISCHER, S., OGUNBUNMI, E.M., DIXON, M.C. & FLEER, E.A.M. (1985). Localization of Ca^{2+} release channels with ryanodine in junctional terminal cisternae of sarcoplasmic reticulum of fast skeletal muscle. *Proc. Natl. Acad. Sci. U.S.A.*, **82**, 7256–7259.

FORD, L.E. & PODOLSKY, R.J. (1970). Regenerative calcium release within muscle cells. *Science*, **167**, 58–59.

FOX, J.W., ELZINGA, M. & TU, A.T. (1979). Amino acid sequence and Disulfide bond assignment of myotoxin *a* isolated from the venom of prairie rattlesnake (*Crotalus viridis viridis*). *Biochemistry*, **18**, 678–684.

HYMEL, L., INUI, M., FLEISCHER, S. & SCHINDLER, H. (1988). Purified ryanodine receptor of skeletal muscle sarcoplasmic reticulum from Ca^{2+}-activated oligometric Ca^{2+} channels in planer bilayers. *Proc. Natl. Acad. Sci. U.S.A.*, **85**, 441–445.

INUI, M., SAITO, A. & FLEISCHER, S. (1987). Purification of the ryanodine receptor and identity with feet structure of junctional terminal cisternae of sarcoplasmic reticulum from fast skeletal muscle. *J. Biol. Chem.*, **262**, 1740–1747.

KIM, D.H., OHNISHI, S.T. & IKEMOTO, N. (1983). Kinetic studies of calcium release from sarcoplasmic reticulum *in vitro*. *J. Biol. Chem.*, **258**, 9662–9668.

KOBAYASHI, J., TANIGUCHI, M., HINO, T. & OHIZUMI, Y. (1988). Eudistomin derivatives, novel phosphodiesterase inhibitors: synthesis and relative activity. *J. Pharm. Pharmacol.*, **40**, 62–63.

KOBAYASHI, M., SHOJI, N. & OHIZUMI, Y. (1987). Gingerol, a novel cardiotonic agent, activate the Ca^{2+}-pumping ATPase in skeletal and cardiac sarcoplasmic reticulum. *Biochem. Biophys. Acta.*, **903**, 96–102.

LAI, F.A., ERICKSON, H.P., ROUSSEAU, E., LIU, Q.-Y. & MEISSNER, G. (1988). Purification and reconstitution of the calcium release channel from skeletal muscle. *Nature*, **331**, 315–319.

LOWRY, O.H., ROSEBROUGH, N.J., FARR, A.L. & RANDALL, R.J. (1951). Protein measurement with the Folin phenol reagent. *J. Biol. Chem.*, **193**, 263–275.

MARTONOSI, A.N. (1984). Mechanisms of Ca^{2+} release from sarcoplasmic reticulum of skeletal muscle. *Physiol. Rev.*, **64**, 1240–1320.

MCPHERSON, P.S. & CAMPBELL, K.P. (1993). The ryanodine receptor/Ca^{2+} release channel. *J. Biol. Chem.*, **268**, 13765–13768.

NAKAMURA, Y., KOBAYASHI, J., GILMORE, J., MASCAL, M., RINEHART, K.L. Jr., NAKAMURA, H. & OHIZUMI, Y. (1986). Bromo-eudistomin D, a novel inducer of calcium release from fragmented sarcoplasmic reticulum that causes contractions of skinned muscle fibers. *J. Biol. Chem.*, **261**, 4139–4142.

PALADE, P. (1987). Drug-induced Ca^{2+} release from isolated sarcoplasmic reticulum: III. Block of Ca^{2+}-induced Ca^{2+} release by organic polyamines. *J. Biol. Chem.*, **262**, 6149–6154.

PESSAH, I.N., STAMBUK, R.A. & CASIDA, J.E. (1987). Ca^{2+}-activated ryanodine binding: mechanisms of sensitivity and intensity modulation by Mg^{2+}, caffeine, and adenine nucleotides. *Mol. Pharmacol.*, **31**, 232–238.

RÜEGG, J.C. (1986). The sarcoplasmic reticulum: storage and release of calcium. In *Calcium in Muscle Activation*. ed. Rüegg, J.C. pp. 29–58. Berlin: Springer-Verlag.

SAITO, A., INUI, M., RAFERMACHER, M., FRANK, J. & FLEISCHER, S. (1988). Ultrastructure of the calcium release channel of sarcoplasmic reticulum. *Cell Biol.*, **107**, 211–219.

SCHNEIDER, M.F. (1981). Membrane charge movement and depolarization-contraction coupling. *Annu. Rev. Physiol.*, **43**, 507–517.

SCHNEIDER, M.F. & CHANDLER, W.K. (1973). Voltage dependent charge movement in skeletal muscle: a possible step in excitation-contraction coupling. *Nature*, **242**, 747–751.

SEINO, A., KOBAYASHI, M., KOBAYASHI, J., FANG, Y.-I., ISHIBASHI, M., NAKAMURA, H., MOMOSE, K. & OHIZUMI, Y. (1991). 9-Methyl-7-bromoeudistomin D, a powerful radio-labelable Ca^{2+} releaser having caffeine-like properties, acts on Ca^{2+}-induced Ca^{2+} release channels of sarcoplasmic reticulum. *J. Pharmacol. Exp. Ther.*, **256**, 861–867.

SILLEN, L.G. & MARTELL, A.E. (1964). *Stability Constants of Metal-ion Complexes*. London: The Chemical Society.

SILLEN, L.G. & MARTELL, A.E. (1971). *Stability Constants of Metal-ion Complexes*, Suppl. 1. London: The Chemical Society.

SMITH, J.S., IMAGAWA, T., MA, J., FILL, M., CAMPBELL, K.P. & CORONADO, R. (1988). Purified ryanodine receptor from rabbit skeletal muscle is the calcium-release channel of sarcoplasmic reticulum. *J. Gen. Physiol.*, **92**, 1–26.

VALDIVIA, H.H., KIRBY, M.S., LEDERER, W.J. & CORONADO, R. (1992). Scorpion toxins targeted against the sarcoplasmic reticulum Ca^{2+}-release channel of skeletal and cardiac muscle. *Proc. Natl. Acad. Sci. U.S.A.*, **89**, 12185–12189.

VOLPE, P., DAMIANI, E., MAIRER, A. & TU, A.T. (1986). Interaction of myotoxin *a* with the Ca^{2+}-ATPase of skeletal muscle sarcoplasmic reticulum. *Arch. Biochem. Biophys.*, **246**, 90–97.

WAGENKNECHT, T., GRASSUCCI, R., FRANK, J., SAITO, A., INUI, M. & FLEISCHER, S. (1989). Three-dimensional architecture of the calcium foot structure of sarcoplasmic reticulum. *Nature*, **338**, 167–170.

(Received January 21, 1994
Revised April 15, 1994
Accepted April 22, 1994)

Br. J. Pharmacol. (1994), **113**, 240–246

Sensitization by dexamethasone of lymphocyte cyclic AMP formation: evidence for increased function of the adenylyl cyclase catalyst

[1]Martin C. Michel, Jörg Knapp & Hanna Ratjen

Departments of Medicine and Pediatrics, University of Essen, Essen, Germany

1 Glucocorticoids and elevations of intracellular adenosine 3':5'-cyclic monophosphate (cyclic AMP) may affect lymphocyte activation, proliferation and effector functions in similar ways. Therefore, we have investigated the effects of the glucorticoid, dexamethasone, on human lymphocyte cyclic AMP formation.

2 Treatment of resting human lymphocytes with the glucocorticoid, dexamethasone, sensitized prostaglandin E_2-stimulated cyclic AMP accumulation in a time- and concentration-dependent manner.

3 In membranes of lymphocytes treated for 24 h with 100 nM dexamethasone, maximal adenylyl cyclase activity stimulated by prostaglandin E_2, isoprenaline, guanosine 5'-triphosphate (GTP), forskolin and $MnCl_2$ was significantly enhanced; the EC_{50} for these agents was not significantly altered.

4 β_2-Adrenoceptor density, immunodetectable α-subunits of the G-proteins G_s and G_i, and pertussis toxin-substrates were not significantly altered by dexamethasone treatment.

5 In dexamethasone-treated lymphocytes, prostaglandin E_2-mediated inhibition of concanavalin A-induced Ca^{2+} elevations was doubled compared to control cells.

6 Based on these data and the observation that enhancement of forskolin- and $MnCl_2$-stimulated adenylyl cyclase activity could quantitatively account for the enhancement of prostaglandin E_2-, isoprenaline- or GTP-stimulated adenylyl cyclase activity, we conclude that dexamethasone treatment sensitizes cyclic AMP formation in resting human lymphocytes by altering the adenylyl cyclase catalyst rather than G-proteins or hormone receptors. This results in an enhanced capability of cyclic AMP generating agonists to inhibit early steps of lymphocyte activation.

Keywords: Glucocorticoid; lymphocyte; adenylyl cyclase; G-protein; immunomodulation

Introduction

Glucocorticoids are potent immunosuppressive drugs the mechanism of action of which appears to involve inhibition of early steps in the activation of resting lymphocytes (Flower, 1988). An increase in intracellular adenosine 3':5'-cyclic monophosphate (cyclic AMP) can also suppress lymphocyte proliferation and effector functions by inhibiting early steps of their activation (Bourne *et al.*, 1974; Kammer, 1988). For example both cyclic AMP elevation and glucocorticoids inhibit expression of interleukin-2 (Northrop *et al.*, 1992; Anastassiou *et al.*, 1992) and interleukin-2 receptors (Tracey *et al.*, 1988; Anastassiou *et al.*, 1992) at a transcriptional level. In non-lymphoid tissues, glucocorticoids can enhance cyclic AMP formation (Malbon *et al.*, 1988). Formation of cyclic AMP results from the complex interaction of receptors, G-proteins and the adenylyl cyclase catalyst (Levitzki, 1988), and expression and/or functional activity of each component of this complex might be affected by glucocorticoids. For example, the gene for the human β_2-adrenoceptor which is expressed in all types of lymphocytes to stimulate cyclic AMP formation (Brodde *et al.*, 1987; Maisel *et al.*, 1989) contains a glucocorticoid response element (Hadcock *et al.*, 1989). Expression of the α-subunit of the adenylyl cyclase-stimulating G-protein G_S can also be enhanced by glucocorticoids in various non-lymphoid cell lines (Rodan & Rodan, 1986; Rizzoli & Bonjour, 1987; Chang & Bourne, 1987). Whether glucocorticoids can also affect expression of the adenylyl cyclase catalyst is not known.

Based on these observations we and others have hypothesized that cyclic AMP may at least partly be involved in the immunosuppressant effects of glucocorticoids (Michel & Brodde, 1989; Gruol *et al.*, 1989). The present study has investigated (a) whether the synthetic glucocorticoid dexamethasone can enhance cyclic AMP formation in human cultured resting lymphocytes, (b) which part(s) of the receptor/G-protein/adenylyl cyclase complex might be regulated by dexamethasone, and (c) whether enhanced cyclic AMP formation following glucocorticoid treatment is relevant for the modulation of lymphocyte function.

[1] Author for correspondence at: Nephrol. Lab IG 1, Klinikum, Hufelandstr. 55, D-45122 Essen, Germany.

Methods

Lymphocyte isolation and cell culture

Mononuclear leukocytes were isolated from EDTA-anticoagulated venous blood of drug-free healthy young volunteers of either sex according to the method of Böyum (1968). Unless otherwise indicated cells were incubated for 24 h in an atmosphere of 95% air/5% CO_2 in RPMI 1640 medium supplemented with 2 mM glutamine, 25 μg ml^{-1} gentamycin and 20% newborn bovine serum in the absence and presence of the indicated dexamethasone concentrations. Following this incubation, non-adherent mononuclear leukocytes (lymphocytes) were washed twice at 400 *g* for 10 min in phosphate-buffered saline.

Cyclic AMP accumulation in intact lymphocytes

Cyclic AMP accumulation in intact lymphocytes was determined during a 15 min incubation at 37°C in the presence of 100 μM of the phosphodiesterase inhibitor, theophyllin as previously described (Brodde *et al.*, 1985). The accumulated cyclic AMP was quantified with a commercially available protein binding assay (Amersham, Braunschweig, Germany).

Adenylyl cyclase activity in lymphocyte membranes

Lymphocyte membranes were prepared by three cycles of freeze/thawing using liquid nitrogen and a water bath at 37°C with subsequent centrifugation for 10 min at 29,000 *g* at 4°C as previously described (Maisel *et al.*, 1990b). The pellet was resuspended by repeated aspiration through a cannula (inner diameter 0.8 mm) yielding membranes of ≈250,000 cells per 20 µl sample. The protein content of the membrane preparation was assessed according to Bradford (1976) using bovine IgG as the standard.

Adenylyl cyclase activity was determined as previously described (Michel *et al.*, 1993b). Briefly, aliquots of the membrane suspension (≈10–14 µg protein) were incubated for 10 min at 37°C in a total volume of 100 µl containing 25 mM Tris, 5 mM $MgCl_2$, 0.5 mM adenosine 5'-triphosphate (ATP), 10 µM guanosine 5'-triphosphate (GTP), 20 µg creatine phosphate and 25 u ml^{-1} creatine phosphokinase at pH 7.4 and the indicated concentrations of agonists. The incubation was stopped by boiling, with subsequent cooling of the samples and centrifugation for 10 min at 13,000 *g*. Following storage at – 20°C the amount of cyclic AMP in the supernatant was determined by a commercially available radioimmunoassay (New England Nuclear, Dreieich, Germany).

Lymphocyte β-adrenoceptor density

β_2-Adrenoceptor density in intact lymphocytes was determined as previously described using six concentrations of [^{125}I]-iodocyanopindolol as the ligand (Brodde *et al.*, 1985). Non-specific binding was defined as binding in the presence of 1 µM of the hydrophilic antagonist (±)-CGP 12,177 and typically was 20% of total binidng of 20 pM of the ligand.

Lymphocyte G-proteins

Lymphocyte G-protein α-subunits were quantified by Western blotting and pertussis toxin-catalyzed ADP-ribosylation. Western blotting was performed according to the method of Burnette (1981) with minor modifications as previously described (Michel *et al.*, 1993a,b). Briefly, membranes were prepared from lymphocytes that had been incubated in the absence and presence of dexamethasone as described above and resuspended at a protein concentration of 2 mg ml^{-1}. Aliquots of the membrane suspension (50 µl) were boiled for 5 min together with 12.5 µl aliquots of sample buffer (4% SDS, 20% glycerol, 10% 2-mercaptoethanol, 125 mM Tris HCl, 0.002% bromphenol blue at pH 8). The mixture was separated by electrophoresis on polyacrylamide/SDS gels according to the method of Laemmli (1970) using 10% acrylamide in the running gel. On gels for the determination of $G_{s\alpha}$ we loaded one lane with membranes from cyc$^-$ cells which lack $G_{s\alpha}$ (Sternweis & Gilman, 1979) in order to control for non-specific bands. Following electroblotting to nitrocellulose membranes (Hybond-ECL 0.45 µm, Amersham), the blots were pre-blocked for 90 min at room temperature with TBS buffer (100 mM NaCl, 20 mM Tris HCl at pH 7.5) supplemented with 2% low-fat dried milk powder. Following two 5 min washes in TTBS (TBS supplemented with 500 µl l^{-1} Tween-20) at room temperature, blots were incubated for 20 h at 4°C in 15 ml TTBS supplemented with 1% dried milk powder and a 1:500 dilution of G-protein antisera (AS/7 for $G_{i\alpha}$ and RM/1 for $G_{s\alpha}$). Following removal of the antisera suspension the blots were washed twice for 10 min each at room temperature in TTBS. Thereafter, each blot was incubated with 100 ml TTBS supplemented with 1% dried milk powder and 80 µl ^{125}I-labelled protein A solution (8.5 µCi $µg^{-1}$, 129 µCi ml^{-1}) for 1 h at room temperature. Following four 10 min washes with TTBS, blots were dried, wrapped in plastic foil and used for autoradiography. Specific bands were identified on the autoradiograms, and corresponding bands were cut from the blots and the incorporated radioactivity was determined in a scintillation counter. Radioactivity incorporated into bands from lanes where no membranes had been loaded was defined as non-specific binding and was subtracted from the total binding.

Pertussis toxin-catalyzed ADP-ribosylation was carried out as previously described in detail (Maisel *et al.*, 1990b). Briefly, aliquots of the lymphocyte membrane suspension (10 µl at 1 mg protein ml^{-1}) were incubated with aliquots of pre-activated pertussis toxin (13 µl at 18 µg toxin ml^{-1}) and reaction mixture (13 µl containing as final concentrations: 139 mM TrisHCl at pH 8, 13.9 mM thymidine, 1.4 mM ATP, 0.14 mM GTP, 3.4 mM $MgCl_2$, 1.4 mM EDTA, 13.9 mM dithiothreitol, 692 µM NADP and 1.4 µM [^{32}P]-NAD) for 1 h at 30°C. The reaction was stopped by addition of 36 µl sample buffer with subsequent boiling. Electrophoretic separation of proteins was performed on gels containing 17% acrylamide. Incorporation of radioactivity into bands from lanes where membranes and reaction mixture had been loaded without pertussis toxin was taken as non-specific incorporation and was subtracted from that in all other lanes.

Ca^{2+} measurements

Intracellular Ca^{2+} concentrations were determined using the fluorescent indicator dye Fura-2 with excitation alternating between 340 and 380 nm and emission recorded at 510 nm in a Hitachi F-2000 spectrofluorometer; experiments were performed in Krebs-Henseleit buffer containing 108 mM NaCl, 4.7 mM KCl, 1.3 mM $CaCl_2$, 1.2 mM $MgSO_4$, 1.2 mM KH_2PO_4, 24.9 mM $NaHCO_3$, and 11 mM glucose. Data were analysed by the ratio method with software provided by the fluorometer manufacturer; details have been described previously (Michel *et al.*, 1992).

Chemicals

[^{32}P]-NAD, [^{125}I]-protein A and the antisera RM/1 and AS/7 were from New England Nuclear, Fura-2 from Molecular Probes (Eugene, OR, U.S.A.), RPMI 1640 and L-glutamine were from ICN (Eschwege, Germany), foetal and newborn bovine serum were from Boehringer Mannheim (Mannheim, Germany), (±)-CGP 12,177 (1-[2-(3-carbamoyl-4-hydroxy) phenoxyethylamino]-3- [4-(1-methyl-4-trifluoromethyl-2-imidazolyl) phenoxy]-2-propanol methanesulphonate) was a gift of Ciba Geigy (Basel, Switzerland), and all other chemicals were from Sigma (Munich, Germany).

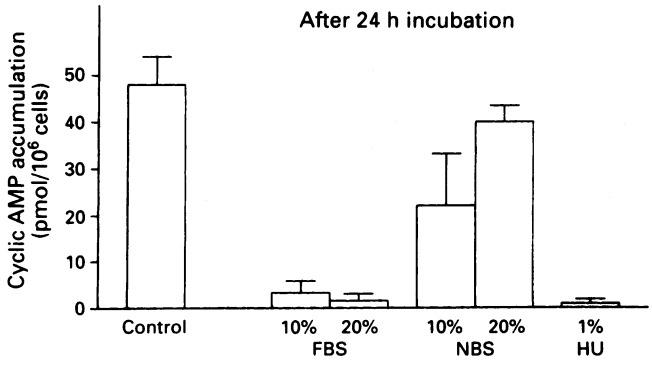

Figure 1 Effects of media supplements on prostaglandin E_2-stimulated cyclic AMP accumulation: Cyclic AMP accumulation stimulated by 10 µM prostaglandin E_2 was determined in intact freshly prepared lymphocytes (control) and in lymphocytes cultured for 24 h in RPMI medium supplemented with the indicated concentrations of foetal or newborn bovine serum (FBS and NBS, respectively) or the chemically defined medium supplement nutridoma HU. Data are mean ± s.e.mean of three experiments.

Data evaluation

Data are presented as mean ± s.e.mean. Statistical significance of differences was assessed by Student's paired t test if two groups were compared and by one-way analysis of variance followed by t tests with Bonferroni correction for multiple comparisons if more than two groups were compared; all statistical analysis was performed using the InStat programme (GraphPAD Software, San Diego, CA, U.S.A.) and a $P<0.05$ was considered significant. Concentration-response curves were analysed by non-linear regression analysis with interative fitting of the experimental data to sigmoidal curves using the InPlot programme (GraphPAD Software); in order to optimize estimates for EC_{50} and maximal effects a constant Hill-slope of one was assumed in these calculations. Pooled data of all experiments were fitted simultaneously, and the statistical significance of differences in EC_{50} and maximal effects were assessed by comparing the 95% confidence intervals (CI) for these parameters obtained during the fitting procedure. Additionally, the concentration-response curves of control and treated cells were compared by two-way analysis of variance to test whether treatment had significantly affected cyclic AMP formation at the $P<0.05$ level.

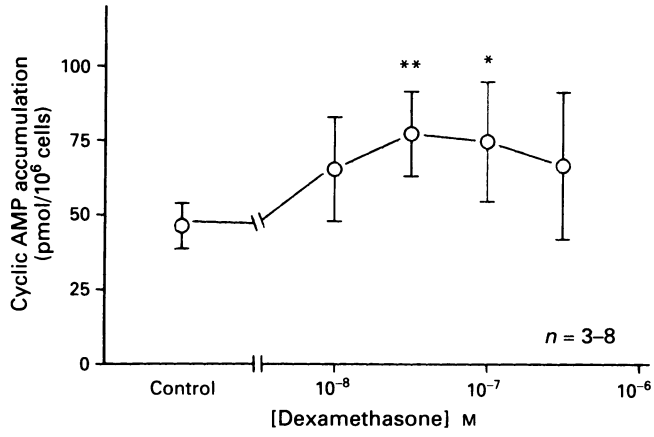

Figure 2 Effect of dexamethasone on prostaglandin E_2-stimulated cyclic AMP accumulation: Lymphocytes were cultured for 24 h in the absence (Control) or presence of the indicated concentrations of dexamethasone. Following washing of the cells, cyclic AMP accumulation stimulated by 10 μM prostaglandin E_2 was determined in intact lymphocytes. Data are mean ± s.e.mean of 3–8 experiments. $*P<0.05$, $**P<0.01$ vs. control in a paired two-tailed t test.

Results

In the first part of our study, we determined optimal conditions to assess glucocorticoid modulation of lymphocyte cyclic AMP formation by measuring 10 μM prostaglandin E_2-stimulated cyclic AMP accumulation in intact lymphocytes. Previous studies have demonstrated that resting human lymphocytes in culture rapidly lose their ability to generate cyclic AMP upon hormonal stimulation (Maisel *et al.*, 1989). Whereas 10% newborn and 10% and 20% foetal bovine serum or the chemically-defined serum substitute nutridoma HU, failed to prevent loss of prostaglandin-stimulated cyclic AMP formation, addition of 20% newborn bovine serum almost completely prevented it (Figure 1). Thus, all further lymphocyte incubations were performed in the presence of 20% newborn bovine serum. Under these conditions prostaglandin-stimulated cyclic AMP accumulation typically ranged between 40–50 pmol per 10^6 cells 15 min^{-1}.

We then tested whether and under what conditions the synthetic glucocorticoid, dexamethasone, enhanced prostaglandin-stimulated cyclic AMP accumulation in intact human lymphocytes. Incubation with 100 nM dexamethasone for 24 h enhanced prostaglandin-stimulated cyclic AMP accumulation by 24.0 ± 6.8 pmol per 10^6 cells 15 min^{-1} ($n=12$, $P=0.0049$). Shorter incubations resulted in smaller and statistically not significant enhancements (data not shown). Thus, a 24 h incubation was chosen for all further experiments. In concentration-response experiments maximal enhancement of prostaglandin-stimulated cyclic AMP accumulation occurred between 30 and 100 nM of dexamethasone (Figure 2). Thus, 100 nM of dexamethasone was used in all further experiments. This enhancing effect was specific for glucocorticoids since other steroid hormones including oestradiol, 5α-dihydro-testosterone and progesterone did not enhance prostaglandin-stimulated cyclic AMP accumulation (data not shown).

To define which part(s) of the receptor/G-protein/adenylyl cyclase catalyst complex had been regulated by dexamethasone, adenylyl cyclase stimulation experiments were performed in membranes obtained from dexamethaxone- and vehicle-treated lymphocytes. Dexamethasone treatment enhanced maximal prostaglandin E_2-stimulated adenylyl cyclase activity in lymphocyte membranes from 290 (95% CI: 221–359) to 561 (95% CI: 490–632) pmol mg^{-1} protein 10 min^{-1} ($P<0.0001$ in a two-way analysis of variance; Figure 3). The EC_{50} of prostaglandin E_2 was 24.3 μM (− log EC_{50} 4.61, 95% CI: 4.97–4.26) in control and 9.1 μM (− log EC_{50} 5.04, 95% CI:

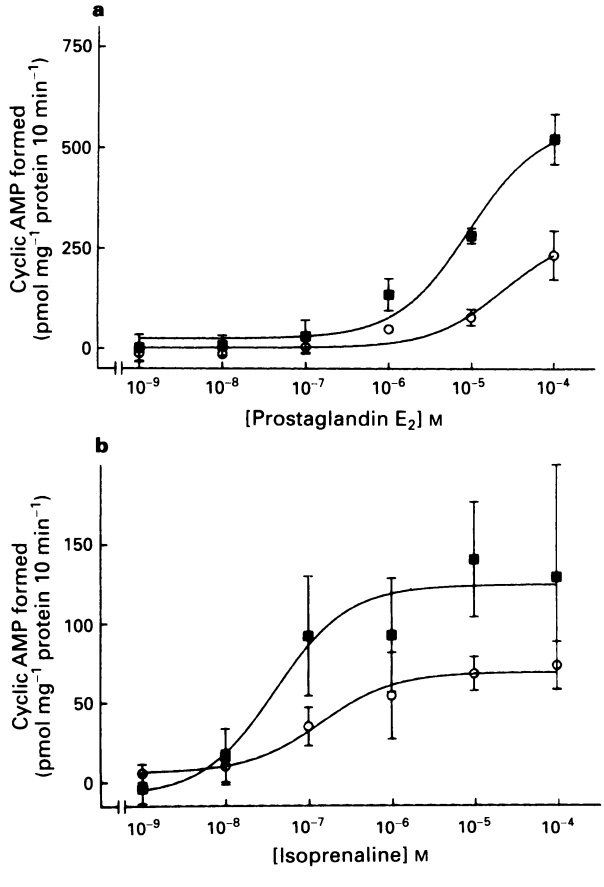

Figure 3 Effects of dexamethasone treatment on hormone-stimulated adenylyl cyclase activity: lymphocytes were cultured for 24 h in the absence (○) and presence (■) of 100 nM dexamethasone. Adenylyl cyclase activity was stimulated in membranes from these cells by prostaglandin E_2 (a) or isoprenaline (b). Basal adenylyl cyclase activity in the presence of 10 μM GTP has been subtracted from each value. Data are mean ± s.e.mean of four experiments. Concentration-response curves for prostaglandin E_2- and isoprenaline-stimulated cyclic AMP formation are significantly enhanced in membranes from dexamethasone-treated cells with $P<0.0001$ and $P=0.0180$, respectively, as determined by two-way analysis of variance.

5.28–4.80) in treated membranes (Figure 3). Similarly isoprenaline-stimulated adenylyl cyclase activity was enhanced from 68 (95% CI: 64–73) to 124 (95% CI: 109–138) pmol mg^{-1} protein 10 min^{-1} ($P = 0.0180$ in a two-way analysis of variance; Figure 3). The EC_{50} for isoprenaline was 143 nM (– log EC_{50} 6.84, 95% CI: 7.06–6.63) in control and 40 nM (– log EC_{50} 7.40, CI: 7.83–6.97) in treated membranes (Figure 3).

Adenylyl cyclase stimulation by the receptor-independent G-protein activator, GTP (10 μM) was enhanced by glucocorticoid treatment from 236 ± 19 to 309 ± 27 pmol mg^{-1} protein 10 min^{-1} ($n = 29$, $P < 0.05$). Dexamethasone treatment also significantly enhanced maximal adenylyl cyclase stimulation by forskolin from 620 (95% CI: 606–635) to 949 (95% CI: 879–1020) pmol mg^{-1} protein 10 min^{-1} ($P = 0.0063$ in a two-way analysis of variance; Figure 4). The potency (– log EC_{50}) of forskolin was not significantly altered (6.18 [95% CI: 6.25–6.11] in membranes from control and 6.07 [95% CI: 6.27–5.87] in those from treated cells; Figure 4). Dexamethasone-treatment also significantly enhanced maximal adenylyl cyclase stimulation by $MnCl_2$ from 371 (95% CI: 347–394) in control to 673 (95% CI: 645–701) pmol mg^{-1} protein 10 min^{-1} in treated cells ($P = 0.0074$ in a two-way analysis of variance; Figure 4). Dexamethasone treatment did not significantly alter the EC_{50} of $MnCl_2$ which was 5.2 mM (– log EC_{50} 2.28, 95% CI: 2.41–2.15) in control and 6.9 mM (– log EC_{50} 2.16, 95% CI: 2.23–2.08) in treated cells (Figure 4). Thus dexamethasone enhancement of adenylyl cyclase stimulation at the level of the catalyst was quantitatively similar to those at the G-protein or receptor level, indicating that the glucocorticoid had mainly regulated the adenylyl cyclase catalyst.

Therefore, we tested directly whether glucocorticoid regulation of adenylyl cyclase-coupled receptors and/or G-proteins were also detectable. Lymphocyte β_2-adrenoceptor density was determined under three conditions: in freshly prepared cells and in those cultured 24 h in the presence of vehicle or dexamethasone. Lymphocytes from each volunteer were always tested in parallel under all three conditions. Neither β_2-adrenoceptor density (Figure 5) nor affinity for the radioligand differed significantly among groups (15.9 ± 0.5 pM in fresh cells, 17.0 ± 1.8 pM in vehicle-treated cells, and 15.4 ± 0.7 pM in dexamethasone-treated cells, $n = 4$). Thus, glucocorticoid regulation of lymphocyte β_2-adrenoceptors was not detectable under our conditions.

Next we assessed the effect of dexamethasone treatment on lymphocyte G-protein α-subunit expression. The $G_{s\alpha}$ antiserum RM/1 recognized a double band in lymphocyte membranes (apparent molecular weights 42 and 44 kDa) with the lower band dominating. Both bands were specific since they were not seen in membranes from cyc^- cells (data not shown). The $G_{i\alpha}$ antiserum AS/7 recognized a single band with an apparent molecular weight of 39 kDa. Pertussis toxin catalyzed the incorporation of ^{32}P into a single band with an apparent molecular weight of 39 kDa. The amounts of ^{125}I-labelled protein A and ^{32}P incorporated into these specific bands were similar in membranes from control and dexamethasone-treated cells in all three assays (Table 1). Thus, glucocorticoid regulation of lymphocyte α-subunits of G_s or G_i was not detectable under our conditions.

Finally, we tested the relevance of sensitized cyclic AMP formation for hormonal modulation of lymphocyte function. An early event in prostaglandin E_2 suppression of lymphocyte activation is inhibition of mitogen-stimulated Ca^{2+} increases which is mediated by cyclic AMP (van Tits *et al.*, 1991; Michel *et al.*, 1992). The inhibition of concanavalin A-stimulated Ca^{2+} increases by 1 μM prostaglandin E_2 was doubled in dexamethasone-treated compared to vehicle-treated lymphocytes (Figure 6).

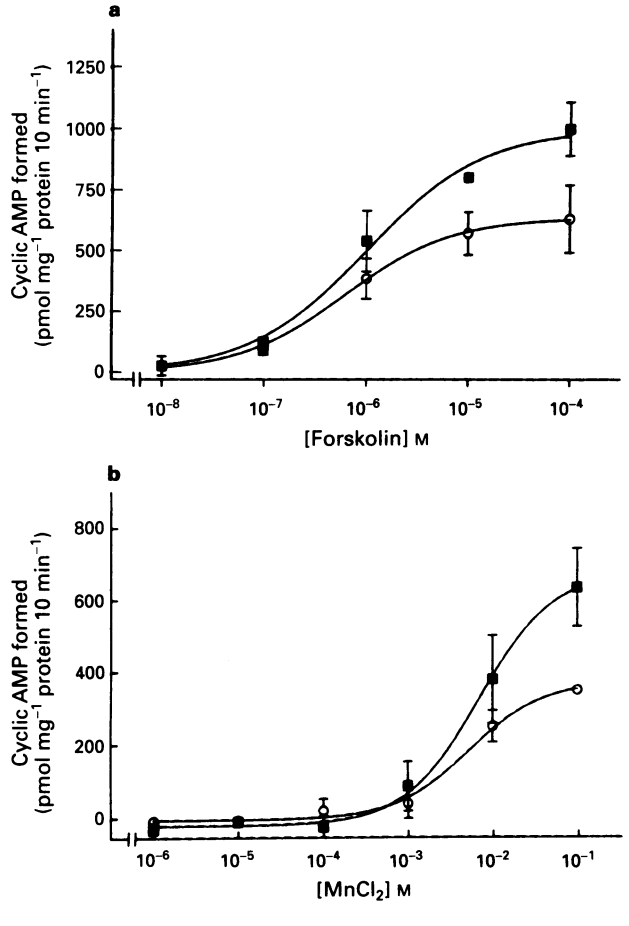

Figure 4 Effects of dexamethasone treatment on receptor-independent stimulation of adenylyl cyclase: lymphocytes were cultured for 24 h in the absence (○) and presence (■) of 100 nM dexamethasone. Adenylyl cyclase activity was stimulated in membranes from these cells by forskolin (a) or $MnCl_2$ (b). Basal adenylyl cyclase activity in the presence of 10 μM GTP has been subtracted from each value. Data are mean ± s.e.mean of four experiments. Concentration-response curves for forskolin- and $MnCl_2$-stimulated cyclic AMP formation are significantly enhanced in membranes from dexamethasone-treated cells with $P = 0.0063$ and $P = 0.0074$, respectively, as determined by two-way analysis of variance.

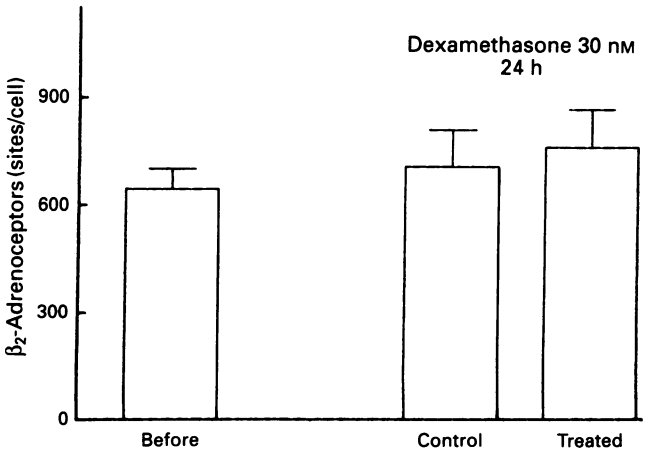

Figure 5 Effect of dexamethasone treatment on lymphocyte β_2-adrenoceptor density: lymphocyte β_2-adrenoceptor density was determined by saturation binding experiments with [^{125}I]-iodocyanopindolol in freshly prepared lymphocytes (Before), and cells which had been cultured for 24 h in the absence (Control) or presence (Treated) of 30 nM dexamethasone. Data are mean ± s.e.mean of four paired experiments and are expressed as [^{125}I]-iodocyanopindolol binding sites/cell.

Table 1 Effect of dexamethasone treatment on lymphocyte G-protein α-subunits

	Control	*Dexamethasone-treated*
Immunodetectable $G_{s\alpha}$	27,277 ± 2490	31,165 ± 2097
Immunodetectable $G_{i\alpha}$	97,937 ± 5741	100,425 ± 8750
Pertussis toxin substrates	4,608 ± 645	5,300 ± 885

Resting human lymphocytes were cultured for 24 h in the absence (control) or presence of 100 nM dexamethasone. Thereafter, G-protein α-subunits were determined in a membrane preparation by quantitative Western blotting or pertussis toxin-catalyzed ADP-ribosylation. Data are mean ± s.e.mean of six experiments. Immunodetectable α-subunits are given as c.p.m. of [^{125}I]-protein A specifically bound per mg lymphocyte membrane protein, pertussis toxin substrates are given as fmol ^{32}P specifically incorporated per mg membrane protein. None of the differences was statistically significant.

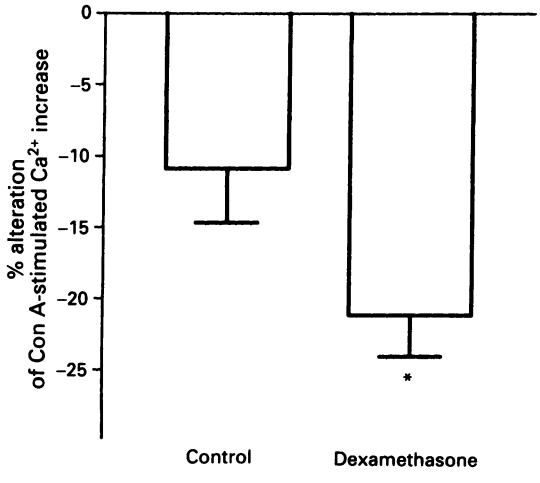

Figure 6 Effects of dexamethasone treatment on inhibition of concanavalin A-stimulated Ca^{2+} increases by prostaglandin E_2: 30 s following addition of 1 μM prostaglandin E_2 or vehicle, concanavalin A (100 μg ml^{-1})-stimulated Ca^{2+} increases were determined in Fura-2 loaded lymphocytes. We calculated % inhibition by the prostaglandin from Ca^{2+} increases in its absence and presence. Parallel experiments were performed in cells which had been cultured for 24 h in the absence (Control) or presence of 100 nM dexamethasone. Data are mean ± s.e.mean from 12 paired experiments with a duplicate determination each in the absence and presence of the prostaglandin. *$P<0.05$ in dexamethasone- vs. vehicle-treated lymphocytes.

Discussion

The cyclic AMP/cyclic AMP-dependent protein kinase system is an important modulator of lymphocyte activation, proliferation, differentiation and effector functions (Bourne *et al.*, 1974; Kammer, 1988). Formation of cyclic AMP is controlled by a cascade consisting of receptors, the stimulatory and inhibitory G-proteins G_s and G_i, and the adenylyl cyclase catalyst. Expression of each component can be dynamically regulated to alter the overall responsiveness of the cascade. Glucocorticoids exert a permissive effect on cyclic AMP-elevating agents in various cell types (Malbon *et al.*, 1988). Therefore, we hypothesized that glucocorticoids might exert their immunomodulatory effects at least partly by affecting cyclic AMP formation.

Previous work had demonstrated that resting human lymphocytes in culture rapidly lose their ability to generate cyclic AMP in response to hormonal stimulation (Maisel *et al.*, 1989). Our data demonstrate that in contrast to a number of other medium supplements, addition of 20% newborn bovine serum can at least partly prevent that loss of responsiveness. Although this addition was sufficient to detect and quantify prostaglandin E_2-stimulated cyclic AMP generation, these conditions may still be suboptimal compared to freshly isolated cells. This may limit the extrapolation of our data to *in vivo* conditions.

Using these culture conditions we demonstrate that the synthetic glucocorticoid, dexamethasone enhances prostaglandin E_2-stimulated cyclic AMP formation in human cultured lymphocytes. Similar enhancement has previously been detected in non-lymphoid cell types (Rodan & Rodan, 1986; Rizzoli & Bonjour, 1987; Chang & Bourne, 1987). The time- and concentration-dependency for the enhancing effect of dexamethasone in human lymphocytes were similar to those reported for dexamethasone effects in other model systems, notably for the enhancement of hormone-stimulated cyclic AMP formation in ROS 17/2.8 cells (Rodan & Rodan, 1986). Optimal stimulatory conditions were then used to determine which parts of the receptor/G-protein/adenylyl cyclase cascade are affected by dexamethasone exposure. This was done in two ways: on the one hand, we performed functional tests on adenylyl cyclase responsiveness using agonists which act on different levels of the receptor/G-protein/adenylyl cyclase cascade; on the other hand, we quantified directly individual components such as receptors and G-protein subunits.

We have used the receptor agonists, prostaglandin E_2 and isoprenaline, to test the whole cascade, GTP as a direct G-protein activator, forskolin as a direct adenylyl cyclase catalyst activator which also has some G-protein effects, and Mn^{2+} as a direct adenylyl cyclase catalyst activator. Treatment with dexamethasone did not significantly alter the potency of any agonist. On the other hand dexamethasone enhanced the maximal adenylyl cyclase responses to all tested agonists. These enhancements were quantitatively similar for all agonists. Since forskolin and $MnCl_2$ stimulate adenylyl cyclase distal to receptors and G-proteins, our data indicate that dexamethasone treatment might primarily affect the adenylyl cyclase catalyst. Whether this is due to increased expression of the catalyst, to an altered enzymatic activity of the enzyme, or both cannot be decided from the present data.

To support this indirect conclusion, we have also directly tested whether dexamethasone treatment affects the expression of lymphocyte β_2-adrenoceptors and/or G-protein α-subunits. Our data demonstrate that dexamethasone-treatment did not significantly alter the number of β_2-adrenoceptors (which mediate the stimulatory effects of isoprenaline) in our model. Glucocorticoids also failed to alter human lymphocyte β_2-adrenoceptor expression *in vivo* (Brodde *et al.*, 1985). The observation that human lymphocyte β_2-adrenoceptors are not regulated by glucocorticoids despite the presence of a glucocorticoid-response element in the regulatory domain of the human β_2-adrenoceptor gene (Hadcock *et al.*, 1989) may be related to the known tissue-dependency of glucocorticoid effects (Malbon *et al.*, 1988).

Cyclic AMP formation could be sensitized at the G-protein level by increased G_s or decreased G_i. Confirming the above functional data, direct quantification of G_s and G_i α-subunits by immunoblotting and ADP-ribosylation did not detect significant increases in G_s or decreases in G_i expression. In RBL-2H3 cells, a rat cell line which is used as a model for mast cells, dexamethasone-treatment also failed to alter expression of G_s or G_i at the protein or the mRNA level (Hide *et al.*, 1991). In contrast glucocorticoids enhance G_s expression in three cell lines which are not related to the white blood cell lineage, ROS 17/2.8 osteosarcoma cells (Rodan & Rodan, 1986), OK-cells derived from opossum kidney (Rizzoli & Bonjour, 1987) and GH_3-cells derived from rat pituitary (Chang & Bourne, 1987). We cannot explain the different behaviour of these cell types at present but speculate that it may be related to the fact that lymphocytes and RBL-2H3 cells belong to stem cell lineage whereas the other cell types do not. The question remains why glucocorticoids

enhance adenylyl cyclase activity in human lymphocytes at the level of the catalyst but apparently do not alter catalyst activity in other model systems. Although we cannot conclusively answer this question at present, we speculate that it may be related to the tissue-specificity of expression of adenylyl cyclase isoforms (Tang & Gilman, 1992). Whether and how such isoforms are differentially regulated by glucocorticoids remains to be studied.

In the final part of our study we asked whether enhanced hormonal stimulation of cyclic AMP formation in lymphocytes following dexamethasone treatment is functionally relevant. We have previously shown that prostaglandins and other cyclic AMP elevating agents inhibit mitogen-induced Ca^{2+} elevations in human lymphocytes (van Tits *et al.*, 1991; Michel *et al.*, 1992). This effect is indeed mediated by cyclic AMP since it is enhanced in the presence of phosphodiesterase inhibitors (van Tits *et al.*, 1991). Our present data demonstrate that the ability of a submaximally effective prostaglandin E_2 concentration to inhibit concanavalin A-stimulated Ca^{2+} increases is almost doubled in dexamethasone-treated lymphocytes. Similarly, cyclic AMP elevation by prostaglandin E_2 or forskolin and the glucocorticoid, methylprednisolone, enhance each others effects on DNA fragmentation and viability in mouse thymocytes (McConkey *et al.*, 1993). Finally, the glucocorticoid cytotoxicity against T-lymphocytes depends on the amount of cyclic AMP-dependent protein kinase present in such cells (Gruol *et al.*, 1989).

Taken together our data demonstrate that glucocorticoids enhance lymphocyte cyclic AMP formation by affecting the catalyst of adenylyl cyclase and that this enhancement is functionally relevant *in vitro*. Elevations of lymphocyte cyclic AMP inhibit lymphocyte activation, proliferation and effector functions *in vitro* (Bourne *et al.*, 1974; Kammer, 1988). *In vivo* cyclic AMP elevating agents such as the β-adrenoceptor agonists cause lymphopaenia in man (Maisel *et al.*, 1990a) and reduce splenic weight in rats (Murray *et al.*, 1993), whereas β-adrenoceptor agonists can increase the number of circulating T-cells in man (Maisel *et al.*, 1991). Whether enhanced lymphocyte cyclic AMP formation is at least partly relevant for the immunosuppressive effects of glucocorticoids *in vivo* cannot be answered from the present *in vitro* data. However, prostaglandin E_1-, GTP-, and forskolin-stimulated adenylyl cyclase activity are also enhanced in lymphocytes obtained from patients treated with glucocorticoids *in vivo* (Michel & Brodde, 1989). Thus, the mechanisms discussed above may also operate *in vivo* in a clinical setting. Their functional role for immunosuppression remain to be assessed.

The skilful technical assistance of Mrs M. Michel-Reher and Mrs A. Thesing is gratefully acknowledged.

References

ANASTASSIOU, E.D., PALIOGIANNI, F., BALOW, J.P., YAMADA, H. & BOUMPAS, D.T. (1992). Prostaglandin E_2 and other cyclic AMP-elevating agents modulate IL-2 and IL-2Rα gene expression at multiple levels. *J. Immunol.*, **148**, 2845–2852.

BOURNE, H.R., LICHTENSTEIN, L.M., MELMON, K.L., HENNEY, C.S., WEINSTEIN, Y. & SHEARER, G.M. (1974). Modulation of inflammation and immunity by cAMP: receptors for vasoactive hormones and mediators of inflammation regulate many leukocyte functions. *Science*, **184**, 19–28.

BÖYUM, A. (1968). Isolation of mononuclear cells and granulocytes from human blood. *Scand. J. Lab. Invest.*, **21**, 77–89.

BRADFORD, M.M. (1976). A rapid and sensitive method for the quantitation of microgram quantities of protein utilizing the principle of protein-dye binding. *Anal. Biochem.*, **72**, 248–254.

BRODDE, O.-E., BECKERINGH, J.J. & MICHEL, M.C. (1987). Human heart β-adrenoceptors: a fair comparison with lymphocyte β-adrenoceptors? *Trends Pharmacol. Sci.*, **8**, 403–407.

BRODDE, O.-E., BRINKMANN, M., SCHEMUTH, R., O'HARA, N. & DAUL, A. (1985). Terbutaline-induced desensitization of human lymphocyte β-adrenoceptors. Accelerated restoration of β-adrenoceptor responsiveness by prednisone and ketotifen. *J. Clin. Invest.*, **76**, 1096–1101.

BURNETTE, W.N. (1981). 'Western blotting': electrophoretic transfer of proteins from sodium dodecyl sulfate-polyacrylamide gels to unmodified nitrocellulose and radiographic detection with antibody and radioiodinated protein A. *Anal. Biochem.*, **112**, 195–203.

CHANG, F.-H. & BOURNE, H.R. (1987). Dexamethasone increases adenylyl cyclase activity and expression of the α-subunit of G_s in GH_3 cells. *Endocrinol.*, **121**, 1711–1715.

FLOWER, R.J. (1988). Lipocortin and the mechanism of action of the glucocorticoids. *Br. J. Pharmacol.*, **94**, 987–1015.

GRUOL, D.J., RAJAH, F.M. & BOURGEOIS, S. (1989). Cyclic AMP-dependent protein kinase modulation of the glucocorticoid-induced cytolytic response in murine T-lymphoma cells. *Mol. Endocrinol.*, **3**, 2119–2127.

HADCOCK, J.R., WANG, H.-Y. & MALBON, C.C. (1989). Agonist-induced destabilization of β-adrenergic receptor mRNA. Attenuation of glucorticoid-induced up-regulation of β-adrenergic receptors. *J. Biol. Chem.*, **264**, 19928–19933.

HIDE, M., ALI, H., PRICE, S.R., MOSS, J. & BEAVEN, M.A. (1991). GTP-binding protein $G_{\alpha z}$: its down-regulation by dexamethasone and its credentials as a mediator of antigen-induced responses in RBL-2H3 cells. *Mol. Pharmacol.*, **40**, 473–479.

KAMMER, G.M. (1988). The adenylate cyclase-cAMP-protein kinase A pathway and regulation of immune response. *Immunol. Today*, **9**, 222–228.

LAEMMLI, U.K. (1970). Cleavage of structural proteins during the assembly of the head of bacteriophage T4. *Nature*, **227**, 680–685.

LEVITZKI, A. (1988). From epinephrine to cyclic AMP. *Science*, **241**, 800–806.

MAISEL, A.S., FOWLER, P., REARDEN, A., MOTULSKY, H.J. & MICHEL, M.C. (1989). A new method for isolation of human lymphocyte subsets reveals differential regulation of β-adrenergic receptors by terbutaline treatment. *Clin. Pharmacol. Ther.*, **46**, 429–439.

MAISEL, A.S., KNOWLTON, K.U., FOWLER, P., REARDEN, A., ZIEGLER, M.G., MOTULSKY, H.J., INSEL, P.A. & MICHEL, M.C. (1990a). Adrenergic control of circulating lymphocyte subpopulations. Effects of congestive heart failure, dynamic exercise, and terbutaline treatment. *J. Clin. Invest.*, **85**, 462–467.

MAISEL, A.S., MICHEL, M.C., INSEL, P.A., ENNIS, C., ZIEGLER, M.G. & PHILLIPS, C. (1990b). Pertussis toxin treatment of whole blood. A novel approach to assess G protein function in congestive heart failure. *Circulation*, **81**, 1198–1204.

MAISEL, A.S., MURRAY, D., LOTZ, M., REARDEN, A., IRWIN, M. & MICHEL, M.C. (1991). Propranolol treatment affects parameters of human immunity. *Immunopharmacol.*, **22**, 157–164.

MALBON, C.C., RAPIEJKO, P.J. & WATKINS, D.C. (1988). Permissive hormone regulation of hormone-sensitive effector systems. *Trends Pharmacol. Sci.*, **9**, 33–36.

MCCONKEY, D.J., ORRENIUS, S., OKRET, S. & JONDAL, M. (1993). Cyclic AMP potentiates glucocorticoid-induced endogenous endonuclease activation in thymocytes. *FASEB J.*, **7**, 580–585.

MICHEL, M.C. & BRODDE, O.-E. (1989). Lymphocyte adenylate cyclase activity in immunosuppressed patients. *Eur. J. Clin. Pharmacol.*, **37**, 41–43.

MICHEL, M.C., BRODDE, O.-E. & INSEL, P.A. (1993a). Are cardiac G-proteins altered in rat models of hypertension? *J. Hypertension*, **11**, 355–363.

MICHEL, M.C., FETH, F., SUNDERMANN, M., RASCHER, W. & BRODDE, O.-E. (1993b). β-Adrenergic desensitization in SK-N-MC cells, a human cell line containing a homogeneous population of β_1-adrenoceptors. *J. Auton. Pharmacol.*, **13**, 425–438.

MICHEL, M.C., VAN TITS, L.J.H., TRENN, G., SYKORA, J. & BRODDE, O.-E. (1992). Dissociation between phytohemagglutinin-stimulated generation of inositol phosphates and Ca^{2+} increase in human mononuclear leukocytes. *Biochem. J.*, **285**, 137–141.

MURRAY, D.R., POLIZZI, S.M., HARRIS, T., WILSON, N., MICHEL, M.C. & MAISEL, A.S. (1993). Prolonged isoproterenol treatment alters immunoregulatory cell traffic and function in the rat. *Brain Behav. Immunol.*, **7**, 47–62.

NORTHROP, J.P., CRABTREE, G.R. & MATTILA, P.S. (1992). Negative regulation of interleukin 2 transcription by the glucocorticoid receptor. *J. Exp. Med.*, **175**, 1235–1245.

RIZZOLI, R. & BONJOUR, J.-P. (1987). Effect of dexamethasone on parathyroid hormone stimulation of cyclic AMP in an opossum kidney cell line. *J. Cell. Physiol.*, **132**, 517–523.

RODAN, W.B. & RODAN, G.A. (1986). Dexamethasone effects on β-adrenergic receptors and adenylate cyclase regulatory proteins G_s and G_i in ROS 17/2.8 cells. *Endocrinol.*, **118**, 2510–2518.

STERNWEIS, P.C. & GILMAN, A.G. (1979). Reconstitution of catecholamine-sensitive adenylate cyclase. Reconstitution of the uncoupled variant of the S49 lymphoma cell. *J. Biol. Chem.*, **254**, 3333–3340.

TANG, W.-J. & GILMAN, A.G. (1992). Adenylyl cyclases. *Cell*, **70**, 869–872.

TRACEY, D.E., HARDEE, M.M., RICHARD, K.A. & PASLAY, J.W. (1988). Pharmacological inhibition of interleukin-1 activity on T cells by hydrocortisone, cyclosporine, prostaglandins, and cyclic nucleotides. *Immunopharmacol.*, **15**, 47–62.

VAN TITS, L.J.H., MICHEL, M.C., MOTULSKY, H.J., MAISEL, A.S. & BRODDE, O.-E. (1991). Cyclic AMP counteracts mitogen-induced inositol phosphate generation and increases in intracellular Ca^{2+}-concentrations in human lymphocytes. *Br. J. Pharmacol.*, **103**, 1288–1294.

(Received April 8, 1994
Accepted May 4, 1994)

Br. J. Pharmacol (1994), **113**, 247–253

Anti-ischaemic efficacy of a nitric oxide synthase inhibitor and a N-methyl-D-aspartate receptor antagonist in models of transient and permanent focal cerebral ischaemia

[1]D.A. Dawson, D.I. Graham, J. McCulloch & I.M. Macrae

Wellcome Surgical Institute and Hugh Fraser Neuroscience Laboratories, University of Glasgow, Glasgow

1 We have recently developed a new model of transient focal ischaemia in the rat utilising topical application of endothelin-1 to the left middle cerebral artery (MCA). In order to validate this approach the present study assessed the neuroprotective efficacy of the NMDA receptor antagonist dizocilpine (MK-801) in the endothelin-1 model. The anti-ischaemic efficacy of the nitric oxide (NO) synthase inhibitor N^G-nitro-L-arginine methyl ester (L-NAME) was subsequently evaluated, and contrasted with its efficacy against permanent focal ischaemia, to determine the utility of the endothelin-1 model for identification of novel pharmacoprotective agents.

2 MK-801 (0.12 mg kg^{-1} bolus, 108 $\mu g\ kg^{-1}\ h^{-1}$ infusion i.v., either 1 or 2.5 h pre-transient MCA occlusion (MCAO)) induced hypotension that persisted for approximately 1.5 h so that mean arterial blood pressure (MABP) at the time of MCAO was significantly lower in the 1 h group compared with control (MABP: 86 ± 11, 68 ± 6 and 84 ± 4 mmHg (mean ± s.d.) for saline, 1 h MK-801 and 2.5 h MK-801 groups respectively). The 2.5 h pretreatment schedule resulted in significant reduction (71%) in the volume of hemispheric damage (assessed 4 h post onset of ischaemia) while the 1 h pretreatment schedule did not (volumes of hemispheric damage: 59 ± 38, 51 ± 51 and 17 ± 28 mm^3 for saline, 1 h and 2.5 h MK-801 groups).

3 Thus the considerable neuroprotective effect of MK-801 in the endothelin-1 model of transient focal cerebral ischaemia was highly sensitive to drug-induced hypotension. This result is in contrast to previous studies of permanent MCAO where MK-801-induced hypotension did not compromise its neuroprotective action.

4 L-NAME (3 mg kg^{-1}, i.v. 30 min pre-MCAO) moderately, but significantly, reduced (16%) the volume of ischaemic damage 4 h post-permanent MCA occlusion, whereas the 29% reduction in volume of damage achieved in the model of transient focal ischaemia did not attain significance due to the greater variability associated with this model. L-NAME did not significantly alter MABP in either model.

5 The modest neuroprotection achieved with NO synthase inhibition suggests NO is of relatively minor importance as a mediator of neurotoxicity following permanent focal cerebral ischaemia. In addition the comparable efficacy of L-NAME against transient focal ischaemia suggests the presence of reperfusion does not enhance the contribution of NO to neuronal injury in the acute (4 h) phase following a focal ischaemic insult.

Keywords: Transient focal ischaemia; glutamate; MK-801; nitric oxide; L-NAME; endothelin-1

Introduction

Animal models of permanent middle cerebral artery (MCA) occlusion have been used extensively to study focal cerebral ischaemia. In particular the repeated demonstration of the anti-ischaemic efficacy of glutamate receptor antagonists in these models has led to the elucidation of the important role of excitotoxic mechanisms in mediating focal cerebral ischaemic damage. However, in man spontaneous resolution of embolic stroke and increased use of thrombolytic therapy means reperfusion following stroke is more common than persistence of the occlusion (Ringelstein *et al.*, 1992). Thus models of transient focal ischaemia have now been developed (see Macrae, 1992, for review) to assess the physiological significance of reperfusion to cerebral injury. We have previously characterized a novel model of transient MCA occlusion in the rat that utilises the potent vasoconstrictor peptide, endothelin-1, to induce temporary occlusion of the MCA (Macrae *et al.*, 1993b). Our model involves direct topical application of endothelin-1 to the exposed proximal portion of the MCA, a procedure that results in profound ischaemia followed by slow, progressive reperfusion that has been characterized over the first 4 h following endothelin-1 application (Macrae *et al.*, 1993b; Gartshore *et al.*, 1994). This model should not be confused with an alternative approach that uses intraparenchymal injection of endothelin-1 to induce cerebral ischaemia (Sharkey *et al.*, 1993). This alternative model (Sharkey *et al.*, 1993) is associated with a different temporal profile of blood flow changes (i.e. profound ischaemia sustained for over 3 h) and as such is more comparable to permanent than transient focal ischaemia.

The development of the endothelin-1 model of transient focal ischaemia and also other models of transient ischaemia means pharmacotherapies with proven efficacy against permanent focal ischaemic damage can now begin to be evaluated in the more clinically relevant context of ischaemia-reperfusion. However, models of transient focal ischaemia are by their very nature associated with greater variability than permanent ischaemia since the incorporation of a period of reperfusion into the design introduces an additional level of complexity above that associated with the ischaemic phase. Thus alterations in key physiological parameters such as blood pressure and cerebral blood flow (CBF) during both the ischaemic and reperfusion phases may impact on final outcome, and it may prove more difficult to demonstrate

[1] Author for correspondence at: Wellcome Surgical Institute, University of Glasgow, Garscube Estate, Bearsden Road, Glasgow G61 1QH.

neuroprotective efficacy in the context of transient compared with permanent MCA occlusion. We therefore wished to compare the efficacy of different treatment strategies in permanent and transient MCA occlusion. The endothelin-1 model of transient focal ischaemia was first validated by assessing the efficacy of the N-methyl-D-aspartate (NMDA) receptor antagonist dizocilpine (MK-801), a drug with proven efficacy against permanent focal ischaemic damage (see McCulloch *et al.*, 1991 for review). The efficacy of a low dose of the nitric oxide (NO) synthase inhibitor N^G-nitro-L-arginine methyl ester hydrochloride (L-NAME) was then compared in our models of permanent and transient MCA occlusion.

It has recently been proposed that glutamatergic excitotoxicity is mediated by NO. Inhibitors of NO synthase antagonize glutamate-induced neuronal injury both *in vitro* (Dawson *et al.*, 1991) and *in vivo* (Fujisawa *et al.*, 1993), but reports of their efficacy in models of permanent focal ischaemia are contradictory (Buisson *et al.*, 1992; Dawson *et al.*, 1992; Yamamoto *et al.*, 1992). The failure to observe neuroprotection consistently with NO synthase inhibitors *in vivo* may partly derive from the dose-dependent cerebral hypoperfusion induced by these drugs (Tanaka *et al.*, 1991; Macrae *et al.*, 1993a). We have previously demonstrated that a relatively high dose of L-NAME (2×30 mg kg^{-1}) has no significant effect on volume of ischaemic damage following permanent MCA occlusion (Dawson *et al.*, 1992). Therefore in the present study the efficacy of a lower dose of L-NAME (3 mg kg^{-1}) was assessed.

Methods

Surgical preparation and induction of ischaemia

Adult male Sprague-Dawley rats were anaesthetized with halothane (5%) in nitrous oxide:oxygen (70:30). Anaesthesia was subsequently maintained with 1% halothane. A tracheostomy was performed and the rats were artificially ventilated via a small respirator pump. The femoral arteries and veins were cannulated for blood sampling, continuous monitoring of blood pressure, and drug administration. Rectal temperature was maintained around 37°C by means of a heating blanket.

For both permanent and transient MCA occlusion, the left MCA was exposed using the sub-temporal approach previously described (Tamura *et al.*, 1981) with the exception that the zygomatic arch was left intact. A fine temperature probe was inserted into the ipsilateral temporalis muscle to estimate brain temperature during exposure and occlusion of the MCA. For permanent MCA occlusion the artery was occluded by bipolar diathermy from where it crossed the inferior cerebral vein to proximal to the origin of the lenticulo-striate branch(es). The artery was then transected to confirm complete occlusion and prevent recanalisation. The method for induction of transient MCA occlusion has been described previously in detail (Macrae *et al.*, 1993b). Briefly the arachnoid membrane overlying the MCA was opened, then endothelin-1 (2.5 nmol in 25 µl water) was applied topically to the proximal portion of the artery. Constriction of the main artery and the lenticulo-striate branch(es) was verified via the operating microscope. Following induction of permanent or transient MCA occlusion, the temporalis muscle temperature probe was removed and the wound closed with sutures.

Quantification of ischaemic damage

Four hours following the onset of permanent or transient MCA occlusion the animals were perfusion-fixed with 40% formaldehyde:acetic acid:methanol (1:1:8) and the brains processed for histological quantification of ischaemic damage (Osborne *et al.*, 1987). Haematoxylin and eosin stained sections at 8 pre-selected stereotactic levels were examined under a light microscope. Regions showing ischaemic cell change and evidence of early infarction (Brown, 1977) were transcribed onto scale drawings normalised to the mean hemisphere volume (570 mm^3) for Sprague-Dawley rats of the weight used. Areas of damage on the line drawings were measured using an image analyser (Quantimet 970, Cambridge Instruments) and converted by integration to the total volume of ischaemic damage.

Experimental groups

In experiment 1, rats underwent transient MCA occlusion with MK-801 pretreatment. MK-801 was administered as a bolus dose (0.12 mg kg^{-1}, i.v.) followed by continuous intravenous infusion (108 µg kg^{-1} h^{-1} at 0.6 ml h^{-1}) throughout the remainder of the experimental period. MK-801 treatment was initiated either 1 h (1 h group, $n = 9$) or 2.5 h (2.5 h group, $n = 9$) prior to endothelin-1 application to the MCA. The control group ($n = 10$) received bolus injection of saline (1 mg kg^{-1}, i.v.) followed by continuous saline infusion (0.6 ml h^{-1}) initiated 1 h pre-MCA occlusion. In experiment 2, L-NAME (3 mg kg^{-1} i.v., $n = 6$) or an equivalent volume of saline ($n = 5$) was administered 30 min prior to permanent MCA occlusion. In experiment 3, L-NAME (3 mg kg^{-1}, i.v., $n = 14$) or saline ($n = 14$) were given 30 min prior to transient MCA occlusion.

Chemicals

N^G-nitro-L-arginine methyl ester hydrochloride (L-NAME) was purchased from Sigma Chemical Co., MK-801 (dizocilpine) was a generous gift from Merck, Sharp and Dohme Research Laboratories. All drugs were dissolved in saline and administered in a volume of 1 ml kg^{-1}.

Statistical analysis

Statistical comparison of blood pressure data was performed using repeated measure 2 way analysis of variance (ANOVA), with subsequent pairwise comparisons by Student's *t* tests with a Bonferroni correction factor for multiple comparisons. For experiment 1 (MK-801), volumes of ischaemic damage were compared by one way ANOVA with subsequent individual comparisons by Dunnett's *t* tests. For experiments 2 and 3 (L-NAME), volumes of ischaemic damage were compared with Student's *t* tests.

Results

Physiological variables

Physiological variables from the 3 separate experiments are shown in Table 1. Values for respiratory parameters were in the normal physiological ranges for all groups. Rectal and temporalis muscle temperatures at the time of MCA occlusion did not differ between the drug and relevant control groups.

Effect of MK-801 on blood pressure and volume of ischaemic damage

MK-801 induced significant hypotension ($P < 0.001$) that persisted for approximately 1.5 h, resulting in significantly lower mean arterial blood pressure (MABP) at the time of MCA occlusion for the group in which MK-801 treatment was initiated 1 h pre-MCA occlusion (Figure 1, Table 1). A similar level of hypotension was induced by MK-801 in the 2.5 h group, but the longer pretreatment interval meant that MABP had returned to control level in this group by the time of MCA occlusion (Figure 1, Table 1).

Table 1 Physiological variables for MK-801 or N^G-nitro-L-arginine methyl ester (L-NAME) pretreatment in reversible or permanent focal cerebral ischaemia

	Group 1			*Group 2*				*Group 3*		
	MCAO	*+1 h*	*+4 h*		*MCAO*	*+1 h*	*+4 h*	*MCAO*	*+1 h*	*+4 h*
MABP (mmHg)				MABP (mmHg)						
Control	86±3	86±2	88±2	Control	90±3	88±2	89±3	85±2	86±3	88±1
MK-801 (1h)	68±2	80±2	88±2	L-NAME	93±5	87±4	90±1	85±2	82±2	89±1
MK-801 (2.5h)	84±1	85±1	86±1							
$PaCO_2$ (mmHg)				$PaCO_2$ (mmHg)						
Control	39±1	37±1	38±1	Control	37±1	40±2	37±1	39±1	37±1	37±1
MK-801 (1h)	37±1	37±1	37±1	L-NAME	36±2	35±2	35±1	35±1	38±1	37±1
MK-801 (2.5h)	38±1	36±1	37±1							
PaO_2 (mmHg)				PaO_2 (mmHg)						
Control	177±8	174±5	184±8	Control	212±14	209±9	220±14	171±8	177±7	184±6
MK-801 (1h)	176±7	180±9	185±5	L-NAME	204±10	199±13	208±10	167±5	174±7	178±7
MK-801 (2.5h)	179±10	177±9	174±3							
Rectal Temp. (°C)				Rectal temp (°C)						
Control	37.0±0.1	37.0±0.1	37.0±0.1	Control	37.0±0.1	37.1±0.1	37.0±0.0	37.2±0.1	37.1±0.1	37.0±0.0
MK-801 (1 h)	37.1±0.1	36.9±0.2	37.1±0.1	L-NAME	37.3±0.1	37.0±0.1	37.0±0.0	37.1±0.1	37.0±0.1	37.0±0.0
MK-801 (2.5h)	37.1±0.0	37.0±0.1	37.0±0.0							
Temporalis temp (°C)				Temporalis temp (°C)						
Control	36.7±0.1			Control	36.5±0.3			36.6±0.1		
MK-801 (1h)	36.7±0.1			L-NAME	36.8±0.2			36.5±0.1		
MK-801 (2.5h)	36.4±0.1									

Physiological variables for (1) MK-801 pretreatment prior to transient middle cerebral artery (MCA) occlusion (2) L-NAME pretreatment prior to permanent MCA occlusion and (3) L-NAME pretreatment prior to transient MCA occlusion. Physiological variables (except temporalis muscle temperature) were measured at the time of MCA occlusion (MCAO), and 1 h and 4 h post-MCA occlusion. Data are presented as mean ± s.e. mean.

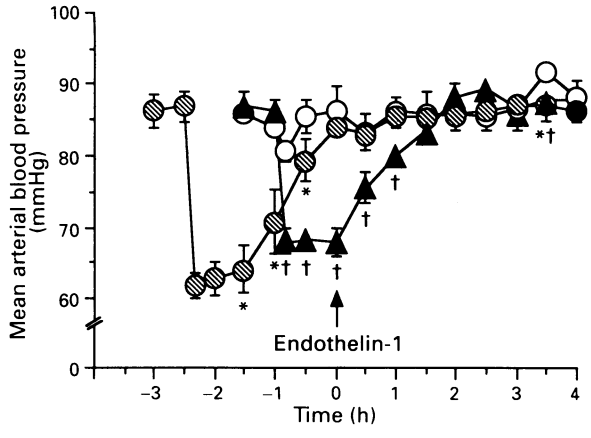

Figure 1 Time course for alterations in mean arterial blood pressure following MK-801 administered prior to transient middle cerebral artery (MCA) occlusion. MK-801 was administered as a bolus (0.12 mg kg^{-1}, i.v.) followed by continuous infusion (108 μg kg^{-1} h^{-1} at 0.6 ml h^{-1}). Treatment was initiated either 2.5 h (hatched symbols) or 1 h (solid symbols) prior to transient MCA occlusion induced by application of endothelin-1 to the exposed MCA. Data are presented as means ± s.e. mean. *$P<0.05$, †$P<0.05$ comparison with saline (open symbols) control at same time point for 2.5 h and 1 h groups respectively.

MK-801-treatment initiated 2.5 h pre-transient MCA occlusion markedly, and significantly, reduced the volumes of ischaemic damage in the whole hemisphere and caudate nucleus by 71% and 85% respectively (Figure 2). The volume of ischaemic damage in the cerebral cortex was reduced by 61% but this just failed to reach statistical significance at the 5% level. In contrast MK-801-treatment initiated 1 h pre-MCA occlusion did not significantly alter the volume of ischaemic damage in either whole hemisphere, cortex or caudate nucleus (Figure 2).

Effect of L-NAME on blood pressure and volume of ischaemic damage

Blood pressure was not significantly altered by administration of L-NAME so that MABP for L-NAME and saline groups were comparable at all time points including MCA occlusion (Figure 3, Table 1).

L-NAME (3 mg kg^{-1}, 30 min pre-MCA occlusion) significantly ($P<0.05$) reduced the volume of ischaemic damage measured 4 h post-permanent MCA occlusion in the whole hemisphere and cerebral cortex compared to saline control (Figure 4). The volume of ischaemic damage in the caudate nucleus was not significantly altered by L-NAME. Although significant, the neuroprotective effect obtained with L-NAME was relatively small with only a 16% reduction in the total volume of ischaemic damage.

In contrast L-NAME (3 mg kg^{-1}, 30 min pre-MCA occlusion) did not significantly reduce the volume of ischaemic damage assessed 4 h post-onset of transient MCA occlusion (Figure 4). There was however an obvious neuroprotective trend, with the volumes of damage reduced by 29%, 26% and 33% respectively in the whole hemisphere, cortex and caudate nucleus.

Discussion

Efficacy of MK-801 against transient focal cerebral ischaemia

The present study demonstrates that MK-801 pretreatment is neuroprotective in the endothelin-1 model of transient MCA occlusion. However, in contrast to permanent MCA occlusion, it appears that drug-induced hypotension present at the onset of ischaemia results in complete loss of the neuroprotective effect since the infusion of MK-801 initiated 2.5 h prior to MCA occlusion significantly reduced the volume of ischaemic damage while the infusion initiated 1 h pre-MCA occlusion did not. The dosing schedule employed in the current study attains a steady state plasma level of MK-801

within 60 min (Gill *et al.*, 1991; Willis *et al.*, 1991), therefore plasma concentrations of MK-801 at the time of MCA occlusion should have been equivalent in both drug groups, the only obvious difference being the relative blood pressures. Thus the lower blood pressure at onset of MCA occlusion in the 1 h MK-801 group appears to have increased the severity of the ischaemic insult and directly counteracted the neuroprotective action of the drug.

In addition to its peripheral action on blood pressure, MK-801 has marked effects on CBF which differ in conscious and anaesthetized animals (Park *et al.*, 1989; Nehls *et al.*, 1990; Roussel *et al.*, 1992) and which could potentially influence outcome following cerebral ischaemia. In conscious rats, MK-801 increases local CBF in specific regions including neocortex and caudate nucleus (Nehls *et al.*, 1990; Roussel *et al.*, 1992), while in artificially-ventilated, anaesthetized rats MK-801 induces widespread homogeneous reductions in CBF (Park *et al.*, 1989). However MK-801 does not induce further reductions in CBF in the ischaemic core region following permanent MCA occlusion in halothane-anaesthetized animals (Park *et al.*, 1989; Greenberg *et al.*, 1991). The cerebrovascular effects of MK-801 are therefore likely to have less impact on outcome following experimental ischaemia in which halothane anaesthesia is maintained (as in the present study) compared with studies in which animals are allowed to regain consciousness. Previous studies have

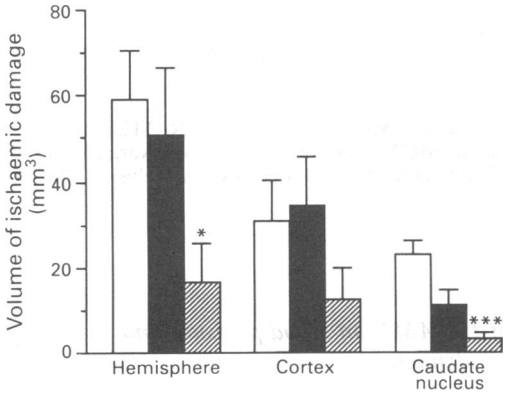

Figure 2 Effect of MK-801 on the volume of ischaemic damage induced by transient middle cerebral artery (MCA) occlusion. MK-801 pretreatment (0.12 mg kg^{-1} bolus, then 108 μg kg^{-1} h^{-1} at 0.6 ml h^{-1} i.v.) started 2.5 h prior to MCA occlusion (hatched column) significantly reduced the volume of ischaemic damage in the cerebral hemisphere and caudate nucleus. In contrast MK-801 treatment initiated only 1 h prior to MCA occlusion (solid column) did not significantly alter the ischaemic damage. Data are presented as means ± s.e. mean. *$P<0.05$, ***$P<0.001$ compared with saline control group (open column) respectively.

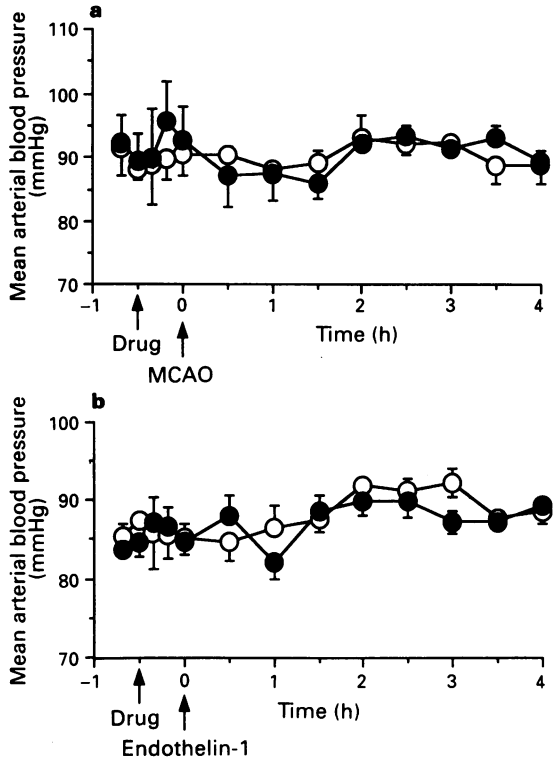

Figure 3 Mean arterial blood pressure following N^G-nitro-L-arginine methylester (L-NAME) administered 0.5 h prior to permanent or transient middle cerebral artery (MCA) occlusion. L-NAME (3 mg kg^{-1}, i.v., ●) pretreatment did not significantly alter blood pressure compared to the saline control group (○) for either (a) permanent MCA occlusion (MCAO) or (b) transient MCA occlusion induced by application of endothelin-1 to the MCA. Data are presented as means ± s.e. mean.

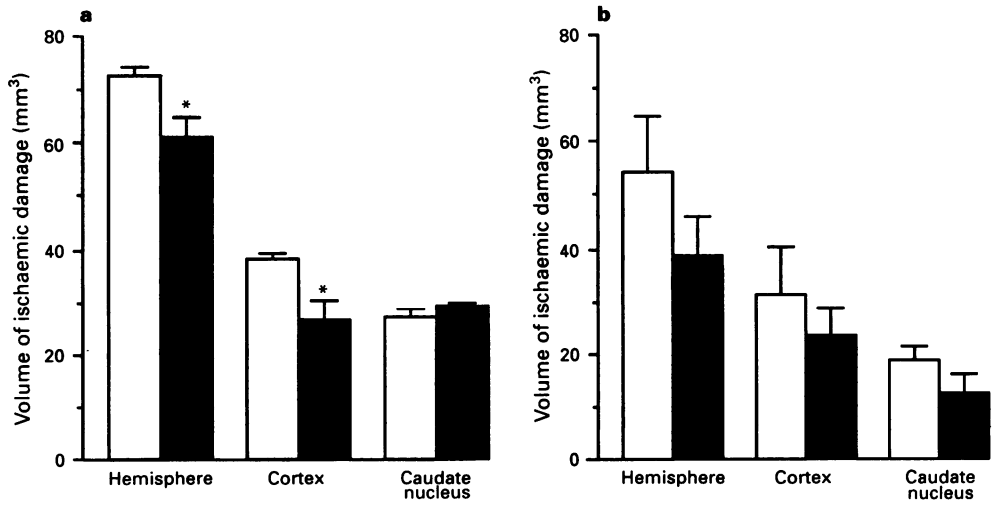

Figure 4 Effect of N^G-nitro-L-arginine methyl ester (L-NAME) on the volume of ischaemic damage induced by permanent and transient middle cerebral artery (MCA) occlusion. (a) L-NAME (3 mg kg^{-1}, i.v., solid columns) pretreatment significantly reduced the volume of ischaemic damage in the cerebral hemisphere and cortex following permanent MCA occlusion. (b) In contrast, L-NAME (3 mg kg^{-1}, i.v., solid columns) did not significantly alter the volume of ischaemic damage induced by transient MCA occlusion, although there was a moderate neuroprotective trend in both the cerebral hemisphere and caudate nucleus. Data are presented as means ± s.e. mean. *$P<0.05$ compared with relevant saline control group (open columns).

reported a beneficial action of MK-801 treatment initiated prior to or during the ischaemic phase of transient MCA occlusion in the normotensive rat (Yang *et al.*, 1991; Buchan *et al.*, 1992). However in these models the rats were conscious for most of the ischaemic period and the reduction in damage observed with MK-801 has been attributed to an increase in CBF in the ischaemic core region rather than a direct anti-excitotoxic action (Buchan *et al.*, 1992). Therefore to the best of our knowledge the present study represents the first demonstration of a significant neuroprotective action of MK-801 in a model of transient MCA occlusion in the normotensive rat, that is independent of the cerebrovascular effects of the drug and probably mediated by a direct anti-excitotoxic action.

Comparative efficacy of MK-801 in models of permanent and transient focal cerebral ischaemia

MK-801 administered pre- or up to 30 min post-permanent MCA occlusion significantly reduces the volume of ischaemic damage assessed at 4 h (Park *et al.*, 1988; Gill *et al.*, 1991) and significant neuroprotection can be achieved despite the presence of drug-induced hypotension at the time of MCA occlusion (Park *et al.*, 1988; Gill *et al.*, 1991). These results are in contrast to the present study where a similar degree of hypotension resulted in complete abolition of the neuroprotective effect of MK-801. Thus although we have demonstrated, in agreement with others (Dezsi *et al.*, 1992; Buchan *et al.*, 1992), that MK-801 can give significant neuroprotection against focal ischaemia-reperfusion injury, the most important aspect of our findings is that the observed neuroprotective effect is more highly sensitive to drug-induced hypotension than in permanent focal ischaemia. The outcome following transient MCA occlusion also appears more sensitive to alterations in other key physiological parameters such as temperature (Morikawa *et al.*, 1992a) than similar models of permanent MCA occlusion.

In models of permanent MCA occlusion the neuroprotective effect of MK-801 is predominantly restricted to the cerebral cortex with no (Gill *et al.*, 1991) or very minor (Park *et al.*, 1988) reduction in damage in the caudate nucleus due to the absence of collateral supply to this region (Gill *et al.*, 1991). In contrast in the present study MK-801 significantly, and markedly, reduced the volume of ischaemic damage in the caudate nucleus following transient MCA occlusion. Thus the restoration of CBF to the caudate nucleus following transient ischaemia renders this region potentially amenable to pharmacological intervention with efficacious drugs such as MK-801.

The role of nitric oxide in focal cerebral ischaemic damage

Permanent focal cerebral ischaemia As investigation into the biological roles of NO proceeds, it is becoming increasingly evident that NO influences a variety of physiological parameters that have the potential to either ameliorate or exacerbate cerebral ischaemic damage. To further complicate the situation, NO is now known to exist in 2 inter-changeable redox forms with distinct pro-excitotoxic (free radical form of NO) and anti-excitotoxic (nitrosonium ion form) actions (Lipton *et al.*, 1993). Endothelial-derived NO, produced immediately after the onset of ischaemia (Tominaga *et al.*, 1993) may be beneficial to outcome by inducing cerebral vasodilatation and improving CBF in the ischaemic region. This effect can be augmented by exogenously-derived NO that improves CBF following permanent MCA occlusion and significantly reduces infarct size (Morikawa *et al.*, 1992b,c; Zhang & Iadecola, 1993). In contrast non-selective inhibition of NO synthase in the immediate post-ischaemic period may induce cerebral hypoperfusion and increase the severity of an ischaemic insult. This may explain why we and others have previously reported no beneficial effect of relatively high doses of NO synthase inhibitors administered solely prior to or immediately following permanent MCA occlusion (Dawson *et al.*, 1993; Yamamoto *et al.*, 1993; Zhang & Iadecola, 1993).
($3\ mg\ kg^{-1}$), that does not significantly alter local CBF in the cortex or caudate nucleus (Macrae *et al.*, 1993a), induced only a relatively small, although significant, reduction in the volume of ischaemic damage assessed 4 h post-permanent MCA occlusion. This result suggests that NO is not a major mediator of neuronal injury in the acute (4 h) phase of permanent focal ischaemia and is supported by the observation that NO levels are only transiently elevated following permanent MCA occlusion, reaching a peak within 5–10 min of the onset of ischaemia and declining to basal levels within 1 h (Kader *et al.*, 1993; Malinski *et al.*, 1993).

The modest neuroprotective effect of L-NAME in the present study (16% reduction in the volume of ischaemic damage) is in direct contrast to the dramatic reductions in lesion size (50%) reported for repeated dosing of NOS inhibitors following permanent MCA occlusion in rats and mice (Nowicki *et al.*, 1991; Buisson *et al.*, 1992). However the apparent neuroprotective efficacy of NO synthase inhibitors in these studies may in fact reflect reduced NO-dependent oedema formation rather than neuronal survival *per se* since the method of quantification of ischaemic damage used in these studies was not corrected for brain swelling and NO synthase inhibitors have been shown to reduce oedema 48 h post-permanent MCA occlusion (Nagafuji *et al.*, 1992). Furthermore NOS inhibitors induce significant hypothermia in conscious rats (Macrae *et al.*, 1993a) which may also contribute to the apparent neuroprotective efficacy of NOS inhibition in conscious animals.

Transient focal cerebral ischaemia In contrast to permanent focal ischaemia, the restoration of CBF following transient focal ischaemia allows a more sustained increase in NO production during the reperfusion phase (Malinski *et al.*, 1993). Thus the potential contribution of NO to neuronal injury may be greater in the context of transient focal ischaemia. However, we were unable to demonstrate greater neuroprotection with L-NAME in transient compared with permanent focal ischaemia. Indeed, under broadly similar experimental conditions, the neuroprotective effect of L-NAME was comparable in both models (total volumes of tissue salvaged were $16\ mm^3$ and $12\ mm^3$ for transient and permanent MCA occlusion respectively), the only difference being that the reduction in tissue damage in the transient ischaemia model did not attain statistical significance due to the greater variability inherent in models of transient versus permanent MCA occlusion. Furthermore the efficacy of L-NAME was poor compared with MK-801 pretreatment in the same model (29% and 71% reductions in volume of damage for L-NAME and MK-801 respectively). These results suggest the contribution of NO to neuronal injury in the *acute* phase following a transient ischaemic insult is moderate and similar to that observed for permanent focal ischaemia. However, our results do not exclude the possibility that NO contributes to the maturation of the lesion in the late reperfusion phase since we have previously demonstrated that lesion volume continues to increase in our endothelin-1 model beyond the 4 h time point used in the present study (Dawson *et al.*, 1993). Indeed preliminary results from other laboratories would suggest that this is indeed the case (Cole *et al.*, 1993).

Several of the consequences of NO synthase inhibition may specifically detract from the inherent neuroprotective efficacy of L-NAME against transient focal ischaemic injury. For example L-NAME-induced vasoconstriction and enhancement of leucocyte adherence to vascular endothelium (Ma *et al.*, 1993) may impair restoration of CBF to previously ischaemic regions, while L-NAME may also increase extracellular glutamate levels during the reperfusion phase (Zhang *et al.*, 1993). Indeed in some methods of transient MCA occ-

lusion (e.g. the intraluminal thread model) L-NAME pretreatment can exacerbate infarct volume (Kuluz et al., 1993). However, L-NAME-induced exacerbation of endothelial damage induced by insertion and retraction of the intraluminal thread may be a major contributory factor to the poor outcome in this particular case. One of the main advantages of our endothelin-1 model of transient MCA occlusion is that mechanical damage to the MCA is avoided, allowing the demonstration of a small (although non-significant) neuroprotective effect of L-NAME pretreatment in the present study.

From this discussion it is evident that NO synthase inhibitors induce a range of physiological responses that can influence outcome following either transient or permanent focal ischaemia. The disparate findings reported in the literature concerning the neuroprotective efficacy of both NO synthase inhibitors and NO donors probably reflects differential interaction between these various factors, the balance of which is dependent on the particular experimental design utilised. However, the anti-ischaemic efficacy of NO synthase inhibitors may be improved in the near future with the development of selective NO synthase inhibitors (Moore et al., 1993) that would allow inhibition of neuronal and inducible NO synthase (putative mediators of excitotoxicity and oedema formation) while conserving endothelial NO synthase activity (to maintain CBF).

Variability in lesion size induced by transient MCA occlusion

In the present study the percentage reduction in ischaemic damage achieved with L-NAME in the transient MCA occlusion model was comparable to that observed in the permanent MCA occlusion model. However this result failed to attain statistical significance. This discrepancy is not surprising since all models of transient focal ischaemia are associated with greater variability than comparable methods of permanent focal ischaemia due to the incorporation of a period of reperfusion into the design (Macrae, 1992). Power analysis calculations ($\alpha = 0.05$, $\beta = 0.2$) have revealed that group sizes of approximately 100 animals would be necessary to detect the observed 29% reduction in total lesion volume demonstrated with L-NAME pretreatment against transient MCA occlusion. The time and expenditure necessary to conduct such a large study make it impractible to carry out. Furthermore we do not think completion of a larger study would improve the information gained from the present study with smaller group sizes, since it is evident from the results presented herein that, as for permanent MCA occlusion, the efficacy of L-NAME as a neuroprotective agent against acute ischaemic damage is considerably less than that of MK-801.

Although all models of transient focal ischaemia are more variable than their permanent counterparts, this comparative lack of power must be balanced against the maximum degree of pharmacoprotection that could potentially be demonstrated in the two model types. For permanent MCA occlusion only the penumbra region, where CBF is less severely reduced, will be amenable to pharmacological intervention. This means that even the most efficacious drugs such a MK-801 can only protect approximately 50% of the total tissue at risk (see Bullock & Fujisawa, 1992). In contrast, for transient MCA occlusion the restoration of CBF (providing it is initiated before ischaemic damage becomes irreversible) renders 100% of the tissue potentially salvagable. Thus in the present study, tissue damage in the caudate nucleus, an end artery region, was successfully reduced by MK-801 pretreatment whereas previous studies have shown that in the presence of permanent MCA occlusion this region is more resistant to neuroprotective agents. Thus highly efficacious drugs such as MK-801 which have the potential to reduce damage substantially (e.g. by over 70% as in the present study) will be able to achieve significant neuroprotection in models of transient focal ischaemia without resorting to large experimental groups.

This work was supported by the Wellcome Trust (Grant No. 034986). We thank the technical and secretarial staff of the department for invaluable assistance and Bayer AG for providing Neuroscience Library facilities.

References

BROWN, A.W. (1977). Structural abnormalities in neurones. *J. Clin. Pathol.*, **30**, S11, 155–169.

BUCHAN, A.M., SLIVKA, A. & XUE, D. (1992). The effect of the NMDA receptor antagonist MK-801 on cerebral blood flow and infarct volume in experimental stroke. *Brain Res.*, **574**, 171–177.

BUISSON, A., PLOTKINE, M. & BOULU, R.G. (1992). The neuroprotective effect of a nitric oxide inhibitor in a rat model of focal cerebral ischaemia. *Br. J. Pharmacol.*, **106**, 766–767.

BULLOCK, R. & FUJISAWA, H. (1992). The role of glutamate antagonists for the treatment of CNS injury. *J. Neurotrauma*, **9**, S443–S461.

COLE, D.J., SCHELL, R.M., ASHWAL, S. & PEARCE, W.J. (1993). Nitric oxide mediated brain injury occurs during the reperfusion phase of temporary focal cerebral ischaemia in rats. *Anesthesiol.*, **79**, 3A, A185.

DAWSON, D.A., GRAHAM, D.I., MCCULLOCH, J. & MACRAE, I.M. (1993). Evolution of ischaemic damage in a new model of focal cerebral ischaemia in the rat. *J. Cereb. Blood Flow Metab.*, **13**, S1, S461.

DAWSON, D.A., KUSUMOTO, K., GRAHAM, D.I., MCCULLOH, J. & MACRAE, I.M. (1992). Inhibition of nitric oxide synthesis does not reduce infarct volume in a rat model of focal cerebral ischaemia. *Neurosci. Lett.*, **142**, 151–154.

DAWSON, V.L., DAWSON, T.M., LONDON, E.D., BREDT, D.S. & SNYDER, S.H. (1991). Nitric oxide mediates glutamate neurotoxicity in primary cortical cultures. *Proc. Natl. Acad. Sci. U.S.A.*, **88**, 6368–6371.

DEZSI, L., GREENBERG, J.H., HAMAR, J., SLADKY, J., KARP, A. & REIVICH, M. (1992). Acute improvement in histological outcome by MK-801 following focal cerebral ischaemia and reperfusion in the cat independent of blood flow changes. J. Cereb. Blood Flow Metab., **12**, 390–399.

FUJISAWA, H., DAWSON, D., BROWNE, S.E., MACKAY, K.B., BULLOCK, R. & MCCULLOCH, J. (1993). Pharmacological modification of glutamate neurotoxicity in vivo. *Brain Res.*, **629**, 73–78.

GARTSHORE, G., DAWSON, D., PATTERSON, J. & MACRAE, I.M. (1994). Local cerebral blood flow measurement by double label autoradiography in the endothelin reperfusion model of focal cerebral ischaemia. *Brain Res. Assoc. Abstr.*, **11**, 75.

GILL, R., BRAZELL, C., WOODRUFF, G.N. & KEMP, J.A. (1991). The neuroprotective action of dizocilpine (MK-801) in the rat middle cerebral artery occlusion model of focal ischaemia. *Br. J. Pharmacol.*, **103**, 2030–2036.

GREENBERG, J.H., UEMATSU, D., ARAKI, N. & REIVICH, M. (1991). Intracellular calcium and pathophysiological changes in cerebral ischaemia. *Arzneim.-Forsch./Drug Res.*, **41**, (I), 3a, 324–332.

KADER, A., FRAZZINI, V.I., SOLOMON, R.A. & TRIFILETTI, R.R. (1993). Nitric oxide production during focal cerebral ischaemia in rats. *Stroke*, **24**, 1709–1716.

KULUZ, J.W., PRADO, R.J., DIETRICH, W.D., SCHLEIEN, C.L. & WATSON, B.D. (1993). The effect of nitric oxide synthase inhibition on infarct volume after reversible focal cerebral ischaemia in conscious rats. *Stroke*, **24**, 2023–2029.

LIPTON, S.A., CHOI, Y.-B., PAN, Z.-Y., LEI, S.Z., CHEN, H.-S.V., SUCHER, N.J., LOSCAIZO, J., SINGEL, D.J. & STAMLER, J.S. (1993). A redox-based mechanism for the neuroprotective and neurodestructive effects of nitric oxide and related nitroso-compounds. *Nature*, **364**, 626–632.

MA, X.-L., LEFER, A.M. & ZIPKIN, R.E. (1993). S-Nitroso-N-acetylpenicillamine is a potent inhibitor of neutrophil-endothelial interaction. *Endothelium*, **1**, 31–39.

MACRAE, I.M. (1992). New models of focal cerebral ischaemia. *Br. J. Clin. Pharmacol.*, **34**, 302–308.

MACRAE, I.M., DAWSON, D.A., NORRIE, J.D. & MCCULLOCH, J. (1993a). Inhibition of nitric oxide synthesis: effects on cerebral blood flow and glucose utilisation in the rat. *J. Cereb. Blood Flow Metab.*, **13,** 985–992.

MACRAE, I.M., ROBINSON, M.J., GRAHAM, D.I., REID, J.L. & MCCULLOCH, J. (1993b). Endothelin-1 induced reductions in cerebral blood flow: dose dependency, time course and neuropathological consequences. *J. Cereb. Blood Flow Metab.*, **13,** 276–284.

MALINSKI, T., BAILEY, F., ZHANG, Z.G. & CHOPP, M. (1993). Nitric oxide measured by a porphyrinic microsensor in rat brain after transient middle cerebral artery occlusion. *J. Cereb. Blood Flow Metab.*, **13,** 355–358.

MCCULLOCH, J., BULLOCK, R. & TEASDALE, G.M. (1991). Excitatory amino acid antagonists: opportunities for the treatment of ischaemic brain damage in man. In *Excitatory Amino Acid Antagonists.* ed. Meldrum, B.S. pp. 287–326. Oxford: Blackwell Scientific Publications.

MOORE, P.K., BABBEDGE, R.C., WALLACE, P., GAFFEN, Z.A. & HART, S.L. (1993). 7-Nitro indazole, an inhibitor of nitric oxide synthase, exhibits anti-nociceptive activity in the mouse without increasing blood pressure. *Br. J. Pharmacol.*, **108,** 296–297.

MORIKAWA, E., GINSBERG, M.D., DIETRICH, W.D., DUNCAN, R.C., KRAYDIEH, S., GLOBUS, M.Y.-T. & BUSTO, R. (1992a). The significance of brain temperature in focal cerebral ischaemia: histopathological consequences of middle cerebral artery occlusion in the rat. *J. Cereb. Blood Flow Metab.*, **12,** 380–389.

MORIKAWA, E., HUANG, Z. & MOSKOWITZ, M.A (1992b). L-Arginine decreases infarct size caused by middle cerebral arterial occlusion in SHR. *Am. J. Physiol.*, **263,** H1632–H1635.

MORIKAWA, E., ROSENBLATT, S. & MOSKOWITZ, M.A. (1992c). L-Arginine dilates rat pial arterioles by nitric oxide-dependent mechanisms and increases blood flow during focal cerebral ischaemia. *Br. J. Pharmacol.*, **107,** 905–907.

NAGAFUJI, T., MATSUI, T., KOIDE, T. & ASANO, T. (1992). Blockade of nitric oxide formation by N^{w}-nitro-L-arginine mitigates ischaemia brain edema and subsequent cerebral infarction in rats. *Neurosci. Lett.*, **147,** 159–162.

NEHLS, D.G., PARK, C.K., MACCORMACK, A.G. & MCCULLOCH, J. (1990). The effects of N-methyl-D-aspartate receptor blockade with MK-801 upon the relationship between cerebral blood flow and glucose utilisation. *Brain Res.*, **511,** 271–279.

NOWICKI, J.P., DUVAL, D., POIGNET, H. & SCATTON, B. (1991). Nitric oxide mediates neuronal death after focal cerebral ischaemia in the mouse. *Eur. J. Pharmacol.*, **204,** 339–340.

OSBORNE, K.A., SHIGENO, T., BALARSKY, A.-M., FORD, I., MCCULLOCH, J., TEASDALE, G.M. & GRAHAM, D.I. (1987). Quantitative assessment of early brain damage in a rat model of focal cerebral ischaemia. *J. Neurol. Neurosurg. Psychiatry*, **50,** 402–410.

PARK, C.K., NELHLS, D.G., GRAHAM, D.I., TEASDALE, G.M. & MCCULLOCH, J. (1988). The glutamate antagonist MK-801 reduces focal ischaemic brain damage in the rat. *Ann. Neurol.*, **24,** 543–551.

PARK, C.K., NEHLS, D.G., TEASDALE, G.M. & MCCULLOCH, J. (1989). Effect of the NMDA antagonist MK-801 on local cerebral blood flow in focal cerebral ischaemia in the rat. *J. Cereb. Blood Flow Metab.*, **9,** 617–622.

RINGELSTEIN, E.B., BINIEK, R., WEILLER, C., AMMELING, B., NOLTE, P.N. & THRON, A. (1992). Type and extent of hemispheric brain infarctions and clinical outcome in early and delayed middle cerebral artery recanalization. *Neurology*, **42,** 289–298.

ROUSSEL, S., PINARD, E. & SEYLAZ, J. (1992). The acute effects of MK-801 on cerebral blood flow and tissue partial pressures of oxygen and carbon dioxide in conscious and alpha-choralose anaesthetized rats. *Neurosci.*, **47,** 959–965.

SHARKEY, J., RITCHIE, I.M. & KELLY, P.A.T. (1993). Perivascular microapplication of endothelin-1: a new model of focal cerebral ischaemia in the rat. *J. Cereb. Blood Flow Metab.*, **13,** 865–871.

TAMURA, A., GRAHAM, D.I., MCCULLOCH, J. & TEASDALE, G.M. (1981). Focal cerebral ischaemia in the rat: 1. Description of technique and early neuropathological consequences following middle cerebral artery occlusion. *J. Cereb. Blood Flow Metab.*, **1,** 53–60.

TANAKA, K., GOTOH, F., GOMI, S., TAKASHIMA, S., MIHARA, B., SHIRAI, T., NOGAWA, S. & NAGATA, E. (1991). Inhibition of nitric oxide synthesis induces a significant reduction in local cerebral blood flow in the rat. *Neurosci. Lett.*, **127,** 129–132.

TOMINAGA, T., SATO, S., OHNISHI, T. & OHNISHI, S.T. (1993). Potentiation of nitric oxide formation following bilateral carotid occlusion and focal cerebral ischaemia in the rat: in vivo detection of the nitric oxide radical by electron paramagnetic resonance spin trapping. *Brain Res.*, **614,** 342–346.

WILLIS, C.L., BRAZELL, C. & FOSTER, A.C. (1991). Plasma and CSF levels of dizocilpine (MK-801) required for neuroprotection in the quinolinate-injected rat striatum. *Eur. J. Pharmacol.*, **196,** 285–290.

YAMAMOTO, S., GOLANOV, E.V., BERGER, S.B. & REIS, D.J. (1992). Inhibition of nitric oxide synthesis increases focal ischaemic infarction in rat. *J. Cereb. Blood Flow Metab.*, **12,** 717–726.

YANG, G.Y., WEINSTEIN, P.R., CHEN, S.F., BABUNA, O.A., SIMON, R.P. & CHAN, P.H. (1991). N-methyl-D-aspartate antagonist, MK-801, reduces reperfusion injury after focal cerebral ischaemia in rats. *J. Cereb. Blood Flow Metab.*, **11,** S2, S288.

ZHANG, F. & IADECOLA, C. (1993). Nitroprusside improves blood flow and reduces brain damage after focal ischaemia. *Neuroreport*, **4,** 559–562.

ZHANG, J., BENVENISTE, J. & PIANTADOSI, C.A. (1993). Inhibition of nitric oxide synthase increase extracellular cerebral glutamate concentration after global ischemia. *Neurosci. Lett.*, **157,** 179–182.

(Received February 17, 1994
Revised April 29, 1994
Accepted May 5, 1994)

Br. J. Pharmacol. (1994), **113**, 254–260

Binding and growth-inhibitory effect of heparin and oligo-heparin (2 kDa) in Balb/c 3T3 cells: lack of effect on PDGF- or serum-induced inositol lipid turnover

Simone Cavari, *Gianna Fiorelli & [1]Simonetta Vannucchi

Istituto di Patologia Generale and *Dipartimento di Fisiopatologia Clinica, University of Firenze, Viale Morgagni 50, 50 134 Firenze, Italy

1 The ability of heparins (bovine heparin sm 1026, Av. mol. wt. 36.9 kDa and bovine heparin EP 756, Av. mol. wt. 12.9 kDa) and heparin fractions of different molecular weights (low molecular weight heparin, LMW 2123/OP, Av. mol. wt. 4.5 kDa and oligo-heparin, Av. mol. wt. 2 kDa) to inhibit the proliferation and signalling of Balb/c 3T3 fibroblasts was investigated.

2 Heparin and heparin fractions of 4.5 and 2 kDa significantly inhibited DNA synthesis as monitored by [^{3}H]-thymidine incorporation.

3 ^{3}H-labelled heparin fractions of 4.5 and 2 kDa were prepared by gel-chromatography fractionation on Sephadex G-75 of an ^{3}H-labelled commercial heparin after treatment with heparinase.

4 The binding of unfractionated and oligo-heparin of 2 kDa to Balb/c 3T3 fibroblasts was studied; we determined the specificity of heparin and oligo-heparin binding to the cells by means of displacement of bound ^{3}H-labelled compound in response to increasing concentrations of unlabelled compounds. Scatchard analysis of binding data obtained using [^{3}H]-heparin as ligand revealed the presence of a single class of high affinity binding sites (K_d = 28 nM) for heparin. Scatchard analysis of binding data obtained using [^{3}H]-oligo-heparin as ligand revealed the presence of a single class of low affinity binding sites (K_d = 3.2 μM) for oligo-heparin.

5 In addition heparin displaced [^{3}H]-oligo-heparin at a concentration of approximately 100 fold of the K_d determined in displacement studies. Furthermore, oligo-heparin significantly displaced [^{3}H]-heparin at a concentration of approximately 10 fold of the K_d determined by displacement studies.

6 Both heparin and oligo-heparin exert their inhibitory effects on Balb/c 3T3 DNA synthesis stimulated by PDGF or serum. However these molecules did not affect the inositol lipid turnover triggered by PDGF at a concentration which did not produce maximal response. The increase of inositol phosphate metabolism produced by 20% serum was also unaffected by heparin. This concentration of serum elicited a response comparable to that induced by a submaximal concentration of PDGF.

Keywords: Balb/c 3T3 fibroblasts; heparin; oligo-heparin; inhibition of proliferation; inositol lipid turnover

Introduction

Heparin is a highly sulphated glycosaminoglycan, with a molecular weight which varies from 5 to 40 kilodaltons (kDa). Heparin acts as an anticoagulant by binding to antithrombin III and thus markedly accelerating the ability of antithrombin III to inactivate the coagulation enzymes thrombin (IIa), factor Xa and factor IXa (Danielsson *et al.*, 1986). Heparin molecules with fewer than 18 saccharides (kDa less than 5.4) are called 'low molecular weight heparins'. These molecules, prepared from standard commercial heparin, have become topics of great clinical interest for two reasons: (1) they progressively lose their ability to prolong the activated partial thromboplastin time (APTT) while retaining their ability to inhibit factor X (factor Xa) with reduction in molecular size (Jordan *et al.*, 1980); (2) with an equivalent antithrombotic effect, they produce less bleeding in experimental models than high molecular weight heparin (Bergquist *et al.*, 1985).

Heparin is known to have other biological effects besides inhibition of blood coagulation. The growth of several normal and transformed cell types, including human and murine fibroblasts, is inhibited by heparin *in vitro* and *in vivo* (Wright *et al.*, 1989b; Ferrao & Mason, 1993; for review see Jackson *et al.*, 1991). The mechanism of the antiproliferative actions of heparin have not been defined. Both anticoagulant and non-anticoagulant forms of heparins are effective in inhibiting smooth muscle cell growth (Pukac *et al.*, 1991). Searching for a mechanism of action that could elucidate the role of heparin as growth inhibitor, we recently reported the effects of heparin on cell proliferation and inositol lipid turnover in a variety of cell lines. We observed that heparin inhibits serum-induced inositol lipid turnover as well as serum-stimulated cell growth in BC3H-1 muscle cells (Vannucchi *et al.*, 1990a,b), whereas in A 431 cells the growth inhibitory effect of heparin is independent of cell signalling induced by epidermal growth factor (EGF) or bradykinin (Vannucchi *et al.*, 1991). Heparin also inhibits platelet-derived growth factor (PDGF)-induced cell proliferation and inositol lipid turnover in v-sis transformants, but it does not affect PDGF mitogenic signalling in normal NIH-3T3 fibroblasts (Cavari *et al.*, 1993). It has been demonstrated that heparin suppresses the induction of c-*fos* and c-*myc* mRNA in murine Balb/c 3T3 fibroblasts by selective inhibition of a protein-kinase C dependent pathway (Wright *et al.*, 1989b). This mitogenic pathway is activated by PDGF but not by EGF, which in these cells utilizes a protein-kinase C independent pathway for gene expression (Besterman *et al.*, 1986). Accordingly, heparin fails to suppress c-*fos* and c-*myc* expression stimulated by EGF in these cells (Wright *et al.*, 1989b).

Since stimulation of inositol lipid degradation appears to be an important step in the mechanism by which PDGF (but not EGF) stimulates mitogenesis in Balb/c 3T3 fibroblasts, we decided to study, first of all, whether Balb/c 3T3 cells bear binding sites for heparin and heparin fractions of low molecular weight, and then the effect of these molecules on cell proliferation and PDGF- or serum-induced inositol lipid turnover. Indeed, it is known that PDGF accounts for only

[1] Author for correspondence.

about 50% of the platelet derived mitogenic activity of serum (Ross *et al.*, 1986).

A brief account of some of this work has already been published (Cavari & Vannucchi, 1993).

Methods

Mitogenesis assay

Balb/c 3T3 fibroblasts were grown in DMEM supplemented with 10% foetal bovine serum. All experiments were performed at pH 7.4 in a humidified atmosphere of 95% air, 5% CO_2 at 37°C. The glycosaminoglycans were added to cell cultures in the presence of 10% foetal bovine serum 24 h before the determination of [^{3}H]-thymidine incorporation. The effects of PDGF, heparin, and oligo-heparin on DNA synthesis were studied in serum-starved cultures. Cells were grown to confluence in 24-well plates and made quiescent by incubation for 24 h in serum-free medium. Immediately thereafter, 1 ml of DMEM containing either PDGF (50 ng ml^{-1}) or 10% serum in the presence or in the absence of heparin and oligo-heparin was added. After 23 h, 0.5 μCi ml^{-1} of [^{3}H]-thymidine was added. After incubation for 1 h, the incorporation of labelled thymidine into DNA was assayed as described previously (Vannucchi *et al.*, 1990a).

Preparation of ^{3}H-labelled heparin fractions

[^{3}H]-heparin (50 μg) was incubated for 1 h at 35°C with 100 units of heparinase I in 0.1 M sodium acetate pH 7.0 (one unit forms 0.1 μmol of unsaturated uronic acid per h at pH 7.5 at 25°C). The sample was boiled for 10 min and gel-filtered on a G-75 Sephadex column (1 × 90 cm) eluted with 1 M NaCl (flux 4 ml h^{-1}); 2 ml fractions were collected. Fractions 15 to 25 and 26 to 32 were pooled, dialyzed against distilled water using a Spectra/por membrane (mwco 1.000, Spectrum Med., Los Angeles, CA, U.S.A.) and lyophilized. The mean molecular weights of the radioactive fractions were calculated by comparison with standard unlabelled heparin fractions of known molecular weight (12.9; 4.9 and 2.0 kDa) on gradient PAGE electrophoresis according to Lyon & Gallagher (1990). The dried gel was submitted to autoradiography. The specific activity of the radioactive fractions, evaluated by measuring the uronic acid content (Bitter & Muir, 1962) of the products was similar to that of the starting material.

Measurement of heparin binding

Binding experiments were performed on confluent cultures of Balb/c 3T3 cells (3 × 10^5 cells per 17-mm dish) as previously described (Vannucchi *et al.*, 1988). The cell number at confluence was determined as follows: triplicate plates were trypsinized and cells counted in a Coulter counter. In all reported experiments, the standard deviation was less than 10% of the mean. Confluent cultures of Balb/c 3T3 cells (3 × 10^5 cells per 17-mm dish) were washed with cold phosphate buffered saline (PBS) and precooled at 4°C for 30 min. The unfractionated [^{3}H]-heparin or the ^{3}H-labelled oligo-heparin fraction were used as ligands in binding experiments. To confluent cell monolayers 1 ml of PBS was added containing 0.1% human serum albumin, increasing concentrations of [^{3}H]-heparin (7.5–30 nM) without unlabelled heparin, and fixed concentration of [^{3}H]-heparin (30 nM) with increasing concentrations of unlabelled ligand (20 nM–40 μM). The same procedure was used to quantify the binding of [^{3}H]-oligo-heparin by incubating increasing concentrations of [^{3}H]-oligo-heparin (50–200 nM) without unlabelled oligo-heparin, and a fixed concentration of [^{3}H]-oligo-heparin (200 nM) with increasing concentrations of unlabelled oligo-heparin (100 nM–200 μM). Non-specific binding was determined in the presence of 1000 fold excess of unlabelled ligand and was negligible (5% of the total binding for heparin and 7.5% of the total binding for oligo-heparin). After 2 h incubation at 4°C the cell monolayers were washed five times with cold PBS (5 ml), then solubilized in 0.2 N NaOH overnight at 37°C. The radioactivity present in cell lysate was determined in a liquid scintillation counter. Binding data were analysed according to the method of Scatchard, using the Ligand computer programme (Munson & Rodbard, 1980). The relative specificity of the binding sites for heparin and oligo-heparin compared to other glycosaminoglycans was studied incubating confluent Balb/c 3T3 cells with 30 nM [^{3}H]-heparin or 200 nM [^{3}H]-oligo-heparin respectively, for 2 h at 4°C, in the absence or in the presence of 100 fold excess of unlabelled glycosaminoglycans.

Analysis of inositol lipid turnover

The experiments involving the measurement of inositol-containing lipids and the water soluble inositol-phosphates, were carried out as previously described (Vannucchi *et al.*, 1990a). Briefly, cells in 35-mm dishes and in log phase growth were first labelled by preincubation with 5 μCi per dish of *myo*-[2-^{3}H]-inositol. After 2 days of incubation cells were confluent and the labelling was continued for an additional 24 h with 5 μCi per dish of [^{3}H]-inositol in serum-free medium. The prelabelling was stopped by washing the monolayers with DMEM. Cells were then incubated with 1 ml of DMEM with 10 mM Li^+. After 10 min, cells were stimulated by appropriate agents. At times thereafter, stimulation was rapidly terminated by addition of 1.2 ml per dish of cold methanol. Extraction of phospholipids and phosphoinositide was carried out as previously described (Vannucchi *et al.*, 1990a).

Materials

[^{3}H]-heparin (400 μCi mg^{-1}, average molecular weight 12 kDa), [^{3}H]-thymidine (82.2 Ci mmol^{-1}) and [^{3}H]-*myo*-inositol were purchased from New England Nuclear. Heparin sm 1026 (kDa 36.9) and heparin EP 756 (kDa 12.9) extracted from bovine intestinal mucosa, low molecular weight heparin (LMW 2123/850, kDa 4.5) and oligo-heparin (kDa 2.0), which were obtained from unfractionated compounds by a patented peroxidalic fragmentation (Volpi *et al.*, 1992), were all provided by Opocrin Research Laboratories (Modena, Italy). Chondroitin sulphate A (CSA), chondroitin sulphate C (CSC) and dermatan sulphate (DS) were obtained from Seikagaku Kogyo Co., Tokyo; heparan sulphate (HS) was from Upjohn International Inc., Kalamazoo, Mich., U.S.A.; hyaluronic acid (HA) and heparinase I (from F. heparinum, E.C.4.2.2.7) were from Sigma Chem. Co., St. Louis, Mo, U.S.A. Sephadex G-75 was from Pharmacia (Uppsala, Sweden). Platelet derived growth factor (PDGF) was from Calbiochem. Gradient PAGE electrophoresis was performed on a standard vertical slab supplied by Pharmacia LKB. Tissue culture media and foetal bovine serum were from GIBCO.

Statistical analysis

Data were expressed as means ± s.d. Statistical differences were analysed by Student's t test and were considered significant at $P<0.01$.

Results

Previous studies have shown that heparin is an inhibitor of Balb/c 3T3 fibroblast proliferation (Wright *et al.*, 1989b). In the present study we tested the antiproliferative activity of heparin fractions of low molecular weight, produced by a radical reaction, compared to the antiproliferative activity exhibited by whole heparin itself. Balb/c 3T3 cell prolifera-

tion assay demonstrated that both the native heparin and the depolymerized heparins have significant ($P<0.005$) antiproliferative activity (Figure 1). However, there were differences in the antiproliferative activities between the compounds tested. Oligo-heparin shows an interesting biological property: it has the higher AXa/APTT ratio among the heparins herein tested; in fact, it is devoid of APTT activity (Table 1). For this reason, we decided to study in greater detail the antiproliferative activity of this compound. As shown in Figure 2 we determined a dose-dependent antiproliferative activity of whole heparin and oligo-heparin. From the results obtained in three different experiments the apparent IC_{50} for heparin was reached by the lower concentration tested (0.5 $\mu g\ ml^{-1}$ = 38.7 nM) with 32.2% median inhibition of [^{3}H]-thymidine incorporation and 95% confidence intervals of 27.8 and 36.6%. The IC_{50} for oligo-heparin was calculated to be 3 $\mu g\ ml^{-1}$ (= 1.5 μM) with median inhibition of 22.5% and 95% confidence intervals of 20.0 and 25.2%. The responses to 100 $\mu g\ ml^{-1}$ of each compound are maximal: at this dose heparin and oligo-heparin produce 65% and 46% inhibition of [^{3}H]-thymidine incorporation, respectively. Both low molecular weight heparin and oligo-heparin obtained by radical depolymerization did not exhibit changes in their primary structure in comparison with heparin fractions obtained by enrichment of native heparin (Volpi *et al.*, 1992). Thus, we investigated whether the oligo-heparin exerted their action through the binding to specific binding proteins present on the cellular membrane or in the extracellular matrix. ^{3}H-labelled heparin fraction of mean molecular weight of 2 kDa was obtained by gel-fractionation on Sephadex G-75 of an ^{3}H-labelled commercial heparin, treated with heparinase I. Pooled fractions were dialyzed and lyophilized. Aliquots were submitted to PAGE electrophoresis (Figure 3) and the fraction of 2 kDa was used for binding studies. Specific [^{3}H]-heparin binding and [^{3}H]-oligo-heparin binding to Balb/c 3T3 cells was time- and temperature-dependent. For both ligands, maximum specific binding was obtained at 4°C after 2 h incubation, and was stable for an additional 1 h (not shown). All subsequent binding studies were conducted at 4°C for 2 h. Binding specificity of unfractionated [^{3}H]-heparin (30 nM) and [^{3}H]-oligo-heparin (200 nM) binding was determined by incubating the cultures in the absence or in the presence of 100 fold excess of the following unlabelled compounds: heparin EP 756; oligo-heparin; hyaluronic acid; heparan sulphate; dermatan sulphate; chondroitin sulphate A and C (Figure 4). The binding of labelled heparin was inhibited by 100 fold excess of unlabelled heparin EP 756, but not by 100 fold excess of heparin-unrelated glycosaminoglycans. Heparin-related glycosaminoglycans (heparan sulphate and oligo-heparin) were the only compounds able to compete for [^{3}H]-heparin binding. The binding of [^{3}H]-oligo-heparin was inhibited by 100 fold excess of heparin. Heparan sulphate and oligo-heparin were also competitors. The heparin-unrelated glycosaminoglycans were able to compete only for oligo-heparin binding.

Scatchard analysis of binding data obtained from four different experiments using [^{3}H]-heparin or [^{3}H]-oligo-heparin as ligands revealed the presence of a single class of binding sites with K_d values of 20, 28, 30 and 35 nM and binding capacity of 1.39, 1.5, 1.73 and 1.84 pmol/10^6 cells for heparin (Figure 5a), and a single class of binding sites with K_d values

Table 1 Properties of heparins used in the experiments

	Mol. wt. (kDa)	*SO_3/COO^-* (MR)	*APTT* (iu mg^{-1})	*AXa* (iu mg^{-1})
EP 756	12.9	2.15	164	114
sm 1026	36.9	–	295	119
LMW 2123/850	4.5	2.19	37	86
Oligo-heparin 2000	2.1	2.03	1	50

Glycosaminoglycan molecular weight (mol. wt.) is expressed in kDa. Degree of sulphation (SO_3/COO^-) is expressed as molar ratio (MR) of sulphate and carboxyl groups determined by potentiometric analysis (Mascelloni *et al.*, 1986). Activated partial thromboplastin time (APTT) is expressed as iu mg^{-1} (Basu *et al.*, 1972). Anti-activated coagulation factor X (AXa) activity was tested in a chromogenic assay and is expressed as iu mg^{-1} (Teien *et al.*, 1976). Abbreviations used: EP 756, heparin; sm, slow moving heparin; LMW, low molecular weight heparin.

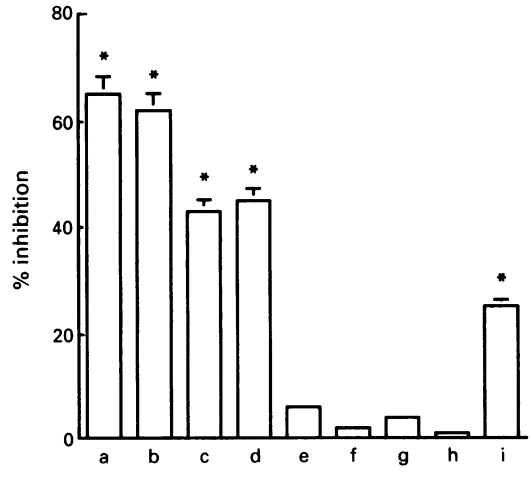

Figure 1 Antiproliferative effects of glycosaminoglycans. Cell growth was assessed as [^{3}H]-thymidine incorporation in the presence of 10 $\mu g\ ml^{-1}$ of the indicated compounds which were added 24 h before pulse labelling (1 h) with [^{3}H]-thymidine: (a) EP 756; (b) heparin sm 1026; (c) LMW 2123/OP; (d) oligo-heparin (2 kDa); (e) chondroitin sulphate A; (f) dermatan sulphate; (g) chondroitin sulphate C; (h) hyaluronic acid; (i) heparan sulphate. Data are expressed as % of inhibition of [^{3}H]-thymidine incorporation compared with controls (no addition, i.e. no inhibition = 0%; full inhibition was 100%). Values are means ± s.d. obtained in three experiments, each performed in quadruplicate. *Statistically different from the control ($P<0.005$; Student's t test).

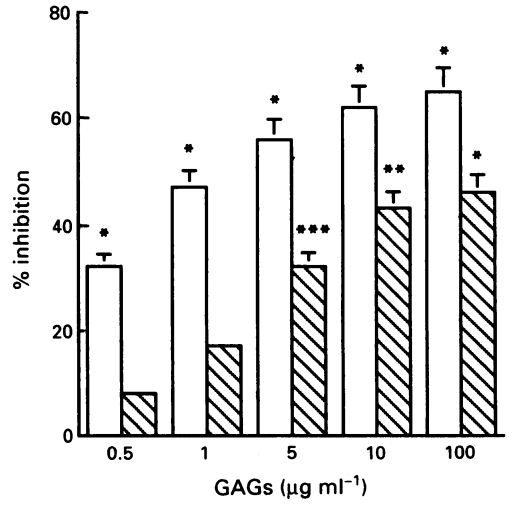

Figure 2 Dose-dependent effect of glycosaminoglycans (GAGs), heparin and oligo-heparin, on Balb/c 3T3 proliferation. Cell growth was assessed as [^{3}H]-thymidine incorporation in the presence of different concentrations of indicated compounds which were added for 24 h before pulse labelling (1 h) with [^{3}H]-thymidine. Data (mean ± s.d.) are derived from three experiments each performed in quadruplicate and are expressed as % inhibition of [^{3}H]-thymidine incorporation. EP 756 (open columns); oligo-heparin (2 kDa) (hatched columns). *Statistically different from control ($P<0.005$; Student's t test). **Statistically different from the control ($P<0.01$; Student's t test). ***Statistically different from the control ($P<0.025$; Student's t test).

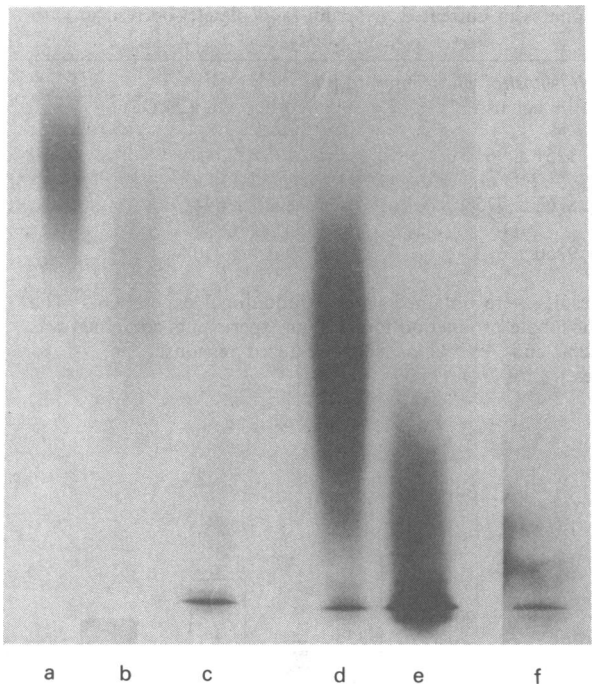

Figure 3 Gradient PAGE electrophoresis of standard heparins and [^{3}H]-heparin fractions from Sephadex G-75: (a) heparin 756 (12.9 kDa); (b) low molecular weight OP 2123/850 (4.5 kDa); (c) oligo-heparin (2.0 kDa); (d) fractions 15–25 from Sephadex G-75; (e) fractions 26-32 from Sephadex G-75; (f) autoradiography of (e).

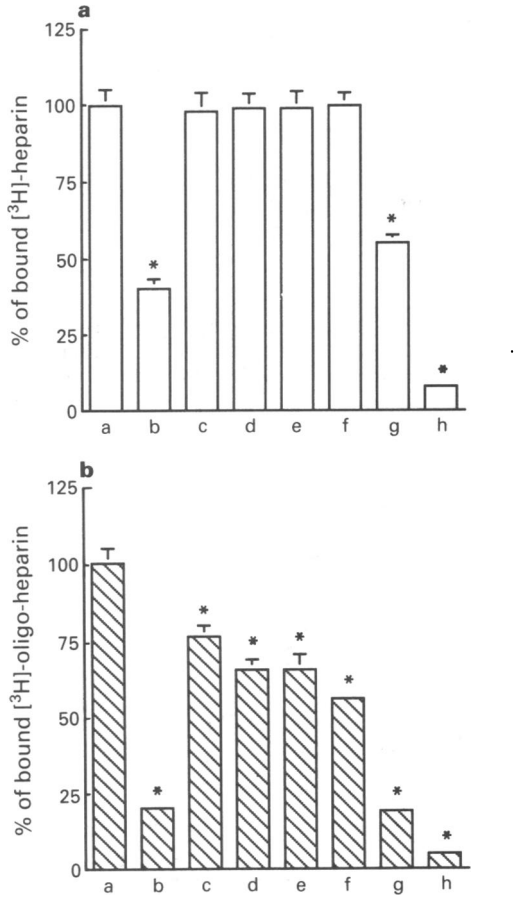

Figure 4 Specificity of unfractionated [^{3}H]-heparin and [^{3}H]-oligo-heparin binding to Balb/c 3T3 fibroblasts. (**a**) Cells were incubated for 2 h at 4°C with [^{3}H]-heparin (4×10^5 d.p.m. ml^{-1} per plate) in the absence (a) or in the presence of 50 μg ml^{-1} per plate of: (b) heparan sulphate; (c) chondroitin sulphate A; (d) dermatan sulphate; (e) chondroitin sulphate C; (f) hyaluronic acid; (g) oligo-heparin (2 kDa); (h) heparin. (**b**) Cells were incubated for 2 h at 4°C with [^{3}H]-oligo-heparin (4×10^5 d.p.m. ml^{-1} per plate) in the absence (a) or in the presence of the compounds listed in (**a**). Results are expressed as % of ^{3}H-labelled compounds bound to cells and are means ± s.d. of triplicate samples. This experiment is representative of three experiments with similar results. *Significantly different from the control ($P < 0.005$; Student's t test).

of 0.3, 0.6, 3.3 and 8.9 μM and binding capacity of 105, 120, 123 and 135 pmol/10^6 cells for oligo-heparin (Figure 5b).

In the antiproliferative experiments the IC_{50} for heparin was 0.5 μg ml^{-1} concentration that corresponds to 38.7 nM, and the IC_{50} for oligo-heparin was 3 μg ml^{-1}, corresponding to 1.5 μM. Taken together, these results suggest that both compounds interact with both binding sites, albeit possibly with different affinities; this difference could explain the different antiproliferative potencies of these compounds. Binding experiments were carried out using confluent cells; therefore, the involvement in our system of binding sites on the extracellular matrix cannot be excluded.

Previous studies showed that in Balb/c 3T3 fibroblasts, heparin inhibits the protein-kinase C-dependent mitogenic pathway, which is activated by PDGF, thrombin and phorbol esters, but has little effect on the EGF-dependent pathway (Wright *et al.*, 1989b). PDGF accounts for approximately 50% of the platelet derived mitogenic activity of serum; the remaining activity appears to be due to an EGF-like molecule and, probably, to other growth factors (Ross *et al.*, 1986). Therefore, we investigated the effects of heparin and oligo-heparin on mitogenic responses of these cells to PDGF or serum. As shown in Figure 6 both heparin and oligo-heparin inhibit DNA synthesis stimulated by PDGF or serum. It has been suggested that heparin acts early in the cell cycle to suppress protein-kinase C-dependent induction of gene expression in vascular smooth muscle cells (Pukac *et al.*, 1990; 1992). Stimulation by PDGF of quiescent Balb/c 3T3 cells leads to tyrosine phosphorylation of PLC-γ and a consequent increase in phosphoinositide turnover (Wahl *et al.*, 1989). Therefore, we next examined directly whether heparin or oligo-heparin could repress PDGF- or serum-induced phosphoinositide degradation in Balb/c 3T3 cells. The results shown in Table 2 demonstrate that treatment with PDGF or serum for 60 min in the absence or in the presence of heparin (100 μg ml^{-1}) or oligo-heparin (100 μg ml^{-1}) significantly increases inositol lipid turnover compared with the control ($P < 0.005$). The effect of the glycosaminoglycan was evaluated with a PDGF concentration (50 ng ml^{-1}) that did not produce the maximal response (Table 2); thus we can exclude the possibility that the lack of effect on the inositol phosphate production induced by PDGF could be because the stimulation was saturated. To evaluate the effect of glycosaminoglycan on serum-induced response, we used a serum concentration (20%) that stimulates the inositol phosphate production at levels in the range of those induced by submaximal concentrations of PDGF. The addition of heparin or oligo-heparin to control or PDGF- or serum-treated cells did not significantly influence the inositol lipid turnover values obtained in the absence of the glycosaminoglycan.

Discussion

The results presented in this paper indicate that heparin and oligo-heparin of 2 kDa specifically bind to Balb/c 3T3 fibroblasts and inhibit proliferation. Several diseases that involve non malignant proliferation of cells include fibroproliferative processes (i.e. pulmonary interstitial fibrosis, and some forms of glomerulonephritis, cirrhosis and myelofibrosis). In these processes normal tissue is replaced by fibroblasts and their extracellular products. Therefore, pharmacological interven-

Table 2 Effects of heparin and oligo-heparin on the levels of inositol phosphates in untreated or serum- and platelet-derived growth factor (PDGF)-stimulated Balb/c 3T3 cells

Condition	*Level of [^{3}H]-inositol phosphates* (d.p.m.) none	+ heparin	+ oligo-heparin (2 kDa)
Basal	1112 ± 80	1251 ± 96	1267 ± 77
PDGF (20 ng ml^{-1})	1413 ± 172	ND	ND
PDGF (50 ng ml^{-1})	7822 ± 388*	8766 ± 775*	8240 ± 804*
PDGF (100 ng ml^{-1})	10764 ± 628*	ND	ND
20% serum	9512 ± 554*	9250 ± 673*	9614 ± 720*

Data represent the mean ± s.d. of duplicate determination. Comparable results were obtained in three additional experiments. The mean percentage change induced by heparin and oligo-heparin in inositol phosphate production for all four experiments combined was respectively −5.92% and +10.8% on PDGF-induced response and +7.2% and +9.5% on serum-induced response.
*Significantly different from the basal condition ($P<0.005$ Student's t test).
ND, not determined.

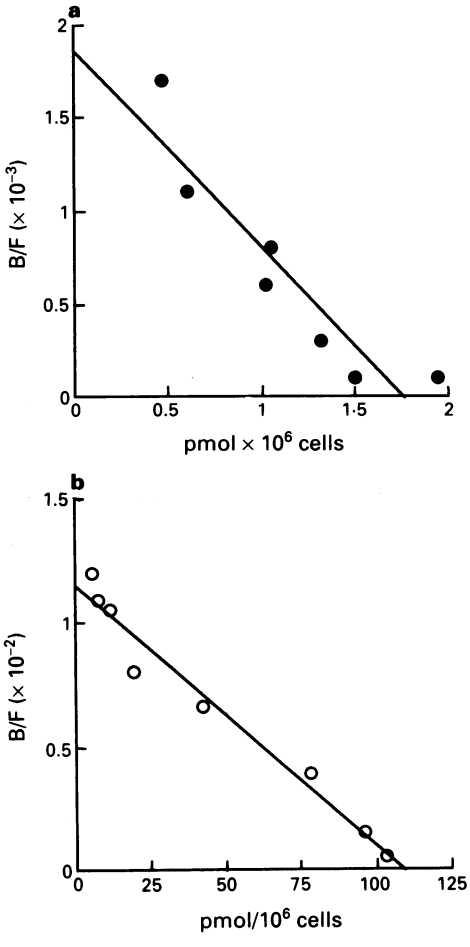

Figure 5 Scatchard analysis of [^{3}H]-heparin (a) and [^{3}H]-oligo-heparin (b) to one Balb/c 3T3 cell monolayer. Each point represents the mean of quadruplicate determinations. In (a) $K_d = 28$ nM; in (b) $K_d = 3.3$ μM. Comparable results were obtained in three additional experiments.

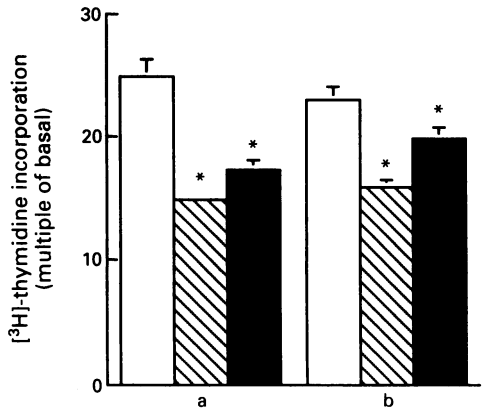

Figure 6 Effects of heparin and oligo-heparin on mitogenic responses. Monolayers of serum-starved Balb/c 3T3 cells were incubated at 37°C for 23 h in the presence of 10% serum (a) or PDGF (50 ng ml^{-1}) (b) without (open columns) or with 100 μg ml^{-1} of heparin (hatched columns) or with 100 μg ml^{-1} of oligo-heparin (2 kDa) (solid columns). Thereafter incorporation of [^{3}H]-thymidine was performed as described under 'Methods'. Data are expressed as means ± s.d. of quadruplicate samples. Comparable results were obtained in three additional experiments. *Significantly different from control ($P<0.005$; Student's t test).

tions aimed to limit uncontrolled fibroblasts proliferation might favourably condition the clinical course of these diseases. Recently it has been shown that the growth of human dermal fibroblasts from patients with progressive systemic sclerosis is inhibited by heparin (Ferrao & Mason, 1993). The antiproliferative features of heparin in structural-functional terms are under investigation; the size requirements are similar for calf and rat vascular smooth muscle cells and rat cervical epithelial cells since hexasaccharide and larger fragments retain activity whereas di- and tetrasaccharides are inactive (Wright *et al.*, 1989a). We have previously reported that both the molecular weight and degree of sulphation of heparin are important in determining growth inhibitory effects in BC3H-1 and A431 cells (Vannucchi *et al.*, 1990a; 1991). However, a pharmacological treatment with the high molecular weight heparin, because of its anticoagulant activity, can lead to haemorrhagic complications as well as thrombocytopaenia. The low molecular weight heparins have reduced ability to catalyze the inactivation of thrombin relative to their ability to inhibit factor Xa because the inactivation of thrombin by heparin is critically dependent on molecular size (Lane *et al.*, 1984). Thus, the growth-inhibitory effect of specific low molecular weight heparin-fractions might be useful in devising new therapeutic strategies exploiting the antiproliferative actions of glycosaminoglycans.

The molecular mechanisms underlying the antiproliferative effect of heparin are still undefined. A major question remains whether heparin acts extra- or intracellularly. It is known that heparin has a direct effect on extracellular matrix, i.e. it regulates the assembly of collagen IV and laminin *in vitro* (Koliakos-Kouzi *et al.*, 1989). Exogenous heparin could act extracellularly on growth by interacting with various components of the extracellular matrix or interfere with cell-substrate attachment processes (San Antonio *et al.*, 1992). However, low molecular weight heparins differ from high molecular weight heparin in their binding to proteins (Lane, 1989): they have lower affinity for proteins such as fibronectin (Dawes & Pavuk, 1991) or Platelet factor 4 and

histidine-rich glycoprotein (Lane *et al.*, 1986). Moreover, they have much lower affinity for the heparin-binding sites on endothelial cells (Vannucchi *et al.*, 1988) and BC3H-1 muscle cells (Vannucchi *et al.*, 1990b). In this paper we show that confluent cultures of Balb/c 3T3 cells bear high affinity binding sites for heparin with K_d values of the same magnitude as the IC_{50} shown in the antiproliferative experiments. The binding sites described using oligo-heparin have an affinity 100 fold lower than that described using heparin, according to the IC_{50} of the oligo-heparin shown in the antiproliferative experiments. However, concerning the antiproliferative effect of oligo-heparin, either extracellular matrix binding sites for all glycosaminoglycans, or heparin specific binding sites, or both, could be involved.

One of the supposed mechanisms for heparin effect on cell proliferation is interaction with growth factors; in fact, it has been shown that the activities of endothelial mitogens are potentiated by heparin (Damon *et al.*, 1989). We have previously demonstrated that heparin inhibited serum-induced phosphoinositide turnover in BC3H-1 muscle cells and the interference with serum growth factors was proposed as a possible mechanism (Vannucchi *et al.*, 1990b). PDGF accounts for approximately 50% of the platelet derived mitogenic activity of serum; the remaining activity appears to be due to other growth factors (Ross *et al.*, 1986). We show here that heparin inhibits both PDGF- and serum-induced cell proliferation; however it fails to inhibit inositol lipid turnover elicited by both submaximal PDGF concentration and 20% serum. These results suggest that heparin and oligo-heparin, either in the medium or bound to cell surface and/or to extracellular matrix components, are unable to inactivate PDGF or to disturb PDGF-PDGF receptor interaction on the cell surface of Balb/c 3T3 fibroblasts. It has been demonstrated that phosphatidylinositol turnover increases as a direct consequence of phospholipase C-γ (PLC-γ) tyrosine phosphorylation in Balb/c 3T3 cells and that PDGF leads to tyrosine phosphorylation of PLC-γ (Wahl *et al.*, 1989). Thus, our results seem to exclude several molecular targets for the inhibitory effect of heparin on Balb/c 3T3 cell proliferation stimulated by PDGF: (1) PDGF itself; (2) binding of PDGF to PDGF receptor; (3) tyrosine phosphorylation of PLC-γ; (4) PLC-γ itself. However, further work is in progress to identify the inhibitory mechanism of heparin on Balb/c 3T3 fibroblast proliferation.

This study was supported by Associazione Italiana Ricerca sul cancro (AIRC) and Ministero della ricerca scientifica e tecnologica (MURST 60%).

References

BASU, D., GALLUS, A., HIRSCH, J. & CADE, J. (1972). A prospective study of the value of monitoring heparin treatment with the activated partial thromboplastin time. *N. Engl. J. Med.*, **287**, 324–327.

BERGQUIST, D., NILSSON, B., HEDNER, U., PEDERSEN, P.C. & OSTERGAARD, P.B. (1985). The effects of heparin fragments of different molecular weight in experimental thrombosis and haemostasis. *Thromb. Res.*, **38**, 589–601.

BESTERMAN, J.M., WATSON, S.P. & CUATRECASAS, P. (1986). Lack of association of Epidermal Growth Factor-, Insulin-, and serum-induced mitogenesis with stimulation of phosphoinositide degradation in Balb/c 3T3 fibroblasts. *J. Biol. Chem.*, **261**, 723–727.

BITTER, J. & MUIR, H.M. (1962). A modified uronic acid carbazole reaction. *Anal. Biochem.*, **4**, 330–334.

CAVARI, S., RUGGIERO, M. & VANNUCCHI, S. (1993). Antiproliferative effects of heparin on normal and transformed NIH/3T3 fibroblasts. *Cell. Biol. Int.*, **17**, 781–786.

CAVARI, S. & VANNUCCHI, S. (1993). Heparin and heparin-related oligosaccharides inhibit proliferation of Balb/c 3T3 fibroblasts. *Eur. J. Histochem.*, **37** (Suppl.), 70–71.

DAMON, D.H., LOBB, R.R., D'AMORE, P.A. & WAGNER, J.A. (1989). Heparin potentiates the action of acidic fibroblast growth factor by prolonging its biological half-life. *J. Cell Physiol.*, **138**, 221–226.

DANIELSSON, A., RAUB, E., LINDAHL, U. & BJORK, I. (1986). Role of ternary complexes in which heparin binds both antithrombin and proteinase, in the acceletation of the reactions between antithrombin and thrombin or factor Xa. *J. Biol. Chem.*, **261**, 15467–15473.

DAWES, J. & PAVUK, N. (1991). Sequestration of therapeutic glycosaminoglycans by plasma fibronectin. *Thromb. Haemost.*, **65**, 829 (abstr.).

FERRAO, A.V. & MASON, R.M. (1993). The effect of heparin on cell proliferation and type-I collagen synthesis by adult human dermal fibroblasts. *Biochim. Biophys. Acta*, **1180**, 225–230.

JACKSON, R.L., BUSCH, S.J. & CARDIN, A.D. (1991). Glycosaminoglycans: molecular properties, protein interactions, and role in physiological processes. *Physiol. Rev.*, **71**, 481–539.

JORDAN, R.E., OOSTA, G.M., GARDNER, W.T. & ROSENBERG, R.D. (1980). The kineteics of hemostatic enzyme-antithrombin interactions in the presence of low molecular weight heparin. *J. Biol. Chem.*, **225**, 10081–10090.

KOLIAKOS-KOUZI, K., KOLIAKIS, G.G., TSILIBARY, E.C., FURCHT, L.T. & CHARONIS, A.S. (1989). Mapping of three major heparin-binding sites on laminin and identification of a novel heparin-binding site on the B1 chain. *J. Biol. Chem.*, **264**, 17971–17978.

LANE, D.A. (1989). Heparin binding and neutralizing protein. In *Heparin, Chemical and Biological Properties, Clinical Applications.* ed. Lane, D.A. & Lindahl, U. pp. 363–383. London, UK: Edward Arnold.

LANE, D.A., DENTON, J., FLYNN, A.M., THUNBERG, L. & LINDAHL, U. (1984). Anticoagulant activities of heparin oligosaccharides and their neutralization by platelet factor 4. *Biochem. J.*, **218**, 725–732.

LANE, D.A., PEJLER, G., FLYNN, A.M., THOMPSON, E.A. & LINDAHL, U. (1986). Neutralization of heparin-related saccharides by histidine-rich glycoprotein and platelet factor 4. *J. Biol. Chem.*, **261**, 3980–3986.

LYON, M. & GALLAGHER, J.T. (1990). A general method for the detection and mapping of submicrogram quantities of glycosaminoglycan oligosaccharides on polyacrylamide gels by sequential staining with azur A and ammoniacal silver. *Anal. Biochem.*, **185**, 63–70.

MASCELLONI, G., RASONI, D., BRUGNOLI, E. & BIANCHINI, P. (1986). Applicazioni analitiche della potenziometria alla caratterizzazione ed analisi dei polisaccaridi ad uso farmaceutico. *III Conv. Naz. Analitica Farmaceutica*, Milan, 11-27/28 (abstr.).

MUNSON, P.J. & RODBARD, D. (1980). LIGAND: a versatile computerized approach for characterization of ligand-binding systems. *Anal. Biochem.*, **107**, 220–239.

PUKAC, L.A., CASTELLOT, J.J., WRIGHT, T.C., CALEB, B.L. & KARNOVSKY, M.J. (1990). Heparin inhibits c-fos and c-myc mRNA expression in vascular smooth muscle cells. *Cell Regul.*, **1**, 435–443.

PUKAC, L.A., HIRSCH, G.M., LORMEAU, J.C., PETITOU, M., CHOAY, J. & KARNOVSKY, M.J. (1991). Antiproliferative effects of novel, non anticoagulant heparin derivatives on vascular smooth muscle cells *in vitro* and *in vivo*. *Am. J. Pathol.*, **139**, 1501–1509.

PUKAC, L.A., OTTLINGER, M.E. & KARNOVSKY, M.J. (1992). Heparin suppresses specific second messenger pathway for protooncogene expression in rat vascular smooth muscle cells. *J. Biol. Chem.*, **267**, 3707–3711.

ROSS, R., RAINES, E.W. & BOWEN-POPE, D.F. (1986). The biology of platelet derived growth factor. *Cell*, **46**, 155–169.

SAN ANTONIO, J.D., LANDER, A.D., WHRIGHT, T.C. & KARNOVSKY, M. (1992). Heparin inhibits the attachment and growth of Balb/c 3T3 fibroblasts on collagen substratta. *J. Cell Physiol.*, **150**, 8–16.

TEIEN, A.M., LIE, M. & ABILGAARD, U. (1976). Assay of heparin in plasma using a chromogenic substrate. *Thromb. Res.*, **8**, 413–416.

VANNUCCHI, S., PASQUALI, F., CHIARUGI, V. & RUGGIERO, M. (1991). Heparin inhibits A-431 cell growth independently of serum and EGF mitogenic signalling. *Febs. Lett.*, **281,** 141–144.

VANNUCCHI, S., PASQUALI, F., CHIARUGI, V. & RUGGIERO, M. (1990a). Inhibition of BC3H-1 cell growth by heparin is related to decreased mitogenic signalling. *Biochem. Biophys. Res.*, **170,** 89–95.

VANNUCCHI, S., PASQUALI, F., FIORELLI, G., BIANCHINI, P. & RUGGIERO, M. (1990b). Effect of heparin on proliferation and signalling in BC3H-1 muscle cells. Evidence for specific binding sites. *Febs. Lett.*, **263,** 137–141.

VANNUCCHI, S., PASQUALI, F., PORCIATTI, F., CHIARUGI, V., MAGNELLI, L. & BIANCHINI, P. (1988). Binding, internalization and degradation of heparin and heparin fragments by cultured endothelial cells. *Thromb. Res.*, **49,** 373–383.

VOLPI, N., MASCELLANI, G. & BIANCHINI, P. (1992). Low molecular weight heparins (5kDa) and oligoheparins (2kDa) produced by gel permeation enrichment or radical process: comparison of structure and physicochemical and biological properties. *Anal. Biochem.*, **200,** 100–107.

WAHL, M.I., OKASHAW, N.E., NISHIBE, S., RHEE, S.C., PLEDGER, W.J. & CARPENTER, G. (1989). Platelet-derived growth factor induces rapid and sustained tryrosine phosphorilation of phospholipase C-gamma in quiescent balb/c 3T3 cells. *Mol. Cell. Biol.*, **9,** 2934–2943.

WRIGHT, T.C., CASTELLOT, J.J., PETITOU, M., LORMEAU, J.C., CHOAY, J. & KARNOVSKY, M.J. (1989a). Structural determinants of heparin's growth inhibitory activity. *J. Biol. Chem.*, **264,** 1534–1542.

WRIGHT, T.C., PUKAC, L.A., CASTELLOT, J.J., KARNOVSKY, M.J., LEVINE, R.A., KIM-PARK, H. & CAMPISI, J. (1989b). Heparin suppresses the induction of c-fos and c-myc mRNA in murine fibroblasts by selective inhibition of a protein kinase C-dependent pathway. *Proc. Natl. Acad. Sci. U.S.A.*, **86,** 3199–3203.

(Received October 18, 1993
Revised April 18, 1994
Accepted May 5, 1994)

Br. J. Pharmacol. (1994), **113**, 261–267

Antagonism by riluzole of entry of calcium evoked by NMDA and veratridine in rat cultured granule cells: evidence for a dual mechanism of action

[1]J.P. Hubert, *J.C. Delumeau, *J. Glowinski, *J. Prémont & A. Doble

Rhône-Poulenc-Rorer, CRVA 13 quai J Guesde, 94403 Vitry-sur-Seine and *Chaire de Neuropharmacologie U114, Collège de France, 11, place M. Berthelot, 75005 Paris, France

1 Intracellular calcium levels were measured in cultured cerebellar granule cells of the rat by use of the fluorescent dye, indo-1/AM.

2 Intracellular calcium levels were increased by depolarizing stimuli such as N-methyl-D-aspartate (NMDA) (100 μM), glutamic acid (20 μM), and veratridine (10 μM). This increase was essentially due to entry of external calcium.

3 Riluzole (10 μM) blocked responses to all the depolarizing agents.

4 Riluzole could still block the increase in intracellular calcium evoked by NMDA or glutamic acid when sodium channels were blocked by tetrodotoxin, suggesting that this effect is not mediated by a direct action of riluzole on the voltage-dependent sodium channel.

5 Pretreatment of the cells with pertussis toxin (0.1 μg ml^{-1}) did not modify the increases in intracellular calcium evoked by NMDA, glutamic acid or veratridine.

6 In pertussis toxin-treated cells, riluzole could no longer block responses to excitatory amino acids, but still blocked responses to veratridine.

7 It is concluded that riluzole has a dual action on cerebellar granule cells, both blocking voltage-dependent sodium channels and interfering with NMDA receptor-mediated responses via a pertussis toxin-sensitive mechanism. Furthermore, these two processes have been shown to be independent.

Keywords: Cerebellar granule cell culture; glutamic acid; indo-1/AM; intracellular calcium; NMDA; riluzole; veratridine

Introduction

Riluzole (2-amino-6-trifluoromethoxybenzothiazole, PK 261-24) is an anticonvulsant drug with an unusual anticonvulsant profile which suggests that it might interfere preferentially with excitatory amino acid-mediated transmission (Mizoule *et al.*, 1985). A number of subsequent studies have shown that riluzole can indeed block excitatory amino acid-evoked events in the central nervous system. These observations were first reported for glutamic acid-evoked guanosine 3':5'-cyclic monophosphate (cyclic GMP) production in cerebellar slices (Benavides *et al.*, 1985), and have since been extended to excitatory amino acid-evoked neuronal firing in the rat facial nucleus (Girdlestone *et al.*, 1989), glutamic acid-evoked calcium entry in cultured neurones (Frandsen *et al.*, 1989), and excitatory amino acid-evoked neurotransmitter release both *in vivo* (Chéramy *et al.*, 1986; 1992; Becquet *et al.*, 1989; 1990) and *in vitro* from brain slices (Benavides *et al.*, 1985; Martin *et al.*, 1993) and cultured neurones (Drejer *et al.*, 1986; 1988; Hubert & Doble, 1989).

However, radioligand binding studies have failed to provide the slightest evidence that riluzole interacts with any of the known binding sites on any excitatory amino acid receptor. Furthermore, riluzole does not antagonize effects of glutamic acid at the metabotropic glutamate receptor coupled to phospholipase C in the striatum or cerebellum (Doble & Perrier, 1989a,b). An interaction of riluozle with an allosteric site on the N-methyl-D-aspartate (NMDA) receptors has however been suggested by recent studies on excitatory amino acid receptors expressed in *Xenopus* oocytes, (Debono *et al.*, 1993). However, it is also possible that indirect effects of riluzole contribute to the blockade of excitatory amino acid-mediated events.

Tsai *et al.* (1987) were the first to suggest that blockade of voltage-dependent sodium channels and subsequent supression of action potential generation may underlie certain effects of riluzole. This hypothesis was recently confirmed directly by Benoît & Escande (1991), who showed that, in frog sciatic nerve, riluzole stabilizes the inactivated state of the voltage-dependent sodium channel. It would, however, seem unlikely that an effect on the sodium channel underlies all of the effects of riluzole on glutamic acid-evoked events, since certain of these are observed in the presence of tetrodotoxin, (Chéramy *et al.*, 1986; Hubert & Doble, 1989; Martin *et al.*, 1993). In parallel with these studies on sodium channels, we have also shown that the inhibition of glutamic acid-evoked transmitter release from cultured cerebellar granule cells is abolished upon pretreatment of the cells with pertussis toxin (Doble *et al.*, 1992). It was concluded that, in this case, the effect of riluzole involves activation of a G-protein-dependent process.

In the present study, we have examined the actions of riluzole on a system where possible interactions with both voltage-dependent sodium channels and excitatory amino acid receptors can be compared. The experimental paradigm chosen was the elevation of intracellular calcium concentrations ($[Ca^{2+}]_i$) in cultured neurones upon depolarization. Cytosolic calcium levels were monitored with the fluorescent dye indo-1 (Grynkiewicz *et al.*, 1985; Delumeau *et al.*, 1991). The results shows that riluzole does indeed interact with both sodium channels and G-protein-dependent processes, that these two actions are independent and that it is mainly the latter that contributes to the inhibition of glutamic acid-evoked calcium entry in these neurones. These results confirm and extend data that we have obtained previously on mouse cultured mesencephalic neurones (Hubert *et al.*, 1992).

[1] Author for correspondence.

Methods

Cell culture

Granule cell cultures were prepared as described by Gallo *et al.* (1982). Cerebella were removed from 7-day old rat pups (Iffa-Credo, Lyon, France), and dissociated enzymatically. The cell suspensions were plated (1.3×10^5 cells cm^{-2}) onto glass slides 45 × 70 mm coated successively with poly-L-ornithine (1.5 $\mu g\ ml^{-1}$) and laminin (2 $\mu g\ ml^{-1}$) in 10 cm Petri dishes in Dulbecco's modified Eagle medium containing 4.5 $g\ l^{-1}$ glucose supplemented with heat-inactivated foetal calf serum (3%), glutamine (1 mM) and Mixed Hormone mixture (7%). The cells were used between 4 and 6 days in a non depolarizing (5.4 mM KCl) culture condition.

Loading with indo-1/AM

Before each experiment, the nutrient medium was replaced with a modified Hank's solution containing (mM): NaCl 130, KCl 5.4, HEPES 20, glucose 5.5, $CaCl_2$ 1.25, $MgCl_2$ 1 and buffered to pH 7.4. The cells were pre-loaded with indo 1/AM by incubation in 4 ml Hank's solution containing 30 µg indo-1/AM, 50 µl 2.5% BSA and 2 µl dimethylsulphoxide (DMSO) for 1 h at 37°C, then washed and maintained at room temperature in the same modified Hank's solution prior to the fluorescence measurements.

Compound application

The cells on their glass slices were placed in a cylindrical Perspex perfusion chamber (diameter 10.6 cm, depth, 3.4 cm) on the stage of a microscope (Nikon Diaphot). The chamber was perfused horizontally at a rate of 2 ml min^{-1} with modified Hank's solution. Individual cells were identified optically and the microperfusor placed directly above them. Compounds were applied directly to the cell from a gravity fed remote controlled mutli-barralled microsuperfusion system. The diameter of the tip of the perfusion barrels was 0.2 mm, and the tip was positioned perpendicular to the flow of medium across the chamber. The material ejected from the pipettes was removed by aspiration from the other side of the cell. Normally, depolarizing agents were applied to the cell for 10 s.

Fluorescence measurements

Cytosolic calcium measurements were carried out by dual-emission microfluorometry with the indo-1/AM probe. The cells, loaded with the fluorescent probe, were excited through a 40 × oil immersion objective using a 100 W xenon light, neutrally attenuated to avoid bleaching, and filtered at 360 nm. Excitation and emission beams were separated by a 380 nm dichroic filter. Emission spectra were then divided into two halves by a 455 nm dichroic filter. From the two halves of the indo-1 emission spectra; two signals were selected by interference filters at 405 nm and 480 nm. These signals were recorded by photometers and passed to an amplifier. The fluorescence ratio F_{405}/F_{480}, which is independent of the probe concentration, was directly calculated from both signals. All optics and photometers for indo-1 were obtained from Nikon-France.

Calibration

Cytosolic calcium concentrations were calculated from the ratio according to the following equation described by Grynkiewicz *et al.* (1985) in which K_D is the dissociation constant of indo-1 for ionized calcium ions (2.5×10^{-7} M), $F_{480(f)}$ is the fluorescence of free indo-1 (1.833 ± 0.182, $n = 15$), $F_{480(b)}$ the fluorescence of indo-1 bound to calcium (0.436 ± 0.106, $n = 15$) and R_{min} (0.244 ± 0.057, $n = 15$) and R_{max} (2.132 ± 0.277, $n = 15$) were determined in the presence of ionomycin

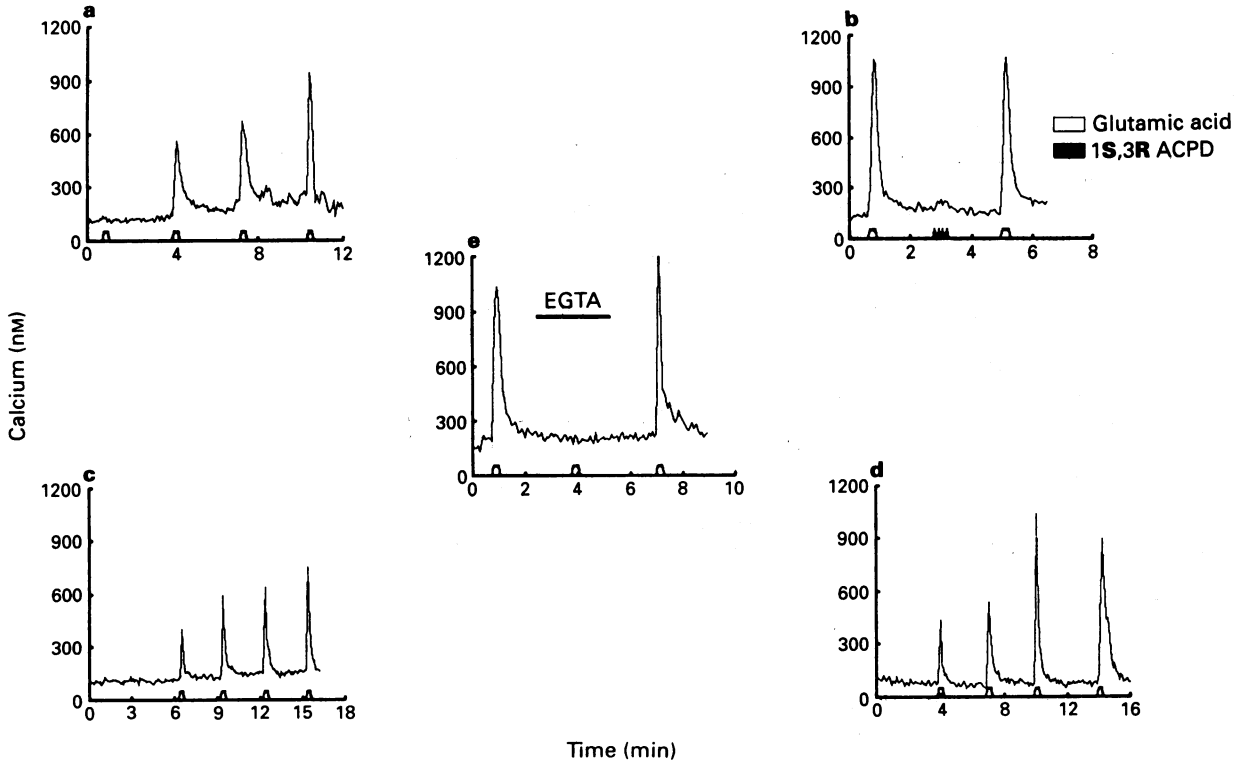

Figure 1 Effect of different depolarizing agents in the increase in intracellular calcium. Data represent a typical recording from a single cell exhibiting a response pattern similar to and representative of those obtained in 12 cells: (a) responses to increasing concentrations of veratridine (3, 10, 30, 100 µM); (b) responses to glutamic acid (20 µM), and *trans* 1S,3R ACPD (300 µM); (c) responses to increasing concentrations of NMDA (10, 30, 100, 300 µM); (d) responses to increasing concentrations of glutamic acid (3, 10, 30, 100 µM); (e) responses to glutamic acid (20 µM) with or without EGTA (3 mM).

(10^{-5} M) and either EGTA (5×10^{-3} M) or $CaCl_2$ (5×10^{-3} M) respectively.

$$[Ca^{2+}]_i = K_D \times \frac{F_{480(f)}}{F_{480(b)}} \times \frac{R - R_{min}}{R_{max} - R}$$

Reagents

Riluzole was synthesized by Dr P. Jimonet at Rhône-Poulenc-Rorer, Vitry, France. Pertussis toxin was purchased from List Biologicals Inc, San Diego, U.S.A. Tetrodotoxin, D-serine, lanthanum chloride, glutamic acid, NMDA (N-methyl-D-aspartic acid), excitatory amino acids and veratridine were from Sigma Chemical Co, St. Louis, U.S.A.; quisqualic acid, (1S,3R) ACPD (1 aminocylopentane-1S, 3R-dicarboxylic acid), CNQX (6-cyano-7-nitroquinoxaline-2,3-dione), and MK 801 ((+)-5-methyl-10, 11-dihydro-5H-dibenzol [a, d] cycloheptine-5-10-imine) from Research Biochemicals Inc, Natick, U.S.A. Cell culture media were purchased from GIBCO, Glasgow, UK, except the NU-Serum which was from Collaborative Research. Indo-1/AM was obtained from Molecular Probes Inc, Eugene, U.S.A.

Results

Rat cerebellar granule cells grown in primary culture had basal intracellular calcium levels of 142 ± 5 nM ($n = 104$). Superfusion of these cells with L-glutamic acid (20 μM) led to a rapid rise in intracellular calcium levels to 906 ± 34 nM ($n = 60$), which quickly returned to basal upon removal of glutamic acid (Figure 1). In the presence of D-serine (10 μM) and $LaCl_3$ (1 μM) in nominally magnesium-free medium, basal calcium levels were 169 ± 6 nM ($n = 106$), which increased to 827 ± 50 nM ($n = 63$) in the presence of NMDA (100 μM, Figure 2). Quisqualic acid (300 μM) had a small stimulatory effect on intracellular calcium 347 ± 42 nM on some, but not all of the cells tested (13/20). (1S,3R) *t* ACPD (300 μM) was inactive ($n = 15$). Veratridine (10 μM) increased intracellular calcium levels to 1079 ± 66 nM ($n = 30$, Figure 1). Depolarization with KCl (20 mM) also raised intracellular calcium levels (694 ± 86; $n = 12$). The EC_{50} values for the different depolarizing agents are summarized in Table 1, and typical dose-response curves in Figure 1. Stimulations by the different depolarizing agents could be reiterated up to six times without observing tachyphylaxis or drift of the basal intracellular calcium concentrations.

Tetrodotoxin (TTX, 1 μM) completely abolished the response to veratridine (10 μM) in these cells (Figure 2). In contrast, the response to glutamic acid (20 μM) was unaffected by tetrodotoxin. The response to glutamic acid could, however, be markedly reduced by the NMDA receptor antagonist MK 801 (1 μM, Figure 3). The NMDA-evoked response was also antagonized by MK 801. The relevant IC_{50} values are given in Table 2. The stimulatory effects of glutamic acid were not modified by inclusion of $LaCl_3$ in the incubation medium, whereas those of veratridine were abolished (data not shown). When external calcium was

Table 1 Increases in intracellular calcium evoked by excitatory amino acids and veratridine

Agonists	EC_{50}(μM)
trans-1S,3R ACPD	NA
Glutamic acid	8 ± 0,6
Quisqualic acid	NA
NMDA	18 ± 1
Veratridine	8.3 ± 0.8

Four-point cumulative concentration-response curves were obtained for each cell and the EC_{50} values determined by computer-assisted iterative non-linear regression analysis. Data are expressed as the mean ± s.e.mean of EC_{50} values obtained from 12 individual cells.

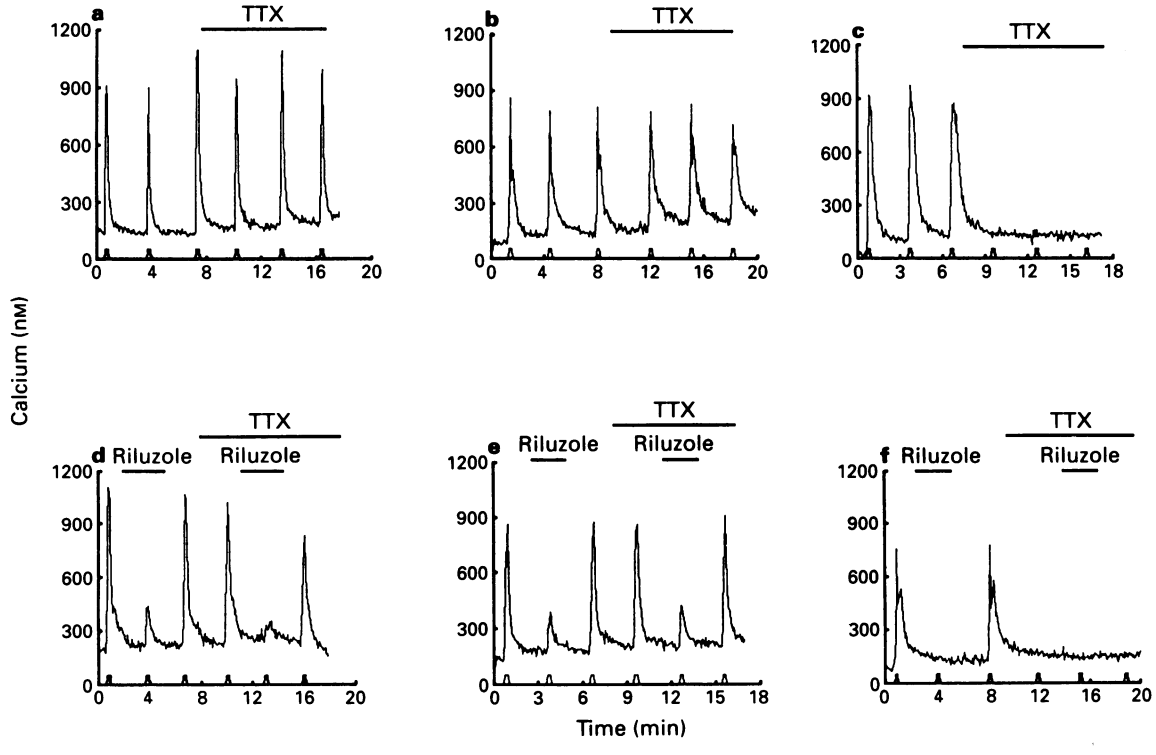

Figure 2 Top: effect of tetrodotoxin (1 μM) on the increase in cytosolic calcium evoked by glutamic acid (20 μM; a), NMDA (100 μM; b), or veratridine (10 μM, c). Bottom: effect of riluzole (1 μM versus glutamic acid (d); 100 μM versus NMDA (e); or 10 μM versus veratridine (f)); the sodium channel blocker TTX (1 μM) was added after the third stimulation. Data represent a typical recording from a single cell exhibiting a response pattern similar to and representative of those obtained in 12 cells from three different preparations.

removed and buffered with EGTA (3 mM), the rise in intracellular calcium evoked by glutamic acid (20 μM) was completely abolished (Figure 1).

Riluzole inhibited the elevation of intracellular calcium evoked by glutamic acid and by veratridine with IC_{50} values of 0.30 ± 0.07, 0.31 ± 0.02 respectively (Figure 3, Table 2). A similar inhibition of the NMDA response was observed at somewhat higher concentrations (Figure 3, Table 2), but K^+-evoked $[Ca^{2+}]_i$ was unaffected (data not shown). The inhibitory effect of riluzole on the glutamic acid response was not modified in the presence of TTX (Figure 2). It was, of course, not possible to study veratridine-evoked responses in the presence of TTX. MK 801 blocked the responses to glutamic acid (IC_{50} = 0.11 ± 0.01 μM) and NMDA (IC_{50} = 0.074 ± 0.020 μM), but not to veratridine (Figure 3, Table 2). When the cells were pretreated for 24 h with pertussis toxin (0.1 μg ml^{-1}), no changes were observed in either basal calcim levels in standard conditions 144 ± 9 nM (n = 24) or in nominally magnesium-free medium 158 ± 13 nM (n = 24) res-

Table 2 Inhibition of depolarization-evoked calcium responses by riluzole and MK 801

	Glutamic acid (12)	*NMDA* (12)	*Veratridine* (12)
Riluzole	0.30 ± 0.07	12.8 ± 2.4	0.31 ± 0.02
MK 801	0.11 ± 0.01	0.074 ± 0.020	NA

The values are expressed as the mean ± s.e.mean (μM) of at least 12 observations from cells taken from three separate preparations. Individual cells were stimulated three times with a fixed concentration of glutamic acid (20 μM), NMDA (100 μM), or veratridine (10 μM). Antagonists were added during the second stimulation. Three concentrations of antagonist were tested on separate populations of 12 cells. The percentage inhibition of the agonist response was calculated and the IC_{50} values determined by regression analysis as a function of the logarithm of the antagonist concentration performed on the total population of observations.

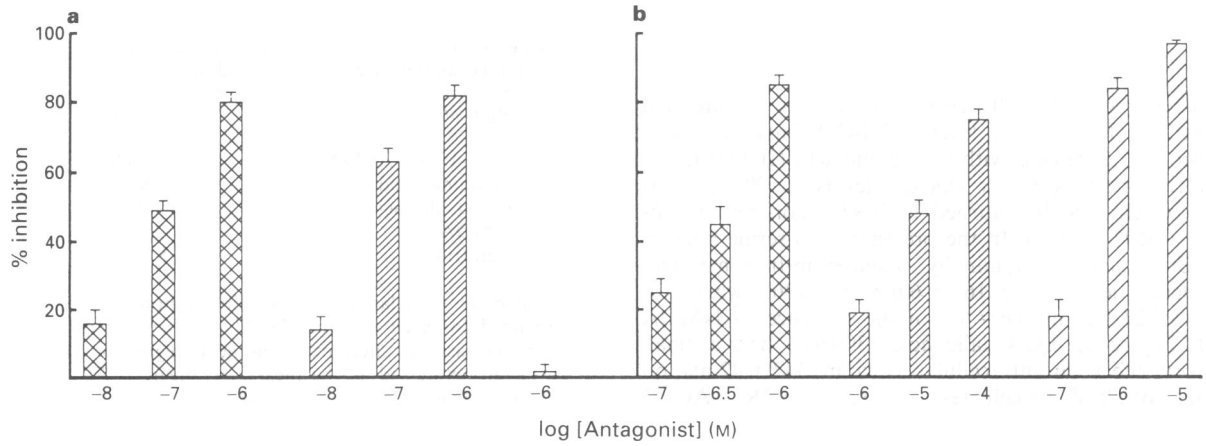

Figure 3 Inhibition of calcium responses to depolarizing agents by riluzole and MK 801. Data are expressed as the mean ± s.e.mean of the percentage inhibition of responses to glutamic acid (20 μM; ▨), NMDA (100 μM; ▨) or veratridine (10 μM; ▨), and were obtained from 12 cells from at least three different preparations at each concentration. (a) Inhibition by MK 801; (b) inhibition by riluzole.

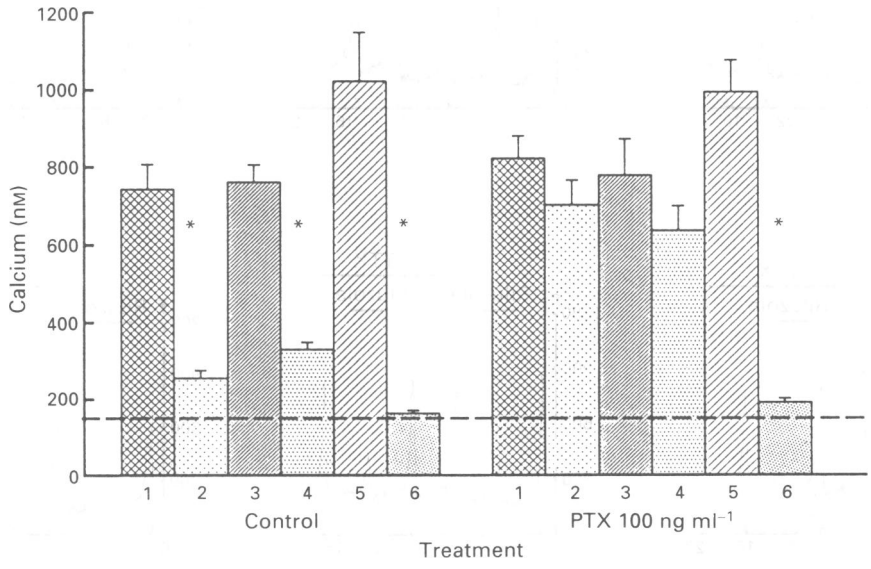

Figure 4 Effect of pertussis toxin on inhibition by riluzole of calcium responses to depolarizing agent. Data are expressed as $[Ca^{2+}]_i$; the dotted horizontal line represents the basal intracellular calcium levels in these cells. Each column represents the mean ± s.e.mean of data from 12 cells from three different preparations. The cells were stimulated three times with glutamic acid (20 μM; (1); NMDA (100 μM) (3)) or veratridine (10 μM; (5)) following the protocol illustrated in Figure 5, and riluzole added during the second application: (2) glutamic acid + 1 μM riluzole; (4) NMDA + 100 μM riluzole; (6) veratridine + 10 μM riluzole. A significant ($P \leqslant 0.005$; Wilcoxon's test) inhibition by riluzole is indicated by the asterisk.

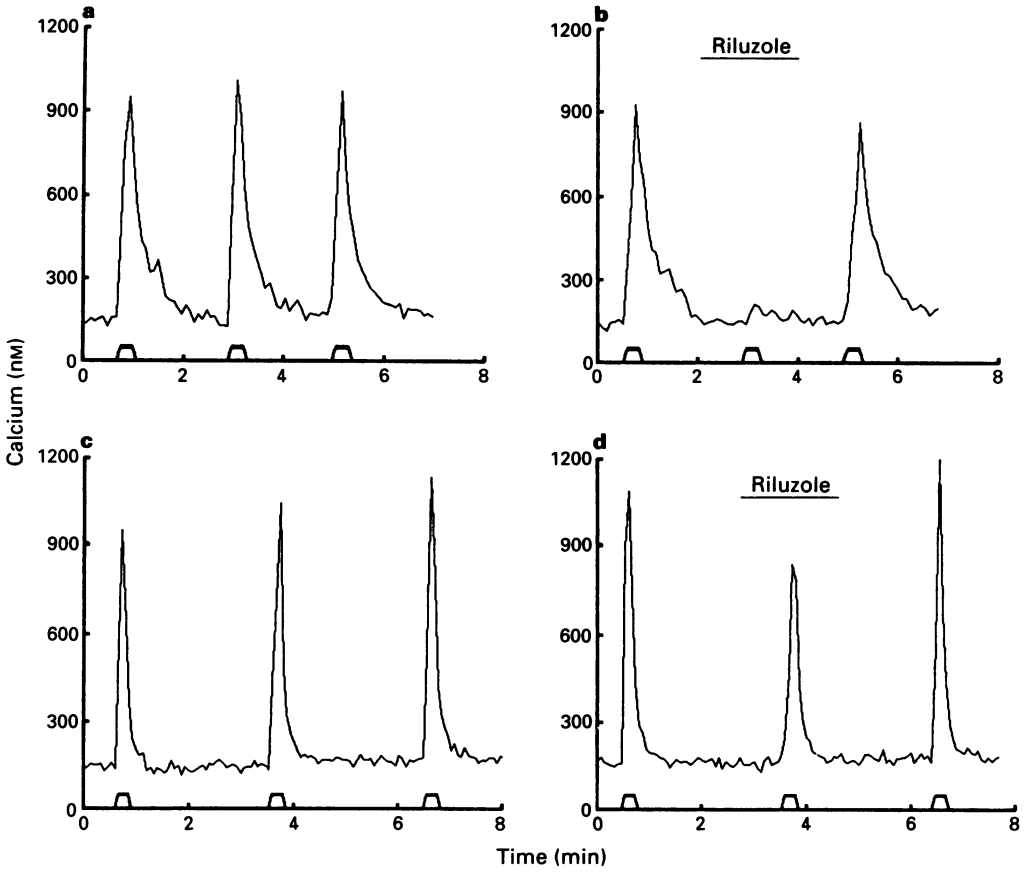

Figure 5 Effect of pretreatment with pertussis toxin on glutamic acid-evoked responses. Pretreatment of granule cells with pertussis toxin (PTX) (0.1 $\mu g\ ml^{-1}$) for 20 h before the fluorescence measurement did not modify the increase in cytosolic calcium evoked by L-glutamic acid (20 μM), ((a) control and (c) PTX). Such a treatment did however, completely abolish the inhibition by riluzole ((1 μM), (b) control, and (d) PTX). Data represent a typical recording from a single cell exhibiting a response pattern similar to and representative of those obtained from three different cell preparations and represent 12 cells.

pectively, or in glutamic acid 822 ± 58 nM ($n = 12$), or in veratridine 995 ± 81 nM ($n = 12$), and in NMDA 783 ± 62 nM ($n = 24$) evoked $[Ca^{2+}]_i$. Such a treatment completely abolished the inhibitory effect of riluzole on the responses evoked by glutamic acid (Figures 4 and 5) and NMDA (Figure 4). The inhibitory effect of MK 801 persisted in the cells pretreated with pertussis toxin (87 ± 3% inhibition at 10^{-6} M; data not shown). On the other hand, responses to veratridine in pretreated cells could still be blocked by riluzole.

Discussion

The feasibility of using a dual-emission microfluorimetric system for the measurement of intracellular calcium in single cerebellar granule cells has been demonstrated by Irving *et al.* (1992). This study extends the use of the technique from previous applications in, for example pituitary cells (Mollard *et al.*, 1989), cultured rat spinal neurones (Schieren & MacDermot, 1988) and astrocytes (Delumeau *et al.*, 1991). We have applied this technique to study the effect of riluzole on depolarization-evoked $[Ca^{2+}]_i$ in single identified neurones. In these cells, $[Ca^{2+}]_i$ can be observed after depolarizing the cells with either excitatory amino acids, potassium ions or the sodium-channel activator, veratridine.

The responses to excitatory amino acids seem to be mediated essentially by receptors of the NMDA subtype, since the metabotropic receptor agonist 1S,3R *t* ACPD and the mixed metabotropic and AMPA receptor agonist, quisqualic acid, did not lead to pronounced increases in intracellular calcium. Furthermore, the highly selective NMDA antagonist, MK 801, completely abolished responses to both glutamic acid and NMDA with indistinguishable IC_{50} values. These findings are partially in agreement with those of Pearson *et al.* (1992) using the fura-2 technique, who found that the dominant $[Ca^{2+}]_i$ response to excitatory amino acids in those cells cultured under these conditions was mediated by NMDA receptors. However, in contrast to Zhao & Peng (1993), we did not observe responses to metabotropic receptor agonists, even though the cells were grown in non-depolarizing conditions. On the other hand, Nicoletti *et al.* (1993) did not observe expression of metabotropic receptors coupled to phospholipase C in cerebellar granule cells cultured in low potassium medium. It is also likely that the rises in intracellular calcium are due to calcium entry via the NMDA receptor channel, since they are not modified by blocking voltage-sensitive calcium channels with lanthanum chloride and are no longer seen in the absence of extracellular calcium. This is supported by recent studies by Simpson *et al.* (1993), who have demonstrated that the rise in intracellular free calcium levels evoked by NMDA receptor activation is essentially due to calcium entry. Moreover, Frandsen *et al.* (1989) demonstrated that glutamic acid directly stimulated $^{45}Ca^{2+}$ entry into cultured cortical neurones. Riluzole was able to antagonize the increase in cytosolic calcium evoked by glutamic acid and NMDA at concentrations previously shown to block the effects of excitatory amino acids in other systems (Benavides *et al.*, 1985; Drejer *et al.*, 1986; Hubert & Doble, 1989) and at which blockade of NMDA responses has been observed in *Xenopus* oocytes (Debono *et al.*, 1993). The IC_{50} value of riluzole against

responses to NMDA was higher than that against responses to glutamic acid or veratridine. If the antagonism of NMDA responses by riluzole reported in the studies od Benavides *et al.* (1985) and Debono *et al.* (1993) were to be competitive, this might be explained in part by the concentration of agonist used in the NMDA experiments (100 μM), which was 5.5 times the EC_{50} value, compared to that used in the glutamic acid experiments (20 μM), which was 2.5 times the EC_{50} value. However, a competitive action of riluzole at the NMDA receptor would be difficult to reconcile with the lack of activity of riluzole in binding studies. Further electrophysiological experiments would be necessary to identify the kinetic mechanisms of the interaction of riluzole with the NMDA receptor. We are currently unable to give a satisfactory explanation for difference in IC_{50} values seen with NMDA and glutamic acid. In order to determine whether the effect of riluzole on NMDA receptor-mediated calcium entry was direct, or, as suggested by Tsai *et al.* (1987), indirect, the effect of riluzole was examined in the presence of either the sodium-channel blocker tetrodotoxin or pertussis toxin, an inactivator of certain G-proteins. Riluzole still blocked responses to glutamic acid and NMDA in the presence of concentrations of tetrodotoxin that totally abolished veratridine-induced depolarization. This suggests that this effect of riluzole is not mediated by a sodium channel blocking effect of this drug. On the other hand, in the presence of pertussis toxin, the activity of riluzole on NMDA and glutamic acid-evoked responses was lost. This is in agreement with our previous work on the release of D-[^{3}H]-aspartate from cerebellar granule cells, where, again, the inhibitory effect of riluzole was abolished by pertussis toxin (Doble *et al.*, 1992). These data suggest that the interaction between riluzole and excitatory amino acid-mediated events may involve activation of a pertussis toxin-sensitive G-protein, perhaps by directly activating a coupled receptor (such an interaction has been observed between adenosine and α-adrenoceptors on astrocytes by Delumeau *et al.* (1991)).

It is somewhat surprising that pertussis toxin should abolish the effect of riluzole on a receptor ion channel such as the NMDA receptor, since these are not generally thought to be regulated by or coupled to G-proteins. However, it has been shown recently by Ben-Ari *et al.* (1992), that NMDA receptor function can be modified by the phosphorylation state of the receptor protein. Furthermore, Murphy *et al.* (1994) propose that phosphorylation by PKC exerts not only a potentiating but also a permissive effect on the NMDA-evoked elevation in cytosolic calcium in striatal neurones. Such a mechanism might underly the non-competitive block of the NMDA receptor by riluzole, if this compound were to activate a G-protein dependent intracellular event which would lead to the dephosphorylation of the NMDA receptor. On the other hand, the ability of riluzole to block the increase in intracellular calcium evoked by veratradine is unaffected by pretreatment of the cells with pertussis toxin. This suggests that this activity does not involve G-proteins, and may reflect a direct action of riluzole on the voltage-dependent sodium channel, as has been demonstrated by Benoît & Escande (1991) in the frog sciatic nerve. It should be pointed out that it is unlikely that riluzole interferes with the mechanism of $[Ca^{2+}]_i$ itself, since this compound does not affect the elevation of intracellular calcium seen upon depolarization of the cells with potassium ions.

In conclusion, these studies demonstrate that riluzole has two distinct mechanisms of action in mammalian neurones. Firstly, this molecule interacts with the voltage-dependent sodium channel, probably by stabilizing the inactivated conformation, as first shown by Benoît & Escande (1991). Secondly, by activation of a G-protein-dependent process, riluzole counteracts the activation by excitatory amino acids of the NMDA receptor. Which of these two mechanisms underlies the anticonvulsant and neuroprotective activities of riluzole seen in animal studies (Mizoule *et al.*, 1985; Malgouris *et al.*, 1989) or in the clinic (Bensimon *et al.*, 1994) remains to be demonstrated.

References

BECQUET, D., FAUDON, M. & HERY, F. (1989). Effect of thalamic parafascicularis nucleus stimulation in regulation of serotoninergic transmission in the cat caudate nucleus: involvement of autoreceptors in the dorsalis raphe nucleus. *Neuroscience*, **33**, 293–300.

BECQUET, D., FAUDON, M. & HERY, F. (1990). In vivo evidence for an inhibitory glutamatergic control of serotonin release in the cat caudate nucleus: involvement of GABA neurones. *Brain Res.*, **519**, 82–88.

BENAVIDES, J., CAMELIN, J.C., MITRANI, N., FLAMAND, F., UZAN, A., LEGRAND, J.J., GUÉRÉMY, C. & LE FUR, G. (1985). 2-Amino-6-trifluoromethoxy benzothiazole. A possible antagonist of excitatory amino acid neurotransmission II. *Neuropharmacology*, **24**, 1085–1092.

BEN-ARI, Y., ANIKSZTEJN, L. & BREGESTOVSKI, P. (1992). Protein kinase C modulation of NMDA currents: an important link for LTP induction. *Trends Neurosci.*, **15**, 333–339.

BENSIMON, G., LACOMBLEZ, L., MENINGER, V. & THE ALS/RILUZOLE STUDY GROUP. (1994). A controlled trial of riluzole in Amyotrophic Lateral Sclerosis. *N. Engl.J. Med.*, **330**, 585–591.

BENOÎT, E. & ESCANDE, D. (1991). Riluzole specifically blocks inactivated Na channels in myelinated nerve fibre. *Pflügers Arch.*, **361**, 1–7.

CHÉRAMY, A., BARBEITO, L., GODEHEU, G. & GLOWINSKI, J. (1992). Riluzole inhibits the release of glutamate in the caudate nucleus of the cat in vivo. *Neurosci. Lett.*, **147**, 209–212.

CHÉRMAY, A., ROMO, R., GODEHEU, G., BARUCH, P. & GLOWINSKI, J. (1986). In vivo presynaptic control of dopamine release in the cat caudate nucleus II. Facilitatory or inhibitory influence of L-glutamate. *Neuroscience*, **9**, 1081–1090.

DEBONO, M.W., LE GUERN, J., CANTON, T., DOBLE, A. & PRADIER, L. (1993). Inhibition by riluzole of electrophysiological responses mediated by rat kainate and NMDA receptors expressed in *Xenopus* oocytes. *Eur. J. Pharmacol.*, **235**, 283–289.

DELUMEAU, J.C., TENCÉ, M., MARIN, P., CORDIER, J., GLOWINSKI, J. & PREMONT, J. (1991). Synergistic regulation of cytosolic calcium concentration by adenosine and α1-adrenergic agonists in mouse striatal astrocytes. *Eur. J. Neurosci.*, **3**, 539–550.

DOBLE, A., HUBERT, J.P. & BLANCHARD, J.C. (1992). Pertussis toxin pretreatment abolishes the inhibitory effect of riluzole and carbachol on D-[^{3}H]aspartate release from cultured cerebellar granule cells. *Neurosci. Lett.*, **140**, 251–254.

DOBLE, A. & PERRIER, M.L. (1989a). Pharmacology of excitatory amino acid receptors coupled to inositol phosphate metabolism in neonatal rat striatum. *Neurochem. Int.*, **15**, 1–8.

DOBLE, A. & PERRIER, M.L. (1989b). Kainic acid-preferring receptors stimulate inositol phosphate formation in cultured cerebellar granule cells. *Br. J. Pharmacol.*, **96**, 316P.

DREJER, J., HONORÉ, T., MEIER, E. & SCHOUSBOE, A. (1986). Pharmacologically distinct glutamate receptors on cerebellar granule cells. *Life Sci.*, **38**, 2077–2085.

DREJER, J., HONORÉ, T. & SCHOUSBOE, A. (1988). Excitatory amino acid-induced release of ^{3}H-GABA from cultured mouse cerebral cortex interneurones. *J. Neurosci.*, **7**, 2910–2916.

FRANDSEN, A., DREJER, J. & SCHOUSBOE, A. (1989). Glutamate induced $^{45}Ca^{++}$ uptake into immature cerebral cortex neurones shows a distinct pharmacological profile. *J. Neurochem.*, **53**, 1959–1962.

GALLO, V., CIOTTI, M.T., COLETTI, A., ALOSI, F. & LEVY, G. (1982). Selective release of glutamate from cerebellar granule cells differentiating in culture. *Proc. Natl. Acad. Sci. U.S.A.*, **79**, 7919–7923.

GIRDLESTONE, D., DUPUY, A., ROY-CONTANCIN, L. & ESCANDE, D. (1989). Riluzole antagonises excitatory amino acid evoked firing in rat facial motoneurones. *Br. J. Pharmacol.*, **97**, 383P.

GRYNKIEWICZ, G., POENIE, M. & TSIEN, R.Y. (1985). A new generation of Ca^{2+} indicators with greatly improved fluorescence properties. *J. Biol. Chem.*, **260**, 3440–3450.

HUBERT, J.P., DELUMEAU, J.C., PRÉMONT, J., DOBLE, A. & GLOWINSKI, J. (1992). Mobilisation du calcium intracellulaire dans des neurones de mésencéphale de rat en culture induite par une dépolarisation. Antagonisme par le riluzole. *Colloque de la Société des Neurosciences*, Strasbourg, France, **83**, A79.

HUBERT, J.P. & DOBLE, A. (1989). Ibotenic acid stimulates D-[^{3}H]aspartate release from cultured cerebellar granule cells. *Neurosci. Lett.*, **96**, 345–350.

IRVING, A.J., COLLINGRIDGE, G.L. & SCHOFIELD, J.G. (1992). Interactions between calcium mobilizing mechanisms cultured rat cerebellar granule cells. *J. Physiol.*, **456**, 667–680.

MALGOURIS, C., BARDOT, F., DANIEL, M., PELLIS, F., RATAUD, J., UZAN, A., BLANCHARD, J.C. & LADURON, P.M. (1989). Riluzole, a novel antiglutamate, prevents memory loss and hippocampal neuronal damage in ischemic gerbils. *J. Neurosci.*, **9**, 3720–3727.

MARTIN, D., THOMPSON, M.A. & NADLER, V. (1993). The neuroprotective agent riluzole inhibits release of L-glutamate and L-aspartate from slices of the hippocampal area CA1. *Eur. J. Pharmacol.*, **250**, 473–476.

MIZOULE, J., MELDRUM, B., MAZADIER, M, CROUCHER, M., OLLAT, C., UZAN, A., LEGRAND, J.J., GUÉRÉMY, C. & LE FUR, G. (1985). 2-amino-6-trifluoromethoxy benzothiazole, a possible antagonist of excitatory amino acid neurotransmission I. *Neuropharmacology*, **24**, 767–773.

MOLLARD, P., GUERINEAU, N., AUDIN, J. & DUFY, B. (1989). Measurement of Ca^{2+} transients using simultaneous dual-emission microspectrofluorimetry and electrophysiology in individual pituitary cells. *Biochem. Biophys. Res. Commun.*, **164**, 1045–1052.

MURPHY, N.P., CORDIER, J., GLOWINSKI, J. & PRÉMONT, J. (1994). Does protein kinase C exert a permissive effect on the N-Methyl-D-Asparate-evoked rise in cytosolic calcium in striatal neurones? *Eur. J. Neurosci* (in press).

NICOLETTI, F., ARONICA, E., DELL'ALBANI, P., CONDORELLI, D.F., HACK, N. & BALAZS, R. (1993). Mechanisms underlying developmental changes in the expression of metabotropic glutamate receptors. *J. Neurochem.*, **61**, S123D.

PEARSON, H., GRAHAM, M.E. & BURGOYNE, R.D. (1992). N-methyl-D-aspartate responses in rat cerebellar granule cells are modified by chronic depolarisation in culture. *Neurosci. Lett.*, **142**, 27–30.

SCHIEREN, I. & MACDERMOTT, A. (1988). Flow cytometric identification and purification of cells by ligand-induced changes in intracellular calcium. *J. Neurosci. Methods*, **26**, 35–44.

SIMPSON, P.B., CHALLISS, R.A.J. & NAHORSKI, S.R. (1993). Involvement of intracellular stores in the calcium responses to N-methyl-D-aspartate and depolarization in cerebellar granule cells. *J. Neurochem.*, **61**, 760–763.

TSAI, C., STEEL, D.J., MCPHERSON, S., TAYLOR, C.A., WOOD, P.L. & LEHMANN, J. (1987). PK 26124 is not a competitive antagonist at NMDA-type receptors. In *Excitatory Amino Acid Transmission*. ed. Hicks, P., Lodge, D. & McClennan, H. pp. 79–82. London: A.R. Liss.

ZHAO, Z. & PENG, L. (1993). Glutamate effects on calcium homeostasis in cerebellar granule cells in primary cultures grown under depolarizing and non-depolarizing conditions. *Synapse*, **13**, 315–321.

(Received January 6, 1994
Revised April 22, 1994
Accepted May 5, 1994)

Br. J. Pharmacol. (1994), **113**, 268–274

Benzodiazepine-induced intestinal motor disturbances in rats: mediation by ω_2 (BZ_2) sites on capsaicin-sensitive afferent neurones

Cécile Bonnafous, *Bernard Scatton & [1]Lionel Buéno

Department of Pharmacology I.N.R.A., 180 Chemin de Tournefeuille, 31300 Toulouse, France and *Synthelabo Recherche, Preclinical Research Department, 31 Avenue Paul Vaillant-Couturier, 92220 Bagneux, France

1 The central and peripheral effects of the ω (benzodiazepine) site ligands, clonazepam, alpidem, zolpidem, triazolam, flumazenil, ethyl β carboline-3-carboxylate (β-CCE) and N-methyl β carboline-3-carboxylate (β-CCM) on intestinal myoelectrical activity were evaluated in conscious rats, chronically fitted with Nichrome electrodes implanted on the duodenum and jejunum. The localization of the ω (benzodiazepine) receptors involved in these effects was evaluated by use of systemic and perivagal capsaicin treatments.

2 When administered intraperitoneally (i.p.) the ω site inverse agonists β-CCE and β-CCM, and the ω site antagonist flumazenil, did not affect the duodeno-jejunal motility. Alpidem and zolpidem, two selective ω_1 site agonists induced an inhibition of migrating myoelectric complexes (MMCs) only at a high dose (5 mg kg^{-1}). In contrast, clonazepam (a mixed ω_1/ω_2 agonist) and triazolam (a preferential ω_2 site agonist) disrupted the MMC-pattern at doses as low as 0.05 mg kg^{-1}, the effect of triazolam being of much longer duration than that of clonazepam. None of these drugs altered MMC-pattern when administered centrally (i.c.v.).

3 Administered i.p. or i.c.v. prior to triazolam, alpidem blocked the effect of triazolam on duodeno-jejunal spike activity. Administered i.p. prior to triazolam, flumazenil suppressed the triazolam-induced MMC-disruption. Previous systemic but not perivagal capsaicin treatment suppressed the effects of clonazepam on MMCs.

4 It is concluded that ω-site agonists but not antagonist or inverse agonists, administered systemically induce intestinal motor disturbances which may be linked to activation of ω_2 (BZ_2) sites located on nonvagal capsaicin-sensitive afferent neurones.

Keywords: Benzodiazepine-sites; intestinal motility; capsaicin-sensitive neurones

Introduction

The benzodiazepines (BZs) have been the most widely prescribed drugs for the treatment of anxiety and related neurotic disorders during the past three decades. The neuropharmacological effects of BZ derivatives are mediated by their interaction with a specific recognition site within the $GABA_A$ receptor macromolecular complex, the so-called ω (BZ) modulatory site. Activation of the ω site increases the chloride conductance of the $GABA_A$ receptor complex leading to hyperpolarization of the target cells.

Several lines of evidence have suggested a heterogeneity of the ω modulatory sites. Binding sites with high affinity for the triazolopyridazine, CL 218,872 (Klepner *et al.*, 1979), the imidazopyridines, zolpidem and alpidem (Arbilla *et al.*, 1985; Langer *et al.*, 1990), and several β carbolines (Braestrup & Nielsen, 1981; Braestrup *et al.*, 1982) are termed ω_1 (BZ_1) and sites with low affinity for these ligands are termed ω_2 (BZ_2) sites (Langer & Arbilla, 1988). Recent advances in molecular biology have demonstrated that $GABA_A$ receptors are made up of different subunits (α,β,γ) probably associated in pentameric complexes and that ω sites are associated with the α subunits (see Olsen & Tobin, 1990 for review). At least six variants of this subunit have been reported and this heterogeneity appears to be responsible for the existence of different ω site subtypes. Ligands that possess affinity for the ω sites can induce different functional effects at $GABA_A$ receptors: while agonists or partial agonists have positive intrinsic activity and enhance the functional response to GABA. The antagonists have no intrinsic activity and the inverse agonists have negative intrinsic activity i.e. inhibit the functional response to GABA.

The ω sites are essentially located in the central nervous system but 'central type' ω sites can also be found in the myenteric plexus (Cherubini & North, 1985; Taniyama *et al.*, 1988). They differ from peripheral type BZ receptors (p sites) located in various organs and in non-neuronal brain tissues which are not associated with the $GABA_A$ receptor macromolecular complex (Benavides *et al.*, 1989; 1990).

The benzodiazepines, in the range of their therapeutic doses have been shown to alter the motility of the small intestine in rats, producing an increased motor activity associated with a disruption of the migrating myoelectric complexes (MMCs) characterizing the fasted state (Martinez *et al.*, 1992; Bonnafous *et al.*, 1993). Similarly, in fasted dogs, diazepam administered intravenously (i.v.) disrupts the MMC-pattern in a time-related manner (Fargeas *et al.*, 1984). Furthermore, in man, vomiting, nausea, diarrhoea and epigastric distress often occur following administration of high doses of benzodiazepines (Harvez *et al.*, 1985).

The purpose of the present study was to determine which subtype of ω site mediates these intestinal motor disturbances. To this end, we studied the effects of a number of ω site ligands with differing selectivity for the ω_1 and ω_2 subtypes on intestinal myoelectrical activity in conscious rats Secondly, we investigated the central vs peripheral localization of those ω sites involved in this effect. The following ligands were used: clonazepam (a non selective ω site agonist), alpidem (a partial ω_1 receptor agonist), zolpidem (a full ω_1 site agonist), triazolam (a preferential ω_2 site agonist), flumazenil (a non selective ω site antagonist), ethyl β carboline-3-carboxylate (β-CCE) and N-methyl β carboline-3-carboxylate (β-CCM) (two ω site inverse agonists).

[1] Author for correspondence.

Methods

Animal preparation

One hundred and twelve male Wistar rats, weighing 200–250 g, were prepared for long-term electromyographic recordings (Ruckebusch & Fioramonti, 1975). Briefly, following induction of anaesthesia with 100 mg kg^{-1} i.p. of ketamine (Imalgene-1000, Rhône-Mérieux, Lyon, France), nichrome wire electrodes (80 μm in diameter) were implanted in the wall of the proximal and distal duodenum (3 and 6 cm from the pylorus) and in the wall of the jejunum (10 and 20 cm from the Treitz' ligament). The insulated electrode wires (80 cm in length) were exteriorized on the back of the neck and protected by a glass tube attached to the skin. Rats were also fitted with permanent polyethylene catheters (PE 10) inserted into the lateral ventricles of the brain (2 mm from the saggital suture and 1 mm from the coronal suture).

Myoelectric recordings and analysis

Electromyographic recordings were initiated five days after surgery. The spiking activity was amplified with an electroencephalograph machine (minihuit ALVAR, France), summated every 20 s by an integrator circuit and automatically plotted 24 h day^{-1} on a potentiometric recorder with a paper speed of 5 cm h^{-1} (Latour, 1973). This 'integrated record' allowed a clear determination of the different patterns of intestinal activity and, particularly, the identification of the migrating myoelectric complexes (MMCs), characterizing the fasted pattern. Intestinal myoelectric activity was analysed over a daily 10 h period, from 09 h 00 min to 19 h 00 min. Modifications appearing after drug injections were appraised by measuring the duration of motor changes i.e. disruption of MMCs. It has been demonstrated that the duration of motor changes is directly correlated to the intensity of electrical activity and mechanical activity (Buéno *et al.*, 1981).

Capsaicin treatments

Systemic capsaicin treatment Capsaicin (Sigma, La Verpillière, France) was systemically administered to a group of eight rats for 4 days. Capsaicin, dissolved in 80% saline, 10% ethanol and 10% Tween 80, was administered subcutaneously. Injections were performed at increasing doses to reach a total dose of 125 mg kg^{-1}. The efficacy of capsaicin treatment was assessed by the eye-wiping test (Holzer *et al.*, 1990): impaired chemosensitivity of corneal afferents which are no longer sensitive to a solution of 1% NH_4OH. Another group of rats ($n = 8$) was treated with the capsaicin vehicle only.

Perivagal capsaicin treatment Eight rats were anaesthetized with ketamine (100 mg kg^{-1}, i.p.) and received atropine sulphate (1 mg kg^{-1}, i.p.) to decrease the acute effects of capsaicin on the respiratory and cardiovascular systems. Cervical vagi were carefully dissected from the carotid artery and isolated. A 1% solution of capsaicin (10 mg ml^{-1}) was applied to each vagus nerve in turn for 30 min. At 10 min intervals, the nerves were swabbed and capsaicin reapplied. The maximum amount of capsaicin applied was 0.5–0.6 mg per rat. After application, the area was thoroughly rinsed with sterile saline (Rayboud *et al.*, 1990). A group of sham animals ($n = 8$) was treated in the same manner but with the capsaicin vehicle alone.

The efficacy of perivagal capsaicin treatment was assessed 15 days later by the CCK satiety test (South & Ritter, 1988). CCK8S (20 μg kg^{-1}) was administered i.p.; on sham animals CCK8S induced satiety as it did on control rats, whereas on perivagal capsaicin-treated rats CCK8S had no effect: animals ate as naive rats. Systemic and perivagal capsaicin treatments were performed 15–20 days before electromyographic recordings.

Drugs

The drugs used for this study were: clonazepam, (Roche, Paris, France), alpidem, zolpidem and triazolam (gifts from Synthélabo, Bagneux, France), flumazenil (Hoffman La Roche, Paris, France); β-CCE and β-CCM (RBI, Natick, U.S.A.).

Experimental procedure

In a first series of experiments, 32 rats were randomly treated by intraperitoneal (i.p.) administration of clonazepam and triazolam at doses of 0.05, 0.1, 0.3 and 0.5 mg kg^{-1}, zolpidem and alpidem at the doses of 0.05, 0.1, 0.3, 0.5 1 and 5 mg kg^{-1} or their vehicle (dimethylsulphoxide: DMSO) (0.3 ml). These drugs or their vehicle (3 μl) were also administered intracerebroventricularly (i.c.v.) to the same rats at the dosage of 10 and 100 μg kg^{-1}.

In a second set of experiments, 24 rats were randomly treated i.p. with either β-CCE, β-CCM at doses of 0.1 and 1 mg kg^{-1}, and either flumazenil at doses of 0.1, 1 and 5 mg kg^{-1}, or their vehicle. They also received DMSO i.c.v. alone or containing one of the three previous drugs at a dose of 10 and 100 μg kg^{-1}.

In the third series of experiments, 16 rats were used and divided into two groups. In the first group ($n = 8$), rats received alpidem at a dose of 0.1 mg kg^{-1}, i.p. and 10 min later, triazolam at a dose of 0.1 mg kg^{-1}, i.p. in the second group ($n = 8$), rats received alpidem i.c.v. at a dose of 10 μg kg^{-1} and 10 min later triazolam at a dose of 0.1 mg kg^{-1}, i.p.

In the fourth series of experiments, eight rats received triazolam at a dose of 0.1 mg kg^{-1}, i.p. preceded or not by the administration of flumazenil at a dose of 5 mg kg^{-1}, i.p.

In the last series of experiments, systemic capsaicin-treated rats ($n = 8$), perivagal capsaicin-treated rats ($n = 8$) and corresponding sham-treated rats ($2 \times n = 8$) were randomly treated with clonazepam and triazolam at a dose of 0.1 mg kg^{-1} or with their vehicle.

Statistical analyses

The duration of MMC-disruption, determined on integrated records from the last MMC to the first MMC reappeared, were expressed as means ± s.e.mean and compared using ANOVA followed by Student's unpaired t test when appropriate. Differences were considered significant for $P < 0.05$.

Results

Control studies

Rats fed only during the night presented a typical pattern of alternating intestinal motility. During day-time, fasted rats exhibited an electrical activity of the duodenum and the jejunum characterized by the cyclic occurrence of migrating myoelectric complexes (MMCs). Each MMC consisted of an irregular spiking activity (phase II) lasting 6–8 min, followed by a short period (4–5 min) of intense and regular spiking activity (phase III), separated by a 3 to 5 min quiescent period (phase I). These MMCs occurred firstly on the proximal duodenum and were propagated aborally at a mean rate of 3.5 ± 0.6 cm min^{-1}.

Comparative effects of ω site subtype agonists on duodenal and jejunal MMC-pattern

When injected i.p., clonazepam and triazolam induced dose-related disturbances of the small intestine fed pattern. These disturbances corresponded to a strong stimulation of duodenal and jejunal spiking activity associated with a transient suppression of the MMC-pattern (Figure 1). At all doses

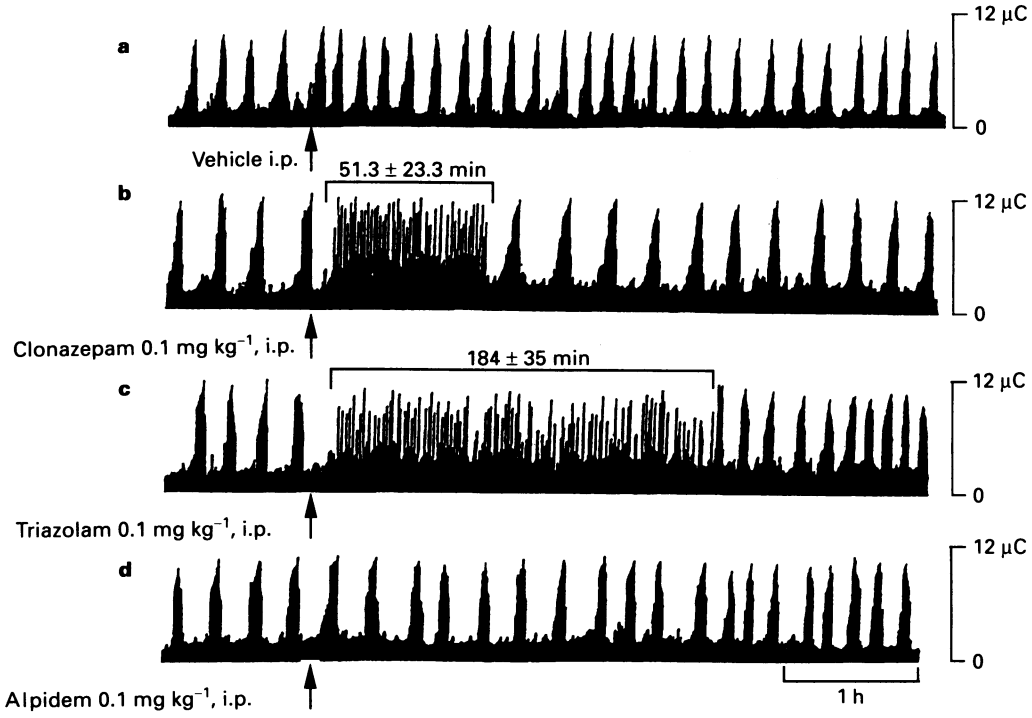

Figure 1 Effect of vehicle (a), clonazepam (b), triazolam (c) and alpidem (d) administered i.p. at a dose of 0.1 mg kg^{-1}, on duodenal myoelectric activity (integrated records) in a fasted rat. Triazolam induced a more prolonged stimulation of duodenal spiking activity than clonazepam; alpidem had no effect.

tested, jejunal electrical pattern was more affected than that of the duodenum: for example, at a dose of 0.1 mg kg^{-1}, clonazepam disrupted MMC for 86.7 ± 15 min and 51.3 ± 23.3 min at the jejunum and duodenum levels, respectively (Figure 2). Triazolam, at similar doses, was always more potent than clonazepam on both duodenum and jejunum (Figure 2). Alpidem and zolpidem had no effect on the fasted pattern (Figure 2) except at the highest dose tested (5 mg kg^{-1}) (alpidem: duodenum; 52 ± 11; jejunum: 56 ± 8; zolpidem: duodenum: 189.1 ± 9.2; jejunum: 151.6 ± 6.6); even at this high dose the effect of these drugs was much smaller in magnitude than that elicited by clonazepam or triazolam. None of the drugs had any effect on the fasted pattern when injected centrally at a dose of 10 and 100 μg kg^{-1}. Values obtained were not significantly different from the time between two consecutive MMCs corresponding to a control fasted pattern. For example, zolpidem at a dose of 10 μg kg^{-1}: duodenum: 14.2 ± 3.1 vs 11.1 ± 2.2 min for control; jejunum: 12.5 ± 0.5 vs 12.3 ± 2.1 min for control.

Effects of i.p. administration of ω site inverse agonists and antagonists on duodenal and jejunal MMC-pattern

Neither β-CCM, β-CCE or flumazenil altered duodenal and jejunal fasted patterns at doses of 0.1, and 1 mg kg^{-1}. For example: respectively β-CCE, β-CCM and flumazenil at a dose of 1 mg kg^{-1}, duodenum: 11.4 ± 4.1, 12.8 ± 2.7, 12.7 ± 4.5 min; jejunum: 10.5 ± 5.5, 13.3 ± 1.1, 15.1 ± 3.2 min vs 12.5 ± 2.4 and 13.1 ± 2.2 min for controls. The same range of values was obtained after 0.1 mg kg^{-1}. In the same way flumazenil at 5 mg kg^{-1} did not modify the MMC-pattern: duodenum: 13.2 ± 1.9, jejunum: 12.7 ± 3.4 vs 12.5 ± 2.4 and 13.1 ± 2.2 for controls. Similarly, none of these compounds had any influence on MMCs when injected i.c.v. at 10 and 100 μg kg^{-1}.

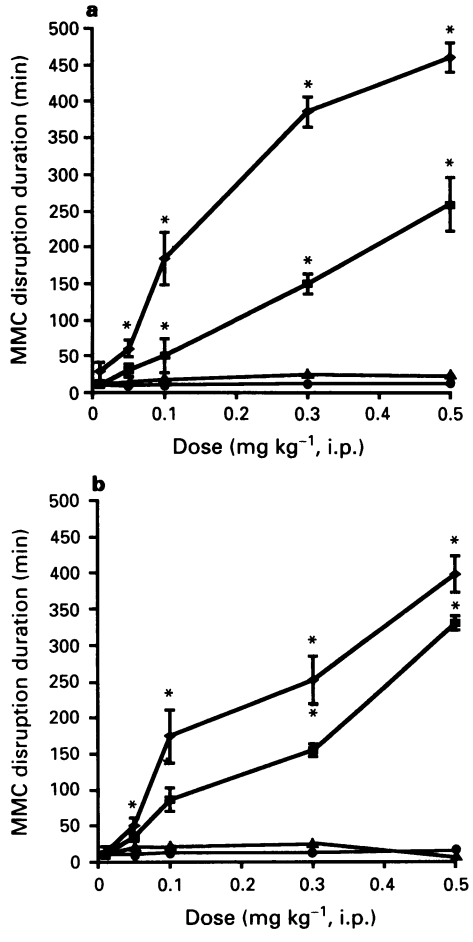

Figure 2 Comparative effects of i.p. administration of clonazepam (■), triazolam (◆), alpidem (●) and zolpidem (▲) on duodenal (a) and jejunal (b) fasted pattern. Clonazepam and triazolam induced a dose-related disruption of the MMC pattern whereas alpidem and zolpidem had no effect. Significantly different (*$P<0.05$) from control values i.e. vehicle-injected i.p. ($n = 8$).

Antagonism by alpidem of triazolam induced MMC-disruption

When administered either i.p. at a dose of 0.1 mg kg^{-1} or i.c.v. at a dose of 10 $\mu g\ kg^{-1}$, 10 min prior to triazolam (0.1 mg kg^{-1}, i.p.), alpidem suppressed triazolam-induced disruption of the duodeno-jejunal MMC-pattern (Figure 3).

Antagonism by flumazenil of triazolam induced MMC-disruption

When administered at a dose of 5 mg kg^{-1} i.p., 10 min prior to triazolam (0.1 mg kg^{-1}), flumazenil antagonized the triazolam induced MMC-disruption on either duodenum or jejunum (Figure 4). Flumazenil had no effect at this dose when administered alone (data not shown).

Effect of systemic and peri-vagal capsaicin treatment on clonazepam-induced MMC-disruption

In sham (vehicle) systemic capsaicin-treated rats, clonazepam (0.1 mg kg^{-1}, i.p.) induced MMC disruption of the duodenum and the jejunum lasting 53.1 ± 23.7 min and 89.4 ± 15.4 min, respectively. However, in systemic capsaicin-treated rats, clonazepam at the same dosage did not alter the small intestine MMC-pattern. In the same way, triazolam (0.1 mg kg^{-1}, i.p.) induced MMC disruption of the duodenum and the jejunum lasting 160 ± 12 and 152.3 ± 19.1 min, respectively (Figure 5).

In contrast, clonazepam and triazolam (0.1 mg kg^{-1}, i.p.) administered to sham perivagal capsaicin-treated rats, disrupted duodenal and jejunal MMCs as it did in control and sham-operated animals (Figure 6).

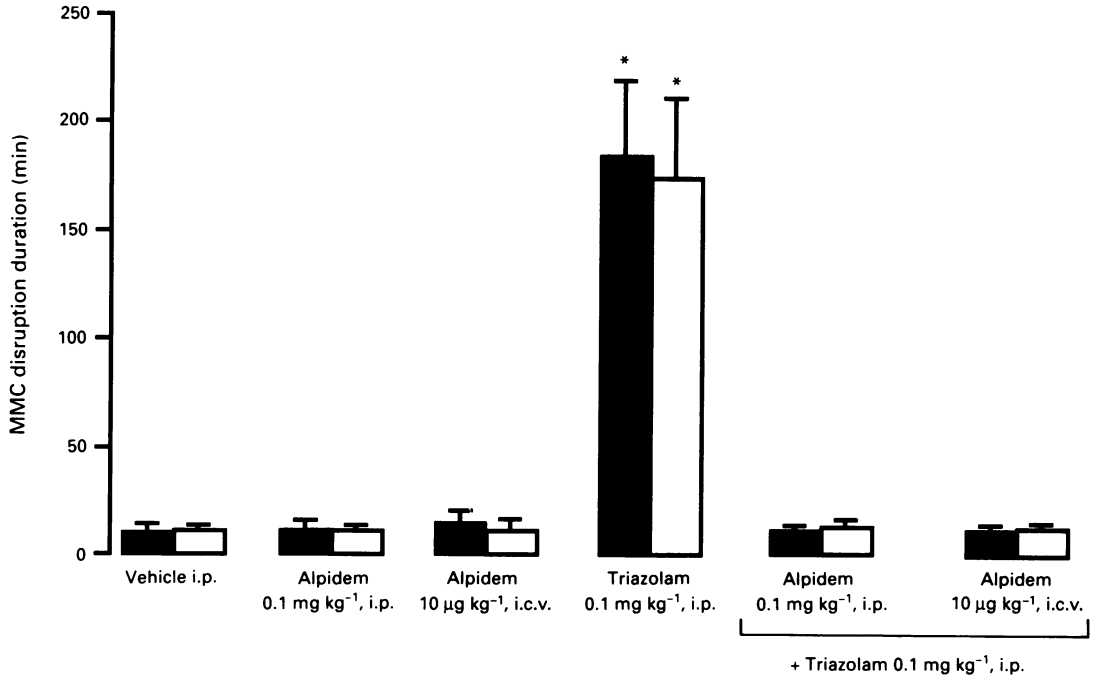

Figure 3 Antagonistic effect of alpidem on triazolam (0.1 mg kg^{-1}, i.p.) induced MMC-disruption at duodenal (solid columns) and jejunal (open columns) levels. Alpidem, administered i.p. or i.c.v. 10 min prior to triazolam, blocked the triazolam-induced MMC-disruption on the small intestine. Significantly different ($^*P < 0.05$) from vehicle values ($n = 8$).

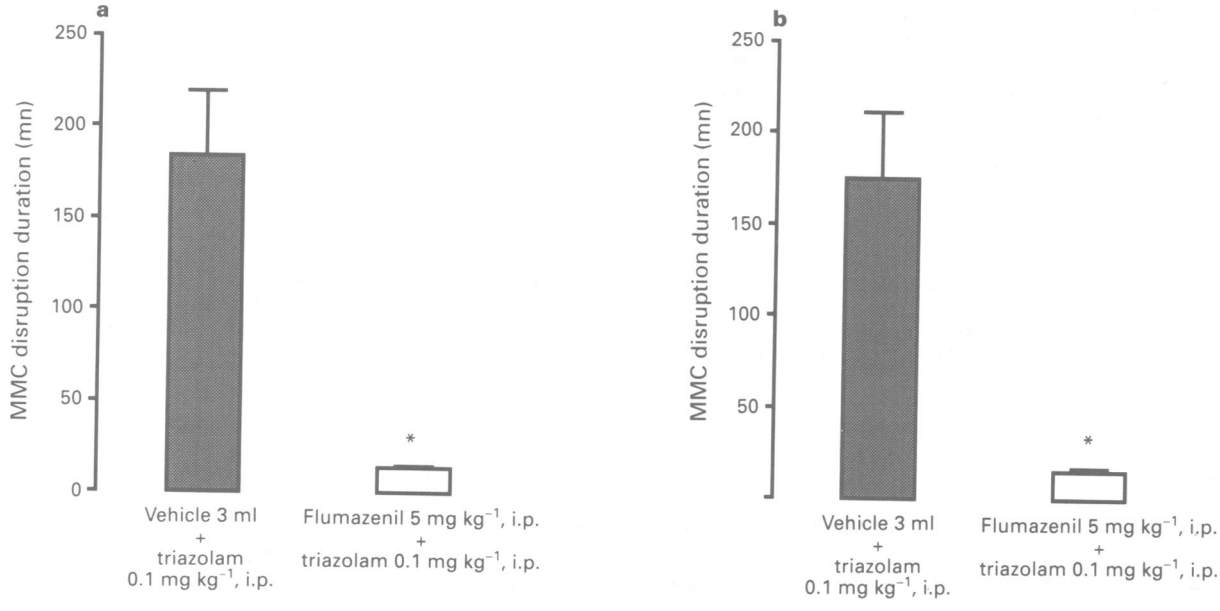

Figure 4 Antagonistic effect of flumazenil on triazolam (0.1 mg kg^{-1}, i.p.) induced MMC-disruption at duodenal (a) and jejunal (b) levels. Flumazenil, administered i.p. 10 min prior to triazolam, blocked the triazolam-induced MMC-disruption on the small intestine. Significantly different ($^*P < 0.05$) from triazolam alone. ($n = 8$).

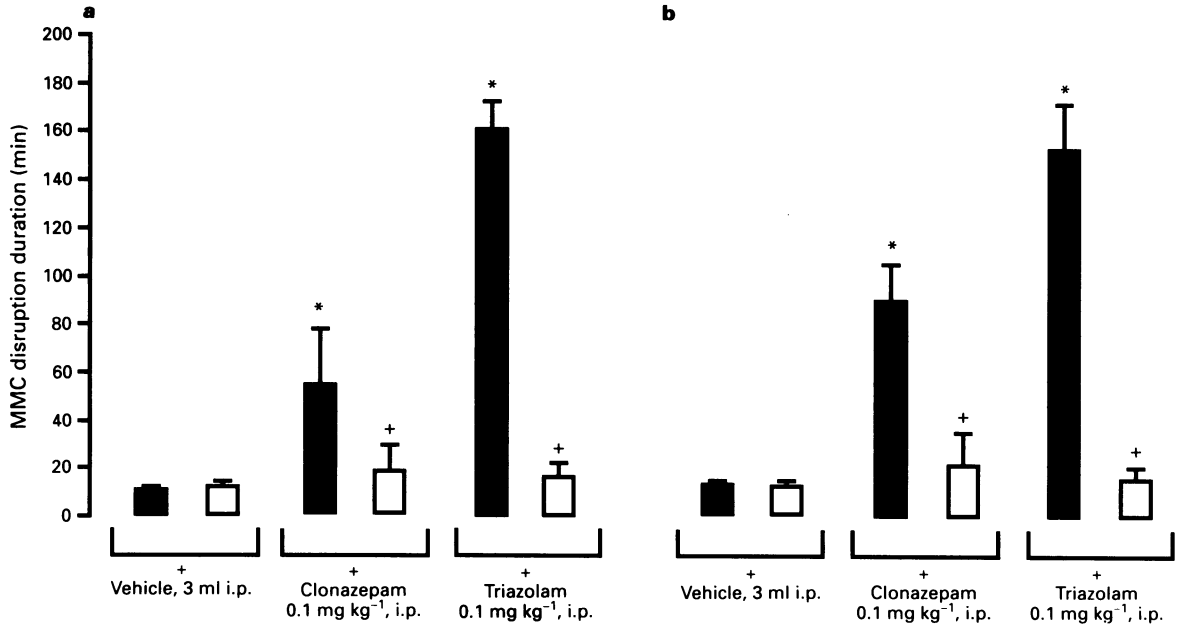

Figure 5 Effect of systemic capsaicin treatment on clonazepam and triazolam-induced small intestine MMC disruption: (a) duodenum; (b) jejunum. Solid columns, sham capsaicin; open columns, systemic capsaicin-treated rats. In vehicle capsaicin-treated rats clonazepam and triazolam induced a significant stimulation of the spiking activity, but had no effect in systemic capsaicin-treated rats. Significantly different ($*P<0.05$) from sham capsaicin-treated rats + vehicle i.p.; significantly different ($\dagger P<0.05$) from sham capsaicin-treated rats + clonazepam (0.1 mg kg^{-1}, i.p.) ($n = 8$).

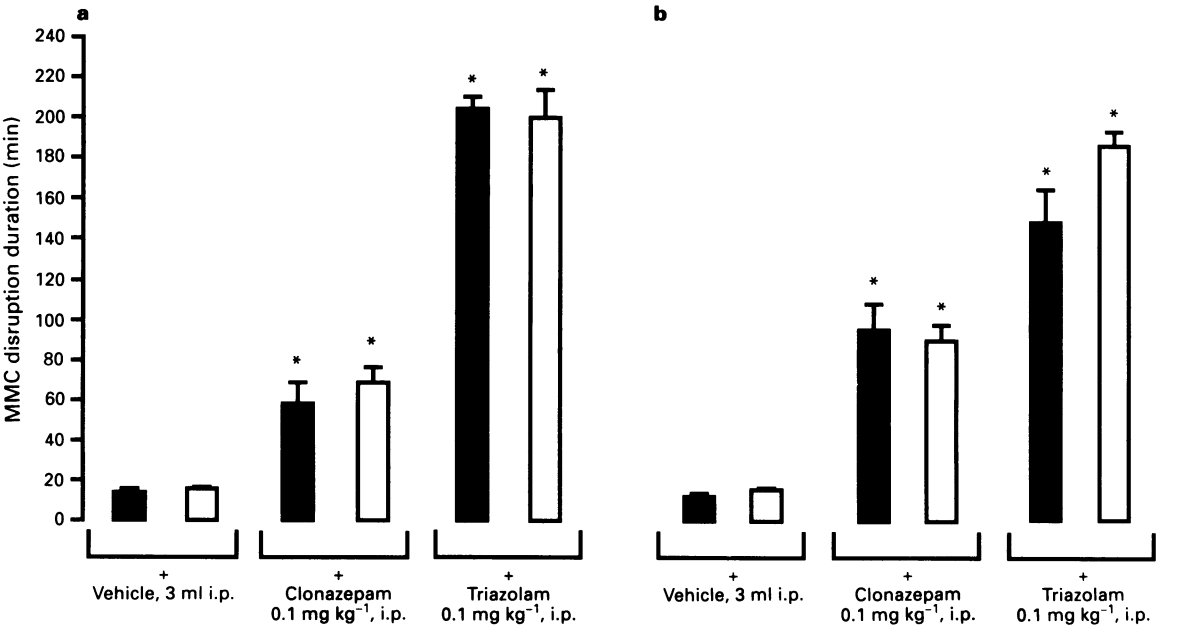

Figure 6 Effect of perivagal capsaicin treatment on clonazepam and triazolam-induced MMC-disruption of the small intestine in fasted rats: (a) duodenum; (b) jejunum. In sham capsaicin-treated rats (solid columns) clonazepam and triazolam induced a significant stimulation of the spiking activity and had the same effect in perivagal capsaicin-treated rats (open columns). Significantly different ($*P<0.05$) from sham capsaicin-treated rats + vehicle i.p. ($n = 8$).

Discussion

In agreement with previous studies (Martinez *et al.*, 1992; Bonnafous *et al.*, 1993), systemic administration of the benzodiazepines, clonazepam and triazolam, induced disturbances of the intestinal MMCs in rats. In contrast, the ω site inverse agonists (β-CCM and β-CCE) and antagonist (flumazenil) had no effect on MMCs. Thus, positive allosteric modulation of $GABA_A$ receptor-mediated transmission is associated with intestinal disturbances of MMCs, whereas negative allosteric modulation of the $GABA_A$ receptor complex does not appear to induce opposite alterations. In agreement with these findings, flumazenil by itself possesses little intrinsic pharmacological activity in animals and man (Hunkeler *et al.*, 1981; Darragh *et al.*, 1983). However, the lack of effect of the inverse agonists β-CCM and β-CCE when administered peripherally or centrally may appear paradoxical since the inverse agonists β carbolines investigated are

known to elicit behavioural and electrophysiological effects that are opposite to those of ω site agonists (Oakley *et al.*, 1980; Braestrup *et al.*, 1982; Thiebot *et al.*, 1988). This discordance may be related to our experimental conditions which do not allow a demonstration of negative functional effects on intestinal motility.

One of the goals of the present study was to identify which subtype of ω sites is involved in the intestinal motor disturbances caused by ω site agonists. To this end, various compounds with differing affinities for ω_1 and ω_2 sites were studied. The present results show that clonazepam, which does not discriminate between ω_1 and ω_2 sites or triazolam which recognizes preferentially ω_2 sites *in vivo* (Benavides *et al.*, 1992) disrupt the jejunal and duodenal MMC-pattern. In contrast, zolpidem and alpidem which are respectively full and partial agonists at ω_1 sites (Langer *et al.*, 1990) do not affect this parameter except at high doses. These data suggest that ω_2 but not ω_1 sites may be involved in the effect of benzodiazepines on small intestine motility. This view is supported by previous *in vivo* binding studies which showed that doses of triazolam that cause marked disturbances of MMC-pattern (e.g. 0.1 mg kg^{-1}) selectively displace by about 50% the *in vivo* binding of [^{3}H]-flumazenil in ω_2-enriched brain areas in the rat (Benavides *et al.*, 1992). Moreover, the three fold lower potency of clonazepam as compared to triazolam in disturbing MMCs, accords with the relative potency of these drugs at displacing [^{3}H]-flumazenil from central ω_2 sites (respectively ED_{50}'s = 0.34 and 0.1 mg kg^{-1}, i.p.) (Benavides *et al.*, 1992). Finally, within the range of doses where zolpidem do not produce MMC-disturbances (0.1–1 mg kg^{-1}, i.p.), this compound was inactive at displacing [^{3}H]-flumazenil from ω_2 sites, yet partially occupied ω_1 sites (Benavides *et al.*, 1992). However, caution should be exercised when making such comparisons as all of these data refer to occupation of ω sites in the CNS and may be different for the myenteric plexus. Binding studies are clearly needed to confirm the pharmacological characteristics of those ω sites located in the myenteric plexus.

When administered by the central or peripheral route prior to triazolam, alpidem antagonizes the triazolam-induced MMC-disruption. The explanation for this finding is not obvious. It may be that ω_1 sites have an opposing effect against ω_2-site-mediated MMC-disruption. Alternatively, alpidem may behave as an antagonist or inverse agonist at ω_2 sites thereby antagonizing the effect of ω_2 site stimulation. In support of this possibility, recent studies have shown that the direction of the modulatory effect of ω site agonists changes in relation to the molecular form of the γ subunit of the $GABA_A$ receptor and that alpidem behaves as an inverse partial agonist in embryonic kidney 293 cells expressing the subunit combination $\alpha_3\beta_1\gamma_1$, which may correspond to a subtype of ω_2 site (Puia *et al.*, 1991). Complementary experiments are clearly needed to clarify this issue.

In the present study, we have also attempted to investigate the localization of those ω sites involved in MMC-disruption. When administered centrally, none of the ω site agonists investigated altered intestinal motility. Since all these substances easily cross the blood-brain barrier, these observations suggest that they act peripherally to induce intestinal motor changes. This view is supported by recent studies which demonstrated the presence of GABA in guinea-pig myenteric plexus and that myenteric neurones themselves are endowed with ω sites which are akin to 'central type' sites (Cherubini *et al.*, 1985; Taniyama *et al.*, 1988). The fact that flumazenil antagonizes triazolam-induced MMC-disruption confirms that BZ receptors involved in this mechanism are of the 'central type'. We have recently demonstrated that peripheral clonazepam-induced MMC-disruption is linked to central release of cholecystokinin triggered by stimulation of peripherally located ω sites (Bonnafous *et al.*, 1993). Altogether, these data suggest that ω-site agonists when administered i.p. act on 'central type' ω_2 sites located on afferent endings of the enteric nerves, thus activating afferent neurones involved in a long reflex responsible for digestive motor changes.

Capsaicin causes a long-term sensory receptor-blocking action which can be used in functional investigations on the sensory pathways (Jancso *et al.*, 1967; Maggi & Meli, 1988). In the digestive tract, capsaicin-sensitive afferent innervation participates in nociception and intestino-intestinal activation of inhibitory reflexes (Holzer *et al.*, 1987; Maggi, 1991). Moreover, the vagus nerve and the vagus afferents play a major role in the regulation of the gastrointestinal functions. Several studies have demonstrated the existence of a central relay in peripheral stimulation of the gastrointestinal tract; for example ileus or peritonitis share a common feature which is the activation of an inhibitory nervous reflex leading to the inhibition of small intestinal motility and gastrointestinal transit (Holzer *et al.*, 1986; Rivière *et al.*, 1993). The fact that peripheral but not perivagal capsaicin treatment prevents clonazepam and triazolam-induced MMC-disruption, suggests that capsaicin-sensitive non vagal afferent neurones are involved in the effects of clonazepam and triazolam on intestinal motility and that MMC-pattern may be triggered by an inhibitory reflex.

The authors thank C. Betoulieres for her technical assistance, SYNTHELABO for supply of compounds and INRA for its financial support.

References

ARBILLA, A., DEPOORTERE, H., GEORGE, P. & LANGER, S.Z. (1985). Pharmacological profile of the imidazopyridine zolpidem at benzodiazepine receptors and electrocorticogram in rats. *Naunyn Schmied. Arch. Pharmacol.*, **330**, 248–251.

BENAVIDES, J., DUBOIS, A., DENNIS, T., HAMEL, E. & SCATTON, B. (1989). ω (Peripheral-type benzodiazepine binding) site distribution in the rat immune system: an autoradiographic study with the photoaffinity ligand ^{3}H-PK14105. *J. Pharmacol. Exp. Ther.*, **249**, 333–339.

BENAVIDES, J., DUBOIS, A., GOTTI, B., BOURDIOL, F. & SCATTON, B. (1990). Cellular distribution of ω_3 (peripheral type benzodiazepine) binding sites in the normal and ischemic rat brain: an autoradiographic study with the photoaffinity ligand ^{3}H-PK14105. *Neurosci. Lett.*, **144**, 32–38.

BENAVIDES, T., PENY, B., DURAND, A., ARBILLAS, S. & SCATTON, B. (1992). Comparative in vivo and in vitro regional selectivity of central w (benzodiazepine) site ligands in inhibiting ^{3}H-flumazenil binding in the rat central nervous system. *J. Pharmacol. Exp. Ther.*, **263**, 884–896.

BONNAFOUS, C., MARTINEZ, J., FARGEAS, M.J. & BUENO, L. (1993). Clonazepam-induced intestinal motor disturbances are linked to central nervous system release of cholecystokinin in rats. *Eur. J. Pharmacol.*, **237**, 237–242.

BRAESTRUP, C. & NIELSEN, M. (1981). (^{3}H) propyl β-carboline-3-carboxylate as a selective radioligand for BZ_1 benzodiazepine receptor subclass. *J. Neurochem.*, **37**, 333–341.

BRAESTRUP, C., SCHMIECHEN, R., NEEF, G., NIELSEN, M. & PETERSEN, E.N. (1982). Interaction of convulsive ligands with benzodiazepine receptors. *Science*, **216**, 1241–1243.

BUENO, L., FERRE, J.P., RUCKEBUSCH, M., GENTON, M. & PASCAUD, X. (1981). Continuous electrical and mechanical activity recording in the gut of the conscious rat. *J. Pharmacol. Methods*, **6**, 129–136.

CHERUBINI, E. & NORTH, R.A. (1985). Benzodiazepines both enhance γ-aminobutyrate responses and decrease calcium action potentials in guinea-pig myenteric neurons. *Neuroscience*, **14**, 309–315.

DARRAGH, A., LAUBE, R., KENNY, M. & BRICK, J. (1983). Tolerance of health volunteers to intravenous administrations of the benzodiazepine antagonist RO 15-1788. *Eur. J. Clin. Pharmacol.*, **14**, 569–570.

FARGEAS M.J., FIORAMONTI, J. & BUENO, L. (1984). Time-related effects of benzodiazepines on intestinal motility on conscious dogs. *J. Pharm. Pharmacol.*, **36**, 130–134.

HARVEZ, S.C., GOODMAN GILMAN, A., GOODMAN, L.S., RALL, T.W. & MURAD, F. (1985). Hypnotics and sedatives. In *The Pharmacological Basis of Therapeutics*. (Goodman and Gilman's) pp. 339–351. New York: Macmillan Publishing Company.

HOLZER, P., LIPPE, I.Th. & HOLZER-PETSCHE. (1986). Inhibition of gastrointestinal transit due to surgical trauma or peritoneal irritation is reduced in capsaicin-treated rats. *Gastroenterology*, **91**, 360–363.

HOLZER, P., PABST, M.A., LIPPE, I.T., PESKAR, B.M., PESKAR, B.A., LIVINGSTON, E.H. & GUTH, P.H. (1990). Afferent nerve-mediated protection against deep mucosal damage in the rat stomach. *Gastroenterology*, **98**, 839–849.

HOLZER, P., SCHUET, W., LIPP, I.T. & SAMETZ, W. (1987). Involvement of capsaicin-sensitive sensory neurons in gastrointestinal function. *Acta Physiol. Hung.*, **69**, 403–411.

HUNKELER, W., MOHLER, H., PIERI, L., POLC, P., BONETTI, E.P., CUMIN, R., SCHAFFNER, R. & HAEFELY, W. (1981). Selective antagonists of benzodiazepines. *Nature*, **290**, 514–516.

JANSCO, N., JANSCO-GABOR, A. & SZOLCSANYI, J. (1967). Direct evidence for neurogenic inflammation and its prevention and by pretreatment with capsaicin. *Br. J. Pharmacol.*, **31**, 138–151.

KLEPNER, C.A., LIPPA, A.S., BENSON, D.I., SANO, M.C. & BEER, B. (1979). Resolution of two biochemically and pharmacologically distinct benzodiazepine receptors. *Pharmacol. Behav.*, **11**, 457–462.

LANGER, S.Z. & ARBILLA, A. (1988). Imidazopyridines as a tool for the characterization of benzodiazepine receptors: a proposal for a pharmacological classification as omega-receptors. *Pharmacol. Biochem. Behav.*, **29**, 763–767.

LANGER, S.Z., ARBILLA, S., TAN, S., LLOYD, K.G., GEORGE, P., ALLEN, J. & WICK, A.E. (1990). Selectivity for omega-receptor subtypes as a strategy for the development of anxiolytic drugs. *Pharmacopsychiatry*, **23**, 102–107.

LATOUR, A. (1973). Un dispositif simple d'analyses quantitative de l'électromyogramme intestinal chronique. *Ann. Rech. Vet.*, **4**, 347–353n.

MAGGI, C.A. (1991). The pharmacology of the efferent function of sensory nerves. *J. Auton. Pharmacol.*, **11**, 173–208.

MAGGI, C.A. & MELI, A. (1988). The sensory-efferent function of capsaicin-sensitive neurons. *Gen. Pharmacol.*, **19**, 1–43.

MARTINEZ, J., FARGEAS, M.J. & BUENO, L. (1992). Gastrointestinal motor alterations induced by precipitated benzodiazepines withdrawal in rats. *J. Pharmacol. Exp. Ther.*, **260**, 1067–1070.

OAKLEY, N.R. & JONES, B.J. (1980). The proconvulsivant and diazepam-reversing effects of ethyl-β-carboline-3-carboxylate. *Eur. J. Pharmacol.*, **68**, 381–382.

OLSEN, R.W. & TOBIN, A.J. (1990). Molecular biology of $GABA_A$ receptors. *FASEB*, **4**, 1469–1480.

PUIA, G., VICINI, S., SEEBURG, P.H. & COSTA, E. (1991). Influence of the recombinant γ-aminobutyric acid $_A$-receptor subunit composition on the action of allosteric modulators of γ-aminobutyric acid-gated Cl^- currents. *Mol. Pharmacol.*, **39**, 691–696.

RAYBOULD, H.E., HOLZER, P., REDDY, N. & TACHE, Y. (1990). Capsaicin-sensitive vagal afferents contribute to gastric acid and vascular responses to intracisternal TRH analog. *Peptides*, **11**, 789–795.

RIVIERE, P.J.M., PASCAUD, X., CHEVALIER, E., LE GALLOU, B. & JUNIEN, J.L. (1993). Fedotozine reverses ileus induced by surgery or peritonitis: action at peripheral κ-opioid receptors. *Gastroenterology*, **104**, 724–731.

RUCKEBUSCH, M. & FIORAMONTI, J. (1975). Electrical spiking activity and propulsion in small intestine in fed and fasted rats. *Gastroenterology*, **68**, 1500–1508.

SOUTH, E.H. & RITTER, R.C. (1988). Capsaicin application to central or peripheral vagal fibers attenuates CCK satiety. *Peptides*, **9**, 601–612.

TANIYAMA, K., HASHIMOTO, S., HANADA, S. & TANAKA, C. (1988). Benzodiazepines and barbiturate potentiate the pro- and postsynaptic γ-aminobutyric acid ($GABA_A$) receptor-mediated response in the enteric nervous system of guinea-pig small intestine. *J. Pharmacol. Exp. Ther.*, **245**, 250–256.

THIEBOT, M.H., SOUBRIE, P. & SANGER, D. (1988). Anxiogenic properties of β-CCE and FG7142: a review of promises and pitfalls. *Psychopharmacology*, **94**, 452–463.

(Received November 29, 1993
Revised April 20, 1994
Accepted May 9, 1994)

Br. J. Pharmacol. (1994), **113**, 275–281

Pharmacological characteristics of liriodenine, isolated from *Fissistigma glaucescens*, a novel muscarinic receptor antagonist in guinea-pigs

Chien-Huang Lin, Gwo-Jyh Chang, Ming-Jai Su, *Yang-Chang Wu, Che-Ming Teng & [1]Feng-Nien Ko

Pharmacological Institute, College of Medicine, National Taiwan University, Taipei and *School of Pharmacy, Kaohsiung Medical College, Kaohsiung, Taiwan

1 The pharmacological activities of liriodenine, isolated from *Fissistigma glaucescens*, were determined in isolated trachea, ileum and cardiac tissues of guinea-pigs.

2 Liriodenine was found to be a muscarinic receptor antagonist in guinea-pig trachea as revealed by its competitive antagonism of carbachol ($pA_2 = 6.22 \pm 0.08$)-induced smooth muscle contraction. It was slightly more potent than methoctramine ($pA_2 = 5.92 \pm 0.05$), but was less potent than atropine ($pA_2 = 8.93 \pm 0.07$), pirenzepine ($pA_2 = 7.02 \pm 0.09$) and 4-diphenylacetoxy-*N*-methylpiperidine (4-DAMP, $pA_2 = 8.72 \pm 0.07$).

3 Liriodenine was also a muscarinic antagonist in guinea-pig ileum ($pA_2 = 6.36 \pm 0.10$) with a pA_2 value that closely resembled that obtained in the trachea.

4 Liriodenine was 10 fold less potent in atrial preparations (left atria, $pA_2 = 5.24 \pm 0.04$; right atria, $pA_2 = 5.35 \pm 0.09$ and 5.28 ± 0.07 for inotropic and chronotropic effects, respectively) than in smooth muscle preparations.

5 High concentration of liriodenine (300 μM) partially depressed the contractions induced by U-46619, histamine, prostaglandin $F_{2\alpha}$, neurokinin A, leukotriene C_4 and high K^+ in the guinea-pig trachea. The inhibitions were characterized by a rightward shift in the concentration-response curves with suppression of their maximal contraction.

6 High concentration of liriodenine (300 μM) did not affect U-46619- or neurokinin A-induced tracheal contraction in the presence of nifedipine (1 μM) or in Ca^{2+}-free (containing 0.2 mM EGTA) medium.

7 Neither cyclic AMP nor cyclic GMP content of guinea-pig trachealis was changed by liriodenine (30–300 μM).

8 It is concluded that liriodenine is a selective muscarinic receptor antagonist in isolated trachea, ileum and cardiac tissues of guinea-pigs. It is more potent in smooth muscle than in cardiac preparations. It also acts as a blocker of voltage-dependent Ca^{2+} channels at a high concentration (300 μM).

Keywords: Muscarinic receptor antagonist; Ca^{2+} channel blocker; guinea-pig trachea; liriodenine; *Fissistigma glaucescens*

Introduction

In most species, the parasympathetic division of the autonomic nervous system is the major determinant of airway tone (Barnes, 1992). Postganglionic parasympathetic nerves release acetylcholine which acts on muscarinic receptors to induce smooth muscle contraction via G-protein-coupled, phosphoinositide-linked mechanisms (Barnes, 1987). Abnormal cholinergic mechanisms, mediated via the vagus nerves. have been suggested as an important factor in the bronchial hyperreactivity associated with asthma (Boushey *et al.*, 1980). Therefore, muscarinic receptor antagonists have an important therapeutic role as bronchodilators in airways obstructive diseases (Gross & Skorodin, 1984).

Medicinal plants have been used as traditional remedies in Asia for hundreds of years. In a large scale screening test, we have isolated many biologically active compounds from plant sources. For example, magnolol (isolated from *Magnolia officinalis*) causes relaxation of rat aorta by releasing endothelium-derived relaxing factor (EDRF) (Teng *et al.*, 1990), dicentrine (isolated from *Lindera megaphylla*) and (−)-discretamine (isolated from *Fissistigma glaucescens*) are selective vascular α_1-adrenoceptor antagonists (Teng *et al.*, 1991; Ko *et al.*, 1993). Atherosperminine (isolated from *Fissistigma glaucescens*) causes relaxation of guinea-pig trachea by acting as a phosphodiesterase inhibitor (Lin *et al.*, 1993).

Recently, we found that liriodenine (Figure 1), an aporphine derivative isolated from *Fissistigma glaucescens* (Lu *et al.*, 1985), inhibited carbachol-induced contraction of guinea-pig trachea in a large scale screening test. In the present study, we investigated the selectivity of this agent for several receptor types and for muscarinic receptors in various tissues.

Methods

Guinea-pig tracheal contraction

Guinea-pigs of either sex weighing 350–600 g were killed by a blow to the head. The trachea was excised, cleaned of adhering fat and connective tissue, cut into 4–5 rings and then opened by cutting longitudinally through the cartilage rings diametrically opposite the tracheal smooth muscle. The segment was mounted in an organ bath containing 5 ml Krebs solution of the following composition (mM): NaCl 118.2, KCl 4.7, $MgSO_4$ 1.2, KH_2PO_4 1.2, glucose 11.7, $CaCl_2$ 1.9 and $NaHCO_3$ 25.0. The tissue bath solution was maintained at 37°C and gassed with 95% O_2 plus 5% CO_2. Tracheal preparations were equilibrated in the medium for 60 min with three changes of Krebs solution and maintained under an optimal tension of 1 g before specific experiment

[1] Author for correspondence at: Pharmacological Institute, College of Medicine, National Taiwan University, No. 1, Jen-Ai Rd., Ist Section, Taipei 10018, Taiwan.

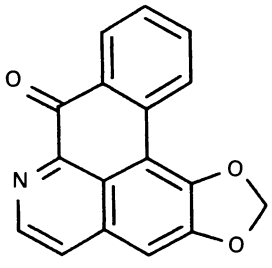

Figure 1 Chemical structure of liriodenine.

protocols were initiated. Contractions were recorded isometrically via a force-displacement transducer connected to a Grass polygraph. All experiments were carried out in the presence of indomethacin (1 μM). Tracheal preparations were precontracted with a single concentration of carbachol (1 μM). Thereafter, the control cumulative concentration-response curves to carbachol were carried out in each preparation. Increasing doses of carbachol were added at 5 min intervals over 30–40 min. After a 60 min washing period, the subsequent cumulative concentration-response curves to carbachol were constructed in the presence of liriodenine or other muscarinic antagonists (with a 30 min preincubation period). Results are expressed as percentages of the maximal response for carbachol before the addition of liriodenine or other muscarinic antagonists.

The contractile effects of calcium were studied in tracheal preparations stabilized in K^+ (120 mM) solution without Ca^{2+}. Calcium was then added from stock dilutions to obtain the desired concentrations, and the effect of each Ca^{2+} concentration was recorded. The maximal tension attained at 3 mM Ca^{2+} was considered as 100%. The high-K^+ solution was prepared by substituting NaCl with KCl in an equimolar amount. In some experiments, the contractile effects of neurokinin A or U-46619 were carried out in the presence of nifedipine (1 μM) or in Ca^{2+}-free (containing 0.2 mM EGTA) solution.

Guinea-pig ileal contraction

Segments of the terminal ileum, from 2 cm of the ileo-caecal valve, were removed quickly and placed in Krebs solution. Ileal segments (2 cm long) were mounted in an organ bath containing Krebs solution at 37°C and gassed with 95% O_2 plus 5% CO_2. The muscle strips were initially under a resting tension of 1 g. Changes in tension were recorded isometrically via a force-displacement transducer connected to a Grass polygraph. The tissues were equilibrated for 60 min and the control concentration-response curves to carbachol at 30 min intervals were carried out in each preparation. Following incubation with liriodenine for 30 min, a new concentration-response curve was obtained for carbachol. Results are expressed as percentages of the maximum control response for carbachol before the addition of liriodenine.

Guinea-pig right and left atria

Male guinea-pigs weighing 250–350 g were killed by cervical dislocation. The hearts were rapidly excised and right and left atria were dissected and mounted in a 10 ml organ bath containing Tyrode solution of the following composition (mM): NaCl 137.0, KCl 5.4, $MgCl_2$ 1.1, $NaHCO_3$ 11.9, NaH_2PO_4 0.33, $CaCl_2$ 2.0 and dextrose 11.0. The solutions were gassed with 95% O_2 plus 5% CO_2 and kept at 36 ± 0.2°C. Contractions of spontaneously beating right atria and electrically driven left atria were measured by connecting one end of the preparations with a fine silk thread to a force-displacement transducer (Type BG 25, Gould) and recorded on a Gould RS 3400 recorder. To obtain the maximal developed tension, an optimal preload (0.5 to 1 g) was used. The left atria were stimulated at a frequency of 2 Hz through bipolar platinum electrodes with rectangular pulses (1 ms duration, twice threshold stength) delivered from a Grass S8800 stimulator. The preparations were equilibrated for 60 min and control cumulative concentration-response curves to carbachol were carried out in each preparation. Following incubation with liriodenine for 30 min, a new concentration-response curve was obtained for carbachol. Results were expressed as percentages of the maximal response for carbachol before the addition of liriodenine.

Cyclic nucleotides measurements

The contents of adenosine 3′:5′-cyclic monophosphate (cyclic AMP) and guanosine 3′:5′-cyclic monophosphate (cyclic GMP) in trachealis were assayed as described previously (Katsuki & Murad, 1977; Bryson & Rodger, 1987). A segment of trachea was mounted in an organ bath containing 5 ml Krebs solution and aerated with 95% O_2 plus 5% CO_2 at 37°C. The tissue was equilibrated for 60 min under an optimal tension of 1 g. After 5 min of incubation with the agents, the segments were rapidly frozen in liquid nitrogen and stored at − 70°C until homogenized in 0.5 ml of 10% trichloroacetic acid, using a potter glass/glass homogenizer. The homogenate was centrifuged at 10,000 *g* for 2 min and the supernatant was removed and extracted with 4 × 3 volumes of diethyl ether, the cyclic AMP or cyclic GMP content was then assayed by using enzyme immunoassay kits. Precipitable protein was determined by the method of the Bio-Rad assay, using bovine serum albumin as standard. Cyclic AMP and cyclic GMP values are presented as pmol mg^{-1} protein.

Data analysis

In each experiment, agonist concentration-response curves in the presence of the indicated concentration of each antagonist were related to the control concentration-response curve, of which the maximal response was taken as 100%. In most experiments, three or four concentrations of liriodenine were tested and the slopes of the resulting Schild plots were used to assess competitive antagonism. The concentration of agonist necessary to give a half-maximal response in the presence of each concentration of antagonist was divided by the concentration giving a half-maximal response in the absence of antagonist to determine the dose-ratio (DR). Data were plotted by the method of Arunlakshana & Schild (1959) as the − log (antagonist concentration) (M) vs the log (DR − 1) and when DR was 2, the − log (antagonist concentration) was taken as pA_2 value from the Schild plot (MacKay, 1978).

The experimental results are expressed as the mean ± s.e. mean and accompanied by the number of observations. Statistical significance was assessed by Student's *t* test and *P* values less than 0.05 were considered significant.

Drugs

Liriodenine (Figure 1) was isolated from the plant *Fissistigma glaucescens* as previously described (Lu *et al.*, 1985). The following drugs were used: carbachol, histamine dihydrochloride, prostaglangin $F_{2\alpha}$ ($PGF_{2\alpha}$), U-46619 (9,11-dideoxymethanoepoxy-9α, 11α-prostaglandin $F_{2\alpha}$), indomethacin, nifedipine, forskolin, sodium nitroprusside, ethyleneglycol-*bis*-(β-aminoethyl ether)-*N*,*N*,*N*′,*N*′′-tetraacetic acid (EGTA), trichloroacetic acid, atropine sulphate were purchased from Sigma Chem. Co.; pirenzepine, methoctramine hydrochloride, 4-diphenylacetoxy-*N*-methylpiperidine methiodide (4-DAMP) and neurokinin A were purchased from RBI; leukotriene C_4 (LTC_4) was purchased from Biomol Research Lab.; cyclic AMP and cyclic GMP enzyme immunoassay kits were purchased from Cayman Chem. Co. Liriodenine and nifedipine were dissolved in dimethylsul-

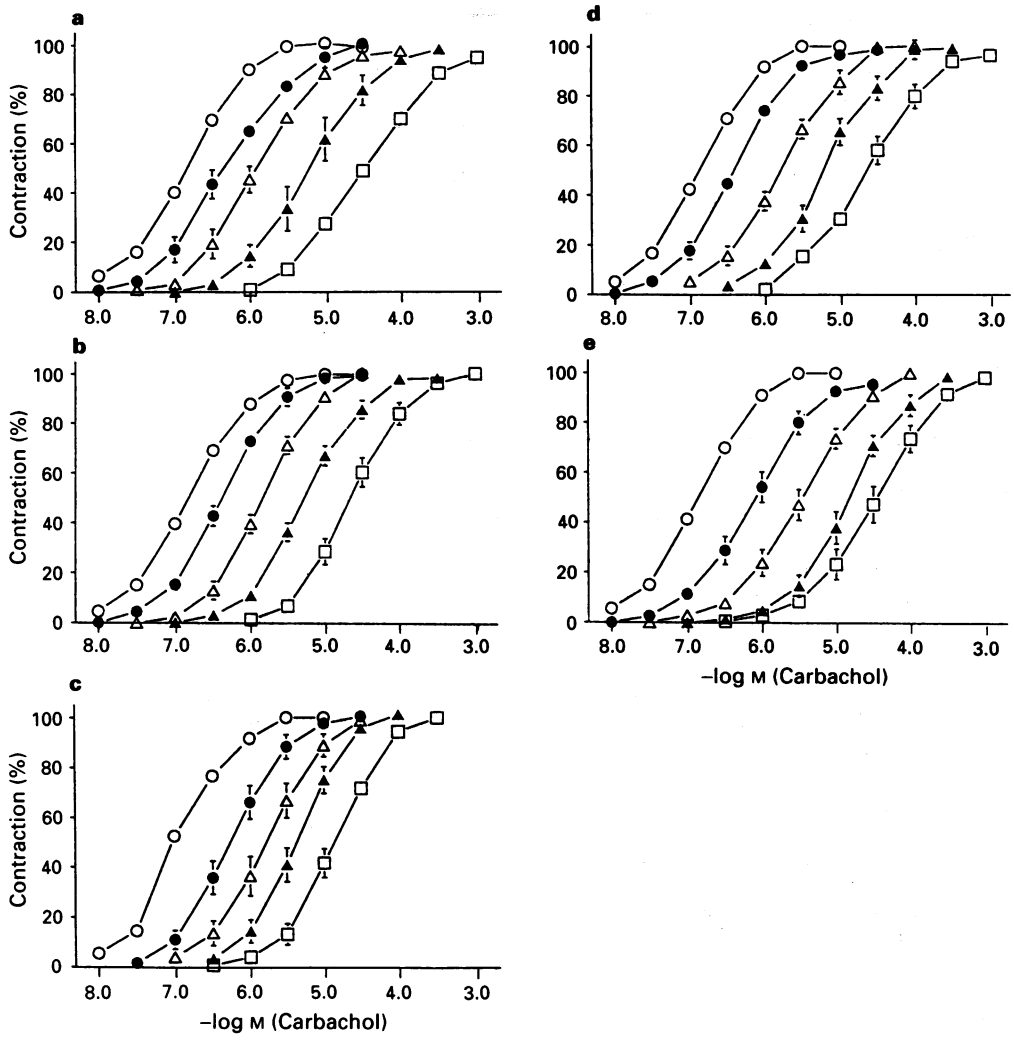

Figure 2 Antagonism of carbachol-induced muscle contraction in guinea-pig trachea. Concentration-response curves for carbachol by 30 min pretreatment of trachea with (a) liriodenine (●, 1 μM; △, 3 μM; ▲, 10 μM; □, 30 μM), (b) atropine (●, 3 nM; △, 10 nM; ▲, 30 nM; □, 100 nM), (c) pirenzepine (●, 0.3 μM; △, 1 μM; ▲, 3 μM; □, 10 μM), (d) methoctramine (●, 3 μM; △, 10 μM; ▲, 30 μM; □, 100 μM), (e) 4-DAMP (●, 3 nM; △, 10 nM; ▲, 30 nM; □, 100 nM) or DMSO (0.1%, control, ○). Each point represents the mean with s.e.mean ($n = 5-7$).

phoxide (DMSO); the final concentration of DMSO in the bathing solution did not exceed 0.1% and had no effect on the muscle contraction.

Results

Muscarinic receptor antagonism in trachea, ileum and cardiac tissue of guinea-pig

Liriodenine was evaluated against a concentration-response curve to carbachol in guinea-pig trachea. Liriodenine (1–30 μM) produced a parallel, rightward shift of the curve consistent with competitive blockade (Figure 2a). The pA_2 value of liriodenine against carbachol was calculated to be 6.22 ± 0.08 (slope range 0.89–1.24) (Table 1). Concentration-response curves for carbachol-induced contraction of guinea-pig trachea were analysed for the muscarinic receptor antagonism by liriodenine in comparison with atropine (non-selective muscarinic antagonist), pirenzepine (selective M_1 antagonist), methoctramine (cardioselective M_2 antagonist) and 4-DAMP (selective smooth muscle M_3 antagonist) (Figure 2b–2e). Liriodenine was slightly more potent than methoctramine ($pA_2 = 5.92 \pm 0.05$), but was less potent than atropine ($pA_2 = 8.93 \pm 0.07$), pirenzepine ($pA_2 = 7.02 \pm 0.09$) and 4-DAMP ($pA_2 = 8.72 \pm 0.07$) (Table 1). In all cases the Schild slopes were not significantly different from 1.0.

Liriodenine (1–30 μM) also caused a concentration-dependent inhibition of carbachol-induced contractions of guinea-pig ileum. The concentration-response curves for car-

Table 1 pA_2 values and slopes of the Schild plots of liriodenine, atropine, pirenzepine, methoctramine and 4-DAMP against muscarinic agonist (carbachol) in guinea-pig trachea, ileum, left atria and right atria

Preparation	*Antagonist*	*pA_2*	*Slope*
Trachea	Liriodenine	6.22 ± 0.08	1.18 (0.89–1.24)
	Atropine	8.93 ± 0.07	0.94 (0.94–1.14)
	Pirenzepine	7.02 ± 0.09	1.02 (0.96–1.09)
	Methoctramine	5.92 ± 0.05	0.96 (0.89–1.04)
	4-DAMP	8.72 ± 0.07	1.12 (0.96–1.22)
Ileum	Liriodenine	6.36 ± 0.10	1.07 (0.85–1.22)
Left atria	Liriodenine	5.24 ± 0.04	1.12 (0.84–1.29)
Right atria	Liriodenine		
(force)		5.35 ± 0.09	0.95 (0.91–1.20)
(rate)		5.28 ± 0.07	1.06 (0.95–1.14)

Results are calculated from Figures 2–4.

bachol were shifted by liriodenine in a parallel fashion with no changes in the maximal response (Figure 3). The pA_2 value of liriodenine against carbachol-induced ileal contraction was calculated to be 6.36 ± 0.10 (slope range 0.85–1.22) (Table 1), and that closely resembled the pA_2 value (6.22 ± 0.08) obtained in the trachea.

Carbachol (0.003–10 μM) caused a concentration-dependent negative inotropic effect in electrically stimulated left atria (Figure 4a). The carbachol-induced responses were antagonized by liriodenine (10–100 μM) with a pA_2 value of 5.24 ± 0.04 (slope range 0.84–1.29) (Figure 4a, Table 1). In spontaneously beating right atria, carbachol (0.003–10 μM) caused negative chronotropic and inotropic effects in a concentration-dependent manner. Liriodenine (10–100 μM) produced a parallel, rightward shift of the curve of carbachol-induced negative chronotropic effect (data not shown) and inotropic effect (Figure 4b). A pA_2 value of 5.28 ± 0.07 (slope range 0.95–1.14) for liriodenine was found at muscarinic receptors in pacemaker cells as determined from carbachol-induced negative chronotropic effect, which was not significantly different ($P > 0.05$) from the value obtained at myocardical receptors in left (5.24 ± 0.04) and right atria (5.35 ± 0.09, slope range 0.91 ± 1.20) (Table 1).

Effects of liriodenine on the contractions of guinea-pig trachea caused by U-46619, histamine, $PGF_{2\alpha}$, neurokinin A, leukotriene C_4 and high K^+

In guinea-pig trachea, U-46619 (10^{-8}–3×10^{-6} M), histamine (10^{-7}–10^{-4} M), $PGF_{2\alpha}$ (3×10^{-8}–3×10^{-5} M), neurokinin A (10^{-9}–10^{-6} M), leukotriene C_4 (3×10^{-10}–3×10^{-6} M) and Ca^{2+} (0.03–3 mM; 120 mM K^+) each caused a concentration-dependent contraction (Figure 5). Liriodenine (100 μM) did not significantly depress all these concentration-response curves, but a higher concentration of liriodenine (300 μM) slightly depressed all the curves (Figure 5). These inhibitions of liriodenine were characterized by a rightward shift in the concentration-response curves with a slight depression of their maxima (Figure 5). Atropine (10^{-7} M), a muscarinic receptor antagonist, did not significantly inhibit these concentration-response curves (data not shown). Furthermore, in the presence of atropine (10^{-7} M), liriodenine (300 μM) still partially depressed these concentration-response curves (data not shown) in a manner that resembled the inhibitory effect of liriodenine (300 μM) alone.

High concentrations of liriodenine (300 μM) slightly inhibited the U-46619 (10^{-6} M)- or neurokinin A (3×10^{-7} M)-induced smooth muscle contraction in guinea-pig trachea. Nifedipine (1 μM), a blocker of voltage-dependent Ca^{2+} channels, also partially inhibited these contractions. A combination of liriodenine (300 μM) and nifedipine (1 μM) did not enhance the inhibition compared with that of nifedipine alone (Figure 6). Additionally, in Ca^{2+}-free and EGTA (0.2 mM)-containing medium, a high concentration of liriodenine (300 μM) did not affect the U-46619-or neurokinin A-induced smooth muscle contraction (Figure 7).

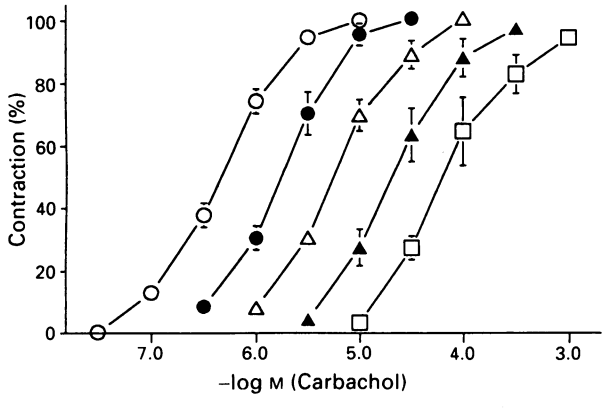

Figure 3 Antagonism of carbachol-induced muscle contraction in guinea-pig ileum. Concentration-response curve for carbachol by 30 min pretreatment of ileum with liriodenine (●, 1 μM; △, 3 μM; ▲, 10 μM; □, 30 μM) or DMSO (0.1%, control, ○). Each point represents the mean with s.e.mean ($n = 6$).

Effects of liriodenine on the cyclic AMP and cyclic GMP formation in guinea-pig trachealis

The cyclic nucleotide contents of trachealis were measured by enzyme immunoassay. As shown in Table 2, forskolin (10 μM) and sodium nitroprusside (10 μM) elevated markedly cyclic AMP and cyclic GMP contents in trachealis, respectively. However, liriodenine (30–300 μM) did not significantly affect the cyclic nucleotide contents.

Discussion

The present experiments have demonstrated that liriodenine, an aporphine alkaloid isolated form *Fissistigma glaucescens*, inhibited the contractile responses of guinea-pig trachea and ileum to the muscarinic agonist, carbachol. It also acted as a muscarinic receptor antagonist in paced left (force) and spontaneously beating right (force and rate) atria of guinea-pigs. It acts as a selective muscarinic receptor antagonist at concentrations less than 100 μM without affecting the contraction of guinea-pig trachea caused by either the thromboxane receptor agonist (U-46619), histamine, $PGF_{2\alpha}$, neurokinin A, leukotrine C_4 or high-K^+ depolarization.

Muscarinic receptors can be differentiated pharmacologically into three distinct subtypes using selective antagonists (Doods *et al.*, 1987). M_1 muscarinic receptors

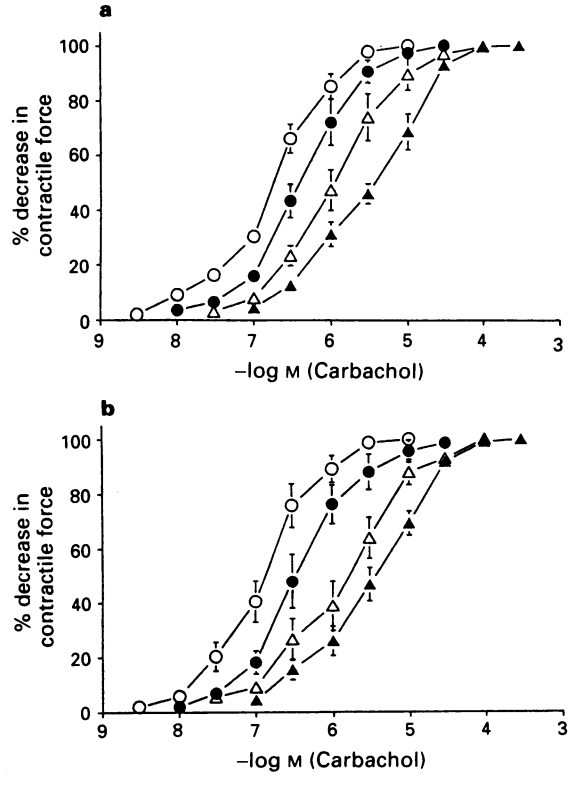

Figure 4 Antagonism of carbachol-induced negative inotropic effect in guinea-pig left or right atria. Concentration-response curve for carbachol by 30 min pretreatment of left atria (a) or right atria (b) with liriodenine (●, 10 μM; △, 30 μM; ▲, 100 μM) or DMSO (0.1%, control, ○). Each point represents the mean with s.e.mean ($n = 6$–7).

have a high affinity for pirenzepine and are abundant in brain and sympathetic ganglia (Hammer *et al.*, 1980). The M_2 subtype has a higher affinity for methoctramine and AF-DX 116 and accounts for most of the muscarinic receptors in the mammalian myocardium (Hammer *et al.*, 1986; Giachetti *et al.*, 1986; Melchiorre *et al.*, 1987; Michel & Whiting, 1988). M_3 muscarinic receptors have a high affinity for 4-DAMP and hexahydrosiladiphenidol (HHSiD) and these receptors

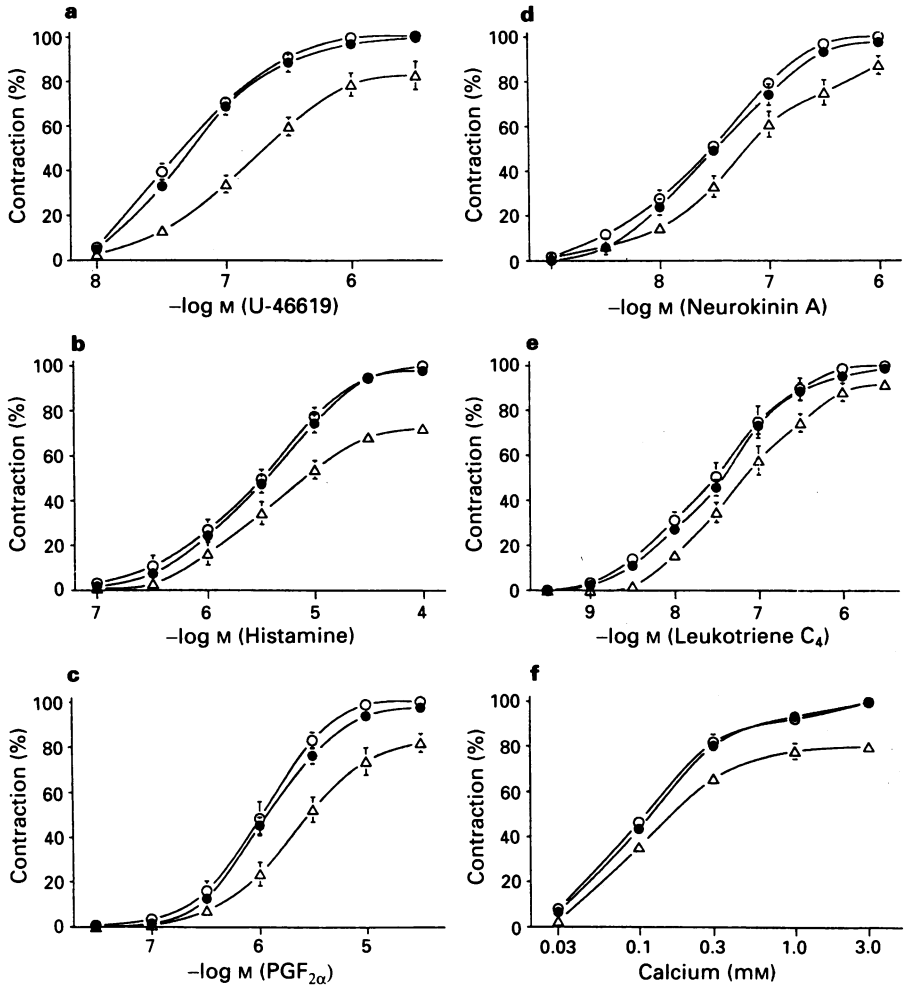

Figure 5 Effects of liriodenine on the contraction induced by U-46619, histamine, prostaglandin $F_{2\alpha}$ ($PGF_{2\alpha}$), neurokinin A, leukotriene C_4 and Ca^{2+} in guinea-pig trachea. Tracheal preparation was preincubated with DMSO (0.1%, control, O) or liriodenine (●, 100 μM; Δ, 300 μM) at 37°C for 30 min, then cumulative concentrations of U-46619 (a), histamine (b), $PGF_{2\alpha}$ (c), neurokinin A (d), leukotriene C_4 (e) and Ca^{2+} (in the presence of 120 mM K^+) (f) were used to trigger the contraction. Each point represents the mean with s.e.mean ($n = 5-6$).

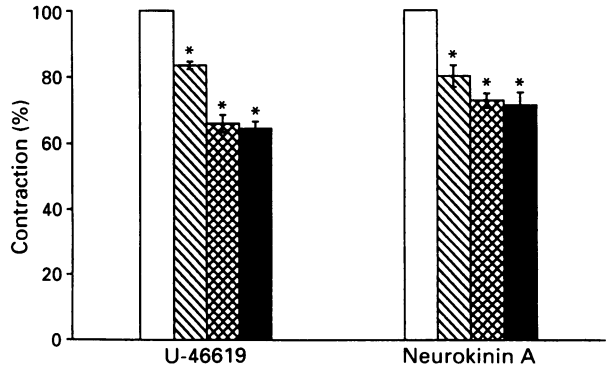

Figure 6 Effects of liriodenine on U-46619- or neurokinin A-induced guinea-pig tracheal contraction in the presence of nifedipine. Trachea was preincubated with DMSO (0.1%, Control, open columns), liriodenine (300 μM, hatched columns), nifepidine (1 μM, cross-hatched columns), or nifedipine (1 μM) plus liriodenine (300 μM) (solid columns) at 37°C for 30 min, then U-46619 (10^{-6} M) or neurokinin A (3×10^{-7} M) was used to trigger the contraction. The values represent mean with s.e.mean ($n = 5$). *$P < 0.01$ as compared with the respective control.

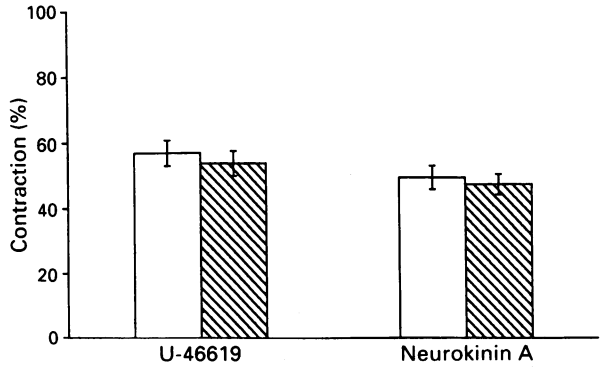

Figure 7 Effects of liriodenine on U-46619- or neurokinin A-induced guinea-pig tracheal contraction in Ca^{2+}-free medium containing 0.2 mM EGTA. Trachea was preincubated with DMSO (0.1%, control, open columns) or liriodenine (300 μM, hatched columns) at 37°C for 30 min, then U-46619 (10^{-6} M) or neurokinin A (3×10^{-7} M) was used to trigger the contraction. Percentages of the control contraction (in normal Krebs solution) are represented as mean with s.e.mean ($n = 5$).

Table 2 Effects of liriodenine on the cyclic AMP and cyclic GMP contents of guinea-pig isolated trachealis

	Cyclic AMP (*pmol mg*$^{-1}$ *protein*)	*Cyclic GMP*
Control	7.5 ± 1.2	1.32 ± 0.15
Forskolin (10 μM)	28.3 ± 2.8*	-
Sodium nitroprusside (10 μM)	-	5.52 ± 0.41*
Liriodenine (μM)		
30	7.2 ± 0.9	1.38 ± 0.21
100	8.0 ± 1.1	1.35 ± 0.17
300	7.9 ± 0.4	1.42 ± 0.17

After preincubation of isolated trachealis with DMSO (0.1%, control), forskolin (10 μM), sodium nitroprusside (10 μM) or various concentrations of liriodenine for 5 min, the reaction was stopped by immersing the tissue into liquid nitrogen. The cyclic AMP and cyclic GMP contents in trachealis were measured. The results are expressed as the mean ± s.e.mean ($n = 5$). *$P < 0.001$ as compared with the respective control.

trigger responses in smooth muscle and exocrine glands (Barlow *et al.*, 1976; Mutschler & Lambrecht, 1984; Lambrecht *et al.*, 1984). The pA_2 values of the known antagonists, atropine, pirenzepine, methoctramine and 4-DAMP in the guinea-pig trachea are listed in Table 1 and are similar to previously published values (Bloom *et al.*, 1987; Roffel *et al.*, 1988; Lambrecht *et al.*, 1989; Hulme *et al.*, 1990). Liriodenine possessed an equal affinity for tracheal and ileal muscarinic receptors. It is 10 times more potent for smooth muscle M_3 muscarinic receptors than for the cardiac M_2 muscarinic receptors that mediate negative inotropic and chronotropic effects. Thus, liriodenine is a selective M_3 receptor antagonist.

Recently, gene studies have indicated that M_1, M_2 and M_3 receptor subtypes are encoded by separate m_1, m_2 and m_3 genes (Bonner, 1989, Buckley *et al.*, 1989). In addition, distinct m_4 and m_5 genes have been detected (Buckley *et al.*, 1989). That different muscarinic receptor subtypes are coupled to various effector systems has been demonstrated since m_1, m_3 and m_5 subtypes expressed in Chinese hamster ovary cells are preferentially coupled to the hydrolysis of phosphoinositides, whereas the m_2 and m_4 subtypes are coupled to inhibition of adenylate cyclase (Ashkenazi *et al.*, 1987; Bonner *et al.*, 1988; Shapiro *et al.*, 1988; Peralta *et al.*, 1988; Bonner, 1989). In view of the considerations outlined above, further investigations will be conducted to evaluate the selectivity of liriodenine on muscarinic receptor subtypes by radioligand binding studies or by inhibition of the generation of second messengers.

High concentrations of liriodenine (300 μM) partially depressed the contraction induced by U-46619, histamine, $PGF_{2\alpha}$, neurokinin A, leukotriene C_4 and high-K^+ depolarization in guinea-pig trachea. In the presence of atropine (10^{-7} M), a high concentration (300 μM) of liriodenine still depressed these contractions, indicating that the inhibitory effect of high concentration of liriodenine was not via muscarinic receptor blockade. In Ca^{2+}-free and EGTA (0.2 mM)-containing medium, liriodenine (300 μM) did not affect U-46619- or neurokinin A-induced tracheal contraction. These results indicate that liriodenine may inhibit Ca^{2+} channels at higher concentrations. This observation was further supported by the lack of suppression of U-46619- and neurokinin A-induced tracheal contraction in the presence of nifedipine (1 μM) by liriodenine (300 μM). Thus, high concentrations of liriodenine may block voltage-dependent Ca^{2+} channels in the trachea.

Increased levels of cyclic nucleotides are associated with relaxation of tracheal smooth muscle (Torphy & Undem, 1991). Forskolin increases cyclic AMP via activation of adenylate cyclase (Ousterhout & Sperelakis, 1987), while sodium nitroprusside increases cyclic GMP levels by direct activation of guanylate cyclase (Gruetter *et al.*, 1979). Neither the cyclic AMP nor cyclic GMP content was changed by liriodenine (Table 2). This indicates that the effects of liriodenine are not mediated by increases of cellular cyclic nucleotide contents.

In conclusion, liriodenine is a novel muscarinic receptor antagonist, with greater selectivity in smooth muscle than in cardiac tissues. In addition, it also may block voltage-dependent calcium channels at higher concentrations. Its structural novelty may provide an original chemical basis for the development of new muscarinic receptor antagonists.

This work was supported by research grants from the National Science Council of the Republic of China (NSC83-0420-B002-004-M03) and National Research Institute of Chinese Medicine.

References

ARUNLAKSHANA, O. & SCHILD, H.O. (1959). Some quantitative uses of drug antagonists. *Br. J. Pharmacol. Chemother.*, **14**, 48–58.

ASHKENAZI, A., WINSIOW, J.W., PERALTA, E.G., PETERSON, G.L., SCHIMERLIK, M.I., CAPON, D.J. & RAMACHANDRAN, J. (1987). An M_2 muscarinic receptor subtype coupled to both adenylyl cyclase and phosphoinositide turnover. *Science*, **238**, 672–675.

BARLOW, R.B., BERRY, K.J., GLENTON, P.A.M., NIKOLAU, N.M. & SOH, S. (1976). A comparison of affinity constants for muscarine sensitive acetylcholine receptors in guinea-pig atrial pacemaker cells at 29°C and in ileum at 29°C and 37°C. *Br. J. Pharmacol.*, **58**, 613–620.

BARNES, P.K. (1987). Cholinergic control of airway smooth muscle. *Am. Rev. Respir. Dis.*, **136** (Suppl. 4), S42–S46.

BARNES, P.J. (1992). Modulation of neurotransmission in airways. *Physiol. Rev.*, **72**, 699–729.

BLOOM, J.W., YAMAMURA, H.I., BAUMGARTENER, C. & HALONEN, M. (1987). A muscarinic receptor with high affinity for pirenzepine mediates vagally induced bronochconstriction. *Eur. J. Pharmacol.*, **133**, 21–27.

BONNER, T.I. (1989). The molecular basis of muscarinic receptor diversity. *Trends Neurosci.*, **12**, 148–151.

BONNER, T.I., YOUNG, A.C., BRANN, M.R. & BUCKLEY, N.J. (1988). Cloning and expression of the human and rat M_5 muscarinic acetylcholine receptor genes. *Neuron*, **1**, 403–410.

BOUSHEY, H.A., HOLTZMAN, M.J., SHELLER, J.R. & NADEL, J.A. (1980). Bronchial hyperreactivity. *Am. Rev. Respir. Dis.*, **121**, 389–413.

BRYSON, S.E. & RODGER, I.W. (1987). Effects of phosphodiesterase inhibitors on normal and chemically-skinned isolated airway smooth muscle. *Br. J. Pharmacol.*, **92**, 673–681.

BUCKLEY, N.J., BONNER, T.I., BUCKLEY, C.M. & BRANN, M.R. (1989). Antagonist binding properties of five cloned muscarinic receptors expressed in CHO K1 cells. *Mol. Pharmacol.*, **35**, 469–476.

DOODS, H.N., MATHY, M.J., DAVIDESKO, D., VAN CHRLDORP, K.J., DE JONHE, A. & VAN ZWIETEN, P.A. (1987). Selectivity of muscarinic antagonists in radioligand and in vivo experiments for the putative M_1, M_2 and M_3 receptors. *J. Pharmacol. Exp. Ther.*, **242**, 257–262.

GIACHETTI, A., MICHELETTI, R. & MONTAGNA, E. (1986). Cardioselective profile of AF-DX 116, a muscarine M_2 receptor antagonist. *Life Sci.*, **38**, 1663–1672.

GROSS, N.J. & SKORODIN, M.S. (1984). Anticholinergic, antimuscarinic bronchodilators. *Am. Rev. Respir. Dis.*, **129**, 856–870.

GRUETTER, C.A., BARRY, B.K., MCNAMARA, D.B., GRUETTER, D.Y., KADOWITZ, P.J. & IGNARRO, L.J. (1979). Relaxation of bovine coronary artery and activation of coronary arterial guanylate cyclase by nitric oxide, nitroprusside and a carciogenic nitrosamine. *J. Cycl. Nucleotide Res.*, **5**, 211–224.

HAMMER, R., BERRIE, C.P., BIRDSALL, N.J.M., BURGEN, A.S.V. & HULME, E.C. (1980). Pirenzepine distinguishes between different subclasses of muscarinic receptors. *Nature*, **283**, 90–92.

HAMMER, R., GIRALDO, E., SCHIAVI, G.B., MONFERINI, E. & LADINSKY, H. (1986). Binding profile of a novel cardioselective muscarinic receptor antagonist, AF-DX 116, to membranes of peripher tissue and brain in the rat. *Life Sci.*, **38,** 1653–1662.

HULME, M.C., BIRDSALL, N.J.M. & BUCKLEY, N.J. (1990). Muscarinic receptor subtypes. *Annu. Rev. Pharmacol. Toxicol.*, **30,** 633–673.

KATSUKI, S. & MURAD, F. (1977). Regulation of adenosine cyclic 3′,5′-monophosphate and guanosine cyclic 3′,5′-monophosphate levels and contractility in bovine tracheal smooth muscle. *Mol. Pharmacol.*, **13,** 330–341.

KO, F.N., YU, S.M., SU, M.J., WU, Y.C. & TENG, C.M. (1993). Pharmacological activity of (−)-discretamine, a novel vascular α-adrenoceptor and 5-hydroxytryptamine receptor antagonist, isolated from *Fissistigma glaucescens*. *Br. J. Pharmacol.*, **110,** 882–888.

LAMBRECHT, G., FEIFEL, R., WAGNER-RODER, M., STROHMANN, C., ZILCH, H., TACKE, R., WAELBROECK, M., CHRISTOPHE, J., BODDECK, H. & MUTSCHLER, E. (1989). Affinity profiles of hexahydro-sila-difenidol analogues at muscarinic receptor subtypes. *Eur. J. Pharmacol.*, **168,** 71–80.

LAMBRECHT, G., MOSER, U., MUTSCHLER, E., WESS, J., LINOH, H., STRECKER, M. & TACKER, R. (1984). Hexahydrosila-difendiol: a selective antagonist on ileal muscarinic receptors. *Naunyn-Schmied. Arch. Pharmacol.*, **325,** R62.

LIN, C.H., KO, F.N., WU, Y.C., LU, S.T. & TENG, C.M. (1993). The relaxant actions on guinea-pig trachealis of atherosperminine isolated from *Fissistigma glaucescens*. *Eur. J. Pharmacol.*, **237,** 109–116.

LU, S.T., WU, Y.C. & LEOU, S.P. (1985). Alkaloids of Formosan Fissistigma and Goniothalamus species. *Phytochemistry*, **24,** 1829–1834.

MACKAY, D. (1978). How should values of pA_2 and affinity constants for pharmacological competitive antagonists be estimated? *J. Pharm. Pharmacol.*, **30,** 312–313.

MELCHIORRE, C., CASSINELLI, A. & QUAGLIA, W. (1987). Differential blockade of muscarinic receptor subtypes by polymethylene tetramines. Novel class of selective antagonists of cardiac M-2 muscarinic receptors. *J. Med. Chem.*, **30,** 201–204.

MICHEL, A.D. & WHITING, R.L. (1988). Methoctramine, a polymethylene tetramine, differentiates three subtypes of muscarinic receptor in direct binding studies. *Eur. J. Pharmacol.*, **145,** 61–66.

MUTSCHLER, E. & LAMBRECHT, G. (1984). Selective muscarinic agonists and antagonists in functional tests. *Trends Pharmacol. Sci.*, **5,** (Suppl. I), 39–44.

OUSTERHOUT, J.M. & SPERELAKIS, N. (1987). Cyclic nucleotides depress action potentials in culture aortic smooth muscle cells. *Eur. J. Pharmacol.*, **144,** 7–14.

PERALTA, E.G., ASHKENAZI, A., WINSLOW, J.W., RAMACHANDRAN, J. & CAPON, D.J. (1988). Differential regulation of PI hydrolysis and adenylyl cyclase by muscarinic receptor subtypes. *Nature*, **334,** 434–437,

ROFFEL, A.F., ELZINGA, C.R.S., VAN AMSTERDAM, R.G.M., DE ZEEUW, R.A. & ZAAGSMA, J. (1988). Muscarinic M_2 receptors in bovine tracheal smooth muscle: discrepancies between binding and function. *Eur. J. Pharmacol.*, **153,** 73–82.

SHAPIRO, R.A., SCHERER, N.M., HABECKER, B.A., SUBERS, E.M. & NATHANSON, N.M. (1988). Isolation, sequence and functional expression of the mouse M_1 muscarinic acetylcholine receptor gene. *J. Biol. Chem.*, **263,** 18397–18403.

TENG, C.M., YU, S.M., CHEN, C.C., HUANG, Y.L. & HUANG, T.F. (1990). EDRF-release and Ca^{2+} channel blockade by magnolol an antiplatelet agent isolated from Chinese herb *Magnolia officinalis*, in rat thoracic aorta. *Life Sci.*, **47,** 1153–1161.

TENG, C.M., YU, S.M., CHEN, C.C., HUANG, Y.L. & HUANG, T.F. (1991). Dicentrine, a natural vascular α_1-adrenoceptor antagonist, isolated from *Lindera megaphylla*. *Br. J. Pharmacol.*, **104,** 651–656.

TORPHY, T.J. & UNDEM, B.J. (1991). Phosphodiesterase inhibitors: new opportunities for the treatment of asthma. *Thorax*, **46,** 512–523.

(Received December 7, 1993
Revised March 28, 1994
Accepted May 12, 1994)

Br. J. Pharmacol. (1994), **113**, 282–288

Effect of 7-nitro indazole on neurotransmission in the rat vas deferens: mechanisms unrelated to inhibition of nitric oxide synthase

Hala S. Allawi, P. Wallace, Ann Pitcher, Zoe Gaffen, P.A. Bland-Ward & [1]P.K. Moore

Pharmacology Group, Biomedical Science Division, King's College University of London, Manresa Road, London, SW3 6LX

1 The effect of the nitric oxide synthase (NOS) inhibitor, 7-nitro indazole (7-NI), on sympathetic and purinergic neurotransmission in the rat isolated vas deferens preparation has been studied.

2 7-NI (50–200 μM) caused a dose- and frequency-dependent inhibition of the phasic (predominantly purinergic) contractile response of the rat vas deferens to electrical (field) stimulation (100 V, 0.5 ms). Greatest inhibition occurred at lower frequencies of stimulation (0.1–10 Hz). The sustained tonic contractile response (predominantly noradrenergic) was inhibited only at a high frequency of stimulation (60 Hz) and only at the highest concentration of 7-NI studied (200 μM).

3 7-NI (100 μM) significantly reduced the contractile response of the vas deferens to exogenous ATP (20 μM–5 mM) and the stable P_{2X} purinoceptor agonist, α,β-methylene ATP (2.5 and 25.0 μM) but was without effect on contractions due to noradrenaline (0.1– 50 μM) indicating a lack of antagonist effect on post-junctional α_1 adrenoceptors.

4 The effect of 7-NI (100 μM) on the phasic contractile response to field stimulation (0.1 and 2.0 Hz) was unaffected by preincubation of preparations with yohimbine (1.0 μM) or propranolol (0.01–10.0 μM) indicating the absence of involvement of α_2- or β-adrenoceptors in this response.

5 7-NI (50–600 μM) caused dose-related inhibition of contractions elicited by addition of a depolarizing concentration of KCl (64 mM).

6 The effect of 7-NI (100 μM) on the phasic contractile response to field stimulation (0.1 and 2.0 Hz) was unaffected by preincubation of preparations with L-arginine (1 mM). Neither L-arginine (1 mM) nor N^G nitro L-arginine methyl ester (L-NAME, 100 μM) affected the response of the vas deferens to field stimulation at 0.1 or 2.0 Hz. Nitric oxide synthase (NOS) enzyme activity, measured as the conversion of [^{3}H]-L-arginine to [^{3}H]-citrulline, was not detectable in rat vas deferens homogenates.

7 7-NI preferentially inhibits the purinergic component of the response of the rat vas deferens to field stimulation. The mechanism of action of 7-NI is not known but is not related to NOS inhibition. It seems likely that 7-NI combines an antagonist action at smooth muscle cell P_{2X}-purinoceptors with the ability to inhibit the cellular influx of calcium ions. Although these hitherto unrecorded effects of 7-NI occur at relatively high concentrations, the effects described may contribute to the pharmacological effects of this NOS inhibitor.

Keywords: 7-Nitro indazole; L-NAME; L-arginine; vas deferens; P_{2X} purinoceptors; α β-methylene ATP; adrenoceptors; calcium influx

Introduction

The fused heterocycle, 7-nitro indazole (7-NI), is a potent inhibitor of nitric oxide synthase (NOS) in rat and mouse cerebellum, olfactory bulb, hippocampus and cerebral cortex both *in vitro* and *ex vivo* following intraperitoneal injection in conscious or anaesthetized animals (Moore *et al.*, 1993a,b; Babbedge *et al.*, 1993a,b; Michel *et al.*, 1993). Furthermore, 7-NI exerts antinociceptive activity in the conscious mouse assessed behaviourally by either the formalin-induced hind-paw licking or acetic acid-induced abdominal constriction procedures (Moore *et al.*, 1993a,b). Alternative inhibitors of NOS such as N^G nitro L-arginine methyl ester (L-NAME) also exhibit antinociceptive activity in the mouse (Moore *et al.*, 1991; Mustafa, 1992) most probably by virtue of preventing the spinal 'wind-up' which follows activation of N-methyl-D-aspartate receptors in the dorsal horn (substantia gelatinosa region) of the spinal cord by the excitatory amino acid, L-glutamate (for review, see Meller & Gebhart, 1993). Thus, it may be reasoned that antinociception in the intact animal due to both 7-NI and L-NAME is secondary to inhibition of a neuronal isoform of NOS (i.e. nNOS) located in nociresponsive neurones of the dorsal spinal cord. Similar inhibition of nNOS may underlie other reported biological effects of 7-NI in the central nervous system including increased dopamine release from the corpus striatum of anaesthetized rats determined by microdialysis (Rose *et al.*, 1994) and reduction of cerebral blood flow in the anaesthetized cat (Kovach *et al.*, 1993).

Unlike L-NAME, 7-NI administration in the anaesthetized rat, mouse (Moore *et al.*, 1993a,b) or cat (Kovach *et al.*, 1993) does not result in a rise in mean arterial blood pressure even though 7-NI is an inhibitor of endothelial cell NOS (i.e. eNOS) *in vitro* (Babbedge *et al.*, 1993a). The absence of cardiovascular side effects of 7-NI underlies our proposal (Moore *et al.*, 1993a,b) that this NOS inhibitor may prove to be a useful tool with which to assess the physiological significance of nitric oxide (NO) in the central nervous system.

The biological effects of indazole and its substituted derivatives have generally attracted very little attention. Thus, there are no published accounts of the effect of 7-NI on autonomic nervous system function in general and on sympathetic or purinergic neurotransmission in particular. Bearing in mind the potential experimental and perhaps clinical applications of 7-NI we considered it of interest to evaluate the effect of this derivative on autonomic neuro-

[1] Author for correspondence.

transmission. The rat vas deferens preparation was chosen since it provides an opportunity to examine the effect of 7-NI on a range of pre- and postjunctional receptors involved in both sympathetic and purinergic neurotransmission. Furthermore, to the best of our knowledge, the presence of NOS and the involvement of NO in responses to field stimulation of this preparation have not previously been studied.

Methods

Preparation of vas deferens and drug treatment

Male Wistar rats (250–320 g) were killed by a blow to the head and exsanguination. Vasa deferentia were excised, cleared of adherent connective tissue and blood vessels, and suspended under a tension of 2 g in 20 ml organ baths containing warmed (37°C) and aerated (95% O_2:5% CO_2) Krebs solution (composition, mM: NaCl 118, KCl 5.4, $NaHCO_3$ 25, $MgSO_4$ 1.2, $CaCl_2$ 2.5, glucose 11.1, pH 7.4). Tension was recorded with a force transducer (Ohmex Ltd.) connected to a pen recorder (Lectromed). Preparations were allowed to equilibrate in the organ bath for 30 min prior to further study. Electrical (field) stimulation (0.1–60 Hz, 100 V, 0.5 ms, 20 s) of the vas deferens was performed with two platinum electrodes positioned on either side of the tissue and connected to an SRI square wave stimulator. Preparations were routinely stimulated at 5 min intervals.

In order to assess the effect of 7-NI (10–600 μM) on contractile responses to noradrenaline (0.1–50 μM) and ATP (20 μM–5 mM) these agonists were applied non-cumulatively at 5 min intervals using a contact time of 1 min which was shown in preliminary experiments to be sufficient for maximal tension development. α, β-Methylene ATP was applied non-cumulatively at 45 min intervals (contact time 3 min). The effect of increasing concentrations of 7-NI (10–600 μM) on the contractile response to KCl (64 mM) was also investigated. In this case preparations were exposed four times to KCl at this concentration in the presence and absence of a single concentration of 7-NI. In further experiments preparations were preincubated in the organ bath for 30 min with yohimbine (1 μM), propranolol (0.01–10 μM) or L-arginine (1 mM) prior to addition of 7-NI. Additionally, some preparations were exposed to L-NAME (100 μM) for 30 min prior to field stimulation at 0.1 or 2.0 Hz. In all cases, preparations were exposed to only a single antagonist or ethanol vehicle.

Measurement of vas deferens NOS enzyme activity in vitro

Male Wistar rats (250–320 g) were killed by a blow to the head and exsanguinated. Vasa deferentia were rapidly removed and homogenized (1:10 w/v) in 20 mM Tris-HCl buffer (pH 7.4) containing 2 mM EDTA using an Ultra-Turrax homogenizer (type 18/2N). After centrifugation (1,000 *g*, 15 min, 4°C) aliquots of supernatant (25 μl) were added to incubation tubes containing NADPH (0.5 mM) and calcium chloride (0.75 mM) and kept on ice. The final incubation volume was 105 μl. The reaction was started by addition of 0.5 μCi [^{3}H]-L-arginine (concentration, 120 nM) and transfer to a water bath at 37°C for 15 min. At the end of this period the enzyme reaction was stopped by addition of 3 ml 20 mM HEPES (pH 5.5) buffer containing 2 mM EDTA and transfer to ice. [^{3}H]-L-arginine was separated from the product [^{3}H]-citrulline by column chromatography using 0.5 ml columns of Dowex AG50WX-8 (Na^+ form) followed by 1 ml distilled water. [^{3}H]-citrulline was quantified by liquid scintillation spectroscopy of a 1 ml aliquot of the flow through as described previously (Moore *et al.*, 1993a,b). In control experiments vas deferens supernatant was added to the incubation after stopping the reaction with HEPES buffer. For comparison, parallel estimates of NOS enzyme activity in rat cerebellar homogenates prepared and incubated as above were also performed. NOS enzyme activity is expressed as pmol citrulline mg^{-1} protein 15 min^{-1}. Protein concentration in vas deferens and cerebellar supernatant was determined using the Folin-phenol reagent with bovine serum albumin as standard (Lowry *et al.*, 1951).

Statistical analysis

The statistical significance of differences between groups of results was determined by analysis of variance coupled with Student's unpaired *t* test. A probability (*P*) value of 0.05 or less was taken to indicate statistical significance. The number of observations are indicated in parentheses.

Drugs and chemicals

7-Nitro indazole was purchased from MTM Research Biochemicals, Lancaster Ltd. and dissolved by sonication in absolute ethanol (Analar grade). Radiolabelled [^{3}H]-L-arginine (specific activity, 62.0 Ci $mmol^{-1}$) was obtained from Amersham, Bucks. All other drugs and chemicals were purchased from Sigma Ltd. Dowex AG50WX-8 H^+ form was converted into the Na^+ form by soaking for 2 h in 2 M sodium hydroxide. (−)-Propranolol hydrochloride, yohimbine hydrochloride, (−)-noradrenaline bitartrate, L-arginine hydrochloride, N^G nitro-L-arginine methyl ester (L-NAME), ATP and α,β-methylene ATP were dissolved in 0.9% w/v NaCl (saline). Drug solutions were prepared fresh each morning. ATP solutions were kept on ice throughout the experiment.

Results

Electrical stimulation of the vas deferens

Repetitive field stimulation of the rat vas deferens (0.1–60 Hz) resulted in frequency-related contractions. At low frequencies (0.1–0.5 Hz) individual monophasic twitch contractions were observed. At higher frequencies of stimulation (1–60 Hz) responses of the vas deferens summated to produce a single tetanic contraction which was biphasic in nature with a rapid (approx. 3–5 s) first phase (i.e. phasic) followed immediately by a more sustained (i.e. tonic) phase. The biphasic character of the response was most obvious at a stimulation frequency of 2 Hz which was therefore routinely chosen for further experiments.

Effect of 7-NI on the field-stimulated vas deferens

Preincubation of vas deferentia with 7-NI (100 μM) did not affect the initial phasic response to field stimulation of the vas deferens as determined by analysis of variance over the entire frequency range (Figure 1a). However, comparison of individual mean responses over the same frequency range revealed a selective inhibitory effect of 7-NI at lower frequencies (0.1–10 Hz) of stimulation (i.e. 2 Hz; 65.3 ± 6.5% inhibition, $n = 6$, $P < 0.01$) compared with higher frequencies (i.e. 60 Hz; 5.1 ± 3.1% inhibition, $n = 6$, $P > 0.05$). At a higher concentration, 7-NI (200 μM) significantly reduced the initial phasic contraction at all frequencies (Figure 1b). Preincubation with an appropriate volume of ethanol did not influence the phasic contractile response of the isolated vas deferens at any of the frequencies studied (Figure 1a,b). A higher concentration of 7-NI (200 μM) also reduced the second (tonic) component of the contractile response of the vas deferens to field stimulation, albeit only at high frequency stimulation (60 Hz), whilst at lower concentration 7-NI (100 μM) was without significant activity at any frequency studied (Figure 2a,b).

In order to examine the effect of concentration of 7-NI upon responses of the vas deferens, preparations were stimulated at 5 min intervals (0.1 and 2.0 Hz) in the presence and absence of increasing amounts of 7-NI (10–200 μM) (Figure 3a,b). 7-NI (10 μM) failed to reduce either the initial phasic or the later tonic contraction of the vas deferens at either frequency examined. At higher concentrations, 7-NI (50–200 μM) caused a dose-related reduction in the phasic contractile response of the vas deferens to field stimulation at both 0.1 and 2.0 Hz. In contrast, 7-NI (10–100 μM) did not influence the tonic contraction of the vas deferens in response to field stimulation at 2 Hz whilst at the highest concentration employed (200 μM) a significant but relatively modest inhibition (38.6 ± 6.6%, $P<0.05$, $n=6$) was apparent. Interestingly, removal of 7-NI (200 μM) from the organ bath at the conclusion of these experiments resulted in a rapid (within 10 min) and complete restoration of both the phasic and tonic components of the response (data not shown).

Effect of 7-NI on the contractile response to noradrenaline, ATP and α,β-methylene ATP

Non-cumulative addition of both noradrenaline (pD_2, 5.30; maximum response, 1.96 ± 0.10 g, $n=6$) and ATP (pD_2 3.15; maximum response, 1.78 ± 0.18 g, $n=6$) resulted in dose-related contractions. Preliminary experiments using α,β-methylene ATP at a single concentration (2.5 μM) revealed the development of rapid desensitization to the contractile effect of this stable ATP analogue. Similar desensitization to α,β-methylene ATP has been observed previously in the isolated vas deferens preparation (e.g. Meldrum & Burnstock, 1983; Sneddon & Westfall, 1984). For this reason responses to α,β-methylene ATP required a dose interval of 45 min and accordingly only two concentrations (2.5 and 25 μM) of this purinoceptor agonist were studied. 7-NI (100 μM) preincubation failed to influence contractions due to noradrenaline but shifted the log dose-response curve for ATP to the right (Figure 4a,b). Due to limitations of solubility the effect of higher doses of ATP in the presence of 7-NI could not be determined and hence a maximum response was not obtained. In separate experiments, 7-NI (100 μM) also reduced contractions due to α,β-methylene ATP (Figure 4c).

Effect of propranolol and yohimbine on the response to 7-NI

The possibility that 7-NI may reduce contractions of the rat vas deferens by an agonist action at pre-junctional α_2-adrenoceptors was examined in preparations pre-equilibrated (30 min) with the selective α_2-adrenoceptor antagonist, yohimbine (1 μM). No effect of yohimbine on the ability of

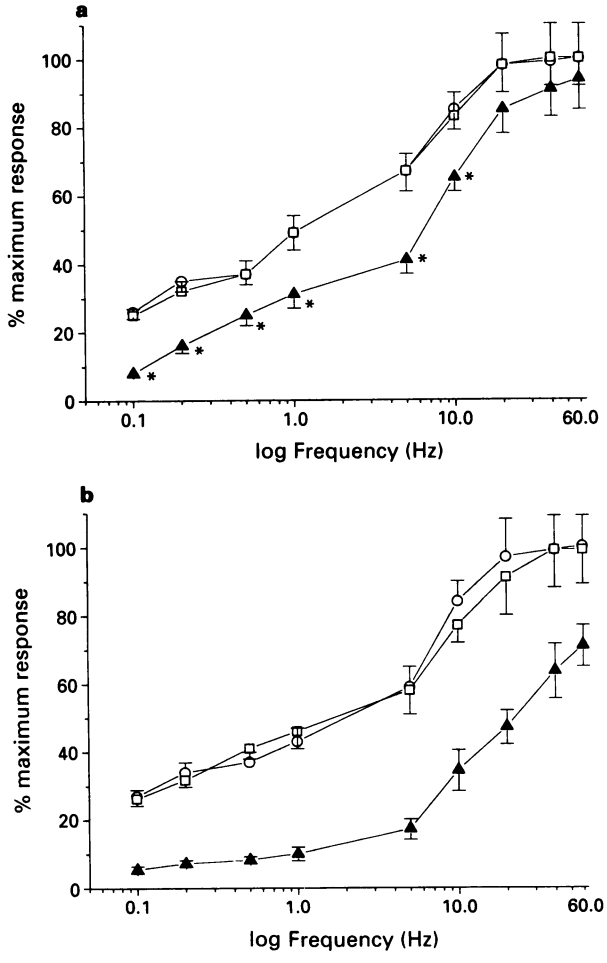

Figure 1 Effect of 100 μM (a) and 200 μM (b) 7-nitro indazole (7-NI) on the initial phasic contraction of the rat vas deferens to electrical field stimulation (0.1–60 Hz). Frequency-response curves were obtained in Krebs solution without drug addition (□) or following 30 min preincubation with 7-NI (▲) or an appropriate volume of ethanol vehicle (○). Analysis of variance indicates no statistically significant difference between the frequency-response curves in (a) ($P>0.05$). Comparison of individual means by Student's t test reveals significant differences at lower frequency stimulation (*$P<0.05$). Analysis of variance indicates a statistically significant ($P<0.01$) effect of the higher concentration of 7-NI (b). Results show % maximal response and are mean ± s.e.mean, $n=6$–8.

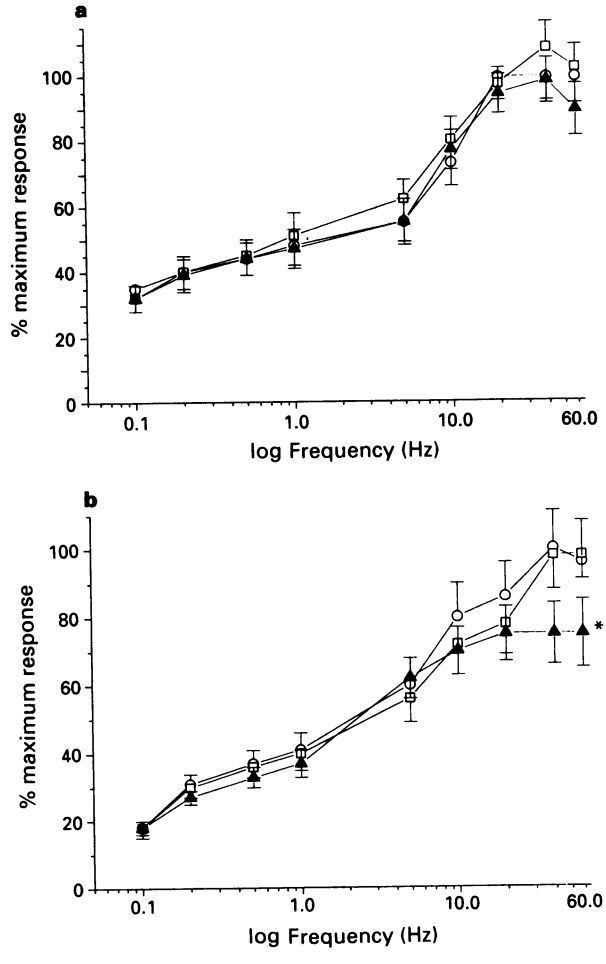

Figure 2 Effect of 100 μM (a) and 200 μM (b) 7-nitro indazole (7-NI) on the secondary tonic contraction of the rat vas deferens to electrical field stimulation (1–60 Hz). Frequency-response curves were obtained in Krebs solution without drug addition (□) or following 30 min preincubation with 7-NI (▲) or an appropriate volume of ethanol vehicle (○). Results show % maximal response and are mean ± s.e.mean, $n=8$. *$P<0.05$ (Student's t test).

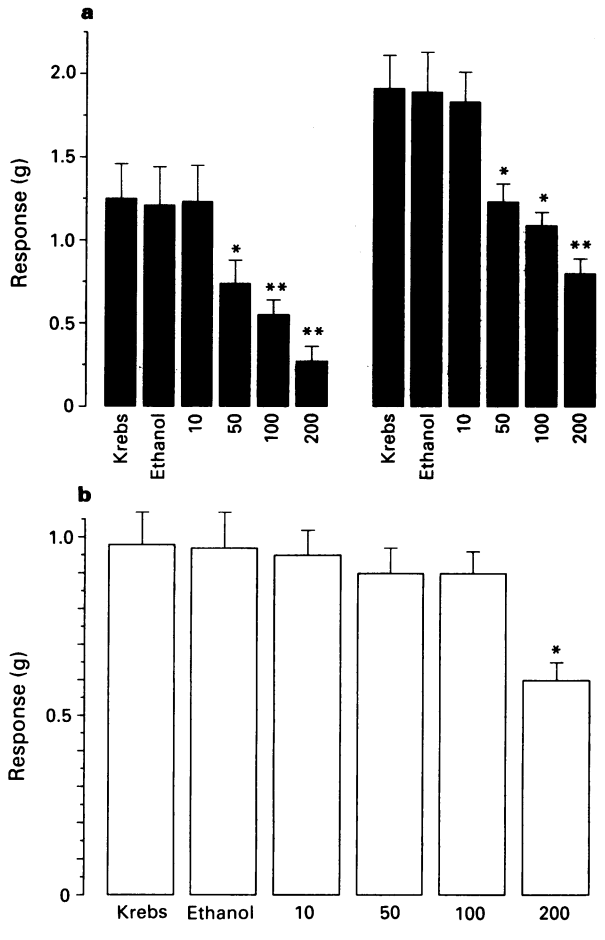

Figure 3 Dose-related effect of 7-nitro-indazole (7-NI, 10-200 μM) on phasic (a) and tonic (b) contractile responses to electrical field stimulation at 0.1 Hz (first set of histograms in a; b) and 2.0 Hz (second set of histograms in a). Preincubation of preparations with an appropriate volume of ethanol did not influence the response to field stimulation. Results show tension developed (g) and are mean ± s.e.mean, $n = 6-8$, $^*P<0.05$, $^{**}P<0.01$ (Student's t test).

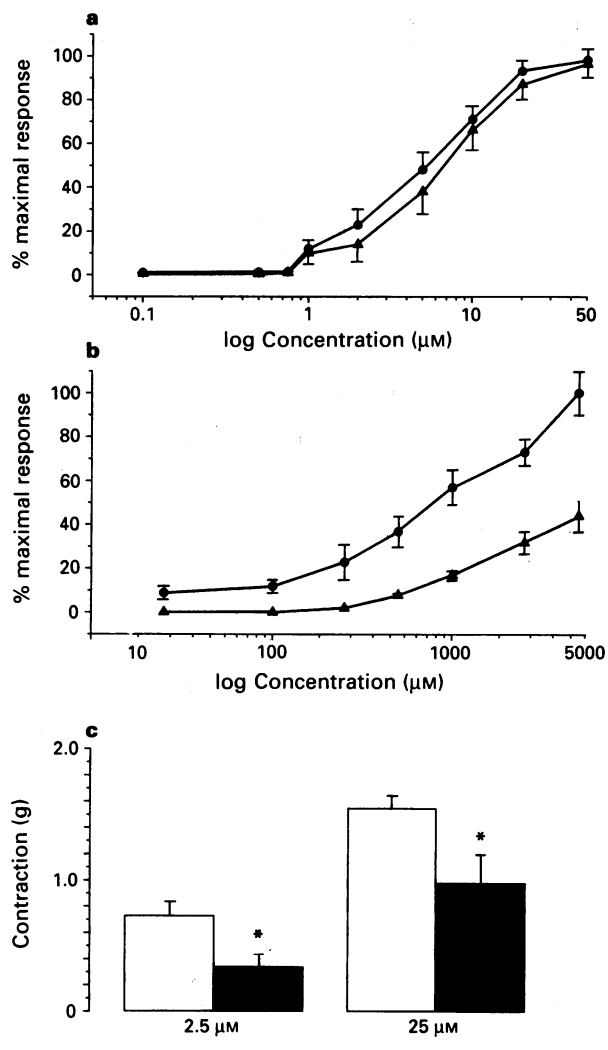

Figure 4 Effect of 7-nitro indazole (7-NI, 100 μM; ▲) and ethanol (●) preincubation on responses of the rat isolated vas deferens to noradrenaline (a) and ATP (b); (c) compares the effect of two concentrations of α,β-methylene ATP on preparations preincubated with 7-NI (100 μM; solid columns) or an appropriate volume of ethanol (open columns). Results indicate % maximal response (a and b) or tension developed in grams (c) and are the mean ± s.e.mean of 6 observations. $^*P<0.05$ (Student's t test).

7-NI (100 μM) to inhibit either the tonic (2.0 Hz) or phasic (0.1 and 2.0 Hz) contractile response of the isolated vas deferens preparation was apparent (Table 1). A higher concentration (10 μM) of yohimbine significantly inhibited the response to exogenous noradrenaline (data not shown) and was therefore not evaluated further in this series of experiments. Since the rat vas deferens preparation also possesses post-junctional β_2 adrenoceptors it seemed worthwhile to investigate a possible β-adrenoceptor agonist effect of 7-NI. However, separate experiments revealed that the non-selective β-adrenoceptor antagonist, propranolol (0.01–10 μM), failed to reverse the ability of 7-NI (100 μM) to inhibit the tonic (2.0 Hz) or phasic (0.1 and 2.0 Hz) components of the field stimulation response (Table 1).

Effect of 7-NI on KCl-induced contractions of the rat vas deferens

KCl (64 mM) evoked a biphasic contractile response comprising an initial rapid rise followed by a more sustained response. The total tension (both phases) developed in response to KCl in the absence of added 7-NI or ethanol was 0.80 ± 0.07 g ($n = 8$). 7-NI (50–600 μM) caused dose-related inhibition of KCl-induced contractions whilst at lower concentrations (10 and 20 μM) 7-NI was without activity (Figure 5). Due to limitation of solubility it was not possible to determine the maximally effective concentration of 7-NI. However, 50% inhibition of KCl-induced contraction was observed at a concentration of 280 μM. 7-NI did not discriminate between the two phases of the KCl response and thus results are shown as inhibition of the overall contraction. Addition of ethanol vehicle did not influence the response of preparations to KCl at volumes up to 0.33 ml/20 ml Krebs solution in the organ bath (equivalent to 400 μM 7-NI). However, even at the highest ethanol volume used (0.49 ml/20 ml Krebs solution) only a small (9.0 ± 1.4%, $n = 6$) reduction in the response to added KCl was observed.

The role of NO in the effect of 7-NI on the field-stimulated rat vas deferens

In order to probe the possible involvement of NO in the response of the rat isolated vas deferens to field stimulation in the presence and absence of 7-NI, further experiments were undertaken to evaluate the effect of the NO precursor, L-arginine, on the responses. Thus, preincubation of rat vas deferens preparations with L-arginine (1 mM) did not influence the contractile response to field stimulation (0.1 or 2.0 Hz) (Table 2). Furthermore, L-arginine (1 mM) did not alter the ability of 7-NI (100 μM) to influence either the tonic or phasic contractile responses to field stimulation at the

Table 1 Effect of propranolol and yohimbine on the response of the field stimulated rat vas deferens to 7-nitro-indazole (7-NI)

	Contractile response (g)		
	Phasic (0.1 Hz)	*Phasic* (2 Hz)	*Tonic* (2 Hz)
Krebs	0.97 ± 0.09	1.87 ± 0.4	1.55 ± 0.31
+ Ethanol	0.96 ± 0.05	1.79 ± 0.32	1.50 ± 0.21
+ 7-NI (alone)	0.20 ± 0.08*	0.85 ± 0.21*	1.45 ± 0.23
+ 7-NI			
+ propranolol (0.01 μM)	0.18 ± 0.05	0.79 ± 0.16	1.45 ± 0.18
+ propranolol (0.1 μM)	0.17 ± 0.06	0.63 ± 0.20	1.44 ± 0.21
+ propranolol (1.0 μM)	0.17 ± 0.05	0.65 ± 0.23	1.37 ± 0.15
+ propranolol (10 μM)	0.15 ± 0.05	0.67 ± 0.17	1.47 ± 0.21
+ yohimbine (1.0 μM)	0.16 ± 0.04	0.69 ± 0.19	1.44 ± 0.09

Effects of yohimbine and propranolol (concentrations shown in parentheses) in combination with 7-NI (100 μM) or an appropriate volume of ethanol vehicle on the tonic and phasic contractile responses of the field stimulated rat vas deferens (0.1 and 2.0 Hz). Preparations were preincubated with drug for 30 min prior to further field stimulation. It should be noted that no tonic response is evident at 0.1 Hz stimulation. Results show mean ± s.e.mean, $n = 6-8$. *$P<0.05$ by Student's t test cf control responses in the presence of ethanol vehicle. Neither propranolol nor yohimbine significantly ($P>0.05$) influenced the response to 7-NI.

Table 2 Effect of N^G-nitro-L-arginine methylester (L-NAME) and L-arginine(L-Arg) on the response of the field stimulated rat vas deferens to 7-nitro indazole (7-NI)

	Contractile response (g)		
	Phasic (0.1 Hz)	*Phasic* (2 Hz)	*Tonic* (2 Hz)
Krebs	1.15 ± 0.19	1.71 ± 0.21	1.41 ± 0.31
Ethanol	1.09 ± 0.17	1.74 ± 0.16	1.44 ± 0.13
Ethanol + L-Arg	0.95 ± 0.18	1.85 ± 0.31	1.51 ± 0.20
L-NAME	0.98 ± 0.31	1.87 ± 0.21	1.50 ± 0.21
7-NI	0.45 ± 0.12*	1.19 ± 0.15*	1.41 ± 0.14
7-NI + L-Arg	0.40 ± 0.15*	1.11 ± 0.17*	1.39 ± 0.17

Effect of L-NAME (100 μM) and L-arginine (1 mM) either alone or in combination with 7-NI (100 μM) or an appropriate volume of ethanol vehicle on the tonic and phasic contractile response of the field stimulated rat vas deferens (0.1 and 2.0 Hz). Preparations were preincubated with drug for 30 min prior to further field stimulation. It should be noted that no tonic response is evidence at 0.1 Hz stimulation. Results show mean ± s.e.mean, $n = 6-8$, *$P<0.05$.

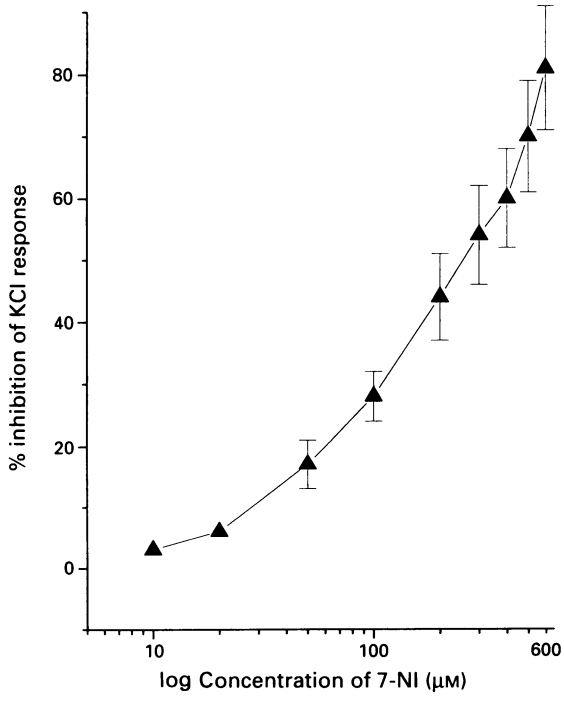

Figure 5 Dose-related effect of 7-nitro indazole (7-NI) on contractions of the rat isolated vas deferens preparation to KCl (64 mM). Results show % inhibition of KCl-induced contractions and are mean ± s.e.mean of experiments on 6 animals.

same frequencies (Table 2). In separate experiments, rat vas deferens homogenates failed to convert [^{3}H]-L-arginine to [^{3}H]-citrulline (limit of detection of assay, 2.2 pmol mg^{-1} protein 15 min^{-1}). For comparison NOS enzyme activity in rat cerebellar homogenates was 37.5 ± 1.9 pmol mg^{-1} protein 15 min^{-1} ($n = 6$).

Effect of L-NAME on the field stimulated rat vas deferens

Preincubation (30 min) of isolated rat vasa deferentia with L-NAME (100 μM) did not affect either the tonic or phasic contractions following field stimulation at 0.1 or 2.0 Hz (Table 2).

Discussion

The major finding of the present study is that high concentrations of 7-NI inhibit the contractile response elicited by field stimulation of the rat isolated vas deferens in a dose- and frequency-dependent manner. 7-NI (50–200 μM) exhibits some degree of selectivity for the initial (phasic) component of the contraction whilst the secondary (tonic) contraction is only modestly reduced even at the highest concentration of 7-NI (200 μM) examined. Neither effect of 7-NI relates to the only other reported pharmacological action of this indazole, *viz.* inhibition of NOS (Moore *et al.*, 1993a,b; Michel *et al.*, 1993) in that, (i) NOS enzyme activity monitored by the conversion of [^{3}H]-L-arginine to [^{3}H]-citrulline was undetectable in homogenates prepared from the rat vas deferens, (ii) inhibition of the contractile response of the rat vas deferens to field stimulation was unaffected by preincubation with a high concentration of L-arginine (substrate for NOS) and (iii) L-NAME, an established inhibitor of NOS, failed to inhibit neurotransmission in the rat isolated vas deferens at a concentration which abolishes non-adrenergic, non-cholinergic (NANC) relaxation in other smooth muscle preparations (e.g. mouse anococcygeus; Gibson *et al.*, 1990).

The biphasic character of the contractile response to repetitive field stimulation of the isolated vas deferens from a variety of species is well established and has been the subject of intensive study over the last decade. The phasic component is antagonized by arylazidoaminopropionyl-ATP (ANAPP$_3$; Fedan *et al.*, 1981) and the P_{2X}-purinoceptor antagonists, suramin (Dunn & Blakely, 1988) and pyridoxalphosphate-6-azophenyl-2',4'-disulphonic acid (PPADS, McLaren *et al.*, 1994) and is thus believed to occur following the release of ATP from sympathetic nerves acting on smooth muscle P_{2X}-purinoceptors (Burnstock & Kennedy, 1985). In contrast, the sustained tonic component results principally from noradrenaline-induced activation of postjunctional α_1-adrenoceptors (Brown *et al.*, 1979; Sneddon & Westfall, 1984; Amobi & Smith, 1987).

Preincubation of rat isolated vas deferens preparations with 7-NI resulted in a dose-related inhibition of the phasic contractile response to field stimulation. At relatively low concentrations of 7-NI (50–100 μM) only the response to lower frequency stimulation (i.e. 0.1–10 Hz) was reduced whilst at higher concentration (200 μM) phasic contractions over the entire frequency-range were attenuated. In other smooth muscle preparations (e.g. rabbit mesenteric artery; von Kügelgen & Starke, 1985) low frequency stimulation is predominantly due to purinergic transmission whereas higher frequency stimulation is mostly due to adrenergic transmission. This, coupled with the observation that 7-NI inhibits the response of the isolated vas deferens to exogenously applied ATP and to the stable P_{2X}-purinoceptor agonist, α,β-methylene ATP (Burnstock & Kennedy, 1985), without affecting contractions due to noradrenaline, is consistent with the hypothesis that 7-NI inhibits the predominantly purinergic component of the response of the vas deferens to field stimulation. It may also be concluded from these results that 7-NI neither promotes the metabolic inactivation of ATP (since it also antagonizes the effect of the stable analogue, α,β-methylene ATP) nor exhibits an antagonist effect on postjunctional α_1-adrenoceptors. However, it should be noted that high concentrations of 7-NI also inhibit the tonic (i.e. noradrenergic) component of the contractile response to high frequency field stimulation. Whether this effect indicates a role for P_{2X}-purinoceptors in the predominantly noradrenergic tonic component of the response or whether 7-NI inhibits noradrenergic transmission by a mechanism unrelated to the direct activation of postjunctional α_1-adrenoceptors (e.g. inhibition of prejunctional noradrenaline release or smooth muscle Ca^{2+} influx) is not known.

The rat isolated vas deferens preparation possesses both prejunctional α_2-(Bullock & Starke, 1990; Brown *et al.*, 1979) and postjunctional α_2-adrenoceptors (Ganguly & Bhattacharya, 1969; Lotti *et al.*, 1980) activation of either of which would be expected to reduce the size of contractions due to field stimulation. In this study, yohimbine (1 μM) failed to reverse the inhibitory effect of 7-NI on the field stimulated rat vas deferens. Since we have previously reported that a lower concentration of yohimbine (0.1 μM) produces significant inhibition of the response of this preparation to the selective α_2-adrenoceptor agonist, xylazine (Moore & Griffiths, 1982), it seems likely that yohimbine was present in sufficient concentration to inhibit α_2-adrenoceptors in the present series of experiments. A higher concentration of yohimbine (i.e. 10 μM) significantly reduced the contractile effect of exogenous noradrenaline suggesting α_1-adrenoceptor blockade and thus could not be studied further. Preincubation of preparations with a range of concentrations of the non-selective β-adrenoceptor antagonist, propranolol, also failed to reverse 7-NI-induced inhibition of the field stimulated rat vas deferens. Thus, the present study provides no evidence for an agonist effect of 7-NI on either α_2- or β_2-adrenoceptors.

The finding that 7-NI inhibits contractions of the rat vas deferens to KCl is also of potential significance. K^+-induced contraction of smooth muscle preparations is believed to result mainly from an increase in membrane permeability to Ca^{2+} ions via voltage-operated channels as a consequence of membrane depolarization (Bolton, 1979). Accordingly, KCl-mediated contraction of the rat vas deferens is inhibited by Ca^{2+} antagonists such as verapamil and nifedipine (Hay & Wadsworth, 1982). Consequently, it seems not unreasonable that 7-NI-mediated relaxation of the vas deferens may also occur by virtue of a similar Ca^{2+} antagonist effect.

In conclusion, the effect of 7-NI on neurotransmission in the rat vas deferens is undoubtedly complex and most probably involves a number of mechanisms. Whether the ability of 7-NI to inhibit the phasic response to field stimulation and to reduce contractions due to ATP and α,β-methylene ATP reflect a direct antagonist action on the P_{2X}-purinoceptor or on post receptor events (e.g. purinoceptor-mediated opening of smooth muscle Ca^{2+} channels) cannot be determined from the present data and requires additional evaluation perhaps using a ligand binding approach. Additionally, the attenuation of KCl-induced contractions and the modest reduction of the tonic response following high frequency field stimulation is suggestive of antagonism of voltage-operated Ca^{2+} channels. In the light of the relative dearth of useful P_{2X}-purinoceptor antagonists, it may be of interest to determine whether the apparent P_{2X}-antagonist activity suggested by the present experiments is restricted to 7-NI or is a more general feature of the indazole ring structure. Of equal importance is the possibility that the effects observed in the present study may contribute to the antinociceptive activity of 7-NI. Unfortunately, there is no available information concerning either the pharmacokinetic profile or the biologically active concentration range of 7-NI in either blood or spinal cord following parenteral administration in experimental animals. However, antagonism of P_{2X}-purinoceptors or voltage-operated Ca^{2+} channels would, at first sight, seem unlikely to play a part in 7-NI-mediated antinociception in that (i) the effect of 7-NI on the rat vas deferens occurs at concentrations (50–600 μM) considerably greater than those required to inhibit NOS enzyme activity at least *in vitro* (e.g. IC_{50} for 7-NI against rat cerebellar NOS of 700 nM; Moore *et al.*, 1993a,b) and (ii) 7-NI-induced antinociception is at least partially reversible with L-arginine (Moore *et al.*, 1993b) which did not influence the response to 7-NI in the present study. As yet we cannot rule out the possibility that a combined effect, for example, on glutamate-induced Ca^{2+} influx into nociresponsive neurones in the dorsal spinal cord coupled with inhibition of NOS enzyme activity in these same neurones may jointly contribute to the antinociceptive effect of 7-NI.

We would like to offer our thanks to Glaxo Group Research (Glaxo Institute for Applied Pharmacology, Cambridge) for financial support in the form of a Studentship to P.A. B.-W.

References

AMOBI, N.T.B. & SMITH, C.H. (1987). Adrenergic and non-adrenergic contributions to the two component tetanus in the rat vas deferens. *Eur. J. Pharmacol.*, **135**, 173–182.

BABBEDGE, R.C., BLAND-WARD, P.A., HART, S.L. & MOORE, P.K. (1993a). Inhibition of rat cerebellar nitric oxide synthase by 7-nitro indazole and related substituted indazoles. *Br. J. Pharmacol.*, **110**, 225–229.

BABBEDGE, R.C., BLAND-WARD, P.A., HART, S.L. & MOORE, P.K. (1993b). Indazoles: a novel group of nitric oxide synthase inhibitors. *Br. J. Pharmacol.*, **109**, 142P.

BOLTON, T.B. (1979). Mechanisms of action of transmitters and other substances on smooth muscle. *Physiol. Rev.*, **59**, 606–718.

BROWN, C.M., MCGRATH, J.C. & SUMMERS, R.J. (1979). The effects of α-adrenoceptor agonists and antagonists on responses of transmurally stimulated prostatic and epididymal portions of the isolated vas deferens of the rat. *Br. J. Pharmacol.*, **66**, 553–564.

BULLOCK, J.M. & STARKE, K. (1990). Presynaptic α_2 autoinhibition in a vascular neuroeffector junction where ATP and noradrenaline act as co-transmitters. *Br. J. Pharmacol.*, **99**, 279–294.

BURNSTOCK, G. & KENNEDY, C. (1985). Is there a basis for distinguishing two types of P_2-purinoceptor? *Gen. Pharmacol.*, **5**, 433–440.

DUNN, P.M. & BLAKELY, A.G.H. (1988). Suramin: a reversible P_2-purinoceptor antagonist in the mouse vas deferens. *Br. J. Pharmacol.*, **93**, 243–245.

FEDAN, J.S., HOGABOOM, G.K., WESTFALL, D.P. & O'DONNELL, J.P. (1981). Comparison of the effects of arylazido aminopropionyl ATP ($ANAPP_3$), an ATP antagonist, on responses of the smooth muscle of the guinea pig vas deferens to ATP and related nucleotides. *Eur. J. Pharmacol.*, **81**, 193–204.

GANGULY, D.K. & BHATTACHARYA, D.D. (1969). Adrenergic receptors in rat vas deferens. *Arch. Int. Pharmacodyn. Ther.*, **185,** 406–412.

GIBSON, A., MIRZAZADEH, S., HOBBS, A.J. & MOORE, P.K. (1990). L-N^G-monomethyl arginine and L-N^G-nitro arginine inhibit non-adrenergic, non-cholinergic relaxation of the mouse anococcygeus muscle. *Br. J. Pharmacol.*, **99,** 602–606.

HAY, D.W.P. & WADSWORTH, R.M. (1982). Effects of some organic calcium antagonists and other procedures affecting Ca^{2+} translocation on KCl-induced contractions in the rat vas deferens. *Br. J. Pharmacol.*, **76,** 103–113.

KOVACH, A.G.B., LOHINAI, Z., BALLA, I., MARCZIS, J., DOMBOVARY, Z., REIVICH, M., DAWSON, T.M. & SNYDER, S.H. (1993). Effect of 7-nitro indazole on rCBF, cerebral NOS catalytic activity and NO content measured by microelectrode. *Endothelium,* **1** (Suppl. 1), 211.

LOTTI, V.J., CHANG, R.S.L. & KLING, P. (1980). $Beta_2$ selective adrenergic responses in the field stimulated rat vas deferens. *Eur. J. Pharmacol.*, **68,** 385–386.

LOWRY, O.J., ROSEBROUGH, N.J., FARR, A.L. & RANDALL, R.J. (1951). Protein measurement with Folin-phenol reagent. *J. Biol. Chem.*, **193,** 265–269.

MCLAREN, G.J., LAMBRECHT, G., MUTSCHLER, E., BAUMERT, P., SNEDDON, P. & KENNEDY, C. (1994). Investigation of the actions of PPADS, a novel P_{2X}-purinoceptor antagonist, in the guinea pig isolated vas deferens. *Br. J. Pharmacol.*, **111,** 913–917.

MELDRUM, L.A. & BURNSTOCK, G. (1983). Evidence that ATP acts as a cotransmitter with noradrenaline in sympathetic nerves supplying the guinea pig vas deferens. *Eur. J. Pharmacol.*, **92,** 161–163.

MELLER, S.T. & GEBHART, G.F. (1993). Nitric oxide (NO) and nociceptive processing in the spinal cord. *Pain,* **52,** 127–136.

MICHEL, A.D., PHUL, R.K., STEWART, T.L. & HUMPHREY, P.P.A. (1993). Characterisation of the binding of [^{3}H]-L-N^G-nitro-arginine in rat brain. *Br. J. Pharmacol.*, **109,** 287–288.

MOORE, P.K. & GRIFFITHS, R.J. (1982). Pre-synaptic and post-synaptic effects of xylazine and naphazoline on the bisected rat vas deferens. *Arch. Int. Pharmacodyn. Ther.*, **260,** 70–77.

MOORE, P.K., OLUYOMI, A.O., BABBEDGE, R.C., WALLACE, P. & HART, S.L. (1991). L-N^G-nitro arginine methyl ester exhibits antinociceptive activity in the mouse. *Br. J. Pharmacol.*, **102,** 198–202.

MOORE, P.K., WALLACE, P., GAFFEN, Z., HART, S.L. & BABBEDGE, R.C. (1993a). 7-Nitro indazole, an inhibitor of nitric oxide synthase, exerts antinociceptive activity in the mouse without increasing blood pressure. *Br. J. Pharmacol.*, **108,** 296–298.

MOORE, P.K., WALLACE, P., GAFFEN, Z., HART, S.L. & BABBEDGE, R.C. (1993b). Characterization of the novel nitric oxide synthase inhibitor 7-nitro indazole and related indazoles: antinociceptive and cardiovascular effects. *Br. J. Pharmacol.*, **110,** 219–224.

MUSTAFA, A.A. (1992). Mechanisms of L-N^G nitro arginine methyl ester-induced antinociception in mice: a role for serotonergic and adrenergic neurones. *Gen. Pharmacol.*, **23,** 1177–1182.

ROSE, S., HINDMARSH, J.G., SILVA, M.T., PITCHER, A., AISLAITNOR, G., MOORE, P.K., GORROD, J.W., JENNER, P. & MARSDEN, C.D. (1994). The novel monosodium salt of 7-nitro indazole inhibits brain nitric oxide synthase and elevates striatal dopamine efflux *in vivo*. *Br. J. Pharmacol.* (in press).

SNEDDON, P. & WESTFALL, D.P. (1984). Pharmacological evidence that adenosine triphosphate and noradrenaline are co-transmitters in the guinea pig vas deferens. *J. Physiol.*, **347,** 561–580.

VON KÜGELGEN, I. & STARKE, K. (1985). Noradrenaline and adenosine triphosphate as co-transmitters of neurogenic vasoconstriction in rabbit mesenteric artery. *J. Physiol.*, **367,** 435–455.

(Received March 30, 1994
Revised May 9, 1994
Accepted May 13, 1994)

Br. J. Pharmacol (1994), **113**, 289–295

Effects of caffeine on intracellular sodium activity in cardiac Purkinje fibres: relation to force

Giovanni Iacono & [1]Mario Vassalle

Department of Physiology, State University of New York, Health Science Center, 450 Clarkson Avenue, Brooklyn, NY 11203, U.S.A.

1 An increase in cytoplasmic calcium by caffeine would lead to Ca extrusion via the Na/Ca exchange. The hypotheses were investigated that, as a consequence, caffeine might increase intracellular sodium activity (a^i_{Na}) and that the relation between a^i_{Na} and force might be conditioned by the Ca load.

2 Action potential, a^i_{Na} and contractile force were recorded in sheep Purkinje fibres during exposure to caffeine under conditions that decrease or increase the Ca load by different mechanisms.

3 In Tyrode solution, caffeine (8 mM) increased a^i_{Na} from 8.05 ± 0.20 to 10.52 ± 0.40 mM (+30.5%) and had a triphasic effect on force: an initial transient increase (+93.6%), a subsequent decrease (−37.1%) (negative inotropy) and slow partial recovery (+8.9%).

4 Decreasing the Ca load by means of manganese (1 mM) decreased a^i_{Na} and force. Adding caffeine re-increased a^i_{Na} and no longer caused a negative inotropic action. Cadmium (0.2 mM) also decreased a^i_{Na}, and caffeine reincreased it although far less than in Tyrode solution.

5 High $[K]_o$ (10 mM) and tetrodotoxin (5 μM) decreased a^i_{Na} as well as force. In their presence, caffeine re-increased a^i_{Na} and no longer had a negative inotropic action.

6 Increasing the Ca load by means of high $[Ca]_o$ (8.1 mM) increased force (+195%) and decreased a^i_{Na}, (−20.3%). Adding caffeine re-increased a^i_{Na} (+28.1%), but immediately decreased force (−32.3%).

7 Addition of pyruvate (10 mM) to caffeine increased force, as it does in the presence of Ca overload.

8 Noradrenaline (0.1–1 μM) decreased a^i_{Na} and increased contractile force. In its presence, caffeine *de*creased a^i_{Na} further and *in*creased force.

9 It is concluded that caffeine increases a^i_{Na}, even during the negative inotropic effect. The decrease in force appears to depend on Ca load. Thus, caffeine no longer decreases force under conditions that decrease Ca load (Mn, high $[K]_o$, TTX) and immediately decreases force when the Ca load is increased (high $[Ca]_o$). However, in the presence of noradrenaline, caffeine *de*creases a^i_{Na} and markedly *in*creases force, as the Ca load is increased, but Ca can be removed from the cytoplasm into the SR.

Keywords: Purkinje fibres; contractile force; caffeine; manganese; cadmium; tetrodotoxin; high potassium; high calcium; calcium overload; pyruvate; noradrenaline

Introduction

In suitable concentrations, caffeine causes or facilitates calcium release from the sarcoplasmic reticulum (SR) and hinders Ca uptake into the SR (Weber & Hertz, 1968). The release of Ca by caffeine is amplified by calcium-induced release of calcium (O'Neill & Eisner, 1990). Caffeine increases the slow inward current I_{Ca} (Kimoto *et al.*, 1974; Goto *et al.*, 1979; Yatani *et al.*, 1984) and the uptake of ^{45}Ca (Shine & Langer, 1971) in cardiac tissues. Furthermore, caffeine decreases the loss of ^{45}Ca from the myocardium (Shine & Langer, 1971) and slows the decrease of force in Ca-free solution (Di Gennaro & Vassalle, 1984). Caffeine decreases ATP-dependent Ca accumulation and Ca-stimulated ATPase activity in sarcolemmal vesicles, suggesting a diminished extrusion of Ca from the cell by that mechanism (Gupta *et al.*, 1990). Caffeine (1–20 mM) induces incomplete relaxation and contracture of myocardial tissues (e.g., Shine & Langer, 1971; Hilgemann *et al.*, 1989; Gupta *et al.*, 1990; MacIntosh *et al.*, 1992).

Indeed, caffeine (5–10 mM) rapidly increases cytoplasmic calcium ($[Ca]_i$), which then declines (O'Neill & Eisner, 1990). The decline might be due to Ca extrusion via Na/Ca exchange and therefore it may be associated with an increase in intracellular sodium activity (a^i_{Na}). In fact, in cardiac fibres, a caffeine bolus induces a Na-dependent transient inward current (Clusin *et al.*, 1983). This inward current is initiated by an increase in $[Ca]_i$, is carried by Na via the electrogenic Na/Ca exchange (Lipp & Pott, 1988; Callewaert *et al.*, 1989) and does not relax completely (Lipp & Pott, 1988). However, the expectation that a continuous exposure to caffeine increases a^i_{Na} is made uncertain by reports that caffeine inhibits I_{Na} (Habuchi *et al.*, 1991) and that *low* concentrations of caffeine (1 mM or less) may stimulate the sarcolemma Na^+-K^+ ATPase (Gupta *et al.*, 1990).

Caffeine also modifies contractile force in a complex manner. In cardiac tissues, caffeine increases and then decreases force (e.g., Shine & Langer, 1971; Vassalle & Lin, 1979; Lin & Vassalle, 1983; Konishi *et al.*, 1984). In Purkinje fibres, the decrease in force is enhanced by an increase in Ca load (e.g., Vassalle & Lin, 1979; Bhattacharyya & Vassalle, 1981; Lin & Vassalle, 1983; Di Gennaro & Vassalle, 1985; Satoh & Vassalle, 1985). In skinned Purkinje fibres, an increase in cytoplasmic Ca beyond an optimal value reduces force (Fabiato, 1985a,b). Alternatively, caffeine could decrease force in Purkinje fibres by depleting SR Ca, as it does in other tissues (see O'Neill & Eisner, 1990).

The general aim of the present experiments was to study in cardiac Purkinje fibres the hypotheses that caffeine increases a^i_{Na} and that the increase in a^i_{Na} may or may not be associated with a negative inotropic action depending on the Ca load. To test these hypotheses, the effects of caffeine on a^i_{Na} and force were studied under conditions that either decrease or increase Ca load. Under conditions that decrease Ca_i, the negative inotropy should be reduced if due to an

[1] Author for correspondence.

excessive Ca load, but it should be increased if due to a SR Ca depletion. The opposite should occur with a high Ca load.

Pyruvate decreases force under normal conditions, but increases it in the presence of Ca overload caused by cardiac steroids or high $[Ca]_o$ (Ishikawa & Vassalle, 1985). Therefore, in the presence of caffeine, pyruvate would be expected to increase force only if the Ca load is excessive. If the Ca in the cytoplasm is reduced by stimulating the Ca uptake into the SR, the negative inotropic effect of caffeine may be eliminated. For this reason, caffeine was tested in the presence of noradrenaline (NA) which increases I_{Ca}, but it also stimulates the Ca uptake into the SR through an adenosine 3':5'-cyclic monophosphate (cyclic AMP)-dependent mechanism (phosphorylation of phospholamban; see Tsien, 1977).

Methods

Sheep of either sex, weighing 14–65 kg (average value 36.8 ± 3.8 kg) were anesthetized with sodium pentobarbitone (30 mg kg^{-1}, i.v.). The heart was quickly excised through an intercostal incision. Free-running strands of Purkinje fibres were cut from the left ventricle and were perfused in a tissue bath with warm (37°C) oxygenated (97% O_2, 3% CO_2) Tyrode solution of the following composition (mM): NaCl 136.9, KCl 4, $NaHCO_3$ 11.9, NaH_2PO_4 0.45, $CaCl_2$ 2.7, $MgCl_2$ 1.05 and glucose 5.5. The concentrations of Ca and K were changed in some experiments, as will be specified.

The preparations were driven at 60 min^{-1} and the stimuli were delivered by a Grass stimulator (model S-4) through a Grass stimulus isolation unit (SIU 4678). One end of the Purkinje strand was immobilized by a stainless steel electrode, while the other end was tied by means of a short silk thread to a rigid rod attached to a force transducer (Grass FTO 3C).

Transmembrane potentials were measured with conventional microelectrodes filled with 3 M KCl and coupled to a WPI dual/differential electrometer (Model FD223). The action potentials and twitch curves were displayed on a Tektronix storage oscilloscope Model 5111 and were recorded on tape by means a Racal Recorder Store 4DS. Intracellular Na^+ activity (a^i_{Na}) was measured with Na^+ selective microelectrodes made with the neutral carrier ETH 227. Construction and calibration of the Na^+ selective microelectrodes were carried out as described (Lee, 1981; Lee & Dagostino, 1982; Dagostino & Lee, 1982; Lee & Vassalle, 1983; Vassalle & Lee, 1984). The signals from the Na^+ selective and conventional microelectrodes were filtered by means of identical low pass filters (with a fixed frequency of 0.24 Hz) (Lee & Dagostino, 1982). The filtered voltage from the conventional microelectrode was then electrically subtracted from the filtered voltage of the Na^+ selective microelectrode. This procedure allows the determination of a^i_{Na} in active fibres (Lee & Dagostino, 1982). Force and a^i_{Na} were recorded simultaneously and continuously at 0.05 mm s^{-1} by means of a Gould recorder (Model 2400S).

The driven fibres were allowed to equilibrate for 1 h before the experiments were initiated. Caffeine, manganese chloride and cadmium chloride were obtained from Sigma Chemical Co., tetrodotoxin from Sankyo (through Calbiochem) and noradrenaline (Levophed bitartrate) from Winthrop-Breon Laboratories. The results are expressed as mean values ± standard error (s.e.); n indicates the number of experiments in fibres obtained from different hearts. Analysis of variance (ANOVA) was performed for all data points and a Bonferroni's test was used to test significance of differences between multiple repeated observations on a single group for caffeine and high $[Ca]_o$ plus caffeine administrations. Student's paired t test was used for other comparisons and a $P<0.05$ was considered significant.

Results

Effects of caffeine on a^i_{Na} and force

In Figure 1, the traces at the top show that 8 mM caffeine monotonically increased a^i_{Na} and caused an initial increase, a subsequent decrease and a late slow re-increase of force. During cafffeine wash-out, there was a transient rebound increase in force, as typically seen during the removal of Ca overload (see Vassalle & Lin, 1979). Caffeine concentration of 1 and 4 mM induced qualitatively similar but quantitatively smaller changes in a^i_{Na} and force (not shown). In subsequent experiments, the caffeine concentration most often used was 8 mM. The effects of caffeine were fully reversible.

The average changes in force ($F = 5.8$, $P<0.0001$) and a^i_{Na} ($F = 71.3$, $P<0.0001$) in the graph of Figure 1 ($n = 12$) show that 8 mM caffeine initially increased force (+89.9%, $P<0.05$) and then, by the tenth minute of exposure, decreased force (−29.9%, $P<0.05$) and increased a^i_{Na} (+8.9%, $P<0.05$) with respect to Tyrode control. Later on, force re-increased while a^i_{Na} continued to increase, but along a steeper slope. The slope of the linear fit of the data increased from 0.0691 ($P<0.005$) during the first half to 0.0999 ($P<0.005$) during the second half of the caffeine exposure (+44.5%). At the end of 30 min exposure, force re-increased by +55.4% ($P<0.05$) with respect to the 10 min value (+8.9% with respect to Tyrode control); and a^i_{Na} increased to 10.52 mM (+30.6% with respect to Tyrode control, $P<0.05$). The dashed lines underline the faster rate of increase of a^i_{Na} and the re-increase in force.

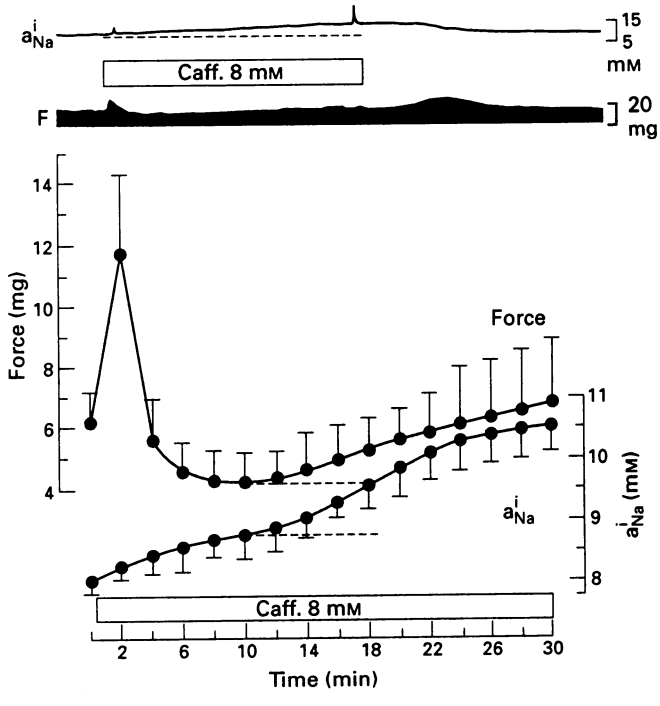

Figure 1 Effects of caffeine on a^i_{Na} and force. The traces at the top show the intracellular sodium activity (a^i_{Na}) and contractile force (F) recorded before, during and after exposure to 8 mM caffeine. The exposure to caffeine is indicated between the traces. The dashed line extrapolates the control value of a^i_{Na}. The graph shows the average changes induced by 8 mM caffeine on force and a^i_{Na}. The left ordinate scale shows contractile force in mg (upper curve labelled force) and the right ordinate scale a^i_{Na} in mM (lower curve labelled a^i_{Na}). The abscissa scale shows the time in min. In both curves, the first symbol is the control value, whereas the other points were obtained in the presence of caffeine, as indicated above the abscissa scale; s.e. mean are shown. The dashed lines extrapolate the values obtained at the tenth minute of exposure to caffeine.

Thus, caffeine monotonically increases a^i_{Na} while having a triphasic effect on force. Neither the initial increase nor the subsequent decrease in force are correlated with the increase in a^i_{Na}.

Effects of caffeine in the presence of slow channel block

The dependence of caffeine negative inotropy on the Ca load was studied by decreasing I_{Ca} by means of the slow channel blocker manganese (Mn). By decreasing $[Ca]_i$ (thereby increasing the Ca gradient across the sarcolemma), Mn would be expected to decrease a^i_{Na} through the Na/Ca exchange. Mn decreased a^i_{Na} by -5.4% ($n = 2$) and force by -49.3% ($n = 3$): adding caffeine increased a^i_{Na} by $+36.8\%$ and the steady-state force by 181.1% and did not have a negative inotropic effect. Thus in the presence of Mn (and of a diminshed Ca load), caffeine increased both a^i_{Na} and force.

Cadmium (Cd, 0.2 mM, $n = 5$) usually abolished force and therefore the effect of caffeine on that parameter could not be determined. Cd decreased a^i_{Na} from 8.37 ± 0.24 to 6.55 ± 0.68 mM (-21.7%, $P < 0.01$) and adding caffeine re-increased a^i_{Na} in 4 experiments (from 6.71 ± 0.87 to 7.34 ± 0.9 mM, $+9.3\%$, $P < 0.02$), while a^i_{Na} continued to decrease in 1 experiment. Thus, the decrease in I_{Ca} by Ca antagonists decreases both force and a^i_{Na}, as expected from a decrease in I_{Ca} and in $[Ca]_i$.

Effects of caffeine in the presence of high $[K]_o$ and tetrodotoxin

High $[K]_o$ decreases a^i_{Na} (see Lee & Vassalle, 1983): the increased Na gradient across the sarcolemma decreases $[Ca]_i$ via the Na/Ca exchange. In Table 1A, high $[K]_o$ decreased a^i_{Na} by -33.7% and caffeine re-increased it by $+24.6\%$. High $[K]_o$ abolished force in 7 experiments and reduced it in 3: in these 3 experiments, caffeine re-increased the steady-state force by $+84.6\%$ and did not have a negative inotropic effect.

Tetrodotoxin (TTX) lowers a^i_{Na} (see Vassalle & Lee, 1984) and therefore $[Ca]_i$: force decreases when a^i_{Na} decreases (Abete & Vassalle, 1987). In Table 1B, TTX decreased a^i_{Na} by -14.1% and force by -68.1%. Caffeine re-increased a^i_{Na} by $+14.4\%$ and force by $+57.1\%$, without inducing negative inotropy. Thus, when a^i_{Na} (and presumably $[Ca]_i$) was decreased by high $[K]_o$ or by TTX, caffeine increased both a^i_{Na} and force.

Table 1 A Effects of high $[K]_o$ on actions of caffeine in cardiac Purkinje fibres

	Tyr	*K* (10 mM)	*+Caff*
$n = 8$			
a^i_{Na} (mM)	8.08 ± 0.21	5.35 ± 0.31**	6.67 ± 0.32**
($n = 3$)			
force (mg)	7.41 ± 1.0	1.63 ± 1.3	3.01 ± 1.1*
$n = 7$			
a^i_{Na} (mM)	7.73 ± 0.15		9.90 ± 0.49**

B Effects of tetrodotoxin (TTX) on actions of caffeine in cardiac Purkinje fibres

	Tyr	*TTX*	*+Caff*
$n = 5$			
a^i_{Na} (mM)	8.61 ± 0.6	7.39 ± 0.44**	8.46 ± 0.77**
Force (mg)	4.4 ± 1.6	1.4 ± 0.4*	2.2 ± 0.7*
$n = 4$			
a^i_{Na} (mM)	7.89 ± 0.13		10.16 ± 0.65**

n, number of experiments. Tyr, K (10 mM), +Caff, results obtained in Tyrode solution, in the presence of 10 mM $[K]_o$ and in the presence of 10 mM $[K]_o$ plus 8 mM caffeine, respectively. a^i_{Na}, value of intracellular sodium activity in mM; force, contractile force in mg. Tyr, TTX, +Caff, results obtained in Tyrode solution, in the presence of 5 μM tetrodotoxin and in the presence of TTX plus 8 mM caffeine, respectively. *$P < 0.05$; **$P < 0.01$ or 0.005.

Effects of caffeine in the presence of high $[Ca]_o$

High $[Ca]_o$ also decreases a^i_{Na} (see Lee & Vassalle, 1983), but (in contrast to Mn, high $[K]_o$ and TTX) increases the Ca load by increasing I_{Ca}. If the negative inotropy of caffeine is related to an excessive Ca load, caffeine may increase a^i_{Na} as usual, but may decrease force from the beginning.

In Figure 2, the traces at the top show that 8.1 mM $[Ca]_o$ decreased a^i_{Na} (-8.0%) and increased force ($+280\%$). In the presence of high Ca_o, caffeine had an immediate negative inotropic effect (-61%) while increasing a^i_{Na} ($+19.7\%$), as in normal $[Ca]_o$. During caffeine wash-out, a^i_{Na} returned to the pre-caffeine value and force re-increased slowly. Reperfusion in Tyrode solution led to a re-increase in a^i_{Na} and a temporary decrease in force below control.

The average changes in force ($F = 4.51$, $P < 0.0001$) and in a^i_{Na} ($F = 7.77$, $P < 0.0001$) are shown in the graph of Figure 2 ($n = 4$). A $[Ca]_o$ of 8.1 mM increased force to a peak ($+271.3\%$, $P < 0.05$) and then to a stable lower value ($+184.8\%$); and decreased a^i_{Na} (-20.3%, $P < 0.05$). In high $[Ca]_o$, caffeine did not transiently increase force and, instead, immediately decreased it (-18.9%). Caffeine then reincreased force by $+10.0\%$ with respect to the minimal value ($P > 0.05$) and a^i_{Na} ($+25.4\%$, $P < 0.05$).

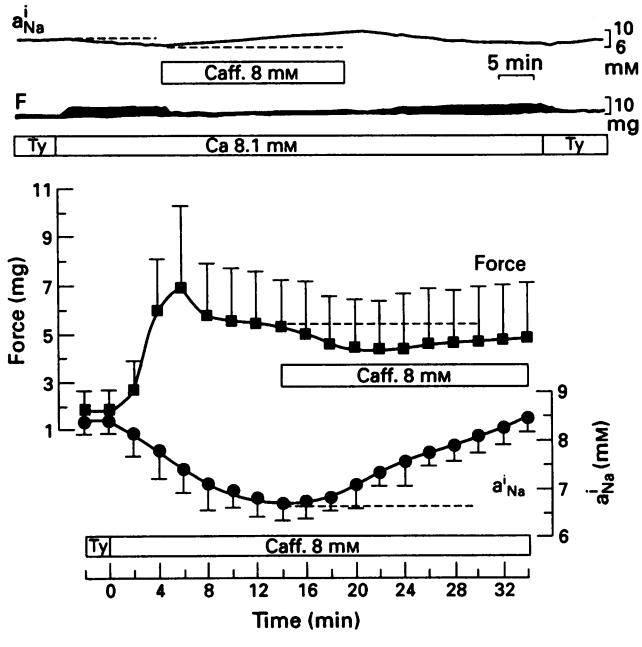

Figure 2 Actions of caffeine on force and a^i_{Na} in the presence of high $[Ca]_o$. The explanation of the traces is the same as in the legend of Figure 1. As indicated below the force trace, the fibre was perfused in Tyrode solution (Ty, beginning and end of the trace) and in high $[Ca]_o$ (Ca 8.1 mM). Caffeine (Caff, 8 mM) was administered as indicated below the a^i_{Na} trace. The dashed lines extrapolate the value of a^i_{Na} in Tyrode solution and in high $[Ca]_o$. The graph shows the average changes in force and a^i_{Na} in the presence of high $[Ca]_o$ and caffeine. The left ordinate scale is for force in mg (upper curve labelled Force) and the left ordinate scale is for a^i_{Na} in mM (lower curve labelled a^i_{Na}). The abscissa scale shows the time in min. The first two values in the graph are the control values (Ty) in Tyrode solution and the subsequent values show the changes in force and a^i_{Na} caused by high $[Ca]_o$ (Ca 8.1 mM, as indicated above the abscissa scale) and by caffeine (Caff, 8 mM, as indicated below the force curve). The dashed lines extrapolate force and a^i_{Na} in high $[Ca]_o$.

Relation between force and a^i_{Na} in normal and high $[Ca]_o$

To determine if the increase in a^i_{Na} and the late re-increase in force during caffeine exposure are correlated, the two variables recorded in normal and high $[Ca]_o$ were plotted on logarithmic scales and the data fitted with regression lines calculated by means of a third order equation.

The caffeine-induced changes in force and in a^i_{Na} were closely correlated both in normal $[Ca]_o$ (Figure 3a, $r = 0.99$) and in high $[Ca]_o$ (Figure 3b, $r = 0.98$). The slope of the relation was much steeper in normal than in high $[Ca]_o$, as force increased as a function of $(a^i_{Na})^{2.2}$ in normal and $(a^i_{Na})^{0.6}$ in high $[Ca]_o$. Thus, a similar increase in a^i_{Na} is associated with a smaller increase in force in high $[Ca]_o$. Even in normal $[Ca]_o$, the re-increase in force in the presence of caffeine is a smaller power function of a^i_{Na} than in other positive inotropic interventions (exponents of 5–6, see Abete & Vassalle, 1987).

The changes in a^i_{Na} with the different procedures carried out

The absolute increase in a^i_{Na} at the end of caffeine exposure was quite different in the different procedures carried out with respect to Tyrode solution (Figure 4). In Tyrode solution, 8 mM caffeine increased a^i_{Na} by approximately the same amount in different controls, from a combined control value of 7.88 ± 0.08 mM (Ty) to a combined value of 10.17 ± 0.17 mM (Caff). The various experimental procedures (TTX, High Ca, Cd, High K) decreased a^i_{Na} from a combined control value of 8.44 ± 0.21 mM (Ty) to a combined value of 6.65 ± 0.52 mM (Exp). Caffeine re-increased a^i_{Na} to a combined value of 7.9 ± 0.58 mM (+Caff).

Thus, in the different procedures, caffeine increased a^i_{Na} but less than in control (−35.3%), and to an absolute value lower than even the control value in Tyrode solution (except for high $[Ca]_o$). The smallest increase in a^i_{Na} occurred in the Cd solution and the largest in the high Ca solution.

Actions of pyruvate in the absence and presence of caffeine

Pyruvate decreases force in normal conditions, but increases it in the presence of Ca overload caused by strophanthidin or high $[Ca]_o$ (Ishikawa & Vassalle, 1985). In 3 tests in 2 experiments, pyruvate (10 mM) decreased contractile force by

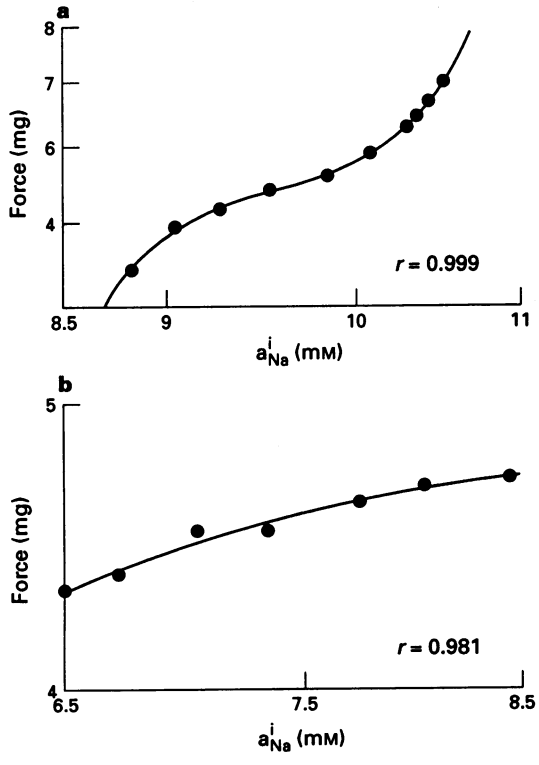

Figure 3 Relations between the slow re-increase in force and in a^i_{Na} in normal and high $[Ca]_o$. The relation between force and a^i_{Na} is shown on logarithmic scales with the data fitted by third order equation in normal $[Ca]_o$ (a) and in high $[Ca]_o$ (b). The ordinates show the scales for force in mg and the abscissae those for a^i_{Na} in mM. r is the correlation coefficient.

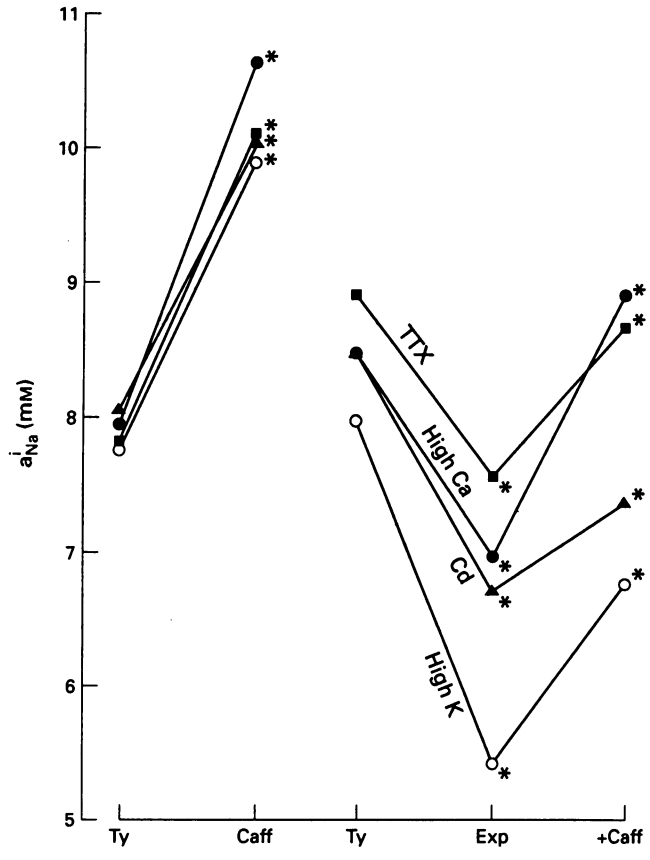

Figure 4 Effects of caffeine on a^i_{Na} in the absence and in the presence of procedures that lower a^i_{Na}. The ordinate scale is for a^i_{Na} in mM. As indicated on the abscissa scale the results were obtained in Tyrode solution (Ty), in the presence of caffeine (Caff), in the various experimental solutions indicated next to the traces (Exp) and in those solutions plus caffeine (+Caff). The following symbols identify the various solutions and their respective control curves: (■) TTX; (●) high Ca; (▲) Cd; and (○) high K. The asterisks indicate statistical difference ($P < 0.05$) with respect to the preceding value.

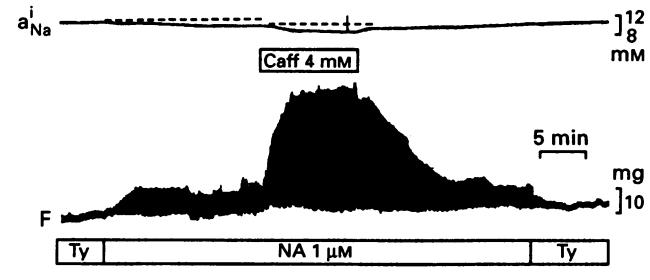

Figure 5 Caffeine decreases a^i_{Na} and increases force in the presence of noradrenaline. Noradrenaline (NA, 1 μM) was administered as indicated below the force trace and caffeine (Caff, 4 mM) as indicated below the a^i_{Na} trace. The dashed lines extrapolate the value of a^i_{Na} in Tyrode solution (Ty) and in the presence of NA.

−44% in Tyrode solution and increased it by +157.7% ($P<0.05$) in the presence of 8 mM caffeine.

Actions of caffeine in the presence of noradrenaline

Noradrenaline (NA) decreases a^i_{Na} (see Lee & Vassalle, 1983) and enhances Ca uptake into the SR by increasing cyclic AMP (see Tsien, 1977). Caffeine enhances the actions of NA by further increasing cyclic AMP through the inhibition of phosphodiesterase (Robison *et al.*, 1971). Therefore, caffeine might increase the NA-stimulated uptake of Ca into the SR and reduce the Ca load of the cytoplasm. As a result, in the presence of NA, caffeine might decrease a^i_{Na} and increase force.

In Figure 5, noradrenaline increased force (+316.6%) and progressively decreased a^i_{Na} (−8.33%). When caffeine was added, force markedly increased (+406.6% with respect to the value in NA) and remained increased as long as caffeine was perfused. At the same time, a^i_{Na} declined further (−10.1% with respect to the value in NA). In 4 experiments, noradrenaline (0.1–1 μM) decreased a^i_{Na} (−0.41 ± 0.23 mM, −4.6%) and caffeine induced a further decrease (−1.30 ± 0.93 mM, −20.1%, $P<0.02$). In 7 experiments, NA increased force (+83.9 ± 43.1%, $P<0.05$) and caffeine (4–8 mM) caused a further increase (+122.2 ± 63.6% with respect to the values in NA, $P<0.05$).

The opposite effects of caffeine on force and a^i_{Na} in the absence and presence of NA indicates that caffeine enhances the direct effect of NA on force and a^i_{Na}.

Discussion

The increase in a^i_{Na} by caffeine

Caffeine could directly increase a^i_{Na}, either by increasing Na influx or by decreasing Na extrusion. As for the increase in Na influx, caffeine decreases I_{Na} (Habuchi *et al.*, 1991). Na extrusion would be decreased if 8 mM caffeine inhibits the Na^+-K^+ ATPase (Gupta *et al.*, 1990). The inhibition of the Na-K pump would cause a *primary* increase in a^i_{Na}, which would have led to a parallel increase in force, as it happens with cardiac steroids (e.g., Lee & Dagostino, 1982).

Still, it could be proposed that the negative inotropic effects result from a simultaneous depletion of SR Ca. However, the abolition of the negative inotropy by decreasing the Ca load and its enhancement by increasing the Ca load would imply that a decreased Ca_i prevents the depletion of SR Ca by caffeine and an increased Ca_i enhances it. No evidence is available to support this possibility. Also, a decrease in Ca_i (due to SR depletion and Ca extrusion) would have decreased a^i_{Na} (which, instead, increased).

A low caffeine concentration (1 mM) also increased a^i_{Na}, although 1 mM caffeine stimulates the sarcolemma Na^+-K^+ ATPase (Gupta *et al.*, 1990). And 8 mM caffeine increased a^i_{Na} even in 10 mM $[K]_o$, which stimulates maximally the Na-K pump activity. These results do not rule out an inhibition of the Na-K pump by high concentrations of caffeine, but suggest that the increase in a^i_{Na} involves other mechanisms.

Another possibility for the increase in a^i_{Na} by caffeine is related to the fact that caffeine increases cellular Ca by several mechanisms (see the Introduction). The consequent extrusion of Ca via the Na/Ca exchange would induce a *secondary* increase in a^i_{Na}. Since the Na/Ca exchange reacts quickly to an increase in $[Ca]_i$, the increase in a^i_{Na} over 30 min of exposure to caffeine suggests that $[Ca]_i$ would increase during this period of time and that the Na/Ca exchange responds to the increase. A continuous increase in Ca extrusion by the Na/Ca exchange is consistent with the fact that in the presence of caffeine the inward tail current that follows depolarizing voltage clamp steps increases in size as a function of caffeine exposure (Vassalle & Di Gennaro, 1984). This current is increased by high $[Ca]_o$ and repetitive activations, and is decreased by low $[Ca]_o$ (Vassalle & Di Gennaro, 1984) and by Na/Ca exchange blocker nickel (Liu & Vassalle, 1993), consistently with an electrogenic extrusion of Ca by the Na/Ca exchanger. As already mentioned, a bolus administration of caffeine induces a large Na-dependent inward transient (Clusin *et al.*, 1983) which is initiated by an increase in $[Ca]_i$ and is due to Na entry via the electrogenic Na/Ca exchange (Lipp & Pott, 1988; Callewaert *et al.*, 1989).

The caffeine-induced increase in a^i_{Na} in the presence of a marked decrease or abolition of force by Cd might be taken to indicate that caffeine does not increase a^i_{Na} by increasing Ca_i. However, the absence of a discernible contraction does not mean that I_{Ca} was reduced to zero or that caffeine could not increase it. I_{Ca} was certainly reduced and indeed the percentage increase in a^i_{Na} by caffeine in the presence of Cd was far smaller than in Tyrode solution (−69.6%) (Figure 4).

The changes in contractile force induced by caffeine and a^i_{Na}

As shown here, in sheep Purkinje fibres, caffeine continuously increased a^i_{Na} while inducing a triphasic change in force similar to that reported in the ventricular myocardium (e.g., Shine & Langer, 1971; Konishi *et al.*, 1984; Di Gennaro & Vassalle, 1984).

The initial increase in force The initial increase in force is unrelated to the far more gradual increase in a^i_{Na}, and it is likely to result from the caffeine-induced release of Ca from the SR (see O'Neill & Eisner, 1990) and an increase in I_{Ca} (Kimoto *et al.*, 1974; Goto *et al.*, 1979; Yatani *et al.*, 1984). Thus, the initial increase in force is dependent on $[Ca]_o$ and is attenuated by Mn and verapamil (Di Gennaro & Vassalle, 1984; Gupta *et al.*, 1990). It may be facilitated by the positive feedback of elevated Ca_i on Ca-induced calcium release from the SR (O'Neill & Eisner, 1990).

The subsequent negative inotropy An increase in cytoplasmic Ca beyond an optimal value results in a smaller contraction (Fabiato, 1985b). If caffeine increases Ca_i beyond an optimal value, this would account for the dependence of the negative inotropic action of caffeine on the Ca load.

Caffeine immediately decreases force (no initial increase) under conditions (high $[Ca]_o$, strophanthidin, low $[Na]_o$, amiloride, etc.) that increase $[Ca]_i$ (Vassalle & Lin, 1979; Bhattacharyya & Vassalle, 1981; Lin & Vassalle, 1983; Satoh & Vassalle, 1985; Gupta *et al.*, 1990). And the negative inotropic effect of caffeine is reduced or abolished under conditions that decrease Ca_i, such as low $[Ca]_o$, local anaesthetics, high $[K]_o$, Mn or verapamil (Bhattacharyya & Vassalle, 1981; Lin & Vassalle, 1983; Di Gennaro & Vassalle, 1984; Satoh & Vassalle, 1985; 1989; Gupta *et al.*, 1990). A brief exposure to zero $[Ca]_o$ decreases force in control conditions, but increases it in the presence of caffeine and even more in the presence of caffeine plus high $[Ca]_o$ (Satoh & Vassalle, 1985). Also, the rebound increase in force during the caffeine wash-out (see Figure 1) is consistent with the removal of Ca overload at the time when a^i_{Na} is still higher than normal.

The present experiments demonstrate that caffeine increases a^i_{Na} also during procedures that decrease a^i_{Na} (Mn, TTX, high $[K]_o$ or high $[Ca]_o$). However, caffeine increases force only during the procedures that decrease $[Ca]_i$ directly (Mn) or indirectly (by lowering a^i_{Na} prior to caffeine, i.e., TTX and high $[K]_o$). In high $[Ca]_o$, the immediate decrease in force by caffeine appears to be related to the enhancement of the Ca load induced by high $[Ca]_o$, in spite of the initially lower a^i_{Na}.

The actions of caffeine may show species-dependence. Thus, in rat ventricular myocytes, even low concentrations of

caffeine cause depletion of SR-Ca due to facilitated release. As a consequence, force transiently decreases during the caffeine wash-out, as less Ca is released on excitation (O'Neill & Eisner, 1990). In contrast, in Purkinje fibres low concentrations of caffeine decrease force and induce oscillatory potentials (Paspa & Vassalle, 1984), a sign of Ca overload. And a decrease in Ca_i consequent to a Ca depletion of the SR *per se* would decrease a^i_{Na}. Low concentrations of caffeine increase the Ca transient during the negative inotropy (Konishi *et al.*, 1984).

The slow re-increase in force during caffeine administration
The explanation for the slow re-increase in force during caffeine exposure is uncertain. It could result from a combination of different caffeine actions such as: sensitization of contractile proteins; increased duration of the Ca transient allowing fuller activation of contractile proteins (see Konishi *et al.*, 1984); slower reuptake of Ca in the SR, as suggested by the slower relaxation of the twitch (e.g., Shine & Langer, 1971); and the rise in a^i_{Na}, which will further slow the rate of recovery of the Ca transient as the reduced Na gradient across the sarcolemma decreases the driving force for the Na/Ca exchange. A role for a^i_{Na} is suggested by the close correlation between the increase in a^i_{Na} and that in force (Figure 3).

The reversal of the negative inotropic effect of pyruvate

Ca uptake in the mitochondria occurs at the expense of oxidative phosphorylation (see Chance, 1965). Therefore, a decreased availability of high energy phosphates might contribute to the decrease in force caused by an increased Ca_i. Providing another substrate (in addition to glucose) in fibres perfused *in vitro* might result in an increased availability of high energy phosphates which improve force development. Whether this is indeed so remains to be seen, but it is established that pyruvate increases force in Purkinje fibres subjected to Ca overload, however induced (strophanthidin or high $[Ca]_o$; Ishikawa & Vassalle, 1985). Thus, the fact that pyruvate also increases force in the presence of caffeine is consistent with the concept that caffeine may increase a^i_{Na} and decrease force by increasing Ca_i.

The interactions between noradrenaline and caffeine

Calcium uptake in the SR is stimulated by cytoplasmic Ca and by cyclic AMP (see Tsien, 1977). The reversal of caffeine effects on force and a^i_{Na} in the presence of NA suggest that the actions of NA prevail because they are potentiated by caffeine through the inhibition of phosphodiesterase (see Robison *et al.*, 1971). It might be speculated that the effect of phosphodiesterase inhibition becomes more apparent when NA increases cyclic AMP, so that caffeine further enhances this effect (see Robison *et al.*, 1971). An increase in cyclic AMP leads to the phosphorylation of phospholamban and to the stimulation of Ca uptake into the SR (see Tsien, 1977). This cyclic AMP-dependent stimulation of Ca uptake may bypass the inhibition by caffeine of the Ca-dependent Ca uptake into the SR. As a result, Ca decreases in the cytoplasm and increases in the SR: as a consequence, a^i_{Na} would decrease and force increase.

Conclusions

A major finding of the present experiments is that in sheep Purkinje fibres caffeine monotonically increases a^i_{Na} during its triphasic effect on contractile force. Caffeine increases a^i_{Na} under different conditions of Ca load. However, caffeine no longer has a negative inotropic effect when Ca_i has been previously decreased (Mn, TTX and high $[K]_o$) and has an immediate negative inotropic effect when Ca_i has been previously increased (high $[Ca]_o$). Pyruvate increases force in the presence of caffeine, as it does when Ca overload is present. In the presence of NA, the actions of caffeine are reversed in that caffeine *de*creases a^i_{Na} and *in*creases force. These findings show that in different conditions caffeine generally increases a^i_{Na} while its negative inotropic effect appears to depend on Ca load.

This work was supported by N.I.H. grant HL 27038. We thank Mr Ping Li for helping with the statistical analysis.

References

ABETE, P. & VASSALLE, M. (1987). Strophanthidin and force regulation by intracellular sodium activity in cardiac Purkinje fibers. *Eur. J. Pharmacol.*, **141**, 51–65.

BHATTACHARYYA, M.L. & VASSALLE, M. (1981). The effect of local anaesthetics on strophanthidin toxicity in canine cardiac Purkinje fibres. *J. Physiol.*, **312**, 125–142.

CALLEWAERT, G., CLEEMAN, L. & MORAD, M. (1989). Caffeine-induced Ca^{2+} release activates Ca^{2+} extrusion via Na^+-Ca^{2+} exchanger in cardiac myocytes. *Am. J. Physiol.*, **257**, C147–C152.

CHANCE, B. (1965). The energy-linked reaction of calcium with mitochondria. *J. Biol. Chem.*, **240**, 2729–2748.

CLUSIN, W.T., FISCHMEISTER, R. & DEHAAN, R.L. (1983). Caffeine-induced current in embryonic heart cells: time course and voltage dependence. *Am. J. Physiol.*, **245**, H528–H532.

DAGOSTINO, M. & LEE, C.O. (1982). Neutral carrier Na^+- and Ca^{2+}-selective microelectrodes for intracellular application. *Biophys. J.*, **40**, 199–207.

DI GENNARO, M. & VASSALLE, M. (1984). Role of calcium on the actions of caffeine in ventricular muscle fibers. *J. Cardiovasc. Pharmacol.*, **6**, 739–747.

DI GENNARO, M. & VASSALLE, M. (1985). Relationship between caffeine effects and calcium in canine cardiac Purkinje fibers. *Am. J. Physiol.*, **248**, H520–H533.

FABIATO, A. (1985a). Rapid ionic modifications during the aequorin-detected calcium transient in a skinned canine cardiac Purkinje cell. *J. Gen. Physiol.*, **85**, 189–246.

FABIATO, A. (1985b). Time and calcium dependence of activation and inactivation of calcium-induced release of calcium from the sarcoplasmic reticulum of a skinned canine cardiac Purkinje cell. *J. Gen. Physiol.*, **85**, 247–289.

GOTO, M., YATANI, A. & EHARA, T. (1979). Interaction between caffeine and adenosine on the membrane current and tension component in the bullfrog atrial muscle. *Jpn. J. Physiol.*, **29**, 393–409.

GUPTA, M.P., MAKINO, N., TAKEO, S., KANEKO, M. & DHALLA, N.S. (1990). Cardiac sarcolemma as a possible site of action of caffeine in rat heart. *J. Pharmacol. Exp. Ther.*, **255**, 1188–1194.

HABUCHI, Y., TANAKA, H., FURUKAWA, T. & TSUJIMURA, Y. (1991). Caffeine-induced block of the Na^+ current in guinea pig single ventricular cells. *Am. J. Physiol.*, **261**, H1855–H1863.

HILGEMANN, D.W., ROOS, K.P. & BRADY, A.J. (1989). Slowly relaxing caffeine responses in rat ventricle: relationship of ryanodine and caffeine actions. *Am. J. Physiol.*, **256**, H1100–H1119.

ISHIKAWA, S. & VASSALLE, M. (1985). Reversal of strophanthidin negative inotropy by metabolic substrates in cardiac Purkinje fibers. *Cardiovasc. Res.*, **9**, 537–551.

KIMOTO, Y., SAITO, M. & GOTO, M. (1974). Effects of caffeine on the membrane potentials, membrane currents and contractility of Bullfrog atrium. *Jpn. J. Physiol.*, **24**, 531–542.

KONISHI, M., KURIHARA, S. & SAKAI, T. (1984). The effect of caffeine on tension development and intracellular calcium transients in rat ventricular muscle. *J. Physiol.*, **355**, 605–618.

LEE, C.O. (1981). Ionic activities in cardiac muscle cells and application of ion-selective microelectrodes. *Am. J. Physiol.*, **241**, H459–H478.

LEE, C.O. & DAGOSTINO, M. (1982). Effect of strophanthidin on intracellular Na ion activity and twitch tension of constantly driven canine cardiac Purkinje fibers. *Biophys. J.*, **40**, 185–198.

LEE, C.O. & VASSALLE, M. (1983). Modulation of intracellular Na^+ activity and cardiac force by norepinephrine and Ca^{2+}. *Am. J. Physiol.*, **244**, C110–C1114.

LIN, C.-I & VASSALLE, M. (1983). Role of calcium in the inotropic effects of caffeine in cardiac Purkinje fibers. *Int. J. Cardiol.*, **3**, 421–434.

LIPP, P. & POTT, L. (1988). Transient inward current in guinea-pig atria myocytes reflects a change in sodium-calcium exchange current. *J. Physiol.*, **397**, 601–630.

LIU, Q.-Y. & VASSALLE, M. (1993). Mechanisms of changes in action potential and currents induced by repetitive activity in isolated myocytes. *FASEB J.*, **7**, A96.

MACINTOSH, B.R., POSNER, P., LOBO, J. & HARMS, R. (1992). Rat atrial muscle response with caffeine: dose-response, force, frequency and postrest contractions. *Can. J. Physiol. Pharmacol.*, **70**, 275–282.

O'NEILL, S.C. & EISNER, D.A. (1990). A mechanism for the effects of caffeine on Ca^{2+} release during diastole and systole in isolated rat ventricular myocytes. *J. Physiol.*, **430**, 519–536.

PASPA, P. & VASSALLE, M. (1984). Mechanism of caffeine-induced arrhythmias in canine cardiac Purkinje fibers. *Am. J. Cardiol.*, **53**, 313–319.

ROBISON, G.A., BUTCHER, R.W. & SUTHERLAND, E.W. (1971). *Cyclic AMP*. New York: Academic Press.

SATOH, H. & VASSALLE, M. (1985). Reversal of caffeine-induced calcium overload in cardiac Purkinje fibers. *J. Pharmacol. Exp. Ther.*, **234**, 172–179.

SATOH, H. & VASSALLE, M. (1989). Role of calcium in caffeine-norepinephrine interactions in cardiac Purkinje fibers. *Am. J. Physiol.*, **257**, H226–H237.

SHINE, K.I. & LANGER, G.A (1971). Caffeine effects upon contraction and calcium exchange in rabbit myocardium. *J. Mol. Cell. Cardiol.*, **3**, 255–270.

TSIEN, R.W. (1977). Cyclic AMP and contractile activity in heart. In *Advances in Cyclic Nucleotide Research*, Vol. 8, ed. Greengard, P. & Robison, G.A. pp. 363–420. New York: Raven Press.

VASSALLE, M. & DI GENNARO, M. (1984). Caffeine actions on currents induced by calcium-overload in Purkinje fibers. *Eur. J. Pharmacol.*, **106**, 121–131.

VASSALLE, M. & LEE, C.O. (1984). The relationship among intracellular sodium activity, calcium, and strophanthidin inotropy in canine cardiac Purkinje fibers. *J. Gen. Physiol.*, **83**, 287–307.

VASSALLE, M. & LIN, C.-I (1979). Effect of calcium on strophanthidin-induced electrical and mechanical toxicity in cardiac Purkinje fibers. *Am. J. Physiol.*, **236**, H689–H697.

WEBER, A. & HERZ, R. (1968). The relationship between caffeine and contracture of intact muscle and the effect of caffeine on reticulum. *J. Gen. Physiol.*, **52**, 750–759.

YATANI, A., IMOTO, Y. & GOTO, M. (1984). The effects of caffeine on the electrical properties of isolated, single rat ventricular cells. *Jpn. J. Physiol.*, **34**, 337–349.

(Received June 28, 1993
Revised April 10, 1994
Accepted May 16, 1994)

Br. J. Pharmacol. (1994), **113**, 296–302

Inhibitory effects of capsaicin on acetylcholine-evoked responses in rat phaeochromocytoma cells

[1]Ken Nakazawa, Kaori Inoue, Schuichi Koizumi, Makoto Ikeda & Kazuhide Inoue

Division of Pharmacology, National Institute of Health Sciences, 1-18-1 Kamiyoga, Setagaya, Tokyo 158, Japan

1 The effects of capsaicin on cellular responses evoked by acetylcholine (ACh) and those by adenosine 5'-triphosphate (ATP) were investigated in rat phaeochromocytoma PC12 cells.

2 Capsaicin (1 to 30 μM) suppressed dopamine release and the intracellular Ca^{2+} increase evoked by 100 μM ACh. The concentration-dependence of the ACh-evoked release of dopamine was not shifted but the maximal response was reduced by capsaicin. Dopamine release evoked by 80 mM KCl was also suppressed by capsaicin (3 and 30 μM), but the extent of suppression was smaller than that of the ACh-evoked release.

3 Under whole-cell voltage-clamp, capsaicin (1 to 30 μM) reversibly inhibited the inward current activated by ACh (30 to 300 μM). The inhibition exhibited dependence on the concentration of ACh, and the current activated by a higher concentration of ACh was less inhibited. Voltage-dependence of block by capsaicin was not observed when it was tested either by applying a ramp pulse during the current activation by ACh or by eliciting the current in cells held at various potentials.

4 High concentrations of capsaicin (30 to 100 μM) enhanced the inward current as well as dopamine release evoked by 30 μM ATP.

5 The results suggest that low concentrations of capsaicin selectively antagonize responses mediated by nicotinic receptor-channels without affecting those mediated by purinoceptor-coupled channels. As the antagonism by capsaicin of the ACh-evoked responses was observed at concentrations as low as 1 μM, the influence on nicotinic receptors should be taken into account when this compound is used as a pharmacological tool to deplete neuropeptides.

Keywords: Capsaicin; acetylcholine; nicotinic receptor-channels; extracellular ATP; rat phaeochromocytoma cells; dopamine release; intracellular Ca^{2+} concentration; voltage clamp

Introduction

Capsaicin has been shown to excite a subpopulation of primary afferent sensory neurones (Bevan & Szolcsanyi, 1990). As this neurone population has characteristics in common with neurones that mediate inflammatory responses, the excitation is believed to be responsible for the chemical irritation observed with this compound (Bevan & Szolcsanyi, 1990). Capsaicin has also been shown to block neurotransmission not mediated by adrenoceptors or acetylcholine receptors in various tissues. This block of 'non-adrenergic non-cholinergic' transmission is considered to be due to neuronal excitation and subsequent depletion of neuropeptides such as substance P (Szolcsanyi & Bartho, 1978; Ellis & Burnstock, 1989) or calcitonin gene-related peptide (CGRP; Franco-Cereceda & Lundberg, 1985; Saito *et al.*, 1987), which exist, presumably, in sensory neurones.

Effects of capsaicin on ion channels have been reported. Capsaicin evoked an inward current through non-selective cation channels in rat vagal (Marsh *et al.*, 1987) or dorsal root ganglion neurones (Docherty *et al.*, 1991), monkey trigeminal ganglion neurones (Ingram *et al.*, 1993), and a rat dorsal ganglion cell line, F-11 cells (Kusano & Gainer, 1993). In contrast, no such inward current was evoked by capsaicin in guinea-pig or chick dorsal root ganglion neurones (Petersen *et al.*, 1987). Capsaicin also affects voltage-gated channels. For Ca^{2+} channels, inhibition was observed in rat dorsal root ganglion neurones (Docherty *et al.*, 1991) whereas both inhibition and potentiation were observed in guinea-pig dorsal root ganglia (Petersen *et al.*, 1989) and F-11 cells (Kusano & Gainer, 1993). Inhibition of Na^+ and K^+ channels were also reported in guinea-pig dorsal root ganglion cells (Petersen *et al.*, 1987). In contrast to the results observed on voltage-gated channels, effects of capsaicin on ligand-gated channels have not been reported.

The present study was aimed at examining the effects of capsaicin on responses mediated through two types of ligand-gated channels: nicotinic receptor channels and ATP-activated channels in PC12 cells. The PC12 cell line was derived from a rat phaeochromocytoma (Greene & Tischler, 1976) and has been widely used to investigate mechanisms underlying catecholamine release and properties of ion channels. We found that capsaicin inhibited ACh-evoked responses at concentrations as low as 1 μM and that it facilitated ATP-evoked responses at higher concentration.

[1] Author for correspondence.

Methods

Cell culture

PC12 (passage 55 to 65) were cultured as previously described (Inoue & Kenimer, 1988; Inoue *et al.*, 1989). Cells cultured in 35 mm-polystyrene dishes for 1 to 3 days were used for experiments.

Dopamine release

Dopamine release was measured by a procedure described previously by Ohara-Imaizumi *et al.* (1991). In brief, the dishes were preincubated with 1 ml of balanced salt solution (BSS) containing (in mM): NaCl 150, KCl 5, $CaCl_2$ 1.8, $MgCl_2$ 1.2, NaH_2PO_4 1.2, D-glucose 10, ethylenediaminetetraacetic acid (EDTA) 0.1, N-2-hydroxyethylpiperazine-N'-2-ethanesulphonic acid (HEPES) 25 (pH was adjusted to 7.4 with NaOH) for 1 h. The preincubation solution was removed and 1 ml BSS was added. After 1 min, the BSS was aspirated and the cells were stimulated for 1 min by ACh or ATP at indicated concentrations in BSS or by 80 mM KCl with or without capsaicin. The solution containing 80 mM KCl was prepared by replacing equimolar NaCl in the BSS. When the effect of capsaicin was examined, an additional

1 min-treatment with the BSS and stimulation were carried out in the presence of this compound. At the end of the incubation, the incubation solution was transferred to test tubes containing 0.25 ml of 1 M $HClO_4$. The dopamine remaining in the cells was extracted by sonication with 0.2 M $HClO_4$. After centrifugation (at 5°C for 2 min, 1000 *g*), supernatants of both the incubation solution and the sonicated cellular solution were collected for measurement of dopamine content. Dopamine content was determined with a high-performance liquid chromatography-electrochemical detector (h.p.l.c.–e.c.d.) system (Bioanalytical Systems). Percentage of release was calculated using the values obtained for the dopamine content in the incubation solution and the content remaining in the cells. All procedures except centrifugation were performed at room temperature (about 25°C).

Intracellular Ca^{2+} concentration

Intracellular Ca^{2+} levels were measured from individual cells using fura-2 (Grynkiewicz *et al.*, 1985) under the conditions described by Ohara-Imaizumi *et al.* (1991) and Nakazawa & Inoue (1992). Cells loaded with fura-2/AM were placed on an inverted microscope (Olympus IMT-2) equipped with a xenon lamp and band pass filters. Fluorescent intensities were recorded by a silicon intensifier target camera (C-2741-08, Hamamatsu Photonics). The intracellular Ca^{2+} concentration was calculated from the ratio of fluorescence intensity measured at wave lengths of 340 and 360 nm (F340 and F360). Drugs were applied by superfusion.

Membrane current measurements

Current recordings were obtained by conventional whole-cell voltage-clamp method (Hamill *et al.*, 1981) under the conditions described elsewhere (Nakazawa *et al.*, 1990). The cells were bathed in an extracellular solution containing (in mM): NaCl 140, KCl 5.4, $CaCl_2$ 1.8, $MgCl_2$ 1.0, HEPES 10, D-glucose 11.1 (pH was adjusted to 7.4 with NaOH). Tip resistances of fire-polished patch pipettes ranged between 3 to 5 MΩ when the pipettes were filled with an intracellular solution containing (in mM): CsCl 150, HEPES 10, ethyleneglycos-*bis*(2-aminoethlether)-*N*,*N*,*N*′,*N*′-tetraacetic acid (EGTA) 5, (pH 7.3 with CsOH). Application of ACh or ATP was made from an emitting tube (2 mm in inner diameter). Cells located near the mouth of the emitting tube (about 1 mm in distance) were selected for recordings, and the ACh- or ATP-containing extracellular solution was applied rapidly (ca. 0.4 ml s^{-1}). To avoid significant desensitization of the nicotinic receptor-channels, the period of each ACh-application was brief (4 to 5 s), and each application was separated by 1 min. Before examining the effects of capsaicin, ACh was applied two or three times and the stability of the response to ACh was confirmed in individual cells. Experiments were performed at room temperature (about 25°C). Data were filtered at 1 kHz and stored on magnetic tape for later analysis.

Statistical analysis

Statistical analysis was made by Scheffe's test for multiple comparison. In the case of the comparison of the current responses obtained from the same cells, the data were analyzed by the paired *t* test. Significant differences are indicated with asterisks ($*P<0.05$, $**P<0.01$; two-tailed test) in figures.

Drugs

Drugs used were capsaicin, (Wako Pure Chemistry, Osaka, Japan), acetylcholine chloride (ACh; Wako), adenosine 5′-triphosphate disodium salt (ATP; Sigma St. Louis, MO, U.S.A.), resiniferatoxin (Wako), guanosine 5′-O(2-thiotriphosphate) trilithium salt (GDPβS; Sigma) and K-252a (8R*, 9S*, 11S*)-(−)-9-hydroxy-9-methoxycarbonyl-8-methyl-2,3,9,10-tetrahydro-8,11-epoxy-1H,8H, 11H-2,7b,11a-triazadibenzo(a,g)cycloocta (cde)trinden-1-one; Kyowa Hakko, Tokyo, Japan). Fura-2/AM was from Dojin (Kumamoto, Japan). Capsaicin was dissolved in ethanol and diluted in the extracellular media so that final concentration of ethanol was <2%. The dopamine release or the ACh-activated current in the present study was not affected by 2% ethanol. K-252a or resiniferatoxin was dissolved in dimethylsulphoxide (DMSO) and added to the intracellular or extracellular solution, respectively (the final concentration of DMSO was ⩽0.1%).

Results

Effects of capsaicin on dopamine release and increase in intracellular Ca^{2+} concentration

ACh (10 to 300 μM) evoked dopamine release from PC12 cells. The ACh-evoked release was regarded as a nicotinic response previously characterized in these cells (e.g., Greene & Rein, 1977) because our preliminary experiments showed that the release was inhibited by 70% by 100 μM hexamethonium and was almost abolished by 300 μM $CdCl_2$ which is a characteristic of nicotinic responses in these cells (Inoue & Kenimer, 1988; see also below). Capsaicin itself (1 to 30 μM) did not affect basal dopamine release, but inhibited the ACh-evoked dopamine release in a concentration-dependent manner (Figure 1a). The concentration-response curve for the ACh-evoked dopamine release was not shifted toward a higher concentration-range, but the maximal response was suppressed (Figure 1b), suggesting that the antagonism by capsaicin is non-competitive.

The influence of capsaicin on the ACh-induced increase in intracellular Ca^{2+} concentration was also tested. When repeated applications of 100 μM ACh were made to control cells, the response to the second application was not significantly different from that to the first response (paired *t* test, $P>0.05$; Figure 2a). In the presence of 3 or 30 μM capsaicin (Figure 2b), however, the response to the second application was less than the response to the first application, and the ratio of the second response to the first response (S_1/S_2) was significantly smaller than that under control conditions (Figure 2c). Thus, the inhibition by capsaicin of the dopamine release by ACh may have resulted from the attenuation of increase in intracellular Ca^{2+} concentration.

Voltage-gated Ca^{2+} channels secondarily activated by depolarization contribute to nicotinic responses in PC12 cells (Ritchie, 1979; Inoue & Kenimer, 1988). As for ACh-stimulated catecholamine release, Ca^{2+} channels play an obligatory role because the release was abolished by Ca^{2+} channel antagonists (Inoue & Kenimer, 1988). Thus, the inhibition by capsaicin of the ACh-evoked release may be due to its reported blockade of Ca^{2+} channels (Petersen *et al.*, 1989; Kusano & Gainer, 1993). We tested whether mechanisms mediated through Ca^{2+} channels are involved in the inhibition of the ACh-evoked responses by stimulating the cells with 80 mM KCl, which evokes dopamine release sensitive to Ca^{2+} channel antagonists (Ritchie, 1979; Nakazawa & Inoue, 1992). Although capsaicin (3 and 30 μM) suppressed the dopamine release evoked by 80 mM KCl (Figure 1c), the magnitude of inhibition was smaller than that of the ACh-evoked release (Figure 1a). For example, the ACh-evoked dopamine release was roughly halved by 3 μM capsaicin (Figure 1a) whereas the KCl-evoked dopamine release was reduced by only 17% by 3 μM capsaicin (Figure 1c). These results suggest that mechanisms involving voltage-gated Ca^{2+} channels do not play a major role in the inhibition of the ACh-evoked release.

Inhibition by capsaicin of ACh-activated current

ACh (30 to 300 μM) elicited a transient inward current in PC12 cells as was previously described (Ifune & Steinbach,

1990). Capsaicin (1 and 3 μM) suppressed this ACh-elicited current (Figure 3). The suppression was reversible, and the ACh-activated current almost fully recovered after a 1 min wash with drug-free solution (Figure 3a). The magnitude of inhibition of the ACh-evoked current (Figure 3b) was roughly the same as that of the inhibition of dopamine release (Figure 1a). A higher concentration (30 μM) of capsaicin abolished the current activated by 100 μM ACh ($n = 2$). Resiniferatoxin (10 nM to 1 μM), a plant product that has structural similarity to capsaicin and is about 10,000 times more potent in activation of the capsaicin-sensitive non-selective cation channels (Bevan & Szolcsanyi, 1990), did not suppress the ACh-activated current in five cells tested: for example, the current activated by 100 μM ACh in the

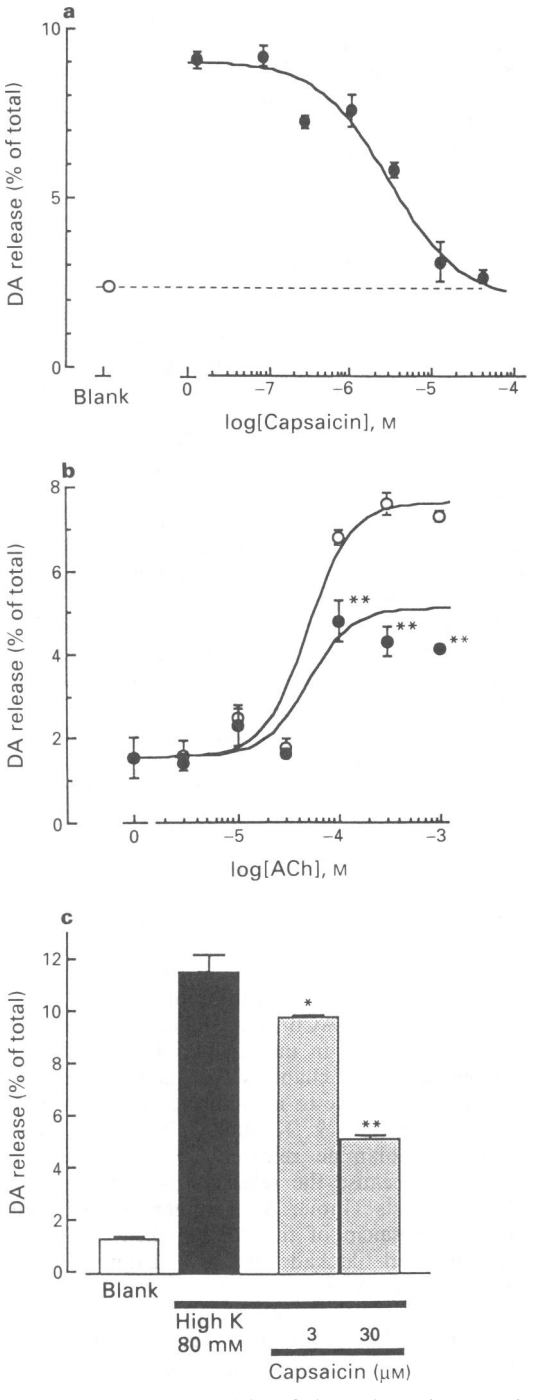

Figure 1 Inhibition by capsaicin of dopamine release evoked by acetylcholine (ACh) (a,b) or 80 mM KCl (c) from PC12 cells. The cells were pretreated with capsaicin 1 min before secretagogue applications. Each symbol or column is the mean with s.e. from three dishes in the same batch. The data are representative of two to three experiments. Asterisks indicate significant difference from the dopamine release without capsaicin (Scheffe's test; $*P < 0.05$, $**P < 0.01$). (a) Concentration-dependence of inhibition by capsaicin of dopamine release evoked by 100 μM ACh. A smooth curve was fitted to the data with a EC_{50} value of 3.7 μM and a Hill coefficient of 1. (b) Comparison of concentration-response relationship for the ACh-evoked dopamine release in the absence (○) and presence of 3 μM capsaicin (●). Curves were fitted to the data assuming that the EC_{50} value (40 μM) and Hill coefficient (3.0) are not changed, but only the maximal response is reduced to 60% of control in the presence of capsaicin. (c) Inhibition by 3 and 30 μM capsaicin of the dopamine release evoked by 80 mM KCl.

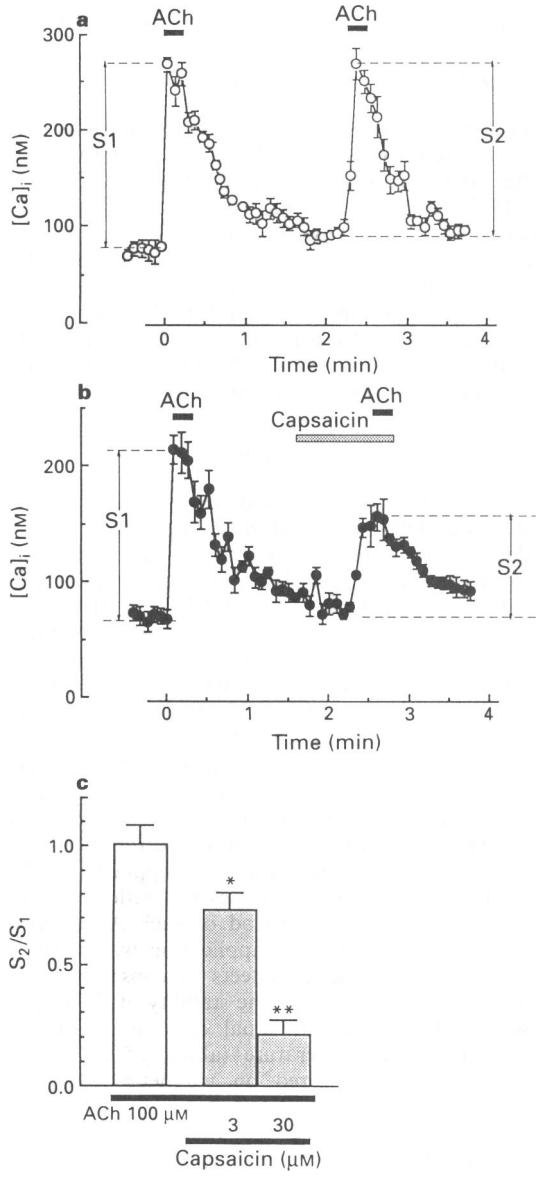

Figure 2 Attenuation by capsaicin of the acetylcholine (ACh)-evoked increase in intracellular Ca^{2+} concentration in PC12 cells. (a,b) Intracellular Ca^{2+} response to repeated applications of 100 μM ACh to the same cells in the absence (a) or presence of 3 μM capsaicin (b). Time course of continuous recordings are illustrated. Each symbol represent the mean with s.e. from 11 (control) or 12 (3 μM capsaicin) cells tested. (c) Comparison of the increase in intracellular Ca^{2+} concentration upon the second application of 100 μM ACh. The Ca^{2+} increase upon the second application (S_1) and that upon the first application (S_2) were measured as shown in (a) and (b), and the ratio of S_2/S_1 was determined in individual cells. Each column represents mean with s.e.. The data without capsaicin and those with 3 μM capsaicin were obtained from the cells shown in (a) and (b), and those with 30 μM capsaicin were from 14 cells tested. Asterisks indicate significant difference from the Ca^{2+} response without capsaicin (Scheffe's test; $*P < 0.05$, $**P < 0.01$).

presence of 1 μM resiniferatoxin was 99.6 ± 8.6% of the current in the absence of this compound (mean ± s.e., $n = 3$).

The magnitude of the current inhibition by capsaicin was increased when the current was activated by a lower concentration of ACh (Figure 4). In the case shown in Figure 4a, the current elicited by 30 μM ACh was decreased to 62% whereas the current elicited by 300 μM ACh was decreased only to 86% of control in the presence of 1 μM capsaicin. The dependence on the concentration of ACh was also obvious with the current inhibition by 3 μM capsaicin (Figure 4c). The current evoked by 30 or 100 μM ACh was more significantly suppressed by 3 μM capsaicin than the current evoked by 300 μM ACh, and the inhibition by 1 μM capsaicin was also significantly larger with the current evoked by 30 μM ACh than with the current evoked by 300 μM ACh (Scheffe's test, $P < 0.01$).

Kusano & Gainer (1993) reported that the inhibition by capsaicin of Ca^{2+} channels in F-11 cells is mediated through guanosine 5'-triphosphate (GTP)-binding proteins. A test was made by including 1 mM GDPβS, a non-hydrolysable analogue of GTP, in the intracellular solution to clarify whether GTP-binding proteins are involved in the block by capsaicin of the ACh-activated current. The current activated by 100 μM ACh in the presence of GDPβS was also inhibited by 3 μM capsaicin in four out of four cells tested. We next tested the contribution of protein kinases by involving 1 μM K-252a, a non-selective protein kinase inhibitor (Kase *et al.*, 1987), in the intracellular solution. The inhibition by 30 μM capsaicin of the ACh (100 μM)-activated current was not abolished by K-252a. The current remaining in the presence of 3 μM capsaicin with intracellular GDPβS (48.1 ± 6.6% of control; mean ± s.e., $n = 4$) or K-252a (53.9 ± 5.6% of control, $n = 5$) was not significantly different from that obtained without these compounds (38.7 ± 1.8% of control, $n = 8$) when compared using Scheffe's test ($P > 0.05$). The inability of GDPβS or K-252a to affect the inhibition by capsaicin may not be due to poor accessibility of these compounds to target intracellular molecules because the enhancement of the ATP-activated current by adenosine was blocked by intracellular GDPβS (Inoue *et al.*, 1994), and that by dopamine was blocked by K-252a (Nakazawa *et al.*, 1993) under similar conditions. The results suggest that neither GTP-binding proteins nor protein kinases are involved in the block by capsaicin of the ACh-activated current.

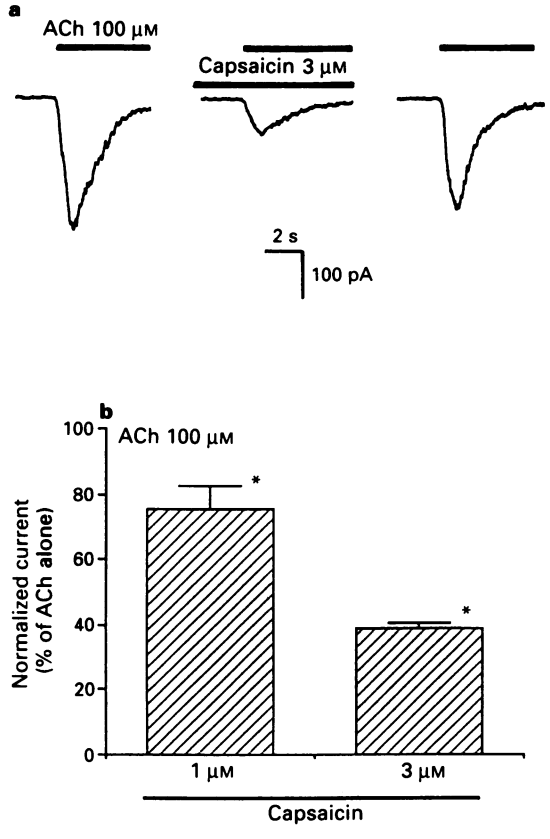

Figure 3 Inhibition by capsaicin of the current evoked by 100 μM acetylcholine (ACh). The cells were held at − 60 mV. (a) Reversible inhibition by 3 μM capsaicin of the ACh-activated current. Capsaicin was continuously present 30 s before and during the ACh-application (middle panel). (b) Concentration-dependence of the current inhibition by capsaicin. Current responses were obtained as in (a), and the peak amplitude of the current during the application of capsaicin was normalized to that before the application. Each column represents mean with s.e. from 6 (1 μM capsaicin) or eight cells (3 μM capsaicin) tested. Asterisks indicate significant difference from the current before the application of capsaicin when the values before normalization were compared in individual cells (paired t test; $^*P < 0.05$).

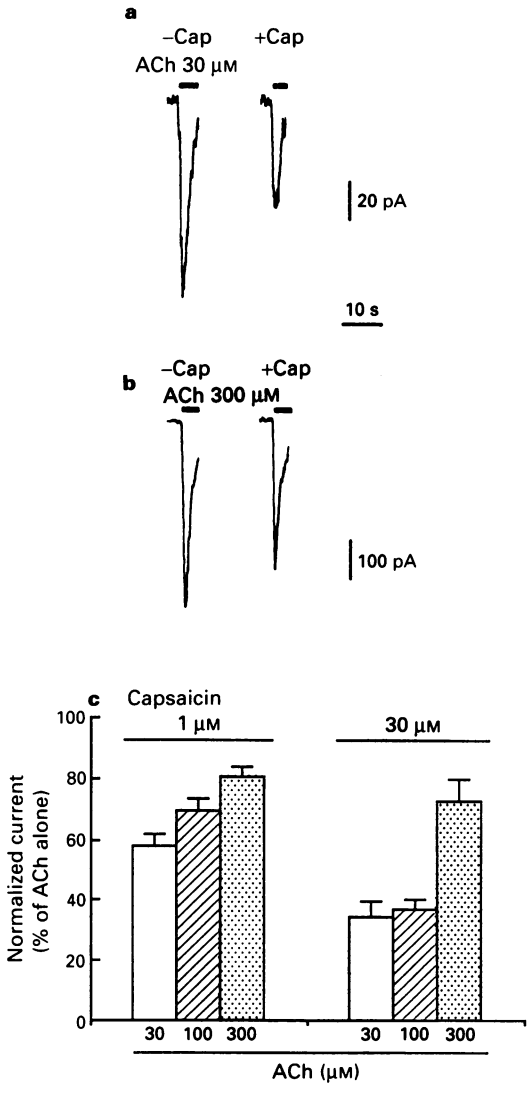

Figure 4 Dependence of the capsaicin-induced inhibition on acetylcholine (ACh) concentration. The cells were held at − 60 mV. The cells were pretreated with capsaicin 30 s before the ACh-application. (a,b) Inhibition by 1 μM capsaicin of the current activated by 30 μM (a) or 300 μM ACh (b). The extent of inhibition was larger with the current activated by 30 μM ACh than that by 300 μM ACh. (c) Summarized data for the current inhibition by 1 or 3 μM capsaicin. The ACh-evoked current was measured as in (a) and (b), and the peak current amplitude with capsaicin was normalized to that without capsaicin before the application. Each column represents the mean with s.e. from five to seven cells tested.

We examined whether the inhibition of the ACh-evoked current by capsaicin exhibits voltage-dependence. Figure 5a compares current-voltage relationships for ACh (100 μM)-activated currents in the absence and presence of 3 μM capsaicin, which was determined using a ramp pulse. The current trace before ACh-application was almost linear between − 70 and + 30 mV (Figure 5a). ACh added an inward current component at potentials more negative than 0 mV, but did not add an outward component at potentials more positive than 0 mV (Figure 5a), suggesting that the ACh-activated current exhibits strong inward rectification. This voltage-dependence was in accord with that previously obtained by

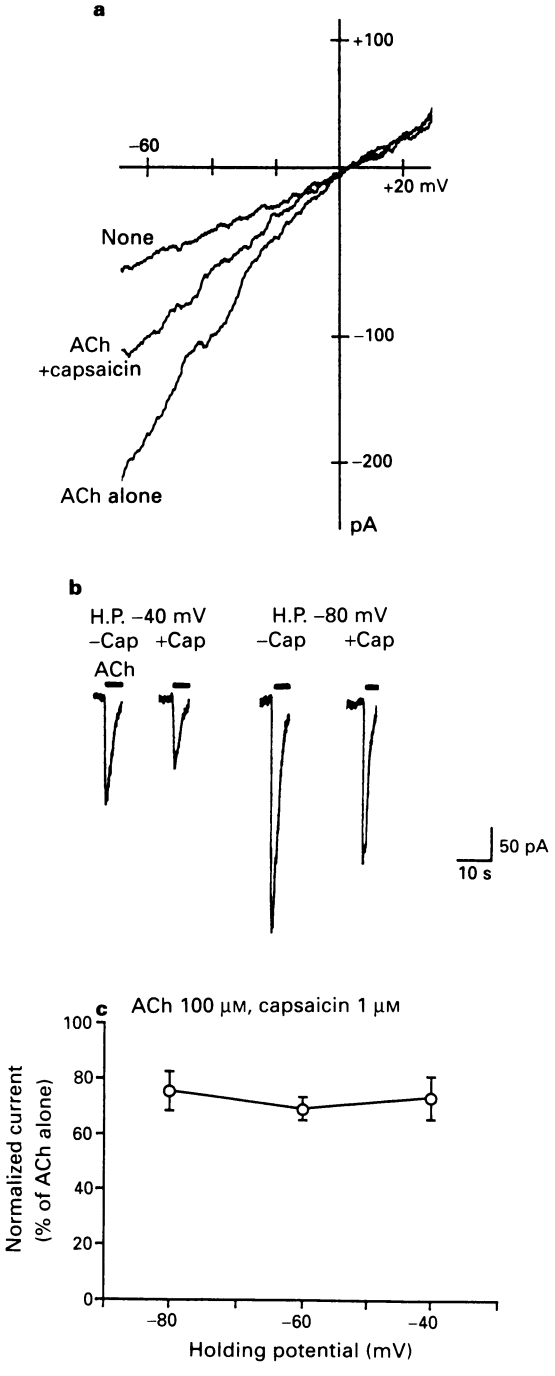

Figure 5 Lack of voltage-dependence of the current inhibition by capsaicin. The cells were pretreated with capsaicin 30 s before the acetylcholine (ACh)-application. (a) Change in instantaneous current-voltage relation by 100 μM ACh in the absence (ACh alone) or presence of 3 μM capsaicin (ACh + capsaicin). A ramp pulse of + 30 to − 70 mV (− 100 mV 200 ms^{-1}) was applied to a cell every 300 ms and the current traces near the peak current were compared with those in the absence of ACh. (b,c) The current inhibition by 1 μM capsaicin of the ACh-activated current at different holding potentials. The cells were continuously held at a potential and exposed to 100 μM ACh. The current responses in a cell held at − 40 and − 80 mV (b) and summarized data at − 40, − 60 and − 80 mV (c). Each column in (c) is the mean with s.e. from 5 cells tested.

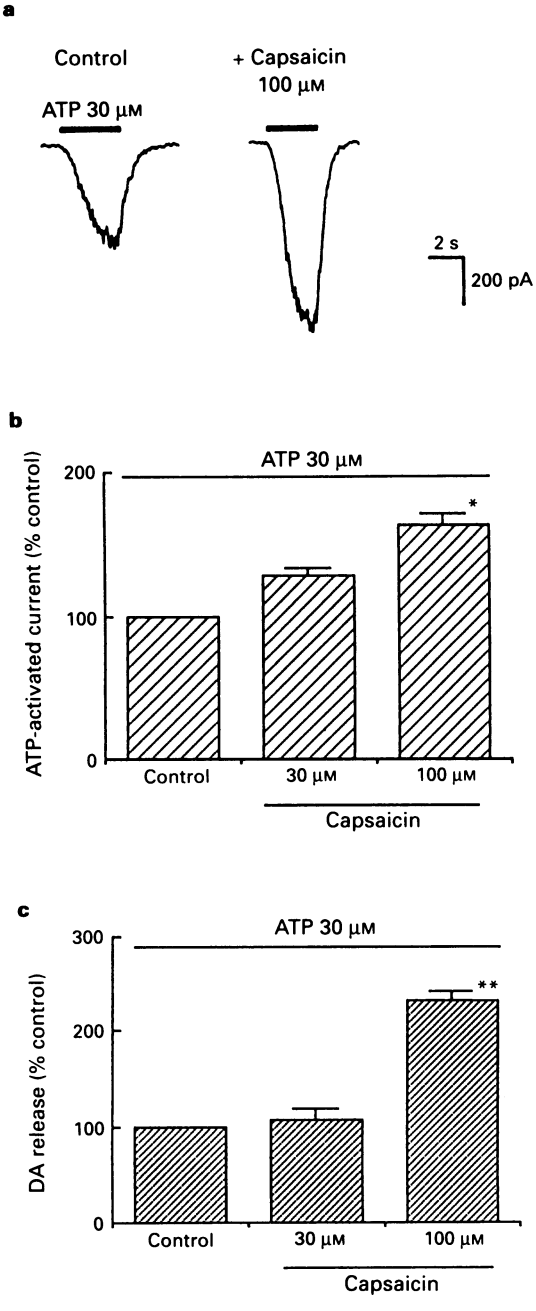

Figure 6 Effects of capsaicin on ATP (30 μM)-evoked inward current (a,b,c) and dopamine (DA) release (c). (a) The enhancement of the ATP-activated current. The current was recorded from a cell held at − 60 mV in the absence (left) and presence of 100 μM capsaicin (right). Capsaicin was present 30 s before and during the ATP-application. (b) Summarized data of enhancement by capsaicin of peak amplitude of the ATP-activated current. The current was recorded as in (a) and normalized to control current. Data were shown as mean ± s.e. of five cells tested with each concentration of capsaicin. An asterisk indicates significant difference from ATP alone by paired t test ($*P<0.05$). (c) Effect of capsaicin on the ATP-evoked dopamine release. The data were obtained and indicated as in Figure 1. Each column represents mean and s.e. from three dishes in the same batch. Data are representative of two experiments. Asterisks indicate significant difference from ATP alone by Scheffe's test for multiple comparison ($**P<0.01$).

Ifune & Steinbach (1990) in PC12 cells. Capsaicin did not affect the voltage-dependence of the ACh-activated current in four out of four cells tested: the current activated in the presence of capsaicin also exhibited inward rectification and the inward component in the negative potential range was uniformly suppressed (Figure 5a).

The voltage-dependence of current inhibition was also tested by applying ACh (100 μM) to cells held at different membrane potentials (Figure 5b,c). The magnitude of the current inhibition by 1 μM capsaicin was not different among the three potentials (−40, −60 and −80 mV; Figure 5c).

Effects of capsaicin on ATP-evoked responses

Extracellular ATP activates non-selective cation channels in PC12 cells (Nakazawa *et al.*, 1990). We investigated the influence of capsaicin on inward currents activated by 30 μM ATP. Capsaicin (1 to 10 μM) did not affect the ATP-activated currents (not shown). A higher concentration of capsaicin (30 and 100 μM), however, enhanced the ATP-activated current (Figure 6a,b). The peak amplitude of the ATP-activated current was increased by about 30% in the presence of 30 μM capsaicin (Figure 6b), and by 60% in the presence of 100 μM capsaicin.

Dopamine release evoked by 30 μM ATP was also affected by capsaicin. ATP (30 μM) evoked a dopamine release of 3.00 ± 0.67% of the total content ($n = 9$). Capsaicin (100 μM) significantly potentiated the ATP-evoked dopamine release by about 130% (Figure 6c; Scheffe's test, $P < 0.01$). The potentiation was not observed with 30 μM capsaicin (Figure 6c).

Discussion

We have investigated the effects of capsaicin on responses mediated by nicotinic receptor-channels and on those mediated by ATP-activated channels in PC12 cells. Capsaicin inhibited dopamine release, the increase in intracellular Ca^{2+} concentration and inward current evoked by ACh at concentrations of 1 to 3 μM, and enhanced dopamine release and inward current evoked by ATP at higher concentrations (30 to 100 μM). These results are novel findings that indicate ligand-gated channels are targets of capsaicin as well as voltage-gated channels (Petersen *et al.*, 1987; 1989; Kusano & Gainer, 1993). Reduction by capsaicin of ACh-evoked accumulation of Ca^{2+} and Na^{+}, which was recently reported in bovine adrenal medullary cells (Toyohira *et al.*, 1992), may also support our findings although the ACh-evoked ion accumulation may have been the result of ion permeation through voltage-gated channels, secondarily activated by depolarization.

The ACh-activated current was inhibited by capsaicin at concentrations as low as 1 μM (Figure 3). Although this potency is weaker than that reported to open the non-selective cation channels in rat sensory neurones (EC_{50} was about 0.3 μM; Bevan & Szolcsanyi, 1990), it was considerably stronger than that found to inhibit Na^{+}, K^{+}, or Ca^{2+} currents in guinea-pig sensory neurones (Petersen *et al.*, 1987; 1989), where capsaicin blocked only a smaller part of the currents at 50 μM. The inhibition of the ACh-activated current was insensitive to K-252a, suggesting that protein kinases are not involved in the channel inhibition. Direct interaction of GTP-binding proteins with the channels, which has been proposed in other types of channels such as Ca^{2+} channels (Hille, 1992), is also not indicated, judging from the lack of influence by GDPβS. Thus, most likely interpretation of the current inhibition in the present study is an effect resulting from interaction of capsaicin with the channel protein itself or some component tightly coupled with the channels.

The inhibition by capsaicin of the ACh-activated current did not exhibit voltage-dependence (Figure 5), suggesting that the compound does not affect the properties of nicotinic receptor channels relating to membrane potential such as mechanisms underlying ion-permeation which are affected by positively charged pore blockers of these channels (Ascher *et al.*, 1978; 1979). In contrast, the current inhibition by capsaicin showed a dependence on the concentration of ACh (Figure 4): the inhibition was partially overcome by increasing the concentration of ACh. The dependence on agonist concentration can be explained by reduction in the affinity of the agonist for its binding-site (Ascher *et al.*, 1978; 1979). Capsaicin may inhibit the association of ACh with nicotinic receptors by either competitive antatgonism or an allosteric effect. Further investigation is necessary to decide the mode of antagonism by capsaicin of nicotinic receptor channels.

Capsaicin suppressed dopamine release evoked by ACh (Figure 1). Judging from the decreased Ca^{2+} concentration (Figure 2), combined with previous results that demonstrated the dependence of the nicotinic responses on extracellular Ca^{2+} (Ritchie, 1979; Inoue & Kenimer, 1988), the suppression may arise from inhibition of ACh-stimulated Ca^{2+}-influx upon the ACh-stimulation. In PC12 cells, it is generally believed that Ca^{2+}-influx through the voltage-gated Ca^{2+} channels, which are secondarily activated by depolarization, is primarily responsible for the increase in intracellular Ca^{2+} concentration upon nicotinic stimulation (Ritchie, 1979; Inoue & Kenimer, 1988). Although capsaicin suppressed the dopamine release evoked by 80 mM KCl (Figure 1c), inhibition of the Ca^{2+} channel-mediated mechanism may not essentially contribute to the antagonism to the ACh-evoked dopamine release because generation of the depolarization itself is hampered by the block of the nicotinic receptor channels. The smaller magnitude of the suppression of the dopamine release evoked by 80 mM KCl (Figure 1c), compared with that of the ACh-evoked release (Figure 1a), may also exclude major contribution of the Ca^{2+} channel-mediated mechanism.

The ATP-evoked current was enhanced by high concentrations of capsaicin (Figure 6a,b). The enhancement of the current may account for the potentiation by capsaicin of the ATP-evoked dopamine release (Figure 6c) because the dopamine release is directly triggered by Ca^{2+}-permeation through ATP-activated channels in PC12 cells (Nakazawa & Inoue, 1992).

The inflammatory effects of capsaicin appear to result from excitation of a subset of sensory neurones (Bevan & Szolcsanyi, 1990). The blockade of nicotinic receptor channels in the present study may not be directly related to the inflammatory effects because the nicotinic receptor-channels generally serve excitatory neurotransmission, and the blockade of the channels will produce inhibitory effects on neurones. The absence of any effect of resiniferatoxin, which is known to be a highly potent capsaicin-like agonist (Bevan & Szolcsanyi, 1990), suggests that there is not a mechanistic relationship between the excitatory effects of capsaicin on sensory neurones and the observed inhibition of acetylcholine receptor channels. The enhancement by capsaicin of the ATP-activated current may not significantly contribute to the inflammation either because the enhancement required a high concentration (30 μM) of capsaicin (Figure 6). However, the block by capsaicin of nicotinic receptor channels may promote undesired responses in pharmacological experiments where capsaicin is used as a tool for depletion of neuropeptides from nerve terminals. In other words, capsaicin-sensitive neurogenic response does not necessarily indicate involvement of peptidergic neurotransmission when nicotinic neurotransmission is not negligible. The concentration of capsaicin that maximally activates non-specific cation channels in rat sensory neurones is >1 μM (Bevan & Szolcsanyi, 1990), and this concentration accords with that utilized for the neuropeptide depletion in isolated tissues (e.g. Saito *et al.*, 1987; Ellis & Burnstock, 1989). Saito *et al.* (1987) reported that capsaicin reversibly inhibited part of the neurogenic contraction at 0.1 μM, but the depletion of the

neurotransmitter responsible for this inhibition (presumably, calcitonin-gene-related peptide) required 1 to 10 μM of capsaicin in smooth muscle of rat vas deferens. Judging from the concentration-dependence of the inhibition of the ACh-activated current (Figure 3b), it is quite likely that the capsaicin-treatment for the neuropeptide depletion simultaneously affects other functions that involve nicotinic responses. It is, therefore, concluded that the possible contribution of a nicotinic mechanism must be carefully examined when capsaicin is used as a pharmacological tool.

We are grateful to Mrs T. Obama for culturing cells with skilled techniques, Miss A. Kawahara for cooperation in some experiments, D.J.G. Kenimer for improving the manuscript, and Drs A. Takanaka and K. Fujimori for continuous encouragement.

References

ASCHER, P., LARGE, W.A. & RANG, H.P. (1979). Studies on the mechanism of action of acetylcholine antagonists on rat parasympathetic ganglion cells. *J. Physiol.*, **295,** 139–170.

ASCHER, P., MARTY, A. & NEILD, T.O. (1978). The mode of action of antagonists of the excitatory response to acetylcholine in *Aplysia* neurons. *J. Physiol.*, **278,** 207–235.

BEVAN, S. & SZOLCSANYI, J. (1990). Sensory neuron-specific actions of capsaicin: mechanisms and applications. *Trends Pharmacol. Sci.*, **11,** 330–333.

DOCHERTY, R.J., ROBERTSON, B. & BEVAN, S. (1991). Capsaicin causes prolonged inhibition of voltage-activated calcium currents in adult rat dorsal root ganglion neurons in culture. *Neuroscience*, **40,** 513–521.

ELLIS, J.L. & BURNSTOCK, G. (1989). Modulation of neurotransmission in the guinea-pig vas deferens by capsaicin: involvement of calcitonin gene-related peptide and substance P. *Br. J. Pharmacol.*, **98,** 707–713.

FRANCO-CERECEDA, A. & LUNDBERG, J.M. (1985). Calcitonin gene-related peptide (CGRP) and capsaicin-induced stimulation of heart contractile rate and force. *Naunyn-Schmied. Arch. Pharmacol.*, **331,** 149–151.

GREENE, L.A. & REIN, G. (1977). Release of ^{3}H-norepinephrine from a clonal line of pheochromocytoma cells (PC12) by nicotinic cholinergic stimulation. *Brain Res.*, **138,** 521–528.

GREENE, L.A. & TISCHLER, A.S. (1976). Establishment of a noradrenergic clonal line of rat adrenal pheochromocytoma cell which respond to nerve growth factor. *Proc. Natl. Acad. Sci. U.S.A.*, **73,** 2424–2428.

GRYNKIEWICZ, G., POENIE, M. & TSIEN, R.Y. (1985). A new generation of Ca^{2+} indicators with greatly improved fluorescence properties. *J. Biol. Chem.*, **260,** 3440–3450.

HAMILL, O.P., MARTY, A., NEHER, E., SAKMANN, B. & SIGWORTH, F.J. (1981). Improved patch-clamp techniques for high-resolution current recordings from cells and cell-free membrane patches. *Pflügers Arch.*, **391,** 85–100.

HILLE, B. (1992). G protein-coupled mechanisms and nervous signaling. *Neuron*, **9,** 187–195.

IFUNE, C.K. & STEINBACH, J.H. (1990). Rectification of acetylcholine-elicited currents in PC12 pheochromocytoma cells. *Proc. Natl. Acad. Sci. U.S.A.*, **87,** 4794–4798.

INGRAM, S.L., MARTENSON, M.E. & BAUMANN, T.K. (1993). Responses of cultured adult monkey trigeminal ganglion neurones to capsaicin. *NeuroReport*, **4,** 460–462.

INOUE, K. & KENIMER, J.G. (1988). Muscarinic stimulation of calcium influx and norepinephrine release in PC12 cells. *J. Biol. Chem.*, **263,** 8157–8161.

INOUE, K., NAKAZAWA, K., FUJIMORI, K. & TAKANAKA, A. (1989). Extracellular adenosine 5′-triphosphate-evoked norephinephrine secretion not relating to voltage-gated Ca channels in pheochromocytoma PC12 cells. *Neurosci. Lett.*, **106,** 294–299.

INOUE, K., WATANO, T., KOIZUMI, S., NAKAZWA, K. & BURNSTOCK, G. (1994). Dual modulation by adenosine of ATP-activated channels through GTP-binding proteins in rat pheochromocytoma PC12 cells. *Eur. J. Pharmacol.* (in press).

KASE, H., IWAHASHI, K., NAKANISHI, S., MATSUDA, Y., YAMADA, K., TAKAHASHI, M., MURAKATA, C., SATO, A. & KANEKO, M. (1987). K252 compounds, novel and potent inhibitors of protein kinase C and cyclic nucleotide-dependent protein kinases. *Biochem. Biophys. Res. Commun.*, **142,** 436–440.

KUSANO, K. & GAINER, H. (1993). Modulation of voltage-activated Ca currents by pain-inducing agents in a dorsal root ganglion neuronal line, F-11. *J. Neurosci. Res.*, **34,** 158–169.

MARSH, S.J., STANSFELD, C.E., BROWN, D.A., DAVEY, R. & MCCARTHY, D. (1987). The mechanism of action of capsaicin on sensory C-type neurons and their axons *in vitro*. *Neuroscience*, **23,** 275–289.

NAKAZAWA, K., FUJIMORI, K., TAKANAKA, A. & INOUE, K. (1990). An ATP-activated conductance in pheochromocytoma cells and its suppression by extracellular calcium. *J. Physiol.*, **428,** 257–272.

NAKAZAWA, K. & INOUE, K. (1992). Roles of Ca^{2+} influx through ATP-activated channels in catecholamine release from pheochromocytoma PC12 cells. *J. Neurophysiol.*, **68,** 2026–2032.

NAKAZAWA, K., WATANO, T. & INOUE, K. (1993). Mechanism underlying facilitation by dopamine of ATP-activated currents in rat pheochromocytoma cells. *Pflügers Arch.*, **422,** 458–464.

OHARA-IMAIZUMI, M., NAKAZAWA, K., OBAMA, T., FUJIMORI, K., TAKANAKA, A. & INOUE, K. (1991). Inhibitory action of peripheral-type benzodiazepines on dopamine release from PC12 pheochromocytoma cells. *J. Pharmacol. Exp. Ther.*, **259,** 484–489.

PETERSEN, M., PIERAU, Fr-K. & WEYRICH, M. (1987). The influence of capsaicin on membrane currents in dorsal root ganglion neurons of guinea-pig and chicken. *Pflügers Arch.*, **409,** 403–410.

PETERSEN, M., WAGNER, G. & PIERAU, Fr-K. (1989). Modulation of calcium-currents by capsaicin in a subpopulation of sensory neurones of guinea pig. *Naunyn-Schmied. Arch. Pharmacol.*, **339,** 184–191.

RITCHIE, A.K. (1979). Catecholamine secretion in a rat pheochromocytoma cell line: two pathways for calcium entry. *J. Physiol.*, **286,** 541–561.

SAITO, A., TOMOBE, Y. & GOTO, K. (1987). Effect of capsaicin on smooth muscles of rat vas deferens: involvement of calcitonin gene-related peptide? *J. Pharmacol. Exp. Ther.*, **242,** 666–672.

SZOLCSANYI, J. & BARTHO, L. (1978). New type of nerve-mediated cholinergic contractions of the guinea-pig small intestine and its selective blockade by capsaicin. *Naunyn-Schmied. Arch. Pharmacol.*, **305,** 83–90.

TOYOHIRA, Y., YANAGIHARA, N., MINAMI, K., TSUTSUI, M., WADA, A. & IZUMI, F. (1992). Inhibitory effects of capsaicin on catecholamine secretion and ionic channels in cultured bovine adrenal medullary cells. *Jpn. J. Pharmacol.*, **58** (Suppl. I), 257P.

(Received January 10, 1994
Revised May 5, 1994
Accepted May 16, 1994)

Br. J. Pharmacol (1994), **113**, 303–309

Inhibition by opioids acting on μ-receptors of GABAergic and glutamatergic postsynaptic potentials in single rat periaqueductal gray neurones *in vitro*

[1]B. Chieng & M.J. Christie

Department of Pharmacology, The University of Sydney, NSW 2006, Australia

1 Membrane properties of rat periaqueductal gray neurones were investigated by use of intracellular recordings from single neurones in brain slices. Morphological properties and anatomical location of each impaled neurone were characterized by intracellular staining with biocytin. The present paper considers the properties of electrically-evoked and spontaneous postsynaptic potentials impinging on periaqueductal gray neurones, and the actions of opioids on postsynaptic potentials in neurones which were not directly hyperpolarized by opioids. The preceding paper considers neurones which were hyperpolarized by opioids.

2 Electrical stimulation in the vicinity of impaled neurones evoked postsynaptic potentials having fast (duration at half-maximal amplitude 37 ± 2 ms, $n = 65$) and in some cases slow (duration at half-maximal amplitude 817 ± 187 ms, $n = 3$) components. Amplitudes of evoked potentials were dependent on stimulus voltage, membrane potential, and were abolished during superfusion with solutions containing tetrodoxotoxin (100 nM to 1 μM, $n = 5$) or Co^{2+} (4 mM, $n = 2$).

3 Fast postsynaptic potentials were mediated predominantly by activation of glutamate and $GABA_A$ receptors. The $GABA_A$-receptor antagonist, bicucuilline (30 μM), inhibited postsynaptic potentials by 44 ± 8% ($n = 14$). The non-NMDA-receptor antagonist, 6-cyano-7-nitroquinoxaline-2,3-dione (10 μM), inhibited postsynaptic potentials by 48 ± 6% ($n = 16$). Combined superfusion of bicuculline (30 μM) and 6-cyano-7-nitroquinoxaline-2,3-dione (10 μM) inhibited postsynaptic potentials by 93 ± 1% ($n = 8$). Additional superfusion of the NMDA-receptor antagonist, (±)-2-amino-5-phosphonovaleric acid (50 μM) inhibited synaptic potentials by 94 ± 1% ($n = 3$).

4 Slow inhibitory postsynaptic potentials were observed in 12% (8/65) of neurones. They reversed polarity between −100 and −110 mV, and were abolished by superfusion with spiperone (1 μM, $n = 2$), but not the α_2-antagonist, idazoxan (3 μM, $n = 2$).

5 Selective μ-receptor agonists inhibited fast postsynaptic potentials in all neurones tested which were not directly hyperpolarized by opioids. Met-enkephalin (30 μM) and Tyr-D-Ala-Gly-MePhe-Glyol (3 μM) inhibited postsynaptic potentials by 53 ± 3% and 49 ± 3%, respectively. This effect was completely antagonised by naloxone (1 μM, $n = 3$). A small inhibition produced by the selective δ-receptor agonist, Tyr-D-Pen-Gly-Phe-D-Pen-enkephalin (3 μM, 26 ± 4%, $n = 14$), was antagonized by naloxone (1 μM), but not by the selective δ-receptor antagonist, naltrindole (10 nM), suggesting non-specific μ-receptor activation by this agonist. The selective κ-receptor agonist, U50488H (3 μM), also consistently inhibited postsynaptic potentials by 45 ± 15% ($n = 4$). However, this effect was not fully reversed by naloxone (1 μM) suggesting a non-specific action.

6 Both glutamatergic and GABAergic components of fast postsynaptic potentials were inhibited by Met-enkephalin (10 or 30 μM). Met-enkephalin inhibited postsynaptic potentials by 55 ± 5% ($n = 12$) in the presence of 6-cyano-7-nitroquinoxaline-2,3-dione (10 μM, predominantly GABAergic component). Met-enkephalin did not affect the response to GABA applied directly by pressure ejection, indicating that opioids exclusively inhibited presynaptic release of GABA. Met-enkephalin (10–30 μM) inhibited postsynaptic potentials by 48 ± 6% ($n = 11$) in the presence of bicuculline (30 μM, predominantly glutamatergic component). In the presence of both bicuculline and 6-cyano-7-nitroquinoxaline-2,3-dione, Met-enkephalin inhibited the small residual component of the synaptic potential by 42 ± 15% ($n = 2$).

7 Frequent spontaneous synaptic potentials were also observed in 11% (10/94) of the neurones which were not directly hyperpolarized by opioids. These were reversibly abolished by bicuculline (30 μM, $n = 5$) and substantially inhibited by Met-enkephalin (30 μM, $n = 6$), but were unaffected by 6-cyano-7-nitroquinoxaline-2,3-dione (10 μM, $n = 2$).

8 In conclusion, fast glutamatergic and GABAergic synaptic potentials were evoked by electrical stimulation throughout the lateral and ventrolateral periaqueductal gray. Slow inhibitory synaptic potentials were also evoked in some neurones. Opioids acting on μ-receptors inhibited both GABAergic and glutamatergic components of synaptic potentials throughout this brain region.

Keywords: Periaqueductal gray; opioid; enkephalin; μ-receptor; δ-receptor; κ-receptor; glutamate; GABA; postsynaptic potentials; presynaptic inhibition

Introduction

The involvement of the periaqueductal gray (PAG) in the analgesic actions of opioids is widely recognised (see Chieng & Christie, 1994). Disinhibition of PAG neurones which project to the ventral medulla has been proposed as the mechanism by which opioids act in this region to induce antinociception (Basbaum & Fields, 1984; Fields *et al.*, 1991).

[1] Author for correspondence.

This has been postulated to occur via opioid inhibition of tonically active GABAergic interneurones in PAG, thereby disinhibiting output neurones which project to the ventral medulla. Although considerable indirect evidence supports this model (see Reichling, 1991), little is known of the direct actions of opioids on membrane properties or synaptic potentials in PAG neurones.

Inhibition of tonically active GABAergic interneurones by opioids has been suggested to account for indirect excitatory effects in several regions of the central nervous system (Madison & Nicoll, 1988; Lacey *et al.*, 1989; Pan *et al.*, 1990; Johnson & North, 1992). In these cases, neurones directly hyperpolarized by opioids (presumably GABAergic) could be distinguished from opioid-insensitive neurones on the basis of distinct morphological and/or physiological properties, as well as by direct inhibition of GABAergic synaptic potentials in neurones which were not directly inhibited by opioids. Within the PAG, opioids acting on μ-receptors directly hyperpolarized a subpopulation of neurones (Behbehani *et al.*, 1990; Chieng & Christie, 1994). However, other physiological and morphological properties of opioid-sensitive neurones did not substantially differ from opioid-insensitive neurones and it is unlikely that opioid-sensitive neurones were GABAergic (Chieng & Christie, 1994). Extracellular recordings from brain slices showed that opioids excited some PAG neurones, probably via an indirect mechanism, which is consistent with opioids producing disinhibition in PAG (Behbehani *et al.*, 1990). The present study used intracellular recordings from brain slices to examine directly the actions of opioids on GABAergic, glutamatergic, and other types of synaptic potentials impinging on lateral and ventrolateral PAG neurones. Other physiological and morphological properties of opioid-sensitive and -insensitive neurones in PAG are described in the preceding paper.

Methods

Methods for preparation of brain slices, intracellular recordings and histochemistry were identical to those described in the accompanying paper (Chieng & Christie, 1994), with the following exceptions.

Electrically-evoked postsynaptic potentials

Bipolar tungsten stimulating electrodes (tip separation approximately 200 μm) were routinely placed within the slice near (200–500 μm) to impaled neurones. Postsynaptic potentials (p.s.ps) were evoked by a single 400 μs stimulus of 10 to 60 V. Membrane potential was maintained in each neurone as uniformly as possible (<5 mV variation) between −85 and −100 mV in order to avoid the generation of full action potentials during stimulation. P.s.ps were evoked at a frequency of 0.03 Hz and four consecutive responses were averaged for subsequent analyses using CLAMPFIT (Axon Instruments). All data are expressed as mean ± s.e. mean.

Pressure application of GABA

In some experiments, a submerged micropipette (10–20 μm diameter) containing GABA (100 mM) was placed above the surface of the slice as near as practicable to the recording electrode. GABA was applied by brief (20 ms) pressure pulses using a Picospritzer (General Valve Corporation, Fairfield, NJ, U.S.A.).

Drugs and reagents

Biocytin, Met-enkephalin and tetrodotoxin were from Sigma (St Louis, MO, U.S.A.); Tyr-D-Ala-Gly-MePhe-Glyol (DAMGO) and Tyr-D-Pen-Gly-Phe-D-Pen (Pen = penicillamine, DPDPE) from NIDA (U.S.A.); *trans*-(+)-3,4-dichloro-N-methyl-N-[2-(1-pyrrolidinyl)-cyclohexyl] benzeneacetamide methane sulphonate (U50488H) from Upjohn; and (±)-2-amino-5-phosphonovaleric acid (APV), (−)-bicuculline methiodide, 6-cyano-7-nitroquinoxaline-2,3-dione (CNQX), naloxone hydrochloride and naltrindole hydrochloride from Research Biochemicals Inc. (Natick, MA, U.S.A.).

Results

With the exception of the characteristics of electrically-evoked p.s.ps, the properties of PAG neurones are described and compared in the preceding paper (Chieng & Christie, 1994).

Properties of fast p.s.ps

Electrical stimulation in the vicinity of the recording electrode invariably induced fast p.s.ps (Figure 1, $n = 65$) and sometimes evoked slow inhibitory p.s.ps (Figure 3, $n = 8$). Fast p.s.ps had a duration at half-maximal amplitude of 37 ± 2 ms ($n = 65$). The amplitude of fast p.s.ps was dependent on the stimulus intensity, and full action potentials were generated when p.s.ps reached threshold (Figure 1a). The amplitude of fast p.s.ps increased when the membrane was hyperpolarized by passing constant current through the recording electrode (e.g. Figure 3a). In all subsequent recordings, p.s.ps were maintained in a subthreshold range by maintaining the membrane potential with little variation (<5 mV) between −85 and −100 mV using direct current

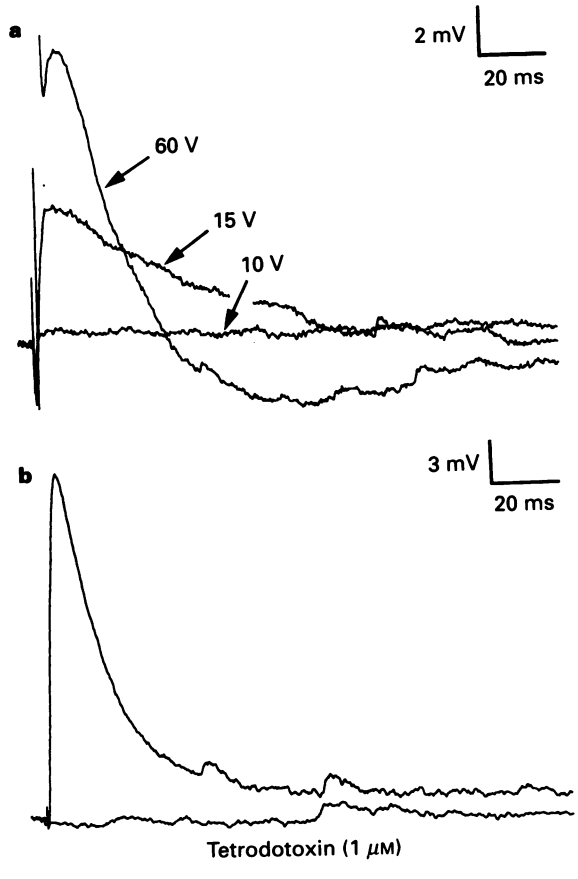

Figure 1 Electrical stimulation (400 μs duration) in the vicinity of the recording electrode evoked fast p.s.ps (displayed traces were not averaged). (a) The amplitude of fast p.s.ps was dependent on the stimulus intensity and an action potential occurred when the p.s.p. amplitude reached threshold. (b) Fast p.s.ps were completely abolished by superfusion with tetrodotoxin (1 μM) implying a presynaptic event.

(−50 to −250 pA). Fast p.s.ps were completely abolished by tetrodotoxin (100 nM to 1 μM, $n = 5$, Figure 1b) or Co^{2+} (4 mM, $n = 2$, data not shown).

In neurones which were not hyperpolarized by opioids, the amplitude of fast p.s.ps was reduced by the non-NMDA glutamate receptor antagonist, CNQX (Figure 2a, Table 1, 10 μM, 48 ± 6% inhibition, range 7 to 80%, $n = 16$). CNQX produced a similar inhibition of fast p.s.ps in neurones which were hyperpolarised by opioids (53 ± 12% inhibition, range 14 to 78%, $n = 5$). Inhibition of fast p.s.ps by APV (Figure 2c, 15 ± 4% inhibition, $n = 4$) was consistently smaller than by CNQX in all neurones tested. All of these neurones were also hyperpolarized by opioids.

The $GABA_A$ antagonist, bicuculline (30 μM) also inhibited fast p.s.ps (Figure 2b, Table 1, 44 ± 8% inhibition, range 0 to 91%, $n = 14$) in neurones which were not hyperpolarized by opioids. Bicuculline produced similar inhibition of fast p.s.ps in neurones which were hyperpolarized by opioids (32 ± 14% inhibition, range 0 to 72%, $n = 5$).

Combined superfusion with CNQX (10 μM) and bicuculline (30 μM) blocked most of fast p.s.ps (93 ± 1% inhibition, $n = 8$, Figure 2d, Table 1), and the small remaining compo-

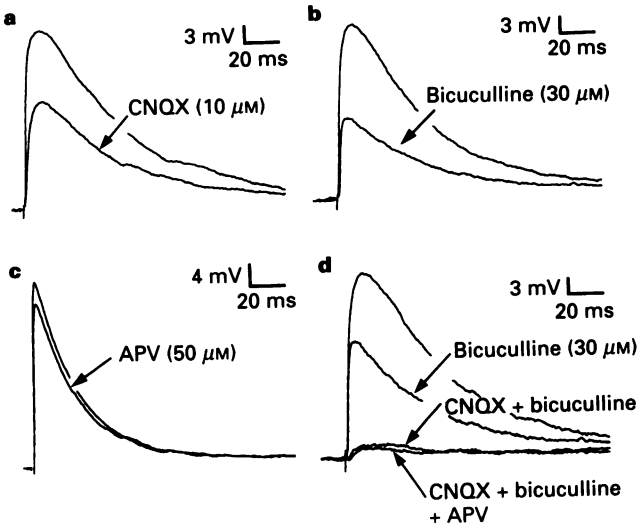

Figure 2 Electrically-evoked fast p.s.ps are comprised of GABAergic, glutamatergic and small residual components. (a) Partial inhibition of a p.s.p. by the non-NMDA-receptor antagonist, CNQX (10 μM). (b) Partial inhibition of a p.s.p. by the $GABA_A$ receptor antagonist, bicuculline (30 μM, same neurone as in a). (c) Partial inhibition of p.s.p. by the NMDA-receptor antagonist, APV (50 μM). (d) Combined superfusion of CNQX and bicuculline inhibited most of the fast p.s.p. (same neurone as in a and b). The remaining component was partially inhibited by APV. For abbreviations, see text.

Table 1 Inhibition of fast p.s.ps in PAG neurones which were not hyperpolarized by opioids

Drugs	*Inhibition of the amplitude of evoked p.s.ps %*	n
Opioids		
Met-enkephalin (30 μM)	53 ± 3**	29
DAMGO (3 μM)	49 ± 4**	23
DAMGO + naloxone (1 μM)	3 ± 3§	3
DPDPE (3 μM)	26 ± 4**	14
DPDPE + naloxone (1 μM)	8 ± 4§	5
DPDPE + naltrindole (10 nM)	24, 23	2
U50488H (3 μM)	45 ± 15*	4
U50488H + naloxone (1 μM)	36 ± 16**§	4
Glutamatergic and GABAergic antagonists		
CNQX (10 μM)	48 ± 6**	16
Bicuculline (30 μM)	44 ± 8**	14
CNQX + bicuculline	93 ± 1**	8
CNQX + bicuculline + APV (50 μM)	94 ± 1**	3
Met-enkephalin (10–30 μM)-mediated inhibition of GABAergic and glutamatergic components of p.s.ps		
GABAergic (in 10 μM CNQX)	55 ± 5†	12
Glutamatergic (in 30 μM bicuculline)	48 ± 6†	11
Residual (in CNQX + bicuculline)	56, 27	2

Values are mean ± s.e.mean
*$P < 0.05$ versus pre-drug p.s.ps; **$P < 0.001$ versus pre-drug p.s.ps §$P < 0.05$ versus pre-antagonist p.s.ps; †$P < 0.0001$ versus pre-Met-enkephalin p.s.ps in the presence of amino acid antagonist (paired t tests).
For abbreviations, see text.

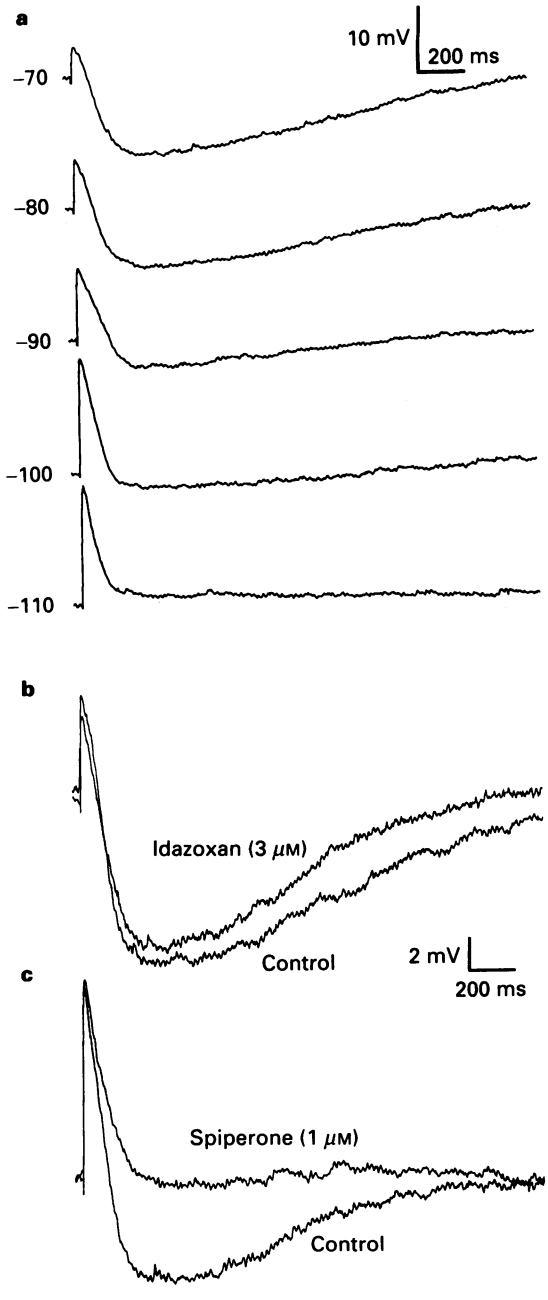

Figure 3 Slow inhibitory p.s.ps (traces were not averaged). (a) The amplitudes of fast and slow p.s.ps depend on membrane potential. The amplitude of fast p.s.ps increased as the membrane potential was made more negative by applying constant current to the recording electrode, whereas the amplitude of slow inhibitory p.s.p. decreased at negative membrane potentials and reversed polarity between −100 mV and −110 mV. (b and c) Slow inhibitory p.s.ps were not affected by α_2-adrenoceptor antagonist, idazoxan (3 μM, b), but were completely abolished by spiperone (1 μM, c).

nent was partially inhibited by APV (50 μM; total inhibition by CNQX, bicuculline and APV = 94 ± 1%, $n = 3$, Figure 2d).

Properties of slow p.s.ps

Slow inhibitory p.s.ps were observed in 8 of the 65 neurones tested. None of these neurones was hyperpolarized by opioids. They had a duration at half-maximal amplitude of 817 ± 187 ms ($n = 3$, Figure 3). Slow p.s.ps were hyperpolarizing at potentials near rest (−8 ± 3 mV between −70 mV and −75 mV) and reversed polarity between −100 and −110 mV (Figure 3a). In some experiments ($n = 3$), slow p.s.ps were not blocked by superfusion with idazoxan (3 μM, Figure 3b, $n = 2$) but were blocked by spiperone (1 μM, Figure 3c, $n = 2$).

Opioids inhibit evoked p.s.ps

The effects of opioids were studied only in neurones which were not hyperpolarized by opioids in order to avoid attenuation of p.s.ps which could be produced by postsynaptic changes in input-resistance or membrane potential. Met-enkephalin inhibited electrically-evoked fast p.s.ps (30 μM; 53 ± 3%; range 31 to 90%, $n = 29$; Figure 4a, Table 1) in all neurones which were not hyperpolarized by opioids. The selective μ-receptor agonist, DAMGO (3 μM), produced similar inhibition (49 ± 3%, $n = 23$, unpaired $t = 0.74$, $P > 0.4$, Figure 4b, Table 1). Inhibition of fast p.s.ps by DAMGO was concentration-dependent with an EC_{50} of approximately 80 nM (Figure 5). The DAMGO-induced inhibition was completely antagonized by 1 μM naloxone (3 ± 3% of the inhibition remained, $n = 3$; Figure 4b, Table 1).

The inhibitory effects of the selective δ-receptor agonist, DPDPE, and κ-receptor agonist, U50488H, on fast p.s.ps were inconclusive. DPDPE (3 μM) produced a smaller inhibition of fast p.s.ps than Met-enkephalin or DAMGO (26 ± 4%, $n = 14$, Table 1) in neurones which were not hyperpolarized by opioids. This inhibition was reversed by naloxone (1 μM; 8 ± 4% of the inhibition remained, $n = 5$, Table 1). However, in the presence of the selective δ-receptor

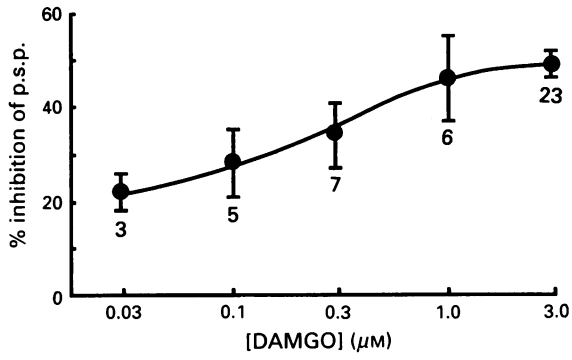

Figure 5 Concentration-response relationship of inhibition of fast p.s.ps by DAMGO. The EC_{50} was approximately 80 nM.

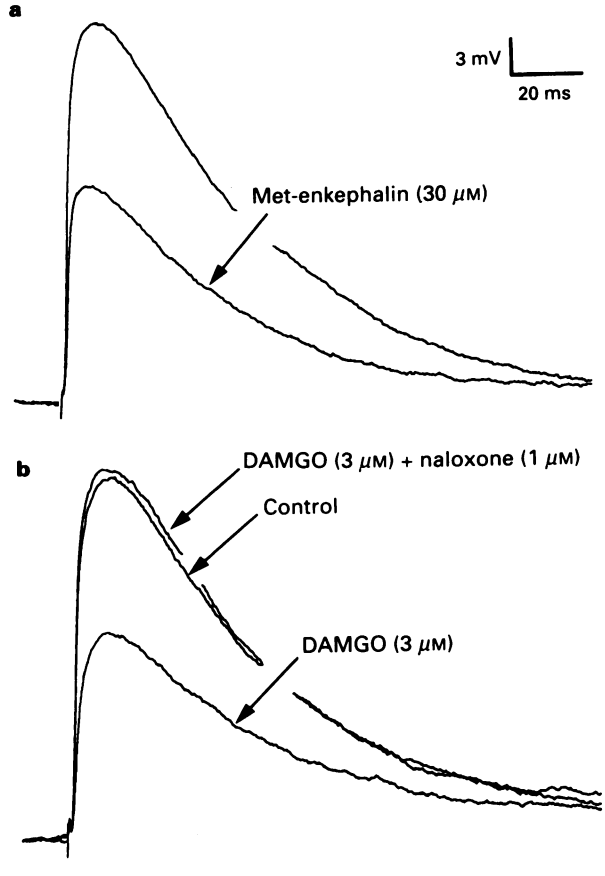

Figure 4 Opioid agonists selective for μ-receptors inhibit fast p.s.ps in a single neurone. Met-enkephalin (30 μM, a) and selective μ-receptor agonist DAMGO (3 μM, b) partially inhibited fast p.s.ps. The DAMGO-induced inhibition was completely reversed by naloxone (1 μM, b). Opioid agonists had no direct effects on other membrane properties of the neurone. For abbreviations, see text.

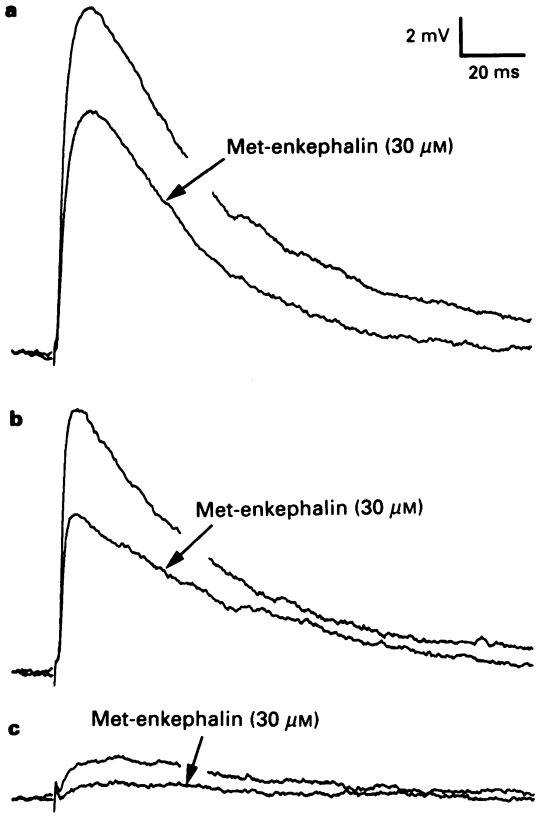

Figure 6 Met-enkephalin inhibits GABAergic, glutamatergic and residual components of fast p.s.ps in a single neurone. (a) In the presence of CNQX (10 μM), the remaining components of fast p.s.ps were predominantly GABAergic (including a small residual component). Met-enkephalin (30 μM) inhibited the GABAergic component of the p.s.p. (b) In the presence of bicuculline (10 μM), the remaining components of fast p.s.ps were predominantly glutamatergic (including a small residual component). Met-enkephalin (30 μM) also inhibited the glutamatergic component of the p.s.p. (c) In the presence of both CNQX (10 μM) and bicuculline (30 μM), the residual component of p.s.p. was also inhibited by Met-enkephalin (30 μM). Opioid agonists had no direct effects on other membrane properties of the neurone. For abbreviations, see text.

antagonist, naltrindole (10 nM) the effects of DPDPE were only partially reversed: 24 ± 1% of the inhibition remained ($n = 2$, Table 1). U50488H (3 μM) also inhibited fast p.s.ps (45 ± 15%, $n = 4$, Table 1), but these effects were not antagonized by naloxone (36 ± 16% of the inhibition remained, $n = 4$, Table 1). The solutions of DPDPE and U50488H used in these experiments were subsequently tested and found to be pharmacologically active on δ- and κ-receptors in mouse vas deferens (N. Lavidis, personal communication) and guinea-pig ileum preparations (data not shown), respectively.

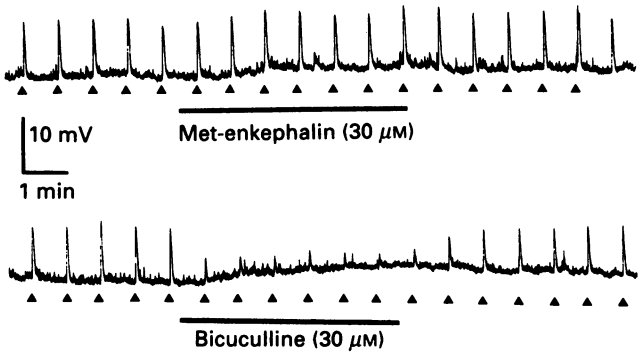

Figure 7 Met-enkephalin did not affect postsynaptic actions of GABA. Direct pressure ejections of GABA (100 mM) through a micropipette onto the impaled neurone produced depolarizations which were not affected by superfusion with Met-enkephalin (30 μM), but were antagonized by bicuculline (30 μM). The bars indicate periods of drug superfusion. The triangles mark the times of pressure ejections (each 20 ms duration).

Opioids inhibit glutamatergic and GABAergic components of evoked-p.s.ps

Opioids inhibited both glutamatergic and GABAergic components of fast p.s.ps in neurones which were not hyperpolarized by opioids. In the presence of CNQX (10 μM) the remaining components of fast p.s.ps were predominantly GABAergic with a small residual component which was resistant to glutamate- and $GABA_A$-receptor antagonists. In the presence of CNQX, Met-enkephalin (10–30 μM) inhibited fast p.s.ps by 55 ± 5% ($n = 12$, Figure 6a, Table 1).

Conversely, in the presence of bicuculline (30 μM), the remaining components of fast p.s.ps were predominantly glutamatergic with a small component which was resistant to glutamate and $GABA_A$-receptor antagonists. In the presence of bicuculline, Met-enkephalin (10–30 μM) inhibited fast p.s.ps by 48 ± 6% ($n = 11$, Figure 6b, Table 1).

In the presence of both CNQX (10 μM) and bicuculline (30 μM), Met-enkephalin (10–30 μM) also inhibited the residual component of fast p.s.ps (42 ± 15%, $n = 2$, Figure 6c, Table 1).

The Met-enkephalin-induced inhibition of the GABAergic component of fast p.s.ps was due to a presynaptic action. Direct application of GABA (100 mM) to neurones by pressure ejection produced depolarizations which were not affected by Met-enkephalin (30 μM, $n = 3$), but were fully antagonized by bicuculline (30 μM, $n = 2$, Figure 7).

Opioids inhibit spontaneous p.s.ps

Frequent (>1 Hz), large amplitude (>3 mV) spontaneous p.s.ps were observed in 11% (10/94) of neurones (Figure 8) which were not directly hyperpolarized by opioids. The amplitude of spontaneous p.s.ps ranged from several mV to

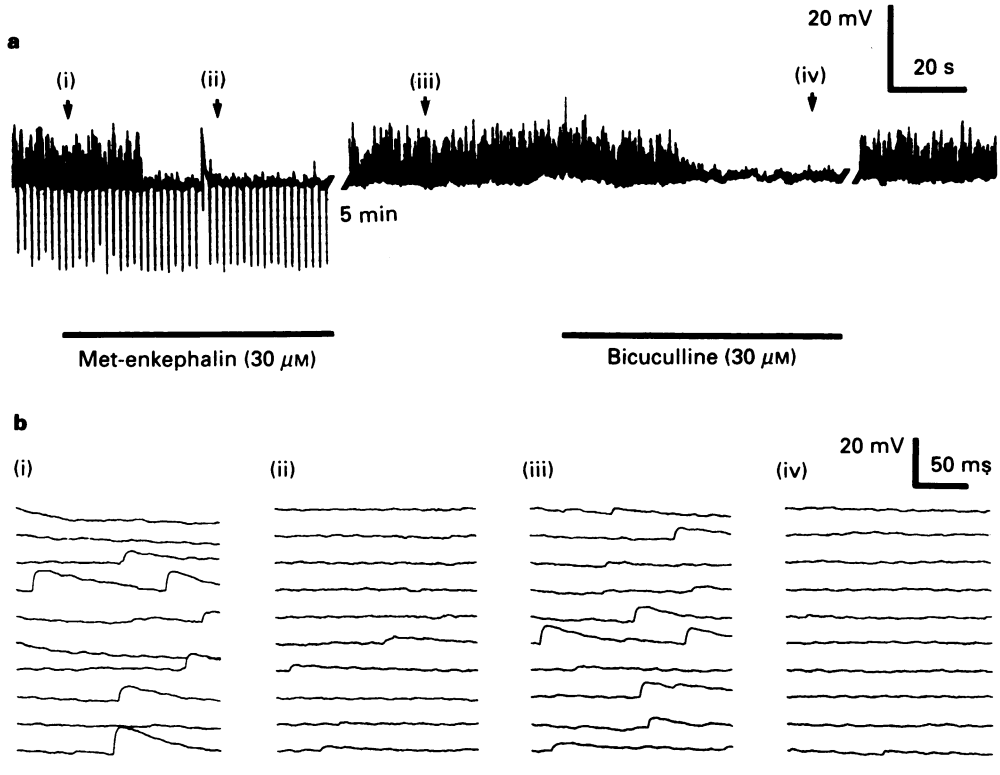

Figure 8 Met-enkephalin inhibited spontaneous p.s.ps. (a) Chart record showing that Met-enkephalin (30 μM) reversibly inhibited spontaneous p.s.ps (upward deflections) without affecting the membrane potential (resting potential −80 mV) or input resistance of the neurone (proportional to downward deflections). Spontaneous p.s.ps were completely abolished by bicuculline (30 μM). Downward deflections are membrane potential responses to current pulses passed through the recording electrode (80 pA, 250 ms) prior to and during superfusion with Met-enkephalin. The bars represent time periods of drug superfusion. (b) Each panel displays ten consecutive 200-ms trace of membrane potential (offset from bottom to top) sampled at times corresponding to the four different time points indicated above on the chart record. Met-enkephalin (30 μM) reduced the amplitude and frequency of spontaneous p.s.ps (ii), while bicuculline (30 μM) nearly abolished p.s.ps (iv).

more than 15 mV at −80 mV. The amplitude of spontaneous p.s.ps increased at more negative holding membrane potentials (data not shown). Bicuculline (30 μM) reversibly abolished spontaneous synaptic potentials ($n = 5$, Figure 8), but CNQX (10 μM) had no effect ($n = 2$, data not shown). Met-enkephalin (10 or 30 μM) inhibited spontaneous synaptic potentials in all neurones tested ($n = 6$, Figure 8).

Discussion

The present study demonstrated that GABAergic, glutamatergic and slow inhibitory (possibly 5-hydroxytryptaminergic) p.s.ps can be evoked by electrical stimulation in the vicinity of neurones located throughout the lateral and ventrolateral PAG. Opioid agonists selective for μ-receptors produced a similar inhibition of both GABAergic and glutamatergic components of synaptic potentials in neurones which were not directly hyperpolarized by opioids.

The amplitude of evoked p.s.ps was dependent on stimulus intensity and membrane potential, and p.s.ps were abolished by agents which block synaptic transmission. Both glutamatergic and GABAergic components of p.s.ps depolarized neurones at resting membrane potentials (−60 to −80 mV), and increased in amplitude at more negative membrane potentials. This was expected because reversal potentials for p.s.ps would be near 0 mV for glutamatergic, and −40 mV for GABAergic components when using electrodes containing 2 M KCl (e.g. Pan *et al.*, 1990).

Activation of $GABA_A$ receptors accounted for 44% of the amplitude of evoked p.s.ps and nonNMDA glutamate receptors accounted for 53%. Under the present recording conditions (1.2 mM Mg^{2+}), the residual component of p.s.ps in the presence of bicuculline and CNQX was partially mediated by NMDA receptors. In the presence of bicuculline, CNQX and APV a small residual component remained. However, it is not clear whether this was due to activation of other receptors, or because of incomplete antagonism of synaptically released GABA and glutamate. Although the proportion of synaptic potentials attributable to activation of $GABA_A$, glutamate, or other receptors varied considerably in different neurones, this was not clearly related to other anatomical, morphological or physiological differences between impaled neurones.

Slow inhibitory p.s.ps were evoked by single electrical stimuli in a small proportion (12%) of PAG neurones. They reversed polarity between −100 and −110 mV, consistent with mediation by an increased potassium conductance. They were blocked by superfusion with spiperone (1 μM), but not the α_2-adrenoceptor antagonist, idazoxan. Whilst these findings are preliminary, they possibly suggest that 5-hydroxytryptaminergic innervation of some PAG neurones mediates slow inhibitory p.s.ps via activation of $5\text{-}HT_{1A}$ receptors. Agonists which activate $5\text{-}HT_{1A}$-receptors have also been reported to hyperpolarize most neurones in the lateral and ventrolateral PAG (Behbehani *et al.*, 1993). It is not clear whether slow inhibitory p.s.ps might be evoked in a higher proportion of PAG neurones using stronger stimuli, or trains of high frequency stimuli (e.g. Egan *et al.*, 1983). The ventrolateral PAG also contains dense terminals of 5-hydroxytryptaminergic, adrenergic and noradrenergic neurones (Clements *et al.*, 1985; Herbert & Saper, 1992). Slow inhibitory p.s.ps which were blocked by spiperone, enhanced by fluoxetine, and mediated by increased potassium conductance were also reported to occur in neurones of the dorsal raphe nucleus (Pan *et al.*, 1989).

Opioids acting on μ-receptors inhibited both evoked- (by more than 55%) and spontaneous- (almost completely) GABAergic p.s.ps. The failure of opioid agonists to affect responses to exogenously applied GABA suggests that actions of opioids in PAG were due to presynaptic inhibition of neurotransmitter release. A possible contribution of κ- and/or δ-receptors to inhibition of p.s.ps cannot be ruled out because the agonists had non-specific effects, and biased sampling of large neurones by intracellular electrodes occurred (see Chieng & Christie, 1994, for discussion). McFadzean *et al.* (1987) also noted that high concentrations of U50488H produced non-specific inhibition of p.s.ps in locus coeruleus neurones.

The origin of opioid-sensitive GABAergic terminals which are responsible for evoked p.s.ps is uncertain. Most GABAergic fibres and terminals in PAG appear to arise from GABAergic interneurones, and appear to innervate most morphological types (Reichling & Basbaum, 1990a,b). It is therefore possible that inhibition of the GABAergic component of synaptic potentials was due to both direct inhibition of terminals and/or inhibition of the somata of local circuit neurones. Secondary components of p.s.ps often occurred up to 40 ms after the initial depolarization (eg. Figure 1b), supporting the possibility that local stimulation of local circuit neurones made some contribution to the observed p.s.ps. However, the decay of GABAergic synaptic potentials was not altered by opioids (data not shown), suggesting that later components were not selectively sensitive to opioids.

GABAergic mediation of spontaneous p.s.ps and their inhibition by Met-enkephalin was more striking than for evoked p.s.ps. It is tempting to speculate that spontaneous GABAergic p.s.ps arose from tonically active, opioid-sensitive neurones in PAG.

Selective μ-receptor agonists inhibited the glutamatergic component of p.s.ps by more than 48%. The origin of opioid-sensitive glutamatergic terminals is unclear. Glutamatergic terminals appear to arise from neurones located in various brain regions (Beart *et al.*, 1990; Beitz & Williams, 1991), but it is not clear whether glutamatergic terminals also arise from intrinsic neurones, nor whether they selectively innervate different types of neurones in PAG.

The present results only partially support the model suggesting that opioids produce disinhibition in PAG by inhibiting GABAergic interneurones (Yaksh *et al.*, 1976; Basbaum & Fields, 1984). Consistent with this model (see Introduction), μ-receptor agonists inhibited GABAergic synaptic potentials impinging on neurones which were not directly hyperpolarized by opioids. Some of these neurones could project to the ventral medulla and inhibition of GABAergic p.s.ps would be expected to produce excitation under normal physiological conditions. However, μ-receptor agonists produced nearly as much inhibition of glutamatergic synaptic potentials impinging on the same neurones. This finding suggests that the actions of opioids in PAG are more complex than suggested by a model of disinhibition.

The PAG is thought to be organised into anatomically and functionally distinct columns of neurones extending along the rostrocaudal axis (see Bandler *et al.*, 1991). The main antinociceptive zone identified by microinjections of opioids was reported to lie within the caudal ventrolateral column (Yaksh *et al.*, 1988). Presynaptic inhibition by opioids was quite uniform throughout the lateral and ventrolateral PAG, consistent with a role in antinociception. Opioids might also modulate other physiological roles of PAG including organisation of autonomic and somatic components of defence and escape behaviours, or perhaps cardio-respiratory functions (see Bandler *et al.*, 1991).

The authors thank Drs N. Lavidis and P.B. Osborne for their helpful comments. Donations of opioid peptides by the National Institute on Drug Abuse (U.S.A.) is gratefully acknowledged. This work was supported by the National Health and Medical Research Council of Australia (910831), National Heart Foundation and the Clive and Vera Ramaciotti Foundation.

References

BANDLER, R., CARRIVE, P. & DEPAULIS, A. (1991). Introduction: Emerging principles of organization of the midbrain periaqueductal gray matter. In *The Midbrain Periaqueductal Gray Matter*. ed. Depaulis, A. & Bandler, R. pp. 1–8. New York: Plenum Press.

BASBAUM, A.I. & FIELDS, H.L. (1984). Endogenous pain control systems: brainstem spinal pathways and endorphin circuitry. *Annu. Rev. Neurosci.*, **7**, 309–338.

BEART, P.M., SUMMERS, R.J., STEPHENSON, J.A., COOK, C.J. & CHRISTIE, M.J. (1990). Excitatory amino acid projections to the periaqueductal gray in the rat: a retrograde transport study utilizing D[^{3}H]aspartate and [^{3}H]GABA. *Neurosci.*, **34**, 163–176.

BEHBEHANI, M.M., JIANG, M. & CHANDLER, S.D. (1990). The effect of [Met]enkephalin on the periaqueductal gray neurons on the rat: an *in vitro* study. *Neurosci.*, **38**, 373–380.

BEHBEHANI, M.M., LIU, H., JIANG, M., PUN, R.Y.K. & SHIPLEY, M.T. (1993). Activation of serotonin$_{1A}$ receptors inhibits midbrain periaqueductal gray neurons of the rat. *Brain Res.*, **612**, 56–60.

BEITZ, A.J. & WILLIAMS, F.G. (1991). Localization of putative amino acid transmitters in the PAG and their relationship to the PAG-raphe magnus pathway. In *The Midbrain Periaqueductal Gray Matter*. ed. Depaulis, A. & Bandler, R., p. 305–327. New York: Plenum Press.

CHIENG, B. & CHRISTIE, M.J. (1994). Hyperpolarization by opioids acting on μ-receptors of a sub-population of rat periaqueductal gray neurones *in vitro*. *Br. J. Pharmacol.*, **113**, 121–128.

CLEMENTS, J.R., BEITZ, A.J., FLETCHER, T.F. & MULLETT, M.A. (1985). Immunocytochemical localization of serotonin in the rat periaqueductal gray: A quantiative light and electron microscopic study. *J. Comp. Neurol.*, **236**, 60–70.

EGAN, T.M., HENDERSON, G., NORTH, R.A. & WILLIAMS, J.T. (1983). Noradrenaline-mediated synaptic inhibition in rat locus coeruleus neurones. *J. Physiol.*, **345**, 477–488.

FIELDS, H.L., HEINRICHER, M.M. & MASON, P. (1991). Neurotransmitters in nociceptive modulatory circuits. *Annu. Rev. Neurosci.*, **14**, 219–245.

HERBERT, H. & SAPER, C. (1992). Organization of medullary adrenergic and noradrenergic projections to the periaqueductal gray matter in the rat. *J. Comp. Neurol.*, **315**, 34–52.

JOHNSON, S.W. & NORTH, R.A. (1992). Opioids excite dopamine neurons by hyperpolarization of local interneurons. *J. Neurosci.*, **12**, 483–488.

LACEY, M.G., MERCURI, N.B. & NORTH, R.A. (1989). Two cell types in rat substantia nigra zona compacta distinguished by membrane properties and the actions of dopamine and opioids. *J. Neurosci.*, **9**, 1233–1241.

McFADZEAN, I., LACEY, M.G., HILL, R.G. & HENDERSON, G. (1987). Kappa opioid receptor activation depresses excitatory synaptic input to rat locus coeruleus neurons *in vitro*. *Neurosci.*, **20**, 231–239.

MADISON, D.V. & NICOLL, R.A. (1988). Enkephalin hyperpolarizes interneurones in rat hippocampus. *J. Physiol.*, **398**, 123–130.

PAN, Z.Z., COLMERS, W.F. & WILLIAMS, J.T. (1989). 5-HT-mediated synaptic potentials in the dorsal raphe nucleus: interactions with excitatory amino acid and GABA neurotransmission. *J. Neurophysiol.*, **62**, 481–486.

PAN, Z.Z., WILLIAMS, J.T. & OSBORNE, P.O. (1990). Opioid actions on single nucleus raphe magnus neurons from rat and guinea-pig *in vitro*. *J. Physiol.*, **427**, 519–532.

REICHLING, D.B. (1991). GABAergic neuronal circuitry in the periaqueductal gray matter. In *The Midbrain Periaqueductal Gray Matter*. ed. Depaulis, A. & Bandler, R., pp. 329–344. New York: Plenum Press.

REICHLING, D.B. & BASBAUM, A.I. (1990a). Contribution of brainstem GABAergic circuitry to descending antinociceptive controls: I. GABA-immunoreactive projection neurons in the periaqueductal gray and nucleus raphe magnus. *J. Comp. Neurol.*, **302**, 370–377.

REICHLING, D.B. & BASBAUM, A.I. (1990b). Contribution of brainstem GABAergic circuitry to descending antinociceptive controls: II. Electron microscopic immunocytochemical evidence of GABAergic control over the projection from the periaqueductal gray to the nucleus raphe magnus in the rat. *J. Comp. Neurol.*, **302**, 378–393.

YAKSH, T.L., AL-RODHAN, N.R.F. & JENSEN, T.S. (1988). Sites of action of opiates in production of analgesia. *Prog. Brain Res.*, **77**, 371–394.

(Received January 4, 1994
Revised April 18, 1994
Accepted May 19, 1994

Br. J. Pharmacol. (1994), **113**, 310–316

Involvement of enzymatic degradation in the inactivation of tachykinin neurotransmitters in neonatal rat spinal cord

[1]H. Suzuki, K. Yoshioka, M. Yanagisawa, *O. Urayama, T. Kurihara, R. Hosoki, [2]K. Saito & M. Otsuka

Department of Pharmacology, Faculty of Medicine, Tokyo Medical and Dental University, Bunkyo-ku, Tokyo 113, Japan and *Department of Laboratory Medicine, Akita University School of Medicine, Akita 010, Japan

1 The possible involvement of enzymatic degradation in the inactivation of tachykinin neurotransmitters was examined in the spinal cord of the neonatal rat.

2 The magnitude of substance P (SP)- or neurokinin A (NKA)-evoked depolarization of a lumbar ventral root in the isolated spinal cord preparation was increased by a mixture of peptidase inhibitors, consisting of actinonin (6 μM), arphamenine B (6 μM), bestatin (10 μM), captopril (10 μM) and thiorphan (0.3 μM). The mixture augmented the response to NKA more markedly than that to SP.

3 In the isolated spinal cord-cutaneous nerve preparation, the saphenous nerve-evoked slow depolarization of the L3 ventral root was augmented by the mixture of peptidase inhibitors in the presence of naloxone (0.5 μM) but not in the presence of both naloxone and a tachykinin receptor antagonist, GR71251 (5 μM).

4 Application of capsaicin (0.5 μM) for 6 min to the spinal cord evoked an increase in the release of SP from the spinal cord. The amount of SP released was significantly augmented by the mixture of peptidase inhibitors.

5 Synaptic membrane fractions were prepared from neonatal rat spinal cords. These fractions showed degrading activities for SP and NKA and the activities were inhibited by the mixture of peptidase inhibitors. The degrading activity for NKA was higher than that for SP and the inhibitory effect of the mixture for NKA was more marked than that for SP. Although some other fractions obtained from homogenates of spinal cords showed higher degrading activities for SP, these activities were insensitive to the mixture of peptidase inhibitors.

6 Effects of individual peptidase inhibitors on the enzymatic degradation of SP and NKA by synaptic membrane fractions were examined. Thiorphan, actinonin and captopril inhibited SP degradation, while thiorphan and actinonin, but not captopril, inhibited NKA degradation. The potency of the inhibition of each peptidase inhibitor was lower than that of the mixture.

7 The present results suggest that enzymatic degradation is involved in the inactivation of tachykinin neurotransmitters in the spinal cord of the neonatal rat.

Keywords: Actinonin; captopril; C-fibre response; inactivation; neurotransmitter; peptidase; spinal cord; tachykinin; thiorphan

Introduction

Substance P (SP) fulfills several criteria for identification of neurotransmitters in mammalian spinal cord dorsal horn (for review see Otsuka & Yoshioka, 1993). Among the criteria, however, the demonstration of inactivation mechanisms of neurally released SP has not been fully satisfied until recently in the spinal cord, although a number of SP-degrading enzymes have been reported to exist in the central nervous system (Lee *et al.*, 1981; Matsas *et al.*, 1983; Oblin *et al.*, 1988). Recently, Yanagisawa *et al.* (1992) showed that a mixture of peptidase inhibitors increased the magnitude of saphenous nerve-evoked C-fibre responses in the isolated spinal cord of the neonatal rat. Based on this finding, they suggested that enzymatic degradation of SP, as well as neurokinin A (NKA), is involved in tachykininergic synaptic transmission in the spinal cord. However, there has been no biochemical evidence that the degradation of exogenously applied or endogenously released tachykinins is indeed blocked by the mixture of peptidase inhibitors in this preparation. Furthermore, the characteristics of peptidases responsible for the degradation of tachykinins have not been clarified. Although effects of peptidase inhibitors on released tachykinins have been examined biochemically in the spinal cord using slice preparations (Geppetti *et al.*, 1989; Mauborgne *et al.*, 1991) or intact animals (Duggan *et al.*, 1992), the isolated spinal cord preparation of neonatal rat has the advantage of enabling us to compare neurochemical effects of peptidase inhibitors with their electrophysiological effects in similar experimental conditions.

In the present study we examined, using the neonatal rat isolated spinal cord, the effects of peptidase inhibitors on the electrophysiological responses, capsaicin-evoked SP release and enzymatic degradation of SP and NKA by membrane fractions derived from the spinal cord. Some of the results have been reported in a preliminary form (Suzuki *et al.*, 1993).

Methods

Electrophysiological experiments

The isolated spinal cord preparation of the neonatal rat was used as described previously (Akagi *et al.*, 1980; Otsuka & Yanagisawa, 1988). The spinal cord below thoracic level was isolated from 1–3 day-old Wistar rats. The spinal cord was hemisected and placed in a recording chamber of 0.2 ml volume and perfused with artificial cerebrospinal fluid (CSF)

[1] Author for correspondence at: Department of Pharmacology, Faculty of Medicine, Tokyo Medical and Dental University, Yushima 1-5-45, Bunkyo-ku, Tokyo 113, Japan.
[2] Present address: Biological Research Laboratories, Sankyo Corporation Ltd., Tokyo 140, Japan.

saturated with a gas mixture of 95% O_2 and 5% CO_2. The composition of artificial CSF was as follows (mM): NaCl 138.6, KCl 3.35, $CaCl_2$ 1.26, $MgCl_2$ 1.16, $NaHCO_3$ 21.0, NaH_2PO_4 0.58, glucose 10.0. Potentials were recorded extracellularly from a lumbar ventral root (L3-5) with a tightly fitting suction electrode. Drugs were dissolved in artificial CSF and applied by perfusion.

The isolated spinal cord-saphenous nerve preparation was also used as described previously (Nussbaumer *et al.*, 1989). The spinal cord below thoracic level, without hemisection, together with lumbar ventral and dorsal roots, dorsal root ganglia, and attached femoral and saphenous nerves on one side, was dissected out, placed in a recording chamber and perfused with artificial CSF. The temperature of the chamber was kept at 27°C for both preparations. Stable reflex responses could be recorded for at least several hours at this temperature (Otsuka & Konishi, 1974).

The composition of the mixture of peptidase inhibitors used in the present electrophysiological study was the same as that used in previous experiments (Yanagisawa *et al.*, 1992) and consisted of actinonin (6 μM), arphamenine B (6 μM), bestatin (10 μM), captopril (10 μM) and thiorphan (0.3 μM). Actinonin and arphamenine B were used at 10 μM instead of 6 μM in the experiments for SP release and tachykinin degradation. These mixtures will be simply referred to as the mixture of peptidase inhibitors in this paper.

Release experiments

Experimental procedures used in the present study were similar to those described previously (Akagi *et al.*, 1980; Sakuma *et al.*, 1991). Under ether anesthesia, the spinal cord below thoracic segments was isolated from 2–4 day-old Wistar rat and hemisected. A pair of hemisected cords were separately fixed in two different perfusion chambers of 1 ml volume and continuously perfused with artificial CSF at a rate of 0.7 ml min^{-1}, respectively. The perfusion medium was thoroughly oxygenated both in the reservoir of artificial CSF and the perfusion chambers by bubbling with a gas mixture of 95% O_2 and 5% CO_2. The temperature in the chambers was maintained at 27°C. After the spinal cords were washed with artificial CSF for about 1.5 h, one hemisected cord was perfused with artificial CSF containing dithiothreitol (DTT, 5 μM) and the other was perfused with artificial CSF containing DTT (5 μM) and the mixture of peptidase inhibitors. Twenty min after the start of perfusion with these solutions, 3 min fractions were collected through a glass wool filter into test tubes containing 500 μl 1 M formic acid. After two 3 min fractions were collected representing basal release, capsaicin (0.5 μM) was bath-applied for 6 min. The collected samples were frozen and lyophilized. Each sample was dissolved in 1 ml of enzyme immunoassay (EIA) buffer and the amount of SP was measured by EIA according to the instruction manual (Cayman Chemical Co.).

Preparation of membrane fractions

Synaptic membranes were prepared from spinal cords of 3 to 5 day old rats as described by Whittaker *et al.* (1964). All procedures were carried out at 4°C. Spinal cords were homogenized in 0.32 M sucrose and centrifuged at 1,000 *g* for 15 min. The supernatant was centrifuged at 10,000 *g* for 15 min and the pellet was resuspended in 0.32 M sucrose and again centrifuged at 10,000 *g* for 15 min. The resultant pellet (P2) was resuspended in water, incubated in an ice bath for 30 min, re-homogenized and centrifuged at 10,000 *g* for 15 min. The supernatant of the water-treated P2 fraction (referred to as P2 sup) was transferred onto discontinuous density gradient of sucrose and ultracentrifuged at 68,200 *g* for 120 min. The fraction containing synaptic vesicles in 0.4 M sucrose layer (SV fraction), the fractions containing synaptic membranes between 0.6 M and 0.8 M sucrose layers and between 0.8 M and 1.0 M sucrose layers (SM fractions) were diluted with water and centrifuged at 200,000 *g* for 30 min and the pellets were resuspended in 0.32 M sucrose.

Immunoblotting for Na^+/K^+-transporting adenosinetriphosphatase, a membrane-embedded protein (Kyte, 1981), using rabbit anti-serum against pig kidney (Wada *et al.*, 1992) revealed that this enzyme was concentrated in the both SM fraction, indicating that these fractions are rich in plasma membranes. Since preliminary experiments showed no difference in the SP- and NKA-degrading activities between the SM fractions of 0.6–0.8 M sucrose layers and that of 0.8–1.0 M sucrose layers, we used either SM fraction for the measurement of the SP- and NKA-degrading activities.

Measurement of SP- and NKA-degrading activities

Samples of SM, SV or P2 sup fractions, containing 5–10 μg protein for SM or SV, and 3 μg protein for P2 sup, were incubated at 27°C in 50 mM Tris-HCl buffer (pH 7.4) in a final volume of 100 μl. The reaction was started by adding SP or NKA at a final concentration of 2 μM and stopped after 120 min by placing the tubes in an ice bath and adding formic acid at a final concentration of 250 mM. After centrifugation, the supernatant was injected into high-performance liquid chromatography (h.p.l.c.) and the amount of the remaining substrate was measured. The h.p.l.c. apparatus consisted of a pump (880-U, Nihon Bunko), a gradient programmer (GP-A40, Nihon Bunko), a column oven (860-CO, Nihon Bunko) set at 40°C and a u.v. detector (UNIDEC 100-VI, Nihon Bunko) monitoring the absorbance at 210 nm. Peptides were separated on a reverse phase column (TSK 120T, Toso) at a flow rate of 1 ml min^{-1} using a linear gradient from 100% solvent A to 40% solvent A/60% solvent B in 30 min. Solvent A was 5% acetonitrile in 0.02% HCl (v/v) and solvent B was 60% acetonitrile in 0.02% HCl (v/v). Under these conditions, NKA and SP were eluted at retention times of 27 min and 29 min, respectively.

Protein was measured by the method of Lowry *et al.* (1951).

Materials

Actinonin, arphamenine B, bestatin, captopril, NKA, SP and thiorphan were purchased from Peptide Institute Inc., Osaka, Japan; capsaicin from Sigma Chemical Co., St. Louis, MO, U.S.A.; tetrodotoxin (TTX) from Sankyo Corporation Ltd., Tokyo, Japan; and SP EIA kit from Cayman Chemical Co., Ann Arbor, MI., U.S.A. GR71251 (D-Pro^9[spiro-γ-lactam] Leu^{10},Trp^{11}]SP) was a gift from Dr R.M. Hagan, Department of Neuropharmacology, Glaxo Group Research Ltd., Park Road, Ware, UK.

Statistical analysis

Values are expressed as mean ± s.e.mean. Statistical significance was assessed by Student's unpaired *t* test (equal or unequal variance).

Results

Effect of peptidase inhibitors on SP- and NKA-evoked depolarization of motoneurones in the neonatal rat spinal cord

Applications of SP or NKA for 30 s to the spinal cord preparation elicited depolarizing responses of lumbar ventral roots in the presence of 0.3 μM TTX in a dose-dependent manner (Yanagisawa & Otsuka, 1990). These responses were augmented by the mixture of the peptidase inhibitors (Figure 1). The responses to NKA at 0.03–0.3 μM were more markedly increased by the mixture of peptidase inhibitors than those evoked by SP (Figure 1).

Effects of naloxone and peptidase inhibitors on slow ventral root potential evoked by saphenous nerve stimulation

In the spinal cord-saphenous nerve preparation, electrical stimulation of the saphenous nerve evoked a slow depolarization lasting 20–30 s of the ipsilateral L3 ventral root (Figure 2). This response will be referred to as saphenous nerve-evoked slow ventral root potential (VRP). The magnitude of the saphenous nerve-evoked slow VRP, expressed as the area under the curve of the depolarizing response (m × Vs), was augmented by about 20% by naloxone at 0.5 μM (Nussbaumer *et al.*, 1989), suggesting the involvement of opioid peptide-mediated inhibition in the slow VRP. In the presence of naloxone, application of the peptidase inhibitor mixture further increased the magnitude of the slow VRP by 25% (Figure 2), confirming the results by Yanagisawa *et al.* (1992). By contrast, application of a tachykinin NK_1 receptor antagonist, GR71251 (Ward *et al.*, 1990; Guo *et al.*, 1993), at 5 μM, depressed the slow VRP by about 50% in naloxone-treated preparations (Figure 3). After the treatment with GR71251 and naloxone eliminating both tachykinin-mediated and opioid peptide-mediated mechanisms, the peptidase inhibitor mixture no longer augmented the slow VRP (Figure 3).

Effects of peptidase inhibitors on the release of endogenous SP from the spinal cord

When a hemisected spinal cord was perfused with artificial CSF, the basal release of SP was about 13.8 fmol mg^{-1} protein in 3 min ($n = 5$) (Table 1). Bath-application of capsaicin (0.5 μM) for 6 min to the spinal cord resulted in an increase in the SP release: during the period of 3–6 min after addition of capsaicin, the SP release became maximum, being about three fold higher than that of the basal level (Table 1) and the increase lasted for more than 10 min (Figure 4). The delay of the increase in the SP release may be largely due to

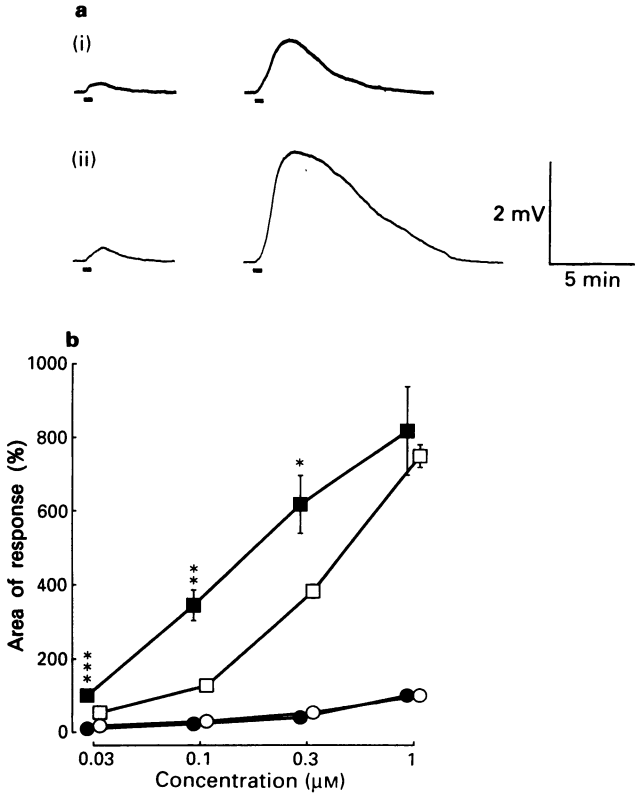

Figure 1 Effects of the mixture of peptidase inhibitors on substance P (SP)- and neurokinin A (NKA)-induced depolarizations of lumbar ventral roots. The experiment was done in the presence of tetrodotoxin (TTX, 0.3 μM). SP and NKA were applied by perfusion for 30 s. The inhibitor mixture consisted of actinonin (6 μM), arphamenine B (6 μM), bestatin (10 μM), captopril (10 μM) and thiorphan (0.3 μM) and was dissolved in artificial CSF. (a) Sample records: (i) responses to SP at 0.3 μM before (left) and 15 min after addition of the inhibitor mixture (right); (ii) responses to NKA at 0.3 μM before (left) and 15 min after addition of the inhibitor mixture (right). (b) Effects of the mixture of peptidase inhibitors on the concentration-response curves for SP and NKA: (○) SP-evoked responses in the absence of the inhibitor mixture and (□) 15 min after addition of the inhibitor mixture; (●) NKA-evoked responses in the absence of the inhibitor mixture and (■) 15 min after addition of the inhibitor mixture. Ordinate scale: area of the depolarizing response (mV × s) expressed as percentage of the response evoked by 1 μM SP or NKA in the absence of the inhibitor mixture. Abscissa scale: concentration of SP or NKA. Each point represents the mean ± s.e.mean ($n = 7$ for SP and $n = 6$ for NKA). Symbols are displaced horizontally to avoid overlapping. $^{*}P<0.05$; $^{**}P<0.01$, $^{***}P<0.001$ when the difference between the NKA-evoked responses in the presence and absence of the peptidase inhibitor mixture was compared with the corresponding difference between the SP responses at each agonist concentration.

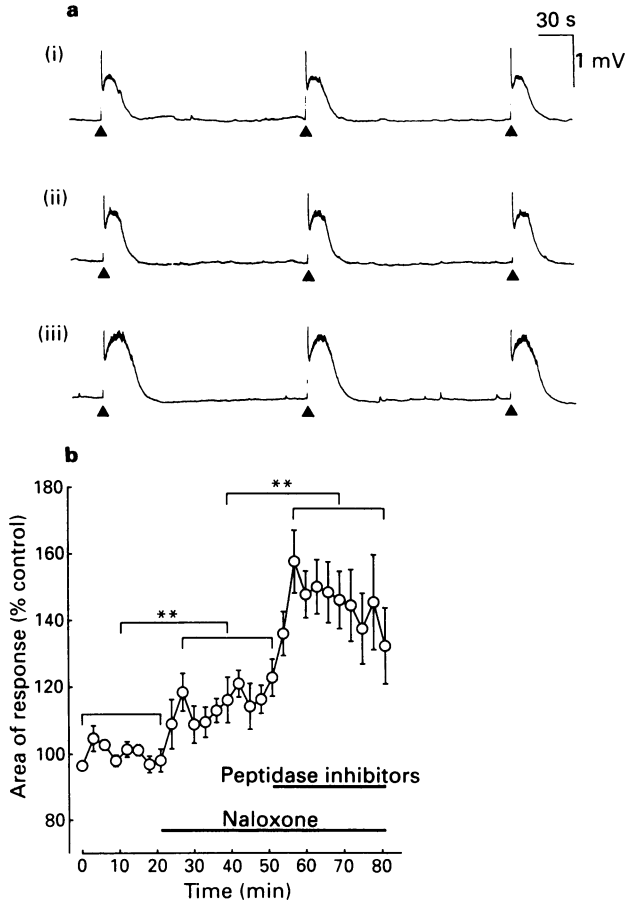

Figure 2 Effects of naloxone and the peptidase inhibitor mixture on the saphenous nerve-evoked slow VRP in isolated spinal cord-saphenous nerve preparations. (a) Sample records: (i) control responses; (ii) responses after addition of naloxone (0.5 μM); (iii) responses after addition of naloxone and the mixture of peptidase inhibitors (the same composition as that in Figure 1). The saphenous nerve was stimulated every 3 min with double square pulses of 100 μs duration and supramaximal intensity at 50 ms interval at ▲. (b) Time course of the responses. Naloxone (0.5 μM) and the mixture of peptidase inhibitors were applied to spinal cords by perfusion during the periods indicated by horizontal bars. Areas of the depolarizing responses in mV × s were measured and expressed as percentages of the average value in normal artificial CSF. Each point represents mean ± s.e.mean ($n = 7$). **Represents a significant difference between the average values of the points under the horizontal bars ($P<0.01$).

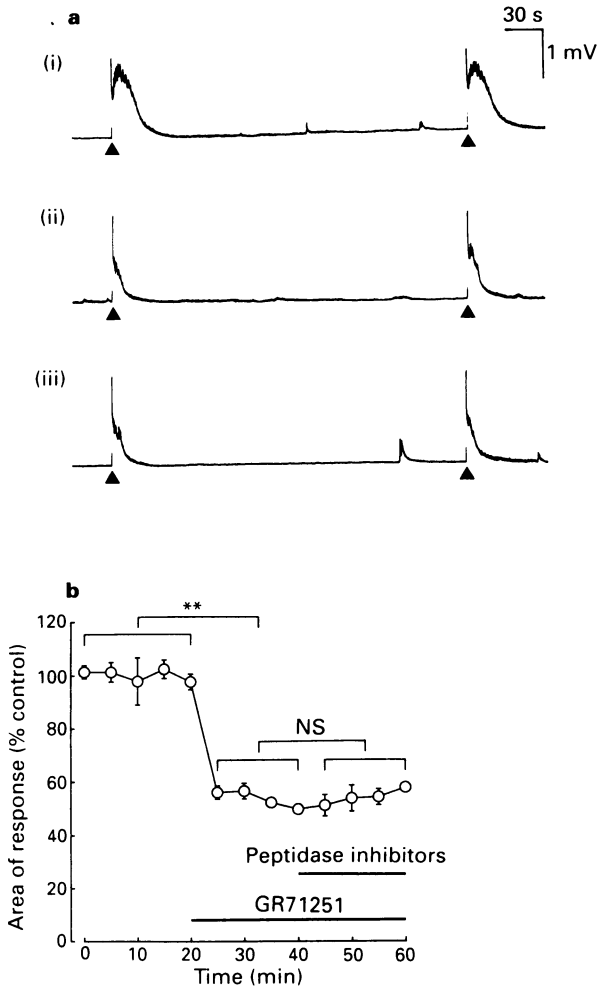

Figure 3 Effects of GR71251 and the mixture of peptidase inhibitors on the saphenous nerve-evoked slow VRP in the isolated spinal cord-saphenous nerve preparations. Naloxone (0.5 μM) was present in perfusion solution throughout the experiments. (a) Sample records: (i) control responses in the presence of naloxone; (ii) responses after addition of GR71251 (5 μM); (iii) responses after addition of GR71251 and the mixture of peptidase inhibitors. Experimental procedures were the same as in Figure 2 except that the saphenous nerve was stimulated every 5 min at ▲. (b) Time course of the responses. Drugs were applied during the periods indicated by the horizontal bars. Each point represents mean ± s.e.mean ($n = 5$). **Represents a significant difference between the average values of the points under the horizontal bars ($P < 0.01$). NS: no significant difference.

Table 1 Capsaicin-evoked substance P (SP) release and the effects of the mixture of peptidase inhibitors

	Control	*+ Inhibitor mixture*
Basal release	13.8 ± 2.9	15.7 ± 2.7
Maximum evoked release (fmol mg^{-1} protein in 3 min collection)	37.5 ± 6.2	86.7 ± 15.5*

Capsaicin (0.5 μM) was applied for 6 min to the spinal cord in the absence or presence of the inhibitor mixture. The maximum evoked release occurred during the period of 3–6 min after addition of capsaicin in the absence of the inhibitor mixture and during the period of 6–9 min in the presence of the inhibitor mixture, respectively. The inhibitor mixture consisted of actinonin (10 μM), arphamenine B (10 μM), bestatin (10 μM), captopril (10 μM) and thiorphan (0.3 μM). Each value represents mean ± s.e.mean ($n = 5$) of the SP release during a 3 min collection period. *$P < 0.05$ when compared with the value of maximum evoked release in the absence of the inhibitor mixture by Student's t test.

the delay in the exchange of the medium in the chamber (Sakuma *et al.*, 1991). When the peptidase inhibitor mixture was applied, the basal SP release was 15.7 fmol mg^{-1} protein in 3 min ($n = 5$), which was not significantly different from the basal release in the absence of the mixture (Table 1). The peptidase inhibitor mixture, however, markedly increased the capsaicin-evoked SP release. During the period of 6–9 min after addition of capsaicin, the SP release was maximum and was about two fold higher than the maximum release in the absence of the mixture (Table 1). Moreover, the time course of the increased SP release was markedly prolonged by the peptidase inhibitor mixture (Figure 4).

Effects of peptidase inhibitors on tachykinin-degrading activities of synaptic membranes

When SP (2 μM) was used as a substrate, the degrading activity of the SM fractions was 88.4 pmol min^{-1} mg^{-1} protein ($n = 26$) (Table 2). The peptidase inhibitor mixture inhibited the SP-degrading activity of the SM fractions to 34.1% ($n = 12$) of the control (Table 2). Both SV and P2 sup fractions showed SP-degrading activities much higher than that of the SM fractions (Table 2). The activities of SV and P2 sup fractions, however, were not inhibited by the peptidase inhibitor mixture.

Effects of individual peptidase inhibitors on the SP degradation were also examined (Table 3). Of five inhibitors, thiorphan (0.3 μM) was the most potent in inhibiting the SP-degradation by the SM fractions, followed by captopril (10 μM) and actinonin (10 μM). Arphamenine B (10 μM) and bestatin (10 μM) had little inhibitory effect. Although thiorphan was the most potent, its inhibitory effect was less potent than that of the peptidase inhibitor mixture (Table 3). The inhibitory effect of actinonin increased dose-dependently in the concentration range from 1 to 100 μM, while that of thiorphan was almost maximal at 0.3 μM (Table 4).

When NKA (2 μM) was used as a substrate instead of SP, the degrading activity of the SM fractions was 137 pmol min^{-1} mg^{-1} protein ($n = 9$) (Table 2), which was significantly higher than that for SP. The peptidase inhibitor mixture caused an inhibition of the degrading activity of the SM fractions for NKA to 10.2%. This inhibition was also

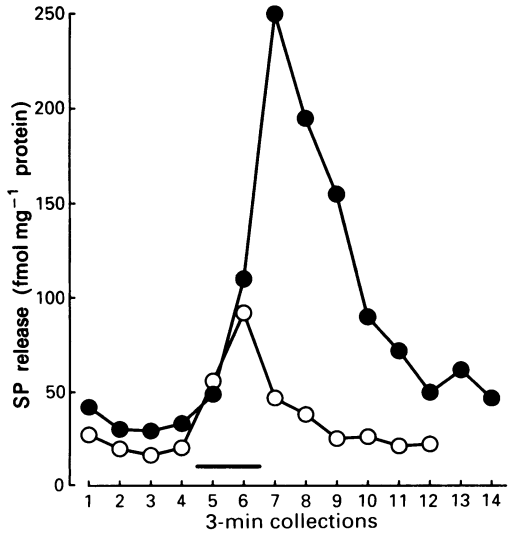

Figure 4 Capsaicin-evoked substance P (SP) release and effect of the peptidase inhibitor mixture. Typical results obtained from a pair of hemisected spinal cords. Ordinate scale: amount of SP release in each 3 min fraction. Abscissa scale: tube numbers. Capsaicin (0.5 μM) was applied for 6 min as indicated by the horizontal bar. Fractions 1 to 4, basal levels; fractions 5 and 6, during perfusion with capsaicin; fractions 7 to 14, after changing to normal artificial CSF: (○) in normal artificial CSF; (●) in artificial CSF containing the peptidase inhibitor mixture (the same composition as that in Table 1).

Table 2 Degrading activities of tissue fractions for substance P (SP) and neurokinin A (NKA) and the effects of the mixture of peptidase inhibitors

	Fraction		
	SM	*SV*	*P2 sup*
SP-degrading activity (pmol min^{-1} mg^{-1} protein)	88.4 ± 5.37 (26)	348.7 ± 10.7 (3)	986.0 ± 53.5 (3)
+ Inhibitor mixture (% control)	34.1 ± 4.8** (12)	104.2 ± 2.5 (3)	96.7 ± 1.7 (3)
NKA-degrading activity (pmol min^{-1} mg^{-1} protein)	137.0 ± 11.1†† (9)		
+ Inhibitor mixture (% control)	10.2 ± 4.1**†† (8)		

SM, synaptic membrane fraction; SV, synaptic vesicle fraction; P2 sup, P2 supernatant. The composition of the inhibitor mixture was the same as that in Table 1. Each value represents mean ± s.e.mean. Numbers in parentheses indicate numbers of experiments. $^{**}P<0.01$ when compared with the control value by Student's t test. $\dagger\dagger P<0.01$ when compared with the corresponding value for SP by Student's t test.

significantly more pronounced than that for SP. Actinonin and thiorphan were effective at 10 μM and 0.3 μM respectively, whereas other inhibitors were ineffective at 10 μM (Table 3). Furthermore, actinonin inhibited the degradation of NKA more markedly than that of SP.

Discussion

The present study showed that the cutaneous nerve-evoked slow VRP was augmented by the mixture of peptidase inhibitors in the presence of naloxone and that this augmentation was not observed after pretreatment with the tachykinin NK_1 receptor antagonist, GR71251. These results suggest that tachykinins released upon nerve stimulation in the neonatal rat spinal cord are partially inactivated by peptidases before acting on their receptors. The fact that naloxone treatment augmented the slow VRP is consistent with the similar observations by Yanagisawa *et al.* (1984) and Nussbaumer *et al.* (1989), suggesting that opioid peptide-mediated inhibition are involved in the slow VRP.

Table 3 Effects of peptidase inhibitors on the degradation of substance P (SP) and neurokinin A (NKA) by the synaptic membrane fractions

	SP-degrading activity (% control)	*NKA-degrading activity* (% control)
Peptidase inhibitor		
Mixture	34.1 ± 4.8** (12)	10.2 ± 4.1**†† (8)
Actinonin	69.8 ± 7.6* (13)	35.1 ± 3.5**†† (4)
Arphamenine B	82.2 ± 14.9 (6)	93.6 ± 8.1 (4)
Bestatin	85.5 ± 9.4 (6)	96.3 ± 10.9 (4)
Captopril	65.8 ± 9.8* (7)	96.5 ± 10.7 (4)
Thiorphan	49.4 ± 5.0** (18)	36.5 ± 12.6** (4)

Values are the SP- and NKA-degrading activities in the presence of inhibitors expressed as percentages of the control degrading activities in the absence of inhibitors. Peptidase inhibitors used were as follows: the mixture of peptidase inhibitors (the same composition as that in Table 1); actinonin 10 μM; arphamenine B 10 μM; bestatin 10 μM; captopril 10 μM; thiorphan 0.3 μM. Each value represents mean ± s.e.mean. Numbers in parentheses indicate numbers of experiments. $^{*}P<0.05$ and $^{**}P<0.01$, when compared with 100% by Student's t test. $\dagger\dagger P<0.01$ when compared with the corresponding value for SP by Student's t test.

The amount of capsaicin-evoked SP release was increased by the peptidase inhibitor mixture. Since capsaicin is known to depolarize C-fibre afferents (Kenins, 1982), this result further suggests that endogenous SP released from C-fibre terminals in the spinal cord is degraded by peptidases. The peak time of the capsaicin-evoked SP release was displaced from 3–6 min after the addition of capsaicin to 6–9 min by the mixture of peptidase inhibitors. This may be explained at least partly by the assumption that the degradation of SP by tissue peptidases during diffusion of SP molecules curtailed the later part of the SP outflow, and that this process was suppressed by peptidase inhibitors.

The present results also showed that SP was degraded by the SM fractions and the SP degradation was inhibited by the mixture of peptidase inhibitors at the same or almost the same concentrations as those used in the release and electrophysiological experiments. In contrast, the SP-degrading activities of P2 sup and SV fractions were insensitive to the peptidase inhibitor mixture. These results suggest that membrane-bound peptidases are involved in the inactivation of SP released from nerve terminals.

The SM fractions also caused degradation of NKA, which was inhibited by peptidase inhibitors. Furthermore, the peptidase inhibitor mixture augmented the NKA-evoked ventral root depolarization. It is therefore likely that the released NKA is at least partly degraded by membrane-bound pep-

Table 4 Concentration-dependent effects of actinonin and thiorphan on the degradation of substance P (SP) by the synaptic membrane fractions

	Actinonin (μM)		
	1	10	100
SP-degrading activity (% control)	93.5 ± 2.2* (8)	69.7 ± 7.6** (13)	52.1 ± 9.2** (8)
	Thiorphan (μM)		
	0.03	0.3	3
	65.8 ± 10.3* (7)	49.4 ± 5.0** (18)	44.5 ± 8.8** (8)

Values are the SP-degrading activities in the presence of inhibitors expressed as percentages of the control degrading activities in the absence of the inhibitors. Each value represents the mean ± s.e.mean. Numbers in parentheses indicate numbers of experiments. $^{*}P<0.05$ and $^{**}P<0.01$ when compared with 100% by Student's t test.

tidases and that the potentiating effect of the inhibitor mixture on the slow VRP is partly due to the inhibition of enzymatic degradation of NKA. The degrading activity of the SM fractions of NKA was higher than that on SP and the inhibition of the NKA degradation by the peptidase inhibitor mixture was more marked than that of the SP degradation (Table 2). These results are consistent with the results of electrophysiological experiments in which NKA-evoked depolarization was more markedly augmented than the SP-evoked depolarization by the peptidase inhibitor mixture (Figure 1). Duggan *et al.* (1992), however, reported that NKA was more resistant to enzymatic degradation than SP in the cat spinal cord. The discrepancy may be due to species differences.

In our preliminary experiments, the saphenous nerve-evoked slow VRP was not significantly augmented by each of the peptidase inhibitors alone. This appears consistent with the observation that the inhibitory effects of each inhibitor on SP- and NKA-degrading activities were less marked than those of the peptidase inhibitor mixture (Table 3). These results suggest that more than one peptidase is involved in the degradation of tachykinins in the spinal cord. Contribution of more than one peptidase to SP degradation was also postulated in the studies on caudate synaptic membranes (Matsas *et al.*, 1983), rat plasma (Ahmad *et al.*, 1992) and human cultured synovial fibroblasts (Bathon *et al.*, 1992).

Of the peptidase inhibitors examined, thiorphan, a specific inhibitor of enkephalinase (Roques *et al.*, 1980), was most potent in inhibiting the SP degradation by the SM fractions, which suggests that enkephalinase is mainly involved in the inactivation of SP in the spinal cord. SP, as well as enkephalins, is a favourable substrate for this enzyme (Turner *et al.*, 1985; Roques *et al.*, 1993), and involvement of enkephalinase in the SP inactivation has also been reported in other areas in the central nervous system and peripheral tissues (Matsas *et al.*, 1983; Oblin *et al.*, 1988; Djokic *et al.*, 1989).

Actinonin is a relatively specific inhibitor of aminopeptidase N and enkephalin aminopeptidase (Hachisu *et al.*, 1987) and captopril inhibits peptidyl dipeptidase A (Ondetti *et al.*, 1977). Aminopeptidase N and peptidyl dipeptidase A are known to degrade SP (Ahmad *et al.*, 1992). These peptidases, therefore, may also contribute to the SP degradation in the spinal cord, because actinonin and captopril showed significant inhibitory activities on the SP degradation by the SM fractions. Actinonin, however, has also been shown to inhibit the activity of enkephalinase at higher concentrations (Hachisu *et al.*, 1987). It is therefore possible that the effects of actinonin at 10 μM and 100 μM are partly due to inhibition of enkephalinase. Arphamenine B inhibits aminopeptidase B (Umezawa *et al.*, 1983) and bestatin inhibits aminopeptidases B and W and leucine aminopeptidase (Umezawa *et al.*, 1976; Tieku & Hooper, 1992). Since both inhibitors were almost ineffective, these aminopeptidases do not seem to contribute significantly to the SP degradation in the neonatal rat spinal cord.

The NKA degradation by the SM fractions, like the SP degradation, was potently inhibited by thiorphan. The NKA degradation, however, was more effectively inhibited by actinonin than the SP degradation. In addition, the NKA degradation was insensitive to captopril. The latter result is consistent with that of Hooper *et al.* (1985) who found that peptidyl dipeptidase A from pig kidney, which is an enzyme sensitive to captopril, hydrolyzed SP but not NKA. The results together suggest that the peptidases responsible for the inactivation are different among tissues and tachykinins.

The mixture of peptidase inhibitors used in the present study did not completely inhibit the degradation of SP and NKA. Some peptidases that are insensitive to the inhibitors used may be involved in the degradation. Furthermore, additional mechanisms other than enzymatic degradation, such as uptake by surrounding cells, may also be involved in the inactivation of tachykinins at synapses, although Segawa *et al.* (1977) showed that SP itself is not taken up by CNS tissues.

We thank Dr R.M. Hagan, Department of Neuropharmacology, Glaxo Group Research Ltd. for the gift of GR71251. This work was supported by grants-in-aid for scientific research from the Ministry of Education, Science and Culture, Japan (Nos. 04255101, 05557117 and 05454147).

References

AHMAD, S., WANG, L. & WARD, P.E. (1992). Dipeptidyl (amino) peptidase IV and aminopeptidase M metabolize circulating substance P in vivo. *J. Pharmacol. Exp. Ther.*, **260**, 1257–1261.

AKAGI, H., OTSUKA, M. & YANAGISAWA, M. (1980). Identification by high-performance liquid chromatography of immunoreactive substance P released from isolated rat spinal cord. *Neurosci. Lett.*, **20**, 259–263.

BATHON, J.M., PROUD, D., MIZUTANI, S. & WARD, P.E. (1992). Cultured human synovial fibroblasts rapidly metabolize kinins and neuropeptides. *J. Clin. Invest.*, **90**, 981–991.

DJOKIC, T.D., NADEL, J.A., DUSSER, D.J., SEKIZAWA, K., GRAF, P.D. & BORSON, D.B. (1989). Inhibitors of neutral endopeptidase potentiate electrically and capsaicin-induced noncholinergic contraction in guinea pig bronchi. *J. Pharmacol. Exp. Ther.*, **248**, 7–11.

DUGGAN, A.W., SCHAIBLE, H.-G., HOPE, P.J. & LANG, C.W. (1992). Effect of peptidase inhibition on the pattern of intraspinally released immunoreactive substance P detected with antibody microprobes. *Brain Res.*, **579**, 261–269.

GEPPETTI, P., SANTICIOLI, P., RUBINI, I., SPILLANTINI, M.G., MAGGI, C.A. & SICUTERI, F. (1989). Thiorphan increases capsaicin-evoked release of substance P from slices of dorsal spinal cord of guinea pig. *Neurosci. Lett.*, **103**, 67–73.

GUO, J.-Z., YOSHIOKA, K., YANAGISAWA, M., HOSOKI, R., HAGAN, R.M. & OTSUKA, M. (1993). Depression of primary afferent-evoked responses by GR71251 in the isolated spinal cord of the neonatal rat. *Br. J. Pharmacol.*, **110**, 1142–1148.

HACHISU, M., HIRANUMA, T., SHIBAZAKI, Y., UOTANI, K., MURATA, S., AOYAGI, T. & UMEZAWA, H. (1987). Composite effects of actinonin when inhibiting enkephalin-degrading enzymes. *Eur. J. Pharmacol.*, **137**, 59–65.

HOOPER, N.M., KENNY, A.J. & TURNER, A.J. (1985). The metabolism of neuropeptides. Neurokinin A (substance K) is a substrate for endopeptidase-24.11 but not for peptidyl dipeptidase A (angiotensin-converting enzyme). *Biochem. J.*, **231**, 357–361.

KENINS, P. (1982). Responses of single nerve fibres to capsaicin applied to the skin. *Neurosci. Lett.*, **29**, 83–88.

KYTE, J. (1981). Molecular considerations relevant to the mechanism of active transport. *Nature*, **292**, 201–204.

LEE, C.-M., SANDBERG, B.E.B., HANLEY, M.R. & IVERSEN, L.L. (1981). Purification and characterisation of a membrane-bound substance-P-degrading enzyme from human brain. *Eur. J. Biochem.*, **114**, 315–327.

LOWRY, O.H., ROSEBROUGH, N.J., FARR, A.L. & RANDALL, R.J. (1951). Protein measurement with the folin phenol reagent. *J. Biol. Chem.*, **193**, 265–275.

MATSAS, R., FULCHER, I.S., KENNY, A.J. & TURNER, A.J. (1983). Substance P and [Leu]enkephalin are hydrolyzed by an enzyme in pig caudate synaptic membranes that is identical with the endopeptidase of kidney microvilli. *Proc. Natl. Acad. Sci. U.S.A.*, **80**, 3111–3115.

MAUBORGNE, A., BOURGOIN, S., BENOLIEL, J.J., HAMON, M. & CESSELIN, F. (1991). Is substance P released from slices of the rat spinal cord inactivated by peptidase(s) distinct from both 'enkephalinase' and 'angiotensin-converting enzyme'? *Neurosci. Lett.*, **123**, 221–225.

NUSSBAUMER, J.-C., YANAGISAWA, M. & OTSUKA, M. (1989). Pharmacological properties of a C-fibre response evoked by saphenous nerve stimulation in an isolated spinal cord-nerve preparation of the newborn rat. *Br. J. Pharmacol.*, **98**, 373–382.

OBLIN, A., DANSE, M.J. & ZIVKOVIC, B. (1988). Degradation of substance P by membrane peptidases in the rat substantia nigra: effect of selective inhibitors. *Neurosci. Lett.*, **84**, 91–96.

ONDETTI, M.A., RUBIN, B. & CUSHMAN, D.W. (1977). Design of specific inhibitors of angiotensin-converting enzyme: new class of orally active antihypertensive agents. *Science*, **196**, 441–444.

OTSUKA, M. & KONISHI, S. (1974). Electrophysiology of mammalian spinal cord in vitro. *Nature*, **252**, 733–734.

OTSUKA, M. & YANAGISAWA, M. (1988). Effect of a tachykinin antagonist on a nociceptive reflex in the spinal cord-tail preparation of the newborn rat. *J. Physiol.*, **395**, 255–270.

OTSUKA, M. & YOSHIOKA, K. (1993). Neurotransmitter functions of mammalian tachykinins. *Physiol. Rev.*, **73**, 229–308.

ROQUES, B.P., FOURNIÉ-ZALAUSKI, M.C., SOROCA, E., LECOMTE, J.M., MALFROY, B., LLORENS, C. & SCHWARTZ, J.-C. (1980). The enkephalinase inhibitor thiorphan shows antinociceptive activity in mice. *Nature*, **288**, 286–288.

ROQUES, B.P., NOBLE, F., DAUGÉ, V., FOURNIÉ-ZALAUSKI, M.C. & BEAUMONT, A. (1993). Neutral endopeptidase 24.11:structure, inhibition, and experimental and clinical pharmacology. *Pharmacol. Rev.*, **45**, 87–146.

SAKUMA, M., YOSHIOKA, K., SUZUKI, H., YANAGISAWA, M., ONISHI, Y., KOBAYASHI, N. & OTSUKA, M. (1991). Substance P-evoked release of GABA from isolated spinal cord of the newborn rat. *Neuroscience*, **45**, 323–330.

SEGAWA, T., NAKATA, Y., YAJIMA, H. & KITAGAWA, K. (1977). Further observation on the lack of active uptake system for substance P in the central nervous system. *Jpn. J. Pharmacol.*, **27**, 573–580.

SUZUKI, H., SENO, N., HOSOKI, R., YANAGISAWA, M., SAITO, K. & OTSUKA, M. (1993). Potentiating effect of peptidase inhibitors on a C fiber-evoked response in the isolated spinal cord preparation of the neonatal rat. *Regul. Pept.*, **46**, 458–460.

TIEKU, S. & HOOPER, N.M. (1992). Inhibition of aminopeptidases N, A and W. A re-evaluation of the actions of bestatin and inhibitors of angiotension converting enzyme. *Biochem. Pharmacol.*, **44**, 1725–1730.

TURNER, A.J., MATSAS, R. & KENNY, A.J. (1985). Are there neuropeptide-specific peptidases? *Biochem. Pharmacol.*, **34**, 1347–1356.

UMEZAWA, H., AOYAGI, T., SUDA, H., HAMADA, M. & TAKEUCHI, T. (1976). Bestatin, an inhibitor of aminopeptidase B, produced by actinomycetes. *J. Antibiot.*, **29**, 97–99.

UMEZAWA, H., AOYAGI, T., OHUCHI, S., OKUYAMA, A., SUDA, H., TAKITA, T., HAMADA, M. & TAKEUCHI, T. (1983). Arphamenines A and B, new inhibitors of aminopeptidase B, produced by bacteria. *J. Antibiot.*, **36**, 1572–1574.

WADA, M., URAYAMA, O., SATOH, S., HARA, Y., IKAWA, Y. & FUJII, T. (1992). A marine algal Na^+-activated ATPase possesses an immunologically identical epitope to Na^+,K^+-ATPase. *FEBS. Lett.*, **309**, 272–274.

WARD, P., EWAN, G.B., JORDAN, C.C., IRELAND, S.J., HAGAN, R.M. & BROWN, J.R. (1990). Potent and highly selective neurokinin antagonists. *J. Med. Chem.*, **33**, 1848–1851.

WHITTAKER, V.P., MICHAELSON, I.A. & KIRKLAND, R.J.A. (1964). The separation of synaptic vesicles from nerve-ending particles ('synaptosomes'). *Biochem. J.*, **90**, 293–303.

YANAGISAWA, M., MURAKOSHI, T., TAMAI, S. & OTSUKA, M. (1984). Tail-pinch method in vitro and the effects of some antinociceptive compounds. *Eur. J. Pharmacol.*, **106**, 231–239.

YANAGISAWA, M. & OTSUKA, M. (1990). Pharmacological profile of a tachykinin antagonist, spantide, as examined on rat spinal motoneurones. *Br. J. Pharmacol.*, **100**, 711–716.

YANAGISAWA, M., YOSHIOKA, K., KURIHARA, T., SAITO, K., SENO, N., SUZUKI, H., HOSOKI, R. & OTSUKA, M. (1992). Enzymatic inactivation of tachykinin neurotransmitters in the isolated spinal cord of the newborn rat. *Neurosci. Res.*, **15**, 289–292.

(Received January 24, 1994
Revised May 4, 1994
Accepted May 23, 1994)

Br. J. Pharmacol. (1994), **113**, 317–323

Effect of dehydration and hyperosmolal hydration on lignocaine and metabolites disposition in conscious rabbits

M. Chamelian, A. Lécrivain, A. Robichaud & [1]P. du Souich

Department of Pharmacology, School of Medicine, University of Montréal, Montréal, P.O. Box 6128, Stat. 'Centre ville', Québec, Canada H3C 3J7

1 The present study aimed to investigate the effect of dehydration and hyperosmolal hydration on the disposition of lignocaine and two of its metabolites, monoethylglycinexylidide (MEGX) and glycinexylidide (GX).

2 Lignocaine was infused to three groups of conscious rabbits: controls, rabbits previously deprived of water for 48 h and rabbits receiving an infusion of 2.5% NaCl.

3 In dehydrated and hyperosmolal-hydrated rabbits, plasma osmolality was 321 ± 1 and 313 ± 1 mOsm kg^{-1}, respectively ($P<0.01$ compared to controls, 285 ± 1 mOsm kg^{-1}). In dehydrated animals, baseline values of plasma arginine vasopressin (AVP) concentrations and plasma renin activity (PRA) were higher than in controls, i.e. 12.4 ± 1.4 pg ml^{-1} and 15.4 ± 1.7 ng AI ml^{-1} h^{-1} vs. 3.4 ± 0.2 pg ml^{-1} ($P<0.01$), and 5.1 ± 0.6 ng AI ml^{-1} h^{-1} ($P<0.01$), respectively; atrial natriuretic peptide (ANP) decreased from 55 ± 11 to 32 ± 4 pg ml^{-1} ($P<0.05$). Compared to controls, hyperosmolal hydration only increased AVP to 15.5 ± 0.7 pg ml^{-1} ($P<0.01$).

4 Under both experimental conditions, lignocaine plasma concentrations were almost double ($P<0.01$) those in controls, due to a lower systemic clearance, e.g. 54 ± 3 and 59 ± 1 vs. 96 ± 5 ml min^{-1} kg^{-1}, respectively. Plasma levels of MEGX increased ($P<0.01$) only in dehydrated animals, although GX plasma concentrations were augmented ($P<0.01$) about three fold in both groups of animals. The changes in lignocaine plasma concentrations were correlated with AVP levels ($R^2 = 0.5168$, $P<0.001$).

5 To document the effect of AVP on hepatic plasma flow, another group of rabbits received on separate occasions two doses of AVP (17 and 84 ng kg^{-1}) while receiving an infusion of indocyanine green. AVP reduced hepatic plasma flow from 38.9 ± 2.7 ml min^{-1} to 19.6 ± 2.5 ml min^{-1} ($P<0.01$). The predicted maximal AVP-induced decrease in hepatic plasma flow was 19.6 ml min^{-1} kg^{-1} (E_{max}), and AVP concentration eliciting 50% of E_{max} (ED_{50}) was 28.7 pg ml^{-1}.

6 It is concluded that both dehydration and hyperosmolal hydration alter the disposition of lignocaine and two of its metabolites.

Keywords: Lignocaine; kinetics; dehydration; hyperosmolality; arginine vasopressin

Introduction

Lignocaine, diethylglycine 2,6-xylidide, was first used as an antiarrhythmic agent almost three decades ago (Gianelly *et al.*, 1967). Soon after, it was observed that lignocaine pharmacological response was directly related to its plasma concentrations (Harrison *et al.*, 1970), and that lignocaine had a rather narrow therapeutic range (Lie *et al.*, 1974). The disposition of lignocaine is characterized by an extensive extraction by the liver (Stenson *et al.*, 1971). Because of its high rate of hepatic extraction, the clearance of lignocaine is considered blood-flow dependent (Wilkinson & Shand, 1975). Therefore, the rate of elimination of lignocaine should decrease whenever hepatic blood flow is reduced (Zito & Reid, 1978). The reduction of hepatic blood flow with aging (Abernathy & Greenblatt, 1983), and under pathological states such as congestive heart failure (Thompson *et al.*, 1973) and left heart failure secondary to myocardial infarction (Lalka *et al.*, 1980) produce a decrease in lignocaine clearance. Moreover, drugs able to diminish hepatic blood flow, such as propranolol, metoprolol or cimetidine, will decrease lignocaine clearance (Ochs *et al.*, 1980; Feely *et al.*, 1982; Conrad *et al.*, 1983).

Several endogenous substances, such as adrenaline, noradrenaline, angiotensin II and arginine vasopressin (AVP) interact closely to modulate peripheral resistances in order to maintain blood pressure (McNeill, 1983). These endogenous substances increase the resistances of the splanchnic vascular bed (Richardson & Withrington, 1981; Khayyal *et al.*, 1985; Boyle & Segel, 1986). Among these products, AVP is a potent vasoconstrictor of the splanchnic vascular bed (Drapanas *et al.*, 1961), and is able to decrease the perfusion pressure of the liver at concentrations as low as 10^{-13} M (Freedman *et al.*, 1978; Altura & Altura, 1984), as well as gastric perfusion by about 56% (Gaskill *et al.*, 1983). In patients with acute or chronic heart failure of any origin, plasma concentrations of AVP are elevated (Parmley, 1985) and that may contribute to alter the kinetics of blood flow-dependent drugs.

The aims of the present study were to investigate the effect of two experimental conditions, dehydration and hyperosmolal hydration on the disposition of lignocaine and two of its metabolites. Dehydration, due to a reduction in circulating volume and an increase in plasma osmolality, enhances plasma levels of AVP and other vasoconstrictor hormones, and hyperosmolal hydration increases the circulating plasma volume and plasma osmolality, which will stimulate the secretion of AVP.

Methods

Animals

Male New Zealand rabbits, purchased from Ferme Cunicole (Mirabel, Québec, Canada), weighing 2.0 to 3.5 kg were used throughout the study. Each rabbit was installed in an individual cage, fed with Rabbit Show Feed (Purina Inc., Ralston) and allowed water *ad libitum*.

[1] Author for correspondence.

Before the experiment, the rabbits were weighed and a catheter was introduced into the vesical bladder (Foley Bard No. 8-10, Laboratories Bard, Mississauga, Ontario, Canada). The animals were installed in individual restraining cages (Plas-Labs, Lansing, Michigan, U.S.A.) and a catheter (Butterfly-21, Abbott Laboratories, Ireland) was placed into the central artery of the ear for blood sampling. Another catheter (PE50, Becton Dickinson, Rutherford, NJ, U.S.A.) was introduced into the lateral vein of an ear to infuse a solution of sodium chloride 0.9% and dextrose 5% (50:50) to replace fluid loss through the lungs and urine. The rate of infusion varied between 5 and 15 ml h^{-1} depending upon the experiment; the infusion was carried out with an infusion pump (Sage Instruments, model No. 355, Orion Research Inc., Cambridge, MA, U.S.A.). Each animal was weighed again at the end of the experiment. Once the rabbits had been prepared and installed in the restraining cages and before any experiment was started, they were left for 1 h in the cages to allow an optimum stabilization.

Experimental protocol

To document the kinetics of lignocaine and the effect of an infusion of lignocaine on baseline conditions (control experiment), six rabbits received lignocaine at the rate of 130 $\mu g\ min^{-1}\ kg^{-1}$ given in a sodium chloride 0.9%:dextrose 5% solution (15 ml h^{-1}) for 360 min. Previous studies have demonstrated that at this rate of infusion and for 360 min, steady state was reached at the predicted levels, confirming that lignocaine kinetics were first order (Marleau *et al.*, 1987; Gariépy *et al.*, 1992). To assay AVP and atrial natriuretic peptide (ANP) plasma concentrations, as well as plasma renin activity (PRA), blood samples (5 ml) were drawn at 60 and 0 min before the infusion of lignocaine and at 300, 330 and 360 min during the infusion of lignocaine. To assay lignocaine and its two metabolites, monoethylglycinexylidide (MEGX) and glycinexylidide (GX), blood was drawn (1 ml) at 240, 270, 300, 330 and 360 min; in addition, in these samples, sodium and potassium plasma concentrations as well as plasma osmolality were measured.

To assess the influence of dehydration-induced increase in AVP on lignocaine disposition, a group of six rabbits was kept for 48 h without water but allowed to eat. Preliminary studies demonstrated that this protocol significantly enhanced plasma osmolality and AVP concentrations. Lignocaine was infused at the rate of 130 $\mu g\ min^{-1}\ kg^{-1}$ for 360 min. The experimental protocol was similar to the one described for the control experiment, with the exception that the rabbits received an infusion of sodium chloride 0.9% at a rate of 5 ml h^{-1}, to compensate only for the volume of blood samples drawn.

Another group of six rabbits, instead of sodium chloride 0.9%:dextrose 5%, received an infusion of sodium chloride 2.5%, 15 ml h^{-1} for 360 min. Lignocaine (130 $\mu g\ min^{-1}\ kg^{-1}$) was infused with the hyperosmolal solution, and blood sampling was carried out as described earlier.

In all experiments, the rabbits' bladder was emptied and thereafter, urine was collected from −60 to 0, 0 to 120, 120 to 240, and 240 to 360 min to measure urinary osmolality. Prostaglandin E_2 (PGE_2) was assayed in urine collected from −60 to 0, pooled urine from 0 to 240 min and from 240 to 360 min.

In a final experiment, to assess the effect of increasing plasma concentrations of AVP on hepatic plasma flow, six rabbits were given intravenously 17 and 84 ng kg^{-1} of AVP, at least at one week interval, in order to generate AVP plasma concentrations ranging between 3 and 350 pg ml^{-1}. Hepatic plasma flow was estimated by infusing indocyanine green (ICG) at a rate of 248.5 $\mu g\ min^{-1}\ kg^{-1}$ for 30 min. AVP was given as an intravenous bolus 10 min after the initiation of the infusion, when ICG steady state was reached (Marleau *et al.*, 1987). Blood samples were drawn (3 ml) prior (time 0) and 10, 12, 16, 20 and 25 min after the beginning of ICG infusion, to assay AVP and ICG serum concentrations.

Analytical methods

Plasma lignocaine and metabolites, as well as serum ICG, were assayed by high performance liquid chromatography (h.p.l.c.) as described by Marleau *et al.* (1987). AVP and ANP plasma concentrations were determined by radioimmunoassay as described by Larose *et al.* (1985b) and Larose *et al.* (1985a), respectively. PRA and PGE_2 were measured using the [^{125}I]-Angiotensin I RIA kit (NEA-022, New England Nuclear, Billerica, MA, U.S.A.) and the Prostaglandin E_2 RIA kit (NEA-020, New England Nuclear, Billerica, MA, U.S.A.), respectively. Osmolality in plasma and urine were determined with an automatic osmometer (Osmette A, Precision Systems Inc., Sudbury, MA, U.S.A.). Sodium and potassium in plasma and urine were assayed with an automatic flame photometer (Model 11943, Instrumentation Laboratory Inc., Lexington, MA, U.S.A.).

Drugs used

Lignocaine, monoethylglycinexylidide (MEGX) and glycinexylidide (GX) were donated by Astra Pharmaceuticals Canada Ltd. Arginine vasopressin (AVP) was purchased from Peninsula Laboratories (Belmont, CA, U.S.A.). Indocyanine green (ICG) was obtained from Aldrich Chemical Company (Milwaukee, Wisconsin, U.S.A.).

Analysis of data

Lignocaine systemic clearance (Cl_{Lig}) and ICG systemic clearance (Cl_{ICG}) were obtained from the ratio of the rate of infusion over the plasma concentration at steady state (Gibaldi & Perrier, 1982). To calculate Cl_{Lig} lignocaine plasma concentration at 360 min was used. Hepatic plasma flow (Q_H) was considered to be equal to ICG systemic clearance (Burczynski *et al.*, 1987; Kanstrup & Winkler, 1987; Shak & Keiding, 1987). Urinary excretion rate of PGE_2 was assessed from the product of PGE_2 urinary concentration times urine volume divided by the interval of urine collection. The predicted maximal reduction in hepatic plasma flow elicited by AVP (E_{max}) and AVP plasma concentration eliciting 50% of E_{max} (ED_{50}) were estimated using the E_{max} model (Holford & Sheiner, 1981).

Statistical tests

In the group of rabbits receiving the infusion of 2.5% NaCl, the studied parameters were always stable after 300 min and for this reason, the mean ± s.e.mean values represent the arithmetic mean of the values measured at 300, 330 and 360 min. The effect of dehydration and of hyperosmolal hydration on lignocaine disposition was assessed by a one way analysis of variance for parallel groups and Dunnett's tables were used to determine the P value (Winer, 1971). The minimal level of statistical significance was established at $P = 0.05$. All results are presented as mean ± standard error of the mean (s.e.mean).

Results

In control rabbits receiving only the infusion of lignocaine, plasma osmolality remained stable all through the study (Table 1). In the group of rabbits subjected to water deprivation for 48 h, plasma osmolality values were significantly higher than those in control animals. The infusion of 2.5% NaCl increased plasma osmolality gradually, to reach values of 296 ± 2 mOsm kg^{-1} at 240 min, and higher than 300 mOsm kg^{-1} after 270 min of infusion of NaCl 2.5% (Table 1). Compared to the control group, mean values of urine

Table 1 Plasma and urine osmolalities in control rabbits, rabbits deprived of water for 48 h and rabbits infused an hyperosmolal solution (NaCl 2.5%)

Time (min)	0 min	*Plasma osmolality* (mOsm kg^{-1}) 270 min	330 min	360 min
Controls	283 ± 2	287 ± 2	287 ± 2	286 ± 1
Dehydrated	318 ± 4*	321 ± 1*	320 ± 1*	324 ± 2*
Hyperosmolal hydration	285 ± 3	313 ± 2†	312 ± 2†	313 ± 2†
Interval of urine collection (min)	−60 to 0 min	*Urine Osmolality* (mOsm kg^{-1}) 0 to 120 min	120 to 240 min	240 to 360 min
Controls	778 ± 96	926 ± 68	759 ± 78	511 ± 122
Dehydrated	1667 ± 109*	1386 ± 99*	1128 ± 136*	1217 ± 148*
Hyperosmolal hydration	887 ± 102	1061 ± 155	1233 ± 155*	1093 ± 114*

Values are mean ± s.e.mean; *$P<0.01$ compared to values in control rabbits; †$P<0.01$ compared to values at time 0 min and to values of control rabbits.

osmolality were higher in both dehydrated rabbits and hyperosmolal-hydrated rabbits (Table 1). Sodium plasma concentrations in dehydrated and hyperosmolal-hydrated rabbits were greater than those in control rabbits, i.e. 165.3 ± 1.4 and 322.0 ± 24.4 mmol l^{-1} versus 137.4 ± 0.4 mmol l^{-1} ($P<0.01$), respectively.

In control rabbits, plasma concentrations of AVP ranged between 0.7 and 6.3 pg ml^{-1} (3.4 ± 0.2 pg ml^{-1}), and remained constant throughout the experiment. In dehydrated rabbits, AVP plasma concentrations were always significantly higher than those in control animals, and in hyperosmolal-hydrated rabbits, AVP plasma concentrations increased progressively to remain stable at 300 min (Figure 1). Baseline values of PRA (−60 min) were similar in all three groups of rabbits, but in dehydrated rabbits mean PRA values increased until the end of the experiment (Figure 1). Hydration with a hyperosmolal solution tended ($P>0.05$) to lower PRA values at 330 min. In dehydrated rabbits, at 330 min, plasma concentrations of ANP were lower than in the control group (Figure 1). Hydration with the hyperosmolal solution did not affect ANP plasma concentrations. Urinary excretion rate of PGE_2 was highly variable, and no differences in the baseline values were detected between the groups (urine collected from −60 to 0 min) (Table 2). In the control group, urinary excretion of PGE_2 increased with the infusion of lignocaine (urine collected from 0 to 240 min); however, this was not observed in dehydrated or hyperosmolal-hydrated rabbits.

In the three groups of rabbits, lignocaine plasma concentrations had already reached steady state at 240 min. In the control group, lignocaine mean steady state plasma concentrations remained constant at around 1.4 μg ml^{-1} (Figure 2). Both in dehydrated and in hyperosmolal-hydrated rabbits, average steady state plasma levels of lignocaine were approximately 60% higher than in control animals, i.e. 2.4 and 2.2 μg ml^{-1} ($P<0.01$), respectively (Figure 2). The increase in steady state plasma concentrations of lignocaine was secondary to the decrease in the clearance of lignocaine, which, at 360 min, averaged 96 ± 5 ml min^{-1} kg^{-1} in control animals, 54 ± 3 ml min^{-1} kg^{-1} ($P<0.01$) in dehydrated rabbits and 59 ± 1 ml min^{-1} kg^{-1} ($P<0.01$) in hyperosmolal-hydrated rabbits.

In control rabbits, MEGX and GX plasma concentrations reached steady state at around 300 min (Figure 2), attaining an average level of 0.22 ± 0.02 and 0.23 ± 0.01 μg ml^{-1}, respectively. Plasma levels of MEGX were increased in dehydrated rabbits by approximately 300% but were not affected in hyperosmolal-hydrated rabbits. On the other hand, both experimental conditions increased plasma levels of GX (Figure 2).

ICG systemic clearance was assumed to reflect hepatic plasma flow based on two facts: (1) the ratio of ICG infusion rate to ICG steady state serum concentration yields a value of ICG clearance that is 7.4% of the value of hepatic plasma flow assessed by the transhepatic extraction ratio method (Pollack *et al.*, 1990), and (2) in the rabbit, ICG clearance values derived at steady state generate values of hepatic plasma flow that are similar to the values estimated using labelled microspheres (Neutze *et al.*, 1968). Two

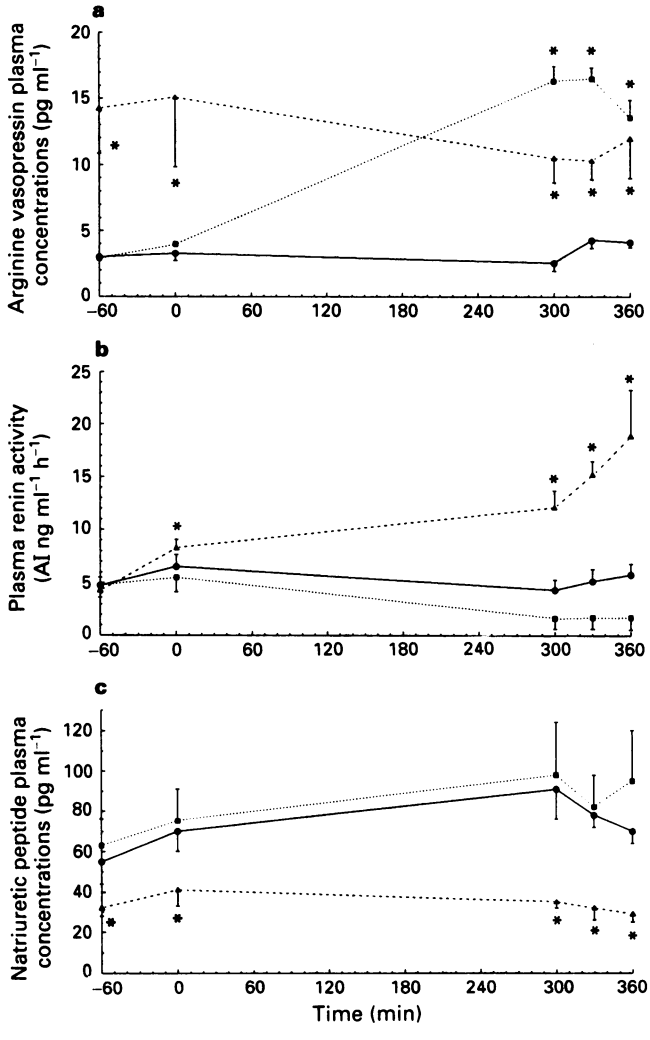

Figure 1 Changes in mean arginine vasopressin (a), plasma renin activity (b), and natriuretic atrial peptide (c), plasma concentrations as a function of time in control rabbits (●), animals deprived of water for 48 h (▲) and rabbits receiving an infusion of 2.5% NaCl solution (■). Mean values ± s.e.mean. *$P<0.01$.

Table 2 Urinary rate of excretion of prostaglandin E_2 (ng min^{-1}) in control rabbits, in rabbits deprived of water for 48 h and in rabbits infused an hyperosmolal solution (NaCl 2.5%)

Interval of urine collection (min)	*−60 to 0 min*	*0 to 240 min*	*240 to 360 min*
Controls	0.048 ± 0.017	0.179 ± 0.013*	0.160 ± 0.054
Dehydrated	0.368 ± 0.192	0.101 ± 0.019	0.153 ± 0.052
Hyperosmolal hydration	0.109 ± 0.057	0.220 ± 0.080	0.118 ± 0.0034

Values are mean ± s.e.mean. *$P<0.05$ compared to −60 to 0 min values.

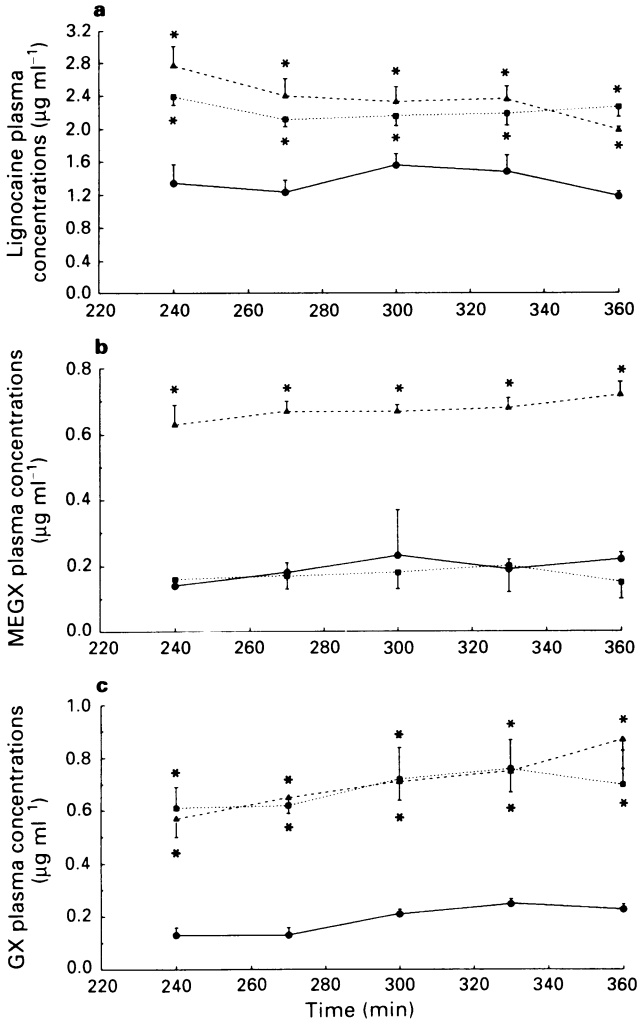

Figure 2 Changes in mean lignocaine (a), monoethylglycinexylidide (MEGX) (b), and glycinexylidide (GX) (c), plasma concentrations as a function of time in control rabbits (●), animals deprived of water for 48 h (▲) and rabbits receiving an infusion of 2.5% NaCl solution (■). Mean values ± s.e.mean. *$P<0.01$.

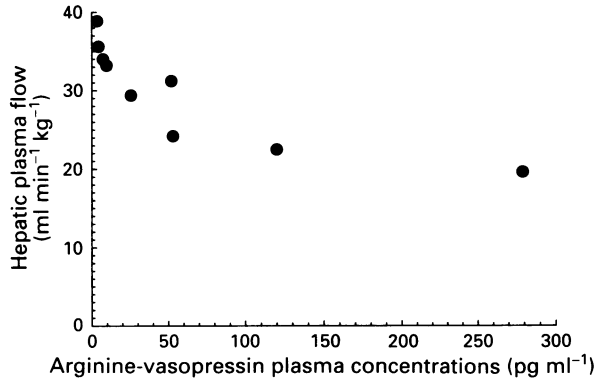

Figure 3 Relationship between the changes in hepatic plasma flow as a function of plasma concentrations of arginine vasopressin (AVP). The relationship is defined by the following equation: $E = E_{bas} + [E_{max} \times C_{AVP}/(E_{max} + ED_{50})]$, where E are the changes in hepatic plasma flow, E_{bas} is the baseline value of hepatic plasma flow, E_{max} is the predicted maximal effect of AVP on hepatic plasma flow, and ED_{50} is the concentration of AVP eliciting 50% of E_{max}, and C_{AVP} are plasma concentrations of AVP. $E_{max} = 19.6$ ml min^{-1}; $ED_{50} = 28.7$ pg ml^{-1}.

minutes after the intravenous injection of 17 or 84 ng kg^{-1} of AVP, plasma peak concentrations of AVP were of the order of 26 ± 2 or 279 ± 22 pg ml^{-1}, which decreased with a half life of approximately 4 min. Baseline hepatic plasma flow was 38.9 ± 2.7 ml min^{-1} kg^{-1} and at peak concentrations of AVP (dose 17 ng kg^{-1}), this value decreased to 29.4 ± 2.3 ml min^{-1} kg^{-1}; however, this difference did not reach statistical significance. After the 84 ng kg^{-1} dose of AVP, hepatic plasma flow was reduced to 19.6 ± 2.5 ml min^{-1} kg^{-1} ($P<0.01$). When the changes in hepatic plasma flow are represented graphically as a function of AVP plasma concentrations, a hyperbola is apparent (Figure 3), suggesting a direct relationship between changes in hepatic blood flow and AVP plasma concentrations. Based on the E_{max} model, it was possible to predict the maximal effect of AVP (E_{max}) on hepatic plasma flow, i.e. it was reduced to values of 19.6 ml min^{-1} kg^{-1}. In addition, the concentration of AVP eliciting 50% of E_{max} (ED_{50}) was 28.7 pg ml^{-1} ($R = 0.93$ and sum of squared residuals = 33.1).

Discussion

The aim of the present study was to assess the effect of endogenous peptides eliciting a potent constriction of the splanchnic vascular bed, i.e. AVP and angiotensin (McNeill, 1976; Richardson & Withrington, 1981; Schrauwen & Houvenaghel, 1982; Altura & Altura, 1984) on the disposition of lignocaine, a flow-dependent drug. To elevate plasma concentrations of AVP and PRA, plasma osmolality was increased by depriving rabbits of water for 48 h. To increase only AVP, another group of rabbits received by infusion a hyperosmolal solution. In addition to osmolal changes, dehydration should reduce the circulating volume and ANP (Trapani *et al.*, 1988), and conversely, hyperosmolal hydration should increase both of them (Kinsey, 1981; Lang *et al.*, 1985; Yandle *et al.*, 1986). Lignocaine plasma levels were augmented in dehydrated rabbits and in hyperosmolal-hydrated rabbits. MEGX levels were increased only in dehydrated animals, although GX levels were enhanced under both experimental conditions.

In man, lignocaine is dealkylated and hydroxylated to generate MEGX, 3-hydroxy- and N-hydroxy-lignocaine, respectively, dealkylation being the major route of degradation, i.e. around 80% of the dose. Dealkylation occurs at very rapid rates and is responsible for the blood flow-

dependent clearance of lignocaine (Stenson *et al.*, 1971; Wilkinson & Shand, 1975). MEGX is also dealkylated and hydroxylated to produce GX, 3-hydroxy- and N-hydroxy-MEGX; however, the major route of MEGX elimination is hydrolysis, to yield 2,6-xylidine. GX biotransformation includes essentially hydrolysis to yield 2,6-xylidine (Drayer *et al.*, 1983). MEGX clearance may be influenced by changes in hepatic blood flow since its rate of elimination parallels that of lignocaine (Bennett *et al.*, 1982); however, GX clearance is around 165 ml min^{-1} of which almost half is renal, thus GX metabolic clearance should be minimally affected by changes in blood flow (Strong *et al.*, 1975). In the rabbit, as in other species (Keenaghan & Boyes, 1972), the metabolism of lignocaine yields the same metabolites (Hollunger, 1960). However, the relative importance of each pathway varies; for instance, in man, steady state MEGX and GX concentrations are around 50 and 20% of lignocaine plasma levels (Prescott *et al.*, 1976; Bennett *et al.*, 1982); in the dog, these figures are 20 and 50% (du Souich *et al.*, 1992) and in the rabbit, in the present study, MEGX and GX concentrations were 15 and 17% of lignocaine plasma concentrations.

In control rabbits, lignocaine clearance was 96 ± 5 ml $min^{-1} kg^{-1}$. However, since lignocaine binds to erythrocytes (ratio of plasma to erythrocyte concentration 1.66), the value of blood lignocaine clearance is around 40% lower, i.e. 60 ml $min^{-1} kg^{-1}$ (Tucker *et al.*, 1970). Hepatic plasma flow estimated in the present and other studies is about 40 ml $min^{-1} kg^{-1}$ (Marleau *et al.*, 1987; Gariépy *et al.*, 1992) therefore, hepatic blood flow should be about 67 ml $min^{-1} kg^{-1}$ assuming an average haematocrit of 0.4. As a consequence, it is possible to assume that most lignocaine biotransformation could happen in the liver.

In dehydrated rabbits, several factors should contribute to reduce hepatic blood flow, such as reduced circulating volume, increased AVP and angiotensin II plasma levels (Brough *et al.*, 1975; McNeill *et al.*, 1976; Richardson & Withrington, 1981), and elevated plasma levels of catecholamines (Richardson & Withrington, 1977). This reduction in hepatic blood flow may explain in part the increase in lignocaine and MEGX plasma concentrations. To explain the increase in GX plasma levels, assuming MEGX de-ethylation was reduced, we may speculate that dehydration decreased the rate of GX elimination.

In the group of animals receiving the infusion of the hyperosmolal solution, the clearance of lignocaine decreased by 39%, and as discussed earlier, a reduction of this magnitude implies a decrease in its dealkylation. The repercussions of a rise in plasma osmolality of the order of 30 mOsm kg^{-1} on mesenteric resistance and intrahepatic blood distribution are unknown. It has been reported that moderate increases in plasma osmolality, of the order of 5 mOsm kg^{-1}, enhance hepatic blood flow by about 10% (Levine *et al.*, 1978; Richardson & Withrington, 1980). On the other hand, Ballet *et al.* (1988) reported that increasing concentrations of AVP were able to augment portal resistances even in the presence of enhanced hepatic blood flow. Since in the present study AVP plasma concentrations increased, we may speculate that high AVP plasma concentrations may override the effect of a hyperosmolal-induced increase in liver blood flow. We may postulate that under the present experimental conditions, hepatic plasma flow was decreased by elevated AVP plasma concentrations and as a consequence, the clearance of lignocaine was diminished. The possibility that AVP decreases lignocaine clearance by reducing splanchnic blood flow is supported by the fact that the changes in lignocaine plasma concentrations were correlated with the changes in AVP ($R^2 = 0.5168$, $P < 0.001$). In hyperosmolal-hydrated rabbits, MEGX plasma levels were not modified. However, since lignocaine clearance was reduced, MEGX formation was probably decreased and therefore, its elimination must also be lessened. To explain the increase in GX concentrations, an increase in MEGX dealkylation cannot be invoked, but rather a decrease in GX elimination.

As discussed earlier, both dehydration and the infusion of a solution of 2.5% NaCl promote multiple homeostatic reactions; since AVP was increased under both experimental conditions, AVP may account, at least in part, for the decrease in MEGX and GX elimination. AVP binds to V_1 and V_2 receptors, the former being on smooth muscle cells, hepatocytes, platelets and kidneys; V_1 receptors are coupled to phospholipase C, responsible for the formation of diacylglycerol and inositol-1,4,5-trisphosphate that will increase intracellular calcium. V_2 receptors are located mainly in the kidneys, where AVP activates adenylate cyclase that will promote the synthesis of adenosine 3':5'-cyclic monophosphate (cyclic AMP) (Hays, 1990). The influence of intracellular increases in diacylglycerol, inositol-1,4,5-trisphosphate or calcium on phase I reactions of biotransformation is unknown. It is possible that stimulation of V_2 receptors may influence the metabolism of lignocaine and its metabolites since it has been shown that cyclic AMP inhibits hepatic phase I reactions (Weiner *et al.*, 1972a,b; Weiner, 1973), and in addition, it appears that the kidneys of rabbits have the ability to metabolize lignocaine (Åkerman *et al.*, 1966). We may speculate that increases in AVP not only reduce splanchnic blood flow, but also decrease the rate of metabolism of selected drugs. Indeed, further studies are needed to verify such a hypothesis.

The observations reported in the current study may be helpful in predicting situations where lignocaine or its metabolites can accumulate and as a consequence, toxicity could be observed. The pathological states where effective plasma volume is reduced, such as patients with left heart failure, hypotension of any cause, congestive heart failure, dehydration and in the elderly, entail an elevation of AVP, angiotensin II and other peptides plasma levels, which can be the cause of accumulation of lignocaine and its metabolites. As a consequence, the risks of toxicity will be augmented. It is interesting to note that Prescott *et al.* (1976) reported that in patients with congestive heart failure, lignocaine plasma concentrations were greatly increased, secondary to a low cardiac output and increased peripheral resistances, but in addition, as observed in the present study, MEGX plasma concentrations were also increased.

This work was supported by the Medical Research Council, grant No. MA-10874. M.C. was a recipient of a fellowship of the FCAR of Québec. The authors thank Mrs Hélène Courteau and Lucie Héroux for their excellent technical assistance.

References

ABERNATHY, D.R. & GREENBLATT, D.J. (1983). Impairment of lidocaine clearance in elderly male subjects. *J. Cardiovasc. Pharmacol.*, **5**, 1093–1096.

ÅKERMAN, B., ÅSTRÖM, A., ROSS, S. & TELC, A. (1966). Studies on the absorption, distribution and metabolism of labelled prilocaine and lidocaine in some animal species. *Acta Pharmacol. Toxicol.*, **24**, 389–403.

ALTURA, B.M. & ALTURA, B.T. (1984). Actions of vasopressin, oxytocin and synthetic analogs on vascular smooth muscle. *Fed. Proc.*, **43**, 80–86.

BALLET, F., CHRÉTIEN, Y., REY, C. & POUPON, R. (1988). Differential response of normal and cirrhotic liver to vasoactive agents. A study in the isolated perfused rat liver. *J. Pharmacol. Exp. Ther.*, **244**, 283–289.

BENNETT, P.N., AARONS, L.J. & BENDING, M.R. (1982). Pharmacokinetics of lidocaine and its deethylated metabolite. Dose and time dependency studies in man. *J. Pharmacokin. Biopharmacol.*, **10**, 265–281.

BOYLE, W.A. & SEGEL, L.D. (1986). Direct cardiac effects of vasopressin in their reversal by a vascular antagonist. *Am. J. Physiol.*, **251**, H734–H741.

BROUGH, R.B., COWLEY, A.W. Jr. & GUYTON, A.C. (1975). Quantitative analysis of the acute response to haemorrhage of the renin-angiotensin vasoconstrictor feedback loop in areflexic dogs. *Cardiovasc. Res.*, **9**, 722–733.

BURCZYNSKI, F.J., GREENWAY, C.V. & SITAR, D.S. (1987). Hepatic blood flow: accuracy of estimation from infusions of indocyanine green in anesthetized cats. *Br. J. Pharmacol.*, **91**, 651–659.

CONRAD, K.A., BYERS, J.M., FINLEY, P.R. & BURNHAM, L. (1983). Lidocaine elimination: effects of metoprolol and of propranolol. *Clin. Pharmacol. Ther.*, **33**, 133–138.

DRAPANAS, T., CROWE, P., SHIM, W.K.T., WORTHINGTON, G. & SCHENK, J. (1961). The effect of pitressin on cardiac output and coronary, hepatic and intestinal blood flow. *Surg. Gynecol. Obstet.*, **113**, 484–489.

DRAYER, P.E., LORENZO, B., WERNS, S. & REIDENBERG, M.M. (1983). Plasma levels, protein binding, and elimination data of lidocaine and active metabolites in cardiac patients of various ages. *Clin. Pharmacol. Ther.*, **34**, 14–22.

DU SOUICH, P., SAUNIER, C., HARTEMANN, D. & ALLAM, M. (1992). Effect of acute and chronic moderate hypoxia on the kinetics of lidocaine and its metabolites and on regional blood flow. *Pulmonary Pharmacol.*, **5**, 9–16.

FEELY, J., WILKINSON, G.R., MCALLISTER, C.B. & WOOD, A.J.J. (1982). Increased toxicity and reduced clearance of lidocaine by cimetidine. *Ann. Intern. Med.*, **96**, 592–594.

FREEDMAN, A.R., KERR, J.C., KENNETH, G.S. & HOBSON, R.W. (1978). Primate mesenteric blood flow: effects of vasopressin and its route of delivery. *Gastroenterolgy*, **74**, 875–878.

GARIÉPY, L., LAROSE, P., BAILEY, B. & DU SOUICH, P. (1992). Effect of lignocaine on arginine-vasopressin plasma levels: baseline or induced by frusemide. *Br. J. Pharmacol.*, **106**, 470–475.

GASKILL, H.V., SIRINEK, K.R. & LEVINE, B.A. (1983). Hemodynamics effects of vasopressin: can large doses be safely given? *Arch. Surg.*, **118**, 434–437.

GIANELLY, R., VAN DER GROEBEN, J.O., SPIVACK, A.P. & HARRISON, D.C. (1967). Effect of lidocaine on ventricular arrhythmias in patients with coronary heart disease. *New Engl. J. Med.*, **277**, 1215–1219.

GIBALDI, M. & PERRIER, D. (1982). Multicompartmental models. *Pharmacokinetics*. pp. 45–112. ed. Swarbrick, J. New York: Marcel Dekker, Inc.

HARRISON, D.C., STENSON, R.E. & CONSTANTINO, R.T. (1970). The relationship of blood levels, infusion rates and metabolism of lidocaine to its antiarrhythmic action. *Symposium on Cardiac Arrhythmias*. pp. 427–447 ed. Sandoe, E., Flensted-Jensen, E. & Olesen, K. Stockholm: A.B. Astra.

HAYS, R.M. (1990). Agents affecting the renal conservation of water. *The Pharmacological Basis of Therapeutics*, 8th edition, pp. 732–742. Goodman, A., Gilman, A., Rall, T.W., Nies, A.S. & Taylor, P. Toronto: Pergamon Press.

HOLFORD, N.H.G. & SHEINER, L.B. (1981). Understanding the dose-effect relationship: clinical application of pharmacokinetic-pharmacodynamic models. *Clin. Pharmacokin.*, **6**, 429–453.

HOLLUNGER, G. (1960). On the metabolism of lidocaine II. The biotransformation of lidocaine. *Acta Pharmacol. Toxicol.*, **17**, 365–373.

KANSTRUP, I.L. & WINKLER, S.G. (1987). Indocyanine green plasma clearance as a measure of changes in hepatic blood flow. *Clin. Physiol.*, **7**, 51–54.

KEENAGHAN, J.B. & BOYES, R.N. (1972). The tissue distribution, metabolism and excretion of lidocaine in rats, guinea pigs, dogs and man. *J. Pharmacol. Exp. Ther.*, **180**, 459–463.

KHAYYAL, M.A., ENG, C., FRANZEN, D., BREALL, J.A. & KIRK, E.S. (1985). Effects of vasopressin on the coronary circulation: reserve and regulation during ischemia. *Am. J. Physiol.*, **248**, H516–H522.

KINSEY, S. (1981). *Équilibre Hydroéléctrolytique. Des Bases Théoriques à la Clinique*, pp. 51–96. Paris: Médecines et Sciences Internationales.

LALKA, D., SLAUGHTER, R.S., GOLDREYER, B.N., CANNOM, D.S., HALTON, D.J. & WYMAN, M.J. (1980). Lidocaine pharmacokinetics and metabolism in acute myocardial infarction patients. *Clin. Res.*, **28**, 239A.

LANG, R.E., THÖLKEN, H., GANTEN, D., LUFT, F.C., RUSKOAHO, H. & UNGER, T. (1985). Atrial natriuretic factor, a circulating hormone stimulated by volume loading. *Nature*, **314**, 264–266.

LAROSE, P., MELOCHE, S., DU SOUICH, P., DE LÉAN, A. & ONG, H. (1985a). Radioimmunoassay of atrial natriuretic factor: human plasma levels. *Biochem. Biophys. Res. Commun.*, **130**, 553–558.

LAROSE, P., ONG, H. & DU SOUICH, P. (1985b). Simple and rapid radioimmunoassay for the routine determination of vasopressin in plasma. *Clin. Biochem.*, **18**, 357–361.

LEVINE, S.E., GRANGER, D.N., BRACE, R.A. & TAYLOR, A.E. (1978). Effect of hyperosmolality on vascular resistance and lymph flow in the cat ileum. *Am. J. Physiol.*, **234**, H14–H20.

LIE, K.I., WELLENS, H.J., VAN CAPELLE, F.J. & DURRER, D. (1974). Lidocaine in the prevention of primary ventricular fibrillation. *New Engl. J. Med.*, **291**, 1324–1326.

MARLEAU, S., ONG, H., GARIÉPY, L. & DU SOUICH, P. (1987). Lidocaine and indocyanine green kinetics: effect of hypoxia and/or hypercapnia. *J. Pharmacol. Exp. Ther.*, **242**, 338–343.

MCNEILL, J.R. (1976). Intestinal vasoconstriction following diuretic-induced volume depletion: role of angiotensin and vasopressin. *Can. J. Physiol. Pharmacol.*, **52**, 829–839.

MCNEILL, J.R. (1983). Role of vasopressin in the control of arterial pressure. *Can. J. Physiol. Pharmacol.*, **61**, 1226–1235.

OCHS, H.R., CARSTEN, G. & GREENBLATT, D.J. (1980). Reduction of lidocaine clearance during continuous infusion and by coadministration of propranolol. *N. Engl. J. Med.*, **303**, 373–377.

PARMLEY, W.W. (1985). Pathophysiology of congestive heart failure. *Am. J. Cardiol.*, **56**, 7A–11A.

POLLACK, G.M., BROUWER, K.L., DEMBY, K.B. & JONES, J.A. (1990). Determinations of hepatic blood flow in the rat using sequential infusions of indocyanine green or galactose. *Drug Metab. Dispos.*, **18**, 197–202.

PRESCOTT, L.F., ADJEPON-YAMOAH, K.K. & TALBOT, R.G. (1976). Impaired lignocaine metabolism in patients with myocardial infarction and cardiac failure. *Br. Med. J.*, **i**, 939–941.

RICHARDSON, P.D.I. & WITHRINGTON, P.G. (1977). The effects of intraportal injections of noradrenaline, adrenaline, vasopressin and angiotensin on the hepatic portal vascular bed of the dog: marked tachyphylaxis to angiotensin. *Br. J. Pharmacol.*, **59**, 293–301.

RICHARDSON, P.D.I. & WITHRINGTON, P.G. (1980). Effects of intraportal infusions of hypertonic solutions on hepatic haemodynamics in the dog. *J. Physiol.*, **301**, 82–83P.

RICHARDSON, P.D.I. & WITHRINGTON, P.G. (1981). Liver blood flow. II. Effects of drugs and hormones on liver blood flow. *Gastroenterology*, **81**, 356–375.

SCHRAUWEN, E. & HOUVENAGHEL, A. (1982). Vascular effects of vasopressin and oxytocin in the pig mesenteric bed. *Pflügers Arch.*, **392**, 301–303.

SHAK, C. & KEIDING, S. (1987). Methodological problems in the use of indocyanine green to estimate hepatic blood flow and ICG clearance in man. *Liver*, **7**, 155–162.

STENSON, R.E., CONSTANTINO, R.T. & HARRISON, D.C. (1971). Interrelationships of hepatic blood flow, cardiac output and blood levels of lidocaine in man. *Circulation*, **43**, 205–211.

STRONG, J.M., MAYFIELD, D.E., ATKINSON, A.J., BURRIS, B.C., RAYMON, F. & WEBSTER, L.T. Jr. (1975). Pharmacological activity, metabolism, and pharmacokinetics of glycinexylidide. *Clin. Pharmacol. Ther.*, **17**, 184–194.

THOMPSON, P.D., MELMON, K.L., RICHARDSON, J.A., COHN, K., STEINBRUNN, W., CUDIHEE, R. & ROWLAND, M. (1973). Lidocaine pharmacokinetics in advanced heart failure, liver disease and renal disease in humans. *Ann. Intern. Med.*, **78**, 499–508.

THOMSON, A.H., ELLIOTT, H.L., KELMAN, A.W., MEREDITH, P.A. & WHITING, B. (1987). The pharmacokinetics and pharmacodynamics of lignocaine and MEGX in healthy subjects. *J. Pharmacokin. Biopharmacol.*, **15**, 101–115.

TRAPANI, A.J., UNDESSER, K.P., KEETON, T.K. & BISHOP, V.S. (1988). Neurohumoral interactions in conscious dehydrated rabbits. *Am. J. Physiol.*, **254**, R338–R347.

TUCKER, G.T., BOYES, R.N., BRIDENBAUGH, P.O. & MOORE, D.C. (1970). Binding of anilide-type local anesthetics in human plasma: I. Relationships between binding, physicochemical properties, and anesthetic activity. *Anesthesiology*, **33**, 287–303.

WEINER, M. (1973). Preliminary characterization of an inhibitor of drug metabolism in response to cyclic adenine nucleotides. *Res. Commun. Chem. Pathol. Pharmacol.*, **6**, 551–564.

WEINER, M., BUTERBAUGH, G.G. & BLAKE, D.A. (1972a). Inhibition of hepatic drug metabolism by cyclic 3',5'-adenosine monophosphate. *Res. Commun. Chem. Pathol. Pharmacol.*, **3**, 249–263.

WEINER, M., BUTERBAUGH, G.G. & BLAKE, D.A. (1972b). Studies on the mechanism of inhibition of drug biotransformation by cyclic adenine nucleotides. *Res. Commun. Chem. Pathol. Pharmacol.*, **4**, 37–50.

WILKINSON, G.R. & SHAND, D.G. (1975). A physiologic approach to hepatic drug clearance. *Clin. Pharmacol. Ther.*, **18**, 377–390.

WINER, B.J. (1971). *Statistical Principals in Experimental Design*, pp. 201–204. New York: McGraw Hill Publications.

YANDLE, T.G., ESPINER, E.A., NICHOLLS, M.G. & DUFF, H. (1968). Radioimmunoassay and characterization of atrial natriuretic peptide in human plasma. *J. Clin. Endocrinol. Metab.*, **63**, 72–79.

ZITO, R.A. & REID, P.A. (1978). Lidocaine pharmacokinetics predicted by indocyanine green clearance. *New Engl. J. Med.*, **298**, 1160–1163.

(Received November 30, 1993
Revised April 26, 1994
Accepted May 23, 1994)

Br. J. Pharmacol. (1994), **113**, 324–330

Endothelium-derived relaxing factor released by 5-HT: distinct from nitric oxide in basilar arteries of normotensive and hypertensive rats

Yoshihiro Yokota, [1]Yuji Imaizumi, *Masahisa Asano, *Tomohiro Matsuda & Minoru Watanabe

Department of Chemical Pharmacology, Faculty of Pharmaceutical Sciences, and *Department of Pharmacology, School of Medicine, Nagoya City University, 3-1 Tanabedori, Mizuhoku, Nagoya 467, Japan

1 The role of the endothelium in cerebrovascular responses to 5-hydroxytryptamine (5-HT) was investigated in spontaneously hypertensive rats (SHR) and normotensive Wistar-Kyoto rats (WKY) *in vitro*.

2 Cumulative addition of 5-HT caused concentration-dependent contractions in ring preparations of SHR basilar arteries; the contractile response was smaller in WKY basilar arteries.

3 Removal of the endothelium enhanced markedly the contractile responses to 5-HT in WKY arteries but had only a slight effect in SHR arteries. The responsiveness to 5-HT in WKY arteries after removal of endothelium was comparable to that in SHR arteries.

4 The endothelium-dependent relaxation induced by acetylcholine in WKY basilar arteries was almost abolished by treatment with 10 μM methylene blue or 10 μM N^G-nitro-L-arginine (L-NOARG). However, the response to 5-HT was not affected by treatment with methylene blue, L-NOARG or indomethacin.

5 Application of 10–20 mM K^+ or 3.2 mM tetraethylammonium (TEA) did not change significantly, or only increased slightly, the resting tension, but markedly enhanced the contractile response to 5-HT in WKY arteries with endothelium. In contrast, the submaximal response to 5-HT in SHR arteries with endothelium was significantly enhanced by 0.3 mM TEA.

6 In the presence of 1 mM TEA, the application of 10 μM L-NOARG further enhanced the responses of 5-HT in WKY arteries with endothelium. In SHR arteries with endothelium, 10 μM L-NOARG *per se* enhanced slightly but significantly the responses to 5-HT.

7 These results indicate that 5-HT-induced contraction in basilar arteries is substantially attenuated by an endothelium-dependent mechanism in WKY, but to a much lesser extent in SHR. The major relaxing factor released by 5-HT from endothelium in WKY is distinct from NO and may exert its effect by activating K^+ channels.

Keywords: Basilar artery; endothelium-derived relaxing factor; endothelium-derived hyperpolarizing factor; nitric oxide; K^+ channel; 5-hydroxytryptamine; spontaneously hypertensive rats

Introduction

Endothelial cells modulate underlying vascular smooth-muscle tone by releasing substances such as endothelium-derived relaxing factor (EDRF; Furchgott & Zawadzki, 1980) and endothelium-derived contracting factor (EDCF; Vanhoutte, 1987). EDRF is either nitric oxide (NO) or an unstable nitroso-related compound (Palmer *et al.*, 1987; Ignarro *et al.*, 1987). The characteristics of EDCF, however, vary with species and tissue (Altiere *et al.*, 1985; Vanhoutte & Katusic, 1988). NO is synthesized from L-arginine by endothelial cells, and its synthesis is inhibited by analogues of L-arginine such as N^G-nitro-L-arginine (L-NOARG). In some isolated vessels, however, L-NOARG has no or little effect on endothelium-dependent relaxation induced by vasodilators, suggesting that NO has little responsibility for relaxation. Since this L-NOARG-resistant relaxation is accompanied by membrane hyperpolarization, it appears to be caused by the release of a factor which hyperpolarizes smooth muscle cells by opening K^+ channels (endothelium-derived hyperpolarizing factor, EDHF) (Chen *et al.*, 1991; Garland & McPherson, 1992; Nagao & Vanhoutte, 1992).

During chronic hypertension, the endothelium changes both morphologically and functionally (Winquist *et al.*, 1984). Relaxation in response to acetylcholine (ACh) is attenuated in the peripheral arteries of spontaneously hypertensive rats (SHR; Konishi & Su, 1983; Watt & Thurston, 1989); these studies suggest that chronic hypertension impairs endothelium-dependent relaxation. However, Luscher & Vanhoutte (1986a) have shown that relaxant response to ACh in precontracted arterial rings is reduced in SHR and that the reduction is normalized after exposure to indomethacin. Moreover, in resting conditions, ACh caused endothelium-dependent contractions; these contractions were inhibited by indomethacin in rings from SHR but not from normotensive Wistar-Kyoto rats (WKY). These authors suggest that the reduced endothelium-dependent relaxations in SHR may be due to a simultaneous release of cyclo-oxgenase-dependent EDCF rather than to a reduced release of EDRF. Little is known concerning the role of EDHF in hypertension.

Studies on the role of endothelial cells in cerebral arteries, especially in response to 5-hydroxytryptamine (5-HT), have yielded conflicting results; it has been reported that cerebral vasoconstriction induced by 5-HT is dependent (Nakagomi *et al.*, 1988) as well as independent (Young *et al.*, 1986) of the endothelium. It has also been reported that the removal of the endothelium potentiates contraction but not membrane depolarization induced by 5-HT in the rabbit basilar artery (Garland, 1987). The present experiments were designed to determine whether the cerebrovascular reactivities to 5-HT are modulated by endothelium and are impaired in SHR. Moreover, efforts were made to determine the characteristics of the modulation by the endothelium.

[1] Author for correspondence.

Methods

Experiments were performed on basilar arteries isolated from age-matched (15–16 weeks) male SHR and normotensive WKY. Rats were killed by stunning and the chest cavity opened. The brain was removed and placed in Krebs solution at room temperature. The basilar artery was carefully dissected from the brain with the aid of a dissecting microscope. The vessel was freed of fat and connective tissues and cut into rings (1 mm in length) with scissors. For some experiments, the endothelial cells were destroyed at this stage by rubbing the intimal surface gently with a stainless steel wire of appropriate diameter (~150 μm) inserted through the lumen. The procedure was performed carefully to minimize damage to the arterial smooth muscle. Removal of the endothelium was confirmed by lack of a relaxation response to 1 μM ACh in rings precontracted with 1 μM 5-HT (see below).

For tension measurement, 2 stainless steel wires (each 50 μm in diameter) were introduced through the lumen of an arterial ring under a dissecting microscope in a 0.9 ml organ chamber filled with Krebs solution. Special care was taken to avoid damage to the artery. One wire was fixed to the silicon rubber attached to the bottom of the chamber and the other was tightly attached to a lever of a force-displacement transducer for isometric tension recording. The transducer was mounted on a micromanipulator movable in x, y and z directions. The 2 wires were carefully kept parallel to each other and the distance was adjusted to apply a resting tension to the vascular ring. The rings were suspended in an organ chamber and superfused at 35°C with Krebs solution bubbled with 95% O_2:5% CO_2 at a rate of 4 ml min^{-1}. The rings were allowed to equilibrate at a predetermined optimal resting tension of 1 mN for at least 60 min before the start of experiments. After this procedure, the rings were repeatedly exposed to 80 mM K^+ solution at intervals of about 30 min until the contraction was reproducible. When the amplitude of the contractile response to 80 mM K^+ was measured changing resting tension by 0.5 mN step from zero to 5 mN, the response was the largest at resting tension in a range of 1–2 mN.

Concentration-response relationships were determined by cumulative addition of 5-HT (0.1 nM –10 μM) to rings with or without endothelium. Experiments were also performed in the presence of 10 μM indomethacin to prevent the production of vasoactive prostanoids. Some experiments were performed in the presence of 10 μM methylene blue or 10 μM L-NOARG inhibitors of guanylate cyclase and nitric oxide synthesis, respectively. To study the contribution of K^+ channels, 10–20 mM K^+ or 0.1–3.2 mM tetraethylammonium (TEA) was added to the perfusion solution 15 min prior to the 5-HT application and was present throughout the experiments. In these experiments, results are expressed as a percentage of the maximal response to 80 mM K^+ solution in each preparation.

In experiments studying relaxation, the rings were precontracted by a single addition of 1 μM 5-HT which caused submaximal tension development. After the contraction reached a plateau, ACh was added cumulatively in a concentration range of 1 nM to 1 μM. In some experiments, 10 μM L-NOARG was added to the perfusion solution 15 min prior to the application of ACh. The relaxation was expressed as a percentage, taking the amplitude of precontraction induced by 1 μM 5-HT as 100%.

The composition of Krebs solution (in mM) was as follows: NaCl 112, KCl 4.7, $CaCl_2$ 2.2, $MgCl_2$ 1.2, $NaHCO_3$ 25, KH_2PO_4 1.2, and glucose 14. High K^+ (10, 15, 20, or 80 mM K^+) solution was prepared by replacing NaCl with equimolar KCl. Drugs used were acetylcholine chloride (ACh) and 5-hydroxytryptamine creatinine sulphate (5-HT; Wako Pure Chemical, Osaka, Japan); methylene blue and indomethacin (Sigma Chemical Co., St. Louis, MO.); tetraethylammonium (TEA; Tokyo Chemical Industry Co., Ltd., Tokyo, Japan); and N^G-nitro-L-arginine (L-NOARG; Peptide Institute Inc., Osaka, Japan). Indomethacin was dissolved in ethanol for stock solutions, L-NOARG in 0.1 M HCl, and other drugs in distilled water. All drugs were further diluted 1,000 fold or more in Krebs solution to give the final concentrations.

Results are given as mean ± s.e.mean. Statistical significance was determined using Student's t test for unmatched pairs. Means were considered significantly different when P was less than 0.05.

Results

Figure 1a shows typical traces of mechanical responses to 5-HT in SHR and WKY basilar arteries with endothelium. Cumulative application of 5-HT elicited concentration-dependent contractile responses that reached maximal values at 1 μM. However, SHR basilar arteries were more sensitive to 5-HT than those from WKY (Figure 1a). The maximal contractile response of SHR arteries to 5-HT (1.88 ± 0.07 mN, $n = 5$) was about 5 times larger than that of WKY arteries (0.40 ± 0.02 mN, $n = 5$, $P < 0.001$ vs. SHR). In contrast, the maximal contractile response to 80 mM K^+ solution in SHR basilar arteries (2.09 ± 0.09 mN, $n = 10$) was only slightly smaller than that from WKY (2.40 ± 0.04 mN, $n = 10$, $P < 0.01$).

As shown in Figure 1b, removal of the endothelium dramatically enhanced the contractile response to 5-HT in WKY, resulting in responses similar to those in SHR. The maximal contractile response to 5-HT in arteries from WKY was approximately doubled by the removal of endothelium (0.96 ± 0.22 mN, $n = 5$). The contractile response to 80 mM K^+ solution was, however, significantly decreased by removal of endothelium in both strains (1.28 ± 0.09 mN in WKY, $n = 10$; 1.12 ± 0.15 mN in SHR, $n = 10$), suggesting that rubbing the vascular endothelium probably causes some damage to the smooth muscles. Another method for disrupting the endothelium, perfusion with 0.1% Triton X-100, appeared to damage the smooth muscle to a similar extent. Therefore, in the present study, the endothelium continued to be removed by rubbing. To normalize data, results are shown as percentages of the maximal response to 80 mM K^+ solution in each normal or rubbed preparation.

The mean dose-response relationships for 5-HT are shown in Figure 2. In WKY and SHR arteries with endothelium, the maximal response to 5-HT was 16.6 ± 0.8 and 91.7 ± 3.0% of the maximal response to 80 mM KCl, respectively. Although the removal of the endothelium significantly enhanced 5-HT-induced contraction relative to that induced by 80 mM K^+ in both WKY and SHR arteries (71.8 ± 5.4 and 101.9 ± 4.1%, respectively; $n = 5$ for each), the enhancement was more pronounced in WKY than in SHR. It is notable that without endothelium, the responsiveness to 5-HT of WKY smooth muscle was only slightly lower than that of SHR. These observations suggest that smooth muscle contraction in response to 5-HT is markedly attenuated by an endothelium-dependent mechanism in WKY but only minimally attenuated in SHR.

To examine the possibility that arachidonic acid metabolites such as prostacyclin (PGI_2) may contribute to the endothelium-dependent attenuation of contractile responses to 5-HT, the effect of 10 μM indomethacin on the response of arteries to 5-HT was examined (Figure 2). Treatment with 10 μM indomethacin did not affect significantly the dose-response relationships for 5-HT in either strain, indicating that the relaxing factor is not a cyclo-oxygenase product. The resting tension was not affected by 10 μM indomethacin in either strain.

Effects of pretreatmemt with methylene blue or L-NOARG on 5-HT-induced contraction were examined in WKY arteries. Rings with endothelium were exposed to 10 μM methylene blue or 10 μM L-NOARG approximately 15 min prior to the cumulative addition of 5-HT. As summarized in

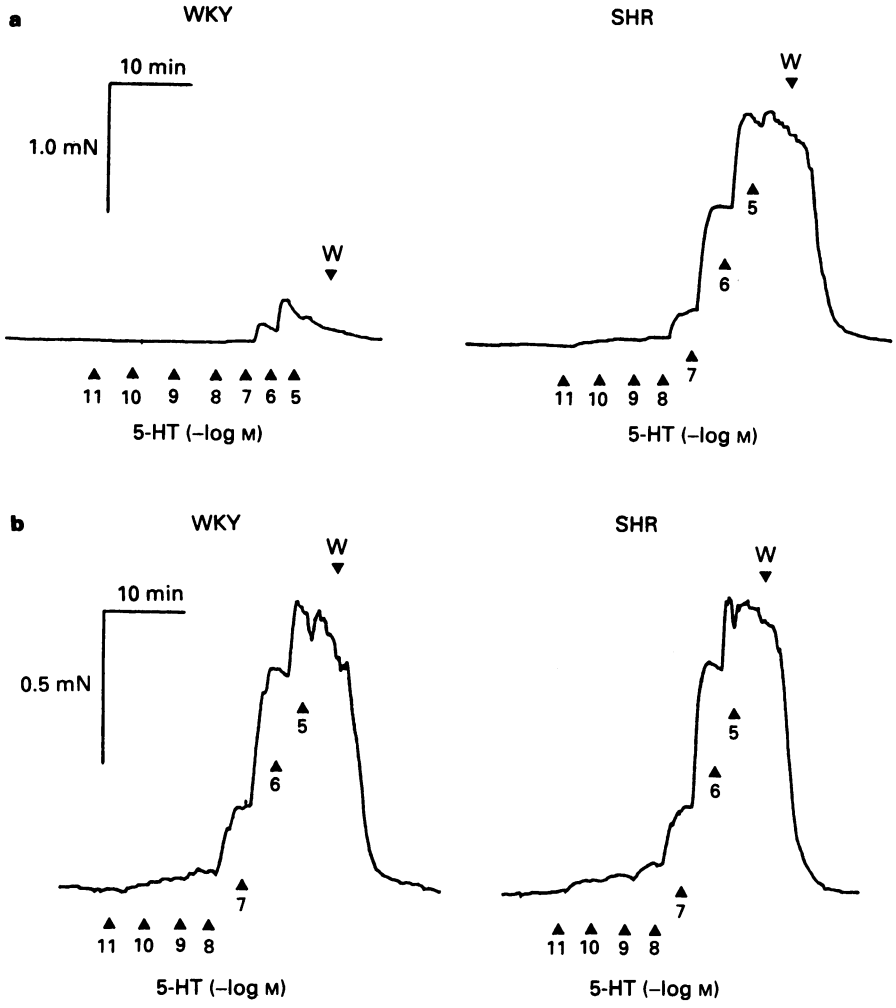

Figure 1 Typical traces of the contractile responses to 5-hydroxytryptamine (5-HT) in rings of basilar arteries from spontaneously hypertensive rats (SHR) and Wistar-Kyoto rats (WKY) with (a) and without (b) endothelium. 5-HT was added cumulatively at concentrations shown below the traces as – log M. W indicates washout of drugs. Note that responsiveness to 5-HT was markedly increased by removal of endothelium in WKY but not in SHR.

Figure 3, neither agent significantly affected resting tension or 5-HT-induced contraction. These results strongly suggest that the substance which is responsible for the endothelium-dependent attenuation of the contractile responses to 5-HT in rat basilar arteries is not NO.

Figure 4 shows the effect of L-NOARG on ACh-induced relaxation in basilar arteries which were precontracted by 1 μM 5-HT. Interestingly, a single addition of 1 μM 5-HT caused a large contraction in both WKY arteries (1.65 ± 0.10 mN, $n = 15$) and SHR arteries (1.85 ± 0.06 mN, $n = 15$). In contrast, a cumulative addition of 5-HT from 10 pM to 10 μM induced only small contractions (see Figures 1 and 2). Although the contraction induced by the single addition of 5-HT in WKY arteries was occasionally phasic and declined gradually after peaking, the contraction had a sustained component in over 60% of the preparations examined. Such a sustained contraction was always observed in WKY rings without endothelium and in SHR rings with and without endothelium. Under these conditions, ACh relaxed the precontracted arteries of both strains in a concentration-dependent fashion. The maximal relaxation induced by ACh was, however, significantly smaller in SHR arteries (41.1 ± 2.1% of an 80 mM K^+-induced contraction, $n = 5$) than in WKY arteries (88.1 ± 2.0%, $n = 5$, $P < 0.001$ vs. SHR). Treatment with 10 μM L-NOARG as well as the removal of endothelium, completely inhibited the ACh-induced relaxation in both strains. A similar inhibitory action was obtained using 10 μM methylene blue (data not shown,

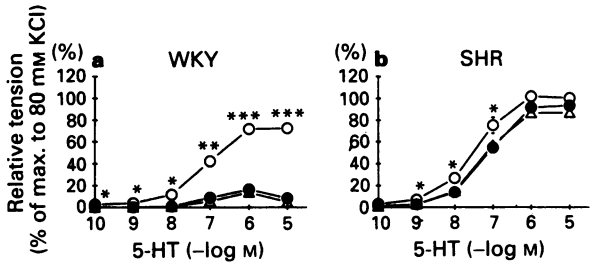

Figure 2 Effects of endothelium removal and treatment with indomethacin on the contractile responses to 5-hydroxytryptamine (5-HT) in rings of basilar arteries from WKY (a) and SHR (b). The maximum amplitude of an 80 mM K^+-induced contraction was taken as 100% in each preparation. Symbols indicate relative amplitude of 5-HT-induced contraction in rings with endothelium (●) ($n = 5$); without endothelium (○) ($n = 5$); with endothelium in the presence of 10 μM indomethacin (△) ($n = 5$). Indomethacin was applied to the rings at least 15 min prior to the addition of 5-HT. $^*P < 0.05$; $^{**}P < 0.01$ and $^{***}P < 0.001$ compared with values with endothelium for each strain.

$n = 5$). These results indicate that the relaxation response to ACh was mediated mainly by the release of NO from endothelium and was significantly reduced in SHR, as has been noted in other vessels (Mayhan *et al.*, 1987).

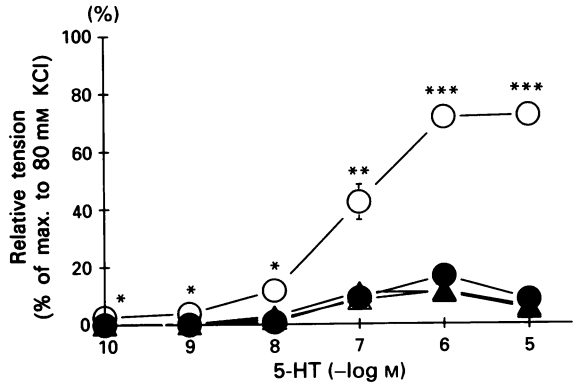

Figure 3 Effects of methylene blue and N^G-nitro-L-arginine (L-NOARG) on 5-hydroxytryptamine (5-HT)-induced contraction in rings of basilar artery with endothelium from WKY. Rings were exposed to 10 μM methylene blue or 10 μM L-NOARG for approximately 15 min prior to the cumulative addition of 5-HT. The maximum amplitude of an 80 mM K^+-induced contraction was taken as 100% in each preparation. Symbols indicate relative amplitude of 5-HT-induced contraction in rings with endothelium (●) ($n = 5$); without endothelium (○) ($n = 5$); with endothelium in the presence of 10 μM methylene blue (△) ($n = 5$); with endothelium in the presence of 10 μM L-NOARG (▲) ($n = 5$). $^*P<0.05$, $^{**}P<0.01$ and $^{***}P<0.001$ compared with the values with endothelium in WKY.

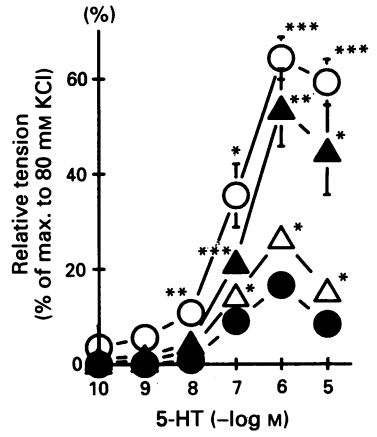

Figure 5 Effect of high K^+ on the contractile responses to 5-hydroxytryptamine (5-HT) in rings of basilar arteries with endothelium from WKY. The maximum amplitude of an 80 mM K^+-induced contraction was taken as 100% in each preparation. Rings were exposed to high K^+ (10, 15 or 20 mM) solution for approximately 15 min prior to the addition of 5-HT. Symbols indicate relative amplitude of 5-HT-induced contraction in normal K^+ solution (●) ($n = 5$); in 10 mM K^+ solution (△) ($n = 5$); in 15 mM K^+ solution (▲) ($n = 5$); in 20 mM K^+ solution (○) ($n = 5$). $^*P<0.05$, $^{**}P<0.01$ and $^{***}P<0.001$ compared with the values in normal K^+ solution.

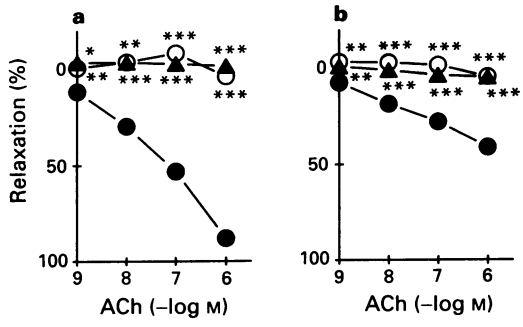

Figure 4 Effects of N^G-nitro-L-arginine (L-NOARG) on endothelium-dependent relaxation induced by acetylcholine (ACh) in rings of basilar arteries from WKY (a) and SHR (b) which had been precontracted with 1 μM 5-hydroxytryptamine (5-HT). Relaxations were expressed as percentages of the 1 μM 5-HT-induced contractions. Rings were exposed to 10 μM L-NOARG for approximately 15 min prior to the addition of ACh. Symbols show relative relaxation in rings with endothelium (●) ($n = 5$); without endothelium (○) ($n = 5$); with endothelium in the presence of L-NOARG (▲) ($n = 5$). $^*P<0.05$, $^{**}P<0.01$ and $^{***}P<0.001$ compared with the values with endothelium for each strain.

Figure 5 shows the influence of an increase in extracellular K^+ concentration on the contractile response of WKY arteries to 5-HT. In 10, 15, or 20 mM K^+ solutions, the tension of basilar arteries developed slightly but significantly by 0.3 ± 0.3, 1.9 ± 1.0 and 9.7 ± 1.4% of the 80 mM K^+-induced contraction, respectively. The contractile response of arteries to 5-HT was significantly enhanced in these high K^+ solutions. In contrast, the maximal response to 5-HT in endothelium-rubbed WKY arteries was not significantly affected by an increase in extracellular K^+ concentration to 20 mM (data not shown, $n = 5$). These results suggested that the endothelium-dependent attenuation of 5-HT-induced contraction may be mediated by the activation of K^+ channels. Therefore, the effect of tetraethylammonium (TEA), a K^+-channel blocker, on the response of WKY arteries to 5-HT was examined (Figure 6).

Figure 6a shows a typical trace of mechanical responses to 5-HT in WKY basilar arteries with endothelium in the presence of 3.2 mM TEA. Application of TEA did not significantly change the resting tension but dramatically augmented the 5-HT-induced contractions which were accompanied by rhythmic oscillations (Figure 6a, right). The enhancement of 5-HT-induced contraction by TEA depended upon the concentration of TEA in the range 0.1 to 3.2 mM (Figure 6b left). At a higher concentration (3.2 mM) TEA significantly enhanced the maximal contraction from 16.6 ± 0.8 to 66.6 ± 3.3% ($P<0.001$) of an 80 mM K^+-induced contraction.

Figure 6b (right) shows the effects of a further addition of 10 μM L-NOARG in the presence of 1 mM TEA on 5-HT-induced responses in WKY arteries with endothelium. Although the application of 10 μM L-NOARG alone did not affect the response (see Figure 3), application in the presence of 1 mM TEA induced an additional enhancement of the response. These results strongly suggest that a TEA-sensitive relaxing factor, which is distinct from NO, predominates in the response to 5-HT in WKY arteries. However, NO is also released and functional when the effect of the major factor is blocked by TEA or high K^+.

In SHR arteries with endothelium, application of 0.3 or 3.2 mM TEA increased the resting tension by 6.3 ± 2.1 and 32.7 ± 3.6% of the 80 mM K^+-induced contraction, respectively. Therefore, only the effect of 0.3 mM TEA on the response to 5-HT was examined. In contrast to WKY arteries, the application of 0.3 mM TEA significantly enhanced the response of SHR arteries to low concentrations of 5-HT and did not affect the maximal response (Figure 7). Moreover, 10 μM L-NOARG, itself, also enhanced the response to low concentrations of 5-HT.

Discussion

It is apparent that the contractile response to 5-HT in WKY is greatly attenuated by endothelium-dependent mechanisms. In contrast to previous observations in the cat and human basilar arteries (Conde *et al.*, 1991), removal of the endothelium markedly augmented 5-HT-induced contractions in WKY basilar arteries. The augmentation of the contraction by removal of endothelium in WKY basilar arteries

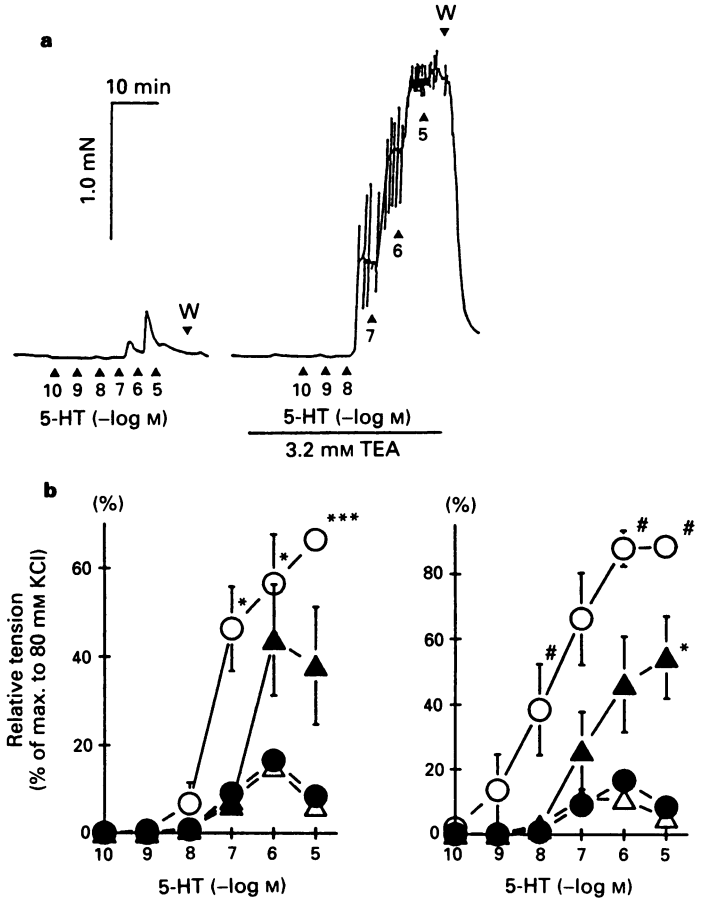

Figure 6 Effects of treatment with tetraethylammonium (TEA) and/or N^G-nitro-L-arginine (L-NOARG) on 5-hydroxytryptamine (5-HT)-induced contraction in rings of basilar arteries with endothelium from WKY. (a) 5-HT was added cumulatively at concentrations shown below the traces as $-\log$ M. Rings were exposed to 3.2 mM TEA for approximately 15 min prior to the addition of 5-HT. W indicates washout of drugs. (b) (left): Summarized data of the results as shown in (a). Symbols indicate relative amplitude of 5-HT-induced contraction in the absence of TEA (●) and in the presence of 0.1 mM TEA (Δ), 0.3 mM TEA (▲), and 3.2 mM TEA (Δ). (b) (right): Effect of L-NOARG on 5-HT-induced contraction in the presence of 1 mM TEA from 15 min prior to the addition of 5-HT. Symbols indicate relative amplitude of 5-HT-induced contraction in the absence of TEA and L-NOARG (●) and in the presence of 10 μM L-NOARG (Δ) or 1 mM TEA (▲) and both 10 μM L-NOARG and 1 mM TEA (○) The maximum amplitude of an 80 mM K^+-induced contraction was taken as 100% in each preparation ($n = 5$). $^*P<0.05$ and $^{***}P<0.001$ compared with the values in the absence of TEA and L-NOARG and $^{**}P<0.05$ compared with the values in the presence of 1 mM TEA.

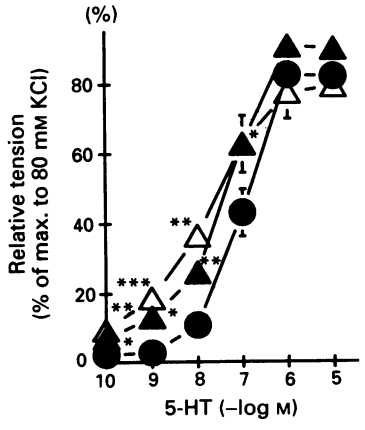

Figure 7 Effects of N^G-nitro-L-arginine (L-NOARG) and tetraethylammonium (TEA) on 5-hydroxytryptamine (5-HT)-induced contraction in rings of basilar arteries with endothelium from SHR. The maximum amplitude of an 80 mM K^+-induced contraction was taken as 100% in each preparation. Rings were exposed to 10 μM L-NOARG or 0.3 mM TEA for approximately 15 min prior to the addition of 5-HT. Symbols indicate relative amplitude of 5-HT-induced contraction in the absence of L-NOARG and TEA (●) ($n = 6$); in the presence of 10 μM L-NOARG (Δ) ($n = 7$); in the presence of 0.3 mM TEA (▲) ($n = 6$). $^*P<0.05$, $^{**}P<0.01$ and $^{***}P<0.001$ compared with values in the absence of L-NOARG or TEA.

appears to be similar to that described in canine and rabbit basilar arteries (Connor & Feniuk, 1989; Garland, 1987; Trezise *et al.*, 1992). Underlying mechanisms in WKY may, however, be distinctive from those in dogs and rabbits. In the present study, treatment with methylene blue of L-NOARG affected neither resting tension nor the 5-HT-induced contraction in WKY basilar arteries. This treatment and the removal of the endothelium markedly enhanced 5-HT-induced contractions in the rabbit and dog, implying that NO released from endothelium attenuates the contraction. Moreover, cyclo-oxygenase products such as prostacyclin (PGI_2) have no role in resting tension or the response to 5-HT in the WKY basilar arteries, since tension changes were not affected by treatment with indomethacin. The results strongly suggest that the major EDRF responsible for the attenuation of 5-HT-induced contraction in basilar WKY arteries was neither NO nor cyclo-oxygenase products.

However, the results do not exclude the possibility that NO has a role as an EDRF in WKY basilar arteries. The ACh-induced relaxation in precontracted basilar arteries of both strains was almost completely inhibited by methylene blue or L-NOARG, and was, therefore, attributable to the release of NO from the endothelium. Moreover, under conditions where the effect of the major relaxing factor was blocked by TEA, NO, which was released concomitantly, significantly contributed to attenuation of the 5-HT-induced

contraction (Figure 6b, right). In rabbit basilar artery, NO, which is released by ACh from endothelium, significantly contributes to the subsequent relaxation (Rand & Garland, 1992). Contribution of NO as a hyperpolarizing factor may be small in the basilar artery of WKY but was not examined directly in the present study. Cyclo-oxygenase products do not appear to have a role even under these conditions (Yokota, unpublished observation).

The major relaxing factor released from the endothelium in rat basilar arteries in response to 5-HT was not determined in the present study. It was, however, found that the relaxing mechanism was not functional in high K^+ solution or in the presence of the K^+-channel blocker, TEA. It has been reported that L-NOARG-resistant relaxation in some vascular tissues is accompanied by membrane hyperpolarization caused by EDHF (Chen *et al.*, 1988; 1991; Garland & McPherson, 1992; Nagao & Vanhoutte, 1992; Pacicca *et al.*, 1992). This hyperpolarization of smooth muscle cells and the associated relaxation are impaired by elevating the extracellular K^+ concentration or by applying TBA (a non-selective K^+-channel blocker). These observations suggest that the endothelium-dependent attenuation of 5-HT-induced contraction in the present study is due to membrane hyperpolarization via K^+-channel activation; however, direct evidence was not obtained. The marked reduction in 5-HT-induced contraction in basilar arteries of both strains by a Ca-channel blocker (Yokota, unpublished observation) indicates the contribution of Ca^{2+}-influx through voltage-dependent Ca channels to the contraction. The Ca^{2+}-influx may be elicited by, or at least enhanced by, membrane depolarization, and may be reduced by hyperpolarization.

At least two kinds of K^+ channels have been postulated as the targets of endogenous relaxants which hyperpolarize vascular smooth muscle cells (Nelson, 1993): ATP-sensitive K^+ channels which are selectively blocked by glibenclamide (Standen *et al.*, 1989), and Ca^{2+}-dependent K^+ channels which have large conductance (BK channels) and are blocked by charybdotoxin with relatively high selectivity (Brayden & Nelson, 1992). In the present study, low concentrations of TEA markedly reduced the attenuation of 5-HT-induced contraction, implying that the activation of BK channels by EDHF may be predominantly important in the response. Further experiments, such as measurements of membrane potential and currents of smooth muscle cells, are required to identify whether activation of K^+ channels by EDHF is responsible for the mechanism in rat basilar artery and, if this is the case, which kind of K^+ channel in the target.

In SHR basilar arteries, a marked contraction was elicited by 5-HT whether the endothelium was present or absent. Since the magnitude of contraction induced by 5-HT or 80 mM K^+ was almost identical in WKY and SHR rings without endothelium, the difference between the 2 strains in the response to 5-HT is mainly due to functional changes in the endothelium of SHR. Luscher & Vanhoutte (1986b) have reported that it is the augmented release of EDCF rather than the decreased release of EDRF that contributes to the reduction of endothelium-dependent attenuation of contractile response to 5-HT in the thoracic aorta of SHR. This may not be so in the basilar artery, since the contractile response in SHR to 5-HT was slightly but significantly increased by the removal of endothelium and was not normalized by treatment with indomethacin. It is, therefore, likely that the release of an EDHF-like substance from endothelium is decreased in SHR. However, the change in sensitivity of smooth muscle cells to the substance cannot be ruled out.

The reason why 0.3 mM TEA significantly increased resting tension in basilar artery of SHR but not that of WKY could be explained in a similar manner as suggested for the carotid artery (Asano *et al.*, 1993). The difference in Ca-channel activity in WKY and SHR vascular smooth muscle cells has been speculated upon (Asano *et al.*, 1986). Since Ca^{2+}-influx at rest through L-type Ca channels in vascular smooth muscle cells in SHR may be larger than those in WKY, the activity of Ca^{2+}-dependent K^+ channels may also be higher in SHR than WKY as indicated by the ^{86}Rb-efflux rate. The block of Ca^{2+}-dependent K^+ channels by TEA may result in membrane depolarization and more Ca^{2+}-influx in SHR.

The response to low concentrations of 5-HT in SHR basilar arteries was significantly augmented by 0.3 mM TEA, whereas the maximal response was not affected. Higher concentrations of TEA were required to augment the response to 5-HT in WKY. The result may be intepreted as follows. The release of an EDHF-like substance in SHR is small and not sufficient to reduce the maximal contractile response to 5-HT but can attenuate submaximal responses. The sensitivity to TEA, therefore, appears to be higher in SHR than in WKY. Similar observations have been made in other vasculature of hypertensive rats (Fujii *et al.*, 1992; Van de Voorde *et al.*, 1992).

Consistent with previous observations, the present study also indicates that the release of NO from endothelium in response to ACh may be greatly reduced in SHR basilar arteries. Interestingly, treatment with L-NOARG alone did not affect the 5-HT-induced contraction in WKY basilar arteries but significantly augmented those from SHR. The augmentation by L-NOARG in WKY was observed only in the presence of TEA. Although this result was unexpected, it may suggest that the relaxation mechanism, including the synthesis and the release of an EDHF-like substance in the SHR endothelium, is more seriously impaired than that of NO.

In conclusion, the endothelium of rat basilar artery exerts an attenuating influence on the responsiveness of smooth muscle to 5-HT. The major mechanism for this is not the release of NO or cyclo-oxygenase products, but may be an activation of K^+ channels, possibly Ca^{2+}-dependent K^+ channels. The attenuation was significantly smaller in SHR than in WKY. The decreased attenuation in SHR may be explained by the inability of endothelium to release an EDHF-like substance but not by augmented release of EDCF.

We thank Mr T Miki, Miss K. Yamashita and Miss R. Azuma for their excellent technical help. We also appreciate Dr Naomi Anderson for her critical reading of the manuscript.

References

ALTIERE, R.J., KIRITSY-ROY, J.A. & CATRAVAS, J.D. (1985). Acetylcholine-induced contractions in isolated rabbit pulmonary arteries: role of thromboxane A_2. *J. Pharmacol. Exp. Ther.*, **236**, 535–541.

ASANO, M., AOKI, K. & MATSUDA, T. (1986). Contractile effects of Bay K 8644, dihydropyridine calcium agonist, on isolated femoral arteries from spontaneously hypertensive rats. *J. Pharmacol. Exp. Ther.*, **239**, 198–205.

ASANO, M., MASUZAWA-ITO, K., MASUDA, T., IMAIZUMI, Y., WATANABE, M. & ITO, K. (1993). Functional role of Ca^{2+}-activated K^+ channels in resting state of carotid arteries from SHR. *Am. J. Physiol.*, **265**, H843–H851.

BRAYDEN, J.E. & NELSON, M.T. (1992). Regulation of arterial tone by activation of calcium-dependent potassium channels. *Science*, **256**, 532–535.

CHEN, G., SUZUKI, H. & WESTON, A.H. (1988). Acetylcholine releases endothelium-derived hyperpolarizing factor and EDRF from rat blood vessels. *Br. J. Pharmacol.*, **95**, 1165–1174.

CHEN, G., YAMAMOTO, Y., NIWA, K. & SUZUKI, H. (1991). Hyperpolarization of arterial smooth muscle induced by endothelial humoral substances. *Am. J. Physiol.*, **260**, H1888–H1892.

CONDE, M.V., MARCO, E.J., FRAILE, M.L., BENITO, J.M., MORENO, M.J., SANZ, M.L. & LOPEZ DE PABLO, A.L. (1991). Different influence of endothelium in the mechanical responses of human and cat isolated cerebral arteries to several agents. *J. Pharm. Pharmacol.*, **43**, 255–261.

CONNOR, H.E. & FENIUK, W. (1989). Influence of the endothelium on contractile effects of 5-hydroxytryptamine and selective 5-HT agonists in canine basilar artery. *Br. J. Pharmacol.*, **96**, 170–178.

FUJII, K., TOMINAGA, M., OHMORI, S., KOBAYASHI, K., KOGA, T., TAKATA, Y. & FUJISHIMA, M. (1992). Decreased endothelium-dependent hyperpolarization to acetylcholine in smooth muscle of the mesenteric artery of spontaneously rats. *Circ. Res.*, **70**, 660–669.

FURCHGOTT, R.F. & ZAWADZKI, J.V. (1980). The obligatory role of endothelial cells in the relaxation of arterial smooth muscle by acetylcholine. *Nature*, **288**, 373–376.

GARLAND, C.J. (1987). The role of membrane depolarization in the contractile response of the rabbit basilar artery to 5-hydroxytryptamine. *J. Physiol.*, **392**, 333–348.

GARLAND, C.L. & MCPHERSON, G.A. (1992). Evidence that nitric oxide does not mediate the hyperpolarization and relaxation to acetylcholine in the rat small mesenteric artery. *Br. J. Pharmacol.*, **105**, 429–435.

IGNARRO, L.J., BYRNS, R.E., BUGA, G.M. & WOOD, K.S. (1987). Endothelium-derived relaxing factor from pulmonary artery and vein possesses pharmacologic and chemical properties identical to those of nitric oxide radical. *Circ. Res.*, **61**, 866–879.

KONISHI, M. & SU, C. (1983). Role of endothelium in dilator responses of spontaneously hypertensive rat arteries. *Hypertension*, **5**, 881–886.

LUSCHER, T.F. & VANHOUTTE, P.M. (1986a). Endothelium-dependent contractions to acetylcholine in the aorta of the spontaneously hypertensive rat. *Hypertension*, **8**, 344–348.

LUSCHER, T.F. & VANHOUTTE, P.M. (1986b). Endothelium-dependent responses to platelets and serotonin in spontaneously hypertensive rats. *Hypertension*, 8 (Suppl. II), 1155–1160.

MAYHAN, W.G., FARACI, F.M. & HEISTAD, D.D. (1987). Impairment of endothelium-dependent responses of cerebral arterioles in chronic hypertension. *Am. J. Physiol.*, **253**, H1435–H1440.

NAGAO, T. & VANHOUTTE, P.M. (1992). Hyperpolarization as a mechanism for endothelium-dependent relaxations in the porcine coronary artery. *J. Physiol.*, **445**, 355–367.

NAKAGOMI, T., KASSELL, N.F., SASAKI, T., LEHMAN, R.M., TORNER, J.C., HONGO, K. & LEE, J.H. (1988). Effect of removal of the endothelium on vasoconstriction in canine and rabbit basilar arteries. *J. Neurosurg.*, **68**, 757–766.

NELSON, M.T. (1993). Ca^{2+}-activated potassium channels and ATP-sensitive potassium channels as modulators of vascular tone. *Trends Cardiovasc. Med.*, **3**, 54–60.

PACICCA, C., VON DER WEID, P.-Y. & BENNY, J.-L. (1992). Effect of nitro-L-arginine on endothelium-dependent hyperpolarizations and relaxations of pig coronary arteries. *J. Physiol.*, **457**, 247–256.

PALMER, R.M.J., FERRIGE, A.G. & MONCADA, S. (1987). Nitric oxide release accounts for the biological activity of endothelium-derived relaxing factor. *Nature*, **327**, 524–526.

RAND, V.E. & GARLAND, C.J. (1992). Endothelium-dependent relaxation to acetylcholine in the rabbit basilar artery: importance of membrane hyperpolarization. *Br. J. Pharmacol.*, **106**, 143–150.

STANDEN, N.B., QUAYLE, J.M., DAVIES, N.W., BRAYDEN, J.E., HUANG, Y. & NELSON, M.T. (1989). Hyperpolarizing vasodilators activate ATP-sensitive K^+ channels in arterial smooth muscle. *Science*, **245**, 177–180.

TREZISE, D.J., DREW, G.M. & WESTON, A.H. (1992). Analysis of the depressant effect of the endothelium on contractions of rabbit isolated basilar artery to 5-hydroxytryptamine. *Br. J. Pharmacol.*, **106**, 587–592.

VAN DE VOORDE, J., VANHEEL, B. & LEUSEN, I. (1992). Endothelium-dependent relaxation and hyperpolarization in aorta from control and renal hypertensive rats. *Circ. Res.*, **70**, 1–8.

VANHOUTTE, P.M. (1987). Endothelium-dependent contractions in arteries and veins. *Blood Vessels*, **24**, 141–144.

VANHOUTTE, P.M. & KATUSIC, Z.S. (1988). Endothelium-derived contracting factor. Endothelin and/or superoxide anion? *Trends Pharmacol. Sci.*, **9**, 229–230.

WATT, P.A.C. & THURSTON, H. (1989). Endothelin-dependent relaxation in resistance vessels from the spontaneously hypertensive rats. *J. Hypertension*, **7**, 661–666.

WINQUIST, R.J., BUNTING, P.B., BASKIN, E.P. & WALLACE, A.A. (1984). Decreased endothelium-dependent relaxation in New Zealand genetic hypertensive rats. *J. Hypertension*, **2**, 541–545.

YOUNG, A.R., MACKENZIE, E.T., SEYLAZ, J. & VERRECCHIA, C. (1986). Receptors involved in the 5-hydroxytryptamine-induced contraction of isolated cerebral arteries. *Acta Physiol. Scand.* (Suppl.), **552**, 54–57.

(Received November 9, 1993
Revised May 15, 1994
Accepted May 27, 1994)

British Journal of Pharmacology

VOLUME 113 (1) SEPTEMBER 1994

BRITISH JOURNAL OF PHARMACOLOGY

The *British Journal of Pharmacology* welcomes contributions in all fields of experimental pharmacology including neuroscience, biochemical, cellular and molecular pharmacology. The Board of Editors represents a wide range of expertise and ensures that well-presented work is published as promptly as possible, consistent with maintaining the overall quality of the journal.

Edited for the British Pharmacological Society by

A.T. Birmingham
(Chairman)

R.W. Horton **W.A. Large**
(Secretaries)

Submission of manuscripts: Manuscripts (two copies) should be sent to The Editorial Office, British Journal of Pharmacology, St. George's Hospital Medical School, Cranmer Terrace, London SW17 0RE.

Authors should consult the Instructions to Authors and the Nomenclature Guidelines for Authors in Vol. **111**, 378–387. These Instructions and Guidelines also appear with the journal Index for Volumes **108–110**, 1993. A checklist of the essential requirements is summarised in each issue of the journal, or as the last page of the issue.

The *British Journal of Pharmacology* is published by Macmillan Press Ltd.

Scope The *British Journal of Pharmacology* is published monthly. It welcomes contribution in all field of experimental pharmacology including neuroscience, biochemical, cellular and molecular pharmacology. The Board of Editors represents a wide range of expertise and ensures that well-presented work is published as promptly as possible, consistent with maintaining the overall qulaity of the journal

This journal is covered by Current Contents, Excerpta Medica, BIOSIS and Index Medicus.

Editorial Manuscripts (plus two copies) and all editorial correspondence should be sent to: The Editorial Office, British Journal of Pharmacology, St George's Hospital Medical School, Cranmere Terrace, London SW17 0RE, UK. Tel: +44 81 767 6765; Fax: +44 81 767 5645.

Advertisements Enquires concerning advertisements should be addressed to: Michael Rowley, Hasler House, High Street, Great Dunmow, Essex CM6 1AP. Tel: +44 371 874613; Fax: +44 371 872273.

Publisher All business correspondence, supplement enquiries and reprint requests should be addressed to British Journal of Pharmacology, Scientific and Medical Division, Macmillan Press Ltd, Houndmills, Basingstoke, Hampshire RG21 2XS, UK. Tel: +44 256 29242; Fax: +44 256 810526. Publisher: Marija Vukovojac. Editorial Assistant: Alice Ellingham. Production Controller: Kath Parr.

Subscription Subscription price per annum (one volume, twelve issues) £540, rest of world £714 (Airmail), £595 (Surface mail) or equivalent in any other currency. Orders must be accompanied by remittance. Cheques should be made payable to Macmillan Magazines and sent to: The Subscription Department, Macmillan Press Ltd, Houndmills, Basingstoke, Hampshire RG21 2XS, UK. Where appropriate, subscribers may make payments into UK Post Office Giro Account No. 519 2455. Full details must accompany the payment. Subscribers from EC territories should add sales tax at the local rate.

British Journal of Pharmacology (ISSN 0007–1188) is published monthly by Macmillan Press Ltd, c/o Mercury Airfreight International Ltd, 2323 Randolph Avenue, Avenel, NJ 07001, USA. Subscription price for institutions is $950 per annum. 2nd class postage is paid at Rahway NJ. Postmaster: send address corrections to Macmillan Press Ltd, c/o Mercury Airfreight International Ltd, 2323 Randolph Avenue, Avenel NJ 07001.

Reprints of any article in this journal are available from Scientific and Medical Division, Macmillan Press Ltd, Houndmills, Basingstoke, Hampshire RG21 2XS, UK. Tel: +44 256 29242; Fax: +44 256 810526.

ISSN 0007–1188

Official publication of the British Pharmacological Society.

PREPARATION OF MANUSCRIPTS

Authors are strongly recommended to read the full *Instructions to Authors* and *Nomenclature Guidelines for Authors* (*Br. J. Pharmacol.* 1994, **111**, 378–387) before submitting a manuscript for publication in the *British Journal of Pharmacology*. The manuscript and cover letter should be checked against the following list before mailing.

The original and one copy of the manuscript must be supplied. Manuscripts must be typed in double-line spacing on one side of A4 paper, in type not smaller than 12 characters per inch or 10 point. Both copies to include Tables and a set of labelled Figures. One set of Figures without numbers or letters is also to be included. The text to be arranged in the following subsections:

1. **Title**—To have no more than 150 characters on a separate page, which should also include a Short Title (50 characters maximum) and the name and address of the author for correspondence.
2. **Summary**—To be arranged in numbered paragraphs (Full Papers) or a single paragraph (Special Reports).
   —to include aims, principal results and conclusions.
   —to include Key words (10 maximum) at end of summary.
3. **Introduction**—To contain concise statements of the problem and the aims of the investigation.
4. **Methods**—To have brief but adequate account of the procedures; *full names of drugs* (*including those referred to by manufacturer's code*), sources of drugs and statistical tests to be stated.
5. **Results**—To have no repetition of data in Figures, Tables and text.
6. **Discussion**—Findings and conclusions to be placed in context of other relevant work.
   NB Simple repetition of results and unwarranted speculation are not acceptable.
7. **Acknowledgements**—Sources of support. Sources of drugs not widely available commercially.
8. **References**—All references in the text to be included in the Reference List and *vice versa*. References in alphabetical order with complete citations; Journals publishing 'in press' papers identified.
   References to manuscripts submitted to other journals but not yet accepted are not allowed.
9. **Tables**—Each on a separate page and prepared in accordance with current requirements of the Journal.
10. **Figures**—Both labelled and non-labelled Figures to be prepared in accordance with current requirements of the Journal (see *Instructions to Authors*, 1993, **108**, 275–281) and provided with Figure Number and Authors' names on back (*in pencil*).
    —each legend to be typed on a separate page and carrying keys to symbols.
    —keys to symbols and histograms must not appear on the figures themselves, but in the respective legends.
    —'box style' figures are not in keeping with the Journal style; line drawings etc must have only left-hand and bottom axes.
11. **Manuscripts**—To be accompanied by a declaration signed by each author that
    (a) results are original
    (b) approval of all persons concerned has been given to submit manuscripts for consideration (see also 12b)
    (c) the same material is neither 'in press' (i.e. is in proof or has definitely been accepted for publication) nor under consideration elsewhere. Furthermore it will not be submitted or published elsewhere before a decision has been reached by the Editorial Board of the *British Journal of Pharmacology* and will not be submitted elsewhere if accepted by the *British Journal of Pharmacology*.
    (d) Copyright assignment is included.
12. **Cover letter**—To state clearly
    (a) Corresponding author's full postal address, telephone, telex or Fax number
    (b) where appropriate, that *either* ethical approval has been given for investigation *or* Company or Institutional permission to publish work has been received.
13. **Reminder**—Packaging to be sufficiently robust to protect Figures and to withstand mailing.

Failure to comply with *Instructions to Authors* may lead to substantial delays in processing, review and publication and may even jeopardize acceptance of the manuscript.

NOMENCLATURE

Authors are reminded that accepted receptor and associated terminology is laid out in *Nomenclature Guidelines for Authors*, as published in the *British Journal of Pharmacology*, *Br. J. Pharmacol.*, 1994, **111**, 385–387.

SPECIAL REPORTS

The purpose of *Special Reports* is to provide rapid publication for **new** and **important** results which the Editorial Board considers are likely to be of special pharmacological significance. *Special Reports* will have publication priority over all other material and so authors are asked to consider carefully the status of their work before submission.

In order to speed publication there is normally no revision allowed beyond very minor typographical or grammatical corrections. If significant revision is required, the Board may either invite rapid re-submission or, more probably, propose that it be re-written as a Full Paper and be re-submitted for consideration. In order to reduce delays, proofs of *Special Reports* will be sent to authors but **essential corrections must reach the Production Office within 48 hours of receipt.** Authors should ensure that their submitted material conforms exactly to the following requirements.

Special Reports should normally occupy no more than two printed pages of the Journal; two illustrations (Figures or Tables, with legends) are permitted. As a guideline, with type face of 12 pitch and double-line spacing, a page of A4 paper could contain about 400 words. The absolute maximum length of the *Special Report* is 1700 words. For each Figure or Table, please deduct 200 words. The manuscript should comprise a Title page with key words (maximum of 10), a Summary consisting of a single short paragraph, followed by Introduction, Methods, Results, Discussion and References (maximum of 10). In all other respects, the requirements are the same as for Full Papers (see current 'Instructions to Authors').

BRITISH JOURNAL OF PHARMACOLOGY VOLUME 113 (1) 1994

SPECIAL REPORTS

PAPERS

Contents continue inside back cover

Typeset by Elite Typesetting Techniques, Southampton, Hampshire
and printed in Great Britain by Unwin Brothers Ltd., The Gresham Press, Old Woking, Surrey